PERIODICAL

WOODS HOLE OCEANOGRAPHIC INSTITUTION

COLLECTED REPRINTS

1953

SEP 1954
LIBRARY
POFI
FISH & WILDLIFE
SERVICE

JULY, 1954

LIBRARY
BUREAU OF COMMERCIAL FISHERIES
U. S. FISH AND WILDLIFE SERVICE
P. O. BOX 3830
HONOLULU 12, HAWAII

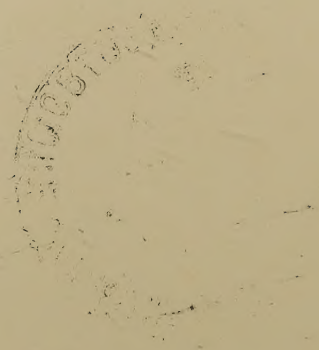

WOODS HOLE OCEANOGRAPHIC INSTITUTION

COLLECTED REPRINTS

1953

1712

JULY, 1954

This volume contains contributions from the

WOODS HOLE OCEANOGRAPHIC INSTITUTION

which appeared in 1953 in publications other than

Papers in Physical Oceanography and Meteorology;

also the Annual Report of the Director

for the year 1953

TABLE OF CONTENTS

Contribution No.

BIGELOW, HENRY B., WILLIAM C. SCHROEDER and STEWART SPRINGER
New and Little Known Sharks from the Atlantic and from the Gulf of Mexico 596

BLANCHARD, DUNCAN C.
Raindrop Size-Distribution in Hawaiian Rains 658
A Simple Recording Technique for Determining Raindrop Size and Time of Occurrence of Rain Showers 659

BUNKER, ANDREW F.
On the Determination of Moisture Gradients from Radiosonde Records . . . 605
Diffusion, Entrainment and Frictional Drag Associated with Non-Saturated, Buoyant Air Parcels Rising through a Turbulent Air Mass. 631

FARMER, HARLOW G. and GEORGE W. MORGAN
The Salt Wedge 638

FRANCIS J. R. D.
A Note on the Velocity Distribution and Bottom Stress in a Wind-Driven Water Current System 639

HELA, ILMO, HILARY B. MOORE and HARDING OWRE
Seasonal Changes in the Surface Water Masses and in their Plankton in the Bermuda Area 677

HOUGH, JACK L.
Pleistocene Climatic Record in a Pacific Ocean Core Sample 641

KETCHUM, BOSTWICK H.
Circulation in Estuaries 642

KETCHUM, BOSTWICK H. and D. JEAN KEEN
The Exchanges of Fresh and Salt Waters in the Bay of Fundy and in Passamaquoddy Bay 593

MALKUS, JOANNE STARR and MELVIN E. STERN
The Flow of a Stable Atmosphere over a Heated Island, Part I 624

MALKUS, WILLEM V. R.
A Recording Bathypitotmeter 634

MILLER, ARTHUR R.
Some Suggestions for more precise Loran Navigation (Dated 1951) 718

MOORE, HILARY B., HARDING OWRE, EVERETT C. JONES and T. DOW
Plankton of the Florida Current. III. The Control of the Vertical Distribution of Zooplankton in the Daytime by Light and Temperature 669

Contribution No.

OFFICER, CHARLES B., JR.
The Refraction Arrival in Water Covered Areas 629

REDFIELD, ALFRED C.
Interference Phenomena in the Tides of the Woods Hole Region 636

ROELOFS, E. W. and D. F. BUMPUS
The Hydrography of Pamlico Sound 547

SAID, RUSHDI
Foraminifera of Great Pond, East Falmouth, Massachusetts 588

SCHEVILL, WILLIAM E. and BARBARA LAWRENCE
Auditory Response of a Bottlenosed Porpoise, *Tursiops truncatus*, to Frequencies above 100 kc. 648

High-Frequency Auditory Response of a Bottlenosed Porpoise, *Tursiops truncatus* (Montagu) 663

SCHOLANDER, P. F. and L. VAN DAM
Composition of the Swimbladder Gas in Deep Sea Fishes 632

SOULE, FLOYD M., P. S. BRANSON and R. P. DINSMORE
Physical Oceanography of the Grand Banks Region and the Labrador Sea in 1951 (Dated 1952) 601

STERN, MELVIN E. and JOANNE STARR MALKUS
The Flow of a Stable Atmosphere over a Heated Island, Part II 625

STOMMEL, HENRY
Computation of Pollution in a Vertically Mixed Estuary 640

Examples of the Possible Role of Inertia and Stratification in the Dynamics of the Gulf Stream System 645

The Role of Density Currents in Estuaries 655

STOMMEL, HENRY and HARLOW G. FARMER
Control of Salinity in an Estuary by a Transition 587

STOMMEL, HENRY, W. S. VON ARX, D. PARSON and W. S. RICHARDSON
Rapid Aerial Survey of Gulf Stream with Camera and Radiation Thermometer 644

TURNER, HARRY J., JR.
The Drilling Mechanism of the Naticidae 630

Fifth Report on Investigations of the Shellfisheries of Massachusetts (Dated 1952) 656

VAN DAM, L. and P. F. SCHOLANDER
Concentration of Hemoglobin in the Blood of Deep Sea Fishes 633

Contribution No.

VISHNIAC, HELEN S. and S. W. WATSON
The Steroid Requirements of *Labyrinthula vitellina* var. *pacifica* 623

VON ARX, WILLIAM S.
Cartographic Principles Applied to Wide-Field Photography 649

WATSON, E. E.
An Experiment to Determine the Hydrodynamic Forces on a Cable inclined to the Direction of Flow 686

WOODCOCK, A. H.
Salt Nuclei in Marine Air as a Function of Altitude and Wind Force . . . 643
Hawaii as a Cloud Physics Laboratory 660

WOODCOCK, A. H., C. F. KIENTZLER, A. B. ARONS and D. C. BLANCHARD
Giant Condensation Nuclei from Bursting Bubbles 673

WORTHINGTON, L. V.
Oceanographic Results of Project Skijump I and Skijump II in the Polar Sea, 1951–1952 628

THE WOODS HOLE OCEANOGRAPHIC INSTITUTION
Report for the year 1953

LIST OF CONTRIBUTIONS

The following contributions, published in 1953, are not included in this volume.

BIGELOW, H. B. and W. C. SCHROEDER
Fishes of the Gulf of Maine 592

SEARS, MARY
Notes on Siphonophores. 2. A Revision of the Abylinae 602

STETSON, HENRY C.
The Sediments of the Western Gulf of Mexico. Part I. The Continental Terrace of the Western Gulf of Mexico: its Surface Sediments, Origin and Development 646

TRASK, PARKER D.
The Sediments of the Western Gulf of Mexico. Part II. Chemical Studies of Sediments of the Western Gulf of Mexico 647

Contribution No. 547

Reprinted from
BULLETIN OF MARINE SCIENCE
OF THE GULF AND CARIBBEAN
Vol. 3, No. 3, pp. 181-205
DECEMBER, 1953

THE HYDROGRAPHY OF PAMLICO SOUND[1,2]

by

E. W. ROELOFS

Institute of Fisheries Research, University of North Carolina

and

D. F. BUMPUS

Woods Hole Oceanographic Institution

ABSTRACT

The horizontal distribution of salinity in Pamlico Sound is influenced by wind and long-term runoff. Vertical salinity gradients are minimal (<0.7 °/₀₀/20 feet) in the main body of the sound, intermediate (>12 °/₀₀ /20 feet) in the river mouths and maximal (>14 °/₀₀/9 feet) in the northern part of Core Sound. Water temperature closely follows air temperature with practically no stratification. Currents in the sound resulting from wind friction reach velocities of 69 cm./sec. Currents resulting from runoff are calculated to be of the order of 0.5 cm./sec. Tidal exchange in the inlets amounts to about 220 x $10^6 m^3$ per tide. This amount, equivalent to 8 times the average river flow, would produce a rise and fall over the whole sound of 5 cm. Estimates of wind "setup" at the northern end of of Pamlico Sound are made.

INTRODUCTION

Pamlico Sound, a broad shallow sheet of water bathing the shores of the northeastern counties of North Carolina, is the largest of the embayments formed behind barrier beaches along the Atlantic Coast of the United States. Compared to other coastal embayments it is relatively shallow. It has a large watershed but the annual fresh-water acquisition is less than the volume of the sound. Access to the sea is had through small unstable inlets. The astronomical tidal effect in the sound is immeasurable. Wind tides are large. The tidal prism occasioned by the semidiurnal tidal rise and fall outside the inlets is about eight times the average one-half daily river flow. Currents in the inlets are strong whereas those in the body of the sound are weak, dependent upon the wind. Vertical gradients in temperature and salinity are virtually lacking.

Studies of the hydrography of these waters have been made during the past 65 years, chiefly in conjunction with oyster culture investigations. Winslow (1886, 1889) made a number of salinity observations.

---

[1]Contribution Number 37 from the Institute of Fisheries Research, University of North Carolina.
[2]Contribution Number 547 from the Woods Hole Oceanographic Institution.

His reports do not include a tabulation of the data, but several general statements were made regarding the salinity distribution and the effects of the wind on the sound waters. Grave (1904) and Coker

FIGURE 1. Orientation chart of Pamlico Sound and tributary waters.

(1907) made some hydrographic observations in the sound, but these are so limited that they added little to the previous knowledge. Seiwell made monthly observations of temperature and salinity from November 1926 to September 1927, covering a "dense network of stations" in the Pamlico Sound area. His data have not been published, but his typewritten report and a number of graphs and charts based on his data have been made available.

The Beach Erosion Board (1935, 1948) has made certain current measurements from time to time in connection with attempts to stabilize the inlets.

The present discussion is based on data obtained since June 1948, when a hydrographic program was initiated at the University of North Carolina, Institute of Fisheries Research. These data permit a discussion of the salinity and temperature in various parts of Pamlico Sound, together with seasonal and yearly variations, as well as certain aspects of the tides and currents which are peculiar to it.

Physiography

Pamlico Sound (Fig. 1), a drowned river valley of the submerged coastal plain, is bordered by the mainland and its tributary rivers on the western side and by the emergent outer banks with their three inlets: Oregon, Hatteras, and Ocracoke Inlet[3], on the eastern side.

At its northern end it connects with Albemarle Sound via Croatan and Roanoke Sounds, which are separated by Roanoke Island. At the southern end it is continuous with Core Sound.

Pamlico Sound is approximately 60 miles long and 15 to 20 miles wide, being narrowest at the northern end (9 miles) and widest opposite Hatteras Island (26 miles). The maximum depth of the main body of the sound is about 22 feet although, because of the extensive shoals around the margin and projecting into the sound, the mean depth is probably not more than 15 feet. The sounds adjoining Pamlico Sound are also shallow, Albemarle Sound being the deepest (15 to 20 feet) and Core Sound the shallowest (average 3 to 4 feet).

The area and volume of these waters are estimated to be as follows:

	Area $\times 10^8 m^2$	Volume $\times 10^8 m^3$
Albemarle Sound	18.2	65.4
Croatan Sound	1.2	3.4
Roanoke Sound	0.96	1.5
Pamlico Sound	43.5	166.0
Core Sound	2.4	2.9
Total	66.3	239.2

[3]Other inlets have been reported previously but have since sanded up (Drane, 1923, and Beach Erosion Board, 1948).

Two large river systems, the Neuse and the Tar-Pamlico, discharge directly into Pamlico Sound. These rivers originate in the north-central Piedmont section of the state, but over two-thirds of the 7,500 square mile combined drainage basin lies in the lower and flatter coastal plain region. Pamlico Sound also receives indirectly the discharge from the Chowan and Roanoke Rivers, the latter having its origin in the Allegheny Mountains of Virginia. These two rivers, draining an area of about 7,000 square miles, empty into the western end of Albemarle Sound which in turn empties into Roanoke and Croatan Sounds. The latter sounds join Pamlico Sound in the vicinity of Oregon Inlet.

In addition to the four river systems mentioned there are many short, wide streams draining the extensive low, swampy areas, characteristic of the North Carolina coast, which contribute to the water supply of the Pamlico Sound complex. The entire drainage area of the sound, including that of the large river systems, is estimated to be in the neighborhood of 20,000 square miles.

Except for Oregon, Hatteras, and Ocracoke Inlets, inlets are an impermanent feature of the outer banks. Even these inlets change in size and position. Shoals have formed both inside and outside the inlets. Those inside are extensive, shallow and cut by narrow, tortuous, continually changing channels. Only small craft piloted with local knowledge can safely navigate their waters.

Salinity

At the beginning of the present study, 36 stations were established in the sound and its tributary waters. The stations were not uniformly distributed throughout the sound but were more numerous in the western area where the oyster industry is concentrated. At each station, surface and bottom temperatures and salinities were recorded. While this method yielded more information than was previously available, coverage of the area seemed inadequate. The large distances involved and the notoriously bad weather of the area prevented regular observations at some of the stations. In January 1951, on the basis of the findings during the earlier two and one-half year period, the sampling method was changed. It had been found earlier that differences in temperature and salinity between surface and bottom were so small as to be of little significance, at least insofar as the needs of the program were concerned. During 1951 and continuing through the spring of 1953, transects were made at various places across the sound taking readings only at the surface at approximately 1.6 mile

intervals. The latter method permitted coverage of a greater portion of the sound and a much larger number of observations.

Horizontal Distribution. Large fluctuations in salinity, dependent on runoff, occur in those parts of the sound adjacent to sources of fresh water. Large gradients in salinity occur near the inlets, where variations in the maximum salinity are dependent on the stage of the tide. Salinity fluctuations are least in the central body of the sound and are dependent on the winds and the long-term cycles of runoff.

In the southwestern part of the sound there is an east-west salinity gradient, the lowest salinities (9.3-19.2 ‰) being naturally found at the mouths of the Neuse and Pamlico Rivers and the highest salinities (up to 35 ‰) occurring at Ocracoke Inlet. In the northern part of the sound a north-south salinity gradient occurs with lower salinities again nearer the source of fresh water, Albemarle Sound.

Except for the net seaward flow required for the eventual discharge of runoff waters, the wind is the dominant force in determining the salinity distribution in the central part of the sound. Figure 2, based on data collected 18-22 April, 1950, exhibits the salinity distribution when there is no appreciable wind. The lowest salinities (15 ‰) are found at the western and northern ends of the sound; the highest salinities (20 ‰) in the north-central area and intermediate salinities in the west-central area.

Northerly winds cause the fresh waters from Albemarle Sound to penetrate farther into Pamlico Sound than is normal. As a result, the north-central part of the sound becomes less saline, as shown in Figure 3, based on data for 25-27 April, 1951.

Southerly winds, particularly those from the southwest have the opposite effect. The saltier waters from the vicinity of the inlets move in a northeasterly direction inside the outer banks, giving rise to a northwest-southeast salinity gradient in both the west-central and north-central sections of the sounds (Figure 4, based on data of 22-25 May, 1951).

Strong southwest winds occasionally move enough water northward to raise the sound water level above that of Oregon Inlet at high tide. During such periods there is a continuous ebb current through the inlet. Fishermen working around the inlet report that such ebb currents may last for two or three days during "sou'westers." Such an ebb current prevailed on 23 April, 1950, during the series of inlet studies reported below. The water which flowed out through Oregon Inlet during the entire period of observation was warmer and more saline

FIGURE 2. Surface salinity distribution in Pamlico Sound following a period having no appreciable winds. Based on data taken 18 - 22 April 1950.

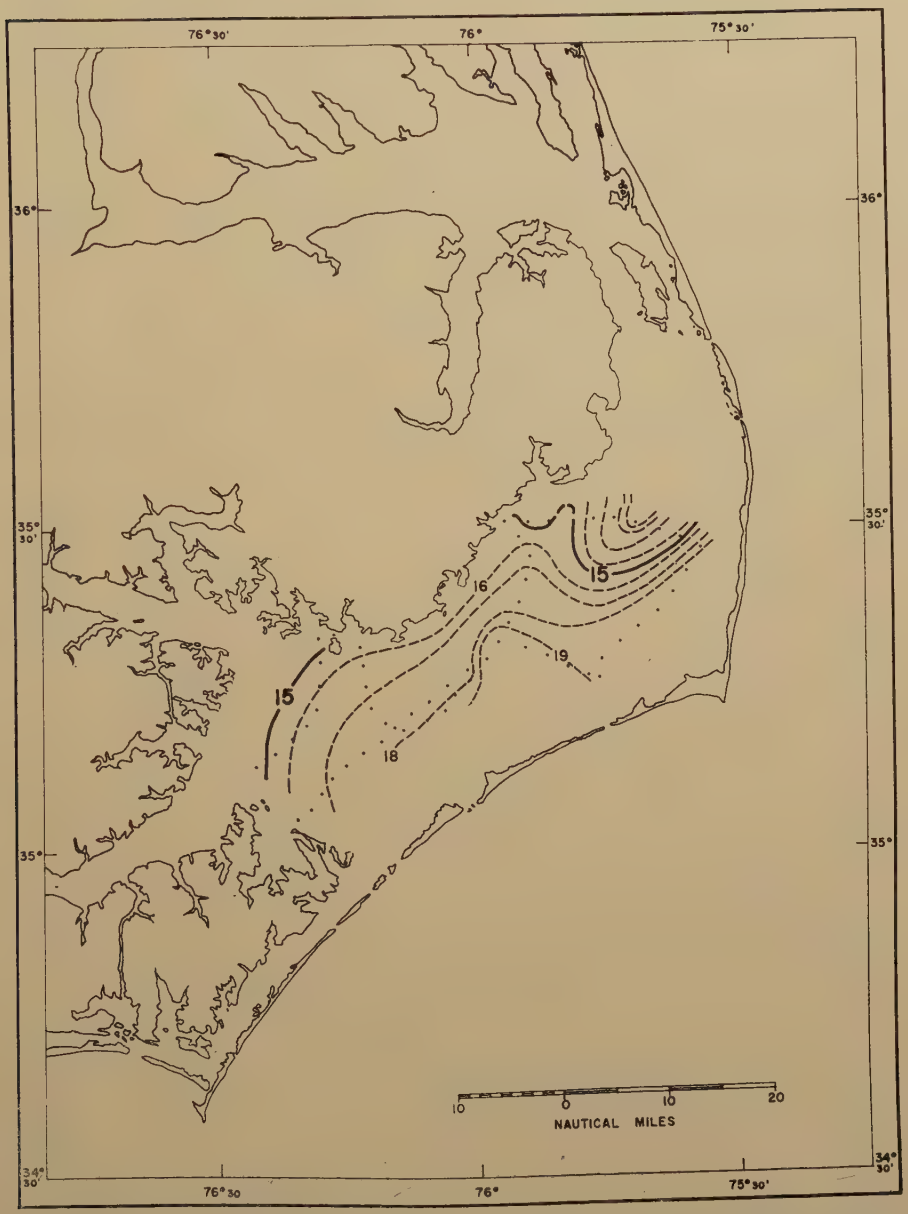

FIGURE 3. Surface salinity distribution in Pamlico Sound following strong northeasterly winds, showing penetration of fresher waters from Albermarle Sound into north-central Pamlico Sound. Based on data taken 25-27 April 1951.

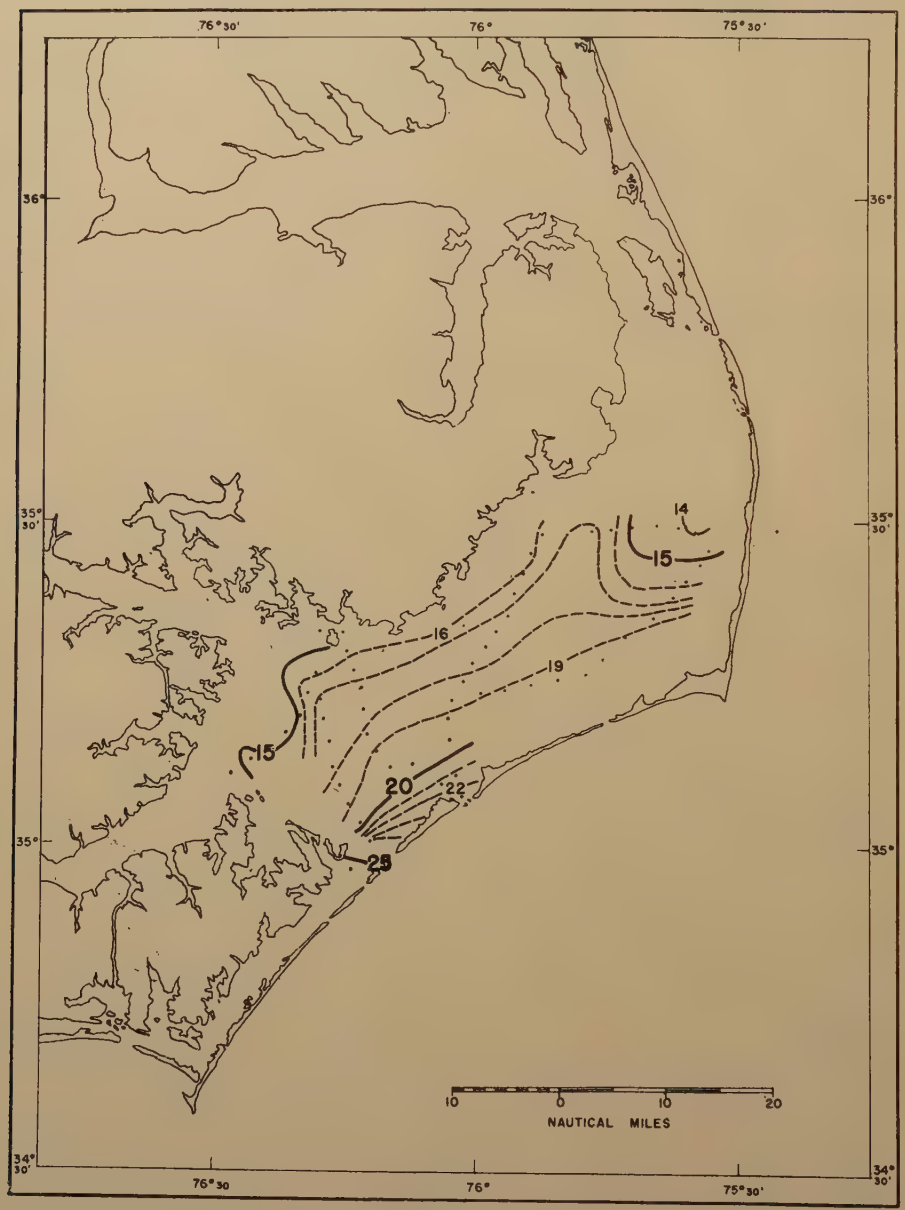

FIGURE 4. Surface salinity distribution in Pamlico Sound following southwesterly winds. Based on data taken 22 - 25 May 1951. Note that the fresher water shown in Figure 3 still persists.

than that found in the immediate vicinity on the previous two days. We believe that most of this water came from the shoals immediately to the south of the inlet. The strong southwest wind on this day could have backed the water of salinity less than 18 ‰ (see Figure 2) into Croatan Sound making this possible. On the following day, 24 April, the temperature and salinity data taken in the sound showed that ocean water had moved in through Hatteras Inlet and had continued northward just inside the outer banks. The waters on the shoals inside the barrier beach between Hatteras and Oregon Inlets contained 12 ‰ more salt than the open sound waters only a short distance away.

The effects of wind were observed by Winslow (1889), who reported that "Easterly winds will cause high water and high densities. Westerly winds will cause low water and low densities. Southerly winds will cause low water and low densities in the southern part of Pamplico Sound [*sic*] and high densities in the northern part. Northerly winds will have an exactly opposite effect in each locality." These general observations agree with the results of the present work except for the effect of southerly winds on salinity distribution as discussed above and shown in Figure 4. Winslow (op. cit.) in his discussion of winds also reported a relationship between Pamlico and Core Sounds which does not seem to be the case considering the present data. He writes, "Anomalous as it may seem, in Core Sound, its general direction being N. E. and S. W., a northeast gale will cause high water and high densities and a southwest gale the reverse—showing that the real outlet of that Sound is into Pamplico and not Beaufort Inlet, as would be supposed." The present study has revealed no such effect of winds on salinity in Core Sound. Salinities in Core Sound are always higher than in the adjacent part of Pamlico Sound. The effect of northerly winds is exactly opposite that reported by Winslow, in that the fresher Pamlico Sound water is "blown" into the upper part of Core Sound On December 1, 1949, for example, the surface water at Harbor Island, about a mile south of a line separating the sounds, contained 14.4 ‰ salt compared with a salinity of 29.3 ‰ opposite Drum Inlet The salinity at Hodges Reef in southern Pamlico Sound was 13.5 ‰. The bottom salinity at Harbor Island was 29.2 ‰, representing a salinity difference of 14.8 ‰ between surface and bottom, a distance of only nine feet. This condition can only be accounted for by a movement of Pamlico Sound water over the surface of the saltier Core Sound water. Vertical mixing did not occur because wave action in

the lee of Harbor Island was insufficient to mix waters of so great a difference in density.

There is a constant salinity gradient in Core Sound from northeast to southwest with higher salinities toward Beaufort Inlet (see Table 1). While Drum Inlet has some local influence, particularly on flood tide, and the rivers and bays entering Core Sound on the west may at times admit fresher water on an ebbing tide to lower the salinities at Bell's Island, the relatively high salinities and the salinity gradient in Core Sound force the conclusion that Beaufort Inlet rather than Pamlico Sound is the chief source of salt water for Core Sound.

It is remotely possible that the inlet situation in the late 1800's might account for the difference in conclusions as to the source of Core Sound water. Drum Inlet was then closed and Whalebone Inlet was open into the extreme southern end of Pamlico Sound. However, Whalebone Inlet was a small shallow inlet, as is Drum Inlet, and it seems doubtful that the presence or absence of either or both would significantly influence the gross hydrography of the area.

TABLE 1

SALINITIES IN PARTS PER THOUSAND IN SOUTHERN PAMLICO SOUND AND CORE SOUND STATIONS. FIGURES IN PARENTHESIS INDICATE DISTANCE IN MILES AND DIRECTION OF STATION POSITIONS IN REFERENCE TO POINT OF JUNCTION BETWEEN THE TWO SOUNDS.

Date	Hodges Reef (3N)	Harbor Island (1 SW)	Drum Inlet (7 SW)	Piney Point (15 SW)	Bell's Island (22 SW)	Wind Direction	Tide Stage
8/18/48	22.8	28.3	32.5	35.5	35.5	N	. . .
9/17/48	24.7	26.6	32.1	34.3	35.2	NE	Low
12/16/48	11.2	11.2	19.1	17.2	17.0	SW	Ebb
3/3/49	12.6	11.6	17.0	21.5	21.3	NE	Ebb
4/13/49	14.6	27.5	27.0	28.4	32.4	SSW	Ebb
6/1/49	20.1	17.6	22.1	25.8	27.5	NE	Fl.
6/27/49	14.8	24.2	31.5	30.9	31.2	SW	Fl.
9/28/49	19.5	20.1	24.4	25.1	28.0	N	Fl.
10/26/49	15.9	17.3	24.4	23.4	22.1	N	Fl.
12/1/49	13.5	14.4	29.3	32.7	33.3	NW	Ebb
9/15/50	14.6	21.8	26.7	22.7	29.3	NW	High
1/9/51	18.3	24.8	28.6	24.5	29.6	NE	Fl.
3/1/51	17.7	19.0	24.1	22.9	24.3	SW	Fl.
5/25/51	19.9	24.4	24.5	29.6	32.7	NW	Ebb
1/11/52	21.2	20.7	25.7	27.8	29.5	NW	Ebb
Average	17.4	20.6	25.9	26.8	28.6		

Vertical Distribution. As mentioned above, surface and bottom salinities were determined during the first two and one-half years of this study. The average difference between surface and bottom salinity in the sound was 0.66 ‰, indicating that there is a net "upstream movement" of more saline water along the bottom as described by other writers for many estuaries.

Pronounced stratification is occasionally found in the Neuse and Pamlico Rivers, where fresher waters flow on top of a more saline layer. In Neuse River, 10 miles above its entrance into the sound, on December 7, 1948, the surface salinity was 2.41 ‰; the bottom, at 24 feet, was 15.39 ‰—a difference of 12.98 ‰. On December 8, 1948 the difference between surface and bottom salinity in Pamlico River, about eight miles above its mouth, was 12.59 ‰. Such differences are not found in the main body of the sound because the size and shallowness of the sound facilitate thorough mixing by the almost incessant winds of the Cape Hatteras area.

Seasonal Variation. There is a seasonal salinity cycle in Pamlico Sound. The salinity is lowest during the period from February through May, after which there is a gradual salinity increase to the highest point in September or October (see Fig. 5). In general, although with some modification, this cycle is exhibited in all parts of the sound.

There are a number of factors influencing salinity; namely, rainfall, evaporation, river discharge, underground water sources, winds, and water exchange with the ocean.

The average rainfall for the area has been estimated from the charts in Linsley, Kohler and Paulhus (1949) as follows:

Period	Rainfall	Volume[4]
December - February	0.30 m	20.0 x $10^8 m^3$
March - May	0.28	18.6
June - August	0.43	28.6
September - November	0.28	18.6
Average Annual	1.29 m	85.8 x $10^8 m^3$

The normal evaporation has also been estimated from the charts in Linsley, Kohler and Paulhus (1949) for the region as follows:

Period	Evaporation[5]	Volume
May - October	0.81 m	53.8 x $10^8 m^3$
November - April	0.33	21.9
Average Annual	1.14 m	75.7 x $10^8 m^3$

[4]Rainfall x 66.3 x $10^8 m^2$ (area of Pamlico Sound complex).
[5]From Class A land plans with a recommended coefficient of 0.7.

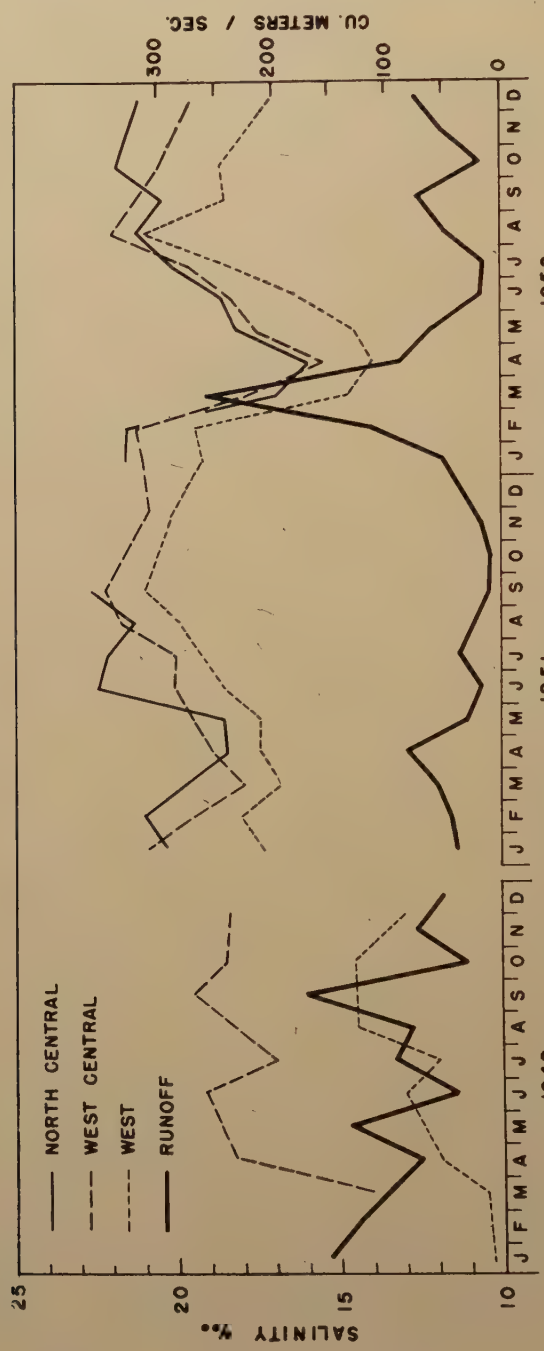

FIGURE 5. Graph of surface salinity of various parts of Pamlico Sound for 1949, 1951, and 1952, together with the runoff from the Neuse River, based on gage readings taken at Kinston, N. C., for the same years. All figures are monthly averages.

This average annual value of 75.7 x $10^8 m^3$ is considerably less than that estimated by the Beach Erosion Board (1935); i.e., 114 x $10^8 m^3$. Perhaps it is reasonable to assume that annually the rainfall into the sound and the evaporation from the sound nearly cancel out. It is also reasonable to assume from the data cited above that evaporation exceeds rainfall in the summer and the reverse in the winter.

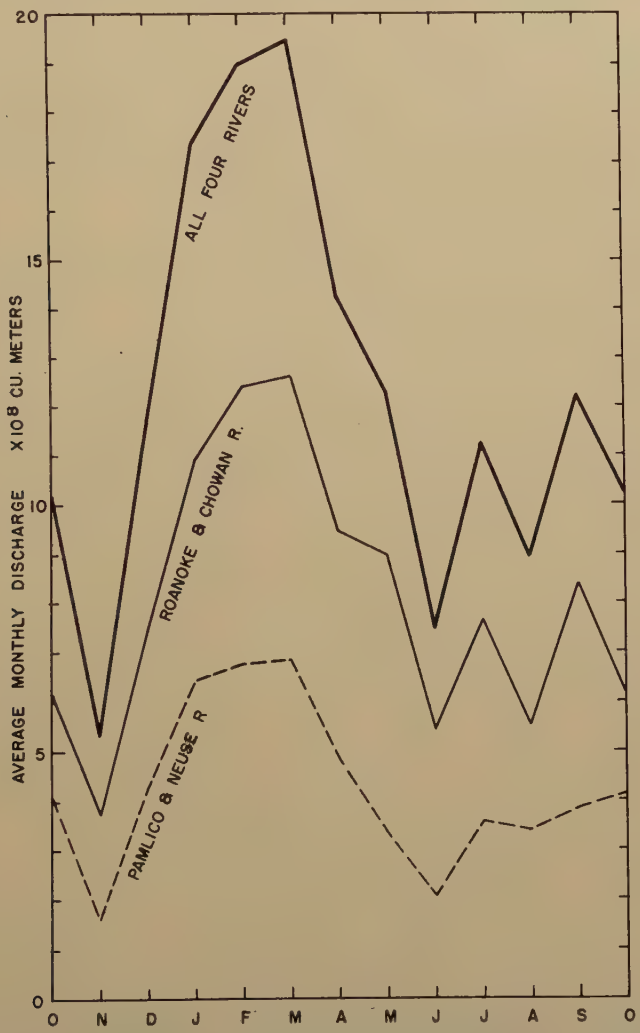

FIGURE 6. Mean monthly river discharge in the Pamlico Sound complex for the years 1941 - 1945.

Underground sources of fresh water for Pamlico Sound are unknown but probably exist (there are numerous artesian wells in Beaufort and Hyde Counties). However, Paulsen (1950) states that water levels in artesian wells are associated with rainfall, so the summer flow from such sources, although relatively small in volume, would be greater than at other seasons, and would counteract rather than intensify the seasonal cycle described above.

There is in Pamlico Sound an inverse relationship between salinity and river discharge or runoff. While there is some variation from year to year, the average runoff, Figure 6, is highest in the winter months and lowest in the summer months. The heavy runoff of the winter months depresses the salinity to a low point in March or April, Fig. 5, and coincident with the summer decrease in runoff, the salinity rises to a high point in late summer or early fall.

The annual discharge directly into Pamlico Sound, mostly from the Neuse and Pamlico Rivers, amounts to 78 x $10^8 m^3$ or only about 40%[6] of the volume of the sound. If the discharge of the northern area—Albemarle Sound—is included, the total annual discharge into the entire sound complex is only slightly greater than the volume of Pamlico Sound. Hence, the discharge during any one month is so small as to produce little salinity change in the sound as a whole. The runoff during the first four months of the year, however, amounts to slightly more than 50% of the total runoff, and the accumulative effect of this winter discharge is a general decrease in salinity as shown above.

No information is available on the seasonal variation in the amount of salt water coming in through the inlets. This is undoubtedly related to the frequency, duration and direction of high winds. What few data are available on flow through the inlets are given in the section on Currents in the Inlets.

Yearly Variation. Year to year variations in rainfall produce fluctuations in runoff and these, in turn, are reflected by variations in the salinity of the sound[7]. During 1948 and 1949, for example, rainfall and runoff were considerably higher than the average for the period

[6]On the basis of the average river flow into and an estimate of the average volume of fresh water contained in Pamlico Sound, it takes approximately five months for a particle of fresh water to pass through.

[7]As Marshall (1951) points out, there is fairly close agreement between rainfall and runoff on a yearly basis; i.e., years during which the rainfall is high, runoff is also high, and vice versa. This relationship, however, does not exist on a monthly basis. Heavy rains in winter generally produce large river discharges, but heavy rains in summer seldom produce large discharges. This apparent anomaly is undoubtedly due to seasonal differences in soil condition, vegetative cover, transpiration, and evaporation.

1931 to 1949. Salinities throughout the sound were low during these two years. In 1951, rainfall and runoff were extremely low and the salinity of the sound was correspondingly higher. The salinity of the western part of the sound, for example, exceeded 20 ‰, whereas in 1949 it never exceeded 15‰. The heavy runoff in the spring of 1952 depressed the salinity of all portions of the sound, but during the summer the reduced runoff resulted in increased salinity. The salinity record of the various parts of the sound and its relationship to the runoff of the Neuse River[8] is given for the years 1949, 1951, and 1952, in Figure 5. The salinities reported by Seiwell (Marshall, 1951) are high, being associated with a period of low runoff.

Temperature

Water temperature in Pamlico Sound shows a seasonal cycle closely related to air temperature. Temperatures are highest during late June, July, and August and are lowest during the winter months. Figure 7 shows the average monthly water temperature in Pamlico Sound during the period of study.

The relationship between air temperature and water temperature is shown in Figure 8. The points in the graph represent the average water temperature in the open sound plotted against the air temperature recorded at Hatteras. The air temperatures used in the graph represent the mean of the temperatures recorded on the day of observation and the previous day. This was done to allow for the lag in water temperature. The correlation coefficient between water temperature and air temperatures thus determined is .972.

There is no appreciable thermal stratification in the sound. Winds and wind-driven currents keep the water in nearly constant agitation and prevent stratification. Differences between observed surface and bottom temperature have never exceeded 2°C. Water flowing in the inlets is isothermal and during the winter months is frequently warmer than the sound water. The reverse is occasionally found in summer; i.e., the ocean waters are cooler than the sound waters. A temperature gradient may therefore be found in the vicinity of the inlets within the area of tidal influence. It is difficult to detect such a gradient in the open sound because of the diurnal variation within the sound. A change of 2 to 3°C. may occur at one station within a given day and

[8]Inasmuch as the runoff figures for all four rivers discharging into the Pamlico Sound complex show nearly identical monthly and seasonal variations, the figures for the Neuse River are considered satisfactory for showing the relationship between runoff and salinity.

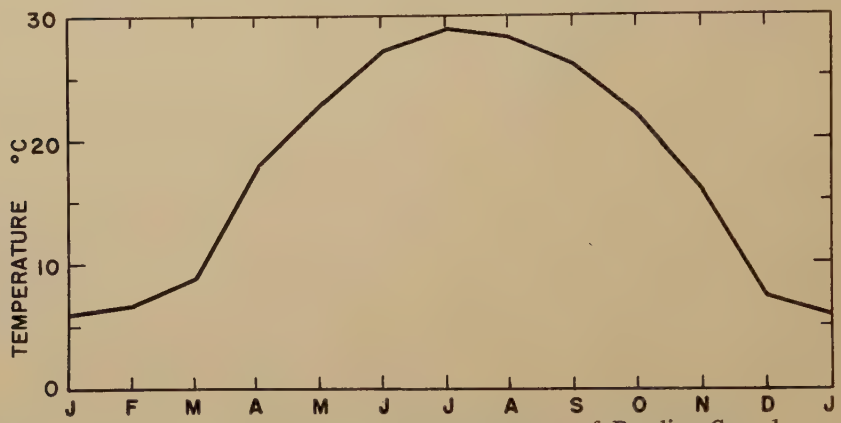

FIGURE 7. Mean monthly surface water temperature of Pamlico Sound.

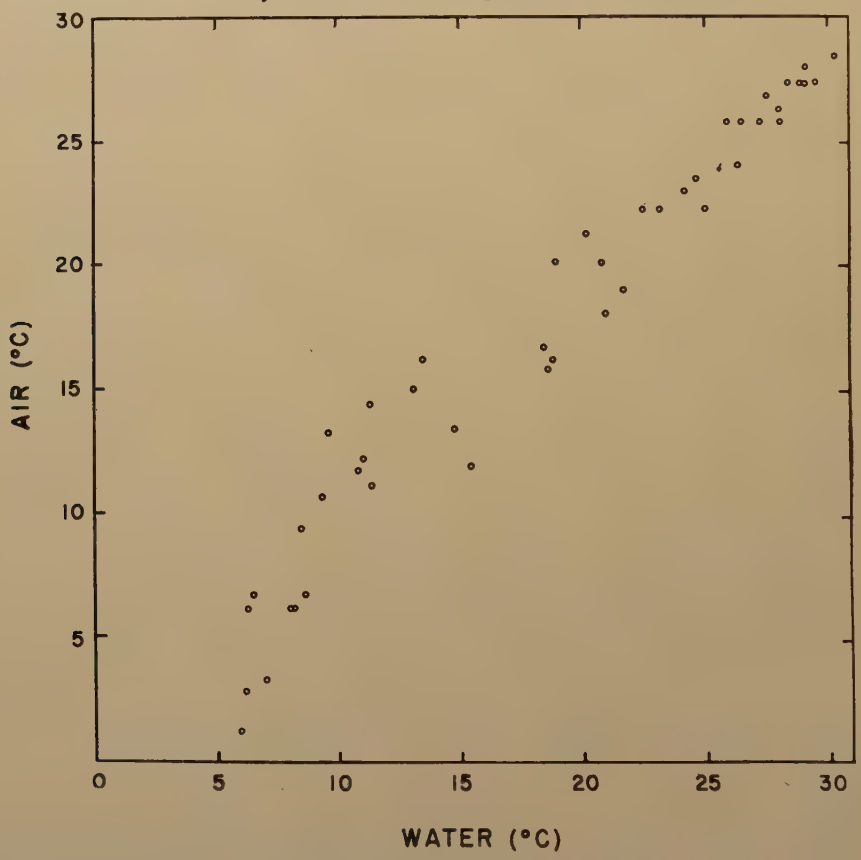

FIGURE 8. Relationship between surface water temperature in Pamlico Sound and air temperature at Hatteras.

as a general rule there is no greater difference between various parts of the sound on the same day.

Currents in Pamlico Sound

The currents in Pamlico Sound, which are relatively weak, depend mainly upon the direction and velocity of the wind, not upon tidal oscillation. Seiwell observed a maximum current of 69 cm./sec. in the mouth of the Neuse River during a squall. In his tabulation of currents during light winds the strongest currents observed were on the western side close to the mouth of the Neuse and Pamlico Rivers with drifts of 10 to 26. cm./sec. at the surface and 8 to 16 cm./sec. to depths of 15 feet. In the central part of the sound, surface currents of 1 to 9 cm./sec. were observed. He found no bottom current in the central part of the sound.

Winslow (1886) made a number of current measurements throughout Pamlico Sound and reported easterly and southeasterly currents in the southern part of the sound, seldom exceeding one-half knot (26 cm./sec.). The strongest current reported was three-fourths knots (38 cm./sec.) in a southwest direction; this occurred during a northeast gale which lasted for several days.

No current measurements were made in the sound during the present study.

However, we can calculate the order of magnitude of the mean current one might expect from the runoff of the Pamlico-Neuse River systems through a 20 mile section in the southwestern part of the sound. The average annual increment of fresh water is $78 \times 10^8 m^3$/year or about 200 cubic meters/sec. Let us assume this volume is augmented by an equivalent amount of salt water since the salinity is roughly half that of sea water. Let us further assume that the water is flowing seaward in only the upper half of the section, i.e., 2.6 m., with a return flow of more saline water beneath. Hence the area of the section is about $8 \times 10^4 m^2$. Then the hydraulic current would amount to only 0.5 cm./sec. Even if our estimate were in error by a factor of 10 the runoff current would easily be over-powered by the currents due to wind friction.

Currents in the Inlets

The only earlier current data in the inlets we have been able to find have been those published for Oregon Inlet in Beach Erosion Board (1935 and 1948) summarized as follows:

OREGON INLET

Date	Cross Section	Maximum Velocity Flood	Maximum Velocity Ebb	Maximum Rate of Flow Inflow	Maximum Rate of Flow Outflow	Total Flow Inflow	Total Flow Outflow
		m/sec	m/sec	m^3/sec	m^3/sec	x$10^6 m^3$	x$10^6 m^3$
9 Sep '31	3650 m^2	0.76	0.70	3800	2520	58.6	46.0
31 Aug '32		.73	.79	3660	2900	52.5	49.8
11 Oct '32		.73	.98	3580	3600	42.8	70.4
24 Aug. '37	3970 m^2	1.13	1.01	5100	4020	78.0	68.7
14 Aug '39	5050 m^2	.85	1.16	4300	3990	46.5	87.9

NOTE: These observations were made when New Inlet was still open.

Current measurements were made at Oregon, Hatteras, and Ocracoke Inlets in April, 1950, with an Ekman Current Meter. Unfortunately, we succeeded in observing a full tidal cycle in Ocracoke Inlet only. The observations at other inlets covered a shorter period. However, they provide some useful information.

The current measurements at Oregon Inlet on 23 April were made at depths of 4 and 18 feet in the narrowest part of the channel where the sounding was 22 feet. They lasted over a period of 6-¾ hours during which time the current was continually ebbing, Figure 9. It appeared to have been ebbing for some time and to continue ebbing even longer. The current velocities at 4 feet varied from 88 cm./sec. to 138 cm./sec., averaging 115 cm./sec., while those at 18 feet varied from 62 cm./sec. to 129 cm./sec., averaging 88 cm./sec., yielding an average for the whole column of about 100 cm./sec. (2 kts.). Thus, about 47 x $10^6 m^3$ of water flowed out during the period of 6-¾ hours. This is assuming that the average velocity in the center of the channel was about 1/3 greater than the average for the whole cross section of 2,600 m^2. No doubt the strong southwest wind, force 4-5, built up a head of water at the northern end of the sound, causing the tide to begin ebbing before predicted high water and to continue ebbing after predicted low water. An estimate of the height of the head of water above mean sea level for the brief period of investigation is presented below.

Current measurements made in Hatteras Inlet on 25 April, at depths of 4 and 15 feet in the narrowest part of the channel where the sounding was 21 feet, were of nearly ten hours duration, Figure 10. The current was on the last half of the ebb when we commenced. The maximum ebb current observed was 94 cm./sec. The ebb continued nearly three hours after the predicted time of low water. The flood commenced about ¾ hour before predicted slack, flood begins

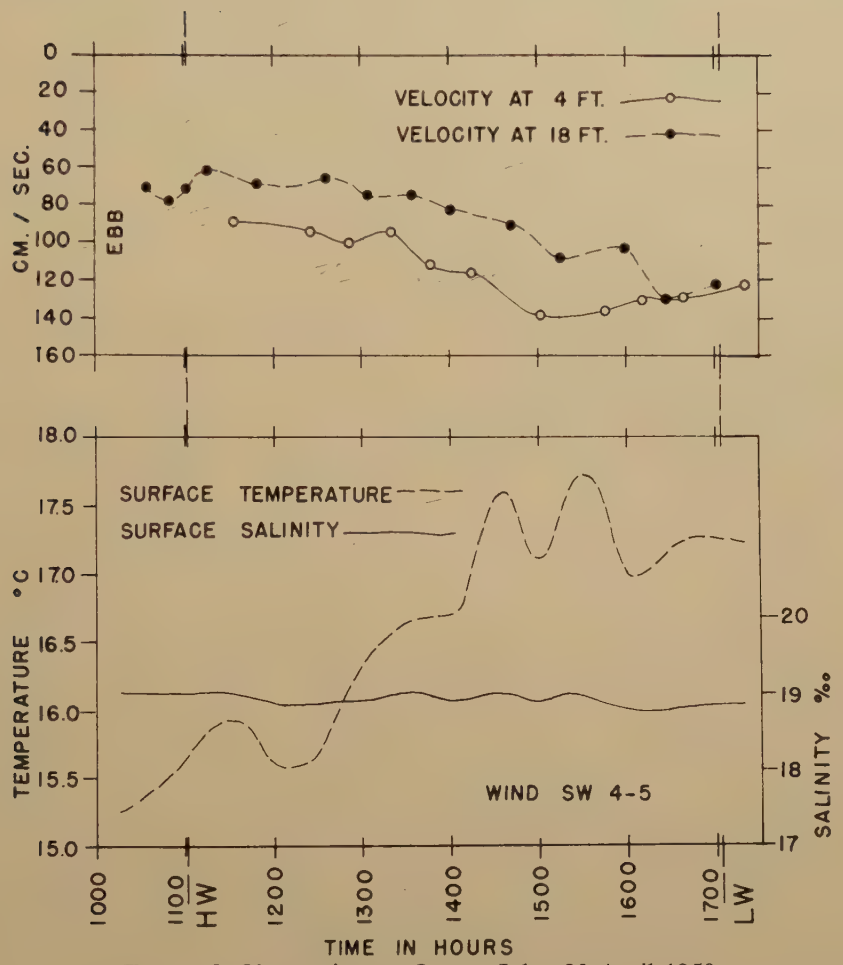

FIGURE 9. Observations at Oregon Inlet, 23 April 1950.

The flood current lasted nearly seven hours, with the maximum flood current being 91 cm./sec. and ended at predicted slack, ebb begins. The average current for the water column (there was little difference between the 4 and 15 foot measurements) was 46 cm./sec. (0.9 kts.). Thus, the total volume of flood, for the 6-¾ hours, assuming the average velocity in the center of the channel was about 1/3 greater than the average for the whole gorge of 7,700 m^2, was 65 x $10^6 m^3$. This volume of water is about equivalent to the volume in a rectangle 5 miles on a side over the shoals immediately inside the inlet.

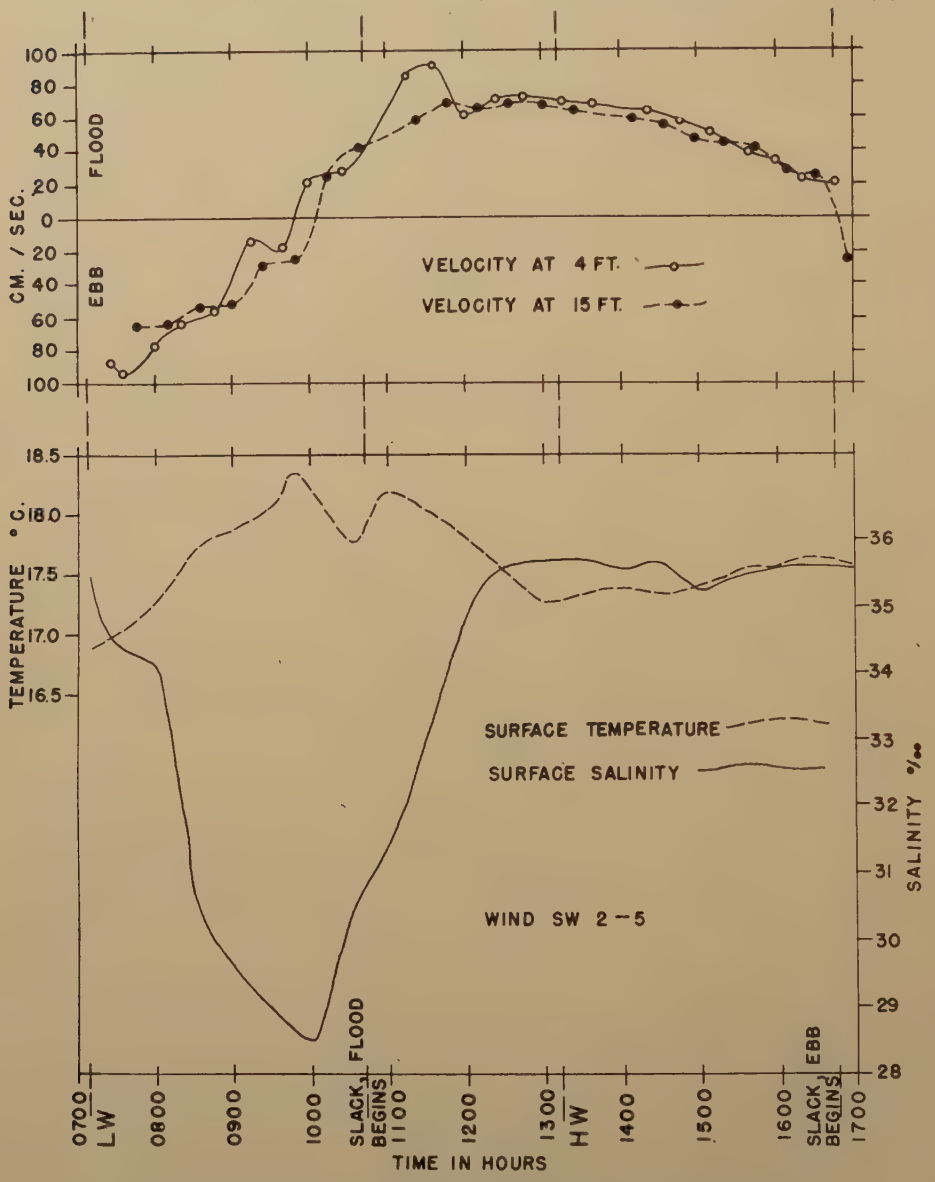

FIGURE 10. Observations at Hatteras Inlet, 25 April 1950.

The trend of the salinity curve in the diagram indicates that, until immediately after we commenced our measurements, the water flowing out on the ebb was undiluted sea water which had moved in dur-

ing the previous flood. Only during the last 2 hours and 40 minutes of the ebb was the salinity less than 35 ‰. The minimum salinity of the ebbing water was 28.5 ‰. Reference to Figure 2, showing the sharp horizontal gradient of salinity about the inlet, suggests that the tidal excursion of the water out of the sound through the inlet was probably less than five miles. During the first two hours of the flood,

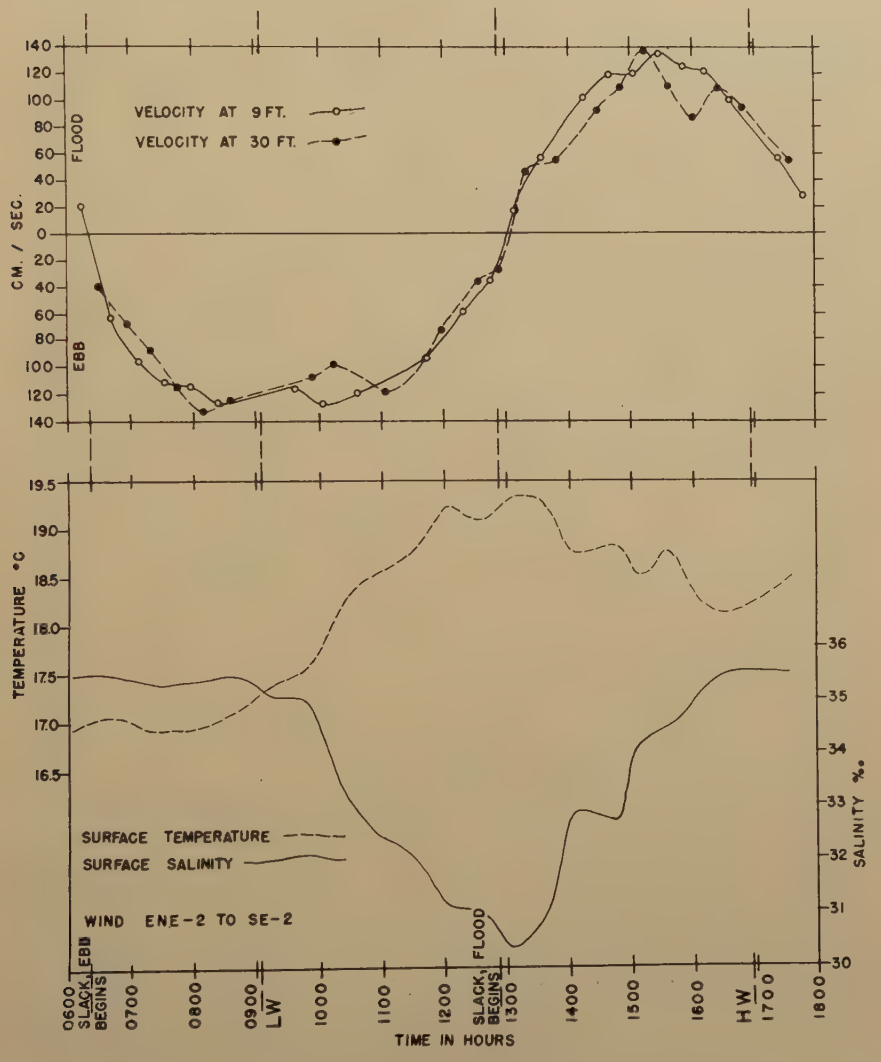

FIGURE 11. Observations at Ocracoke Inlet, 27 April 1950.

diluted sea water was pushed back in through the inlet, allowing nearly five hours for undiluted sea water to flow in.

The current measurements at Ocracoke Inlet on 27 April at depths of 9 and 30 feet in the narrowest part of the channel where the sounding was 38 feet continued for 11-¾ hours, Figure 11. The measurements commenced at the turn from flood to ebb and ended just before the end of the next flood. The ebb commenced at predicted slack, ebb begins, lasted 6-¾ hours with a maximum flow of 134 cm./sec., average of 92 cm./sec. (1.8 kts.). This yielded a transport (assuming gorge of 9,000 m^2) of 150 x $10^6 m^3$ of water. The current turned just a few minutes after predicted slack, flood begins. The flood was observed for nearly 5 hours with a maximum flow of 137 cm./sec., averaging 80 cm./sec. (1.6 kts.), yielding a transport of 96 x $10^6 m^3$ of water. The ebb began 2.5 hours before predicted low water, the flood nearly 4 hours before predicted high water.

As noted for Hatteras Inlet, undiluted sea water flowed out during the first 3.5 hours of the ebb. The minimum salinity flowing out was 30.4 ‰, well above values within 5 miles of the inlet. During the first 3 hours of the flood diluted sea water was pushed back in through the inlet.

The above mentioned current observations are tabulated below:

	Max. Velocity		Av. Velocity		Observed Transport	
	Flood cm/sec	Ebb cm/sec	Flood cm/sec	Ebb cm/sec	Flood x$10^6 m^3$	Ebb x$10^6 m^3$
Oregon Inlet	...	138	...	100	...	47
" "	...	...	...	...	56*	64*
Hatteras Inlet	91	94	46	...	65	...
Ocracoke Inlet	137	134	80	92	96	150

*Average of 5 sets of Beach Erosion Board figures on p. 198.

Thus, a rough figure for the inflow through the inlets might be 440 x $10^6 m^3$/diem which is approximately eight times the average daily effluent of fresh water from all four rivers.

There probably is no systematic mechanism which regulates the daily salinity increment into the sound. Although the amount of water flowing in and out through the inlets is much larger than the river effluent, much of it appears to oscillate back and forth through the inlets and over the shoals immediately inside. The length and strength of flood and ebb depends on the present and recent winds as well as the semidiurnal tides. The amount of exchange through the inlets must be small, however, for the average salinity of the sound (Fig. 8)

follows roughly the mean monthly runoff from the rivers, as shown above. Inasmuch as the average salinity of Pamlico Sound is roughly 20 ‰ we might assume on an annual basis that the sound is composed of 3 parts runoff and 4 parts sea water. Thus somewhat on the order of 40-50 x $10^6 m^3$ of undiluted sea water must be added each day, which is about one-tenth of the tidal prism.

Tide

Except near the inlets, the periodic (astronomical) tides are negligable, U.S.C.&G.S. (1950, p. 298), Beach Erosion Board (1935, p. 25). The nonperiodic rise and fall of water is largely due to the strong winds which blow in the region. The ranges of tide at the inlets are as follows, U.S.C.&G.S. (1949a):

	Mean Range of Tide	Spring Range of Tide
Oregon Inlet	1.8 feet	2.2 feet
Hatteras Inlet	2.0 feet	2.4 feet
Ocracoke Inlet	1.9 feet	2.3 feet

Estimate of Tidal Range in Pamlico Sound. For purposes of conjecture, what is the range of the tide assuming the water flowing in through the inlets were distributed uniformly over the entire surface of Pamlico Sound?

$$\text{If } H = E/A$$

where H is the range of the tide, E is the tidal exchange and A is the area of the sound, we see that, with an inflow of about 220 x $10^6 m^3$ per tide and the area of Pamlico Sound of 44 x $10^8 m^2$, the tidal range is about 5 cm.

Estimate of Wind Tide at the Northern End of Pamlico Sound. It is evident that southwest winds can produce a head of water in the northern end of Pamlico Sound, thus raising the level in the sound higher than the level in the sea outside Oregon Inlet. This is probably the reason that there are no predictions for the time of slack water for Oregon Inlet in the Current Tables (U.S.C.&G.S., 1949b) although there are such for Hatteras and Ocracoke Inlets where the setup is probably much less.

Keulegan (1951) gives an equation for wind tide or setup in natural conditions, where he means by setup the displacement of the waters in an enclosed body of water due to wind friction, as follows:

$$\frac{S}{L} = 3.3 \times 10^{-6} \left(1 + 63 \left(\frac{H}{L}\right)^{1/2}\right) \frac{V^2}{gH}$$

where S, the setup, equals $h_2 - h_1$, the windward and leeward displacements h_1 and h_2, respectively. L is the length of the bay; V, the velocity of the wind; H, the mean depth; and g, the acceleration of gravity in cgs units.

Since the depths vary considerably over the 60 mile length of Pamlico Sound, partial computations have been made for S, S_1 for the windward 46 miles (7.4×10^6cm.) where the mean depth is 5.2 m., S_2 for the next 8 miles (1.29×10^6cm.) where the mean depth is 4 m. and for S_3 the leeward section of the sound, 6 miles (0.94×10^4cm.) where the mean depth is roughly 1 m.

Thus for several wind velocities:

	Vel.	(kts)	5	10	20	40
	S_1	(cm)	6	18	73	292
	S_2	(cm)	2	6	23	92
	S_3	(cm)	4	13	53	212
Σ	S	(cm)	12	37	149	596
Rise in Level	h_1	(cm)	6	18	75	298
		(ft)	0.2	0.6	2.5	9.8

Hence a southwest wind of about 13 knots is required to provide a setup of about 1 foot. This neglects the funneling effect, caused by the shape of the sound, which must be appreciable. Northeasterly winds will provide a similar rise in level along the southwestern shores.

An estimate of the height of the head of water above mean sea level in the northern part of the sound on a given occasion can be made from the current measurements at Oregon Inlet on 23 April 1950.

If we assume the velocity through the inlet is proportional to the elevation inside minus the elevation outside, this expression would appear as follows:

$$V^2 \sim (h_p - h_s)$$

where V is the velocity at a given time, h_p is the elevation in the sound above mean sea level which we wish to discover, and h_s is the elevation in the sea above or below mean sea level. Since the mean range of tide at Oregon Inlet is 1.8 feet (55 cm.) and the velocity through the inlet at high water was approximately 70 cm./sec. and at low water 120 cm./sec., we have:

$$\text{AT HW} \quad 70^2 \sim (h_p - 27)$$
$$\text{AT LW} \quad 120^2 \sim (h_p + 27)$$

Solving, $h_p = 55$ cm. (1.8 feet) above mean sea level. By Keulegan's method, with an estimated wind of force 4-5 (ca 19 kts.), one would have predicted a setup of 70 cm.

REFERENCES

Beach Erosion Board
1935. Beach erosion at Kitty Hawk, Nags Head and Oregon Inlet, N. C., 74th Cong., 1st Session. H. R. No. 155.
1948. North Carolina shoreline, beach erosion study. 80th Cong. 2nd Session. H. R. No. 763.

Coker, R. E.
1907. Experiments in oyster cultivation in Pamlico Sound, North Carolina. Bull. N. C. geol. econ. Surv. *15*, 74 p.

Drane, B. S.
1923. Report on the proposal to construct certain additional inlets on the North Carolina coast. *In* Report of special committee on inlets which investigated the proposal to construct certain additional inlets on the North Carolina coast. Issued by North Carolina Fisheries Commission Board at Morehead City.

Grave, C.
1904. Investigations for the promotion of the oyster industry of North Carolina. Rep. U. S. Comm. Fish. for 1903 (1905), p. 247-315.

Keulegan, G. H.
1951. Wind tides in small closed channels. J. Res. nat. Bur. Stand. *46* (5), p. 358-381.

Linsley, R. K., Jr., M. S. Kohler, and J. L. H. Paulhus
1949. Applied hydrology. McGraw-Hill, New York.

Marshall, N.
1951. Hydrography of North Carolina marine waters. *In* Taylor, H. F. & Associates. Survey of marine fisheries of North Carolina. University of North Carolina Press, Chapel Hill, p. 1-76.

Paulsen, C. G.
1950. Water levels and artesian pressure in observation wells in the United States in 1946. Part 2. Southeastern States. Wat. Supp. Pap. No. 1072, Wash.

Seiwell, H. R.
1927. A brief report on the physical hydrography of Pamlico Sound and its tributaries. Typed report to the Dept. Geol., Univ. N. C. and U. S. Bureau of Fisheries. Unpublished.

U. S. Coast and Geodetic Survey
1949a. Tide tables, Atlantic Ocean for the year 1950.
1949b. Current tables, Atlantic coast, North America for the year 1950.

U. S. Geological Survey Water Supply Papers
1942-1946. Surface water supply of the United States, Pt. 2, South Atlantic slope and eastern Gulf of Mexico basins. Nos. 952 (1942), 972 (1943), 1002 (1944), 1032 (1945), 1052 (1946).

Winslow, F.
1886. Report on the waters of North Carolina with reference to their possibilities for oyster culture, together with the results obtained by the surveys directed by the resolution of the General Assembly, ratified March 11, 1885. Raleigh: North Carolina State Printer and Binder. 151 p.
1889. Reports on the sounds and estuaries of North Carolina with reference to oyster culture. Bull. U.S. Cst geod. surv. No. 10, 136 p.

Contribution No. 587

CONTROL OF SALINITY IN AN ESTUARY BY A TRANSITION[1]

By

HENRY STOMMEL and HARLOW G. FARMER

Woods Hole Oceanographic Institution
Woods Hole, Massachusetts

ABSTRACT

A theoretical reason is developed to explain why the mouth of a vertically stratified estuary should act as a constraint on the amount of salt water available for mixing in the estuary. Flume experiments designed to test this idea are described. The effect of tides on the control action and application to various estuaries is discussed.

THEORY

There is a curious way in which a control[2] acts to limit the possible amount of mixture. Consider an estuary E (Fig. 1) opening into the ocean O (without tides) through a transition T. If the entire system is sufficiently deep, and if the discharge (q_0 per unit width of the transition) of the river R is not too great, there is a two layer flow through the transition. If there is no mixing between the two fluids, then the lower layer is stagnant and the upper layer at T is entirely fresh.

Suppose that some agency for vertical mixing of the two layers exists in the estuary E and that the amount of mixing is progressively increased. The upper layer is now somewhat brackish, the discharge of both layers through T is increased, and the interface is nearer to the mid-depth. Increased mixing in E decreases the salinity difference of the two layers at T and increases the discharge; but there is a point beyond which increased mixing has no further effect on either the discharges through or the salinities at T.

It is natural to suppose that some estuaries will be overmixed in this sense and that the salinity control will be exercised by the nature of the transition rather than by diffusion, whether it be horizontal, vertical, or otherwise.

The criterion for "overmixing" can be obtained from the equation for a stationary interfacial wave,

[1] Contribution No. 587 of the Woods Hole Oceanographic Institution; work done in this paper was supported by public funds made available by the Office of Naval Research.

[2] The notation and theory is a continuation of an earlier paper in this Journal (Stommel and Farmer, 1952).

Reprint from SEARS FOUND. JOURN. MAR. RES.

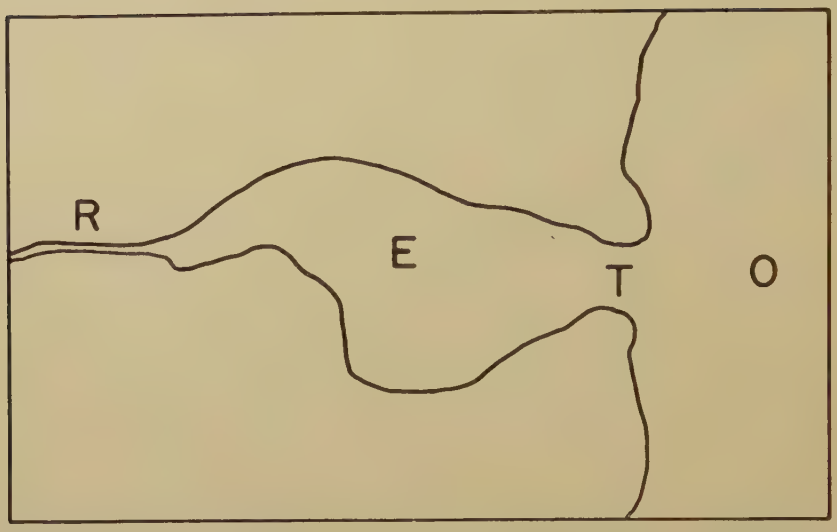

Figure 1. Schematic diagram of an estuary, E, connecting the river, R, to the ocean, O, through a transition in width, T.

$$\frac{q_2^2}{(1-\eta)^3} + \frac{\alpha q_1^2}{\eta^3} = g\beta D^3 , \tag{1}$$

from the equation of continuity,

$$q_1 + q_2 = q_0 , \tag{2}$$

and from the equation for the conservation of salt,

$$q_1 s_1 + q_2 s_2 = 0 . \tag{3}$$

To relate salinity and density we may take a simplified equation of state

$$\rho = \rho_0 (1 + a\, s) . \tag{4}$$

Thus

$$\beta \equiv \frac{\rho_2 - \rho_1}{\rho_2} \backsimeq a\,(s_2 - s_1), \quad \alpha \equiv \frac{\rho_1}{\rho_2} \backsimeq 1 - a\,(s_2 - s_1) . \tag{5}$$

The equation (1) may now be written in the following form:

$$\varphi(\eta) = \nu^2\eta^3 + (1-\eta)^3 - (1-\nu)^3\eta^3(1-\eta)^3\mathfrak{F}^{-1} = 0 , \tag{6}$$

where

$$\nu = \frac{s_1}{s_2} , \qquad \mathfrak{F} = q_0^2/\,(gas_2D^3) .$$

This is an approximation of equation (1).

The real roots of $\varphi(\eta) = 0$ between $\eta = 0$ and $\eta = 1$ cease to exist as $\nu \to 1$, and this point determines the state of overmixing. The value of η at which there is a double root occurs when

$$\frac{\partial \phi}{\partial y} = 0 = 3\{\nu^2\eta^2 - (1-\eta)^2 - (1-\nu)^3(1-\eta)^2\eta^2(1-2\eta)\mathcal{F}^{-1}\}. \quad (7)$$

If we multiply equation (7) by η and substract from (6) we obtain

$$(1-\nu)^3\eta^4 = \mathcal{F}. \quad (8)$$

Elimination of ν gives the following form

$$\mathcal{F}\eta^8 = (\eta^4 - (1-\eta)^4)^3. \quad (9)$$

As $\mathcal{F} \to 0$, $\eta \to 1/2$. This means that, for weak river flows in estuaries with large transitions, the overmixing leads to an interface at half depth. In order to investigate approximately the effect of $\mathcal{F} > 0$ we introduce $\epsilon = \eta - 1/2$; ϵ is a small quantity as long as $\mathcal{F}$ is small. Substituting this into equation (9) and retaining only the large terms, we obtain

$$256\epsilon^3 - \mathcal{F}(1 + 16\epsilon) = 0. \quad (10)$$

For small values of $\mathcal{F}$ the roots of this expression are approximately

$$\epsilon = \sqrt[3]{\mathcal{F}/256}. \quad (11)$$

In states of overmixing we can thus evaluate at what values of $\mathcal{F}$ the quantity η deviates significantly from 1/2. The ratio of salinities of the upper and lower layers, ν, is given by

$$\nu = 1 - \sqrt[3]{\mathcal{F}/\eta^4}. \quad (12)$$

EXPERIMENTAL STUDIES IN A FLUME

The experimental flume used in this work has been described elsewhere (Stommel and Farmer, 1952). Vigorous mixing was produced by large rotary beaters.

Two sets of runs were made past a transition to test the theory of overmixing. The transition was a short narrow section of width W_1, the channel opening to full width both upstream and downstream. The length of the narrow section was 42 cm in series G, and 100 cm in series H. In all runs the total depth D was 31.5 cm; q_0 is the river discharge per unit width of the transition, ρ_0 the density of river discharge, ρ_1 the density of the overmixture, and ρ_2 the density of the sea water. ν is defined as

$$\nu = \frac{\rho_1 - \rho_0}{\rho_2 - \rho_0},$$

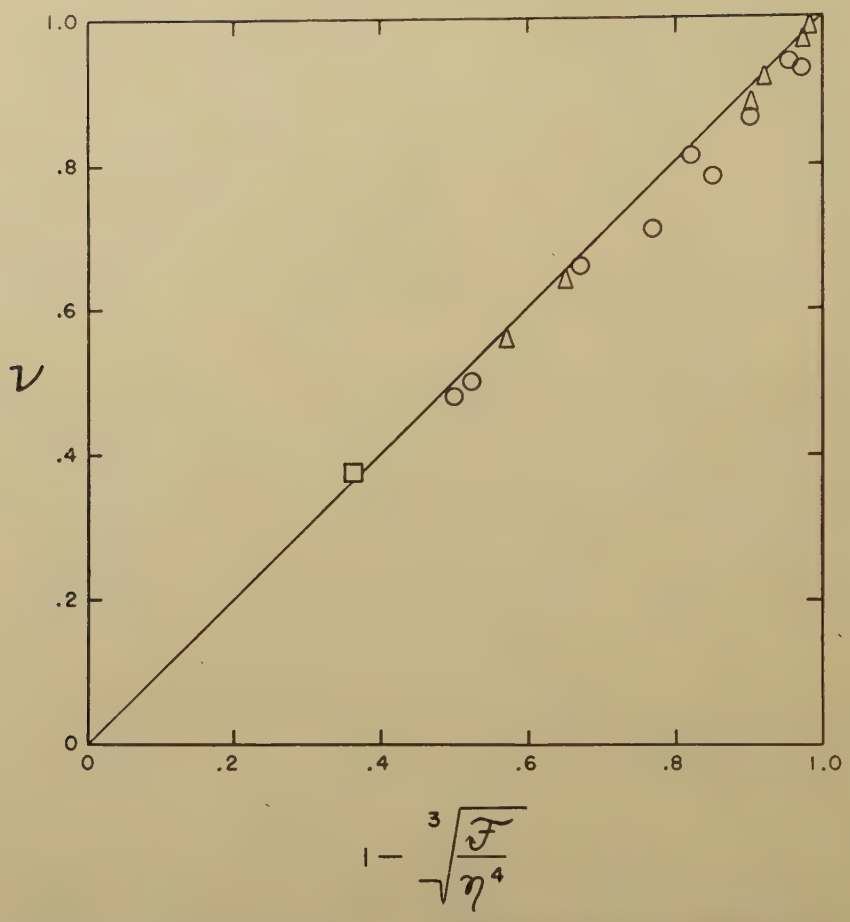

Figure 2. Comparison of observed values of ν and computed value. The meaning of the different points is explained in the text.

and ν_c is computed from the theory. The data are plotted in Fig. 2: the circles are G runs, the triangles are H series, and the square is the only run (G-6) where ε is of sensible order of magnitude.

Four tests were also made with a tide imposed on the overmixed condition; Fig. 3 shows the results of these experiments. In test 2, with the two-minute tidal period, and in test 3, the sea water of density ρ_2 was swept out of the transition for a portion of the tidal cycle and there was a reversal of flow in the upper layer. It is evident that serious disagreement in ρ_1 of the steady and unsteady tests was not experienced until test 4. In this test the surface profile was distorted by a bore and there was no vertical stratification.

TABLE I. Overmixing Experimental Runs

Run	q_0 (cm^2/sec)	W_1 (cm)	ρ_0	ρ_1	ρ_2	ν	ν_c
G–1	43.5	8.7	1.0170	1.0213	1.0259	.48	.50
–3	14.5	8.7	1.0170	1.0233	1.0259	.71	.77
–4	14.5	8.7	1.0000	1.0214	1.0259	.81	.82
–5	1.5	8.7	1.0000	1.0243	1.0259	.94	.95
–6	145.0	8.7	1.0000	1.0097	1.0259	.37	.36
–7	0.7	17.7	1.0000	1.0247	1.0259	.93	.97
–8	7.1	17.7	1.0000	1.0229	1.0255	.86	.90
–9	43.0	17.7	1.0000	1.0171	1.0255	.66	.67
–10	7.1	17.7	1.0170	1.0239	1.0255	.78	.85
–11	43.0	17.7	1.0170	1.0212	1.0255	.50	.52
H–1	0.7	17.5	1.0000	1.0240	1.0248	.97	.97
–2	7.1	17.5	1.0000	1.0221	1.0248	.88	.90
–3	71.0	17.5	1.0000	1.0140	1.0248	.56	.57
–4	0.5	27.8	1.0000	1.0248	1.0250	.99	.98
–5	4.6	27.2	1.0000	1.0230	1.0250	.92	.92
–6	46.0	27.2	1.0000	1.0160	1.0250	.64	.65

OVERMIXING IN ESTUARIES

The only type of estuary to which the concept of overmixing can properly be applied is that in which there is vertical stratification and in which there is evidence of a net flow (averaged over a tidal cycle) downstream in the upper layer and a net flow upstream in the bottom layer. It is important not to attempt to apply this hydraulic condition to vertically mixed estuaries, such as the Raritan River, Delaware Bay, Bristol Channel-Severn estuary, where there appears to be no hydraulic control action at the mouth.

Not all vertically stratified estuaries are likely to be overmixed. Rather obvious examples are Alberni Inlet, which is too deep to be thoroughly mixed by tides, and the Mississippi River passes, in which the tidal action is too small. However, in estuaries where there are tides of several feet or more and where the depth is not more than about ten meters, it is reasonable to suppose that overmixing may occur; that is, the salinity of the estuary upstream of a transition is determined by the control or "throttling" action of the transition on the two layer flow through it, not by the magnitude of large scale horizontal turbulent exchange in the sense of Ketchum (1951) and Arons and Stommel (1951).

Hachey (1939) has summarized the data available on the salinity of the upper layer in St. John Harbor (New Brunswick, Canada). In Fig. 4 the difference in salinity of the upper and lower layers is plotted as a function of river discharge. The straight line is computed from

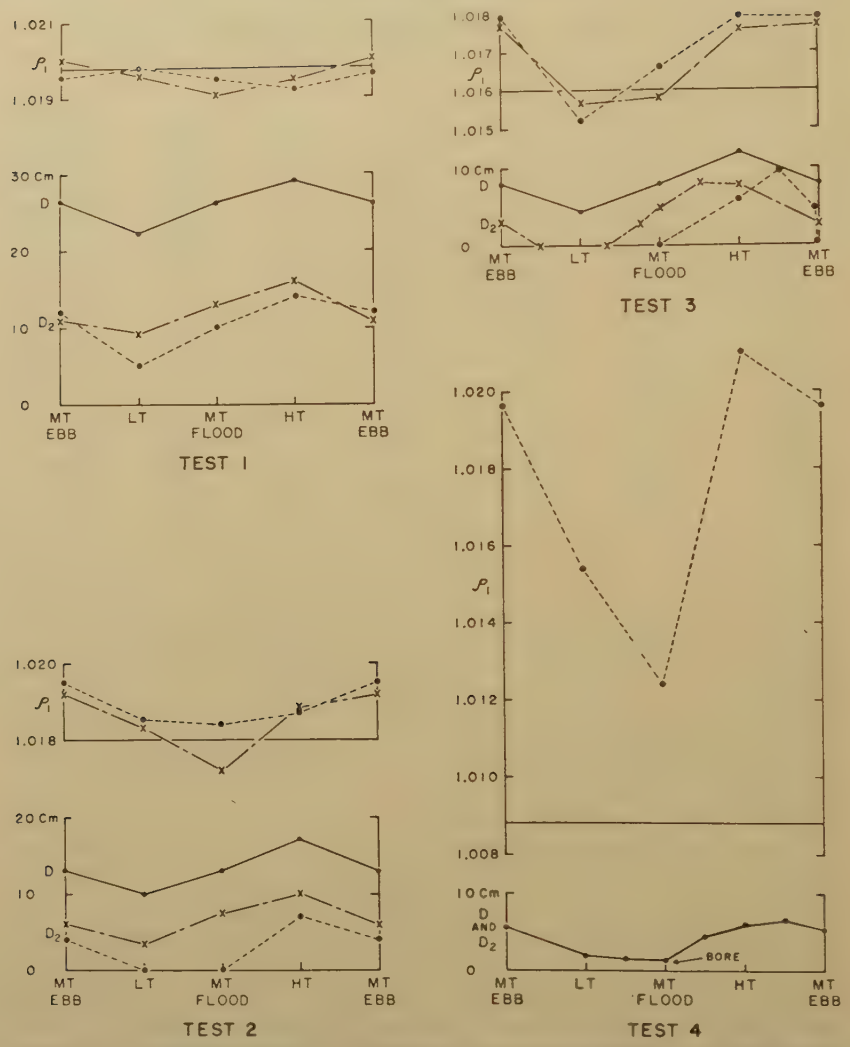

Figure 3. Experimental tests on the influence of tides on overmixing. X's refer to tides of 6-minute period and O's refer to tides of 2-minute period. The solid straight lines indicate the observed ρ_1 without the influence of tides. Data: $\rho_2 = 1.0237$; $\rho_0 = 1.0009$; $q_0 = 7.1$ cm²/sec (test 1); and 3.5 cm²/sec (tests 2, 3, 4); $W_1 = 17.7$ cm.

equation (12) on the supposition that the abrupt widening at the mouth of the harbor acts as a control, that the width of the channel is 2,000 feet, that the depth of the water is 30 feet, and that the mixing action of the reversing-falls upstream is so efficient that overmixing

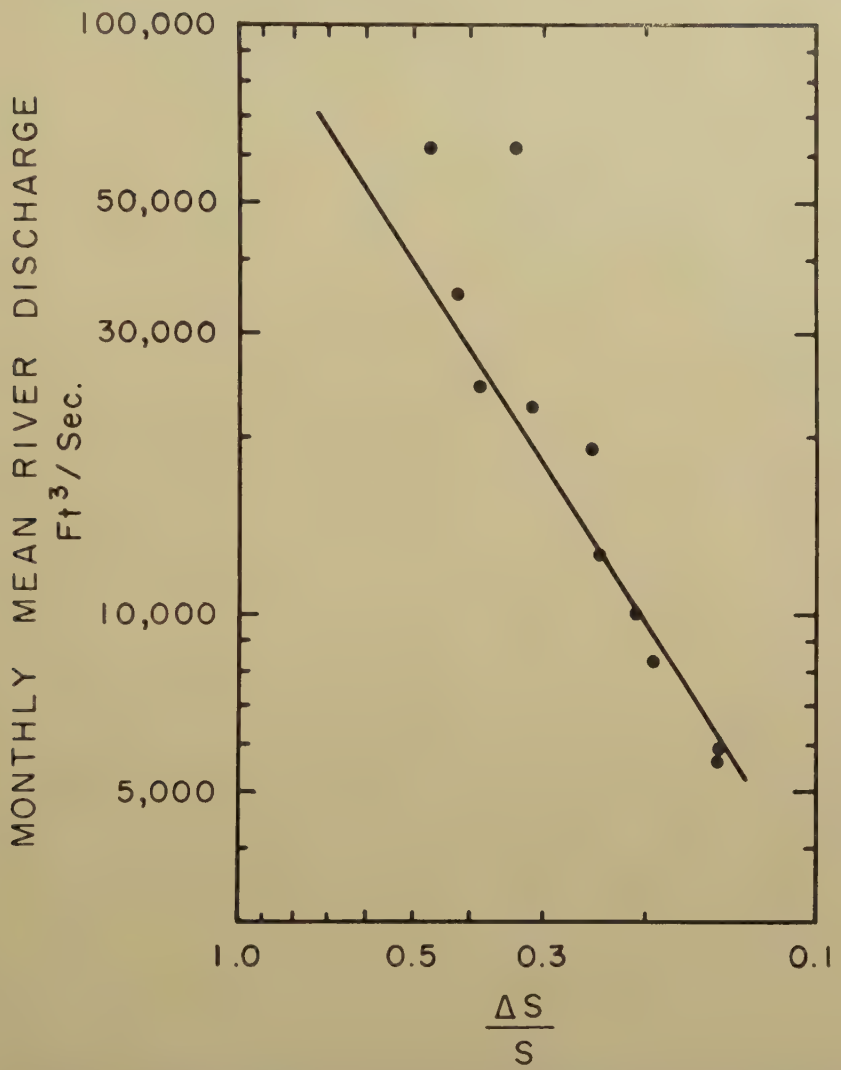

Figure 4. Ratio of vertical salinity difference between the bottom and surface layers in St. John Harbor, plotted against the monthly mean river discharge of the St. John river. The points are from data by Hachey (1939). The straight line is computed from the theory of overmixing.

occurs. Considering the crude nature of both the theory and data, the agreement is fairly good, and it is concluded that St. John Harbor is overmixed.

Data on the dependence of stratification at the mouth of an estuary upon the river discharge are difficult to find in the literature. Very fragmentary data suggest that the following estuaries may be overmixed:

St. Johns River, Jacksonville, Fla.
Columbia River, Oregon
Savannah River, South Carolina
New Waterway, Holland
New York Harbor, N. Y.

It is suggested that future surveys of estuaries where the possibility of overmixing exists include considerable detailed survey work on sections that are likely to exert control action. The observations should give vertical salinity and temperature soundings over a complete tidal cycle for several different stages of river discharge throughout the year. Construction of a graph, such as that shown in Fig. 3, will immediately determine whether or not a condition of overmixing exists in a particular estuary.

REFERENCES

Arons, A. B. and Henry Stommel
1951. A mixing length theory of tidal flushing. Trans. Amer. geophys. Un., *32* (3): 419–421.

Hachey, H. B.
1939. Hydrographic features of the waters of Saint John Harbour. J. Fish. Res. Bd. Canada, *4* (5): 424–440.

Ketchum, B. H.
1951. The exchange of fresh and salt waters in tidal estuaries. J. mar. Res., *10* (1): 18–38.

Stommel, Henry and H. G. Farmer
1952. Abrupt change in width in two-layer open channel flow. J. mar. Res., *11* (2): 205–214.

Contribution No. 588

71. FORAMINIFERA OF GREAT POND EAST FALMOUTH, MASSACHUSETTS[1]

RUSHDI SAID
Gizeh, Egypt

ABSTRACT—Results are given of a quantitative study of the Foraminifera of Great Pond, East Falmouth, Massachusetts. Three foraminiferal populations are noted: a **Trochammina** assemblage in areas temporarily exposed by tidal action, an **Elphidium** population in regions where salinity fluctuated greatly but has never been recorded below 20 o/oo, and an **Ammobaculites** assemblage in areas with salinities lower than 20 o/oo. The small foraminiferal numbers are probably due to the amount of food and to oxygen content.

1 Contribution No. 588 from the Woods Hole Oceanographic Institution.

Reprinted from CONTRIBUTIONS FROM THE CUSHMAN FOUNDATION FOR FORAMINIFERAL RESEARCH
Volume IV, Part 1, February, 1953

Printed by Dorr's Print Shop, Bridgewater, Massachusetts, U. S. A.

INTRODUCTION

Great Pond, a narrow embayment on the south shore of Cape Cod, is about a mile and a half in length, less than a quarter of a mile in width, and has a maximum depth of nine feet in high tide. The northern part of the Pond is divided into two narrow arms, the eastern one of which receives the outflow of Coonamessett River. The Pond is connected by a short, narrow channel with Vineyard Sound to the south.

The distribution of salinity is subject to seasonal and tidal changes, but in general the salinity gradually decreases towards the north and away from Vineyard Sound. In the main body of the Pond, salinity gradients decrease steadily but gradually towards the north. In the eastern arm salinity gradients are rapid and steep. The greatest change in bottom salinity per unit distance is at the southern tip of the eastern arm where, at least during part of the high tide, a 10 o/oo change in salinity occurs in a distance of less than 600 feet. Figure 3 shows the salinity gradients.

Seasonal temperature changes are marked and the bottom is subjected to large annual fluctuations, from nearly freezing in winter to about 77°F in August. The greatest change in temperature per unit distance also occurs in the southern part of the eastern arm (Fig. 3).

The Pond receives a large amount of fresh water. The exchange of its water with that of Vineyard Sound has been discussed by Ketchum (1951). The bottom is covered with uncompacted black, sticky mud whose composition approximates the muds described by Bourcart and Francis-Boeuf (1942) from French estuaries. The texture is due to organic matter in various stages of decomposition. The loss of weight by ignition of the sediment is 22%. The nature of the mud results in an environment in which the decomposition of organic matter releases both hydrogen sulfide and methane gas. The southernmost part of the Pond is sandy and is submerged for a brief period during high tides.

Throughout the year the organic production in the Pond is much higher than that in Vineyard Sound. It reaches a maximum in summer. The percentage of phytoplankton and zooplankton increases from the Sound towards the eastern arm. The phytoplankton species in the arm are different from those in the Pond whereas the zooplankton species in both the Pond and the arm are the same.

Acknowledgments.—The author is indebted to Alfred C. Redfield and Henry C. Stetson for suggesting the problem and to Edward M. Hulburt, John P. Barlow, and Harry J. Turner for use of their unpublished data on the salinity, temperature and plankton populations of the Pond. He wishes also to thank John P. Barlow for assistance in the field.

Collection of samples.—Thirty-one samples (eighteen cores and thirteen grabs) were collected from Great Pond during the summer of 1951. The core samples were obtained by means of a removable plastic liner, 30 cm. in length, affixed to the end of a long wooden rod. Thus short cores could be acquired with a minimum amount of effort in a simple skiff equipped with only an outboard motor. Grab samples were obtained either by hand in shallow waters or by a simple snapper device in deeper waters. Only the topmost six inches of the cores were examined. Figure 1 shows the areal distribution of samples and the type of bottom of the Pond.

SYSTEMATIC WORK

Fourteen species of Foraminifera were obtained in Great Pond:

Ammobaculites cassis (Parker)
Ammobaculites sp.
Elphidium incertum (Williamson)
E. frigidum (Cushman)
E. subarcticum (Cushman)
Buccella calida (Cushman and Cole)
Labrospira crassimargo (Norman)
Miliammina fusca (H. B. Brady)
Nonion tisburyensis (Butcher)
Reophax sp. cf. *R. arctica* (H. B. Brady)
Rotalia beccarii (Linne)
Trochammina inflata (Montagu)
T. lobata (Cushman)
T. macresens (H. B. Brady)

Except for the common New England species *Elphidium incertum, Buccella calida, Trochammina inflata, T. lobata, and Rotalia beccarii,* typical subarctic forms predominate. Cape Cod appears to be the southernmost occurrence from which they have been recorded. All species are either wholly restricted to or exceptionally well developed in brackish estuarine areas. Most species have been described and figured by Phleger and Walton (1950). Also, *Ammobaculites* sp. is the same as that described and figured by these authors (p. 277, pl. 1, fig. 15).

The Woods Hole region lies within a district in which the distribution of Foraminifera of various habitats has been critically studied (Parker, 1948 and 1952; Phleger and Walton, 1950; Said, 1951; and Phleger, 1952). Three major biotopes are represented: the continental shelf, the bay, and the estuary. The total number of Foraminifera and the number of species decreases from the shelf to the estuary. There are several species characteristic of each biotope; however, many species are present in all three biotopes (Parker, 1952, list).

THE DISTRIBUTION OF FORAMINIFERA

Method of Study.—Sixty grams of dried core samples and forty grams of dried grab samples were wet-sieved. Material finer than 0.07 mm. (200 mesh) was

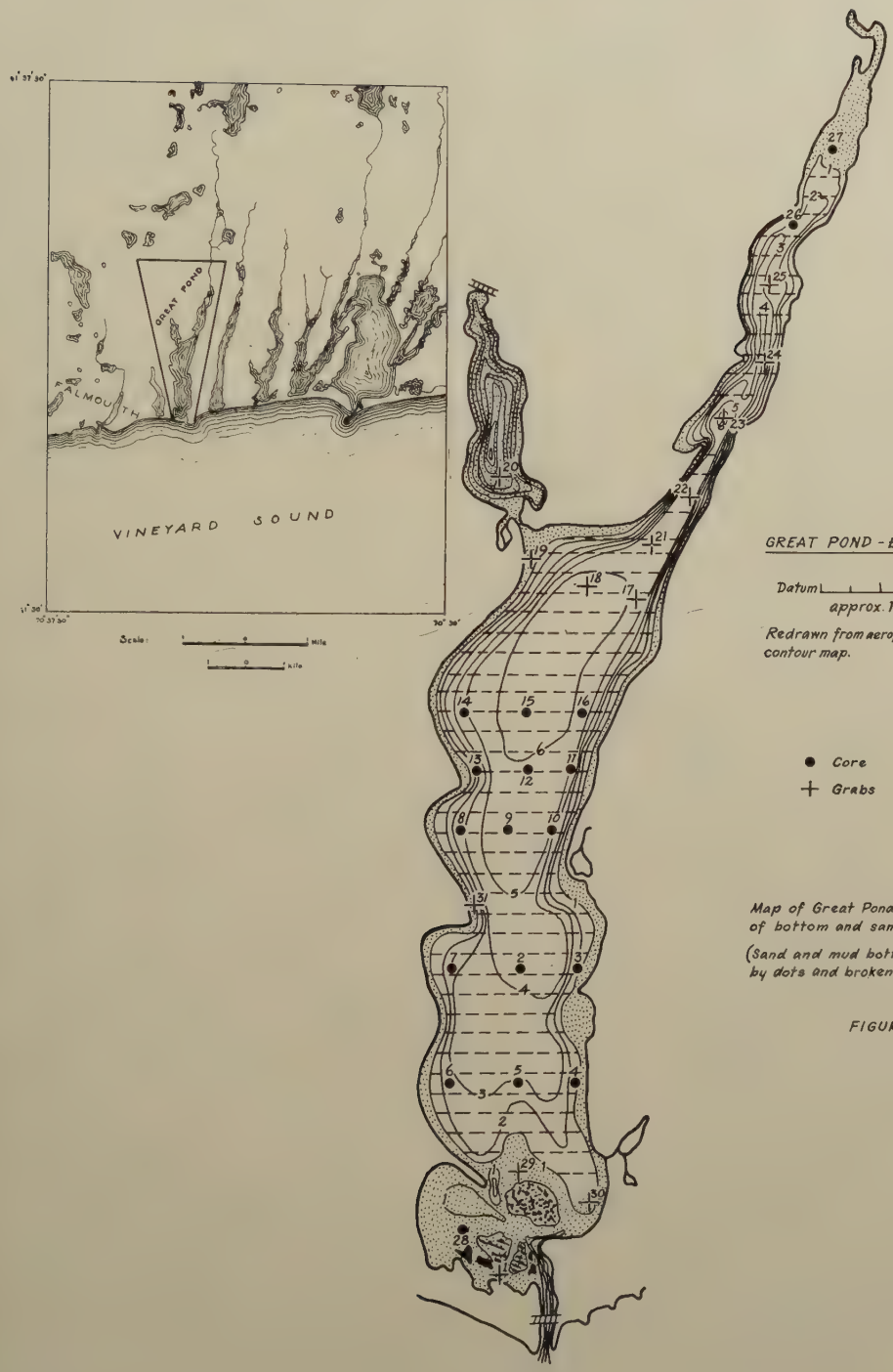

Map of Great Pond showing nature of bottom and sample locations.

(Sand and mud bottoms are represented by dots and broken lines respectively.)

FIGURE 1.

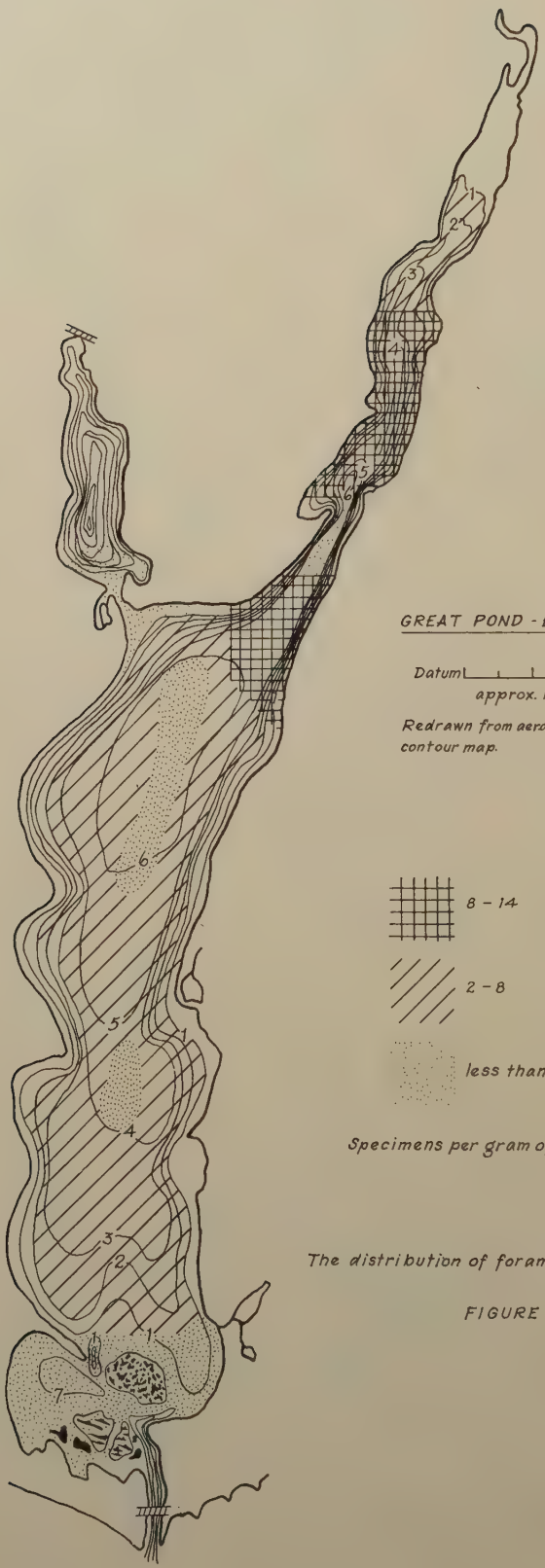

The distribution of foraminifera in Great Pond.

FIGURE 2.

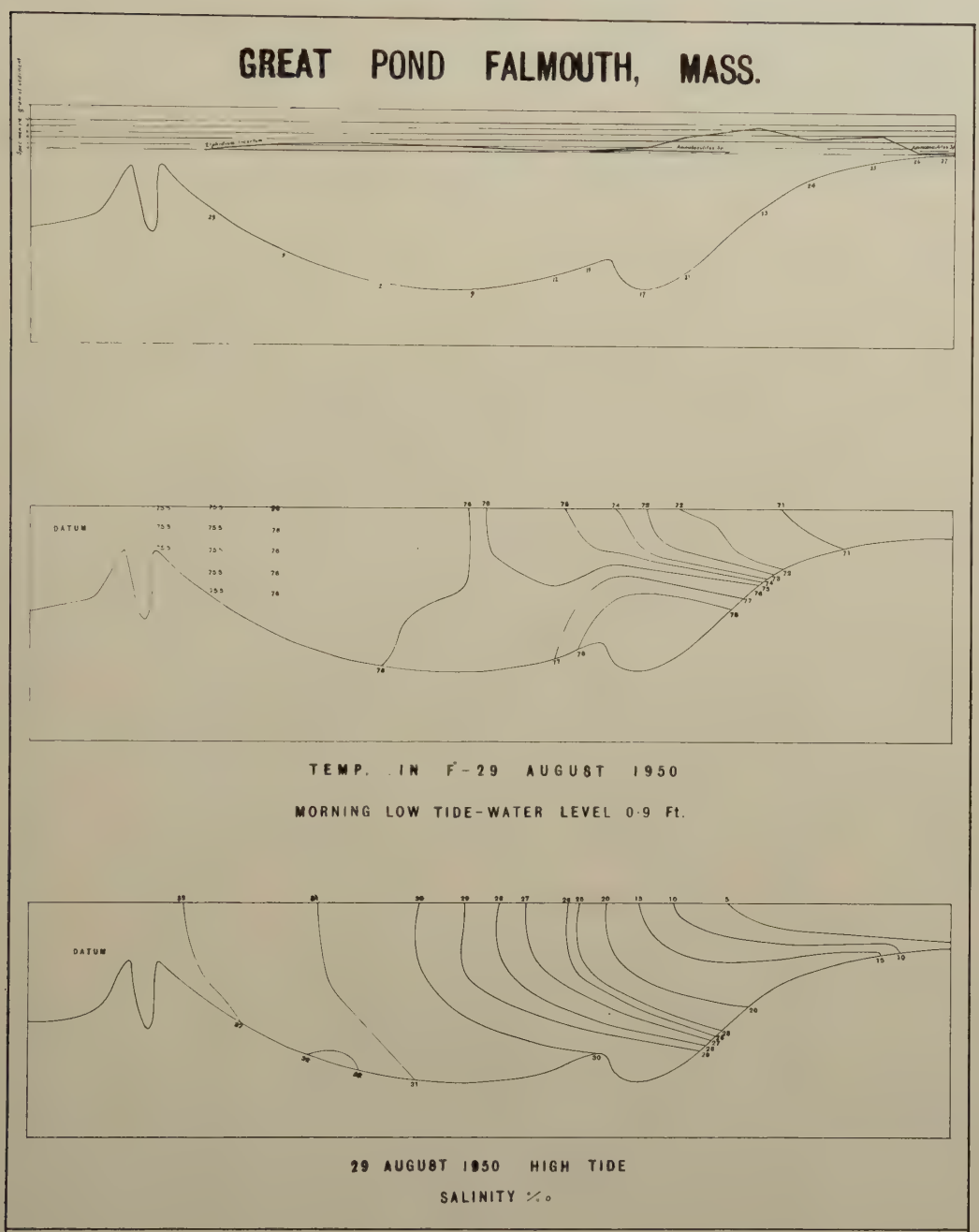

Figure 3: Longitudinal profiles of Great Pond showing from top to bottom: frequency fluctuations of some of the common species of Foraminifera; temperature isotherms and salinity gradients.

TABLE I

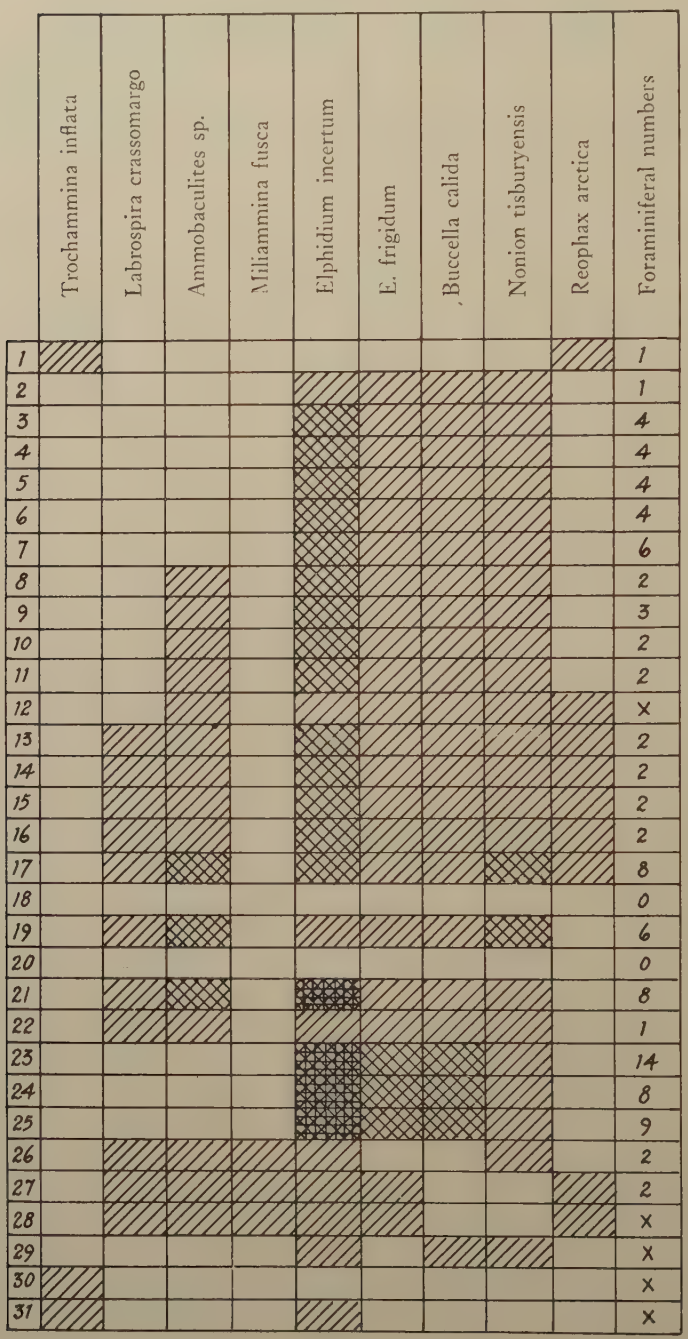

Specimens in one gram of sediment

discarded. The coarser fractions were then treated by carbon tetrachloride for separation of the Foraminifera. The Foraminifera in each sample were then counted, using the method previously described by the author (1950). Table 1 presents the results of this quantitative work in terms of numbers of specimens per gram of sediment. Only nine of the fourteen species recorded in the area were sufficiently abundant to be counted separately. These species only appear in Table 1. The remainder of the species occur in small numbers and nowhere exceed 5% of the total number of Foraminifera.

Total numbers of Foraminifera.—The total foraminiferal numbers in all samples were low, the average foraminiferal number of all samples being 3 specimens per gram. This is much lower than the 200 to 300 per gram content in the continental shelf of the Eastern Atlantic Ocean (Parker, 1948), or the 40 to 50 per gram in Narragansett Bay (Said, 1951). This small number of Foraminifera in the Pond may be due to an environment unfavorable for a flourishing benthonic foraminiferal assemblage, in spite of the fact that organic production is high. In the Great Pond type of basin where the bottom is almost unaerated it appears that oxygen plays an important role in limiting the number of benthonic forms. The nature of the bottom of the Pond is apparently of importance in governing the growth of benthonic foraminiferal populations. In aerated basins where the turnover, exchange of water, and type of bottom sediment permit an abundance of oxygen at the bottom, the oxygen seems to play an insignificant role in the appearance of Foraminifera. This has been pointed out by the author in his study on the distribution of Foraminifera in the Red Sea (1950). In basins where the bottom is unaerated, oxygen appears to be an important limiting factor.

Figure 2 shows the distribution of Foraminifera in Great Pond, and Figure 3 represents the frequency fluctuations of some of the more common species of Foraminifera appearing in the Pond from the Vineyard Sound northward to the eastern arm. The abundance and distribution of Foraminifera coincide with those of the zooplankton population. The largest foraminiferal numbers occur in the southern portion of the eastern arm (Samples no. 23 - 25), an area characterized also by the highest numbers of zooplankton. That this area of maximum development of benthonic Foraminifera shows the greatest fluctuations of both temperature and salinity is interesting. In spite of the fact that this part of the arm is restricted in areal extent, the salinity varies from 30 to 40 o/oo within a distance of not more than 600 feet. One small area may be subjected to such radical changes as 15 to 30 o/oo in one tidal cycle. In spite of these great salinity and temperature variations the samples show remarkable uniformity both in the foraminiferal species and in the total foraminiferal numbers, suggesting that these species are extremely stenohaline and stenothermal.

Size of Foraminifera.—The foraminifers in the Pond are of smaller size than the average in the Vineyard Sound, probably as the result of the unaerated bottom. For example, *Elphidium incertum* is about one-half the size of those in the Sound, a dwarfing apparently due to the smaller amount of oxygen present.

Number of species.—The number of species in the Pond is limited by several unfavorable conditions; namely, the unaerated bottom, the vigorous fluctuations of salinity and temperature, and periods of dryness for at least part of the day.

The foraminiferal numbers increase northward from the Sound to the arm in the same manner as previously noted in Narragansett Bay (Said, 1951). A similar observation has been made of the zooplankton populations (John P. Barlow, oral communication).

Distribution of species.—There are three distinct populations in the Pond: an *Elphidium* assemblage abundant in the main body of the Pond and the southern reaches of the arm; an *Ammobaculites* assemblage with other arenaceous Foraminifera in the northern reaches of the arm; and a *Trochammina* assemblage common in the sub-tidal shallow flat in the southern reaches of the Pond.

The *Elphidium* assemblage is comprised of calcareous forms which form either the entire assemblage or at least a large percentage of it. In the latter case there is an influx of some arenaceous species in a few localities with a general trend in increase of these arenaceous forms to the north of the main body of the Pond. In the southern reaches of the arm the assemblage is composed entirely of calcareous forms of great uniformity.

The *Ammobaculites* assemblage (with other arenaceous species) occurs in the northern reaches of the arm. Few calcareous forms are present. The change from a calcareous assemblage (*Elphidium*) to an arenaceous assemblage is sudden and apparently related to salinity inasmuch as the *Elphidium* assemblage, while tolerating great salinity fluctuations, does not seem to withstand waters less saline than 20 o/oo. This low salinity is present at least part of the time in the northern arenaceous Foraminifera zone, but has not been recorded at any time in the main body of the Pond.

The *Trochammina* assemblage occurs in a sandy and very shallow area subjected to less fluctuations in salinity than any other part of the Pond. It is also wetted daily by the tides. This zone is probably similar to the *Spartina glabra* zone of Johnson (1925, pp. 522-528).

SUMMARY AND CONCLUSIONS

Great Pond is a shallow embayment which represents one of the better known estuaries of the eastern

coast of North America. The study of the distribution of Foraminifera in the Pond should therefore give definite results as to the response of the contained species to the physical conditions of the environment.

All species recorded are of the subarctic type, and it seems probable that the low temperature to which the Pond is subjected during the winter months thus determines the kind of species that can persist. Temperature cannot, however, account for the distribution pattern within the area. A similar observation has been made by Phleger and Walton (1950) and Said (1951).

The foraminiferal numbers in the Pond are the lowest ever recorded in recent marine sediments. The small numbers are believed to be the result of an almost unaerated bottom. The most important single factor determining the appearance and abundance of benthonic Foraminifera seems to be the hydrographic conditions of the basin. Although oxygen appears to be of no consequence in the distribution of Foraminifera in aerated basins (Said, 1951), it becomes an important factor in unaerated basins. The influence of oxygen is limited not only to lowering the foraminiferal numbers but also has an effect in the dwarfing of the foraminiferal fauna. Lalicker (1948) summarized the knowledge of the dwarfing of protozoan faunas and has cited examples from the geologic record. The amount of oxygen and the hydrographic condition of the basin of deposition seem to be much more important than any factor hitherto considered. Dwarfing is probably due to retardation of growth because of a lower metabolic rate under unfavorable condition.

Salinity seems to play an important role in the distribution of Foraminifera. Salinity fluctuations and the oxygen content may account for the small number of species in the Pond, inasmuch as there are only fourteen species in contrast to over 200 species in nearby Vineyard Sound. There are three biofacies in the Pond: a *Trochammina* assemblage, which flourishes in areas with the least salinity fluctuation; an *Elphidium* assemblage which thrives in that part of the Pond where there is vigorous salinity change but the salinity is always greater than 20 o/oo; and an *Ammobaculites* assemblage. *Ammobaculites* also appears in areas with higher salinities but in smaller numbers. It is possible that its numbers increase when the salinity becomes lower than 20 o/oo due to the elimination of other competing species.

Explanation of the distribution of species due to salinity is probably an oversimplification for the nature of the bottom is also an important factor. *Trochammina* appears only in sandy bottoms. *Elphidium incertum clavatum*, common in the New England coast and a species which is always present in association with *E. incertum*, was not observed in the Great Pond apparently due to the fact that the bottom of the Pond is muddy. The species has been observed only on sandy bottoms (Said, 1951). The effect of tidal submergence which subdivided similar embayments into floral zones (Johnson, 1925) is probably important in determining the kind of species that could live in areas which are only briefly wetted. *Trochammina* appears to be able to endure wetting by tidal action for a brief period.

Although salinity appears to be the controlling factor in the distribution of species, the drastic salinity variations common in the southern part of the eastern arm do not seem to affect the character of the fauna in that area. On the contrary, this region is characterized by the most uniform and most abundant foraminiferal fauna in the Pond.

The total foraminiferal numbers increase northward as do the numbers of zooplankton population in the Pond. The low oxygen content reduces numbers, leaving the Great Pond with much lower numbers than Vineyard Sound even though organic production is high.

REFERENCES

Bourcart, J. and Francis-Boeuf, C., 1942, La Vase: Hermann, Paris.

Johnson, D. W., 1925, The New England Acadian Shoreline: New York, John Wiley, pp. 522-528.

Ketchum, B. H., 1951, The flushing of tidal estuaries: Sewage and Industrial Wastes, vol. 23, pp. 198-209.

Lalicker, C. G., 1948, Dwarfed protozoan faunas: Journ. Sed. Petrology, vol. 18, pp. 51-55.

Parker, F. L., 1948, Foraminifera of the Continental Shelf from the Gulf of Maine to Maryland: Bull. Mus. Comp. Zool., Harvard, vol. 100, pp. 214-241.

———, 1952, Foraminiferal distribution in the Long Island Sound-Buzzards Bay area, *ibid*, vol. 106, pp. 427-473.

Phleger, F. B, 1952, Foraminifera ecology off Portsmouth, New Hampshire: *ibid*, pp. 315-390.

Phleger, F. B and Walton, W. R., 1950, Ecology of Marsh and Bay Foraminifera, Barnstable, Mass.: Amer. Journ. Sci., vol. 248, pp. 274-294.

Said, R., 1950, The distribution of Foraminifera in the northern Red Sea: Contrib. Cushman Found. Foram. Res., vol. 1, pp. 9-29.

———, 1951, Foraminifera of Narragansett Bay: *ibid*, vol. 2, pp. 75-86.

———, 1951, Ecology of Foraminifera: The Micropaleontologist, vol. 5, pp. 12-14.

Contribution No. 593

The Exchanges of Fresh and Salt Waters in the Bay of Fundy and in Passamaquoddy Bay[1]

By Bostwick H. Ketchum and D. Jean Keen
Woods Hole Oceanographic Institution, Woods Hole, Mass.
(Received for publication February 26, 1952)

ABSTRACT

The results of 385 previously published hydrographic stations in the Bay of Fundy are summarized, and the average distribution of salinity at various depths is derived from these data.

The total quantity of river water accumulated within the Bay of Fundy is equivalent to the quantity introduced by the rivers during a period of about 76 days.

The exchange ratios for tidal excursion segments of the Bay of Fundy range from 0.17 in the neighborhood of Cape Chignecto to 0.056 in the segment immediately south of Grand Manan. In the upper tidal reaches of the Petitcodiac River and of Minas Basin the exchange ratios are about 0.95.

The estuary of the St. Croix River has been studied and calculations indicate that about 15 tides, or 8 days are required on the average to replace one day's river flow. The exchange ration in this case range from 0.905 to 0.30.

From a summary of existing data in Passamaquoddy Bay it is calculated that the total accumulation of river water is equal to the quantity introduced by the rivers in a period of about 16 days.

CONTENTS

	Page
Acknowledgments	97
Introduction	98
The Bay of Fundy	
Observed distribution	101
Tidal exchange calculation	101
Comparison of calculations with observations	107
Discussion	111
Passamaquoddy Bay	113
The St. Croix estuary	115
Passamaquoddy Bay	115
Exchanges with the Bay of Fundy	118
Discussion	119
References	121
Appendix	123

ACKNOWLEDGMENTS

This investigation was suggested by Dr. A. G. Huntsman, and the authors greatly appreciate his co-operation and many suggestions, which were particularly valuable because of his long experience in the region.

At the invitation of Dr. A. W. H. Needler, the senior author enjoyed the facilities of the Atlantic Biological Station during August, 1951. The cordial

[1]Contribution No. 593 from the Woods Hole Oceanographic Institution, Woods Hole, Massachusetts.

J. Fish. Res. Bd. Can., **10** (3), 1953.
Printed in Canada.

co-operation of many members of the staff, and particularly of Dr. H. B. Hachey and the Oceanographic Group is gratefully acknowledged.

INTRODUCTION

THE GREAT TIDES of the Bay of Fundy, and the enormous effect they have in mixing the river effluents to considerable depths in the area, have been emphasized by all hydrographers who have studied the Bay. It seemed desirable to determine whether the techniques for evaluating the circulation in estuaries, which have been developed for much smaller and generally shoaler regions, would be applicable to the Bay of Fundy.

The Bay of Fundy, shown in Figure 1, is a narrow, funnel-shaped arm of the Gulf of Maine, varying in width from about 40 miles at Grand Manan, to about

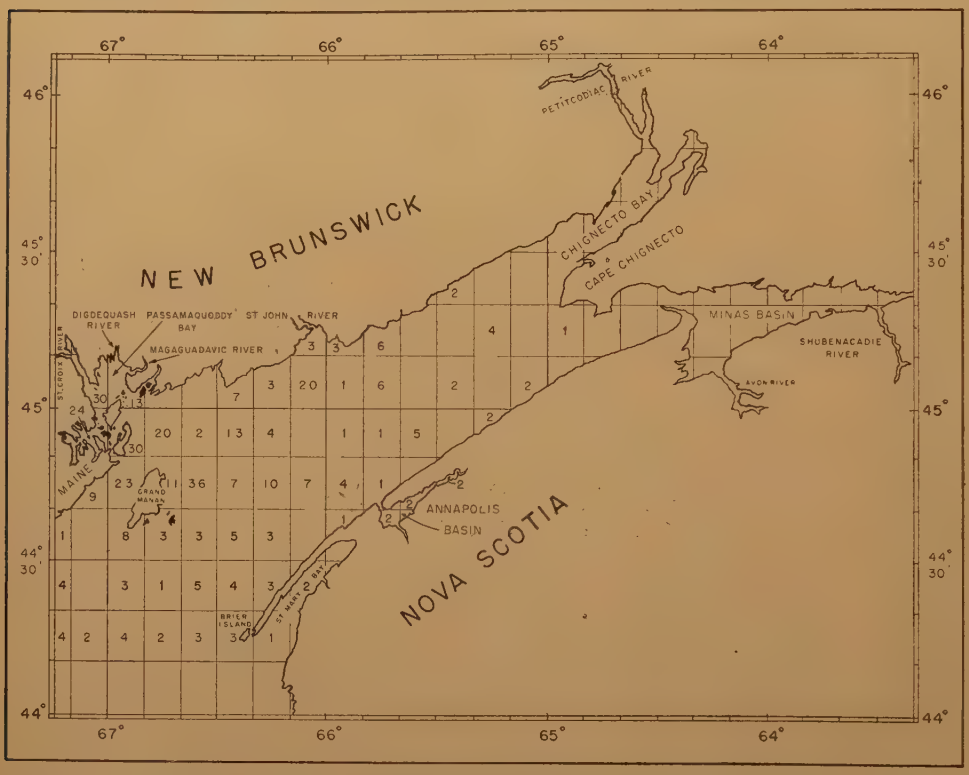

FIGURE 1. The Bay of Fundy. The numbers in the ten-minute squares show the number of stations available.

25 miles at Cape Chignecto. The maximum depth decreases, over this same distance, from about 116 fathoms to about 25 fathoms. Above Cape Chignecto the Bay subdivides into two arms, Chignecto Bay and Minas Basin.

The general pattern of circulation of the surface waters of the Bay of Fundy has been described by Mavor (1922, 1923), Hachey (1931) and Watson (1936).

The transport of drift bottles has confirmed the pattern deduced from the distribution of density. The results show a counterclockwise circulation, with more saline water occupying the southern part and flowing into the Bay along the Nova Scotia shore. Fresher water occupies the northern part and flows seaward along the New Brunswick shore and south of Grand Manan. The drift bottles released close to the Nova Scotia shore were generally picked up to the east of the point of release. The bottles released farther than 5 to 10 miles from the Nova Scotia shore usually drifted northward and were recovered in New Brunswick. These results indicated that some water transport across the Bay occurs throughout its length. Many of the drift bottles released by Bigelow (1927) and by Fish and Johnson (1937) in the Gulf of Maine were found in the Bay of Fundy, predominantly along the Nova Scotia shore. These results confirm the inflow of water along this shore and establish the source of this surface water as, in part at least, an offshoot of the Gulf of Maine eddy. Some contribution of surface water from the Scotian Shelf may also occur and Mavor (1922) mentions this as the source of the high salinity inflow. Bigelow (1927, p. 832), however, concludes that the Nova Scotian current flows into the Gulf of Maine in volume during only a few weeks in spring.

The circulation around Grand Manan is less firmly established. Both Mavor and Watson concluded that there was a clockwise circulation around Grand Manan, though the latter commented that it was small. Fish and Johnson (1937) released 24 drift bottles between West Quoddy Head and Whale Cove, Grand Manan. Of the eight recovered, five drifted to the north or east of the point of release, three drifted southwest to the coast of Maine. Although they drew probable lines of drift in a clockwise direction around Grand Manan, their results are subject to other interpretations. McLellan (1951) concludes from hydrographic data that there is no conclusive evidence of residual currents in Grand Manan Channel, though MacGregor and McLellan (1951) observed net southward movements a couple of weeks later. Their observed drift would indicate a counterclockwise circulation around Grand Manan. They suggest that the residual current may be variable depending upon meteorological conditions.

The deep water in the Bay of Fundy has a relatively high salinity (32.5 to $> 33\ ‰$) and is derived from the deep water in the Gulf of Maine. Bigelow (1927) showed that, at depths of 100 meters, water of salinity greater than 33 ‰ and moderately high temperature (4–5°C.) was continuous with similar water in the Gulf of Maine. Watson (1936) observed that the salinity of the water at 100 meters off Grand Manan increased from 32.5 ‰ at the end of April to 33.2 ‰ in September. He concluded that there must be a "steady inflow of salt deep water from the Gulf of Maine which more than compensates for the dilution from vertical mixing".

The river effluents entering the Bay of Fundy are derived from seven main drainage basins, which are illustrated by Watson (1936) who gives mean monthly rates of flow for each. The drainage into Chignecto Bay comprises about 9 per cent and that into Minas Basin about 15 per cent of the total mean annual flow. The fresh water entering at the head of the Bay of Fundy is thus only about one-

quarter of the total river drainage. Most of the remainder (60 per cent) is contributed by the St. John River, which enters the New Brunswick side of the Bay about midway between Cape Chignecto and Grand Manan. Both Hachey (1935) and Watson (1936) show that the diluted water issuing from the mouth of the St. John estuary extends southward for 40 to 50 miles and is identifiable at the surface east of Grand Manan. The St. John water, by the time it has reached this degree of extension, has a salinity of 31.5 $^0/_{00}$, which, as Hachey (1935) calculates, shows an admixture of about 64 times its own volume of sea water (of salinity 32.0 $^0/_{00}$). This large volume of sea water, which at the time of spring freshet in 1932, was greater than four million cubic feet per second, must be provided by an inflow of sea water, either below the diluted surface water or to the east of it.

The presence of the large effluent from the St. John along the north shore, and the necessarily enormous counter-flow of sea water, must contribute in a substantial way to the development and maintenance of the seaward-directed current of diluted water along this shore, and to the general counterclockwise circulation of the Bay.

The tidal wave is augmented within the Bay of Fundy so that the mean range increases from about 14 feet at Brier Island to nearly 40 feet in the inner end of Minas Basin, (Dawson, 1917). Along the south shore of the Bay the mean range of tides is somewhat greater than it is along the north shore (Marmer, 1926; Redfield, 1950). This Kelvin wave effect would augment the tendency for the waters to circulate in a counterclockwise direction.

The available data do not give conclusive evidence concerning the rate of the circulation within the Bay of Fundy. Hachey (1934) has deduced, from the temperature distribution, that the rate of replacement of Bay of Fundy waters differs from year to year. The differences are correlated with the prevailing winds and with variations in the discharge of the St. John River. His data, however, do not lend themselves to direct computations of velocity. Watson (1936) concluded that the St. John River effluent had a net seaward drift of 34 cm./sec. (0.7 knots). Mavor (1922) derived non-tidal drifts of 2.34 to 6.53 miles per tidal cycle (0.19 to 0.52 knots), from Dawson's (1908) current measurements. Mavor also obtained, from drift bottle returns, net drifts ranging from 4 to 5 miles per day (0.17 to 0.21 knots).

The objective of this investigation was to determine, from available data, the distribution of river water within the Bay of Fundy and Passamaquoddy Bay, and to evaluate the rate of its transport by the methods used by Tully, 1949; Ketchum, 1950; Ketchum, Redfield and Ayers, 1951. The empirical calculations of exchange ratios and of total accumulation of river water by the method described by Ketchum (1951) have also been made, and the results compared with those obtained from the observed distribution of salinity.

It should be emphasized that the conclusions drawn in this paper represent average distributions and average exchanges of water across complete cross-sections of the Bay. The foregoing summary of the circulation should make it clear that the actual conditions in various parts of the cross-sections will vary considerably from these averages.

The salinity results of 385 hydrographic stations have been obtained from the published literature referred to in the introduction and from the files of oceanographic data at the Woods Hole Oceanographic Institution. These data have been summarized by grouping the results within ten-minute squares, and the number of observations in each such square in the area studied is indicated in Figure 1. Data are available over the major part of the Bay. They are sparse in the northeastern area, and no salinity information has been found for Chignecto Bay and Minas Basin.

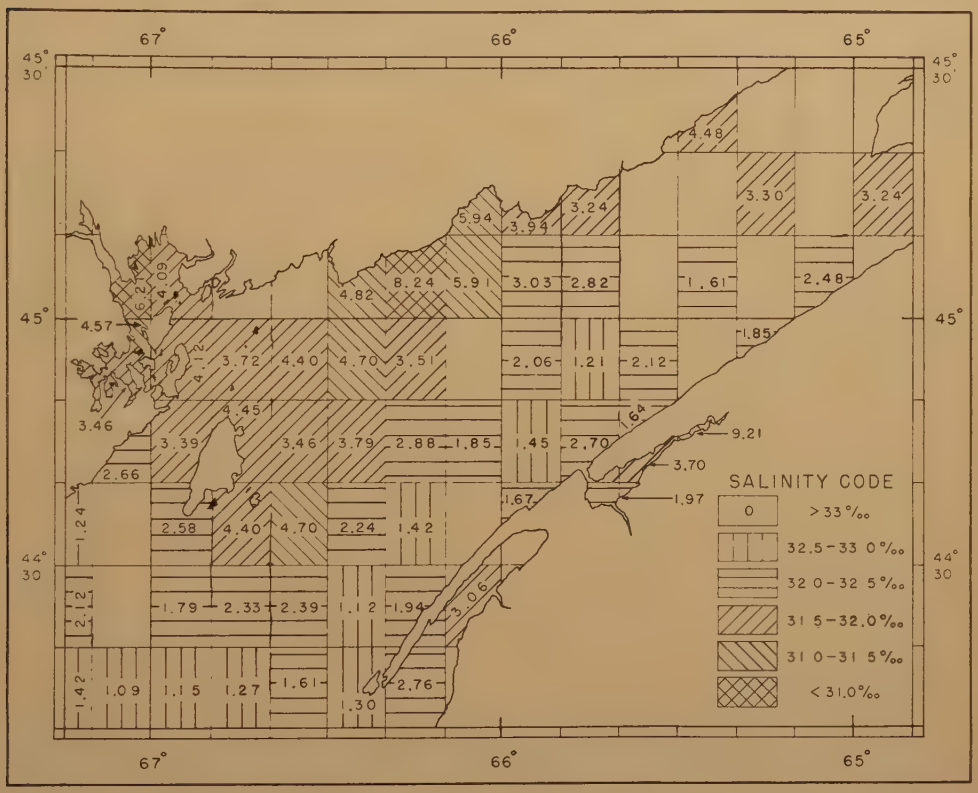

FIGURE 2. The distribution of average salinity and river water, 0–25 meters.

OBSERVED DISTRIBUTION

SALINITY

In each ten-minute square average salinities, weighted for depth of observations, have been computed for depth ranges of 0 to 25, 25 to 50, 50 to 100, and greater than 100 meters. The results are given in Figures 2, 3, 4, and 5, where the salinity range is shown by the hatching pattern, and the percentage of fresh water is given by the number in each square. In the upper 25 meters (Figure 2) water with a salinity greater than 32 ‰ predominates throughout the southern

part of the Bay along the Nova Scotian shore except for the stations directly opposite Minas Basin where the observed salinity was slightly less than 32 ‰. In contrast, the water throughout the northern part of the Bay has a salinity lower than 32 ‰. The greatly freshened water resulting from the admixture of the St. John River outflow extends to the southwest, from St. John Harbor as far as the shoals in the neighborhood of Grand Manan. Average fresh-water contents greater than 4 per cent (salinities < 31.7 ‰) are thus found more than 50 miles from the mouth of the St. John River. It is clear that these average values faithfully reflect the counterclockwise circulation previously described and

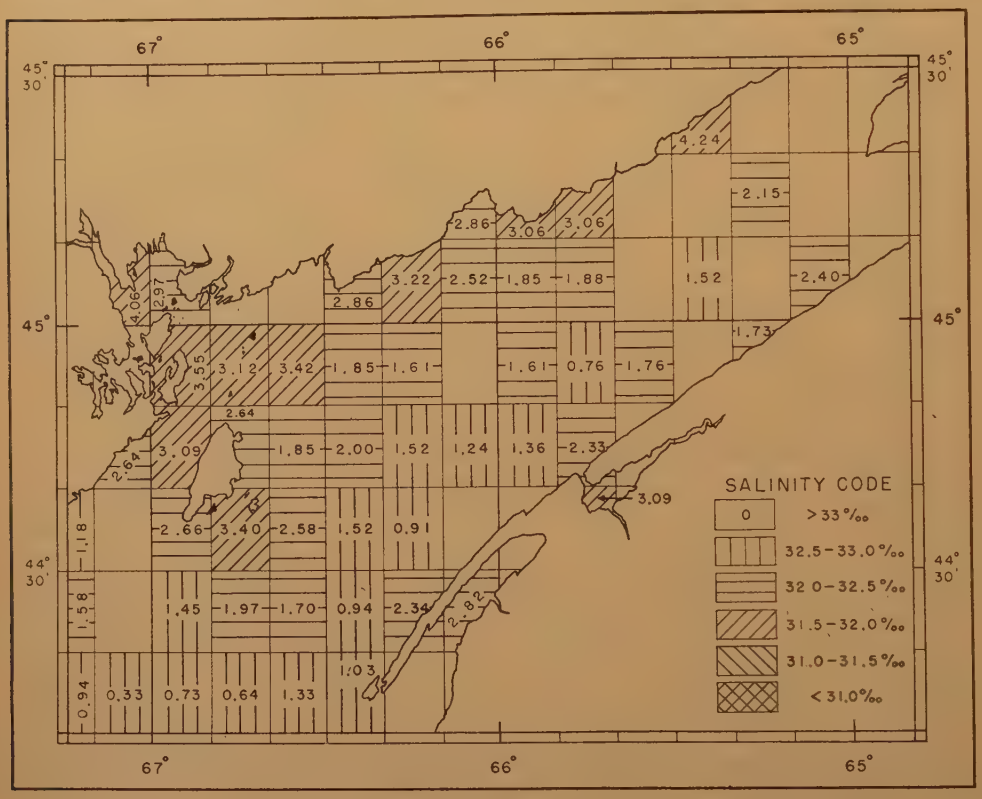

FIGURE 3. The distribution of average salinity and river water, 25–50 meters.

summarized in the introduction. It is of some interest that the surface water to the west of Grand Manan Island is fresher than the surface water to the southward. This indicates that some river water from either the St. John or from Passamaquoddy Bay is present. This observation does not confirm the clockwise circulation around Grand Manan that has been previously reported.

The mean distribution of salinity between 25 and 50 meters is generally similar to that of the surface water except that the water is more saline throughout the Bay. The freshest water is found along the New Brunswick shore, both

to the east and west of the St. John River. Directly opposite the St. John, however, more saline water is found—as though an indraft of high-salinity water occurred in this location. Other areas, with higher salinity than in any of the surrounding water at these depths, are found east of Grand Manan and in the northern part of Passamaquoddy Bay.

Between 50 and 100 meters the increase in salinity is even more marked, but the pattern of fresher water throughout the northern part of the Bay is maintained. Only a small part of the Bay contains water at depths greater than 100 meters, and all of this water has a salinity greater than 32.5 ‰.

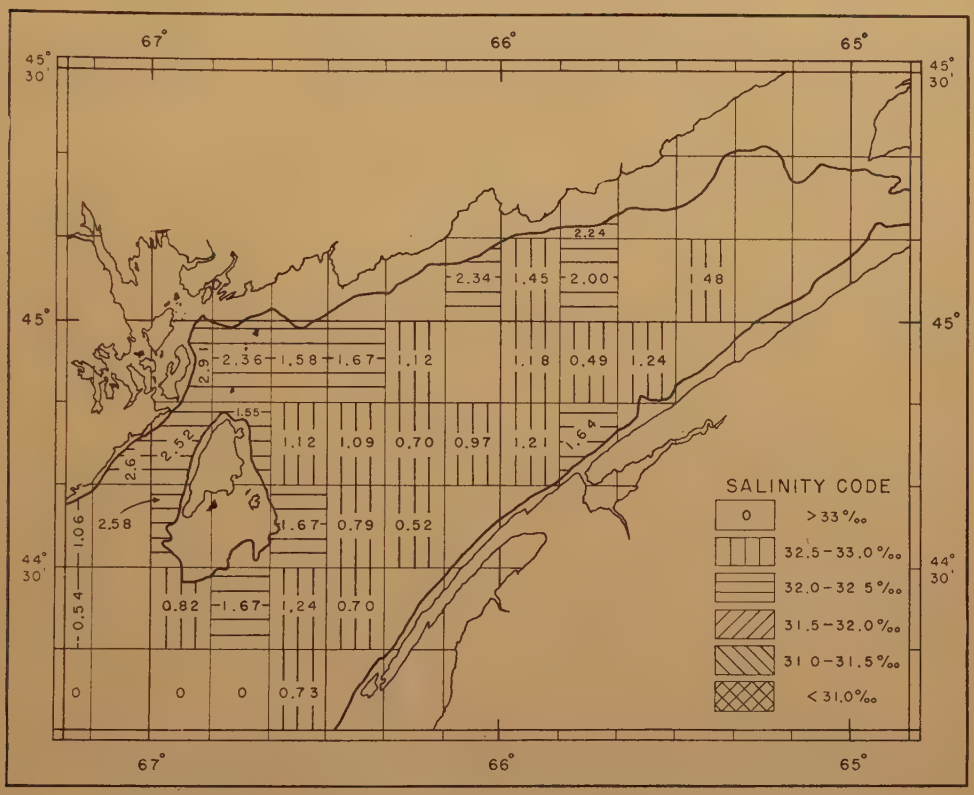

FIGURE 4. The distribution of average salinity and river water, 50–100 meters.

FRESH WATER

From the average-salinity data the proportion of fresh water in each sample has been calculated, using 33 ‰ as the salinity of the source sea water. Water of this salinity is found only at depths of 100 meters or more near the mouth of the Bay. Bigelow's results indicate that this salinity is characteristic of the tongue of water penetrating at these depths from the Gulf of Maine. In all of Watson's sections across the mouth of the Bay, water of this salinity appeared. The percentage of fresh water in each ten-minute square for various depths is also shown in Figures 2 to 5.

In order to compute transport from the distribution of fresh water, complete cross-sections must be used. The Bay was therefore subdivided by sections running southeast to northwest, located 11.5 miles apart. The lines thus form diagonals of some of the ten-minute squares, but a row of complete squares is included between each pair of lines. The average salinity for various depths of each segment was computed from the data previously described, and the average proportion of fresh water computed for each of the segments. The total volume and the volume to various depths was obtained by planimetering the areas between depth contours on charts Nos. 0609 and 0610 of the U.S. Navy Hydro-

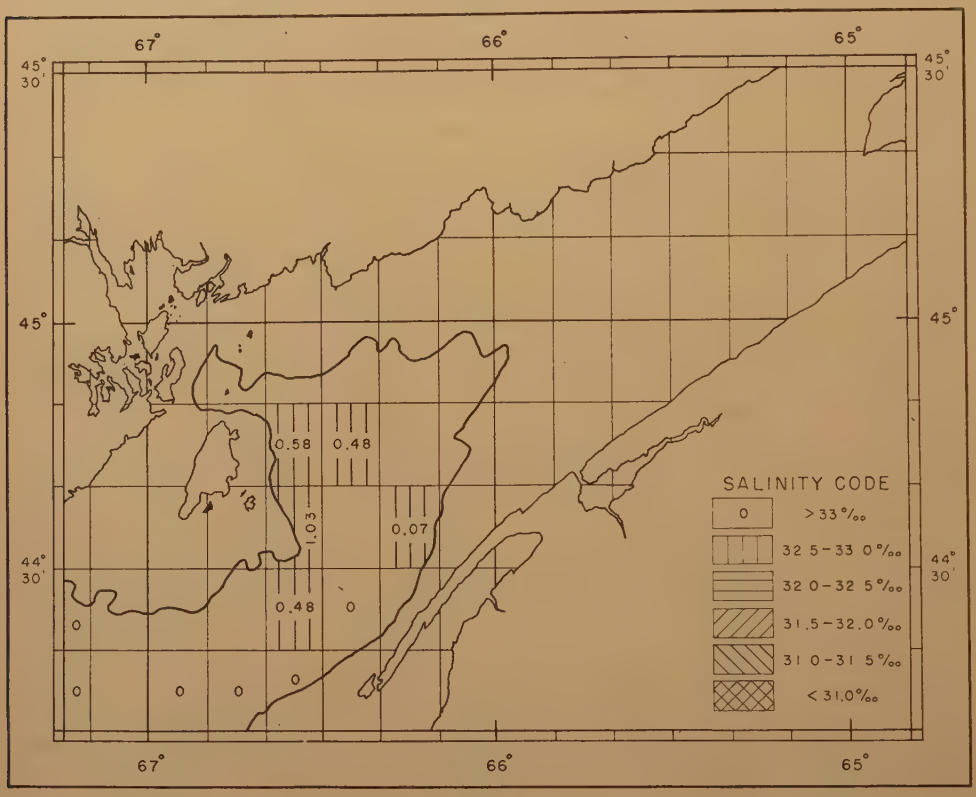

FIGURE 5. The distribution of average salinity and river water, > 100 meters.

graphic Office. From these data the proportion and total volume of fresh water within the Bay have been computed and the results are given in Table I. In Figure 6 the proportions and the accumulated volumes of fresh water are shown for various distances from Cape Chignecto.

The water is diluted with river effluents to depths of 100 meters. A small amount of fresh water is found even at greater depths. The upper 25 meters contains about half of the total fresh water in the Bay, although its volume is only 29 per cent of the total. The percentage of fresh water in the surface decreases

gradually from the neighborhood of Cape Chignecto until the freshening effect of the St. John River appears, where it increases greatly. The fresh-water content then gradually decreases again throughout the remainder of the length of the Bay. It is of interest that the percentage of fresh water in the total volume of water in each segment does not vary greatly, ranging from 2.64 per cent at Cape Chignecto

TABLE I The mean salinities, volumes of river water and flushing times for the various segments of the Bay of Fundy.

Segment	Depth	Total volume	Mean salinity	River water	River water	Mean flushing time
		$10^9 ft.^3$	‰	%	$10^9 ft.^3$	*days*
A	0–25	860	32.00	3.03	26.0	4.98
	25–50	586	32.22	2.36	13.4	
B	0–25	873	32.094	2.75	24.0	
	25–50	759	32.206	2.41	18.3	5.59
	50–100	130	32.51	1.49	1.9	
C	0–25	949	32.23	2.32	22.0	
	25–50	851	32.34	1.99	16.95	5.75
	50–100	373	32.43	1.74	6.5	
D	0–25	1,069	31.965	3.14	33.6	
	25–50	982	32.317	2.07	20.3	8.51
	50–100	900	32.51	1.48	13.3	
E[a]	0–25	1,225	31.82	3.58	44.1	
	25–50	1,132	32.323	2.05	23.2	11.3
	50–100	1,540	32.535	1.41	21.7	
F	0–25	1,398	31.94	3.20	44.7	
	25–50	1,265	32.37	1.92	24.3	11.8
	50–100	2,044	32.64	1.09	22.3	
	> 100	689	32.895	0.32	2.2	
G[b]	0–25	1,540	31.94	3.20	49.4	
	25–50	1,382	32.25	2.28	31.4	15.5
	50–100	2,446	32.53	1.43	35.0	
	> 100	2,084	32.90	0.30	6.25	
H[c]	0–25	1,486	32.09	2.77	41.1	
	25–50	1,238	32.296	3.13	26.4	12.6
	50–100	1,762	32.435	1.71	30.1	
	> 100	1,474	32.965	0.11	1.62	
Total		31,037			600.02	76.03

a Annapolis Basin included.
b Northern part of Passamaquoddy Bay included.
Southern part of Passamaquoddy Bay included.

to 1.66 per cent south of Grand Manan. The freshening effect of the St. John River is observable at all depths of the water column opposite its entrance (segments D and E, Table I).

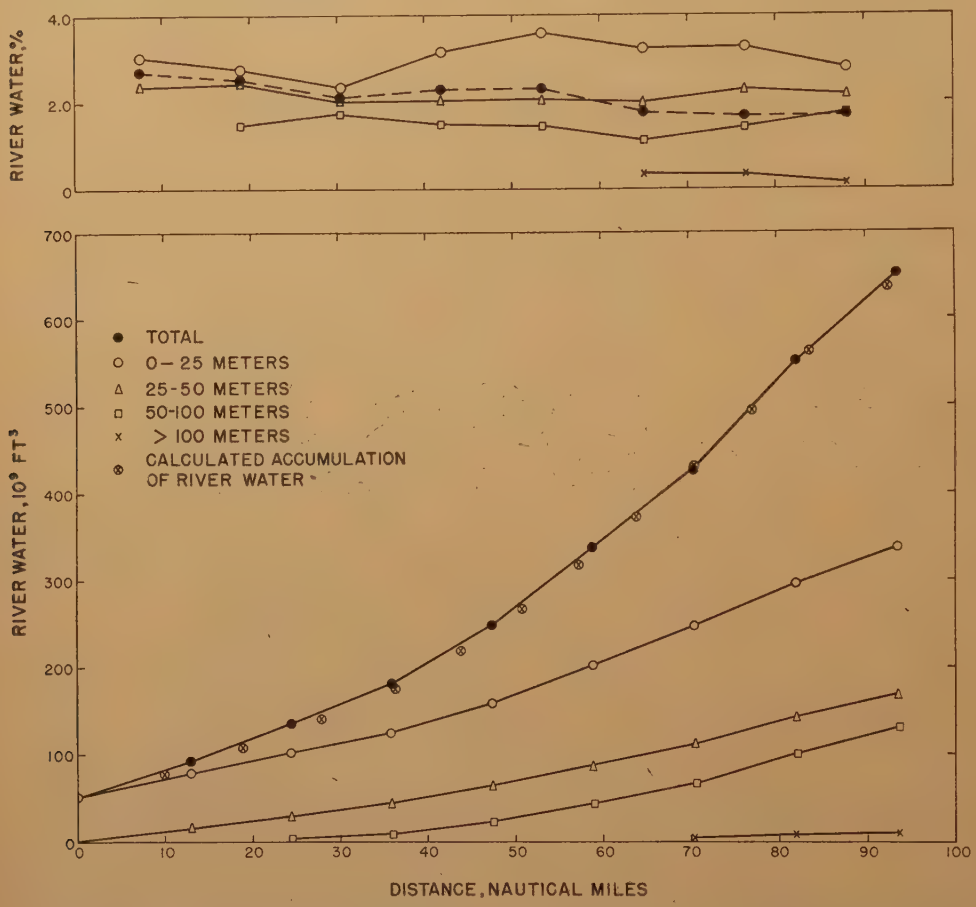

FIGURE 6. *Upper figure:* The proportions of river water at various depths, plotted at increasing distances from Cape Chignecto. *Lower figure:* The total volume of river water enclosed.

THE FLUSHING TIME

The average length of time required to remove one day's contribution of river water is defined by the ratio of the quantity of river water accumulated within the estuary to the quantity introduced daily by the rivers, and has been called the "flushing time". The average river flow for the months of April, May, June, and July, as given by Watson (1936) has been used in the computation. This period was selected because 76 per cent of the data used—293 of the 385 stations—was obtained during the period June to September. The river-flow data for the earlier months were included in the average because of the time interval

required to traverse the Bay. During this period the rivers contribute 7.9×10^9ft.^{3} per day, or 4.08×10^9ft.^{3} per tidal cycle.

The corresponding times are included in Table I, and indicate that about 76 days are required to exchange the average particle of river water in the area. Since the part of the Bay considered is about 93 miles long these results give an overall average rate of transport of about 1.22 nautical miles per day. For the various segments the rate of transport ranges from 2.3 miles per day at Cape Chignecto to 0.74 miles per day near Grand Manan. These values are, of course, somewhat less than those quoted above which were for the surface water alone. Some of the river water is entrained by the counterdrift of sea water, and the time required for this water to make the complete circuit of the Bay is included in our average.

Tidal Exchange Calculation

The empirical method for computing exchange ratios and the accumulation of fresh water in an estuary, as previously described by Ketchum (1951) has also been applied to the Bay of Fundy.

In this calculation it is necesssry to subdivide the estuary into segments which are horizontally defined by the width of the estuary and the average excursion of a particle of water on the flooding tide. In each segment so defined the exchange ratio, r_n, is given by:

$$r_n = \frac{P_n}{P_n + V_n} \tag{1}$$

in which P_n is the intertidal volume, and V_n is the low tide volume of the nth segment.

If the mixing is sufficiently vigorous so that all of the water within the segment is diluted with river water, the total quantity of fresh water, Q_n, accumulated within each segment is equal to:

$$Q_n = \frac{R}{r_n} \tag{2}$$

in which R is the quantity of fresh water introduced by the rivers during a complete tidal cycle. It has been shown that the water below 100 meters in the Bay of Fundy is only slightly diluted, and the segmentation has been made excluding the waters at greater depths.

Segmentation

The Bay of Fundy has been subdivided into tidal excursion segments from the head of tide in the Petitcodiac River and in Minas Basin to a diagonal line to the southwest of Grand Manan. The location of the segments so obtained is shown in Figure 7 and their lengths are included in Table II. The northern arm of the Bay is thus subdivided into seven segments, including two in the Cumberland Basin (2a and 2b), and Minas Basin is subdivided into six segments. The

Bay of Fundy between Cape Chignecto and the southern end of Grand Manan is divided into twelve segments.

These segments are computed from the displacement expected from the volume of water introduced as the tide floods, and the length of each should equal the mean excursion during the flooding tide. This method will give erroneous results if the tidal currents are restricted to part of the water column. Comparisons with direct current measurements are therefore desirable to check the size of the segments. It will be noted that Segment 2 in the Petitcodiac River has a length of 23 miles. The tidal bore in the Petitcodiac River runs for a distance of

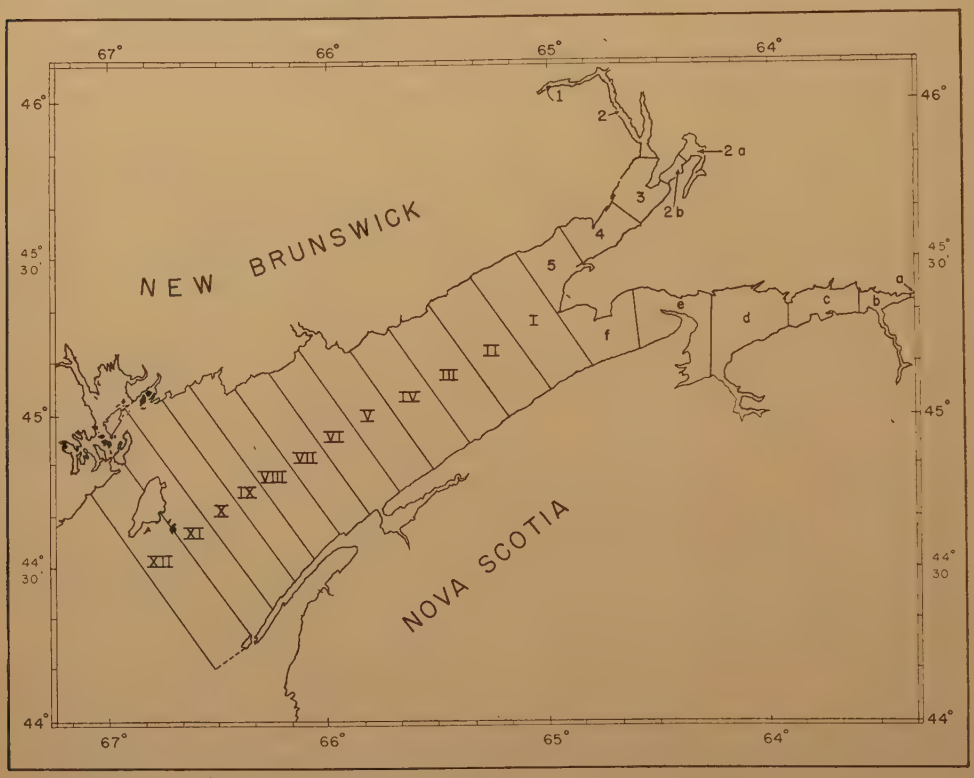

FIGURE 7. The location of the tidal-excursion segments in the Bay of Fundy area.

21 miles in the neighbourhood of this segment. (U.S. Navy Dept., 1939). At the mouth of the Petitcodiac River the maximum tidal velocities are 3 to 4 knots giving excursions[1] of 10 to 14 miles, and in Chignecto Bay the tidal currents have average velocities of about 2 knots, producing excursions of about 8 miles. In this region our tidal segments range from 9.3 to 11.5 miles in length. In Minas Basin the tidal currents have average velocities of 3 to 4 knots, giving mean excursions of 12 to 16 miles. Our segment lengths range from 13.7 at the upper end to 15.3 miles for the outermost segments.

[1]Calculated as $\frac{2}{\pi} \times$ average maximum velocity $\times$ 6.2 hours. Maximum spring-tide velocities are multiplied by 0.85 to convert them to average maximum velocities.

Within the Bay of Fundy the length of the segments decreases from 10 miles at Cape Chignecto to 6.5 miles at Grand Manan. The final segment is again greater, being 9 miles in length. The average length is 7.7 miles. The current tables of the U.S. Coast and Geodetic Survey give average velocities at strength of currents within this area which range from 1.5 to 2 knots, giving excursions ranging from 5.9 to 7.9 miles. In Grand Manan Channel the velocity is 2.4 knots, or 9.5 miles for the excursion. To the south of Grand Manan the observed currents are 2.6 to 3.3 knots, giving excursions of 10.3 to 13 miles. These stations are outside of our outermost segment which was 9 miles in length, but they indicate that the excursions in this area may be expected to increase. It appears, therefore, that the tidal excursions computed from volume displacements by this method are comparable to excursions derived from measured currents.

TABLE II. Intertidal and high-tide volumes and exchange ratios of various tidal exchange segments of the Bay of Fundy. (For location of segments, see Figure 7.)

	Segment	Distance [a]	Length of segment	Intertidal volume	High tide volume	Exchange ratio
		miles	*miles*	$10^9 ft.^3$	$10^9 ft.^3$	r_n
Chignecto Bay	0	64.2	—	0.32	0.34	0.95
	1	54.8	9.4	3.81	4.0	0.95
	2	31.3	23.5	33.8	37.8	0.85
	2a	34.8	—	6.7	7.4	0.91
	2b	29.8	5.0	23.9	30.6	0.78
	3	20.8	10.5	122	190	0.64
	4	9.3	11.5	100	290	0.346
	5	0	9.3	100	390	0.256
Minas Basin	a	66.9	—	2.63	2.8	0.94
	b	57.5	9.4	29.4	32.2	0.92
	c	43.8	13.7	102.8	135	0.76
	d	29.8	14.0	205	340	0.604
	e	15.3	14.5	220	560	0.392
	f	0	15.3	170	730	0.233
Bay of Fundy	I	10.0	10.0	200	1380	0.151
	II	19.0	9.0	200	1520	0.132
	III	28.0	9.0	200	1720	0.116
	VI	36.5	8.5	200	1920	0.104
	V	44.0	7.5	200	2120	0.094
	VI	51.0	7.0	200	2320	0.086
	VII	57.5	6.5	200	2520	0.080
	VIII	64.0	6.5	200	2720	0.074
	IX	70.5	6.5	200	2920	0.069
	X	77.0	6.5	200	3120	0.064
	XI	83.5	6.5	200	3320	0.060
	XII	92.5	9.0	280	3600	0.056

[a] From Cape Chignecto to outer boundary of segment.

EXCHANGE RATIOS

The volumes within each of these segments and the appropriate exchange ratios are presented in Table II. In the Petitcodiac River and the upper end of Minas Basin, where the range of tides becomes 40 feet, the exchange ratios are 0.95 and 0.94 respectively. In the neighbourhood of Cape Chignecto the exchange ratio is 0.15, and it falls gradually as a result both of increasing depth and decreasing tidal range to a value of 0.056 in the segment immediately south of Grand Manan.

ACCUMULATION OF FRESH WATER

The fact that the St. John River contributes the major portion of the fresh water to the Bay near its center complicates the calculation of the accumulation of fresh water. Water at all depths in the neighbourhood of the St. John River is

TABLE III. Volume of river water accumulated within the various segments of the Bay of Fundy.

	Segment	River flow	St. John[a] water	River water accumulated	Cumulative river water
		$10^9 ft.^3/T.C.$	$10^9 ft.^3$	$10^9 ft.^3$	$10^9 ft.^3$
Chignecto Bay	0	0.32	0.003	0.34	0.343
	1		0.061	0.34	0.744
	2		0.571	0.38	1.695
	2a		0.112	0.35	
	2b		0.461	0.41	
	3		2.87	0.50	6.40
	4		4.37	0.90	11.67
	5		5.89	1.25	18.81
Minas Basin	a	0.45	0.042	0.48	0.522
	b		0.484	0.49	1.50
	c		2.04	0.59	4.13
	d		5.14	0.75	10.02
	e		8.45	1.15	19.62
	f		11.0	1.92	32.55
Bay of Fundy	I	0.77	20.0	5.14	76.5
	II		23.0	5.8	105.3
	III		26.0	6.6	137.9
	IV		29.0	7.4	174.3
	V	4.08		43.4	217.7
	VI			47.4	265.1
	VII			51.4	316.5
	VIII			55.5	372.0
	IX			59.6	431.6
	X			63.9	495.5
	XI			67.9	563.4
	XII			73.4	636.8

[a]River water introduced into upper part of estuary in counter-flow of sea water; 1.51% of high-tide volume.

diluted with river effluent. It is this diluted sea water which provides the source of the countercurrent and is involved in the mixing in the upper part of the Bay. Inspection of the figures showing the distributions of salinity and fresh water indicates that the source sea water for the part of the Bay to the northeast of the St. John River has a salinity of approximately 32.5 rather than the salinity of 33 $^{0}/_{00}$ which appears appropriate for the lower part of the Bay. This decreased salinity corresponds to the incorporation of 1.51 per cent river water, most of which must originate in the St. John. The Bay of Fundy has therefore been treated as though it were two estuaries in tandem. All of the water in the upper part of the estuary is assumed to contain 1.51 per cent river water derived from the St. John River. To this volume of river water we have added the quantity of river water which would be expected to accumulate as a result of the river flow from the drainage basins discharging into Chignecto Bay and Minas Basin.

The results of the computation of the total accumulation of fresh water in the Bay of Fundy are presented in Table III. These calculations have been made using, as above, the river flow for the period April to July, as given by Watson (1936). The computed accumulation of fresh water is 636.8 x 10^9 cubic feet, which corresponds to nearly 81 times the daily contribution of all of the drainage basins. Between Cape Chignecto and the line south of Grand Manan the calculated accumulation is 585 x 10^9ft.^{3}. The computed flushing time of this part of the area is thus about 74 days. These values correspond to those computed from the salinity distribution; namely, 600 x 10^9ft.^{3} for the accumulation and 76 days for the flushing time.

Comparison of Calculations with Observations

fresh water

A direct comparison between the calculated and observed accumulation of water in the Bay of Fundy is shown in Figure 8. The quantity of fresh water computed to be present in Chignecto Bay and Minas Basin is included, although the salinity data necessary to check these computations are not available. The quantities of river water deduced from the salinity distribution were read for the appropriate distances from Figure 6.

The numbers recorded above the correlation line indicate the average flushing time in days for the observed quantity of fresh water. The numbers below the correlation line show the distance in nautical miles from Cape Chignecto. The correlation between calculated and observed accumulation of river water is very close throughout the entire length of the Bay of Fundy.

It will be remembered that the tidal-exchange calculation was made excluding the water below a depth of 100 meters. If this deeper water were included in the computation the results for the first seven segments would not be affected, but six shorter segments would be substituted for the final five segments. The total computed accumulation of river water would be increased by 76 x 10^9ft.^{3}. The data in Table I show that only 10 x 10^9ft.^{3} are to be found at depths greater than 100 meters. On both the basis of the observed distribution of salinity and the tidal excursions discussed previously, therefore, the exclusion of this deeper water from the calculations seems justifiable.

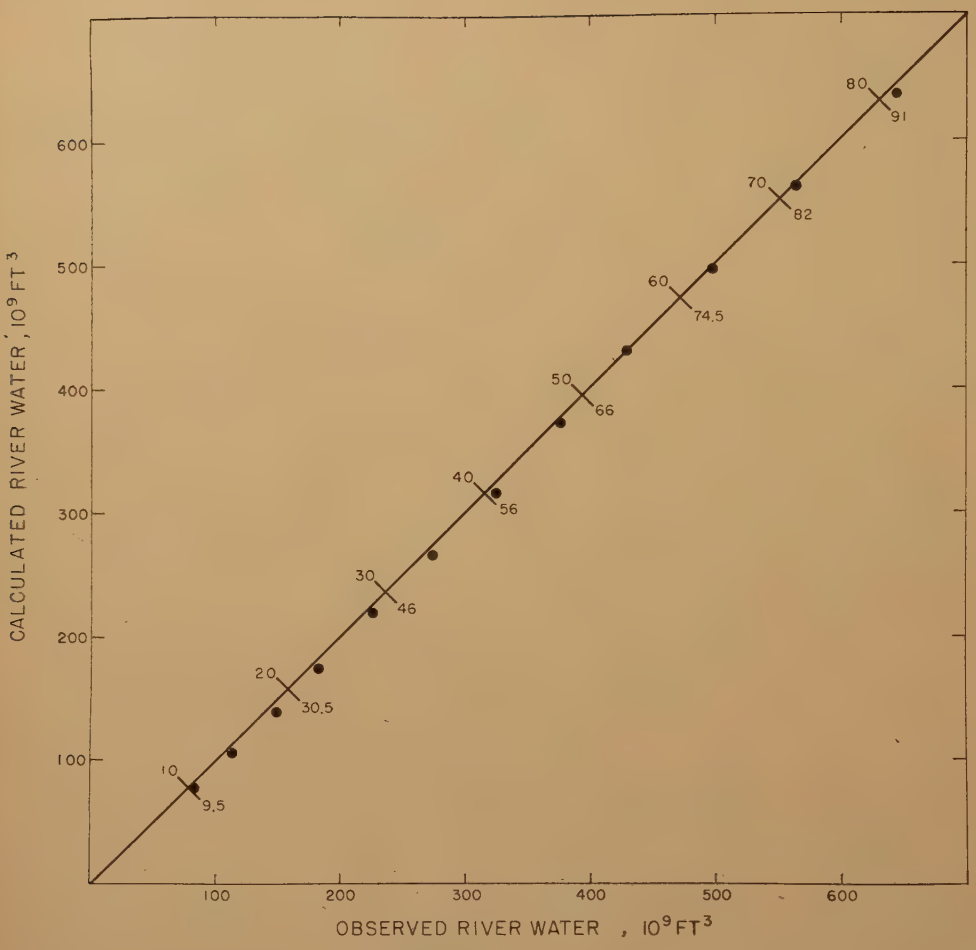

FIGURE 8. Comparison between the observed and the calculated accumulation of river water in the Bay of Fundy. The numbers above the correlation line show the average flushing time in days; those below the line show the distance, in nautical miles, from Cape Chignecto.

EXCHANGE RATIOS

An exchange ratio (r) can also be computed from observed distribution of fresh water as follows:

$$r = \frac{R}{Q} \qquad (3)$$

where Q is the observed quantity of fresh water as derived from the salinity distribution and R is the volume of water introduced by the river during a tidal cycle. This calculation must also be made separately for each of the tidal-excursion segments, since any variation in the size of the segments considered will have a direct effect on the value of Q. It will be recognized that this equation is identical with equation (2), but we are using different basic data for the calcul-

ation. In this case the observed distribution of river water is used to calculate an exchange ratio; in applying equation (2), an exchange ratio calculated from tidal volumes was used to compute a theoretical distribution of river water.

In Figure 9 the exchange ratios calculated from the tidal volumes and from the observed distribution of fresh water are plotted for various distances from Cape Chignecto. Close agreement between the exchange ratios calculated by the two methods is obtained. The values decrease in a regular way from about 0.15 at Cape Chignecto to about 0.056 south of Grand Manan.

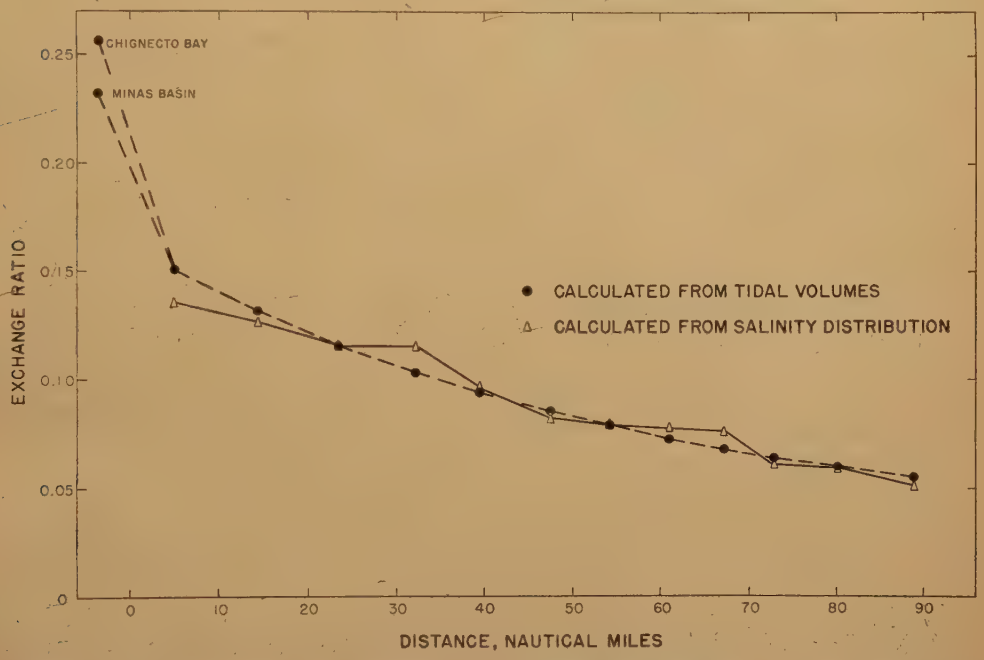

FIGURE 9. The exchange ratios calculated from the observed distribution of river water and from the tidal volumes for various distances from Cape Chignecto.

DISCUSSION

It should be emphasized that the exchanges and the derived flushing times given above are averages for complete cross-sections of the estuary. The circulation in the Bay of Fundy clearly indicates that there is a net inflow of more saline water along the Nova Scotia shore, with the river water mainly escaping along the New Brunswick shore. It is clear that, depending upon which side of the estuary is being considered, the actual exchanges will vary from the average by large amounts. They will be greater along the New Brunswick shore and less along the Nova Scotia shore. There appears to be no very certain method of determining how great this variation from the average may be.

It should also be pointed out that although the foregoing conclusions were based upon the distribution of river water, the same exchanges may be expected for any material or organism freely transported by the water. The effect of the

circulation on the biological populations present could be evaluated by methods similar to those discussed by Ketchum (1952), using the average exchange ratios presented in this paper.

One of the purposes of this investigation was to determine whether the simplified empirical method of calculating exchanges in a tidal estuary and the resultant accumulation of river water would apply to the Bay of Fundy. The agreement between the calculated and observed accumulations of river water is very close when the calculation is made excluding the water deeper than 100 meters. One of the basic assumptions in the empirical calculation is that the water is thoroughly mixed in a segment defined by the sides of the estuary and the average excursion of a particle of water on the flood tide. It seems logical that this sets the maximum distance over which complete mixing can be expected. If, however, mixing is complete over a shorter distance, the computed accumulation of river water would be less than the actual accumulation. The fact that the computed and observed distributions agree in the Bay of Fundy indicates that mixing is sufficiently vigorous so that the assumption of the tidal-excursion segment as a mixing length gives valid results.

The Bay of Fundy is much larger than the estuaries previously discussed. The success of the tidal-exchange calculation in this region indicates that it is not limited to the smaller estuaries and suggests that it may be useful in any estuary having vigorous tidal mixing. Some characteristics of the estuaries previously discussed by Ketchum (1951) are compared with the Bay of Fundy in Table IV.

TABLE IV. Some characteristics of the estuaries in which the tidal-exchange calculation has been satisfactory.

Characteristic	Previous range[a]	Bay of Fundy
Surveyed length—*nautical miles*	1.5 to 20	90
Surface area—*sq. nautical miles*	1 to 45	3,300
Max. high tide depth—*feet*	9 to 1000	630
Depth of diluted water —*feet*	5 to 40	> 300
Range of tides—*feet*	1.5 to 6.4	14 to 40
Tidal prism volume—$10^6 ft.^3$	7.6 to 9200	3,670,000
River flow per tidal cycle—$10^6 ft.^3$	0.5 to 120	4,080
Ratio $\frac{\text{Prism volume}}{\text{River flow}}$	15 to 279	900

[a]The extreme values for Raritan River and Bay, Alberni Inlet, and Great Pond, previously discussed by Ketchum, 1951.

The volume of the tidal prism in the Bay of Fundy is about 400 times greater than that in Raritan Bay, the largest previous value. The volume of river water introduced during a tidal cycle is nearly 40 times greater than that introduced into Alberni Inlet, the largest previous value. The ratio of tidal-prism volume to river flow is 60 times as great as the smallest, and more than three times as great as the largest value discussed in the previous paper.

In the estuaries previously studied the depth of the water which was measure-

ably diluted with river water was 40 feet or less. In the Bay of Fundy dilution of the sea water with river water is detectable at depths greater than 100 meters. This observation emphasizes the vigorous vertical mixing which occurs in the Bay of Fundy.

PASSAMAQUODDY BAY

The details of the circulation of waters in Passamaquoddy Bay have been less thoroughly studied than in the Bay of Fundy. Passamaquoddy Bay, shown in Figure 10, is a nearly enclosed body of water which receives the drainage from three major basins, the St. Croix, the Digdequash, and the Magaguadavic. Although a number of hydrographic observations have been made within the Bay, no systematic attempt at a quantitative description of the circulation has been made. Watson comments that most of the fresh water escapes from Passamaquoddy Bay through the Western Passage, but he makes no attempt to evaluate the quantity of this discharge. Copeland (1909), and Craigie (1914), conducted salinity and temperature surveys of the St. Croix River. Hachey (1934a, 1935) has described the mixing of fresh and salt water in estuaries, with special reference to parts of Passamaquoddy Bay.

The St. Croix Estuary

The St. Croix is the largest of the three rivers, producing one and one-half times as much fresh water as the other two combined. Entering as it does on the western side of Passamaquoddy Bay, the effluent from the St. Croix would tend to establish and maintain a counterclockwise circulation in much the same way the St. John does for the Bay of Fundy. The waters in the estuary of the St. Croix, and in the Bay off its mouth, are fresher than those found in any other part of Passamaquoddy Bay.

The exchanges of water in the St. Croix estuary have been evaluated by methods similar to those used for the Bay of Fundy. The results of the tidal-exchange calculation are given in Table V. The river is divided into five segments

Table V. The St. Croix Estuary. Intertidal and high-tide volumes, exchange ratios and accumulation of river water when the river flow is 104×10^6 ft.^{3} per tidal cycle. For location of segments see Figure 10; segments A, B, C, are in Oak Bay.

Segment No.	Distance from mouth	Intertidal volume	High-tide volume	Exchange ratio	River water Local	River water Cumulative
	miles	$10^9 ft.^3$	$10^9 ft.^3$	r_n	$10^9 ft.^3$	$10^9 ft.^3$
0	13.1	0.104	0.115	0.905	0.115	0.115
I	10.2	0.786	0.905	0.870	0.120	0.235
A	12.0	0.20	0.25	0.80	0.130	—
B	10.3	1.13	1.33	0.860	0.121	—
C	8.4	1.37	2.70	0.506	0.206	0.692
II	6.2	2.21	5.82	0.38	0.273	0.965
III	2.8	2.60	8.40	0.31	0.336	1.301
IV	0	3.60	12.0	0.30	0.348	1.649

from the head of tide at Calais to the mouth at St. Andrews. Three additional tidal segments are found in Oak Bay. The location of these segments is shown in Figure 10. The exchange ratio decreases from 0.905 at Calais to 0.30 at St. Andrews.

FIGURE 10. Passamaquoddy Bay. The letters in the five-minute squares correspond to those in Table IV. The numbered segments in the St. Croix River correspond to those in Table V and VI.

The St. Croix River is gauged near Baileyville, Maine, and the office of the Geological Survey at Augusta, Maine, has made available the river-flow data prior to its publication. For the first 17 days of August, 1951, the gauged flow averaged 2,320 ft.^{3}/sec., or 104 x 10^6ft.^{3}/tidal cycle. Using this value for the river flow, the quantity of river water accumulated in the estuary between Calais and St. Andrews is calculated to be about 1,650 x 10^6 cubic feet.

During August, 1951, a series of salinity and temperature observations were

made in the estuary of the St. Croix, and the results are given in the appendix. The data from the stations marked with an asterisk were used in computing the average high-tide salinities and volumes of fresh water in the various tidal-excursion segments. The mean salinity and fresh-water content of the tidal-excursion segments are given in Table VI. The salinity results indicate that about

TABLE VI. Mean salinities and volumes of river water accumulated in the various tidal-exchange segments of the St. Croix Estuary, August, 1951.

Segment No.	Stations used	Mean salinity	River water	River water	
				Local	Cumulative
		‰	%	$10^9 ft.^3$	$10^9 ft.^3$
0	R–1	12.785	60.0	0.069	0.069
I	R–2	26.18	18.2	0.165	0.234
A, B, C	R–3a	28.86	9.82	0.420	0.654
II	R–3, R–4	29.83	6.78	0.394	1.048
III	R–4, R–4a	30.72	4.00	0.282	1.330
IV	R–5, R–6	31.14	2.69	0.323	1.653

1,650 x 10^6 cubic feet of river water was present in the stretch between Calais and St. Andrews. A direct comparison between the computed and observed quantities of river water in the St. Croix estuary is given in Figure 11. The agree-

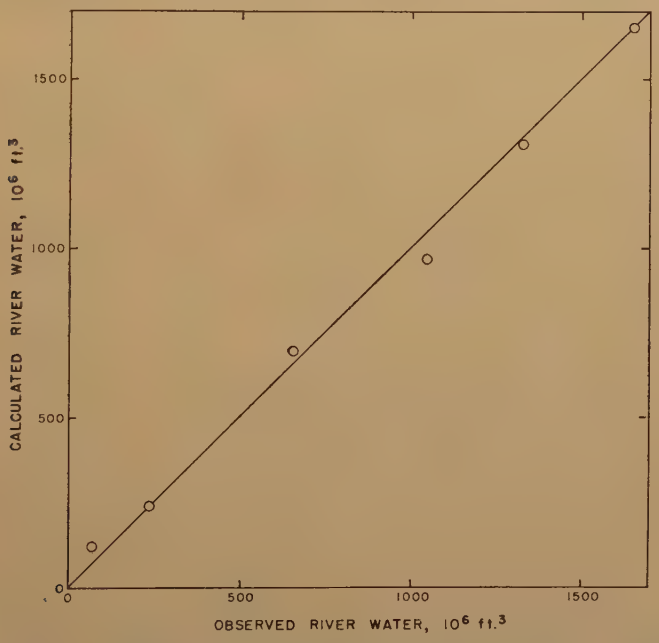

FIGURE 11. Comparison between the observed and the calculated volumes of fresh water in the St. Croix Estuary.

ment between the observed and calculated values indicates that the exchange ratios computed from tidal volumes are adequate to explain the observed distribution.

The flushing times of the various segments range from a little more than one tidal cycle for the segment near Calais, to about three tidal cycles near St. Andrews. For the entire length of the estuary considered, about 15 tides, or 8 days are required, on the average, to replace one day's river flow.

Passamaquoddy Bay

Passamaquoddy Bay proper has been subdivided into volumes bounded by lines drawn at five-minute intervals. The available salinity data have been summarized for the following depth ranges: surface to 25 meters, 25 to 50 meters, and greater than 50 meters. The volume, mean salinity, and percentage of river water for each one of these parts of Passamaquoddy Bay are listed in Table VII.

Table VII. Average salinities and quantities of river water in various segments of Passamaquoddy Bay. (The location of the segments is shown in Figure 10.)

Segment	Depth	Total volume	Mean salinity	River water[a]	River water	Mean flushing time
	meters	$10^9 ft.^3$	‰	%	$10^9 ft.^3$	*days*
A	0–25	12.49	(31.47)	(2.72)	0.34	
	25–50	1.36	(31.65)	(2.16)	0.029	1.98[b]
B	0–25	25.50	31.47	2.72	0.695	
	25–50	3.58	31.65	2.16	0.077	4.15[b]
	> 50	0.01	—	—	—	
D	0–25	35.67	31.235	3.45	1.230	
	25–50	6.49	31.615	2.27	0.147	
	> 50	0.02	—	—	—	3.45[c]
E	0–25	33.65	31.61	2.29	0.77	
	25–50	13.79	32.21	0.43	0.059	4.45[b]
	> 50	1.70	—	—	—	
F	0–25	16.48	31.49	2.66	0.44	
	25–50	10.69	31.72	1.95	0.208	
	> 50	5.20	32.10	0.77	0.039	1.78[c]

[a] Reference salinity 32.35 ‰.
[b] Using river flow of Digdequash and Magaguadavic Rivers (0.186 x 10^9ft.^{3}/day).
[c] Using river flow of Digdequash, Magaguadavic and St. Croix Rivers (0.387 x 10^9ft.^{3}/day).

For the calculations of the percentage of fresh water a base salinity of 32.35 ‰ has been used. This was the average salinity of the water deeper than 25 meters in the channel between Deer Island and Campobello Island. It was assumed that this deep water was the source sea water for mixing inside of Passamaquoddy Bay.

The deep water in the area marked E in Figure 10 was always more saline than any other water within the Bay. This is in agreement with Huntsman's conclusion (personal communication) that the high-salinity water enters Passamaquoddy Bay through Letite Passage.

The total volume of river water within the Bay, exclusive of the St. Croix estuary, was about 4×10^9 ft.^{3}. On the basis of the drainage of the Digdequash and Magaguadavic Rivers alone this corresponds to a mean flushing time of 21.6 days. If, on the other hand, it is assumed that the river flow from the St. Croix becomes uniformly mixed throughout this area, a mean flushing time of about 10 days is obtained.

Inspection of Figure 10 suggests that the St. Croix outflow should be included in the calculations for the areas marked D and F, but should not be included for the others. The calculation has been made in this way in Table VII, and gives a mean flushing time for Passamaquoddy Bay of 15.8 days.

Although it is impossible to determine precisely how the river flow should be utilized in interpreting the circulation in a complex area such as this, it seems probable that a flushing time of about 15 days should be approximately correct.

Exchanges with the Bay of Fundy

It may also be desirable to evaluate the relative discharge from Passamaquoddy Bay through the two main passages. Available current observations are inadequate to provide the necessary information. An approximation can be made, however, from the salinity data provided by Watson (1936). In July, 1932, he made simultaneous observations at high and low, half flood, and half ebb tides, from two boats in the two passages. We have drawn cross-sections of the passages at the location of his station and determined the total cross-sectional area. From the averages of his salinity data it is possible to calculate the mean proportion of fresh water and consequently the part of the cross-sectional area which would be occupied by the fresh water if it were possible to separate it from the salt. The results are presented in Table VIII and show that of the total cross-sectional area of 782,000 square feet in the Western Passage, 0.82 per cent or 6,430 ft.^{2} would be occupied by the fresh water. Similarly, of 209,000 square feet of Letite Passage, 0.99 per cent or 2,070 ft.^{2} were occupied by fresh water. If it is assumed that the transport through the passages is proportional to the quantity of fresh water present, then 75.6 per cent of the river water contributed to Passamaquoddy Bay escapes through the Western Passage, and 24.4 per cent escapes through Letite Passage. It should be recognized that this assumption implies that the non-tidal drift through the two passages is equal. There are no data to substantiate this assumption.

From the proportion of fresh water in each cross-section the total volume of water which must escape in order to discharge one river flow during a complete tidal cycle is given by:

$$E = 100R/F$$

in which E is the total volume of water escaping each tidal cycle, R is the volume

TABLE VIII. Transport of water through the passages into Passamaquoddy Bay in July, 1932, when the total river flow was 2,932 ft.^{3}/sec., or 131 $\times$ 10^6ft.^{3} per tidal cycle.

	LOCATION OF SECTIONS			
	Western Passage		Letite Pass.	E. Quoddy Head
	Inner end	Outer end	Inner end	to Muscabin Point
Area of section (A) 10^4ft.^{2}	7.82	49.3	20.9	506
Fresh water (F) %	0.82	0.23	0.99	0.17
Area fresh $\left(\frac{AxF}{100}\right)$ 10^4ft.^{2}	0.643	0.112	0.207	0.96
River flow (R) 10^6ft.^{3}/tidal cycle	99	99	32	131
Escaping volume $\left(E = \frac{100R}{F}\right)$ 10^6ft.^{3}/T.C.	12,100	43,000	3,200	77,000
Non-tidal drift $\left(E\right)$ 10^3ft./T.C.	15.5	55.2	15.5	15.2

of river water exchanged per tidal cycle, and F is the mean per cent of fresh water in the mixture (Hachey, 1935; Ketchum, 1951). These calculations have been made for the inner ends of the passages, for a station near the outer end of the Western Passage, and for a cross-section running from East Quoddy Head to Muscabin Point. For the inner end of Western Passage the escaping volume of mixed water is 122 times as great as the river flow. This increases almost four-fold within the Passage so that at the southern end the escaping volume is 435 times the river flow. In Letite Passage the escaping volume is 100 times the river flow. The combined volume of fresh water discharged through both passages must also escape through the section running between East Quoddy Head and Muscabin Point. Here the entrained sea water is 588 times the river-flow volume. Using the average river flow for July, 1932, as given by Watson, the corresponding volumes of mixed water range from 12 x 10^9 to 77 x 10^9ft.^{3} per tidal cycle (270,000 to 1,720,000 ft.^{3}/sec.). These results are included in the data given in Table VIII.

The non-tidal drift of the water results from inequalities of either the duration or velocity of flood and ebb currents. The non-tidal drift must be sufficient to remove the fresh water added by the rivers during a tidal cycle. It has been mentioned that the assumption concerning the proportion of water moving through each passage imposes the condition that the non-tidal drifts be equal. The computed rate of this drift is 15,500 ft., or about 2.5 miles per tidal cycle of 12.4 hours. It is interesting that the non-tidal drift for the section between East Quoddy Head and Muscabin Point, through which all of the water must pass, is nearly equal to that calculated for the inner ends of the two passages. At the outer end of the Western Passage the computed rate of non-tidal drift is much greater. This is necessary to remove the large volume of sea water which becomes

entrained in the flow within the Passage. The velocities of the tidal currents show a similar increase. The maximum velocity for mean tides near the inner end of the Passage is 1.9 knots, while the comparable value for the velocity at the outer end is 3.1 knots (United States Coast and Geodetic Survey).

Discussion

The same general comments which were made in the discussion of the Bay of Fundy data (page 113) apply to the St. Croix estuary and Passamaquoddy Bay. The observation that about eight days are required on the average to exchange the water within the St. Croix estuary between Calais and St. Andrews, and that an additional 16 days are required for the exchange of water in Passamaquoddy Bay may aid in the interpretation of the interesting distributions of biological populations in these areas.

The major uncertainty in this area appears to be the actual quantities of water exchanged through the various passages between Passamaquoddy Bay and the Bay of Fundy. The conclusions we have drawn concerning this process are based upon assumptions which it is impossible to check with the available data. It seems clear, however, that the mixing in the Western Passage of Passamaquoddy Bay is very vigorous, since in traversing a little over two miles of this Passage this water becomes mixed with about four times its own volume of sea water. This is in agreement with observable hydrographic conditions, since this is a region of rapid tidal flow, and boils and whirlpools are frequently observed which indicate locations where active admixture of deep water is taking place. It would be very desirable to have complete series of current measurements and samples to determine the salinity of the water in each of the two main passages. From such data the actual transports, and the proportion of river water escaping through the two passes could be determined.

REFERENCES

Bigelow, Henry B. 1927. Physical oceanography of the Gulf of Maine. *Bull. U.S. Bur. Fish.*, **40**, 511–1027.

Copeland, G. G. 1909. The temperatures and densities and other subjects of Passamaquoddy Bay and its environs. Their bearing on the oyster industry. *Cont. Canad. Biol., 1906–1910*, No. 18, 281–294.

Craigie, E. Horne, 1916. Hydrographic investigations in the St. Croix River and Passamaquoddy Bay in 1914. *Cont. Canad. Biol., 1914–1915*, No. 15, 151–161.

Dawson, Bell. 1917. Tides at the head of the Bay of Fundy. Ottawa, 34 pp.

1908. Tables of hourly direction and velocity of currents and time of slack water in the Bay of Fundy and its approaches. Ottawa, 15 pp.

Fish, C. J., and Johnson, M. W. 1937. The biology of the zooplankton population in the Bay of Fundy and Gulf of Maine with special reference to production and distribution. *J. Biol. Bd. Canada*, **3**, 189–322.

Hachey, H. B. 1931. The general hydrography of the waters of the Bay of Fundy. MS Report No. 389, Atlantic Biol. Sta., St. Andrews, N.B. (unpublished).

1934. The replacement of the Bay of Fundy waters. *J. Biol. Bd. Canada*, **1**, 121–131.

1934a. Movements resulting from mixing of stratified waters. *Ibid.*, 133–143.

1935. Tidal mixing in an estuary. *Ibid.*, 171–178.

KETCHUM, B. H. 1950. Hydrographic factors involved in the dispersion of pollutants introduced into tidal waters. *J. Boston Soc. Civil Eng.*, **37**, 296–314.

1951. The flushing of tidal estuaries. *Sewage and Ind. Wastes*, **23**, 198-209.

1951a. The exchanges of fresh and salt waters in tidal estuaries. *J. Mar. Res.*, **10**, 18–38.

1952. Relation between the circulation and planktonic populations in estuaries. (Ined.).

KETCHUM, B. H., J. C. AYERS, and R. F. VACCARO. 1952. Processes contributing to the decrease of coliform bacteria in a tidal estuary. *Ecology* **33**, 247–258.

KETCHUM, B. H., A. C. REDFIELD, and J. C. AYERS. 1951. The oceanography of the New York Bight. *Pap. Phys. Oceanog. and Meteorol.*, **12** (1), 46 pp.

MARMER, H. A. 1926. The Tide, New York; D. Appleton, 282 pp.

MAVOR, J. W. 1922. The circulation of the water in the Bay of Fundy, Part I. Introduction and drift bottle experiments. *Cont. Can. Biol.*, N.S. **1**, 103–124.

1923. The circulation of the water in the Bay of Fundy, Part II. The distribution of temperature, salinity and density in 1919, and the movements of the waters which they indicate in the Bay of Fundy. *Ibid.*, 355–375.

MACGREGOR, D. G. and H. J. MCLELLAN. 1951. Current measurements in Grand Manan Channel. MS Report, Atlantic Oceanographic Group, St. Andrews, N.B. (unpublished).

MCLELLAN, H. J. 1951. A survey of water conditions in the Grand Manan Channel in September, 1950. MS Report, Atlantic Oceanographic Group, St. Andrews, N.B. (unpublished).

REDFIELD, A. C. 1950. The analysis of tidal phenomena in narrow embayments. *Pap. Phys. Oceanog. and Meteorol.*, **11** (4), 36 pp.

TULLY, J. 1949. Oceanography and prediction of pulp mill pollution in Alberni Inlet. *Bull. Fish. Res. Board Canada, No.* **83**, 169 pp.

U.S. Coast and Geodetic Survey, Current Tables, revised annually.

U.S. Navy Dept., HO99, 1939. Sailing directions for Nova Scotia.

WATSON, E. E. 1936. Mixing and residual currents in tidal waters, as illustrated in the Bay of Fundy. *J. Biol. Bd. Canada*, **2** (2), 141–208.

APPENDIX

Salinities and Temperatures in the St. Croix Estuary, August, 1951.

Date	Station	Location	Time after HW, ref. St. Andrews		Depth	Salinity	Temp.
			hours	*min.*	*meters*	‰	°C.
Aug. 15	R–1	45°11.1′N		33[a]	0	1.19	20.56
		67°15.6′W			5	24.38	15.00
Aug. 15	R–2	45°09.7′N		48[a]	0	14.11	
		67°13.6′W			4	27.36	
					9	28.35	
					14	29.38	
Aug. 15	R–3	45°09.7′N	1	33[a]	0	24.07	16.67
		67°09.5′W			4	28.49	14.56
					9	30.55	13.33
					14	30.91	13.29
Aug. 15	R–3	45°09.7′N	4	53	0	23.26	16.67
		67°09.5′W			5	27.65	14.80
					15	29.94	13.89
Aug. 15	R–3a	45°11.6′N	3	08[a]	0	26.94	16.50
		67°10.0′W			5	28.46	14.39
					10	29.92	14.10
					14	29.90	14.00
Aug. 15	R–3b	45°10.9′N	2	28	0	28.26	15.28
		67°08.7′W			5	28.37	14.85
Aug. 15	R–4	45°07.9′N	5	38	0	25.41	16.67
		67°07.6′W			5	28.59	13.85
					10	30.61	13.61
					15	30.75	13.57
					25	30.90	13.47
Aug. 21	R–4	45°07.9′N		19[a]	0	29.88	15.00
		67°07.6′W			5	29.83	14.05
					10	30.41	13.67
					20	30.97	13.42
					30	31.20	13.28
Aug. 21	R–4a	45°06.4′N		46[a]	0	30.30	14.44
		67°06.6′W			5	30.57	13.86
					10	30.79	13.47
					20	31.06	12.94
					25	31.44	12.89
Aug. 15	R–5	45°04.9′N	6	08	0	28.01	15.56
		67°06.0′W			5	29.51	13.75
					10	30.70	13.33
					15	31.15	13.16
					25	31.53	13.11
Aug. 21	R–5	45°04.9′N	1	11[a]	0	30.93	13.89
		67°06.0′W			5	31.08	13.44
					10	31.13	13.29
					20	31.33	12.96
					25	31.46	12.83

[a]Data used to calculate accumulation of river water in the St. Croix Estuary.

Salinities and Temperatures in the St. Croix Estuary, August, 1951 (continued).

Date	Station	Location	Time after HW, ref. St. Andrews		Depth	Salinity	Temp.
			hours	*min.*	*meters*	‰	°C.
Aug. 21	R–6	45°03.5′N	1	41[a]	0	30.62	14.17
		67°05.4′W			5	30.73	13.97
					10	30.90	13.42
					15	31.04	13.22
					25	31.51	12.91
Aug. 21	R–7	45°01.2′N	2	16	0	30.39	14.44
		67°03.2′W			5	30.41	13.36
					10	31.22	12.92
					20	31.60	12.86
					30	31.58	12.83
Aug. 17	DR–1	45°10.5′N		03	0	15.44	15.56
		66°57.7′W			5	28.69	13.97
Aug. 17	DR–2	45°09.5′N		18	0	28.82	14.56
		66°57.9′W			2.5	28.82	14.18
					7.5	31.15	13.28
Aug. 17	DR–3	45°08.8′N		43	0	29.09	14.17
		66°57.9′W			5	29.54	13.41
					10	31.24	13.21
					15	31.36	13.07
Aug. 17	DR–4	45°08.1′N	1	04	0	29.83	14.33
		66°57.3′W			5	29.85	13.47
					10	31.26	13.17
					15	31.46	13.06

[a]Data used to calculate accumulation of river water in the St. Croix Estuary.

Contribution No. 596

Bulletin of the Museum of Comparative Zoology

AT HARVARD COLLEGE

Vol. 109, No. 3

NEW AND LITTLE KNOWN SHARKS FROM THE ATLANTIC AND FROM THE GULF OF MEXICO

By

Henry B. Bigelow, William C. Schroeder
and Stewart Springer

CAMBRIDGE, MASS., U.S.A.

PRINTED FOR THE MUSEUM

July, 1953

No. 3. — *New and Little Known Sharks from the Atlantic and from the Gulf of Mexico*[1]

By

Henry B. Bigelow, William C. Schroeder
and Stewart Springer

Experimental trawlings in which we took part, were carried on in the northern sector of the Gulf of Mexico, by "Oregon" of the U. S. Fish and Wildlife Service, 1950–1952, and on the continental slope off southern New England, by the dragger "Cap'n Bill II" chartered by Woods Hole Oceanographic Institution, during the summer of 1952. These have brought to light three sharks of the genera *Etmopterus* and *Scymnodon* which appear to represent species new to science, as do a series, contributed by Dr. Max Poll, of the *Etmopterus* recently reported by him (Poll, 1951) from tropical West Africa, as *E. hillianus*. The "Oregon" and "Cap'n Bill II" trawlings have also yielded specimens of *Apristurus atlanticus*, of *Squalus fernandinus* and of *Centrophorus uyato*, none of which had been recorded previously from the western side of the North Atlantic; also series of *Apristurus profundorum* and of *Scyliorhinus retifer* that add to knowledge of those species.

Myers (1952, p. 108) has recently emphasized the desirability of including a statement of the problem in hand in papers on systematic biology. Thinking the point well taken, we may add that the following pages continue the attempt, on which we have long been engaged, to learn what kinds of elasmobranch fishes exist today, where they live, and how they live.

All the drawings in this paper are by H. B. Bigelow and Jessie H. Sawyer.

Family SCYLIORHINIDAE

Genus Scyliorhinus

Scyliorhinus retifer (Garman) 1881

Previous locality records for positively identified specimens of the chain dogfish had been confined to the outer edge of the continental shelf and upper part of the slope, between the offings of Cape Lookout, North Carolina, and of New York, at depths of 40–125 fathoms (Bigelow and Schroeder, 1948, p. 210). Recent captures by "Oregon" and by the draggers "Eugene H" and "Cap'n Bill II" in 1950, 1951 and 1952 extend the known range of the species to the northern part of the Gulf of Mexico in the one direction and to the offing of southern

[1] Contribution No. 596, Woods Hole Oceanographic Institution.

New England and to the southwestern edge of Georges Bank (Lat. 40°02′N, Long. 69°37′W) in the other. The greatest depth from which *retifer* has yet been recorded in the northern part of its range is 125 fathoms; it ranges deeper, however, in the Gulf of Mexico, where "Oregon" trawled it at 240–260 fathoms.

Genus APRISTURUS

Examination of a Gulf of Mexico specimen of *Apristurus* apparently referable to *A. atlanticus* Koefoed 1932, known only from off Morocco previously, and of six specimens of *A. profundorum* that were trawled on the continental slope off southern New England by "Cap'n Bill II" during the summer of 1952, enable us to offer a key to the North Atlantic species of the genus, more satisfactory than our earlier attempt (Bigelow and Schroeder, 1948, p. 221).

Key to North Atlantic species of *Apristurus*

1. First to third gill openings nearly as long as distance between inner ends of nostrils; upper and lower labial furrows form about a right angle at each corner of mouth ..... *riveri* Bigelow and Schroeder, 1944
   North coast of Cuba

   First to third gill openings less than half as long as distance between nostrils; upper labial furrow forms an acute angle of about 45° with lower labial furrow at each corner of mouth 2
2. Origin of anal fin under or behind rear end of base of first dorsal; origin of first dorsal fin is above rear part of bases of pelvic fins; base of anal fin only about 2 to 2½ times as long as base of first dorsal fin.....
   profundorum (Goode and Bean) 1895, p. 00

   Origin of anal fin about under origin of first dorsal; origin of first dorsal fin is opposite or behind rear end of bases of pelvic fins; base of anal fin is very nearly 4 times as long as base of first dorsal fin.....
   atlanticus (Koefoed) 1932, p. 00

APRISTURUS PROFUNDORUM (Goode and Bean) 1895

Two specimens, only, of this deep water scyliorhinid had been reported previously from the western side of the North Atlantic, both of them taken off Delaware Bay (the type locality) by the "Albatross" many years ago, and both of them in damaged condition when we saw them (Bigelow and Schroeder, 1948, p. 222, Fig. 38). We can now

report eight more, 113 mm. to 596 mm. long, trawled by the dragger "Cap'n Bill II" along the continental slope from southeast of Nova Scotia to southern New England between Lats. 42°39′ and 39°46′N, and between Longs. 63°54′ and 71°35′W, at 395-530 fathoms during June and July, 1952. This additional material allows us to amend our earlier account in the following respects.

A. Relative sizes of first and second dorsal fins: On the type specimen (this was pictured by us earlier) the base of the second dorsal fin is about as long as the base of the first dorsal, with the second dorsal a very little larger in area than the first dorsal. And since the second dorsal is definitely the larger of the pair on a newly hatched specimen, we had regarded this as a juvenile character. But the present series shows that the relative areas of these fins in *profundorum* is subject to considerable variation from specimen to specimen, irrespective of size, the transverse breadths of the first and second dorsals, measured at the rear end of the base, being as follows for six of the "Cap'n Bill II" specimens of different sizes.

total length	*breadth of 1st dorsal*	*breadth of 2nd dorsal*	*ratio of breadth 2nd dorsal to 1st dorsal*
mm.	*mm.*	*mm.*	
596	17.5	18	1.0
514	14.5	17	1.2
267	8	10	1.3
258	7.5	9	1.2
254	7	8	1.1
232	6.5	9	1.4
113	4	4.8	1.2

B. Length of caudal fin: The percentage of the total length that is occupied by the caudal fin is as follows for seven specimens of different sizes: 113 mm., 30%; 146 mm., 25%; 232 mm., 33.6%; 254 mm., 32.3%; 267 mm., 30.7%; 510 mm. (the type[2]) 25%; 514 mm., 25%. Evidently the variation in the relative length of the caudal does not depend on the size of the individual.

C. Lengths of gill openings: The relationship between the length of the third gill opening and the distance between the nostrils is as follows for the specimens listed under *A*.

[2] The 146 mm. specimen, U. S. National Museum, No. 83894, was measured by us earlier; for measurements of the type, of 510 mm., No. 35646, see Bigelow and Schroeder, 1948, p. 222.

total length	*length 3rd gill opening*	*distance between nostrils*	*ratio, distance between nostrils to length of 3rd gill opening*
mm.	*mm.*	*mm.*	
596	7	22.5	3.2
514	6	21	3.5
267	3.2	10.5	3.3
258	4.5	11	2.4
254	3.5	10.5	3
232	3	11	3.7
113	2	4.5	2.3

The resultant ratios of 2.3 to 3.7 for the gill lengths *vs.* the internarial distance indicate that an appreciable variation exists in these proportions irrespective of the size of the shark.

D. Labial furrows: The upper and lower labial furrows make an angle of about 45° at each corner of the mouth in all of the "Cap'n Bill II" specimens. This is a matter of interest because of the difference in this respect between *A. profundorum* and *A. riveri,* which is employed as an alternative character in the preceding Key to Species (p. 214).

E. Relationship between horizontal diameter of eye and distance between the nostrils:

total length	*diameter of eye*	*distance between nostrils*	*ratio, distance between nostrils to diameter of eye*
mm.	*mm.*	*mm.*	
596	19.5	23	1.2
514	15	21	1.4
267	7	11	1.6
258	8	11	1.4
254	7	10.5	1.5
232	7	11	1.6
113	5	4	0.8

Thus, there appears to be no trend in the ratio of these proportions as between young and grown specimens although in the new born one (113 mm.) the eye is relatively much larger, as would be expected.

F. Teeth: The number of teeth in the 596 mm. specimen is $\frac{40\text{-}40}{41\text{-}41}$, the outermost in each jaw being difficult to count; this contrasts with $\frac{25\text{-}25}{25\text{-}25}$ recorded for the type specimen, of 510 mm. Both the uppers and the lowers agree closely with our earlier account of those of the type

specimen (Bigelow and Schroeder, 1948, p. 223).

Proportional dimensions in per cent of total length of female, 596 mm. long from Lat. 39°46′N., Long. 71°35′W., 395–405 fathoms, and of male, of 254 mm. long from Lat. 39°52′N., Long. 70°43′W., 415–440 fathoms. Museum of Comparative Zoology Nos. 37425 and 37416, respectively.

Trunk at origin of pectoral: breadth 9.2, 9.5; height 8.4, 8.3.
Snout: length in front of mouth 10.2, 11.8.
Eye: horizontal diameter 3.2, 3.7.
Mouth: breadth 6.9, 5.5.
Nostrils: distance between inner ends 3.8, 4.1.
Labial furrow lengths: upper 3.9, 3.1; lower 2.7, 2.5.
Gill opening lengths: 1st 1.2, 1.2; 3rd 1.2, 1.4; 5th 1.2, 1.4.
First dorsal fin: vertical height 2.8, 2.8; length of base 7.0, 5.9.
Second dorsal fin: vertical height 3.5, 3.3; length of base 6.1, 6.7.
Anal fin: length of base 14.9, 15.0.
Caudal fin: upper margin 25.0, 32.3; lower anterior margin 12.9, 11.8.
Pectoral fin: outer margin 11.9, 11.8; inner margin 5.4, 6.3; width 7.5, 6.3.
Distance from snout to: 1st dorsal 51.2, 44.8; 2nd dorsal 66.2, 57.2; upper caudal 75.0, 67.7; pectoral 22.8, 27.5; pelvics 46.0, 42.9; anal 59.2, 52.7.
Interspace between: 1st and 2nd dorsals 8.0, 6.3; 2nd dorsal and caudal 2.7, 4.0; anal and caudal 0.0, 0.0.
Distance from origin to origin of: pectorals to pelvics 23.1, 15.3; pelvics to anal 13.2, 9.8.

Range. A. profundorum is now known from the continental slope off Delaware Bay (type locality), off southern New England and off the southern part of Georges Bank and the offing of Cape Sable, Nova Scotia at 395–530 fathoms; also off the coast of Iceland, if we are correct in our view that the *Scyllium laurussonii* of Saemundsson (1922, p. 173, Pl. 4, fig. 1) cannot be distinguished from *profundorum.*

Apristurus atlanticus (Koefoed) 1932
Figure 1

This species had been known only from the type specimen 247 mm. long, trawled by the "Michael Sars" off the coast of Morocco, Lat. 28°8′N, Long. 13°35′W from 1365 meters (Koefoed 1932, p. 18,

Pl. 3, fig. 3). We can now report a second specimen, from the northern part of the Gulf of Mexico, which agrees with *atlanticus* in all the features that seem likely to be of specific importance in *Apristurus*. Consequently we refer it to that species, though with some reservation, for Koefoed's original account does not include any information as to shape of nostrils, as to labial furrows, teeth, or dermal denticles; or as to color other than that dark appears to be implied.

Description. Female, 297 mm. long, northern part of Gulf of Mexico, Lat. 27°32′N., Long. 93°02′W., 400–450 fathoms, "Oregon" Station 534, April 11, 1952.

Proportional dimensions in per cent of total length.

Trunk at origin of pectoral: breadth 11.1; height 9.5.

Snout: length in front of mouth 11.5.

Eye: horizontal diameter 3.4.

Mouth: breadth 7.8.

Nostrils: distance between inner ends 4.5.

Labial furrow lengths: upper 2.2; lower 1.9.

Gill opening lengths: 1st 1.2; 3rd 1.2; 5th 1.2.

First dorsal fin: vertical height 2.7; length of base 4.4.

Second dorsal fin: vertical height 3.4; length of base 5.7.

Anal fin: length of base 16.5

Caudal fin: upper margin 28.5; lower anterior margin 11.1.

Pectoral fin: outer margin 11.8; inner margin 6.4; distal margin 10.8.

Distance from snout to: 1st dorsal 51; 2nd dorsal 62; upper caudal 71.5; pectoral 24.6; pelvics 40.5; anal 51.6.

Interspace between: 1st and 2nd dorsals 6.7; 2nd dorsal and caudal 3.7.

Distance from origin to origin of: pectorals to pelvics 16.8; pelvics to anal 10.4.

Trunk, noticeably soft, about ⅛ as high opposite pectorals (where highest) as it is long to origin of caudal fin; somewhat broader there than high, but compressed, thence rearward, so that the caudal peduncle is only about 3/7 as broad as it is high. Dorsal profile sloping gently forward from shoulder region to rather thin-tipped and very flexible snout. Snout ovoid anteriorly, its length to mouth a little less than ½ of head (47%) to origins of pectorals. Eye oval, its horizontal diameter a little less than ⅓ as long as snout in front of mouth (30%). Spiracle between ¼ and ⅕ (22%) as long as eye; close behind eye and about level with the longitudinal axis of eye. Nostrils about 1.4 times

as long as eye, their outer ends at outer edge of head; anterior nasal flap broadly triangular with blunted tip; distance from tip of snout to level of outer (anterior) ends of nostrils about ½ as long as length of snout to mouth; and distance between inner ends of nostrils about 40 per cent as great as length of snout to mouth. Mouth moderately arched, the gape occupying about 70 per cent of breadth of head. Upper labial furrow about ¾ as long as distance between inner ends of nostrils; lower labial furrow about ⅔ as long as upper; the upper and lower labial furrows making an acute angle of about 45° at corner of mouth.

Anterior margins of gill openings concave, but not enough so as to expose the tips of the gill filaments; the longest (4th) about 40 per cent as long as eye, and about 30 per cent as long as distance between nostrils. Teeth $\frac{35\text{-}35}{31\text{-}31}$ in specimens seen; uppers and lowers similar, those along central ⅔ of mouth mostly with 5 or 7 cusps, but those near outer corners of mouth with 3–5 cusps; the median cusp longest and curved slightly outward in most cases, the lateral cusps graduated in length, nearly straight, and radiating outward; about 4 rows of teeth in function simultaneously in each jaw. Dermal denticles minute, clothing the trunk closely and the fins out nearly to margins; the denticles rising steeply from skin over trunk as a whole; leaflike, the blades without evident sculpture, their margins tridentate, those on lower surface of snout with shorter median tooth than those on back, sides, and belly.

First dorsal fin rounded, of shape shown in Figure 1; its base about 1.3 times as long as eye, its origin about 70 per cent of distance rearward from snout toward origin of caudal, and about over origin of anal. Distance from rear end of base of first dorsal to origin of second dorsal about twice as long as eye and about 1½ times as long as base of first dorsal. Second dorsal similar in shape to first; its base about 1.3 times as long as base of first; its length from mid point of base to tip about 1½ times as great as length of first dorsal, similarly measured; its origin about over mid point of base of anal. Distance from rear end of base of second dorsal to origin of caudal a little less than ⅔ (65%) as long as base of second dorsal. Caudal about 1.2 times as long as head to origin of pectorals; upper margin nearly straight; tip rounded — truncate, with moderate subterminal excavation; lower posterior margin slightly sinuous, forming a blunted angle of about 115° with lower anterior margin; the latter being weakly convex.

Anal trapezoid in shape, anterior margin weakly convex; distal margin nearly straight; base nearly three times (2.9) as long as base of second dorsal; origin about under origin of first dorsal. No measurable interspace between rear end of base of anal and origin of lower side of caudal fin. Pelvics rhomboid; the margins nearly straight, the corners rounded; outer margin about 2½ times as long as anterior margin; base about 60 per cent as long as base of anal; interspace between rear end of base of pelvics and origin of anal about ⅕ as long as base of anal. Distance between origin of pelvics and axils of pectorals about 1.1 times as long as base of pelvics (in female). Pectorals with broadly rounded corners and weakly convex margins, of shape shown in Figure 1. Extreme length of pectoral from point of origin, about as great as distance from front of eye to pelvic origin; the fin conspicuously broad based, the base being about as long as maximum breadth of pectoral fin.

Color. The "Oregon" specimen is uniformly dark sooty gray, after preservation in alcohol, both on trunk and on fins out to their margins, and about as dark below as above. The type specimen is described as "brown" (Koefoed, 1932, p. 19).

Size. The two specimens that have been seen are respectively 247 mm. (the type) and 297 mm. ("Oregon" specimen) long; but as both are females their sizes give no clue to how large this shark may grow.

Remarks. A. atlanticus resembles *A. profundorum* very closely in its general appearance. But the differences between the two listed in the preceding key (p. 214) are so sharp-cut that identification of any given specimen of *Apristurus* of this general type as the one species or as the other should present no special difficulty.

Range. Present indications are that *atlanticus* is restricted to the tropical-subtropical belt of the Atlantic, east and west, including the Gulf of Mexico, localities of record for it being off the coast of Morocco[3], and the northern part of the Gulf of Mexico at the locality listed above, (p. 218) at depths of 746 fathoms and 400–450 fathoms respectively. Nothing is known about its habits.

Family SQUALIDAE

Genus SQUALUS

SQUALUS FERNANDINUS Molina 1782

Figure 2

The only members of this well known genus that have been reported

[3] "Michael Sars" N. Atlant. Exped. 1910, Sta. 41.

reliably from the western side of the Atlantic, north of the equator, or from the Gulf of Mexico, are the common spiny dog (*Squalus acanthias* Linnaeus 1758) of northern seas, and the Cuban dog (*Squalus cubensis* Howell-Rivero 1936). But word was to be expected, sooner or later, of spiny dogfishes of the *fernandinus-blainville* group somewhere along our South Atlantic coasts, or in the Gulf of Mexico, for these little sharks are common not only in the Mediterranean but along tropical West Africa as well.[4] And we can now report the captures of two small specimens of this group off South Carolina (Lat. 33°00′N, Long. 77°07′W), by "Albatross" III of the U. S. Fish and Wildlife Service, in a trawl haul from 206 fathoms, and of a third (a female of 640 mm.) trawled by "Oregon" in the northern part of the Gulf of Mexico, Lat. 27°44′N, Long. 85°02′W, at 215 fathoms, September 29, 1951; "Oregon" Sta. 490.

Comparison has failed to show anything to differentiate these specimens, as to species, from an excellent female of *fernandinus*, of 914 mm., in the Museum of Comparative Zoology, from the island of Juan Fernandez, which is the type locality of the species.[5] The only other reliable record for a shark of the *fernandinus-blainville* group, for the western side of the Atlantic, north or south, is for a 320 mm. specimen that was taken from the stomach of an albatross off the coast of Argentina, Lat. 34°44′S, Long. 53°W (Lahille, 1928, p. 327; Bigelow and Schroeder, 1948, p. 479, Footnote 65).

Among the North Atlantic members of its genus, *fernandinus* differs from *acanthias* in that the exposed base of its first dorsal fin spine stands about even with the inner corner of the pectoral or a little anterior to it, when the fin is laid back (considerably posterior to the inner corner of the pectoral in *acanthias*); that the mid points of the bases of the pelvics are about opposite the mid point of the interspace between the two dorsals (Fig. 2; much nearer the second dorsal than the first dorsal in *acanthias*); and that the flap-like expansion of the anterior (inner) margin of the nostril bears a small accessory lobe. *Fernandinus* agrees with *cubensis* in the foregoing respects. But there should be no danger of confusing the one species with the other, for the distal margin of the pectoral is only weakly concave in *fernandinus*, and the inner corner of the fin rounded, whereas the distal pectoral

[4] Poll (1951, p. 59) reports *fernandinus* at 19 stations along the West African coast between latitudes 9°32′N, and 19°52′S.

[5] For an illustration of this Juan Fernandez specimen, see Bigelow and Schroeder, 1948, p. 456, Fig. 87E.

margin is deeply concave and the inner pectoral corner sharp-pointed in *cubensis*.

In our earlier discussion of the species of the genus *Squalus* (Bigelow and Schroeder, 1948, p. 454, 455) we retained *blainville* Risso 1826 of the Mediterranean provisionally, as distinct from *fernandinus*, because perhaps it has a relatively longer second dorsal spine than that of *fernandinus*, and a larger eye relative to the length of the snout and relative to the distance between the nostrils. But it appears that the second dorsal spine may vary considerably in length in the Mediterranean form, for while Rey (1928, p. 43) writes that it may exceed the length of the anterior margin of the fin in *blainville*, his excellent illustration of the latter (Rey, 1928, Pl. 4, Fig. 2), which we had overlooked, pictures its tip as falling about as far short of the apex of the fin as is the case in our Gulf of Mexico specimen of *fernandinus*, and almost as far short of the apex of the fin as in the Juan Fernandez specimen.[6] Neither does it seem likely that the size of the eye relative to the length of the snout in front of the mouth (horizontal diameter of eye about 60 per cent as long as snout in *blainville*, *vs.* 40–50 per cent in *fernandinus*[7]) can be used as the basis of specific separation. Poll's (1951, p. 59) definite reference of *blainville* to the synonymy of *fernandinus* seems, therefore, to be correct.

Squalus cubensis Howell-Rivero 1936

The Cuban dogfish, made easily recognizable among North Atlantic spiny dogs of the genus *Squalus* by the sharply pointed inner corner of its pectoral fin, was known only from the north coast of Cuba, from Trinidad (probably), and from Rio de Janeiro (Bigelow and Schroeder, 1948, p. 477). We can now report it from the northern part of the Gulf of Mexico, when "Oregon" trawled two specimens, 375 and 465 mm. long, one at Station 257, Lat. 28°41′N, Long. 86°03′W, on January 27, 1951, 165 fathoms; the other at Station 278, Lat. 29°49′N, Long. 85°45′W, 112 fathoms on February 24, 1951. The geographic distribution of the locality records for this species suggests that it will prove to be widespread throughout the West Indian, Gulf, and Caribbean regions, and along the northern and northeastern coasts of South America.

[6] In the Juan Fernandez specimen the spine, measured from the level at which it emerges from the skin, is about 77 per cent as long as the free anterior margin of the fin. Our earlier illustration (Bigelow and Schroeder, 1948, Fig. 87E) pictures it as too short.

[7] In our Western Atlantic and Gulf of Mexico specimens, the varietal range in this respect is from 40 to 50 per cent. In the Juan Fernandez specimen it is 48 per cent, stated erroneously as 40 per cent in alternative 3B of our earlier key to the Western Atlantic species of *Squalus*. (Bigelow and Schroeder, 1948, p. 455.)

Genus CENTROPHORUS Müller & Henle 1837

The genus *Centrophorus* was proposed by Müller and Henle (1837, p. 398) for a squalid shark identified by them as the *Squalus granulosus* of Bloch and Schneider 1801, of which Müller and Henle published a detailed account with illustrations four years later (1841, p. 88, Pl. 33), based in part on a dried specimen from Bloch's collection, as well as on other specimens from Sicily. Its most distinctive characters, among squalid sharks, are: upper and lower teeth both one-cusped, but unlike in the two jaws, the cusps of the lowers being blade-like and directed sharply outward along each half of the jaw, the cusps of the uppers more narrowly triangular to awl shaped along the median section of the jaw, but more nearly similar to the lowers toward each corner of the mouth; dorsal fin spines lying along anterior margins of the fins, the second longer than the first, and both of them at least moderately prominent; both the dorsal fins short, neither member of the pair much larger than the other; pectoral fins with the inner corner sharp pointed and considerably extended. And the passage of time has added nothing to make us doubt the validity of the foregoing set of characters as distinctive of the genus *Centrophorus*. Garman (1913, pp. 189, 211), it is true, abandoning the shape of the pectorals as a primary generic character, retained the genus *Lepidorhinus* Bonaparte 1838, not only for the reception of its type species, *Squalus squamosus* Bonnaterre 1788, but also for *Centrophorus steindachneri* Pietschmann 1907,[8] both of which fall in *Centrophorus* as defined here because the pectoral corners of each are sharp pointed though only slightly extended. Garman also placed *Centrophorus foliaceus* Günther 1877 and *Centrophorus rossi* Alcock 1898 in *Lepidorhinus* but both of these fall in the genus *Scymnodon* in our view, because with rounded inner pectoral corners (p. 230). But to abandon the shape of the pectorals as a primary generic character is to ignore the most conspicuous feature by which we can subdivide the considerable group of squaloids that agree in having one-cusped blade like teeth in both jaws and simple, dermal denticles.

The species in question with the inner corners of the pectorals more or less produced, have been redistributed more recently by Fowler (1941, p. 229, 242) between *Centrophorus* Müller and Henle 1837, and *Entoxychirus* Gill 1862. But, as we have already remarked (1948, p. 451, footnote 8), "the differences on which this division is based, i.e., the relative degrees to which the inner corners of the pectorals

[8] For a good illustration of *steindachneri*, see Pietschmann, 1908, Pl. 1, fig. 1.

are produced and the shapes of the dermal denticles, do not seem to us sufficient for generic separation."

Sharks, referable to *Centrophorus* as defined here, that have been named from the North Atlantic and Mediterranean, are *Squalus squamosus* Bonnaterre 1788; *S. granulosus* Bloch and Schneider 1801 (discussed above); *Galeus* [*Squalus*] *uyato* Rafinesque 1810; *Centrophorus lusitanicus* Bocage and Capello 1864; *Machephilus dumerilii* Johnson 1867; and *Centrophorus braganzae* Regan 1906. The *Squalus infernus* of Blainville 1825 was also placed in *Centrophorus* by Garman (1913, p. 197), as a synonym of *uyato*, perhaps on the strength of Blainville's (1825, p. 60) suggestion that it might be identical with Rafinesque's *uyato*. But Blainville's (1825, p. 59) description of its upper teeth as with a rather long erect, pointed median cusp flanked on either side by a small accessory cusp, combined with his failure to mention the shape of the inner corners of the pectorals, suggest that *infernus* was not a *Centrophorus*.[9] Its tooth characters, as described by Blainville, suggest, rather, an *Etmopterus* (p. 237), but the proportional dimensions given for it by him differ considerably from those of any member of that genus known from the Atlantic.

Garman (1913, pp. 197, 212) was no doubt correct in referring *braganzae* to the synonymy of *uyato*, and *dumerilii* to that of *squamosus*. Rey (1928, p. 436) has reduced the list of accepted species still farther by placing both *lusitanicus* and *uyato* in the synonymy of *granulosus*. And while Nobre (1935, p. 449)[10] has revived *lusitanicus* as a distinct species, Rey's treatment of it seems to be preferable, so far as we can judge from Bocage and Capello's (1864, p. 260, fig. 1) original description and illustration of it. *C. squamosus* (Bonnaterre) 1788, differs both from *granulosus* and from *uyato* in the shape of its pectoral fins, in a relatively larger second dorsal fin relative to the first dorsal, and also in its dermal denticles (see below).

The status of *uyato*, if perhaps more puzzling, is the most pertinent to our present study. The original account and illustration of it, by Rafinesque (1810, p. 13, Pl. 14, fig. 2) tell us only that it resembles *Squalus* in general, but has minute, sharp teeth, and that the inner corners of the pectorals are somewhat extended, and angular. About all we learn from the brief first-hand accounts that have appeared since Rafinesque's time is that the eastern Atlantic in low and mid latitudes and the Mediterranean do harbor a *Centrophorus*, to which

[9] We might note, in passing, that while Blainville (1825, p. 59) quotes "Pl. 14, Fig. 1" for his *infernus*, his Pl.14 actually pictures a Thresher (Fig. 1) and a *Lamna* (Fig. 2).

[10] His Plate 61, figure 194, is credited both to *granulosus* (p. 448) and to *lusitanicus* (p. 449).

the name *uyato* Rafinesque 1810 seems to apply. It appears to differ from *C. granulosus* (Bloch and Schneider) 1801, type species of the genus, in its sharp, pointed, dermal denticles and in a longer second dorsal spine; perhaps in some of its proportional dimensions as well, though such information as is available does not afford satisfactory comparison between the two in this last respect.[11] Comparison, however, of the specimens of *uyato* described below, with a dried skin of *granulosus*, about 860 mm. long, from Europe (no definite locality), in the Museum of Comparative Zoology, shows that the two species actually differ widely as regards their dermal denticles, those of *granulosus* being block-like, quadrate, and close set in quincunx mosaic (Fig. 3A), but those of *uyato* very small, conical, thorn like, recurved, and so sparsely distributed that the skin is exposed between them (Fig. 3C). And the denticles of *C. squamosus* (Fig. 3B) are of so different a type, being scale like and overlapping, that a glance at the skin with a hand lens is sufficient for identification, among these three species (Fig. 3).

Provisional Key to North Atlantic-Mediterranean Species of *Centrophorus*

1. Inner corners of pectorals only a little extended though sharp-pointed, reaching only about even with origin of first dorsal fin when pectoral is laid back; base of first dorsal fin nearly or fully twice as long as base of second dorsal. Dermal denticles scale-like, overlapping (Fig. 3B) . . . . . *squamosus* (Bonnaterre) 1788[12]

   Inner corners of pectorals considerably extended, reaching nearly or quite as far as the mid base of the first dorsal when the pectoral is laid back; base of first dorsal fin only about 1⅓–1½ times as long as base of second dorsal; dermal denticles not overlapping 2

2. Cutting edges of cusps of lower teeth with fine serrations more or less evident[13]; second dorsal spine reaches not more than ½ way along free anterior margin of second dorsal fin; dermal denticles block-like, sessile from end to end, the exposed surface nearly parallel with the skin so that

[11]Poll's (1951, p. 60, fig. 33; p. 65, fig. 34) recent illustrations of *uyato* in side view, and of the lower surface of its head, are not accompanied by a description.

[12]For excellent illustrations of *squamosus*, see Jensen, 1899, Pl. 3; and Saemundsson, 1932, Pl. not numbered (*Centrophorus squamosus*). The Museum of Comparative Zoology has recently received an excellent specimen of *squamosus* about 49 inches long from west of Iceland, 218 fathoms, from Dr. Arni Fridricksson.

[13]Described and pictured as finely serrate by Müller and Henle (1841, p. 88, Pl. 33); also by Bocage and Capello (1866, p. 26, Pl. 1, Fig. 3D); and so described by Garman (1913, p. 202). But microscopic examination of the teeth of the specimen Garman had at hand shows no regular serrations but only a certain amount of raggedness.

the latter feels no rougher when stroked from rear to front than when stroked from front to rear; and so close spaced in regular quincuncial mosaic that they are very nearly in contact, one with the next, concealing the skin; the exposed surface nearly square in outer view, with rounded edges and angles, cornering antero-posteriorly, and weakly convex dorso-ventrally, the anterior ½ to ⅔ sculptured radially with 5 to 7 low ridges separated by shallow rounded furrows, converging anteriorly, so that two adjacent ridges often fuse one with the other (Fig. 3A); lining of mouth dark-spotted, only..... *granulosus* (Bloch and Schneider) 1801

Cutting edges of lower teeth perfectly smooth; second dorsal spine reaching at least ⅔ the way along free anterior margin of second dorsal fin; dermal denticles (Fig. 3C) conical-thorn shaped, sharp-pointed, so loosely spaced that the skin is widely exposed between them, and with the tips elevated so that the skin is much rougher to the touch when stroked from rear to front than when stroked from front to rear; the outer surface sculptured with 3 to 5 sharp radial ridges converging toward the tip; lining of mouth uniformly either sooty gray, very dark blue, or perhaps black..... ..... *uyato* (Rafinesque) 1810, p. 227

Besides the North Atlantic species just discussed, nine of the squalid sharks that have been named from Indo-Pacific waters fall in the genus *Centrophorus* as defined here; namely, *C. tesselatus* Garman 1906, *C. steindachneri* Pietschmann 1907, *C. acus* Garman 1913 and *C. atromarginatus* Garman 1913 from Japanese waters; *C. moluccensis* Bleeker 1860 from the East Indies; *C. nilsoni* Thompson 1930 from New Zealand; *C. scalpratus* McCulloch 1915 and *C. harrisonii* McCulloch 1915 from Victoria, Australia; and *Atractophorus armatus* Gilchrist 1922 from southern Africa.[14] These stand in evident need of revision which we are now not able to undertake.

Up to the present time, records for the genus *Centrophorus* in the Atlantic had been from the eastern side only; those for *granulosus* from the Canaries, Madeira, Spain (both coasts) and Portugal; those for *uyato* from Senegal and the Mediterranean; those for *squamosus* from Madeira, the Azores, the Mediterranean, Portugal, the waters southwest of Ireland, the Faroe Bank, and south and southwest of

[14] Fowler (1941, p. 233, 234) also includes *Centrophorus kaikurae* Whitley, 1934, and *Centrophorus waitei* Thompson 1930 in the genus *Centrophorus*. But the illustrations of the former by Thompson (1930, Pl. 42, Figs. a–i, as *C. calceus* Lowe 1839), show it as with rounded pectoral inner corners, and with a very long first dorsal fin, long pointed snout, and pitchfork shaped dermal denticles; these refer it to the genus *Deania* according to the classification adopted earlier by us. And *waitei* seems referable provisionally to *Scymnodon*, though Thompson's illustration of it (1930, Pl. 44, Fig. A) seems to have been of a specimen with damaged fins, the caudal being pictured as with a pointed tip, and the pectoral as paddle shaped, bilaterally symmetrical, broadest about midway of its length and tapering to a narrowly rounded tip, which does not accord with any known group of squalids.

Iceland.

The known range of the genus has now been extended to the northern part of the Gulf of Mexico, by the capture there of three specimens which appear to be specifically identical with the specimen in the Museum of Comparative Zoology from "France" on which Garman (1913, p. 197, as *uyatus*) based his description of *uyato*. As this is the first report of the presence of the genus *Centrophorus* in the western side of the Atlantic, a description follows from which the reader may judge the correctness of our identification.

CENTROPHORUS UYATO (Rafinesque) 1810

Figure 4

Study material. Female, 420 mm. long, "Oregon" Sta. 278, Lat. 28°39′N, Long. 85°46′W, 112 fathoms, February 24, 1951; juvenile male, about 429 mm., and female about 442 mm., "Oregon" Sta. 515, Lat. 29°17′N, Long. 87°42′W, 208 fathoms, April 1, 1952. Also juvenile male, 480 mm., Nice, France, in Museum of Comparative Zoology.

Description. Proportional dimensions, in per cent of total length, of female, 442 mm., Gulf of Mexico; and juvenile male, 480 mm., Nice, France (Mus. Comp. Zool. No. 943).

Trunk at origin of pectoral: breadth 10.8, 9.9; height 11.3, 11.4.

Snout: length in front of mouth 11.8, 10.5.

Eye: horizontal diameter 5.6, 5.9.

Mouth: breadth 7.5, 7.3.

Nostrils: distance between inner ends 4.1, 3.8.

Labial furrow: 5.6, 5.1.

Gill opening lengths: 1st 2.5, 2.1; 4th 2.9, 2.7; 5th 3.1, 3.1.

First dorsal fin: vertical height 6.3, 6.9; length of base[15] 7.7, 8.2.

Second dorsal fin: vertical height 4.9, 4.6; length of base[15] 6.5, 5.7.

Caudal fin: upper margin 23, 22.8; lower anterior margin 13.3, 13.2.

Pectora fin: outer margin 12.0, 12.0; inner margin 13.5, 12.6; distal margin 11.8, 11.1.

Distance from snout to: 1st dorsal[15] 32.8, 34.2; 2nd dorsal[15] 62.8, 66.2; upper caudal 77.0, 77.2; pectoral 22.8, 22.7; pelvics 53.5, 56.1.

Interspace between: 1st and 2nd[15] dorsals 21.2, 25.8; 2nd dorsal and caudal 6.8, 7.1; rear base of pelvics and caudal 14.0, 14.0.

Distance from origin to origin of: pectorals to pelvics 30.7, 33.4; pelvics to caudal 19.4, 20.6.

[15] to base of spine.

Trunk fusiform, tapering both rearward and forward from region of first dorsal fin; ovoid in cross section, the belly somewhat flattened (unless in gravid females or after a full meal); caudal peduncle without lateral longitudinal ridges. Height at first dorsal (where highest) about 1/5 as great as length to origin of caudal; the breadth there about 1/2 as great as the height or a little more; breadth close in front of first gill openings (where broadest) a little more than 1 1/2 times as great (1.7 times in 442 mm. female) as at level of first dorsal fin. Head nearly straight in dorsal profile, its length to origin of pectorals nearly 1/3 (30% in 442 mm. female) of trunk to origin of caudal fin. Snout thin tipped, narrowing forward to rounded tip (Fig. 4); its length in front of mouth a little less than 1/2 of head (47% in 442 mm. female) to origin of pectorals. Eyes noticeably large, a little more than twice as long as high, and about 1/4 as long as head. Distance from front of eye to tip of snout about 1.2 times as long as eye. Spiracles about 1/3 as long as eye, posterior to latter by a distance about 1/5 as long as eye, and at a slightly higher level than longitudinal axis of eye.

Nostrils about 1/4 as long as eye; nearly transverse; their outer (anterior) ends posterior to tip of snout by a distance about 4/5 as long as eye; anterior nasal flap rather broadly triangular with rounded tip; and without accessory lobe. Mouth very low-arched, the gape (when closed) occupying about 2/3 of breadth of head or a little more; labial furrows noticeably short, the upper furrows extending inward a little less than half of distance toward the mid line of head; the lower furrows a little shorter; their rearward extensions traceable about half the distance toward the first gill openings. Anterior margins of first to fourth gill openings weakly concave, the fifth the most oblique; longest gill (fifth) about 1.2 times as long as first, and a little more than 1/2 (52–55%) as long as horizontal diameter of eye. Teeth $\frac{18\text{-}1\text{-}19}{16\text{-}1\text{-}16}$ in female of 442 mm. one-cusped and smooth edged; uppers with triangular cusp on quadrate base; the median upper tooth erect and symmetrical, the next few teeth either side of the symphysis nearly so, but successive teeth thence outward along each side of the jaw with cusps increasingly oblique, so that the upper teeth along the outer 1/4 or so of the jaw are similar to the lowers in shape. Lower teeth (except for median tooth) considerably larger than uppers, the cusps triangular, directed strongly outward all along each half of the jaw, their inner cutting margins at an angle of about 15° with the general contour of jaw. Lower median tooth much smaller than the others, its

cusp curving obliquely toward the one side or the other. Teeth $\frac{18\text{-}18}{16\text{-}16}$ in male of 480 mm., no median tooth.[16] Dermal denticles small (average length about 0.2 mm. on 442 mm. specimen), evenly distributed in random arrangement, mostly spaced so loosely that skin is widely exposed between them, but rarely the tip of one overlapping the base of the next; the denticles clothing entire trunk and fins out to margins; anterior ends of denticles thick, sessile, but tips elevated so that skin is rough to the touch; blades thick, ovoid narrowing rearward to sharp pointed tip; their upper surface conspicuously corrugated with median ridge flanked either side by two (usually) lateral ridges, the furrows converging toward tip, and the extreme margin also elevated a little. Denticles on lower surface in general similar to those on sides and back, but those on fins smaller, narrower, very sharp tipped, and less conspicuously sculptured, or even smooth.

Origin of first dorsal (first sensible elevation above general profile of back) posterior to origins of pectorals by a distance about as long as from tip of snout to center of eye; its base about twice as long as distance between nostrils, or about 1.2 times as long as from tip of snout to eye; anterior margin weakly convex, distal margin moderately concave, rear tip rather narrowly acuminate, free lower margin about as long as from rear end of base to point of emergence of spine. Interspace from rear end of base of first dorsal to origin of second dorsal (first sensible elevation) about as long as from snout to level of second gill opening. Second dorsal similar to first in shape, but only about $\frac{3}{4}$ as long as first dorsal at base and correspondingly smaller in area. Dorsal fin spines with a longitudinal groove close to anterior edge on either side; the rear surface of the spines slightly furrowed also. Both of the spines are well exposed; the second about $1\frac{1}{3}$ times as long as the first, its tip about even with the apex of the fin. Interspace between rear end of base of second dorsal and origin of upper side of caudal a little longer than base of second dorsal. Caudal fin about as long as head to origin of pectorals; about $\frac{1}{2}$ as broad as long or a little less, the upper margin nearly straight, tip obliquely truncate; lower posterior margin with obtuse subterminal excavation, the lower anterior corner a little extended as a low, rounded lobe; the lower anterior margin weakly convex, about 3/5 (58–60%) as long as upper margin. Interspace between lower origin of caudal and rear ends of bases of pelvics about as long as distance from snout to level of spiracles

[16]For a recent account of the spacial relationships between the successive rows of teeth in *C. uyato*, see Landholt, 1947, p. 353.

or slightly more than ½ (54%) as long as from origins of pelvics to axils of pectorals. Pelvics approximately as large as second dorsal, their origin at a perpendicular about ½ to ⅔ of the distance rearward from rear end of first dorsal base toward origin of second dorsal. Anterior pelvic margin moderately convex, outer corner rounded, distal and inner margins weakly concave, rear corner pointed, reaching back about to below second dorsal fin spine. Pectorals with moderately convex outer margin, rounded outer corner, the distal margin nearly straight outwardly, but inwardly curving rearward to narrowly acuminate, sharp pointed inner-rear corner; the latter reaching back nearly or quite as far as rear end of base of first dorsal when pectoral is laid back; inner pectoral margin thus about as long as from tip of snout to rear of eye.

Color. Back and upper parts of the sides mouse gray after preservation in alcohol, paling to greyish white along the lower parts of the sides and on the lower surface as a whole; outer parts of the dorsal and caudal fins in general are sooty, but rear tips of dorsals, also extreme distal margin and acuminate rear corner of pectorals pale; a pale spot at base of each dorsal fin spine also; and one on the top of the head between the eyes. Region of gill openings bluish (perhaps brighter blue in life); lining of mouth uniformly very dark gray blue;[17] lining of body cavity black.

Size. This shark has been reported up to about 38½ inches (980 mm.) long (Poll 1951, p. 64). How much larger it may grow is not known.

Genus SCYMNODON Bocage and Capello 1864

Sharks of this genus are characterized among the Squalidae by dorsal fin spines at the anterior edges of the fins with at least the tips projecting; by one-cusped teeth above as well as below, the uppers much narrower than the lowers, at least along the central part of the mouth; by more or less acutely dentate dermal denticles; and by rounded inner pectoral corners. Their closest affinities seem to be with *Centrophorus* from which they differ chiefly in the shape of the pectoral fins, and with *Centroscymnus*, from which they are separated by their dentate dermal denticles.[18] In the type species of the genus,

[17]The linings of the mouth and of the body cavity are described as dark turquoise by Bonaparte (1841, text to Pl. 57).

[18]The distinction between *Scymnodon* and *Centroscymnus* applies only to adults, if Tortonese's (1952, p. 386, fig. 1) recent identification of a juvenile male with dentate denticles is correct, as *C. coelolepis*.

ringens Bocage and Capello (1864, p. 261, fig. 5 p. 263; 1866, p. 32, Pl. 1, fig. 1), the broadly triangular cusps of the lower teeth are described as symmetrical and erect along the central part of the jaw, but as directed increasingly outward, toward its corners;[19] and the genus *Scymnodon* was characterized accordingly in Bocage and Capello's original (1864) diagnosis.[20] But the genus has been expanded, by subsequent authors,[21] to include species in which the lower teeth are more or less strongly oblique all along the jaw, from the symphysis to either corner of the mouth.

Three species referable to *Scymnodon* as defined above are known from the eastern side of the North Atlantic, *ringens* Bocage and Capello 1864,[22] *crepidator* (Bocage and Capello) 1864,[23] and *jonsonii* Saemundsson (1922).[24] Fowler (1941, pp. 226, 227) credits a third species, *Scymnodon squamulosus* (Günther) 1877, to the Atlantic, quoting Regan (1908, p. 48) as authority. But the locality stated for *squamulosus* by Regan was Japan, nor has it ever been reported elsewhere, so far as we know.

Available information, including notes on a specimen in the British Museum, identified by Günther as *crepidator*, kindly contributed by Mr. N. B. Marshall, also makes it likely that the cusps are erect (or nearly so) on a larger number of the teeth along the mid section of the lower jaw in *ringens*, and the dermal denticles more pronouncedly tridentate, than in *crepidator*, though a more detailed comparison between the two species is much to be desired in these respects. If the illustrations of the two that have appeared are to be relied upon, *crepidator* differs further from *ringens* in smaller eyes, but a considerably longer snout relative to other bodily proportions.[25] The illustrations suggest also that the caudal is truncate at the tip, and with a

[19]For the best description and illustration of the teeth of *S. ringens* with which we are acquainted, see Rey, 1928, pp. 455, 456, fig. 152.

[20]In their subsequent account (1866, p. 32, Pl. 1, fig. 1C) they characterized the lower teeth as erect, and so pictured them all around the jaw.

[21]Garman 1913, pp. 207–208; Fowler 1941, pp. 225–226; Bigelow and Schroeder 1948, pp. 450–451.

[22]For descriptions and illustrations see Bocage and Capello 1866, p. 31, Pl. 1, fig. 1; and Rey 1928, p. 454.

[23]For descriptions and illustrations see Bocage and Capello 1866, p. 27, Pl. 2, fig. 2; and Rey 1928, p. 449. *Crepidator*, referred by its describers to the genus *Centrophorus*, was made the type of a new genus *Centroselachus* by Garman 1913, p. 206. But it falls within the limits of *Scymnodon* as defined here. See Bigelow and Schroeder 1948, p. 494, footnote 1.

[24]For description and illustrations see Saemundsson 1922, p. 192, Pl. 5, figs. 1, 2. According to Saemundsson, the first mention of this species was in Schmidt, 1901, p. 23, where it was listed as "*Centrophorus* nov. spec." on the authority of Jensen.

[25]Eye about 1/5 to 1/4 and snout about 1/5 to 1/4 of head in *ringens;* eye about 1/3 and snout about 1/3 of head in *crepidator*.

definite lower anterior lobe in *crepidator*, contrasting with narrowly rounded tip, and without lower anterior lobe as it is described[26] and pictured[27] in *ringens*. But it is a question whether the pictured differences can be accepted as specific, for the tracing by Mr. Marshall of the caudal of the British Museum specimen labelled *crepidator* shows the fin as intermediate in shape in these respects, i.e. with rounded tip, but with definite lower anterior lobe. In both *ringens* and in *crepidator* the upper tooth band along each side of the upper jaw follows an arc of long radius, the convexity directed rearward, with these two lateral arcs connected by a shorter but similar arc in the region of the symphysis. And in both of them the entire pelvic fin on each side is anterior to a perpendicular at the point of emergence of the second dorsal fin spine. *Jonsonii*[28] differs conspicuously both from *ringens* and from *crepidator* in that its pelvic fins are described and pictured as with their bases very nearly opposite the base of the second dorsal fin.[29]

The following seven squalids also, that have been named from the Pacific and Indian Oceans, and from the Straits of Magellan, appear to fall in the genus *Scymnodon* as defined here: *foliaceous* (Günther) 1877, Japan and also reported from the Philippines;[30] *macracanthus* (Regan) 1906, Straits of Magellan; *plunketi* (Waite) 1910, New Zealand; *rossi* (Alcock) 1898, India; *sherwoodi* Archey 1921, New Zealand; *squamulosus* (Günther) 1877, Japan; and *waitei* (Thompson) 1910, New Zealand. *Macracanthus* is set apart, among these, by "well developed and strongly projecting" first and second fin-spines;[31] *foliaceous* by a strongly projecting second dorsal fin-spine.[32] If the original illustration is to be relied upon, *waitei* is even more sharply separated from its genus mates by a pointed caudal fin. The remaining members of the Pacific-Indian Ocean group (*rossi*, *plunketi*, *sherwoodi* and *squamulosus*) resemble one another closely in most respects. But *squamulosus* is the only one of these that we have seen, and the published accounts of the other three are not detailed enough to serve as basis for the revision of which they stand in evident need.

[26]Bocage and Capello 1866, p. 39, footnote.

[27]Bocage and Capello 1866, Pl. 1, fig. 1; Rey 1928, p. 455, Fig. 151.

[28]Saemundsson (1922, p. 192, Pl. 5, figs. 1, 2), who has given the only detailed account of this species, left it in the genus *Centrophorus*. But his description of its pectoral fin as with rounded posterior corner places it in *Scymnodon* according to the scheme followed here.

[29]Saemundsson 1922, p. 195 (Table of Measurements), Pl. 5, fig. 1.

[30]By Smith and Radcliffe 1912, p. 679.

[31]Regan 1906, p. 436.

[32]As pictured and described by its author. Jordan and Fowler's (1903, p. 631) description as *foliaceus*, of a Japanese specimen with only the tips of the fin spines exposed suggests that they may have been dealing with *squamulosus*, in which this is the case.

The experimental trawlings by "Cap'n Bill II" on the continental slope off southern New England and off Georges Bank during the summer of 1952 have now yielded three specimens of a *Scymnodon* which seem not to be referable either to *ringens* or to *crepidator* for the reasons stated below (p. 236), and which differ from *jonsonii* in the fact that their pelvic fins are wholly anterior to the base of the second dorsal fin (for further discussion, see p. 232). Neither do the specimens in question seem to fall within the probable limits of variation of any of the representatives of the genus that have been described from other seas. We therefore propose for it the new specific name *melas*. We must confess, however, that we would do so with more confidence, if the published accounts and illustrations of *ringens* and of *crepidator* were more satisfactory and informative.

SCYMNODON MELAS, n. sp.
Figure 5

Type specimen. Female, 462 mm. long, trawled by the dragger "Cap'n Bill II" on the continental slope off Georges Bank, Lat. 40°00′N, Long. 68°52′W, at 420–480 fathoms, July 12, 1952, Museum of Comparative Zoology, No. 37452.

Additional material. Two juvenile males, 330 mm. and 339 mm. long, trawled by "Cap'n Bill II" on the slope off southern New England, Lat. 39°52′N, Long. 70°43′W, 415–440 fathoms, and Lat. 39°51′N, Long. 70°48′W, 450–495 fathoms, both on August 24, 1952, also in Museum of Comparative Zoology.

Description. Proportional dimensions, in per cent of total length, of female of 462 mm. (type) and male, 339 mm.

Trunk at origin of pectoral: breadth 13.2, 12.1.

Snout: length in front of mouth 8.2, 9.8.

Eye: horizontal diameter 4.1, 4.1.

Mouth: breadth 7.8, 7.7.

Nostrils: distance between inner ends 3.9, 3.5.

Labial furrow length from corner of mouth: 7.3, 7.4.

Gill opening lengths: 1st 1.3, 1.3; 2nd 1.3, 1.3; 3rd 1.3, 1.3; 4th 1.3, 1.3; 5th 1.6, 1.6.

First dorsal fin: vertical height 3.0, 3.2; length of base 5.0, 4.7.

Second dorsal fin: vertical height 3.2, 3.5; length of base 6.1, 4.7.

Caudal fin: upper margin 23, 22.

Pectoral fin: extreme length 12.3, 12.1.

Distance from snout to: 1st gill opening 17.9, 19.2; 1st dorsal origin

35.5, 34.2; 2nd dorsal origin 62.8, 64; upper caudal origin 77, 78; pectoral origin 22.5, 23.3; pelvic origins 59.8, 59.3.

Interspace between: 1st and 2nd dorsals 22.3, 25.1; 2nd dorsal and caudal 8.2, 9.2; base of pelvics and caudal 10.4, 9.7.

Distance from origin to origin of: pectorals to pelvics 37.2, 36.1; pelvics to caudal 10.8, 10.9.

Trunk at first dorsal (where highest) about 1/6 as high as it is long to origin of caudal; slightly flattened sidewise, rearward from pectoral fins; its thickness at first dorsal only about ½ as great as its height there, but much thicker anteriorly, the breadth of the head, abreast of the first gill opening being almost twice as great as that of the body at the first dorsal. Head, to origin of pectorals, between ¼ and ⅓ (29%) of length of trunk to origin of caudal; flattened above, the dorsal profile sloping downward slightly; only a little narrowed at eyes. Snout moderately fleshy, but not very flexible; its anterior outline obtusely angular with rounded tip; its length in front of mouth 37 per cent of head, and its length to eyes 19 per cent. Eye oval, a little more than twice as long as high, its horizontal diameter ½ as long as snout in front of mouth. Spiracle about ⅓ as long as eye, its outward margin about on a level with upper margin of eye, and forward margin posterior to eye by a distance ½ to ⅔ as long as eye. Nostrils about ½ as long as eye, close to front of snout, and moderately oblique; the anterior nasal flap narrowly triangular, crossing the nasal aperture at about the mid-length of the latter. Mouth very little arched, the gape occupying a little less than ⅔ (about 60%) of breadth of head; anterior (upper) labial furrows extending between ½ and 3/5 of distance toward symphysis; rearward extensions of labial furrows reaching about ½ of distance toward first gill openings. Longest gill opening (5th) nearly ½ (44–46%) as long as distance between nostrils; first gill about 4/5 (80%) as long as fifth. Anterior margin of first gill concave, but not enough to expose the gill filaments, the 3rd to 5th gill openings nearly straight; first and second gills almost vertical, but the 3rd to 5th increasingly oblique.

Teeth smooth edged; $\frac{20\text{-}1\text{-}20}{21\text{-}21}$ in female of 462 mm. (type); $\frac{20\text{-}20}{20\text{-}20}$ in juvenile male of 339 mm.; the upper teeth slender, sharp pointed and erect along central ⅔ of mouth, but successively broader, more blade-like, and with cusp curving increasingly outward toward corners; the individual teeth largest along median third, or so, of each side of mouth; smaller both in region of symphysis and toward corner

of mouth, the outermost teeth much the smallest. Lower teeth triangular, with blade-like cusp, directed so strongly outward, all along each half of the tooth band, that the inner edges of the successive cusps form a practically unbroken cutting edge following the general contour of the jaw from the symphysis outward. No median lower tooth in the specimens seen. About 2 to 3 rows of teeth are in function simultaneously in the upper jaw, but one row only in the lower jaw.

The upper tooth band extends considerably beyond the outer limit of the gape on either side, i.e. into the mouth, and when viewed from below with mouth wide spread, is seen to follow an arc of long radius along either side of the mouth, the convexity facing inward (i.e. into the mouth), with these two lateral tooth-arcs interconnected around the symphysis of the jaws, as is the case in *S. ringens*. It is along the regions of transition between the median tooth-arc and the two lateral arcs that the individual teeth are the largest.

The lower tooth band extends considerably farther outward than the upper, on either side, and its arc of curvature is uniform, from the one end to the other.

Dermal denticles unevenly spaced, some close set, others more scattered, clothing the entire trunk (except for the lips) as well as the fins out very nearly to the margins of the latter; their arrangement random; the individual denticles rising rather steeply from the skin, on short pedicels; tridentate at margin but not definitely striate radially; their marginal teeth broadly triangular and sharp pointed, the median tooth considerably the largest; denticles on the belly similar to those on sides and back; those on lower surface of head and on fins smaller than those on body, more close set, less erect, pointing rearward at an angle of about 45°, not tridentate or only weakly so.

First dorsal fin about as long at base as length of eye, its upper contour continuously rounded, the rear corner sharp pointed, the free lower margin about as long as the base; origin of first dorsal about opposite to the tips of the pectorals (when these are laid back). Interspace between first and second dorsal fins about as long as head. Base of second dorsal fin about $1\frac{1}{5}$ times as long as base of first dorsal and its area correspondingly larger; its anterior margin weakly convex; apex broadly rounded, distal margin nearly straight; rear corner sharp pointed; free lower margin about as long as the base; origin about over rear ends of bases of pelvics. First and second dorsal fin spines with only their points exposed.

Interspace between base of second dorsal and origin of caudal about ⅓ as long as interspace between first and second dorsals. Distance from rear corner of second dorsal to origin of caudal about ½ as long as eye.

Caudal about as long as head to origin of pectoral and about ½ as broad as long; upper margin nearly straight proximally but increasingly convex distally; the tip obliquely truncate; the lower rear margin with conspicuous subterminal excavation, a little more obtuse than a right angle; the lower anterior corner expanded as a broadly triangular lobe with slightly blunted apex; the lower anterior margin weakly convex, about ½ as long as upper margin.

Distance from lower origin of caudal to rear ends of bases of pelvics a little less than ⅖ as long as from origins of pelvics to axils of pectorals (38% on female of 462 mm.). Pelvics a very little longer at base than second dorsal; anterior margin weakly convex; distal margin nearly straight; their entire base anterior to origin of second dorsal. Pectorals with weakly convex margins and broadly rounded corners, reaching back very nearly as far as the origin of the first dorsal when the pectoral is laid back. The distal margins of all the fins are frayed; the dorsals and pelvics very narrowly, the pectorals somewhat more broadly so, the lower lobe of the caudal and the tip of the latter considerably more broadly still. On the 462 mm. specimen these fringes are rather regular. But they are irregular on the two smaller specimens, evidence that the present state of the fin margins is not normal, but was the result of rough treatment in the trawl.

Color. Uniformly almost black in life and after preservation in alcohol, below as well as above, without any evident pattern of darker and of paler markings. Lining of body cavity dark bluish gray, lining of mouth grayish white, teeth white.

Size. We dare not guess how large this shark may grow, for the largest specimen (the type) is a female.

Remarks. S. melas falls with *S. ringens* in shortness of snout, and large eyes, but differs quite sharply from *S. ringens* (according to available information as to the latter) in the shape of its caudal with truncate tip and definite lower anterior lobe; in the strong obliquity of the cusps of the lower teeth all along each side of the jaw from symphysis to outer corner;[33] apparently in pectoral fins considerably larger in area though perhaps no longer. It resembles *crepidator* more nearly in the shape of the caudal fin and in the shapes of the lower

[33]For an excellent illustration of the teeth of *ringens*, see Rey, 1928, p. 456, Fig. 152.

teeth, but differs conspicuously from *crepidator* (as the latter is pictured) in a much shorter snout, but much larger eyes, and in its smooth bladed but pronouncedly tridentate dermal denticles.[34] Furthermore, the upper labial furrows of *crepidator* are described by Günther (1870, p. 421) as nearly meeting in the mid line of the snout, and they are so shown in the sketch of the British Museum specimen, whereas their inner ends are separated by an interspace about as long as the eye in all three of our specimens of *melas*.

Among the members of the genus *Scymnodon* (as defined here) that have been named from the Pacific and Indian Oceans, *melas* shares its sharply tridentate dermal denticles with the Japanese *squamulosus* (Günther) 1877; also its very oblique lower teeth, the shape of its caudal, and its bodily proportions in general. But comparison with two excellent specimens of *squamulosus* from Japan, in the Museum of Comparative Zoology, shows that the two forms are clearly distinct, the lining of the mouth of *squamulosus* being blackish (grayish white in *melas*); its dermal denticles so much smaller than those of *melas* of a corresponding size that its skin feels velvety to the touch (rough in *melas*); and only the extreme tips of the dorsal fin spines of *squamulosus* are visible, if, indeed, they are not buried wholly in the skin, hence to be detected by touch only.

Habits and Range. The depths at which our three specimens were taken, added to the fact that it has never been taken any shoaler on grounds that are as intensively trawled as are the offshore parts of the Scotian Banks and of Georges Bank, are evidence that *melas* is restricted to depths greater than perhaps 300–350 fathoms. Nothing more is known of its habits. It is known so far only from the localities listed above (p. 233). But it may prove much more plentiful than the meagre record might suggest, for fishermen may well have confused it with the common black dogfish (*Centroscyllium fabricii*).

The discovery of this new *Scymnodon* extends the known range of this genus to the western side of the North Atlantic.

Genus ETMOPTERUS Rafinesque 1810

These little dark-colored deep-water squalids are characterized by having a prominent spine at the anterior margin of each dorsal fin,

[34] These are described and pictured as with up to seven radial ridges but with marginal teeth only weakly indicated in *crepidator;* and the sketch of the British Museum specimen mentioned above shows them as with three ridges only and no definite marginal teeth.

upper teeth with several cusps, but lower teeth with only one cusp, and those in each side of the jaw directed so sharply outward that the inner margins of the successive cusps form an almost unbroken cutting edge. Some members, also, of the genus, are luminescent; several of them are much darker colored below than above, and several have conspicuous dark markings of characteristic shape on the flanks, color-characters unusual among sharks.

The dozen species that had been described from one part of the oceans or another are divided by Fowler (1941, p. 246) into two subgenera, (a) *Etmopterus* Rafinesque 1810, with "second dorsal origin over or a little before ventral base; ventral origin slightly nearer subcaudal than pectoral origin," and (b) *Acanthidium* Lowe 1839, with "second dorsal origin behind ventral base; first dorsal origin midway between orbit and second dorsal origin." Examination of available material does not seem to us to justify subdivision of the genus on this basis. We think it likely, however, that the *E. paessleri* of Lönnberg 1907 from the Straits of Magellan and reported subsequently from Argentine waters by Lahille (1921, p. 63) will prove distinct generically, for its dermal denticles were described as having several smaller lateral spines surrounding the central spine, and the lateral cusps on its upper teeth as "nicht sichtbar". Further exploration, however, of this matter seems idle, since knowledge of *paessleri* is still limited to Lönnberg's original account, which did not include illustrations either of its dermal denticles or of its upper teeth.

Up to the present time, four species have been described from the North Atlantic with its tributary seas: — (a) *spinax* (Linnaeus) 1758 of North African and European waters from the Cape Verdes, Morocco and the Azores to Norway, including the Mediterranean and reported from southern Africa;[35] (b) *pusillus* (Lowe) 1839, Madeira (type locality), Cape Verde Islands, Canaries, Azores,[36] and also in Japanese waters or represented there by a very close ally;[37] (c) *hillianus* (Poey) 1861, West Indian-Cuban region, southern Florida, northward off the Atlantic slope of America to the offing of Chesapeake Bay;[38] and (d) *princeps* Collett, 1904, described originally from the Faroe region, and

[35]Gilchrist, 1922, p. 49.

[36]Goode and Bean's (1895, p. 10, Pl 2, fig. 5) report of *pusillus* from St. Kitts, West Indies, is shown, by their illustration, to have been based in reality on a specimen of *hillianus*. And Jordan and Evermann's report of it from Cuba (1896, p. 219; 1896a, p. 55) doubtless refers equally to *hillianus*, which they did not recognize as a separate species.

[37]First described as *E. frontimaculatus* by Pietschmann (1907, p. 395; 1908, p. 654, Pl. 1, fig. 2, Pl. 2, fig. 2); subsequently as *E. pusillus* by Tanaka (1912, Vol. 5, Pl. 22; Vol. 6, p. 88).

[38]The *Etmopterus* reported from tropical West African waters by Poll (1951) as *hillianus* has proved to represent a new species described here as *E. polli* (pp. 240, 241).

reported subsequently from the offing of the Straits of Gibraltar.[39]

We thought it likely, earlier (Bigelow and Schroeder 1948, p. 488, footnotes 3, 4) that *princeps*, originally described from poorly preserved material, would prove to be identical with *spinax*. But receipt of the specimens listed below (p. 247), trawled on the continental slope off southern New England and off southern Nova Scotia, which agree in detail with Collett's account and illustrations, proves that *princeps* is in fact an easily recognizable species (p. 250).

The experimental trawlings of the "Oregon", in the northern part of the Gulf of Mexico have now brought to light two additional members of the genus that cannot be referred to any species of *Etmopterus* previously known, whether from the Atlantic or from the Indo-Pacific. They are described here as *E. schultzi*, n. sp. (p. 252), and as *E. virens*, n. sp. (p. 257). Examination, too, of the *Etmopterus* recently reported by Poll (1951) from tropical West Africa as *hillianus* has shown that a new specific name is needed for it also. We propose *polli* in honor of its discoverer (p. 241).

Final decision, whether the sharks that have been described as *spinax*, from southern African waters, and as *pusillus* from Japan, are actually identical with the *spinax* and with the *pusillus* of the North Atlantic must await a comparison of specimens from these widely separated seas. The status of *paessleri* is discussed above (p.238). Other species, referable to *Etmopterus*, that have been named from seas other than the North Atlantic, are: *lucifer* Jordan and Snyder 1902,[40] reported originally from Japan, where it appears to be common, and subsequently off Natal, southeastern Africa, from the East Indies, and widespread in Philippine waters; *granulosus* (Günther) 1880,[41] reported originally off the Coast of Chile, and subsequently off Natal, southeastern Africa,[42] and credited by Barnard (1925, p. 50) to the Hawaiian Islands; *brachyurus*, Smith and Radcliffe 1912,[43] from the Philippines; and *villosus* Gilbert 1905[44] from the Hawaiian region, the last two of which are known from the type specimens only. *Lucifer* is the only member of the Indopacific-Southern African-southern South American list of species that we have seen.

[39]Koefoed, 1932, p. 21, Sta. 25, Lat. 35°46'N, Long. 8°16'W, 2055 meters; as "*Spinax princeps*".

[40]Jordan and Snyder, 1902, p. 79; for list of locality references up to 1941, see Fowler, 1941, Vol. 13, p. 246.

[41]Günther, 1880, p. 19, Pl. 2, fig. C.

[42]Cape Point; Gilchrist, 1922, p. 49.

[43]Smith and Radcliffe, 1912, p. 679, Pl. 52; Fowler, 1941, p. 248.

[44]Gilbert, 1905, p. 580, Pl. 66; Fowler, 1941, p. 250.

Key to Species of *Etmopterus* of the North and Equatorial Atlantic, Mediterranean and Gulf of Mexico

1. Upper side of caudal fin very nearly as long as from tip of snout to rear edge of pectorals when latter are laid back; margins of fins fringed normally ..... *schultzi*, n. sp.
   Gulf of Mexico, p. 252

   Upper side of caudal fin very little longer, if any, than from tip of snout to origins of pectorals, and considerably shorter in some; margins of fins not fringed normally, though often much frayed out 2

2. Distance from rear ends of bases of pelvics to origin of lower side of caudal is about as long as from tip of snout to origins of pectorals 3

   Distance from rear ends of bases of pelvics to origin of lower side of caudal is at least no longer than from tip of snout to first gill openings 4

3. Rear end of base of first dorsal is about as near to origins of pelvics as it is to axils of pectorals; black and pale markings on rear part of trunk as in Figure 6A ..... *hillianus* (Poey) 1861
   Cuban-West Indian region and northward along the American Atlantic slope to the offing of Chesapeake Bay.

   Rear end of base of first dorsal is considerably nearer to axils of pectorals than it is to origins of pelvics; black and pale markings on rear part of trunk as in Figure 6D ..... *virens*, n. sp., p. 257
   Gulf of Mexico

4. Dermal denticles on back and sides of anterior part of trunk low, truncate, their apex either flat or weakly convex, without conspicuous median spine ..... *pusillus* (Lowe) 1839
   Eastern Atlantic from equatorial West Africa[45] to Canaries, Madeira and Azores.

   Dermal denticles on back and sides of anterior part of trunk with conspicuous median spine, either conical, thorn-like or bristle-like in form .. 5

5. Distance from rear ends of bases of pelvics to origin of lower side of caudal nearly or quite as long as upper side of caudal, and about as long as interspace between first and second dorsals ..... *polli*, n. sp.
   Equatorial West Africa, p. 241

   Distance from rear ends of bases of pelvics to origin of lower side of caudal is not more than ⅔ as long as upper side of caudal, and is shorter than interspace between first and second dorsals 6

6. Belly at least slightly but definitely darker than sides and back with abrupt line of transition; the black of the lower surface extending upward

[45]We have received a fine specimen of *pusillus*, 167 mm. long, from Dr. Max Poll, from equatorial West Africa, Lat. 6°08′S, Long. 11°24′E. For an excellent colored illustration of *pusillus*, see Braganza, 1904, Pl. 2, fig. 2.

on rear part of sides as a sharply outlined flank mark of shape shown in Figure 6C; dermal denticles slender, bristle-like. . .*spinax* (Linnaeus) 1758
Eastern Atlantic, including Mediterranean, from the Cape Verde Islands, Morocco and the Azores to Norway; also reported from southern Africa (p. 238, footnote 35)

Back and sides black or blackish brown like belly; no definite flank mark; dermal denticles low, conical to thorn-like ..... *princeps*, Collett, 1904
Faroes-Hebrides region and offing of Straits of Gibraltar in Eastern Atlantic, American slope off southern Nova Scotia, off Georges Bank, and off southern New England in Western. p. 246.

Etmopterus polli, n. sp.
Figure 7

Type specimen. Male, 197 mm. long; tropical West Africa, Lat. 6°08′S, Long. 11°24′E, 350–380 meters, M.C.Z. No. 38001, received from Dr. Max Poll. *Additional material:* five males and five females, 106–232 mm. long from the above locality and from Lat. 10°45′S, Long. 13°10′E, 350 meters, also contributed by Dr. Max Poll and all in Museum of Comparative Zoology.

Description. Proportional dimensions, in per cent of total length, of male 197 mm. long (type), and male of 213 mm.

Trunk at origin of pectoral: breadth 12.2, 9.9; height 10.1, 9.4.
Snout length in front of: outer nostrils 1.3, 1.4; mouth 9.6, 9.4.
Eye: horizontal diameter 5.1, 4.7.
Mouth: breadth 7.1, 6.6.
Nostrils: distance between inner ends 3.5, 3.3.
Labial furrow length: 4.6, 4.7.
Gill opening lengths: 1st 1.8, 1.4; 3rd 1.8, 1.4; 5th 1.8, 1.6.
First dorsal fin: vertical height 4.6, 4.7; length of base 5.6, 6.1.
Second dorsal fin: vertical height 4.8, 5.2; length of base 7.6, 8.0.
Caudal fin: upper margin 21.9, 23.4; lower anterior margin 12.2, 9.9.
Pectoral fin: outer margin 10.1, 8.9; inner margin 6.6, 6.1; distal margin 7.6, 6.7.
Distance from snout to: 1st dorsal 34.6, 33.3; 2nd dorsal 57.5, 54.5; upper caudal 78.1, 76.6; pectoral 23.9, 23.5; pelvis 49.3, 48.8.
Interspace between: 1st and 2nd dorsals 17.2, 15.0; 2nd dorsal and caudal 13.2, 14.1; pelvic base and caudal 15.7, 17.9.
Distance from origin to origin of: pectorals to pelvics 25.4, 25.3.
Trunk at first dorsal (where highest) between 1/6 and 1/7 (16%)

as high as it is long to origin of caudal; its thickness there about ⅔ as great as height, narrowing thence rearward and increasingly flattened sidewise with caudal peduncle about ½ as thick as high; trunk thickest anteriorly, breadth of head at level of first gill openings being about 1¼ times as great as breadth at first dorsal. Head, to origin of pectorals a little less than ⅓ (30%) of length of trunk to origin of caudal; flattened above and narrowed only a little abreast of the eyes; dorsal profile of head nearly straight, sloping evenly forward. Snout fleshy as is usual in the genus, its anterior outline forming an angle of a little more than 90°, with rounded tip. Length of snout to mouth opening about ½ (53%) of head, its length to eye about ⅕ (21%). Eye oval with pointed rear corner, between 2 and 3 times as long as high, its horizontal diameter about ½ (51%) as long as snout in front of mouth opening. Spiracle about 29 per cent as long as eye; behind eye by a distance about ½ as long as eye, and about level with upper edge of eye. Nostril close to outer anterior margin of snout; about 60 per cent as long as eye; anterior nasal flap narrowly pointed, much as in *schultzi* (p.253); crossing nasal aperture a little outward from mid-length of latter. Mouth moderately arched, the gape occupying about ⅔ (63%) of breadth of head. Upper labial furrows extending inward about 30 per cent of distance toward mid-line of head; rearward extensions of labial furrows reaching back from corner of mouth about ½ the distance toward first gill openings.

Gill openings about ½ as long as distance between inner ends of nostrils, anterior margins concave, but not enough so as to expose tips of gill filaments.

Teeth smooth edged, of the usual etmopterid shapes; $\frac{29}{16\text{-}1\text{-}16}$ in type specimen, $\frac{27 \text{ to } 34}{28 \text{ to } 30}$ in other specimens 207–232 mm. long. Upper teeth mostly with 5-7 cusps, the median cusp much the longest, the outermost cusp on each side much the shortest; a few teeth with only 3 cusps. Lower teeth with the cusp directed so strongly outward that the inner cutting edges are practically parallel with the general contour of the jaw; median lower tooth in type but not in ten other specimens examined. Mostly three rows in function simultaneously in upper jaw, one row in lower jaw.

Dermal denticles slender, thorn-like, stiff, thus intermediate in shape between the conical thorn-like denticles of *princeps* and the bristle-like denticles of *hillianus* and *schultzi;* rising steeply, with the tips curving rearward, making the skin rough to the touch; the bases 4-angled but

mostly hidden in the skin. The denticles are sparsely distributed, in random arrangement on the anterior parts in general, but are in about 12 regular longitudinal rows along the tail sector of the trunk. Space between nostrils, and mid-belt of snout thence rearward to mouth either entirely naked, or with only an occasional denticle, so that the skin there feels glossy smooth to the touch. Basal 1/3–1/2 of fins sparsely denticulate, but their marginal zones naked.

First dorsal fin at base about 1.1 times as long as eye in type, 1.3 times in specimen 213 mm. long, of the characteristic etmopterid shape; its origin posterior to origin of pectorals by a distance about 2/3 as long as from tip of snout to mouth. Interspace between first and second dorsals (to first sensible elevation above general profile of back) nearly 3/4 (73%) as long as head to origin of pectorals in type, nearly 2/3 (64%) in specimen 213 mm. long. Origin of second dorsal about over rear ends of bases of pelvics (in male); its base about 1 1/3 times as long as base of first dorsal; its rear margin moderately concave; free lower margin about 3/4 as long as base; its rear corner sharp. Dorsal fin spines slender and needle-sharp, the second about 1.7 times as long as the first, its tip about level with the apex of the second dorsal fin. Distance from rear end of base of second dorsal fin to origin of upper side of caudal fin a little shorter than interspace between first and second dorsals; and a little more than 1/2 (55%) as long as head to origin of pectorals in type, 3/5 as long in specimen of 213 mm. Upper side of caudal fin about as long as from tip of snout to third gill openings; the tip obliquely truncate; lower rear margin with subterminal excavation forming an angle of about 150°, the lower anterior corner forming a low, well-rounded lobe as pictured (Fig. 7). Lower anterior margin of caudal about 1/2 (56%) as long as upper margin. Distance from origin of lower side of caudal to rear ends of bases of pelvics nearly as long as from tip of snout to first gill openings, and about as long as interspace between first and second dorsals. Pelvics a little shorter at base than second dorsal; outer corner well rounded; rear end of pelvic bases about under second dorsal spine. Pectorals reaching a little beyond first dorsal fin spine when laid back, truncate at tip with rounded corners.

The horny rays along the distal margins of all the fins are frayed out, but in such varying degree as to suggest that their present state has resulted from rough treatment, rather than that it represents the normal condition.

Claspers of mature males cylindrical, tapering to slender tips, the

latter fleshy with one sharp spur exposed on the outer side, when not in function.

Color. Back and upper part of sides dark grayish brown, merging into black along lower surface of head, on belly, and in a narrow median band along ventral side of tail sector of trunk. The upper parts are of nearly as dark a shade as the belly; the sides seem to be plain-colored at first sight. Close examination, however, under a strong light, shows that the black of the lower surface spreads upward and rearward in a narrow band along the lower edge of the anterior part of the caudal peduncle on each side; also upward close behind the respective pelvic fin, then rearward as a definitely outlined, flank mark of the shape illustrated (Fig. 7), which is preceded anteriorly, after a short gap, by a second narrow oval black band, corresponding to the anterior extension of the flank mark to be seen on *E. spinax* (Fig. 6C); *E. hillianus* (Fig. 6A), *E. lucifer* (Fig. 6B), and *E. virens* (Fig. 6D). The top of the head is marked with a small vaguely outlined pale yellowish spot, and there is a pale spot close above the rear part of the eye in some specimens, but perhaps not in all. The margins of the pectoral, dorsal and pelvic fins are pale and translucent, but the tip of the caudal is smoky. Teeth cream white; lining of mouth dark bluish gray; lining of body cavity black.

It is interesting that the black dots and dashes that mark the side of several other members of the genus (pp. 255, 261) either are not represented at all on *polli*, or if they are present, are entirely concealed from view by the dark and dense pigmentation.

Size. The claspers of males 212–232 mm. long appear to be fully formed, suggesting a maximum length of perhaps 250–300 mm. at most.

Remarks. The specimens described here as *E. polli* were reported originally by Poll (1951, pp. 65–69) as *E. hillianus*. But a comparison with the considerable series of *hillianus* in the Museum of Comparative Zoology, from the type region (Cuba), has shown that the West African form differs quite sharply from *hillianus* in stouter and more sparsely distributed dermal denticles resulting in a rougher skin; in the nakedness of the midzone of the lower surface of its snout (densely denticulate in *hillianus*); in a somewhat longer head relative to the tail sector of the body (head about 1.4 times distance from pelvic base in *polli* but only about 1.1 times as long in *hillianus*). *Polli* seems also to lack the pattern of black dots and dashes (perhaps luminescent) to be seen on the sides of *hillianus*, and while the anterior portion of the

black flank mark is continuous with the posterior portion in *hillianus* it is separate from the posterior portion in *polli* (cf. Fig. 6A with Fig. 7). Neither is there any likelihood of confusing *polli* with the new species *virens* (p. 257), so noticeably does it differ from the latter in its uniformly dark coloration; in the shape of the black flank marks on the rear part of the trunk (cf. Fig. 7 with Fig. 10); and especially in the relatively much shorter tail sector of its trunk, to list only the most conspicuous differences. *E. polli* recalls *E. princeps*, *E. pusillus*, *E. schultzi*, and newly-caught specimens of *E. spinax* among North Atlantic species, and *E. granulosus* of mid-latitudes of the southern hemisphere, in its dark coloration and proportional dimensions in general. But it differs from *spinax* in the nakedness of the mid-zone of the lower side of its snout (denticulate in *spinax*), in the linear arrangement of the denticles on the tail sector of its trunk (random there in *spinax*), in that the interspace between its pelvics and the lower side of its caudal is about as long as from tip of snout to second gill openings (only about as long as from tip of snout to corners of mouth in *spinax*), and in the shape of its black flank marks (cf. Fig. 6C with Fig. 7). More slender dermal denticles, narrower nasal flap, somewhat shorter caudal relative to length of head, smaller, more truncate pectorals reaching considerably farther rearward, the presence of the black flank mark and of the pale interocular spot on the top of the head, and much smaller size at sexual maturity mark it off from *princeps*. Distinctive differences between *polli* and *pusillus* are the thorn-like dermal denticles of the former (mostly truncate in *pusillus*); nakedness of its internarial space and of the mid-belt of the snout thence rearward to the mouth (uniformly denticulate in *pusillus*); much shorter interspace between its first and second dorsal fins, relative to the length of the head and to the total length of the fish; pectoral fins reaching considerably farther rearward; also in the presence on the rear part of its trunk of definitely outlined black flank marks.[46] Comparison with our considerable series of *E. schultzi* (p.252)shows *polli* as differing from the latter in a considerably shorter caudal fin in relation to other proportional dimensions; in a longer head but shorter interspace between the first and second dorsals; in the truncate shape of its pectorals (rounded in *schultzi*); in the shape of its caudal fin with more prominent lower anterior corner; in stiffer and more thorn-like dermal denticles; in the nakedness of its inter-

[46]We have, for comparison, a female *pusillus* about 280 mm. long, in a fair state of preservation, from Madeira, and a female of 167 mm., in excellent condition, from tropical West Africa, Lat. 6°08′S; Long. 11°24′E, received from Dr. Poll.

narial space and of the mid-belt of the lower surface of the snout thence rearward to the mouth; in the presence of the definitely outlined black flank mark on the rear part of the trunk (indistinct in *schultzi*, p.255); and in that the present frayed out state of the margins of its fins seem not to represent the normal condition.

Polli falls with *granulosus* in the nakedness of the mid-belt of the lower surface of its snout. But our West African specimens differ from *granulosus* as characterized and pictured by Günther (1880, p. 19, Pl. 2, fig. C),[47] in that the distance from snout to lower jaw occupies only about 35–40 per cent of the length of the head (to pectoral fins) in them, but ½ the length of the head in *granulosus;* that the distance from the rear ends of the bases of the pelvics to the lower origin of the caudal fin is longer than the interspace between the first and second dorsal fins in *polli* but shorter than the interdorsal space in *granulosus*; and that the base of the second dorsal fin is about ½ as long as the interdorsal space in *polli* but only about ⅓ that long in *granulosus*. Günther also describes the skin of *granulosus* as "granular", suggesting that its dermal denticles resemble the truncate denticles of *pusillus* (p. 240) rather than the thorn-like or bristle-like denticles of other members of the genus — except on the tail where he characterizes them as "minute spinelets." And he adds that the back of the tail is "naked" in *granulosus,* which is not the case in our specimens of *polli*.

Range. Specimens referable to *polli* have been reported only off the coast of tropical West Africa, between latitudes 5°39′S, and 11°53′S; from depths of 164 to 279 fathoms (300–510 meters, Poll, 1951, pp. 65–68, as *E. hillianus*). But the species must be decidedly common there, at the proper depth, for trawl hauls at 9 stations, by the Belgian expedition of 1948–1949 yielded 162 specimens, most of which, at least, were of this species.[48]

Etmopterus princeps Collett 1904
Figure 8

Our good fortune in obtaining the excellent series listed below, during the experimental trawlings carried out by the Woods Hole Oceanographic Institution on "Caryn" during the summer of 1949 and on "Cap'n Bill II" during the summer of 1952, enables us to add to Collett's original account of this species which was based on rather

[47]This is all we have to go upon.

[48]One specimen, at least, proves to be a *pusillus* (p.245, footnote 46), so it is possible that there may have been others of that species that were overlooked among the more numerous *polli*.

poor material. They also extend the known range of *princeps* to the western side of the North Atlantic.

Study material. Forty-seven specimens, 7½–24 inches (190–605 mm.) long, of both sexes, including a male with fully formed claspers; trawled on the continental slope off southern Nova Scotia, off Georges Bank and off southern New England, as above, at depths of 310–520 fathoms, between latitudes 42°39′ and 39°52′N, and between longitudes 63°58′ and 70°05′W.

Description. Proportional dimensions, in per cent of total length, of mature male 545 mm. long and female of 593 mm., both in Museum of Comparative Zoology.

Trunk at origin of pectoral: breadth 10.3, 12.2; height 7.9, 9.3.
Snout, length in front of: nostrils 1.1, 2.0; mouth 9.4, 9.8.
Eye: horizontal diameter 4.0, 4.0.
Mouth: breadth 7.9, 7.7.
Nostrils: distance between inner ends 2.8, 3.5.
Labial furrow length from angle of mouth: upper 4.4, 6.1.
Gill opening lengths: 1st 1.8, 2.0; 3rd 1.8, 1.7; 5th 1.6, 1.4.
First dorsal fin: vertical height 3.1, 3.4; length of base 5.1, 5.4.
Second dorsal fin: vertical height 4.6, 5.1; length of base 7.5, 7.6.
Caudal fin: upper margin 22.8, 22.0.
Pectoral fin: outer margin 9.7, 9.8; width 5.7, 6.9.
Distance from snout to: 1st dorsal 31.7, 34.3; 2nd dorsal 60.3, 60.6; upper caudal 77.2, 78.0; pectoral 21.6, 25.0; pelvics 53.7, 55.3.
Interspace between: 1st and 2nd dorsals 23.5, 20.9; 2nd dorsal and caudal 9.4, 9.8; pelvic base and caudal 14.7, 11.8.
Distance from origin to origin of: pectorals to pelvics 32.1, 30.4.

Trunk at first dorsal (where highest) about 1/7–1/8 as high as its length to origin of caudal fin, moderately flattened sidewise rearward from pectorals, its thickness at first dorsal about 3/5–3/4 its height there. Head flattened above, narrowed somewhat abreast of eyes, and noticeably broad; its width at level of corners of mouth and of first gill openings a little less than ½ (47%) as great as distance from snout to origin of pectorals; its length (to pectorals) between ⅕ and ¼ of total length in specimens in which the snout is not distorted. Tail sector from center of cloaca to origin of caudal fin about between ⅕ and ¼ as long as body sector (snout to cloaca) and 45–70 per cent as long as head to origin of pectorals.

Snout thick, fleshy (as usual in this genus), low-wedge shaped in

front with rounded tip, in specimen in which it is not distorted; its length in front of mouth 2/5–1/2 (39–50%) of length of head.[49] Eye about 2½ times as long as high, its horizontal diameter about 2/5 as long as snout in front of mouth opening. Spiracles about ⅓ as long as eye, at about level of eyes, and posterior to eyes by a distance about ⅔ as long as eye. Mouth very low-arched or nearly straight, its corners with short but conspicuous labial furrows extending inward about ⅓ of distance towards the respective symphysis, and continued rearward and outward, from each corner of mouth for a distance about as long as the eye. Nostrils close to front of snout, strongly oblique, about as long as eye; inner anterior margin expanded as a broadly triangular flap with blunted tip, crossing outer part of nasal aperture. First to third gill openings ⅓–½ as long as eye, the fifth a little shorter. Anterior margins of first to third gills so deeply concave that the tips of the respective gill filaments are more or less exposed to view, at least on large specimens.

Teeth smooth edged; $\frac{32}{50}$ in adult male of 545 mm.; $\frac{30}{40}$ in male of 404 mm.; $\frac{29}{48}$ in female of 593 mm.; a range suggesting that the number tends to increase with growth; the lower jaw with or without a median tooth. Upper teeth mostly with 5 cusps in adults, the median cusp much the largest, the outermost much the smallest; those of middle sized specimens either with the outer pair of cusps minute, or with only 3 cusps; small specimens with 3 cusps only. Lower teeth with cusps directed outward at an angle of as much as 70–75° in some cases, in others almost parallel with jaw, the inner margins of successive teeth together forming a nearly continuous cutting edge; those toward corners of jaws much smaller than those along central part.

Dermal denticles low, thorn-like, with slightly blunted tip, and nearly erect except with points turning a little rearward; more or less prominently striate longitudinally, on quadri-radiate bases that are mostly hidden in the skin; the denticles so sparsely distributed that the skin is exposed between them, the arrangement random over the anterior part of the trunk, but giving place to longitudinally linear arrangement on caudal peduncle and out along caudal fin. On adults the entire trunk, including the skin around the gill openings, and between them, is rough with denticles except for the area between the nostrils on the lower side of the snout which is sparsely denticulate,

[49] On one of our larger specimens, an adult male of about 545 mm., the tip of the snout is shrivelled, having dried by accident; hence it is now shorter than when the specimen was first taken; see legend to Figure 8.

or on some specimens naked, and along the upper lip, which is naked and velvety to the touch. On half-grown specimens and smaller this naked labial belt is broader, the internarial area is wholly naked, and the mid-belt of the lower side of the snout thence rearward may bear only a few scattered denticles. In this case, the pattern of mucous pores (obscured by the denticles on adults) is clearly visible. All but the outermost zone of the pectoral, dorsal and pelvic fins is rough with denticles, also the upper side of the caudal out to its margin. But the lower side of the caudal, outward from the caudal axis, is mostly naked. The fins are of the ordinary type, i.e. the margins not normally fringed, though very thin and more or less frayed out on all the specimens we have seen. First dorsal of usual etmopterid shape, its base about ¼–⅓ (average 30% on four specimens) as long as interspace between first and second dorsals; its origin posterior to a perpendicular at axils of pectorals by a distance between ¼ and ⅓ as long as interspace between dorsals. Interspace between dorsals from a little shorter to a little longer than head. Base of second dorsal about 1½ times as long as base of first dorsal, including the respective fin spines (1.4 times on 545 mm. male); distal margin weakly concave, free lower margin about as long as anterior margin from point of emergence of fin spine. Second dorsal spine about twice as long as first dorsal spine, its origin slightly but definitely posterior to rear ends of bases of pelvics. Interspace between second dorsal and origin of caudal ⅖ to about ½ (40–47%) as long as interspace between first and second dorsals. Caudal about as long (0.9–1.1 times) as head and about as long (0.97–1.05) as interspace between dorsals; about ⅓ as broad as long, with definite lower anterior corner, not, however, extended as a separate lobe; lower posterior outline slightly sinuous with well marked subterminal indentation, the tip obliquely truncate. Pelvics a little longer at base than base of second dorsal; rear pelvic corners angular. Pectoral with nearly straight anterior margin merging into moderately rounded distal inner margin around to axil; extreme length of pectoral from origin about ⅓ to a little less than ½ (33–44%) as great as length of head, its base, from origin to axil, about as wide as from tip of snout to level of center of eye. Claspers of mature males moderately stout, attached to the pelvic fins very nearly to the tips of the latter, and extending only a little beyond; tips of the claspers widely expanded when in function, with 4 sharp thorns, one of them covered with skin. On one mature male (Fig. 8) the left-hand clasper, with its thorns, is spread, exposing the orifice of the sperm channel, but the tip of the

other clasper is closed and conical, with the thorns concealed entirely.

Color. The trunk, as a whole, of half-grown specimens and adults is very dark, blackish brown, or uniform black; the belly is somewhat darker than the back on some specimens after preservation in alcohol, but not on others; no definite flank mark. The outer parts of all the fins are about as dark as the trunk (if the pigmented skin has not been rubbed off by rough treatment) except that the lower rear corner of the second dorsal fin is whitish over a larger or smaller area on some partly grown specimens, perhaps on all, though not on adults. The anterior surface of the outer part of each gill arch (exposed by the deeply excavated anterior contour of the respective gill opening), is whitish; the teeth white and therefore conspicuous against the sooty or black lining of the mouth; the lining of the body cavity sooty or black. It is interesting that no trace is to be seen of the rows of dark dots and dashes, or of the pale interocular spot, that characterize various other members of the genus.

Size. A male, about 545 mm. long, appears to be fully mature sexually, which suggests that the original specimens, about 750 mm. long, from the Faroe region, were about as large as the species grows.

Luminescence. There is no reason to suppose that *princeps* is luminescent — at least we have seen no evidence of light emission by any of the specimens that we have handled while they were still alive.

Remarks. Comparison of our series of *princeps* with two specimens of *spinax* from Norway and two from the Mediterranean, in good condition, bears out Collett's (1904, 1905) belief that the former differs from the latter in a wider head relative to the length of the snout, in longer gill openings, in shape of dermal denticles, and in color. Thus the breadth of the head is 1.2–1.4 times as great as the length of the snout (to the mouth) in four *princeps*, but only about as great as the length of the snout in the four specimens of *spinax;* the longest gill openings are ⅓–½ as long as the eye in *princeps* but about $^1/_7$–⅓ only in the *spinax;* the conical, thorn-like denticles of *princeps* differ noticeably from the bristle-like denticles of *spinax;* and none of our *princeps* show any trace of the black flank marks to be seen on the rear part of the sides in *spinax*, more or less conspicuously, depending on whether the color of the upper parts of the specimens examined has faded.

Superficial examination is all that is needed to distinguish *princeps* from all the remaining North and Tropical Atlantic species of its genus. The most conspicuous features marking it off from *hillianus,*

and from *virens* are its uniformly black or blackish brown color, without definite flank markings, and its large gill openings; likewise the much greater length to which it grows. Its short thorn-like denticles mark it off further from *hillianus*, and a relatively much shorter tail sector of its trunk from *virens*. It resembles *pusillus* and the new species *schultzi* (p. 252) and *polli* (p. 241) in its uniformly dark coloration. But a much shorter caudal fin, longer gill openings, much larger size at maturity, fins that are not fringed normally, and short, thorn-like denticles separate it from *schultzi;* its conical thorn-like denticles, a caudal fin at least as long as the head, the shape of the caudal and a more rounded pectoral separate it from *pusillus*.

Turning now to the species of *Etmopterus* that have been named from more distant seas, we find *princeps* set apart from *E. paessleri* by the teeth and dermal denticles — if, indeed, *paessleri* falls properly in this genus at all (p. 238); from *villosus* by the position of its first dorsal fin nearer to the spiracles than to the second dorsal (nearer to the second dorsal than to the spiracles in *villosus*); from *brachyurus*[50] by a much shorter tail sector of the trunk as compared with the body sector; from *lucifer* similarly by a much shorter tail sector, as well as by uniformly dark coloration, with neither black flank marks nor pale interocular spot. *Princeps* appears to agree very closely indeed with *granulosus* in relative dimensions, as it also does in color. But, to judge from Günther's (1880, p. 19) description, which is all we have to go upon,[51] the dermal denticles on the anterior part of the body of *granulosus* ("granules") differ in shape from those on the tail, where he characterized them as "in the form of minute spinules." That is to say, they reproduce the condition to be seen in *pusillus* rather than the condition in *princeps*, where the denticles are conical thorn-like on the posterior part of the sides as well as anteriorly. We cannot carry our comparison farther, lacking either a detailed description of *granulosus* or specimens of the latter, for comparison with *princeps*.

Habits. Evidently *princeps* is confined to deep water, recorded depths for it being 310–520 fathoms in the Western Atlantic, 410–602 fathoms in the region of the Faroes and Hebrides, and 1134 fathoms off the Straits of Gibraltar.

Range. The recent captures, listed above, extend the known range of

[50] As described and pictured for the type specimen of *brachyurus* by Smith and Radcliffe (1912, p. 679, Pl. 52) and by Fowler (1941, p. 249).

[51] The dermal denticles of *granulosus* have not been figured either by Günther (1880) or by Barnard (1925).

E. princeps from the Faroe-Hebrides region, and from the offing of the Straits of Gibraltar to the Western Atlantic slope off southern Nova Scotia, off Georges Bank and off southern New England.

Etmopterus schultzi, n. sp.
Figure 9

Type. Male, 270 mm. long, "Oregon" Sta. 279, Lat. 29°11′N, Long. 86°53′W; 305 fathoms, February 24, 1950 (U. S. Nat. Mus. No. 113,381). Also 38 males and females, 195 to 300 mm. long, from "Oregon" trawlings in northern part of Gulf of Mexico, 220 to 400 fathoms.[52]

Description. Proportional dimensions, in per cent of total length, of male of 270 mm. (type) and female, 255 mm.

Trunk at origin of pectoral: breadth 9.6, 10.2; height 7.8, 9.0.

Snout length in front of: outer nostrils 1.5, 1.6; mouth 9.4, 9.1.

Eye: horizontal diameter 4.8, 5.1.

Mouth: breadth 7.8, 7.5.

Nostrils: distance between inner ends 3.3, 3.1.

Labial furrow length: 4.1, 4.3.

Gill opening lengths: 1st 1.1, 1.6; 2nd 1.1, 1.6; 3rd 1.1, 1.6; 4th 1.1, 1.6; 5th 1.1, 1.6.

First dorsal fin: vertical height 2.6, 2.3; length of base 4.5, 4.3.

Second dorsal fin: vertical height 5.5, 5.1; length of base 8.2, 8.6.

Caudal fin: upper margin 25.5, 23.0.

Pectoral fin: outer margin 7.4, 7.5; inner margin 3.9, 4.3; width 5.9, 5.5.

Distance from snout to: 1st dorsal 31.1, 32.9; 2nd dorsal 54.1, 55.7; upper caudal 74.5, 77.0; pectoral 21.1, 19.6.

Interspace between: 1st and 2nd dorsals 18.5, 18.5; 2nd dorsal and caudal 12.2, 13.0; base of pelvics and caudal 15.2, 12.6.

Distance from origin to origin of: pectorals to pelvics 29.6, 33.3.

Trunk thickest opposite pectorals, narrowing rather evenly rearward, its height at first dorsal (where highest) about 15 per cent as great as its length to origin of caudal. Head about 28 per cent of trunk to caudal; body sector (snout to center of cloaca) about 3½

[52] "Oregon" Station 270, Lat. 29°23′N, Long. 82°25′W, 220 fath., Feb. 17, 1950; Sta. 271, Lat. 29°24′N, Long. 86°56′W, 300 fath., Feb. 18, 1950; Sta. 279, Lat. 29°11′N, Long. 86°53′W, 305 fath., Feb. 24, 1950; Sta. 319, Lat. 29°20′N, Long. 87°25′W, 315 fath., April 28, 1951; Sta. 321, Lat. 29°27′N, Long. 87°19′W, April 28, 1951; Sta. 482, Lat. 28°57′N, Long. 88°43′W, 210 fath., Sept. 7, 1951; Sta. 542, Lat. 27°41′N, Long. 94°59′W, 250–300 fath., April 16, 1952; and Sta. 549, Lat. 26°59′N, Long. 96°07′W, 300–400 fath., April 18, 1952.

times as long as tail sector from center of cloaca to origin of caudal. Head flattened above, slightly narrowed at eyes, its breadth abreast mouth and first gills about 1.4–1.5 as great as distance from front of snout to mouth. Snout thick, fleshy, soft, obtusely rounded in front, its length in front of mouth a little less than ½ (44%) of head to origin of pectorals. Eye about twice as long as high, its horizontal diameter about ½ (51%) as long as snout in front of mouth. Spiracles about ¼ as long as eye; a little above horizontal axis of eye, and behind latter by a distance about ⅕ (22%) as long as eye. Nostrils very close to anterior margin of snout, as characteristic of the genus; about ½ as long as eye; anterior (inner) margin expanded as a narrow pointed lobe crossing nasal aperture; inner subdivision of nasal aperture about twice as long as outer subdivision. Mouth very low arched, the gape occupying about ⅔ of breadth of head; labial furrows reaching inward about ⅕ of distance toward symphysis; extended as a conspicuous furrow outward and rearward beyond corner of mouth for a distance about 45 per cent as long as eye. Gill openings about ⅛ as long as distance between nostrils, and about ¼ as long as eye (about ⅓ as long in specimen of 254 mm.)[53], their anterior outlines concave, but not enough so as to expose the tips of the gill filaments.

Teeth smooth edged, $\frac{38}{32}$ in type specimen, $\frac{32}{32}$ in female of 254 mm.; uppers mostly with 7 cusps, a few with 8 (4 laterals on the one side, 3 on the other), a few with only 5 or 6; median cusp considerably the longest and stoutest, the lateral cusps on each side graded in length outward. Lower teeth with the cusp directed so strongly outward as to form a practically unbroken cutting edge approximately parallel with the jaw. Dermal denticles minute, bristle-like, curving so strongly rearward that the distal half of their length is approximately parallel with the skin; the tips hair-fine, and flexible; the bases quadriradiate, but mostly concealed in the skin. The denticles are close spaced over the trunk as a whole, including the entire lower surface of the head, excepting only along the upper and lower lips;[54] in random distribution, not in linear arrangement anywhere. All the fins, also, are closely denticulate out very nearly to the fringed marginal zone (Fig. 9E).

Base of first dorsal fin about ¼ (24%) as long as interspace between first and second dorsals; its upper contour rounded, the free lower margin about ⅔ as long as the base; its origin posterior to axils of

[53] The softness of the skin makes precise measurements difficult.

[54] On specimens preserved in alcohol the denticles are so covered with coagulated mucus that it is necessary to scrub them clean, to expose their shape and arrangement.

pectorals by a distance about as long as from corners of mouth to origins of pectorals. Interspace between first and second dorsals nearly as long as head, and a little less than ¾ (74%) as long as caudal fin. Second dorsal about 1½ times as large as first dorsal in linear dimensions, its anterior margin nearly straight, distal margin weakly concave, apex bluntly angular; free lower margin about as long as anterior margin from point of emergence of fin spine; origin about even with rear ends of bases of pelvics. Second dorsal spine extending out nearly to level of apex. Interspace between second dorsal and caudal about ⅔ (66%) as long as interspace between first and second dorsals. Caudal about 1.2 times as long as head, and 1.4 times as long as interspace between first and second dorsals; about 3½ times as long as broad, its tip rounded; the lower rear margin increasingly concave toward tip but without definite subterminal notch; lower anterior corner a little more obtuse than a right angle, not produced as a lobe; lower anterior edge nearly straight. Interspace between lower origin of caudal and rear ends of bases of pelvics about ½ as long as interspace between rear ends of bases of pelvics and axils of pectorals. Pelvics subquadrate, their anterior and distal margins nearly straight; anterior margin about as long as base. Pectorals with weakly convex anterior margin, grading insensibly into broadly and evenly rounded distal and inner margins around to axil; maximum length of pectoral about 2/5 as great as distance from snout to level of first gill openings, the rear margin falling considerably short of the first dorsal spine when the pectoral is laid back.

The outstanding feature of the species is that the outer ends of the horny terminal rays (ceratotrichia) of all the fins are not only thicker than in other species of the genus, but are free from the skin so that they form a conspicuous fringe. Since this is true of all the specimens examined, though some of them were still alive when we first handled them, we see no reason to doubt that this is the normal state. But the fact that the edges of the skin, whence the rays emerge, are somewhat ragged in varying degree from place to place, suggests that the fringe-like conditions may be a growth character. However, we have not been able to check the state of the fins either on unborn embryos, or even on very young free-living specimens. In the case of the pectorals, the fringe around the distal margin occupies about ⅕–⅙ of the length of the fin, grading down to nothing at origin and axil. The fringe is narrower (hence less conspicuous) on the dorsals and pelvics; very narrow indeed along the upper edge of the caudal, though it is evident

even there on close examination.

Color. Back and upper parts of sides very dark sooty gray, with brownish cast, the top of the head with a vaguely outlined pale yellowish spot between the eyes; the belly black. On specimens preserved in alcohol the line of demarkation between the slightly darker belly and the slightly paler sides above is rather definite in most cases. On the type specimen — when slightly dried — the black of the lower surface extends upward and forward as a vaguely outlined band on either side above the paler base of the respective pelvic fin, reminiscent of the much more conspicuous and more definitely outlined black flank mark to be seen on several other members of the genus, such as *virens*, *lucifer*, *spinax* and *polli*. But some other specimens, which seem to have retained their normal coloration better, show no sign of this. The lower margin of the caudal axis, near the tip, is narrowly edged with black. The fins otherwise are paler generally than the trunk, except that the tip of the caudal is dark-margined at least on some specimens. Other than that, the free rays that edge the fins are colorless and nearly translucent so that the marginal fringe of the pectorals shows whitish against the dark sides when the fins are laid back. Faded specimens also show two irregular lines of short, very narrow, black dots and dashes along each side, the upper row extending from over the origin of the pectoral fin back to about opposite the tip of the second dorsal, the lower row from abreast the tip of the pectoral back about halfway toward a perpendicular at the origin of the pelvics. There also are a few black dots on the top of the head and others, wide spaced, in a single row along the mid-line of the back rearward to the caudal peduncle. But these black markings are so obscured by the generally dark color that those on the sides are discernible only here and there on the type, or on other specimens that have retained their color, while the dorsal dots are not to be seen on them at all. The teeth are white; the lining of the mouth is sooty to black, and the lining of the body cavity as well.

Size. A female 275 mm. long contains several large eggs (apparently not fertilized), and the claspers of the type specimen, of 270 mm., appear to be nearly full grown, suggesting a maximum length perhaps not much greater than 300 mm.

Luminescence. The black dots and dashes on the back and sides bear so close a resemblance to those of *E. spinax* and of *E. lucifer*[55] as to

[55]See Johann (1899, p. 136–160, Pls. 10, 11) for the luminescent organs and luminescence of *spinax;* Oshima (1911, p. 1) for *lucifer*.

suggest that they are luminescent in *schultzi* also. But we saw no sign of light emission by any of the specimens, even when first taken from the trawl.

Remarks. E. schultzi falls with *E. princeps* and with *E. pusillus*, among North Atlantic species, in its nearly plain dark coloration. But it differs conspicuously from *princeps* in a relatively much longer caudal fin, also in its fringed fins, in its bristle-like denticles, and in much smaller size at maturity; also in having the pale interocular spot which *princeps* lacks; from *pusillus* (with which it shares a uniformly denticulate internarial region and the pale interocular spot) in a considerably longer caudal, from both *princeps* and *pusillus* in its fringed fins and its soft, bristle-like dermal denticles. The nature of its denticles would seem to ally it to *spinax* and to *hillianus*, if this be regarded as a primary specific character. But it differs from both of these in its fringed fins; also in its plain coloration; further from *hillianus* in a much shorter tail sector of the trunk relative to the body sector; from *spinax* (which it resembles more closely in its proportional dimensions) in rounded pectorals, their outer margins falling far short of the first dorsal spine when the pectorals are laid back; and in that it lacks the black flank marks which are visible on *spinax* even in fresh specimens on which the back and sides are nearly as dark as the belly.[56] A relatively much longer caudal fin separates *schultzi* quite obviously from the new species *E. polli* (p.241); its lack of black flank marks is an equally precise differential character, though one less conspicuous, for these black markings are not easy to see on *polli* though regularly characteristic of that species.

Plain coloration, without conspicuous flank marks, combined with its bodily proportions, seem to ally *schultzi* the most nearly to *granulosus* and to *brachyurus*, among species of its genus of other seas. But its caudal fin is considerably longer, relatively, and the tail sector of its trunk relatively much shorter than those of *brachyurus;* while a longer caudal plus the fact that the space between its nostrils is denticulate separate it from *granulosus*. And there is nothing in the published accounts of *brachyurus* or of *granulosus* to suggest that the fins are fringed normally in either of these species, as they are in *schultzi*.[57]

[56]See Smitt (1895, p. 1163, Pl. 51, fig. 3) for description and excellent colored illustration of *spinax*.

[57]For descriptions and illustrations of *granulosus*, see Günther, 1880, p. 19, Pl. 2, fig. C; Barnard, 1925, p. 49; 1927, Pl. 2, fig. 8; and Smith, 1949, p. 58, fig. 50. For *brachyurus* see Smith and Radcliffe, 1912, p. 679, Pl. 52; and Fowler, 1941, p. 248.

Habits. Evidently this little shark is confined to water at least moderately deep, for the captures were all made at depths of between 210 and 400 fathoms. Beyond this, all that we know of its habits is that its food includes squids (field notes).

Range. So far known only from the northern part of the Gulf of Mexico, between latitudes 26°59′ and 29°20′N; and between longitudes 82°25′ and 96°07′W ("Oregon" Stations 270, 271, 279, 319, 321, 482, 542, 549). *E. schultzi* must be decidedly common at appropriate depths in this part of the Gulf for the total number of specimens taken was more than one hundred, of all sizes (field notes).

Etmopterus virens, n. sp.
Figures 6D, 10

Type. Adult male 203 mm. long, "Oregon" Sta. 501, northern part of Gulf of Mexico, Lat. 29°52′N, Long. 91°33′W, 220 fathoms, Dec 11, 1951; U. S. National Museum No. 160,859. Also 42 others, males and females, including an embryo ready for birth, from the same general region, "Oregon" Stations 321, Lat. 29°27′N, Long. 87°19′W, 220 fathoms; Sta. 351, Lat. 29°13′N, Long. 88°00′W, 200 fathoms; Sta. 382, Lat. 29°12′N, Long. 88°08′W, 190–210 fathoms; and Sta. 489, Lat. 27°44′N, Long. 85°09′W, 254 fathoms; in U. S. National Museum and Museum of Comparative Zoology.

Description. Proportional dimensions, in per cent of total length, of male of 203 mm. (type) and female, 153 mm.

Trunk at origin of pectoral: breadth 8.8, 7.8; height 8.4, 7.2.

Snout length in front of: outer nostrils 1.7, 2.0; mouth 11.1, 10.5.

Eye: horizontal diameter 5.7, 5.2.

Mouth: breadth 7.6, 6.9.

Nostrils: distance between inner ends 3.5, 3.3.

Labial furrow length: 4.0, 3.9.

Gill opening lengths: 1st 1.0, 1.0; 2nd 1.0, 1.0; 3rd 1.0, 1.0; 4th 1.0, 1.0; 5th 1.2, 1.3.

First dorsal fin: vertical height 2.5, 2.6; length of base 4.4, 4.6.

Second dorsal fin: vertical height 4.9, 3.9; length of base 6.9, 6.5.

Caudal fin: upper margin 23.2, 24.2.

Pectoral fin: outer margin 10.6, 9.5; inner margin 5.4, 5.2; width 7.4, 6.9.

Distance from snout to: 1st dorsal 32.5, 30.7; 2nd dorsal 55.6, 53.5; upper caudal 76.8, 75.8; pectorals 23.1, 21.5; pelvics 46.8, 47.0.

Interspace between: 1st and 2nd dorsals 18.7, 18.3; 2nd dorsal and caudal 14.3, 15.7; base of pelvics and caudal 21.2, 20.1.
Distance from origin to origin of: pectorals to pelvics 23.6, 25.4.

Body thickest at pectorals, narrowing rearward to thin caudal peduncle, its height at first dorsal (where highest) about 15 per cent as great as length of trunk to origin of caudal; its thickness at first dorsal about 75–80 per cent as great as its height there. Breadth of head at corner of mouth about as great as length of snout to mouth. Head to origin of pectorals a little more than ¼ (30%) of trunk to origin of caudal fin, its length about 1.2 times as great as length of interspace between first and second dorsals. Body sector, to cloaca, about 2.3 times as long as tail sector from cloaca to origin of lower caudal. Head flattened above, the nape elevated a little. Snout fleshy, its anterior contour forming an angle of about 90° with broadly rounded apex, its lateral outlines narrowed a little abreast of eyes, the pattern of mucous pores on its lower surface visible thanks to the nakedness of the skin there (see below, p. 259). Eyes about 1.7 times as long as high, and about ½ as long as snout to front of mouth Spiracles about ⅓ as long as eye, a little above mid-level of eyes, and behind latter by a distance about ⅓ as great as length of eye. Nostrils close to anterior margins of snout as usual in this genus, about 60 per cent as long as eye, only slightly oblique, the lobe-like expansion of the inner anterior margin slender (even more so than in *E. schultzi*,) reaching across nasal aperture; inner subdivision of latter about twice as long as outer subdivision. Mouth very little bowed, occupying about 4/5 breadth of head, the labial furrows reaching inward only about 28 per cent of distance toward the respective symphysis, and each extending rearward and outward from corner of mouth as a well marked furrow for a distance about ⅔ as long as horizontal diameter of eye. First to fourth gill openings between ¼ and ⅓ (29%) as long as distance between inner ends of nostrils and about ⅕–⅙ as long as eye; anterior margins concave but not enough so as to expose the gill filaments to view; fifth gill opening 1.2 times as long as first-fourth gills.

Teeth smooth edged, $\frac{34}{32}$ in type specimen, $\frac{29}{24}$ in female of 153 mm.; no median tooth in lower jaw in either case; upper teeth mostly with 5 cusps, occasionally with only 4 (1 lateral cusp on the one side, 2 on the other), the median cusp much the longest, the outermost cusp on each side very small. Lower teeth with cusps directed so strongly outward, toward the corner of the mouth, that the inner edges of the

functional row form an almost continuous cutting edge parallel with the jaw. Dermal denticles low, conical to thorn-like, moderately to strongly curved rearward, recalling those of *E. princeps* (p.248,Fig. 8E), and of *E. lucifer*, rather than those of *hillianus*, of *spinax*, or of *schultzi* (p. 253);on moderately expanded quadri-radiate bases more or less concealed in the skin; the denticles rather sparsely distributed on anterior parts of trunk in general in random arrangement, but with indefinite indications of a linear arrangement on sides rearward from level of second dorsal; more closely crowded on lower part of the sides and on the black dotted area of the abdomen than above. Skin on lower surface of snout as a whole back to mouth naked (an important specific character); likewise lower lip as well as skin in region of gill openings. Caudal fin rather densely denticulate along fleshy axis but naked along margins; the other fins denticulate only close in to their bases.

The fins are of the ordinary type, i.e. the margins not regularly fringed, but with edges so delicate that they are more or less frayed on all our specimens. First dorsal fin evenly rounded along anterior upper margin; its base nearly as long as the eye, its free lower margin about as long as base, its rear corner rounded, its origin (first sensible elevation above general profile of back) posterior to origins of pectorals by a distance about as long as from spiracle to fifth gill opening. Interspace from rear end of base of first dorsal to first sensible elevation of second dorsal about as long as from snout to second gill opening; or about ¾ as long as upper side of caudal fin. Anterior edge of visible base of second dorsal spine posterior to rear ends of bases of pelvics by a distance about ⅔ as long as eye on adult as illustrated by the type, but very close behind rear ends of pelvic bases on small specimens. Posterior margin of second dorsal fin deeply concave, its rear corner slenderly pointed, the free lower margin a very little shorter than the eye, the base (measured from anterior base of spine) about as long as from spiracle to second gill opening, and about 1.4 times as long as base of first dorsal measured from anterior base of spine. Distance from rear end of base of second dorsal to origin of upper side of caudal about as long as from tip of snout to rear of eye, or about ¾ as long as interspace between first and second dorsals. Caudal about as long as head to origin of pectorals, its axis only slightly raised, its extreme breadth a little less than ⅓ as great (29–30%) as its length; its upper outline weakly convex, increasingly so rearward; the tip obliquely truncate with rounded corner; lower posterior margin moderately con-

cave, without definite subterminal notch; the lower anterior corner rounded, a little produced; lower anterior margin weakly convex, about as long as from spiracle to fifth gill opening. Distance from origin of lower side of caudal fin to rear ends of bases of pelvic fins about $^{9}/_{10}$ as long as head to origins of pectorals, and a little longer than distance from origins of pelvics to axils of pectorals. Bases of pelvics about as long as base of first dorsal; the margins nearly straight, the outer anterior corner rounded, the rear corner narrowly pointed; rear end of bases of pelvics definitely anterior to anterior base of second dorsal spine on type specimen, but only slightly so on small specimens. Pectorals nearly square-tipped, with rounded corners reaching when laid back nearly or quite to a perpendicular at base of first dorsal fin-spine; anterior margin of pectoral slightly convex, inner margin rather strongly so to axil; base strongly oblique, about $^{2}/_{3}$ (68–69%) as wide as anterior margin of pectoral. Claspers of mature male cylindrical, free only at their extreme outer ends from inner margin of pelvic fin, the tip with three hard thorns.

Color. Perhaps the most striking feature of this new species is its pattern of darker and paler markings, easier represented pictorially (Figs. 6D, 10) than described verbally. In general, the upper parts of the trunk are sooty brown above the level of the origins of the pectoral fins, darkest along the back, but interrupted on each side by two narrow longitudinal stripes of pale bluish gray, the one stripe high up on the side, bowing down a little below the second dorsal fin and reaching forward to over the first gill opening; the other stripe (paler and hence more conspicuous) running rearward from close behind the upper end of the base of the pectoral fin past the base of the respective pelvic fin where it unites with the upper longitudinal pale stripe. The members of the lower pair of pale stripes (one on each side) are interconnected across the black belly by a pale belt close in front of the pelvics (conspicuous in ventral view); also by a pale area of considerable extent behind the pelvics. There also is a pale yellowish oval spot on the upper surface of the head between the orbits (as in *pusillus*, in *hillianus*, in *schultzi* and in *polli*). The region of the gill openings is pale brownish gray; so, too, are comma-shaped patches extending downward from before and behind the gill openings; there is a pale oval patch behind each eye, and a considerable pale area on the lower surface of the rear half of the tail sector of the trunk. Contrasting sharply with these pale areas, the lower surface of the snout is very dark bluish gray or blue black; the lower surface of the head,

rearward from the mouth, is black, as is the belly also, back to the pelvics (except for the pale cross belt just mentioned). Other conspicuous black markings are: (A) a flank mark, in the form of a bar that extends above the pelvic along each side, forward to about even with the origin of the pelvics and rearward about as far as the rear end of the base of the second dorsal, with the flank marks of the two sides joining to form a black belt crossing the lower surface of the trunk a little rearward from the pelvics; (B) a second belt crossing the lower surface of the tail sector of the trunk a little in front of the origin of the caudal fin, and extending rearward along each side in the shape illustrated (Figs. 6D, 10); and (C) a narrow stripe on either side along the lower edge of the caudal axis near the tip of the latter. The tip of the caudal fin is blackish, also, as is its lower anterior corner. But the other fins as a whole are pale gray, and with their outer parts translucent. The lining of the mouth is sooty to black, also the lining of the body cavity; the teeth are white. One of the most interesting characteristics of *virens* is that the belly of fresh-caught specimens shines with bright green iridescence, hence the name we propose for it. But this is entirely lost after preservation in alcohol.

The dark hue of the upper parts of *virens* in general, of the lower surface of the snout, and of the corners of the caudal fin is due to ordinary pigmentation. But the dark hue of the lower surface rearward from the mouth to the pelvics, and of the markings on the sides on the tail sector of the trunk result chiefly from the presence of great numbers of inky black depressions of the skin, irregularly roundish in shape, and of various sizes, but large enough on the whole and loosely enough scattered, to be visible individually under an ordinary hand-lens. The paler skin between them is richly provided, too, with much smaller black spidery chromatophores. And the black peritoneum, showing through the body wall, plays its part, likewise, in producing the black of the belly. Besides the broad-scale black areas just outlined, each side of the trunk is marked from the origin of the pectoral fin back to the origin of the caudal fin, with a complex series of black dots and narrow black dashes as follows: A) in a longitudinal row (double for part of its length) following the upper edge of the lower of the two pale side stripes from close to the axil of the respective pectoral fin to above the origin of the pelvic fin; B) in a shorter longitudinal row midway up each side, from below the first dorsal fin to above the origin of the pelvic fin; C) in a double row running along, close above the upper pale side stripe from below the first dorsal fin

to below the rear end of the base of the second dorsal whence it continues rearward as a single row as far as the origin of the caudal fin. There also are two groups of longitudinal black dashes on each side of the head between the eye and the first gill opening, the one group behind the other, with each group consisting of 3 dashes, one above another. Small specimens also have a mid-dorsal row of dots (the successive dots so close together as to form a nearly continuous line) extending forward from the origin of the first dorsal fin nearly as far as the spiracles; also a loose cluster of black dots close behind the pale interocular spot, with another such cluster in front of the latter and partially enclosing it. But the heads of the larger specimens show only faint traces of these mid-dorsal markings.

Microscopic examination shows that each of these black dots and dashes actually represents either a pit or a trough-like depression of the skin, in which they agree with the similar black markings on the sides and back of *E. spinax* and of *E. lucifer*.[58]

Size. The facts that the claspers of the type specimen 203 mm. long, and those of another male of 225 mm. appear to be fully formed and in functional condition, and that a female of 230 mm. contained an embryo 45 mm. long and about ready for birth show that this is one of the smallest of known sharks, and suggest a maximum length perhaps not greater than 300 mm.

Luminescence. The black pits and furrows on the back and sides of *E. virens*, like the similar structures on *E. schultzi* (p. 255) recall the luminescent organs of *E. spinax* and of *E. lucifer* (p. 255, Footnote). And while we saw no signs of the emission of light by *virens*, any more than by *schultzi* (p. 256), the possibility remains that they may so function, for the specimens that were in the best condition were all taken during the daytime.

Remarks. Among North Atlantic species, *virens* falls the most nearly with *hillianus* in its proportional dimensions and in its color. But it differs quite sharply from *hillianus* in its low, conical denticles (bristle-like in *hillianus*); in the nakedness of the skin on the lower surface of its snout and in the region of its gill openings (rough with denticles in *hillianus*); and in a shorter snout, the distance from its tip to the level of the spiracles being about as long as from spiracles to axils of the pectorals in *hillianus*, but only about as long as from spiracles to origins of pectorals in *virens*. A still more conspicuous difference lies in the shapes of the black markings on the sides of the rear part of the

[58] See footnote 55, p. 255.

trunk in the two species (Fig. 6), while the freshly taken specimens of *hillianus* that we have seen showed no trace of the green iridescence that is so conspicuous a feature of the belly of fresh-caught *virens* (p. 261). Among species of *Etmopterus* from other seas, *virens* falls the nearest to *lucifer* in the great length of the tail sector of its trunk, and in its color pattern. But it differs from *lucifer* a) in lower and stouter dermal denticles; b) in a longer caudal fin (about 1.3 times as long as interspace between first and second dorsals in *virens;* only about 90 per cent as long as interspace between dorsals in *lucifer*); c) in the shape of its nasal flap (Fig. 10C), that of *lucifer* being broadly triangular, i.e. more nearly as it is in *princeps* (Fig. 8C); d) more conspicuously in the shapes of the black markings on the posterior part of the trunk (Fig. 6).

Habits. All that is known of the habits of this little shark is that it appears to be confined to at least moderately deep water, all the specimens yet seen having been trawled between 190 fathoms and 254 fathoms; and that it feeds on squids.

Range. Known only from the northern side of the Gulf of Mexico, at the stations listed (p. 257); but evidently quite common there, at suitable depths, for we saw more than a hundred specimens taken from the trawl, of all sizes.

BIBLIOGRAPHY

Alcock, Alfred

1898. A note on the deep sea fishes . . . Ann. Mag. Nat. Hist. ser. 7, vol. 2, pp. 136–156.

1899. Fishes, Part 6, Pl. 26, fig. 3; *in* Ills. Zool. H. M. Indian Marine Surveying Steamer "Investigator" . . . Calcutta.

Archey, Gilbert

1921. A new species of shark. Trans. New Zealand Inst., vol. 53, pp. 195–196, pl. 39.

Barnard, K. H.

1925. A monograph of the marine fishes of South Africa, Part 1. Ann. S. Afr. Mus., vol. 21, part 1, 418 pp.

1927. A monograph of the marine fishes of South Africa, Part 2. Ann. S. Afr. Mus., vol. 21, part 2, pp. 419–1065, 37 pls.

Bigelow, Henry B. and W. C. Schroeder

1944. New sharks from the Western North Atlantic. Proc. New England Zool. Club, vol. 23, pp. 21–36.

1948. Fishes of the Western North Atlantic, Chap. 3, Sharks. Mem. Sears Found. Mar. Res., no. 1, part 1, pp. 59–576.

Blainville, H. M. D. de

1825. Poissons, *in* Faune Française, 96 pp., 22 pls.

Bleeker, Pieter

1860. Elfde Bidjdrage tot de Kenntnis der Vischfauna van Amboina. Verhand. [Act.] Soc. Sci. Ind. Neerland., vol. 8, no. 5, p. 3.

Bloch, M. E. and I. G. Schneider

1801. Systema Ichthyologiae, . . . , L + 584 pp.; Atlas, 110 pls.

Bocage, J. V. Barboza du and F. de B. Capello

1864. Sur quelques éspeces inédites de Squalidae . . . Proc. Zool. Soc. London, 1864, pp. 260–263.

1866. Notes pour Servir a l' Ichthyologie du Portugal. Poissons Plagiostomes, Part 1. 40 pp., 3 pls., Lisboa [French and Portuguese].

Bonaparte, C. L.

1838. Selachorum tabula analytica. Nuov. Ann. Sci. Nat. Bologna, vol. 2, pp. 195–214. Also as Mem. Soc. Sci. Neuchatel, vol. 2, 1839, no. 4, pp. 1–12.

1841. Text, to Pl. [57], *in* Iconographia faune Ital., vol. 3, Pesci.

BONNATERRE, [P. J.]

1788. Ichthyologie, in Tab. Encyc. Méthod. Troi règnes de la Nature, lvi, 215 pp., pls. A, B, + 1–100. Paris.

BRAGANZA, CARLOS DE

1904. Resultados das investigações scientificas . . . do Yacht "Amelia", Part 2, Ichthyol., 107 pp., 2 pls.

COLLETT, R.

1904. Diagnosis of four hitherto undescribed fishes from the depths south of the Faroe Islands. Videns. Selskabs Forhand. Christiania, 1904, no. 9, 7 pp.

1905. Fiske . . . "Michael Sars" Togter i Nordhavet 1900–1902. Rept. Norwegian Fisher. and Marine Invest., vol. 2, part 2, no. 3, 147 pp., 2 pls.

FOWLER, HENRY W.

1941. The Fishes of the Groups Elasmobranchii, Holocephali, Isospondyli and Ostariophysi . . . Contributions to the Biology of the Philippine Archipelago and Adjacent Seas. Bull. 100, U. S. Nat. Mus., vol. 13, ix + 879 pp.

GARMAN, SAMUEL

1906. New Plagiostomia. Bull. Mus. Comp. Zool., vol. 46, pp. 201–208.

1913. The Plagiostomia . . . Mem. Mus. Comp. Zool., vol. 36, xiii, 515 pp.; Atlas, 75 pls.

GILBERT, CHARLES H.

1905. The deep sea fishes of the Hawaiian Islands. Bull. U. S. Fish Comm., vol. 23, part 2, pp. 575–714, 36 pls.

GILCHRIST, J. D. F.

1922. Deep sea fishes procured by the S. S. "Pickle" Part 1. Fisher. Mar. Biol. Surv. Union S. Africa Rept. 2 (1921), Spec. rept. 3, pp. 41–79; pls. 7–12.

GILL, THEODORE

1862. On the classification of the families and genera of the Squali of California. Proc. Acad. Nat. Sci. Philadelphia, 1862, pp. 483–501.

GOODE, GEORGE BROWN, and T. H. BEAN

1895. Oceanic Ichthyology . . . Smithsonian Contrib. Knowl., vol. 30, xxxv + 26 + 553 pp.; vol. 31, Atlas, 123 pls. Also, 1896, as vol. 22, Mem. Mus. Comp. Zool.

GÜNTHER, ALBERT

1870. Catalogue Fishes British Museum, vol. 8, xxv, 549 pp.

1877. Preliminary notes on new fishes collected in Japan . . . Ann. Mag. Nat. Hist., ser. 4, vol. 20, pp. 433–446.

1880. Report on the shore fishes . . . "Challenger" Rept. Zool., vol. 1, part 6, 82 pp., 32 pls.

1887. Report on the deep sea fishes. "Challenger" Rept. Zool., vol. 22, part 57, lxv, 268 pp., 66 pls.

HOWELL-RIVERO, LUIS

1936. Some rare and little known fishes from Cuba. Proc. Boston Soc. Nat. Hist., vol. 41, pp. 41–76, pls. 9–13.

JENSEN, A. S.

1899. On *Centrophorus squamosus*, in Saemundsson, Zool. Meddel. fra Island; vid. Meddel. Naturhist. Forening, Copenhagen [vol. 54], 1899, p. 411–419, pl. 3.

JOHANN, LEOPOLD

1899. Über eigenthümliche epitheliale Gebilde (Leuchtorgane) bei *Spinax niger*. Zeit. Wiss. Zool., vol. 66, pp. 136–160, pls. 10, 11.

JOHNSON, J. Y.

1867. Description of a new species of Spinacidae . . . Proc. Zool. Soc. London, 1867, pp. 713–715.

JORDAN, D. S. and B. W. EVERMANN

1896. A check list of the fishes and fish like vertebrates of North and Middle America. Rept. U. S. Comm. Fish [1895], pp. 209–584.

1896a. Fishes of North and Middle America. Bull. 47, U. S. Nat. Mus., part 1, lx + 1240 pp.

JORDAN, D. S. and H. W. FOWLER

1903. A review of the elasmobranchiate fishes of Japan. Proc. U. S. Nat. Mus., vol. 26, pp. 593–674, 2 pls.

JORDAN, D. S. and J. O. SNYDER

1902. Descriptions of two new species of squaloid sharks from Japan. Proc. U. S. Nat. Mus., vol. 25, pp. 79–82.

KOEFOED, EINAR

1932. Fishes from the sea bottom. Rept. Sci. Res. "Michael Sars" N. Atlant. Exped. 1910, vol. 4, part 1, 147 pp., 6 pls.

LAHILLE, FERNANDO

1921. Enumeracion sistematica . . . peces cartilaginosos . . . Argentinas. Physis, Buenos Aires, vol. 5, pp. 63–64.

1928. Nota sobre unos peces elasmobranquios. An. Mus. Nac. Buenos Aires, vol. 34, pp. 299–339, 5 pls.

Landholt, H. H.

1947. Ueber den Zahnwechsel bei Selachien. Rev. Suisse Zool., vol. 54, pp. 305–367.

Linnaeus, C.

1758. Systema naturae, 10th Ed., vol. 1, 824 pp. Holmiae.

Lönnberg, Einar

1907. Fische — *in* Ergeb. Hamburg Magalhaens. Sammelreise, vol. 8, No. 6, pp. 1–16, 1 pl.

Lowe, R. T.

1839. A supplement to a synopsis of the fishes of Madeira. Proc. Zool. Soc. London, part 7, 1839, pp. 76–92.

McCulloch, A. R.

1915. Report on some fishes obtained by the F. I. S. "Endeavour" . . . Biol. Res. "Endeavour", vol. 3, part 3, pp. 97–170, pls. 13–37, Commonwealth of Australia.

Molina, Juan Ignacio

1782. Saggio sulla storia naturale del Chile, 367 pp., 1 map, Bologna.

Müller, Johannes and F. G. J. Henle

1837. Ueber die Gattungen der Haifische und Rochen . . . Arch. Naturgesch. Jahrg. 3, vol. 2, pp. 394–401, 434.

1841. Systematische Beschreibung der Plagiostomen. Berlin, xxii + 200 pp., 60 pls.

Myers, George

1952. The nature of systematic biology . . . Systematic Zoology, vol. 1, no. 3, pp. 106–111.

Nobre, Augusto

1935. Vertebrados. Fauna marinha de Portugal, vol. 1, lxxxiv, 574 pp., 77 pls.

Oshima, H.

1911. Some observations on the luminous organs of fishes. Journ. Coll. Sci. Tokyo, vol. 27, no. 15, 25 pp., 1 pl.

Pietschmann, Viktor

1907. Zwei neue Selachia aus Japan. Anz. Akad. Wiss. Wien, vol. 44, pp. 394–396.

1908. Japanische Plagiostomen. Sitzber. Akad. Wiss. Wien, vol. 117, part 1, pp. 637–710, pls. 1, 2.

Poey, Felipe

1861. Memorias sobra la Historia Natural de la Isla de Cuba. Vol. 2, 442 pp., 19 pls. [dates of publication given on p. 427].

Poll, Max

1951. Poissons. 1, Generalités; 2, Sélaciens et Chimeres. Res. Sci. Exped. Oceanogr. Belge Eaux Côtes Afric. Atlant. Sud., vol. 4, fasc. 1, pp. 1–154, pls. 1–13.

Rafinesque, C. G.

1810. Caratteri di alcuni Nuove generi e specie di animalie e piante della Sicilia . . . iv, 105 pp., 20 pls. Palermo.

Regan, C. T.

1906. Descriptions of some new sharks in the British Museum collection. Ann. Mag. Nat. Hist., ser. 7, vol. 18, pp. 435–440.

1908. A synopsis of the sharks of the family Squalidae. Ann. Mag. Nat. Hist., ser. 8, vol. 2, pp. 39–57.

Rey, Luis Lozano

1928. Fauna Iberica, Peces. Vol. 1, 690 pp., 20 pls. Inst. Nac. Ciencias, Madrid.

Saemundsson, B.

1922. Zoologiske Meddelelser fra Island. Vidensk. Meddel. Naturhist. Foren. Copenhagen, vol. 74, pp. 159–200, pls. 3–5.

1932. Centrophorus jonsonii. Faune Ichthyol., Conseil Internat. Perm. Explor. Mer. Pl. not numbered.

Schmidt, Johannes

1901. Fiskeri undersøgelser ved Island og Faerøerne. Skrift. Komm. Havunders., Copenhagen, no. 1, 148 pp., 10 pls.

Smith, H. M. and Lewis Radcliffe

1912. The squaloid sharks' of the Philippine Archipelago . . . Proc. U. S. Nat. Mus., vol. 41, pp. 677–685, pls. 50–54.

Smith, J. L. B.

1949. The sea fishes of southern Africa. 550 pp., 102 pls. Central News Agency, S. Africa.

Smitt, F. A.

1895. Scandinavian fishes . . . Part 2, pp. 567–1240, pls. 28–53.

TANAKA, SHIGEHO
1912. Figures and descriptions of the fishes of Japan. Vol. 5, pp. 71–86, pls. 21–25; vol. 6, pp. 87–108, pls. 26–30.

THOMPSON, E. F.
1930. New records of the genera Centrophorus and Hoplichthys in New Zealand. Rec. Canterbury Mus., vol. 3, no. 4, pp. 275–279, pls. 42–44.

TORTONESE, ENRICO
1952. Studi sui Plagiostomi . . . . . Arch. Zool. Ital., vol. 37, pp. 383-398.

WAITE, E. R.
1910. Notes on New Zealand fishes. Trans. New Zealand Inst., vol. 42, pp. 384–391, pls. 37, 38.

WHITLEY, GILBERT
1934. Notes on some Australian sharks. Mem. Queensland Mus., vol. 10, part 4, pp. 180–200, pls. 27–30.

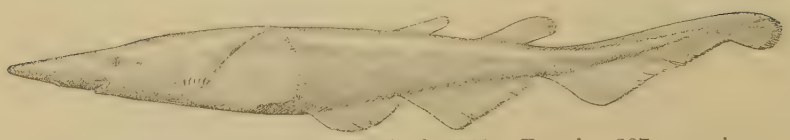

Fig. 1. *Apristurus atlanticus* Koefoed 1932. Female, 297 mm. long, northern part of Gulf of Mexico, Lat. 27°32′N, Long. 93°02′W, 400–450 fathoms, "Oregon" Sta. 534.

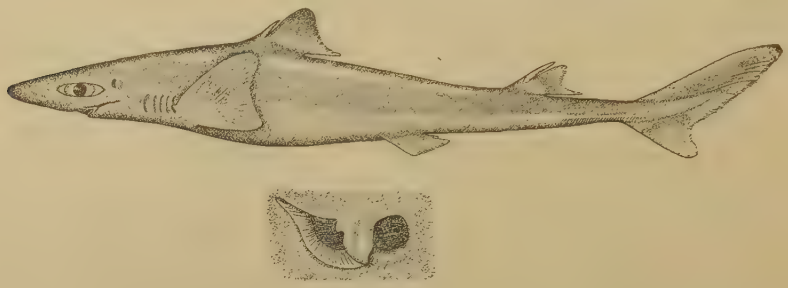

Fig. 2. *Squalus fernandinus* Molina 1782. Juvenile male, 395 mm. long, off South Carolina, Lat. 33°00′N, Long. 77°07′W, May 1949, collected by "Albatross" III. Below, left-hand nostril of same, x about 3.

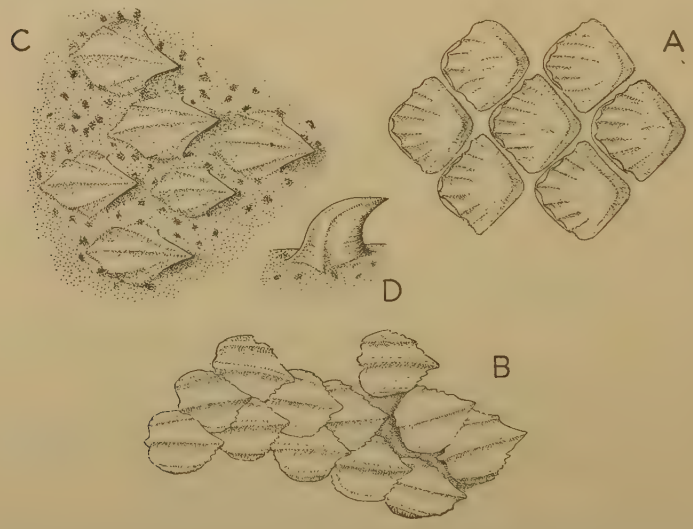

Fig. 3. Dermal denticles of three species of *Centrophorus*, from side, below first dorsal fin. A: *granulosus* Bloch and Schneider 1801, specimen in Museum of Comparative Zoology, x about 12. B: *squamosus* Bonnaterre 1788, 1200 mm. long; west of Iceland, specimen in Museum of Comparative Zoology, x about 6. C–D: *uyato* Rafinesque 1810, female, 445 mm. long, northern part of Gulf of Mexico, Lat. 29°17′N, Long. 87°42′W, 208 fathoms, "Oregon" Sta. 515, x about 40.

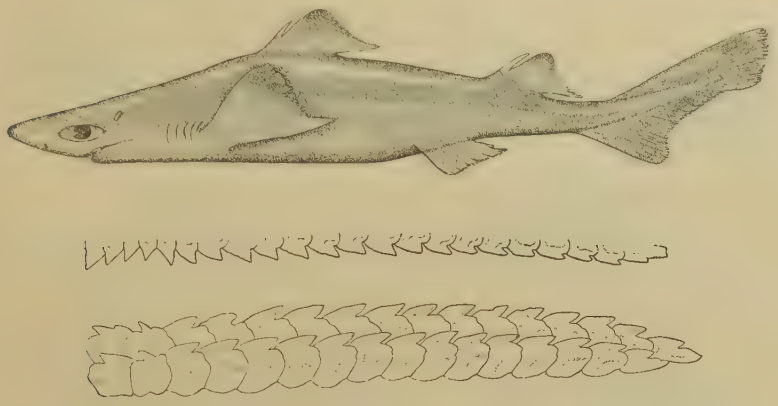

Fig. 4. *Centrophorus uyato*(Rafinesque)1810. Juvenile male, about 429 mm. long, northern part of Gulf of Mexico, Lat. 29°17′N, Long. 87°42′W, 208 fathoms, "Oregon" Sta. 515. Below: upper and lower tooth bands of left-hand side of mouth, viewed from anterior side,of female 445 mm. long, same specimen as in Fig. 3C, x about 3.4.

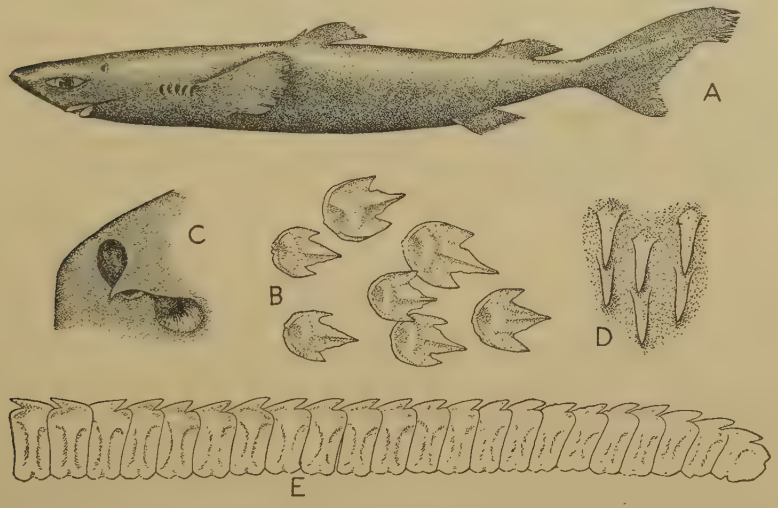

Fig. 5. *Scymnodon melas*, n. sp. A: type specimen, 462 mm. long, continental slope off Georges Bank, Lat. 40°00′N, Long. 68°52′W, 420–480 fathoms, July 12, 1952, Museum of Comparative Zoology No. 37452. B: group of dermal denticles of same from side below first dorsal fin, x about 10. C: right-hand nostril of same, x about 2. D: teeth of same from upper jaw, near center, x about 4. E: lower tooth band of same, from right-hand side of mouth, anterior view, x about 4.

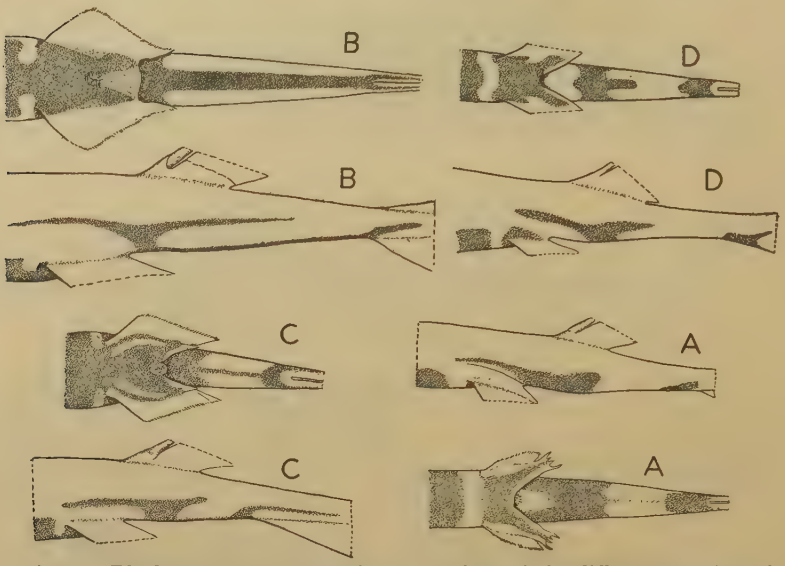

Fig. 6. Black pattern on posterior part of trunk in different species of *Etmopterus*. A: *E. hillianus* Poey 1861; north coast of Cuba, x about 0.4. B: *E. lucifer* Jordan and Snyder 1902, Japan, x about 0.4. C: *E. spinax* (Linnaeus) 1758, Norway, x about 0.4. D: *E. virens*, n. sp., type specimen; northern part of Gulf of Mexico, x about 0.4.

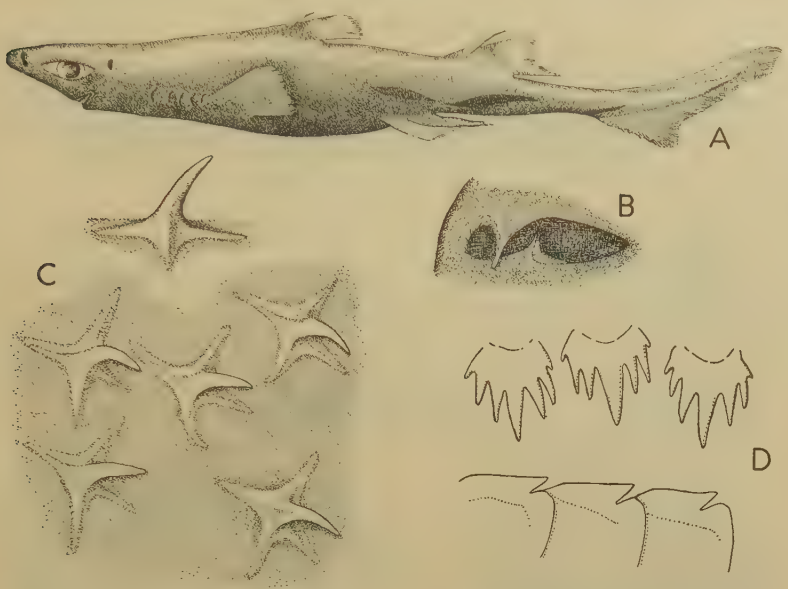

Fig. 7. *Etmopterus polli*, n. sp. A: type specimen, 197 mm. long, off equatorial West Africa, Lat. 6°08′S, Long. 11°24′E, 350–380 meters, Museum of Comparative Zoology No. 38001. B: right-hand nostril of same, x about 5. C: dermal denticles of male, 232 mm. long, from same locality as the type specimen, x about 45. D: upper and lower teeth of male, 197 mm. long, same locality as type specimen, about midway between symphysis and outer corner of mouth, x about 14.

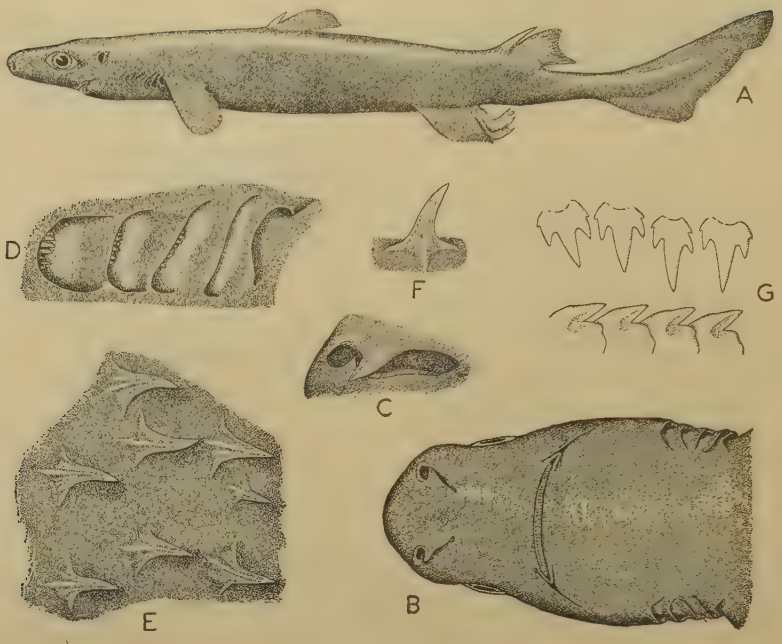

Fig. 8. *Etmopterus princeps* Collett 1904. A: adult male, about 545 mm. long, off southern Nova Scotia, Lat. 41°25′N, Long. 65°56′W, 400–490 fathoms, tip of snout somewhat restored from a slightly smaller specimen from nearby. B: lower surface of snout of same, x about 0.4. C: right-hand nostril of same, x about 1.2. D: gill openings of same, left-hand side, x about 1.2. E: group of dermal denticles of same, from side below first dorsal fin, x about 15. F: side view of a dermal denticle of same, x about 15. G: upper and lower teeth of same, about midway between symphysis and corner of mouth, x about 4.

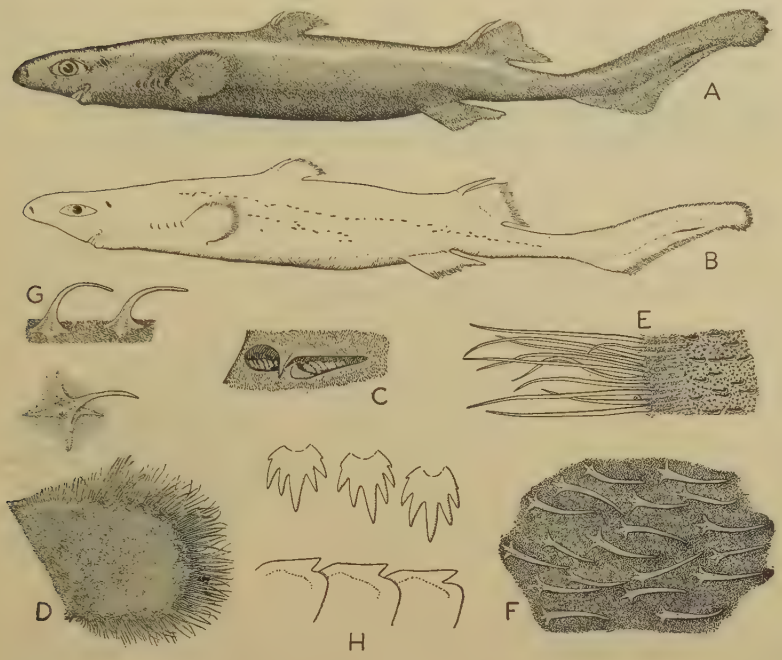

Fig. 9. *Etmopterus schultzi,* n. sp. A: type specimen, 270 mm. long, northern part of Gulf of Mexico, Lat. 29°11′N, Long. 86°53′W, 305 fathoms, "Oregon" Sta. 279, U. S. National Museum No. 113,381. B: outline drawing of same showing the black dashes and dots, perhaps luminescent. C: right-hand nostril of same, x about 3. D: left-hand pectoral fin of adult male about 280 mm. long, "Oregon" Sta. 549, x about 1.2. E: margin of pectoral of same, to higher scale, to show free, fringe-like terminations of the horny rays, x about 6. F: group of dermal denticles of same, from side below first dorsal fin, x about 22. G: dermal denticles of same in side view, and viewed obliquely with base freed from the skin, x about 24. H: upper and lower teeth of male 245 mm. long from about midway between symphysis and outer corner of mouth; "Oregon" Sta. 542, Lat. 27°41′N, Long. 94°59′W, x about 10.

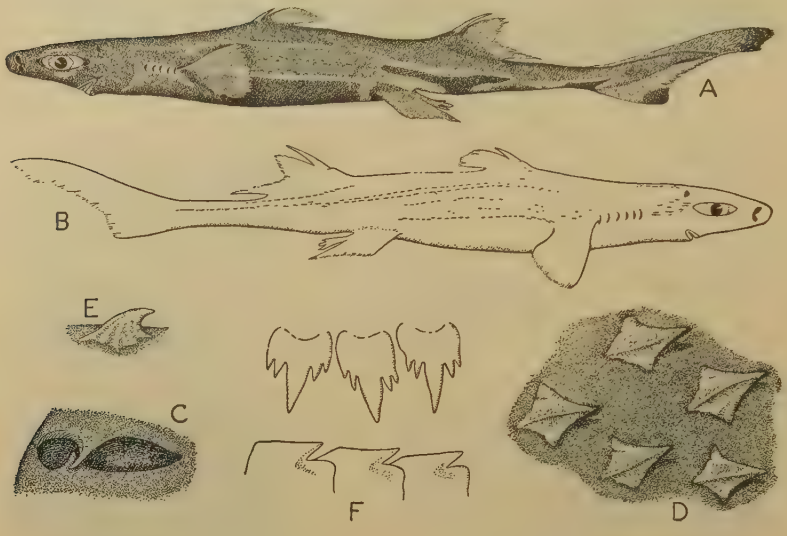

Fig. 10. *Etmopterus virens*, n. sp. A: type specimen, 203 mm. long, northern part of Gulf of Mexico, Lat. 29°52′N, Long. 91°33′W, 220 fathoms, "Oregon" Sta. 501; U. S. National Museum No. 160,859. B: outline drawing of right-hand side of same, to show the pattern of black dots and dashes, perhaps luminescent. C: right-hand nostril of same, x about 3. D: group of dermal denticles of another specimen of about the same size, from the side below the first dorsal fin, x about 36. E: dermal denticle of same in side view, x about 36. F: upper and lower teeth, from about midway between symphysis and corner of mouth, x about 10.

Contribution No. 601

PHYSICAL OCEANOGRAPHY OF THE GRAND BANKS REGION AND THE LABRADOR SEA IN 1951

By Floyd M. Soule, P. S. Branson and R. P. Dinsmore [1]

The 180-foot tender-class cutter *Evergreen* again served as oceanographic vessel of the ice patrol during 1951. No marked alterations affecting the oceanographic work were made in the vessel since the 1950 season.

The oceanographic work of the 1951 season began with the *Evergreen's* departure from Argentia on 2 April to make a current survey of the waters over and immediately seaward of the southwestern, southern, and eastern slopes of the Grand Banks with the survey extending northeastward as far as Flemish Cap. The work of collection of data began at station 4307, located at 43°32.5′ N., 51°32′ W., on the late afternoon of 3 April and progressed eastward around the Tail of the Banks and thence northward to Flemish Cap where the final station of the survey, number 4385, was completed 12 days later. The *Evergreen* then proceeded to Argentia, arriving there on the morning of 17 April. This survey was made under most unfavorable weather conditions for oceanographic work. Only once, for the brief period of 3 hours, was it necessary to heave to because of weather; but conditions frequently reached the point of being just short of limiting conditions for oceanographic work. Because of the relative strength and direction of wind, sea, and current, out of the 79 stations occupied, the wire angle was 40° or greater at 20 of the stations, and of these the wire angle exceeded 45° at 12 stations.

The *Evergreen* departed Argentia on 28 April for the purpose of making a second current survey, the area to include the waters over and immediately seaward of the northeastern slope of the Grand Banks; and to occupy the triangle containing the branch point where the Labrador Current divides into its eastern and western branches. The survey was planned to begin with the counterclockwise occupation of the triangle beginning and ending at its northeastern corner and thence to work southeastward around the northeastern shoulder of the Grand Banks occupying an experimental network of stations between the triangle and Flemish Cap.

[1] Contribution No. 601 of the Woods Hole Oceanographic Institution.

204964—53—4

Sailing, originally planned for 27 April, was postponed until the following day while a gale blew itself out. It was expected, therefore, that at least the first part of the survey could be carried out with quiet weather. This proved to be unwarranted optimism. The work of collection of data began at station 4386, located at 49°58′ N., 48°58′ W., on the afternoon of 29 April. At 1016 the following day it was necessary to heave to on account of weather. Operations were resumed at 0438 on 1 May. At 0746 on 1 May oceanographic work was interrupted while the *Evergreen* proceeded toward Fogo Island to assist in locating a man reported adrift on the ice. Oceanographic work was resumed 9 hours later. At 2135 on 3 May it was necessary to heave to again on account of weather, this time for 7½ hours. Weather again forced an interruption of the work on 8 May when the ship was hove to from 1251 to 1826. These interruptions do not tell the complete story of the boisterous weather which was a succession of gales. Of the 79 stations occupied, 19 were occupied in winds of force 6 or greater, including 4 with force 8. The final station of the survey, number 4464, located at 46°47.5′ N., 44°51′ W., was completed on the morning of 10 May. The *Evergreen* then proceeded to pick up a carboy of water at 45°41.5′ N., 44°39′ W., for use as a substandard of salinity. A course was then set for Argentia with arrival there on the morning of 12 May.

The *Evergreen* departed Argentia on the evening of 21 May to make a third current survey of the Grand Banks region. This survey was planned to cover the waters over and immediately seaward of the eastern and northeastern slopes of the Grand Banks, including occupations of sections T, U, and W, and extending to the area just northward of the latitude of Flemish Cap, with the work beginning at the southern end of the area and progressing northward. Accordingly the work of collection of data began at station 4465, located at 43°20′ N., 50°15′ W., on the early morning of 23 May. There was a delay of an hour and a half on the evening of 31 May while a defective electrode cable for the von Arx current meter was replaced. At 1136 on 3 June, after completion of station 4553, it was necessary to heave to an account of weather. Work was resumed at station 4554 at 0350 on 4 June. No further interruptions occurred and the work of collection of data was completed at station 4559, located at 47°13′ N., 49°18′ W., on the afternoon of 4 June. The *Evergreen* then proceeded to Boston, arriving there on the evening of 7 June.

Since the ice observation and ice patrol services had been discontinued for the season on 24 May because of the absence of ice in positions of potential hazard to shipping, no further current surveys of the Grand Banks area were made. The post-season

cruise began with the departure of the *Evergreen* from Port Union, Newfoundland, on the afternoon of 13 July. The oceanographic work included the occupation of three sections disposed in the form of a triangle with corners at approximately 50°00′ N., 49°00′ W.; 48°44′ N., 52°58′ W.; and 47°24′ N., 50°00′ W. The occupation of the triangle was followed by a repetition of the section across the Labrador Sea from South Wolf Island, Labrador, to Cape Farewell, Greenland. The work of collection of data on the post-season cruise began on the morning of 14 July at station 4560, located at 50°01.5′ N., 48°58′ W. The triangle was completed without incident at station 4589, located at 49°59.5′ N., 48°58′ W., on the morning of 17 July. The section across the Labrador Sea was begun at station 4590, located at 53°42.5′ N., 55°46′ W., on the evening of 18 July. Work progressed northeastward along the section without incident as far as station 4603, located at 56°36.5′ N., 50°30′ W., which was occupied on the evening of 20 July. From this station on winds from the easterly quadrants continued to freshen. Although progress was slow, work at stations continued until 2230 on 22 July when, after completing station 4610, located at 59°25′ N., 44°49′ W., the ship was hove to to await daylight. Progress was resumed at 0250 on 23 July and the work of collection of data was completed at station 4613, located at 59°43.5′ N., 43°58′ W., at 0818 on 23 July.

On the evening of 23 July a carboy of water for eventual use as a substandard of salinity was collected at 58°58′ N., 45°23′ W. After various diversions the *Evergreen* arrived at Woods Hole on the afternoon of 1 August to discharge oceanographic equipment and personnel and conclude the oceanographic field work for 1951.

The oceanographic work was under the supervision of Oceanographer Floyd M. Soule who was assisted by Lt. Peter S. Branson and Lt. (jg) Robertson P. Dinsmore.

In all, 307 stations were occupied during the season and post-season cruises. The 24 stations comprising the section across the Labrador Sea were occupied from the surface to as near bottom as was practicable. At the remaining 283 stations the observations extended to a depth of about 1,500 meters where the depth of water permitted. As in previous years the intended depths of observation, in meters, were 0, 25, 50, 75, 100, 150, 200, 300, 400, 600, 800, 1,000 and thence by 500-meter intervals. The dynamic topography has been referred to the 1,500-decibar surface for the section across the Labrador Sea. For all other stations, the dynamic heights have been referred to the 1,000-decibar surface.

Temperatures were measured with deep sea reversing thermometers, most of them of Richter and Wiese manufacture. Some of the protected thermometers were manufactured by Negretti and

Zambra, some by the GM Manufacturing Co., and some by the Kahl Scientific Instrument Corp. The depths of observation were based on Richter and Wiese unprotected thermometers.

The thermometers were used in pairs and a program was followed of periodically shifting the thermometers comprising the pairs. This provided a series of comparisons of each thermometer with several other thermometers and served not only to identify thermometers which were not functioning properly but also to determine consistent errors in the scale corrections in use and to ascertain the degree of precision of the temperature measurements. In judging this precision, 1,847 comparisons were considered. These gave a probable difference between the corrected readings of a pair of thermometers of $\pm$ 0.013° C. As many of the thermometers had recent laboratory comparisons with thermometers tested by the National Bureau of Standards and, as in most cases, the temperatures are the means of the corrected readings of a pair of thermometers, it is considered that the tabulated observed temperatures have a probable error of $\pm$ 0.01° C.

As in previous years, the routine salinity determinations were made with a Wenner salinity bridge which had been calibrated by the measurement of a series of samples whose salinities were assumed to be known from comparisons with Copenhagen standard water by means of silver nitrate titration.[2] Thus the accuracy of the tabulated observed salinities is only that permitted by silver nitrate titration although their precision is much better and probably about $\pm$ 0.005‰. For the most part, the salinities are tabulated to the nearest 0.01‰. Each cell of the bridge was standardized at the beginning and end of each run with a substandard of salinity from a carboy of sea water kept under an oil seal. Intermediate standardizations were made every 10 to 15 measurements. In addition, Copenhagen water was measured as an unknown one or more times during the run. These measurements of Copenhagen standard water were used to determine minor corrections to the salinities determined for each survey and to adjust the assumed value of the salinity of the carboy of sea water used as a substandard. None of the surveys required salinity corrections of as much as 0.005‰ and the figures illustrating the dynamic topography are in accordance with the tabulated temperatures and salinities.

[2] Since a substitution method is used, only relative conductivity is involved in the bridge calibration. If C is conductivity and A and B are constants and S is the salinity corresponding to conductivity C, then for the range of salinity from 30 to 40 ‰ the isothermal conductivity-salinity relationship may be approximated by $C = C'(A + BS)$. Early work by E. Ruppin (O. Krümmel, Handbuch der Ozeanographie, Band I, p. 291, Stuttgart, 1907) and A. L. Thuras (J. Acad. Sci., 8, p. 685, Washington, 1918) resulted in mean values such that $C = C_{35}(0.10925 + 0.02545\ S)$. More recent work by Thomas, Thompson, and Utterback (1934), as digested by Lafond in U. S. Navy Hydrographic Office Publication No. 614, results in a similar expression for this range of salinity at a temperature of 25° C. of $C = C_{35}(0.11055 + 0.025361\ S)$. From the 1950 calibration of the salinity bridge, made at a temperature of about 28.9°C., the similar expression derived was $C = C_{35}(0.11436 + 0.025304\ S)$.

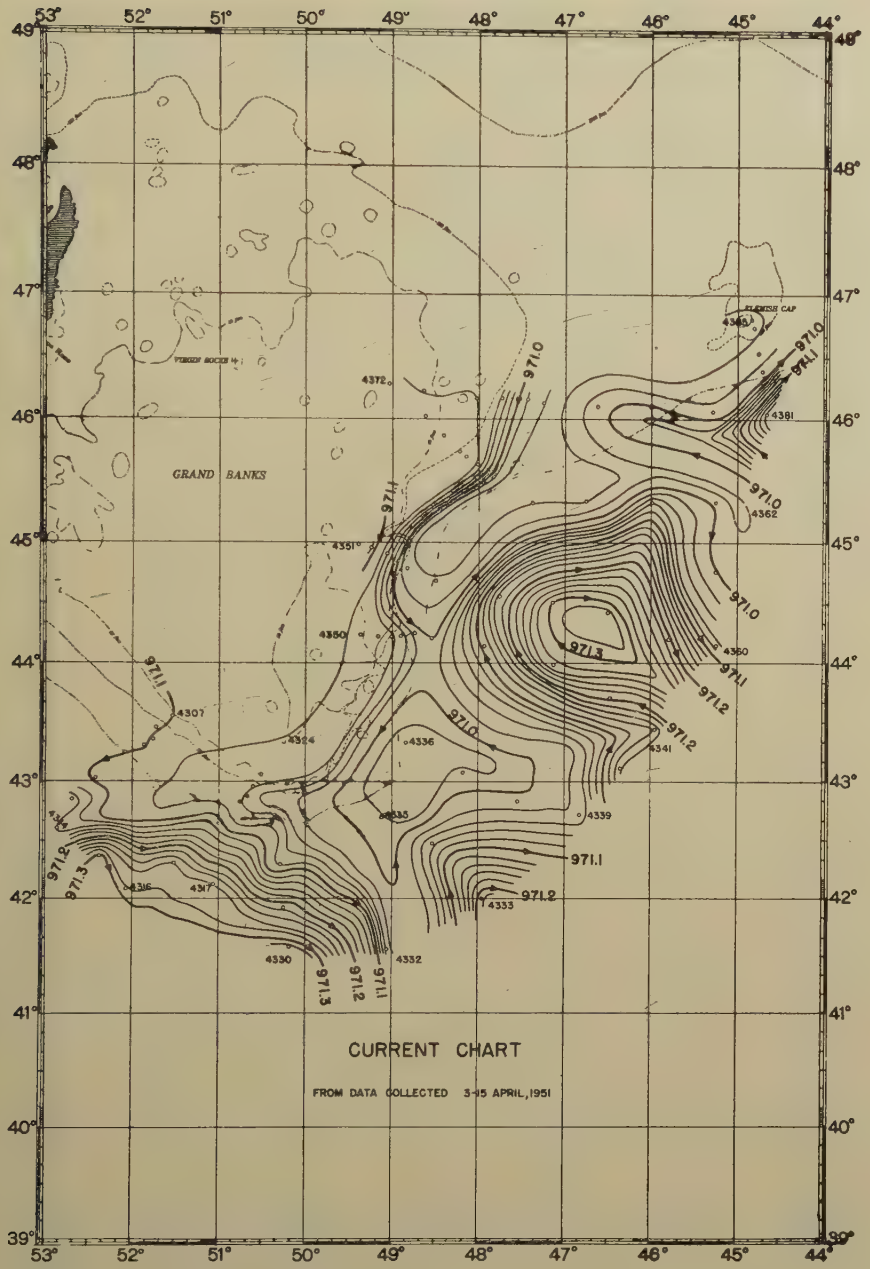

FIGURE 7.—Dynamic topography of the sea surface relative to the 1,000-decibar surface from data collected 3–15 April, 1951. Oceanographic station positions are indicated and the station numbers given at turning points.

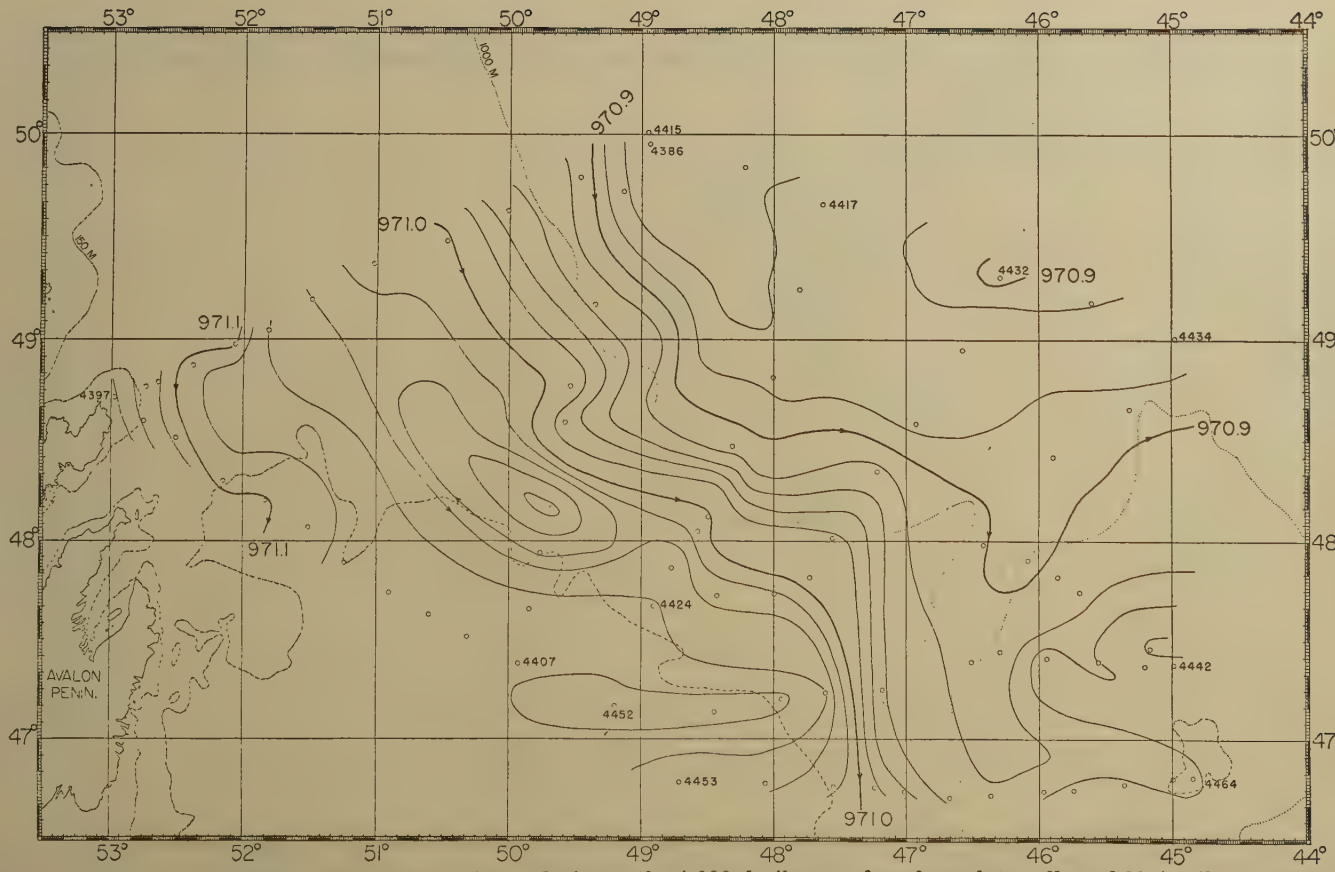

FIGURE 8.—Dynamic topography of the sea surface relative to the 1,000-decibar surface from data collected 29 April to 10 May 1951. Oceanographic station positions are indicated and the station numbers given at turning points.

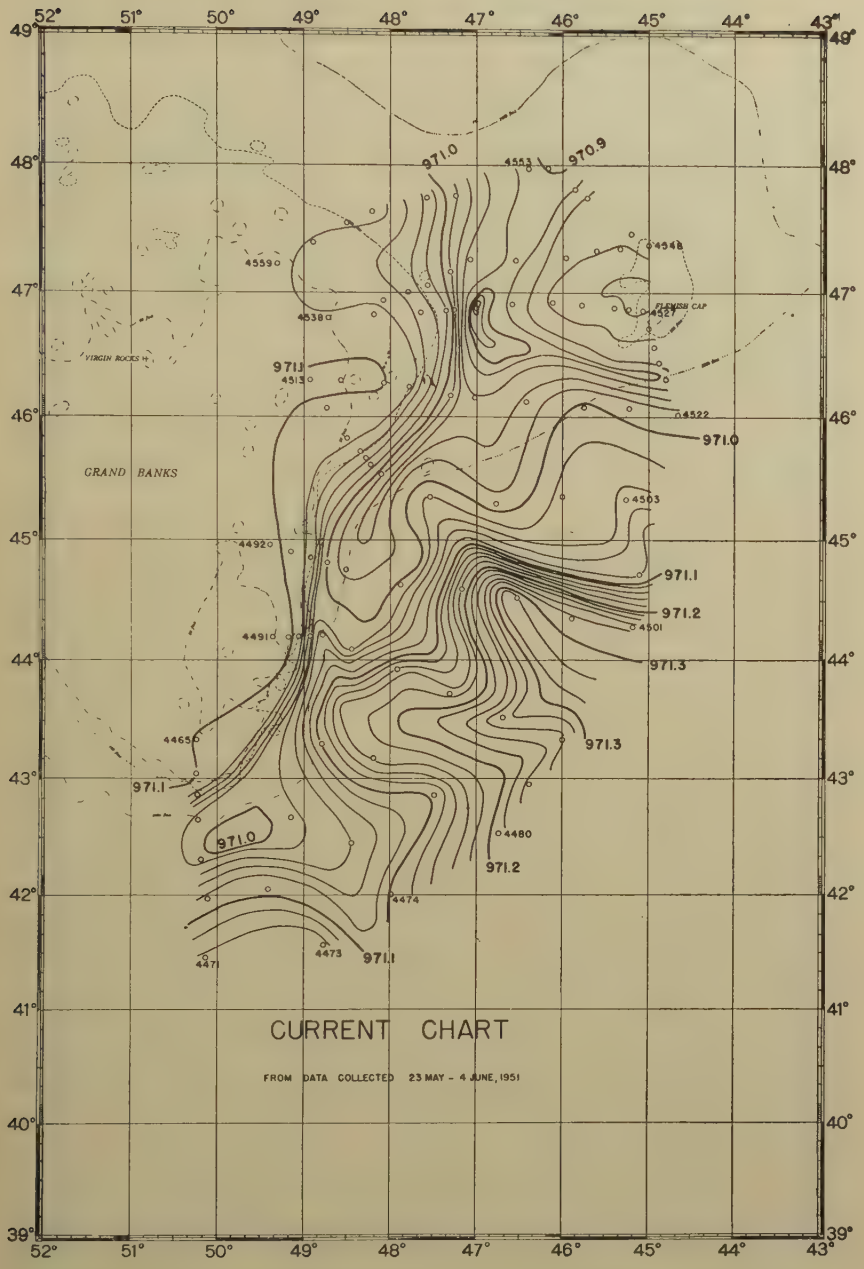

FIGURE 9.—Dynamic topography of the sea surface relative to the 1,000-decibar surface from data collected 23 May to 4 June 1951. Oceanographic station positions are indicated and the station numbers given at turning points.

Figures 7, 8 and 9 show the dynamic topography of the sea surface relative to the 1,000-decibar surface as found during the first, second and third surveys respectively. In figure 7 the margins of the Atlantic Current are to be seen in the southwestern part of the surveyed area, in the salient whose axis points northwestward from 44° N., 46° W., and again at the 46th parallel just southward of Flemish Cap. The salient, which is the dominating feature of figure 7, seems to have been effective in blocking the southward flow of the Labrador Current. The shape of the salient in figure 7 is not such as to produce the considerable diversion of the Labrador Current eastward north of the 44th parallel which is shown in the chart. However, what past evidence is available indicates that such salients or meanders progress in a northeasterly direction and it is probable that the diversion of the Labrador Current was accomplished at some time prior to the first survey when the Atlantic Current salient was centered more to the southwest.

Had any bergs been in the area immediately northward of that covered by this survey figure 7 would have indicated two potential danger areas for close surveillance by the patrol. One of these, at the southern edge of the surveyed area, was in the neighborhood of the 49th meridian where bergs might have moved southward after following the eastern edge of the Grand Banks. The other was centered at about 45° N., 45° W., where bergs diverted eastward north of 44° N., could again move south and southeastward toward the steamer lanes of the North Atlantic Track Agreement. Very little Labrador Current, however, reached southward of the 44th parallel and an outstanding feature of this survey, not shown by the dynamic topography, was the exceptionally high temperature of the water in the area. Negative temperatures were found at only 15 of the 79 stations and all of these were north of 44° N. The number of stations at which temperatures lower than 3° C. were found was 32, and those where temperatures were in excess of 15° C. totaled 17. These figures are to be compared with a similar cruise in 1950 when, of 69 stations occupied, 47 had temperatures below 3°, 34 had negative temperatures, and 3 had temperatures above 15°.

The second survey was made in an area from which relatively few previous observations are available. Our knowledge of the circulation here is based largely on inference. From the 1,000-meter isobath in figure 8 it will be seen that a large part of the area is situated in shallow water so that, if the dynamic topography is to be referred to the 1,000-decibar surface, 57 of the 79 stations must be adjusted for their shallow depth. Thus the picture of circulation deduced from the density distribution and

shown in figure 8 does not have a reliability comparable to that of the dynamic topographic charts of the adjacent area to the south.

The western part of the surveyed area containing the triangle beginning at station 4386 and with corners at stations 4397 and 4407 and closing at station 4415 is comparable to the earlier occupations of this triangle in 1948, 1949, and 1950. Considering this triangle in this survey it would appear that any bergs entering the area and crossing the 49th parallel east of about 51° W., would follow the eastern branch of the Labrador Current, that those crossing this parallel west of about 51°50′ W., would follow the western branch, and that those crossing at intermediate longitudes would strand on the northern edge of the Grand Banks or be set in toward the banks at about the 47th parallel. Of those following the eastern branch, bergs crossing the 49th parallel eastward of 48°50′ W., would drift eastward and northeastward north of the latitude of Flemish Cap.

The dynamic topographic chart resulting from the third survey, figure 9, presents a different picture from that of the first survey made about 7 weeks earlier. In the third survey Labrador Current water was reaching the Tail of the Banks. The Atlantic Current water salient, while not having the strength nor the high temperatures encountered during the first survey, was still prominent and effective in diverting eastward some of the Labrador Current water northward of the 44th parallel. Were it not for the absence of bergs entering the area, figure 9 would have indicated midseason conditions with danger areas southwestward of the Tail of the Banks, southward of the surveyed area at about longitude 48° W., and eastward of the surveyed area north of about latitude 44°30′ N. The northern part of the surveyed area overlaps the southeastern part of the area covered by the second survey and comparisons of the results of the two surveys in this area will be made in the discussion of the volumes of flow of the Labrador Current.

It should be noted that in the past there has been evidence of a gradual progress northeastward of meanders such as the salient of Atlantic Current water. The rate of progression has been estimated to be of the order of magnitude of a few miles a day. With an interval of about 7 weeks elapsing between the first and third surveys, one might expect that the meanders found during the first survey would be displaced perhaps 200 miles to the northeastward in the third survey. Thus there is no assurance that the salient of Atlantic Current water found during the third survey is the same meander shown in figure 7. If it is, we have here an unusual case of stagnation or stability of current pattern.

204964—53—5

Certain sections across the Labrador Current in the Grand Banks region have been repeatedly occupied in the process of making current surveys during the ice patrol season over the period of years beginning with 1934 and the accumulated data form the basis for establishing seasonal normals for this part of the year, and a means of comparing the Labrador Current found during any survey with that found during another. The sections have been designated T, U, and W which are located as follows: section T running southeasterly from about 46°20′ N., 49°00′ W.; section U extending eastward from the Grand Banks at about the 45th parallel; and section W running southerly off the Grand Banks at about the 50th meridian. In bulletin number 36 of this series, tentative normal seasonal variation curves were published for the volume of flow and the mean temperature of the Labrador Current at each of these sections. In the following discussion, the units used in volume transport are millions of cubic meters per second, mean temperature and minimum observed temperature are given in degrees Centigrade, and the heat transport is expressed in units of millions of cubic meter degrees Centrigrade per second.

Only the first and third surveys included occupations of sections T, U, and W. However, other sections located northward of section T and for which normals have not been established were occupied during the second and third cruises and on the post-season cruise. On the second cruise the triangle off Cape Bonavista was occupied and the sections forming its sides have been designated NW, SW, and SE to indicate the northwest, southwest, and southeast sides respectively. A section running easterly from the Grand Banks to Flemish Cap was occupied and has been called section F and two sections running northeasterly from the Grand Banks intermediate between section F and the Bonavista triangle have been called G and H. On the third cruise sections F and G were occupied in addition to T, U, and W and on the post-season cruise the Bonavista triangle was occupied in addition to the section across the Labrador sea from South Wolf Island to Cape Farewell, Greenland. No seasonal variation normals are available for the Labrador Current off South Wolf Island, but the section has been occupied in the summer time in 14 of the 24 years beginning with 1928 (see p. 89, Bulletin No. 36 of this series). In the absence of normals for this section, the values found in 1951 have been compared with the averages of these 14 occupations.

In table 1 the results obtained in 1951 have been summarized and compared with normal values where they are available. From table 1 it is apparent that during both the first and third surveys the volume of flow of the Labrador Current in the Grand Banks

Table 1. Summary of velocity sections across Labrador Current occupied in 1951

Section	Volume transport			Mean temperature			Min. observed temp.			Heat transport		
	1951	Normal	Anomaly	1951	Normal	Anomaly	1951	Normal	Anomaly	1951	Normal	Anomaly
1st survey:												
T	2.74	3.55	−0.61	1.90	1.95	−0.05	−1.28	−1.41	+0.13	5.20	6.92	−1.72
U	3.21	5.28	−2.07	1.71	1.55	+0.16	−1.11	−1.22	+0.11	5.50	8.18	−2.68
W	0.21	4.24	−4.03	1.59	2.11	−0.52	+1.42	−0.53	+1.95	0.34	8.95	−8.61
2d survey:												
NW	3.48			1.19			−1.64			4.15		
SW	0.61			−0.71			−1.58			−0.43		
SE	2.52			1.23			−1.33			3.09		
H	3.34			2.24			−1.08			7.48		
G	2.81			2.06			−1.17			5.79		
F	1.66			1.97			−1.12			3.27		
3d survey:												
G	2.99			2.21			−1.29			6.60		
F	3.33			1.90			−1.24			6.31		
T	1.35	2.65	−1.30	1.14	2.90	−0.16	−0.86	−1.57	+0.71	1.53	7.68	−6.15
U	2.07	3.82	−1.75	1.89	2.36	−0.47	−1.29	−1.24	−0.05	3.92	9.02	−5.10
W	2.18	4.13	−1.95	3.53	3.16	+0.37	−0.42	−0.40	−0.02	7.70	13.05	−5.35
Post season:												
NW	4.39			1.67			−1.58			7.33		
SW	0.61			1.17			−1.56			0.72		
SE	3.55			1.79			−1.57			6.35		
S. Wolf Island	5.30	4.27	+1.03	2.63	2.47	+0.16	−1.34			13.93	11.19	+2.74

region was subnormal. The departures from normal mean temperature are not as striking and the subnormality of the heat transport is attributed to the reduced volume transport. Sections U and W were expected to show smaller than normal transports because of the diversion of the Labrador Current by the Atlantic Current salient as shown in figures 7 and 9, but it is evident from table 1 that the amount of Labrador Current reaching section T also was less than normal. The minimum observed temperatures were somewhat warmer than normal.

Considering the Bonavista triangle, during the second survey about 80 percent of the water entering the triangle followed the eastern branch of the Labrador Current. Approximately 85 percent followed this branch during the post-season cruise. The volume transport past section G was about the same during the second and third surveys, but a considerable part of this water recurved northeastward north of section F during the second survey whereas this diversion occurred farther south in the third survey. The circulation deduced from the values given in Table 1 is shown schematically in figure 10 for each of the surveys made in 1951. The computed figures for volume transport have been rounded to the nearest 0.1 million cu. m/sec. and adjusted for the triangles so that the sum of the transport past sections SW and SE equals the transport past section NW[3]. In the first survey it is considered that the increase in volume at section U over that at section T is the result of a contribution from the west, rather than a closed eddy on the east, because of the lower mean temperature found at section U. The recirculation of water in the closed eddy centered near 43° N., 49° W., in figure 7 seems, from the low mean temperature found at section W, not to have extended as far westward as this section.

In the second survey, the greater flow past section H than that at either sections SE or G indicates additional circulation associated with the margins of the Labrador Sea, as does also the higher mean temperature.

In the third survey the addition of water from the westward between sections G and F, resulting in the lower mean temperature at section F, is an indication that this water is not associated with the Grand Banks eddy which by the first of June has undergone appreciable warming. Similarly the addition of water from the Grand Banks between sections T and U is called upon to explain the higher mean temperature at the latter section rather than

[3] Regarding the reliability of the computed volumes of transport, it should be noted that a consistent error of 0.01 $^0/_{00}$ in salinity at one of a pair of stations will produce an error in the dynamic height of that station of about 7.2 dynamic mm and an error of about 0.36×10^6 cu. m/sec. in the volume of flow between the two stations if 1,000 decibars is the reference surface. These errors become 10.8 dynamic mm and 0.81×10^6 cu. m/sec. respectively if 1,500 decibars is the reference surface.

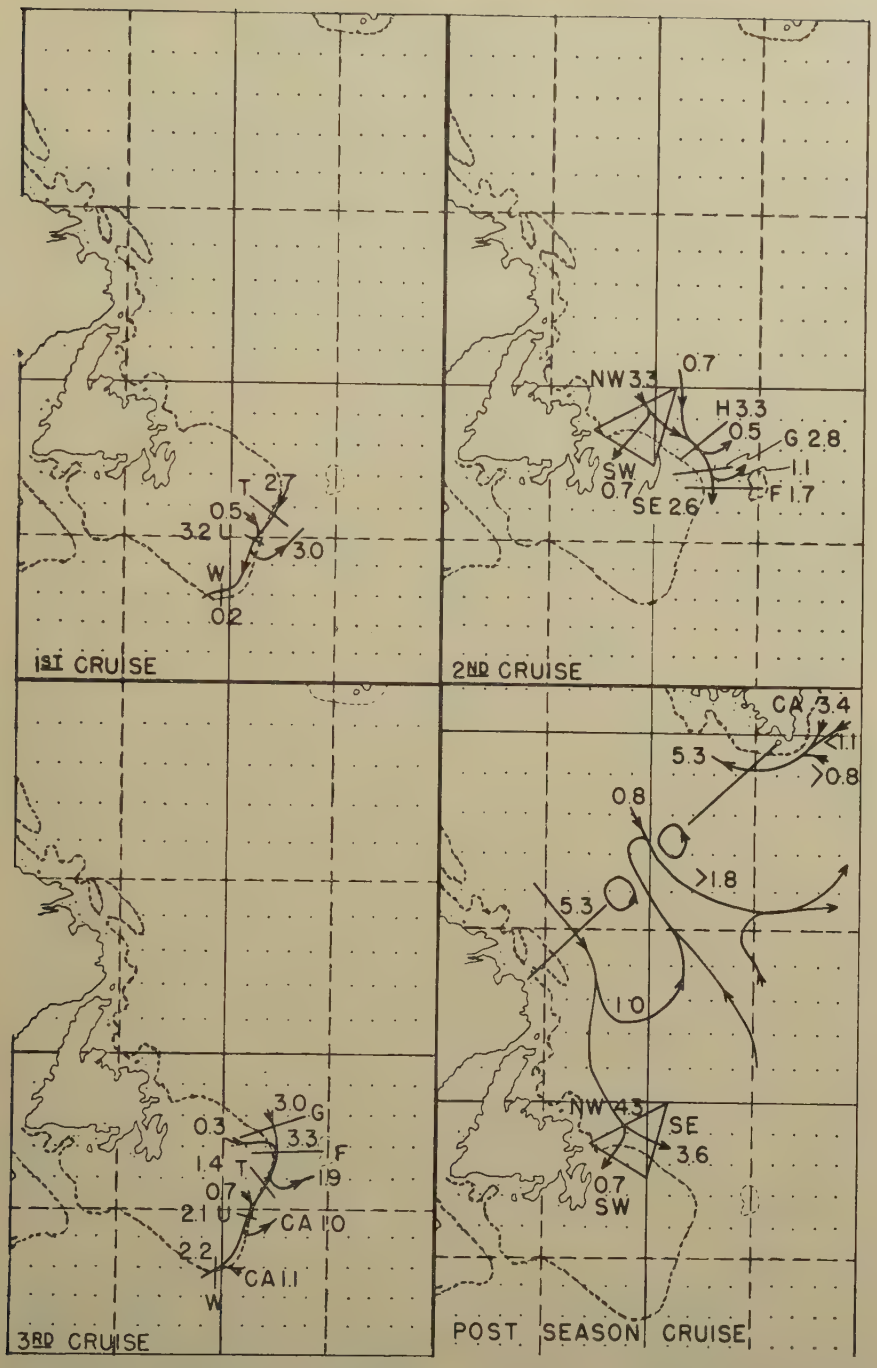

FIGURE 10.—Schematic representation of circulation deduced from sections occupied during 1951. Numerals indicate volume transport in units of cu. m/sec. x 10^{-6}.

interpreting the higher volume at section U as being the result of recirculation of mixed water from the eastward. The marked increase in mean temperature at section W indicates the presence of a considerable proportion of recirculating mixed water.

Except for noting the increase in transport at the Bonavista triangle during the post-season cruise over that found during the second survey, and the higher than average transport (both volume and heat) and mean temperature at the South Wolf Island section, discussion of the circulation found during the post-season cruise will be deferred until after the data on the complete South Wolf–Cape Farewell section have been presented.

The temperature-salinity relationships found in the past in the Grand Banks region at levels below 75 meters have established the Labrador Current water and the Atlantic Current water as water masses, and usually the mixed water derived from these water masses has been sufficiently uniform to permit it to be considered as a virtual water mass. The T–S curves for individual stations occupied during the first and third surveys have been examined and classified as Labrador Current water, mixed water, or Atlantic Current water. During the first survey a small group of stations classified as mixed water followed a consistent pattern similar to the characteristic mixed water found in the past. The remaining mixed water stations, however, had T–S curves which varied from normal mixed water to nearly Atlantic Current water, indicating the presence of water mixed from the parent water masses in varying proportions. The stations at which the abnormal mixed water was found formed a belt bordering the Atlantic Current water and extended to the edge of the Grand Banks on its southwestern slope. The area containing stations at which the usual mixed water was found extended from the Tail of the Banks to Flemish Cap as a zone between the abnormal mixed water and the Labrador Current water. During the third survey no such belt of abnormal mixed water was found.[4]

In figure 11 the T–S relationships found during 1951 have been shown for each of the three water masses in comparison with similar T–S curves representing the mean of conditions found during the 8-year period 1934–41. In drawing the curve for

[4] Since individual station curves are not identical, a check was made to determine whether or not the mixed water was a virtual water mass and not merely an apparent water mass derived from the bias of earlier work. The probable departures of temperature and salinity, at a given level at an individual station, from temperature and salinity at that level on the mean curves shown in figure 11 were computed for each level for each mean curve for 1951. These probable differences were then used as the axes of elipses constructed with their centers at the appropriate level on the mean curve. While the elipse patterns overlapped, each mean curve fell outside the envelopes of the elipses of the other two curves. Taken level for level the elipses of the three curves did not overlap except at 600 meters and below for mixed water and Labrador Current water, and at 1,500 meters for mixed water and Atlantic Current water. It was concluded that in 1951 the mixed water was a virtual water mass.

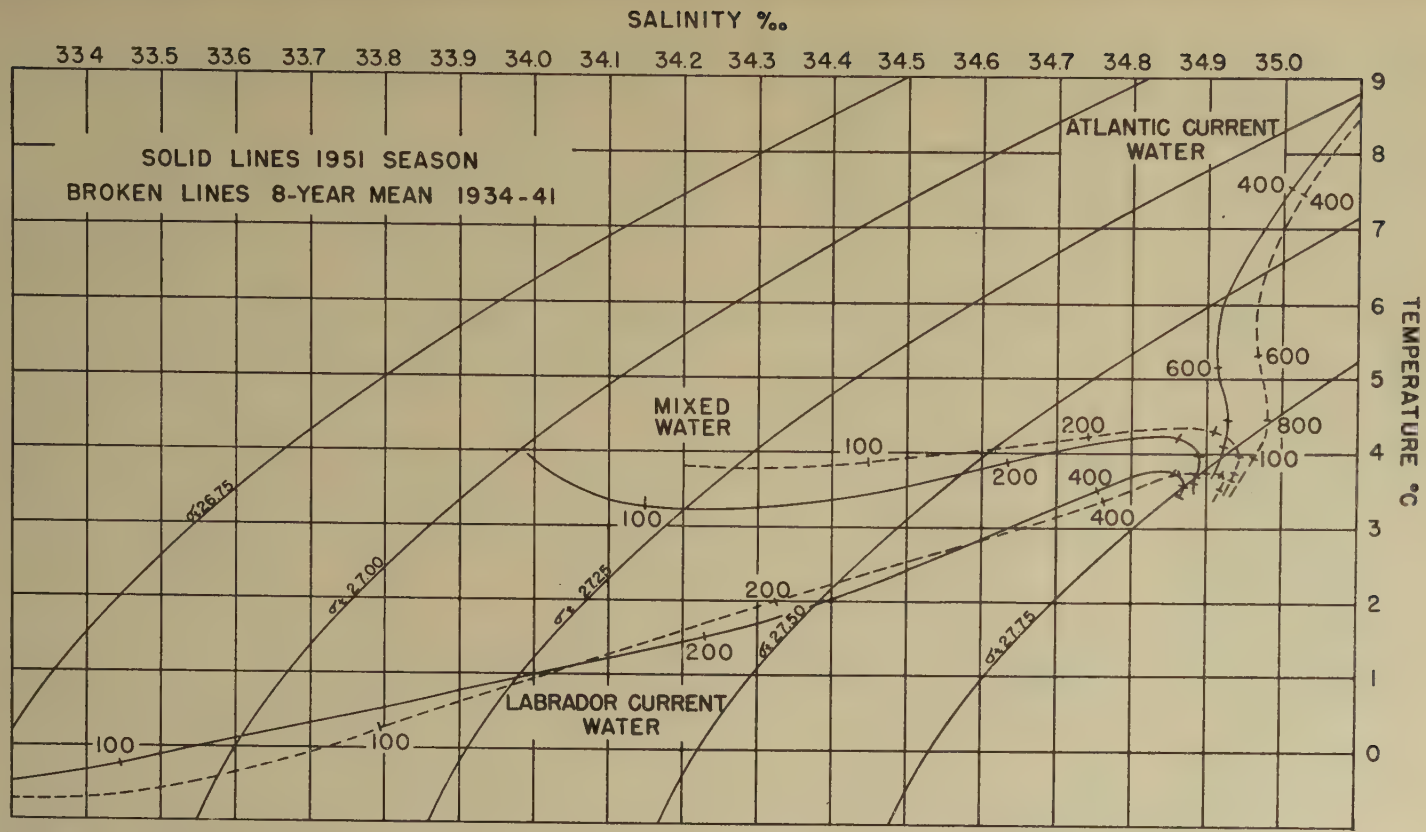

FIGURE 11.—Temperature-salinity relationships for Labrador Current water, Atlantic Current water, and mixed water found in the Grand Banks region. Solid lines show conditions during the 1951 season and broken lines represent the 8-year mean for the period 1934–41. An approximate depth scale in meters is given.

mixed water for 1951 the abnormal mixed water found during the first survey was excluded from consideration. An approximate depth scale in meters is shown on each curve in figure 11. It will be seen from figure 11 that, level for level, each water mass was lighter during 1951 than the 8-year mean and that lower salinities were responsible for these differences in densities. The differences were greater in the upper levels than in the deeper levels, but they still averaged 0.02 to 0.03 in σ_t between 400 and 1,000 meters.

The second survey was not included in the analysis of the T–S relationships of the water masses of the Grand Banks region inasmuch as the data considered previously were from the area south of Flemish Cap. The stations lying seaward of the Labrador Current in the second survey were examined to find out whether they approximated the characteristics of the mixed water of the Grand Banks region. Only stations 4440 to 4445 and 4459 to 4464 did. These 12 stations were located in the vicinity of Flemish Cap and lie in the region where the dynamic topography indicates the water entered the area from the Grand Banks region farther to the south. It is considered probable that the characteristic mixed water of the Grand Banks region is not formed northward of Flemish Cap.

In comparing the results of the von Arx current meter (geomagnetic electrokinetograph, abbreviated GEK) with the currents deduced from density distribution a method was presented in Bulletin No. 34 of this series wherein the currents as measured by GEK during the run between two oceanographic stations were converted into an equivalent difference in dynamic height at the two stations using the expression $\Delta D = 0.01391\ LC \sin \phi_m$ where ΔD is the difference in dynamic height in dynamic meters between two points separated by a distance L nautical miles, C is the average component of the current normal to the line between stations expressed in nautical miles per hour and ϕ_m is the mean latitude.

If C is not zero there is an angular difference Θ between the ship's heading and the course made good. The jog component M_J measured by GEK is normal to the ship's heading. We require the component C normal to the course made good. L and ϕ_m are known. Let the mean component of the current in the direction of the ship's heading be M_C (derived from the values computed each half hour). Let the time elapsed during the run be t hours. The mean M_J can be derived from scaling the trace at short intervals of time. The total movement of the ship from the current acting during t is subtracted vectorially from L at the station of arrival to reach the dead

reckoned point of arrival and from it the dead reckoned distance R and the angle Θ. From figure 12:

$$M_J t/L = \sin\Theta = Ct/R \text{ or } R = LCt/M_J t$$

also $$(M_C t + R)/L = \cos\Theta$$

whence $$(M_C t + R)^2 = L^2 - M_J{}^2 t^2$$

substituting the value of R and rearranging:

$$CL = M_J\,(\sqrt{L^2 - M_J{}^2 t^2} - M_C t)$$

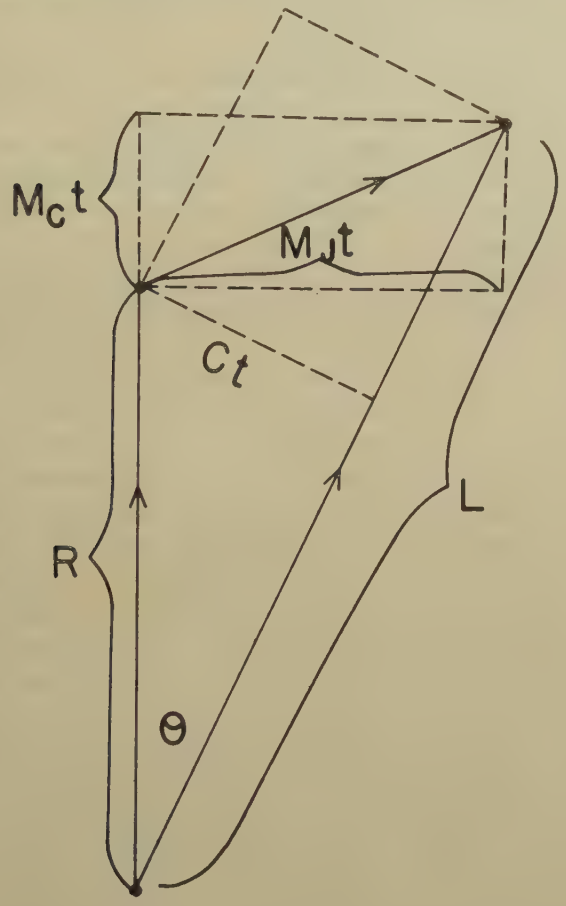

FIGURE 12.—Derivation of CL in terms of measured components.

This expression is general if the convention is adopted that M_e is positive if directed with the ship's heading and negative if counter to the ship's heading.

In earlier comparisons only general agreement had been obtained between currents derived from GEK measurements and density distribution. In addition to the possibility that one or more of the various assumptions made might be significantly erroneous, it was recognized that in contrast with the average

204964—53—6

conditions represented by the dynamic topography, instantaneous current vectors would result from the GEK observations. These were considered to be the sum of the steady state and the momentary value of fluctuating currents. The fluctuating currents were expected to include periodic currents, such as tidal currents, and aperiodic currents, such as transient wind effects. To simplify the interpretation of the comparison as far as possible the first part of the June survey of 1950 was selected as having been made during exceptionally quiet weather when wind effects were assumed to have been negligibly small.

The above described method was used to compute equivalent differences in dynamic height, station to station, from the GEK observations (ΔD GEK) for stations 4175 to 4205 and compared with the differences in dynamic height of the surface above the 1,000-decibar surface (ΔD 1,000 dcb). The disagreement between the GEK and dynamic topography was of the same order of magnitude as in the 1948 measurements. To see if there were any relation between ΔD GEK and the density distribution two plots were made, one of ΔD GEK $-$ ΔD 1,000 dcb versus ΔD 1,000 dcb, and the other ΔD GEK $-$ ΔD 1,000 dcb versus gradient as determined from the dynamic topography. Both plots showed a random distribution of points with no evident relationship.

In order to study the general trend of ΔD GEK, cumulative plots were made of ΔD GEK, ΔD 1,000 dcb, ΔD 1,500 dcb and ΔD 2,000 dcb against distance. These plots showed that, although in general the profile of the sea surface thus constructed from the various derivations of ΔD tended to be similar, errors at any one point were masked by the fact that the curves were displaced from one another because of the cumulative differences in the values for each station interval.

To better examine the station to station differences, lines of ΔD GEK $-$ ΔD 1,000 dcb, ΔD GEK $-\Delta$D 1,500 dcb, ΔD GEK $-\Delta$D 2,000 dcb and ΔD GEK (uncorrected for drift) $-$ ΔD 1,000 dcb were plotted against distance. Disregarding the magnitude of the proportionality constant, there was little to choose between the different reference levels of dynamic computation in comparison with the GEK. Observations permitting the use of the deeper reference levels, however, were available only from the southern part of the survey. This southern section showed, surprisingly enough, that variations between the GEK and the dynamic heights were smallest in the area of shoalest water, a finding which is probably coincidental.

The proportionality factor of the current meter varied widely from station to station and was less than unity at 22 of the 30

interstation intervals as compared to the usually accepted values of unity or greater.

The average value of ΔD GEK — ΔD 1,000 dcb was computed to be + 8.6 dynamic mm with a probable departure from average of ± 103.2 mm. The average interstation interval was 28½ miles. When the equivalent difference in dynamic height was uncorrected for drift the average became + 7.7 ± 107.6 dynamic mm. From this it is concluded that the correction for drift is unimportant and need not be considered until the larger sources of discrepancy have been remedied.

By applying the cumulative values of ΔD GEK to the dynamic height at station 4175, quasi-dynamic heights were computed for the remainder of the stations and a chart of dynamic topography was drawn using these values. Comparison of this chart with one drawn exclusively from density considerations showed agreement only in the coarsest features of the circulation pattern and this method of constructing a current chart was not considered satisfactory.

In order to distribute the discrepancies between ΔD GEK and ΔD 1,000 dcb and thus preserve more of the circulation pattern found by considering only the density distribution, the computed quasi-dynamic heights were set equal to the dynamic heights at four points, stations 4175, 4185, 4195 and 4205, and the differences proportioned between these stations by adjusting ΔD GEK. This method produced a current chart which was closer to the chart constructed from density computations, but which still left much to be desired.

If a major source of the discrepancies was the measurement by dynamic topography of the steady state, as compared with the measurement by the current meter of the sum of the steady state and the fluctuating currents; and if, because of the weak winds which characterized this particular survey, the aperiodic currents were a negligible part of the fluctuating currents; then the discrepancies might be expected to represent in large measure the periodic fluctuations. An analysis was therefore undertaken as follows. The GEK current vectors, usually determined each half hour, were superimposed on the dynamic topographic chart and at each of these points the geostrophic current vector was scaled from the chart. The vector differences were then resolved into their north-south and east-west components and plotted against time beginning at station 4175. For the first 2 days there seemed to be a poorly defined period of about 18 hours in the north-south component. No other periods were apparent from inspection of the curves. If the errors of measurement contributed a negligibly small part to the discrepancies between the GEK measurements and the dynamic

topography, these results may indicate that the periodic currents of periods of more than a few hours were small enough to have been masked by larger aperiodic fluctuations, or that the area considered was large enough to include geographical differences in the periodic currents.

Since direction of the GEK vector is better than its magnitude, some means of constructing a current chart was sought in which the complete vector was used instead of using only one component of the vector.

The method of producing a current chart from current vectors gotten from the GEK is essentially the determination of the stream function (ψ) for many points on the chart. Contouring the chart for lines of equal value of the stream function will result in a current pattern, since the stream function is defined by this premise. The validity of the results depends on three major assumptions: that the GEK vectors are truly representative of the current, that the currents over the survey area are horizontal and free from vertical motion, and that the points at which a GEK current fix is obtained are spaced closely enough to permit representative sampling of all important spatial current fluctuations.

The first assumption is dependent upon the instrument and is reasonably safe in that sufficient observations have shown a good correspondence between GEK vectors and true currents.

The second assumption of horizontal flow is also an assumption in the computation of currents by the method of dynamic topography. However, there is a difference in that in computing the stream function any errors introduced due to divergence will be cumulative from station to station and may become very important after a number of stations if not kept under control. Maintaining control of the divergence is an important phase which is reflected both in laying out the track of the survey and the method of computing the stream function.

The third assumption of adequate sampling merely requires that GEK stations be made frequently along a track line such that all major current variations are in evidence.

The stream function (ψ) of fluid flow at a point x, y is defined mathematically as:

$$\psi_{x,\,y} = \int_{x_0,\,y_0}^{x,\,y} (u\,dy - v\,dx)$$

where x_0, y_0 is an arbitrary starting point where $\psi = o$; u and v are the x and y components respectively of the velocity.

If the GEK stations are spaced closely enough along a track line

such that no important features of the current pattern are missed, the equation then becomes:

$$\psi_{x,\,y} = \sum_{x_0,\,y_0}^{x,\,y} (u\,\Delta y - v\,\Delta x)$$

where u and v are the average x and y components of the velocity over the distance Δy and Δx.

The basic procedure is first to resolve the current vectors into x and y components and then numerically integrate along the track line from station to station beginning from an arbitrarily chosen starting station where ψ is let equal to zero. This series of computations will result in values of ψ for each station.

Where the track line crosses or approaches upon itself or returns to the starting point will serve as a test of the three assumptions since the value of ψ must be the same. If the values do not agree, then steps must be taken to bring them into accord. This may be done by discarding certain questionable vectors, by assigning relative weights to more desirable vectors, or by apportioning the difference over a segment of the track line which would give the best fit.

A similar method is to divide the survey into a grid of x and y lines. Each row of squares is denoted by a value of b and each column of squares by a. The size of the square is dependent on the interval of the stations and the scale of the chart. All the components falling within each square are averaged and assumed to apply at the midpoint of the square. Δx and Δy may then be equated to unity and the computations performed as before. This method expedites the process and averages out random errors, but may tend to smooth out true currents over a greater width than they actually occupy.

An intensive survey over a small area where the track line crosses many times provides numerous instances where ψ must be brought back into agreement with previously determined values. To do this by trial and error may become very laborious and often impossible. A method employing a statistical approach devised by Pritchard [5] is herein summarized for practical application to this case. This method determines the most probable value of the stream function for each midpoint of a grid such as described in the preceding paragraph. Values of ψ_x and ψ_y for each square are found by interpolation from the equations:

$$(\psi_y)_{a,\ b+\frac{1}{2}} = \sum_{y=o}^{y=b} u\,\Delta y \text{ and } (\psi_x)_{a+\frac{1}{2},\ b} = \sum_{x=o}^{x=a} v\,\Delta x$$

[5] Pritchard, D. W., "Streamlines from a discrete vector field," Jour. Mar. Res. Vol. VII, pp. 296–303, New Haven, 1948.
The notation used herein has been changed to avoid confusion.

A separate value of ψ_y and ψ_x is thus computed for each square, there being n squares in the x direction and m squares in the y direction. ψ_x and ψ_y must now be composed to produce the complete stream function for each square. Theory for this process utilizes the statistical method of least squares to obtain a distribution of ψ which will best fit the observed data. This derivation is not shown but the result is to compute constants of Aa and Bb which when added respectively to ψ_x and ψ_y determine ψ. The constants of A (A_1, A_2, $\cdots$) are computed for each horizontal row ($b = 1$, $b = 2$, $\cdots$) by the formula:

$$A_b = \left(\sum_{a=1}^{a=n} \psi_y - \sum_{a=1}^{a=n} \psi_x - \sum_{a=1}^{a=n} \psi_{x(b-1)} - \sum_{a=1}^{a=n} \psi_{y(b=1)} \right) n$$

and constants of B (B_1, B_2, $\cdots$) are computed for each vertical column ($a = 1$, $a = 2$, $\cdots$) by the formula:

$$B_a = \sum_{b=1}^{b=m} \psi_x - \sum_{b=1}^{b=m} \psi_y + \sum_{b=1}^{b=m} A \Big) m$$

Then the stream function may be computed from the following equation:

$$\psi_{a,\,b} = \psi_{x(a,\,b)} + A_b = \psi_{y(a,\,b)} + B_a$$

If the three primary assumptions are strictly true, then a value of ψ obtained from either equation will be the same. In practice, however, this will rarely be true and the mean is considered to be the most probable value.

Once the stream function has been determined for each square or station, the current map is produced by contouring the chart along lines of equal ψ in multiples of 5, 10, or 20 to suit the scale of the chart. The contours or streamlines will, of course, show the current direction at a particular position. The speed of the current is represented by the crowding of the streamlines, and is computed by dividing the interval of the streamline units by the distance between the streamlines in units which were used for Δx and Δy. These units may be any convenient arbitrarily selected units of length.

Current charts utilizing the above methods have agreed rather well with maps of dynamic topography made simultaneously. The former reflect to a much greater degree transitory and tidal currents.

It should be noted that in producing a map by directly integrating current components from station to station, the cumulative error may reach such proportions as to produce a fictitious overall picture, while smaller areas will be reasonably valid when studied separately.

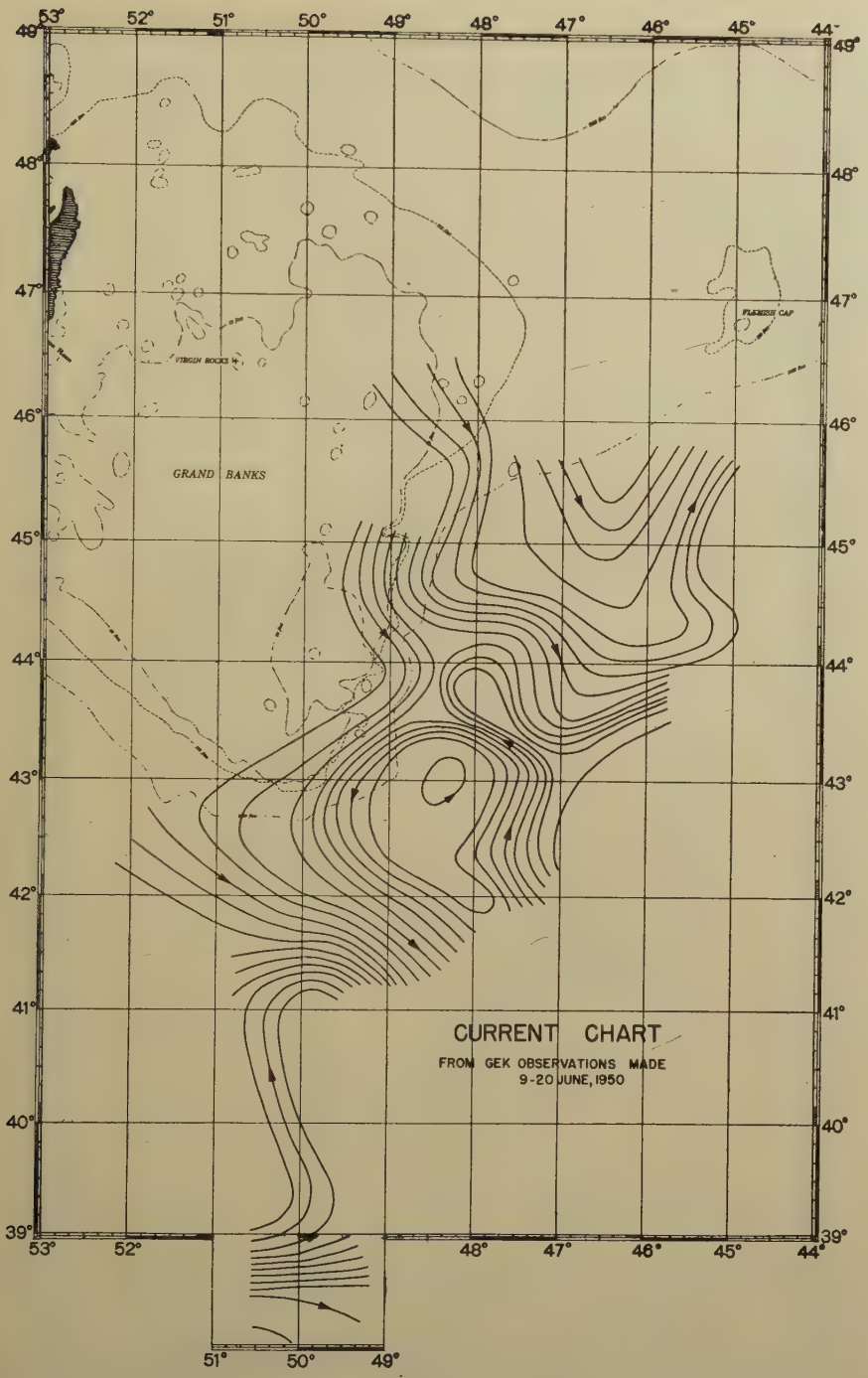

FIGURE 13.—Current chart constructed by contouring the stream function as derived from observations made with the von Arx current meter (GEK) 9–20 June 1950. Speed in knots is 6.9 divided by distance between contours in minutes of longitude.

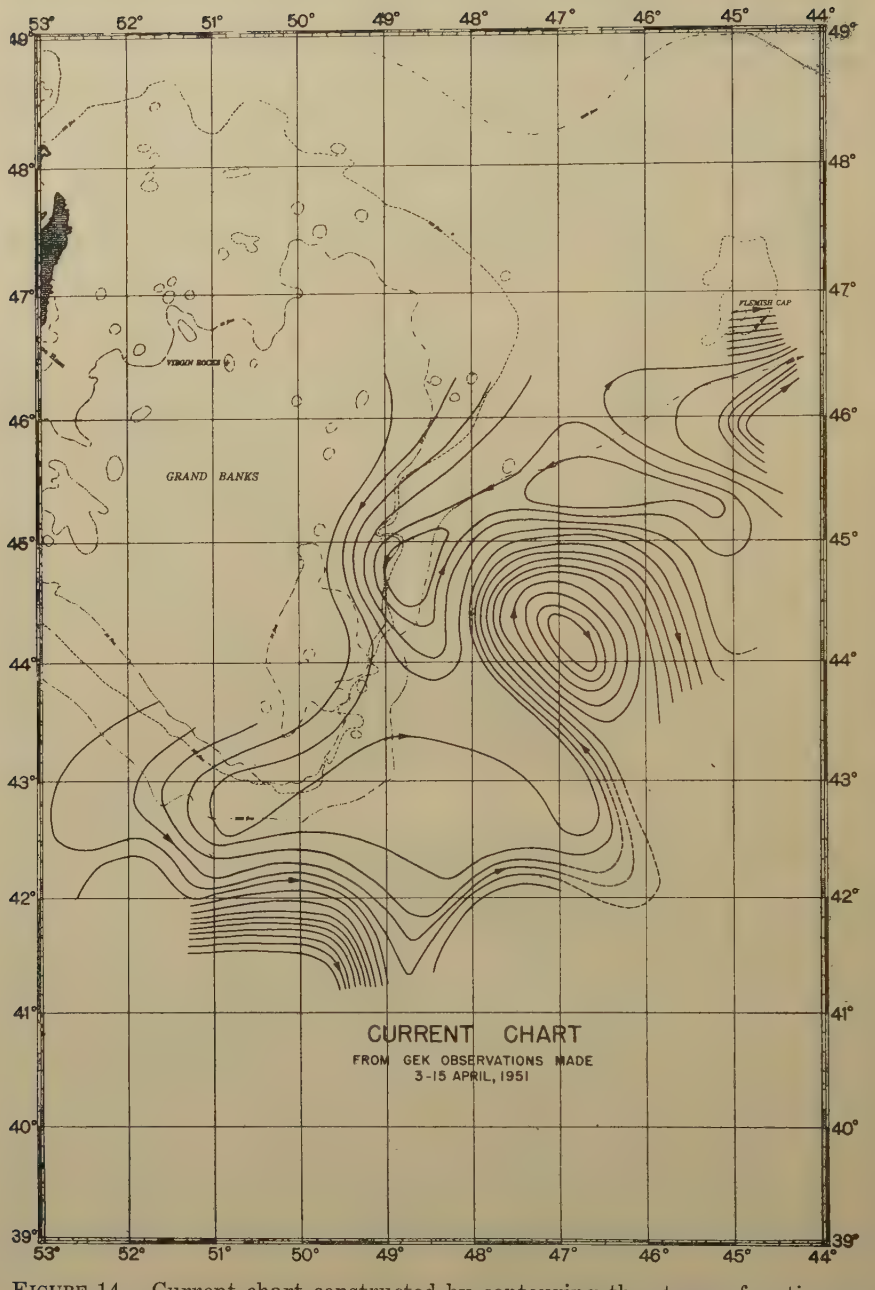

FIGURE 14.—Current chart constructed by contouring the stream function as derived from observations made with the von Arx current meter (GEK) 3–15 April 1951. Speed in knots is 5.4 divided by distance between contours in minutes of longitude.

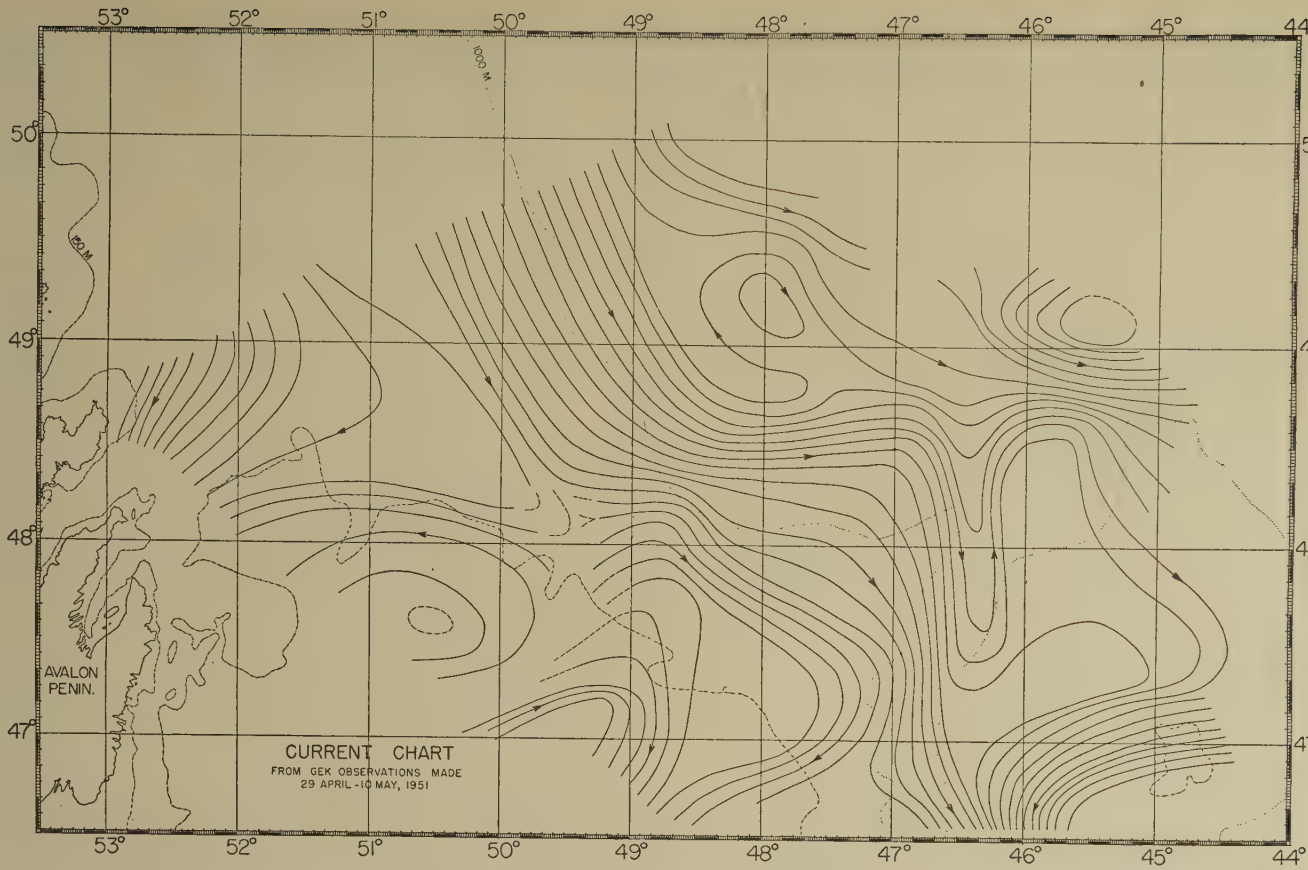

FIGURE 15.—Current chart constructed by contouring the stream function as derived from observations made with the von Arx current meter (GEK) 29 April–10 May 1951. Speed in knots is 2.9 divided by distance between contours in minutes of longitude.

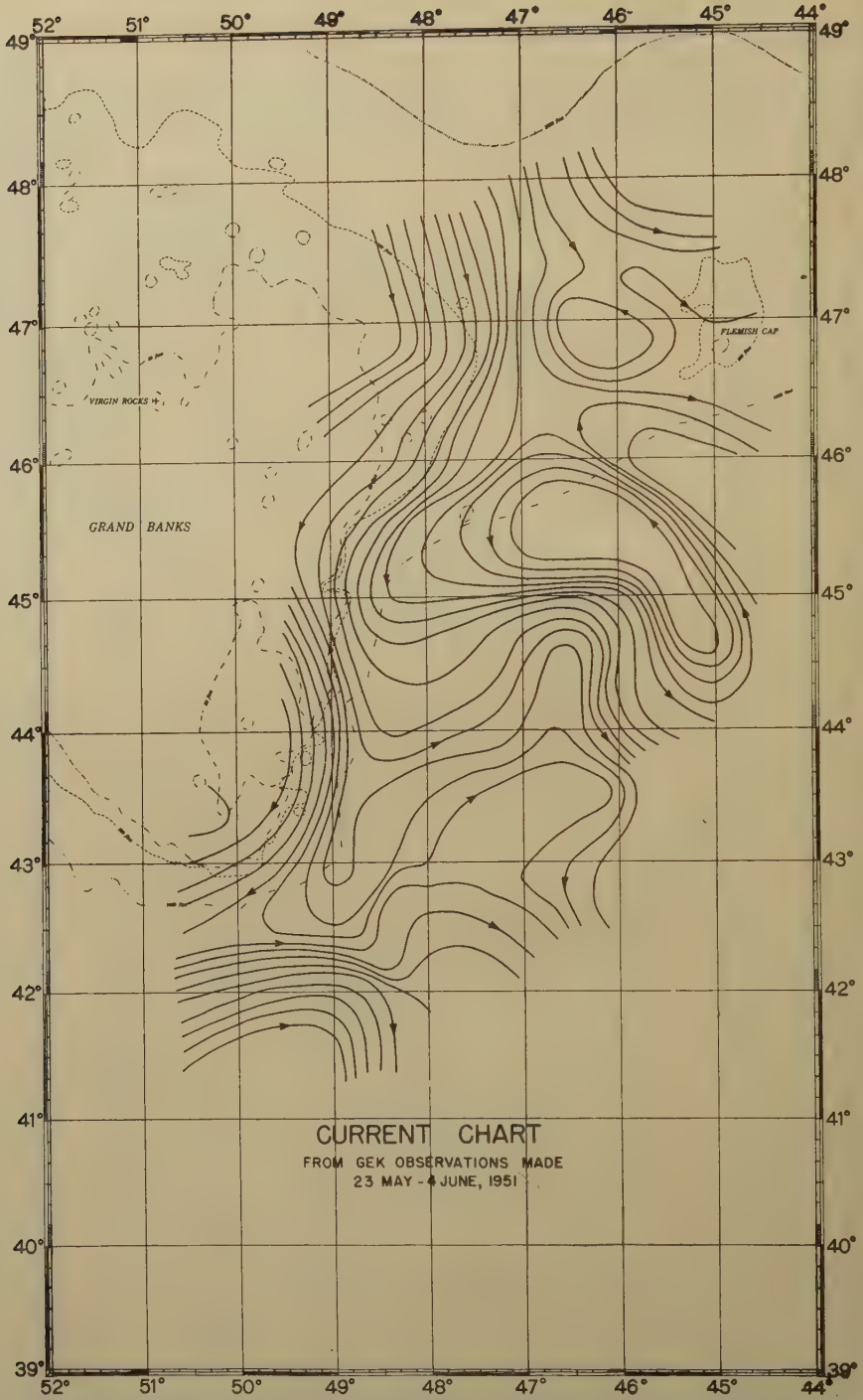

FIGURE 16.—Current chart constructed by contouring the stream function as derived from observations made with the von Arx current meter (GEK) 23 May–4 June 1951. Speed in knots is 5.4 divided by distance between contours in minutes of longitude.

Using the procedure described above, current charts have been constructed from the GEK vectors observed during the surveys made 9–20 June 1950, 3–15 April 1951, 29 April–10 May 1951, and 23 May–4 June 1951. The resulting charts are shown in figures 13 to 16 and are to be compared with the dynamic topographic charts shown in figure 18, Bulletin No. 36 of this series, and figures 7, 8, and 9 of this bulletin. In preparing figures 13 to 16, no correction has been applied to the magnitudes of the GEK vectors for the departure of the proportionality factor from unity or of the vertical intensity of the earth's magnetic field from 50,000 γ. The current speeds indicated by the GEK charts, therefore, are not exact but the directions and current patterns should be comparable to those shown in the charts of dynamic topography.

In figure 13 the difference in current pattern from that shown by the dynamic topography are greatest in the vicinity of 43° N., 49° W., and near 45° N., 47° W. Near the eastern edge of the Grand Banks at about 45° N., figure 13 shows a number of contour lines which are not present farther north. While the sources of such a discrepancy include the possibility of cumulative error of the GEK vectors and convergent flow, probably a major source is the treatment as synoptic a series of observations of fluctuating currents made over a considerable period of time. The relative speed of the current near the southern extreme of the survey is lower than expected and may be an instance of the smoothing out of peak velocities arising from the averaging process described above.

Figure 14 shows a difference in current pattern from that of figure 7 in the area near 43° N., 49° W., and marked differences in relative speed shown by these figures are present in the extreme western and northeastern parts of the surveyed area.

In comparing figure 15 with figure 8, we find general agreement in the eastern branch of the Labrador Current and disagreement in the vicinity of Flemish Cap and Cape Bonavista. In each of these cases the disagreement is considered to be the result of periodic fluctuating currents. It is to be noted that the disagreement between the GEK and dynamic topography seems to be no worse for this survey than for the southern part of the survey made in June 1950, although the latter was made during exceptionally quiet weather and the former during exceptionally boisterous weather.

The comparison of figure 16 with figure 9 shows areas of disagreement near 43° N., 48° W., and 46° N., 46° W. While it is noted that the areas of disagreement consistently occur along the outer margins of the North Atlantic Current in the four charts presented here, the degree of consistency is insufficient to warrant conclusions as to the principal cause of the disagreements.

In previous bulletins of this series the position of the outer boundary of the North Atlantic Current water in the Grand Banks region has been reported and related to factors assumed to be associated with the relative strengths of the North Atlantic Current and the Labrador Current. The boundary has been taken as the horizontal projection of the line of intersection of the isothermal surface of 6° and the isohaline surface of $34.95^0/_{00}$. As the boundary is characteristically sinuous, its position has been described by the area between it and reference rhumb lines made up of the 45th parallel from the boundary to 49° W., the 49th meridian thence to 43° N., and a line from 43° N., 49° W., through 42° N., 47° W., extended to the boundary. To compensate for the effect of the Labrador Current on the position of the boundary, the area was adjusted by the subtraction of 10,000 square kilometers for each million cubic meters per second volume of flow of the Labrador Current past section U. The adjusted area was assumed to represent effects on the position of the boundary the causes of which were associated with the North Atlantic eddy. A further assumption was made that changes in the strength of the Gulf Stream were proportional to changes in the difference in sea level between Bermuda and Charleston, S. C. Monthly mean sea levels at each of these stations, corrected to normal barometric pressure for the station, were used to derive a value for the change in difference in sea level by taking sea level at Charleston minus the departure from average at Bermuda. Over the period from 1934 to 1941 a good correlation was found to exist between the sea level difference, Charleston, minus the Bermuda departure, and the adjusted area in the Grand Banks region 13½ months later. During this period 27 surveys gave the relation

$$A = 6.8(H - 5.07) + 1.34$$

where A is the adjusted area in units of 10,000 square kilometers and H is the sea level difference Charleston minus the Bermuda departure, in feet.

Since resumption of the oceanographic program of the International Ice Patrol after World War II eight surveys of the Grand Banks region have been made, one in 1948, two in 1949, three in 1950, and two in 1951. These surveys show a poorer correlation, with three of the eight cases showing a discrepancy as to sign. The differences between the post-war series and the earlier series are large enough to suggest a revision of the above expression for the relationship between the adjusted area and the sea level difference.

Before deriving a new expression for A, consideration was given to the changes in conditions and to their physical significance. If a true relationship exists, it should apply to both series of observations. The fact that the relationship depends on the departure

from normal of the difference in sea level across the Bermuda-Charleston section focuses attention on that normal. No extended uninterrupted series of tide gauge records exist for the Bermuda end of the section and so it is not yet possible to draw any conclusions regarding changes in mean sea level at that end of the section. At the Charleston end of the section tide gauge records have continued with reference to the same bench mark since the fall of 1921. They show an increase in sea level with an abrupt rise of about 0.14 foot between 1932 and 1933 to a mean value of 5.07 for the 8-year period 1933–40 (used in studying the relationship with the 27 surveys made 1934–41) with a further increase to a mean of 5.40 for the 4-year period 1947–50 (used in connection with the 8 recent surveys made during 1948–51). It is not known whether sea level at both ends of the section rose or whether the change occurred only at the Charleston end. Nor is it known what part of the change at Charleston represents a sinking of the coast. This is believed to be of a smaller order of magnitude. It is also considered that the rate of change of total volume of water in the oceans is negligibly small. If the sinking of the coast can be neglected and if most of the changes in sea level across the section take place at the outer edge of the North Atlantic eddy, the change can be interpreted as indicating a weaker circulation of the Gulf Stream system during the post-war period. Examination of the tide gauge records, therefore, indicate that the figure of 5.07 may continue to be used as the normal sea level from which departures may be considered.

In the Grand Banks sector of the North Atlantic eddy the outer margin of North Atlantic Current water, as defined by the unadjusted area, was somewhat nearer the center of the eddy but maintained a position which averaged nearly the same for the post-war period as for the earlier period (7.1×10^4 as compared with 6.8×10^4 square kilometers). During the post-war period the volume of flow of the Labrador Current past section U has been decidedly subnormal compared with the earlier period (about 3.0 as compared with about 6.8×10^6 cu.m/sec.). Qualitatively, then, these changes are in agreement, with the position of the boundary in the Grand Banks sector undergoing little change since both the Labrador Current and the North Atlantic eddy were weaker than previously.

If a contraction of the boundary of the North Atlantic eddy follows weakening of the circulation in the eddy, the peripheral branches fed by the eddy might be expected to be profoundly affected by such a contraction, especially if the branching is conditioned by the configuration of the land or bottom. The Irminger Current, recurving to the westward in the vicinity of Iceland, contributes Atlantic water to make the West Greenland Current a

relatively warm current. Observations of the West Greenland Current off Cape Farewell have been made during each of 14 summertime occupations of the section extending from the Labrador coast to Cape Farewell. These include 6 of the 8 years 1934–41 and each of the 4 years 1948–51. The Irminger Current component of the West Greenland Current was subnormal in 1948 and almost totally absent from this section in each of the three subsequent years. This agrees qualitatively with the conception of a contracted weakened North Atlantic eddy.

It has been concluded, therefore, that the differences between conditions found during the post-war period and the earlier period do not represent permanent changes but more probably represent longer period departures from normal. In computing the relationship between the adjusted area A and the sea level difference, Charleston-Bermuda departure, H, the previous normal value of $H = 5.07$ has been used in combining all observations to derive the expression

$$A = 6.4(H - 5.07) + 1.85$$

for computing the adjusted area with a probable error of $\pm$ 1.9 $\times 10^4$ square kilometers. In figure 17 the values of A computed by the use of this formula are shown as circles connected by broken lines and are compared with the values of A derived by adjusting the observed area by the subtraction of the volume of flow of the Labrador Current past section U. The latter are shown as black dots and are connected by solid lines. The shape of the connecting lines follows the changes in H. In arriving at the "observed" values of A there are several possible sources of error such as in estimating the location of the boundary in those parts of a survey where the boundary is outside the limits of the survey, and in determining the volume of flow of the Labrador Current past section U, and in assuming that that part of the volume of flow past section U which is water from the Grand Banks eddy is of importance equal to that of the true Labrador Current in determining the position of the boundary. In arriving at the computed values of A, all modifying factors which may be interposed in 13½ months and along 1,500 miles have been neglected. For example, no account has been taken of the possible development in or progress through the Grand Banks sector of a meander. In view of these uncertainties, the agreement between the observed and computed values of A is considered to be good.

In the studies that thus far have been made of the triangle off Cape Bonavista one of the points of interest which has received attention is whether or not the area is one in which the current pattern at the surface is sufficiently similar to that at subsurface levels to permit the movement of deep draft bergs to be deduced

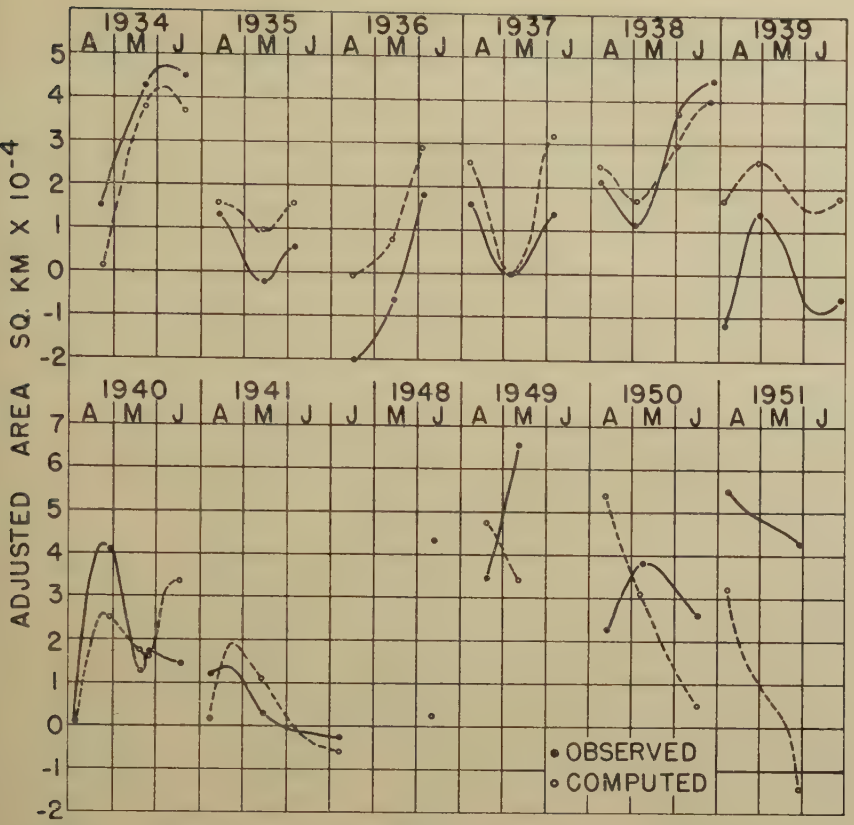

FIGURE 17.—Correspondence between adjusted area in Grand Banks sector and sea level difference, Charlston-Bermuda departure, 13½ months earlier. Dots show adjusted area derived from observed boundary. Circles show adjusted area computed from $A = 6.4(H - 5.07) + 1.85$. Shape of curves derived from changes in H.

from a consideration of the dynamic topography of the sea surface alone. The dynamic topography at the 100-decibar surface has been compared with that at the surface in surveys made in previous years and in general the current patterns have been found to be similar. The current patterns found at the surface and at the 100-decibar surface have been compared and found to be similar for each of the two occupations of the triangle made in 1951. The dynamic topography of the surface found during the second cruise has been shown in figure 8. That found during the post-season cruise is shown in figure 18. The dynamic topography of the sea surface obtained from the triangle indicates that any bergs entering the area from the north would have followed the eastern branch of the Labrador Current if they had crossed the 49th parallel eastward of about 53° W., whereas those crossing the 49th parallel westward of that longitude would have either followed the western branch or stranded on the northern slope of the Grand Banks. It

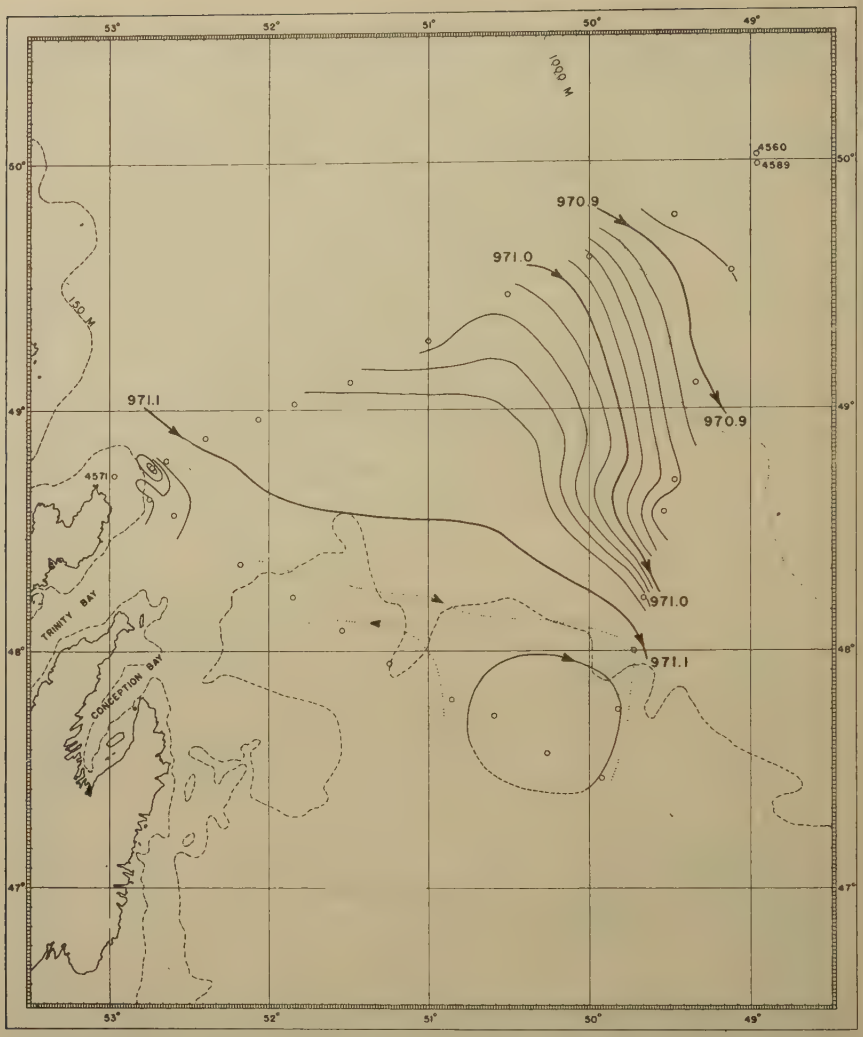

FIGURE 18.—Dynamic topography of the sea surface relative to the 1000-decibar surface from data collected 14–17 July 1951. Oceanographic station positions are indicated and the station numbers given at turning points.

is noted also, that the topography indicates that some of the bergs following the eastern branch would have stranded on the northeastern shoulder of the Grand Banks between about 48° N., and 47°30′ N.

The von Arx current meter was operated on the run from Port Union to the first station of the triangle (number 4560). As this run was very nearly over the reverse path followed in occupying the first section of the triangle (stations 4560 to 4571) the two sets of current vectors are comparable except as to time. The differences obtained verify the existence here of transitory (probably tidal) currents.

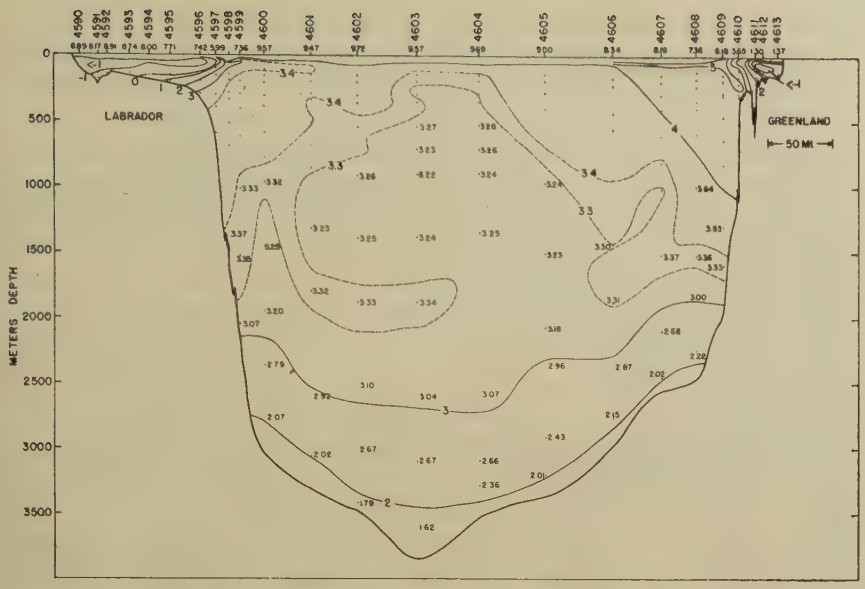

FIGURE 19.—Temperature distribution between South Wolf Island, Labrador, and Cape Farewell, Greenland, 18–23 July 1951.

Figure 19 shows the temperature distribution along the section across the Labrador Sea from South Wolf Island, Labrador, to Cape Farewell, Greenland, from data collected during the post-season cruise of 1951. The temperature minimum layer which characterizes the Labrador Current over the shelf was not as cold as usual. The warm tongue which extends inshore and downward to the continental slope beneath the core of the Labrador Current is to be seen in figure 19 between the 3.4° isotherms. This tongue contained maximum temperatures slightly warmer than 3.5° and thus was colder than usual by several tenths of a degree. The temperature minimum which is a feature of the intermediate water of the Labrador Sea in summer was somewhat warmer than the usual 3.17°. The warmer offshore part of the West Greenland Current, usually contributed by the Irminger Current, was colder than usual again with temperatures exceeding 5° only in a small tongue extending inshore and downward toward the edge of the shelf at station 4610. Temperatures as high as 6° were not found except in the upper 50 meters.

The deficiency of Irminger Current water indicated by the subnormal temperatures of the West Greenland Current is also shown in figure 20 by the subnormal salinity of this part of the West Greenland Current. This figure shows the salinity distribution found in 1951 along the Greenland end of the South Wolf Island-Cape Farewell section. The salinity maximum, which was remarkably constant at 35.04‰ until 1949, was only 34.96‰ in 1951 as compared with 34.97 in 1949 and 34.99 in 1950. The small

cross sectional area of water of salinity in excess of 34.95‰ is noted as additional evidence of the almost total absence of Irminger Current water at this section.

The dynamic topography of the sea surface relative to the 1500-decibar surface in the vicinity of the South Wolf Island-Cape Farewell section, found during the 1951 post-season cruise, is shown in figure 21. The Labrador Current has two major bands, one inshore of the shoal off Hamilton Inlet and the other over the continental slope. In the central part of the section there is evidence of a small amount of water from the extreme northwestern margins

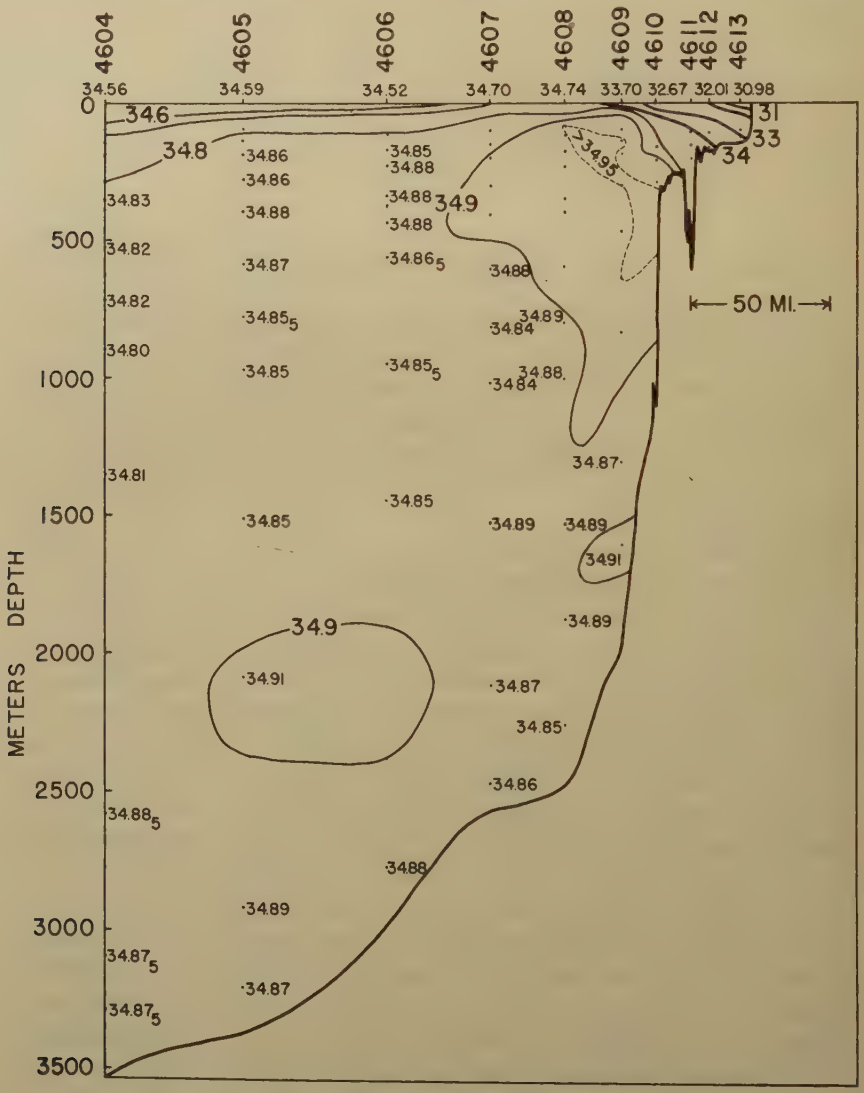

FIGURE 20.—Salinity distribution off Cape Farewell, Greenland, 21–23 July 1951.

of the North Atlantic eddy entering and leaving the Labrador Sea. There is also an indication of a weak counterclockwise eddy between this water and the West Greenland Current.

The volume of flow, mean temperature, and heat transport of the Labrador Current past this section has already been presented

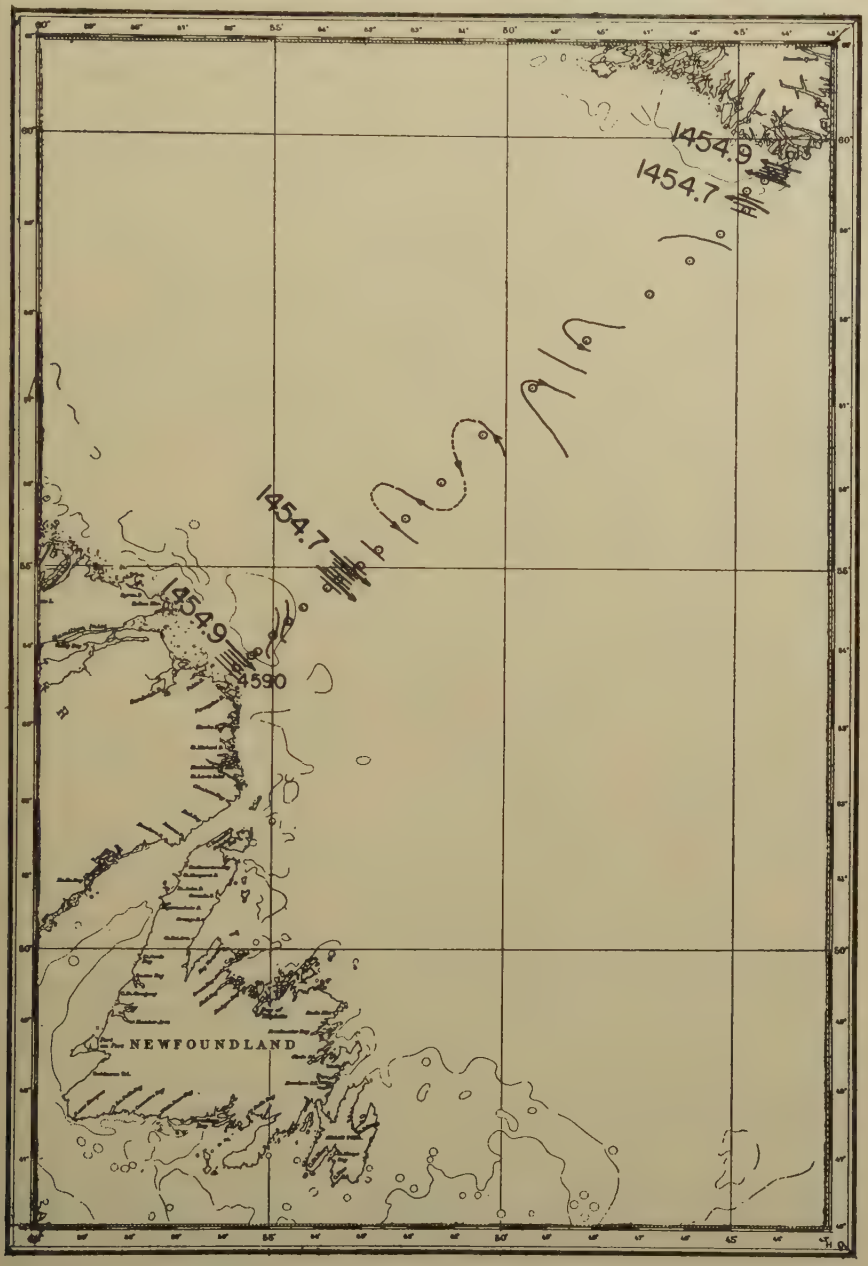

FIGURE 21.—Dynamic topography of the sea surface relative to the 1500-decibar surface, from data collected 18–23 July 1951.

in table 1 and discussed in connection with other measurements of the Labrador Current. The rest of the section has been examined in a similar manner. The West Greenland Current, which lies between approximately station 4605 and the beach at Cape Farewell, was computed to have a volume of flow of 5.28 million cu.m/sec., a mean temperature of 3.68° C and a heat transport of 19.41 million cu.m. degrees C/sec. These units will be used in the remainder of the discussion without further repetition. In Bulletin No. 35 of this series mean curves of seasonal variation were presented for the volume of flow of the West Greenland Current and its components of East Greenland Current (assumed to have a constant mean temperature of 3.2° C) and of Irminger Current (assumed to have a constant mean temperature of 5.5° C). If these curves are taken as normals, then for the time of year when the section was occupied in 1951 the normal volume of flow would have been 4.48 (made up of 1.47 East Greenland Current water and 3.01 Irminger Current water) with a mean temperature of 4.74° C, and a heat transport of 21.26. Thus in 1951 the West Greenland Current was above normal in volume transport and subnormal in mean temperature and slightly subnormal in heat transport.

A critical examination of the velocity section, however, leads to the conclusion that of the 5.28 volume of flow of the West Greenland Current only the inshore 4.50 is contributed from the northeastward of Cape Farewell and at least 0.78 is a more direct contribution from the waters nearby and to the southeastward of Cape Farewell. The volume transport of 4.50 is therefore considered to include the contributions from the East Greenland Current and the Irminger Current and may possibly also include some water from the outer margins of the North Atlantic eddy which has recurved westward before reaching the vicinity of Iceland. The mean temperature of the 4.50 volume of flow was 3.77°. Assuming the same constant mean temperatures of the East Greenland Current and Irminger Current components which were used in deriving the mean seasonal variation curves we arrive at the volume transports of 3.38 and less than 1.12 for the contributions from the East Greenland and Irminger Currents respectively. These values are to be compared with the seasonal normals of 1.47 and 3.01 mentioned above. Reference is made to figure 10 for a schematic representation of the circulation deduced above.

Between the outer margins of the Labrador Current and the West Greenland Current there was computed to be a net southeasterly flow of 0.81. This is considered to have its origin in the early recurving of the outer margin of the West Greenland Current passing the Cape Farewell section. Thus the net flow out of the Labrador Sea at this section exceeded the inflow past the

section by about 0.8, which represents the contributions through the northern openings less such an amount as sank below the reference surface of 1,500 decibars.

SUMMARY

1. The surface circulation in the Grand Banks region in 1951 has been discussed on the basis of three dynamic topographic charts made during the season.

2. A more detailed picture of the circulation in the upper 1,000 meters in the Grand Banks region has been presented on the basis of volume of flow, mean temperature, and minimum observed temperature of the Labrador Current at 14 occupations of 8 selected sections made during the 1951 season.

3. The temperature-salinity relationships for the three water masses found in the Grand Banks region in 1951 have been compared with conditions found in other years.

4. Observations made with a von Arx geomagnetic electrokinetograph in 1950 and 1951 have been given further study in comparison with the dynamic topography based on concurrently collected temperature and salinity observations. A method of applying the stream function to the construction of a contoured current chart from the GEK vectors has been described and four charts made by its use have been presented.

5. The relationship between the location of the northern boundary of North Atlantic Current water in the Grand Banks region, the strength of the Labrador Current, and the changes in the difference in sea-level between Bermuda and Charleston have been reviewed in the light of 27 surveys made during the period 1934–41 and 8 surveys made 1948–51. A weakened post-war circulation in the North Atlantic eddy, deduced from changes in the sea level difference at the Bermuda-Charleston section, has been proposed as a possible explanation for the deficiency of the Irminger Current component of the West Greenland Current at Cape Farewell.

6. An increase in temperature of the intermediate water of the Labrador Sea in 1951 over 1950 has been noted and the thermal characteristics of the section from South Wolf Island, Labrador, to Cape Farewell, Greenland, have been compared with those found in earlier occupations of this section.

7. The circulation in the southern part of the Labrador Sea has been inferred from examination of the volume transport and mean temperature of the Labrador Current and West Greenland Current and, with the supporting evidence of temperature and salinity observations, it has been concluded that the Irminger Current component of the West Greenland Current continued to be deficient in 1951.

The data collected during the 1951 season and post-season cruises are tabulated below. The individual station headings give the station number, date, geographical position, depth of water, and the dynamic height of the sea surface used in the construction of the dynamic topographic charts shown in figures 7, 8, 9, 18, and 21. The depths of water are uncorrected sonic soundings based on a sounding velocity of 800 fathoms per second. Where the depths of the scaled values are enclosed in parentheses, the data are based on extrapolated vertical distribution curves of temperature or salinity or both. Asterisks appearing before observed temperatures indicate that these temperatures were determined from the depth of reversal and the corrected reading of an unprotected thermometer. The symbol σ_t signifies 1,000 (density — 1) at atmospheric pressure and temperature *t*.

Table of Oceanographic Data

STATIONS OCCUPIED IN 1951

Station 4307; Apr. 3; latitude 43°32.5′ N., longitude 51°32′ W.; depth 89 meters, dynamic height 971.100

Observed values			Scaled values			
Depth, meters	Temperature °C.	Salinity ‰	Depth, meters	Temperature °C.	Salinity ‰	σ_t
0	2.17	33.41	0	2.17	33.41	26.72
26	3.87	32.97	25	3.80	32.98	26.22
51	7.98	34.18	50	7.70	34.13	26.65
77	9.63	34.78	75	9.55	34.75	26.85

Station 4308; Apr. 3; latitude 43°27.5′ N., longitude 51° 44′ W.; depth 169 meters, dynamic height 971.111

Observed values			Scaled values			
Depth, meters	Temperature °C.	Salinity ‰	Depth, meters	Temperature °C.	Salinity ‰	σ_t
0	3.88	33.42	0	3.88	33.42	26.57
26	3.87	33.42	25	3.85	33.42	26.57
52	4.31	33.48	50	4.20	33.47	26.58
78	7.38	34.18	75	7.00	34.10	26.73
104	9.55	34.65	100	9.50	34.64	26.77
156	6.93	34.42	150	7.20	34.45	26.98

Station 4309; Apr. 3; latitude 43°22′ N., longitude 51°46′ W.; depth 340 meters, dynamic height 971.093

Observed values			Scaled values			
Depth, meters	Temperature °C.	Salinity ‰	Depth, meters	Temperature °C.	Salinity ‰	σ_t
0	6.08	33.61	0	6.08	33.61	26.47
20	6.12	33.62	25	6.10	33.62	26.48
40	6.13	33.62	50	6.15	33.63	26.47
60	6.23	33.71	75	8.00	34.21	26.68
80	8.43	34.37	100	7.15	34.66	27.15
			(150)	5.30	34.50	27.26
			(200)	4.95	34.47	27.29
			(300)	4.50	34.45	27.32

Station 4310; Apr. 3–4; latitude 43°19.5′ N., longitude 51° 53′ W.; depth 649 meters, dynamic height 971.110

Observed values			Scaled values			
Depth, meters	Temperature °C.	Salinity ‰	Depth, meters	Temperature °C.	Salinity ‰	σ_t
0	6.38	33.70	0	6.38	33.70	26.50
18	6.57	33.72	25	6.60	33.72	26.49
35	6.59	33.73	50	7.70	34.04	26.58
53	8.35	34.17	75	9.85	34.67	26.74
71	9.83	34.66	100	9.86	34.70	26.77
107	9.70	34.70	150	7.55	34.64	27.07
142	7.90	34.66	200	5.90	34.52	27.21
213	5.59	34.50	(300)	4.70	34.47	27.31
			(400)	4.10	34.61	27.49
			(600)	3.40	34.80	27.71

Station 4311; Apr. 4; latitude 43°15.5′ N., longitude 52°06′ W.; depth 1,737 meters, dynamic height 971.099

Observed values			Scaled values			
Depth, meters	Temperature °C.	Salinity ‰	Depth, meters	Temperature °C.	Salinity ‰	σ_t
0	8.78	34.47	0	8.78	34.47	26.77
25	8.79	34.47	25	8.79	34.47	26.76
49	8.80	34.47	50	8.80	34.47	26.76
73	8.82	34.57	75	8.80	34.57	26.84
97	7.12	34.30	100	7.15	34.30	26.87
147	7.81	34.48	150	7.80	34.49	26.92
196	6.72	34.66	200	6.70	34.66	27.21
293	5.63	34.64	300	5.50	34.64	27.35
377	4.33	34.66	400	4.25	34.67	27.52
519	4.09	34.78	600	4.10	34.83	27.66
633	4.16	34.85	800	4.25	34.92	27.72
810	4.25	34.925	1,000	4.05	34.92	27.74
1,283	3.66	34.90				

Station 4312; Apr. 4; latitude 42°03′ N., longitude 52°26′ W.; depth 2,798 meters, dynamic height 971.093

Observed values			Scaled values			
Depth, meters	Temperature °C.	Salinity ‰	Depth, meters	Temperature °C.	Salinity ‰	σ_t
0	13.35	35.49	0	13.35	35.49	26.72
23	13.36	35.49	25	13.35	35.49	26.72
46	13.36	35.48	50	13.30	35.48	26.72
69	11.58	35.09	75	11.45	35.07	26.77
91	11.11	35.03	100	10.70	34.97	26.83
137		34.70	150	7.60	34.60	27.04
183	5.97	34.43	200	5.85	34.45	27.16
274	5.64	34.62	300	5.95	34.74	27.37
335	6.47	34.88	400	5.30	34.85	27.54
512	4.18	34.78	600	4.15	34.85	27.67
695	4.17	34.92	800	4.05	34.91	27.73
878	4.01	34.90	1,000	3.85	34.90	27.74
1,349	3.55	34.88				

STATIONS OCCUPIED IN 1951—Continued

Station 4313; Apr. 4; latitude 42°51′ N., longitude 52°42′ W.; depth 3,475 meters, dynamic height 971.146

Observed values			Scaled values			
Depth, meters	Temperature °C.	Salinity ‰	Depth, meters	Temperature °C.	Salinity ‰	σ_t
0	11.17	34.97	0	11.17	34.97	26.75
25	11.18	34.97	25	11.18	34.97	26.75
50	11.19	34.98	50	11.19	34.98	26.74
75	11.29	35.00	75	11.29	35.00	26.74
100	11.51	35.13	100	11.51	35.13	26.79
150	10.82	34.94	150	10.82	34.94	26.78
201	8.32	34.86	200	8.30	34.86	27.14
301	5.77	34.63	300	6.35	34.68	27.27
356	6.28	34.67	400	5.30	34.69	27.41
535	4.53	34.81	600	4.55	34.87	27.65
714	4.60	34.96	800	4.40	34.95	27.72
926	4.08	34.93	1,000	4.00	34.93	27.75
1,485	3.79	34.95				

Station 4314; Apr. 4; latitude 42°36′ N., longitude 52°52′ W.; depth 3,841 meters, dynamic height 971.139

0	15.56	35.94	0	15.56	35.94	26.58
24	14.79	35.76	25	14.70	35.75	26.63
47	12.52	35.19	50	12.50	35.18	26.65
71	12.35	35.16	75	12.30	35.14	26.66
94	11.22	35.01	100	10.85	34.99	26.81
140	.....	34.92	150	8.00	34.88	27.20
187	6.76	34.73	200	6.60	34.71	27.27
281	6.15	34.65	300	6.05	34.65	27.29
745	4.67	34.94	400	5.60	34.72	27.40
1,286	3.93	34.96	600	4.90	34.88	27.61
			800	4.55	34.94	27.70
			1,000	4.30	34.95	27.73

Station 4315; Apr. 4; latitude 42°22.5′ N., longitude 52°23′ W.; depth 3,841 meters, dynamic height 971.305

0	16.79	36.20	0	16.79	36.20	26.51
25	16.93	36.21	25	16.93	36.21	26.48
49	16.74	36.20	50	16.70	36.20	26.53
74	16.32	36.12	75	16.30	36.11	26.55
98	15.70	35.96	100	15.65	35.96	26.58
148	.....	35 90	150	14.45	35.89	26.79
196	13.38	35.65	200	13.30	35.63	26.83
294	10.91	35.33	300	10.80	35.32	27.08
249	11.80	35.39	400	9.40	35.13	27.17
451	8.70	35.06	600	6.50	34.96	27.48
752	4.87	34.93	800	4.65	34.93	27.68
1,269	4.04	34.96	1,000	4.35	34.94	27.72

Station 4316; Apr. 5; latitude 42°05′ N., longitude 52°04′ W.; depth 3,896 meters, dynamic height 971.281

0	17.41	36.35	0	17.41	36.35	26.47
24	17.40	36.34	25	17.40	36.34	26.47
48	17.41	36.34	50	17.40	36.34	26.47
72	17.39	36.33	75	17.35	36.33	26.47
96	16.08	36.09	100	15.90	36.07	26.60
193	15.24	35.93	150	15.40	35.97	26.65
318	12.20	35.53	200	15.15	35.91	26.66
478	7.77	35.04	300	12.70	35.60	26.94
641	4.40	34.79	400	8.55	35.27	27.42
821	4.64	34.95	600	4.75	34.82	27.58
1,305	4.05	34.96	800	4.60	34.94	27.69
			1,000	4.45	34.94	27.71

Station 4317; latitude 42°08′ N., longitude 51°04′ W. Apr. 5; depth 316 meters, dynamic height 971.258

0	18.07	36.39	0	18.07	36.39	26.34
27	18.08	36.38	25	18.10	36.39	26.33
53	16.02	35.94	50	16.35	36.02	26.47
79	15.63	35.89	75	15.65	35.89	25.52
105	15.80	36.03	100	15.80	36.02	26.59
159	14.64	35.82	150	14.85	35.86	26.68
211	13.71	35.78	200	13.95	35.79	26.82
316	10.35	35.28	300	10.85	35.36	27.10
417	7.73	35.03	400	8.15	35.06	27.32
627	4.36	34.80	600	4.45	34.81	27.61
838	4.48	34.94	800	4.45	34.92	27.70
1,049	4.35	34.975	1,000	4.40	34.97	27.74
1,577	3.72	34.94				

Station 4318; Apr. 5; latitude 42°19′ N., longitude 51°31′ W.; depth 3,017 meters, dynamic height 971.258

0	17.16	36.26	0	17.16	36.26	26.46
29	17.10	36.26	25	17.10	36.26	26.47
56	17.07	36.25	50	17.10	36.26	26.47
85	15.83	35.98	75	16.25	36.08	26.53
113	15.39	35.95	100	15.60	35.91	26.56
170	14.16	35.66	150	14.60	35.72	26.63
227	13.10	35.60	200	13.60	35.63	26.77
339	10.06	35.25	300	11.40	35.40	27.03
443	5.86	34.68	400	7.40	34.92	27.32
663	3.96	34.80	600	3.95	34.76	27.62
1,328	3.93	34.90	800	4.00	34.87	27.71
			1,000	3.95	34.90	27.73

Station 4319; Apr. 5; latitude 42°41′ N., longitude 51°00′ W.; depth 1,628 meters, dynamic height 971.101

0	7.61	34.07	0	7.61	34.07	26.62
28	7.56	34.26	25	7.55	34.23	26.75
55	8.61	34.50	50	8.45	34.46	26.80
83	9.23	34.64	75	9.10	34.62	26.83
110	9.30	34.68	100	9.30	34.67	26.83
166	7.82	34.65	150	8.20	34.66	27.00
220	9.21	35.13	200	8.70	34.96	27.15
330	5.29	34.66	300	6.10	34.76	27.37
426	4.55	34.73	400	4.60	34.70	27.50
632	4.73	34.95	600	4.75	34.93	27.66
836	3.84	34.89	800	3.95	34.90	27.73
1,046	3.57	34.88	1,000	3.55	34.88	27.75
1,574	3.46	34.885				

Station 4320; Apr. 5; latitude 42°50.5′ N., longitude 50°45′ W.; depth 1,060 meters, dynamic height 971.068

0	5.84	33.78	0	5.84	33.78	26.63
25	7.70	34.21	25	7.70	34.21	26.72
50	8.14	34.36	50	8.14	34.36	26.77
75	8.99	34.58	75	8.99	34.58	26.81
100	9.57	34.79	100	9.57	34.79	26.88
150	6.93	34.52	150	6.93	34.52	27.07
200	6.09	34.55	200	6.09	34.55	27.20
300	4.68	34.65	300	4.68	34.65	27.43
397	3.69	34.67	400	3.70	34.67	27.58
594	4.04	34.85	600	4.05	34.85	27.68
791	3.82	34.87	800	3.85	34.87	27.72
987	3.63	34.87	1,000	3.60	34.87	27.75

STATIONS OCCUPIED IN 1951—Continued

Station 4321; Apr. 5-6; latitude 42°53′ N., longitude 50°40′ W.; depth 622 meters, dynamic height 971.056

Observed values			Scaled values			
Depth, meters	Temperature °C.	Salinity ‰	Depth, meters	Temperature °C.	Salinity ‰	σ_t
0	7.21	34.11	0	7.21	34.11	26.71
26	7.57	34.29	25	7.55	34.28	26.79
52	7.59	34.32	50	7.60	34.32	26.82
78	6.36	34.14	75	6.45	34.16	26.85
104	4.90	34.01	100	5.05	34.02	26.92
156	6.01	34.44	150	5.90	34.38	27.09
209	6.77	34.75	200	6.70	34.74	27.27
313	4.62	34.68	300	4.85	34.69	27.47
400	3.96	34.70	400	3.95	34.70	27.57
596	3.77	34.81	600	3.75	34.81	27.68

Station 4322; Apr. 6; latitude 42°58′ N., longitude 50°36′ W.; depth 169 meters, dynamic height 971.068

Observed values			Scaled values			
Depth, meters	Temperature °C.	Salinity ‰	Depth, meters	Temperature °C.	Salinity ‰	σ_t
0	2.76	32.94	0	2.76	32.94	26.29
23	2.45	33.10	25	2.45	33.20	26.52
46	4.72	33.84	50	5.00	33.89	26.82
69	6.12	34.10	75	6.35	34.14	26.85
93	6.87	34.24	100	6.85	34.23	26.85
139	5.71	34.18	(150)	5.40	34.16	26.98

Station 4323; Apr. 6; latitude 43°12′ N., longitude 50°23′ W.; depth 89 meters, dynamic height 971.075

Observed values			Scaled values			
Depth, meters	Temperature °C.	Salinity ‰	Depth, meters	Temperature °C.	Salinity ‰	σ_t
0	2.47	33.18	0	2.47	33.18	26.50
26	2.42	33.20	25	2.45	33.20	26.52
52	2.44	33.22	50	2.45	33.22	26.53
78	1.15	33.32	75	1.35	33.30	26.67

Station 4324; Apr. 6; latitude 43°20′ N., longitude 50°15′ W.; depth 68 meters, dynamic height 971.079

Observed values			Scaled values			
Depth, meters	Temperature °C.	Salinity ‰	Depth, meters	Temperature °C.	Salinity ‰	σ_t
0	2.11	32.88	0	2.11	32.88	26.29
25	1.72	32.88	25	1.72	32.88	26.32
51	1.42	32.96	50	1.40	32.96	26.40

Station 4325; Apr. 6; latitude 42°59′ N., longitude 50°13′ W.; depth 89 meters, dynamic height 971.058

Observed values			Scaled values			
Depth, meters	Temperature °C.	Salinity ‰	Depth, meters	Temperature °C.	Salinity ‰	σ_t
0	1.88	32.78	0	1.88	32.78	26.23
26	1.79	33.10	25	1.80	33.09	26.47
51	1.50	33.30	50	1.50	33.30	26.66
77	1.46	33.30	75	1.45	33.30	26.67

Station 4326; Apr. 6; latitude 42°48.5′ N., longitude 50°20′ W.; depth 403 meters, dynamic height 971.034

Observed values			Scaled values			
Depth, meters	Temperature °C.	Salinity ‰	Depth, meters	Temperature °C.	Salinity ‰	σ_t
0	7.29	34.03	0	7.29	34.03	26.63
25	7.11	34.10	25	7.11	34.10	26.72
50	6.98	34.25	50	6.98	34.25	26.85
75	5.35	34.04	75	5.35	34.04	26.89
100	5.13	34.01	100	5.13	34.01	26.90
150	6.48	34.45	150	6.48	34.45	27.07
200	4.63	34.49	200	4.63	34.49	27.33
300	3.60	34.65	300	3.60	34.65	27.57
			(400)			

Station 4327; Apr. 6; latitude 43°39′ N., longitude 50°24′ W.; depth 1,481 meters, dynamic height 971.079

Observed values			Scaled values			
Depth, meters	Temperature °C.	Salinity ‰	Depth, meters	Temperature °C.	Salinity ‰	σ_t
0	3.00	33.03	0	3.00	33.03	26.34
22	11.20	34.95	25	11.85	35.03	26.66
44	12.53	35.30	50	12.50	35.31	26.75
66	12.36	35.32	75	12.10	35.32	26.84
88	11.63	35.30	100	11.10	35.23	26.95
176	7.51	34.51	150	8.75	34.76	26.99
264	4.90	34.46	200	6.60	34.48	27.08
393	3.47	34.69	300	4.30	34.50	27.38
588	3.75	34.83	400	3.45	34.69	26.61
783	3.87	34.89	600	3.75	34.84	27.70
980	3.64	34.87	800	3.85	34.89	27.73
1,423	3.45		1,000	3.60	34.87	27.75

Station 4328; Apr. 6; latitude 42°18′ N., longitude 50°17′ W.; depth 2,834 meters, dynamic height 971.075

Observed values			Scaled values			
Depth, meters	Temperature °C.	Salinity ‰	Depth, meters	Temperature °C.	Salinity ‰	σ_t
0	11.75	34.90	0	11.75	34.90	26.58
25	12.64	35.28	25	12.64	35.28	26.70
48	12.59	35.28	50	12.60	35.28	26.71
73	12.93	35.38	75	12.90	35.38	26.73
97	7.78	34.44	100	7.75	34.43	26.88
146	7.34	34.36	150	7.30	34.37	26.90
194	7.08	34.67	200	7.00	34.67	27.18
291	4.90	34.56	300	4.85	34.60	26.40
327	4.84	34.74	400	4.80	34.89	27.63
512	4.76	34.97	600	4.70	34.97	27.71
712	4.54	34.97	800	4.20	34.95	27.75
903	3.92	34.905	1,000	3.80	34.90	27.75
1,402	3.52	34.885				

Station 4329; Apr. 7; latitude 41°55′ N., longitude 50°15′ W.; depth 3,475 meters, dynamic height 971.215

Observed values			Scaled values			
Depth, meters	Temperature °C.	Salinity ‰	Depth, meters	Temperature °C.	Salinity ‰	σ_t
0	16.39	36.02	0	16.39	36.02	26.46
27	16.37	36.02	25	16.40	36.02	26.46
53	16.42	36.06	50	16.45	36.05	26.46
79	15.76	35.91	75	15.90	35.95	26.51
105	14.92	35.75	100	15.10	35.78	26.56
159			150	13.45	35 52	26.72
211	11.52	35.27	200	11.85	35.31	26.88
316	9.16	35.13	300	9.45	35.15	27.18
380	7.88	35.07	400	7.50	35.05	27.40
575	4.35	34.80	600	4.30	34.81	27.63
775	4.14	34.88	(800)	4.10	34.89	27.71
			(1,000)	3.90	34.90	27.74

Station 4330; Apr. 7; latitude 41°35′ N., longitude 50°11′ W.; depth 3,841 meters, dynamic height 971.323

Observed values			Scaled values			
Depth, meters	Temperature °C.	Salinity ‰	Depth, meters	Temperature °C.	Salinity ‰	σ_t
0	17.95	36.40	0	17.95	36.40	26.38
22	17.97	36.41	25	17.95	36.41	26.38
43	17.96	36.41	50	17.95	36.42	26.39
65	17.86	36.45	75	17.95	36.45	26.42
87	17.85	36.45	100	17.95	36.45	26.42
131	17.92	36.43	150	17.90	36.45	26.43
174	17.83	36.44	200	17.10	36.27	26.48
261	15.12	35.86	300	14.15	35.83	26.81
331	13.57	35.81	(400)	10.00	35.37	27.26
			(600)	4.15	34.81	27.64
			(800)	4.10	34.94	27.75
			(1,000)	3.90	34.93	27.76

STATIONS OCCUPIED IN 1951—Continued

Station 4331; Apr. 7; latitude 42°05′ N., longitude 49°24′ W.; depth 2,926 meters, dynamic height 971.118

Observed values			Scaled values			
Depth, meters	Temperature °C.	Salinity ‰	Depth, meters	Temperature °C.	Salinity ‰	σ_t
0	17.62	36.27	0	17.62	36.27	26.36
23	17.60	36.26	25	17.60	36.26	26.35
45	17.53	36.245	50	17.50	36.24	26.36
68	15.75	35.92	75	15.35	35.86	26.57
91	14.77	35.75	100	14.80	35.77	26.63
137	15.17	35.89	150	15.00	35.84	26.63
1 2	13.91	35.63	200	11.70	35 40	26.98
273	5.47	34.63	300	4.65	34.43	27.28
212	6.97	34.64	400	4.10	34.88	27.70
301		34.43	600	4.25	34.97	27.76
379	4.13	34.85	800	3.90	34.94	27.77
520	4.35	34.98	1,000	3.60	34.92	27.79
954	3.62	34.92				

Station 4332; Apr. 7; latitude 41°33′ N., longitude 49°04′ W.; depth 3,255 meters, dynamic height 971.034

0	5.66	33.44	0	5.66	33.44	26.38
28	5.39	33.73	25	5.45	33.70	26.62
55	5.12	33.78	50	5.15	33.77	26.71
83	4.91	33.89	75	5.00	33.85	26.79
110	3.46	33.84	100	3.95	33.86	26.90
166	2.98	34.14	150	3.10	34.08	27.16
222	2.57	34.27	200	2.65	34.22	27.32
332	3.54	34.64	300	3.15	34.52	27.51
426	4.56	34.85	400	4.35	34.81	27.62
638	4.18	34.94	600	4.25	34.93	27.62
851	4.10	34.95	800	4.10	34.95	27.76
			(1,000)	4.00	34.95	27.77

Station 4333; Apr. 8; latitude 42°00′ N., longitude 47°56′ W.; depth 3,841 meters, dynamic height 971.217

0	15.87	35.87	0	15.87	35.87	26.46
23	15.87	35.88	25	15.80	35.88	26.48
46	11.93	34.995	50	11.90	35.00	26.63
68	11.86	35.01	75	12.20	35.08	26.63
91	13.43	35.50	100	13.30	35.48	26.72
136	12.74	35.36	150	12.55	35.40	26.81
182	12.27	35.52	200	11.65	35.40	26.98
273	6.21	34.44	300	5.50	34.32	27.10
298	5.49	34.32	400	6.25	34.64	27.25
486	6.71	34.92	600	5.15	34.92	27.62
700	4.10	34.92	800	4.15	34.94	27.74
869	4.25	34.955	1,000	4.15	34.95	27.75
1,285	3.89	34.92				

Station 4334; Apr. 8; latitude 42°28′ N., longitude 48°32′ W.; depth 3,292 meters, dynamic height 971.056

0	7.71	33.71	0	7.71	33.71	26.33
26	8.33	34.13	25	8.30	34.11	26.55
51	5.21	33.98	50	5.25	33.99	26.86
76	3.76	33.86	75	3.75	33.86	26.92
101	4.90	34.21	100	4.90	34.20	27.07
153	7.36	34.83	150	7.35	34.82	27.25
204	4.70	34.45	200	4.85	34.45	27.28
305	3.55	34.48	300	3.55	34.48	27.43
397	3.23	34.56	400	3.25	34.56	27.53
589	4.73	34.94	600	4.70	34.94	27.68
778	4.17	34.935	800	4.10	34.93	27.74
			(1,000)	3.95	34.92	27.75

Station 4335; Apr. 8; latitude 42°41.5′ N., longitude 49°07′ W.; depth 2,543 meters, dynamic height 970.981

0	6.83	33.64	0	6.83	33.64	26.40
28	5.70	33.73	25	5.80	33.72	26.59
55	5.52	33.72	50	5.55	33.72	26.62
82	3.07	34.00	75	3.60	33.91	26.98
109	2.63	34.16	100	2.70	34.11	27.22
220	4.46	34.70	150	3.10	34.36	27.39
329	5.00	34.89	200	4.20	34.60	27.47
308	4.70	34.92	300	4.80	34.88	27.62
502	4.55	34.96	400	4.75	34.94	27.67
723	4.02	34.93	600	4.30	34.95	27.73
920	3.84	34.92	800	3.90	34.92	27.76
1,442	3.57	34.91	1,000	3.80	34.92	27.77

Station 4336; Apr. 8; latitude 43°20.5′ N., longitude 48°50′ W.; depth 1,866 meters, dynamic height 970.972

0	7.21	33.58	0	7.21	33.58	26.29
25	5.80	33.56	25	5.80	33.56	26.46
50	4.63	33.60	50	4.63	33.60	26.63
75	3.43	33.70	75	3.43	33.70	26.83
100	2.80	34.04	100	2.81	34.04	27.16
150	3.54	34.43	150	3.54	34.43	27.39
201	3.96	34.72	200	3.95	34.71	27.58
301	4.22	34.86	300	4.20	34.86	27.68
389	4.11	34.88	400	4.10	34.88	27.70
581	3.99	34.90	600	3.95	34.90	27.73
772	3.69	34.89	800	3.65	34.89	27.75
967	3.68	34.90	1,000	3.65	34.90	27.76
1,459	3.59	34.915				

Station 4337; Apr. 9; latitude 43°05.5′ N., longitude 48°11 W.; depth 3,109 meters, dynamic height 970.986

0	10.11	34.29	0	10.11	34.29	26.40
21	6.19	33.78	25	5.70	33.75	26.62
42	4.71	33.70	50	4.40	33.78	26.80
63	3.97	34.04	75	3.60	34.09	27.12
85	3.43	34.14	100	3.40	34.19	27.22
170	3.56	34.48	150	3.45	34.40	27.38
255	4.51	34.78	200	3.95	34.59	27.48
334	4.32	34.85	300	4.45	34.83	27.62
			(400)	4.30	34.87	27.67
			(600)	4.20	34.90	27.71
			(800)	4.05	34.90	27.72
			(1,000)	3.90	34.90	27.74

Station 4338; Apr. 9; latitude 42°51′ N., longitude 47°32′ W.; depth 3,676 meters, dynamic height 971.016

0	8.43	33.57	0	8.43	33.57	26.12
16	7.71	34.32	25	7.25	34.36	26.90
33	7.05	34.41	50	7.25	34.49	27.00
49	7.28	34.49	75	6.40	34.40	27.05
65	6.16	34.34	100	7.05	34.65	27.16
99	7.03	34.65	150	4.90	34.42	27.25
131	4.21	34.29	200	6.65	34.82	27.35
197	6.69	34.82	300	4.80	34.76	27.53
363	4.16	34.72	400	4.15	34.75	27.59
547	4.40	34.91	600	4.35	34.91	27.70
732	4.08	34.91	800	3.95	34.91	27.74
923	3.81	34.90	1,000	3.75	34.90	27.75
1,413	3.58	34.91				

STATIONS OCCUPIED IN 1951—Continued

Station 4339; Apr. 9; latitude 42°42.5′ N., longitude 46°49′ W.; depth 4,024 meters, dynamic height 971.028

Observed values			Scaled values			
Depth, meters	Temperature °C.	Salinity ‰	Depth, meters	Temperature °C.	Salinity ‰	σ_t
0	14.31	34.96	0	14.31	34.96	26.11
27	14.16	35.15	25	14.15	35.14	26.28
53	8.53	34.46	50	9.40	34.58	26.74
80	6.23	34.30	75	6.30	34.31	26.99
106	7.49	34.67	100	7.25	34.58	27.07
159	6.97	34.82	150	7.15	34.81	27.27
212	5.18	34.64	200	5.45	34.67	27.38
318		34.86	300	5.15	34.82	27.54
412	5.12	34.93	400	5.10	34.92	27.62
519	4.93	34.94	600	4.50	34.97	27.73
562	4.66	34.97	800	4.15	34.95	27.75
715	4.24	34.96	1,000	3.95	34.94	27.76
1,122	3.87	34.93				

Station 4340; Apr. 9; latitude 43°07.5′ N., longitude 46°21′ W.; depth 4,390 meters, dynamic height 971.158

0	16.75	35.94	0	16.75	35.94	26.32
24	16.22	35.88	25	16.20	35.88	26.39
48	14.96	35.72	50	14.90	35.72	26.57
71	14.61	35.78	75	14.40	35.77	26.72
95	13.36	35.51	100	13.50	35.54	26.73
142	14.54	35.72	150	12.40	35.42	26.86
190	9.62	35.05	200	9.20	35.00	27.10
285	6.03	34.62	300	5.80	34.59	27.27
237	7.83	34.83	400	5.15	34.52	27.30
447	4.90	34.51	600	3.90	34.88	27.72
596	3.88	34.87	(800)	4.05	34.94	27.75
			(1,000)	3.90	34.93	27.76

Station 4341; Apr. 9; latitude 43°27′ N., longitude 45°57′ W.; depth 4,390 meters, dynamic height 971.141

0	15.41	35.34	0	15.41	35.34	26.16
24	15.18	35.66	25	15.15	35.66	26.47
48	13.09	35.32	50	12.70	35.23	26.65
73	9.15	34.57	75	8.75	34.53	26.81
97	7.69	34.36	100	7.70	34.36	26.84
146	8.18	34.49	150	8.30	34.53	27.87
194	9.55	35.06	200	9.50	35.06	27.10
291	7.93	34.96	300	7.65	34.94	27.30
347	6.42	34.81	400	5.85	34.86	27.48
501	5.21	34.91	600	4.80	34.92	27.66
678	4.53	34.92	800	4.15	34.92	27.73
859	4.03	34.92	1,000	3.85	34.91	27.75
1,335	3.66	34.90				

Station 4342; Apr. 10; latitude 43°4.5′ N., longitude 46°28′ W.; depth 4,170 meters, dynamic height 971.203

0	15.93	35.80	0	15.93	35.80	26.40
23	15.36	35.79	25	15.30	35.79	26.53
45	14.98	35.74	50	15.05	35.75	26.55
68	15.35	35.865	75	15.35	35.87	26.58
91	15.18	35.855	100	14.85	35.80	26.64
136	12.52	35.45	150	12.05	35.36	26.88
273	7.70	34.75	200	10.25	35.10	27.00
291	7.06	34.68	300	7.00	34.68	27.18
445	6.64	34.935	400	6.75	34.88	27.38
607	5.49	34.95	600	5.55	34.95	27.59
777	4.83	34.995	800	4.70	34.99	27.72
1,234	3.71	34.90	1,000	4.00	34.95	27.77

Station 4343; Apr. 10; latitude 43°59′ N., longitude 47°08′ W.; depth 4,097 meters, dynamic height 971.272

0	16.52	36.08	0	16.52	36.08	26.47
22	16.53	36.10	25	16.55	36.10	26.48
44	16.30	36.10	50	16.25	36.10	26.56
66	16.27	36.11	75	16.25	36.11	26.56
88	16.21	36.09	100	16.00	36.02	26.55
133	14.90	35.80	150	14.60	35.79	26.68
177	14.29	35.78	200	13.65	35.68	26.80
265	11.04	35.26	300	10.60	35.25	27.06
269	11.37	35.35	400	9.00	35.13	27.24
403	8.97	35.12	600	5.10	34.89	27.59
538	5.76	34.90	800	4.15	34.89	27.70
700	4.53	34.89	1,000	3.85	34.89	27.73
1,151	3.74	34.89				

Station 4344; Apr. 10; latitude 44°08.5′ N., longitude 47°56′ W.; depth 3,658 meters, dynamic height 971.105

0	13.75	35.13	0	13.75	35.13	26.36
19	14.57	35.61	25	14.60	35.65	26.58
37	14.62	35.68	50	13.40	35.45	26.68
56	12.67	35.33	75	12.00	35.25	26.80
150	10.85	35.14	100	11.35	35.09	26.80
224	7.72	34.88	150	10.85	35.14	26.93
348	5.93	34.89	200	8.65	34.95	27.15
478		34.90	300	5.30	34.88	27.44
579	5.03	34.97	400	5.70	34.89	27.52
775	4.07	34.91	600	4.90	34.97	27.69
1,357	3.59	34.89	800	4.00	34.91	27.74
			1,000	3.85	34.90	27.74

Station 4345; Apr. 10; latitude 44°12.5′ N., longitude 48°33′ W.; depth 2,177 meters, dynamic height 971.002

0	7.72	33.73	0	7.72	33.73	26.34
22	7.43	33.75	25	7.40	33.76	26.41
45	7.08	33.91	50	6.70	33.89	26.60
67	2.89	33.60	75	4.25	33.63	26.69
180	1.60	34.24	100	2.20	33.76	26.98
270	2.99	34.61	150	1.70	34.06	27.26
319	4.00	34.80	200	1.80	34.33	27.47
504	4.17	34.90	300	3.80	34.74	27.62
708	3.82	34.89	400	4.10	34.87	27.70
896	3.76	34.905	600	4.00	34.90	27.73
1,381	3.47	34.885	800	3.75	34.90	27.75
			1,000	3.65	34.90	27.76

Station 4346; Apr. 10; latitude 44°15′ N., longitude 48°45 W.; depth 1,609 meters, dynamic height 971.010

0	0.99	32.90	0	0.99	32.90	26.38
24	6.11	33.74	25	6.10	33.74	26.57
48	4.56	33.77	50	4.20	33.76	26.80
73	1.47	33.49	75	1.35	33.49	26.83
97	0.86	33.52	100	0.85	33.54	26.90
146	1.97	34.04	150	1.95	34.06	27.25
195	1.45	34.22	200	1.50	34.24	27.42
292	3.25	34.56	300	3.20	34.58	27.55
384	3.59	34.73	400	3.60	34.75	27.65
555	4.13	34.89	600	4.05	34.89	27.71
714	3.75	34.88	800	3.55	34.88	27.75
900	3.44	34.87	1,000	3.40	34.87	27.77
1,371	3.40	34.87				

STATIONS OCCUPIED IN 1951—Continued

Observed values			Scaled values			
Depth, meters	Temperature °C.	Salinity ‰	Depth, meters	Temperature °C.	Salinity ‰	σ_t
Station 4347; Apr. 10; latitude 44°14′ N., longitude 48°54′ W.; depth 558 meters, dynamic height 971.050						
0	1.93	32.87	0	1.93	32.87	26.29
25	−0.13	33.12	25	−0.13	33.12	26.61
50	−0.33	33.16	50	−0.33	33.16	26.65
75	−0.66	33.18	75	−0.66	33.18	26.69
100	−0.37	33.24	100	−0.37	33.24	26.72
150	−0.25	33.49	150	−0.25	33.49	26.92
201	0.86	34.02	200	0.90	34.01	27.28
301	2.13	34.44	300	2.10	34.44	27.53
400	3.77	34.76	400	3.75	34.76	27.64
497	3.98	34.84				
Station 4348; Apr. 10; latitude 44°14′ N., longitude 49°00′ W.; depth 169 meters, dynamic height 971.066						
0	2.25	32.78	0	2.25	32.78	26.20
25	1.46	33.18	25	1.46	33.18	26.58
50	0.73	33.20	50	0.73	33.20	26.47
75	0.87	33.24	75	0.87	33.24	26.67
101	−0.10	33.20	100	−0.10	33.20	26.68
151	−0.21	33.41	150	−0.20	33.41	26.86
Station 4349; Apr. 10; latitude 44°16′ N., longitude 49°10′ W.; depth 78 meters, dynamic height 971.068						
0	2.43	32.72	0	2.43	32.72	26.13
25	1.04	33.12	25	1.04	33.12	26.56
51	0.06	33.16	50	0.05	33.16	26.64
71	0.03	33.16	75	0.00	33.16	26.64
Station 4350; Apr. 10; latitude 44°15′ N., longitude 49°23′ W.; depth 53 meters, dynamic height 971.073						
0	1.20	32.70	0	1.20	32.70	26.21
26	0.17	32.94	25	0.15	32.94	26.46
41	0.25	32.96	50	0.30	32.97	26.48
Station 4351; Apr. 11; latitude 44°59.5′ N., longitude 49°24′ W.; depth 73 meters; dynamic height 971.112						
0	1.27	32.68	0	1.27	32.68	26.19
25	0.44	32.85	25	0.44	32.85	26.38
51	−0.34	32.89	50	−0.35	32.89	26.43
Station 4352; Apr. 11; latitude 44°57.5′ N., longitude 49°15′ W.; depth 123 meters, dynamic height 971.121						
0	1.25	32.62	0	1.25	32.62	26.14
25	0.65	32.66	25	0.65	32.66	26.21
51	0.19	32.71	50	−0.20	32.71	26.29
76	−0.49	32.84	75	−0.50	32.84	26.41
102	−0.70	33.01	100	−0.70	33.00	26.55
Station 4353; Apr. 11; latitude 44°54.5′ N., longitude 49°04′ W.; depth 631 meters, dynamic height 971.061						
0	1.73	32.58	0	1.73	32.58	26.08
20	2.88	33.12	25	2.50	33.10	26.43
40	−1.11	33.01	50	−1.00	33.10	26.63
61	−0.83	33.21	75	−0.80	33.23	26.73
81	−0.79	33.24	100	−0.65	33.29	26.77
121	−0.46	33.37	150	−0.15	33.51	26.94
161	0.02	33.57	200	0.60	33.87	27.18
242	1.43	34.22	300	3.15	34.61	27.58
308	3.25	34.65	400	3.65	34.79	27.67
417	3.71	34.80	(600)	3.90	34.85	27.70

Observed values			Scaled values			
Depth, meters	Temperature °C.	Salinity ‰	Depth, meters	Temperature °C.	Salinity ‰	σ_t
Station 4354; Apr. 11; latitude 44°47′ N., longitude 48°50′ W.; depth 1,463 meters, dynamic height 970.967						
0	9.26	34.01	0	9.26	34.01	26.32
24	9.16	34.03	25	9.15	34.03	26.35
48	8.24	34.43	50	7.95	34.43	26.85
72	4.85	34.18	75	4.70	34.18	27.08
96	3.95	34.23	100	3.95	34.25	27.22
145	4.24	34.52	150	4.25	34.54	27.41
194	4.15	34.70	200	4.20	34.72	27.57
290	4.52	34.86	300	4.50	34.86	27.64
232	4.79	34.83	400	4.40	34.88	27.66
373	4.47	34.88	600	3.90	34.90	27.74
714	3.78	34.90	800	3.70	34.90	27.76
1,210	3.41	34.87	1,000	3.55	34.89	27.76
Station 4355; Apr. 11; latitude 44°41′ N., longitude 48°30 W.; depth 2,195 meters, dynamic height 970.966						
0	7.51	33.63	0	7.51	33.63	26.29
19	7.11	33.80	25	6.95	33.80	26.51
39	6.39	33.80	50	5.45	33.81	26.71
58	4.54	33.83	75	3.90	34.00	27.02
77	3.86	34.01	100	3.85	34.24	27.22
116	3.86	34.38	150	4.05	34.55	27.44
155	4.08	34.58	200	4.35	34.73	27.55
232	4.61	34.84	300	4.50	34.88	27.65
263	4.42	34.84	400	4.40	34.91	27.69
419	4.36	34.92	600	4.10	34.93	27.74
593	4.15	34.93	800	3.85	34.91	27.75
768	3.90	34.915	1,000	3.70	34.91	27.77
1,251	3.57	34.905				
Station 4356; Apr. 11; latitude 44°34′ N., longitude 47°45′ W.; depth 3,566 meters, dynamic height 971.170						
0	15.04	35.70	0	15.04	35.70	26.52
18	15.06	35.72	25	15.10	35.72	26.52
36	15.10	35.72	50	15.30	35.86	26.58
53	15.36	35.90	75	14.90	35.75	26.59
71	15.03	35.78	100	13.70	35.57	26.71
107	13.21	35.50	150	10.90	35.16	26.94
143	11.03	35.16	200	10.25	35.21	27.09
214	10.05	35.22	300	8.05	35.07	27.34
383	6.36	34.94	400	6.30	34.94	27.48
567	6.25	34.99	600	6.00	34.98	27.55
747	4.41	34.93	800	4.25	34.93	27.72
949	4.05	34.93	1,000	4.00	34.93	27.75
1,478	3.57	34.90				
Station 4357; Apr. 11; latitude 44°30.5′ N., longitude 47°08′ W.; depth 3,786 meters dynamic height 971.302						
0	16.37	36.11	0	16.37	36.11	26.53
21	16.40	36.11	25	16.40	36.11	26.52
43	16.41	36.11	50	16.35	36.10	26.54
64	16.10	36.08	75	16.15	36.07	26.54
86	16.16	36.07	100	16.10	36.05	26.55
129	15.86	36.00	150	15.65	35.92	26.56
172	15.37	35.98	200	14.45	35.71	26.66
258	12.29	35.44	300	11.35	35.36	27.01
360	10.25	35.26	400	9.35	35.19	27.22
544	6.22	34.93	600	5.65	34.94	27.57
732	4.95	34.955	800	4.55	34.94	27.70
924	4.09	34.90	1,000	3.95	34.91	27.74
1,414	3.69	34.91				

STATIONS OCCUPIED IN 1951—Continued

Station 4358; Apr. 12; latitude 44°26′ N., longitude 46°39′ W.; depth 3,841 meters, dynamic height 971.322

Observed values			Scaled values			
Depth, meters	Temperature °C.	Salinity ‰	Depth, meters	Temperature °C.	Salinity ‰	σ_t
0	16.33	36.14	0	16.33	36.14	26.56
20	16.45	36.14	25	16.45	36.14	26.54
41	16.42	36.125	50	16.45	36.13	26.53
61	16.46	36.14	75	16.40	36.13	26.54
82	16.40	36.12	100	16.40	36.12	26.53
124	16.45	36.14	150	16.50	36.15	26.53
165	16.53	36.16	200	15.10	35.96	26.71
247	13.36	35.67	300	11.95	35.46	26.98
261	12.81	35.58	400	9.45	35.19	27.21
391	9.66	35.21	600	6.00	34.96	27.54
522	6.77	34.96	800	4.95	34.95	27.66
694	5.44	34.96	1,000	4.20	34.92	27.73
1,198	3.80	34.90				

Station 4359; Apr. 12; latitude 44°12′ N., longitude 45°48′ W.; depth 4,115 meters, dynamic height 971.210

Observed values			Scaled values			
Depth, meters	Temperature °C.	Salinity ‰	Depth, meters	Temperature °C.	Salinity ‰	σ_t
0	14.68	35.41	0	14.68	35.41	26.38
24	14.63	35.42	25	14.65	35.42	26.39
49	13.56	35.50	50	13.50	35.49	26.69
73	12.70	35.335	75	12.60	35.32	26.74
147	10.68	35.09	100	11.95	35.23	26.80
293	7.73	34.88	150	10.60	35.08	26.92
312	6.44	34.71	200	9.45	34.96	27.03
465	5.62	34.91	300	7.30	34.80	27.24
766	5.47	34.915	400	5.80	34.87	27.50
1,134	3.86	34.905	600	5.50	34.91	27.57
			800	5.35	34.91	27.58
			1,000	4.30	34.91	27.70

Station 4360; Apr. 12; latitude 44° 09′ N., longitude 45°14′ W.; depth 4,481 meters, dynamic height 971.067

Observed values			Scaled values			
Depth, meters	Temperature °C.	Salinity ‰	Depth, meters	Temperature °C.	Salinity ‰	σ_t
0	13.70	35.12	0	13.70	35.12	26.36
21	13 78	35.13	25	13.80	35.11	26.34
42	12.68	34.98	50	12.00	34.94	26.56
63	11.02	34.91	75	10.75	34.91	26.77
84	10.56	34.91	100	9.75	34.83	26.98
127	8.08	34.69	150	7.80	34.71	27.10
170	7.61	34.73	200	7.25	34.75	27.21
254	6.33	34.78	300	4.80	34.67	27.45
277	4.67	34.59	400	4.65	34.87	27.64
367	5.40	34.94	600	4.05	34.90	27.72
426	4.13	34.82	800	3.85	34.89	27.73
528	4.14	34.90	(1, 000)	3.80	34.89	27.74
773	3.91	34.89				

Station 4361; Apr. 12; latitude 44°46.5′ N., longitude 45° 15′ W.; depth 4, 042 meters, dynamic height 971.004

Observed values			Scaled values			
Depth, meters	Temperature °C.	Salinity ‰	Depth, meters	Temperature °C.	Salinity ‰	σ_t
0	11.71	34.43	0	11.71	34.43	26.23
24	11.43	34.50	25	11.40	34.51	26.34
48	10.26	34.74	50	10.20	34.74	26.73
71	8.91	34.68	75	8.50	34.63	26.92
95	5.90	34.37	100	5.70	34.38	27.12
143	5.02	34.55	150	5.05	34.57	27.35
191	5.31	34.72	200	5.30	34.74	27.45
286	4.94	34.86	300	4.85	34.88	27.61
392	4.59	34.92	400	4.55	34.92	27.69
589	4.42	34.90	600	4.35	34.90	27.69
789	3.97	34.91	800	3.90	34.91	27.75
990	3.67	34.90	1,000	3.65	34.90	27.76
1,498	3.46	34.90				

Station 4362; Apr. 12; latitude 45°20′ N., longitude 45°15′ W.; depth 3,658 meters, dynamic height 970.988

Observed values			Scaled values			
Depth, meters	Temperature °C.	Salinity ‰	Depth, meters	Temperature °C.	Salinity ‰	σ_t
0	11.45	34.52	0	11.45	34.52	26.34
24	10.89	34.78	25	10.85	34.78	26.65
49	9.44	34.56	50	9.30	34.55	26.74
73	6.86	34.20	75	6.80	34.20	26.84
97	5.73	34.32	100	5.55	34.33	27.10
146	4.29	34.45	150	4.30	34.46	27.35
195	4.41	34.58	200	4.40	34.59	27.44
292	4.43	34.78	300	4.40	34.79	27.59
356	4.23	34.84	400	4.10	34.86	27.69
536	3.87	34.88	600	3.80	34.88	27.73
719	3.68	34.88	800	3.55	34.88	27.75
904	3.51	34.87	1,000	3.45	34.87	27.76
1,374	3.35	34.87				

Station 4363; Apr. 13; latitude 45°20′ N., longitude 45°59′ W.; depth 3,566 meters, dynamic height 971.053

Observed values			Scaled values			
Depth, meters	Temperature °C.	Salinity ‰	Depth, meters	Temperature °C.	Salinity ‰	σ_t
0	14.50	35.51	0	14.50	35.31	26.49
25	14.88	35.52	25	14.48	35.52	26.50
50	14.20	35.59	50	14.20	35.59	26.62
75	12.62	35.34	75	12.62	35.34	26.75
100	9.12	34.72	100	9.12	34.72	26.90
397	4.77	34.90	150	5.90	34.60	27.27
595	4.76	34.92	200	4.70	34.55	27.37
796	4.31	34.93	300	4.65	34.72	27.52
996	4.01	34.925	400	4.75	34.90	27.64
1, 499	3.48	34.91	600	4.75	34.92	27.66
			800	4.25	34.93	27.72
			1,000	4.00	34.92	27.75

Station 4364; Apr. 13; latitude 45°21′ N., longitude 46°45, W.; depth 3,017 meters, dynamic height 970.957

Observed values			Scaled values			
Depth, meters	Temperature °C.	Salinity ‰	Depth, meters	Temperature °C.	Salinity ‰	σ_t
0	7.84	33.61	0	7.84	33.61	26.23
25	11.00	34.74	25	11.00	34.74	26.59
50	3.82	33.60	50	3.82	33.60	26.72
75	3.26	33.98	75	3.26	33.98	27.03
100	2.71	34.18	100	2.71	34.18	27.27
151	2.83	34.43	150	2.85	34.43	27.46
201	4.13	34.69	200	4.10	34.69	27.55
301	3.75	34.78	300	3.75	34.78	27.65
393	4.60	34.94	400	4.60	34.94	27.69
589	4.10	34.93	600	4.05	34.93	27.74
788	4.00	34.92	800	3.83	34.92	27.76
987	3.73	34.92	1,000	3.70	34.92	27.78
1,488	3.51	34.915				

Station 4365; Apr. 13; latitude 45°20.5′ N., longitude 47°23′ W.; depth 2,652 meters, dynamic height 970.959

Observed values			Scaled values			
Depth, meters	Temperature °C.	Salinity ‰	Depth, meters	Temperature °C.	Salinity ‰	σ_t
0	9.23	34.00	0	9.23	34.00	26.32
25	10.17	34.41	25	10.17	34.41	26.48
50	9.39	34.43	50	9.39	34.43	26.62
75	3.70	34.01	75	3.70	34.01	27.05
100	2.12	34.09	100	2.12	34.09	27.25
150	3.59	34.47	150	3.59	34.47	27.43
200	4.50	34.76	200	4.50	34.76	27.56
300	4.52	34.90	300	4.52	34.90	27.67
380	4.29	34.90	400	4.25	34.90	27.70
571	4.12	34.93	600	4.05	34.93	27.75
764	3.77	34.91	800	3.70	34.90	27.76
958	3.53	34.88	1,000	3.50	34.88	27.76
1,447	3.42	34.90				

STATIONS OCCUPIED IN 1951—Continued

Station 4366; Apr. 13; latitude 45°33′ N., longitude 47°50′ W.; depth 1,353 meters, dynamic height 970.988

Observed values			Scaled values			
Depth, meters	Temperature °C.	Salinity ‰	Depth, meters	Temperature °C.	Salinity ‰	σ_t
0	3.17	32.72	0	3.17	32.72	26.08
24	0.78	33.26	25	0.75	33.27	26.69
47	−0.51	33.34	50	−0.50	33.35	26.82
71	−0.11	33.51	75	0.10	33.55	26.95
95	1.25	33.87	100	1.40	33.93	27.17
142	3.29	34.26	150	2.60	34.31	27.39
189	4.18	34.54	200	4.30	34.58	27.44
284	4.53	34.82	300	4.70	34.87	27.63
313	4.90	34.90	400	4.60	34.93	27.68
460	4.51	34.94	600	4.30	34.91	27.70
606		34.91	800	3.70	34.86	27.73
747		34.86	(1,000)	3.35	34.87	27.77
948	3.40	34.865				

Station 4367; Apr. 13; latitude 45°39′ N., longitude 48°00′ W.; depth 622 meters, dynamic height 971.077

Observed values			Scaled values			
Depth, meters	Temperature °C.	Salinity ‰	Depth, meters	Temperature °C.	Salinity ‰	σ_t
0	2.52	32.41	0	2.52	32.41	25.89
25	0.06	32.62	25	0.06	32.62	26.21
51	−1.14	32.89	50	−1.15	32.88	26.46
76	−1.17	33.02	75	−1.15	33.02	26.58
101	−0.87	33.14	100	−0.90	33.13	26.66
152	0.10	33.63	150	0.05	33.62	27.02
203	0.75	33.96	200	0.70	33.94	27.23
304	2.36	34.34	300	2.60	34.44	27.49
319	3.75	34.65	400	3.60	34.72	27.63
456	3.71	34.78				

Station 4368; Apr. 13; latitude 45°43′ N., longitude 48°08′ W.; depth 165 meters, dynamic height 971.086

Observed values			Scaled values			
Depth, meters	Temperature °C.	Salinity ‰	Depth, meters	Temperature °C.	Salinity ‰	σ_t
0	2.48	32.38	0	2.48	32.38	25.86
22	0.32	32.55	25	0.10	32.56	26.15
45	−1.24	32.80	50	−1.25	32.84	26.43
67	−1.19	32.98	75	−1.05	33.05	26.60
89	−0.79	33.21	100	−0.65	33.26	26.75
134	−0.33	33.38	(150)	−0.20	33.42	26.87

Station 4369; Apr. 13; latitude 45°46′ N., longitude 48°14′ W.; depth 112 meters, dynamic height 971.096

Observed values			Scaled values			
Depth, meters	Temperature °C.	Salinity ‰	Depth, meters	Temperature °C.	Salinity ‰	σ_t
0	2.06	32.46	0	2.06	32.46	25.96
26	1.94	32.48	25	2.00	32.48	25.97
53	−0.52	32.71	50	−0.30	32.67	26.26
79	−1.28	32.96	75	−1.30	32.92	26.50
100	−0.97	33.17	100	−0.95	33.18	26.70

Station 4370; Apr. 13; latitude 45°53.5′ N., longitude 48°25′ W.; depth 89 meters, dynamic height 971.088

Observed values			Scaled values			
Depth, meters	Temperature °C.	Salinity ‰	Depth, meters	Temperature °C.	Salinity ‰	σ_t
0	1 89	32.55	0	1.89	32.55	26.04
25	0.48	32.64	25	0.48	32.64	26.21
50	0.09	32.70	50	0.09	32.70	26.27
75	−0.88	33.02	75	−0.88	33.02	26.57

Station 4371; Apr. 14; latitude 46°02.5′ N., longitude 48°38′ W.; depth 73 meters, dynamic height 971.087

Observed values			Scaled values			
Depth, meters	Temperature °C.	Salinity ‰	Depth, meters	Temperature °C.	Salinity ‰	σ_t
0	1.78	32.60	0	1.78	32.60	26.09
23	0.36	32.70	25	0.30	32.70	26.26
45	−0.02	32.71	50	−0.15	32.73	26.31

Station 4372; Apr. 14; latitude 46°17.5′ N., longitude 49°03′ W.; depth 68 meters, dynamic height 971.086

Observed values			Scaled values			
Depth, meters	Temperature °C.	Salinity ‰	Depth, meters	Temperature °C.	Salinity ‰	σ_t
0	2.24	32.57	0	2.24	32.57	26.03
23	2.11	32.58	25	2.05	32.59	26.07
46	0.54	32.72	50	0.35	32.75	26.30

Station 4373; Apr. 14; latitude 46°14′ N., longitude 48°39′ W.; depth 89 meters, dynamic height 971.078

Observed values			Scaled values			
Depth, meters	Temperature °C.	Salinity ‰	Depth, meters	Temperature °C.	Salinity ‰	σ_t
0	2.26	32.52	0	2.26	32.52	25.99
26	0.72	32.66	25	0.80	32.66	26.20
51	0.31	32.71	50	0.35	32.70	26.25
77	−0.40	32.94	75	−0.35	32.91	26.45

Station 4374; Apr. 14; latitude 46°11′ N., longitude 48°01′ W.; depth 115 meters, dynamic height 971.080

Observed values			Scaled values			
Depth, meters	Temperature °C.	Salinity ‰	Depth, meters	Temperature °C.	Salinity ‰	σ_t
0	1.92	32.47	0	1.92	32.47	25.98
25	0.45	32.53	25	0.45	32.53	26.12
50	−0.39	32.68	50	−0.39	32.68	26.27
75	−1.11	32.88	75	−1.11	32.88	26.46
100	−0.95	33.11	100	−0.95	33.11	26.64

Station 4375; Apr. 14; latitude 46°10.5′ N., longitude 47°44′ W.; depth 169 meters, dynamic height 971.058

Observed values			Scaled values			
Depth, meters	Temperature °C.	Salinity ‰	Depth, meters	Temperature °C.	Salinity ‰	σ_t
0	2.53	32.49	0	2.53	32.49	25.94
24	0.02	32.60	25	0.00	32.61	26.21
48	−1.17	32.96	50	−1.20	32.97	26.54
71	−0.93	33.19	75	−0.85	33.22	26.72
95	−0.40	33.40	100	−0.35	33.43	26.87
143	0.03	33.58	150	0.10	33.59	26.98

Station 4376; Apr. 14; latitude 46°09.5′ N., longitude 47°26, W.; depth 626 meters, dynamic height 970.980

Observed values			Scaled values			
Depth, meters	Temperature °C.	Salinity ‰	Depth, meters	Temperature °C.	Salinity ‰	σ_t
0	6.03	33.28	0	6.03	33.28	26.21
25	−0.66	32.94	25	−0.66	32.94	26.50
50	−0.75	33.22	50	−0.75	33.22	26.72
74	0.05	33.73	75	0.05	33.74	27.11
99	0.46	33.80	100	0.45	33.80	27.13
149	1.41	34.15	150	1.40	34.16	27.37
198	1.63	34.32	200	1.65	34.32	27.48
297	2.61	34.56	300	2.65	34.57	27.60
388	3.67	34.78	400	3.65	34.79	27.67
586	3.81	34.86	600	3.80	34.86	27.72

Station 4377; Apr. 14; latitude 46°0.5′ N., longitude 47°10′ W.; depth 1,225 meters, dynamic height 970.961

Observed values			Scaled values			
Depth, meters	Temperature °C.	Salinity ‰	Depth, meters	Temperature °C.	Salinity ‰	σ_t
0	5.44	33.07	0	5.44	33.07	26.12
25	2.11	33.24	25	2.11	33.24	26.58
49	1.38	33.53	50	1.35	33.53	26.86
74	1.13	33.86	75	1.15	33.86	27.14
99	1.32	34.02	100	1.30	34.02	27.26
148	1.39	34.23	150	1.40	34.23	27.42
197	1.95	34.37	200	2.00	34.38	27.49
296	3.49	34.71	300	3.50	34.73	27.64
394	3.91	34.84	400	3.90	34.84	27.69
588	3.77	34.87	600	3.75	34.87	27.73
780	3.55	34.86	800	3.50	34.86	27.75
978	3.44	34.86	1,000	3.40	34.86	27.76
1,177	3.42	34.86				

STATIONS OCCUPIED IN 1951—Continued

Station 4378; Apr. 14; latitude 46°06.5′ N., longitude 46°37′ W.; depth 1,060 meters, dynamic height 970.991

Observed values			Scaled values			
Depth, meters	Temperature °C.	Salinity ‰	Depth, meters	Temperature °C.	Salinity ‰	σ_t
0	11.99	34.29	0	11.99	34.29	26.06
24	11.43	34.92	25	11.40	34.29	26.66
48	10.99	34.96	50	10.95	34.96	26.77
73	9.11	34.76	75	8.90	34.74	26.95
97	6.40	34.61	100	6.35	34.61	27.22
145	5.96	34.70	150	5.90	34.70	27.35
193		34.78	200	5.60	34.79	27.45
290	5.05	34.86	300	4.95	34.86	27.59
372	4.41	34.87	400	4.30	34.87	27.67
555	3.95	34.88	600	3.85	34.88	27.72
735	3.75	34.89	800	3.70	34.89	27.75
933	3.66	34.885	(1,000)	3.65	34.89	27.75

Station 4379; Apr. 15; latitude 46°06.5′ N., longitude 46°00′ W.; depth 1829 meters, dynamic height 971.006

Observed values			Scaled values			
Depth, meters	Temperature °C.	Salinity ‰	Depth, meters	Temperature °C.	Salinity ‰	σ_t
0	13.30	34.82	0	13.30	34.82	26.22
25	11.97	35.04	25	11.97	35.04	26.64
50	12.85	35.31	50	12.85	35.31	26.69
76	10.13	34.80	75	10.15	34.85	26.83
101	6.63	34.39	100	6.65	34.40	27.01
151	6.48	34.72	150	6.50	34.71	27.28
202	5.59	34.76	200	5.60	34.76	27.43
303	5.15	34.89	300	5.15	34.89	27.59
400	4.17	34.84	400	4.15	34.84	27.66
597	3.94	34.89	600	3.90	34.89	27.73
791	3.75	34.89	800	3.70	34.89	27.75
990	3.48	34.86	1,000	3.45	34.86	27.75
1,485	3.40	34.88				

Station 4380; Apr. 15; latitude 46°07.5′ N., longitude 45°17′ W.; depth 2,834 meters, dynamic height 970.987

Observed values			Scaled values			
Depth, meters	Temperature °C.	Salinity ‰	Depth, meters	Temperature °C.	Salinity ‰	σ_t
0	12.43	34.69	0	12.43	34.69	26.29
25	9.77	34.47	25	9.77	34.47	26.59
50	11.00	34.89	50	11.00	34.89	26.71
76	5.11	34.11	75	5.10	34.11	26.98
101	5.67	34.44	100	5.65	34.43	27.16
152	5.07	34.61	150	5.10	34.61	27.38
203		34.72	200	4.95	34.71	27.47
304	4.75	34.86	300	4.75	34.86	27.61
404	3.96	34.82	400	3.95	34.82	27.67
602	3.77	34.86	600	3.75	34.86	27.72
			(800)	3.60	34.86	27.74
			(1,000)	3.45	34.87	27.76

Station 4381; Apr. 15; lattuide 46°03′ N., longitude 44°38′ W.; depth 3658 meters, dynamic height 971.187

Observed values			Scaled values			
Depth, meters	Temperature °C.	Salinity ‰	Depth, meters	Temperature °C.	Salinity ‰	σ_t
0	16.26	36.03	0	16.26	36.03	26.50
21	16.23	36.02	25	16.20	36.03	26.50
43	15.93	36.06	50	15.80	36.07	26.62
64	15.60	36.08	75	15.40	36.05	26.71
85	15.21	35.99	100	14.85	35.91	26.72
129	13.73	35.76	150	13.50	35.72	26.87
172	13.25	35.68	200	12.65	35.62	26.96
257	10.99	35.46	300	9.80	35.31	27.25
330	9.20	35.22	400	8.05	35.16	27.41
503	6.70	35.09	600	5.75	35.04	27.63
870	4.32	34.945	800	4.50	34.96	27.72
1,379	3.69	34.92	1,000	4.10	34.94	27.75

Station 4382; Apr. 15; latitude 46°24′ N., longitude 44°43′ W.; depth 1463 meters, dynamic height 970.986

Observed values			Scaled values			
Depth, meters	Temperature °C.	Salinity ‰	Depth, meters	Temperature °C.	Salinity ‰	σ_t
0	12.18	34.07	0	12.18	34.07	26.28
24	10.72	34.55	25	10.70	34.56	26.51
48	10.08	34.67	50	10.05	34.67	26.71
71	8.87	34.58	75	8.35	34.50	26 85
95	4.98	34.22	100	4.75	34.22	27.11
143	3.94	34.37	150	4.00	34.44	27.36
191	5.02	34.72	200	5.05	34.76	27.50
286	4.87	34.86	300	4.75	34.87	27.62
214	4.47	34.80	400	4.30	34.88	27.68
477	4.00	34.88	600	3.75	34.87	27.73
655	3.72	34.87	800	3.55	34.87	27.75
862	3.55	34.87	(1,000)	3.50	34.87	27.76

Station 4383; Apr. 15; latitude 46°32′ N., longitude 44°46′ W.; depth 220 meters, dynamic height 970.966

Observed values			Scaled values			
Depth, meters	Temperature °C.	Salinity ‰	Depth, meters	Temperature °C.	Salinity ‰	σ_t
0	11.47	34.33	0	11.47	34.33	26.18
23	9.83	34.45	25	9.80	34.45	26.58
47	8.93	34.29	50	8.80	34.29	26.61
70	6.94	34.34	75	6.00	34.33	27.04
94	4.04	34.18	100	3.80	34.19	27.18
140	3.18	34.40	150	3.20	34.44	27.44
187	3.27	34.56	(200)	3.25	34.59	27.55

Station 4384; Apr. 15; latitude 46°44′ N., longitude 44°48′ W.; depth 169 meters, dynamic height 970.948

Observed values			Scaled values			
Depth, meters	Temperature °C.	Salinity ‰	Depth, meters	Temperature °C.	Salinity ‰	σ_t
0	11.34	34.33	0	11.34	34.33	26.21
25	8.82	34.48	25	8.82	34.48	26.75
50	5.05	34.00	50	5.05	34.00	26.90
74	5.60	34.36	75	5.60	34.36	27.12
99	3.02	34.30	100	3.00	34.30	27.35
149	3.22	34.43	150	3.20	34.43	27.43

Station 4385; Apr. 15; latitude 46°48′ N., longitude 44°50′ W.; depth 132 meters, dynamic height 970.958

Observed values			Scaled values			
Depth, meters	Temperature °C.	Salinity ‰	Depth, meters	Temperature °C.	Salinity ‰	σ_t
0	10.96	34.31	0	10.96	34.31	26.27
24	10.46	34.48	25	10.45	34.48	26.48
48	7.46	34.23	50	7.20	34.23	26.80
73	5.02	34.24	75	4.90	34.24	27.10
97	2.99	34.22	100	2.80	34.21	27.30

Station 4386; Apr. 29; latitude 49°58′ N., longitude 48°58′ W.; depth 1,902 meters, dynamic height 970.846

Observed values			Scaled values			
Depth, meters	Temperature °C.	Salinity ‰	Depth, meters	Temperature °C.	Salinity ‰	σ_t
0	4.45	34.37	0	4.45	34.37	27.26
24	4.20	34.39	25	4.15	34.39	27.30
48	2.50	34.51	50	2.50	34.52	27.57
72	2.79	34.60	75	2.80	34.61	27.61
95	2.91	34.64	100	2.95	34.65	27.63
143	3.29	34.74	150	3.30	34.74	27.67
190	3.33	34.78	200	3.35	34.79	27.70
285	3.47	34.84	300	3.45	34.84	27.73
373	3.47	34.84	400	3.45	34.84	27.73
562	3.34	34.83	600	3.35	34.83	27.73
755	3.40	34.84	800	3.35	34.85	27.75
949	3.39	34.87	1,000	3.35	34.87	27.77
1,449	3.36	34.88				

STATIONS OCCUPIED IN 1951—Continued

Station 4387; Apr. 29; latitude 49°48′ N., longitude 49°29′ W.; depth 1,408 meters, dynamic height 970.918

Observed values			Scaled values			
Depth, meters	Temperature °C.	Salinity ‰	Depth, meters	Temperature °C.	Salinity ‰	σ_t
0	0.28	33.57	0	0.28	33.57	26.96
24	0.29	33.63	25	0.30	33.63	27.00
48	0.63	33.66	50	0.60	33.67	27.02
72	0.43	33.90	75	0.45	33.94	27.24
97	1.21	34.12	100	1.25	34.14	27.36
145	2.01	34.36	150	2.05	34.38	27.49
193	2.39	34.52	200	2.45	34.53	27.57
290	2.97	34.67	300	3.00	34.68	27.65
607	3.39	34.83	400	3.30	34.76	27.69
766	3.37	34.84	600	3.40	34.83	27.73
1,024	3.39	34.86	800	3.35	34.85	27.75
1,286	3.32	34.86	1,000	3.35	34.86	27.76

Station 4388; Apr. 30; latitude 49°38′ N., longitude 50°01′ W.; depth 622 meters, dynamic height 970.948

Observed values			Scaled values			
Depth, meters	Temperature °C.	Salinity ‰	Depth, meters	Temperature °C.	Salinity ‰	σ_t
0	0.60	33.20	0	0.60	33.20	26.65
23	0.56	33.20	25	0.55	33.20	26.65
45	0 39	33.26	50	0.25	33.32	26.76
68	−0.21	33.70	75	−0.05	33.81	27.17
90	0.88	33.94	100	0.95	33.98	27.24
135	1.19	34.12	150	1.40	34.19	27.39
180	1.79	34.34	200	2.00	34.41	27.52
270	2.66	34.60	300	2.95	34.67	27.65
335	3.32	34.74	400	3.55	34.81	27.70
524	3.71	34.86	(600)	3.70	34.87	27.74

Station 4389; Apr. 30; latitude 49°30′ N., longitude 50°28′ W.; depth 338 meters, dynamic height 971.003

Observed values			Scaled values			
Depth, meters	Temperature °C.	Salinity ‰	Depth, meters	Temperature °C.	Salinity ‰	σ_t
0	0.12	33.01	0	0.12	33.01	26.53
24	0.03	33.04	25	0.05	33.04	26.55
48	0.14	33.10	50	0.15	33.10	26.58
72	−0.26	33.10	75	−0.30	33.11	26.61
95	−0.36	33.42	100	−0.35	33.45	26.89
144	0.09	33.77	150	0.20	33.81	27.16
191	1.31	34.18	200	1.50	34.23	27.41
286	2.73	34.61	300	2.90	34.64	27.63

Station 4390; Apr. 30; latitude 49°23′ N., longitude 51°01′ W.; depth 348 meters, dynamic height 971.017

Observed values			Scaled values			
Depth, meters	Temperature °C.	Salinity ‰	Depth, meters	Temperature °C.	Salinity ‰	σ_t
0	0.43	32.89	0	0.43	32.89	26.40
28	0.42	32.90	25	0.45	32.90	26.41
54	−0.54	33.02	50	−0.45	32.99	26.53
82	−1.00	33.24	75	−0.95	33.18	26.70
108	−0.43	33.46	100	−0.65	33.38	26.85
164	0.85	33.91	150	0.65	33.82	27.14
218	1.23	34.18	200	1.10	34.09	27.33
326	3.06	34.70	300	2.55	34.56	27.60

Station 4391; May 1; latitude 49°12.5′ N., longitude 51°30′ W.; depth 311 meters, dynamic height 971.040

Observed values			Scaled values			
Depth, meters	Temperature °C.	Salinity ‰	Depth, meters	Temperature °C.	Salinity ‰	σ_t
0	0.32	32.66	0	0.32	32.66	26.23
21	0.40	32.80	25	0.45	32.81	26.35
42	0.70	32.88	50	0.65	32.88	26.39
63	0.47	32.88	75	−0.25	33.04	26.56
83	−0.70	33.18	100	−0.65	33.30	26.78
124	−0.47	33.46	150	0.20	33.66	27.04
165	0.64	33.78	200	1.10	34.00	27.26
227	1.41	34.18	(300)	2.35	34.54	27.59

Station 4392; May 1; latitude 49°03′ N., longitude 51°49′ W.; depth 304 meters, dynamic height 971.060

Observed values			Scaled values			
Depth, meters	Temperature °C.	Salinity ‰	Depth, meters	Temperature °C.	Salinity ‰	σ_t
0	0.29	32.16	0	0.29	32.16	25.83
25	0.31	32.16	25	0.31	32.16	25.82
50	0.05	32.60	50	0.05	32.60	26.20
75	−0.45	33.10	75	−0.45	33.10	26.61
100	−0.52	33.42	100	−0.52	33.42	26.88
150	0.23	33.71	150	0.23	33.71	27.08
200	0.93	34.01	200	0.93	34.01	27.27
295	1.70	34.32	300	1.75	34.33	27.47

Station 4393; May 1; latitude 48°59′ N., longitude 52°04′ W.; depth 300 meters, dynamic height 971.101

Observed values			Scaled values			
Depth, meters	Temperature °C.	Salinity ‰	Depth, meters	Temperature °C.	Salinity ‰	σ_t
0	−0.27	32.77	0	−0.27	32.77	26.34
25	−0.37	32.76	25	−0.31	32.76	26.34
50	−0.40	32.78	50	−0.40	32.78	26.36
74	−0.29	32.82	75	−0.30	32.82	26.38
99	−1.28	32.91	100	−1.30	32.92	26.50
149	−1.50	33.12	150	−1.50	33.12	26.66
199	−0.24	33.52	200	−0.20	33.53	26.95
288	1.16	34.16	(300)	1.30	34.22	27.42

Station 4394; May 1; latitude 48°53′ N., longitude 52°23′ W.; depth 352 meters, dynamic height 971.089

Observed values			Scaled values			
Depth, meters	Temperature °C.	Salinity ‰	Depth, meters	Temperature °C.	Salinity ‰	σ_t
0	0.41	32.38	0	0.41	32.38	26.00
25	0.21	32.39	25	0.21	32.39	26.02
50	−0.31	32.70	50	−0.31	32.70	26.28
74	−1.64	32.99	75	−1.65	33.00	26.57
99	−1.61	33.09	100	−1.60	33.09	26.64
149	−1.08	33.29	150	−1.05	33.30	26.79
199	0.44	33.73	200	0.45	33.74	27.08
298	1.34	34.24	300	1.35	34.24	27.43

Station 4395; May 1; latitude 48°47.5′ N., longitude 52°39′ W.; depth 220 meters, dynamic height 971.123

Observed values			Scaled values			
Depth, meters	Temperature °C.	Salinity ‰	Depth, meters	Temperature °C.	Salinity ‰	σ_t
0	0.91	31.74	0	0.91	31.74	25.45
25	0.30	32.02	25	0.30	32.02	25.72
51	−1.53	32.56	50	−1.50	32.55	26.20
76	−1.29	32.76	75	−1.30	32.75	26.36
101	−1.24	32.82	100	−1.25	32.82	26.42
152	−0.68	33.18	150	−0.70	33.17	26.68
203	0.23	33.64	200	0.15	33.62	27.01

Station 4396; May 1; latitude 48°46.5′ N., longitude 52°44′ W.; depth 159 meters, dynamic height 971.130

Observed values			Scaled values			
Depth, meters	Temperature °C.	Salinity ‰	Depth, meters	Temperature °C.	Salinity ‰	σ_t
0	1.10	31.62	0	1.10	31.62	25.34
25	0.29	32.02	25	0.29	32.02	25.72
50	−1.52	32.48	50	−1.52	32.48	26.15
75	−1.38	32.68	75	−1.38	32.68	26.30
100	−1.32	32.74	100	−1.32	32.74	26.35
150	−0.77	33.14	150	−0.77	33.14	26.66

Station 4397; May 1; latitude 48°43′ N., longitude 52°58′ W.; depth 77 meters, dynamic height 971.165

Observed values			Scaled values			
Depth, meters	Temperature °C.	Salinity ‰	Depth, meters	Temperature °C.	Salinity ‰	σ_t
0	1.46	31.22	0	1.46	31.22	25.00
25	0.57	31.48	25	0.57	31.48	25.26
49	−0.58	31.94	50	−0.60	31.95	25.69
67	−0.91	32.18	(75)	−1.05	32.27	25.97

STATIONS OCCUPIED IN 1951—Continued

Station 4398; May 1; latitude 48°36′ N., longitude 52°45′ W.; depth 187 meters, dynamic height 971.139

Observed values			Scaled values			
Depth, meters	Temperature °C.	Salinity ‰	Depth, meters	Temperature °C.	Salinity ‰	σ_t
0	1.18	31.60	0	1.18	31.60	25.33
23	−0.34	31.99	25	−0.35	32.01	25.73
47	−0.94	32.23	50	−1.05	32.27	25.97
70	−1.52	32.53	75	−1.50	32.56	26.21
93	−1.48	32.64	100	−1.45	32.66	26.29
140	−1.22	32.82	(150)	−1.15	32.86	26.44

Station 4399; May 1; latitude 48°30.5′ N., longitude 52°30′ W.; depth 243 meters, dynamic height 971.118

0	0.84	31.75	0	0.84	31.75	25.47
22	−0.12	32.10	25	−0.20	32.12	25.82
44	−0.60	32.21	50	−0.80	32.27	25.96
66	−1.41	32.46	75	−1.45	32.51	26.17
88	−1.52	32.58	100	−1.45	32.66	26.29
137	−1.25	32.97	150	−1.35	33.05	26.60
175	−1.58	33.14	200	−0.55	33.35	26.81
206	−0.28	33.40				

Station 4400; May 1; latitude 48°18′ N., longitude 52°09′ W.; depth 183 meters, dynamic height 971.088

0	0.41	32.31	0	0.41	32.31	25.94
28	0.04	32.26	25	0.10	32.27	25.93
57	−1.47	32.62	50	−1.05	32.50	26.15
85	−1.37	32.74	75	−1.40	32.70	26.32
112	−1.37	32.86	100	−1.35	32.80	26.40
169	−0.41	33.44	150	−0.80	33.24	26.74

Station 4401; May 2; latitude 48°12′ N., longitude 51°50′ W.; depth 187 meters, dynamic height 971.103

0	−0.05	32.21	0	−0.05	32.21	25.88
25	−0.18	32.28	25	−0.18	32.28	25.94
50	−0.18	32.30	50	−0.18	32.30	25.96
75	−1.41	32.66	75	−1.41	32.66	26.29
100	−1.31	32.80	100	−1.31	32.80	26.40
150	−1.28	32.98	150	−1.28	32.98	26.54
175	−0.66	33.24				

Station 4402; May 2; latitude 48°04′ N., longitude 51°31′ W.; depth 188 meters, dynamic height 971.087

0	0.34	32.30	0	0.34	32.30	25.93
24	0.32	32.30	25	0.30	32.30	25.94
49	0.03	32.34	50	0.00	32.35	26.00
73	−1.27	32.81	75	−1.25	32.83	26.42
98	−1.10	32.94	100	−1.10	32.95	26.51
147	−0.76	33.20	150	−0.75	33.30	26.71
171	−0.74	33.20				

Station 4403; May 2; latitude 47°53.5′ N., longitude 51°14′ W.; depth 174 meters, dynamic height 971.078

0	0.64	32.38	0	0.64	32.38	25.99
27	0.62	32.38	25	0.65	32.38	25.99
52	−0.39	32.62	50	−0.30	32.60	26.21
79	−1.30	32.87	75	−1.25	32.83	26.42
105	−1.08	33.00	100	−1.15	32.98	26.54
158	−0.63	33.25	150	−0.70	33.21	26.72

Station 4404; May 2; latitude 47°44.5′ N., longitude 50°54′ W.; depth 128 meters, dynamic height 971.077

0	1.01	32.44	0	1.01	32.44	26.02
29	1.00	32.43	25	1.00	32.44	26.02
59	−0.23	32.64	50	0.20	32.55	26.14
88	−0.99	33.03	75	−0.75	32.85	26.42
117	−0.91	33.08	100	−0.95	33.05	26.59

Station 4405; May 2; latitude 47°39′ N., longitude 50°36′ W.; depth 114 meters, dynamic height 971.076

0	0.99	32.46	0	0.99	32.46	26.03
25	0.95	32.46	25	0.95	32.46	26.03
51	0.63	32.51	50	0.65	32.51	26.09
76	−0.92	32.90	75	−0.95	32.88	26.45
102	−0.82	33.12	100	−0.80	33.11	26.63

Station 4406; May 2; latitude 47°31′ N., longitude 50°19′ W.; depth 115 meters, dynamic height 971.077

0	1.57	32.50	0	1.57	32.50	26.02
26	1.53	32.50	25	1.55	32.50	26.02
52	1.11	32.56	50	1.20	32.55	26.10
79	−0.75	33.02	75	−0.55	32.97	26.51
105	−0.77	33.01	100	−0.75	33.02	26.56

Station 4407; May 2; latitude 47°23′ N., longitude 49°56′ W.; depth 96 meters, dynamic height 971.077

0	1.37	32.52	0	1.37	32.51	26.04
28	1.40	32.51	25	1.40	32.51	26.04
58	1.14	32.5	50	1.25	32.51	26.05
86	−0.82	33.03	75	−0.05	32.82	26.37

Station 4408; May 2–3; latitude 47°39.5′ N., longitude 49°51′ W.; depth 115 meters, dynamic height 971.070

0	1.11	32.47	0	1.11	32.47	26.03
27	1.11	32.49	25	1.10	32.49	26.04
53	0.96	32.54	50	1.05	32.53	26.09
79	−0.75	32.99	75	−0.60	32.91	26.46
105	−0.79	33.18	100	−0.75	33.15	26.66

Station 4409; May 3; latitude 47°56.5′ N., longitude 49°46′ W.; depth 183 meters, dynamic height 971.044

0	1.13	32.72	0	1.13	32.72	26.23
27	1.13	32.72	25	1.15	32.72	26.23
54	0.87	32.88	50	0.95	32.84	26.34
80	−1.24	33.17	75	−0.95	33.11	26.64
106	−0.68	33.36	100	−0.80	33.32	26.80
160	0.46	33.82	150	0.30	33.73	27.08

Station 4410; May 3; latitude 48°09.5′ N., longitude 49°41′ W.; depth 225 meters, dynamic height 971.084

0	−0.06	32.43	0	−0.06	32.43	26.06
24	−0.09	32.44	25	−0.05	32.44	26.07
47	−0.25	32.46	50	−0.40	32.50	26.13
71	−1.33	32.86	75	−1.35	32.89	26.47
94	−1.28	32.98	100	−1.15	33.01	26.57
141	−0.32	33.35	150	−0.20	33.42	26.87
188	0.35	33.69	(200)	0.50	33.74	27.08

STATIONS OCCUPIED IN 1951—Continued

Station 4411; May 3; latitude 48°35.5′ N., longitude 49°35′ W.; depth 622 meters, dynamic height 970.970

Observed values			Scaled values			
Depth, meters	Temperature °C.	Salinity ‰	Depth, meters	Temperature °C.	Salinity ‰	σ_t
0	0.75	32.67	0	0.75	32.67	26.21
25	0.78	32.71	25	0.78	32.71	26.24
50	0.37	33.18	50	0.37	33.18	26.64
74	0.31	33.78	75	0.30	33.79	27.13
100	0.74	33.95	100	0.74	33.95	27.24
149	1.09	34.13	150	1.10	34.13	27.36
199	1.99	34.40	200	2.00	34.40	27.51
299	2.73	34.61	300	2.75	34.61	27.62
376	3.66	34.81	400	3.65	34.82	27.70
574	3.53	34.86	(600)	3.50	34.86	27.75

Station 4412; May 3; latitude 48°46′ N., longitude 49°33′ W.; depth 1,188 meters, dynamic height 970.993

Observed values			Scaled values			
Depth, meters	Temperature °C.	Salinity ‰	Depth, meters	Temperature °C.	Salinity ‰	σ_t
0	0.81	32.76	0	0.81	32.76	26.28
24	0.92	32.82	25	0.95	32.83	26.33
47	−0.36	33.09	50	−0.40	33.13	26.64
71	−0.53	33.45	75	−0.50	33.50	26.94
95	0.29	33.72	100	0.45	33.76	27.10
142	0.94	34.03	150	0.95	34.06	27.31
189	1.17	34.19	200	1.30	34.23	27.42
284	2.35	34.51	300	2.55	34.55	27.59
			(400)	3.35	34.76	27.68
			(600)	3.70	34.86	27.73
			(800)	3.50	34.87	27.76
			(1,000)	3.40	34.86	27.76

Station 4413; May 3; latitude 49°10.5′ N., longitude 49°22′ W.; depth 1,546 meters, dynamic height 970.933

Observed values			Scaled values			
Depth, meters	Temperature °C.	Salinity ‰	Depth, meters	Temperature °C.	Salinity ‰	σ_t
0	0.94	33.10	0	0.94	33.10	26.54
24	0.58	33.46	25	0.60	33.46	26.85
48	0.77	33.69	50	0.75	33.70	27.04
72	0.78	33.95	75	0.80	33.98	27.25
96	1.91	34.17	100	1.95	34.19	27.35
144	1.98	34.36	150	2.00	34.38	27.49
192	2.29	34.50	200	2.35	34.52	27.58
288	3.14	34.68	300	3.20	34.69	27.64
516	3.66	34.83	400	3.50	34.78	27.68
719	3.64	34.87	600	3.65	34.85	27.72
874	3.50	34.86	800	3.55	34.87	27.75
1,222	3.33	34.865	1,000	3.40	34.86	27.76

Station 4414; May 3; latitude 49°40′ N., longitude 49°11′ W.; depth 1,664 meters, dynamic height 970.865

Observed values			Scaled values			
Depth, meters	Temperature °C.	Salinity ‰	Depth, meters	Temperature °C.	Salinity ‰	σ_t
0	1.49	33.72	0	1.49	33.72	27.01
28	1.95	33.94	25	1.85	33.91	27.13
54	2.86	34.32	50	2.75	34.26	27.34
82	2.80	34.58	75	2.80	34.54	27.55
109	2.90	34.65	100	2.85	34.63	27.62
164	3.27	34.76	150	3.20	34.73	27.67
219	3.41	34.785	200	3.40	34.87	27.69
328	3.35	34.805	300	3.35	34.80	27.71
363	3.57	34.84	400	3.55	34.84	27.72
543	3.44	34.835	600	3.40	34.84	27.74
724	3.42	34.85	800	3.40	34.85	27.75
922	3.39	34.845	1,000	3.35	34.85	27.75
1,442	3.31	34.885				

Station 4415; May 3; latitude 50°01.5′ N., longitude 48°58′ W.; depth 2,103 meters, dynamic height 970.854

Observed values			Scaled values			
Depth, meters	Temperature °C.	Salinity ‰	Depth, meters	Temperature °C.	Salinity ‰	σ_t
0	1.93	33.76	0	1.93	33.76	27.01
23	2.69	34.21	25	2.70	34.21	27.30
45	2.74	34.21	50	2.75	34.29	27.36
68	2.70	34.58	75	2.70	34.60	27.61
90	2.84	34.64	100	2.90	34.66	27.65
136	3.13	34.72	150	3.15	34.73	27.67
182	3.23	34.76	200	3.25	34.78	27.70
272	3.37	34.82	300	3.40	34.83	27.73
603	3.38	34.82	(400)	3.50	34.84	27.73
905	3.35	34.86	600	3.35	34.82	27.73
			800	3.35	34.84	27.74
			(1,000)	3.30	34.87	27.78

Station 4416; May 4; latitude 49°51′ N., longitude 48°14′ W.; depth 2,415 meters, dynamic height 970.854

Observed values			Scaled values			
Depth, meters	Temperature °C.	Salinity ‰	Depth, meters	Temperature °C.	Salinity ‰	σ_t
0	3.29	34.15	0	3.29	34.15	27.20
26	3.31	34.17	25	3.30	34.17	27.22
51	2.98	34.48	50	3.00	34.47	27.49
77	2.92	34.51	75	2.95	34.51	27.52
103	3.00	34.67	100	3.00	34.65	27.63
153	3.32	34.77	150	3.30	34.77	27.70
205	3.36	34.79	200	3.35	34.79	27.70
308	3.41	34.82	300	3.40	34.82	27.73
531	3.41	34.84	400	3.40	34.83	27.73
711	3.35	34.835	600	3.40	34.84	27.74
898	3.36	34.85	800	3.35	34.84	27.74
1,380	3.33	34.88	1,000	3.30	34.86	27.77

Station 4417; May 4; latitude 49°40′ N., longitude 47°38′ W.; depth 2,652 meters, dynamic height 970.867

Observed values			Scaled values			
Depth, meters	Temperature °C.	Salinity ‰	Depth, meters	Temperature °C.	Salinity ‰	σ_t
0	4.45	34.36	0	4.45	34.36	27.25
23	4.41	34.36	25	4.40	34.36	27.26
45	4.38	34.36	50	4.20	34.37	27.29
68	3.07	34.54	75	3.00	34.55	27.55
91	2.90	34.56	100	2.90	34.58	27.58
136	3.08	34.65	150	3.15	34.67	27.63
181	3.26	34.71	200	3.30	34.72	27.66
272	3.35	34.37	300	3.45	34.80	27.70
288	3.49	34.79	400	3.45	34.82	27.72
429	3.45	34.82	600	3.30	34.82	27.74
568	3.32	34.825	800	3.30	34.83	27.74
729	3.31	34.825	1,000	3.30	34.84	27.75
1,162	3.40	34.85				

Station 4418; May 4–5; latitude 49°15′ N., longitude 47°49′ W.; depth 2,377 meters, dynamic height 970.866

Observed values			Scaled values			
Depth, meters	Temperature °C.	Salinity ‰	Depth, meters	Temperature °C.	Salinity ‰	σ_t
0	4.33	34.32	0	4.33	34.32	27.23
25	4.32	34.33	25	4.32	34.33	27.24
50	4.33	34.33	50	4.33	34.33	27.23
74	2.34	34.31	75	2.35	34.41	27.49
99	2.80	34.54	100	2.80	34.54	27.55
148	3.70	34.74	150	3.70	34.75	27.64
198	3.87	34.82	200	3.85	34.82	27.68
297	3.69	34.84	300	3.60	34.82	27.72
320	3.48	34.80	400	3.45	34.82	27.72
484	3.41	34.825	600	3.35	34.83	27.73
653	3.37	34.83	800	3.30	34.85	27.76
831	3.36	34.85	1,000	3.30	34.85	27.76
1,305	3.33	34.86				

Station 4419; May 5; latitude 48°49′ N., longitude 48°01′ W.; depth 2,286 meters, dynamic height 970.873

Observed values			Scaled values			
Depth, meters	Temperature °C.	Salinity ‰	Depth, meters	Temperature °C.	Salinity ‰	σ_t
0	2.98	33.96	0	2.98	33.96	27.08
24	3.31	34.06	25	3.30	34.06	27.13
49	3.91	34.25	50	3.90	34.25	27.22
73	3.40	34.51	75	3.40	34.52	27.49
98	3.50	34.66	100	3.50	34.66	27.59
146	3.08	34.69	150	3.10	34.69	27.65
194	3.41	34.76	200	3.45	34.77	27.68
292	3.82	34.855	300	3.80	34.85	27.71
303	3.79	34.855	400	3.70	34.85	27.72
452	3.66	34.85	600	3.45	34.85	27.74
601	3.49	34.85	800	3.35	34.84	27.74
772	3.40	34.84	1,000	3.30	34.85	27.76
1,236	3.32	34.86				

Station 4420; May 5; latitude 48°28.5′ N., longitude 48°19′ W.; depth 1,829 meters, dynamic height 970.904

Observed values			Scaled values			
Depth, meters	Temperature °C.	Salinity ‰	Depth, meters	Temperature °C.	Salinity ‰	σ_t
0	1.10	32.85	0	1.10	32.85	26.34
21	1.04	32.86	25	1.15	33.05	26.50
42	2.56	34.01	50	2.70	34.15	27.25
64	2.73	34.27	75	2.40	34.33	27.42
85	2.08	34.38	100	2.20	34.43	27.52
127	2.52	34.53	150	2.60	34.57	27.60
169	2.69	34.60	200	2.90	34.66	27.65
254	3.35	34.75	300	3.40	34.77	27.69
251	3.36	34.75	400	3.55	34.82	27.71
365	3.50	34.795	600	3.40	34.84	27.74
471	3.72	34.86	800	3.40	34.85	27.75
608	3.43	34.84	1,000	3.35	34.86	27.76
984	3.38	34.86				

Station 4421; May 5; latitude 48°07.5′ N., longitude 48°31′ W.; depth 622 meters, dynamic height 971.001

Observed values			Scaled values			
Depth, meters	Temperature °C.	Salinity ‰	Depth, meters	Temperature °C.	Salinity ‰	σ_t
0	1.14	32.82	0	1.14	32.82	26.31
25	0.96	32.80	25	0.96	32.80	26.31
50	−0.59	33.31	50	−0.59	33.31	26.78
76	−0.13	33.58	75	−0.15	33.57	26.99
101	0.35	33.78	100	0.35	33.78	27.12
151	0.98	34.10	150	0.95	34.10	27.34
201	1.22	34.18	200	1.20	34.18	27.39
302	2.26	34.46	300	2.25	34.46	27.54
387	2.84	34.62	400	2.90	34.64	27.63
571	3.67	34.83	(600)	3.65	34.84	27.71

Station 4422; May 5; latitude 48°03′ N., longitude 48°35′ W.; depth 322 meters, dynamic height 971.003

Observed values			Scaled values			
Depth, meters	Temperature °C.	Salinity ‰	Depth, meters	Temperature °C.	Salinity ‰	σ_t
0	0.90	32.50	0	0.90	32.50	26.06
25	0.79	32.80	25	0.79	32.80	26.32
50	−0.68	33.33	50	−0.68	33.33	26.81
75	−0.25	33.52	75	−0.25	33.52	26.95
100	0.32	33.74	100	0.32	33.74	27.09
150	0.98	34.06	150	0.98	34.06	27.31
200	1.43	34.23	200	1.43	34.23	27.41
300	2.38	34.50	300	2.38	34.50	27.56

Station 4423; May 5; latitude 47°51.5′ N., longitude 48°46′ W.; depth 220 meters, dynamic height 971.046

Observed values			Scaled values			
Depth, meters	Temperature °C.	Salinity ‰	Depth, meters	Temperature °C.	Salinity ‰	σ_t
0	0.46	32.48	0	0.46	32.48	26.08
25	0.36	32.465	25	0.36	32.465	26.07
50	−0.05	32.68	50	−0.05	32.68	26.26
75	−0.34	33.12	75	−0.34	33.12	26.62
100	−0.59	33.38	100	−0.59	33.38	26.84
150	0.59	33.87	150	0.59	33.87	27.18
200	1.00	34.10	200	1.00	34.10	27.34

Station 4424; May 5; latitude 47°40′ N., longitude 48°55′ W.; depth 169 meters, dynamic height 971.062

Observed values			Scaled values			
Depth, meters	Temperature °C.	Salinity ‰	Depth, meters	Temperature °C.	Salinity ‰	σ_t
0	1.64	32.53	0	1.64	32.53	26.04
25	1.35	32.54	25	1.35	32.54	26.08
49	1.02	32.58	50	1.00	32.59	26.14
74	−1.08	33.02	75	−1.10	33.03	26.58
99	−0.79	33.18	100	−0.75	33.20	26.71
148	0.49	33.80	150	0.50	33.83	27.15

Station 4425; May 5; latitude 47°43.5′ N., longitude 48°26′ W.; depth 225 meters, dynamic height 971.036

Observed values			Scaled values			
Depth, meters	Temperature °C.	Salinity ‰	Depth, meters	Temperature °C.	Salinity ‰	σ_t
0	1.22	32.61	0	1.22	32.61	26.15
25	0.79	32.64	25	0.79	32.64	26.19
50	−0.61	32.94	50	−0.61	32.94	26.49
75	−0.69	33.25	75	−0.69	33.25	26.74
100	−0.25	33.52	100	−0.25	33.52	26.95
150	0.86	33.98	150	0.86	33.98	27.25
200	1.14	34.16	200	1.14	34.16	27.38

Station 4426; May 5; latitude 47°44′ N., longitude 48°00′ W.; depth 260 meters, dynamic height 971.023

Observed values			Scaled values			
Depth, meters	Temperature °C.	Salinity ‰	Depth, meters	Temperature °C.	Salinity ‰	σ_t
0	0.92	32.56	0	0.92	32.56	26.11
24	0.79	32.61	25	0.80	32.62	26.17
49	0.88	33.10	50	0.85	33.12	26.57
73	−0.01	33.48	75	0.00	33.50	26.92
97	0.31	33.70	100	0.35	33.73	27.08
146	0.78	34.00	150	0.80	34.02	27.29
194	1.18	34.18	200	1.25	34.20	27.41
243	1.72	34.32				

Station 4427; May 5; latitude 47°49′ N., longitude 47°44′ W.; depth 297 meters, dynamic height 970.994

Observed values			Scaled values			
Depth, meters	Temperature °C.	Salinity ‰	Depth, meters	Temperature °C.	Salinity ‰	σ_t
0	1.18	32.83	0	1.18	32.83	26.32
23	0.99	32.98	25	0.95	33.00	26.47
47	0.48	33.26	50	0.45	33.29	26.72
70	0.06	33.52	75	0.10	33.58	26.97
93	0.57	33.85	100	0.65	33.89	27.19
140	1.05	34.08	150	1.20	34.12	27.35
187	1.58	34.29	200	1.70	34.34	27.48
266	2.52	34.54				

Station 4428; May 6; latitude 48°01′ N., longitude 47°34′ W.; depth 382 meters, dynamic height 970.986

Observed values			Scaled values			
Depth, meters	Temperature °C.	Salinity ‰	Depth, meters	Temperature °C.	Salinity ‰	σ_t
0	1.52	32.86	0	1.52	32.86	26.31
27	1.35	33.04	25	1.40	33.02	26.45
53	−0.17	33.49	50	−0.10	33.44	26.87
80	0.14	33.66	75	0.05	33.62	27.02
106	0.79	33.94	100	0.65	33.90	27.20
159	1.33	34.17	150	1.25	34.13	27.35
212	1.91	34.38	200	1.75	34.33	27.47
318	3.22	34.72	300	3.00	34.67	27.65

STATIONS OCCUPIED IN 1951—Continued

Station 4429; May 6; latitude 48°21′ N., longitude 47°14′ W.; depth 1,957 meters, dynamic height 970.927

Observed values			Scaled values			
Depth, meters	Temperature °C.	Salinity ‰	Depth, meters	Temperature °C.	Salinity ‰	σ_t
0	1.18	32.78	0	1.18	32.78	26.28
27	1.12	32.91	25	1.10	32.89	26.36
53	1.40	34.15	50	1.40	34.02	27.25
80	1.50	34.26	75	1.45	34.25	27.43
106	1.79	34.34	100	1.70	34.32	27.47
160	2.43	34.52	150	2.30	34.49	27.56
213	2.88	34.64	200	2.80	34.62	27.62
319	3.29	34.75	300	3.25	34.74	27.67
381	3.48	34.76	400	3.45	34.77	27.68
568	3.55	34.83	600	3.55	34.84	27.72
753	3.61	34.86	800	3.55	34.86	27.74
946	3.44	34.855	1,000	3.40	34.86	27.76
1,435	3.33	34.87				

Station 4430; May 6; latitude 48°35′ N., longitude 46°56′ W.; depth 2,451 meters, dynamic height 970.874

0	3.44	33.92	0	3.44	33.92	27.00
24	3.48	33.96	25	3.50	33.96	27.03
47	3.70	34.10	50	3.70	34.15	27.16
71	3.62	34.45	75	3.55	34.50	27.45
94	3.18	34.60	100	3.20	34.62	27.59
141	3.30	34.70	150	3.35	34.72	27.65
188	3.49	34.77	200	3.50	34.78	27.68
282	3.50	34.82	300	3.50	34.83	27.72
431		34.84	400	3.50	34.84	27.73
904	3.39	34.855	600	3.45	34.85	27.74
1,356	3.32	34.875	800	3.40	34.85	27.75
			1,000	3.35	34.86	27.76

Station 4431; May 6; latitude 48°57′ N., longitude 46°35′ W.; depth 2,780 meters, dynamic height 970.862

0	4.55	34.32	0	4.55	34.32	27.21
26	4.52	34.32	25	4.55	34.32	27.21
51	4.46	34.32	50	4.45	34.32	27.22
77	3.12	34.49	75	3.20	34.48	27.47
102	2.92	34.63	100	2.90	34.62	27.62
153	3.32	34.76	150	3.30	34.76	27.69
204	3.43	34.78	200	3.45	34.79	27.69
306	3.48	34.82	300	3.50	34.82	27.72
395	3.54	34.84	400	3.50	34.84	27.73
591	3.40	34.84	600	3.40	34.84	27.74
787	3.40	34.85	800	3.40	34.85	27.75
985	3.37	34.85	1,000	3.35	34.85	27.75
1,483	3.35	34.89				

Station 4432; May 6; latitude 49°19′ N., longitude 46°18′ W.; depth 3,072 meters, dynamic height 970.901

0	4.96	34.29	0	4.96	34.29	27.14
24	4.96	34.295	25	4.95	34.30	27.15
45	4.72	34.30	50	4.70	34.30	27.17
69	4.52	34.32	75	4.40	34.36	27.26
89	4.06	34.46	100	3.80	34.49	27.42
134	3.30	34.56	150	3.20	34.57	27.55
178	3.14	34.59	200	3.20	34.63	27.59
267	3.40	34.76	300	3.45	34.78	27.68
372	3.54	34.80	400	3.50	34.81	27.71
561	3.53	34.845	600	3.50	34.84	27.73
754	3.43	34.835	800	3.40	34.84	27.74
948	3.43	34.86	1,000	3.40	34.86	27.76
1,441	3.32	34.86				

Station 4433; May 6; latitude 49°10.5′ N., longitude 45°38′ W.; depth 2,780 meters, dynamic height 970.882

0	4.29	34.30	0	4.29	34.30	27.22
26	4.21	34.33	25	4.20	34.33	27.25
52	4.17	34.34	50	4.15	34.34	27.26
79	3.26	34.46	75	3.40	34.43	27.41
105	2.83	34.58	100	2.85	34.56	27.57
156	2.86	34.66	150	2.85	34.66	27.65
209	3.08	34.72	200	3.05	34.71	27.67
314	3.20	34.76	300	3.20	34.76	27.70
394	3.30	34.78	400	3.30	34.78	27.70
588	3.55	34.84	600	3.55	34.84	27.72
782	3.49	34.82	800	3.45	34.82	27.72
981	3.44	34.845	1,000	3.40	34.85	27.75
1,480	3.33	34.845				

Station 4434; May 7; latitude 49°00.5′ N., longitude 44°59′ W.; depth 1,719 meters dynamic height 970.861

0	4.75	34.21	0	4.75	34.21	27.10
25	4.04	34.34	25	4.04	34.34	27.28
50	3.70	34.37	50	3.70	34.37	27.34
74	2.87	34.57	75	2.85	34.57	27.58
99	2.84	34.65	100	2.85	34.65	27.64
149	3.13	34.73	150	3.15	34.73	27.67
199	3.27	34.76	200	3.25	34.76	27.69
298	3.36	34.80	300	3.35	34.80	27.21
366	3.49	34.82	400	3.50	34.83	27.72
550	3.46	34.84	600	3.45	34.84	27.73
738	3.44	34.83	800	3.40	34.84	27.74
931	3.39	34.85	1,000	3.35	34.86	27.76
1,424	3.31	34.895				

Station 4435; May 7; latitude 48°39.5′ N., longitude 45°20′ W.; depth 1,152 meters, dynamic height 970.896

0	4.45	33.90	0	4.45	33.90	26.88
25	4.35	33.93	25	4.35	33.93	26.91
50	3.77	34.28	50	3.77	34.28	27.26
75	3.10	34.40	75	3.10	34.40	27.42
100	3.18	34.52	100	3.18	34.52	27.51
150	3.18	34.66	150	3.18	34.66	27.62
200	3.20	34.70	200	3.20	34.70	27.65
300	3.61	34.80	300	3.61	34.80	27.69
385	3.79	34.84	400	3.80	34.84	27.70
577	3.50	34.83	600	3.50	34.83	27.72
770	3.47	34.85	800	3.45	34.85	27.74
968	3.36	34.845	1,000	3.30	34.85	27.76
1,091	3.34	34.86				

Station 4436; May 7; latitude 48°24.5′ N., longitude 45°54′ W.; depth 1,152 meters, dynamic height 970.891

0	4.61	34.02	0	4.61	34.02	26.97
25	4.34	34.02	25	4.34	34.02	26.99
50	4.00	34.10	50	4.00	34.10	27.09
75	3.00	34.32	75	3.00	34.32	27.37
100	3.01	34.45	100	3.01	34.45	27.47
150	3.27	34.65	150	3.27	34.65	27.60
200	3.67	34.77	200	3.67	34.77	27.66
300	3.79	34.84	300	3.79	34.84	27.70
400	3.83	34.87	400	3.83	34.87	27.73
598	3.57	34.85	600	3.55	34.85	27.73
796	3.43	34.85	800	3.40	34.85	27.75
996	3.38	34.86	1,000	3.35	34.86	27.76

Station 4437; May 7; latitude 47°59′ N., longitude 46°26′ W.; depth 1,170 meters dynamic height 970.903

Observed values			Scaled values			
Depth, meters	Temperature °C.	Salinity ‰	Depth, meters	Temperature °C.	Salinity ‰	σ_t
0	4.10	33.98	0	4.10	33.98	26.98
23	3.69	33.97	25	3.60	33.97	27.03
45	2.46	34.11	50	3.20	34.13	27.28
68	1.77	34.20	75	1.80	34.23	27.39
91	1.91	34.30	100	1.95	34.32	27.46
136	2.12	34.42	150	2.25	34.46	27.54
181	2.56	34.56	200	2.70	34.60	27.61
272	3.25	34.72	300	3.40	34.75	27.67
285	3.26	34.72	400	3.80	34.85	27.71
437	3.84	34.86	600	3.70	34.86	27.73
595	3.74	34.86	(800)	3.55	34.86	27.74
760	3.60	34.86	(1000)	3.45	34.86	27.75

Station 4438; May 7; latitude 47°54.5′N., longitude 46°05′ W.; depth 1,051 meters, dynamic height 970.891

Observed values			Scaled values			
Depth, meters	Temperature °C.	Salinity ‰	Depth, meters	Temperature °C.	Salinity ‰	σ_t
0	4.02	33.85	0	4.02	33.85	26.89
25	3.47	33.95	25	3.47	33.95	27.02
50	3.24	34.20	50	3.24	34.20	27.24
74	2.52	34.30	75	2.50	34.31	27.40
99	2.74	34.49	100	2.75	34.49	27.52
148	2.99	34.61	150	3.60	34.61	27.60
198	3.47	34.73	200	3.50	34.73	27.64
297	3.79	34.83	300	3.80	34.83	27.69
401	3.78	34.84	400	3.75	34.84	27.70
605	3.58	34.86	600	3.55	34.86	27.74
812	3.43	34.86	800	3.40	34.86	27.76
			(1000)	3.35	34.86	27.76

Station 4439; May 7; latitude 47°48.5′N., longitude 45°52′ W.; depth 421 meters, dynamic height 970.908

Observed values			Scaled values			
Depth, meters	Temperature °C.	Salinity ‰	Depth, meters	Temperature °C.	Salinity ‰	σ_t
0	3.99	33.77	0	3.99	33.77	26.83
25	3.49	33.78	25	3.49	33.78	26.88
49	3.20	33.98	50	3.15	33.98	27.07
74	2.92	34.12	75	2.90	34.12	27.22
98	2.60	34.22	100	2.60	34.23	27.32
148	3.33	34.56	150	3.35	34.57	27.53
197	3.35	34.66	200	3.35	34.67	27.61
295	3.75	34.84	300	3.75	34.84	27.70
398	3.81	34.86	400	3.80	34.86	27.72

Station 4440; May 7; latitude 47°44′N., longitude 45°42′ W.; depth 325 meters, dynamic height 970.964

Observed values			Scaled values			
Depth, meters	Temperature °C.	Salinity ‰	Depth, meters	Temperature °C.	Salinity ‰	σ_t
0	3.84	33.71	0	3.84	33.71	26.80
25	3.50	33.75	25	3.50	33.75	26.86
50	2.84	33.86	50	2.84	33.86	27.01
75	2.92	34.13	75	2.92	34.13	27.22
100	2.21	34.21	100	2.21	34.21	27.35
150	3.89	34.62	150	3.89	34.62	27.52
200	3.61	34.68	200	3.61	34.68	27.59
300	3.70	34.83	300	3.70	34.83	27.70

Station 4441; May 7; latitude 47°27′N., longitude 45°11′ W.; depth 230 meters, dynamic height 970.964

Observed values			Scaled values			
Depth, meters	Temperature °C.	Salinity ‰	Depth, meters	Temperature °C.	Salinity ‰	σ_t
0	7.59	33.90	0	7.59	33.90	26.48
25	6.77	33.89	25	6.77	33.89	26.59
49	6.75	33.89	50	6.75	33.89	26.60
74	6.38	33.94	75	6.25	33.94	26.71
99	4.10	34.06	100	4.10	34.06	27.05
148	3.14	34.38	150	3.15	34.39	27.40
207	3.60	34.66	200	3.60	34.63	27.55

Station 4442; May 8; latitude 47°22′N., longitude 45°00′ W.; depth 188 meters, dynamic height 970.954

Observed values			Scaled values			
Depth, meters	Temperature °C.	Salinity ‰	Depth, meters	Temperature °C.	Salinity ‰	σ_t
0	6.96	33.94	0	6.96	33.94	26.61
29	6.68	33.95	25	6.75	33.95	26.65
59	5.76	33.91	50	6.10	33.92	26.71
88	4.30	34.06	75	5.00	33.95	26.86
117	3.40	34.40	100	3.80	34.19	27.18
176	3.56	34.50	150	3.45	34.46	27.43

Station 4443; May 8; latitude 47°22′N., longitude 45°13′ W.; depth 216 meters, dynamic height 970.950

Observed values			Scaled values			
Depth, meters	Temperature °C.	Salinity ‰	Depth, meters	Temperature °C.	Salinity ‰	σ_t
0	7.09	33.89	0	7.09	33.89	26.55
25	6.57	33.88	25	6.57	33.88	26.61
50	6.45	33.90	50	6.45	33.90	26.65
75	4.90	33.98	75	4.90	33.98	26.90
100	3.48	34.20	100	3.48	34.20	27.22
151	3.94	34.56	150	3.95	34.56	27.46
201	4.01	34.67	200	4.00	34.67	27.55

Station 4444; May 8; latitude 47°23′N., longitude 45°33′ W.; depth 272 meters, dynamic height 970.940

Observed values			Scaled values			
Depth, meters	Temperature °C.	Salinity ‰	Depth, meters	Temperature °C.	Salinity ‰	σ_t
0	5.20	33.72	0	5.20	33.72	26.67
23	4.90	33.71	25	4.90	33.71	26.69
45	4.66	33.72	50	4.55	33.72	26.73
68	3.81	34.00	75	3.60	34.06	27.10
91	3.36	34.17	100	3.35	34.24	27.26
136	3.55	34.49	150	3.65	34.54	27.47
182	3.98	34.64	200	4.00	34.69	27.56
236	4.01	34.79				

Station 4445; May 8; latitude 47°24′N., longtidue 45°57′ W.; depth 320 meters, dynamic height 970.952

Observed values			Scaled values			
Depth, meters	Temperature °C.	Salinity ‰	Depth, meters	Temperature °C.	Salinity ‰	σ_t
0	5.46	33.74	0	5.46	33.74	26.65
23	5.47	33.78	25	5.50	33.78	26.68
46	5.45	33.83	50	5.45	33.85	26.74
69	4.62	33.99	75	4.35	34.03	26.99
92	3.96	34.16	100	3.85	34.22	27.21
137	3.53	34.38	150	3.65	34.43	27.38
184	3.85	34.59	200	3.85	34.64	27.53
276	3.80	34.82	(300)	3.80	34.85	27.71

Station 4446; May 8; latitude 47°26′N., longitude 46°18′ W.; depth 622 meters, dynamic height 970.912

Observed values			Scaled values			
Depth, meters	Temperature °C.	Salinity ‰	Depth, meters	Temperature °C.	Salinity ‰	σ_t
0	3.18	33.58	0	3.18	33.58	26.75
21	3.13	33.60	25	3.15	33.68	26.84
41	2.91	33.97	50	2.65	34.02	27.16
62	2.34	34.08	75	2.25	34.14	27.28
82	2.22	34.18	100	2.65	34.35	27.42
123	3.14	34.54	150	3.10	34.60	27.58
165	3.10	34.62	200	3.10	34.66	27.63
247	3.19	34.70	300	3.55	34.76	27.66
353	3.85	34.84	400	3.80	34.84	27.70
545	3.76	34.86	(600)	3.70	34.86	27.73

STATIONS OCCUPIED IN 1951—Continued

Station 4447; May 8; latitude 47°23′N., longitude 46°31′ W.; depth 1042 meters, dynamic height 970.918

Observed values			Scaled values			
Depth, meters	Temperature °C.	Salinity ‰	Depth, meters	Temperature °C.	Salinity ‰	σ_t
0	3.74	33.77	0	3.74	33.77	26.85
21	3.25	33.79	25	3.25	33.82	26.94
43	3.22	33.99	50	3.25	34.03	27.10
64	3.24	34.14	75	3.10	34.18	27.24
86	2.89	34.23	100	2.65	34.30	27.38
128	2.36	34.42	150	2.30	34.45	27.53
171	2.32	34.48	200	2.45	34.53	27.57
257	2.83	34.62	300	3.25	34.71	27.65
272	3.02	34.67	400	3.80	34.85	27.71
438	3.88	34.87	600	3.80	34.87	27.73
613	3.81	34.87	800	3.55	34.87	27.75
793	3.59	34.87	(1000)	3.45	34.87	27.76

Station 4448; May 8; latitude 47°15′N., longitude 47°11′ W.; depth 1,024 meters, dynamic height 970.943

0	2.46	33.37	0	2.46	33.37	26.65
25	2.68	33.64	25	2.68	33.64	26.85
50	2.45	33.99	50	2.45	33.79	27.14
76	2.40	34.14	75	2.40	34.14	27.27
101	1.89	34.23	100	1.90	34.23	27.38
152	2.18	34.40	150	2.15	34.40	27.50
202	2.40	34.49	200	2.40	34.48	27.54
303	3.27	34.70	300	3.25	34.69	27.63
385	3.64	34.79	400	3.65	34.79	27.67
580	3.86	34.83	600	3.80	34.83	27.69
776	3.61	34.855	800	3.55	34.85	27.73
930	3.44	34.855	(1000)	3.35	34.85	27.75

Station 4449; May 9; latitude 47°14′N., longitude 47°36′ W.; depth 220 meters, dynamic height 971.060

0	1.34	32.55	0	1.34	32.55	26.08
26	1.06	32.58	25	1.10	32.58	26.12
52	−1.17	32.91	50	−1.15	32.90	26.47
79	−0.74	33.20	75	−0.80	33.16	26.67
105	−0.38	33.37	100	−0.45	33.33	26.80
156	0.59	33.85	150	0.45	33.79	27.12
209	1.16	34.14	200	1.05	34.10	27.34

Station 4450; May 9; latitude 47°12′ N., longitude 47°05′ W.; depth 169 meters, dynamic height 971.088

0	1.67	32.56	0	1.67	32.56	26.06
24	1.67	32.57	25	1.65	32.57	26.07
48	1.39	32.56	50	1.35	32.56	26.09
71	−0.96	32.84	75	−0.95	32.88	26.45
95	−0.92	33.10	100	−0.90	33.14	26.67
143	0.09	33.58	(150)	0.20	33.64	27.02

Station 4451; May 9; latitude 47°08′ N., longitude 48°27′ W.; depth 125 meters, dynamic height 971.087

0	1.93	32.58	0	1.93	32.58	26.06
28	1.77	32.58	25	1.80	32.58	26.07
56	0.22	32.64	50	0.60	32.62	26.18
84	−0.99	33.12	75	−0.80	32.96	26.51
112	−0.61	33.27	100	−0.80	33.21	26.72

Station 4452; May 9; latitude 47°10′ N., longitude 49°12′ W.; depth 88 meters, dynamic height 971.089

0	2.58	32.60	0	2.58	32.60	26.03
26	2.44	32.61	25	2.45	32.61	26.05
51	1.98	32.65	50	2.05	32.65	26.12
77	−0.58	33.02	75	−0.55	32.98	26.52

Station 4453; May 9; latitude 46°46.5′ N., longitude 48°44′ W.; depth 82 meters, dynamic height 971.044

0	2.73	32.64	0	2.73	32.64	26.05
24	2.23	32.66	25	2.20	32.66	26.10
48	1.99	32.67	50	1.85	32.67	26.14
69	0.00	32.97	(75)	−0.45	33.07	26.59

Station 4454; May 9; latitude 46°46′ N., longitude 48°04′ W.; depth 117 meters, dynamic height 971.051

0	3.36	32.67	0	3.36	32.67	26.02
26	1.82	32.66	25	1.85	32.66	26.13
51		32.68	50	1.70	32.68	26.16
77	1.10	32.76	75	1.15	32.75	26.26
103	−0.69	33.17	100	−0.60	33.10	26.61

Station 4455; May 9; latitude 46°45′ N., longitude 47°33′ W.; depth 169 meters, dynamic height 971.024

0	2.30	32.57	0	2.30	32.57	26.03
25	1.16	32.58	25	1.16	32.58	26.12
51	0.74	32.86	50	0.75	32.95	26.44
76	−1.12	33.08	75	−1.10	33.07	26.61
102	−0.53	33.36	100	−0.60	33.35	26.82
153	0.74	33.95	150	0.65	33.90	27.20

Station 4456; May 9; latitude 46°45′ N., longitude 47°15′ W.; depth 320 meters, dynamic height 970.986

0	3.04	32.81	0	3.04	32.81	26.17
25	1.79	32.84	25	1.79	32.84	26.28
49	1.30	33.06	50	1.30	33.09	26.51
74	1.14	33.68	75	1.10	33.69	27.00
98	0.74	33.86	100	0.75	33.87	27.18
147	1.08	34.12	150	1.15	34.12	27.35
197	1.97	34.35	200	2.00	34.36	27.48
295	2.38	34.50	300	2.40	34.50	27.56

Station 4457; May 9; latitude 46°43.5′ N., longitude 47°02′ W.; depth 860 meters, dynamic height 970.963

0	2.49	32.86	0	2.49	32.86	26.24
23	1.80	32.88	25	1.75	32.88	26.32
46	1.40	33.15	50	1.30	33.23	26.63
69	0.80	33.78	75	0.80	33.82	27.13
92	0.78	33.91	100	0.85	33.95	27.23
137	1.16	34.12	150	1.35	34.18	27.38
183	1.97	34.34	200	2.10	34.40	27.50
275	2.78	34.62	300	3.05	34.70	27.66
331	3.48	34.77	400	3.70	34.83	27.70
514	3.79	34.88	600	3.65	34.87	27.74
707	3.50	34.87	(800)	3.40	34.87	27.77

Station 4458; May 9; latitude 46°41.5′ N., longitude 46°41′ W.; depth 1,197 meters, dynamic height 970.936

0	2.72	33.26	0	2.72	33.26	26.54
23	2.24	33.26	25	2.15	33.26	26.59
46	1.48	33.67	50	1.50	33.76	27.04
68	2.60	34.07	75	2.50	34.08	27.21
91	1.91	34.09	100	1.95	34.12	27.30
136	2.52	34.33	150	2.45	34.35	27.43
182	2.32	34.43	200	2.55	34.49	27.54
273	3.74	34.77	300	3.80	34.80	27.67
332	3.85	34.82	400	3.80	34.84	27.70
509	3.81	34.86	600	3.65	34.87	27.74
693	3.55	34.88	800	3.50	34.88	27.76
877	3.49	34.875	1,000	3.40	34.87	27.77
1,019	3.42	34.87				

STATIONS OCCUPIED IN 1951—Continued

Station 4459; May 10; latitude 46°42′ N., longitude 46°22′ W.; depth 622 meters, dynamic height 970.922

Observed values			Scaled values			
Depth, meters	Temperature °C.	Salinity ‰	Depth, meters	Temperature °C.	Salinity ‰	σ_t
0	4.74	33.58	0	4.74	33.58	26.60
25	4.23	33.58	25	4.23	33.58	26.65
50	3.66	33.73	50	3.66	33.73	27.33
75	2.18	34.06	75	2.18	34.06	27.23
100	2.49	34.32	100	2.49	34.32	27.41
150	3.22	34.57	150	3.22	34.57	27.55
201	3.80	34.72	200	3.80	34.72	27.61
301	4.03	34.84	300	4.05	34.84	27.67
389	3.86	34.85	400	3.85	34.85	27.70
487	3.72	34.87				

Station 4460; May 10; latitude 46°43.5′ N., longitude 45°58′ W.; depth 324 meters, dynamic height 970.935

Observed values			Scaled values			
Depth, meters	Temperature °C.	Salinity ‰	Depth, meters	Temperature °C.	Salinity ‰	σ_t
0	6.94	33.94	0	6.94	33.94	26.61
25	6.54	33.93	25	6.54	33.93	26.65
50	6.73	34.00	50	6.73	34.00	26.69
75	3.84	34.12	75	3.84	34.12	27.13
100	3.19	34.24	100	3.19	34.24	27.28
150	3.95	34.54	150	3.95	34.54	27.44
200	3.96	34.68	200	3.96	34.68	27.55
300	3.85	34.86	300	3.85	34.86	27.71

Station 4461; May 10; latitude 46°44′ N., longitude 45°44′ W.; depth 265 meters, dynamic height 970.953

Observed values			Scaled values			
Depth, meters	Temperature °C.	Salinity ‰	Depth, meters	Temperature °C.	Salinity ‰	σ_t
0	7.59	34.12	0	7.54	34.12	26.66
25	7.36	34.10	25	7.36	34.10	26.68
50	7.61	34.16	50	7.61	34.16	26.69
74	6.12	34.13	75	6.00	34.13	26.88
99	4.40	34.13	100	4.40	34.13	27.07
149	4.84	34.59	150	4.85	34.59	27.39
198	4.18	34.65	200	4.15	34.65	27.51
248	3.88	34.72				

Station 4462; May 10; latitude 46°45.5′ N., longitude 45°22′ W.; depth 220 meters, dynamic height 970.948

Observed values			Scaled values			
Depth, meters	Temperature °C.	Salinity ‰	Depth, meters	Temperature °C.	Salinity ‰	σ_t
0	6.66	33.92	0	6.66	33.92	26.64
23	6.17	33.87	25	6.10	33.87	26.68
46	5.86	33.86	50	5.80	33.87	26.71
69	5.49	33.92	75	5.40	33.96	26.82
92	5.15	34.20	100	4.95	34.28	27.13
139	4.19	34.52	150	4.05	34.55	27.44
185	3.82	34.61	(200)	3.75	34.63	27.53

Station 4463; May 10; latitude 46°47′ N., longitude 45°00′ W.; depth 169 meters, dynamic height 970.929

Observed values			Scaled values			
Depth, meters	Temperature °C.	Salinity ‰	Depth, meters	Temperature °C.	Salinity ‰	σ_t
0	6.94	33.97	0	6.94	33.97	26.64
25	6.57	33.98	25	6.57	33.98	26.69
50	6.15	33.94	50	6.15	33.94	26.72
75	3.37	34.13	75	3.37	34.13	27.17
101	3.01	34.30	100	3.00	34.30	27.35
151	3.24	34.49	150	3.25	34.49	27.47

Station 4464; May 10; latitude 46°47.5′ N., longitude 44°51′ W.; depth 133 meters, dynamic height 970.936

Observed values			Scaled values			
Depth, meters	Temperature °C.	Salinity ‰	Depth, meters	Temperature °C.	Salinity ‰	σ_t
0	6.68	33.90	0	6.68	33.90	26.61
26	6.25	33.88	25	6.30	33.88	26.65
51	5.66	33.92	50	5.70	33.92	26.77
77	4.43	34.05	75	4.50	34.03	26.98
102	3.67	34.27	100	3.70	34.27	27.26
127	3.38	34.31				

Station 4465; May 23; latitude 43°20′ N., longitude 50°15′ W.; depth 57 meters, dynamic height 971.097

Observed values			Scaled values			
Depth, meters	Temperature °C.	Salinity ‰	Depth, meters	Temperature °C.	Salinity ‰	σ_t
0	7.16	32.86	0	7.16	32.86	25.74
23	3.11	32.89	25	3.10	32.89	26.21
42	3.13	32.91	(50)	3.15	32.92	26.24

Station 4466; May 23; latitude 43°03′ N., longitude 50°15′ W.; depth 76 meters, dynamic height 971.100

Observed values			Scaled values			
Depth, meters	Temperature °C.	Salinity ‰	Depth, meters	Temperature °C.	Salinity ‰	σ_t
0	4.49	32.67	0	4.49	32.67	25.90
25	3.94	32.67	25	3.94	32.67	25.96
50	1.26	32.78	50	1.26	32.78	26.27
75	0.67	32.90	75	0.67	32.90	26.39
			(100)	0.35	33.04	26.53

Station 4467; May 23; latitude 42°52′ N., longitude 50°15′ W.; depth 329 meters, dynamic height 971.076

Observed values			Scaled values			
Depth, meters	Temperature °C.	Salinity ‰	Depth, meters	Temperature °C.	Salinity ‰	σ_t
0	5.46	32.67	0	5.46	32.67	25.80
25	2.93	32.65	25	2.93	32.65	26.04
50	0.89	32.72	50	0.89	32.72	26.24
75	−0.32	32.98	75	−0.32	32.98	26.51
100	−0.42	33.35	100	−0.42	33.35	27.82
150	1.37	33.93	150	1.37	33.93	27.18
200	2.65	34.22	200	2.65	34.22	27.32
300	3.58	34.63	300	3.58	34.63	27.55

Station 4468; May 23; latitude 42°39.5′ N., longitude 50°14′ W.; depth 1,957 meters, dynamic height 971.013

Observed values			Scaled values			
Depth, meters	Temperature °C.	Salinity ‰	Depth, meters	Temperature °C.	Salinity ‰	σ_t
0	8.20	33.23	0	8.20	33.23	25.88
25	7.60	33.69	25	7.60	33.69	26.32
50	6.00	33.86	50	6.00	33.86	26.68
75	3.93	33.84	75	3.93	33.84	26.88
100	3.07	34.12	100	3.07	34.12	27.20
150	3.81	34.39	150	3.81	34.39	27.34
201	4.30	34.60	200	4.30	34.59	27.45
301	4.35	34.76	300	4.35	34.76	27.58
398	4.92	34.94	400	4.90	34.94	27.66
595	4.29	34.93	600	4.30	34.93	27.71
793	4.10	34.93	800	4.05	34.93	27.74
993	3.72	34.90	1,000	3.70	34.90	27.76
1,492	3.43	34.87				

Station 4469; May 23; latitude 42°19′ N., longitude 50°12′ W.; depth 3,017 meters, dynamic height 971.008

Observed values			Scaled values			
Depth, meters	Temperature °C.	Salinity ‰	Depth, meters	Temperature °C.	Salinity ‰	σ_t
0	9.82	33.19	0	9.82	33.19	25.59
24	7.72	33.39	25	7.65	33.39	26.08
49	5.69	33.41	50	5.65	33.41	26.36
73	4.77	33.96	75	4.60	33.97	26.93
97	2.83	34.10	100	2.85	34.12	27.22
146	3.31	34.35	150	3.30	34.37	27.38
195	3.40	34.50	200	3.40	34.52	27.49
292	4.02	34.76	300	4.10	34.78	27.62
385	5.04	34.98	400	5.00	34.98	27.68
578	4.35	34.95	600	4.30	34.95	27.73
772	3.97	34.925	800	3.90	34.92	27.76
968	3.88	34.92	1,000	3.85	34.92	27.76
1,461	3.52	34.915				

STATIONS OCCUPIED IN 1951—Continued

Station 4470; May 23; latitude 41°58′ N., longitude 50°08′ W.; depth 3,585 meters, dynamic height 971.085

Observed values			Scaled values			
Depth, meters	Temperature °C.	Salinity ‰	Depth, meters	Temperature °C.	Salinity ‰	σ_t
0	12.56	33.71	0	12.56	33.71	25.50
25	10.89	34.49	25	10.89	34.49	26.41
50	12.36	35.11	50	12.36	35.11	26.63
74	12.28	35.34	75	12.25	35.34	26.82
99	11.25	35.24	100	11.20	35.24	26.94
148	9.23	34.99	150	9.15	34.98	27.09
197	7.03	34.77	200	7.00	34.77	27.26
296	6.44	34.90	300	6.45	34.90	27.43
555	4.79	34.96	400	5.70	34.95	27.57
744	4.43	34.97	600	4.65	34.96	27.71
936	4.18	34.96	800	4.35	34.97	27.75
1,425	3.76	34.94	1,000	4.10	34.96	27.77

Station 4471; May 23; latitude 41°26.5′ N., longitude 50°09′ W.; depth 3,786 meters, dynamic height 971.143

Observed values			Scaled values			
Depth, meters	Temperature °C.	Salinity ‰	Depth, meters	Temperature °C.	Salinity ‰	σ_t
0	12.84	33.70	0	12.84	33.70	25.44
27	8.63	33.75	25	8.80	33.74	26.18
53	7.65	33.95	50	7.65	33.91	26.49
80	11.46	35.16	75	11.00	35.00	26.79
106	9.99	34.91	100	10.15	34.95	26.90
160	11.20	35.37	150	11.05	35.30	27.01
213	9.61	35.17	200	10.05	35.22	27.13
319	6.84	34.87	300	7.45	34.96	27.34
392	6.39	34.93	400	6.05	34.90	27.49
587	4.63	34.90	600	4.55	34.90	27.67
783	4.24	34.92	800	4.15	34.92	27.73
980	3.86	34.905	1,000	3.80	34.90	27.75
1,474	3.38	34.86				

Station 4472; May 24; latitude 42°03′ N., longitude 49°25′ W.; depth 3,109 meters, dynamic height 971.093

Observed values			Scaled values			
Depth, meters	Temperature °C.	Salinity ‰	Depth, meters	Temperature °C.	Salinity ‰	σ_t
0	12.58	33.74	0	12.58	33.74	25.52
24	11.54	34.64	25	11.55	34.67	26.44
49	12.50	35.20	50	12.55	35.22	26.67
73	12.59	35.40	75	12.55	35.40	26.81
97	11.07	35.10	100	10.90	35.08	26.87
146	9.20	34.94	150	9.20	34.94	27.06
195	9.70	35.20	200	9.60	35.19	27.18
292	5.43	34.69	300	5.40	34.70	27.41
368	5.27	34.84	400	5.10	34.88	27.59
553	4.55	34.94	600	4.45	34.94	27.71
739	4.27	34.94	800	4.20	34.94	27.74
931	4.09	34.94	1,000	4.00	34.94	27.76
1,421	3.71	34.93				

Station 4473; May 24; latitude 41°34′ N., longitude 48°47′ W.; depth 3,292 meters, dynamic height 971.151

Observed values			Scaled values			
Depth, meters	Temperature °C.	Salinity ‰	Depth, meters	Temperature °C.	Salinity ‰	σ_t
0	12.02	33.70	0	12.02	33.70	25.60
26	10.88	34.41	25	10.90	34.39	26.34
52	12.33	35.04	50	12.20	35.00	26.57
78	13.86	35.66	75	13.80	35.64	26.74
104	13.46	35.61	100	13.55	35.62	26.78
155	11.18	35.22	150	11.40	35.25	26.92
207	10.70	35.31	200	10.80	35.31	27.07
311	6.70	34.77	300	7.00	34.81	27.29
393	6.23	34.92	400	6.20	34.93	27.49
591	4.97	34.97	600	4.90	34.97	27.69
792	4.19	34.92	800	4.15	34.92	27.73
991	3.83	34.90	1,000	3.80	34.90	27.75
1,492	3.65	34.92				

Station 4474; May 24, latitude 42°00′ N., longitude 47°58′ W.; depth 3,658 meters, dynamic height 971.105

Observed values			Scaled values			
Depth, meters	Temperature °C.	Salinity ‰	Depth, meters	Temperature °C.	Salinity ‰	σ_t
0	13.12	33.27	0	13.12	33.27	25.06
26	11.90	34.53	25	11.95	34.50	26.23
51	10.51	34.80	50	10.60	34.80	26.71
77	8.76	34.64	75	8.90	34.64	26.87
102	8.26	34.66	100	8.30	34.66	26.98
155	9.02	34.98	150	9.00	34.95	27.10
206	7.49	34.82	200	7.70	34.84	27.21
308	5.27	34.70	300	5.30	34.70	27.42
334	6.31	34.94	400	5.90	34.97	27.57
510	5.21	34.99	600	4.90	34.98	27.69
693	4.60	34.96	800	4.30	34.94	27.72
875	4.14	34.93	1,000	3.95	34.92	27.75
1,346	3.62	34.90				

Station 4475; May 25; latitude 42°27.5′ N., longitude 48°26′ W.; depth 3,383 meters, dynamic height 971.042

Observed values			Scaled values			
Depth, meters	Temperature °C.	Salinity ‰	Depth, meters	Temperature °C.	Salinity ‰	σ_t
0	9.38	32.95	0	9.38	32.95	25.46
27	6.12	33.33	25	6.20	33.30	26.20
53	5.45	33.65	50	5.50	33.64	26.56
80	2.12	33.70	75	2.40	33.68	26.90
106	3.77	34.10	100	3.45	34.01	27.08
159	4.16	34.41	150	4.10	34.38	27.30
212	3.64	34.44	200	3.70	34.43	27.38
318	4.90	34.83	300	4.70	34.78	27.55
353	4.52	34.81	400	4.50	34.83	27.61
533	4.49	34.92	600	4.45	34.94	27.71
719	4.41	34.95	800	4.10	34.94	27.75
908	3.81	34.91	1,000	3.75	34.91	27.76
1,395	3.67	34.92				

Station 4476; May 25; latitude 42°40.5′ N., longitude 49°09′ W.; depth 2,268 meters, dynamic height 971.016

Observed values			Scaled values			
Depth, meters	Temperature °C.	Salinity ‰	Depth, meters	Temperature °C.	Salinity ‰	σ_t
0	10.41	33.38	0	10.41	33.38	25.64
22	8.02	33.33	25	7.75	33.34	26.02
44	6.51	33.70	50	5.75	33.74	26.61
66	3.65	33.82	75	3.15	33.88	26.99
88	2.88	33.97	100	3.00	34.06	27.16
131	3.50	34.37	150	4.50	34.58	27.42
174	5.64	34.82	200	5.55	34.87	27.53
262	5.32	34.92	300	5.20	34.93	27.61
396	4.91	34.93	400	4.90	34.93	27.65
594	4.41	34.95	600	4.40	34.95	27.72
792	3.94	34.89	800	3.90	34.89	27.73
991	3.77	34.89	1,000	3.75	34.89	27.74
1,489	3.58	34.87				

Station 4477; May 25; latitude 43°19′ N., longitude 48°47′ W.; depth 1,737 meters, dynamic height 971.106

Observed values			Scaled values			
Depth, meters	Temperature °C.	Salinity ‰	Depth, meters	Temperature °C.	Salinity ‰	σ_t
0	13.38	34.08	0	13.38	34.08	25.62
24	14.12	35.08	25	14.15	35.10	26.25
49	13.36	35.27	50	13.35	35.27	26.55
73	12.22	35.23	75	12.15	35.22	26.75
97	10.18	34.91	100	10.15	34.92	26.88
145	10.00	35.09	150	9.90	35.09	27.06
194	9.04	35.04	200	8.85	35.03	27.18
291	5.59	34.70	300	5.40	34.70	27.41
383	4.44	34.73	400	4.35	34.74	27.56
577	3.84	34.83	600	3.80	34.84	27.70
773	3.81	34.86	800	3.80	34.86	27.72
968	3.73	34.87	1,000	3.70	34.87	27.74
1,456	3.53	34.87				

STATIONS OCCUPIED IN 1951—Continued

Station 4478; May 25; latitude 43°10.5′ N., longitude 48°11′ W.; depth 3,164 meters, dynamic height 971.169

Observed values			Scaled values			
Depth, meters	Temperature °C.	Salinity ‰	Depth, meters	Temperature °C.	Salinity ‰	σ_t
0	15.04	35.50	0	15.04	35.50	26.36
25	15.28	35.78	25	15.28	35.78	26.52
51	15.53	35.86	50	15.55	35.86	26.53
76	15.25	35.84	75	15.25	35.84	26.58
101	14.41	35.75	100	14.45	35.75	26.69
151	12.81	35.47	150	12.80	35.48	26.82
202	11.59	35.45	200	11.60	35.45	27.03
303	7.74	34.90	300	7.80	34.91	27.25
347	7.26	34.96	400	6.65	34.96	27.46
531	5.36	34.96	600	4.85	34.94	27 66
723	4.32	34.91	800	4.10	34.91	27.73
913	3.92	34.90	1,000	3.80	34.90	27.75
1,404	3.46	34.88				

Station 4479; May 25; latitude 42°51.5′ N., longitude 47°28′ W.; depth 3,823 meters, dynamic height 971.106.

Observed values			Scaled values			
Depth, meters	Temperature °C.	Salinity ‰	Depth, meters	Temperature °C.	Salinity ‰	σ_t
0	13.30	34.64	0	13.30	34.64	26.07
25	12.34	34.51	25	12.34	34.51	26.16
50	11.42	34.71	50	11.42	34.71	26.49
74	10.74	34.73	75	10.70	34.73	26.63
99	9.61	34.59	100	9.50	34.59	26.73
148	6.86	34.50	150	6.80	34.50	27.07
198	6.43	34.66	200	6.40	34.66	27.25
297	6.01	34.82	300	5.90	34.82	27.45
344	4.57	34.72	400	4.70	34.78	27.55
518	4.82	34.92	600	4.50	34.92	27.69
693	4.21	34.92	800	3.95	34.90	27.73
880	3.84	34.89	1,000	3.70	34.89	27.75
1,367	3.55	34.89				

Station 4480; May 25–26; latitude 42°32′ N., longitude 46° 44′ W.; depth 4,207 meters, dynamic height 971.212

Observed values			Scaled values			
Depth, meters	Temperature °C.	Salinity ‰	Depth, meters	Temperature °C.	Salinity ‰	σ_t
0	16.01	35.40	0	16.01	35.40	26.07
26	16.05	35.90	25	16.05	35.89	26.43
51	15.89	35.94	50	15.90	35.94	26.50
77	15.55	35.97	75	15.55	35.97	26.61
103	14.49	35.76	100	14.65	35.80	26.68
153	13.17	35.56	150	13.25	35.58	26.81
205	11.05	35.22	200	11.20	35.25	26.95
308	8.18	34.90	300	8.40	34.94	27.18
387	4.11	34.44	400	4.15	34.47	27.37
579	5.47	34.96	600	5.35	34.96	27.62
771	4.61	34.95	800	4.50	34.95	27.71
967	4 09	34.92	1,000	4.00	34.92	27.75
1,461	3.64	34.90				

Station 4481; May 26; latitude 42°57′ N., longitude 46°23′ W.; depth 4,463 meters, dynamic height 971.246

Observed values			Scaled values			
Depth, meters	Temperature °C.	Salinity ‰	Depth, meters	Temperature °C.	Salinity ‰	σ_t
0	14.90	34.84	0	14.90	34.84	25.89
25	15.43	35.74	25	15.43	35.74	26.46
52	15.92	36.01	50	15.90	36.01	26.56
77	15.90	36.04	75	15.90	36.04	26.58
103	15.70	36.01	100	15.70	36.02	26.62
154	13.34	35.55	150	13.60	35.60	26.75
205	11.68	35.34	200	11.85	35.36	26.92
308	9.00	35.00	300	9.15	35.01	27.12
401	7.73	35.00	400	7.75	35.00	27.33
600	4.87	34.86	600	4.85	34.86	27.60
799	4.74	34.98	800	4.75	34.98	27.70
998	4.27	34.915	1,000	4.25	34.91	27.71
1,494	3.71	34.895				

Station 4482; May 26; latitude 43°20′ N., longitude 46°00′ W.; depth 4,663 meters, dynamic height 971.251

Observed values			Scaled values			
Depth, meters	Temperature °C.	Salinity ‰	Depth, meters	Temperature °C.	Salinity ‰	σ_t
0	15.72	35.35	0	15.72	35.35	26.10
25	15.55	35.79	25	15.55	35.79	26.47
50	15.74	35.98	50	15.74	35.98	26.58
75	16.08	36.12	75	16.08	36.12	26.61
101	15.23	35.90	100	15.25	35.91	26.63
150	13.25	35.54	150	13.25	35.54	26.78
201	12.47	35.42	200	12.50	35.42	26.84
302	9.92	35.16	300	9.95	35.16	27.11
399	7.60	34.94	400	7.60	34.94	27.30
600	4.68	34.81	600	4.65	34.81	27.59
801	4.51	34.93	800	4.50	34.93	27.69
1,002	4.34	34.96	1,000	4.30	34.96	27.74

Station 4483; May 26; latitude 43°31.5′ N., longitude 46° 42′ W.; depth, 4,298 meters, dynamic height 971.275

Observed values			Scaled values			
Depth, meters	Temperature °C.	Salinity ‰	Depth, meters	Temperature °C.	Salinity ‰	σ_t
0	16.94	35.93	0	16.94	35.93	26.26
26	16.60	36.12	25	16.65	36.12	26.47
51	16.05	36.06	50	16.05	36.06	26.57
77	16.03	36.10	75	16.05	36.10	26.60
103	15.62	36.01	100	15.70	36.02	26.62
153	14.60	35.81	150	14.65	35.82	26.70
205	13.07	35.51	200	13.25	35.54	26.78
308	9.06	34.90	300	9.35	34.94	27.03
374	8.90	35.09	400	8.50	35.07	27.27
563	6.03	34.97	600	5.65	34.96	27.59
755	4.76	34.94	800	4.60	34.94	27.69
949	4.27	34.93	1,000	4.15	34.93	27.73
1,444	3.65	34.90				

Station 4484; May 26; latitude 43°43.5′ N., longitude 47° 18′ W.; depth 3,969 meters, dynamic height 971.166

Observed values			Scaled values			
Depth, meters	Temperature °C.	Salinity ‰	Depth, meters	Temperature °C.	Salinity ‰	σ_t
0	13.99	34.64	0	13.99	34.64	25.93
26	13.42	35.07	25	13.40	35.07	26.39
52	13.86	35.32	50	13.85	35.30	26.47
78	12.35	35.05	75	12.55	35.07	26.56
103	11.64	35.04	100	11.70	35.04	26.70
154	9.95	34.98	150	10.10	34.99	26.94
206	6.14	34.41	200	6.30	34.47	27.12
309	8.00	35.05	300	7.90	35.01	27.32
342	7.23	34.98	400	6.55	34.97	27.48
521	5.65	34.97	600	5.15	34.96	27.65
705	4.66	34.94	800	4.40	34.93	27.70
896	4.26	34.93	1,000	4.10	34.93	27.74
1,310	3.81	34.92				

Station 4485; May 26; latitude 43°54′ N., longitude 47°55′ W.; depth 3,658 meters, dynamic height 971.142

Observed values			Scaled values			
Depth, meters	Temperature °C.	Salinity ‰	Depth, meters	Temperature °C.	Salinity ‰	σ_t
0	5.40	32.56	0	5.40	32.56	25.72
26	1.61	32.55	25	1.70	32.55	26.06
52	−0.64	33.01	50	−0.60	32.97	26.51
78	−0.73	33.08	75	−0.70	33.07	26.60
104	−0.54	33.24	100	−0.60	33.20	26.70
154	4.42	33.98	150	4.10	33.92	26.94
206	7.70	34.66	200	7.70	34.65	27.06
309	1.65	34.22	300	1.95	34.25	27.40
349	1.77	34.26	400	2.60	34.43	27.48
521	4.60	34.86	600	4.50	34.90	27.67
692	4.41	34.92	800	4.20	34.94	27.74
880	4.13	34.94	1,000	3.90	34.92	27.76
1,290	3.40	34.865				

STATIONS OCCUPIED IN 1951—Continued

Station 4486; May 27; latitude 44°5.5′ N., longtitude 48°27′ W.; depth 3,200 meters, dynamic height 971.019

Observed values			Scaled values			
Depth, meters	Temperature °C.	Salinity ‰	Depth, meters	Temperature °C.	Salinity ‰	σ_t
0	4.68	32.50	0	4.68	32.50	25.75
24	4.86	33.00	25	4.85	33.03	26.15
48	4.57	33.53	50	4.55	33.57	26.62
72	3.89	33.86	75	3.75	33.89	26.94
96	2.93	34.03	100	2.85	34.06	27.17
145	2.69	34.34	150	2.70	34.36	27.42
192	3.24	34.53	200	3.35	34.56	27.52
288	4.33	34.80	300	4.30	34.80	27.62
394	3.90	34.79	400	3.90	34.79	27.65
587	4.09	34.87	600	4.10	34.87	27.70
779	4.09	34.89	800	4.05	34.89	27.71
985		34.86	1,000	3.90	34.86	27.71
1,430	3.52	34.87				

Station 4487; May 27; latitude 44°13′ N., longitude 48°47′ W.; depth 1,646 meters, dynamic height 971.053

Observed values			Scaled values			
Depth, meters	Temperature °C.	Salinity ‰	Depth, meters	Temperature °C.	Salinity ‰	σ_t
0	4.81	32.57	0	4.81	32.57	25.80
25	3.64	32.50	25	3.64	32.50	25.85
51	1.04	32.88	50	1.05	32.87	26.36
75	−0.24	33.30	75	−0.24	33.30	26.76
101	0.18	33.61	100	0.15	33.61	27.00
151	1.67	34.14	150	1.65	34.14	27.33
202	2.04	34.34	200	2.05	34.34	27.46
303	2.55	34.51	300	2.55	34.50	27.55
414	3.57	34.73	400	3.45	34.71	27.63
619	3.88	34.85	600	3.85	34.84	27.69
823	3.85	34.88	800	3.85	34.88	27.72
1,031		34.85	1,000	3.70	34.85	27.72
1,465	3.46	34.83				

Station 4488; May 27; latitude 44°13′ N., longitude 48°56′ W.; depth 585 meters, dynamic height 971.031

Observed values			Scaled values			
Depth, meters	Temperature °C.	Salinity ‰	Depth, meters	Temperature °C.	Salinity ‰	σ_t
0	5.52	32.52	0	5.52	32.52	25.67
25	2.74	32.60	25	2.74	32.60	26.02
50	−0.69	32.97	50	−0.69	32.97	26.52
75	−0.71	33.18	75	−0.71	33.18	26.69
100	−0.43	33.36	100	−0.43	33.36	26.82
150	0.40	33.74	150	0.40	33.74	27.09
201	0.97	34.00	200	0.95	34.00	27.26
301	2.59	34.49	300	2.60	34.49	27.53
152	0.38	33.76	400	3.35	34.71	27.64
550	3.65	34.80				

Station 4489; May 27; latitude 44°12.5′ N., longitude 49°04′ W.; depth 139 meters, dynamic height 971.099

Observed values			Scaled values			
Depth, meters	Temperature °C.	Salinity ‰	Depth, meters	Temperature °C.	Salinity ‰	σ_t
0	6.28	32.60	0	6.28	32.60	25.65
24	1.63	32.70	25	1.55	32.71	26.19
48	0.36	32.85	50	0.25	32.86	26.39
72	−0.73	33.01	75	−0.75	33.04	26.58
96	−0.51	33.24	100	−0.45	33.26	26.74
133	−0.08	33.44				

Station 4490; May 27; latitude 44°13′ N., longitude 49°11′ W.; depth 55 meters, dynamic height 971.102

Observed values			Scaled values			
Depth, meters	Temperature °C.	Salinity ‰	Depth, meters	Temperature °C.	Salinity ‰	σ_t
0	5.68	32.62	0	5.68	32.62	25.74
24	2.28	32.80	25	2.25	32.80	26.22
46	2.05	32.80	(50)	2.05	32.80	26.24

Station 4491; May 27; latitude 44°13′ N., longitude 49°23′ W.; depth 52 meters, dynamic height 971.114

Observed values			Scaled values			
Depth, meters	Temperature °C.	Salinity ‰	Depth, meters	Temperature °C.	Salinity ‰	σ_t
0	7.85	32.48	0	7.85	32.48	25.34
22	4.27	32.74	25	4.15	32.75	26.00
40	3.52	32.76	(50)	3.35	32.77	26.10

Station 4492; May 27; latitude 44°59′ N., longitude 49°24′ W.; depth 66 meters, dynamic height 971.105

Observed values			Scaled values			
Depth, meters	Temperature °C.	Salinity ‰	Depth, meters	Temperature °C.	Salinity ‰	σ_t
0	5.91	32.47	0	5.91	32.47	25.59
26	3.88	32.59	25	3.90	32.59	25.91
52	1.26	32.68	50	1.40	32.67	26.17

Station 4493; May 27; latitude 44°55.5′ N., longitude 49°10′ W.; depth 119 meters, dynamic height 971.096

Observed values			Scaled values			
Depth, meters	Temperature °C.	Salinity ‰	Depth, meters	Temperature °C.	Salinity ‰	σ_t
0	5.45	32.52	0	5.45	32.52	25.68
25	2.49	32.64	25	2.49	32.64	26.07
50	0.53	32.76	50	0.53	32.76	26.30
76	−0.13	32.83	75	−0.10	32.83	26.38
101	−0.33	33.05	100	−0.30	33.04	26.56

Station 4494; May 27; latitude 44°52.5′ N., longitude 48°56′ W.; depth 631 meters, dynamic height 971.075

Observed values			Scaled values			
Depth, meters	Temperature °C.	Salinity ‰	Depth, meters	Temperature °C.	Salinity ‰	σ_t
0	4.86	32.56	0	4.86	32.56	25.78
25	2.29	32.57	25	2.29	32.57	26.03
49	0.12	32.85	50	0.05	32.86	26.40
74	−1.29	33.04	75	−1.30	33.05	26.60
99	−0.52	33.30	100	−0.50	33.31	26.78
148	0.21	33.66	150	0.25	33.67	27.05
197	0.96	34.02	200	1.00	34.04	27.29
296	1.67	34.31	300	1.70	34.32	27.47
372	2.75	34.57	400	2.95	34.62	27.61
564	3.49	34.76				

Station 4495; May 28; latitude 44°49.5′ N., longitude 48°44′ W.; depth 1,527 meters, dynamic height 971.000

Observed values			Scaled values			
Depth, meters	Temperature °C.	Salinity ‰	Depth, meters	Temperature °C.	Salinity ‰	σ_t
0	4.86	32.33	0	4.86	32.33	25.60
25	3.24	32.76	25	3.24	32.76	26.10
50	1.58	33.00	50	1.58	33.00	26.43
75	0.27	33.61	75	0.27	33.61	27.00
100	2.77	34.03	100	2.77	34.03	27.15
151	3.42	34.46	150	3.40	34.46	27.44
200	3.94	34.62	200	3.95	34.62	27.51
300	4.61	34.84	300	4.60	34.84	27.61
391	4.27	34.87	400	4.20	34.87	27.69
585	3.80	34.865	600	3.75	34.87	27.73
777	3.59	34.88	800	3.55	34.88	27.75
976	3.48	34.86	1,000	3.45	34.86	27.75
1,181	3.45	34.86				

Station 4496; May 28; latitude 44°46.5′ N., longitude 48°31′ W.; depth 2,030 meters, dynamic height 970.972

Observed values			Scaled values			
Depth, meters	Temperature °C.	Salinity ‰	Depth, meters	Temperature °C.	Salinity ‰	σ_t
0	7.23	33.10	0	7.23	33.10	25.91
25	5.60	33.38	25	5.60	33.38	26.34
50	5.86	33.91	50	5.86	33.91	26.74
75	3.83	34.14	75	3.83	34.14	27.14
100	4.01	34.34	100	4.01	34.34	27.28
151	2.82	34.42	150	2.80	34.42	27.46
201	3.39	34.58	200	3.40	34.58	27.53
301	3.90	34.80	300	3.90	34.80	27.66
402	3.86	34.82	400	3.85	34.82	27.68
599	3.83	34.88	600	3.80	34.88	27.73
795	3.68	34.88	800	3.65	34.88	27.74
995	3.44	34.85	1,000	3.45	34.85	27.74
1,497	3.46	34.85				

STATIONS OCCUPIED IN 1951—Continued

Station 4497; May 28; latitude 44°38′ N., longitude 47°53′ W.; depth 3,347 meters, dynamic height 971.004

Observed values			Scaled values			
Depth, meters	Temperature °C.	Salinity ‰	Depth, meters	Temperature °C.	Salinity ‰	σ_t
0	6.26	32.50	0	6.26	32.50	25.57
25	3.93	32.92	25	3.93	32.92	26.16
50	5.31	33.61	50	5.31	33.61	26.56
75	2.99	33.57	75	2.99	33.57	26.77
100	0.69	33.90	100	0.69	33.90	27.20
150	1.73	34.16	150	1.73	34.16	27.34
199	2.64	34.44	200	2.65	34.45	27.50
299	4.30	34.82	300	4.30	34.82	27.63
404	4.39	34.90	400	4.40	34.90	27.68
602	4.04	34.91	600	4.05	34.91	27.73
799	3.78	34.90	800	3.75	34.90	27.75
999	3.61	34.90	1,000	3.60	34.90	27.77
1,500	3.45	34.90				

Station 4498; May 28; latitude 44°35.5′ N., longitude 47°10′ W.; depth 3,749 meters, dynamic height 971.187

Observed values			Scaled values			
Depth, meters	Temperature °C.	Salinity ‰	Depth, meters	Temperature °C.	Salinity ‰	σ_t
0	14.71	35.45	0	14.71	35.45	26.40
25	14.34	35.62	25	14.34	35.62	26.61
51	14.06	35.66	50	14.05	35.66	26.70
76	14.31	35.74	75	14.30	35.74	26.71
101	14.78	35.89	100	14.80	35.89	26.71
151	14.38	35.79	150	14.40	35.80	26.74
202	11.58	35.35	200	11.75	35.38	26.95
303	9.41	35.16	300	9.50	35.18	27.19
398	6.48	34.84	400	6.45	34.84	27.39
599	4.98	34.95	600	4.95	34.95	27.66
801	4.26	34.93	800	4.25	34.93	27.72
1,005	3.90	34.92	1,000	3.90	34.92	27.76
1,476	3.54	34.89				

Station 4499; May 28; latitude 44°32.5′ N., longitude 46°32′ W.; depth 4,024 meters, dynamic height 971.327

Observed values			Scaled values			
Depth, meters	Temperature °C.	Salinity ‰	Depth, meters	Temperature °C.	Salinity ‰	σ_t
0	15.79	35.96	0	15.79	35.96	26.55
24	15.34	36.05	25	15.35	36.05	26.72
48	15.27	36.04	50	15.25	36.04	26.73
72	15.28	36.05	75	15.30	36.05	26.73
96	15.29	36.05	100	15.30	36.05	26.73
145	15.29	36.05	150	15.30	36.05	26.73
193	15.27	36.05	200	15.25	36.04	26.73
289	13.58	35.72	300	13.30	35.68	26.87
370	11.44	35.40	400	10.60	35.30	27.10
563	6.90	34.98	600	6.40	34.97	27.50
764	5.17	34.96	800	4.95	34.96	27.67
970	4.39	34.94	1,000	4.30	34.93	27.71
1,363	3.60	34.88				

Station 4500; May 29; latitude 44°22′ N., longitude 45°54′ W.; depth 3,841 meters, dynamic height 971.284

Observed values			Scaled values			
Depth, meters	Temperature °C.	Salinity ‰	Depth, meters	Temperature °C.	Salinity ‰	σ_t
0	6.61	32.66	0	6.61	32.66	25.65
26	14.32	35.72	25	14.25	35.60	26.61
51	14.75	35.86	50	14.70	35.86	26.72
76	14.76	35.88	75	14.75	35.88	26.72
101	14.75	35.89	100	14.75	35.89	26.72
153	14.78	35.90	150	14.75	35.90	26.73
204	14.70	35.89	200	14.75	35.90	26.73
305	11.24	35.33	300	11.45	35.37	27.00
442	7.45	34.94	400	8.35	35.00	27.24
642	5.22	34.92	600	5.50	34.92	27.57
826	4.52	34.93	800	4.60	34.93	27.68
1,041	3.99	34.91	1,000	4.05	34.91	27.73
1,373	3.65	34.90				

Station 4501; May 29; latitude 44°17.5′ N., longitude 45°13′ W.; depth 4,207 meters, dynamic height 971.271

Observed values			Scaled values			
Depth, meters	Temperature °C.	Salinity ‰	Depth, meters	Temperature °C.	Salinity ‰	σ_t
0	16.97	36.00	0	16.97	36.00	26.31
26	16.17	35.96	25	16.15	35.96	26.47
52	16.32	36.15	50	16.30	36.14	26.56
78	16.35	36.17	75	16.35	36.17	26.58
103	16.19	36.14	100	16.25	36.14	26.58
156	14.44	35.79	150	14.65	35.83	26.70
208	12.67	35.42	200	12.95	35.47	26.79
311	9.13	34.96	300	9.45	35.00	27.06
426	6.67	34.79	400	7.10	34.81	27.28
633	5.09	34.92	600	5.30	34.91	27.54
838	4.41	34.91	800	4.50	34.91	27.68
1,088	4.08	34.91	1,000	4.20	34.91	27.72
1,500	3.57	34.86				

Station 4502; May 29; latitude 44°43′ N., longitude 45°06′ W.; depth 4,353 meters, dynamic height 971.078

Observed values			Scaled values			
Depth, meters	Temperature °C.	Salinity ‰	Depth, meters	Temperature °C.	Salinity ‰	σ_t
0	7.36	32.62	0	7.36	32.62	25.52
25	3.45	33.21	25	3.45	33.21	26.44
50	9.63	34.60	50	9.63	34.60	26.73
74	11.43	35.16	75	11.45	35 16	26.84
99	7.65	34.54	100	7.60	34.54	26.99
148	7.13	34.56	150	7.10	34.57	27.09
198	8.27	34.98	200	8.25	34.98	27.24
297	5.87	34.79	300	5.80	34.79	27.43
375	5.00	34.84	400	4.95	34.86	27.59
561	4.78	34.96	600	4.70	34.96	27.70
746	4.33	34.95	800	4.20	34.95	27.75
941	3.99	34.93	1,000	3.90	34.92	27.76
1,395	3.49	34.89				

Station 4503; May 29; latitude 45°19.5′ N., longitude 45°14′ W.; depth 4,207 meters, dynamic height 971.042

Observed values			Scaled values			
Depth, meters	Temperature °C.	Salinity ‰	Depth, meters	Temperature °C.	Salinity ‰	σ_t
0	9.31	33.42	0	9.31	33.42	25.86
25	4.26	32.88	25	4.26	32.88	26.10
48	5.03	33.40	50	5.00	33.43	26.45
73	2.70	33.60	75	2.70	33.61	26.83
97	2.99	33.87	100	3.00	33.90	27.03
146	3.23	34.22	150	3.30	34.26	27.29
194	6.33	34.84	200	6.30	34.84	27.41
291	5.21	34.84	300	5.10	34.84	27.56
356	4.51	34.82	400	4.45	34.84	27.63
543	4.38	34.92	600	4.25	34.91	27.71
736	3.97	34.90	800	3.85	34.90	27.74
934	3.72	34.90	1,000	3.65	34.90	27.76
1,307	3.53	34.89				

Station 4504; May 29; latitude 45°22.5′ N., longitude 46°00′ W.; depth 3,475 meters, dynamic height 971.028

Observed values			Scaled values			
Depth, meters	Temperature °C.	Salinity ‰	Depth, meters	Temperature °C.	Salinity ‰	σ_t
0	7.80	33.29	0	7.80	33.29	25.97
27	7.66	33.80	25	7.70	33.75	26.36
54	6.93	33.88	50	7.25	33.87	26.51
81	4.68	33.86	75	5.35	33.87	26.77
108	3.05	33.75	100	3.25	33.78	26.91
163	3.61	34.36	150	3.35	34.20	27.23
216	4.22	34.60	200	4.05	34.56	27.45
324	4.30	34.80	300	4.30	34.77	27.60
420	4.30	34.84	400	4.30	34.83	27.64
630	3.91	34.88	600	3.95	34.88	27.71
842	3.61	34.88	800	3.60	34.88	27.75
1,059	3.46	34.86	1,000	3.45	34.86	27.75
1,457	3.41	34.88				

STATIONS OCCUPIED IN 1951—Continued

Station 4505; May 29; latitude 45°18′ N., longitude 46°48′ W.; depth 3,109 meters, dynamic height 970.986

Observed values			Scaled values			
Depth, meters	Temperature °C.	Salinity ‰	Depth, meters	Temperature °C.	Salinity ‰	σ_t
0	7.38	33.43	0	7.38	33.43	26.15
26	5.41	33.50	25	5.45	33.50	26.46
52	5.29	33.88	50	5.30	33.84	26.74
78	5.01	34.19	75	5.05	34.16	27.03
104	4.19	34.22	100	4.20	34.21	27.16
157	4.43	34.63	150	4.40	34.57	27.43
209	4.65	34.75	200	4.60	34.74	27.53
313	4.03	34.80	300	4.10	34.80	27.64
400	3.74	34.78	400	3.74	34.78	27.65
600	3.76	34.84	600	3.76	34.84	27.70
802	3.54	34.85	800	3.50	34.85	27.74
1,008	3.62	34.88	1,000	3.60	34.88	27.75
1,441	3.35	34.84				

Station 4506; May 30; latitude 45°22′ N., longitude 47°32′ W.; depth 2,725 meters, dynamic height 971.021

Observed values			Scaled values			
Depth, meters	Temperature °C.	Salinity ‰	Depth, meters	Temperature °C.	Salinity ‰	σ_t
0	7.61	33.30	0	7.61	33.30	26.01
26	6.60	33.33	25	6.60	33.32	26.17
51	6.55	33.88	50	6.55	33.88	26.62
77	3.18	33.83	75	3.20	33.83	26.95
103	5.30	34.39	100	5.15	34.32	27.14
153	5.45	34.63	150	5.45	34.62	27.34
205	4.96	34.70	200	5.00	34.69	27.45
308	4.71	34.85	300	4.75	34.85	27.60
395	4.29	34.85	400	4.25	34.85	27.66
586	4.11	34.88	600	4.10	34.88	27.70
772	3.89	34.87	800	3.85	34.87	27.72
969	3.69	34.87	1,000	3.60	34.87	27.75
1,423	3.59	34.88				

Station 4507; May 30; latitude 45°33′ N., longitude 48°06′ W.; depth 1,280 meters, dynamic height 970.990

Observed values			Scaled values			
Depth, meters	Temperature °C.	Salinity ‰	Depth, meters	Temperature °C.	Salinity ‰	σ_t
0	4.55	32.82	0	4.55	32.82	26.02
25	2.62	32.88	25	2.62	32.88	26.25
50	0.24	33.29	50	0.24	33.29	26.73
76	0.15	33.68	75	0.15	33.67	27.05
101	0.74	33.89	100	0.70	33.88	27.18
150	1.43	34.18	150	1.45	34.18	27.37
200	1.63	34.29	200	1.60	34.29	27.45
301	2.49	34.54	300	2.50	34.54	27.58
326	2.80	34.60	400	3.40	34.74	27.66
497	3.74	34.83	600	3.70	34.87	27.74
672	3.72	34.88	800	3.60	34.88	27.75
856	3.55	34.87	1,000	3.45	34.86	27.75
1,045	3.48	34.86				

Station 4508; May 30; latitude 45°37′ N., longitude 48°14′ W.; depth 348 meters, dynamic height 971.034

Observed values			Scaled values			
Depth, meters	Temperature °C.	Salinity ‰	Depth, meters	Temperature °C.	Salinity ‰	σ_t
0	3.54	32.48	0	3.54	32.48	25.85
24	2.56	32.54	25	2.50	32.54	25.99
47	−0.42	32.98	50	−0.40	33.05	26.58
71	−0.31	33.48	75	−0.20	33.53	26.95
94	0.18	33.71	100	0.25	33.74	27.10
141	0.69	33.92	150	0.75	33.94	27.23
189	0.84	34.00	200	0.90	34.02	27.29
283	1.69	34.29	(300)	1.90	34.36	27.49

Station 4509; May 30; latitude 45°40′ N., longitude 48°18′ W.; depth 156 meters, dynamic height 971.044

Observed values			Scaled values			
Depth, meters	Temperature °C.	Salinity ‰	Depth, meters	Temperature °C.	Salinity ‰	σ_t
0	3.67	32.48	0	3.67	32.48	25.84
25	0.37	32.78	25	0.37	32.78	32.78
50	−0.83	33.25	50	−0.83	33.25	33.25
75	−0.28	33.49	75	−0.28	33.49	33.49
99	−0.13	33.53	100	−0.10	33.53	33.53
144	−0.05	33.55	150	−0.05	33.55	33.55

Station 4510; May 30; latitude 45°43′ N., longitude 48°21′ W.; depth 104 meters, dynamic height 971.069

Observed values			Scaled values			
Depth, meters	Temperature °C.	Salinity ‰	Depth, meters	Temperature °C.	Salinity ‰	σ_t
0	3.86	32.46	0	3.86	32.46	25.80
24	2.03	32.65	25	1.90	32.66	26.13
49	−0.34	32.94	50	−0.40	32.95	26.50
73	−0.86	33.12	75	−0.85	33.13	26.65
93	−0.85	33.20	(100)	−0.80	33.22	26.72

Station 4511; May 30; latitude 45°49.5′ N., longitude 48°31′ W.; depth 89 meters, dynamic height 971.084

Observed values			Scaled values			
Depth, meters	Temperature °C.	Salinity ‰	Depth, meters	Temperature °C.	Salinity ‰	σ_t
0	4.86	32.58	0	4.86	32.58	25.80
25	3.31	32.62	25	3.31	32.62	25.98
51	0.28	32.72	50	0.40	32.71	26.26
76	−0.47	33.03	75	−0.45	33.02	26.55

Station 4512; May 30; latitude 46°04.5′ N., longitude 48°45′ W.; depth 68 meters, dynamic height 971.097

Observed values			Scaled values			
Depth, meters	Temperature °C.	Salinity ‰	Depth, meters	Temperature °C.	Salinity ‰	σ_t
0	5.67	32.61	0	5.67	32.61	25.74
25	4.61	32.62	25	4.61	32.62	25.85
49	2.36	32.64	50	2.30	32.64	26.09

Station 4513; May 30; latitude 46°19′ N., longitude 48°55′ W.; depth 68 meters, dynamic height 971.103

Observed values			Scaled values			
Depth, meters	Temperature °C.	Salinity ‰	Depth, meters	Temperature °C.	Salinity ‰	σ_t
0	5.83	32.63	0	5.83	32.63	25.73
27	4.27	32.64	25	4.45	32.64	25.89
55	2.68	32.64	50	3.00	32.64	26.03

Station 4514; May 30; latitude 46°21.5′ N., longitude 48° 34′ W.; depth 89 meters, dynamic height 971.107

Observed values			Scaled values			
Depth, meters	Temperature °C.	Salinity ‰	Depth, meters	Temperature °C.	Salinity ‰	σ_t
0	5.99	32.63	0	5.99	32.63	25.71
25	3.86	32.62	25	3.86	32.62	25.93
51	2.19	32.67	50	2.25	32.66	26.10
76	−0.27	32.97	75	−0.20	32.96	26.49

Station 4515; May 30; latitude 46°17.5′ N., longitude 48°05′ W.; depth 115 meters, dynamic height 971.101

Observed values			Scaled values			
Depth, meters	Temperature °C.	Salinity ‰	Depth, meters	Temperature °C.	Salinity ‰	σ_t
0	4.77	32.46	0	4.77	32.46	25.71
25	2.96	32.50	25	2.96	32.50	25.91
50	0.34	32.72	50	0.34	32.72	26.27
76	−0.91	33.08	75	−0.90	33.07	26.52
101	−0.77	33.18	100	−0.80	33.18	26.62

Station 4516; May 30; latitude 46°15.5′ N., longitude 47°47′ W.; depth 169 meters, dynamic height 971.090

Observed values			Scaled values			
Depth, meters	Temperature °C.	Salinity ‰	Depth, meters	Temperature °C.	Salinity ‰	σ_t
0	3.65	32.42	0	3.65	32.42	25.79
25	2.86	32.46	25	2.86	32.46	25.90
50	−0.03	32.81	50	−0.03	32.81	26.37
75	−1.19	32.99	75	−1.19	32.99	26.55
101	−0.71	33.28	100	−0.70	33.28	26.77
151	0.01	33.53	150	0.00	33.52	26.94

STATIONS OCCUPIED IN 1951—Continued

Station 4517; May 30; latitude 46°11′ N., longitude 47°18′ W.; depth 622 meters, dynamic height 970.989

Observed values			Scaled values			
Depth, meters	Temperature °C.	Salinity ‰	Depth, meters	Temperature °C.	Salinity ‰	σ_t
0	3.83	32.77	0	3.83	32.77	26.05
25	2.61	32.87	25	2.61	32.87	26.24
50	0 16	33.35	50	0.16	35.35	26.78
75	0.07	33.63	75	0.07	33.63	27.01
100	0.60	33.83	100	0.60	33.83	27.14
150	1.04	34.06	150	1.04	34.06	27.31
200	1.71	34.45	200	1.71	34.45	27.57
300	2.85	34.59	300	2.85	34.59	27.59
396	3.55	34.76	400	3.55	34.76	27.66
593	3.66	34.84	600	3.65	34.84	27.71

Station 4518; May 31; latitude 46°10′ N., longitude 47°00′ W.; depth 1,307 meters, dynamic height 970.942

Observed values			Scaled values			
Depth, meters	Temperature °C.	Salinity ‰	Depth, meters	Temperature °C.	Salinity ‰	σ_t
0	3.88	32.90	0	3.88	32.90	26.15
25	1.65	32.98	25	1.65	32.98	26.40
50	1.25	33.58	50	1.21	33.58	26.90
76	1.82	34.06	75	1.85	34.05	27.24
101	1.64	34.21	100	1.65	34.21	27.39
151	2.22	34.45	150	2.20	34.45	27.54
202	2.45	34.52	200	2.40	34.52	27.58
303	2.99	34.68	300	2.95	34.67	27.65
301	2.97	34.66	400	3.40	34.77	27.69
500	3.60	34.83	600	3.65	34.86	27.73
699	3.66	34.87	800	3.55	34.87	27.75
899	3.47	34.87	1,000	3.40	34.87	27.77
1,192	3.34	34.87				

Station 4519; May 31; latitude 46°08′ N., longitude 46°24′ W.; depth 512 meters, dynamic height 970.964

Observed values			Scaled values			
Depth, meters	Temperature °C.	Salinity ‰	Depth, meters	Temperature °C.	Salinity ‰	σ_t
0	4.48	32.76	0	4.48	32.76	25.97
25	4.31	32.76	25	4.31	32.76	26.00
50	1.59	33.43	50	1.59	33.43	26.76
75	0.88	34.02	75	0.88	34.02	27.29
100	1.89	34.23	100	1.89	34.23	27.38
150	3.90	34.58	150	3.90	34.58	27.48
199	4.27	34.74	200	4.25	34.74	27.57
299	4.21	34.83	300	4.20	34.83	27.65
392	4.24	34.89	400	4.20	34.89	27.70
490	3.98	34.88				

Station 4520; May 31; latitude 46°06′ N., longitude 45°44′ W.; depth 1,866 meters, dynamic height 971.005

Observed values			Scaled values			
Depth, meters	Temperature °C.	Salinity ‰	Depth, meters	Temperature °C.	Salinity ‰	σ_t
0	6.55	33.04	0	6.55	33.04	25.96
25	6.41	33.36	25	6.41	33.36	26.23
50	7.41	33.92	50	7.41	33.92	26.53
76	3.40	33.82	75	3.50	33.82	26.92
101	1.94	33.86	100	1.95	33.86	27.08
151	4.53	34.50	150	4.55	34.50	27.35
202	4.14	34.57	200	4.15	34.57	27.45
303	3.85	34.77	300	3.85	34.77	27.64
403	4.06	34.85	400	4.05	34.85	27.68
601	3.93	34.87	600	3.90	34.87	27.72
800	3.55	34.86	800	3.55	34.86	27.74
1,000	3.50	34.87	1,000	3.50	34.87	27.76
1,500	3.38	34.89				

Station 4521; May 31; latitude 46°04.5′ N., longitude 45°13′ W.; depth 3,109 meters, dynamic height 970.986

Observed values			Scaled values			
Depth, meters	Temperature °C.	Salinity ‰	Depth, meters	Temperature °C.	Salinity ‰	σ_t
0	7.74	33.08	0	7.74	33.08	25.83
25	6.22	33.63	25	6.22	33.63	26.46
51	1.97	33.63	50	2.00	33.63	26.90
76	5.12	34.25	75	4.90	34.24	27.10
101	7.42	34.79	100	7.40	34.78	27.21
152	6.63	34.82	150	6.65	34.82	27.35
203	6.26	34.90	200	6.25	34.90	27.46
304	5.32	34.96	300	5.35	34.96	27.62
393	4.96	34.96	400	4.85	34.96	27 68
586	3.68	34.85	600	3.65	34.85	27.72
780	3.65	34.87	800	3.60	34.87	27.75
977	3.44	34.86	1,000	3.40	34.86	27.76
1,473	3.34	34.88				

Station 4522; May 31; latitude 46°01′ N., longitude 44°38′ W.; depth 3,658 meters, dynamic height 970.984

Observed values			Scaled values			
Depth, meters	Temperature °C.	Salinity ‰	Depth, meters	Temperature °C.	Salinity ‰	σ_t
0	8.42	33.61	0	8.42	33.61	26.15
25	7.99	33.87	25	7.99	33.87	26.41
50	5.28	33.74	50	5.28	33.74	26.66
76	2.71	33.78	75	2.70	33.78	26.95
101	4.53	34.30	100	4.55	34.28	27.17
151	4.40	34.51	150	4.40	34.51	27.38
202	4.11	34.64	200	4.10	34.64	27.51
303	4.34	34.84	300	4.35	34.84	27.64
404	4.26	34.86	400	4.20	34.86	27.68
603	3.67	34.87	600	3.65	34.87	27.74
801	3.52	34.85	800	3.50	34.85	27.74
1,002	3.44	34.82	1,000	3.40	34.84	27.74
1,502	3.33	34.85				

Station 4523; May 31; latitude 46°20′ N., longitude 44°46′ W.; depth 2,286 meters, dynamic height 970.923

Observed values			Scaled values			
Depth, meters	Temperature °C.	Salinity ‰	Depth, meters	Temperature °C.	Salinity ‰	σ_t
0	7.52	33.86	0	7.52	33.86	26.47
25	5.09	33.93	25	5.09	33.93	26.84
50	4.38	34.02	50	4.38	34.02	26.99
75	3.37	34.24	75	3.37	34.24	27.26
101	3.21	34.32	100	3.25	34.32	27.34
151	3.53	34.60	150	3.50	34.60	27.54
201	3.96	34.78	200	3.95	34.78	27.63
302	3.56	34.82	300	3.55	34.82	27.71
393	3.69	34.84	400	3.65	34.84	27.71
586	3.52	34.84	600	3.50	34.84	27.73
779	3.45	34.84	800	3.45	34.84	27.73
976	3.50	34.85	1,000	3.45	34.85	27.74
1,470	3.37	34.84				

Station 4524; May 31; latitude 46°28′ N., longitude 44°52′ W.; depth 593 meters, dynamic height 970.946

Observed values			Scaled values			
Depth, meters	Temperature °C.	Salinity ‰	Depth, meters	Temperature °C.	Salinity ‰	σ_t
0	7.30	33.92	0	7.30	33.92	26.55
24	6.56	33.87	25	6.55	33.87	26.61
47	5.19	33.96	50	5.05	33.97	26.88
71	4.02	34.04	75	3.90	34.06	27.07
94	3.40	34.22	100	3.30	34.26	27.29
141	2.93	34.47	150	3.00	34.51	27.52
188	3.56	34.66	200	3.60	34.69	27.60
282	3.67	34.78	300	3.65	34.78	27.66
344	3.67	34.78	400	3.65	34.79	27.67
483	3.65	34.80				

Station 4525; June 1; latitude 46°35′ N., longitude 44°56′ W.; depth 216 meters, dynamic height 970.957

Observed values			Scaled values			
Depth, meters	Temperature °C.	Salinity ‰	Depth, meters	Temperature °C.	Salinity ‰	σ_t
0	7.89	33.89	0	7.89	33.89	26.43
26	6.49	33.90	25	6.55	33.90	26.63
51	4.61	33.94	50	4.65	33.94	26.89
77	4.27	34.03	75	4.30	34.02	27.00
103	3.95	34.23	100	4.00	34.21	27.18
154	2.97	34.42	150	3.00	34.40	27.43
195	3.27	34.60	200	3.25	34.62	27.58

Station 4526; June 1; latitude 46°43.5′ N., longitude 45°00′ W.; depth 169 meters, dynamic height 970.966

Observed values			Scaled values			
Depth, meters	Temperature °C.	Salinity ‰	Depth, meters	Temperature °C.	Salinity ‰	σ_t
0	8.48	33.91	0	8.48	33.91	26.36
25	7.61	33.90	25	7.61	33.90	26.48
51	6.11	33.96	50	6.15	33.96	26.73
76	4.82	34.04	75	4.90	34.03	26.94
102	3.15	34.22	100	3.15	34.21	27.26
153	3.34	34.44	150	3.30	34.43	27.42

Station 4527; June 1; latitude 46°52′ N., longitude 45°04′ W.; depth 170 meters, dynamic height 970.985

Observed values			Scaled values			
Depth, meters	Temperature °C.	Salinity ‰	Depth, meters	Temperature °C.	Salinity ‰	σ_t
0	8.25	33.89	0	8.25	33.89	26.38
25	8.01	33.90	25	8.01	33.90	26.43
49	7.03	33.93	50	7.00	33.93	26.59
74	6.65	33.94	75	6.60	33.94	26.66
98	4.52	34.02	100	4.35	34.03	26.99
147	3.35	34.34	150	3.35	34.36	27.36

Station 4528; June 1; latitude 46°52.5′ N., longitude 45°13′ W.; depth 201 meters, dynamic height 970.984

Observed values			Scaled values			
Depth, meters	Temperature °C.	Salinity ‰	Depth, meters	Temperature °C.	Salinity ‰	σ_t
0	8.33	33.88	0	8.33	33.88	26.36
24	8.03	33.90	25	8.00	33.90	26.43
49	6.85	33.92	50	6.80	33.92	26.62
73	5.53	33.92	75	5.45	33.93	26.80
98	4.60	34.06	100	4.55	34.07	27.01
147	3.47	34.32	150	3.45	34.34	27.33
186	3.27	34.50	(200)	3.25	34.55	27.52

Station 4529; June 1; latitude 46°53′ N., longitude 45°20′ W.; depth 220 meters, dynamic height 970.967

Observed values			Scaled values			
Depth, meters	Temperature °C.	Salinity ‰	Depth, meters	Temperature °C.	Salinity ‰	σ_t
0	8.36	33.86	0	8.36	33.86	26.35
25	7.04	33.91	25	7.04	33.91	26.57
50	6.90	33.97	50	6.90	33.97	26.64
75	6.46	34.09	75	6.46	34.09	26.79
100	4.05	34.10	100	4.05	34.10	27.09
149	3.25	34.43	150	3.25	34.43	27.42
199	3.41	34.60	200	3.40	34.60	27.55

Station 4530; June 1; latitude 46°54.5′ N., longitude 45°46′ W.; depth 276 meters, dynamic height 970.974

Observed values			Scaled values			
Depth, meters	Temperature °C.	Salinity ‰	Depth, meters	Temperature °C.	Salinity ‰	σ_t
0	7.96	33.77	0	7.96	33.77	26.33
20	8.01	33.81	25	7.80	33.84	26.41
39	7.19	34.00	50	7.15	34.02	26.65
59	7.09	34.04	75	6.00	34.07	26.84
79	5.71	34.08	100	4.85	34.17	27.06
118	4.11	34.24	150	2.70	34.29	27.36
157	2.59	34.31	200	3.75	34.64	27.54
205	3.81	34.67				

Station 4531; June 1; latitude 46°56′ N., longitude 46°07′ W.; depth 320 meters, dynamic height 970.967

Observed values			Scaled values			
Depth, meters	Temperature °C.	Salinity ‰	Depth, meters	Temperature °C.	Salinity ‰	σ_t
0	7.90	33.84	0	7.90	33.84	26.39
26	7.91	33.84	25	7.90	33.84	26.39
51	7.22	33.96	50	7.25	33.95	26.56
77	5.98	34.15	75	6.15	34.14	26.87
102	3.82	34.16	100	4.00	34.16	27.14
153	3.30	34.43	150	3.30	34.41	27.41
204	3.91	34.68	200	3.90	34.66	27.55
306	3.84	34.84	300	3.85	34.84	27.69

Station 4532; June 1; latitude 46°55′ N., longitude 46°34′ W.; depth 622 meters, dynamic height 970.924

Observed values			Scaled values			
Depth, meters	Temperature °C.	Salinity ‰	Depth, meters	Temperature °C.	Salinity ‰	σ_t
0	5.51	33.18	0	5.51	33.18	26.20
25	5.92	33.68	25	5.92	33.68	26.54
48	2.80	33.92	50	2.50	33.93	27.09
73	1.89	34.11	75	1.90	34.13	27.30
97	2.10	34.29	100	2.15	34.30	27.42
146	3.01	34.51	150	3.05	34.52	27.52
194	3.43	34.66	200	3.45	34.68	27.60
291	4.05	34.86	300	4.05	34.86	27.69
294	4.13	34.86	400	3.80	34.86	27.72
482	3.67	34.86	(600)	3.55	34.86	27.74

Station 4533; June 1; latitude 46°53′ N., longitude 47°00′ W.; depth 1,170 meters, dynamic height 970.994

Observed values			Scaled values			
Depth, meters	Temperature °C.	Salinity ‰	Depth, meters	Temperature °C.	Salinity ‰	σ_t
0	3.44	32.95	0	3.44	32.95	26.23
25	2.53	34.33	25	2.53	34.33	27.41
50	2.72	34.56	50	2.72	34.56	27.58
76	2.94	34.66	75	2.95	34.66	27.64
101	3.04	34.70	100	3.05	34.70	27.66
151	3.19	34.72	150	3.20	34.72	27.67
202	3.38	34.77	200	3.35	34.77	27.69
303	3.53	34.80	300	3.50	34.80	27.70
460	3.50	34.83	400	3.45	34.82	27.72
684	3.56	34.86	600	3.50	34.85	27.74
910	3.46	34.86	800	3.50	34.86	27.75
1,139	3.34	34.87	1,000	3.40	34.86	27.76

Station 4534; June 1; latitude 46°52.5′ N., longitude 47°15′ W.; depth 622 meters, dynamic height 970.994

Observed values			Scaled values			
Depth, meters	Temperature °C.	Salinity ‰	Depth, meters	Temperature °C.	Salinity ‰	σ_t
0	3.92	32.70	0	3.92	32.70	25.99
25	2.36	32.84	25	2.36	32.84	26.24
50	−0.25	33.22	50	−0.25	33.22	26.70
75	−0.13	33.58	75	−0.13	33.58	26.99
100	0.45	33.82	100	0.45	33.82	27.15
150	1.20	34.13	150	1.20	34.13	27.35
201	1.89	34.37	200	1.85	34.37	27.50
301	2.74	34.61	300	2.70	34.61	27.62
354	3.00	34.68	400	3.20	34.72	27.67
550	3.62	34.82	600	3.65	34.84	27.71

Station 4535; June 1; latitude 46°52′ N., longitude 47°21′ W.; depth 309 meters, dynamic height 971.027

Observed values			Scaled values			
Depth, meters	Temperature °C.	Salinity ‰	Depth, meters	Temperature °C.	Salinity ‰	σ_t
0	3.81	32.49	0	3.81	32.49	25.83
25	2.26	32.78	25	2.26	32.78	26.70
50	−0.14	33.12	50	−0.14	33.12	26.62
75	−0.79	33.37	75	−0.79	33.37	26.84
100	0.15	33.66	100	0.15	33.66	27.04
150	1.03	34.07	150	1.03	34.07	27.32
201	1.60	34.30	200	1.60	34.30	27.46
301	1.85	34.35	300	1.85	34.35	27.48

STATIONS OCCUPIED IN 1951—Continued

Station 4536; June 1; latitude 46°51′ N., longitude 47°39′ W.; depth 169 meters, dynamic height 971.052

Observed values			Scaled values			
Depth, meters	Temperature °C.	Salinity ‰	Depth, meters	Temperature °C.	Salinity ‰	σ_t
0	4.01	32.51	0	4.01	32.51	25.83
25	2.30	32.57	25	2.30	32.57	26.03
49	−1.20	32.97	50	−1.25	32.98	26.54
74	−1.24	33.17	75	−1.25	33.18	26.70
99	−0.76	33.32	100	−0.75	33.34	26.82
148	0.57	33.86	150	0.60	33.88	27.18

Station 4537; June 1; latitude 46°50′ N., longitude 48°11′ W.; depth 117 meters, dynamic height 971.085

Observed values			Scaled values			
Depth, meters	Temperature °C.	Salinity ‰	Depth, meters	Temperature °C.	Salinity ‰	σ_t
0	4.97	32.55	0	4.97	32.55	25.76
25	4.52	32.53	25	4.52	32.53	25.80
50	1.99	32.65	50	1.99	32.65	26.12
76	−0.81	32.90	75	−0.80	32.90	26.46
101	−0.76	33.14	100	−0.75	33.13	26.65

Station 4538; June 2; latitude 46°48′ N., longitude 48°43′ W.; depth 95 meters, dynamic height 971.082

Observed values			Scaled values			
Depth, meters	Temperature °C.	Salinity ‰	Depth, meters	Temperature °C.	Salinity ‰	σ_t
0	5.16	32.61	0	5.16	32.61	25.79
24	4.97	32.61	25	4.95	32.61	25.82
49	2.06	32.66	50	2.00	32.66	26.12
83	−0.04	32.98	75	0.45	32.90	26.41

Station 4539; June 2; latitude 46°57′ N., longitude 48°04′ W.; depth 132 meters, dynamic height 971.077

Observed values			Scaled values			
Depth, meters	Temperature °C.	Salinity ‰	Depth, meters	Temperature °C.	Salinity ‰	σ_t
0	4.44	32.47	0	4.44	32.47	25.75
24	3.82	32.48	25	3.80	32.48	25.83
49	1.87	32.49	50	1.75	32.49	26.00
73	−0.94	33.02	75	−0.95	33.04	26.58
98	−0.88	33.16	100	−0.85	33.16	26.67
117	−0.75	33.22				

Station 4540; June 2; latitude 47°00.5′ N., longitude 47°48′ W.; depth 169 meters, dynamic height 971.058

Observed values			Scaled values			
Depth, meters	Temperature °C.	Salinity ‰	Depth, meters	Temperature °C.	Salinity ‰	σ_t
0	4.06	32.43	0	4.06	32.43	25.76
26	1.65	32.55	25	1.80	32.54	26.04
52	−0.82	32.87	50	−0.65	32.84	26.42
79	−1.30	33.09	75	−1.30	33.06	26.61
105	−1.11	33.24	100	−1.15	33.21	26.73
157	0.47	33.81	150	0.25	33.74	27.10

Station 4541; June 2; latitude 47°04′ N., longitude 47°34′ W.; depth 220 meters, dynamic height 971.027

Observed values			Scaled values			
Depth, meters	Temperature °C.	Salinity ‰	Depth, meters	Temperature °C.	Salinity ‰	σ_t
0	3.92	32.39	0	3.92	32.39	25.75
23	1.91	32.61	25	1.60	32.65	26.14
46	−0.84	32.96	50	−0.95	33.02	26.57
69	−1.09	33.19	75	−1.00	33.24	26.75
93	−0.43	33.38	100	−0.30	33.45	26.89
139	0.44	33.80	150	0.60	33.86	27.17
185	1.03	34.09	(200)	1.20	34.18	27.39

Station 4542; June 2; latitude 47°10′ N., longitude 47°18′ W.; depth 320 meters, dynamic height 970.981

Observed values			Scaled values			
Depth, meters	Temperature °C.	Salinity ‰	Depth, meters	Temperature °C.	Salinity ‰	σ_t
0	4.07	32.48	0	4.07	32.48	25.80
24	1.67	33.02	25	1.35	33.03	26.46
48	0.03	33.10	50	−0.05	33.13	26.62
71	−0.19	33.55	75	−0.15	33.60	27.01
95	0.45	33.84	100	0.55	33.87	27.19
143	1.11	34.13	150	1.20	34.16	27.38
191	1.71	34.32	200	1.80	34.35	27.49
286	2.68	34.60	300	2.80	34.63	27.62

Station 4543; June 2; latitude 47°18′ N., longitude 47°04′ W.; depth 1,005 meters, dynamic height 970.935

Observed values			Scaled values			
Depth, meters	Temperature °C.	Salinity ‰	Depth, meters	Temperature °C.	Salinity ‰	σ_t
0	3.63	32.97	0	3.63	32.97	26.23
25	3.01	33.18	25	3.01	33.18	26 46
50	2.00	33.75	50	2.00	33.75	26.99
75	0.24	33.84	75	0.24	33.84	27.18
100	1.14	34.08	100	1.14	34.08	27.31
150	2.05	34.40	150	2.05	34.40	27.51
199	2.40	34.52	200	2.40	34.52	27.58
299	3.15	34.72	300	3.15	34.72	27.67
389	3.55	34.81	400	3.50	34.81	27.71
583	3.70	34.88	600	3.70	34.88	27.74
777	3.51	34.87	800	3.45	34.87	27.76
883	3.43	34.87	(1,000)	3.35	34.87	27.77

Station 4544; June 2; latitude 47°15′ N., longitude 46°32′ W.; depth 842 meters, dynamic height 970.918

Observed values			Scaled values			
Depth, meters	Temperature °C.	Salinity ‰	Depth, meters	Temperature °C.	Salinity ‰	σ_t
0	4.77	33.21	0	4.77	33.21	26.31
24	3.18	33.22	25	3.20	33.24	26.49
49	3.78	34.02	50	3.80	34.05	27.07
73	2.98	34.27	75	2.85	34.27	27.34
97	1.83	34.32	100	1.85	34.33	27.46
146	2.32	34.49	150	2.35	34.50	27.56
195	2.85	34.61	200	2.85	34.62	27.62
292	3.52	34.77	300	3.55	34.78	27.67
383	3.67	34.83	400	3.65	34.84	27.71
576	3.68	34.87	600	3.65	34.87	27.74
770	3.51	34.87	800	3.45	34.87	27.76

Station 4545; June 2; latitude 47°18′ N., longitude 45°57′ W.; depth 318 meters, dynamic height 970.949

Observed values			Scaled values			
Depth, meters	Temperature °C.	Salinity ‰	Depth, meters	Temperature °C.	Salinity ‰	σ_t
0	7.28	33.62	0	7.28	35.62	26.32
25	6.75	33.68	25	6.75	33.68	26.43
51	6.84	34.02	50	6.85	34.01	26.68
76	3.07	34.04	75	3.10	34.04	27.13
102	3.38	34.24	100	3.35	34.23	27.25
151	3.07	34.46	150	3.10	34.46	27.47
202	3.77	34.66	200	3.75	34.66	27.56
304	3.90	34.83	300	3.90	34.83	27.68

Station 4546; June 2; latitude 47°19′ N., longitude 45°35′ W.; depth 261 meters, dynamic height 970.957

Observed values			Scaled values			
Depth, meters	Temperature °C.	Salinity ‰	Depth, meters	Temperature °C.	Salinity ‰	σ_t
0	6.42	33.28	0	6.42	33.28	26.17
25	6.24	33.53	25	6.24	33.53	26.38
50	6.33	33.85	50	6.33	33.85	26.62
74	6.32	33.90	75	6.30	33.90	26.67
99	1.99	34.13	100	2.00	34.14	27.30
149	2.66	34.41	150	2.70	34.50	27.53
198	4.06	34.73	200	4.10	34.73	27.58
248	4.11	34.78				

Station 4547; June 2; latitude 47°21′ N., longitude 45°19′ W.; depth 220 meters, dynamic height 970.960

Observed values			Scaled values			
Depth, meters	Temperature °C.	Salinity ‰	Depth, meters	Temperature °C.	Salinity ‰	σ_t
0	6.55	33.41	0	6.55	33.41	26.25
25	6.62	33.66	25	6.62	33.66	26.43
50	5.41	33.74	50	5.41	33.74	26.65
76	3.84	34.10	75	3.85	34.10	27.11
101	2.80	34.21	100	2.80	34.21	27.30
152	3.63	34.46	150	3.60	34.45	27.41
202	3.83	34.61	200	3.85	34.60	27.50

STATIONS OCCUPIED IN 1951—Continued

Station 4548; June 2; latitude 47°23′ N., longitude 45°00′ W.; depth 183 meters, dynamic height 970.953

Observed values			Scaled values			
Depth, meters	Temperature °C.	Salinity ‰	Depth, meters	Temperature °C.	Salinity ‰	σ_t
0	8.08	33.87	0	8.08	33.87	26.39
24	7.22	33.90	25	7.20	33.90	26.54
48	6.15	33.86	50	6.05	33.86	26.67
72	5.02	34.05	75	4.85	34.08	26.96
95	3.89	34.21	100	3.85	34.24	27.22
162	3.65	34.53	150	3.70	34.48	27.42

Station 4549; June 3; latitude 47°28′ N., longitude 45°11′ W.; depth 220 meters, dynamic height 970.956

0	7.52	33.80	0	7.52	33.80	26.42
25	7.30	33.80	25	7.30	33.80	26.45
50	6.21	33.94	50	6.21	33.94	26.71
75	4.60	33.95	75	4.60	33.95	26.91
100	3.80	34.14	100	3.80	34.14	27.14
148	3.91	34.52	150	3.90	34.52	27.44
198	3.81	34.64	200	3.80	34.64	27.54

Station 4550; June 3; latitude 47°45′ N., longitude 45°42′ W.; depth 320 meters, dynamic height 970.940

0	6.37	33.17	0	6.37	33.17	26.08
20	5.53	33.44	25	5.55	33.50	26.36
40	5.68	33.66	50	5.00	33.74	27.09
61	3.81	33.84	75	2.60	34.04	27.33
81	2.50	34.10	100	2.40	34.21	27.41
121	2.27	34.29	150	2.25	34.38	27.54
161	2.22	34.42	200	3.60	34.63	27.62
242	4.17	34.82	(300)	4.05	34.86	27.69

Station 4551; June 3; latitude 47°50′ N., longitude 45°51′ W.; depth 430 meters, dynamic height 970.920

0	5.64	33.06	0	5.64	33.06	26.08
26	3.76	33.17	25	3.85	33.17	26.36
51	1.96	33.90	50	2.05	33.88	27.09
76	1.29	34.11	75	1.30	34.11	27.33
101	2.03	34.28	100	2.00	34.27	27.41
153	3.11	34.56	150	3.10	34.55	27.54
204	3.23	34.67	200	3.20	34.66	27.62
305	3.90	34.86	300	3.90	34.85	27.70
410	3.81	34.86	400	3.75	34.86	27.72

Station 4552; June 3; latitude 47°57′ N., longitude 46°10′ W.; depth 1,051 meters, dynamic height 970.892

0	5.07	33.24	0	5.07	33.24	26.29
25	3.92	33.81	25	3.92	33.81	26.86
50	3.98	34.20	50	3.98	34.20	27.17
76	2.68	34.34	75	2.70	34.34	27.40
101	2.71	34.46	100	2.70	34.46	27.50
150	2.94	34.60	150	2.95	34.60	27.59
200	3.49	34.76	200	3.49	34.76	27.67
301	3.73	34.85	300	3.75	34.85	27.71
399	3.56	34.83	400	3.50	34.83	27.72
596	3.54	34.86	600	3.50	34.86	27.75
792	3.48	34.87	800	3.45	34.87	27.76
1,008	3.34	34.87	1,000	3.35	34.87	27.77

Station 4553; June 3; latitude 47°58.5′ N., longitude 46°23′ W.; depth 1,188 meters, dynamic height 970.915

Observed values			Scaled values			
Depth, meters	Temperature °C.	Salinity ‰	Depth, meters	Temperature °C.	Salinity ‰	σ_t
0	4.51	33.32	0	4.51	33.32	26.41
25	4.58	33.57	25	4.58	33.57	26.41
50	4.10		50	4.10	33.90	26.92
76	3.56	34.23	75	3.55	34.22	27.23
101	2.76	34.40	100	2.75	34.39	27.44
151	2.87	34.56	150	2.85	34.56	27.57
201	3.20	34.69	200	3.20	34.69	27.64
302	3.77	34.84	300	3.80	34.84	27.70
402	3.83	34.87	400	3.85	34.87	27.72
604	3.52	34.86	600	3.50	34.86	27.75
806	3.46	34.86	800	3.45	34.86	27.75
1,011	3.35	34.86	1,000	3.35	34.86	27.76

Station 4554; June 4; latitude 47°45.5′ N., longitude 47°14′ W.; depth 400 meters, dynamic height 970.989

0	2.42	32.79	0	2.42	32.79	26.20
24	2.42	32.79	25	2.40	32.79	26.20
48	1.21	33.10	50	1.05	33.14	26.58
72	−0.17	33.46	75	−0.20	33.51	26.94
96	0.44	33.83	100	0.50	33.85	27.17
144	1.10	34.09	150	1.15	34.12	27.35
192	1.61	34.30	200	1.70	34.33	27.47
288	2.62	34.56	300	2.75	34.58	27.59
360	3.19	34.70	(400)	3.40	34.76	27.68

Station 4555; June 4; latitude 47°45′ N., longitude 47°34′ W.; depth 320 meters, dynamic height 971.037

0	3.97	32.48	0	3.97	32.48	25.81
24	2.96	32.48	25	2.90	32.48	25.91
49	0.24	32.99	50	0.20	33.01	26.52
73	−0.87	33.32	75	−0.85	33.32	26.80
97	−0.28	33.48	100	−0.70	33.50	26.95
145	0.60	33.82	150	0.65	33.84	27.15
194	1.05	34.06	200	1.10	34.08	27.32
291	2.18	34.44	300	2.30	34.47	27.55

Station 4556; June 4; latitude 47°38′ N., longitude 48°12′ W.; depth 220 meters, dynamic height 971.093

0	2.84	32.40	0	2.85	32.40	25.85
27	2.82	32.40	25	2.85	32.40	25.85
52	2.43	32.43	50	2.50	32.42	25.89
79	−1.27	33.02	75	−1.15	32.93	26.50
105	−1.29	33.16	100	−1.30	33.13	26.66
158	−0.03	33.61	150	−0.25	33.53	26.95
210	0.78	33.95	200	0.65	33.87	27.18

Station 4557; June 4; latitude 47°32′ N., longitude 48°30 W.; depth 169 meters, dynamic height 971.082

0	3.30	32.38	0	3.30	32.38	25.79
25	3.25	32.40	25	3.25	32.40	25.82
49	1.94	32.71	50	1.90	32.72	26.17
74	−0.40	32.94	75	−0.40	32.94	26.49
98	−1.32	33.14	100	−1.30	33.15	26.68
147	0.19	33.69	150	0.25	33.72	27.09

STATIONS OCCUPIED IN 1951—Continued

Station 4558; June 4; latitude 47°23′ N., longitude 48°54′ W.; depth 135 meters, dynamic height 971.077

Observed values			Scaled values			
Depth, meters	Temperature °C.	Salinity ‰	Depth, meters	Temperature °C.	Salinity ‰	σ_t
0	3.72	32.44	0	3.72	32.44	25.81
24	3.66	32.45	25	3.65	32.45	25.82
48	0.74	32.66	50	0.50	32.68	26.24
73	-1.27	32.99	75	-1.25	33.01	26.57
97	-0.88	33.17	100	-0.85	33.18	26.69
121	-0.69	33.24				

Station 4559; June 4; latitude 47°13′ N., longitude 49°18′ W.; depth 86 meters, dynamic height 971.082

Observed values			Scaled values			
Depth, meters	Temperature °C.	Salinity ‰	Depth, meters	Temperature °C.	Salinity ‰	σ_t
0	3.70	32.42	0	3.70	32.42	25.79
26	3.70	32.44	25	3.70	32.44	25.81
51	1.65	32.57	50	1.85	32.56	26.05
77	-0.82	33.10	75	-0.65	33.05	26.58

Station 4560; July 14; latitude 50°01.5′ N., longitude 48°58′ W.; depth 1,866 meters, dynamic height 970.857

Observed values			Scaled values			
Depth, meters	Temperature °C.	Salinity ‰	Depth, meters	Temperature °C.	Salinity ‰	σ_t
0	8.05	33.22	0	8.05	33.22	25.89
22	4.00	34.22	25	3.75	34.24	27.23
43	2.87	34.32	50	2.90	34.39	27.43
65	2.94	34.54	75	3.00	34.58	27.57
86	3.01	34.62	100	3.10	34.67	27.64
129	3.28	34.74	150	3.30	34.76	27.69
172	3.34	34.78	200	3.35	34.79	27.70
258	3.41	34.82	300	3.40	34.84	27.74
314	3.46	34.84	400	3.40	34.84	27.74
467	3.40	34.84	600	3.35	34.85	27.75
620	3.39	34.85	800	3.30	34.86	27.77
798	3.33	34.86	1,000	3.30	34.86	27.77
1,283	3.27	34.87				

Station 4561; July 14; latitude 49°47′ N., longitude 49°29′ W.; depth 1,307 meters, dynamic height 970.872

Observed values			Scaled values			
Depth, meters	Temperature °C.	Salinity ‰	Depth, meters	Temperature °C.	Salinity ‰	σ_t
0	8.04	32.87	0	8.04	32.87	25.62
26	2.25	34.13	25	2.50	34.08	27.21
52	1.91	34.33	50	1.90	34.32	27.46
78	2.77	34.51	75	2.65	34.49	27.53
104	3.01	34.62	100	3.00	34.61	27.60
155	3.27	34.74	150	3.25	34.73	27.66
207	3.40	34.80	200	3.40	34.79	27.70
311	3.43	34.83	300	3.45	34.83	27.72
411	3.43	34.84	400	3.45	34.84	27.73
616	3.43	34.84	600	3.40	34.84	27.74
821	3.40	34.86	800	3.40	34.86	27.76
1,027	3.36	34.86	1,000	3.35	34.86	27.76
1,250	3.29	34.86				

Station 4562; July 14; latitude 49°37′ N., longitude 50°01′ W.; depth 622 meters, dynamic height 970.968

Observed values			Scaled values			
Depth, meters	Temperature °C.	Salinity ‰	Depth, meters	Temperature °C.	Salinity ‰	σ_t
0	8.49	32.70	0	8.49	32.70	25.41
24	0.25	33.00	25	0.20	33.02	26.52
49	-0.55	33.44	50	-0.55	33.46	26.91
73	-0.15	33.68	75	-0.10	33.70	27.08
97	0.42	33.87	100	0.45	33.89	27.20
146	1.70	34.25	150	1.75	34.27	27.43
194	2.39	34.47	200	2.45	34.49	27.54
291	3.20	34.71	300	3.25	34.72	27.66
376	3.26	34.76	400	3.30	34.77	27.70
564	3.44	34.83	(600)	3.45	34.83	27.72

Station 4563; July 14; latitude 49°28′ N., longitude 50°31′ W.; depth 320 meters, dynamic height 971.031

Observed values			Scaled values			
Depth, meters	Temperature °C.	Salinity ‰	Depth, meters	Temperature °C.	Salinity ‰	σ_t
0	9.67	32.68	0	9.67	32.68	25.22
23	2.38	32.84	25	1.75	32.85	26.30
47	-0.60	33.01	50	-0.80	33.03	26.57
70	-1.31	33.17	75	-1.30	33.20	26.72
94	-1.10	33.34	100	-1.00	33.38	26.86
141	0.05	33.72	150	0.20	33.78	27.13
187	0.99	34.02	200	1.30	34.11	27.33
281	2.88	34.66	300	3.20	34.78	27.71

Station 4564; July 15; latitude 49°17′ N., longitude 51°00′ W.; depth 331 meters, dynamic height 971.027

Observed values			Scaled values			
Depth, meters	Temperature °C.	Salinity ‰	Depth, meters	Temperature °C.	Salinity ‰	σ_t
0	9.67	32.67	0	9.67	32.67	25.21
24	3.60	32.88	25	3.50	32.88	26.17
50	1.50	32.94	50	1.50	32.94	26.38
74	-0.69	33.33	75	-0.70	33.34	26.82
100	-0.43	33.59	100	-0.45	33.59	27.01
149	0.81	33.91	150	0.80	33.92	27.21
198	1.34	34.19	200	1.35	34.20	27.40
298	2.84	34.64	300	2.85	34.65	27.64

Station 4565; July 15; latitude 49°07′ N., longitude 51°31′ W.; depth 304 meters, dynamic height 971.075

Observed values			Scaled values			
Depth, meters	Temperature °C.	Salinity ‰	Depth, meters	Temperature °C.	Salinity ‰	σ_t
0	10.37	33.12	0	10.37	32.12	24.67
25	2.90	32.62	25	2.90	32.62	26.02
49	0.44	32.74	50	0.45	32.75	26.30
74	-0.45	33.08	75	-0.45	33.09	26.60
99	-1.06	33.19	100	-1.05	33.21	26.73
148	-0.10	33.68	150	-0.10	33.70	27.08
197	0.84	33.94	200	0.85	33.96	27.24
286	2.00	34.40	(300)	2.20	34.47	27.56

Station 4566; July 15; latitude 49°02′ N., longitude 51°51′ W.; depth 311 meters, dynamic height 971.084

Observed values			Scaled values			
Depth, meters	Temperature °C.	Salinity ‰	Depth, meters	Temperature °C.	Salinity ‰	σ_t
0	10.51	32.17	0	10.51	32.17	24.68
23	2.43	32.69	25	1.75	32.70	26.17
46	-1.03	32.85	50	-1.20	32.88	26.46
69	-1.55	33.02	75	-1.55	33.06	26.62
91	-1.48	33.14	100	-1.40	33.20	26.73
137	-1.01	33.39	150	-0.85	33.47	26.93
182	-0.23	33.67	200	0.15	33.77	27.13
273	1.46	34.18	(300)	1.90	34.32	27.46

Station 4567; July 15; latitude 48°58′ N., longitude 52°04′ W.; depth 293 meters, dynamic height 971.092

Observed values			Scaled values			
Depth, meters	Temperature °C.	Salinity ‰	Depth, meters	Temperature °C.	Salinity ‰	σ_t
0	10.07	33.16	0	10.07	32.16	24.75
23	3.49	32.58	25	3.15	32.60	25.99
46	-0.63	32.79	50	-1.00	32.83	26.41
69	-1.58	33.01	75	-1.60	33.04	26.60
92	-1.53	33.13	100	-1.50	33.16	26.69
138	-1.23	33.32	150	-1.05	33.40	26.88
184	-0.21	33.66	200	0.15	33.77	27.13
258	1.27	34.12				

Station 4568; July 15; latitude 48°53′ N., longitude 52°24′ W.; depth 344 meters, dynamic height 971.096

Observed values			Scaled values			
Depth, meters	Temperature °C.	Salinity ‰	Depth, meters	Temperature °C.	Salinity ‰	σ_t
0	9.90	32.14	0	9.90	32.14	24.76
25	1.79	32.64	25	1.79	32.64	26.12
49	-1.28	32.84	50	-1.30	32.85	26.44
74	-1.52	33.00	75	-1.50	33.01	26.58
99	-1.46	33.11	100	-1.45	33.11	26.65
148	-0.19	33.36	150	-0.90	33.36	26.84
197	-0.19	33.64	200	-0.15	33.66	27.06
296	1.83	34.35	300	1.90	34.37	27.50

STATIONS OCCUPIED IN 1951—Continued

Station 4569; July 15; latitude 48°48′ N., longitude 52°39′ W.; depth 220 meters, dynamic height 971.111

Observed values			Scaled values			
Depth, meters	Temperature °C.	Salinity ‰	Depth, meters	Temperature °C.	Salinity ‰	σ_t
0	11.33	31.50	0	11.33	31.50	24.02
23	1.43	32.52	25	1.25	32.55	26.08
46	−0.61	32.81	50	−1.00	32.85	26.43
69	−1.56	33.00	75	−1.55	33.03	26.59
93	−1.85	33.10	100	−1.50	33.13	26.67
139	−1.12	33.36	150	−0.95	33.42	26.90
185	−0.22	33.58	(200)	0.25	33.64	27.02

Station 4570; July 15; latitude 48°46′ N., longitude 52°44′ W.; depth 157 meters, dynamic height 971.195

Observed values			Scaled values			
Depth, meters	Temperature °C.	Salinity ‰	Depth, meters	Temperature °C.	Salinity ‰	σ_t
0	11.94	31.56	0	11.94	31.56	23.96
24	2.08	32.51	25	1.80	32.54	26.04
48	−0.70	32.74	50	−0.75	32.77	26.36
72	−1.37	32.90	75	−1.40	32.91	26.49
96	−1.58	33.00	100	−1.60	33.02	26.59
139	−1.42	33.14	150	−1.30	33.17	26.70

Station 4571; July 15; latitude 48°44′ N., longitude 52°58′ W.; depth 98 meters, dynamic height 971.147

Observed values			Scaled values			
Depth, meters	Temperature °C.	Salinity ‰	Depth, meters	Temperature °C.	Salinity ‰	σ_t
0	12.35	31.27	0	12.35	31.27	23.66
25	1.71	32.40	25	1.71	32.40	25.94
51	−0.68	32.62	50	−0.65	32.62	26.24
86	−1.26	32.76	75	−1.15	32.72	26.33

Station 4572; July 15; latitude 48°48′ N., longitude 52°45′ W.; depth 174 meters; dynamic height 971.143

Observed values			Scaled values			
Depth, meters	Temperature °C.	Salinity ‰	Depth, meters	Temperature °C.	Salinity ‰	σ_t
0	12.79	31.26	0	12.79	31.26	23.56
25	−0.04	32.42	25	−0.04	32.42	26.06
50	−1.10	32.62	50	−1.10	32.62	26.26
75	−1.27	32.77	75	−1.27	32.77	26.38
100	−1.22	32.84	100	−1.22	32.84	26.43
150	−1.41	33.03	150	−1.41	33.03	26.59

Station 4573; July 15; latitude 48°34′ N., longitude 52°36′ W.; depth 263 meters, dynamic height 971.129

Observed values			Scaled values			
Depth, meters	Temperature °C.	Salinity ‰	Depth, meters	Temperature °C.	Salinity ‰	σ_t
0	12.26	31.52	0	12.26	31.52	23.67
25	0.88	32.54	25	0.88	32.54	26.10
50	−0.36	32.73	50	−0.36	32.73	26.31
74	−1.32	32.85	75	−1.35	32.85	26.44
99	−1.53	32.96	100	−1.55	32.96	26.54
149	−1.37	33.14	150	−1.35	33.04	26.60
198	−0.77	33.41	200	−0.75	33.42	26.89
248	0.39	33.80				

Station 4574; July 15; latitude 48°21.5′ N., longitude 52°11′ W.; depth 185 meters, dynamic height 971.115

Observed values			Scaled values			
Depth, meters	Temperature °C.	Salinity ‰	Depth, meters	Temperature °C.	Salinity ‰	σ_t
0	11.36	31.48	0	11.36	31.48	24.00
25	1.68	32.47	25	1.68	32.47	25.99
50	−1.16	32.72	50	−1.16	32.72	26.33
75	−1.39	32.89	75	−1.39	32.89	26.47
101	−1.47	32.98	100	−1.45	32.97	26.54
151	−0.95	32.25	150	−1.00	33.24	26.75

Station 4575; July 15; latitude 48°14′ N., longitude 51°52′ W.; depth 183 meters, dynamic height 971.117

Observed values			Scaled values			
Depth, meters	Temperature °C.	Salinity ‰	Depth, meters	Temperature °C.	Salinity ‰	σ_t
0	11.53	31.46	0	11.53	31.46	23.95
25	−0.03	32.43	25	−0.03	32.43	26.06
50	−1.28	32.70	50	−1.28	32.70	26.32
75	−1.45	32.87	75	−1.45	32.87	26.46
100	−1.56	32.97	100	−1.56	32.97	26.55
150	−1.31	33.18	150	−1.31	33.18	26.70

Station 4576; July 15–16; latitude 48°05.5′ N., longitude 51° 33′ W.; depth 220 meters, dynamic height 971.107

Observed values			Scaled values			
Depth, meters	Temperature °C.	Salinity ‰	Depth, meters	Temperature °C.	Salinity ‰	σ_t
0	11.25	31.39	0	11.25	31.39	23.95
25	4.09	32.17	25	4.09	32.17	25.55
50	−0.87	32.80	50	−0.87	32.80	26.39
75	−1.45	33.03	75	−1.45	33.03	26.59
100	−1.35	33.16	100	−1.35	33.16	26.69
149	−0.04	33.58	150	−0.05	33.59	26.99
199	0.27	33.71	200	0.30	33.71	27.07

Station 4577; July 16; latitude 47°57.5′ N., longitude 51°15′ W.; depth 155 meters, dynamic height 971.103

Observed values			Scaled values			
Depth, meters	Temperature °C.	Salinity ‰	Depth, meters	Temperature °C.	Salinity ‰	σ_t
0	11.56	31.58	0	11.56	31.58	24.04
25	3.11	32.20	25	3.11	32.20	25.67
50	−0.77	32.71	50	−0.77	32.71	26.31
75	−1.16	32.99	75	−1.16	32.99	26.55
100	−0.96	33.18	100	−0.96	33.18	26.70
140	−0.15	33.54	(150)	0.05	33.63	27.02

Station 4578; July 16; latitude 47°48′ N., longitude 50°51′ W.; depth 114 meters, dynamic height 971.111

Observed values			Scaled values			
Depth, meters	Temperature °C.	Salinity ‰	Depth, meters	Temperature °C.	Salinity ‰	σ_t
0	11.49	31.52	0	11.49	31.52	24.00
25	5.23	32.29	25	5.23	32.29	25.52
50	−0.38	32.65	50	−0.38	32.65	26.26
74	−0.88	32.97	75	−0.90	32.97	26.53
99	−0.88	33.14	100	−0.85	33.14	26.66

Station 4579; July 16; latitude 47°44′ N., longitude 50°36′ W.; depth 150 meters, dynamic height 971.129

Observed values			Scaled values			
Depth, meters	Temperature °C.	Salinity ‰	Depth, meters	Temperature °C.	Salinity ‰	σ_t
0	11.52	31.65	0	11.52	31.65	24.10
23	8.22	32.14	25	7.70	32.17	25.12
45	2.50	32.39	50	1.80	32.44	25.96
68	0.16	32.74	75	−0.25	32.89	26.43
90	−0.78	33.11	100	−0.80	33.14	26.66
122	−0.79	33.20				

Station 4580; July 16; latitude 47°34′ N., longitude 50°16′ W.; depth 119 meters, dynamic height 971.115

Observed values			Scaled values			
Depth, meters	Temperature °C.	Salinity ‰	Depth, meters	Temperature °C.	Salinity ‰	σ_t
0	11.39	31.88	0	11.39	31.88	24.30
25	5.24	32.30	25	5.24	32.30	25.53
51	1.39	32.56	50	1.50	32.56	26.08
76	−0.49	32.92	75	−0.45	32.91	26.46
102	−0.72	33.10	100	−0.70	33.09	26.61

Station 4581; July 16; latitude 47°28.5′ N., longitude 49°56′ W.; depth 70 meters, dynamic height 971.116

Observed values			Scaled values			
Depth, meters	Temperature °C.	Salinity ‰	Depth, meters	Temperature °C.	Salinity ‰	σ_t
0	11.88	31.80	0	11.88	31.80	24.15
22	4.85	32.30	25	4.20	32.33	25.67
43	1.95	32.55	(50)	1.40	32.62	26.13

Station 4582; July 16; latitude 47°45.5′ N., longitude 49°50′ W.; depth 115 meters, dynamic height 971.122

Observed values			Scaled values			
Depth, meters	Temperature °C.	Salinity ‰	Depth, meters	Temperature °C.	Salinity ‰	σ_t
0	11.67	31.73	0	11.67	31.73	24.13
25	5.59	32.33	25	5.59	32.33	25.52
50	1.01	32.64	50	1.01	32.64	26.18
75	−0.52	32.98	75	−0.52	32.98	26.52
100	−0.95	33.12	100	−0.95	33.12	26.65

STATIONS OCCUPIED IN 1951—Continued

Station 4583; July 16; latitude 48°00′ N., longitude 49°44′ W.; depth 169 meters, dynamic height 971.110

Observed values			Scaled values			
Depth, meters	Temperature °C.	Salinity ‰	Depth, meters	Temperature °C.	Salinity ‰	σ_t
0	11.66	31.73	0	11.66	31.73	24.13
23	3.23	32.46	25	2.90	32.53	25.95
46	0.71	32.83	50	0.15	32.84	26.38
69	−1.47	32.86	75	−1.50	32.88	26.47
92	−1.57	32.96	100	−1.55	33.01	26.58
138	−0.86	33.25	150	−0.55	33.32	26.79

Station 4584; July 16; latitude 48°13′ N., longitude 49°41′ W.; depth 217 meters, dynamic height 971.074

Observed values			Scaled values			
Depth, meters	Temperature °C.	Salinity ‰	Depth, meters	Temperature °C.	Salinity ‰	σ_t
0	11.53	32.14	0	11.53	32.14	24.48
25	2.15	32.77	25	2.15	32.77	26.20
50	−0.70	32.92	50	−0.70	32.92	26.48
76	−1.47	33.08	75	−1.45	33.08	26.63
101	−1.34	33.23	100	−1.35	33.23	26.75
151	−0.31	33.56	150	−0.35	33.56	26.98
202	0.80	33.92	200	0.75	33.91	27.21

Station 4585; July 16; latitude 48°34′ N., longitude 49°32′ W.; depth 633 meters, dynamic height 970.923

Observed values			Scaled values			
Depth, meters	Temperature °C.	Salinity ‰	Depth, meters	Temperature °C.	Salinity ‰	σ_t
0	10.64	32.44	0	10.64	32.44	24.87
24	−0.70	33.52	25	−0.70	33.53	26.97
49	0.79	33.96	50	0.85	33.97	27.25
73	1.73	34.25	75	1.75	34.26	27.42
97	2.10	34.38	100	2.10	34.39	27.49
146	2.52	34.50	150	2.55	34.51	27.56
194	2.80	34.60	200	2.80	34.61	27.61
291	3.07	34.69	300	3.10	34.70	27.66
380	3.43	34.80	400	3.40	34.81	27.72
574	3.45	34.83	600	3.45	34.83	27.72

Station 4586; July 16; latitude 48°42′ N., longitude 49°28′ W.; depth 1,097 meters, dynamic height 970.946

Observed values			Scaled values			
Depth, meters	Temperature °C.	Salinity ‰	Depth, meters	Temperature °C.	Salinity ‰	σ_t
0	9.89	32.55	0	9.89	32.55	25.08
23	7.79	32.66	25	7.30	32.73	25.62
47	2.93	34.14	50	2.75	34.16	27.26
70	2.15	34.24	75	2.05	34.25	27.39
94	1.79	34.28	100	1.80	34.29	27.44
140	2.07	34.41	150	2.25	34.46	27.54
187	2.76	34.61	200	2.90	34.65	27.64
281	3.31	34.76	300	3.40	34.78	27.69
345	3.52	34.80	400	3.50	34.82	27.72
526	3.54	34.84	600	3.50	34.85	27.74
712	3.50	34.86	800	3.45	34.86	27.75
907	3.37	34.86	(1,000)	3.35	34.86	27.76

Station 4587; July 17; latitude 49°06′ N., longitude 49°20′ W.; depth 1,600 meters, dynamic height 970.904

Observed values			Scaled values			
Depth, meters	Temperature °C.	Salinity ‰	Depth, meters	Temperature °C.	Salinity ‰	σ_t
0	9.11	32.56	0	9.11	32.56	25.21
26	0.69	33.86	25	0.70	33.81	27.13
53	1.56	34.11	50	1.50	34.10	27.31
78	1.68	34.27	75	1.65	34.25	27.42
105	2.10	34.39	100	2.00	34.37	27.49
157	2.83	34.58	150	2.75	34.56	27.58
210	3.07	34.68	200	3.05	34.67	27.64
315	3.39	34.78	300	3.35	34.77	27.69
402	3.53	34.84	400	3.50	34.84	27.73
601	3.44	34.84	600	3.40	34.84	27.74
799	3.37	34.83	800	3.35	34.84	27.74
998	3.32	34.84	1,000	3.30	34.84	27.75
1,496	3.30	34.86				

Station 4588; July 17; latitude 49°34′ N., longitude 49°08′ W.; depth 1,701 meters, dynamic height 970.880

Observed values			Scaled values			
Depth, meters	Temperature °C.	Salinity ‰	Depth, meters	Temperature °C.	Salinity ‰	σ_t
0	9.87	32.97	0	9.87	32.97	25.40
25	2.77	34.06	25	2.77	34.06	27.18
51	2.52	34.35	50	2.50	34.34	27.42
76	2.61	34.56	75	2.60	34.54	27.57
102	2.94	34.58	100	2.90	34.57	27.58
152	3.32	34.73	150	3.35	34.73	27.65
204	3.40	34.78	200	3.40	34.78	27.69
306	3.39	34.81	300	3.40	34.81	27.72
386	3.42	34.83	400	3.40	34.83	27.73
578	3.40	34.83	600	3.35	34.83	27.73
770	3.35	34.85	800	3.35	34.85	27.75
966	3.32	34.85	1,000	3.30	34.85	27.76
1,463	3.33	34.86				

Station 4589; July 17; latitude 49°59.5′ N., longitude 48°58′ W.; depth 1,866 meters, dynamic height 970.862

Observed values			Scaled values			
Depth, meters	Temperature °C.	Salinity ‰	Depth, meters	Temperature °C.	Salinity ‰	σ_t
0	9.21	33.20	0	9.21	33.20	25.70
24	4.06	34.29	25	4.00	34.30	27.25
49	3.08	34.45	50	3.10	34.46	27.47
73	3.13	34.65	75	3.15	34.66	27.62
98	3.26	34.73	100	3.30	34.73	27.66
147	3.42	34.79	150	3.40	34.79	27.70
195	3.37	34.80	200	3.40	34.80	27.71
293	3.38	34.84	300	3.40	34.84	27.74
370	3.40	34.84	400	3.40	34.84	27.74
557	3.39	34.84	600	3.35	34.84	27.74
747	3.33	34.84	800	3.30	34.84	27.75
938	3.27	34.84	1,000	3.25	34.84	27.75
1,421	3.31	34.86				

Station 4590; July 18; latitude 53°42.5′ N., longitude 55°46′ W.; depth 100 meters, dynamic height 1,454.957

Observed values			Scaled values			
Depth, meters	Temperature °C.	Salinity ‰	Depth, meters	Temperature °C.	Salinity ‰	σ_t
0	8.89	27.07	0	8.89	27.07	20.96
23	−1.11	32.14	25	−1.10	32.15	25.87
46	−1.18	32.38	50	−1.20	32.44	26.11
69	−1.34	32.66	75	−1.35	32.68	26.30
78	−1.34	32.69	(100)	−1.30	32.81	26.41

Station 4591; July 19; latitude 53°52′ N., longitude 55°28′ W.; depth 217 meters, dynamic height 1,454.886

Observed values			Scaled values			
Depth, meters	Temperature °C.	Salinity ‰	Depth, meters	Temperature °C.	Salinity ‰	σ_t
0	8.17	30.44	0	8.17	30.44	23.70
24	0.40	32.48	25	0.25	32.53	26.13
49	−1.02	32.91	50	−1.05	32.92	26.49
73	−1.18	33.06	75	−1.20	33.07	26.62
98	−1.11	33.18	100	−1.10	33.19	26.71
147	−0.96	33.33	150	−0.95	33.34	26.83
181	−0.68	33.49	(200)	−0.35	33.58	26.99

Station 4592; July 19; latitude 53°57′ N., longitude 55°21′ W.; depth 169 meters, dynamic height 1,454.890

Observed values			Scaled values			
Depth, meters	Temperature °C.	Salinity ‰	Depth, meters	Temperature °C.	Salinity ‰	σ_t
0	8.91	30.46	0	8.91	30.46	23.60
25	0.10	32.49	25	0.10	32.49	26.09
49	−1.18	32.76	50	−1.20	32.77	26.38
74	−1.16	32.93	75	−1.15	32.94	26.51
99	−1.18	33.08	100	−1.20	33.09	26.63
148	−0.63	33.52	150	−0.60	33.54	26.97

STATIONS OCCUPIED IN 1951—Continued

Station 4593; July 19; latitude 54°08.5′ N., longitude 55°00′ W.; depth 165 meters, dynamic height 1,454.887

Observed values			Scaled values			
Depth, meters	Temperature °C.	Salinity ‰	Depth, meters	Temperature °C.	Salinity ‰	σ_t
0	8.74	30.77	0	8.74	30.77	23.87
24	1.41	32.34	25	1.25	32.38	25.95
48	-1.07	32.74	50	-1.10	32.75	26.35
71	-1.17	32.95	75	-1.15	32.98	26.54
95	-1.16	33.13	100	-1.15	33.16	26.69
143	-0.62	33.50	150	-0.55	33.57	27.00

Station 4594; July 19; latitude 54°19′ N., longitude 54°42 W.; depth 180 meters, dynamic height 1,454.855

0	8.00	31.18	0	8.00	31.18	24.30
26	-0.45	32.68	25	-0.35	32.62	26.22
52	-1.10	33.05	50	-1.10	33.03	26.58
78	-0.91	33.27	75	-0.95	33.25	26.76
105	-0.79	33.41	100	-0.80	33.39	26.86
156	0.01	33.76	150	-0.10	33.72	27.10

Station 4595; July 19; latitude 54°30′ N., longitude 54°21′ W.; depth 220 meters, dynamic height 1,454.852

0	7.71	31.06	0	7.71	31.06	24.24
25	-0.79	32.78	25	-0.79	32.78	26.38
50	-0.96	33.09	50	-0.96	33.09	26.62
75	-1.09	33.24	75	-1.09	33.24	26.75
100	-0.89	33.41	100	-0.89	33.41	26.89
150	-0.23	33.65	150	-0.23	33.65	27.05
200	1.10	34.09	200	1.10	34.09	27.33

Station 4596; July 19; latitude 54°44.5′ N., longitude 53°50′ W.; depth 320 meters, dynamic height 1,454.834

0	7.42	30.92	0	7.42	30.92	24.18
24	-1.19	32.86	25	-1.20	32.87	26.46
49	-1.19	33.07	50	-1.20	33.08	26.62
73	-1.12	33.25	75	-1.10	33.26	26.76
97	-0.92	33.38	100	-0.85	33.40	26.87
146	1.14	33.95	150	1.25	33.99	27.24
194	2.02	34.29	200	2.15	34.32	27.44
291	3.23	34.66	300	3.30	34.68	27.62

Station 4597; July 19; latitude 54°50.5′ N., longitude 53°34′ W.; depth 637 meters, dynamic height 1,454.775

0	5.99	31.32	0	5.99	31.32	24.67
25	0.25	32.64	25	0.25	32.64	26.22
50	-0.67	33.48	50	-0.67	33.48	26.93
75	0.49	33.84	75	0.49	33.84	27.16
100	1.65	34.11	100	1.65	34.11	27.31
150	2.22	34.37	150	2.22	34.37	27.48
200	2.96	34.60	200	2.96	34.60	27.59
300	3.33	34.73	300	3.33	34.73	27.65
394	3.44	34.745	400	3.40	34.75	27.67
592	3.51	34.81	600	3.50	34.81	27.71

Station 4598; July 19; latitude 54°56′ N., longitude 53°18′ W.; depth 1,584 meters; dynamic height 1,454.705

0	5.99	31.58	0	5.99	31.58	24.88
24	7.48	34.06	25	7.50	34.11	26.67
47	4.22	34.44	50	3.95	34.46	27.38
71	2.85	34.53	75	2.85	34.54	27.55
95	2.97	34.58	100	3.00	34.59	27.58
142	3.22	34.68	150	3.25	34.69	27.63
189	3.39	34.75	200	3.40	34.75	27.67
284	3.50	34.79	300	3.50	34.79	27.69
340	3.54	34.80	400	3.50	34.81	27.71
515	3.52	34.81	600	3.50	34.82	27.72
693	3.52	34.82	800	3.50	34.84	27.73
878	3.49	34.85	1,000	3.45	34.85	27.74
1,363	3.37	34.84	(1,500)	3.35	34.84	27.74

Station 4599; July 19; latitude 55°01′ N., longitude 53°06′ W.; depth 2,195 meters, dynamic height 1,454.672

0	7.36	32.44	0	7.36	32.44	25.38
25	3.56	34.07	25	3.56	34.07	27.12
49	2.93	34.50	50	2.95	34.51	27.52
74	3.07	34.65	75	3.10	34.65	27.62
99	3.24	34.69	100	3.25	34.69	27.63
148	3.42	34.73	150	3.45	34.73	27.64
197	3.49	34.78	200	3.50	34.78	27.68
296	3.49	34.80	300	3.50	34.80	27.70
409	3.49	34.82	400	3.45	34.82	27.72
611	3.49	34.83	600	3.45	34.83	27.72
813	3.46	34.84	800	3.45	34.84	27.73
1,014	3.33	34.83	1,000	3.30	34.83	27.74
1,529	3.35	34.86	1,500	3.35	34.86	27.76
2,049	3.07	34.87	2,000	3.10	34.87	27.80

Station 4600; July 19; latitude 55°13′ N., longitude 52°44′ W.; depth 3,054 meters, dynamic height 1,454.657

0	9.57	34.06	0	9.57	34.06	26.31
26	6.62	34.39	25	6.70	34.39	27.00
52	3.30	34.64	50	3.30	34.62	27.58
78	3.22	34.69	75	3.20	34.68	27.63
104	3.35	34.72	100	3.30	34.72	27.66
155	3.56	34.77	150	3.55	34.77	27.67
206	3.57	34.79	200	3.55	34.79	27.68
310	3.53	34.81	300	3.55	34.81	27.70
389	3.50	34.81	400	3.50	34.81	27.71
582	3.51	34.85	600	3.50	34.85	27.74
774	3.43	34.84	800	3.40	34.84	27.74
965	3.32	34.83	1,000	3.30	34.83	27.74
1,456	3.25	34.84	1,500	3.25	34.84	27.75
1,954	3.20	34.88	2,000	3.10	34.88	27.80
2,386	2.79	34.86	2,500	2.60	34.85	27.82
2,774	2.07	34.83	(3,000)	1.55	34.83	27.89

Station 4601; July 20; latitude 55°36′ N., longitude 52°07′ W.; depth 3,310 meters, dynamic height 1,454.630

0	9.47	34.55	0	9.47	34.55	26.71
24	8.17	34.54	25	8.00	34.54	26.93
48	3.72	34.64	50	3.65	34.65	27.56
72	3.36	34.70	75	3.35	34.71	27.64
96	3.32	34.74	100	3.35	34.75	27.67
144	3.41	34.80	150	3.40	34.80	27.71
193	3.42	34.82	200	3.40	34.82	27.725
289	3.46	34.83	300	3.45	34.83	27.725
337	3.37	34.82	400	3.35	34.83	27.73
509	3.41	34.85	600	3.35	34.84	27.74
682	3.34	34.84	800	3.30	34.85	27.76
859	3.32	34.85	1,000	3.30	34.85	27.76
1,318	3.23	34.84	1,500	3.25	34.85	27.76
1,796	3.32	34.86	2,000	3.30	34.87	27.78
2,605	2.92	34.88	2,500	3.05	34.88	27.80
3,056	2.02	34.89	3,000	2.15	34.89	27.89

STATIONS OCCUPIED IN 1951—Continued

Station 4602; July 20; latitude 56°03′ N., longitude 51°24′ W.; depth 3,475 meters, dynamic height 1,454.648

Observed values			Scaled values			
Depth, meters	Temperature °C.	Salinity ‰	Depth, meters	Temperature °C.	Salinity ‰	σ_t
0	9.72	34.39	0	9.72	34.39	26.54
25	7.03	34.41	25	7.03	34.41	26.97
50	4.42	34.57	50	4.42	34.57	27.43
75	4.00	34.66	75	4.00	34.66	27.54
101	3.72	34.69	100	3.70	34.69	27.59
150	3.52	34.72	150	3.52	34.72	27.64
200	3.49	34.78	200	3.49	34.78	27.68
301	3.48	34.81	300	3.50	34.81	27.71
361	3.48	34.84	400	3.45	34.84	27.73
544	3.31	34.84	600	3.30	34.84	27.75
727	3.31	34.85	800	3.30	34.84	27.75
913	3.26	34.84	1,000	3.25	34.84	27.75
1,389	3.25	34.85	1,500	3.25	34.86	27.77
1,877	3.33	34.88	2,000	3.35	34.88	27.77
2,514	3.10	34.89	2,500	3.10	34.89	27.81
3,015	2.67	34.90	3,000	2.70	34.90	27.85
3,417	1.79	34.86				

Station 4603; July 20; latitude 56°36.5′ N., longitude 50°30′ W.; depth 3,841 meters, dynamic height 1,454.635

Observed values			Scaled values			
Depth, meters	Temperature °C.	Salinity ‰	Depth, meters	Temperature °C.	Salinity ‰	σ_t
0	9.57	34.50	0	9.57	34.50	26.65
25	8.88	34.55	25	8.88	34.55	26.80
49	3.85	34.64	50	3.80	34.64	27.54
74	3.53	34.72	75	3.50	34.72	27.64
98	3.43	34.76	100	3.40	34.76	27.68
147	3.34	34.78	150	3.35	34.78	27.69
197	3.31	34.81	200	3.30	34.81	27.73
295	3.29	34.82	300	3.30	34.82	27.74
351	3.33	34.82	400	3.30	34.82	27.74
532	3.27	34.83	600	3.25	34.82	27.74
716	3.23	34.82	800	3.20	34.82	27.75
905	3.22	34.83	1,000	3.20	34.83	27.75
1,385	3.24	34.84	1,500	3.25	34.85	27.76
1,885	3.34	34.88	2,000	3.25	34.88	27.78
2,596	3.04	34.90	2,500	3.10	34.90	27.82
3,103	2.67	34.90	3,000	2.80	34.90	27.84
3,608	1.62	34.86	3,500	1.85	34.87	27.90

Station 4604; July 21; latitude 57°10′ N., longitude 49°25′ W.; depth 3,530 meters, dynamic height 1,454.664

Observed values			Scaled values			
Depth, meters	Temperature °C.	Salinity ‰	Depth, meters	Temperature °C.	Salinity ‰	σ_t
0	9.69	34.56	0	9.69	34.56	26.68
23	8.36	34.56	25	8.10	34.56	26.93
47	4.56	34.57	50	4.40	34.57	27.43
71	3.78	34.60	75	3.70	34.61	27.53
95	3.55	34.66	100	3.50	34.67	27.60
142	3.38	34.75	150	3.35	34.76	27.68
189	3.32	34.79	200	3.30	34.79	27.71
284	3.30	34.80	300	3.30	34.80	27.72
350	3.30	34.83	400	3.30	34.81	27.73
528	3.28	34.82	600	3.25	34.81	27.73
711	3.26	34.82	800	3.25	34.81	27.73
895	3.24	34.80	1,000	3.20	34.80	27.73
1,349	3.25	34.81	1,500	3.25	34.81	27.73
2,580	3.07	34.885	2,000	3.30	34.83	27.74
3,091	2.66	34.875	2,500	3.15	34.88	27.79
3,284	2.36	34.875	3,000	2.75	34.88	27.83
			(3,500)	1.90	34.87	27.90

Station 4605: July 21; latitude 57°44.5′ N., longitude 48°14′ W.; depth 3,365 meters, dynamic height 1,454.616

Observed values			Scaled values			
Depth, meters	Temperature °C.	Salinity ‰	Depth, meters	Temperature °C.	Salinity ‰	σ_t
0	9.00	34.59	0	9.00	34.59	26.81
23	8.53	34.59	25	8.05	34.59	26.96
46	3.86	34.69	50	3.85	34.70	27.58
69	3.89	34.76	75	3.90	34.77	27.64
93	3.82	34.78	100	3.80	34.79	27.66
138	3.74	34.83	150	3.75	34.84	27.70
184	3.79	34.86	200	3.80	34.86	27.72
277	3.66	34.86	300	3.65	34.86	27.73
391	3.61	34.88	400	3.65	34.88	27.74
584	3.48	34.87	600	3.45	34.87	27.76
777	3.31	34.855	800	3.30	34.86	27.77
968	3.24	34.85	1,000	3.20	34.85	27.77
1,507	3.23	34.85	1,500	3.20	34.85	27.77
2,079	3.18	34.91	2,000	3.20	34.91	27.82
2,361	2.96	34.90	2,500	2.85	34.90	27.84
2,912	2.43	34.89	3,000	2.35	34.88	27.86
3,202	2.01	34.87				

Station 4606; July 21–22; latitude 58°16′ N., longitude 46°54′ W.; depth 2,980 meters, dynamic height 1,454.632

Observed values			Scaled values			
Depth, meters	Temperature °C.	Salinity ‰	Depth, meters	Temperature °C.	Salinity ‰	σ_t
0	8.34	34.52	0	8.34	34.52	26.87
28	7.04	34.65	25	7.25	34.64	27.12
55	3.99	34.74	50	4.40	34.72	27.54
84	3.76	34.76	75	3.80	34.76	27.64
111	3.91	34.82	100	3.85	34.80	27.66
167	3.84	34.85	150	3.85	34.84	27.69
223	3.88	34.88	200	3.85	34.87	27.72
334	3.75	34.88	300	3.80	34.88	27.73
437	3.67	34.88	400	3.70	34.88	27.74
368	3.72	34.88	600	3.55	34.86	27.74
556	3.60	34.865	800	3.45	34.86	27.75
941	3.40	34.855	1,000	3.35	34.85	27.75
1,438	3.30	34.85	1,500	3.30	34.85	27.76
1,888	3.31	34.90	2,000	3.30	34.90	27.80
2,375	2.87	34.90	2,500	2.65	34.90	27.86
2,768	2.15	34.88				

Station 4607; July 22; latitude 58°40′ N., longitude 46°01, W.; depth 2,550 meters, dynamic height 1,454.627

Observed values			Scaled values			
Depth, meters	Temperature °C.	Salinity ‰	Depth, meters	Temperature °C.	Salinity ‰	σ_t
0	8.18	34.70	0	8.18	34.70	27.03
24	8.15	34.72	25	8.15	34.72	27.05
49	5.90	34.82	50	5.80	34.82	27.46
73	4.63	34.84	75	4.55	34.84	27.62
99	4.30	34.87	100	4.30	34.87	27.67
147	4.25	34.90	150	4.25	34.90	27.70
196	4.13	34.90	200	4.15	34.90	27.71
295	4.09	34.91	300	4.10	34.91	27.73
403	4.02	34.92	400	4.00	34.92	27.75
606	3.60	34.88	600	3.60	34.88	27.75
810	3.37	34.84	800	3.35	34.85	27.75
1,011	3.29	04.84	1,000	3.30	34.84	27.75
1,516	3.37	34.89	1,500	3.40	34.89	27.78
2,102	2.68	34.87	2,000	2.90	34.87	27.82
2,459	2.02	34.86	(2,500)	1.90	34.86	27.89

STATIONS OCCUPIED IN 1951—Continued

Station 4608; July 22; latitude 58°57.5′ N., longitude 45°20′ W.; depth 2,469 meters, dynamic height 1,454.647

Observed values			Scaled values			
Depth, meters	Temperature °C.	Salinity ‰	Depth, meters	Temperature °C.	Salinity ‰	σ_t
0	7.36	34.74	0	7.36	34.74	27.18
28	6.98	34.76	25	7.10	34.75	27.23
57	5.06	34.89	50	5.15	34.85	27.56
85	4.91	34.95	75	4.95	34.93	27.64
114	4.79	34.945	100	4.85	34.95	27.67
171	4.62	34.93	150	4.65	34.94	27.69
228	4.61	34.94	200	4.60	34.94	27.69
342	4.53	34.94	300	4.55	34.94	27.70
392	4.48	34.935	400	4.45	34.93	27.70
591	4.18	34.92	600	4.15	34.92	27.73
793	3.90	34.89	800	3.85	34.89	27.73
998	3.64	34.88	1,000	3.65	34.88	27.74
1,510	3.36	34.89	1,500	3.35	34.89	27.78
1,863	3.00	34.89	2,000	2.75	34.88	27.83
2,249	2.22	34.85				

Station 4609; July 22; latitude 59°13′ N., longitude 44°51′ W.; depth 1,920 meters, dynamic height 1,454.663

Observed values			Scaled values			
Depth, meters	Temperature °C.	Salinity ‰	Depth, meters	Temperature °C.	Salinity ‰	σ_t
0	6.18	33.70	0	6.18	33.70	26.52
23	5.44	34.83	25	5.40	34.84	27.52
46	5.37	34.92	50	5.35	34.93	27.59
69	5.35	34.96	75	5.25	34.96	27.64
92	4.86	34.92	100	4.85	34.93	27.65
137	4.86	34.96	150	4.80	34.96	27.69
184	4.73	34.94	200	4.70	34.95	27.69
276	4.66	34.96	300	4.65	34.95	27.70
296	4.68	34.95	400	4.60	34.95	27.70
460	4.62	34.94	600	4.55	34.95	27.71
636	4.53	34.95	800	4.30	34.93	27.71
823	4.27	34.93	1,000	3.95	34.90	27.73
1,299	3.53	34.87	1,500	3.35	34.90	27.79
1,593	3.33	34.91				

Station 4610; July 22; latitude 59°25′ N., longitude 44°49′ W.; depth 1,097 meters, dynamic height 1,454,733

Observed values			Scaled values			
Depth, meters	Temperature °C.	Salinity ‰	Depth, meters	Temperature °C.	Salinity ‰	σ_t
0	3.65	32.67	0	3.65	32.67	25.99
26	2.76	33.01	25	2.75	32.97	26.31
51	3.28	34.46	50	3.20	34.40	27.41
78	4.18	34.63	75	4.10	34.61	27.49
103	4.79	34.80	100	4.75	34.79	27.56
155	4.95	34.86	150	4.95	34.86	27.59
206	5.08	34.94	200	5.10	34.94	27.63
309	4.81	34.95	300	4.80	34.94	27.67
282	4.75	34.92	400	4.75	34.95	27.68
442	4.69	34.96	600	4.40	34.94	27.71
616	4.35	34.94	(800)	4.25	34.92	27.72

Station 4611; July 23; latitude 59°32.5′ N., longitude 44°26′ W.; depth 338 meters, dynamic height 1,454.789

Observed values			Scaled values			
Depth, meters	Temperature °C.	Salinity ‰	Depth, meters	Temperature °C.	Salinity ‰	σ_t
0	1.30	32.38	0	1.30	32.38	25.95
24	−0.20	32.81	25	−0.30	32.83	26.39
50	−1.07	33.35	50	−1.05	33.35	26.84
74	−0.63	33.66	75	−0.60	33.67	27.08
99	1.49	34.11	100	1.50	34.12	27.33
148	1.92	34.24	150	1.95	34.24	27.39
198	2.11	34.29	200	2.10	34.29	27.41
			(300)	2.20	34.36	27.47

Station 4612; July 23; latitude 59°37′ N., longitude 44°17′ W.; depth 174 meters, dynamic height 1,454.833

Observed values			Scaled values			
Depth, meters	Temperature °C.	Salinity ‰	Depth, meters	Temperature °C.	Salinity ‰	σ_t
0	2.55	32.01	0	2.55	32.01	25.56
27	0.69	32.44	25	0.75	32.37	25.97
54	−0.95	33.14	50	−0.75	33.04	26.58
80	−1.23	33.42	75	−1.20	33.38	26.87
107	−0.98	33.50	100	−1.05	33.47	26.94
160	1.61	34.14	150	1.05	34.02	27.28

Station 4613; July 23; latitude 59°43.5′ N., longitude 43°58′ W.; depth 143 meters, dynamic height 1,454.907

Observed values			Scaled values			
Depth, meters	Temperature °C.	Salinity ‰	Depth, meters	Temperature °C.	Salinity ‰	σ_t
0	1.37	30.98	0	1.37	30.98	24.82
24	1.36	31.01	25	1.35	31.07	24.89
48	−0.24	32.58	50	−0.30	32.65	26.24
7[illegible]	−0.73	32.92	75	−0.75	32.93	26.49
9[illegible]	−0.89	33.01	100	−0.85	33.06	26.59
121	−0.62	33.39				

☆ U. S. GOVERNMENT PRINTING OFFICE: 1953—204964

Contribution No. 605

On the Determination of Moisture Gradients from Radiosonde Records [1, 2]

ANDREW F. BUNKER

Woods Hole Oceanographic Institution, Woods Hole, Massachusetts

ABSTRACT

The humidity indicated by the rapidly rising radiosonde lags behind the true humidity of the air, making moisture gradient determinations uncertain by a factor of 4. Application of isothermal laboratory determinations of the lag to the readings may be misleading because the radiosonde, in rising through the atmosphere, usually passes from warm air to cooler air. The lag of the strip may be quite different under these circumstances. By comparison of radiosonde reports with airplane humidity soundings, it is found that in the case of the radiosonde moving from warm, dry air (about −5°C) to cooler, moister air (about −18°C) the lag may increase to 165 seconds. When it passes to cooler, drier air, the lag decreases to 10 to 20 seconds. Using these lags and assuming an exponential approach to the final value, more nearly correct values of the humidity at particular heights can be computed from the radiosonde records.

I. INTRODUCTION

A VAST file of upper-air data has been accumulated during the past two decades from radiosonde reports from all parts of the globe. The usefulness of this material is restricted by the performance of the humidity element, which, in spite of tremendous improvements, has a few shortcomings. The particular characteristic discussed in this paper is the time of response of the electric humidity strip to changes in humidity and temperature. Knowledge of the lag of the element is of prime importance if exact values of the humidity or humidity gradients are desired, as is often the case in research work.

A. Wexler (1949) has studied exhaustively the lag of the humidity strip at many temperatures and humidities and has found it to follow a very complex pattern. He gives values of the lag which show that it varies not only with the temperature and humidity, but also with the direction and magnitude of the humidity change. A point not checked is the lag time when the change in humidity is small and continuous and occurs non-isothermally. As the radiosonde in actual use always moves through regions of continually changing temperature and humidity, it is important to determine the lag under this condition. It may be reasoned that if a humidity strip is warmer than the surrounding air, by virtue of its large thermal lag, it will heat the air immediately in contact with it, thereby changing its relative humidity. If this relative humidity change is in the same direction as the change in the outside atmosphere with height, then the effective lag of the strip is greatly reduced. However, if the two changes are in opposite directions, the effective lag is, of course, increased. It is apparent that no one correcting factor can be applied to Wexler's published lag to cover all the situations occurring in the atmosphere.

It is found upon investigation that the radiosonde always reports a more rapid decrease of mixing ratio with height than actually exists. This peculiarity arises because the radiosonde is a relative humidity measuring device and the most frequently occurring condition in a turbulently mixed layer of the atmosphere is a rise in relative humidity coupled with a decrease in temperature with height. The effect of the lag and the warming of the air next to the strip is to report relative humidities that are too small, and hence, mixing ratios that decrease with height, even when the actual mixing ratios remain constant with height. It is of interest to note at this point that a rapidly rising dew point recorder with considerable lag would report a slight increase in mixing ratio under similar circumstances. A comparison of the relative humidity and mixing ratio values of the Portland, Maine, 1500Z, February 3, 1950 radiosonde ascent with the values obtained from a dew point recorder carried by a DC-3 aircraft circling Portland at 1900Z is presented in FIGURE 1. The various features of a turbulently mixed ground layer and the radiosonde's interpretation of the relative humidity and mixing ratio are shown clearly.

II. DETERMINATION OF EFFECTIVE LAG

The lag of the humidity strip under the conditions of its ascent through the atmosphere has been

[1] Contribution No. 605 from the Woods Hole Oceanographic Institution.

[2] This work was carried out under Contract No. N6onr-27702 (NR-082-021) of the Office of Naval Research with the Woods Hole Oceanographic Institution.

determined through comparison with the humidities obtained by airplane-carried psychrographs. An airplane equipped with a humidity measuring device can climb at a controlled, low rate. This assures that no appreciable errors due to lag occur. From an airplane ascent made at the time and place of release of a radiosonde-carrying balloon exact values of the humidity can be established at several heights. The difference between the airplane and the radiosonde values will be a measure of the effective lag with the given thermal and humidity lapse rates.

The easiest way of computing the lag is to assume that the humidity strip follows the exponential decay law as do thermometers. Apparently, the strip does not hold strictly to the law, but varies somewhat irregularly. Nevertheless, the function may be considered a sufficiently good representation of the strip's response for present purposes. Following Middleton (1942),

$$\theta_i - \theta_e = -\beta\lambda(1 - e^{-t/\lambda}) \qquad (1)$$

where θ_i is the indicated relative humidity at a particular height, and θ_e, the humidity of the environment at that height. β is the time rate of change of humidity relative to an ascending balloon, i.e., $\theta_e = \theta_1 + \beta t$, λ is the lag of the element, and t, the time interval. If θ_e and β are known from the airplane observations, then λ can be found.

This calculation has been carried out for five sets of simultaneous airplane and radiosonde data available in the files of the Oceanographic Institution. The first set was obtained over Portland, Maine on February 3, 1950. The airplane humidity measurements were obtained with a dew point temperature recorder only a few hours after the release of the radiosonde balloon by the U. S. Weather Bureau. As a steady NW wind was blowing, no significant change in the humidity structure of the layer occurred. In the main body of the ground layer the dry-bulb temperature dropped adiabatically from − 5°C to − 18°C near the base of the ground layer inversion, and an increase with height of the relative humidity of 40% (corresponding to a slight decrease in the mixing ratio) occurred. Under these circumstances the heating of the air by the strip opposed the increasing humidity of the air and the lag increased greatly, to 165 seconds. The lag found in the low-

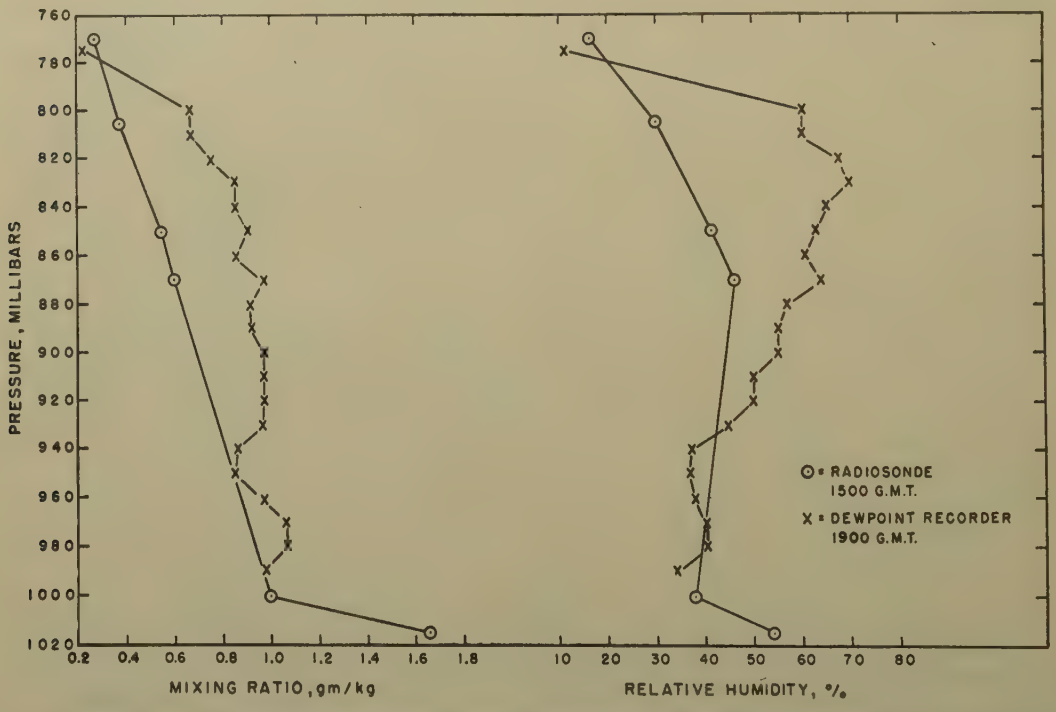

FIG. 1. Comparison of radiosonde and dew-point recorder determinations of the relative humidities and mixing ratios in the turbulently mixed ground layer over Portland, Maine.

TABLE I. LAGS OF HUMIDITY STRIPS DETERMINED IN FLIGHT

Date of determination	Lag, in seconds	Humidity change	Temperature °C	Lapse rate °C/100 m	Lag determined by Wexler (1949) (seconds)
February 3, 1950	165	Increase	−5 to −18	1.0	40
	10	Decrease	−4 to −5	1.0	20
January 17, 1950	105	Increase	−1 to −12	0.9	40
	20	Decrease	1 to −1	1.0	20
November 5, 1952	150	Increase	14 to −4	1.0	Not determined
September 5, 1950	60	Increase	17 to 12	0.9	Not determined
November 7, 1952	~0	Increase	24 to 14	1.0	Not determined

est 130 m, where the relative humidity decreased rapidly, was 10 seconds.

On January 17, 1950, airplane observations were made in the Boston area. These have been compared to the Portland radiosonde. A lag of 105 seconds was found for the upper region of the ground layer where the relative humidity rise occurs. In the lowest 200 m, where a humidity decrease occurs, the lag drops to 20 seconds. The temperature of the air was 1°C near the surface and − 12°C at 1450 m.

On September 5, 1950, an airplane equipped with a psychrograph made several ascents through the ground layer of air over the island of Nantucket at about the time of release of the U. S. Weather Bureau radiosonde balloon. From the records of the two ascents, a lag of 60 seconds was computed. On this occasion the air temperature varied from 17°C at the ground to 7°C at 1300 m. TABLE I presents these findings together with the lag determined by Wexler which most nearly corresponds to the conditions found in the atmosphere.

During a flight to Bermuda in November 1952, two soundings were made in the areas close to radiosonde stations that are suitable for lag determinations. One, made on November 5, 1952, near weather ship "H", shows a lag of 150 seconds under conditions of humidity increase and temperatures from 14°C to − 4°C. The other sounding, taken 40 miles off Bermuda in air with a temperature of 24°C falling to 14°C and a humidity increase, shows no measurable lag of the element. In fact, computation yields a very small negative value for the lag. This, of course, indicates that the small true lag is masked by minor variations of the humidity in the two regions.

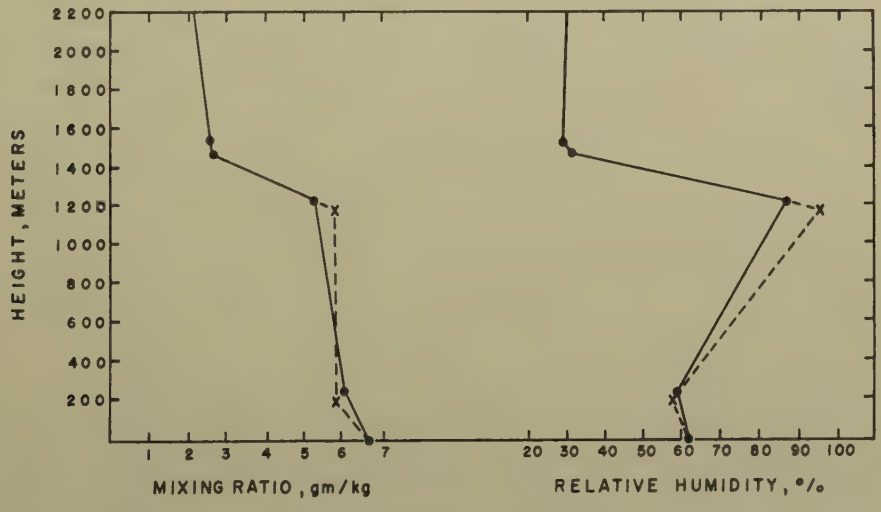

FIG. 2. Original and corrected Bermuda radiosonde. The correction was computed on the basis of a 20 second lag in the lowest region and a 60 second lag in the upper region.

III. Determination of the True Values of the Humidity

The rate of change of humidity relative to the rising balloon can be computed most easily from the following form of equation (1):

$$\beta = \frac{\theta_i - \theta_1}{t - \lambda(1 - e^{-t/\lambda})}, \qquad (2)$$

where θ_1 is an initial reading of the humidity strip. This reading may be either the value obtained in the instrument shelter prior to release, or the value at the base of a column of air with a particular humidity gradient. Once the value of λ is determined, the true humidities of the air can be found at all heights up to the point where the gradient changes. The value of λ may be selected from Table I.

For greater accuracy, further tests should be made for conditions not covered by the present tests. The values presented together with Wexler's values are sufficient to improve greatly the accuracy of mixing ratio gradients determined from radiosonde records.

The Bermuda January 18, 1951, 0300Z radiosonde is presented here as an example of a sounding that is made more intelligible by correction for the lag of the humidity element. Weather observers reported $\frac{7}{10}$–$\frac{8}{10}$ sky coverage of stratocumulus *translucidus* with a base at 1000 m to 1500 m, yet the radiosonde reported a relative humidity at the cloud level of but 87%. If the radiosonde is corrected for the lag of the humidity element, a relative humidity of 97% is obtained. This value is much more compatible with the presence of clouds. A value of 60 seconds was employed for the lag in the region in which the relative humidity increased as the temperature decreased from 13°C to 4°C. The correction modifies the mixing ratio gradient from -8×10^{-9} cm^{-1} to -1×10^{-9} cm^{-1}, a value more consistent with gradients determined from airplane observations. Figure 2 has been drawn to show the original and the corrected values of the relative humidity and the mixing ratio.

Mixing ratio gradients determined from the February 3, 1950 radiosonde reports without correction for lag are found to be 4×10^{-8} cm^{-1}, while the gradient determined from the dew-point recorder values is 1×10^{-9} cm^{-1}. Thus the two determinations differ by a factor of 4. The September 5, 1950 radiosonde yields a value in error by a factor of only 1.5, as the strip response is faster at the higher temperatures occurring on this day.

References

Wexler, Arnold, 1949: "Low-temperature performance of radiosonde electric hygrometer elements." *Journ. Res. Nat. Bur. Stand.*, Vol., 43, pp. 49–56.

Middleton, W. E. K., 1942: *Meteorological Instruments.* Toronto: University of Toronto Press. 213 pp., 160 figs.

Contribution No. 623

Reprinted from THE JOURNAL OF GENERAL MICROBIOLOGY
Vol. 8, No. 2, April 1953
(*All rights reserved*)
PRINTED IN GREAT BRITAIN

VISHNIAC, H. S. & WATSON, S. W. (1953). *J. gen. Microbiol.* **8**, 248–255.

The Steroid Requirements of *Labyrinthula vitellina* var. *pacifica*

BY HELEN S. VISHNIAC* AND S. W. WATSON

Haskins Laboratories, New York 17, *N.Y., and the Woods Hole Oceanographic Institution, Woods Hole, Massachusetts, U.S.A.*†

SUMMARY: *Labyrinthula vitellina* var. *pacifica* requires a steroid as growth factor. Cholesterol, Δ^4-cholestenone, fucosterol, and β-sitosterol are active. When cholesterol is modified by (1) the C3‡ hydroxyl group becoming *trans* to the C10 methyl group, (2) esterification of the C3 hydroxyl group, or (3) saturation of the C5, 6 double bond, the resulting compound is inactive. Modification of the side chain of cholesterol or cholestenone by the addition of a C24 ethyl or vinyl group does not destroy activity but unsaturation at C22, 23 does, as do the more marked changes found in diosgenin, deoxycorticosterone acetate, and methyltestosterone. Bile salts are inactive. The specificity of the requirement indicates that active steroids function as essential metabolites rather than solely as protective agents. Active steroids may be obtained by this micro-organism in nature from host plants or from diatoms and bacteria associated with the hosts.

The isolation in pure culture of the labyrinthula strains by Watson (to be published) made possible the investigation of their nutritional requirements. One isolate, *L. vitellina* var. *pacifica*, has been found to require a steroid for growth. Since such requirements are rare among micro-organisms, a detailed investigation of steroid specificity has been made.

MATERIALS AND METHODS

Stock cultures of isolates of *L. macrocystis* var. *atlantica* and *L. minuta* var. *atlantica* were maintained at 20° in tubes containing the semi-solid medium given in Table 1. The addition of 1·0 mg % (w/v) of cholesterol rendered this medium suitable for the maintenance of *L. vitellina* var. *pacifica*.

The agar in this medium appears to be necessary as a physical support without which these organisms settle to the bottom of the tube, or cling to its sides, where they grow poorly. High viscosity methylcellulose (0·5 % (w/v), Hercules Powder Company) gave fair results as an alternative supporting agent but did not form a sufficiently homogeneous gel to give consistent or maximal growth. The constant motion provided by a rotating apparatus constructed after Baker (1949) substituted for mechanical support and allowed the smallest strain (*L. minuta* var. *atlantica*) to grow as well in a liquid as in an agar-containing medium. Tubes of liquid medium were placed in a rack held at an angle of 11·5° to the horizontal and rotated at 21 r.p.m. by this apparatus. This method of cultivation appears most promising for more critical studies

* Present address: Department of Microbiology, Yale University, 310 Cedar St, New Haven 11, Conn.

† Contribution No. 623 from the Woods Hole Oceanographic Institution.

‡ For the structure of steroids and the numbering system used see Deuel (1951).

of non-steroid nutritional requirements of labyrinthula and is being further studied.

Since it was most convenient to use agar as supporting agent for the present investigations, only preliminary experiments on non-steroid nutritional requirements have been made. The agar used (Difco agar) contains significant amounts of various vitamins and inorganic compounds. The latter are also contributed

Table 1. *Composition of stock medium. Quantities made up to* 100 *ml. with distilled water and* pH *value adjusted to* 8·0–8·2 *with* KOH *after the medium had been boiled for* 20 *min. and cooled to room temperature*

NaCl	2·5 g.	Thiamine	0·2 mg.
$MgSO_4.7H_2O$	0·5 g.	Nicotinic acid	0·1 mg.
K_2HPO_4	0·01 g.	Ca pantothenate	0·1 mg.
Ethylenediamine tetracetic acid*	0·05 g.	Pyridoxin.HCl	0·04 mg.
$CaCO_3$	0·025 g.	Pyridoxamin.2HCl	0·02 mg.
Mn (as manganous sulphate)	2·0 mg.	*p*-Aminobenzoic acid	0·01 mg.
Zn (as sulphate)	2·0 mg.	Biotin	0·5 μg.
Fe (as ferrous sulphate)	0·2 mg.	Cobalamin (vitamin B_{12})	0·05 μg.
Gelatin hydrolysate	0·1 g.	Folic acid	2·5 μg.
Agar	0·2 g.		

* 'Versene'-free acid, Bersworth Chemical Co., Framingham, Mass.

to the medium by the gelatin hydrolysate. The gelatin hydrolysate used was made from Eastman gelatin hydrolysed with sulphuric acid and partially neutralized with barium hydroxide before filtration and final neutralization with KOH. The strains which we have maintained on the stock medium (Table 1) grow only slightly better and more consistently when the vitamins listed are added than when they are omitted. It seems probable that these strains do require one or more of the known vitamins. Our preliminary experiments indicated that the sodium, chloride, phosphate, magnesium, calcium, manganese, zinc and iron contents of the stock medium are approximately optimal.

Gelatin hydrolysate serves as carbon and nitrogen source. Glucose, sodium succinate hexahydrate, fumaric acid (neutralized with KOH), glycerol, and sodium acetate trihydrate were ineffective as substrates in the presence of a non-toxic concentration of NH_4Cl (0·02 %, w/v) added aseptically after autoclaving. The carbon sources tested were at the concentration of 0·2 % (w/v). Monosodium glutamate (0·25 %, w/v) supported a slight amount of growth. The initial pH value of the medium could not be lowered without decreasing growth.

Under the conditions given stock cultures should be transferred once a week, although they will survive for a month if kept in the refrigerator after a 4- or 5-day period of growth at 20°. The temperature tolerance of *L. minuta* var. *atlantica* extends from about 2° (refrigerator) to 30°; cultures incubated at 37° failed to grow at that temperature or when transferred to a room temperature of about 21–24°. *L. vitellina* var. *pacifica* and *L. macrocystis* var. *atlantica* grew rapidly at 20° but were killed by incubation at 30–31°.

RESULTS

L. vitellina var. *pacifica* was originally isolated on serum agar and did not grow in the absence of serum. The discovery that cream, but not yeast extract or a tryptic digest of casein, would substitute for serum suggested that a lipid growth factor was required. Non-toxic concentrations of bile salts (1·0, 5·0 mg./100 ml.), lecithin (1·0, 5·0, 10·0 mg./100 ml.), Tween 40 (1·0 mg./100 ml.; polyoxyethylene sorbitan palmitate, Atlas Powder Co.), Tween 80 (1·0 mg./100 ml.; polyoxyethylene sorbitan oleate, Atlas Powder Co.), or glycerol mono-oleate (1·0 mg./100 ml.) failed to support continued growth. Cholesterol (1·0 mg./100 ml.) was effective in preliminary experiments.

The stock medium (without cholesterol) was used in studying the specificity of this steroid requirement. Ten ml. lots of medium were distributed in 25 ml. glass-capped Erlenmeyer flasks which were in turn sealed with transparent cellulose tape between two Pyrex glass kitchen trays. Steroids were added as freshly made solutions in commercial absolute ethanol, before autoclaving. Ergosterol was also used as an unsterilized ethanolic solution added after autoclaving. No contaminations occurred in this experiment. The amount of ethanol added is critical; 0·1 ml. ethanol/10 ml. medium added after autoclaving completely suppressed growth in the presence of cholesterol. Ethanol is not completely removed by autoclaving; 0·25 ml. ethanol/10 ml. medium added before autoclaving inhibited growth although half this amount did not. No more than 0·05 ml. ethanol/10 ml. medium was added after autoclaving, nor more than 0·125 ml./10 ml. before autoclaving, in these experiments. The addition of the steroids as ethanolic solutions gave fairly uniform dispersion. No better results were obtained by using bile salts to solubilize cholesterol. The inoculum consisted of one or two drops of a 1/10 dilution of a stock culture in basal medium. Inoculated flasks were incubated in an incubator controlled at 18–20°.

The steroid preparations used were: cholesterol (U.S.P.); cholesteryl acetate (recrystallized from a preparation of Dr N. A. Milas); cholesteryl laurate (m.p. 74–75°, gift of Dr M. Calvin, Radiation Laboratory, University of California); cholesteryl palmitate, *epi*cholesterol, progesterone, estrone, and deoxycorticosterone acetate (gifts of Dr H. Sobotka, Mt. Sinai Hospital); coprosterol (m.p. 92–99°), β-cholestanol (m.p. 145°), Δ^4-cholestenone (m.p. 79–80°), and cholestanone (m.p. 129–130°) (gifts of Dr Ivan Salamon, Sloan Kettering Institute for Cancer Research); ergosterol (The Matheson Co., Inc., East Rutherford, N.J., recrystallized before use); ergosterol, zymosterol (m.p. 108–115°, $[\alpha]_D + 34[CHCl_3]$), and 5-dihydroergosterol (gifts of Dr O. N. Breivik, the Fleischmann Laboratories); fucosterol, brassicasterol, and β-sitosterol (gifts of Dr W. Bergman, Sterling Chemistry Laboratories, Yale University); β-sitosterol (L. Light and Co., Ltd., Colnbrook, Bucks, England); mixed soya sitosterols (β and γ) and stigmasterol (The Glidden Co., Chicago, Ill.); calciferol (Nutritional Biochemicals Corp., Cleveland, Ohio); methyltestosterone and ethinyl estradiol (Schering Corp., Bloomfield, N.J.); cortisone (gift of Dr T. H. Jukes, Lederle Laboratories); diosgenin (gift of Dr Monroe

E. Wall, Eastern Regional Research Laboratory, United States Department of Agriculture); and progesterone (gift of Dr K. Schindler).

Table 2. *Steroids as growth factors for* Labyrinthula vitellina *var.* pacifica

	Steroid added to 10 ml. basal medium	Optical density
None; no inoculum	0	0·07
Cholesterol No inoculum	0·05 mg.	0·07
None; inoculated	0	0·07, 0·08
Cholesterol	0·005 mg.	0·09*
	0·01 mg.	0·17–18
	0·025 mg.	0·31
	0·05 mg.	0·31, 0·36, 0·41
	0·1 mg.	0·37
	0·25 mg.	0·41
	0·5 mg.	0·50
Δ^4-Cholestenone	0·0025 mg.	0·09*
	0·005 mg.	0·19, 0·12†
	0·01 mg.	0·30
	0·025 mg.	0·33
	0·05 mg.	0·37
	0·1 mg.	0·37, 0·41
	0·25 mg.	0·33
Fucosterol	0·005 mg.	0·12–13†
	0·01 mg.	0·25
	0·025 mg.	0·31
	0·05 mg.	0·33
β-Sitosterol	0·005 mg.	0·08*
	0·01 mg.	0·16
	0·025 mg.	0·30
	0·05 mg.	0·34–36, 0·29
	0·1 mg.	0·32–33
	0·25 mg.	0·38–40

* Indicates absence of growth, † slight growth (150 organisms or more in a low power microscope field) where the optical density data do not clearly provide this information.

The positive results are given in Table 2 in terms of the optical density of the cultures reached after 8 days of incubation. Cholesterol, Δ^4-cholestenone, fucosterol and β-sitosterol were active as growth factors. The following compounds showed slight activity at the concentrations given parenthetically: *epi*cholesterol (0·1 mg./10 ml.), so yasitosterols (0·025 mg./10 ml.; higher concentrations toxic), ergosterol (added after autoclaving, 0·01–0·1 mg./10 ml. but not consistently), brassicasterol (0·01–0·1 mg./10 ml.), and stigmasterol (0·1 mg./10 ml.). We consider these compounds to be really inactive because of the low level of growth (optical densities usually less than 0·19) and the relatively high concentrations required for even this little growth. The purity of these steroid preparations was not high and steroids deteriorate more or less rapidly in any case; contaminants or degradation products were probably responsible for the slight apparent activity. When the occurrence of growth was doubtful a microscopic examination of the culture was always made. The

other compounds tested were inactive, although not completely inhibitory over at least a portion of the experimental range of concentrations. They were as follows: cholesteryl acetate (toxic at 0·1 mg./10 ml.), cholesteryl laurate and cholesteryl palmitate (toxic at 0·025 mg./10 ml.), 3-β-cholestanol (inhibitory at 0·1 mg./10 ml.), coprosterol (toxic at 0·05 mg./10 ml.), cholestanone (inhibitory at 0·1 mg./10 ml.), 5-dihydroergosterol, zymosterol (toxic at 0·05 mg./10 ml.), calciferol (toxic at 0·025 mg./10 ml.), cortisone, deoxycorticosterone acetate (toxic at 0·05 mg./10 ml.), estrone (toxic at 0·01 mg./10 ml.), ethinyl estradiol (toxic at 0·01 mg./10 ml.), methyltestosterone (inhibitory at 0·025 mg./10 ml.) and diosgenin. Progesterone was so toxic that no growth occurred at the lowest concentration tested—0·005 mg./10 ml. of medium. A compound was judged to be toxic when it completely inhibited growth in the presence of 0·05 mg. cholesterol/10 ml. medium. The significance of the apparent inactivity of the more toxic compounds is doubtful for the same reasons that cause us to doubt the significance of slight activities.

Comparison of the structures of active and inactive compounds leads to the following conclusions:

(1) The oxidation of the hydroxyl group of C3 to a keto group, and the simultaneous shift of the double bond from 5:6 to 4:5 does not affect activity since cholestenone was active.

(2) The configuration of the hydroxyl group at C3 must be *cis* to the C10 methyl group; *epi*cholesterol was inactive.

(3) Esterification of the hydroxyl group destroys activity; none of the cholesteryl esters was active.

(4) Saturation of the 5:6 double bond destroys activity; neither coprosterol nor its C5 stereoisomer, cholestanol, were active. Saturation of the 4:5 double bond of cholestenone likewise destroys activity; cholestanone was inactive.

(5) The side chain of cholesterol may be modified by the addition of an ethyl group at C24, but only one of the two possible C24 stereoisomers resulting is active; the activity of mixed β- and γ-sitosterols occurred at a level indicating activity of β-sitosterol alone.

(6) A vinyl group at C24 is also permissible; fucosterol was active.

(7) Unsaturation of the side chain at C22, 23 destroys activity; stigmasterol was inactive although β-sitosterol (22-dihydrostigmasterol) was active.

(8) Changing the side chain of cholesterol to that of a saponin destroys activity; diosgenin was inactive.

(9) Shortening the side chain of cholestenone to that of deoxycorticosterone acetate or methyltestosterone destroys activity. The other compounds tested differed in more than one respect from active compounds.

DISCUSSION

The physiologic importance of steroids in higher animals is well recognized. However, while steroids are found in many groups of micro-organisms (Deuel, 1951), they do not occur in all micro-organisms. Sifferd & Anderson (1936) isolated significant amounts of a steroid mixture from *Azotobacter chroococcum* which had been grown on a steroid-free medium; Guirard, Snell & Williams

(1946) isolated a steroid fraction from several *Lactobacillus* spp. Yet Anderson, Schoenheimer, Crowder & Stodola (1935), applying even more searching techniques to *Mycobacterium tuberculosis*, were able to confirm the many earlier reports which stated that no steroids could be found in these bacteria. *Corynebacterium diphtheriae* (Chargaff, 1933*b*), the BCG strain of *Mycobacterium tuberculosis* (Chargaff, 1933*a*), and *Bacterium coli* (Behring, 1930) also appear to lack steroids. Heilbron (1942), reviewing the work of his laboratory on the steroid composition of algae, reported that the blue-green algae contained no steroids. It is therefore difficult to postulate a general essential role of steroids in micro-organisms.

Evidence that steroids may nevertheless be essential metabolites for a few micro-organisms has been provided by nutritional experiments. The degree to which such requirements represent a special metabolic evolution will become clearer when more such organisms are known, and when we have some idea of the biochemical role of these compounds. Unfortunately, the demonstration that cholesterol is a necessary ingredient in a medium does not prove that it has a metabolic role within the micro-organism. The toxicity of unsaturated fatty acids was first noted by Hutner (1942) to be annulled by cholesterol, among other compounds. This subject has been discussed in detail recently by Pollock (1949) and by Kodicek (1949). Ordinary bacteriological broths may require the addition of cholesterol solely as a protective agent for sensitive organisms (see Lwoff 1947, on the subject of peptone media for *Moraxella* and *Neisseria*). A medium initially fatty acid-free can be made toxic by unsaturated fatty acids produced by a micro-organism before visible growth has occurred (as *Haemophilus pertussis*, see Pollock, 1949). Organisms which require oleic acid as a growth factor may therefore require cholesterol, or other substances with a similar 'buffer' action, to maintain a low but constant supply of oleic acid. It follows that pure cultures, media of known composition, and knowledge of the specificity of the requirement, are necessary if one is to conclude for a given micro-organism that a steroid is an essential metabolite rather than solely a protective agent.

None of these desiderata has yet been attained in the nutritional studies which indicate cholesterol requirements in amoebae (see Lwoff, 1951). It is difficult to evaluate Devloo's (1938) claim that yeast 'W' required 'biosterol' in the light of present-day steroid chemistry. The specificity studies of Cailleau (1937) on the steroid requirement of a pure culture of *Trichomonas columbae*, however, indicate a true metabolic requirement which may be general in this group of protozoa. *Eutrichomastix colubrorum* (Cailleau, 1938*b*) in pure culture, and *Trichomonas batrachorum* (Cailleau, 1939) and *T. foetus* (Cailleau, 1938*a*) in mixed cultures also required cholesterol. Unpublished data of Hutner and Sanders have confirmed the cholesterol requirement of *T. foetus* in pure culture. The only other steroid-requiring micro-organisms which have been reported are the pleuropneumonia-like organisms studied by Edward & Fitzgerald (1951), which required cholesterol; of the related compounds tested stigmasterol and cholestanol were active.

The metabolic role of cholesterol in these organisms, and in labyrinthula,

is unknown. The specificity of the requirement rules out the possibilities suggested by the activity of cortisone (Gaines, Broquist & Williams, 1951) and dehydro*epi*androsterone (Gaines & Totter, 1950) in replacing leucovorin and pteroylglutamic acid for *Leuconostoc citrovorum* and *Streptococcus faecalis*. Furthermore, folic acid was present in our basal medium for labyrinthula. It is also interesting to note that the specificity of the steroid requirement of *L. vitellina* var. *pacifica* differs from that of *Trichomonas columbae*. *T. columbae* utilized 5:6 saturated sterols, cholesteryl esters and ergosterol as growth factors; labyrinthula did not. Conversion of the C3 hydroxyl group to a keto group destroyed activity for *Trichomonas columbae* but not for labyrinthula. The pleuropneumonia-like organisms of Edward & Fitzgerald utilized cholestanol and stigmasterol, but not cholesteryl esters, ergosterol, or coprosterol, thus exhibiting still another pattern of specificity.

Where does *L. vitellina* var. *pacifica* obtain steroids in nature? This variety was found associated with *Zostera marina*, *Ulva* spp., and material from phytoplankton and zooplankton tows. The common steroids of higher plants (as *Zostera marina*) are the sitosterols and stigmasterol; of these β-sitosterol is active. 'Sitosterol' is also commonly present in the green algae (Heilbron, 1942), including *Ulva lactuca*. Diatoms and bacteria are conspicuous associates of the host plants. The diatom *Nitzschia closterium* contains fucosterol (Heilbron, 1942) which is active. Evidence that bacteria may provide utilizable steroids (though labyrinthula is not phagotrophic) was presented by isolation plates of non-nutrient sea-water agar on which *L. vitellina* var. *pacifica* grew in and around bacterial colonies but not when more distant from bacteria.

We are very grateful to those (indicated in the text) whose generosity in donating steroids made this study possible. We also wish to thank Michael Bach for assistance and Dr S. H. Hutner and Dr W. Vishniac for discussion of this work. The Haskins Laboratories investigations of microbial nutrition are assisted by grants from the Lederle Laboratories Division of the American Cyanamid Co. and the Rockefeller Foundation.

REFERENCES

Anderson, R. J., Schoenheimer, R., Crowder, J. A. & Stodola, F. H. (1935). Die Chemie der Tuberkelbazillen-Lipoide. XL. Über das Vorkommen von Sterinen in Tuberkelbazillen. *Hoppe-Seyl. Z.* **237**, 40.

Baker, P. B. (1949). A rotating test-tube apparatus for experimental fermentations. *Nature, Lond.* **163**, 732.

Behring, H. v. (1930). Enthalten Bakterien Sterine? *Hoppe-Seyl. Z.* **192**, 112.

Cailleau, R. (1937). La nutrition des flagellés tétramitidés. Les sterols, facteurs de croissance pour les trichomonades. *Ann. Inst. Pasteur*, **59**, 7.

Cailleau, R. (1938*a*). Le cholestérol et l'acide ascorbique, facteurs de croissance pour le flagellé tétramitidé *Trichomonas foetus* Riedmuller. *C.R. Soc. Biol., Paris*, **127**, 861.

Cailleau, R. (1938*b*). L'acide ascorbique et le cholestérol, facteurs de croissance pour le flagellé *Eutrichomastix colubrorum*. *C.R. Soc. Biol., Paris*, **127**, 1421.

Cailleau, R. (1939). Le cholestérol, facteur de croissance pour le flagellé *Trichomonas batrachorum*. *C.R. Soc. Biol., Paris*, **130**, 1089.

Chargaff, E. (1933*a*). Über die Lipoide des Bacillus Calmette-Guerin (BCG). *Hoppe-Seyl. Z.* **217**, 115.

CHARGAFF, E. (1933*b*). Über das Fett und das Phosphatid der Diphtheriebakterien. *Hoppe-Seyl. Z.* **218**, 233.

DEUEL, Jr. H. J., (1951). *The Lipids.* I. *Chemistry.* New York: Interscience Pub., Inc.

DEVLOO, R. (1938). Un stérol indispensable à la levure W. *Arch. int. Physiol.* **46**, 157.

EDWARD, D. G. ff. & FITZGERALD, W. A. (1951). Cholesterol in the growth of organisms of the pleuropneumonia group. *J. gen. Microbiol.* **5**, 576.

GAINES, D. S., BROQUIST, H. P. & WILLIAMS, W. L. (1951). Certain relationships between pteroylglutamic acid, citrovorum factor, and cortisone. *Proc. Soc. exp. Biol., N.Y.* **77**, 247.

GAINES, D. S. & TOTTER, J. R. (1950). Pteroylglutamic acid-like effect of dehydro-*iso*androsterone on growth of certain micro-organisms. *Proc. Soc. exp. Biol., N.Y.* **74**, 558.

GUIRARD, B. M., SNELL, E. E. & WILLIAMS, R. J. (1946). The nutritional role of acetate for lactic acid bacteria. I. The response to substances related to acetate. *Arch. Biochem.* **9**, 361.

HEILBRON, I. M. (1942). Some aspects of algal chemistry. *J. chem. Soc.* p. 79.

HUTNER, S. H. (1942). Some growth requirements of *Erysipelothrix* and *Listerella*. *J. Bact.* **43**, 629.

KODICEK, E. (1949). The effect of unsaturated fatty acids on Gram-positive bacteria. *Symp. Soc. Exp. Biol.* **3**, *Selective Toxicity and Antibiotics*, p. 217.

LWOFF, A. (1947). Sur le role du serum dans le développement de *Moraxella lacunata* et de *Neisseria gonorrhae*. *Ann. Inst. Pasteur*, **73**, 735.

LWOFF, M. (1951). Nutrition of parasitic amebae. In *Biochemistry and Physiology of Protozoa*, **1**, 235. New York: Academic Press, Inc.

POLLOCK, M. R. (1949). The effects of long-chain fatty acids on the growth of *Haemophilus pertussis* and other organisms. *Symp. Soc. exp. Biol.* **3**, *Selective Toxicity and Antibiotics*, p. 193.

SIFFERD, R. H. & ANDERSON, R. J. (1936). Über das Vorkommen von Sterinen in Bakterien. *Hoppe-Seyl. Z.* **239**, 270.

(*Received* 18 *August* 1952)

Contribution No. 624

THE FLOW OF A STABLE ATMOSPHERE OVER A HEATED ISLAND, PART I

By Joanne Starr Malkus and Melvin E. Stern

Woods Hole Oceanographic Institution[1,2]

(Manuscript received 5 August 1952)

ABSTRACT

The effect upon a stable atmosphere of a heat source (5–10 km width), which is a specified function of the coordinates, is investigated theoretically. A two-dimensional problem is chosen, with the x-coordinate in the direction of the mean undisturbed surface wind U, and the z-direction vertical. The heat source, a finite-width pulse in x, has maximum amplitude at the ground ($z = 0$) and decays with height. A steady state, in which the heat supplied by the source is continuously carried away downstream, is assumed, and the equations of motion are linearized by the method of perturbations. By Fourier analysis of the pulse function, the perturbation equations are made separable, and solutions for the streamline flow are obtained. It is shown that "lee waves," *i.e.*, extended downstream oscillations in the streamlines, occur only if the undisturbed wind or stability undergoes a change in the vertical. The results of the analysis are compared with observations made over Nantucket Island, a flat sandy strip about 5 km in width.

1. Introduction

A study of the convective motions arising when a stable airstream flows over a localized heat source has been undertaken as part of a broad-scale investigation of atmospheric convection. Interest in the problem began when periodically-spaced rows of small cumuli were frequently observed on sunny summer days. These clouds extended great distances downwind of several islands in the Woods Hole area which are too flat (10–50 m elevation) to act significantly as mountain barriers. The flow of gravitationally stable air over such islands has lent itself to both theoretical and observational analyses, which have proved of meteorological interest for three principal reasons. The first is that an island provides a relatively simple situation for inquiry about the relation between some types of convective clouds and their initial energy sources in organized, unsaturated motions in the sub-cloud layer. The second is that such a flat, isolated segment of terrain offers somewhat controlled conditions under which to study the modification of an air mass as it flows from water onto land, including various coastal phenomena such as the sea breeze; and thirdly, the problem is of interest because of its relation to other superficially quite different meteorological problems, especially that of flow over mountains. As will be seen later, these three aspects become intimately coupled with one another.

Preliminary observational work (Malkus *et al.*, 1949) showed that heating from below was a necessary, but not sufficient, condition for the formation of cloud rows. The regular spacing of the clouds indicated the possibility of wave-like vertical oscillations in the streamlines before condensation, perhaps similar to those in the lee of mountains in which stability is the predominant restoring force. The first theoretical question raised, then, concerns the conditions necessary for the production of "lee waves" in the motion field. It is sought to determine what magnitude and distribution of heating by the island, and what upstream conditions of the air, are required for oscillations of sufficient amplitude to bring about saturation at the wave crests under ordinary moisture distributions. Then, if the air is in addition conditionally unstable (as is frequent in summer in these regions), cumulus clouds may be expected to break out at these spots. It will first be determined whether a perturbation treatment, with use of a fairly simple theoretical model, is able to predict such major features of the flow as the appearance or non-appearance of cloud rows, and the cloud spacing within the rows. These predictions are briefly tested by comparison with observations. Detailed observational studies of a typical island are published elsewhere (Malkus and Bunker, 1952). The answers to the first theoretical questions, and the comparison with observations of these model predictions, lead eventually to the framing of more fundamental questions, primarily concerning the relation between cloud-scale convective motions and the so-called "turbulent ground layer." These questions bear intimately upon each of the three cited aspects of the island problem. In the answers to them, in Part II of this work[3], the several aspects of the problem become unified, and the

[1] Contribution No. 624 from the Woods Hole Oceanographic Institution.

[2] Dr. Malkus is on leave from the Illinois Institute of Technology.

[3] *Ed. note:* Part II will appear in the April 1953 issue of the JOURNAL.

most arbitrary and unrealistic assumptions of the present treatment are removed.

2. The theoretical model

A schematic illustration of the problem is given in fig. 1. A basic premise of the model is that the hydrodynamic equations, without viscosity or turbulence, can be used to predict the mean convective motions. In addition, a two-dimensional, time-independent field of motion is considered, where the x-axis is chosen in the direction of the mean undisturbed wind U, and the z-axis points upward. Physically, the meaning of these assumptions is that the island is very extensive in the direction normal to the mean wind, and that a steady state has been reached in which the heat supplied to the air by the island is continuously carried off downstream or removed by cooler waters. This condition may be expected to prevail near noon on sunny summer days. Since the islands investigated are 5–10 km in width and the wavelengths of the oscillations are rarely longer than this, effects of the earth's rotation are omitted.

The five basic equations which relate the five dependent variables u, w, p, T and ρ, the total (undisturbed plus disturbed) horizontal velocity, vertical velocity, pressure, absolute temperature and density, respectively, consist of two equations of motion, the equation of continuity, the equation of state, and some form of the energy equation. For this latter equation, the first law of thermodynamics is used (similar to the method of Langwell, 1951), and the introduction of heat is achieved therein in a manner which will shortly be discussed in detail. In the problem studied, these equations have the following form:

$$du/dt = -\rho^{-1}\,\partial p/\partial x, \tag{1}$$

$$dw/dt = -\rho^{-1}(\partial p/\partial z) - g, \tag{2}$$

$$\rho^{-1}\,d\rho/dt = -(\partial u/\partial x + \partial w/\partial z), \tag{3}$$

$$p = \rho RT, \tag{4}$$

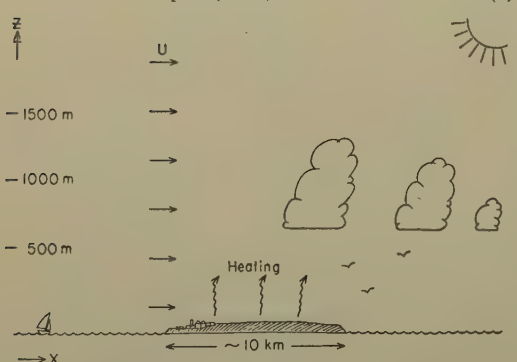

FIG. 1. Schematic picture of airflow over a heated island, showing choice of coordinate axes and typical heights and distances. In corresponding theoretical model, island is assumed to extend infinite distance normal to x-axis.

and

$$V = C_v\frac{dT}{dt} + Jp\frac{d}{dt}\left(\frac{1}{\rho}\right) = C_p\left(\frac{T}{\theta}\right)\frac{d\theta}{dt}, \tag{5}$$

where V is the number of calories per gram per second supplied to the air at a given point, R the gas constant for dry air, J the heat equivalent of work, C_v and C_p are the specific heats of dry air at constant volume and constant pressure, respectively, θ is potential temperature, and the rest of the symbols have their standard meanings.

The following assumptions are now introduced:

$$\begin{aligned} u &= U + u', \quad T = \bar{T} + T', \\ w &= w', \qquad p = \bar{p} + p', \\ \rho &= \bar{\rho} + \rho', \quad V = V', \end{aligned} \tag{6}$$

$$\bar{T} = \bar{T}_0 - \alpha z, \tag{7}$$

$$\partial\bar{p}/\partial z = -\bar{\rho}g, \tag{8}$$

$$\partial(U, \bar{p}, \bar{T}, \bar{\rho})/\partial x = 0, \tag{9}$$

$$\partial(u, w, p, T, \rho; u', w', p', T', \rho')/\partial t = 0, \tag{10}$$

where (6) divides each variable into two components, one representative of the undisturbed flow at great distance upwind of the island, the other due to the perturbation introduced by the heat source. The crux of this assumption is that the rate of heat addition V can be treated as a perturbation quantity V'. This implies that the kinetic energy originally in the basic current is considerably larger than the energy added to the air as it passes over the island. For the island sizes and heating rates considered, this assumption is valid, and the calculated magnitudes of u' and w' further support it. First-order perturbation quantities are represented throughout the analysis by primed symbols. Products of primed quantities and products of their derivatives are thus assumed to be of second order and are neglected. Equation (7) states that the undisturbed temperature decreases with elevation at a lapse rate α, where $\bar{T}_0$ represents the undisturbed temperature at $z = 0$. Equation (8) states that the undisturbed current is in hydrostatic equilibrium; equation (9) requires that the parameters of the undisturbed flow are independent of x, and equation (10) expresses the steady-state hypothesis.

For simplicity in the present derivation, two additional assumptions are made. The first is that the undisturbed wind U is independent of elevation. When the wind-shear terms are carried through, as is readily done, observations show that they are usually considerably smaller than the terms appearing with them, since in this problem only the first 3 km or so of air above the ground are being investigated. The second is the assumption that in the continuity equation (3) the term $\rho^{-1}\,d\rho/dt$ may be neglected.

Physically, this states that the velocity of sound in the fluid is very, very large compared to the basic-current speed U, and that the fluid is compressible only with respect to heating and lifting. Mathematically, it serves to remove those terms containing in their denominators the velocity of sound squared, which terms would anyway be dropped at the end as negligible.

When the foregoing approximations are made, and (6), (8), (9) and (10) are substituted into (1) through (4), the latter become

$$U\,\partial u'/\partial x = -\bar{\rho}^{-1}\,\partial p'/\partial x, \tag{1a}$$

$$U\,\partial w'/\partial x = -\bar{\rho}^{-1}\,\partial p'/\partial z - (\rho'/\bar{\rho})g, \tag{2a}$$

$$\partial u'/\partial x + \partial w'/\partial z = 0, \tag{3a}$$

and

$$\bar{p}' = \rho' R\bar{T} + \bar{\rho} R T'. \tag{4a}$$

By differentiating (1a) with respect to z, and (2a) with respect to x, and using (3a) and (1a), we eliminate the pressure. Then

$$\nabla^2 w' + \frac{\partial w'}{\partial z}\left(\frac{1}{\bar{\rho}}\frac{\partial \bar{\rho}}{\partial z}\right) = -\frac{g}{U\bar{\rho}}\frac{\partial \rho'}{\partial x}, \tag{11}$$

where $\nabla^2 = \partial^2/\partial x^2 + \partial^2/\partial z^2$.

By means of (4a), and use of (7), (8), (1a) and (3a), the density may be eliminated, so that

$$\nabla^2 w' + \frac{\partial w'}{\partial z}\left(\frac{\alpha}{\bar{T}}\right) = \frac{g}{U\bar{T}}\frac{\partial T'}{\partial x}. \tag{12}$$

It is interesting to note that the derivation so far is equally as applicable, except perhaps because of omission of wind-shear terms, to the airflow over mountains as to the heated island. In the mountain problem (see, for example, Scorer, 1949) it is easy to eliminate the temperature perturbation from (12) by means of the adiabatic relation between temperature and pressure changes. In the vicinity of the island, the adiabatic relation clearly does not hold, since heat is being added to the air. The present approach to the island problem involves the introduction of the first law of thermodynamics in the form (5), with the hope that something may be said concerning the distribution of the heating rate V. Another approach attempts to eliminate the velocity perturbation w' in terms of T' (or *vice versa*) by use of the eddy heat-conduction equation. More concerning this method will be said in Part II.

When (5) is expanded by perturbations, and relations (4), (1a), (3a), (7) and (8) are used, the form of the first law of thermodynamics becomes

$$\frac{V'}{C_p} = U\frac{\partial T'}{\partial x} + w'(\Gamma - \alpha) - \frac{JU^2}{C_p}\frac{\partial w'}{\partial z}, \tag{13}$$

where $\Gamma = Jg/C_p$, the dry-adiabatic lapse rate. Solving for $\partial T'/\partial x$ and substituting into (12), one obtains a partial differential equation for w' as a function of x and z, namely,

$$\nabla^2 w' - \frac{\partial w'}{\partial z}s + \frac{gs}{U^2}w' = \frac{gV'}{U^2 C_p \bar{T}}, \tag{14}$$

where $s = (\Gamma - \alpha)/\bar{T} = \bar{\theta}^{-1}\,\partial\bar{\theta}/\partial z$, the undisturbed stability. Scorer (1949) has shown that the $\partial w'/\partial z$ term is unimportant except at great heights, and it is henceforth omitted. At this point, it is convenient to introduce a new dependent variable ψ, so that

$$w' = d\psi/dt = U\,\partial\psi/\partial x, \tag{15}$$

where ψ is the displacement, due to the perturbation, of a streamline from its undisturbed level. The conventional stream function is then $U\psi$, where the undisturbed current U is constant. The differential equation to be solved now becomes

$$\left(\nabla^2 + \frac{gs}{U^2}\right)\frac{\partial\psi}{\partial x} = \frac{gV'}{U^3 C_p T_m}, \tag{16}$$

where $1/\bar{T}$ in the inhomogeneous term has been replaced by $1/T_m$, where T_m is the mean, undisturbed, absolute temperature of the air layer. The stability s is henceforth considered constant. Hence, we have an equation with constant coefficients.

It is not surprising that, except for the inhomogeneous term, equations (14) and (16) are essentially the same as those derived by Queney (1947) and Scorer (1949) for the mountain-wave problem, because the same oscillating system, namely the stable atmosphere, is being described. The new feature introduced is the inhomogeneous term, which is seen to depend upon the time rate of heat addition to each gram of air. It should be noted that the "forcing function" in (16) varies inversely with U, *i.e.*, it will be greater the more time the air spends over the island. To solve the equation, some statement must now be made concerning the dependence of V' upon x and z. Owing to the important role played by this parameter in the physics of the problem, its determination and the implications thereof will be discussed in detail.

3. The form of the heating function

It has been assumed, in this and other similar atmospheric studies where the non-viscous hydrodynamic equations are used, that the mean motion (upon averaging over sufficient time to eliminate turbulent fluctuations) is, at least to a first approximation, streamline in character. This assumption by no means implies, however, that the effects of turbulence upon the motion are insignificant. On the contrary, it is clear from observations that turbulent mixing plays a vital role in the convective processes studied: specifically, it is by eddy transfer that a

large part of the heat energy supplied to the lowest levels of the air is distributed upward, so that it becomes available to cause oscillations of the type to be described. Therefore, while the records show that solar radiation is a necessary condition for convective motions near the island, the energy apparently needs to undergo several transformations before convection can set in. The first step in the transformation is the absorption of the short-wavelength solar radiation by the ground and its re-radiation in infra-red wavelengths. What fraction of this re-radiated energy is made directly available for convection, and what fraction must be spread upwards by turbulence from the surface, is not yet well known; nevertheless, it appears from observation that the formation of a well-mixed layer from the ground up to cloud base (300–800 m) normally precedes the development of cloud-scale convective motions.

At the outset, rather than to become involved with the mechanism of the heat supply, it seems plausible merely to assume *a priori* a reasonable distribution of the heating function V' in space. In this way it may be determined which, if any, significant features of the flow are predictable merely from the presence and magnitude of the heating and the initial air structure, and which require a more exact knowledge of the form and mechanism of the heating. In Part II of this work, the mechanism of the heating is investigated in greater detail, and an attempt is made to predict the distribution of V' in space from physical principles.

For the remainder of Part I, it will merely be assumed that V' depends upon x in such a way as to be positive over the island and zero or negative elsewhere, and decays with z so as to be crudely consistent with the presence of turbulent mixing. While an exponential decay with z is perhaps not the most realistic *a priori* assumption possible, it greatly simplifies the mathematics and therefore will be used in the first examples calculated. The adequacy and implications of this assumption will be examined later, when more realistic heating functions are sought. It is now assumed that

$$V' = Qe^{-z/h}\, q(x), \tag{17}$$

where Q is the amplitude of the heating rate at the surface in calories per gram per second, and will be obtained from observations; h is the height at which the heating rate decays to $1/e$ of its surface value, and may be associated with the thickness of the mixed ground layer. When (17) is introduced into (16), it becomes clear that the choice of $q(x)$ will prescribe the methods which are available to separate the partial differential equation into one or more ordinary differential equations, and thereby to solve the problem. If $q(x)$ is assumed to be a strictly aperiodic function of x, such as, for example, a rectangular or bell-shaped pulse, the evaluation of a Fourier integral will eventually be required. This was the technique used by Queney (1947) and Scorer (1949) in the mountain problem, where in their case the isolated pulse in x (the mountain) served as a boundary condition. In the present problem, the direct evaluation of such an integral proves to be considerably more difficult, however, primarily due to the existence of the inhomogeneous term in the differential equation. A detailed comparison between the problem of the mountain and that of the island is undertaken in Part II of this study.

A type of heating function representing an approximation to the isolated pulse would be a pulse in x which repeats only after great distance. If these heat sources are made sufficiently far apart, the airflow over each "island" may be expected to be little affected by the presence of the neighboring "islands." A function $q(x)$ of this type, being periodic, can be expressed as the sum of a Fourier series and, it is to be hoped, may be well approximated by a not excessive number of terms. Since, with little formal development this method readily lends itself to computation of specific cases, it is now taken up in detail.

4. Solution for a heat source repeating at large intervals in the horizontal

Direct measurements of the form of $q(x)$ over islands have not been made. The degree of resemblance to reality of the flow patterns obtained under various *a priori* assumptions concerning it may provide clues as to its distribution. Furthermore, the detailed shape of $q(x)$ for an island of fixed width should not play a critical role in the solution to the differential equation, since qualitatively similar flow patterns have been observed over islands of widely differing terrain and over the same island as the wind blows in different directions across it (see cases presented in table 2, below, or for more details see observations presented by Malkus and Bunker, 1952). A tentative assumption for $q(x)$, then, could be a rectangular pulse of unit amplitude, width d (island width), repeating after an interval $2L$. The distance between island centers is assumed ten times the width of one island, so that $d/L = \frac{1}{5}$. If the origin of x is chosen at the center of one of the islands, $q(x)$ is an even function and its expansion in a Fourier series is

$$q(x) = \mathrm{Re} \sum_{n=1}^{\infty} \frac{2}{n\pi} \sin \frac{n\pi d}{2L} \exp \frac{in\pi x}{L}, \tag{18}$$

where Re denotes "real part of," $i = (-1)^{\frac{1}{2}}$, and the $n = 0$ term has been omitted, so that an amount of heat energy is removed by the water between islands equal to that supplied by the islands.

The vertical displacement ψ of each streamline is now similarly decomposed into a series of sine and cosine terms, namely,

$$\psi = \mathrm{Re} \sum_{n=1}^{\infty} \psi_n \exp \frac{in\pi x}{L}, \tag{19}$$

where ψ_n is the amplitude of the z dependence of each harmonic of ψ, and is complex. When (19) and (18) are substituted into (17), and this expression is substituted into (16), the following ordinary differential equation for each ψ_n as a function of z is readily obtained:

$$\frac{d^2\psi_n}{dz^2} + \left(\frac{gs}{U^2} - \frac{n^2\pi^2}{L^2}\right)\psi_n = -i\frac{gQ}{U^3C_pT_m}\frac{2L}{n^2\pi^2}\sin\frac{n\pi d}{2L}e^{-z/h}. \tag{20}$$

The solution to (20) is easily reached, and is

$$\psi_n = -iP_n\left[\exp -z/h + C_1 \exp z\left(\frac{n^2\pi^2}{L^2} - \frac{gs}{U^2}\right)^{\frac{1}{2}} + C_2 \exp -z\left(\frac{n^2\pi^2}{L^2} - \frac{gs}{U^2}\right)^{\frac{1}{2}}\right], \tag{21}$$

where

$$P_n = \frac{\dfrac{gQ}{U^3C_pT_m}\dfrac{2L}{n^2\pi^2}\sin\dfrac{n\pi d}{2L}}{\dfrac{1}{h^2} + \dfrac{gs}{U^2} - \dfrac{n^2\pi^2}{L^2}}, \tag{22}$$

and C_1 and C_2 are the (complex) constants of integration. These may be functions of n.

To prescribe the flow, it now only remains to apply the boundary conditions. The lower boundary condition is unequivocal and applicable to all cases considered. It states that, at $z = 0$, each harmonic of ψ is zero at all values of x. To obtain a second relation between C_1 and C_2, an upper boundary condition may be specified. Due to the extremely critical role that the choice of the second boundary condition proves to play in determining the form of the flow, two types of model will be discussed specifically, the first in which the undisturbed current extends unaltered to great heights, and the second in which an alteration in one or more of the parameters (such as wind speed or stability) occurs at some upper elevation.

The model of infinite vertical extent.—Since, in this model, the undisturbed airstream is unbounded in the vertical, an "upper boundary condition" may of necessity be somewhat weak. The requirement that the amplitude of each harmonic of the streamline displacement, ψ_n, remain finite as z becomes very large is an essential one, but unfortunately does not determine a unique relation between C_1 and C_2 of (21) for all values of gs/U^2 for all harmonics. For the higher harmonics (larger wave-numbers), $n^2\pi^2/L^2 > gs/U^2$, so that the exponents in (21) are real. Hence, in this situation, to prevent the solution from becoming very large at large heights, C_1 must be set equal to zero. The most important harmonics in the solution, however, prove to be those lower ones for which $gs/U^2 > n^2\pi^2/L^2$. For these, the exponents are purely imaginary, and neither exponential term in (21) becomes infinite at great heights. Nevertheless, it can be shown that C_1 is also zero for these wave numbers. When the multiplication indicated in (19) is made between each ψ_n and $\exp in\pi x/L$, the two terms

$$\exp in\pi x/L \exp iz[(gs/U^2) - (n^2\pi^2/L^2)]^{\frac{1}{2}}$$

and

$$\exp in\pi x/L \exp -iz[(gs/U^2) - (n^2\pi^2/L^2)]^{\frac{1}{2}}$$

appear. These represent waves in the streamlines which slope in the upstream and downstream directions, respectively. It is for this reason that the former component must be omitted from the solution, for otherwise there is a finite disturbance at an arbitrarily large distance upwind of an island, provided great enough heights are considered. This clearly violates the requirement that the flow be undisturbed far upstream. The result obtained by these considerations[4] is the same as that reached by Queney (1947) and Scorer (1949), following somewhat different reasoning.

Therefore, the complete solution for the infinite model becomes

$$\psi = \sum_{n=1}^{n_1} P_n\left[(e^{-z/h} - \cos Bz)\sin\frac{n\pi x}{L} + \sin Bz\cos\frac{n\pi x}{L}\right] + \sum_{n=n_1+1}^{\infty} P_n\{\exp -z/h - \exp -z[(n^2\pi^2/L^2) - (gs/U^2)]^{\frac{1}{2}}\}\sin n\pi x/L, \tag{23}$$

where $B = [(gs/U^2) - (n^2\pi^2/L^2)]^{\frac{1}{2}}$, and n_1 denotes the highest harmonic for which $gs/U^2 > n^2\pi^2/L^2$. In sample calculations in specific cases, it is found that, for the infinite model, only the first six harmonics of ψ contribute non-negligibly to the result, and for normal values of the parameters $n_1 \approx 20$. Hence, in practice, only the first sum in (23) need be considered.

An example of the flow in the infinite model has been calculated for typical values of the parameters, and the streamlines are plotted in fig. 2. The amplitude at the ground, Q, of the heating function was chosen to correspond to a heat flux into the air of approximately 1.4 cal cm^{-2} min^{-1} ($Q = 2 \times 10^{-4}$ cal g^{-1}

[4] The writers are indebted to Dr. R. S. Scorer for bringing to their attention this very simple way of resolving what had been a perplexing difficulty in this and similar problems.

sec^{-1}) when the height of exponential decay, h, of the heating rate is taken as 1 km, in rough correspondence with the thickness of the mixed layer. Insolation records show that this figure for heating is about the normal maximum near the noon hour on sunny summer days (see Malkus and Bunker, 1952). As a check on these magnitudes, the temperature gradient along the ground which corresponds to this heating rate is readily obtained from (13), since w' vanishes at the surface. It comes out to be $\frac{1}{6}$C per kilometer, which the observations show to be a conservative value, even with such a slow vertical decay of heating.

The most striking feature of fig. 2 is the absence of repeated lee oscillations in the streamline pattern. The question then arises as to whether lee waves may be produced by heating in an infinite layer when the distribution of V' varies considerably from that chosen, or when the heating function has a downwind tilt with elevation, as might well be expected from the configuration of the mixed ground layer. These possibilities are investigated in Part II, when comparison with the airflow over mountains is made. It is found that lee waves may occur at large heights in an infinite layer when the island is sufficiently narrow, but a tilt of the heating function or other changes in its contours will have no such effect. Also of interest in fig. 2 are the orders of magnitude of ψ, w' and u'. The maximum vertical streamline displacement is 115 m and occurs at the 800 m level, just to lee of the island center. The maximum vertical velocity (average value over about 1.5-km horizontal distance) is 18 cm/sec, and occurs at a height of 1 km. The maximum value of u' is at the ground, as expected, and is 1.3 m/sec.

Although it may not necessarily be expected to find lee oscillations in an infinite layer, certain other phenomena commonly associated with differential heating might be anticipated to appear within it, such as a "sea-breeze circulation." It is seen, from the perturbation velocities (arrows) in fig. 2, that the predicted u' and its derivative with x are in the sense exactly opposite to that commonly observed. In the model, the wind near the surface *decreases* as the island is approached from the windward, and *increases* as the lee shore is passed. This "backwards" sea breeze reverses at a height between 600–800 m, which is somewhat higher than the usual level recorded. The height of maximum w' at 1 km is also considerably higher than indicated by observations.

It is interesting to compare the temperature distribution along the ground arising from the heating function assumed in the model and the form of the actual gradients and other features observed in the study of a real island by Malkus and Bunker (1952). Without going into details at present, we may state that the observations immediately indicate several deficiencies in the present assumed distribution of heating. Firstly, the heating in real cases was rarely evident above 1 km. Secondly, the temperature increased far more sharply as the air first crossed the upwind shore of the island. As is well known from other studies of the heating of air at a coast line (Wexler, 1946; Malkus *et al.*, 1951) the temperature increase is very rapid at first, and slows up as the air temperature comes nearer that of the warmed surface. A heating function, therefore, which is sharply positive at the upwind shore, and sharply negative at the lee shore, would probably be a considerably better fit to the observations, and might be expected to lead to a more realistic prediction of the sea breeze. For the moment, however, rather than attempt to guess at or infer a more realistic distribution of heating, which is the main subject considered in Part II, we will first determine whether it is possible, using

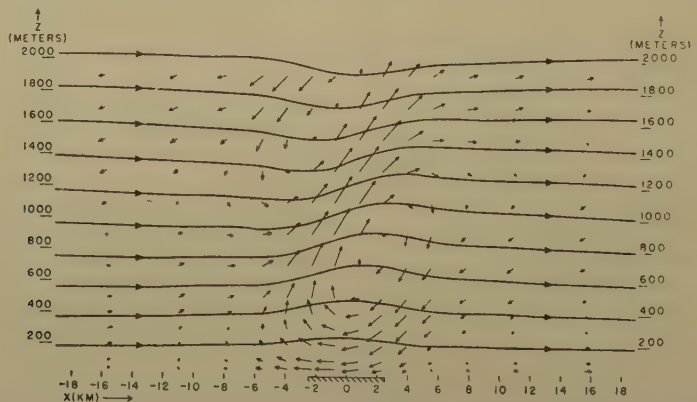

FIG. 2. Flow over island for model of infinite height. Streamlines denoted by heavy solid lines; arrows show perturbation velocities. Vertical scale is exaggerated ten times relative to horizontal. Island is shown by hatched region at base of figure. In this example, pulse function in x repeats after 50-km horizontal distance, and each pulse (island) is 5 km wide. Undisturbed windspeed is 5 m/sec, and undisturbed lapse rate 0.5C per 100 m. Amplitude of heating function corresponds to flux from island to air of 1.4 cal cm^{-2} min^{-1} and was assumed to decay to $1/e$ of surface value at 1 km.

the present assumed heating function, to arrive at a model of airflow over the heated island which gives rise to lee oscillations in the streamlines.

In accord with the experience of Scorer (1949), a variation in the vertical of one or more of the basic-current parameters may next be investigated. A continuous change with height of the stability s, or wind speed U, of (20) would be the most realistic, but the calculation is prohibitive for all but very special variations of the parameters. A two-layer model, with a different value of gs/U^2 in the upper layer from that of the lower, is a second possibility, and the solution to (20) has formally been set up for this situation. Due to the great labor involved in the actual computation, however, and to the fact that the most essential information about this model may, be inferred from a far simpler though less realistic one, only the extreme example of a change in the vertical is considered here, namely an air layer topped by a rigid lid at some height l. This might be thought of as corresponding to the case where the wind speed U becomes extremely large (nearly infinite) at l and above. An infinite U in the upper layer corresponds to a rigid lid, because the amplitude of ψ is proportional to P_n which, in turn, is inversely proportional to U^3. Thus, ψ would be zero in an upper layer of infinite U, which is exactly equivalent, as far as the effect upon the lower layer, to placing a lid or creating a node at $z = l$. The very great alteration in the field of flow which thereby occurs illustrates the critical dependence upon the upper boundary condition of airflow over heat sources of the scale discussed.

The model with a rigid lid at some height l.—In this case, the upper boundary condition is straightforward and merely states that, at $z = l$, $\psi_n = 0$. The complete solution for ψ, if all the other previous conditions remain unaltered, now becomes

$$\psi = \sum_{n=1}^{n_1} P_n\left(\exp -z/h - \cos Bz + C \sin Bz\right) \sin\left(\frac{n\pi x}{L}\right) + \sum_{n=n_1+1}^{\infty} P_n\{\exp -z/h - \exp -z[(n^2\pi^2/L^2) - (gs/U^2)]^{\frac{1}{2}} + C' \sinh z[(n^2\pi^2/L^2) - (gs/U^2)]^{\frac{1}{2}}\} \sin n\pi x/L, \quad (24)$$

where

$$C = (\cos Bl - e^{-l/h})/\sin Bl,$$

$$C' = \frac{\exp -[(n^2\pi^2/L^2) - (gs/U^2)]^{\frac{1}{2}}l - \exp -l/h}{\sinh [(n^2\pi^2/L^2) - (gs/U^2)]^{\frac{1}{2}}l},$$

and n_1 again denotes the highest harmonic for which $gs/U^2 > n^2\pi^2/L^2$. Examination of the coefficient of $\sin Bz$ in the first summation shows that the nature of the solution is now radically altered from what it was for the infinite layer. The denominator of this coefficient is $\sin Bl$, so that the $\sin Bz$ term may reach very large positive or negative values[5] for one or more harmonics of the solution. This may occur for any wave number up to $n = n_1$, and hence all harmonics in the first sum of (24) must be included in the calculation; those where $n > n_1$ again prove to contribute negligibly. Fortunately, for most lid heights between about 1.5–3.5 km, and normal values of stability and wind speed, the harmonics of the solution are amplified relative to one another in such a way as to contribute updrafts over the island and a positive sea-breeze circulation. Computation reveals that those harmonics n_j, which are amplified relative to the others, appear as downstream oscillations or lee waves with the wavelength $2L/n_j$, that is, the lower the harmonic amplified, the longer the lee wave. Since, for those harmonics where $n > n_1$, (24) shows the presence of $\sinh l[(n^2\pi^2/L^2) - (gs/U^2)]^{\frac{1}{2}}$ in the denominator of the $\sinh z[(n^2\pi^2/L^2) - (gs/U^2)]^{\frac{1}{2}}$ term, only a very few harmonics of ψ will become very large in a real case. For conditions the same as those used in fig. 2 (except for the presence of the lid), no harmonics are amplified for lid heights of 0–1.22 km, one for lids between 1.22–2.44 km, two for lids between 2.44–3.66 km, and so forth. It can also be seen by inspection of (24), that when the lid height is kept constant and gs/U^2 is increased, the wavelengths of the amplified harmonics are shortened, as observed, and n_1 is increased, to give more possible superposed wavelengths in the lee waves.

The displacement of the streamlines ψ, and also u' and w', were calculated from (24), with a lid at 2.6 km and the same values of the other parameters as used in fig. 2. The resulting streamlines are shown in fig. 3. The wavelengths of the two amplified harmonics are 2.7 km and 7 km, in this example. The wavelength 2.7 km corresponds very well to the observed spacing of cumulus clouds downwind of the islands on days with conditions similar to those of the model, and the longer superposed wavelength of 7 km might account for the observation that every second or third cloud is frequently taller than its neighbors. The clouds sketched lightly in the figure are merely to indicate where cumuli may find preferred locations and what their relative vertical development may be. It should be remembered that cumulus rows may be expected to appear in the manner indicated only if the air is sufficiently moist and also conditionally unstable. On one occasion, when this latter condition was lacking, eyebrow-like lenticulars appeared in the lee of the island, very much resembling those found

[5] Examination of the Fourier integrals in the case of the isolated island shows that those amplitudes do not become infinite. The orders of magnitude of the streamline displacements in the example to follow in fig. 3 are the same as those indicated by examination of the integrals.

downwind of mountain ridges [see Malkus and Bunker (1952), case of 28 August 1950].

Since the theoretical treatment has considered only unsaturated air, the question must be raised as to how much the condensation process may be expected to alter the flow. Since the small cumuli are observed to form nearly simultaneously, it is reasonable to regard the release of latent heat by each one as a small heat source, proportional in magnitude to the initial lifting. Such small periodic heat sources, placed at the points of maximum lifting, should do nothing more than intensify the perturbation motions existing prior to saturation, much in the manner of a "periodic island" in phase with the existing disturbance.

The magnitudes of ψ, w' and u' in the lid model are of considerable interest. The streamlines, at heights around 600–800 m, experience a total lifting of nearly 500 m. Whether or not this is normally adequate to cause condensation can be seen by reference to the Nantucket Island observations by Malkus and Bunker (1952). It was found that the lifting condensation level for the lowest air varied between 200–400 m, on those days when cumulus rows appeared. The cumulus rows often first formed as early as 0800 to 0900, when the insolation rate had only risen to about half the 1.4 cal cm^{-2} min^{-1} used in construction of fig. 3. That the barrier or mountain effect cannot have had a significant influence in causing these cumulus rows is most strikingly demonstrated by the fact that Nantucket Island never exceeds an elevation of 30 m above sea level. As shown by Scorer (1949), the amplitude of mountain-produced lee waves is roughly equal to the height of the mountain itself. Additional observational evidence of the critical role played by heating in these cases has been presented by

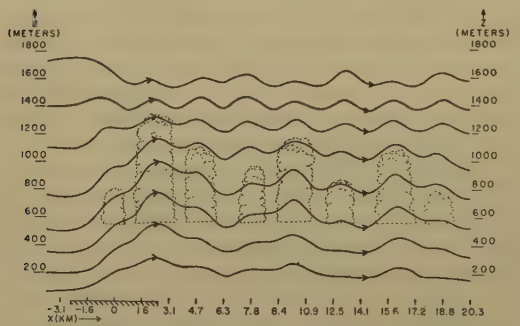

FIG. 3. Streamlines for model with lid at 2.6 km. Values of other parameters same as for case shown in fig. 2. Due to large response of atmosphere to some of higher harmonics in pulse-type heat source, all harmonics up to $n = 20$ were calculated, those higher being shown negligible. Clouds sketched lightly in places where they may be expected to form if sufficient moisture is available. Their development has been indicated in proportion to lifting the air has undergone, maximum lifting of an air parcel being nearly 500 m. Island is indicated by hatched region in lower left of figure. Vertical scale is exaggerated 15.6 times relative to horizontal.

Malkus, *et al.* (1949). The results of the present theory are, therefore, in this respect quite consistent with the observational evidence.

The value of u' at $z = 0$ at the shore of the island (sea breeze) is now about 2 m/sec, and u' and its derivative with respect to x are in the expected sense. The maximum w' is 72 cm/sec, a large increase over the infinite layer. Also significant is the fact that the greatest updraft and the greatest downdraft are found side-by-side, just at the lee shore of the island. To illustrate, table 1 gives the vertical velocities at their height of greatest magnitude, 800 m, as a function of distance downwind from the island center. Even without clouds present, a horizontal shear of vertical wind of 0.8 m sec^{-1} km^{-1} is indicated, of the same order of magnitude as that obtaining across cumuli. When a cloud develops in the updraft, the downdraft and shear may also be expected to be intensified. This factor, added to the fact that the lee shore of the island is the region of greatest turbulence due to minimum low-level stability and maximum passage of the air over the land, might constitute a hazard to low-flying aircraft. An updraft and succeeding sharp downdraft in approximately this position showed up strikingly in several of the 1950 aircraft flights discussed by Malkus and Bunker (1952). In Part II of this paper, the edge region of the island will be considered further.

Considerable physical insight may be gained by analogy between the vertical dimension of the atmospheric problem and the forced oscillations of a flexible string. In this analogue, tension and inertia provide the restoring force. If the string is of infinite extent in one direction, any imposed deformation, composed of any group of wavelengths, merely travels indefinitely without change of speed or shape, after at most one reflection from the node at the fixed end. This corresponds to the infinite layer studied. The lowest levels of the air correspond to those portions of the string near the fixed end, where the wave pattern is caused by superposition of oncoming and reflected wave.

When the string is fixed to a rigid support at the other end, the second boundary also acts as a node and an energy reflector. Those imposed waves for which an integral number of half-wavelengths are contained between boundaries are amplified, and all others diminished by destructive interference. This means that, when a blow which is a composite of many different wavelengths is applied, the string will

TABLE 1. Vertical velocities at 800 m as a function of distance downwind from island center.

	←——Over island——→				←Off shore→	
km downwind:	0	0.8	1.5	2.3	2.9	3.9
w' (cm/sec):	+36	+60	+72	0	−24	−4

TABLE 2. Predicted wavelengths of lee waves *vs.* observed wavelengths.

Date	$s_1 \times 10^7$ (cm^{-1})	U_1 (m/sec)	$\left(\frac{gs}{U^2}\right)_1 \times 10^{10}$ (c.g.s.)	Height of sharpest transition (m)	$s_2 \times 10^7$ (cm^{-1})	U_2 (m/sec)	$\left(\frac{gs}{U^2}\right)_2 \times 10^{10}$ (c.g.s.)	Effective lid height (m)	$\frac{(\eta^2\pi^2/l^2)}{\times 10^{10}}$ ($\eta = 1$)	λ_x Predicted (km)	λ_x Obs. (km)
Aug. 8 1950	1.25	3.0 from North	13.9	1600	to 3 km 1.65	to 3 km 6.5 from North	to 3 km 4.0	2000	2.5	1.8	1.5
Aug. 14 1950	1.00	1.5 from South	44.0	900	to 3 km 1.30	to 3 km 4.0 from South	to 3 km 8	1000	10	1.1	1.0

respond much more markedly to some of its components than to others. This is exactly what happens to the atmosphere in the lid case, the lid providing the upper reflector. Some harmonics in the heat source are responded to far more than others. The problem studied here has one more dimension than that of the string, and the deformation of the streamlines in x may be compared independently to a disturbance on a doubly infinite string. The "bump" in the streamlines is traveling through the air at a speed $-U$. Clearly, deformations with other speeds in x are possible, but this particular one was selected by the steady-state hypothesis. In contrast to two separate strings, however, a relation between the x-wavelength and the z-wavelength of each harmonic of the atmospheric wave is implied. This relation is readily perceived from the first summation in (24). The wavelength of each harmonic in x is

$$\lambda_x = 2L/n, \tag{25}$$

while the wavelength in z, for those harmonics in which the sin Bz term predominates, is very closely

$$\lambda_z \approx 2\pi/B = 2\pi/[(gs/U^2) - (n^2\pi^2/L^2)]^{\frac{1}{2}}. \tag{26}$$

But for these wavelengths, nodes must occur at $z = 0$ and $z = l$; hence,

$$l = \eta\lambda_z/2, \tag{27}$$

where η is an integer whose maximum possible value will be seen to give the greatest number of harmonics which can be amplified.

After combination of (27) and (26) and substitution into (25), the result is

$$\lambda_{\eta x} = 2\pi/[(gs/U^2) - (\eta^2\pi^2/l^2)]^{\frac{1}{2}}, \tag{28}$$

where $\lambda_{\eta x}$ gives the wavelengths of the lee waves and η goes through integral values 1, 2, 3, *etc.*, until the radical in (28) becomes imaginary. It should be noted that, for normal values of gs/U^2 and l^2, η can only go through the values 1 and perhaps 2 before the x-wavelength becomes imaginary, corresponding to an n in (26) giving an imaginary wavelength for λ_z, *i.e.*, $n > n_1$, so that the solution in z is of the exponential form given by the second summation in (24). It is also interesting to note that, as the height of the lid l becomes large, (28) approaches an expression for the wavelength of the oscillations which can be derived immediately from "single parcel" considerations [see, for example, Haurwitz (1941), p. 354, problem 7]. It was qualitative agreement between observed cloud

FIG. 4. Cloud rows of 8 August 1950. Island in foreground is Tuckernuck (see map in fig. 6), small island just west of Nantucket. Camera is pointed SW at 1430 EST from aircraft at about 3000 ft. Cloud row is oriented north-south. Spacing of the clouds was determined from other photographs made from ground camera located on Tuckernuck Island. (After Malkus and Bunker, 1952.)

FIG. 5. Photograph from Tuckernuck Island, looking east-northeast toward Nantucket see (fig. 6), showing major Nantucket cloud row at 1248 EST 14 August 1950. Cloud base is at 450 m. This photograph was used, in conjunction with others made from plane which showed cloud shadows relative to surface landmarks, to determine cloud spacing. (After Malkus and Bunker, 1952.)

spacing and the results of this "parcel equation" which initiated this theoretical study.

The two-layer model, in which a current possessing a different value of gs/U^2 is superposed in place of a lid upon the original basic current considered, would correspond to two strings, tied together end to end, which had different properties, e.g., different mass per unit length. Since partial reflection occurs at the boundary between the two strings, it may be expected for analogous reasons that the solution for the corresponding atmospheric case is qualitatively similar to the lid case just discussed. In other words, when the airstream flowing across the island may be separated into two layers with widely differing mean values of gs/U^2, reflection of energy from the boundary region, and thereby lee waves, might be expected. The writers have shown that these waves will be significant only when gs/U^2 in the upper layer is considerably smaller than in the lower, in agreement with the results of Scorer (1949; 1951).

When, in real cases, the mean value of gs/U^2 in the upper layer is, say, one-half or less than in the lower layer, and the transition is rapid, it may be possible to use (28) to predict the wavelengths of the lee waves to a good approximation by defining an "equivalent lid" height. This hypothesis is based on an analogy with the vibrating string attached to a non-rigid support (or a very massive second string). It is found possible to place an "equivalent rigid support" at some distance beyond the actual end of the string, in proportion to the non-rigidity of the real support. Hence, in the atmospheric case, the "equivalent lid" should be placed somewhat above the transition level, by an amount roughly inversely proportional to the decrease in the quantity gs/U^2. Next, some predictions of wavelengths on this basis are compared with observations.

5. Comparison of predicted wavelengths of lee waves with observations

Of the seven case studies made during the summer of 1950 of a typical small, flat island in the Woods Hole region (reported on by Malkus and Bunker, 1952), only two showed clear-cut examples of lee waves in which the cloud spacing could also be measured with some accuracy. In each of these, there was a rather rapid decrease of gs/U^2 at some height between 1 and 2 km, due in each case to a rather sharp increase in wind speed. These cases are summarized in table 2. The subscript "1" refers to the lower layer, "2" to the upper layer. The stabilities, winds, *etc.* are mean values for the layers indicated, although the variation through each layer was slight. A photograph of the cloud rows on 8 August is shown in fig. 4. Fig. 5 is a corresponding photograph for the 14th, and fig. 6 shows the location of the latter clouds on a map of the island. The dynamics of the individual clouds have been studied, and the results are published elsewhere (Malkus, 1952).

The figures for 14 August 1950 are quite reliable, due to accurate airplane soundings (one made far upwind of the island), pilot-balloon runs by the Woods Hole group, and several checks on the measured cloud spacing. The figures for 8 August are considerably poorer, since radiosondes and radio wind observations had to be called upon as no adequate airplane soundings were available and the pilot-balloon runs ended at 2 km. Furthermore, there were so many clouds on that occasion that their spacing was difficult to determine accurately from the photographs. Nevertheless, the agreement between observed and predicted wavelength is fairly good. It is fortunate that the two cases represent exactly opposite directions of basic-current flow over the island, so that the cloud formations cannot be attributed to topography, warmer downwind waters or any other peculiarity of locale. Furthermore, in one case the upper wind remained in the same direction as the lower and strengthened, and in the other, it completely reversed and strengthened.

In concluding the discussion of the observational checks, we should mention that, in each of the cases presented in table 2, the term in (28) contributed by the "effective lid" is 25 per cent or less of the gs/U^2 term; as good or better agreement with observations of wavelength would have been obtained had the $\eta^2\pi^2/l^2$ term been omitted from (28) entirely, and the simple equation used which is derived from the "single parcel period." Although it may turn out that this simple equation is adequate to forecast wavelengths on most days when lee waves are seen (it will work best when the effective lid is rather high or gs/U^2 in the lower layer large), it is clear that the

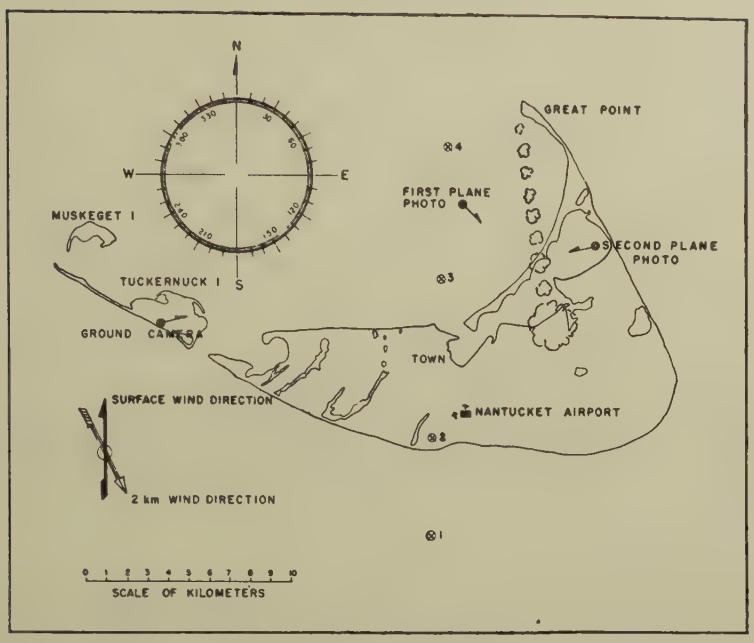

FIG. 6. Map showing major Nantucket cloud row, 14 August 1950. Clouds reconstructed in nearly exact location and to scale. Fig. 5 was taken from Tuckernuck Island (marked "ground camera"), and two aerial pictures (not shown) used in plotting cloud positions were taken from places marked. Helical airplane soundings were made around locations of the numbered crosses, and horizontal traverses were made along line joining them. (After Malkus and Bunker, 1952.)

"parcel method" tells nothing whatsoever about the mechanism of the lee waves, under what conditions they may be excited, or how many wavelengths are present. For these important purposes, an analysis using the equations of motion similar to the present one is required.

6. Conclusion

Rather strong evidence has been presented here that some cumuli, at least, have their origins in organized convective motions in originally unsaturated air, and that a fairly simple perturbation treatment is able to predict some of the important features of these motions. Specifically, the foregoing analysis has succeeded in formulation of several necessary conditions for the formation of waves in the lee of a heated region, such as an adequate-amplitude heating function, and, most significantly, a marked decrease in the air parameter gs/U^2 at an upper level. It has succeeded in a good prediction of the wavelengths when the above conditions have been fulfilled and the presence of lee waves established by the appearance of cloud rows. Conversely, the analysis should also be tested by additional checks to determine whether, on days when other conditions remained favorable (such as heating and moisture distribution) and no cloud rows appeared, such a decrease in gs/U^2 was absent. Unfortunately, the results of such a check were negative. At least two observational case studies were made in which all conditions mentioned, including a decrease in gs/U^2, were met and not a cumulus appeared. Nor did the observations offer any other evidence of lee oscillations. Interestingly enough, these were days on which the turbulent ground layer over the island was noticeably shallow and poorly developed. This failure, and the unrealistic sea-breeze prediction of the infinite layer, must be regarded as serious deficiencies in the present model. The particular places in which this model fails to predict properly point to the main source of its inadequacies, namely the *a priori* assumption of a heating function and its distribution in space. Part II of this work is concerned with remedying this inadequacy and with determining a more realistic distribution of heating by means of physical principles consistent with the presence of a turbulent ground layer. To determine a more satisfactory heating function, the flow over heated islands is related to that over mountains, and thereby a more general discussion is possible concerning the conditions for the formation of lee waves, which have only been illustrated by example in the foregoing work. It will be found that this treatment automatically removes the major deficiencies of the present model and provides greatly increased insight into the airflow over a piece of terrain heated relative to its surroundings.

Acknowledgments.—The writers would like to express their gratitude to the Office of Naval Research, which supported this investigation. The theoretical work was begun under Contract No. Nonr-174(00) with the Illinois Institute of Technology, and continued under Contract No. N6onr-27702(NR-082-021) with the Woods Hole Oceanographic Institution.

They would like to thank Major Philip D. Thompson, USAF, for numerous helpful suggestions concerning the theoretical work. Gratitude is also due Mrs. Mabel Hempstead for carrying out many of the calculations, and Miss Evelyn M. Parker for assistance in preparation of the manuscript.

REFERENCES

Haurwitz, B., 1941: *Dynamic meteorology.* New York, McGraw-Hill Co., 365 pp.

Langwell, P. A., 1951: Forced convection cell circulation in clear air. *Trans. Amer. geophys. Union*, **32**, 7–14.

Malkus, J. S., 1952: The slopes of cumulus clouds in relation to external wind shear. *Quart. J. r. meteor. Soc.*, **78**, 530–542.

——, and A. F. Bunker, 1952: Observational studies of the air flow over Nantucket Island during the summer of 1950. *Pap. phys. Ocean. Meteor., Mass. Inst. Tech. and Woods Hole ocean. Instn.*, **12**, No. 2, 50 pp.

——, and K. McCasland, 1949: *Observational studies of convection.* Woods Hole Ocean. Instn., Ref. No. 49–51, 22 pp.

——, 1951: A formation of pileus-like veil clouds over Cape Cod, Mass. *Bull. Amer. meteor. Soc.*, **32**, 61–66.

Queney, P., 1947: Theory of perturbations in stratified currents with applications to air flow over mountain barriers. *Dep. Meteor. Univ. Chicago, Misc. Rep.*, No. 23, 81 pp.

Scorer, R. S., 1949: Theory of waves in the lee of mountains. *Quart. J. r. meteor. Soc.*, **75**, 41–56.

——, 1951: Forecasting the occurrence of lee waves. *Weather*, **6**, 99–103.

Wexler, R., 1946: Theory and observation of land and sea breezes. *Bull. Amer. meteor. Soc.*, **27**, 272–287.

Contribution No. 625

THE FLOW OF A STABLE ATMOSPHERE OVER A HEATED ISLAND, PART II

By Melvin E. Stern and Joanne Starr Malkus

Woods Hole Oceanographic Institution[1,2]

(Original manuscript received 5 August 1952; revised manuscript received 5 January 1953)

ABSTRACT

In Part I, the convective motions produced by the flow of a stable air stream over a small flat island were studied when the distribution of heating as a function of the coordinates was assumed. In Part II, the mechanism of the heating is examined. It is found that the heat source obeys an eddy-conduction equation and is established by turbulent eddying in the mixed ground layer. The streamline displacement may be divided into two components, one obeying the equation for air flow over a mountain ridge and the other obeying a heat-conduction equation, the latter component being important only in the near vicinity of the island. An "equivalent mountain" corresponding to the heated island may be specified analytically; it depends only upon the temperature distribution along the surface, the wind speed, the eddy conductivity in the ground layer, and the undisturbed stability. Its amplitude is related to the maximum streamline displacement. The "equivalent mountain" for Nantucket Island is calculated for two extreme observational cases. The complete streamline picture is constructed for several examples of an air stream whose properties remain unaltered to great heights. The basic current possessing a change in stability or wind speed at an upper level is also discussed, and the forecasting of lee waves is related to the development of the mixed ground layer *via* the height of the "equivalent mountain." An expression for the sea breeze is also derived.

1. Introduction

The flow of a stable air stream over a flat, heated island has received considerable attention not only because of the rows of cumulus clouds often produced on sunny days, but also because the island serves as a somewhat simplified laboratory to study atmospheric heat transfer and the modification of an air mass as it moves from water to land. A theoretical study (Part I of this work, by Malkus and Stern, 1953) and a detailed observational program (Malkus and Bunker, 1952) precede the present theoretical discussion. At first, the investigations were directed mainly toward determining under what conditions lee waves (made visible as downwind rows of cumuli, if sufficient moisture is present) would be produced.

Preliminary observations showed that the heating of the air by the island was a necessary, but not sufficient, condition. The theoretical work in Part I predicted that the critical factor in the production of lee waves lay in the vertical structure of the air stream before it reached the island; namely, a change with height in the undisturbed wind speed or lapse rate was required. The wavelength of the lee waves was also predicted by this analysis.

The more detailed observational investigation supported the theoretical prediction concerning the wavelengths of lee waves. In part, it also supported the prediction concerning the conditions required for their formation, since on those days when cloud rows were observed, a change was reported in the undisturbed air stream at an upper level. However, many equally sunny days with equal moisture content were studied on which a similar change in the air stream was noted, and not a cumulus appeared. This led to a re-examination of the theoretical model, with a view towards eliminating its most obvious deficiencies. The most serious of these was that the space distribution of heating supplied to the air had had to be assumed *a priori*. In Part I, the "heating function" was taken as a rectangular pulse in the horizontal, coinciding with the extent of the island. Its amplitude was assumed to decay exponentially with height. Although this particular assumption could be shown not to affect the production or non-production of lee waves, nor to influence their wavelengths, it led to several unrealistic features in the predicted flow; namely, it led to a reversed sea-breeze circulation and a vertical-velocity maximum at excessively large heights above the ground.

The purpose of the present theoretical study, therefore, is to remove the *a priori* introduction of the heating function. An attempt is made to solve for its approximate distribution from the eddy-conduction equation. This procedure relates the heat supply for convective motions to a process: small-scale eddying in the ground layer, the mechanism of which can be at least crudely described in terms of such operationally defined parameters as eddy conductivity, wind speed, and lapse rate. It is thus hoped to gain further insight into the relation between convective motions

[1] Contribution No. 625 from the Woods Hole Oceanographic Institution.

[2] Dr. Malkus is on leave from the Illinois Institute of Technology.

and their energy sources in the sub-cloud layer, which may eventually help in the understanding of less restricted meteorological problems. By proceeding thus in the case of the island, it is found that many of the undesirable features of the model presented in Part I automatically disappear.

2. Determination of a more realistic heating function

The equation derived in Part I for the vertical displacement, ψ, of a streamline from its undisturbed level, upwind of the island, is

$$\left(\frac{\partial^2}{\partial x^2}+\frac{\partial^2}{\partial z^2}+\frac{gs}{U^2}\right)\frac{\partial\psi}{\partial x}=\frac{g}{U^2}\frac{V}{c_pT_m}, \qquad (1)$$

where s is the undisturbed stability, assumed constant, U the constant undisturbed wind speed, g the acceleration of gravity, c_p the specific heat of dry air at constant pressure, and T_m is the undisturbed mean absolute temperature of the air layer. V is the rate, in cal g^{-1} sec^{-1}, at which heat is supplied to the air at a point in space. The streamline displacement is simply related to the perturbation vertical velocity w'; namely,

$$w'=d\psi/dt=U(\partial\psi/\partial x). \qquad (2)$$

The conventional stream function is, then, ψ.

The x axis is chosen in the direction of U, and z points vertically upward. The problem has been restricted to two dimensions, by the assumption that the island is very long in the direction normal to the $x-z$ plane; and a steady state is achieved, since the heat is carried off by the current as rapidly as it is supplied. The observations over Nantucket Island have supported the use of these assumptions. For the present analysis, it is more convenient to rewrite the equation in terms of new dimensionless coordinates χ and ζ which are $(gs/U^2)^{\frac{1}{2}}$ times x and z.

The equation thus becomes

$$(\nabla^2+1)\frac{\partial\psi}{\partial\chi}=\frac{V}{c_pT_mUs}\left(\frac{gs}{U^2}\right)^{-\frac{1}{2}}, \qquad (3)$$

where $\nabla^2=\partial^2/\partial\chi^2+\partial^2/\partial\zeta^2$.

In Part I, V was simply assumed to depend on the coordinates in an arbitrary manner; its functional dependence was substituted into the differential equation, and the equation was then solved for the streamline field. It is now appropriate to discuss a mechanism by which a "heating function" for convective motions is produced.

Attention will be temporarily confined to the mixed ground layer, which builds up during the day to a height of several hundred meters above the island. It is well known that, throughout most of this layer, small-scale eddying is the predominant transfer process. It will be assumed that the heating in this region can be described by the eddy-conduction equation. This equation states that

$$K(\partial^2\theta/\partial z^2)=d\theta/dt, \qquad (4)$$

where θ is the potential temperature and K the eddy conductivity, the interpretation of which will be discussed presently. The eddy conductivity can be determined operationally by measurement of the sensible heat fluxes and gradients, or it can be discussed in the framework of mixing lengths and w'', the fluctuations of vertical velocity of the time and space scale corresponding to turbulent eddies. It must be emphasized that the following analysis, using (4) and the coefficient K, is independent of and only subsequently related to the perturbation treatment of ψ and w', the mean convective motions, prescribed by (1), (2) and (3). It is a basic assumption that the convective motions w' and the important turbulent fluctuations w'' are sufficiently separated in scale, so that a space averaging technique which measures w' will almost completely average out w''.

It will also be assumed presently that, in the region over the island where turbulent fluctuations w'' are the most effective transporters of heat, the convective motions w' are small, and that at heights above the ground layer over the island, and at all heights over the water, transports by small-scale eddying are far smaller than they are in the ground layer itself. This means that convective motions in the lee of the island (lee waves) would be adiabatic motions, similar to waves in the lee of mountains. A test of these assumptions would be provided, if the measured K in the lowest several hundred meters (where contributions due to w' are negligible or omitted) were far greater immediately above the island than elsewhere. The Nantucket observations (Malkus and Bunker, 1952) lend strong support to this picture. The K in (4), therefore, is assumed to be the mean value which could be measured for the lowest few hundred meters over the island; the eddy conductivity is assumed to be far smaller than this value elsewhere.

Now, the connection will be made between (4) and (1) and (2). The rate at which heat is added to the air, V, in calories per gram per second, is $c_p(T/\theta)(d\theta/dt)$. This can also be written, to first order, as

$$V/c_p=d\theta/dt=U(\partial T'/\partial x)+w'(\Gamma-\alpha), \qquad (5)$$

where Γ is the dry-adiabatic lapse rate, α the undisturbed lapse rate far upwind of the island, and T' is the temperature perturbation. Physically, (5) is a statement of the first law of thermodynamics, and was introduced as such in Part I. This law states that the thermal energy added to unit mass of air, V, is used in two ways: first, to raise the internal energy of the air, which is made evident as a horizontal temperature increase in the direction of motion; second, in work done upon the surroundings, which appears in the

second term, $w'(\Gamma - \alpha)$, representing an increase in potential energy of the stratified gas.

From (4) and (5), it follows that

$$\frac{V}{c_p} = K\frac{\partial^2 T'}{\partial z^2} = U\frac{\partial T'}{\partial x} + w'(\Gamma - \alpha). \qquad (6)$$

It might appear immediately possible to substitute (6) back into (1) and (2), thus eliminating ψ in terms of T', and thereby deriving a fourth-order differential equation, describing T' as a function of the coordinates. This, however, would imply a K which is characteristic of the undisturbed air stream, and which changes only by a perturbation amount over the island. Observations clearly deny this use of perturbation techniques. They do, however, indicate a better and simpler approach.

At this point, physical knowledge of the ground layer, described previously, can be introduced to advantage; namely, it will be assumed that the temperature field in this region, where V is significantly different from zero, is created and maintained by small-scale turbulence, and is not altered significantly by convective motions of the scale of w'. This implies that, in (6), $w'(\Gamma - \alpha) \ll U(\partial T'/\partial x)$ for this region. This is clearly true at and very near the surface, since most of the convective motions increase upward only very slowly. The Nantucket observations showed that the two terms in (6) might become equal at an elevation of about 500 m. It will be seen that most of the heat supplied the air is furnished considerably below this height. The assumption concerning the relative magnitudes of the two terms $w'(\Gamma - \alpha)$ and $U(\partial T'/\partial x)$ is tested and justified by the work to follow (see especially fig. 11).

Upon omitting the w' term from (6), and differentiating twice with respect to z, we get

$$K(\partial^2 V/\partial z^2) = U(\partial V/\partial x), \qquad (7)$$

or that, over the island, where K is large and w' small, the heating function V obeys an eddy-conduction equation. Outside the ground layer, V is very small, and (6) can be written $U(\partial T'/\partial x) = -w'(\Gamma - \alpha)$, meaning that nearly adiabatic convective motions predominate, and produce the observed horizontal temperature gradients.

In addition, it is seen from (6) that the boundary value of V is simply related to the temperature gradient along the ground, by means of the relation

$$V(x, 0) = c_p U\frac{\partial T'}{\partial x}(x, 0). \qquad (8)$$

The distribution of the heating function throughout the ground layer can, therefore, be specified once the surface temperature-profile is known. It is then possible to obtain the explicit solution for this, and substitute it into the differential equation for w' or ψ, and solve for the field of motion. Actually, with the introduction of Fourier integrals, in the next section, it is seen that this rather prohibitive procedure may be short-circuited. However, a sample distribution of V which is constant along the island surface (in this way similar to the heating function assumed in Part I) has been calculated, and is shown in fig. 1. Even with a rather large value of $a = (K/U)^{\frac{1}{2}}$, it will be seen that most of the heating is achieved in the lowest 500 m. Therefore, although at greater heights the V calculated from (7) may be even 100 per cent in error, this will not appreciably affect the field of mean motion, since it represents a very small fraction of the

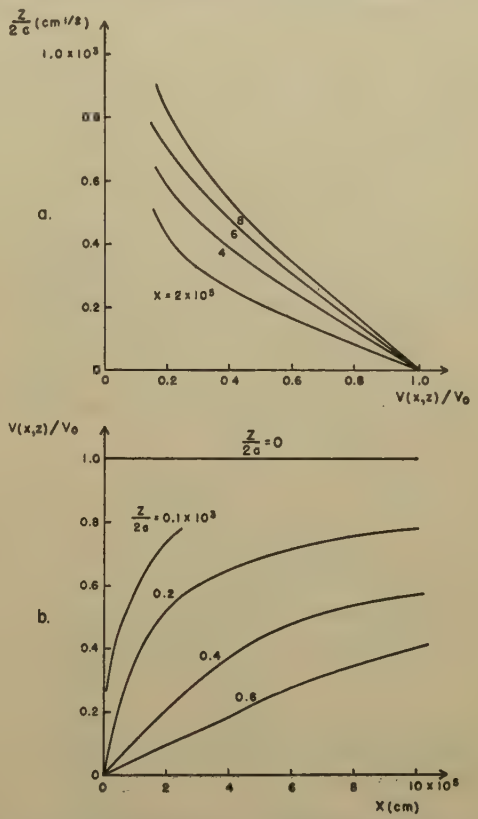

FIG. 1. Height dependence of rectangular-shaped heating function, which has constant value over the island. In top portion, vertical axis is $z/2a$, where $a = (K/U)^{\frac{1}{2}}$. When, for example, $K = 10^6$ cm^2/sec and $U = 2 \times 10^2$ cm/sec, point marked $z/2a = 1.0 \times 10^3$ cm$^{\frac{1}{2}}$ is equivalent to vertical elevation of 1 km. Horizontal axis is ratio $V(x, z)/V_0$, where V_0 is constant value which heating function maintains along island surface. Horizontal distance x is measured in direction of wind, beginning from the windward shore. Note that, due to its downwind slope, heating function decays less rapidly with height as distance from windward edge increases. In bottom portion, vertical coordinate is ratio $V(x, z)/V_0$, and horizontal coordinate is x, distance downwind from windward shore, in centimeters. Although this figure only shows behavior of heating function over island, its values over downwind waters could also be obtained from solution of (7), and are illustrated for differently shaped heating-function in fig. 11.

thermal energy that is added to the air. Other examples of different heating functions are given later in this paper (see fig. 11), as well as more details concerning the solution of (7).

Finally, (7) is rewritten in terms of the new coordinates, χ and ζ; namely,

$$\partial V/\partial \chi = b^2(\partial^2 V/\partial \zeta^2), \tag{9}$$

where $b^2 = a^2(gs/U^2)^{\frac{1}{2}}$, $a^2 = K/U$, and the boundary condition (8) in the new coordinates is

$$\frac{V}{c_p}(\chi, 0) = \left(\frac{gs}{U^2}\right)^{\frac{1}{2}} U \frac{\partial}{\partial \chi} T'(\chi, 0). \tag{10}$$

3. Solution of the equation

To separate (3) into an ordinary linear differential equation, the χ-dependence of V, ψ and T' will be defined as a sum of periodic functions, by means of Fourier integrals in the form

$$V = \mathrm{Re} \int_0^\infty e^{ik\chi} \bar{V}(k, \zeta)\, dk, \tag{11}$$

where Re denotes "real part of"; k is the angular frequency of each "harmonic," or 2π divided by the wavelength, and $\bar{V}$, $\bar{\psi}$ and $\bar{T}$ are the amplitudes of the ζ dependence of each harmonic of the heating function, streamline displacement, and temperature, respectively.

If the relations typified by (11) are substituted into (3) and (9), they become

$$\left(\frac{d^2}{d\zeta^2} + 1 - k^2\right) ik\bar{\psi} = \frac{1}{UsT_m} \frac{\bar{V}}{c_p}, \tag{12}$$

and

$$\left(b^2 \frac{d^2}{d\zeta^2} - ik\right) \bar{V} = 0. \tag{13}$$

The thermal boundary condition becomes

$$\frac{\bar{V}}{c_p}(k, 0) = U\left(\frac{gs}{U^2}\right)^{\frac{1}{2}} (ik)\, \bar{T}(k, 0). \tag{14}$$

The upper boundary condition to be applied to (13) is that $\bar{V}$ should be bounded at great heights. Its solution then becomes

$$\frac{\bar{V}}{c_p}(k, \zeta) = U\left(\frac{gs}{U^2}\right)^{\frac{1}{2}} ik\, \bar{T}(k, 0)\, e^{\frac{-i^{\frac{1}{2}}k^{\frac{1}{2}}\zeta}{b}}, \tag{15}$$

where $i^{\frac{1}{2}} = \exp(\frac{1}{4}\pi i)$. It is important to note that, similar to the assumed heating function in Part I (Malkus and Stern, 1953), the heating function of (15) also decays exponentially with height. The rate of decay, however, is now dependent upon the scale of the heating function, in that the higher the "harmonic" or the shorter the wavelength, the more rapidly it dies out with elevation. The heating declines more slowly with height, the larger the eddy conductivity, *i.e.*, the greater the development of small-scale turbulence, and more rapidly the greater the wind speed U. Also, each harmonic of the heating function described by (15) has a forward tilt with elevation, proportional to its rate of decay with height. These features are in excellent agreement with the behavior of the mixed ground layer revealed by the Nantucket observations (Malkus and Bunker, 1952), and represent immense improvement over the assumed heating function of the earlier theoretical treatment presented in Part I. A typical example of the space dependence of the heating function has been illustrated in fig. 1. Note, in contrast to the heating function of Part I, that the decay with z is much more rapid for all normal values of $a = (K/U)^{\frac{1}{2}}$, and that the rate of vertical decay now depends upon x.

Upon substitution of (15) into (12), the differential equation for $\bar{\psi}$ becomes

$$\left(\frac{d^2}{d\zeta^2} + 1 - k^2\right)\bar{\psi} = \frac{\bar{T}(k, 0)}{sT_m} e^{\frac{-i^{\frac{1}{2}}k^{\frac{1}{2}}\zeta}{b}}, \tag{16}$$

where $\bar{\psi}$, the height dependence of the amplitude of each harmonic of the displacement, is now expressed in terms of the temperature profile along the ground.

Equation (16) is a simple second-order equation in ζ, with an exponential forcing function, of the same type as the equation for each "harmonic" solved in Part I. When (16) is solved for $\bar{\psi}$, and the solution is substituted into (11), the result is

$$\psi = \mathrm{Re} \int_0^\infty e^{ik\chi} \bar{M}(k) \left[e^{\frac{-i^{\frac{1}{2}}k^{\frac{1}{2}}\zeta}{b}} - f(\zeta, k)\right] dk, \tag{17}$$

where

$$\bar{M}(k) = \frac{1}{sT_m} \frac{\bar{T}(k, 0)}{(ik/b^2) + 1 - k^2}, \tag{18}$$

and $f(\zeta, k)$ is a linear combination of $\exp[-\zeta(k^2-1)^{\frac{1}{2}}]$ and $\exp[\zeta(k^2-1)^{\frac{1}{2}}]$, *i.e.*, the solution of the homogeneous part of (12). The particular linear combination for $f(\zeta, k)$ depends on the boundary conditions. For flat islands, it is required that the displacement of the streamlines be zero at the ground; therefore $f(0, k) = 1$.

Equation (17) is now separated into two parts; namely, $\psi = \psi_1 - \psi_2$, where

$$\psi_1 = \mathrm{Re} \int_0^\infty e^{ik\chi} \bar{M}(k)\, e^{\frac{-i^{\frac{1}{2}}k^{\frac{1}{2}}\zeta}{b}}\, dk, \tag{19}$$

and

$$\psi_2 = \mathrm{Re} \int_0^\infty e^{ik\chi} \bar{M}(k)\, f(\zeta, k)\, dk. \tag{20}$$

In the particular case where there is no change in the undisturbed wind speed and stability in the vertical (infinite model), $f(\zeta, k)$ is determined by a "weak" boundary condition, namely, that there shall be no disturbance at large heights far upstream (see Malkus and Stern, 1953; also Queney, 1947; Scorer, 1949).

Then

$$\psi_2 = \mathrm{Re} \int_0^\infty e^{ikx} e^{-ik(1-k^2)^{\frac{1}{2}}} \bar{M}(k)\, dk. \qquad (21)$$

Returning to the more general solution given by (19) and (20), we readily see that these functions satisfy the relations

$$\mathrm{I}\begin{cases} \left(b^2 \dfrac{\partial^2}{\partial \zeta^2} - \dfrac{\partial}{\partial \chi}\right)\psi_1 = 0, \\ \psi_1(\chi, 0) = M(\chi), \end{cases} \quad \mathrm{II}\begin{cases} (\nabla^2 + 1)\psi_2 = 0, \\ \psi_2(\chi, 0) = M(\chi) \end{cases} \qquad (22)$$

where

$$M(\chi) = \mathrm{Re} \int_0^\infty e^{ik\chi} M(k)\, dk$$

$$= \frac{1}{sT_m} \mathrm{Re} \int_0^\infty \frac{e^{ik\chi} \bar{T}(k, 0)}{(ik/b^2) + 1 - k^2}\, dk. \qquad (23)$$

The function $M(\chi)$ is computed from a knowledge of the temperature distribution along the surface, and is called the "mountain function" because the perturbation ψ_2 is the same as that which would be produced by a mountain of shape $M(\chi)$ placed along the ground. To obtain the total solution, one subtracts this from the solution of the conduction equation, ψ_1. This solution is known from the literature (see Carslaw, 1945), and is

$$\psi_1 = \frac{2}{\pi^{\frac{1}{2}}} \int_{\frac{1}{2}\zeta b^{-1}\chi^{-\frac{1}{2}}}^\infty M\left(\chi - \frac{\zeta^2}{4b^2\eta^2}\right) e^{-\eta^2}\, d\eta. \qquad (24)$$

The solution ψ_1 is characterized by a rapid decay in the vertical and horizontal, and therefore contributes to the convective motions only in the very near vicinity of the island. It is important, because its presence is the principal difference between the mountain problem and the heated-island problem. It enables the boundary condition at the ground, namely, $\psi = 0$, to be fulfilled, while the flow at greater distances from the island is dominated by ψ_2, the mountain component.

Considerable information about ψ may be gained without detailed calculation, by examination of $M(\chi)$, the mountain function. The nature of the flow may then be visualized, and computations made by reference to the literature on air flowing over a mountain (Queney, 1947, 1948; Scorer, 1949). Since ψ_2, the mountain solution, is subtracted from ψ_1, the heat-conduction solution, the "equivalent mountain" may be thought of as upside down, or to correspond to a depression in the ground. This clearly must be the case, as downdrafts are needed near the ground to cancel the updrafts produced by the heating, that are given by ψ_1. Since the mountain solution oscillates between positive and negative values with height (see, for example, Queney, 1948, fig. 2), the total solution will show updrafts increasing upwards, as expected.

4. The equivalent mountain

The work in the preceding section has shown that those air motions not confined to the immediate vicinity of the island will come from the mountain component ψ_2 of the solution. Therefore, to predict the presence and development of lee waves and downwind rows of cumuli, it is this part of the solution which must be examined. The mountain function is now evaluated from (23). For broad islands and large values of $b^2 = (K/U)(gs/U^2)^{\frac{1}{2}}$, the largest harmonics of the integrand in (23) are clustered about $k = 0$, so that $(ik/b^2) + 1 - k^2 \approx 1$, and

$$M(x) = T(x, 0)/(\Gamma - \alpha). \qquad (25)$$

Hence, in these cases, the mountain is geometrically similar to the temperature profile and is $1/(\Gamma - \alpha)$, or about 0.2×10^5, times as high in centimeters as T exceeds the water temperature in degrees (or from 200–1000 m tall). The height and shape of the mountain are, under these conditions, unaffected by the

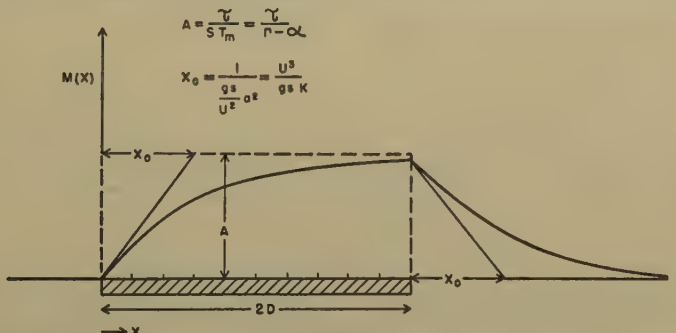

FIG. 2. Equivalent mountain corresponding to rectangular-shaped temperature profile. Elevation of mountain $M(x)$ as function of x is shown by heavy line. Vertical scale, in centimeters, may be determined in a particular case by solving for $A = \tau/\Gamma - \alpha$, where τ is amount by which island surface temperature exceeds that of water. Distance of exponential decay, $x_0 = U^3/gsK$ cm, in this example is 0.3 times island width $2D$. This would represent distance of 3 km if $2D$ were 10 km, $U = 2$ m/sec, $s = 10^{-7}$ cm^{-1} and $K = 2.6 \times 10^5$ cm^2/sec, which are typical values of parameters. For 2C temperature elevation of island, maximum height reached by "mountain" would be 667 m.

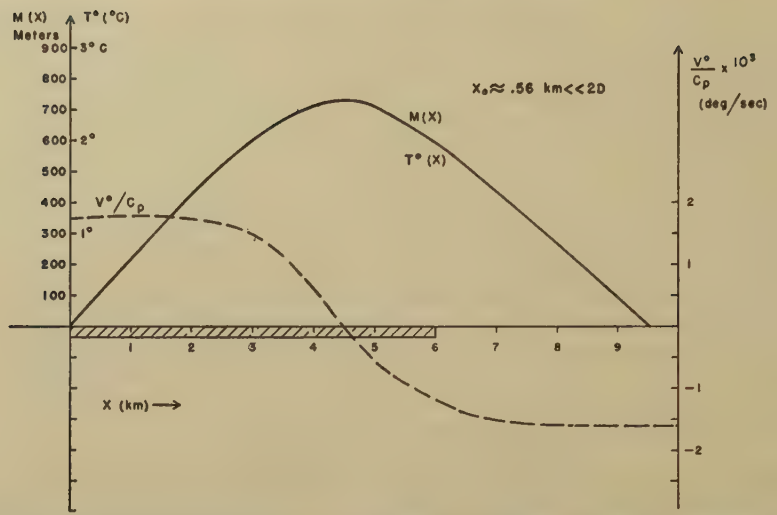

FIG. 3. Equivalent mountain for Nantucket Island on 14 August 1950 (Case 4 studied by Malkus and Bunker, 1952). $T^\circ(x)$ was observed temperature profile along island surface. Mountain function $M(x)$ is shown to have similar shape, due to small value of x_0. Value of V°/c_p, heating function along ground divided by specific heat of air at constant pressure, was calculated from observed values of $U\,\partial T'/\partial x$ along surface. Horizontal extent of island is shown by hatched region.

eddy conductivity K and the wind speed U, provided, of course, that b^2 is large enough and the island broad enough for the approximation to hold. When the island is not broad and/or b^2 not large, so that the above approximation is no longer valid, the mountain slope is distorted from that of the temperature profile, and its height is reduced. It is then necessary to evaluate (23) more exactly. This may be done by using the Fourier convolution theorem (see, for example, Sneddon, 1951), which for present purposes may be stated as

$$\mathrm{Re}\int_0^\infty e^{ikx}\,\bar{T}(k,0)\,\bar{g}(k)\,dk = \int_{-\infty}^{\infty} T^\circ(x-\xi)\,g(\xi)\,d\xi, \quad (26)$$

where $T^\circ(x)$ is the temperature excess along the ground, and where

$$\bar{g}(k) = \int_{-\infty}^{\infty} e^{-ik\xi}\,g(\xi)\,d\xi = \frac{1}{(ik/b^2)+1-k^2}. \quad (27)$$

It is then simple to solve for $g(\xi)$, by inverting (27) and evaluating the integral in the complex k plane. The integral in (23) then finally becomes

$$M(x) = \frac{1}{sT_m}\,\frac{2b^2}{(1-4b^4)^{\frac{1}{2}}}\int_0^\infty e^{-\xi/2b^2} \times\left[\sinh\xi\,\frac{(1-4b^4)^{\frac{1}{2}}}{2b^2}\right] T^\circ(x-\xi)\,d\xi. \quad (28)$$

Therefore, the mountain function is specified once T°, the temperature excess along the ground, is known. For a constant temperature excess, the integral is readily evaluated; for other profiles, the procedure becomes quite laborious. The constant temperature excess is therefore chosen in illustration of the major features of the flow and of the effect of the various parameters thereupon, and it is assumed for the present that

$$T^\circ(x) = \begin{cases} 0 & x<0 \\ \tau & \text{for } 2d>x>0 \\ 0 & x>2d \end{cases}, \quad (29)$$

where the windward edge of the island is placed at $x=0$; its length is $2d$, and it has a constant temperature excess τ. Then (28) becomes

$$M(x) = \frac{\tau}{sT_m}\,\frac{2b^2}{(1-4b^4)^{\frac{1}{2}}}\begin{cases}\displaystyle\int_0^x e^{-\xi/2b^2}\left[\sinh\xi\,\frac{(1-4b^4)^{\frac{1}{2}}}{2b^2}\right]d\xi & \text{for } x\le 2d, \\ \displaystyle\int_{x-2d}^x e^{-\xi/2b^2}\left[\sinh\xi\,\frac{(1-4b^4)^{\frac{1}{2}}}{2b^2}\right]d\xi & \text{for } x\ge 2d,\end{cases} \quad (30)$$

$$= \frac{\tau}{sT_m}\,\frac{2b^4}{\beta}\left[\frac{e^{-\xi(1+\beta)/2b^2}}{1+\beta} - \frac{e^{-\xi(1-\beta)/2b^2}}{1-\beta}\right]_{\text{limits}}, \quad (31)$$

where $\beta = (1 - 4b^4)^{\frac{1}{2}}$. The Nantucket observations have indicated b^2's ranging from 0 to 0.3. Therefore, we first investigate the form of the equivalent mountain when $4b^4 \ll 1$, and then show that for larger values the solution approaches the simple result given by (25). When this approximation is made, the equivalent mountain shape becomes

$$M(\chi) = \frac{\tau}{sT_m} \begin{cases} 1 - e^{-\chi b^2} & \text{for } \chi \leq 2d, \\ e^{-\chi b^2}(e^{2db^2} - 1) & \text{for } \chi \geq 2d, \end{cases} \tag{32}$$

after introduction of the limits indicated in (30). Finally, by replacing the dimensionless units by c.g.s. units and returning to the coordinates x and z, we get

$$M(x) = \frac{\tau}{\Gamma - \alpha} \begin{cases} 1 - e^{-xa^2 gs/U^2} & \text{for } x \leq 2D, \\ e^{-xa^2 gs/U^2}(e^{2Da^2 gs/U^2} - 1) & \text{for } x \geq 2D, \end{cases} \tag{33}$$

where $2D = 2d/(gs/U^2)^{\frac{1}{2}}$ is the width of the island in centimeters, and $a^2 = K/U$. An illustration is given in fig. 2. The amplitude of the mountain is given by

$$A = \tau/sT_m = \tau/\Gamma - \alpha, \tag{34}$$

and its shape is determined by the parameter

$$x_0 = \frac{1}{(gs/U^2)a^2} = \frac{U^3}{gsK}, \tag{35}$$

where x_0 is the conventional decay distance of an exponential function. If, for example, $U = 2$ m/sec, $s = 10^{-7}$ cm^{-1} and $K = 2.67 \times 10^5$ cm^2/sec, $b^2 = 0.067$ and $x_0 = 3$ km. This corresponds to the example in fig. 2, if $2D = 10$ km. Therefore, the elevation of the mountain becomes proportional to the excess ground temperature at about 3 km downwind of the windward shore. It is important to note that changes in wind speed or eddy conductivity change x_0, but not A. Hence, to summarize, when $x_0 \ll 2D$, corresponding to the broad island discussed previously, the mountain shape and height are determined completely from the temperature profile along the ground and the undisturbed lapse rate α, and are independent of the detailed features of the mixed ground layer. When x_0 is comparable to $2D$ but smaller, as in the example presented in fig. 2, (33) shows[3] that the conductivity and wind speed change the shape of the windward and leeward slopes of the mountain, but its maximum height changes only insignificantly. When x_0 approaches and exceeds $2D$, the maximum height of the mountain becomes appreciably less than A, and x_0 dominates. Since the wind-speed cubed enters x_0, and the conductivity enters only to the first power, it appears justified to have used a constant mean value of the latter for the lowest layers. The maximum displacement of the mountain may be computed without recourse to the eddy conductivity, where the following condition is fulfilled: $K > U^3/2Dgs$. Two examples of the mountain function for actual cases are shown in figs. 3 and 5.

5. Discussion of the mountain function in actual cases

The mountain function was calculated for two real cases, which probably represent extremes. The pertinent parameters, observed or calculated from observations, for these cases are shown in table 1. Each case is discussed in detail by Malkus and Bunker (1952), and the first one (14 August) has already been partially described in Part I of this paper.

In Case 4, x_0 is much less than the island width. $M(x)$ can therefore be calculated directly from the

[3] Since x_0 decreases as b^2 increases, by the time $4b^4 \approx 1$ the edge effect is already confined to very small regions around the shores. Therefore, the correction required by the failure of the approximation $4b^4 \ll 1$ would produce a secondary effect which is so small that it can hardly be shown on the scale of the diagrams.

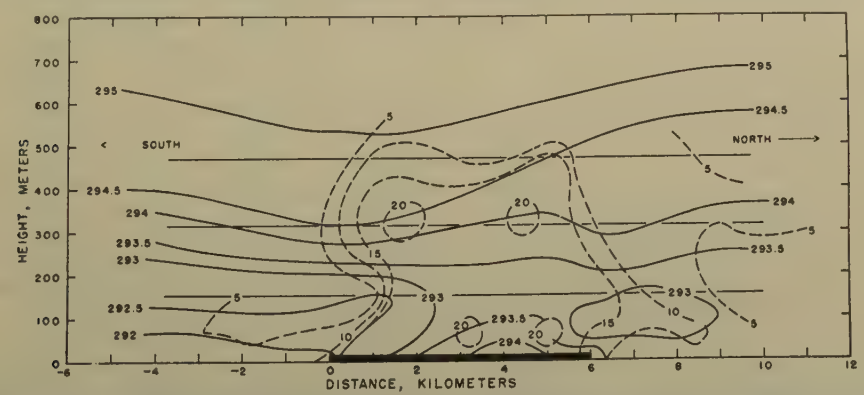

Fig. 4. Observed cross-section of air over Nantucket Island from which fig. 3 was constructed, made from horizontal airplane traverses across island. Potential-temperature isotherms are solid lines; dashed lines are isopleths of turbulence index (taken from airplane accelerometer record; exact definition of this property is given by Malkus and Bunker, 1952). Note high elevation reached by large values of turbulence, indicating deep mixed ground layer. [After Malkus and Bunker (1952).]

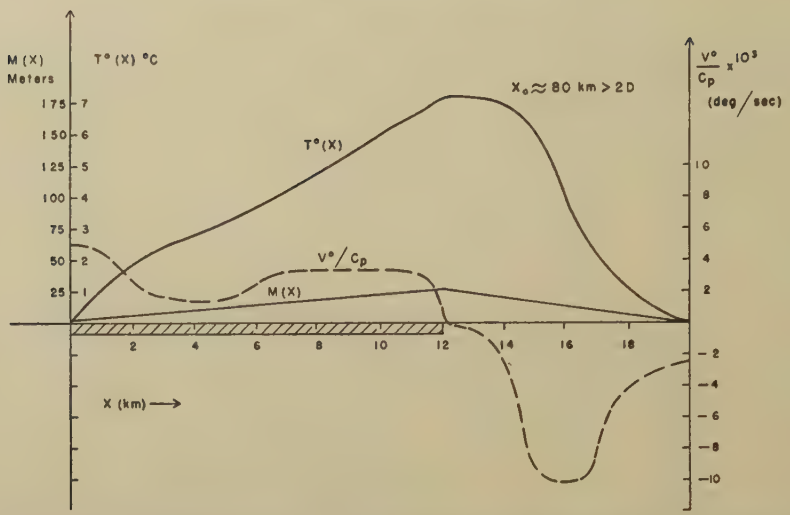

FIG. 5. Equivalent mountain for Nantucket Island on 9 August 1950 (Case 3 studied by Malkus and Bunker, 1952). Observed temperature profile along ground, $T°(x)$, is given by heavy solid line. Heating function along the ground divided by specific heat at constant pressure, $V°/c_p$, was calculated from observed surface values of $U\,\partial T'/\partial x$ and is shown by dashed line. Extent of island is indicated by hatched region.

observed $T°$, with use of (25), and has the same shape as the $T°$ profile. The observed distribution of surface temperature, the resulting mountain function, and the heating function along the ground are shown in fig. 3. The height to which the equivalent mountain rises is about 700 m, somewhat higher than the sample mountains used by Scorer (1949) in his discussion of lee waves. Fig. 4 shows the cross section of the air over the island, observed by Malkus and Bunker (1952), from which the calculations were made. This was a day of a notably deep and well-developed mixed layer,

TABLE 1. Summary of observed cases.

Case	$\alpha = -\frac{\partial T}{\partial z}$ (deg C/cm)	$s = \frac{\Gamma - \alpha}{T_m}$ (cm^{-1})	U (m/sec)	K (cm^2/sec)	x_0 (km)	$2D$ (km)	$A_{max} = \frac{\gamma_{max}}{\Gamma - \alpha}$ (m)
Case 4, 14 August 1950	0.72×10^{-4}	10^{-7} (lowest km)	1.5	6×10^5	0.56	≈10	700
Case 3, 9 August 1950	-2.7×10^{-4}	10^{-6} (lowest 150 m)	9.0	1×10^5	80	≈20	135

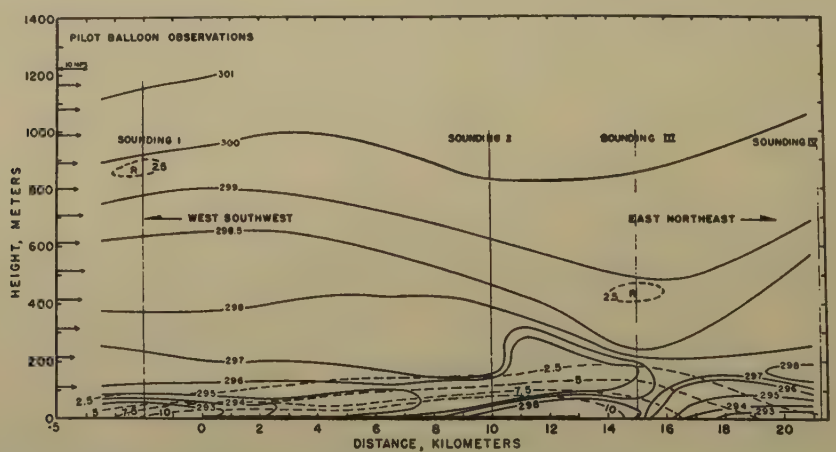

FIG. 6. Observed cross-section of air over Nantucket Island from which fig. 5 was constructed, made from four spiral airplane soundings whose central positions are shown by light vertical lines. Potential-temperature isotherms are solid lines; lines of constant turbulence index are dashed. Note low levels to which the turbulence is confined, indicating only very shallow mixed ground layer. [After Malkus and Bunker (1952).]

and light winds. The effects of surface heating were noticeable on the airplane soundings up to 1.1 km. As was brought out in Part I (see especially figs. 5 and 6 therein), the best cloud rows of the 1950 season were observed on this day.

Case 3 provides a marked contrast. The value of x_0 far exceeds the island width $2D$. Strictly speaking, since the observed temperature profile (see fig. 5) was not rectangular in shape, the derived method for finding $M(x)$ does not apply. However, an upper limit for it is readily set. If the observed temperature profile, with a maximum of 7C, is replaced by a rectangular profile of height 5C, the amplitude of the mountain, from (34), is 135 m. $M(x)$ would reach 0.72 of this value at 80 km, or 25 m at 20 km. The height of the equivalent mountain, therefore, cannot exceed 25 m, and is so drawn in fig. 5. The values of the heating function along the ground, computed from $U\,\partial T'/\partial x$, are also shown. Although the heating at the surface was far greater in this case than in the one preceding, the airplane soundings showed that most of the heating was confined to the lowest 200–300 m of the air. Therefore, it is probable that the total flux of sensible heat from island to air was roughly the same in the two cases, a supposition supported by the soundings and the records of a heat-flux recorder operated at the ground. Fig. 6 shows the observed cross-section of the air over the island, from which the calculations were made. The day was notable for the shallow, weakly developed ground layer, strong low-level stability, and high southwest wind. No cumulus clouds formed in the vicinity of the island.

6. Streamlines of the airflow over a broad island when the undisturbed wind speed and stability are constant

It has been shown that the streamline flow may be determined by subtracting a mountain solution from a heat-conduction solution. The mountain solution is determined, in principle, once $M(x)$ is obtained. Queney (1948) has shown that, when the half-width of the mountain is small compared to $(gs/U^2)^{-\frac{1}{2}}$, a system of stationary waves appears in the lee of the mountain. However, when the half-width becomes large compared with this number (and Coriolis forces can be neglected), the waves in the lee become negligibly small and do not appear until increasingly large elevations are attained, so that the significant motions become confined to the region above the mountain. There is an oscillation in the displacement of the streamlines from positive to negative with elevation, the amplitude of which is roughly equal to the height of the mountain. For an island in the Cape Cod group, the corresponding mountain half-width is about 5×10^5 cm, and $(gs/U^2)^{\frac{1}{2}}$ ranges from 3×10^{-5} to 7×10^{-5} cm^{-1}. Since the product of these numbers is much greater than unity, the flow pattern ordinarily will be of the second type.

Fulfillment of the foregoing criterion for the large half-width is tantamount to setting $\exp[-i\zeta(1-k^2)^{\frac{1}{2}}] \approx \exp(-i\zeta)$ in (21). It is to be emphasized that this simplification is in no way vital to the theory presented, since it is readily shown that the necessary correction up to the greatest altitudes ($\approx$3 km) for which the streamlines have been computed is quite negligible, while the disturbances at greater heights are deducible from the work of Queney. The mountain component of the solution, ψ_2, is then, for present purposes,

$$\psi_2 = \mathrm{Re}\, e^{-i\zeta} \int_0^\infty e^{ikx}\, \bar{M}(k)\, dk. \tag{36}$$

Upon substitution of $\bar{M}(k)$ from (18), this may be written as

$$\psi_2 = (\tau/sT_m)(\cos\zeta\ \mathrm{Re}\, I + \sin\zeta\ \mathrm{Im}\, I), \tag{37}$$

where

$$I = \frac{1}{\tau}\int_0^\infty \frac{e^{ikx}\,\bar{T}(k,0)}{(ik/b^2)+1-k^2}\,dk. \tag{38}$$

In (37), Re I denotes the real part of the integral I, and Im I the imaginary part. From (23), it is seen that Re I is proportional to the mountain function $M(\chi)$, of which a number of examples have already been given. Therefore, it is only necessary to calculate the component Im I, which is of great importance in determining the sea breeze, as will be seen later. In evaluation of (38), the same distribution of temperature along the ground as given by (29) will be used, except that the origin $\chi = 0$ is now placed at the island center. Since

$$T^\circ(\chi) = \mathrm{Re}\int_0^\infty \bar{T}(k,0)\, e^{ikx}\,dk = \tfrac{1}{2}\int_{-\infty}^{\infty} \bar{T}(k,0)\, e^{ikx}\,dk,$$

and, hence, upon inversion,

$$\bar{T}(k,0) = \pi^{-1}\int_{-\infty}^{\infty} T^\circ(\xi)\, e^{-ik\xi}\,d\xi,$$

(38) may first be written, after some manipulation, as

$$I = \frac{1}{\pi\tau}\int_{-\infty}^{\infty} T^\circ(\chi-\xi)\,d\xi \int_0^\infty \frac{e^{ik\xi}}{(ik/b^2)+1-k^2}\,dk. \tag{39}$$

The second integral may be evaluated by integration in the complex k plane. The result is

$$\mathrm{Im}\int_0^\infty \frac{e^{ik\xi}}{(ik/b^2)+1-k^2}\,dk = \frac{-1}{a_2-a_1}\left[e^{-\frac{1}{2}a_1}\,\mathrm{Ei}\,(-a_1\xi) - e^{-\frac{1}{2}a_2}\,\mathrm{Ei}\,(-a_2\xi)\right], \tag{40}$$

where

$$\left.\begin{matrix} a_1 \\ a_2 \end{matrix}\right\} = \frac{1}{2b^2}\left[1 \pm (1 - 4b^4)^{\frac{1}{2}}\right],$$

and

$$\text{Ei } u = \int_u^\infty (e^{-t}/t)\, dt = \text{exponential integral.} \quad (41)$$

When (40), together with the assumed temperature profile, is substituted in (39), the result of integration is

$$\text{Im } I = \frac{1}{\pi(a_2 - a_1)}\left[e^{-\xi a_1}\,\text{Ei}\,(-\xi a_1) - e^{-\xi a_2}\,\text{Ei}\,(-\xi a_2)\right]_{x-d}^{x+d}. \quad (42)$$

Figs. 7 and 8 are graphs showing the real and imaginary parts of the integral I, when $b^2 = (K/U)(gs/U^2)^{\frac{1}{2}}$ takes the values 0.05 and 0.50, respectively (on 14 August 1950, $b^2 = 1/3$). The relatively small change in these curves produced by an order of magnitude alteration in b^2 is particularly to be noted. The maximum amplitude of Re I (and thus of the mountain) changes by only 10 per cent, while the maximum amplitude of Im I changes by a factor of three.

The component of the streamline displacement, ψ_2, is simply obtained from these curves as indicated by (37). To obtain the total solution, this must be subtracted from a heat-conduction component, ψ_1, as given by (24). This latter solution ordinarily contributes little to the streamline displacements, except at small heights in the near vicinity of the island. When the mountain function $M(x)$ is of nearly rectangular shape (as, for example, in fig. 8), as a good approximation it follows from (24) that

$$\frac{\psi_1(x, z)}{\psi_1(x, 0)} = \begin{cases} 1 - \text{erf } \frac{1}{2}z/ax^{\frac{1}{2}}, & (x \leq 2D) \\ \text{erf } \frac{1}{2}z/a(x - 2D)^{\frac{1}{2}}, & (x \geq 2D) \end{cases} \quad (43)$$

where

$$\text{erf } u = 2\pi^{-\frac{1}{2}} \int_0^u e^{-t^2}\, dt = \text{error function,}$$

$a = (K/U)^{\frac{1}{2}}$, and where x and z are expressed in c.g.s. units, with $x = 0$ at the windward shore. For those conditions in which the mountain function deviated somewhat from a rectangular shape, as in fig. 7, $M[\chi - (\zeta^2/4b^2\eta^2)]$ in (24) was expanded in a Taylor series and integrated for small ζ.

The complete streamlines for three examples have been computed and plotted. The first two (figs. 9 and 10) were constructed from fig. 8 and, hence, have the same shape equivalent mountain. The value of $b^2 = (K/U)(gs/U^2)^{\frac{1}{2}} = 1/2$ probably represents an upper limit for observed cases. Of particular interest are the resulting very pronounced edge effects, and the large vertical velocities associated with them. These are the results of the steep sides of the "mountain", or, more physically, of the large temperature gradients at the shore coupled with the high value of $K(gs)^{\frac{1}{2}}/U^2$. Fig. 9 shows the streamlines for an island 1C warmer than the surrounding waters, when $\alpha = 0.5 \times 10^{-4}$ deg C/cm, $K = 7.2 \times 10^6$ cm^2/sec, and $U = 4.2$ m/sec. The maximum vertical motions come out to be about 1 m/sec. Since the "mountain" of 14 August 1950 was 700 m tall and had even slightly steeper sides than the mountain of fig. 8, in an atmosphere of constant stability and wind speed in the vertical, it would be expected to produce a streamline

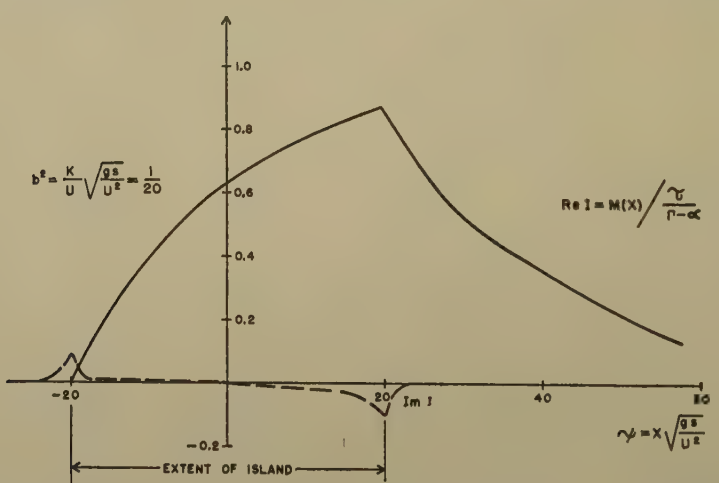

FIG. 7. Integral I as function of χ, dimensionless parameter of horizontal position, when $b^2 = (K/U)(gs/U^2)^{\frac{1}{2}} = 0.05$. Value of mountain function $M(x)$ can be obtained from Re I (solid line), by converting dimensionless ordinate shown into centimeters by means of multiplication by $\tau/(\Gamma - \alpha)$. Mountain component ψ_2 of streamline displacement (in dimensionless units) is found by multiplying Re I by $\cos (gs/U^2)^{\frac{1}{2}}z$, and adding to product of Im I (dashed line) and $\sin (gs/U^2)^{\frac{1}{2}}z$. Result is converted to centimeters by multiplication by $\tau/(\Gamma - \alpha)$. Because of low value of b^2, "mountain" does not reach maximum amplitude A. Streamline picture of fig. 11 was calculated with aid of this diagram.

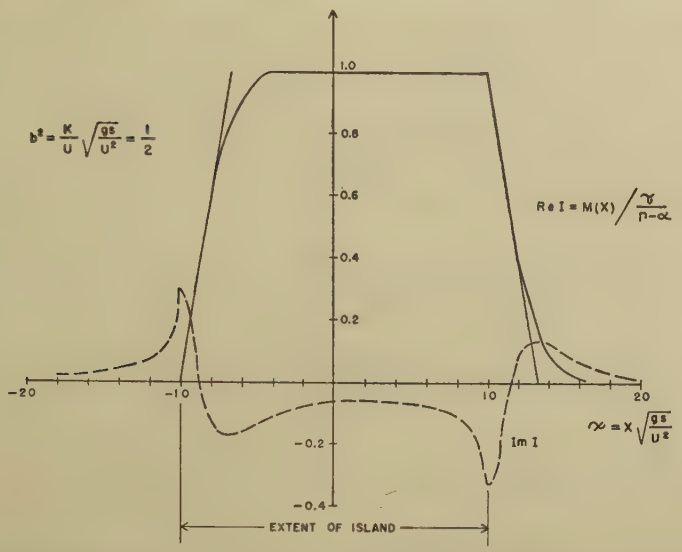

FIG. 8. Integral I as function of χ, when $b^2 = (K/U)(gs/U^2)^{\frac{1}{3}} = 0.5$. In this case, "mountain" reached maximum amplitude after only 15 per cent of distance across island. Streamline pictures of figs. 9 and 10 were calculated with aid of this diagram.

displacement of about 700 m and updrafts of about 36 cm/sec (due to having streamlines with the same slope as in fig. 9 and a U of 1.5 m/sec, compared to 4.2 m/sec). If the stability and wind speed should undergo suitable alteration in the vertical, these perturbations might be larger, as shall be discussed presently.

Fig. 10 shows the flow pattern in another situation, where $b^2 = 1/2$, so that the same shape "equivalent mountain" applies, but in which the island temperature excess is only 0.5C, and two of the parameters of the undisturbed air stream are different. The wind speed was now taken as 1.7 m/sec, and the eddy conductivity as 1.4×10^6 cm^2/sec, a more normal value. The maximum lifting is now about 150 m, and the highest updrafts about 50 cm/sec.

A final example was chosen, in which $b^2 = 0.05$. The equivalent mountain for this case is shown in fig. 7. Its sides are far less steep than those of the mountain in fig. 8. For an island of 1C temperature excess, undisturbed lapse rate one-half the dry adiabatic, and wind speed of 5 m/sec, the streamline picture is as shown in fig. 11. Although the maximum streamline displacement is only slightly less than that in fig. 9, the sharp drafts at the island edges are nearly missing, being only about 15 cm/sec. Therefore, in real cases, these drafts may be expected to be well developed only when $K(gs)^{\frac{1}{3}}/U^2$ is large (for the conditions of fig. 11, K would be 8.3×10^5 cm^2/sec, which is a fairly large value, but U is also large).

The field of motion shown in fig. 11 at last permits a test of the assumption made earlier, that the con-

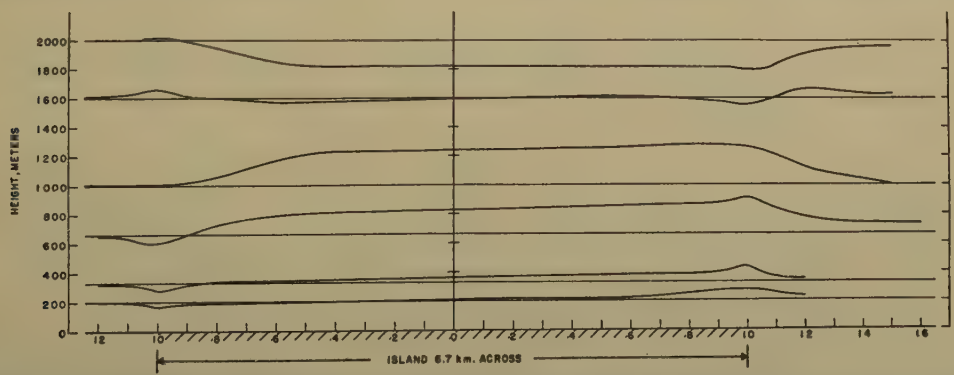

FIG. 9. Complete streamline picture for typical example of air flow over small heated island, when gs/U^2 is constant with elevation and equal to 9×10^{-10} cm^{-2}. Mountain component, ψ_2, of streamline displacement was calculated with use of fig. 8. Value of $b^2 = (K/U)(gs/U^2)^{\frac{1}{3}} = 0.5$, so that if $U = 4.2$ m/sec, $K = 7.2 \times 10^6$ cm^2/sec. Temperature across island surface is assumed constant and 1C in excess of water temperature, so that equivalent mountain (from fig. 8) is 200 m high, since $\Gamma - \alpha = 0.5 \times 10^{-4}$ deg C/cm. Island is hatched area, and streamlines are shown by solid lines.

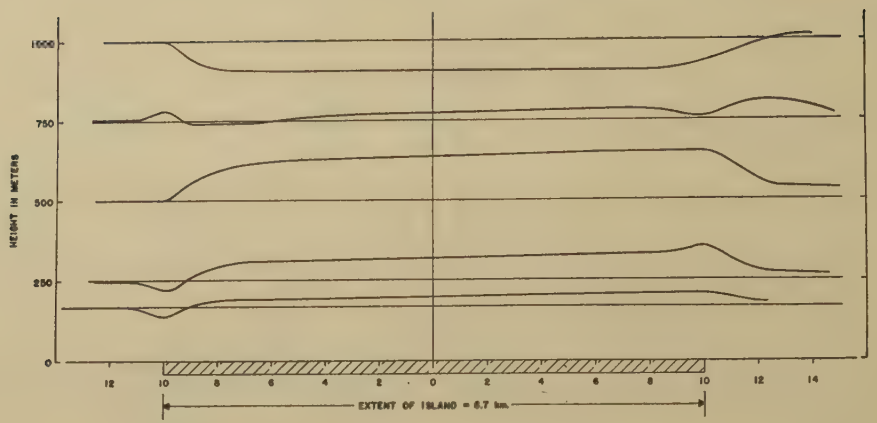

FIG. 10. Complete streamline picture for typical example of air flow over heated island, for conditions similar to those of fig. 9, except that now island is 0.5C warmer than surrounding waters; $gs/U^2 = 36 \times 10^{-10}$ cm^{-2}; $U = 1.7$ m/sec, and $K = 1.4 \times 10^6$ cm^2/sec. Equivalent mountain has same shape, but one-half amplitude, of that corresponding to fig. 9. Parameter b^2 is still 0.5, and fig. 8 was used in calculation of ψ_2.

vective vertical velocities w' are small in the region above the island where the heating function V is significant. To test this, values of V have been denoted by dashed lines on fig. 11. For a constant island temperature, the heating function along the ground has the form of a Dirac delta function, with a positive peak at the windward shore and a negative peak at the leeward. Above the ground, it decays very rapidly and slants, so that nowhere do appreciable values of V coincide with the more sloping portions of the streamlines.[4] If average values across the entire island are taken, the heating function at 300 m has fallen to 0.45 of its average value along the ground. At this level, the average value of $c_p w'(\Gamma - \alpha)$, the vertical motion term to be compared with it, is 0.4 times the average value of the heating function at that level. The assumption is clearly far better than this indicates, because the heating function leans in such a way that lower-than-average vertical motions at any level coincide with higher-than-average values of the heating function.

Another important test of the adequacy of this model, and its derived heating function, lies in whether or not it predicts a realistic sea-breeze circulation. It will be remembered that the models of Part I, based upon assumed distributions of heating, failed notably in this respect. The next section, therefore, is concerned with this topic.

[4] The analytic expression for the space distribution of the heating function is readily obtained by taking the general solution to the heat equation, given by (24) with $V(x, z)$ instead of ψ_1, substituting into it each delta function, and integrating for a temperature jump of τ degrees at $x = 0$, $z = 0$. The result is

$$V(x, z) = 2\pi^{-\frac{1}{2}}(c_p U\tau)e^{-z^2/4a^2x}zx^{-\frac{3}{2}} \quad \text{for} \quad x > 0,$$
$$= 0 \quad \text{for} \quad x < 0.$$

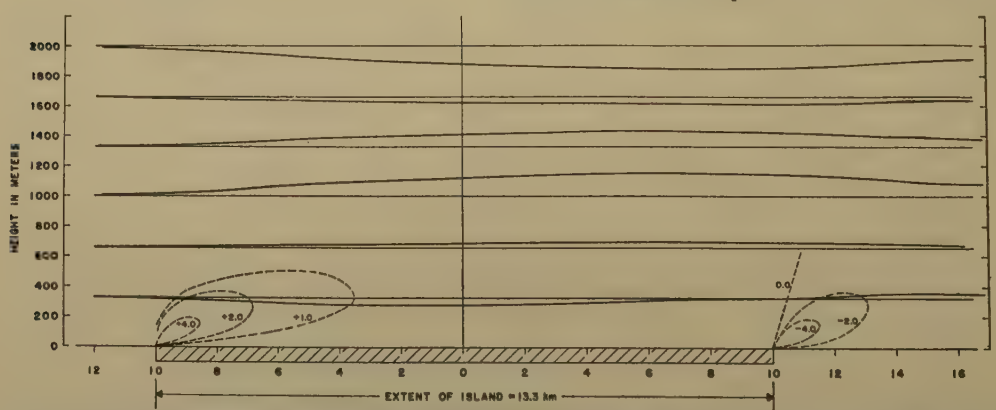

FIG. 11. Complete streamline picture for example of air flow over heated island, when $b^2 = 0.05$, $U = 5$ m/sec, $gs/U^2 = 9 \times 10^{-10}$ cm^{-2}, $K = 8.3 \times 10^5$ cm^2/sec. Temperature excess across island surface is 1C. Fig. 7 was used in calculation of mountain part of solution. In this case, equivalent mountain has shape of solid curve in fig. 7, and is slightly less than 200 m high. Island is hatched area, and streamlines are shown by solid lines. Dashed lines are space distribution of heating function V. Latter values can be converted to cal gm^{-1} sec^{-1} by multiplying them by $(c_p U\tau/\pi) \times 10^{-6} = 6.8 \times 10^{-5}$.

7. Application of the theory to study of the sea breeze

In examining figs. 9 to 11, it is seen in each case that the sea-breeze circulation is in the expected sense. Near the ground, on the windward shore, the vertical velocity decreases with height and, therefore, $\partial u'/\partial x > 0$. Hence, there will be an increase of horizontal wind as the island is approached. On the lee shore, on the other hand, $\partial w'/\partial z > 0$ near the ground, so that $\partial u'/\partial x < 0$, and the wind will be decreased or reversed. The height at which the sea breeze reverses, and the horizontal perturbation u' changes sign, is also reasonable. At the windward shore, this reversal occurs at 600, 250 and 500 m, respectively, in figs. 9, 10 and 11. It can be shown from the analysis to follow that, in general, at this shore, the reversal will occur at a height of $\frac{1}{2}\pi(gs/U^2)^{-1}$. Moreover, the theory permits definite quantitative conclusions regarding the variation of the sea breeze with the various atmospheric parameters.

After substitution of (2) in the equation of continuity, $\partial u'/\partial x = -\partial w'/\partial z$, the horizontal velocity perturbation becomes

$$u'(x, z) = -U\partial\psi(x, z)/\partial z. \tag{44}$$

The model used in section 6 is again considered, *i.e.*, the island is at a constant temperature τ above the surrounding waters. The sea breeze at the windward edge is of particular interest, since it is especially pronounced in this region, and since it can be calculated there with relatively little difficulty.

Since the heat-conduction component, ψ_1, is zero on the windward side of the island, it is necessary to evaluate only $\partial\psi_2/\partial z$ in (44). This may be obtained by differentiation of (37) with respect to z. When the result is expressed in c.g.s. units, and substituted in (44), the sea breeze becomes

$$u'(-d, 0) = \tau/(\Gamma - \alpha)\,(gs)^{\frac{1}{2}}\,(\mathrm{Im}\ I)_{\chi=-d}, \tag{45}$$

where $(\mathrm{Im}\ I)_{\chi=-d}$ is the amplitude of the broken-lined curve in figs. 7 and 8, at the left (upwind) edge of the island. Its analytical representation is given by (42), when $\chi = -d$ is substituted in the limits. Therefore,

$$u' = \frac{\tau}{\Gamma - \alpha}(gs)^{\frac{1}{2}}\frac{1}{\pi(a_2 - a_1)} \times \left[e^{-\xi a_1}\,\mathrm{Ei}\,(-\xi a_1) - e^{-\xi a_2}\,\mathrm{Ei}\,(-\xi a_2)\right]_{-2d}^{0}. \tag{46}$$

For d of the order of 10 or greater (island widths of 1–3 km or more), the lower limit contributes negligibly compared to the upper one. Hence,

$$u' = \frac{\tau}{T_m}\left(\frac{g}{s}\right)^{\frac{1}{2}}\frac{1}{\pi(a_2 - a_1)}\lim_{\xi\to 0}\left[\mathrm{Ei}\,(-\xi a_1) - \mathrm{Ei}\,(-\xi a_2)\right].$$

The indeterminate form in the above equation may be evaluated, and we obtain

$$u' = \frac{\tau}{T_m}\left(\frac{g}{s}\right)^{\frac{1}{2}}\frac{\ln\,(a_2/a_1)}{\pi(a_2 - a_1)}, \tag{47}$$

where a_2 and a_1 are given by (40).

It was previously noted that, in many situations, the air parameters are such that $4b^4 \ll 1$. Under these conditions, (47) has the much simpler form

$$u' = \frac{\tau}{T_m}\left(\frac{g}{s}\right)^{\frac{1}{2}}\frac{2}{\pi}b^2\ln\frac{1}{b^2}, \tag{48}$$

or

$$u' = \frac{g\tau}{T_m}\frac{2}{\pi}\frac{K}{U^2}\ln\frac{U^2}{K(gs)^{\frac{1}{2}}}. \tag{49}$$

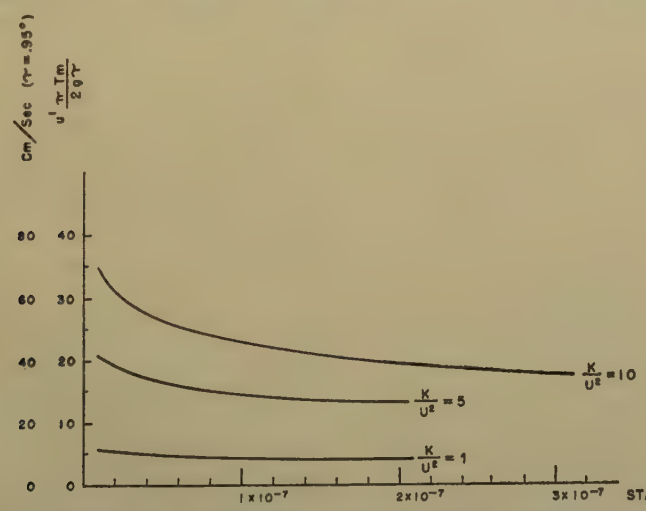

FIG. 12. Variation of amplitude of sea breeze at windward shore, as function of undisturbed stability s (cm^{-1}). Ordinate is in units of $u'\pi T_m/2g\tau$ (sec), while adjacent scale shows value u' must have in cm/sec for particular temperature excess ($\tau = 0.95$C). K is effective eddy conductivity of ground layer (cm^3 sec^{-1}) and U (cm/sec) is undisturbed wind speed.

In the studies of sea breezes at coastlines, the dependence of the strength of the circulation upon stability and wind speed has been a subject of considerable controversy (see, for example, Balkema, 1950). For the special case of the island, (49) shows this dependence very clearly, as well as that upon temperature excess τ, and on eddy conductivity K. These results are presented graphically in fig. 12. This figure shows that, other conditions remaining the same, the sea breeze varies inversely with the basic wind and stability, and directly with the eddy conductivity. It should be pointed out that the present discussion of the sea breeze was based on the assumption of a basic wind and a two-dimensional steady-state model. A future paper is planned, in which the modifications due to the diurnal temperature wave and the Coriolis force are considered.

If observations are made of the sea breeze and temperature along the ground, it is possible to compute the effective mean value of the eddy conductivity K. This calculation is facilitated by fig. 9, which is a plot of the transcendental part of (47). The ordinate is determined from the observations, and b^2 is read off the graph. From this, K is readily computed, and for typical observed values of the parameters comes out well within the magnitudes measured by Malkus and Bunker (1952).

8. The production of lee waves and forecasting of cloud rows

We will now consider the situation in which the wind speed and stability of the undisturbed air stream are constant only up to some height h, of the order of 1–3 km, above which there is a rapid change. The important effect of this change will be in the modification of the boundary condition which the mountain component ψ_2 must satisfy. Since the heat conduction component ψ_1, and the mountain function $M(x)$, are determined by the properties of the ground layer, they will not be altered by a change in air structure which occurs above the top of this layer. If the alteration occurred within the ground layer, a positive exponential would need to be added to the solution of (12), some reflection of the upward transported heat and of ψ_1 would occur, and the mountain function and derived solutions would have to be modified. Barring an excessively low h, then, the same mountain function $M(x)$ and eddy conduction solution ψ_1 may be used as previously, and it only remains to inquire what effect upon ψ_2 is produced by the change in air structure, in order to obtain the new streamline picture. The answer to this question has already been suggested by the work in Part I of this paper, coupled with that of Scorer (1949; 1951) on the airflow over mountains. Scorer has shown that, if the undisturbed wind speed increases upwards by a sufficient amount, a system of stationary sinusoidal waves is excited in the lee, the amplitude of which is directly related to the mountain height.

In the case of the island also, Part I showed that the existence and wavelengths of lee waves depended upon s and U, and their vertical variations. For a highly idealized model, namely that of an infinitely large wind speed above h (equivalent to a lid at h), a formula for the wavelengths was derived, which checked very well with observations in those cases where pronounced lee waves were observed. This model failed, however, because its heating function was assumed arbitrarily and did not alter with changes in the low-level mixing processes, so that lee waves were predicted on many days when no such oscillations could be detected.

In contrast with the mountain flow, in which the ground deformation is a permanent feature, and an alteration in gs/U^2 is the only requirement for sizeable lee waves, an additional criterion must be provided in the case of differential heating by an island. This criterion can now be quantitatively stated in terms of the height of the "equivalent mountain" associated with the island, and thereby explicitly related to the turbulent processes occurring in the lowest air. It has been shown that, for a given island, the height of the "equivalent mountain" may vary by more than an order of magnitude from one sunny summer day to the next, depending upon the extent and development

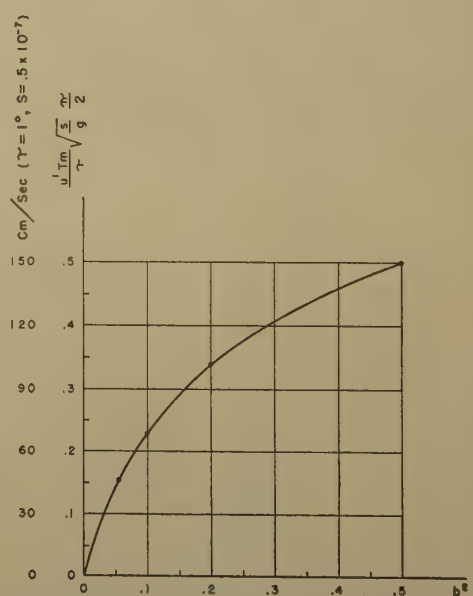

FIG. 13. Variation of sea breeze with $b^2 = (K/U^2)(gs)^{\frac{1}{2}}$. Ordinate $(u'T_m/\tau)(s/g)^{\frac{1}{2}}(\pi/2)$ is in dimensionless units, while adjacent scale shows corresponding value of u' (cm/sec) for particular values of τ, temperature excess of island, and s, undisturbed stability.

of the ground layer (which was seen to be the most sensitively dependent upon the wind speed).

Therefore, while a change in gs/U^2 at levels of 1–3 km is a necessary condition for cloud rows from the Cape Cod islands, it is by no means sufficient. Since the observations show that such wind increases as cited by Scorer are very common in this area, the development of the mixed ground layer (and consequent high equivalent mountain) is probably the more critical factor in predicting the occurrence of these cumuli. It so happens, in this region, that days of light winds and deep mixed layer usually occur in a high-pressure cell, about the second or third day following the passage of a cold front. On these occasions, a wind change at about 1–2 km is common. Directly following a cold front, the northerly wind is generally too strong and the air too dry for cumulus rows. The most unfavorable conditions (equal insolation assumed) are days of strong southwest wind, on which the lowest air has also become very stable after a long over-water trajectory. Such a case was that of 9 August 1950. Although lee waves would have been predicted for this case from the theoretical model of Part I, the present improved treatment revealed that the equivalent mountain was only 25 m high. On this type of day, therefore, it is quite unnecessary to examine the soundings for alterations in the basic current at upper levels, since any lee waves present will have negligible amplitudes. The case of 14 August 1950, on the other hand, was ideal for cumulus rows. Not only was the island in the weak-wind area of the cold high following a polar-front passage three days earlier, so that an excellent mixed layer developed, but the wind reversed direction and increased at about 1 km. The wavelength formula of Part I, in this case, gave results which were correct within observational error.

9. Conclusion

The separation of the solution to the present problem into two parts has led to clearer understanding of the air flow over heated terrain in several ways. The first component of the streamline displacement is intimately related to the turbulent-conduction mechanism, while the second, or so-called "mountain solution," is related only indirectly to this mechanism. In the first place, the separation enables a significant component of the motions over a heated island to be predicted, at least qualitatively, by reference to the extensive literature on the mountain-ridge problem, and therefore without laborious calculation by means of Fourier analysis in each case. Second, it has been found that the factors responsible for the height and shape of the mountain are critical in the formation of significant lee waves. In examining these factors, attention was directed to the development of the turbulent ground layer. Its role in convection near the island is now much clearer. By means of vertical distribution of heat due to turbulent eddying, the mean streamlines over the island are deformed upward in a mountain-like shape, causing the airflow above to be deformed just as if a physical mountain were present. Flow over this "barrier" was seen to give rise to good-sized downstream oscillations, under conditions which were specified and checked by observations already existing.

Finally, the model presents a clarified picture of the relation between the heating distribution within the ground layer and the more extensive motions resulting as its consequence. Arising from such a picture are specific predictions, which readily lend themselves to checks by future observational programs. A number of these concerned the sea-breeze circulation, the strength of which has been related to the low-level air structure. The relations between the island-produced cumulus clouds and their initial sources of energy are also better understood. The present theory hypothesizes that only those directly over the island may have a significant source of energy in the upward transport of sensible heat and moisture *via* the mixed layer, while those downstream must be formed in "forced convective" updrafts whose energy is taken not from the heated island, but from the kinetic energy of the air stream itself.

In conclusion, it may be suggested that the present treatment be applied to other meteorological problems. The air flow over a mountain barrier is frequently complicated by heating. The "equivalent mountain" solution which must be subtracted from the actual mountain solution should be calculable by the method derived. Also, flow over larger-scale heat sources may perhaps be treated by finding an "equivalent mountain range," thus relating the flow to the large-scale mountain problem studied by Queney and others, in which the Coriolis force is of importance and oscillations also take place in a horizontal plane.

Acknowledgments.—The writers would like to thank Prof. Paul Queney for the extremely valuable discussions concerning the relation of the island problem to that of the mountain, and the resolution of the upper boundary condition in the infinite model. Considerable insight into the conditions necessary for the production of lee waves was obtained from correspondence and conversations with Dr. R. S. Scorer. The writers have had access to an unpublished manuscript on the air flow over an island by Prof. B. Haurwitz, who has also made important suggestions in the course of the research. Gratitude is also due to Mr. Andrew Bunker, for information concerning the mixed ground layer and for several calculations from the observations. The work described in this paper was carried out under Contract N6onr-27702 (NR-082-021) between the Office of Naval Research and the Woods Hole Oceanographic Institution.

REFERENCES

Balkema, F., 1950: An investigation on some aspects of the effect of land and sea breeze. *K. ned. meteor. Inst. Meded. Verh.*, B, No. 2, 50 pp.

Carslaw, H. S., 1945: *Introduction to the mathematical theory of conduction of heat in solids.* 2nd ed. New York, Dover Publ.

Malkus, J. S., and M. E. Stern, 1953: The flow of a stable atmosphere over a heated island, Part I. *J. Meteor.*, **10**, 30–41.

Malkus, J. S., and A. F. Bunker, 1952: Observational studies of the air flow over Nantucket Island during the summer of 1950. *Pap. phys. Ocean. Meteor., Mass. Inst. Tech. and Woods Hole ocean. Instn.*, **12**, No. 2, 50 pp.

Queney, P., 1947: Theory of perturbations in stratified currents with applications to air flow over mountain barriers. *Dep. Meteor. Univ. Chicago, Misc. Rep.*, No. 23, 81 pp.

——, 1948: The problem of air flow over mountains: A summary of theoretical studies. *Bull. Amer. meteor. Soc.*, **29**, 16–25.

Scorer, R. S., 1949: Theory of waves in the lee of mountains. *Quart. J. r. meteor. Soc.*, **75**, 41–56.

——, 1951: Forecasting the occurrence of lee waves. *Weather*, **6**, 99–103.

Sneddon, I. N., 1951: *Fourier transforms.* New York, McGraw-Hill, 542 pp.

Contribution No. 628

OCEANOGRAPHIC RESULTS OF PROJECT SKIJUMP I AND SKIJUMP II IN THE POLAR SEA, 1951-1952

L. V. Worthington

Abstract--Oceanographic observations made from ice floes by United States naval aircraft in 1951 and 1952 indicate that the circulation of the Polar Sea is more complicated than the cyclonic system suggested by Nansen. The chief feature observed is a large anticyclonic eddy north of Alaska. Some evidence is produced of the existence of a submarine ridge running across the center of the North Polar Basin.

Introduction--Project Skijump I was inaugurated in 1951 by the Office of Naval Research to study the oceanography of the Polar Sea, using aircraft. During the spring of 1951 a Navy R-4D was used. Twelve landings were made on the ice and three hydrographic stations were occupied. During that season the area studied was limited by the range of the R-4D.

For the season of 1952 two Navy P-2V aircraft were added to the R-4D. These planes were capable of landing on the ice and refueling the R-4D, and it was thought that the oceanographic survey could be extended much farther from the base at Point Barrow, Alaska. The positions of the hydrographic stations made in both years are illustrated in Figure 1. Stations 1, 2, and 3 were made on April 1, April 21, and May 3, 1951.

Stations 4, 5, and 6 were made on successive days (March 11-13, 1952), with the R-4D remaining on the ice during the nights of March 11 and 12 and a P-2V coming out to her from Point Barrow each day.

Station 7 was made on March 25, the R-4D remaining on the ice as before. The following day the R-4D and a P-2V landed at station 8; the P-2V refueled the R-4D and returned to Point Barrow. The hydrographic station was made during the night of March 26. On the morning of March 27 the R-4D's port landing gear collapsed in an attempt to take off and she had to be abandoned. This concluded the oceanographic section of Skijump II. With the plane it was necessary to abandon the winch, the Nansen bottles, and much other equipment. The best operating month from the point of view of light, ice conditions, and air temperatures is April, which was lost on account of this misfortune.

Methods--The technique of making hydrographic stations from a plane is unusual and may, therefore, be worth going into in some detail. The holes through the ice were made with a 5-hp, gasoline-driven, post-hole digger. This machine bored a clean 12.5-inch hole through five feet of ice in about ten minutes. This diameter was found to be large enough for Nansen bottles. The chain-saw and ice-chisel method used in 1951 took as much as 2 1/2 hr for ice of the same thickness.

Analysis of salinity samples taken in 1951 showed that some had been frozen, causing highly saline water to settle to the bottom of the Nansen bottle, where it was drawn off into the sample bottle. Accordingly, in 1952 every effort was made to see that the Nansen bottles were not exposed to freezing temperatures. The plane, when on station, was heated by a gasoline-burning space heater which was kept running continuously a few feet from the plane. The heater had three ducts, two of which were brought into the plane through one of the ports while the third was directed to the top of the ice hole. A tent surrounded the hole enclosing it with the interior of the plane. The heater kept the top of the hole free from slush ice at all times during the station work.

Table 1--Comparison of paired thermometers

Difference in corrected temperature	Number of observations
°C	
0.00	7
0.01	10
0.02	1
0.03	1
Total	19

The after part of the plane where the Nansen bottles were racked was kept as near 5° C as possible, enough to preclude freezing but not so much as to necessitate a long wait for the thermometers to reach equilibrium. Comparisons of paired thermometers were made during the last two stations with the results (excluding one defective thermometer) shown in Table 1.

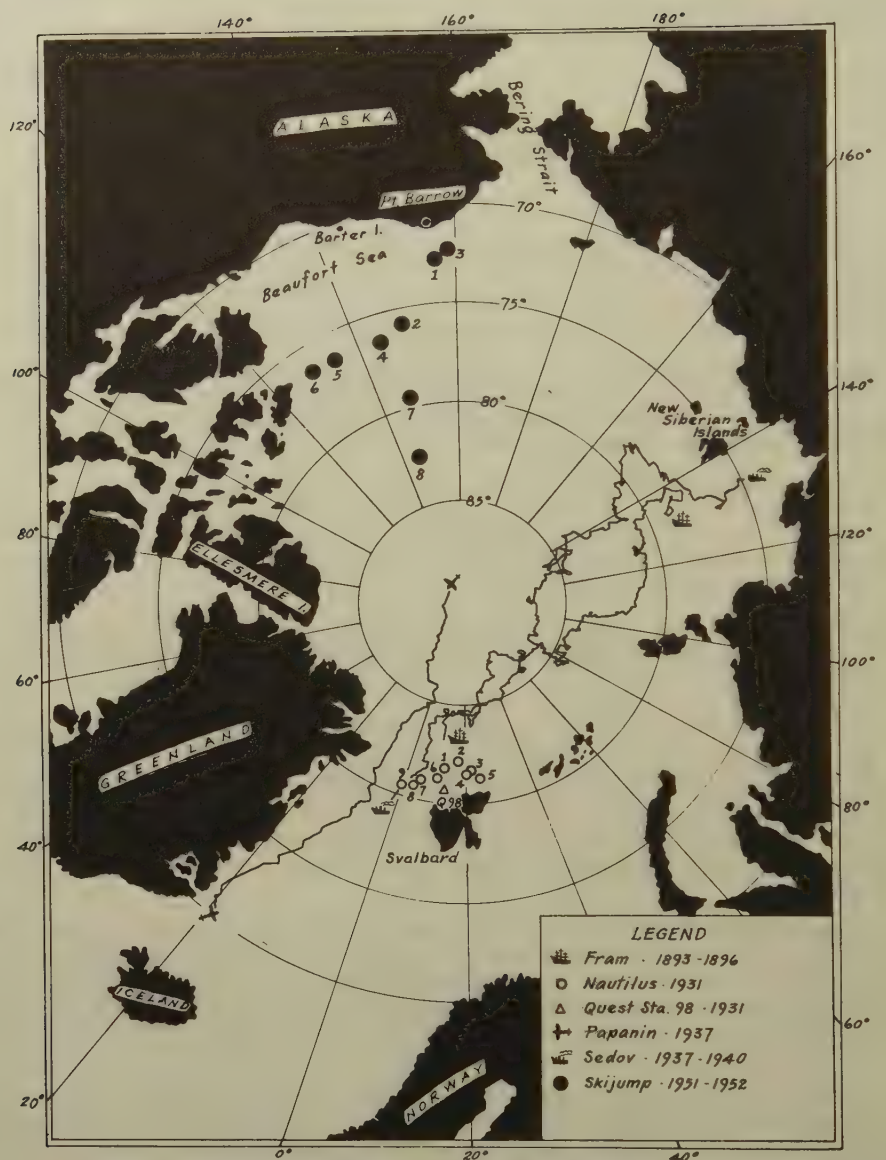

Fig. 1--Expeditions on which oceanographic measurements were made in the deep Polar Basin

The winch was mounted forward owing to its weight, but the observer had a clutch control aft which enabled him to bring the bottles to hand smoothly in most cases. The winch held 3400 m of 1/16-inch 7 × 7 stainless steel cable with a breaking strain of 480 lb. A strip of friction tape was wrapped around the wire before each bottle was attached to adapt the small diameter wire to the clamp on the bottle. As only one bottle slid down the wire, this procedure is regarded as satisfactory. A 15-lb weight was used at the end of the wire, and all wire angles were nearly zero. On all shallow series the wire was moved up and down by hand for a few seconds to ensure proper flushing of the bottles.

The results were somewhat marred by a Nansen bottle which became defective at Station 7 and did not close properly. This escaped detection until the samples were titrated in Woods Hole.

Table 2--Hydrographic station data

Date	Station	Location		Depth	Temperature	Salinity
		Lat. N	Long. W			
1951		° ′	° ′	m	°C	°/oo
Apr. 1	1	72 52	156 32	2	-1.64	30.26
				10	-1.56	....
				20	-1.30	30.10
				50	-0.92	30.09
				100	-1.51	31.87
				200	-1.20	....
Apr. 21	2	75 45	150 00	2	-1.58	29.72
				10	-1.61	29.70
				20	-1.60	....
				50	-1.52	29.50[a]
				100	-1.21	31.96
				150	-1.49	32.55
				200	-1.48	33.53
				300	-0.07	34.47
				400	0.36	34.77
				600	0.37	34.72[a]
				800	0.10	34.85
				999	-0.06	34.70[a]
				1295	-0.26	....
				1594	-0.38	....
				2092	-0.42	....
				3200	(bottom, by sounding)	
May 3	3	72 36	158 32	2	-1.64	30.78
				10	-1.68	30.77
				20	-1.68	30.78
				50	-1.68	31.83
				100	-1.77	32.56
				150	-0.38	34.39
				171	(bottom, by wire)	
1952						
Mar. 11-12	4	76 25	144 19	2	-1.60	29.34
				10	....	29.31
				25	-1.62	....
				50	-1.15	30.03
				75	-1.15	31.78
				100	-1.25	....
				150	-1.46	32.80
				200	-1.45	....
				300	-0.15	33.95
				500	0.52	34.70
				600	0.38	34.86
				800	0.16	34.92
				1300	-0.22	34.90
				1700	-0.37	34.94
				2200	-0.52[a]	34.92
				3000	-0.35	34.99
Mar. 12	5	76 26	134 00	2	-1.64	30.03
				10	....	30.02
				25	-1.65	30.03
				50	-1.72	31.37
				75	-1.63	31.70
				100	-1.34	32.40
				150	-1.49	33.01
				200	-1.07	33.90
				400	-0.35	34.79

[a]Questionable.

(Continued)

Table 2--Hydrographic station data (concluded)

Date	Station	Location		Depth	Temperature	Salinity
		Lat. N	Long. W			
1952		° ′	° ′	m	°C	°/oo
Mar. 12	5	76 26	134 00	500	0.51	34.85
				700	0.14	34.87
				1000	....	34.88
				1300	-0.20	....
				1700	-0.36	34.93
				2100	-0.42	34.96
Mar. 13	6	76 20	128 20	2	-1.64	30.38
				10	-1.66	30.41
				25	-1.68	30.49
				50	-1.61	31.51
				75	-1.31	32.11
				100	-1.45[a]	32.71
				150	-1.45	33.40
				200	-0.74	34.32
				300	0.12	34.71
				400	0.39	34.83
				500	0.39	34.87
				600	0.27	34.87
Mar. 25	7	79 36	147 10	2	-1.60	29.33
				10	-1.59	....
				25	-1.61	29.31
				50	-1.21	30.59
				75	-1.03	31.73
				100	-1.21	32.20
				150	-1.48	32.85
				200	-1.35	33.62
				300	-0.10	34.46
				400	0.44	....
				500	0.56	....
				600	0.41	34.86
				700	0.24	34.87
				1000	-0.10	35.02[a]
				1400	-0.25	34.94
				1800	-0.37	....
				2300	-0.41	34.96
				2950	(bottom, by sounding)	
Mar. 26-27	8	82 22	145 20	3	-1.68	30.44
				25	-1.67	30.60[a]
				51	....	30.34
				75	-1.34	31.89
				100	-1.31	32.57
				150	-1.45	33.00
				200	-1.27	33.86
				300	-0.09	....
				400	0.30	34.79
				500	0.43	34.85
				600	0.31	....
				800	0.11	34.99[a]
				1000	-0.12	34.88[a]
				1500	-0.30	....
				2100	-0.42	....

[a]Questionable.

There were other cases of pollution that could perhaps have been avoided by a more rigorous testing of Nansen bottles. A tabulation of the hydrographic station data is given in Table 2.

Oceanography--The deep Polar Basin was discovered by Nansen in 1893 in his historic expedition aboard the Fram [NANSEN, 1902]. The Fram was deliberately allowed to be frozen into the ice field, and drifted during the years 1893-1896 from a point north of the New Siberian Islands across the eastern half of the basin to a point north of Svalbard, where she got free of the ice.

The submarine Nautilus attempted to penetrate the Polar Sea beneath the ice in 1931 [SVERDRUP and SOULE, 1933]. She was prevented from submerging by the loss of a diving plane and was thus limited to a small but most interesting area north of Svalbard.

In 1937 a Russian expedition under Papanin landed a plane on the ice close to the pole and drifted, in the course of 274 days, out of the Polar Sea. The expedition was taken off its ice floe by ship after it had been carried to latitude 71° N by the East Greenland Current.

In 1937-1940 the Russian icebreaker Sedov roughly paralleled the Fram's track. Complete published data from the two Russian expeditions are not available, but WÜST [1942] was able to piece together some information from various sources including the Russian newspapers. The tracks of these expeditions together with the positions of Skijump's stations are shown in Figure 1. A further expedition in the Maud [SVERDRUP, 1929] attempted to drift across the Polar Sea in 1922. This was certainly the best-equipped expedition to set out, but by great misfortune the Maud was unable to penetrate the deep Polar Basin, being confined by adverse ice drift to the waters of the Siberian Shelf.

What is known of the general character of the Polar Sea has been derived from those expeditions. The surface water is cold (-1.5° to -1.9° C) and of low salinity (29 to 33 °/oo). This water is formed in the basin itself and is called North Polar water [NANSEN, 1902].

Beneath the surface water is a transition layer (of varying thickness) to Atlantic water. This water enters the basin to the west of Svalbard with temperatures up to 4° and salinities of slightly more than 35 °/oo. A wedge of Atlantic water with temperatures greater than 0° has been observed at all deep stations in the Polar Sea. The deeper 0° isotherm is found between 700 and 900 m, and provides a convenient lower boundary for this water.

Below the Atlantic water is found the Polar Deep water. This water is formed in the Norwegian Sea and consists chiefly of Atlantic water with a slight admixture of North Polar water. As it enters the basin near Svalbard it has a slightly lower salinity than the intermediate water, about 34.94 °/oo. Winter conditions in parts of the Norwegian Sea render the whole water column isothermal at temperatures below -1°, forming Norwegian Sea deep water which is nearly identical with Polar deep water.

North Polar water--Nansen considered that the freshness of the North Polar water was maintained by the inflow of fresh water from the great Siberian rivers, and to a lesser extent by the precipitation over the Polar Sea. He based this on salinity values that increased steadily in the surface layer as the Fram drifted away from the Siberian Shelf. It appears from Skijump data that the freshness of the surface layer depends more upon distance from the source of saline water than upon proximity to the Siberian coast. Skijump Stations 4 and 7 had lower salinities (29.34 and 29.32 °/oo) than any of those observed along the Fram's drift except on the Siberian Shelf itself.

From evidence found in the Atlantic water, Station 4 is judged to be in the center of an eddy and is thus farther in point of time from the source of saline water than any other station yet made in the Polar Sea. In Figure 2 the surface salinities found in Skijump are plotted and the 30 °/oo isohaline sketched in.

Atlantic water--As the warmer, more saline Atlantic water flows into the Polar Sea, it submerges beneath the North Polar water. Upon entering near Svalbard it has a maximum temperature of more than 4° at 50 m [Quest Sta. 98, in Fig. 1 of MOSBY, 1938]. As it progresses farther into the basin, its maximum temperature diminishes and is found at greater depths.

The lowest observed maximum in the Polar Sea, +0.32°, was found by Nansen at 81°30'N, 125° E, at a depth of 400 to 500 m. Nansen's maxima increased steadily from this point as the Fram drifted toward Svalbard. Nansen's theory of the Atlantic water circulation was based on these maxima. He concluded, lacking observations from the western half of the basin, that the Atlantic water revolved cyclonically around the perimeter of the basin, gradually losing heat, and that the maxima on the Canadian-Alaskan side would fall below 0°. Nansen's conception is confirmed, at least in the neighborhood of Svalbard, by the results of the Nautilus cruise, where it is

Fig. 2--Salinity °/oo of the surface layer, Skijump 1951-1952

stated: "This distribution indicates that the greater part of the Atlantic water follows the border of the shelf towards the northeast, but a weaker branch runs toward the northwest. . ." [SVERDRUP and SOULE, 1933].

That Skijump maxima ranged between +0.39° and +0.52° does not in itself contradict Nansen's theory since large variations in the maxima have been found in different years at nearly the same locations. For example, the Fram's maximum at Station 26, 84° 06′N, 12° 26′ E, was +0.93°, while Sedov's maximum at 83° 59′N, 9° 02′ W, is 1.2. Thus, it is not possible to use the temperature maxima from the different expeditions as an index of water circulation.

What does complicate Nansen's circulation picture is the anticyclonic eddy north of Alaska indicated by Skijump stations. Dynamic computations show water transports relative to the 600-decibar surface of 3.75×10^6 m^3/sec flowing southward between Stations 4 and 6 and 2.66×10^6 m^3/sec flowing eastward between Stations 4 and 8. A tentative system of Atlantic water circulation is illustrated in Figure 3, in which Nansen's picture is modified to include the eddy; clearly, however, other interpretations are possible.

Fig. 3--Atlantic water circulation in the North Polar Basin

A further phenomenon observed in Skijump was a small negative thermal gradient between 50 and 150 m. Two temperature curves showing this condition are drawn in Figure 4. The gradients appear to be the last remnants of a seasonal thermocline. It is judged that a seasonal thermocline can only have been formed in the Beaufort Sea, which was extraordinarily ice-free in the summers of 1950 and 1951. The gradient was most marked on Station 7 and least marked on Stations 5, 6, and 8.

Table 3 shows the temperatures at the top and bottom of these negative gradients, together with the difference between them. The slightly warmer water is apparently carried by the eddy into areas which are covered with ice even in midsummer. The large gradient found at Station 7 is not surprising when it is considered that, apart from Station 1, Station 7 is the closest station to the southern Beaufort Sea in terms of water transport.

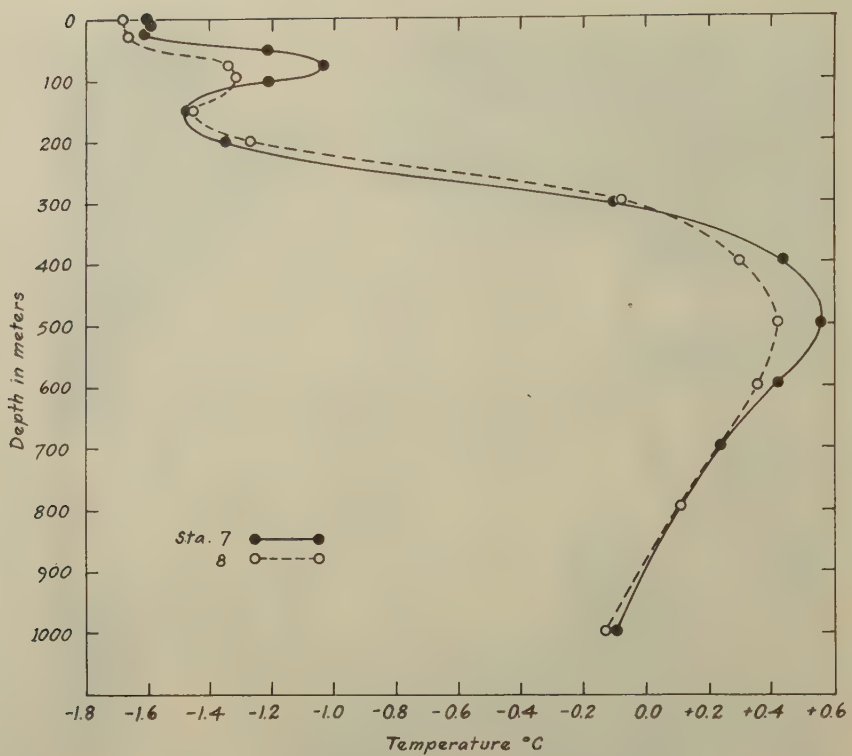

Fig. 4--Two temperature curves showing remnants of a summer thermocline (75-150 m)

Table 3--Temperature at top and bottom of negative gradients

Station	Temperature		
	Top	Bottom	Difference
	°C	°C	°C
1	-0.92	-1.51	0.59[a]
2	-1.21	-1.49	0.28
3		No gradient	
4	-1.15	-1.46	0.31
5	-1.34	-1.49	0.15
6	-1.31	-1.45	0.14
7	-1.03	-1.48	0.45
8	-1.31	-1.45	0.14

[a]Possibly false.

Polar Deep water--Previous sources, Fram in 1893-1896 and Nautilus in 1931, have agreed that the minimum temperature in the Polar Deep water lies between -0.79° and -0.91°. The colder values are found near Svalbard where the deep water flows in, and the warmer towards the easterly end of the Fram's drift. The minimum was found by Nansen between 2500 and 3000 m, below which depth the water becomes adiabatically warmer.

The minimum temperature found in Skijump stations was -0.52° at 2200 m on Station 4. There are in fact indications that this figure is low due to misreading or malfunction of the thermometer. The thermometer in question was malfunctional on the next series and was not used subsequently. If we accept the reading of -0.52°, we must accept a positive gradient of 0.17° between 2200 and 3000 m, a value considerably over the adiabatic rate.

On this basis it appears that the probable temperature minimum in the Beaufort Sea is about -0.45° at 2300 m. This value is 0.34° higher than any minimum previously recorded. Further, since the adiabatic heating starts at a shallower level than in Nansen's observations, it seems likely that Beaufort Sea bottom temperatures are as much as 0.50° warmer than those on the other side of the basin.

There are two possible explanations for this: (1) The deep water entering the basin from the Norwegian Sea has been warmer in recent years than it was in Nansen's time, and (2) there is a submarine ridge, running roughly from Ellesmere to the New Siberian Islands, which separates the deepest water of the Beaufort Sea from the remainder of the basin.

In support of the former hypothesis is the overall weakening of the severity of the Arctic climate as reflected in the intermediate water by the temperature maxima observed by the Sedov, which are higher in the same location than those observed by the Fram, as noted above.

In support of the latter hypothesis are the observed temperatures in the deep water. Nansen's nearest deep observation to Svalbard shows a temperature of -0.87° at 3000 m. This agrees perfectly with the deep temperatures found on the Nautilus expedition, which range between -0.82° and -0.91° in the 2000 to 3000 m level. This, however, does not prove that changes have not taken place between 1931 and the present.

There is some indication that soundings give further support to the existence of a ridge. CRARY and Others [1952] found depths up to 3838 m in the Beaufort Sea (74° 45′ N, 150° 55′ W). On Skijump Station 7 about 300 miles to the north the depth had diminished to 2950 m. Unfortunately, no sounding was obtained on Station 8, but the depth was in excess of 2100 m by wire.

The sill depth of the ridge should not exceed 2300 m, the depth of the temperature minimum, below which the water is homogeneous or very nearly so. It is not possible on the basis of present observations to estimate how shallow a ridge could be.

Acknowledgment--This research was sponsored by the Office of Naval Research under Contract N6onr-27701.

References

CRARY, A. P., R. D. COTELL, and JACK OLIVER, Geophysical studies in the Beaufort Sea, 1951, Trans. Amer. Geophys. Union, v. 33, pp. 211-216, 1952.

MOSBY, H., Svalbard waters, Geofys. Pub., v. 12, no. 4, 85 pp., 1938.

NANSEN, FRIDTJOF, The oceanography of the North Polar Basin, Norwegian North Polar Exped., 1893-1896, Sci. Results, v. 3, no. 9, 427 pp., 1902.

SVERDRUP, H. U., The waters on the North Siberian Shelf, Norwegian North Polar Exped. with the Maud, 1918-1925, Sci. Results, v. 4, no. 2, 75 pp. plus 4 pl. and 14 fig., 1929.

SVERDRUP, H. U., and F. M. SOULE, Scientific results of the Nautilus Expedition, 1931, Papers Phys. Ocean. Met., v. 2, no. 1, 76 pp., 1933.

WÜST, GEORG, Die morphologischen und ozeanographischen Verhältnisse des Nordpolarbeckens, Veröffentlichungen des Deutschen Wissenschaftlichen Instituts zu Kopenhagen, Reihe I, Arktis. no. 6, pp. 1-21, Gebruder Borntraeger, Berlin-Zehlendorf, 1942.

Woods Hole Oceanographic Institution,
Woods Hole, Massachusetts

(Communicated manuscript received January 26, 1953, and, as revised, April 23, 1953; open for formal discussion until January 1, 1954.)

Contribution No. 629

Reprinted for private circulation from
GEOPHYSICS
Vol. XVIII, No. 4, October, 1953

THE REFRACTION ARRIVAL IN WATER COVERED AREAS*

CHARLES B. OFFICER, JR.†

ABSTRACT

A solution is given for the refraction arrival in water covered areas in terms of the evaluation of a branch line integral for an impulsive point source. The physical significance of the mathematical solution is discussed, and experimental verification of the theoretical predictions is presented. The character, frequency, and range dependence of the refraction arrival agree with theory.

Using the results of this theory and the conventional interpretation techniques for refraction seismograms, it is possible to determine the velocities and depths of the seismic refraction horizons from the record of a single receiver. The velocities of the refraction layers can be determined from the frequency of the refraction arrivals, the depth of water, and the velocity of sound in water. Then, from the travel times the depths of the horizons can be computed.

This method could be of importance in reconnaissance measurements of geologic structure over the continental shelves.

INTRODUCTION

The formal theory for the transmission of sound in a system consisting of a water layer overlying one or two unconsolidated sedimentary layers (having the elastic properties of liquids) has been given by Pekeris (1948). His solution consists of the evaluation of a series of poles and a branch line integral in the complex domain. The poles correspond to the normal modes of propagation with their dispersive wave properties, and their evaluations agree with the experimental results of Worzel and Ewing (1948) for the characteristics of the water wave arrival. By re-examining his branch line integral, one obtains an evaluation which correctly predicts the experimentally measured characteristics of the refraction arrival.

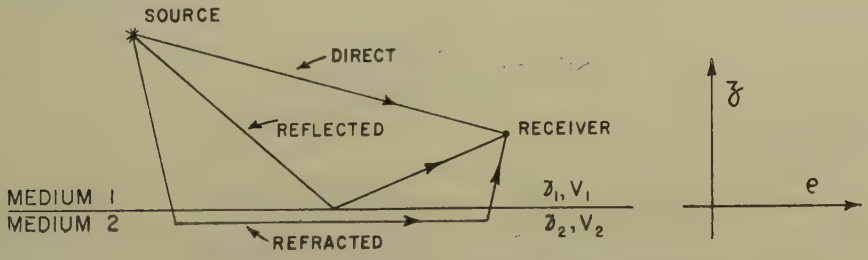

FIG. 1 Direct-, reflected-, and refracted-wave paths.

THEORY OF THE REFRACTION ARRIVAL ACROSS A SINGLE BOUNDARY

The solution of the problem of wave propagation from a point source in a semi-infinite medium of velocity v_1, overlying a semi-infinite medium of higher

* Woods Hole Oceanographic Institution Contribution No. 629. Manuscript received by the Editor March 17, 1953.

† Woods Hole Oceanographic Institution, Woods Hole, Mass.

velocity, v_2, has been given by Jeffreys (1926) and by Muskat (1933). From their analysis three waves are obtained—the direct wave from source to receiver, the reflected wave from the interface between the two media, and the refracted wave, incident and emergent in the first medium at the critical angle and travelling in the second medium parallel to the interface (see Figure 1). As the solution of this problem has a close relation to that of refraction in water covered areas, it will be reviewed briefly here, following the method of Muskat (1933).

Let ρ, z be the cylindrical coordinates with source located at $(0, h)$ and let γ_1 and γ_2 denote the densities of the two media respectively. Then the displacement potential, Φ, will be described by the differential equation

$$\left(\nabla^2 + \frac{\omega^2}{v^2}\right)\Phi = 0 \tag{1}$$

where ω is the circular frequency and Φ is related to the displacement components in the z and ρ directions by

$$w = \frac{\partial \Phi}{\partial z} \quad \text{and} \quad q = \frac{\partial \Phi}{\partial \rho}. \tag{2}$$

Fundamental solutions of equation (1) are given by

$$\begin{aligned} z > 0 \qquad & \Phi = e^{\alpha z} J_0(\xi\rho) \\ z < 0 \qquad & \Phi = e^{\bar{\alpha} z} J_0(\xi\rho) \end{aligned} \tag{3}$$

where

$$\alpha^2 - \xi^2 + \frac{\omega^2}{{v_1}^2} = 0 \quad \text{and} \quad \bar{\alpha}^2 - \xi^2 + \frac{\omega^2}{{v_2}^2} = 0. \tag{4}$$

The source can be expressed by

$$\Phi_0 = \frac{e^{i(\omega/v_1)[\rho^2 + (h-z)^2]^{1/2}}}{[\rho^2 + (h-z)^2]^{1/2}} \tag{5}$$

or in integral form by

$$\Phi_0 = \int_0^\infty \frac{e^{-\alpha(h-z)} J_0(\xi\rho)\xi d\xi}{\alpha}. \tag{6}$$

The complete solution, satisfying the boundary conditions at infinity, will then be

$$\begin{aligned} z > 0 \qquad & \Phi_1 = \Phi_0 + \int_0^\infty A(\xi) e^{-\alpha z} J_0(\xi\rho) d\xi \\ z < 0 \qquad & \Phi_2 = \int_0^\infty B(\xi) e^{\bar{\alpha} z} J_0(\xi\rho) d\xi \end{aligned} \tag{7}$$

where A and B are arbitrary functions determined by the boundary conditions at $z=0$,

$$\frac{\partial \Phi_1}{\partial z} = \frac{\partial \Phi_2}{\partial z} \quad \text{and} \quad \gamma_1 \Phi_1 = \gamma_2 \Phi_2 \tag{8}$$

resulting in

$$z > 0 \qquad \Phi_1 = \Phi_0 + \int_0^\infty \frac{\xi(\alpha k - \bar{\alpha})}{\alpha(\alpha k + \bar{\alpha})} e^{-\alpha(h+z)} J_0(\xi\rho) d\xi \tag{9}$$

$$\Phi_2 = 2\int_0^\infty \frac{\xi e^{\bar{\alpha} z - \alpha h}}{\alpha k + \bar{\alpha}} J_0(\xi\rho) d\xi \tag{10}$$

where $k=\gamma_2/\gamma_1$.

The second term of Φ_1 can be evaluated in the complex plane as two branch line integrals. The first branch line integral around the branch point $\alpha=0$ gives the reflected wave

$$\Phi_{r_1} = -\frac{1}{\rho} e^{-i(\omega/v_1)[\rho+(h+z)^2/2\rho]} \tag{11}$$

and the second integral around the branch point $\bar{\alpha}=0$ gives the refraction wave

$$\Phi_{r_2} = -\frac{2iv_1^2}{kv_2\omega\beta^2\rho^2} e^{-i\omega[\rho/v_2+\beta(h+z)/v_1]} \tag{12}$$

where $\beta=(1-v_1^2/v_2^2)^{1/2}$. In the above evaluation the approximation has been made that ρ is large compared with h and z so that the expression $\rho+(h+z)^2/2\rho$ is an approximation for $(\rho^2+(h+z)^2)^{1/2}$. Generalizing the above solutions to an arbitrary pulse $f(t)$ gives

$$\Phi_{r_1} = \frac{-1}{2\pi\rho}\int_{-\infty}^{\infty} d\omega \int_0^\infty f(\mu) e^{i\omega[\mu+t-\rho/v_1-(h+z)^2/2\rho v_1]} d\mu \tag{13}$$

and

$$\Phi_{r_2} = \frac{-iv_1^2}{\pi k v_2 \beta^2 \rho^2}\int_0^\infty \frac{d\omega}{\omega} \int_0^\infty f(\mu) e^{i\omega[\mu+t-\rho/v_2-\beta(h+z)/v_1]} d\mu. \tag{14}$$

The refraction wave, equation (14), in this case is distorted with respect to the initial wave in such a way that its velocity components resemble the displacement components of the initial wave. It does not have any frequency selective characteristics except what may be in the initial wave.

The plane wave solution for this problem does not yield a refraction arrival, for it is only when there are waves spreading out from a point source that there

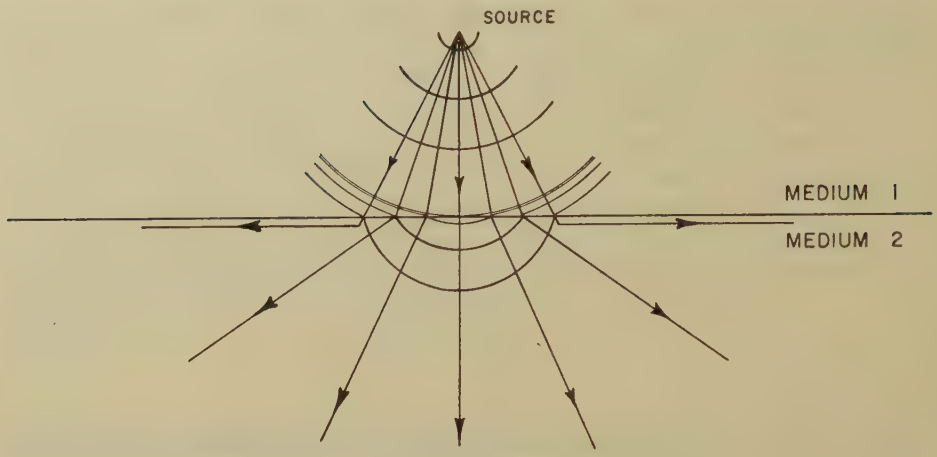

FIG. 2. Refraction at a boundary.

will be a continuum of energy travelling parallel to the interface in the second medium, see Figure 2.

THEORY OF THE REFRACTION ARRIVAL IN A TWO LAYERED MEDIA

Following Pekeris (1948) the formal solution for sound propagation in a water layer underlain by a uniform "liquid" bottom can be given as follows. Let ρ_1 and ρ_2 be the densities of the water and the bottom respectively and c_1 and c_2 be the velocities respectively with $c_2 > c_1$, and let d = depth of the source, z = depth of the receiver, and H = depth of water. Then, the velocity potential, Φ, must satisfy the differential equations

$$\nabla^2\Phi = \frac{1}{c_1^2}\frac{\partial^2\Phi}{\partial t^2} \tag{15}$$

in the water, and

$$\nabla^2\Phi = \frac{1}{c_2^2}\frac{\partial^2\Phi}{\partial t^2}$$

in the bottom where Φ is related to the acoustic pressure, p, and the vertical and horizontal velocity components, w and u, by the relations

$$p = \rho\frac{\partial\Phi}{\partial t}, \quad w = -\frac{\partial\Phi}{\partial z}, \quad \text{and} \quad u = -\frac{\partial\Phi}{\partial r}. \tag{16}$$

Fundamental solutions of equations (15) and (16) are

$$\Phi = e^{i\omega t}J_0(kr)F(z)G(k) \tag{17}$$

where F is given by the following for regions 1, 2, and 3 of Figure 3,

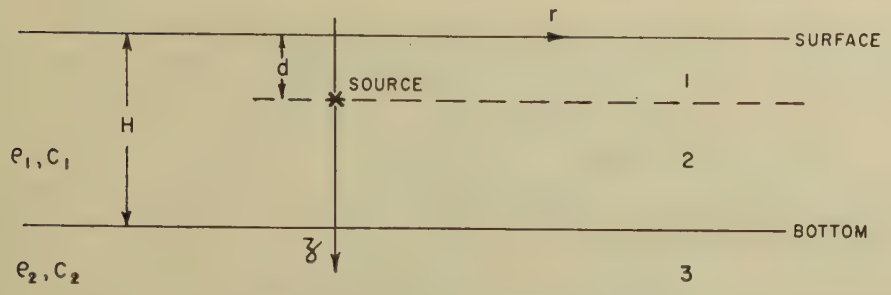

FIG. 3. Geometry of source in water layer of thickness H.

$$\begin{aligned} F_1 &= A \sin \beta_1 z \\ F_2 &= B \sin \beta_1 z + C \cos \beta_1 z \\ F_3 &= De^{-i\beta_2 z} \end{aligned} \tag{18}$$

satisfying the boundary conditions at infinity and at $z=0$. β_1 and β_2 are given by

$$\begin{aligned} \beta_1 &= \sqrt{\frac{\omega^2}{c_1^2} - k^2} && k < \frac{\omega}{c_1} \\ &= -i\sqrt{k^2 - \frac{\omega^2}{c_1^2}} && k < \frac{\omega}{c_1} \\ \beta_2 &= \sqrt{\frac{\omega^2}{c_2^2} - k^2} && k < \frac{\omega}{c_2} \\ &= -i\sqrt{k^2 - \frac{\omega^2}{c_2^2}} && k < \frac{\omega}{c_2}. \end{aligned} \tag{19}$$

At $z=H$, the boundary conditions

$$\rho_1 F_1 = \rho_2 F_2 \quad \text{and} \quad \frac{\partial F_2}{\partial z} = \frac{\partial F_3}{\partial z} \tag{20}$$

must be satisfied, and at $z=d$ the conditions

$$F_1 = F_2 \tag{21}$$

and

$$\frac{\partial F_1}{\partial z} - \frac{\partial F_2}{\partial z} = 2k \tag{22}$$

must be satisfied. Condition (22) insures a point source at $z=d$ when Φ is integrated over k from 0 to ∞ (Press and Ewing, 1950). Substituting (20), (21), and (22) into (18) and integrating over k from 0 to ∞ gives

$$\Psi_1 = 2\int_0^\infty J_0(kr)\,kdk\,\frac{\sin\beta_1 z}{\beta_1}\left[\frac{\beta_1\cos\beta_1(H-d)+ib\beta_2\sin\beta_1(H-d)}{\beta_1\cos\beta_1 H+ib\beta_2\sin\beta_1 H}\right] \tag{23}$$

$$\Psi_2 = 2\int_0^\infty J_0(kr)\,kdk\,\frac{\sin\beta_1 d}{\beta_1}\left[\frac{\beta_1\cos\beta_1(H-z)+ib\beta_2\sin\beta_1(H-z)}{\beta_1\cos\beta_1 H+ib\beta_2\sin\beta_1 H}\right] \tag{24}$$

$$\Psi_3 = 2b\int_0^\infty J_0(kr)\,kdk\,\frac{\sin\beta_1 d e^{-i\beta_2(z-H)}}{\beta_1\cos\beta_1 H+ib\beta_2\sin\beta_1 H} \tag{25}$$

where Φ is related to Ψ by $\Phi = e^{i\omega t}\Psi(r, z, \omega)$ and where $b = \rho_1/\rho_2$.

Ψ_2 (or Ψ_1) can most easily be evaluated in the complex k-plane (see Figure 4). The lines drawn from k_1 and k_2 parallel to the negative imaginary

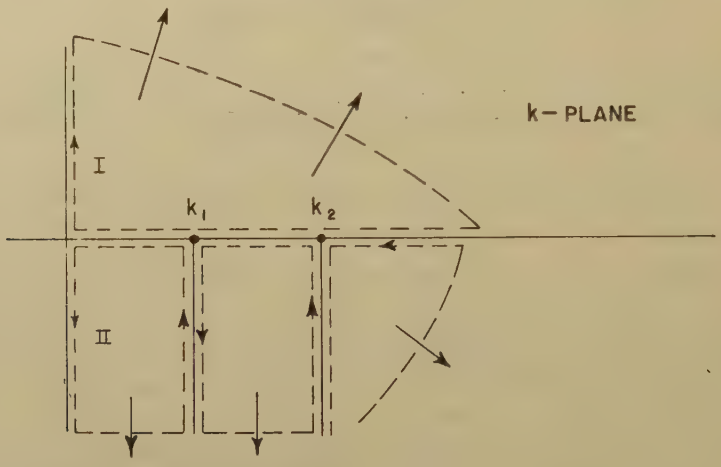

FIG. 4. Branch lines in complex k-plane corresponding to multiple-valued fractions β_1 and β_2.

axis are the branch lines corresponding to the multiple-valued functions β_1 and β_2 where $k_1 = \omega/c_1$ and $k_2 = \omega/c_2$. Substituting $2J_0(kr) = H_0^{(1)}(kr) + H_0^{(2)}(kr)$ into (24), where $H_0^{(1)}$ and $H_0^{(2)}$ are the first and second Hankel Functions respectively, and integrating $H_0^{(1)}$ over path I in Figure 4, and $H_0^{(2)}$ over path II gives the desired integral in terms of the sum of the residues and the two branch line integrals. $H_0^{(1)}$ vanishes at infinity in the first quadrant and $H_0^{(2)}$ in the fourth quadrant, and the integrals along the imaginary axis cancel since $H_0^{(1)}(iq) = -H_0^{(2)}(-iq)$. The first branch line integral, corresponding to $\beta_1 = 0$, has zero value since F has the same value on both sides of the branch line. The residues give the dispersive normal mode wave trains and are discussed fully by Pekeris (1948) both for a periodic point source and for the more general case of an explosive point source. The interest in this paper is in the evaluation of the second branch line integral, corresponding to $\beta_2 = 0$.

Let us designate this integral by Υ; then

$$\Upsilon = \int_{-i\infty}^{k_2} H_0^{(2)}(kr)\,[F(\beta_1, \beta_2) - F(\beta_1, -\beta_2)]\,kdk$$

$$= -2ib \int_{-i\infty}^{k_2} H_0^{(2)}(kr)\, \frac{\beta_2 \sin(\beta_1 d) \sin(\beta_1 z)}{\beta_1^2 \cos^2(\beta_1 H) + b^2\beta_2^2 \sin^2(\beta_1 H)}\, kdk. \qquad (26)$$

Since $H_0^{(2)}$ vanishes exponentially for large imaginary parts of its argument, the value of the integrand is appreciable only when the argument of $H_0^{(2)}$ is small. Then, changing the variable of integration to

$$k = \frac{\omega}{c_1}\eta = k_1\eta \qquad (27)$$

where

$$\eta = \frac{c_1}{c_2} - i\theta \qquad (28)$$

over the path of integration, we will have for θ small,

$$\beta_1 = \sqrt{k_1^2 - k^2} = k_1(1 - \eta^2)^{1/2} \approx k_1\left(1 - \frac{c_1^2}{c_2^2}\right)^{1/2} = k_1\mu \qquad (29)$$

$$\beta_2 = \sqrt{k_2^2 - k^2} = k_1\left(\frac{c_1^2}{c_2^2} - \eta^2\right)^{1/2} \approx k_1\left(2i\theta\frac{c_1}{c_2}\right)^{1/2} = k_1\left(2\theta\ \frac{c_1}{c_2}\right)e^{i(\pi/4)} \qquad (30)$$

$$H_0^{(2)}(kr) = H_0^{(2)}(k_1 r\eta) = \sqrt{\frac{2c_2}{\pi k_1 r c_1}}\, e^{i(\pi/4 - k_2 r)} e^{-k_1 r\theta} \qquad (31)$$

and

$$\beta_1^2 \cos^2(\beta_1 H) + b^2\beta_2^2 \sin^2(\beta_1 H) \approx \beta_1^2 \cos^2(\beta_1 H) = k_1^2\mu^2 \cos^2(k_1\mu H) \qquad (32)$$

where $\mu = (1 - c_1^2/c_2^2)^{1/2}$. Since β_2 is very small, the approximation to be given in equation (33) is valid generally, except in the regions of zeros of $\cos(\beta_1 H)$. Substituting (28), (29), (30), (31), and (32) into (26) gives

$$\Upsilon = \frac{4ibk_2}{\sqrt{\pi k_1 r}}\, \frac{\sin(k_1\mu d)\sin(k_1\mu z)}{\mu^2\cos^2(k_1\mu H)}\, e^{-ik_2 r} \int_0^\infty \theta^{1/2} e^{-k_1 r\theta} d\theta$$

$$= \frac{2ibk_2}{(k_1 r)^2}\, \frac{\sin(k_1\mu d)\sin(k_1\mu z)}{\mu^2\cos^2(k_1\mu H)}\, e^{-ik_2 r}. \qquad (33)$$

The case of principal interest is that for which equation (33) is generalized to a pulse. As representative of an explosion, we shall take an exponential pulse of the form

$$\begin{aligned} f(t) &= e^{-\lambda t} \qquad t > 0 \\ &= 0 \qquad t < 0 \end{aligned} \qquad (34)$$

where $f(t)$ can be given by the Fourier integral

$$f(t) = \frac{1}{2\pi}\int_{-\infty}^{\infty} \frac{e^{i\omega t}}{(\lambda + i\omega)}\, d\omega. \tag{35}$$

Then the expression for the generalized branch line integral, T, will be

$$\begin{aligned} T &= \frac{1}{2\pi}\int_{-\infty}^{\infty} \frac{\Upsilon(r, z, \omega)}{\lambda + i\omega} e^{i\omega t} d\omega \\ &= \frac{1}{2\pi}\int_{-\infty}^{\infty} \frac{2ibk_2}{(k_1 r)^2} \frac{\sin(k_1\mu d)\sin(k_1\mu z)}{\mu^2\cos^2(k_1\mu H)} \frac{e^{i[\omega t - k_2 r]}}{(\lambda + i\omega)} d\omega. \end{aligned} \tag{36}$$

This integral will have its major contributions at values of ω satisfying the equation

$$\cos(k_1\mu H) = 0. \tag{37}$$

However, at these points the approximation of equation (32) will no longer be valid. That expression will then be given by

$$\begin{aligned} &\beta_1^2\cos^2(\beta_1 H) + b^2\beta_2^2\sin^2(\beta_1 H) \\ &\quad \approx b^2\beta_2^2\sin^2(\beta_1 H) = b^2k_1^2\left(2\theta\frac{c_1}{c_2}\right)e^{i(\pi/4)}\sin^2(k_1\mu H). \end{aligned} \tag{38}$$

Substituting (38) into (26) gives for Υ_0,

$$\begin{aligned} \Upsilon_0 &= \frac{2k_2c_2}{bc_1\sqrt{\pi k_1 r}} \frac{\sin(k_1\mu d)\sin(k_1\mu z)}{\sin^2(k_1\mu H)} \int_0^{\infty} \theta^{-1/2} e^{-k_1 r\theta}\, d\theta \\ &= \frac{2c_2k_2}{bc_1k_1r} \frac{\sin(k_1\mu d)\sin(k_1\mu z)}{\sin^2(k_1\mu H)} e^{-ik_2 r} \\ &= \frac{2}{br} \frac{\sin(k_1\mu d)\sin(k_1\mu z)}{\sin^2(k_1\mu H)} e^{-ik_2 r} \end{aligned} \tag{39}$$

and for T_0,

$$T_0 = \frac{1}{2\pi}\int_{-\infty}^{\infty} \frac{2}{br} \frac{\sin(k_1\mu d)\sin(k_1\mu z)}{\sin^2(k_1\mu H)} \frac{e^{i[\omega t - k_2 r]}}{(\lambda + i\omega)} d\omega \tag{40}$$

where T_0 is to be evaluated in the neighborhood of values of the integrand ω_0 satisfying equation (37). For the source and receiver on the bottom, i.e., $z = d = H$, this will be of the form,

$$\begin{aligned} T_0 &= \sum_{\omega_0} \frac{A_0}{\pi br} \frac{\cos\left[\omega_0 t - k_{20} r - \tan^{-1}\left(\frac{\omega_0}{\lambda}\right)\right]}{(\lambda^2 + \omega_0^2)^{1/2}} && t \geqq \frac{r}{v_2} \\ &= 0 && t < \frac{r}{v_2}. \end{aligned} \tag{41}$$

T_0 is the expression for the velocity potential of the refraction arrival from an impulsive point source. It is a train of waves travelling with the velocity of the lower medium, $c_2 = \omega_0/k_{20}$. It is composed of the set of discrete frequencies, ω_0. It varies in range as r^{-1}, as contrasted with r^{-2} for the steady-state case; and its amplitude is greater the greater the density contrast between the two media. The $(\lambda^2+\omega_0^2)^{1/2}$ term merely expresses the excitation of the source at the frequencies ω_0.

It has come to the author's attention that Sato (1952) has obtained a similar solution for the refracted SH waves in a single layered medium.

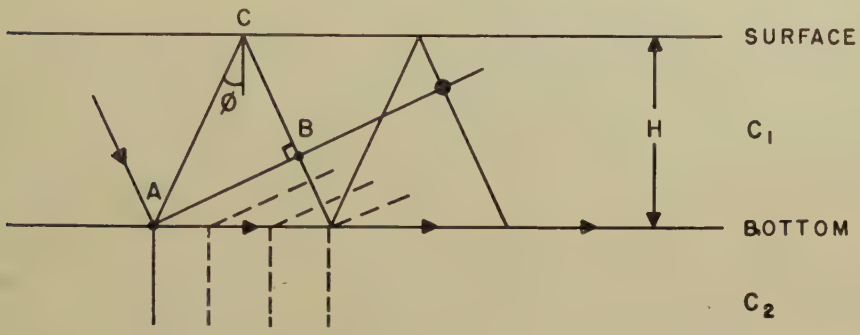

FIG. 5. Interference of refraction waves set up by multiple reflections within water layer of thickness H.

PHYSICAL SIGNIFICANCE OF THE FREQUENCY SELECTIVITY

The refraction arrival at a distant point will have maximum intensity for those frequencies for which there is constructive interference of the refraction waves set up by the multiple reflections from the free surface (see Figure 5.)* This corresponds to a phase difference of 2π between the waves at A and B, or

$$\frac{\omega_0}{c_1}\left[\overline{AC} + \overline{CB}\right] - \pi = 2(n-1)\pi \tag{42}$$

since the reflection coefficient on the bottom is zero at the critical angle, ϕ, and the reflection coefficient at the free surface is π. Then, from the geometry of Figure 5,

$$\frac{\omega_0}{c_1}\left[2H\cos\phi\right] = (2n-1)\pi. \tag{43}$$

Substituting $\phi = \sin^{-1}(c_1/c_2)$ and $f_0 = \omega_0/2\pi$ where f_0 is the frequency in cycles per second, gives

* This is similar to the argument used to describe the physical significance of the normal modes in the water channel (Press and Ewing, 1948 and Officer, 1951).

$$f_0 = \frac{(2n - 1)c_1c_2}{4H\sqrt{c_2^2 - c_1^2}}. \tag{44}$$

We may obtain the same expression from Equation (37):

$$\frac{\omega}{c_1} H \sqrt{1 - \frac{c_1^2}{c_2^2}} = (2n - 1)\frac{\pi}{2} \tag{45}$$

or

$$f_0 = \frac{(2n - 1)c_1c_2}{4H\sqrt{c_2^2 - c_1^2}}. \tag{46}$$

From the above discussion it should be clear why there is a frequency dependence for the refraction arrival in the layered case and not in the single boundary case. In the layered media the refraction is set up from the mutual interference of the multiple reflections at the critical angle in the overlying channel. This occurs at the discrete frequencies, ω_0. The range dependence is spherical, r^{-1} for the velocity potential (r^{-2} for intensity). For the single boundary the refraction is set up from the single critical angle ray; it has no frequency dependence. It is similar to a Lloyd mirror effect and correspondingly falls off as r^{-2} for the velocity potential (r^{-4} for intensity).

REFRACTION ARRIVALS IN MULTIPLE LAYERED MEDIA

In multiple layered media the branch line integral describes the refraction arrival from the lowest horizon. Its solution is exactly equivalent to equation (41). The refraction arrival from the intermediate layers are contained in the normal mode evaluation of the poles. Depending on the thicknesses and physical

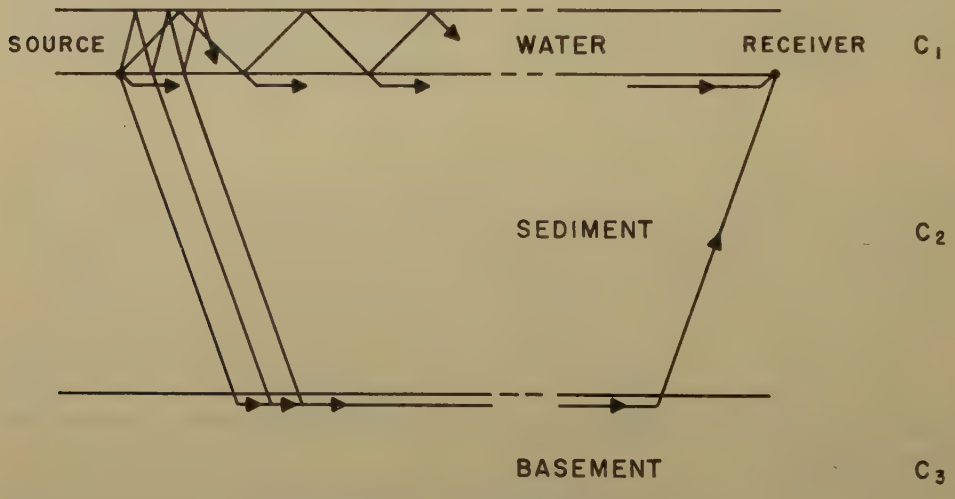

FIG. 6. Refraction over continental shelf areas.

properties of the media, these arrivals may be set up in the manner shown in Figure 5 with the frequency dependence of equation (44), or they may be determined solely by the method of Press and Ewing (1952).

Over the continental shelf areas a relatively simple geologic structure is usually found. It consists of a section of unconsolidated sediment and sometimes semiconsolidated and consolidated sediment down to the crystalline basement. The ratio of thickness of sediment to water is 5:1 or greater. Refractions are obtained from the top of the unconsolidated sediment, one or two intermediate horizons if present, and the basement (see Figure 6). Due to the thickness of the sediment, the ratio of the thickness of sediment to water, and the excess absorption in the sediment, the frequency selectivity for the lower horizon, i.e., the basement, will be determined by the constructive interference of the multiple reflections in the water channel alone. For the same reasons the sediment refraction will be determined by the multiple reflections in the water channel and not from reflections from the basement. Thus, the frequency selectivity for both arrivals will be given by equation (44).

OBSERVATIONS

In order to test the range dependence predicted by equation (41) for the primary refraction arrival, a series of measurements was made in Buzzard's Bay, Massachusetts. One-half pound charges of TNT-tetryl were fired on the bottom at various distances from the receiver, also on the bottom. Two receiving systems were used, both consisting of a Brush Development Co. Type AX-58 hydrophone, an underwater sound amplifier (Dow, 1952), a pen motor driver, and a Sanborn recorder. Both systems were calibrated through the hydrophone at the frequency of the refraction arrival.

If α is the range coefficient for the velocity potential of the refraction arrival, then the average intensity I will be given by

$$I = Ar^{-2\alpha} \tag{47}$$

or, in terms of decibels,

$$10 \log I = 10 \log A - 20\alpha \log r \tag{48}$$

so that a plot of the intensity, expressed in decibels, versus log r should be a straight line with slope 20α. Figure 7 is such a plot for one of the receiving systems. Both gave a value of 1.25 for α. This compares well with the theoretical value of 1.0 from equation (41), especially considering that there would be an increase over the theoretical value from such effects as absorption, scattering in the medium, and rough surface reflection and refraction.*

Table I gives a comparison of the experimentally measured frequencies of

* Perkins (1952) has a plot of log of the relative amplitude of the refraction arrival versus log of the shot-detector distance for a profile made on Bikini Atoll. For the refraction arrival from the igneous basement a value of 1.28 for α can be read from his graph.

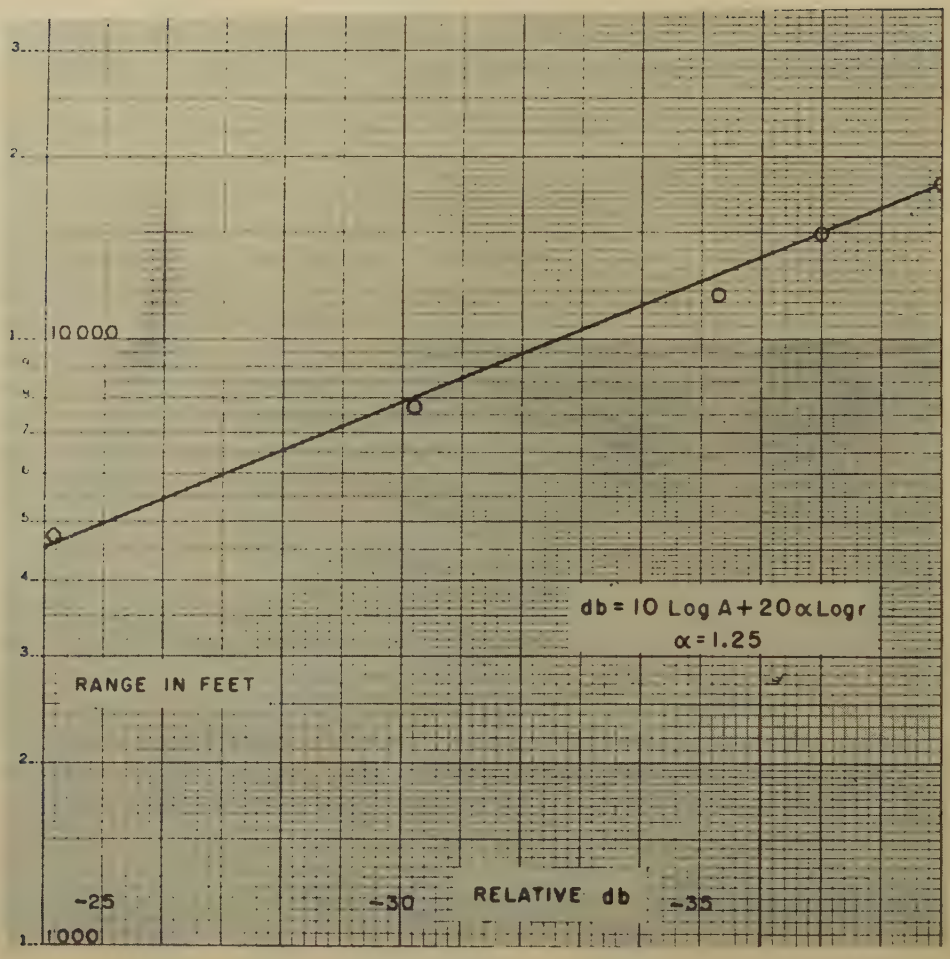

FIG. 7. Refraction arrival intensity vs. range.

the basement and sediment refraction arrivals and those predicted from equation (44) for four profiles made in Buzzard's Bay and on the continental shelf south of Cape Cod. In addition it contains a summary of the refraction results. The frequencies quoted for the experimental data are averaged from all the records for each profile; there is a variation of ± 1–2 cycles per second for a particular mode among the records of a given profile, except for the second mode of the sediment refraction on Profile 1, where the error in reading the frequency of the arrival itself is much larger. The agreement between the theoretical and experimental values is good. Figure 8 is a graph of Equation (44); frequency is plotted against depth of water for various velocity contrasts c_n/c_1 for the first three modes.

The character of the refraction arrival in water covered areas is in agreement

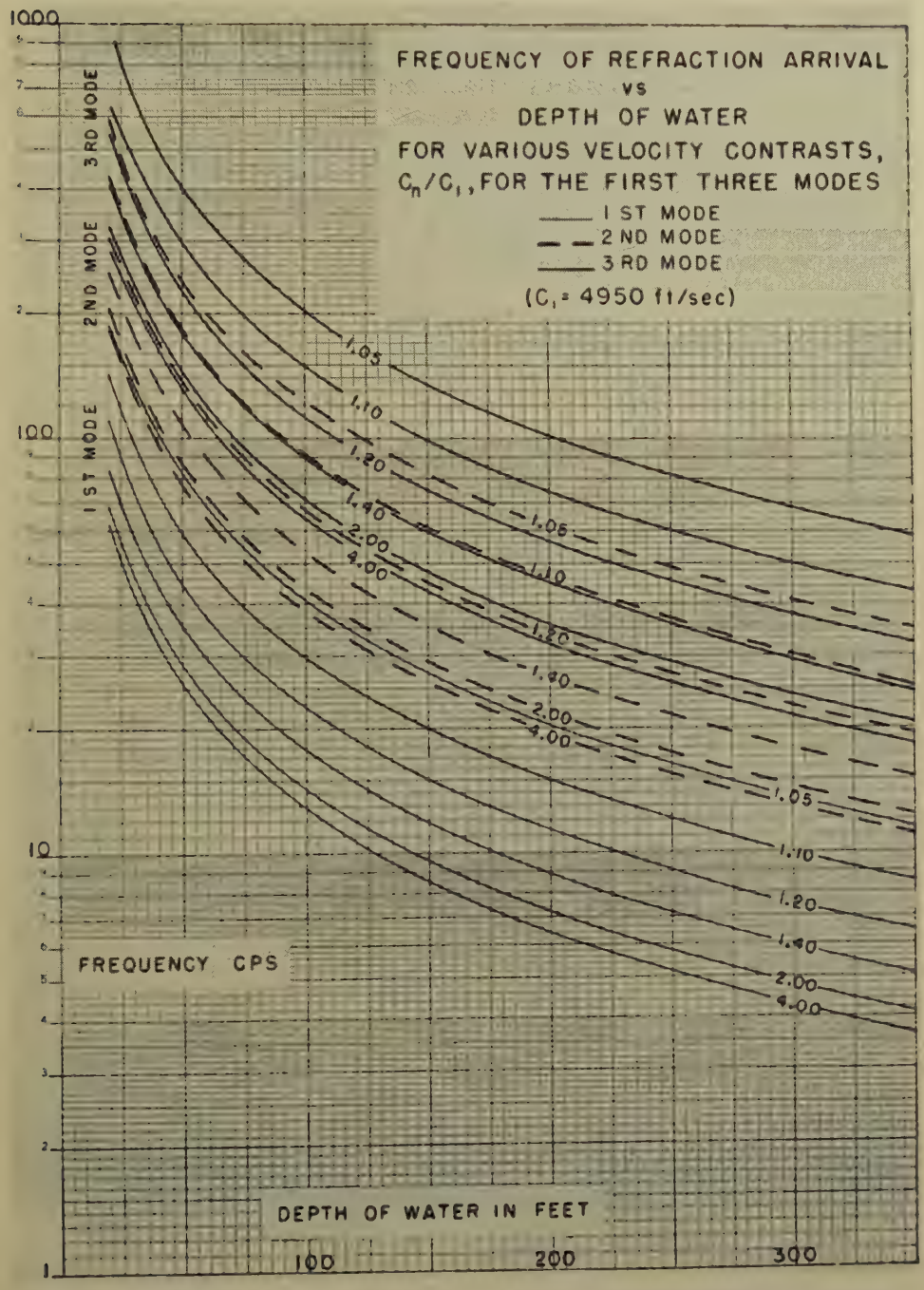

FIG. 8. Chart for determining refraction velocity from frequency of refraction arrival and water depth.

TABLE I

COMPARISON OF COMPUTED AND OBSERVED FREQUENCIES OF REFRACTION ARRIVALS

Refraction Results						Frequencies of Refraction Arrivals (in cps)							
						Basement		Sediment					
Profile	Depth of Water (ft)	Thickness of Sediment (ft)	Water Velocity (ft/sec)	Sediment Velocity (ft/sec)	Basement Velocity (ft/sec)	1st Mode		1st Mode		2nd Mode		3rd Mode	
						Theory	Expt.	Theory	Expt.	Theory	Expt.	Theory	Expt.
1	52	270	4890	5100	19650	26	27	83	83	250	215±		
2	107	1270	4890	5870	17600	12	14	21	21	65	62		
3	162	2200*	4900	5490	19350*			18	18	53	56		
4	252	2690*	4930	6160	18750*			8	9	25	23	41	44
						1st Mode							
						Theory	Expt.						
From Oliver & Drake (1951) (Fig. 9)	75	1500	4950	6490	17425	17	17	25	24	76	75		
						2nd Mode							
						Theory	Expt.						
						52	54						

* Values quoted from Ewing et al. (1950).

with the prediction of Equations (41) and (44). It travels with the velocity of the lower medium. It is composed of a train of waves of one or more discrete frequencies, according to the series, 1, 3, 5, . . . , determined by the velocities of sound in the water and the refraction medium and the depth of water. It has a sharp beginning and stays at fairly constant amplitude during its reception. Its velocity potential falls off with range as r^{-1}.

From the theory for normal mode propagation in the channel itself, i.e., the evaluation of the poles, an arrival is predicted which also travels with the velocity of the lower medium (Pekeris, 1948). However, this wave starts out at zero amplitude and builds up gradually as a continuous wave train to a maximum during the reception of the Airy phase following the incidence of the sound wave through the water. It is a dispersive wave train, decreasing in frequency to the Airy phase. These features are not observed on refraction profiles over the con-

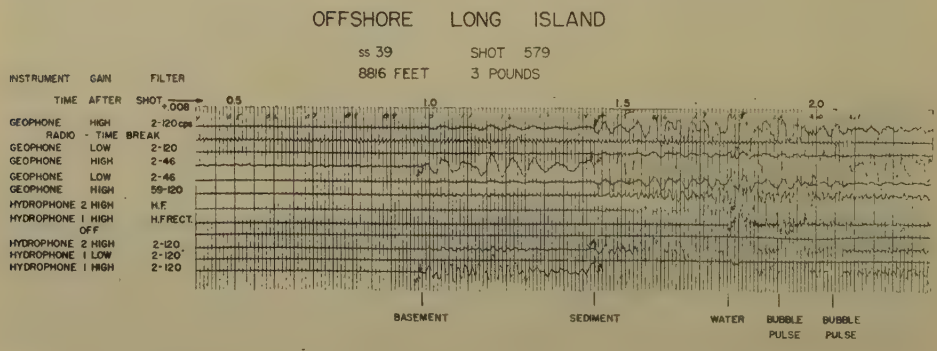

FIG. 9. Sample record showing refraction arrivals recorded at sea off Long Island by Oliver and Drake. Reproduced by permission of Geological Society of America.

tinental shelf (Ewing et al., 1950 or Oliver and Drake, 1951, Figure 9), although they have been observed on some profiles in very shallow water (Pekeris, 1948).

CONCLUSIONS

Knowing the frequencies of the refraction arrivals, the depth of water, and the velocity of sound in water, one can calculate the velocities and depths of the seismic refraction horizons from a single refraction record. From Figure 8, or a similar graph, the velocities of the refraction layers can be determined from the frequencies of the arrivals. Then from the travel times the depths of the horizons can be computed.

This method could be of importance in reconnaissance measurements of geologic structure over the continental shelves or of similar structures on land. In either case knowledge of the frequency of the refraction arrival increases the potential information available on a record.

ACKNOWLEDGMENTS

The author expresses his thanks to Dr. J. B. Hersey for cooperation in the research program and to Prof. F. Press for reading and criticizing the manuscript.

RFERENCES

Dow, W. (1952) An experimental portable listening device for detection, measurement, and recording of underwater sound, Woods Hole Oceanographic Institution, Reference No. 52-10.

Ewing M., Worzel, J. L., Steenland, N. C., and Press, F. (1950) Geophysical investigations in the emerged and submerged Atlantic coastal plain. Part V., Woods Hole, New York, and Cape May sections, *Bull. Geol. Soc. Am.*, vol. 61, pp. 877–892.

Jeffreys, H. (1926) On compressional waves in two superposed layers, *Proc. Cambr. Phil. Soc.*, vol. 23, pp. 472–481.

Muskat, M. (1933) The theory of refraction shooting, *Physics*, vol. 4, pp. 14–28.

Officer, C. B. (1951) Normal mode propagation in three layered liquid half-space by ray theory, *Geophysics*, vol. 16, pp. 207–212.

Oliver, J. E. and Drake, C. L. (1951) Geophysical investigations in the emerged and submerged Atlantic coastal Plain, Part VI, The Long Island area, *Bull. Geol. Soc. Am.*, vol. 62, pp. 1287–1296.

Pekeris, C. L. (1948) Theory of propagation of explosive sound in shallow water in *Propagation of Sound in the Ocean*, Mem. 27, Geol. Soc. Am.

Perkins, B. (1952) Letter to the Editor, *Geophysics*, vol. 17, pp. 411–412.

Press, F. and Ewing, M. (1948) A theory of microseisms with geologic applications, *Trans. Am. Geophys. U.* vol. 29, pp. 163–174.

———, (1950) Propagation of explosive sound in a liquid layer overlying a semi-infinite elastic solid, *Geophysics*, vol. 15, pp. 426–446.

———, (1952) Note on refracted waves in a layer (abstract), *Bull. Geol. Soc. Am.*, vol. 63, pp. 1356.

Sato, Y. (1952) Study on surface waves, VI. Generation of Love and other types of SH Waves, *Bull. Earthquake Res. Inst., Tokyo Univ.*, vol. 30, pp. 101–120 (in English).

Worzel, J. L. and Ewing, M. (1948) Explosion sounds in shallow water, in *Propagation of Sound in the Ocean*, Mem. 27, Geol. Soc. Am.

Contribution No. 630

Reprinted from Ecology, Vol. 34, No. 1, January, 1953
Printed in U. S. A.

THE DRILLING MECHANISM OF THE NATICIDAE[1]

It has never been conclusively determined whether carnivorous prosobranchs of the family Naticidae drill holes through the shells of other molluscs by means of (1) chemical secretions from the salivary glands or similar organs, (2) mechanical rasping with the radula, or (3) a combination of both. The drilling process has not been observed directly because most species refuse to feed above the surface of the sand, and the few that will feed in the open water cover the drilling organs with the foot so that the drilling process is hidden.

A number of investigators have been of the opinion that the hole is made with a flat, disc-like pad that is situated on the ventral surface of the proboscis at the distal extremity. This organ occurs only in this group of prosobranchs, and its size agrees closely with that of the hole. Schiemenz (1891) obtained a reddening of blue litmus paper when touched to fresh pads and concluded that the hole is dissolved with acid secreted by this organ which he named the "boring gland" (*Bohrdruse*).

Hirsh (1915) and Boettger (1930) both held to this view although neither was able to demonstrate the actual secretion of a sufficient amount of free acid to dissolve a hole in the short time in which it is normally accomplished. Later Ankel (1937) placed "boring glands" on glossy shells and demonstrated faint etching of the surface, but was unable to determine the presence of any of the common acids. He finally concluded (1938) that a specific enzyme, "Calcase," might be the active agent.

An opposite view was held by Fischer (1922) who maintained, after histological studies had proved that the pad was mainly a muscular organ, that the hole is bored mechanically with the radula working as a rasp. However, he did suggest that its action might be facilitated by a softening of the calcareous shells with sulphuric acid secreted by the salivary glands. Pelseneer (1925) showed that the salivary secretions contain no acid and concluded that the drilling process is purely mechanical.

The discovery of drilled egg capsules of the marine snail Sipho by Thorson (1935) and of bored egg cases of rays by Jensen (1951) demonstrated that the Naticidae could penetrate noncalcareous substances. Jensen determined that both materials were resistant to sulphuric acid in concentrations as high as two per cent, and also that the edges of the holes were furrowed with minute scratches which he believed were made by the radula teeth.

There appear to be no published records of experiments to determine the ability of the Naticidae to drill through other inert materials. For this reason, two experiments were performed with the American clam drill, *Polynices duplicata*, to test its ability to perforate lamellibranch shells coated with paraffin wax and plaster of Paris. A number of clams (*Mya arenaria*) coated with histological paraffin in layers approximately 0.5 mm thick, were placed in a sea-water aquarium containing starved *P. duplicata*. The Polynices readily attacked the coated clams and drilled typical holes without any interference from the wax layers. This established the fact that the drilling process is basically mechanical but did not preclude the auxiliary use of chemical secretions to soften the hard calcareous shell after the wax had been scraped away. A number of clams were then coated with plaster of Paris as a further test. Plaster of Paris is a fine powder which consists of partially dehydrated calcium sulphate. When mixed with an appropriate quantity of water it sets within a few minutes and reaches its full degree of hardness after only a few hours. It is insoluble in dilute acids and organic solvents. The *Polynices* readily attacked clams coated with Plaster of Paris and drilled typical holes through the coatings without apparent difficulty.

The results of these experiments indicate clearly that the Naticidae drill holes through the shells of their prey by mechanical rasping with the radula, unaided by chemical secretions. The function of the so-called "boring gland" is not apparent, but its structure and location suggest that it may be an adhesive pad that holds the anterior extremity of the proboscis firmly against the shell to facilitate the action of the radula.

References

Ankel, W. E. 1937. Wie bohrt *Natica?* Biol. Centralbl., **57.**

——. 1938. Erwerb und Aufnahme der Nahrung bei den Gastropoden. Zool. Anz., Suppl., **11.**

Boettger, C. R. 1930. Die Lage der Bohrstelle beim Angriff der Raubschnecken aus der Familie Naticidae. Zeit. wiss. Zool., **136.**

Fischer, P. H. 1922. Sur les Gastropodes perceurs. J. Conchyliol., **67.**

Hirsch, G. Chr. 1915. Die Ernahrungsbiologie fleischfressender Gastropoden. Zool. Jahrb., Abt. Allg. Zool., **35.**

Jensen, Ad. S. 1951. Do the Naticidae (Gastropoda Prosobranchia) drill by chemical or by mechanical means? Vidensk. Medd., Dansk. naturh. Foren., **113.**

Pelseneer, P. 1925. Gastropodes marins carnivores Natica et Purpura. Ann. Soc. Roy. Zool. Belgique, **55.**

Schiemenz, P. 1891. Wie bohrt Natica die Muscheln an? Mitt. Zool. St. Neapel., **10.**

Thorson, G. 1935. Studies on the egg capsules and development of arctic marine prosobranchs. Medd. om Grønl. **100** (5).

Harry J. Turner, Jr.
Woods Hole Oceanographic Institution,
Woods Hole, Massachusetts

[1] Contribution No. 630 from the Woods Hole Oceanographic Institution.

Contribution No. 631

DIFFUSION, ENTRAINMENT AND FRICTIONAL DRAG ASSOCIATED WITH NON-SATURATED, BUOYANT AIR PARCELS RISING THROUGH A TURBULENT AIR MASS

By Andrew F. Bunker

Woods Hole Oceanographic Institution[1,2]

(Manuscript received 10 September 1952)

ABSTRACT

The entrainment equations of Houghton and Cramer have been extended to include the effects of diffusion of heat and momentum and the frictional pressure drag. The equations developed from these considerations show that certain combinations of parcel size, temperature difference, vertical velocity, and turbulence permit buoyant air parcels to pass from the bottom to the top of the turbulent ground layer. Other combinations lead to rapid dissipation of the parcel's temperature difference and velocity. The equations have been checked against three sets of observations within unstable, dry air masses. Observed properties of buoyant parcels existing in super-adiabatic atmospheres agree, within observational error, with combinations leading to extended survival of air bubbles as predicted by the equations. One set of data leads to the approximation of the value of the coefficient of pressure drag, 0.1, associated with an air parcel moving through the air.

1. Survival of convective parcels within an unstable, turbulent air stream

The question frequently arises, during studies of turbulence in the ground layer of the atmosphere, "What are the stability and turbulence conditions which will allow a non-saturated buoyant bubble or parcel of any given size to ascend to the top of the layer?" The problem is one of evaluating the retarding and dissipative influences of friction, entrainment and diffusion that are in critical balance with the bubble's buoyancy and inertia. If, for example, the atmospheric turbulence is too great or the parcel size too small, the temperature excess and momentum will be dissipated before the parcel can rise an appreciable distance through the layer. The height variation of the temperature lapse-rate, turbulence, and parcel size will have an effect on the survival of the parcel. All of these and many other factors must be accounted for in any satisfactory theory of convection within a turbulent medium.

The equations of Houghton and Cramer (1951), describing the entrainment of outside air into jets, have been applied to air parcels and extended to include the effects mentioned, under the assumption that entrainment operates similarly with thickness-radius ratios of less than one. Differential equations

[1] Contribution No. 631 of the Woods Hole Oceanographic Institution.

[2] This research was conducted under Contract No. N6onr-277, Task Order No. II, NR-082-021, between the Office of Naval Research and the Woods Hole Oceanographic Institution.

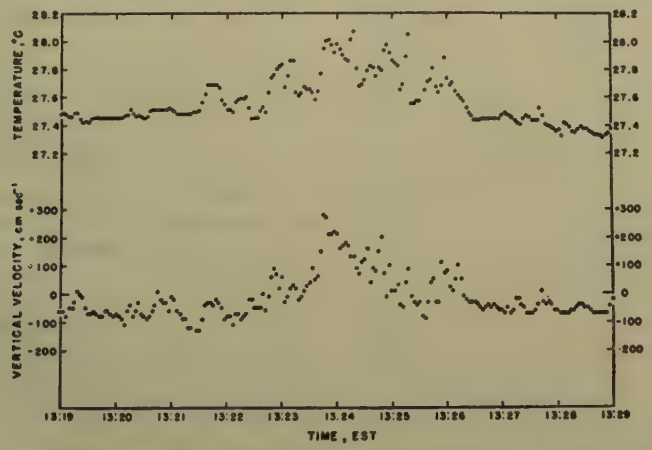

FIG. 1. Time cross-section, showing temperature and vertical-velocity fluctuations associated with passage of large buoyant parcel through 100-m surface.

have been developed which take into account the entrainment of environmental air, the diffusion to the outside air of the jet's temperature excess and momentum, the pressure drag of the surrounding air, and the buoyancy of the air. These equations are similar to theirs, but contain additional terms. Since many simplifications have been made in deriving the equations, they cannot describe with precision the motions and temperatures of the ascending parcel, but are sufficient to predict intensification or dissipation of velocities and temperature excesses. Integration of the equations, accomplished by numerical means, yields changes in the vertical velocities and temperature excesses which may be compared with observed values.

Observations of radii, heights, thicknesses, temperature excesses, vertical velocities of air parcels, and coefficients of turbulent mass exchange have been made on three days with convective activity. One set of data was obtained from instruments mounted on the Brookhaven, Long Island, meteorological tower (Ludlam, 1948). On 31 August 1951, combination bivanes, anemometers and thermometers recorded the total air velocity, the vertical velocity of the air, and the air temperature at two levels of the tower. Fig. 1 is a time cross-section of the largest bubble observed during the afternoon of 31 August 1951, at the 100-m level. Temperatures are plotted in degrees Celsius, while vertical velocities are plotted in centimeters per second. The vertical velocity "zero" is determined by the average velocity for over an hour. On "convective" days, such as this day, it is possible to observe the properties of individual bubbles as they pass the instruments. They are readily detected by their great temperature excesses and vertical velocities, which are roughly an order of magnitude larger than those of the turbulent eddies of the surrounding atmosphere. The appearance of such convecting bubbles or parcels is quite distinct from the smaller turbulent gusts, which show a much smaller correlation between temperature and vertical velocity deviations. By observation of passages at two heights, it is determined which sizes of parcels are able to pass from one level to the next and what changes occur in the size, temperature excess, and the vertical velocities. Sufficient supplementary observations and measures of the turbulence at different levels, for insertion in the equations, were obtained from both airplane and tower measurements of the heat flow through the atmosphere.

On 1 September 1948 and 3 February 1950, airplane observations of the water-vapor flux and gradients were made, in connection with diffusion experiments (Bunker, 1952), in unstable air masses in which buoyant parcels existed. Measurements and estimates of the sizes, velocities, and temperature excesses of the surviving parcels have been made and may be substituted into the equations.

2. Extension of entrainment theory to include diffusion and friction

Houghton and Cramer (1951) have developed equations describing the entrainment of outside air into jets of unsaturated air, as well as into cumulus clouds. Their equations were not intended as a theory of convection, since they do not include diffusion or frictional effects. The present work uses the findings and notation of Houghton and Cramer, and modifies them to consider the influence of a turbulent environment.

Proceeding in a similar manner, we consider a volume element of the rising column with cross section $d\sigma$ and height dz. Air entering the bottom has an average temperature T', a density ρ', and a vertical velocity w', while outside air has the temperature T, the density ρ, and zero vertical velocity. According to theory, the lighter air of the jet ($T' > T$) stretches, and entrains outside air, so that air leaves the volume with the temperature and density $T' + (\delta T'/\delta z)\,dz$ and $\rho' + (\delta\rho'/\delta z)\,dz$, where δ represents the change due to entrainment, diffusion and frictional influences. The velocity of the air leaving the volume is $w' + (Dw'/Dz)\,dz$, where D stands for the combined change due to buoyancy acceleration, entrainment, diffusion of momentum and frictional forces.

With these conventions, we obtain the same form of mass continuity equation; namely,

$$\Delta m = w'\,\delta\rho'/\delta z + \rho'\,Dw'/Dz, \tag{1}$$

where Δm is the mass of environmental air added per unit volume per unit time.

The energy equation can be developed by considering both the entrainment and diffusion of heat into and out of the elemental volume. The energy equation may be written

$$c_p T'\rho' w'\,d\sigma + c_p T\,\Delta m\,dz\,d\sigma + c_p\rho'\,d\sigma\,dz\,\partial T'/\partial t = c_p(\rho' w'\,d\sigma + \Delta m\,dz\,d\sigma)(T' + \delta T'/\delta z\,dz). \tag{2}$$

In this equation, $\partial T'/\partial t$ means the time-rate-of-change of temperature due to diffusion alone. The derivative may be replaced through use of the diffusion equation,

$$\partial T'/\partial t = (A/\rho')\,\partial^2 T'/\partial x^2. \tag{3}$$

The second derivative may be evaluated by assuming the temperature variation across a jet to approximate an elliptical curve. Observations show very irregular temperature traces across jets, but mean curves do approximate ellipses. The second derivative of an ellipse is equal to $-b^4/a^2y^3$, when a and b are the major and minor axes. Applied to jets, a is the radius of the jet and b is the maximum value, T'_{max}, of a mean temperature curve. Equation (3) then becomes

$$\partial T'/\partial t = (A/\rho')(b^4/a^2y^3). \tag{4}$$

A further simplification results if an average value of

$\partial T'/\partial t$ between x equal to 0 and a is entered in the energy equation (2):

$$\overline{\partial T'/\partial t} = -(A/\rho')T'_{\max}/0.6\,L^2 = -2.12\,AT'/\rho'L^2 \approx -2AT'/\rho'L^2, \quad (5)$$

where L is the radius of the jet.

The energy equation (2) becomes (6) with substitution of $-2AT'/\rho'L^2$ for $\partial T'/\partial t$ and the collection of terms, omitting second-order terms:

$$\Delta m = -(\rho' w'\,\delta T'/\delta z)/[(T' - T) - 2A/L^2]. \quad (6)$$

A practical problem arises, when it is desired to determine a value of the coefficient of turbulent mass exchange to place in (6). Only a value of the horizontal mass-exchange coefficient inside the parcel can completely satisfy the definition and use of the coefficient as it appears in (3). Such a value would be extremely difficult, if not impossible, to determine. However, an approximate value can be found by making two assumptions. One is that the turbulence of the outside air is isotropic, that is, the horizontal coefficient equals the vertical coefficient. This assumption undoubtedly holds true in the adiabatic portion of the ground layer, but breaks down near the ground and possibly near the inversion at the top of the layer. The other assumption is that the horizontal turbulence inside the parcel is practically the same as the horizontal turbulence outside the parcel. At the moment, the validity of this assumption cannot be proven. The determination of the coefficient reduces, then, to measurements of the flow of a property through a surface and the vertical gradient of the property, and substitution in the diffusion equation. Measurements of heat or water-vapor flows can be made easily with psychrographs carried by airplanes, yielding coefficients characteristic of these properties (see Bunker, 1952). In the development of the following momentum equation, the same value of the coefficient is used, although a controversy exists regarding the identity of the coefficients of turbulent mass exchange for heat, momentum, water vapor and other properties of the air.

The momentum equation may be developed in a similar manner, but the effect of frictional drag must be considered. The momentum change per unit time of an infinitesimal mass of a rising solid cylinder of total mass M, retarded by a force F, may be expressed as $dm\,\Delta v/t = dm\,F/M$. Assuming that a rising air column can be treated in a similar way, we obtain

$$dm\,\Delta v/t = dm\,F/M = (\rho\,d\sigma\,dz)(C_d w'^2 \rho\,d\sigma)/2\rho\,d\sigma\,H, \quad (7)$$

where C_d is the drag coefficient and H the vertical dimension of the jet. It is open to question whether this assumption correctly describes the drag on the air in the column. It is believed that errors introduced by this simplification of the drag term do not appreciably affect the final velocity curve of the entire column, although it might greatly affect the velocity in various regions of the column. The expression of the drag in terms of the velocity squared and C_d, the drag coefficient, is the one customarily employed in hydrodynamics. The momentum-balance equation then becomes

$$\rho' w'^2\,d\sigma + \rho' w'(\partial w'/\partial z)\,d\sigma\,dz - (2\,Aw'/\rho'L^2)\rho'\,d\sigma\,dz - \rho' w'^2\,d\sigma - \rho' w'(Dw'/Dz)\,dz\,d\sigma - \Delta m\,dz\,d\sigma - \rho' C_d w'^2\,d\sigma\,dz/2H = 0. \quad (8)$$

This equation reduces to

$$\Delta m = \rho'\,\partial w'/\partial z - 2\,A/L^2 - \rho'\,Dw'/Dz - \rho' C_d w'/2H. \quad (9)$$

These equations, (1), (6) and (9), may be solved for Dw'/Dz and $\delta T'/\delta z$, through use of the buoyancy equation,

$$\partial w'/\partial z = g(T' - T)/w'T, \quad (10)$$

and the equation of state, without the pressure term, since $p' \approx p$:

$$(1/\rho')(\delta\rho'/\delta z) = -(1/T')(\delta T'/\delta z). \quad (11)$$

We find

$$Dw'/Dz = -A/\rho L^2 + (T' - T)g/(2Tw') - w' C_d/4H, \quad (12)$$

and

$$\delta T'/\delta z = -A(T' - T)/w\rho L^2 - (T' - T)^2 g/2w'T + C_d(T' - T)/4H. \quad (13)$$

Equations (12) and (13) will allow the computation of the velocity and temperature-height curves, whenever original values of size, temperature, velocity and turbulence are given. These equations differ from the Houghton-Cramer equations by the addition of the first and third terms, which include the effect of diffusion and drag.

A few moments' examination of these equations will show that certain combinations of sizes, turbulence, velocities and temperature differences may result in rapid dissipation of convecting parcels. Large values of the turbulent intensity, combined with small values of temperature differences and dimensions, lead to this result. The opposite effect results when weak turbulence is combined with large sizes and temperature differences. In the following section, observed values of these parameters are substituted in the equations, to see if survival or dissipation is forecast by the equations.

3. Comparison of equations with data obtained on Brookhaven meteorological towers

On 30 and 31 August 1951, extensive observations were made on the Brookhaven meteorological tower, during a joint experiment by the meteorological groups

of Brookhaven, New York University and the Woods Hole Oceanographic Institution (Panofsky, 1953). The regular Brookhaven tower and smoke-generator equipment were used, together with the heat-flux meter and airplane psychrograph of the Woods Hole Oceanographic Institution. The observations pertinent to the present discussion of convective motion within a turbulent stream are the simultaneous recordings of the rapid fluctuations of the temperatures, inclinations and velocities of the winds, and recordings of the gradients. From the observations of the fluctuations of temperature and vertical velocity, it is possible to detect convecting parcels and note their velocities, temperature excesses, and their lateral and vertical extent. Since observations were made at both the 25-m and 100-m levels, it is possible to notice differences in the sizes, velocities and temperatures of the convecting jets at the two levels. At the lower level, the gusts are smaller and more frequent with sizes ranging around 40–50 m in radius, temperature excesses around 0.5C, and vertical velocities around 90 cm/sec. At the 100-m level, the buoyant bubbles are less frequent and more easily separated from the surrounding air. It is noted that jets of radius 40 m have temperature excesses of about 0.3C and vertical velocities of about 60 cm/sec. Jets of radius 250 m, which are common at the higher level, have larger temperature excesses of about 0.6C and vertical velocities of 100 to 140 cm/sec. It has not been possible to study identical parcels at different levels, but it is sufficient for the present check to determine the temperature and velocity characteristics of the various-sized parcels. The vertical extent H of the jets has been estimated from the observations, since no direct measurements could be made. After checking of vertical velocities and radii of bubbles observed at the 25 and 100-m levels, and noting of the fact that jets at the 100-m level, with radii up to 250 m, could not be identified at the 25-m level, it is concluded that the vertical extent of many bubbles is of the order of magnitude of $\frac{1}{10}$ their radii. The following two computations are based on this ratio, although measurements from airplanes at higher levels indicate that ratios of $\frac{1}{4}$ to $\frac{1}{2}$ occur under conditions of instability and moderately intense turbulence. Warm, moist bubbles of approximately these dimensions were observed frequently during the diffusion experiments, already mentioned, carried out in unstable air blowing over warm water.

The first test of the equations consists of finding out whether computed temperature and velocity variations duplicate the changes observed to occur in the 40-m radius parcels. For this test, the radius of the bubble is held constant during the integration from the 25- to the 100-m level. The equations (12) and (13) are numerically integrated.

A value for the drag coefficient of 0.1 was tried as a reasonable value, since it lies between the value for a solid sphere, 0.3, and the value for a streamlined airfoil, 0.01. This drag coefficient of 0.1 yields results in agreement with the observations. Computations show that if the drag coefficient were increased to 0.3, and other parameters were held the same, a parcel of the character studied in table 1 would nearly halt by the time it reached the 60-m level, but retain its large temperature difference. If a drag of 0.01 were used, the parcel would retain most of its vertical velocity but lose its temperature excess. From the equations, it is seen that the "best" drag coefficient depends to a considerable degree upon the thickness-radius ratio used, and is consequently affected by inaccuracies in the ratio determination.

The value of the coefficient of turbulent mass exchange used in the equations was determined from the temperature gradients and the heat flow through the air surrounding the convecting parcels. The heat flow was determined from a one-hour series of measurements, with the Woods Hole Oceanographic Institution heat-flow meter, of one-second values of the vertical velocity and temperature of the air. The velocities and temperatures of buoyant parcels were excluded from the heat-flow determination. A heat flow of 1.1 cal cm^{-2} sec^{-1} was measured. As the Brookhaven bivane and anemometer give a value of the heat flow 2.2 times greater (Panofsky, 1953), it not being known which of the two instruments is the more accurate, an average between the two instruments gives a heat-flow value of 1.8 cal cm^{-2} sec^{-1}. When this heat flow is substituted into the diffusion equation,

$$F = -c_p A\, \partial\theta/\partial z, \qquad (14)$$

TABLE 1. Computed velocities and temperature excesses. (Constant radius.)

z (m)	w' (cm/sec)	Dw'/Dz (sec^{-1})	$T'-T_0$ (deg C)	$\delta T/\delta z$ (C/cm)	A (g cm^{-1} sec^{-1})	ΔT_0 (deg C)	L (m)
25	90	-0.50×10^{-2}	0.500	-6.18×10^{-5}	150	0.057	40
35	85	-0.43×10^{-2}	0.495	-6.57×10^{-5}	150	0.055	40
45	81	-0.37×10^{-2}	0.484	-6.91×10^{-5}	150	0.053	40
55	77	-0.34×10^{-2}	0.451	-6.93×10^{-5}	150	0.052	40
65	74	-0.31×10^{-2}	0.431	-7.08×10^{-5}	150	0.051	40
75	71	-0.29×10^{-2}	0.413	-6.85×10^{-5}	150	0.050	40
85	68	-0.27×10^{-2}	0.393	-6.87×10^{-5}	150	0.074	40
100	65		0.360		150		40

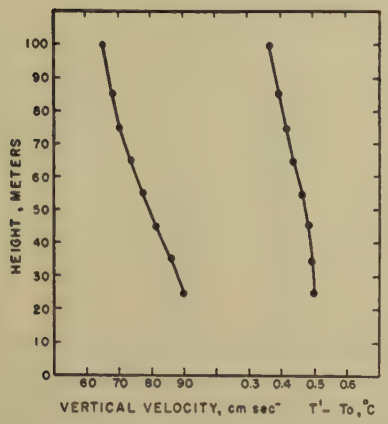

FIG. 2. Computed velocities and temperatures of parcel moving from 25-m level to 100-m level. 40-m radius of parcel and coefficient of turbulent mass exchange of 150 g cm^{-1} sec^{-1} are constant.

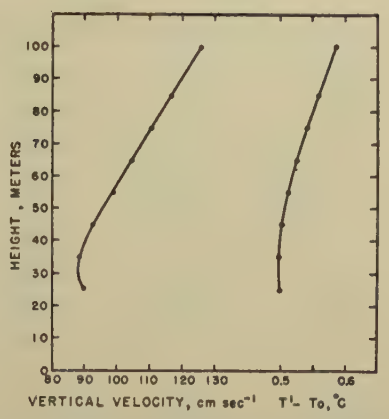

FIG. 3. Computed velocities and temperatures of parcel moving from 25-m level to 100-m level. Radius was increased from 40 to 265 m. Turbulent-exchange coefficient was held constant at 150 g cm^{-1} sec^{-1}.

the coefficient A is found to be 150 g cm^{-1} sec^{-1}. It was found that practically no variation of the coefficient occurred between the 25- and the 100-m levels. With use of these values, the velocities and temperatures in table 1 were found.

In this table, the computed quantities are entered in columns headed by the symbols as used in the equations. The only new symbol used is ΔT_0. It designates the increase in the parcel's temperature excess due to the parcel's upward passage through a super-adiabatic atmosphere with a potential-temperature lapse rate of 5×10^{-5} C/cm. The velocities and temperature excesses have been plotted against the height in fig. 2. The computations show that parcels will retain their identity in passing from the 25- to the 100-m level, and that they are retarded and lose 30 per cent of their temperature excess.

The second test was to use the same initial conditions, but let the radius expand and also the thickness, since the ratio of $\frac{A}{\rho_0}$ is to be maintained, as the bubble rises through the air. The increase is stated as a linear function for this calculation, although the actual process is visualized as a discontinuous one resulting from the chance proximity of two or more smaller bubbles. That is, several parcels may converge, so that they act as a single buoyant parcel. The greater radius of the parcel decreases the rate of diffusive transport of momentum and heat out of the parcel, thereby increasing its chances of survival and of reaching the top of the layer. A calculation similar to the previous one has been made with the new condition. The resulting values are presented in table 2 and fig. 3.

It is seen that the parcel starts to decelerate, but as the size increases the diffusion losses become smaller and the parcel accelerates again. Further, it will be noted that the temperature excess actually increases as the bubble moves through the air which has a super-adiabatic lapse rate. The final velocity and temperature excess agree with the observed properties of parcels of radius 265 m at the 100-m level.

4. Survival of convective parcels throughout ground layer on 1 September 1948

The following data were obtained from an airplane, equipped for observing water-vapor diffusion in the air as it blew off the coast of southeastern Massachusetts, out over the waters of Buzzards Bay. An unstable air mass, heated over the land, possessed convective currents which produced about 2/10 sky coverage of

TABLE 2. Computed velocities and temperature excesses. (Increasing radius.)

z (m)	w' (cm/sec)	Dw'/Dz (sec^{-1})	$T'-T_0$ (deg C)	$\delta T/\delta z$ (C/cm)	A (g cm^{-1} sec^{-1})	ΔT_0 (deg C)	L (m)
25	90.0	-0.500×10^{-2}	0.500	-6.18×10^{-5}	150	0.029	40
30	87.5	0.093×10^{-2}	0.498	-4.56×10^{-5}	150	0.028	55
35	88.0	0.350×10^{-2}	0.503	-4.42×10^{-5}	150	0.055	70
45	91.5	0.549×10^{-2}	0.514	-4.15×10^{-5}	150	0.053	100
55	97.0	0.590×10^{-2}	0.525	-4.07×10^{-5}	150	0.052	130
65	102.9	0.638×10^{-2}	0.536	-3.97×10^{-5}	150	0.051	160
75	109.3	0.634×10^{-2}	0.547	-3.92×10^{-5}	150	0.050	190
85	115.6	0.636×10^{-2}	0.558	-3.89×10^{-5}	150	0.074	220
100	126.1		0.573		150		265

TABLE 3. Computed vertical velocities and temperature excesses. (1 September 1948.)

s (m)	w' (cm/sec)	Dw'/Ds (sec^{-1})	$T'-T_0$ (deg C)	$\delta T/\delta s$ (C/cm)	A ($g\ cm^{-1}\ sec^{-1}$)	ΔT_0 (deg C)	L (m)	H (m)
100	100.0	6.30×10^{-3}	0.500	-4.88×10^{-4}	5000	0.005	500	250
125	115.7	3.58×10^{-3}	0.385	-2.64×10^{-4}	4885	0.005	500	250
150	124.7	2.44×10^{-3}	0.324	-1.78×10^{-4}	4775	0.005	500	250
175	130.8	1.76×10^{-3}	0.284	-1.34×10^{-4}	4662	0.005	500	250
200	135.2	1.33×10^{-3}	0.255	-1.06×10^{-4}	4550	0.005	500	250
250	141.8	0.75×10^{-3}	0.216	-0.72×10^{-4}	4325	0.010	500	250
300	145.5	0.48×10^{-3}	0.185	-0.55×10^{-4}	4100	0.010	500	250
350	147.9	0.33×10^{-3}	0.167	-0.45×10^{-4}	3875	0.010	500	250
400	149.6	0.15×10^{-3}	0.155	-0.38×10^{-4}	3650	0.020	500	250
500	151.1	0.18×10^{-3}	0.137	-0.29×10^{-4}	3200	0.020	500	250
600	152.9	0.21×10^{-3}	0.128	-0.24×10^{-4}	2750	0.040	500	250
800	157.0	0.45×10^{-3}	0.120	-0.20×10^{-4}	1850	0.040	500	250
1000	166.0	0.66×10^{-3}	0.120	-0.16×10^{-4}	950	0.040	500	250
1200	179.0		0.112		50	0.040	500	250

cumulus clouds. The air blew out over the sea, and the instability of the air changed to neutral equilibrium 12 km offshore. Beyond this point, no convective activity existed. The size of the coefficient dropped from the high value of 15,000 g cm^{-1} sec^{-1} to 340 g cm^{-1} sec^{-1} beyond the 12-km mark (Bunker, 1952). The decrease was caused in part by the stability change, and in part by the cessation of convective motions. A coefficient of 5000 g cm^{-1} sec^{-1} has been adopted as the value characteristic of the turbulence at the 100-m level. Acceptance of this value depends on an estimate that one-third of the water-vapor flux was accomplished by turbulence, and two-thirds by buoyant parcels. The approximate value of two-thirds was computed from the sky coverage by cumulus clouds, estimated velocities, and measured mixing-ratio differences between the moist buoyant parcels and the surrounding air. The diameter of one cloud was measured to be 1000 m, while its thickness was 250 m. A thickness-radius ratio of one-half is used for the following computation, on the assumption that the convecting parcel had the same dimensions as the cloud that it finally produced. Temperature measurements in the air over the land indicated that horizontal variations of the order of 0.5C existed.

An integration was performed on the equations, with use of a coefficient that decreased from 5000 g cm^{-1} sec^{-1} at 100 m to 50 g cm^{-1} sec^{-1} at 1200 m. This decrease in the coefficient was computed from mean curves of flux-height relation and gradient-height relation, determined from many series of soundings (Bunker, 1952). The integrations, table 3 and fig. 4, show that parcels of this size, temperature excess and turbulence will survive the dissipating action of the turbulent air and will accelerate until they are brought to rest by the stability of the inversion capping the

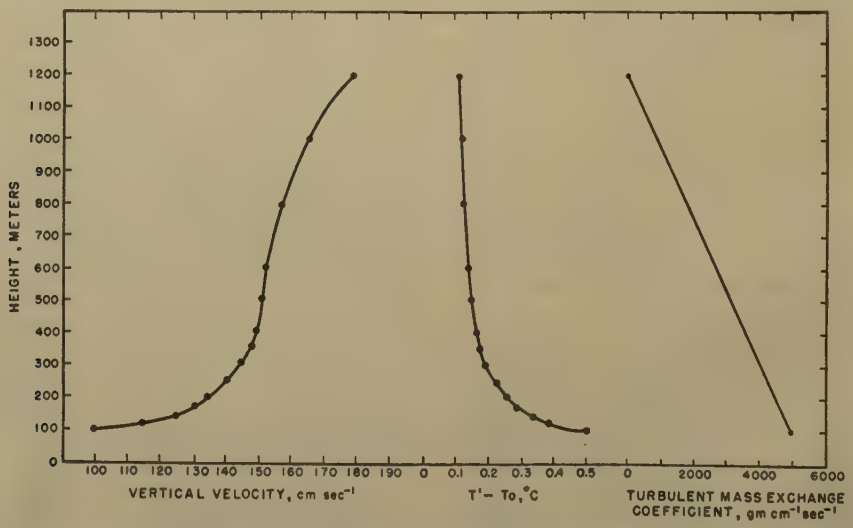

FIG. 4. Computed velocities and temperatures of 500-m parcel rising from 100-m level to top of ground layer at 1200 m. Coefficient of turbulent mass exchange decreased from 5000 to 50 g cm^{-1} sec^{-1}.

TABLE 4. Computed vertical velocities and temperature excesses. (3 February 1950.)

s (m)	w' (cm/sec)	Dw'/Ds (sec^{-1})	$T'-T$ (deg C)	$\delta T/\delta s$ (C/cm)	A ($g\ cm^{-1}\ sec^{-1}$)	L (m)
600	100	5.17×10^{-3}	0.300	-1.62×10^{-4}	2500	1500
700	138	2.37×10^{-3}	0.200	-0.40×10^{-4}	2050	1500
800	158	1.73×10^{-3}	0.170	-0.22×10^{-4}	1600	1500
900	163	1.34×10^{-3}	0.153	-0.13×10^{-4}	1150	1500
1000	175	1.13×10^{-3}	0.141	-0.10×10^{-4}	800	1500
1100	186	1.07×10^{-3}	0.132	-0.07×10^{-4}	450	1500
1200	196		0.125		50	

ground layer, or until they condense into a cumulus cloud.

5. Survival of parcels throughout ground layer on 3 February 1950

On this day, a clear, unstable air mass moved from land out over the Gulf of Maine, with the subsequent production of 2/10 sky coverage by small cumulus clouds about 20 km offshore. Airplane measurements were made of water-vapor flows, gradients, convective parcel sizes, temperature and velocities, allowing the computation of the coefficient of turbulent mass exchange of the surrounding air, 2500 $g\ cm^{-1}\ sec^{-1}$ at 600 m (Bunker, 1952). It was noted that numerous moist, warm parcels were rising through the air mass. They were observed to be 0.3C warmer than the surrounding air and to have gust velocities of about 100 cm/sec at the 600-m level. These vertical velocities were determined from the records of an accelerometer carried by the sounding aircraft, and must be considered as only approximate. Radii of the parcels were determined to be roughly 1500 m. A thickness-radius ratio of 0.1 has been used in the following computation. Table 4 is presented, to show that parcels with these properties are capable of rising to the top of a ground layer with the stated coefficient of turbulent mass exchange.

6. Concluding remarks

The success of the present computations in predicting the survival of parcels observed to exist under given turbulent conditions indicates that this approach should be pursued further. Better observations of the various parameters describing the parcels and their environment should be obtained, to test the equations more critically. This involves more accurate determinations of the exchange coefficients inside and outside the parcels, and more accurate descriptions of the dimensions and motions of the parcels. Improved airplane- and tower-observing techniques will be required for the task. With improved observations, undoubtedly many of the simplifications adopted in the present development will have to be abandoned in favor of more exact forms.

REFERENCES

Bunker, A. F., 1952: Measurements of the vertical water vapor transport and distribution within the unstable atmospheric ground layers and the turbulent mass exchange coefficient. *Pap. phys. Ocean. Meteor., Mass. Inst. Tech. and Woods Hole ocean. Instn.*, 12, No. 3, 40 pp.

Houghton, H. G., and H. E. Cramer, 1951: A theory of entrainment in convective currents. *J. Meteor.*, 8, 95–102.

Ludlum, D. M., 1948: Micrometeorology at Brookhaven. *Weatherwise*, 1, No. 5, 95–98 and 107.

Panofsky, H. A., 1953: The cooperative turbulence study of August 30–31, 1951 at Brookhaven National Laboratory. (In press.)

CORRIGENDA

"Diffusion, entrainment and frictional drag associated with non-saturated, buoyant air parcels rising through a turbulent air mass," by Andrew F. Bunker. In (5), on page 214, $T' - T$ should replace T'. In (6), on page 214, the bracket should be closed after $(T' - T)$. In (8), on page 214, a factor w' should be inserted into the sixth term. In (13), on page 214, the w' of the second term on the right should be squared. In (12) and (13), on page 214, the ρ's should be primed. These errors occurred in the manuscript stage, and all computations presented were computed from the correct equations.

Contribution No. 632

Reprinted from Biological Bulletin, Vol. 104, No. 1, 75–86, February, 1953
Printed in U. S. A.

COMPOSITION OF THE SWIMBLADDER GAS IN DEEP SEA FISHES [1]

P. F. SCHOLANDER AND L. VAN DAM

Woods Hole Oceanographic Institution, Woods Hole, Massachusetts, and Lerner Marine Laboratory, Bimini, Bahamas

In an earlier study of the composition of the swimbladder gas in bottom-dwelling marine fishes caught at depths down to 220 meters, it was found that at all depths the partial pressure of nitrogen in the swimbladder was usually close to that of the surrounding sea water, *i.e.*, 0.8 of an atmosphere (Scholander, Claff, Teng and Walters, 1951). CO_2 was present only in traces, and thus the pressure build-up above 0.8 atmosphere seemed to be due to oxygen only. A slight but definite increase in the nitrogen pressure with depth was apparent from the data, but this was considered at least partly to be an artifact due to changes in the gas composition after the catch.

Non-bottom-dwelling species were often found to have a partial pressure of nitrogen in their bladders far above 0.8 of an atmosphere. These fishes were in buoyancy equilibrium at a very shallow depth, and hence might have acquired their high nitrogen values when equilibrating at much lesser depths than that at which they were caught, *i.e.*, as a consequence of vertical migrations.

In the summer of 1952 we had the opportunity to extend the survey down to a depth of some 950 meters, *i.e.*, about four to five times deeper than before, with the result that now a fuller and more accurate picture of the performance of the gas gland in relation to depth can be presented.

Material

Material for the present investigation was obtained at the Lerner Marine Laboratory, Bimini, Bahamas, December 24, 1951, to January 2, 1952, and during two trawling cruises from the Woods Hole Oceanographic Institution. The latter were conducted off the New England coast by the dragger *Cap'n Bill II* from July 10 to 17 and 23 to 30, 1952. Some 260 specimens were analyzed, covering 29 species of fish caught between 120 and 950 meters' depth.

At the Lerner Marine Laboratory the fishes were obtained at depths of 300–420 meters. They were caught at the bottom on a baited hook fastened to a heavily weighted wire line and were pulled to the surface within 3–5 minutes by means of a motor driven reel. The wire passed over a meter wheel which indicated the depth. Gas samples from the following species were analyzed:

Epinephelus	Grouper
Epinephelus mystacinus	Black grouper
Lutianus vivanus	Long-fin red snapper

[1] Contribution Number 632 from the Woods Hole Oceanographic Institution.

Fishing on the *Cap'n Bill* was done by means of an otter trawl, dragging the bottom for 30 minutes. The time of ascent of the net from the bottom to the surface may be estimated at about 30 minutes for the greatest depths. The depth of the stations was continuously indicated on a fathometer. Gas samples from the following fishes were taken and analyzed on board:

		Known depth range in meters
Alepocephalus sp.		890
Antimora viola	Blue hake	560–1830
Argentina silus	Herring smelt	60–670
Coryphaenoides rupestris	Round-nose ratfish	700–2200
Cottunculus thomsonii	Deep sea sculpin	190–1570
Dicrolene sp.		840–890
Macrourus bairdii	Common ratfish	140–2300
Macrourus berglax	Smooth-spined ratfish	180–1240
Merluccius bilinearis	Silver hake	0–870
Notacanthus phasganorus		870
Peristedion miniatum	Deep sea robin	170–350
Sebastes marinus	Rosefish	30–1680
Simenchelys parasiticus	Slime eel	360–1620
Synaphobranchus pinnatus	Long-nosed eel	240–2660
Tautogolabrus adspersus	Cunner	0–130
Urophycis chesteri	Long-finned hake	60–990
Urophycis chuss	Squirrel hake (ling)	0–540
Urophycis regius	Spotted hake	160
Urophycis tenuis	White hake (ling)	0–540

The data on the depth range are taken from Bigelow and Welsh (1924) and from Goode and Bean (1895), or are from our own records.

Methods and Reliability of Data

The micro-gas-analytical method used gives the carbon dioxide and oxygen percentages through absorption with KOH and alkaline pyrogallol [2] respectively (Scholander *et al.*, 1951). The accuracy is about ± 0.2 to ± 0.3 per cent of the true value. The unabsorbed fraction ("nitrogen") of the gas sample, in addition to nitrogen, may contain noble gases and organic gases.

The amount of organic gases was determined by combustion in a separate chamber and subsequent analysis for CO_2 in the one-half cc. analyzer (Scholander, 1947). The plungers of the syringes with which the samples for these analyses were taken had been lubricated with concentrated lithium chloride solution, and care was taken throughout to avoid organic contaminations. The results are given in Table I and show that the amount of CO_2 formed by combustion of the swimbladder gas is usually no more than a few hundredths of one per cent. Hence organic gases play no significant role in the build-up of the gas pressure in the swimbladder of deep sea marine fishes. The traces of organic gases present in the samples may have been derived from bacterial activity in the gut of the fish.

[2] In the described technique the oxygen is absorbed by running a large excess of fresh pyrogallol down over the gas bubble. This procedure keeps carbon monoxide formation down to sub-detectable values, even in samples of pure oxygen, and agrees with results obtained by Kilday (1950), who used essentially the same absorption principles in a Haldane-type macro-method.

No carbon monoxide could be detected in gas samples from *Urophycis chesteri* and *Macrourus berglax*. Other species were not tested.

Schloesing and Richard (1896) analyzed the swimbladder gas of *Muraena helena* caught at 88 meters' depth and found that the argon over nitrogen-plus-argon ratio was 1.85%. Similarly in *Synaphobranchus pinnatus*, caught at 1385 meters' depth, the ratio was 1.94%. With a ratio in air of 1.18%, this means about a 60% increase in the argon over nitrogen-plus-argon ratio in these fishes. The samples were small and the analyses were not considered very accurate, although probably significant as to the increase mentioned. We have as yet no data on the content of argon in our material.

In our discussion of the correlation of the gas composition with depth we have assumed (a) that the fish are in a steady state of equilibrium at the depth of the catch, *i.e.*, that they have remained at this depth for a substantial period of time, and (b) that this gas composition has not changed materially since the time the fish was caught.

TABLE I

Carbon dioxide content of swimbladder gas before and after combustion

Species	Depth of catch (m.)	% N_2	% CO_2		ΔCO_2
			Before Combustion (a)	After Combustion (b)	(b)−(a)
Antimora viola	820	7.8	1.31	1.32	0.01
	820	7.2	0.84	0.90	0.06
Coryphaenoides rupestris	720	10.0	0.18	0.19	0.01
	720	11.6	0.67	0.72	0.05
	720	—	0.85	0.96	0.11
Macrourus bairdii	820	8.2	0.03	0.16	0.13
	610	8.2	0.65	0.67	0.02
Sebastes marinus	440	11.2	0.37	0.38	0.01
	440	—	0.34	0.41	0.07
Synaphobranchus pinnatus	820	6.2	1.96	1.98	0.02
Urophycis tenuis	610	7.8	0.37	0.40	0.03
	610	5.8	0.20	0.20	0.00
	610	6.2	0.18	0.19	0.01

As to the first assumption, we know that the Bimini fishes were at the bottom when they were caught, and Bigelow and Welsh (1924) consider most of our northern deep sea species as decidedly bottom-dwelling species. To what extent these fishes might migrate up and down along the bottom slope is not known.

As to the second assumption, there is good evidence that the changes in gas composition that take place from the time the fish is caught until the time the gas

sample is secured are so small that they could not change the conclusions significantly. Thus, the Bimini fishes, which were secured between five and ten times faster than the northern fishes, gave results which superimposed on the northern data. Two sets of experiments showed that changes in the gas composition after the catch occur only slowly. Bloated and more or less moribund individuals of eight species of our deep sea fishes, left on deck, in or out of water, showed an increase of at most one per cent in the nitrogen percentage in 30 minutes. In two species of fishes from much shallower depths, as reported earlier, the increase was larger, but still insignificant when compared with the total nitrogen.

In other experiments oxygen was injected into the peritoneal cavity of two remoras (*Echeneis naucrates*) and one puffer (*Spheroides maculatus*), caught in shallow water. The amount injected was about ten times the amount of swimbladder gas normally present in fishes of similar weights. In these fully alive fish the nitrogen per cent of the injected gas increased in half an hour by 1.4 and 0.4%, respectively. A fish at 1000 meters' depth contains 100 times as much gas as a surface fish, and if such an amount could have been injected into these remoras or the puffer the percentage nitrogen increase would have been entirely negligible.

Also, simple calculation shows that even if the entire amount of nitrogen dissolved in the tissues of a fish were transferred into the swimbladder, which was then expanded 100 times, the increase in the nitrogen would amount to only a few tenths of a per cent. Finally, the amount of oxygen present in a swimbladder at 100 atmospheres' depth is so great that respiratory oxygen removal could not materially change the nitrogen percentage either. We feel, therefore, that our data must reflect essentially the conditions which existed in the swimbladder when the fish was caught.

Composition of the Swimbladder Gas in Relation to Depth

In Figure 1 a composite diagram is presented of the previous (Scholander *et al.*, 1951) and present data, extending from the surface forms to the deep sea forms at 950 meters. The diagonal straight line represents a nitrogen percentage which corresponds to a partial pressure of nitrogen of 0.8 atmosphere, *i.e.*, that of the surrounding sea water. We assume here that nitrogen values to the right of this line are due to something other than diffusion equilibrium and that the balance of the pressure is due to oxygen secretion. It is clear from the figure that the nitrogen values found at greater depths deviate increasingly from the line showing the atmospheric nitrogen tension.

Figure 2 shows the partial pressures of the nitrogen and oxygen as calculated from the percentages found and from the depths at which the fish were taken. In fishes living near the surface the nitrogen and oxygen tensions were generally found to be close to those in air, indicating that here the diffusion exchange between the swimbladder and the outside water dominates the picture. From the surface value of 0.8 atmosphere the nitrogen pressure increases in an over-all linear fashion with depth, often attaining values as much as 10 to 15 atmospheres higher than the nitrogen tension in the surrounding sea water.

Much of the considerable spread in the data in Figure 2 is due to specific differences among the fishes. In Figure 3 we have plotted the nitrogen for four species of fish, covering a wide range of depth. It is indicated that the increase in

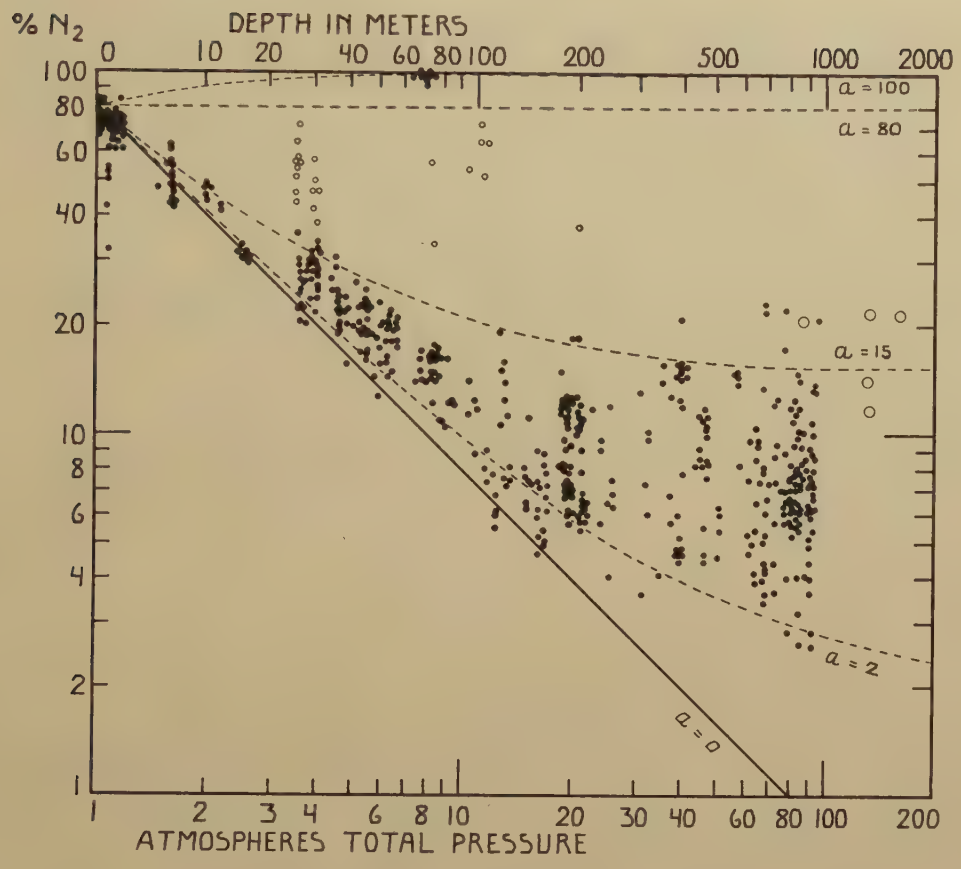

FIGURE 1. Composite graph of the nitrogen concentration found in swimbladder gas from fishes at various depths. The diagonal full-drawn line represents the percentage of nitrogen which at any given depth would give a partial pressure of nitrogen of 0.8 atmosphere. Both the present and previous data (Scholander *et al.*, 1951), as well as Hüfner's data (1892) for *Coregonus* (near 100% N_2), are given by solid circles. The large open circles are data on *Simenchelys parasiticus* (1674 m.) and *Synaphobranchus pinnatus,* given by Schloesing and Richard (1896). The small open circles are data from scup and silver hake, where the high nitrogen most likely is due to vertical migration. The dotted lines represent percentages of the total gas pressure due to nitrogen corresponding to values for *a* of equation (1). The empirical data indicate that *a* in our material lies usually between 2 and 15.

nitrogen tension with depth in each species is more or less linear, the curves for the different species having individual slopes. These differences are also apparent in Figures 4 and 5.

Sebastes is a fish that apparently stays at the bottom in the daytime, but moves off the bottom at night. This could tend to produce a nitrogen value higher than that corresponding to the bottom depth (Scholander *et al.*, 1951). However, high nitrogen is also found in species like the deep sea sculpin, *Cottunculus,* and many others which are most likely always in close proximity to or on the bottom. Many

of these fishes caught at depths of 900–1000 meters have a nitrogen percentage so high that they would have to move up to 100 meters' depth, or shallower, if their nitrogen were to be explained by simple diffusion from the sea water. Such vertical migrations are clearly out of the question for most of our fishes, and we are therefore forced to assume that nitrogen as well as oxygen can be deposited in the swimbladder against very considerable pressure gradients. This, of course, corroborates Hüfner's findings (1892) of nitrogen secretion in the whitefish.

Relation Between Gas Deposition by Diffusion and Secretion

The swimbladder gas may be resolved into two main components. One is derived from diffusion exchange with the outside sea water. The other constitutes

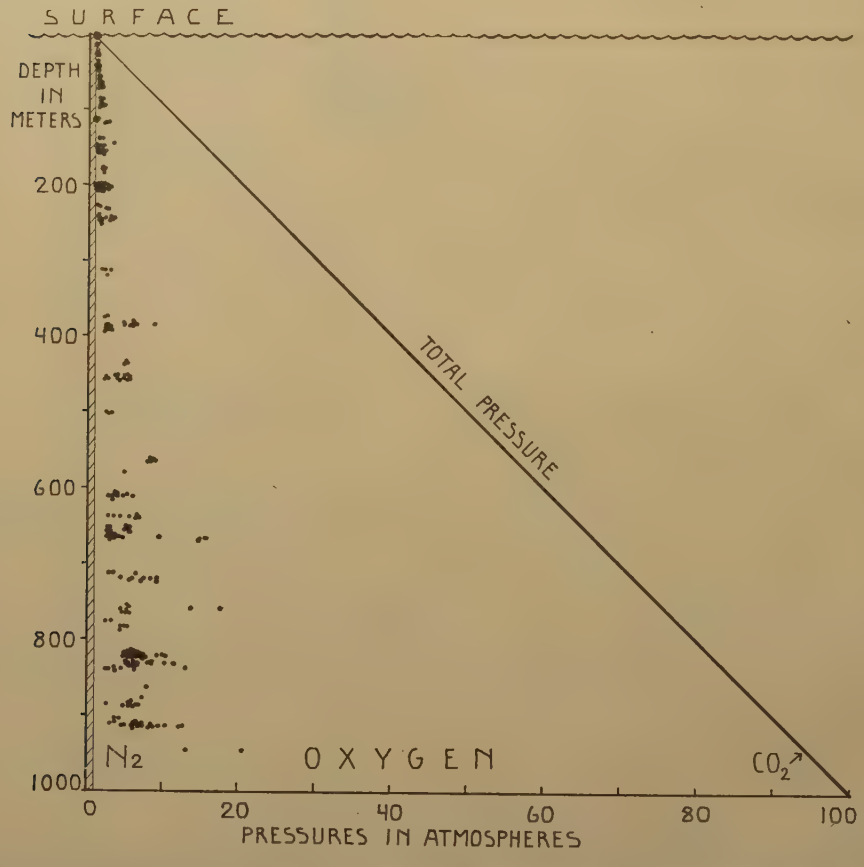

Figure 2. The partial pressures of nitrogen, oxygen and CO_2 calculated from the percentages and the depths. The shaded area is equal to the partial pressure of nitrogen in the sea water. The partial pressure of nitrogen in the swimbladder is to the left of each point, of oxygen to the right. The partial pressure of the CO_2 is usually less than what is represented by the thickness of the drawn diagonal line. The over-all picture suggests a linear increase in the partial pressure of the nitrogen with depth.

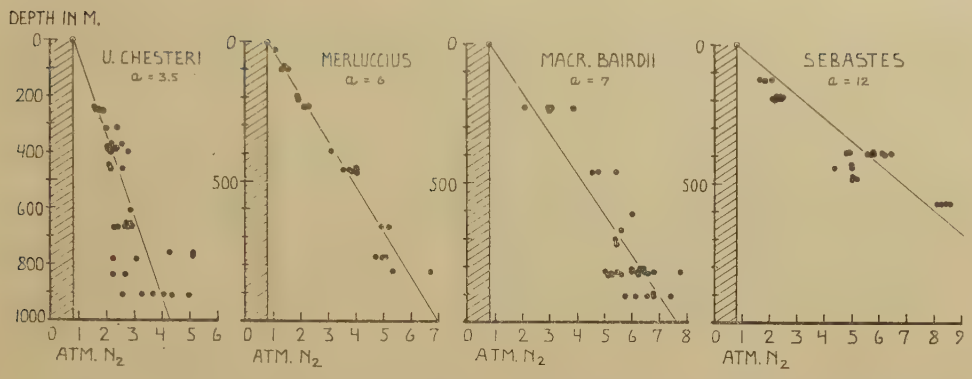

FIGURE 3. Partial pressures of nitrogen in the swimbladders of *Urophycis chesteri, Merluccius bilinearis, Macrourus bairdii,* and *Sebastes marinus.* The data suggest that the nitrogen in excess of 0.8 atmosphere increases linearly with depth from a value of zero at the surface. The different slopes of the lines indicate that the proportions of nitrogen and oxygen secreted are different in different species.

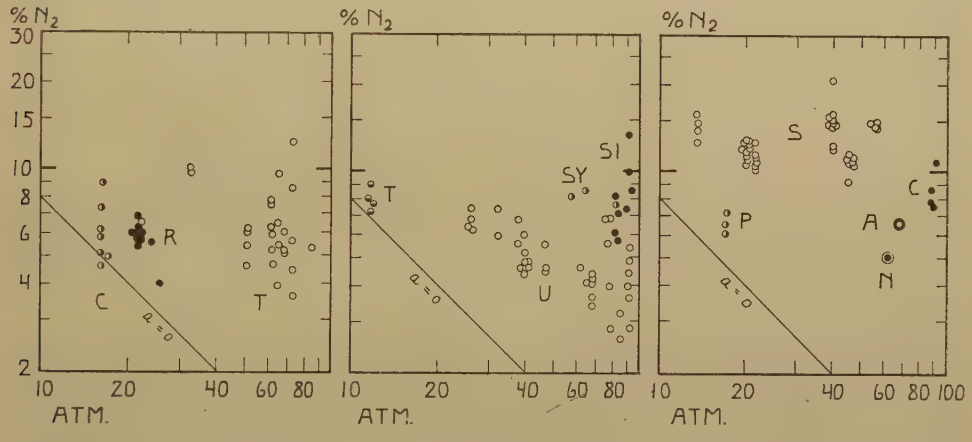

FIGURE 4. Gas composition in the swimbladder in relation to total pressure. Left: *Urophycis chuss* (C), *Urophycis regius* (R), *Urophycis tenuis* (T). Middle: *Tautogolabrus adspersus* (T), *Urophycis chesteri* (U), *Simenchelys parasiticus* (SI), *Synaphobranchus pinnatus* (SY). Right: *Peristedion miniatum* (P), *Sebastes marinus* (S), *Cottunculus thompsonii* (C), *Notacanthus phasganorus* (N), *Argentina silus* (A). These fishes were taken off the New England coast. The N_2 percentages of *Simenchelys* and *Synaphobranchus* obtained by Schloesing and Richard (1896) are entered on Figure 1. They are about twice as great as those shown from our data on these species.

what may be called the secreted [3] part which is responsible for the pressure build-up. As the nitrogen tension is known to be constant and very near to 0.8 atmosphere at all depths (Rakestraw and Emmel, 1938; Hamm and Thompson, 1941), we shall

[3] We shall use the word "secretion" to mean any process whereby gases are deposited into the swimbladder so as to increase potentially or really the partial pressure above that in the ambient medium.

discuss below mainly the nitrogen deposition in the swimbladder. The same considerations may be applied also to the oxygen deposition, although here the picture may be somewhat blurred by the fact that the oxygen tension in the sea water varies considerably.

If a fish remains for a long time at a definite hydrostatic pressure where it maintains a neutral buoyancy, one may assume that the gas entering the swimbladder will be equal to that leaving the swimbladder in amount as well as in composition. Where such a steady-state situation obtains, the quantitative relation of the gas composition to the depth may be empirically described as the resultant of (1) a diffusion exchange term and (2) a gas secretion term.

The diffusion exchange component would lead to a partial pressure of nitrogen equal to the partial pressure in sea water, 0.8 atmosphere, times a factor, F, expressing the completeness of equilibrium between the swimbladder gas and the sea water, *i.e.*, $0.8 \times F$.

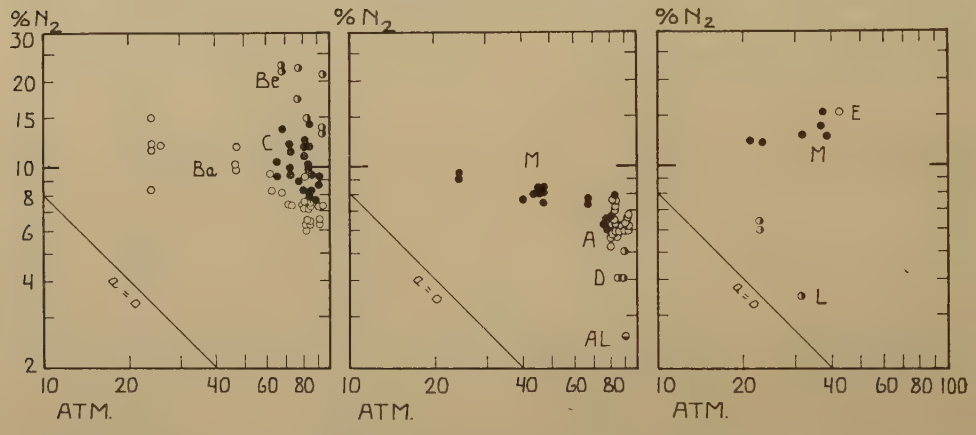

FIGURE 5. Gas composition in the swimbladder in relation to total pressure. Left: *Macrourus bairdii* (BA), *Macrourus berglax* (BE), *Coryphaenoides rupestris* (C). Middle: *Merluccius bilinearis* (M), *Antimora viola* (A), *Dicrolene* sp. (D), *Alepocephalus* (AL). Right: *Epinephelus mystacinus* (M), *Lutianus vivanus* (L), *Epinephelus* (E). The last three fishes were taken off Bimini. All the others were caught off the New England coast.

The gas secretion component represents an additional quantity of nitrogen which has entered the swimbladder as the result of secretion and which increases the partial pressure by an amount represented by $\frac{a}{100} \times D$, where a is the percentage of nitrogen present in the swimbladder as the result of secretion and D is the depth in atmospheres.

The total partial pressure, P_{N_2}, is thus given by

$$P_{N_2} = (0.8 \times F) + \left(\frac{a}{100} \times D\right) \qquad (1)$$

The factor F is introduced into the diffusion term for the following reason. Near the surface D is small and in most fishes the gas diffusion exchange with the

sea water is so complete that a near-air composition is maintained in the swimbladder. This does not hold for all species, however. Even when kept in a shallow tank for a long time tautogs usually have much less than 80% N_2 in their swimbladders (Safford, 1940; Scholander *et al.*, 1951, Fig. 7). This fish, then, seems to have an exceptionally well developed isolation of its swimbladder with respect to diffusion, and this may be expressed by a factor F which is smaller than one. Although difficult to verify, it seems likely that deep sea fishes would have developed a high degree of isolation of their swimbladders against diffusion (low F) as a means for reducing gas loss.

We may now scrutinize somewhat further the idea that the nitrogen deposited into the swimbladder to develop a pressure $\left(\frac{a}{100} D\right)$ is a more or less constant fraction of the oxygen pressure $\left(\frac{100 - a}{100} D\right)$. In Figure 1 we have plotted curves for a series of a values (0, 2, 15, 80 and 100), according to equation (1). It will be seen that curves calculated using the a values of 2 and 15 describe fairly well the upper and lower limits of nitrogen admixture in the deposited swimbladder gas of our marine fishes. A fish like *Coregonus* which deposits near to 100% nitrogen would be expected to present a nitrogen percentage increasing with depth. A fish with an a value of 80 would maintain this percentage at all depths. We have no explanation why there seems to be a gap in the a values between some 20 and 90–100. As indicated by Figure 3 and by Hüfner's data, a seems to be a species characteristic.

Hüfner (1892) found that six out of nine whitefish (*Coregonus acronius*) from 60 to 80 meters' depth in the Bodensee had a nitrogen content in their swimbladders of 99–100%. At the surface these fishes were bloated with enough gas to make them buoyant at the bottom, and they must hence have deposited their nitrogen against a hydrostatic pressure of some 6–8 atmospheres (*cf.*, Scholander *et al.*, 1951). The data have been entered in Figure 1 and agree with the ideas embodied in equation (1). It is a pleasure to record that these seemingly incredible findings have lately been fully corroborated and extended by observations on fishes from the Great Lakes made by Mr. R. L. Saunders from the laboratory of Dr. F. E. J. Fry, Department of Zoology, University of Toronto.

Composition of the Gas Secreted

We have so far discussed the gas composition as it is found in the swimbladder at various depths, which leads us to believe that deep sea fishes deposit in their swimbladders not pure oxygen, but oxygen together with a fraction, a, of inert gases ("nitrogen"), a being high in some species and low in others. We shall now consider to what extent the a values might reveal what is the composition of the gas that has actually been secreted.

The gas pressure in the swimbladder in excess of the one atmosphere due to the combined pressure of nitrogen + oxygen in the sea water is the resultant of (1) the gas secretion into the bladder and (2) the diffusion losses through its wall. The swimbladder in deep sea fishes is capable of maintaining with low gas loss a pressure gradient of one hundred or more atmospheres through the thin air bladder

wall, and it is therefore clear that the exit mechanism for the gases constitutes a potent diffusion barrier. It seems likely that the secreted gases at sub-maximal depths are produced with a pressure substantially higher than the ambient hydrostatic pressure. Only if the diffusion coefficients for the different gases were the same could the gas composition in the swimbladder equal the composition of the secreted gas. The diffusion coefficient for nitrogen through a variety of animal tissues has been found to be only around one half of that of oxygen (Krogh, 1919). The steady state requires that the molar amount of each gas leaving the bladder through diffusion loss should equal the molar amount secreted. A steady state can therefore occur only when the swimbladder has backed up enough partial pressure for each gas component to allow it to pass the diffusion barrier in an amount equal to that secreted. The pressures of nitrogen and oxygen accumulated in the swimbladder above the ambient partial pressures were empirically found to be $\frac{a}{100} \times D$ atmospheres and $\frac{100 - a}{100} \times D$ atmospheres respectively (equation (1)). The diffusion losses, and therefore secretion, of these gases would hence be $\frac{a}{100} \times D \times n$ and $\frac{100 - a}{100} \times D \times o$, where n and o are the diffusion coefficients for nitrogen and oxygen respectively. Recalculated on a per cent basis, the secreted nitrogen percentage, N_{2_s}, would relate to a according to

$$N_{2_s} = \frac{100\,a}{\frac{o}{n}(100 - a) + a}. \qquad (2)$$

With the ratio of $o/n = 2/1$, the secreted N_2 percentage would be $\frac{100\,a}{200 - a}$. This means that for low values of a, like the ones found, it might be anticipated that the secreted mixture would have a *nitrogen* percentage equal to about $\frac{1}{2}\,a$. Conversely, if a were near 100, as found in *Coregonus,* the *oxygen* percentage of the secreted gas would be about twice as high as the oxygen percentage found. Thus, if the nitrogen percentage in the swimbladder of a fish at 1000 meters' depth is found to be 4.8%, then a is 4.0% and the secreted mixture is likely to be 2% N_2 and 98% O_2. If in a *Coregonus* the a value is 95, the secreted gas is likely to be 90% N_2 and 10% oxygen.

Schloesing and Richard (1896) found the argon fraction in the swimbladder "nitrogen" to be some 60% higher than in air. From the solubility of argon in water and its molecular weight one would expect argon to have twice as high a diffusion coefficient through animal tissue as nitrogen. If, therefore, argon and nitrogen entered the swimbladder in the same ratio as in air one would expect a lower argon fraction in the swimbladder rather than a higher. Evidently, therefore, these two gases enter the swimbladder in proportions different from those in air. We are totally in the dark as to how the presumably inert argon and nitrogen have attained the high pressures found in the swimbladder.

We wish to express our gratitude to Dr. Alfred C. Redfield for his stimulating

interest. We were fortunate to have all possible cooperation from Dr. William C. Schroeder, who conducted the deep sea cruises off the New England coast. He identified our specimens and supplied us with information on the depth ranges of the fishes. The Captain and the crew of the dragger *Cap'n Bill II* did everything to facilitate our work on board.

We are indebted to Dr. C. M. Breder, Jr., at the American Museum of Natural History, for arranging our stay at the Lerner Marine Laboratory. We wish to extend our thanks to Mr. Michael Lerner for his generous cooperation in securing deep sea material at Bimini and to Mr. Marshall Bishop for providing us with the most excellent facilities in the laboratory. We wish to thank Mr. Vladimir Walters, of New York University, for his excellent assistance, and we are much obliged to Mrs. Susan I. Scholander for help in the field and in the preparation of the final manuscript.

Summary

1. The composition of the swimbladder gas has been determined in 26 species (260 specimens) of marine deep-sea fishes taken at known depths between 200 and 950 meters.

2. The partial pressure of nitrogen in the bladder steadily increases with depth until it reaches some 5–15 atmospheres at a depth of 900 meters, revealing that not only oxygen but also nitrogen is transported into the swimbladder against a considerable gradient. This corroborates the findings of Hüfner (1892) that the whitefish (*Coregonus*) is able to secrete pure nitrogen against a hydrostatic pressure of 6–8 atmospheres.

3. The data, together with previous observations from shallower depths, show that the nitrogen tension at all depths may be expressed by (1) a diffusion term of 0.8 atmosphere, plus (2) a secretion term which, although different for different species of fish, is in each species a constant percentage of the total secreted gas pressure. Among our fish the secretion term ranges from about 2% to 15% nitrogen. In the whitefish it is apparently 100%. In a steady-state situation the percentage nitrogen actually secreted into the swimbladder is probably lower than the nitrogen percentage indicated by the secretion term because oxygen is more easily lost by diffusion through animal tissue than is nitrogen.

Literature Cited

Bigelow, H. B., and W. W. Welsh, 1924. Fishes of the Gulf of Maine. Bull. U. S. Bureau Fisheries, vol. 40, pt. 1.

Goode, G. B., and T. H. Bean, 1895. Oceanic ichthyology. Smithsonian Contr. Knowledge, vols. 30–31.

Hamm, R. E., and T. G. Thompson, 1941. Dissolved nitrogen in the sea water of the Northeast Pacific with notes on the total carbon dioxide and the dissolved oxygen. *J. Marine Res.*, **4**: 11–27.

Hüfner, G., 1892. Zur physikalischen Chemie der Schwimmblasengase. *Arch. Anat. Physiol., Physiol. Abth.*, 54–79.

Kilday, Marthada V., 1950. A quantitative study of the carbon monoxide formed during the absorption of oxygen by alkaline pyrogallol. *J. Research Natl. Bureau Standards*, **45**: 43–59.

Krogh, A., 1919. The rate of diffusion of gases through animal tissues, with some remarks on the coefficient of invasion. *J. Physiol.*, **52**: 391–408.

RAKESTRAW, N. W., AND V. M. EMMEL, 1938. The relation of dissolved oxygen to nitrogen in some Atlantic waters. *J. Marine Res.*, **1**: 207–216.

SAFFORD, VIRGINIA, 1940. Asphyxiation of marine fish with and without CO_2 and its effect on the gas content of the swimbladder. *J. Cell. Comp. Physiol.*, **16**: 165–173.

SCHLOESING, T., AND J. RICHARD, 1896. Recherche de l'argon dans les gaz de la vessie natatoire des poissons et des physalies. *C. R. Acad. Sci. Paris*, **122**: 615–617.

SCHOLANDER, P. F., 1947. Analyzer for accurate estimation of respiratory gases in one-half cubic centimeter samples. *J. Biol. Chem.*, **167**: 235–250.

SCHOLANDER, P. F., C. L. CLAFF, C. T. TENG AND V. WALTERS, 1951. Nitrogen tension in the swimbladder of marine fishes in relation to the depth. *Biol. Bull.*, **101**: 178–193.

Contribution No. 633

Reprinted from the JOURNAL OF CELLULAR AND COMPARATIVE PHYSIOLOGY
Vol. 41, No. 3, June 1953

CONCENTRATION OF HEMOGLOBIN IN THE BLOOD OF DEEP SEA FISHES

L. VAN DAM AND P. F. SCHOLANDER
Woods Hole Oceanographic Institution, Woods Hole, Massachusetts
(Contribution number 633 from the Woods Hole Oceanographic Institution)

It has long been known that deep sea fishes can secrete gas into their swimbladders against considerable pressures. Richard (1895) and Schloesing and Richard (1896) analyzed the swimbladder gas from deep sea eels, *Simenchelys parasiticus* and *Synaphobranchus pinnatus,* taken at 1674 and 1385 meters' depth respectively, and in a recent study fishes with swimbladders were found to be common down to a depth of at least 1000 meters, or at 100 atmospheres' pressure (Scholander and van Dam, '53). In agreement with the data of Schloesing and Richard we found also that at a pressure of about 100 atmospheres some 90% of the swimbladder gas consists of oxygen.

An important function of the gas secretion is to maintain the fish at a neutral buoyancy at any depth. In order to compensate for a given buoyancy decrease a molar amount of gas must be secreted which is proportional to the hydrostatic pressure at which the buoyancy adjustment must be accomplished. Thus, at 100 atmospheres' depth 100 times more gas must be secreted than at the surface in order to effect the same increase in swimbladder volume. This consideration led us to look for conditions which might possibly speed up or facilitate the gas secretion in deep sea fishes. Such a condition, if the oxygen secreted into the swimbladder is transported by the hemoglobin, could be an increased hemoglobin content.

Since the iron content of the blood may be assumed to reflect very nearly its hemoglobin content and hence its oxygen com-

bining capacity, we have measured the iron content of the blood in 11 species of deep sea fishes in order to determine if these fish have developed a higher oxygen capacity of the blood to facilitate oxygen secretion.

MATERIAL AND METHODS

The fishes were caught by trawling during two cruises off the New England coast in July, 1952, as previously described (Scholander and van Dam, '53). The blood was drawn by hypodermic syringe from the heart, which was usually still pulsating. A larger than normal spread in our data may have

TABLE 1

Iron content in the blood of deep sea fishes

SPECIES	NUMBER OF INDIVIDUALS	DEPTH IN METERS	MG FE PER 100 CM^3 BLOOD		
			Low	High	Average
Cottunculus thomsonii	3	750–915	10.4	14.1	11.9
Coryphaenoides rupestris	3	390–865	9.2	16.9	11.9
Macrourus berglax	3	860–945	12.8	18.3	16.5
Merluccius bilinearis	1	930	24.0	24.0	24.0
Notacanthus phasganorus	1	610	18.0	18.0	18.0
Sebastes marinus	2	500	24.7	25.1	24.9
Simenchelys parasiticus	3	640–915	20.0	23.7	22.0
Synaphobranchus pinnatus	2	710–865	14.5	29.1	21.8
Urophycis chesteri	2	610–865	16.6	21.7	19.2
Urophycis chuss	2	125	20.4	21.3	20.9
Urophycis tenuis	6	610–640	20.4	26.0	24.0

been brought about by the presence of a severe gas embolism in the blood of some of the fishes, disturbing the normal plasma to cell ratio. The samples (1–2 ml) were stored in small stoppered vials for analysis on shore. No anti-coagulant was used.

The coagulated and more or less rotted sample was transferred quantitatively into a glass homogenizer, and 1 cm^3 of the homogenate was digested by wet ashing in a mixture of concentrated sulfuric and nitric acid. The concentration of iron in the clear and colorless digest was determined in a Klett-Summerson photo electric colorimeter, essentially following the procedure of Wong ('28).

RESULTS

Our analytical data are shown in table 1. The mean value of the iron content in the blood of 11 species of deep sea fishes is 19.6 mg %. Hall and Gray ('29) give iron values from 15 species of shallow water marine fishes. Their mean value is 26.7 mg %. If we disregard their data on fishes of the mackerel family with an exceptionally high iron content, their average is 22.3 mg %. There is, therefore, no indication that deep sea fishes have higher hemoglobin concentration in their blood than shallow water species.

SUMMARY

The iron content of the blood has been determined in 11 species of deep sea fish, caught at depths of 125 to 945 meters. The values fall well inside the range of those found in shallow water fishes. There is no indication, therefore, that deep sea fishes have developed a high oxygen capacity of the blood as a possible means of facilitating the secretion of oxygen against high pressures.

LITERATURE CITED

Hall, F. G., and I. E. Gray 1929 The hemoglobin concentration of the blood of marine fishes. J. Biol. Chem., *81:* 589–594.

Richard, J. 1895 Sur les gaz de la vessie natatoire des poissons. C. R. Acad. Sci. Paris, *120:* 745–747.

Schloesing, T. and J. Richard 1896 Recherche de l'argon dans les gaz de la vessie natatoire des poissons et des physalies. C. R. Acad. Sci. Paris, *122:* 615–617.

Scholander, P. F., and L. van Dam 1953 Composition of the swimbladder gas in deep sea fishes. Biol. Bull., *104:* 75–86.

Wong, S. Y. 1928 Colorimetric determination of iron and hemoglobin in blood. II. J. Biol. Chem., *77:* 409–412.

Contribution No. 634

A RECORDING BATHYPITOTMETER[1]

By

WILLEM V. R. MALKUS

Woods Hole Oceanographic Institution[2]
Woods Hole, Massachusetts

ABSTRACT

The stability of a cable towed through the sea has suggested the use of its weighted end as a platform for velocity measurement. This report describes an instrument, lowered on standard hydrographic wire, which uses mechanical sensors to record speed, temperature, and pressure on a waxed paper roll. Initial measurements are presented which indicate that the vertical profile of an ocean current can be determined in approximately one hour.

INTRODUCTION

The direct determination of change of an ocean current with depth has become an urgent need in modern oceanography. The vertical structure of a velocity field is probably the most sensitive indicator of the physical processes which dominate its evolution. Most theories on the development of currents due to wind stress, and theories on the mixing processes that modulate this development, can be tested critically by their ability to predict this variation with depth. Also, it is essential to supplement with other data the information concerning fluid transport obtained by the geostrophic relation from density measurements; for while these density measurements are indicative of the average fluid motions, the forces responsible for the time-dependent meanders raise the most recent questions.

Such direct velocity measurements have not been made extensively because of the difficulty of creating a stable reference platform in a tossing sea. Another problem is the time element in making observations to great depth; if the velocity field is fluctuating continuously, establishing the mean velocity might require a longer period than the persistence of the investigated structure at the place of measurement.

This report describes a technique of measurement with an instrument that permits the determination of the vertical structure of a current in one hour.

[1] This work was performed under the auspices of the Office of Naval Research, Contract N6onr–27701.

[2] Contribution No. 634 from the Woods Hole Oceanographic Institution.

THE CATENARY PLATFORM

The catenary-like curve of a long wire weighted at its end and towed by a ship acts as a filter for the short period roll and pitch of a ship. The horizontal and vertical stability of the weighted end has suggested its use as a platform for velocity measurements. The difference between such a measurement and the ship's mean velocity through the surface water is the change in velocity of the ocean current between the surface and the depth of the platform. The absolute surface velocity may be found by making a lowering into quiet waters below the current, or, if none exists, by lowering to a point just above the bottom. Three difficulties confront this suggestion. The first concerns the time necessary for the catenary to come to equilibrium at a specific depth. If this time is longer than a few minutes, then the time involved in the complete measurement might be excessive. The second difficulty is the necessity of maintaining a constant mean surface velocity during the measurement. The third is the problem of shallow and surface measurements where the catenary has lost its value as a stable platform.

These problems have been resolved by using the standard 3/32″ hydrographic wire with a 150-pound instrument in the ship's mean speed range of 3½–5½ knots. It is found that the catenary attains its new equilibrium two to three minutes after changing the instrument depth 100 m. Surface velocity can be determined and maintained by a carefully checked ship's pit log, or other secondary measurement and by cautious correction of the helm.

AN INSTRUMENT

A simple rugged device whose calibration could be checked on board was sought for the velocity measurement. The pitot seemed like such a device, but it indicates speed only, not direction. The instrument developed is tentative in character due to the assumption that ocean currents have little or no change in direction with depth and that their speed alone is worth investigating. It is necessary, therefore, to determine or estimate the direction of the surface current with the Geomagnetic Electrokinetograph (von Arx, 1950), by drift measurements, by Loran or Navigation, or from the thermal structure. The ship is then headed into the current and the simple speed versus depth measurements are interpreted as indicative of the velocity. A more refined tool must embody a direction indicator as well, but this is complicated by the normal long-period fluctuations in ship direction undamped by the catenary. The pitot measurement is relatively insensitive to either small angular changes in course or to a small constant deviation of ship motion from due upstream.

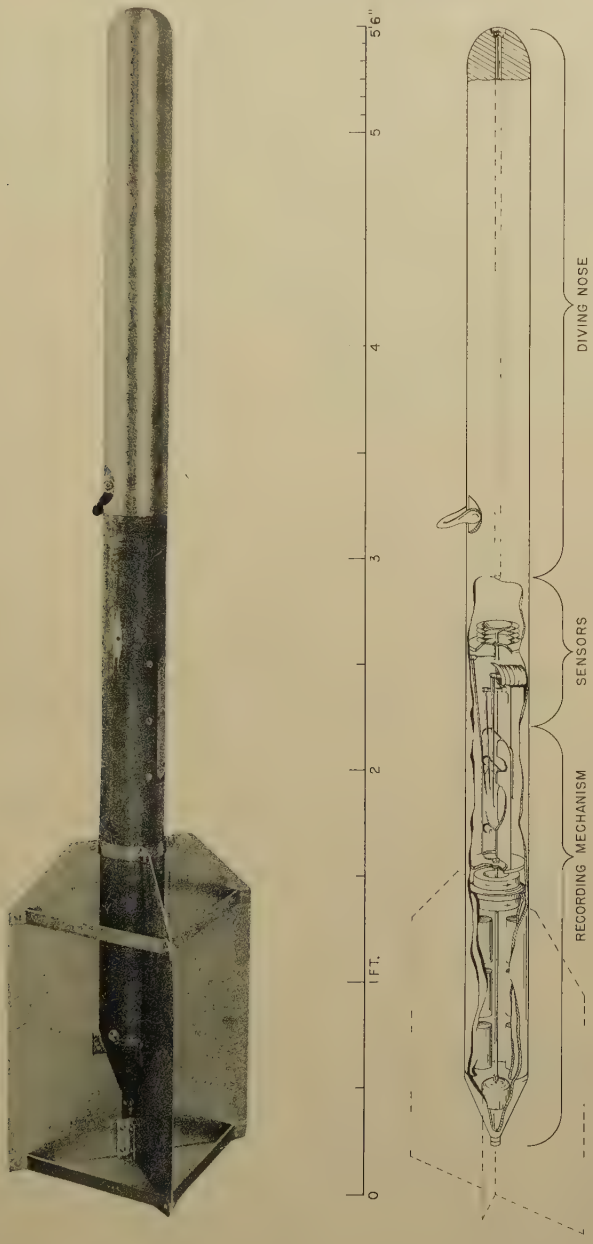

Figure 1. A schematic drawing and photograph of the complete bathypitotmeter.

The decision to record the measurements on commercially available rolls of waxed paper has influenced to a large extent the character of the sensors and auxiliary equipment used in the particular instrument which was constructed. Briefly, a sylphon bellows, activated by the pitot pressure, drives a stylus across the waxed paper. A pressure case contains batteries and a small electric motor. The motor is magnetically coupled through the pressure case to the paper, which is open to the sea. A second stylus is driven by a bourdon pressure element to measure depth. A third stylus is driven by a flushed bimetal strip to record temperature, while a fourth stylus provides a reference line to remove errors due to lateral drift of the paper. Back lash is avoided by the use of flexural couplings between sensor and stylus; these couplings also remove the problems of corrosion created by pivoted linkages. A schematic diagram and a photograph of the instrument appear in Fig. 1. The component details will be discussed in separate paragraphs.

THE SENSORS

Fig. 2 shows the three sensors and a detail of a flexural amplifier. The phosphor bronze flexure coupling is ¼″ wide, .008″ shim stock with full range deflection of ± 10° in this application. The amplification factor of the flexure is controlled by the distance between the shims and the length of the pen and can be made very large if stiffer sensors are desired. The high natural frequency of a stiff sensor reduces the problem of stylus vibration which attends the use of any sensitive indicator.

The pitot sylphon, with sturdy positive and negative stops to avoid excessive strain when the instrument is diving, has a full range of 5½ knots. Its full scale response time is less than a second.

The temperature element is a $6 \times 1.0 \times 0.1''$ bimetal; while it is thermally insulated from the water in the instrument case by the formica block in which it is mounted, it is continuously flushed by small louvres that are open to the surrounding sea. Its response time to 1/e of its final value is approximately one second. However, the attainment of final equilibrium of all sensors is limited by the frictional drag of a stylus on the paper. With the paper in motion and with the normal vibration of the whole instrument, this equilibrium is reached in less than ten seconds.

The depth-indicating bourdon is interchangeable to permit several depth scales.

Fig. 3 shows the "shallow" grid that is used to interpret a record for measurement down to 800 m.

Calibration of the pitot is accurate to ± 1/20 knot, though changes in velocity of .02 knot are easily detected between 3 and 5½ knots.

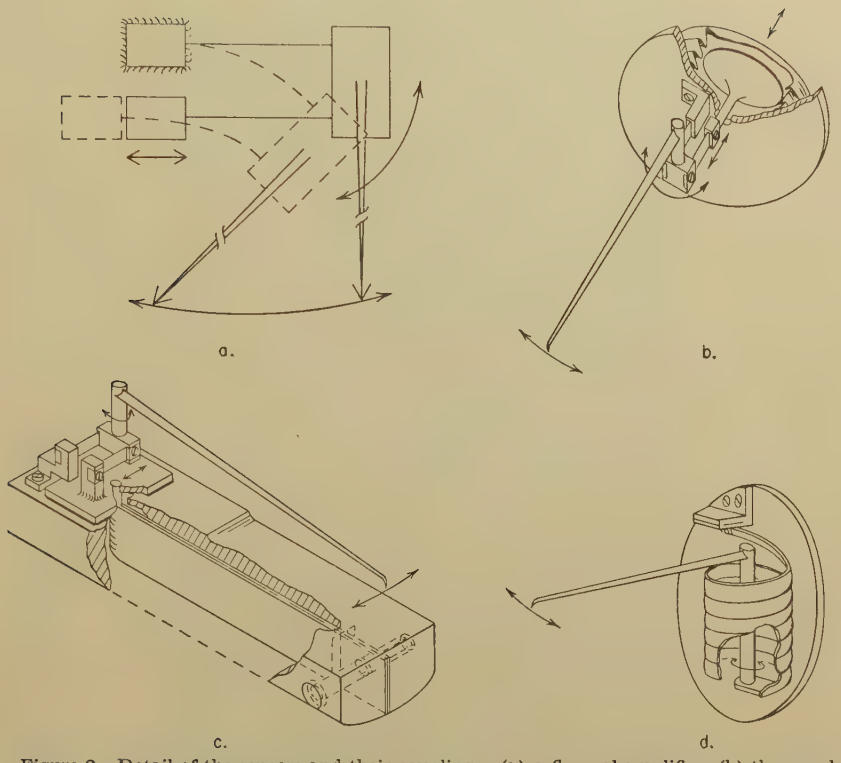

Figure 2—Detail of the sensors and their couplings: (a) a flexural amplifier; (b) the speed sensor; (c) the temperature sensor; (d) the pressure sensor.

Recalibration of the pitot aboard ship can be performed with a water manometer. Calibration of the bimetal is initially correct to $\pm$ 0.1° F, but the drift with time and use has not been ascertained.

THE RECORDING MECHANISM

An "O" ring sealed stainless steel pressure case with 1/8″ walls and an inside diameter of 2½″ contains batteries and the paper drive motor. A salt water switch on the tail actuates the motor when the instrument is in the sea. The batteries will last for at least 100 operating hours and can be quickly changed at sea. A permanent magnet pair, one in the pressure case and one in the sea, transmits the motion to the paper roll at 1″ or 5/16″ a minute, depending on the choice of an external gear. The spools which contain the paper are removed and inserted as in a camera. The waxed paper, which comes

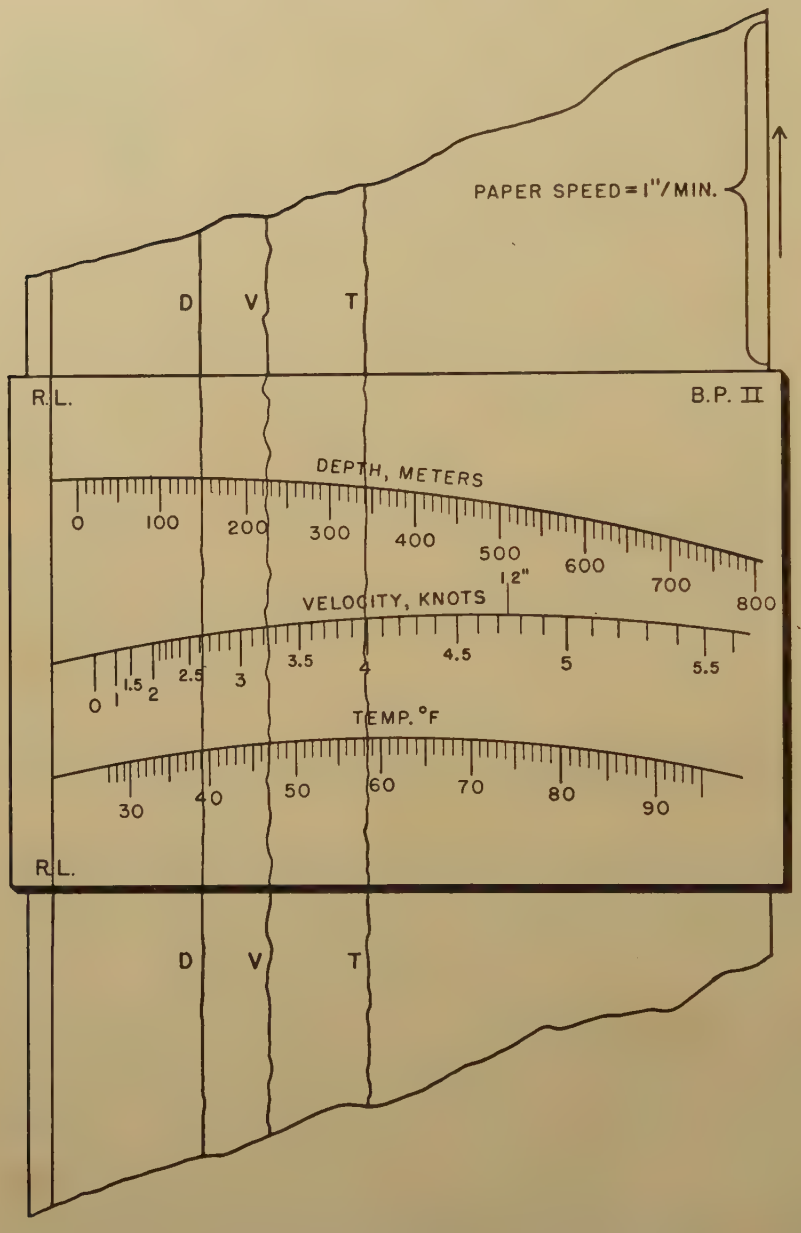

Figure 3—A calibrated grid superimposed on the waxed paper record.

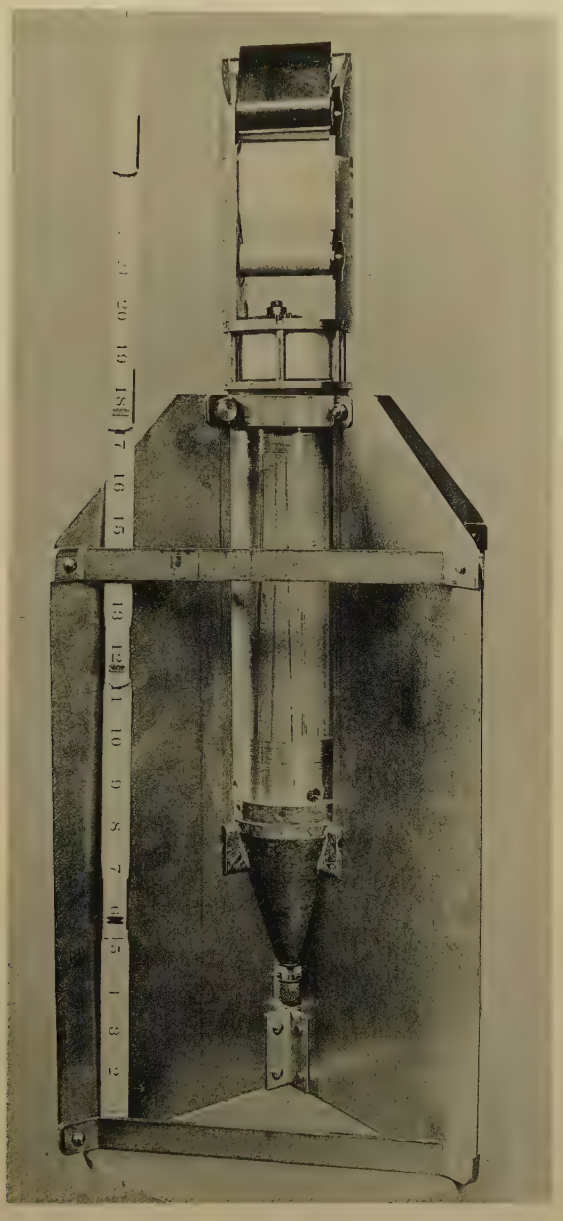

Figure 4. The recording mechanism.

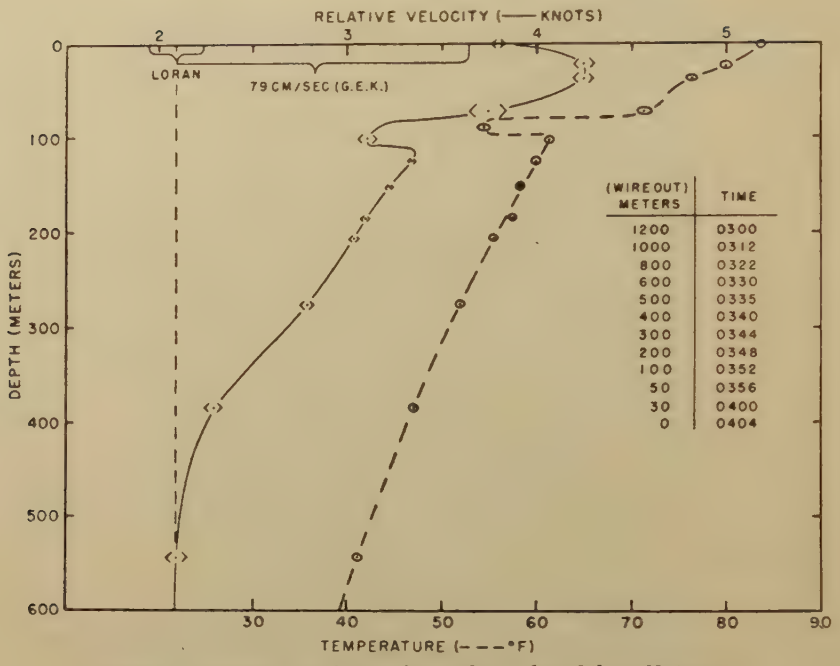

Figure 5—A sample record from the northern edge of the gulf stream.

to the surface with its back thoroughly soaked, is permitted to dry several minutes before a reading. Four knurled screws near the tail permit the withdrawal of the recording mechanisms (Fig. 4) from the body of the instrument for loading and recovery of the paper.

A SAMPLE RECORD

The following record, presented to clarify the operational use of the instrument, does not necessarily represent a typical section of a current.

In a northern edge of the Gulf Stream, off Cape Hatteras, the vessel was headed into the current at a surface speed of 3.8 knots. The direction of the surface current was established by a careful G. E. K. observation just before this operation. Triple Loran observations were made to ascertain the ship's way with respect to the earth.

After 1200 m of hydrographic wire had been reeled out, the bathypitotmeter was allowed 20 minutes to swing to its first equilibrium at 542 m depth. At this time it was assumed that the measurement commenced. The wire was then retrieved in 12 steps as indicated. The waxed paper was dried and read through a grid to produce the record given in Fig. 5. It is significant, perhaps, that fluctuations

around the mean at all depths were small and slow. They are indicated on the record by the double ended arrows at each velocity datum and by ellipses at each temperature datum.

The Loran observations, with a bracket estimating their probable error, support the indication of the lowest measurement that the water at 500 m had little or no velocity relative to the earth. The G. E. K. observations, drawn as a long bracket from the Loran "zero," is further evidence that the absolute velocity as well as the relative velocity of the stream at each depth was determined. The discrepancy between the indicated G. E. K. surface velocity and the actual surface velocity is a measure of the average total transport of fluid at this section (Malkus and Stern, 1952).

The record contains several uncommon features, such as the thermal inversion at 90 m and a maximum velocity at 30 m below the surface, but it gives evidence of how such phenomena may be observed and correlated.

The work of Mr. Angelo Cangiamila in preparing the instrument for use and in the observational program is gratefully aclnowledged. The trouble-free operation of the instrument is attributed to the ingenuity of Mr. Myron Howland, who is responsible for its construction.

REFERENCES

Malkus, W. V. R. and M. E. Stern

1952. Determination of ocean transports and velocities by electromagnetic effects. J. mar. Res., *11* (2): 97–105.

von Arx, W. S.

1950. An electromagnetic method for measuring the velocities of ocean currents from a ship underway. Pap. phys. Oceanogr. Meteor., *11* (3): 1–62.

Contribution No. 636

INTERFERENCE PHENOMENA IN THE TIDES OF THE WOODS HOLE REGION[1]

By

ALFRED C. REDFIELD

Woods Hole Oceanographic Institution

ABSTRACT

The relations of mean range of tide, time of high water, and time of slack water along Vineyard and Nantucket Sounds may be attributed to the interference of tidal waves entering the sounds from their opposite ends. Interference of the semidiurnal constituents is maximal in the neighborhood of Woods Hole where the great reduction of these constituents, relative to the diurnal constituents, results in a pronounced diurnal inequality in the range of successive tides at appropriate phases of the moon. The tide gauge record at Woods Hole is distorted in form as a result of the development of shallow water harmonics combined with the reduction of the fundamental semidiurnal constituent by interference. The inequality in the duration of flood and ebb currents in Woods Hole Passage may be attributed to the effect of these harmonics on the tide levels in Great Harbor.

In discussing the complicated system of tides in Nantucket and Vineyard Sounds in 1855, Bache stated that "observations already made pointed to the interference of the several tide-waves having access to this space as the source of the seeming irregularities." In the present paper it will be shown that a number of characteristics of the tides in this region can be explained by interference between two systems of waves which enter Vineyard Sound, one directly from the ocean, the other from the Gulf of Maine via Nantucket Sound. The characteristics in question are: (1) The relation of time of high water and slack water and the mean range of tide along Vineyard and Nantucket Sounds; (2) The relative values of the diurnal and semidiurnal tidal constants at Woods Hole; (3) The specific form of the tide gauge curve at Woods Hole; and (4) The relative duration of flow eastward and westward in Woods Hole passage.

COTIDAL LINES

The simultaneous positions of the crest of high water, as the tidal wave approaches the New England Coast, were first drawn by Bache (1855) and were later amplified by Harris (1904). The cotidal lines for the region, modified to take account of the more complete information presently available (U. S. Coast and Geodetic Survey, 1951), are shown in Fig. 1.

[1] Contribution No. 636 from the Woods Hole Oceanographic Institution

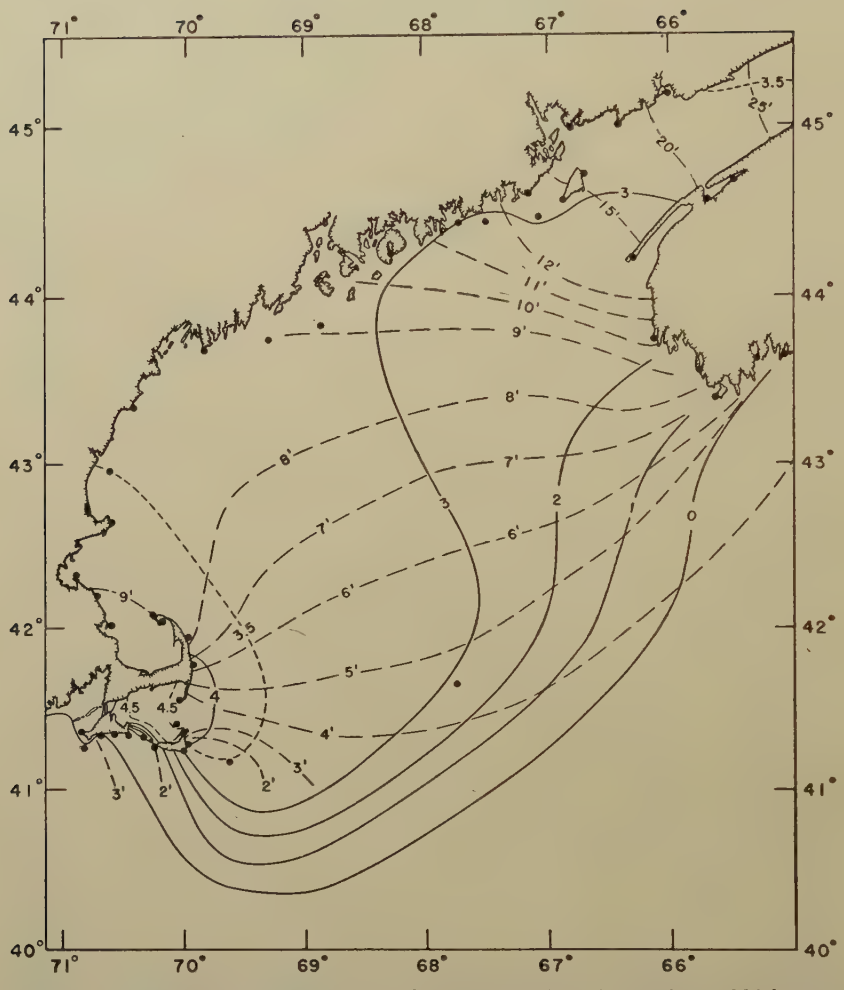

Figure 1. Cotidal and corange lines for the Gulf of Maine. Mean times of high water shown by continuous and broken lines in lunar hours relative to moon transit at Greenwich. Mean range of tide shown by dashed lines in feet.

High water occurs almost simultaneously at outlying points along the coast between Long Island, New York, and Nova Scotia. From offshore the crest of high water moves progressively along Vineyard Sound and enters Nantucket Sound from the west after a lapse of four hours. A similar movement into Nantucket Sound occurs through Muskeget Channel.

On entering the Gulf of Maine, the tidal wave is deflected to the left with the result that the delay in high water is greatest along the Massachusetts Coast. There the crest of high water moves southward and reaches the entrance to Nantucket Sound at Monomoy Point and Great Point about four hours after its occurrence on the outer coast.

Within Nantucket Sound high water is latest in an area bounded by Hyannisport, Dennisport, and Nantucket Harbor, where it occurs almost 4½ hours after high water at No Mans Land. In this region the wave that enters through Vineyard Sound and that from the Gulf of Maine meet from opposite directions.

THE TIME OF HIGH WATER, SLACK WATER, AND MEAN RANGE OF TIDE IN VINEYARD AND NANTUCKET SOUNDS

Cotidal and corange lines for Vineyard and Nantucket Sounds are shown in Figs. 2 and 3. Not only is the time of high water delayed as the tidal wave progresses along Vineyard Sound but the mean range of tide decreases from a value of 3.0 feet at Gay Head and No Mans Land to a minimum of 1.3 feet at Falmouth. Eastward of Falmouth the mean range increases to 3.7 feet at Monomoy Point. The interval by which slack water (current turns west) follows high water is about three hours in Vineyard Sound. Along the Falmouth shore, this interval decreases rapidly, and east of Succonessett slack water precedes high water by an interval which increases to about two hours at Monomoy Point.

Theory. These relations are superficially similar to those that would be expected by the interference of two progressive waves moving in opposite directions along the channel. They may be examined quantitatively by methods recently employed in the analysis of tidal phenomena in narrow embayments in which it is assumed that the reflection of the primary tidal wave by the barrier at the head of the embayment produces the mathematical equivalent to a second wave moving through the barrier in the opposite direction (Redfield, 1950). The assumptions necessary to the treatment are:

1. That irregularities in the cross section of the channel alter the velocity of the respective waves, thus distorting the geographical distribution of phase differences along the channel, but that they do not alter the fundamental relations of elevation, motion, and phase difference within the wave;
2. That damping is proportional to the phase change within the wave rather than to the distance traveled;
3. That the damping coefficient is constant along the length of the channel.

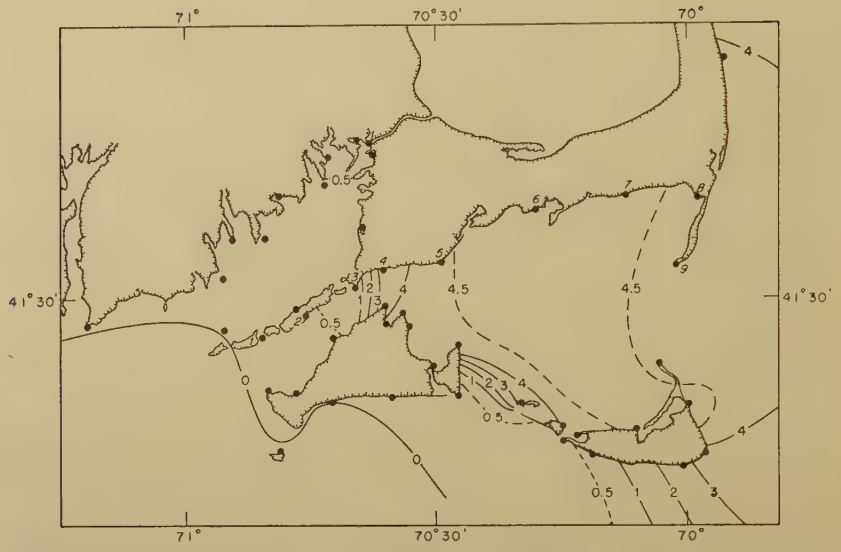

Figure 2. Cotidal lines for Vineyard and Nantucket Sounds. Mean times of high water shown in lunar hours relative to moon's transit at Greenwich.

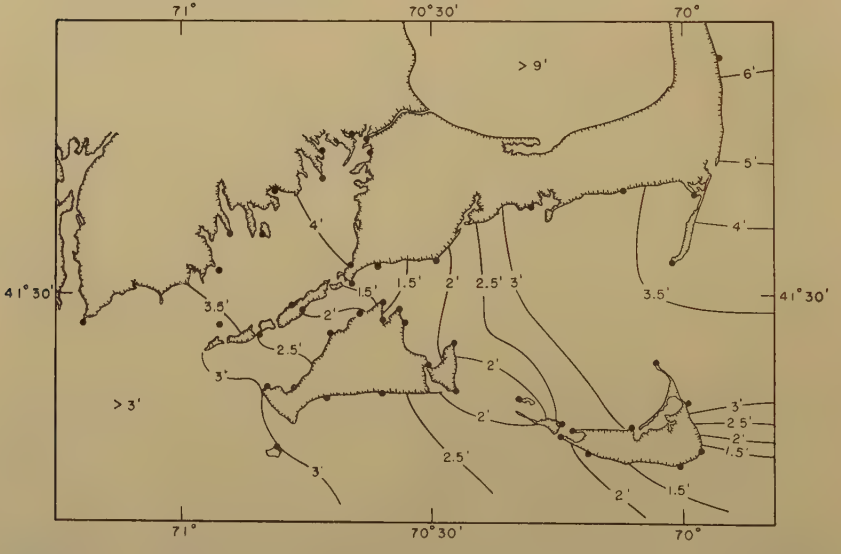

Figure 3. Corange lines for Vineyard and Nantucket Sounds, showing mean range of tide in feet.

In a strait separating an island from the mainland it may be expected that tidal waves will enter, meet, and pass in opposite directions. The following treatment should apply, provided the strait is sufficiently narrow to prevent the development of marked effects of the Coriolis force or the production of rotatory currents. It is evident that some point must exist where waves of like period are always in phase. The time of high water at this point of phase equality is taken as the origin of time. Letting σ be the change in phase per unit time, the time angle σt gives the phase at any point relative to the phase at the position of phase equality.

The position of phase equality is also taken as the origin from which phase differences due to position are measured. In a regular channel, phase differences may be expressed by kx, where k is the change of phase per unit of distance and x is the distance measured from the origin. Since phase changes in an irregular channel are not necessarily proportional to distance, x cannot be taken to represent distance in a geographic sense. However, k may be defined as a phase difference of 360° and x as that part of a cycle which a wave will complete in passing between any designated points. Consequently, kx denotes the phase difference due to position between any point and the position of phase equality.

Damping is assumed to be proportional to the phase change along the channel. The attenuation of each wave in its direction of progression is given by $e^{-\mu x}$, where the damping coefficient μ represents the attenuation per cycle and x is the fraction or multiple of the cycle completed.

To find the time of high water at any point. The elevation of the surface η at any time and place along the channel is given by the sum of the elevations of the respective waves, η_1 and η_2. If A and $(1+f)$ A are the amplitudes of the respective waves at the position of phase equality,

$$\eta_1 = A \cos(\sigma t - kx)\, e^{-\mu x} \text{ and } \eta_2 = (1+f)\, A \cos(\sigma t + kx)\, e^{\mu x},$$

η_2 being the elevation of the wave taken to be moving in the negative direction with respect to x.

Since $\eta = \eta_1 + \eta_2$,

$$\eta = A\left[\cos(\sigma t - kx)\, e^{-\mu x} + (1+f)\cos(\sigma t + kx)\, e^{\mu x}\right]. \qquad (1)$$

High water occurs when $\delta\eta/\delta t = 0$ or when $\sin(\sigma t - kx)\, e^{-\mu x} + (1+f)\sin(\sigma t + kx)\, e^{\mu x} = 0$, from which it follows that the local time angle of high water, σt_H, is given by

$$\tan^{-1}\left[-\tan kx\, \frac{(1+f)\, e^{\mu x} - e^{-\mu x}}{(1+f)\, e^{\mu x} + e^{-\mu x}}\right].$$

Letting F represent the term $\dfrac{(1+f)\,e^{\mu x} - e^{-\mu x}}{(1+f)\,e^{\mu x} + e^{-\mu x}}$,

this becomes

$$\sigma t_H = \tan^{-1}\left[-\tan kx \cdot F\right]. \tag{2}$$

To find the elevation at any point at high water. From (1) the elevation at any time and place may be written

$$\eta = A\,(\cos\sigma t\cos kx + \sin\sigma t\sin kx)\,e^{-\mu x} + (1+f)\,(\cos\sigma t\cos kx - \sin\sigma t\sin kx)\,e^{\mu x}.$$

At high water it follows from (2) that

$$\cos\sigma t_H = \frac{1}{\sqrt{1+F^2\tan^2 kx}} \text{ and}$$

$$\sin\sigma t_H = \frac{-F\tan kx}{\sqrt{1+F^2\tan^2 kx}}.$$

Consequently the elevation at high water η_H may be written

$$\eta_H = \tag{3}$$

$$A\,\frac{(\cos kx - F\tan kx\sin kx)\,e^{-\mu x} + (1+f)\,(\cos kx + F\tan kx\sin kx)\,e^{\mu x}}{\sqrt{1+F^2\tan^2 kx}}.$$

To find the time of slack water at any point. The velocity of the current due to the respective waves at any time and place is given by

$$u_1 = A\,\frac{b}{h}\left(\frac{1}{\sqrt{\mu^2+k^2}}\right)e^{-\mu x}\cos(\sigma t - kx) \text{ and}$$

$$u_2 = -(1+f)\,A\,\frac{b}{h}\left(\frac{1}{\sqrt{\mu^2+k^2}}\right)e^{\mu x}\cos(\sigma t + kx),$$

where h is the depth and b the cross section of the channel.

At any point along the channel slack water occurs when $u_1 + u_2 = 0$, or when

$$e^{-\mu x}\cos(\sigma t - kx) - (1+f)\,e^{\mu x}\cos(\sigma t + kx) = 0, \text{ or}$$

$$\cos\sigma t\cos kx\,[e^{-\mu x} - (1+f)\,e^{\mu x}] + \sin\sigma t\sin kx\,[e^{-\mu x} + (1+f)\,e^{\mu x}] = 0.$$

Letting σt_s denote the local time angle of slack water, it follows that

$$\sigma t_s = \tan^{-1}\cdot\frac{F}{\tan kx}. \tag{4}$$

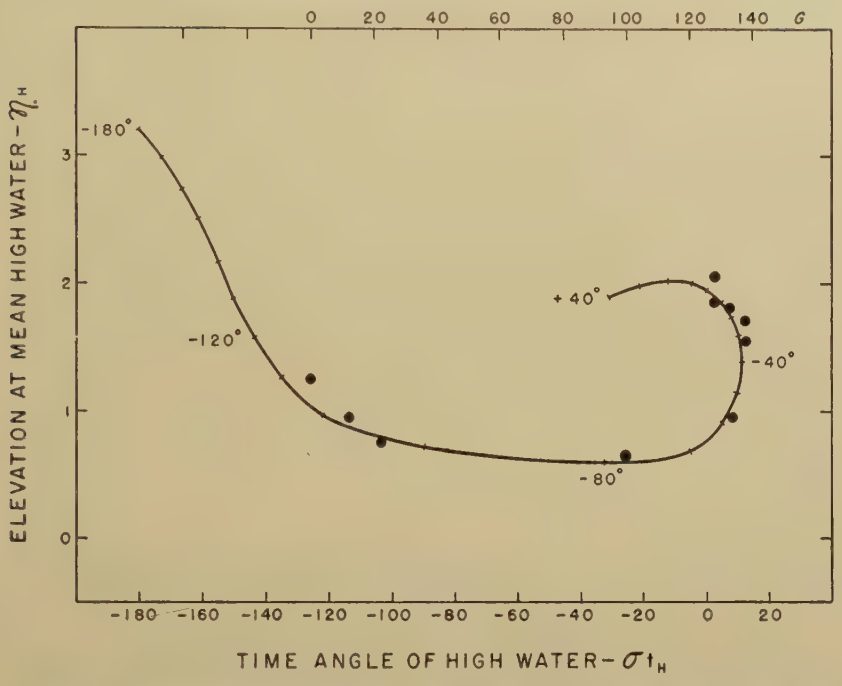

Figure 4. Relation between elevation at high water (ηH) and time angle at high water (σtH) along Vineyard and Nantucket Sounds. Curve estimated from equations (2) and (3) taking $\mu = 3$, $f = 2$, and $A = 0.65$ feet. Points represent stations recorded in Table I.

Applications. In this treatment, effects of the earth's rotation and the deformation of the tidal wave by shallow water and damping are neglected. In its application to Vineyard and Nantucket Sounds, the influence of tidal flow through the Muskeget Channel is not taken into account. For this reason, attention is limited to stations along the northern side of the Channel where there is a relatively unbroken boundary.

To test the application of equations (2), (3), and (4) to tidal relations in Vineyard and Nantucket Sounds, data from the tide and current tables of the U. S. Coast and Geodetic Survey relative to nine stations along the northern coast of the sounds have been selected. In Table I, times of high water and slack water at these stations are expressed by the Greenwich epoch G which is related to σt by $G = \sigma t + K$, where K is the Greenwich epoch of high water at the point of phase equality. The elevation at high water, η_H, is given as equal to one-half the mean range of tide.

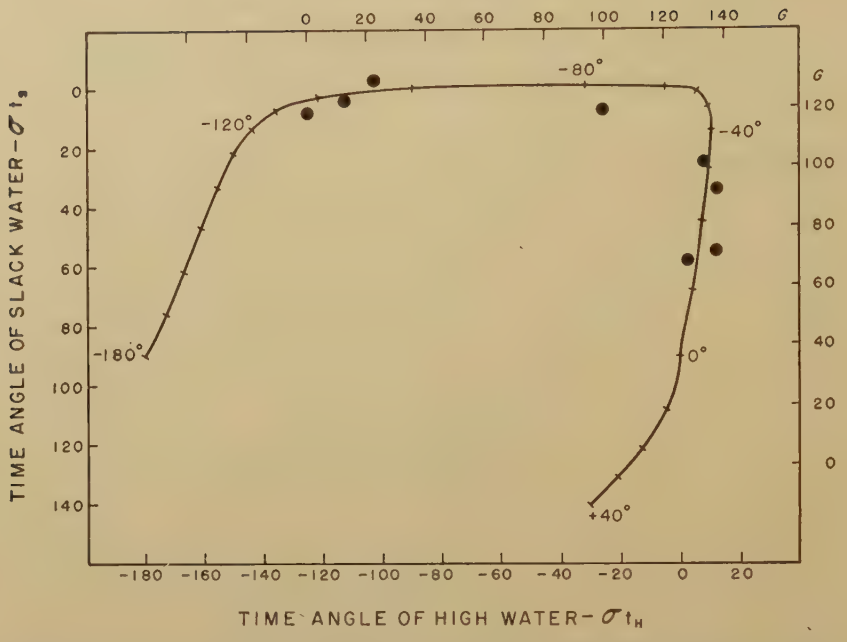

Figure 5. Relation between time angle at high water (σt_H) and time angle at slack water (σt_s) along Vineyard and Nantucket Sounds. Curve estimated from equations (3) and (4), taking $\mu = 3.0$, $f = 2$, and $A = 0.65$ feet. Points represent stations recorded in Table I. Note: Time angles of slack water should have negative signs.

By assuming arbitrarily chosen values for the constants μ, A, and f, and solving equations (2) and (3) for the values of σt_H and η_H corresponding to a series of values for kx, a curve may be drawn which shows the unique relations of the time of high water and the elevation at high water determined by the constants chosen, as in Fig. 4.

Along the curve a scale of values of kx corresponding to each combination is marked. The relations σt_H and σt_S or η_H and σt_S may be treated similarly, the former combination being shown in Fig. 5.

Appropriate pairs of observed parameters may be plotted on such diagrams and tested for correspondence with the theoretical curves. If η_H is plotted as its logarithm, the "shape" of the curves is determined solely by μ and f, and the values of A and K are found by the vertical and horizontal displacements of the observed points required to secure the best fit. A final test of fit is obtained by comparing the values of kx which may be assigned to the positions of observation by the analysis of different pairs of parameters.

The curves shown in Figs. 4 and 5 are drawn with $\mu = 3$, $f = 2$, $A = 0.65$ feet, and $K = 126°$. The observed points are distributed

TABLE I. Tidal Data for North Shore of Vineyard and Nantucket Sounds

No.	Station*	Mean Range (feet)	High Water interval (hours)	Slack Water interval† (hours)	η_H (feet)	G_H (degrees)	G_S (degrees)	kx (degrees)
1	Quicks Hole	2.5	7.66	11.62	1.25	1	118	−105
2	Tarpaulin Cove	1.9	8.02	11.76	0.95	13	122	−98
3	Nobska Point	1.5	8.53	12.00	0.75	23	129	−94
4	Falmouth Heights	1.3	11.00	11.66	0.65	100	119	−78
5	Succonnessett Point	1.9	12.16	11.38	0.95	134	111	−58
6	Hyannisport	3.1	12.33	10.76	1.55	138	92	−30
7	Dennisport	3.4	12.35	10.02	1.70	138	71	−20
8	Stage Harbor	3.6	12.20	—	1.80	133	—	−16
9	Monomoy Point	3.7	12.00	9.94	1.85	128	68	−10

* Positions of stations are identified by number in Fig. 2.
† Slack before current turns west.

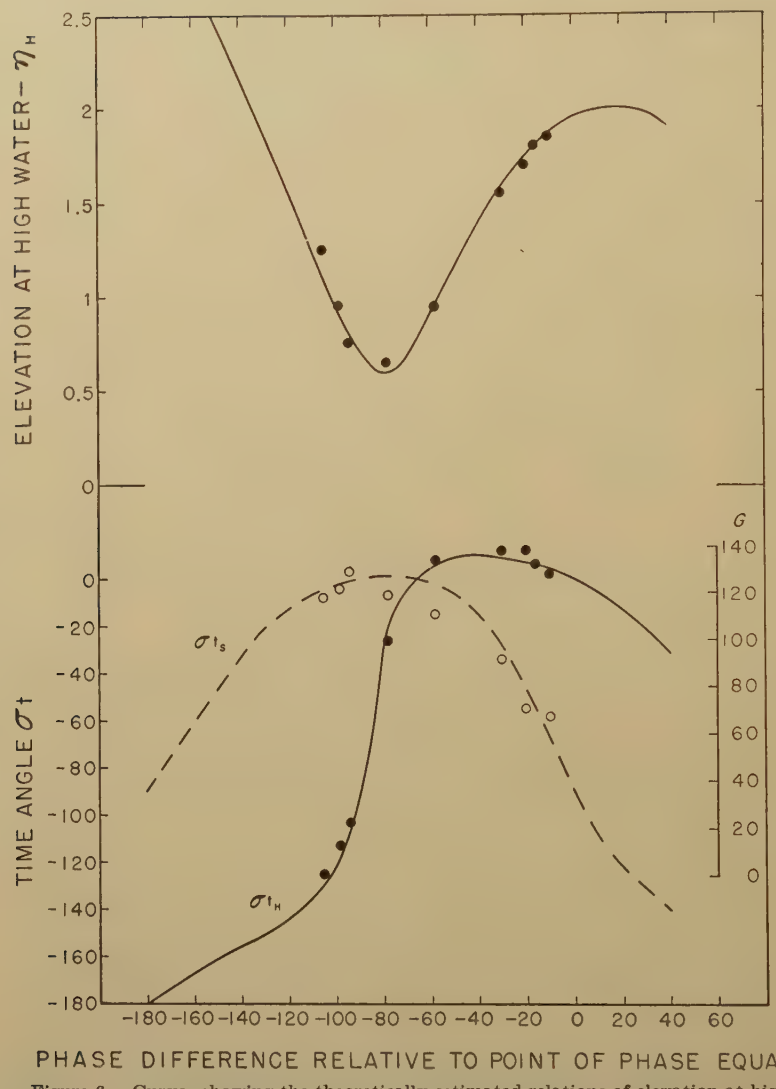

Figure 6. Curves showing the theoretically estimated relations of elevation at high water (ηH), time angle of high water ($\sigma t H$), and time angle of slack water (σt_s) to the phase difference along the channel. The plotted points represent observations at stations recorded in Table I.

closely along these curves. From the scales marked along the curves, approximate values of kx may be obtained for each position of observation and may be adjusted so as to reconcile the differences given by the two curves. The adjusted values, entered in Table I, represent

the phase difference of the waves at each station relative to the position of phase equality. In Fig. 6 the estimated values of η_H, σt_H, and σt_S are plotted as curves against the corresponding values of kx. The positions of observation are spaced along the abscissa in accordance with the values of kx assigned to each, and the measured values of the several properties of the tide at each position are plotted for comparison with the theoretical curves. Fig. 6 shows that the observed values for mean range of tide, time of high water, and time of slack water are consistent with the values estimated from the several equations.

The values of the constants chosen to represent the properties of the tide in Vineyard and Nantucket Sounds have been found by trial to give a reasonably good description of the observations. They are not necessarily those which give the best fit in any statistical sense. The value of the damping coefficient μ is somewhat greater than that deduced from Long Island Sound and the Bay of Fundy, where μ was between 1 and 1.5 (Redfield, 1950). This is reasonable in view of the limited depth of Nantucket and Vineyard Sounds. The value of f is concordant with the facts that the general range of tide is much greater in the Gulf of Maine than it is along the outer coast south of New England. The position of phase equality appears to lie to the east of Monomoy Point. At this position it may be expected that the value of G for mean high water is 126°, that the elevation at high water due to the wave moving eastward through Vineyard and Nantucket Sounds is 0.65 feet, and that the elevation at high water due to the wave moving westward from the Gulf of Maine is 1.95 feet above mean sea level.

Along the southern shore of Vineyard and Nantucket Sounds the general trend of tidal phenomena is similar to that on the opposite coast. In general the ranges of tide are somewhat greater along the shore of Marthas Vineyard than are those at corresponding points on the mainland; this may be attributed to effects of the earth's rotation. Along the shore of Nantucket, Tuckernuck, and Muskeget Islands, the relations are presumably determined primarily by interference between the wave originating in the Gulf of Maine and that entering Muskeget Channel, which should produce similar but not necessarily the same relations as those found along the northern coasts of the sounds.

In view of the correspondence of theory and observation along the northern coast and the qualitative agreement along the southern shore, it is concluded that the relations between the time of high water, slack water, and mean range of tide along Vineyard and Nantucket Sounds are satisfactorily accounted for by the interference of tidal waves of unequal amplitude which traverse the sounds in opposite directions.

THE AMPLITUDE OF THE DIURNAL AND SEMIDIURNAL TIDAL CONSTITUENTS AT WOODS HOLE

The foregoing analysis is based on the mean values for range of tide, high water interval, and slack water interval. Since the tidal phenomena in the North Atlantic are dominated by the M_2 constituent, it may be assumed that the analysis applies to a single wave having a speed number of 29° per hour (Proudman and Doodson, 1924). Thus, the interference phenomena described are those which affect the semidiurnal constituents of the tide. Nobska Point, at the entrance to Great Harbor, Woods Hole, is situated about ¼ wave length from the point of phase equality, and consequently the amplitude of the semidiurnal constituents is maximally reduced by interference in its neighborhood.

The diurnal waves that enter the sounds from opposite ends may be expected to be in phase at about the same position as the semidiurnal waves, since they move with similar velocity. However, the phase difference of the diurnal waves along the channel will be only half as great since the wave length is double. Consequently, the phase difference between Nobska Point and the position of phase equality will be approximately ⅛ wave length, and the reduction of the amplitude by interference will be much less than that in the case of the semidiurnal constituents.

The correctness of this reasoning is indicated by a comparison of the amplitude H of the principle tidal constituents at Woods Hole and at Atlantic City, which is on the outer coast where the local geographic conditions may be expected to have a minimal effect upon the ocean tide. The values of the principle constituents at these stations, based on analyses of complete records during the year 1940, are shown in Table II. With the exception of the small Q_1 component, the amplitudes at Woods Hole are reduced relative to those at Atlantic City. The proportional reduction of the semidiurnal constituents is substantially greater than that of the diurnal constituents. Taking the ratio of the sums of the amplitudes of each species to give a weighted expression, the combined amplitudes of the diurnal constituents at Woods Hole is 76% of those at Atlantic City, while the ratio for the semidiurnal constituents is 44%. The reduction of the semidiurnal constituents is thus more than twice that of the diurnal constituents, and this may be attributed to the interference phenomena associated with the topography of Vineyard and Nantucket Sounds.

The consequence of the unequal reduction of the diurnal and semidiurnal constituents at Woods Hole is to increase the diurnal inequality of the tidal range. This gives rise to a condition approaching the

mixed tides characteristic of the Pacific Ocean, where great inequality exists between the elevation of successive high (and low) waters at the time of the moon's maximum semimonthly declination and where periods of equality follow when the moon is over the equator. This characteristic of the tide at Woods Hole has not impressed local observers because the range of tide there is small and is subject to relatively great variation from meteorological causes. However, it appears clearly from measurements of tidal records (see Fig. 7).

TABLE II. Amplitude (H) of the Principle Constituents of the Tide at Woods Hole and Atlantic City

	Constituent	Woods Hole	Atlantic City	Ratio
Diurnal	K_1	0.224	0.344	0.652
	O_1	0.203	0.236	0.854
	P_1	0.075	0.113	0.664
	Q_1	0.053	0.039	1.36
	Sum (C_1)	0.555	0.732	0.76
Semidiurnal	M_2	0.759	1.928	0.393
	S_2	0.200	0.393	0.509
	N_2	0.246	0.447	0.551
	K_2	0.043	0.096	0.448
	Sum (C_2)	1.248	2.864	0.44

The ratio of the sum of the diurnal constituents C_1 to the sum of the semidiurnal constituents C_2 serves as a ready index of the tendency for diurnal inequality of the tide at any place. The following tabulation compares this index for Woods Hole with that for positions on the outer coasts of the Atlantic (Atlantic City, N. J.) and Pacific (Claoquot, B. C.). There is added the index for Victoria, B. C., where the tide is almost completely diurnal owing to the suppression of the semidiurnal constituents by interference similar to that ascribed to the Woods Hole tide (Redfield, 1950).

		C_1	C_2	C_1/C_2
Atlantic City	1940	0.732	2.864	0.255
Woods Hole	1940	0.555	1.248	0.444
Claoquot	1939	2.63	5.11	0.516
Victoria	1939	4.15	1.88	2.22

The index for Woods Hole approaches closely that for the example chosen for the Pacific Ocean.

THE FORM OF THE TIDE GAUGE CURVE AT WOODS HOLE

Records of the elevation of the sea surface by the tide gauge at the Woods Hole Oceanographic Institution on Great Harbor show a striking departure from the usual sinusoidal curve. The rise of the

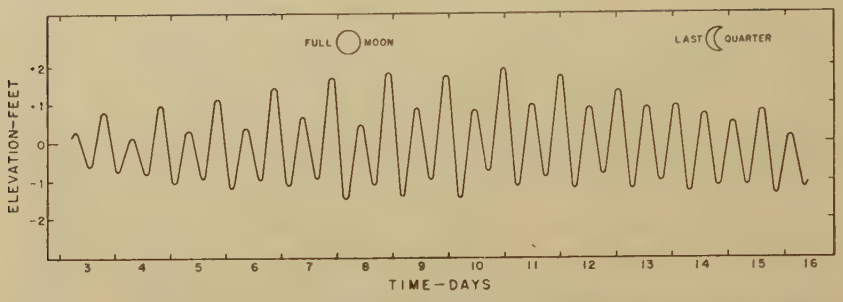

Figure 7. Diagram showing elevation of the tide at Woods Hole at successive high and low water during June 3–16, 1952. The form of the curve and the spacing of high and low waters are not represented exactly.

tide occupies about 5.4 hours, while 7.0 hours intervene between high water and the following low water. During the ebb, at about half tide, the fall is interrupted and the surface level remains constant or rises slightly for nearly an hour (see Fig. 8). The effect varies from day to day and appears to be most pronounced when the range of tide is relatively great.

The distortion of the record during the fall in tide level appears to be due to phenomena similar to those responsible for double high- and double low-waters which are discussed by Doodson and Warburg (1941) in relation to conditions near Southampton. A nearby case of double low-water is cited by Harris (1907) for Providence, Rhode Island. These phenomena in general are explained as follows. In shallow water tidal waves are distorted in such a way that they may

Figure 8. Record from tide gauge at Great Harbor, Woods Hole, September 30, 1952.

be described by the sum of a series of harmonics. At points where the fundamental constituent is suppressed by interference, certain of the harmonics are undisturbed or are reinforced, and thus they may stand out as recognizable distortions of the sinusoidal wave. The phase relations of these distortions depend on the topographic conditions which determine the interference patterns of the fundamental and its harmonics. Where the semidiurnal constituent M_2 is the principle constituent of the tide, the quarter diurnal constituent M_4 will be the harmonic largely responsible for the distortion of the

curve. If σt represents the phase of the M_2 wave, the phase of the M_4 wave is given by $2\sigma t + \theta$. If the angle θ is 180°, double high-waters may result; if it is 0°, double low-waters are possible. If θ is 90°, or thereabout, the effect is to steepen the rise of tide and to delay its fall when half tide level is reached. This is apparently the condition in the present case, and this is the phase relation which may be expected when harmonics are generated by progressive waves that undergo distortion in shallow water. These distortions are sufficient to reverse the slope of the record only when interference reduces substantially the amplitude of the fundamental wave relative to the harmonic.

An exact harmonic analysis of the tide at Woods Hole has been made by the U. S. Coast and Geodetic Survey for the years 1933 and 1940. The constants for the M_2 and S_2 components and their harmonics for 1933 are as follows:

	H	k
M_2	0.703	254.7
M_3	0.011	176.0
M_4	0.162	74.6
M_6	0.052	337.8
M_8	0.009	329.0
S_2	0.185	253.2
S_4	0.017	70.0

The principle harmonic present, M_4, has an amplitude of 23% of its fundamental M_2. The phase displacement of the M_2 and M_4 components may be estimated from the values of k so that $\theta = 75°$. The M_6 component also has sufficient amplitude to affect the shape of the tide gauge record appreciably. A curve calculated from the M_2, M_4, and M_6 components shows distortion which is similar to that of the record but which is less pronounced than that usually observed.

A curve which is a reasonable facsimile of the record is shown in Fig. 9, Curve B. The constants used in constructing this curve are given on page 138 and are such that $\theta = 90°$ in the case of both the M_4 and M_6 constituents. The nature of the distortion is shown by a comparison of Curve B with Curve A, which is that for the M_2 constituent alone.

The harmonics present in the tide at Woods Hole, and their exaggeration relative to the fundamental waves, may be explained by the distortion of tidal waves by the shoal water of Vineyard and Nantucket Sounds. Wherever the harmonics may be generated, the suppression of the semidiurnal wave, which is required to make their presence evident by the distortion of the tide record, is explained by the interference of the semidiurnal waves which traverse the sounds in opposite directions.

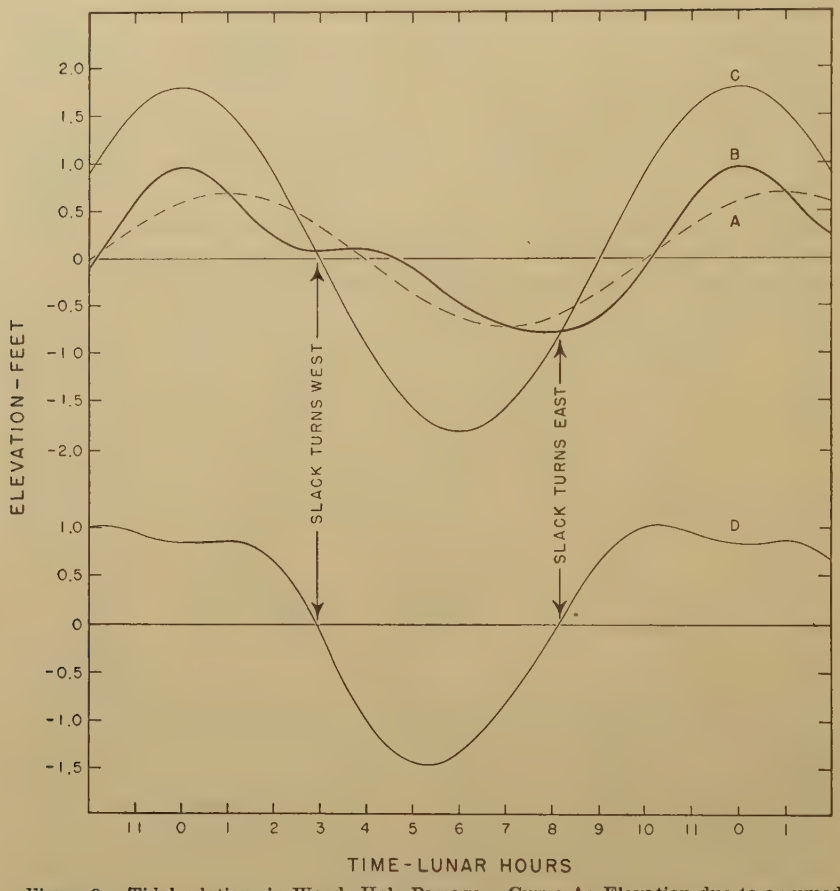

Figure 9. Tidal relations in Woods Hole Passage. Curve A: Elevation due to assumed M_2 constituent at Great Harbor. Curve B: Elevation of sea surface at Great Harbor resulting from sum of assumed M_2, M_4, and M_6 constituents. Curve C: Elevation at Uncatena Island represented by a single (M_2) constituent. Curve D: Hydrostatic head between Uncatena Island and Great Harbor. Time: Lunar hours relative to time of high water at Uncatena Island.

At Woods Hole, just ¼ wave length from the position of phase equality, the semidiurnal waves are maximally reduced by interference. If quarter-diurnal waves accompany these fundamentals at Woods Hole, they would be ½ their wave length from the position of phase equality and they would reinforce one another.

Harmonic analysis of the tide at a number of stations scattered about the area would be required to clarify the geographical origin of the phenomena. The existing information, however, is sufficient to

indicate that the form of the tide record at Woods Hole is due primarily to the M_4 and M_6 constituents. The suppression of the fundamental semidiurnal components, required to develop the observed distortion of the record, is explained adequately by the interference of the fundamental waves which traverse the sound in opposite directions.

THE TIDAL CURRENT IN WOODS HOLE PASSAGE

The movement of water through Woods Hole Passage is due to a hydraulic current resulting from inequalities of range and time of tide in Buzzards Bay and Vineyard Sound. These inequalities arise from the topography of these tidal basins.

Buzzards Bay is a relatively short closed embayment in which reflection of the advancing tidal wave produces a tide of the standing wave type. High water is delayed less than 45 minutes between its mouth and its head. The mean range of tide increases as the head of the bay is approached, being 3.4 feet at Penikese Island and 4.1 feet at Onset.

Vineyard Sound is a part of a long system of channels in which the tide advances as a progressive wave. The wave arising in the Gulf of Maine, and traversing the sounds in the opposite direction, produces interference effects. The length of the channel is such that off Woods Hole Passage the range of tide is greatly reduced. Because of the high degree of damping, the west-moving wave is so reduced in amplitude that interference is incomplete and the progressive character of the tidal wave which enters Vineyard Sound remains evident.

At the eastern end of Woods Hole Passage, in Great Harbor, the mean range of tide is 1.8 feet as compared to 3.6 feet at the western end, at Uncatena Island. The time of high water at Great Harbor is only 5 minutes later than at Uncatena Island, but low water is 1.7 hours later. Evidently the major condition responsible for the hydraulic head is the difference in level which amounts to about 1.0 foot at high water and nearly 1.5 feet at low water.

A striking characteristic of the currents in Woods Hole Passage is the unequal duration of flow in opposite directions. The duration of the eastward current exceeds that of the westward current by about two hours. This characteristic may be explained as the result of the peculiar form of the tide curve in Great Harbor which appears to arise from the presence of the harmonics in the tidal complex.

If the mean elevations on either side of the Passage were determined solely by the relative amplitudes and times of the semidiurnal tidal constituents in Great Harbor and Buzzards Bay, the differences in elevation and the resulting flow would follow a symmetrical sinusoidal curve, and the duration of the eastward and westward currents would

TABLE III. Comparison of Tidal Characteristics of Woods Hole Passage Estimated from Mathematical Model and Predicted by the Tide and Current Tables. *Lunar hours or feet.*

	Model	Tables	Difference
Uncatena Island HW	0	0	0
Great Harbor HW	0.1	0.1	0
Great Harbor LW	7.9	7.9	0
Current Turns West	2.9	2.6	+ 0.3
Current Turns East	8.2	7.6	+ 0.6
Current Flows West	5.3	5.0	+ 0.3
Current Flows East	6.7	7.0	− 0.3
Maximum Current West	5.6	5.7	− 0.1
Maximum Current East	11.0	10.8	+ 0.2
Mean Range:			
Uncatena	3.6	3.6	0
Great Harbor	1.73	1.8	0.07

	Maximum Head	Maximum Currents*
West	1.49 feet	3.6 knots
East	1.02 feet	2.7 knots
Ratio	1.46	1.33

* Current pole measurements (Haight, 1936)

be equal. The harmonics in Great Harbor produce an additional component of flow through the Passage. The time relations of this component of flow are such that it is eastward at both periods when slack water would result from the interaction of the semidiurnal components alone. In this way, the duration of the eastward current may be prolonged at the expense of that of the westward current.

Fig. 9 demonstrates this principle and approximates the observed conditions. The tidal elevations at Uncatena Island are represented by a single semidiurnal constituent, M_2, those at Great Harbor by the combination of a semidiurnal, M_2, a quarter diurnal, M_4, and a sixth diurnal constituent, M_6. The harmonic constants are as follows:

		H	k
Uncatena Island	M_2	1.8 feet	233°
Great Harbor	M_2	0.7 feet	263°
	M_4	0.3 feet	76°
	M_6	0.1 feet	339°

Note that the elevations due to the M_2 components, Curves A and C, are equal and that slack water would occur at hours 2.5 and 8.5 in the absence of the higher harmonics. At these times the elevations due to the combined harmonic constituents are negative, producing a hydrostatic head favoring flow eastward from Uncatena Island to

Great Harbor. Equal elevations occur 0.4 hours later during the falling tides and 0.3 hours earlier during the rising tides. This produces inequality in the duration of east and west flow.

The hydrostatic head between Uncatena Island and Great Harbor is shown in the lower part of Fig. 9. This curve resembles that which describes current measurements made by the U. S. Coast and Geodetic Survey off Devils Foot Island (Haight, 1936: fig. 32, Station 13035) in indicating that the westward current is not only shorter in duration but is also of greater maximum velocity. Table III shows how closely the characteristics of the tides in Woods Hole Passage, as represented by the mathematical model, agree with the predictions of the tide and current tables.

Acknowledgment is made to the U. S. Coast and Geodetic Survey which, through the kindness of Dr. Harry Marmer, has made available unpublished harmonic constants used in the preparation of this paper. Thanks are due Mr. Henry Stommel of the Woods Hole Oceanographic Institution for aid in the mathematical treatment of the interference of tidal waves.

SUMMARY

1. The relations of mean range of tide, time of high water, and time of slack water along Vineyard and Nantucket Sounds may be attributed to the interference of tidal waves entering the sounds from their opposite ends.

2. These waves are in phase at a position to the east of Monomoy Point. At this position the wave approaching from the Gulf of Maine has twice the amplitude of that which has traversed the sounds.

3. The damping coefficient of the tidal waves in the sounds is of the order of 3.0.

4. Interference of the semidiurnal constituents is maximal in the neighborhood of Woods Hole. The great reduction of the semidiurnal constituents relative to the diurnal constituents results in a pronounced diurnal inequality in the range of successive tides at appropriate phases of the moon.

5. The tide gauge record at Woods Hole is distorted in form as a result of the development of shallow water harmonics combined with the reduction of the fundamental semidiurnal constituent by interference.

6. The inequality in the duration of flood and ebb currents in Woods Hole Passage may be attributed to the effect of these harmonics on the tide levels in Great Harbor.

REFERENCES

Bache, A. D.
1855. Report of the Superintendent of the Coast Survey for the year 1854. Washington, D. C. 288 pp.

Doodson, A. T. and H. D. Warburg
1941. Admiralty Manual of Tides. London. 270 pp.

Haight, F. J.
1936. Currents in Narragansett Bay, Buzzards Bay, and Nantucket and Vineyard Sounds. Spec. Publ. U. S. Cst. geod. Surv., No. 208. Washington, D. C. 103 pp.

Harris, R. A.
1904. Manual of Tides. Part IVB. Cotidal lines for the world. Rep. U. S. Cst. geod. Surv., Appendix No. 5: 313–400.
1907. Manual of Tides. Part V. Currents, shallow water tides, meteorological tides and miscellaneous matters. Rep. U. S. Cst. geod. Surv., Appendix No. 6: 213–545.

Proudman, J. and A. T. Doodson
1924. The principal constituent of the tides of the North Sea. Phil. Trans., (A) *224:* 185–219.

Redfield, A. C.
1950. The analysis of tidal phenomena in narrow embayments. Pap. phys. Oceanogr. Meteorol., *11* (4): 1–36.

U. S. Coast and Geodetic Survey
1951. Tide Tables East Coast North and South America for the year 1952. Serial No. 742. Washington, D. C. 249 pp.
1951. Current Tables Atlantic Coast North America for the year 1952. Serial No. 751. Washington, D. C. 174 pp.

Contribution No. 638

PROCEEDINGS OF THIRD CONFERENCE

ON

COASTAL ENGINEERING

CAMBRIDGE, MASSACHUSETTS

OCTOBER 1952

Edited by

J. W. JOHNSON

PROFESSOR OF HYDRAULIC ENGINEERING

UNIVERSITY OF CALIFORNIA
BERKELEY

PUBLISHED BY

COUNCIL ON WAVE RESEARCH
THE ENGINEERING FOUNDATION

1953

CHAPTER 5

THE SALT WEDGE[1]

Harlow G. Farmer
Woods Hole Oceanographic Institution
Woods Hole, Massachusetts

George W. Morgan
Assistant Professor of Applied Mathematics
Brown University
Providence, Rhode Island

INTRODUCTION

The "salt wedge" is an idealized model of a phenomenon encountered in some estuaries. It consists of a layer of fresh river water flowing over and past an underlying layer of heavier salt water. The following study is an attempt to predict the shape of the salt wedge and its length measured from some significant point in the estuary in terms of quantities, such as the densities of the fresh and salt water, the average river depth and velocity, etc., which are usually available.

THEORETICAL ANALYSIS[2]

To simplify the mathematical treatment we assume that all variations in the direction of the estuary or channel width are negligible and that there is no velocity component in this direction. The channel has a plane horizontal bottom and its cross-section is rectangular and uniform.

We stipulate the existence of a sharp interface between the fresh water and the salt wedge, i.e., a density discontinuity, and the absence of mixing between the layers.

The equations of motion can then be written for each layer in the following form (Fig. 1):

---

[1]Contribution No. 638 from the Woods Hole Oceanographic Institution. This work was supported from funds made available by the Office of Naval Research, through their Contract No. N6onr-27701 (NR-083-004) with the Woods Hole Oceanographic Institution.

---

[2]For a more detailed account of the theory and additional investigations, see: L. Sanders, L. C. Maximon, G. W. Morgan, On the stationary "salt wedge" - a two layer free surface flow. Technical Report No. 1, Contract Nonr-56202 (NR-083-067). The theoretical results presented in this paper were obtained in the course of research sponsored by the Office of Naval Research under the above Contract with Brown University.

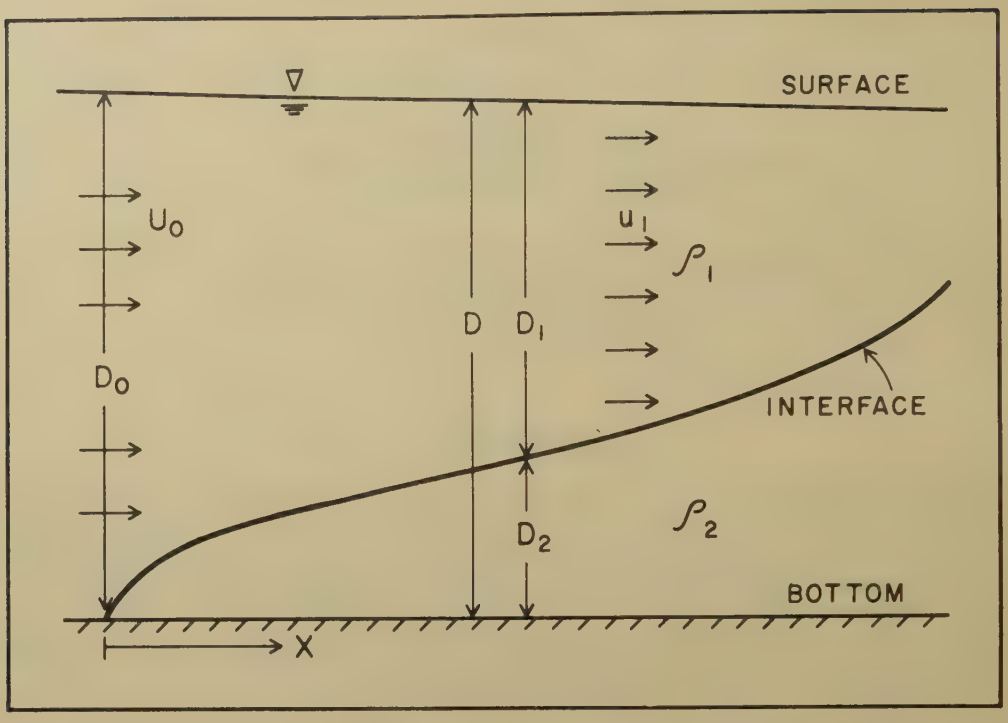

Fig. 1. Schematic diagram of salt wedge.

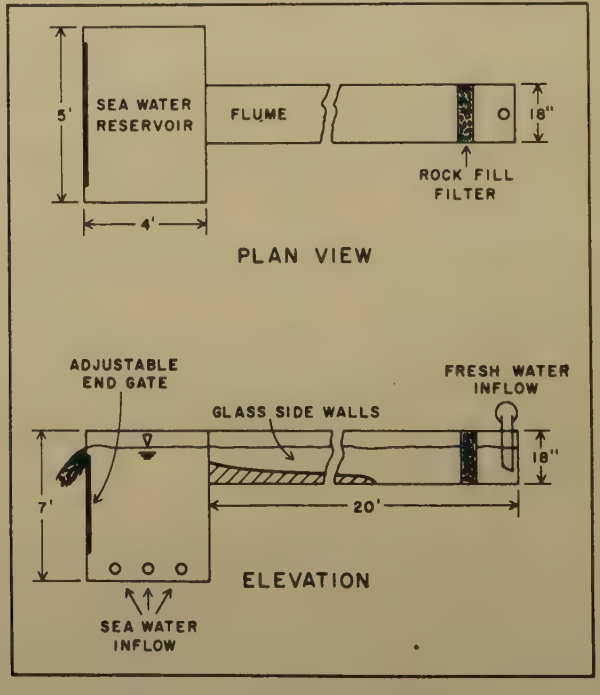

Fig. 2. Schematic diagram of experimental apparatus.

$$\frac{\partial}{\partial x}(p_i + \rho_i u_i^2) + \frac{\partial}{\partial z}(\rho_i u_i w_i) = \frac{\partial}{\partial x}(A_i \frac{\partial u_i}{\partial x}) + \frac{\partial}{\partial z}(A_i \frac{\partial u_i}{\partial z}) \qquad (1)$$

$$\frac{\partial}{\partial z}(p_i + \rho_i w_i^2) + \frac{\partial}{\partial x}(\rho_i u_i w_i) = -\rho_i g + \frac{\partial}{\partial x}(A_i \frac{\partial w_i}{\partial x}) + \frac{\partial}{\partial z}(A_i \frac{\partial w_i}{\partial z}) \qquad (2)$$

$$\frac{\partial u_i}{\partial x} + \frac{\partial w_i}{\partial z} = 0 \qquad (3)$$

where the subscript i takes on the values 1 or 2 referring to the upper or lower layer, respectively;

ρ is the density,
p is the pressure,
u is the horizontal velocity component,
w is the vertical velocity component,
g is the gravitational acceleration, and
A is an eddy viscosity.

These equations apply to turbulent flow, the quantities u, w, p representing time averages of the actual time-dependent quantities.

If we neglect the inertia and shear forces in the vertical direction we can integrate the vertical momentum equation. Applying the condition $p = 0$ at the free surface $z = D$, we obtain

$$p_1 = \rho_1 g (D - z) \qquad (4)$$

and

$$p_2 = \rho_2 g (D_2 - z) + \rho_1 g D_1 \qquad (5)$$

where $z = D_2$ is the interface and $D_1 = D - D_2$, see Figure 1.

The solution is too difficult because of the presence of the unknown boundaries D, D_2. We therefore make a further approximation in our analysis by demanding that the laws of conservation of mass and momentum be satisfied only in the large rather than at every point of the flow, i.e., we integrate the equations over the depth. We then obtain the following equations from (1)

$$\rho_1 g D_1 \frac{d}{dx}(D_1 + D_2) + \rho_1 \frac{d}{dx}\int_{D_2}^{D} u_1^2\, dz = \tau_1 - \tau_2 \qquad (6)$$

$$g D_2 \frac{d}{dx}(\rho_1 D_1 + \rho_2 D_2) + \rho_2 \frac{d}{dx}\int_{o}^{D_2} u_2^2\, dz = \tau_2 - \tau_o \qquad (7)$$

Here τ_o, τ_1, τ_2 are the values of $A\frac{\partial u}{\partial z}$ at $z = 0$, D, D_2 respectively, and we have neglected the term $\frac{\partial}{\partial x}(A\frac{\partial u}{\partial x})$ compared with $\frac{\partial}{\partial z}(A\frac{\partial u}{\partial z})$.

The continuity equation (3) gives

$$\frac{d}{dx}\int_{D_2}^{D} u_1 dz = 0 \qquad (8)$$

or

$$\int_{D_2}^{D} u_1 dz = q \qquad (8a)$$

and

$$\frac{d}{dx}\int_{o}^{D_2} u_2 dz = 0 \qquad (9)$$

or

$$\int_{o}^{D_2} u_2 dz = 0 \qquad (9a)$$

since there can be no net flow within the stationary wedge.

Equations (6) to (9) can now be treated in an approximate manner by assuming plausible velocity distributions u_1, u_2. Since the flow is turbulent it is reasonable to suppose that u_1 is fairly uniform over the depth except near the interface where sharp velocity gradients may be

expected; i.e., $u_1 = \frac{q}{D_1}$. Since there is zero net flow across any section of the wedge and since the velocities in the wedge are caused by friction at the interface, we may expect that u_2 will be small compared with u_1 except possibly near the interface and that, therefore, the integral and the term τ_0 in equation (7), representing inertia forces and bottom shear forces, respectively, are negligible. We may also drop the free surface friction term τ_1.

We still know nothing concerning the nature of the interface shear force τ_2. At this point we content ourselves with developing a semi-empirical theory and take recourse to experimental results to determine an approximate law for τ_2.

It is convenient to rewrite equations 6, 7, 8a, 9a in non-dimensional terms by means of the following definitions:

$$D_1 = D_o n_1, \quad D_2 = D_o n_2, \quad z = D_o z', \quad D = D_o D'$$

$$x = Lx', \quad u_1 = U_o u_1', \quad \tau_2 = \rho_2 U_o^2 \tau'$$

$$\beta = \frac{\rho_2 - \rho_1}{\rho_2}, \quad \alpha = \frac{U_o^2}{g D_o \beta} \text{ and } \lambda = \frac{L}{D_o}$$

where D_o is a reference depth, taken to be the total depth at the tip of the wedge, L is the total length of the wedge, (to be defined later), and U_o is the uniform velocity of the fresh water at the tip of the wedge.

Incorporating the assumptions just discussed equations (6) and (7) become:

$$\frac{1-\beta}{\beta\alpha\lambda} n_1 \frac{d}{dx'}(n_1 + n_2) - \frac{(1-\beta)}{\lambda n_1^2} \frac{dn_1}{dx'} = -\tau' \qquad (10)$$

$$\frac{1}{\beta\alpha\lambda} n_2 \frac{d}{dx'}\left[(1-\beta) n_1 + n_2\right] = \tau' \qquad (11)$$

after putting

$$u_1' = \frac{1}{n_1} \qquad (12)$$

To determine the shear law we insert observed values of n_1, n_2, etc. in equations (10) and (11) and calculate τ'.

The values of τ' found in this manner for various positions along a given wedge and for various wedges are found to be somewhat erratic, but it appears that over the range of α and β covered by our experiments τ' can be taken as approximately constant, say equal to K. This says that the shear force at the interface varies from wedge to wedge as the square of the fresh water velocity at the tip and is approximately constant over a given wedge.

Now, recalling that u_1' is constant with depth, equations (10) to (12) can be converted into the following two non-linear equations for the two unknowns n_1 and n_2.

$$(1 - \beta)\, n_2\, (n_1^3 - \alpha)\, \frac{dn_1}{dx'} = - \lambda \alpha K n_1^2 \left[(1 - \beta)\, n_1 + n_2 \right] \qquad (13)$$

$$n_2 \frac{d}{dx'} \left[(1 - \beta)\, n_1 + n_2 \right] = \lambda \alpha \beta K \qquad (14)$$

To solve these we make use of the fact that β is very small (approximately 0.025) and develop n_1, n_2 in power series of β; i.e., we assume the following forms of solutions:

$$n_1 = n_{10} + \beta n_{11} + \beta^2 n_{12} + \ldots \qquad (15)$$

$$n_2 = n_{20} + \beta n_{21} + \beta^2 n_{22} + \ldots \qquad (16)$$

For small β we may hope that n_1, n_2 will be given sufficiently accurately by the first term of the power series.

Inserting the series into equations (13) and (14) and equating the coefficients of like powers of β we obtain as the equations to be satisfied by n_{10} and n_{20}:

$$n_{20}\, (n_{10}^3 - \alpha)\, \frac{dn_{10}}{dx'} = - \lambda \alpha K n_{10}^2\, (n_{10} + n_{20}) \qquad (17)$$

$$n_{20} \frac{d}{dx'} (n_{10} + n_{20}) = 0 \qquad (18)$$

If we take the origin x = 0 at the tip of the wedge, our boundary conditions are

$$n_{10}(0) = 1 , \qquad n_{20}(0) = 0 \tag{19}$$

Equation (18) gives

$$n_{10} = 1 - n_{20} \tag{20}$$

and then (17) becomes

$$n_{20}\left[(1 - n_{20})^3 - \alpha\right] \frac{dn_{20}}{dx'} = \lambda K \alpha (1 - n_{20})^2 \tag{21}$$

Equation (21) can be integrated to give

$$\lambda \alpha K x' = -\frac{1}{6} n_{20}^2 (3 - 2n_{20}) - \alpha \left[\frac{n_{20}}{1 - n_{20}} + \log (1 - n_{20})\right] \tag{22}$$

The left-hand side of equation (22) is $\alpha K \frac{x}{D_o}$. Hence, provided K can be found, and presuming α is given, equation (22) is an expression for the shape of the wedge. The value of K must be found by observing n_{20} for one or more experiments and calculating K from the equation (22) for these experiments.

So far we have no information concerning λ, the length of the wedge; in fact this length is not yet defined. In the experimental set-up the channel leads to a reservoir which represents the ocean and the transition section from channel to reservoir determines the location of the wedge. We therefore define the length of the wedge to be the distance from the wedge tip to the reservoir. Experimentally the slope of the interface is found to be very large near the tip, to decrease with increasing x and then to increase again as the reservoir is approached. It is also observed that $\frac{n_1^3}{\alpha}$, which equals $\frac{gD_1^3\beta}{q^2}$, approaches unity as one approaches the reservoir.

Equation (21) shows that the slope of the interface is infinite at the tip and again when $(1 - n_{20})^3 = \alpha$ or when

$$\frac{n_{10}^3}{\alpha} = 1. \qquad (23)^3$$

We cannot, of course, expect our equations to hold near these regions, but, in order to obtain an estimate of the length of the wedge we formally associate the point at which $\frac{n_{10}^3}{\alpha} = 1$ with the section of transition to the reservoir. Hence the depth of the wedge at the reservoir, say n_{20}^*, is given by

$$n_{20}(1) = n_{20}^* = 1 - \sqrt[3]{\alpha} \qquad (24)$$

Substituting $n_{20} = n_{20}^*$ and $x' = 1$ into equation (22), we obtain a formula for λ in terms of n_{20}^*:

$$\lambda K \alpha = \frac{1}{6}(n_{20}^*)^2 (3 - 2n_{20}^*) - \alpha \left[\frac{n_{20}^*}{1 - n_{20}^*} + \log (1 - n_{20}^*) \right] \qquad (25)$$

Equation (25) together with equation (24) provides an alternate method of finding K by measuring λ for one or more experiments.

A convenient method of comparison between theory and experiment is afforded by plotting $\frac{n_{20}}{n_{20}^*}$ against x'. The theoretical curves are found to be practically independent of α for all permissible values of α, i.e., for α ranging between zero and one. They are approximately given by

$$x' = \left(\frac{n_{20}}{n_{20}^*} \right)^2 \left(3 - 2 \frac{n_{20}}{n_{20}^*} \right) \qquad (26)$$

If one wishes to apply the theory to actual estuaries where the values of U_o and D_o differ drastically from those in the experimental set-up, it is necessary to first obtain a value of K from observation. Inasmuch as K is a kind of measure of the turbulent shear at the interface its value will be different for various estuaries and, of course, will be different from that in the experimental set-up. It may be hoped, however,

---

[3] For a separate discussion of this criterion at transitions see Stommel and Farmer, 1952.

that the value of K will remain reasonably constant for a given experimental set-up or estuary although U_o, D_o, β may vary.

EXPERIMENTATION

Figure 2 shows in outline form the experimental apparatus used in the salt wedge studies. The flume has plate glass side walls and a level bottom. The reservoir and flume are connected together through a six inch long elliptically shaped transition. The total depth of water in the reservoir and flume is controlled by the weir on the overflow side of the reservoir. The concrete reservoir, representing the ocean source in the apparatus, is constantly supplied with sea water. The salinity of the sea water remains at a satisfactorily constant 32 °/oo and the density is determined from its temperature and salinity. Fresh water is metered with a Rotometer before discharging into the upstream end of the flume. In order to vary the density difference of the two waters in the flume, sea water may be drawn from the concrete reservoir source, separately metered, and then mixed with the fresh water before discharging into the flume. The specific gravity of the fresh and salt water mixtures was taken by hydrometer, and these values were used as density. The wedge profiles were measured with point gauges, the level of the interface being taken in the troughs of the internal waves which were present at the interface.

A total of 45 different salt wedges was established in the flume, β being held a constant 0.025 for 27 runs, and in the remaining 18 it was varied from 0.0170 to 0.000684. A full account of the experimental data is given by Farmer, 1951.

DISCUSSION OF RESULTS

Figure 3 shows the approximate theoretical curve for the shape of the wedge as given by equation (26), as well as one set each of experimental data from the flume and observational results, Rhodes, 1950, from the Mississippi River South West Pass.

Figure 4 is a typical curve of dimensionless length $\lambda = \frac{L}{D_o}$ versus discharge q for a given density difference β and a fixed K and D_o, the values chosen being of the order of magnitude pertinent to the Mississippi River. The value K = .001 was determined for the salt wedge in South West Pass, D_o = 48 ft., q = 66 $ft^2/sec.$, L = 10 miles and β = .0196. D_o was taken as the total depth at the tip of the wedge.

Figure 5 shows the variation of λ with β for a fixed value of $\frac{U_o^2}{gD_o}$ and K.

Comparison of theory with experimental results based on K = 0.006 gives fairly good agreement for the interface shape. Theoretical predictions of the length of the wedges agree with experiment to within approximately 15%.

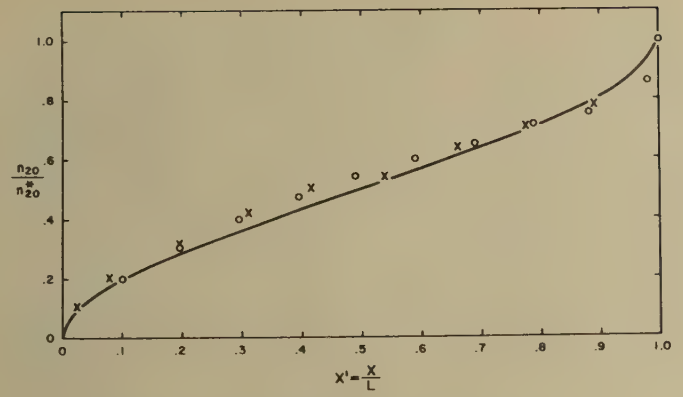

Fig. 3. Non-dimensional shape of salt wedge; the solid line is given by Equation (26), O's refer to Mississippi River South West Pass and x's refer to experimental run A-8.

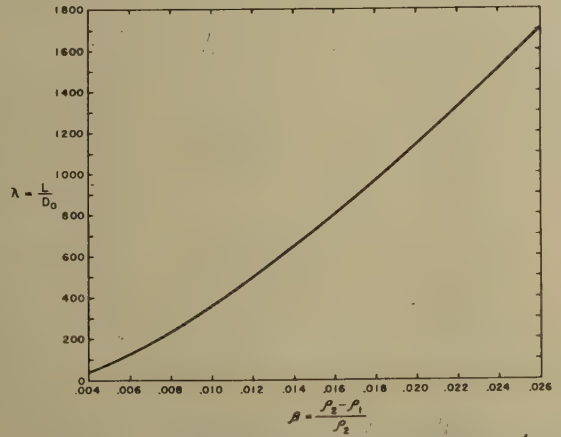

Fig. 5. Non-dimensional length L/D_o versus β. U_o^2/gD_o = .00125, K =.001.

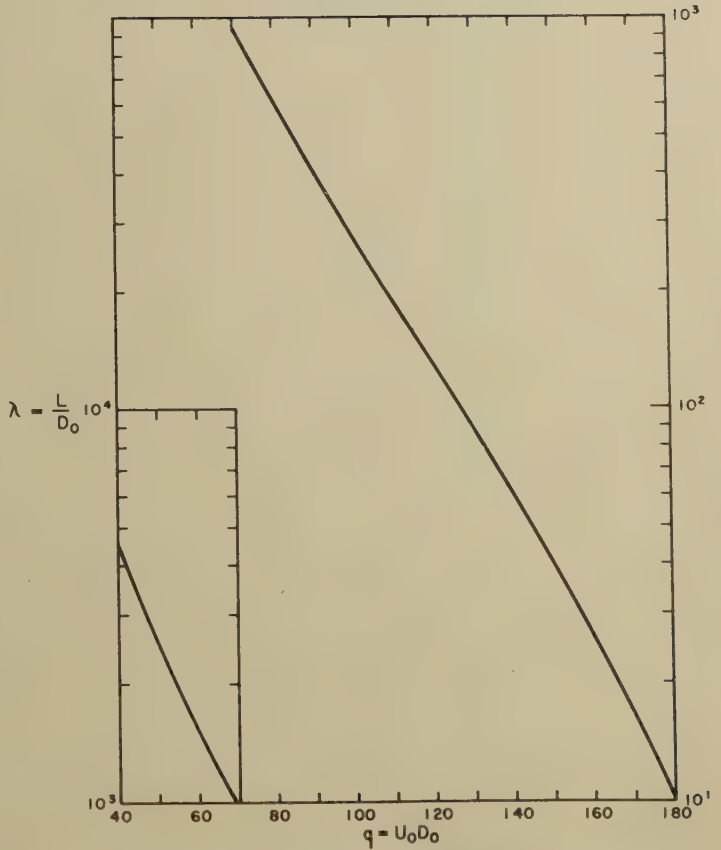

Fig. 4. Non-dimensional length L/D_o versus discharge per unit width q. D_o = 48 ft., β = .0196, and K = .001.

Observational data were limited to a few isolated curves for the Mississippi River. In this connection it must be pointed out that in the range of α encountered in the Mississippi the length, as predicted by theory, is very sensitive to slight changes in river depth D_o. Since the bottom is not horizontal, the question of what value of D_o to choose in attempting to apply the theory becomes a difficult one and will require further study.

REFERENCES

Farmer, Harlow G. (1951). An experimental study of salt wedges: Woods Hole Oceanographic Institution Technical Report, Reference No. 51-99, Manuscript Report to Office of Naval Research.

Rhodes, Ralph F. (1950). Effect of salinity on current velocities: Committee on Tidal Hydraulics, Report No. 1, Corps of Engineers, U. S. Army.

Stommel, Henry and Farmer, H. G. (1952). Abrupt change in width in two layer open channel flow: J. Mar. Res. XI (2), 205-214.

Contribution No. 639

A NOTE ON THE VELOCITY DISTRIBUTION AND BOTTOM STRESS IN A WIND-DRIVEN WATER CURRENT SYSTEM[1]

By

J. R. D. FRANCIS

ABSTRACT

The shear stress of the wind on a water surface is sometimes found by measuring the slope of the surface in a lake or wind tunnel. The stress on the bottom of the lake due to the return water current is an error term which has been variously estimated. An experimental method of determining the error is described, and the results indicate that it is but some 1½% of the wind stress.

One way of finding the aerodynamic stress of wind on a water surface τ_s is to observe the slope α of the surface along the direction of the wind. The wind causes both the slope and also a drift current towards the lee side in the upper layers of water; consequently, along the bottom of an enclosed lake or sea a return current exists which brings the water back again to the windward side and exerts on the bottom a shear stress τ_b. These two stresses act on the water in the same direction and are balanced by the hydrostatic force due to the rise in water level downwind. Thus, $\tau_s + \tau_b = g\rho\alpha h$, where h is the mean depth of water. It will be seen, therefore, that a measurement of α cannot alone be used to find τ_s, an important oceanographic quantity.

If it can be assumed that the flow throughout the water is laminar, the ratio τ_b/τ_s can be found by analytical methods. These are fully worked by Hellstrom (1941) and Keulegan (1951), where it is found that $\tau_b = 0.50\ \tau_s$. However, the water-flows in a lake or sea or even in a laboratory wind-wave tunnel are turbulent in all practical cases, and τ_b/τ_s may therefore be different from the laminar flow value. Hellstrom uses values of 0.15 to 0.80 depending on the depth of the water, and they are based on Boussinesq's theory for turbulent flow. Keulegan uses a purely arbitrary constant value of 0.25 for his wind tunnel experiments. Francis (1951), in some wind tunnel experiments of a similar nature, took measurements of the mean velocity of the return water current, and by applying the usual drag formula $\tau_b = c\rho u^2$ (u = water speed, c = drag coefficient), he found that τ_b never exceeded 3% of τ_s. In this last case, a conservatively high value of c

[1] Contribution No. 639 from the Woods Hole Oceanographic Institution.

Reprint from SEARS FOUND JOURN MAR. RES.

was used in order to allow empirically for the oscillatory motion imposed by the wind-generated surface waves on the much slower mean velocity. It was thought that the turbulence added by the oscillations might increase the drag.

An attempt was made to measure τ_b directly in the small wind-wave tunnel mentioned above while the water currents were being wholly generated by wind. A flat smooth plate was arranged just to float

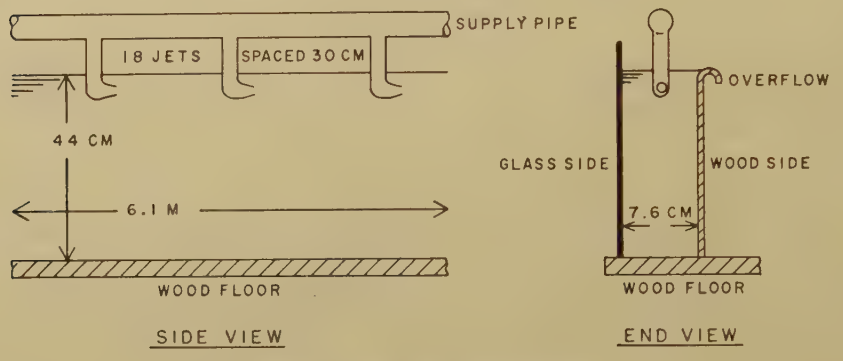

Figure 1. Tank used in experiments.

in the surface of a pool of heavy fluid at the bottom of the tunnel. The plate was constrained by a spring system so that the shear stress on the plate could be measured by its deflection. The experiment was a failure because the wave motions caused the plate to oscillate badly; not even a mean position could be determined. Better success has now been achieved with another experimental technique which uses horizontal jets of water to apply to the water surface the momentum that was applied before by the wind. This artifice ensures a surface without waves and water-flows in the tank that are noticeably steadier. The total amount of water in the tank is kept constant by a uniform overflow all along the top of one side of the tank; thus the jets add momentum but not mass to the water already there. Below the upper few centimetres there is no motion caused by the water overflow. A slight correction is made because of the finite size of the jets, since the momentum is really applied to a thin layer at the surface, making the effective surface for shear somewhat below the actual surface.

Fig. 1 shows the tank, which is 6.1 m long, 12.7 cm wide, and 44 cm deep from bottom to overflow. Eighteen jets, spaced 30 cm apart, were supplied with sea water through a 5 cm pipe parallel to the tank length and above the water level. The jet outlets, just in the surface of the water, were of an oval, flattened shape, the total cross-sectional

area of all the jets being 10.7 cm². The shear stress measuring-device is shown in Fig. 2. Its design is based upon the equipment used by Sheppard (1946) for measuring stress in the atmosphere. The circular moving plate is brass, 7.6 cm in diameter, and is of an inverted dish shape. It floats on carbon tetrachloride (density 1.70 gm cm^{-3}) in a shallow dish with only 5 mm clearance all round. A piece of small

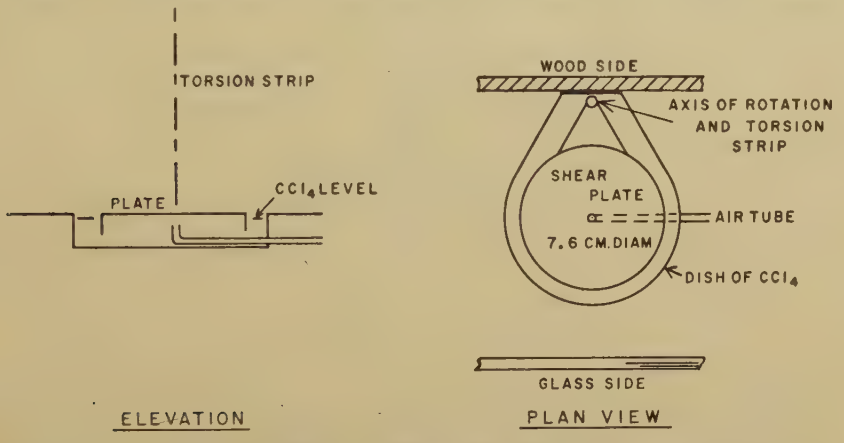

Figure 2. Detail of shear plate.

bore tube allows air to be blown into the underside of the plate so that its buoyancy may be adjusted with some precision to place the top of the plate, the surface of the CCl_4, and the top of the circumscribing dish all in one plane. A false floor 1.2 cm thick is laid in the tank so that the apparatus does not project into the flow. The plate is pivoted on a vertical axis at the side of the tank; and the spring restraint is a vertical torsion strip 2.1 mm by 0.3 mm by 17 cm long. It is clamped at its upper end clear of the water, with an adjustment for the no-load position of the plate. The position of the plate is observed by a travelling telescope (cathetometer) which views a mark on the periphery through the glass side of the tank. The torsion constant of the apparatus was measured by putting weights in a paper pan on a fine cotton thread attached to the plate; the resulting calibration was linear, with negligible scatter for load increasing and decreasing.

The jet discharge Q through the total orifice area a was calibrated against the pressure in the supply pipe by collecting the water in a large tank. The momentum supplied by the jets per second (the available thrust force) is therefore $\rho Q^2/a$. Not all of this is available for driving the water currents; some of it is counterbalanced by the backward thrust of the further end of the tank where the high velocity

stream strikes; some of it is counterbalanced by the thrust of the water on the backs of the jet pipes which must project into the fast surface stream; and some is counterbalanced by the shear stress of the fast upper stream on the sides of the tank. The last correction is necessary only because of the limited width of the tank in the shallow zone where there are fast velocities solely due to the dispersing jets. Below a depth of about 12 cm the velocities are low and the stresses on the

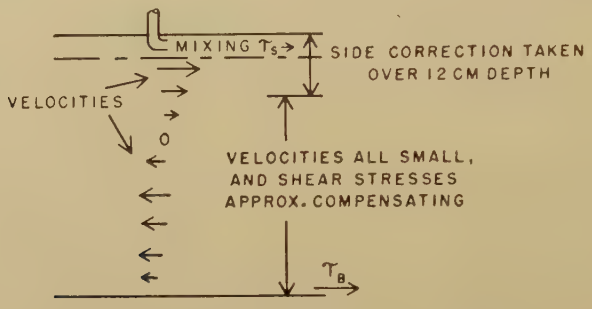

Figure 3. Position of hanging side correction plate.

sides caused by the forward velocity must nearly balance the stress in the opposite direction caused by the backward return current below (see Fig. 3). The correction terms were all measured directly, the first by placing a false flat end plate on a pendulum and measuring the deflection; the second by mounting a jet pipe on a pendulum and immersing to the appropriate depth; and the third by suspending similarly a smooth flat plate 90 cm long and 12 cm deep parallel to, and 0.4 cm away from, the glass side of the tank.

The observations for two different water-flows are summarized below.

Table of Forces on Water in Tank of Plan Area 7720 cm²

Q Water flow ($cm^3 . sec^{-1}$)	$\rho Q^2/a$ Input by jets (dynes × 10^3)	Corrections (dynes × 10^3) End	Side	Jets	Net input force (dynes × 10^3)	Net τ_s (dynes. cm^{-2})	Measured τ_b (dynes. cm^{-2})	τ_b/τ_s (%)
2230	480	98	72	54	256	33.1	0.46	1.4
2900	800	173	98	82	447	57.9	0.77	1.3

τ_b is the average of measurements at two places on the floor of the tank.

There was still a little oscillation of the shear plate, due presumably to large scale turbulence in the tank, but the mean deflection of the plate could be easily estimated. Lower jet speeds, however, gave such small deflections of the plate that the results are not significant. It will be seen that the bottom stress is small compared with the top

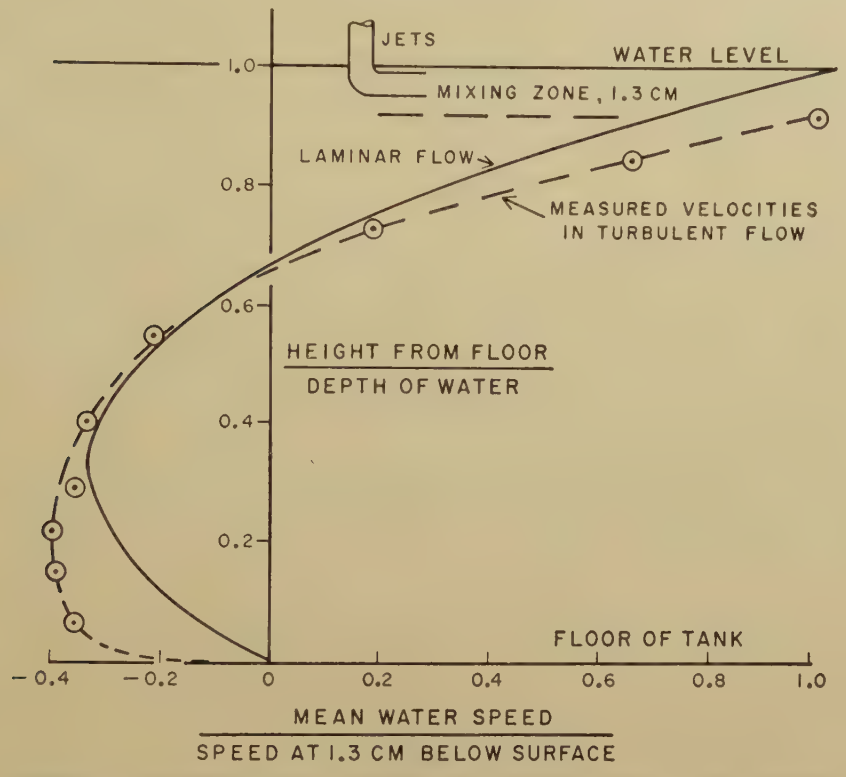

Figure 4. Comparison between theoretical and measured velocity profiles (measured velocity at 1.3 cm below surface = 26.3 cm sec^{-1}).

stress and can be neglected in most cases, for in practice the measurement of slope α is fraught with errors that are greater than this correction.

Velocity profile. The distribution of mean velocity was determined at one jet speed by a total head tube traversed on the centreline of the tank. The static pressure was taken at a tapping in the side of the tank in the plane of the traverse. The pressures were measured by a micrometer point in a glass stilling well.

The profile is shown in Fig. 4 together with the parabolic one for laminar flow. Both profiles are defined by nondimensional parameters, the reference velocity being that at 1.3 cm below the water surface. A reference velocity at or nearer the surface would be atypical of the drift system as a whole, for the occasional high speed jet gives a very nonuniform flow there. It will be seen that the two

profiles have a strong family likeness, the height of zero velocity being nearly the same. In the lower (return) current, however, the measured profile is a flatter one which gives larger gradients near the bottom.

The experimental work described above was done while I was holding a fellowship at, and granted by, the Woods Hole Oceanographic Institution.

REFERENCES

Francis, J. R. D.
1951. The aerodynamic drag of a free water surface. Proc. roy. Soc. London, (A) *206:* 387–406.

Hellstrom, B.
1941. Wind effects on lakes and rivers. Ingen. Vetensk. Akad. Handl., No. 158.

Keulegan, G. H.
1951. Wind tides in small closed channels. J. Res. Nat. Bur. Stand., Wash., *46:* 358–381.

Sheppard, P. A.
1946. The aerodynamic drag of the earth's surface and the value of von Karman's constant in the lower atmosphere. Proc. roy. Soc. London, (A) *188:* 208–222.

Contribution No. 640

Reprinted from Sewage and Industrial Wastes, Vol. 25, No. 9, September, 1953
Printed in U. S. A.

COMPUTATION OF POLLUTION IN A VERTICALLY MIXED ESTUARY *

By Henry Stommel

Woods Hole Oceanographic Institution, Woods Hole, Mass.

Papers recently published by Ketchum (1) and Arons and Stommel (2) have presumed to give a theoretical account of the distribution of fresh water in an estuary. Pritchard (3), however, justly has pointed out that these treatments are at best applicable only to estuaries so intensely tidally mixed that they exhibit no vertical stratification. In such cases the salt is carried upstream against the main river flow by turbulence. Ketchum proposed a mixing process, which he called "exchange ratio," and was able to compute the salinity distribution in the Raritan. Using the published data (4) on the Severn estuary, the author and Harlow G. Farmer found that the method of the "exchange ratio" gave a grossly incorrect salinity distribution. Inasmuch as the Severn is unstratified, and appears to fit all the requirements of Ketchum's analysis, it is quite clear that the method of the exchange ratio is not nearly so general as was proposed.

The method of Arons and Stommel (2) is open to similar objections. The Severn salinities can be plotted on the family of curves given in that paper, but it is found that the mixing length is of the order of magnitude of the depth, or about 1/1000th of the tidal excursion. This discrepancy suggests that, at least so far as the Severn is concerned, the hypothesis about the mixing length made by Arons and Stommel does not hold in general. In short, it does not appear likely that any good purpose can be served at present by making *a priori* suppositions about the turbulent mixing process. From a practical point of view the proper procedure is to use the distribution of river water as a means of discovering the magnitude of the turbulent diffusion coefficients at various places in the estuary, and to devise a method using these coefficients which will yield the dilution of pollution at any point in the estuary. An attempt at such a method is described in the following. It is important to re-emphasize that it is intended to apply only to vertically unstratified estuaries in which the mixing is due to tides.

Steady-State Equations

In considering an estuary such as that shown in Figure 1, it is assumed that the x-axis is directed along the axis of the channel; also that the cross-sectional area, $S(x)$, may vary with the position along the axis.

Now it is supposed that a pollutant, which is miscible with water, whose average (over a tide) concentration, $c(x)$, varies with x, is in a steady-state distribution in the estuary. By the term "steady state" is meant that the average of the concentration c over a tidal cycle does not change from tide to tide. This will be true if there has been little change in the river discharge during the time involved, and the discharge of pollutant into the estuary has remained constant. If the total river discharge into the estuary, at some point remote in the $-x$ direction, is Q, then the flux of pollutant by advection toward the sea is $Q\,c$.

* Contribution No. 640 from the Woods Hole Oceanographic Institution.

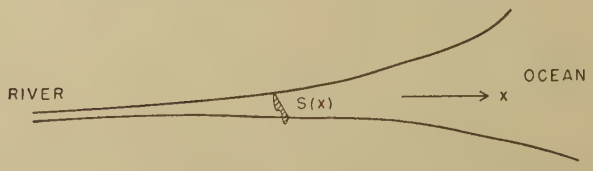

FIGURE 1.—Basic dimensions for estuary computations.

In addition, there is a turbulent flux due to the tidally-produced turbulence in the estuary. This turbulent flux may be written in the customary fashion; that is, $-SA\,dc/dx$, where $A(x)$ is a turbulent eddy diffusivity, the value of which must be determined before the distribution of the pollutant can be calculated. Contrary to the methods of Ketchum (1) and of Arons and Stommel (2), A is not specified *a priori*.

The net seaward flux, $F(x)$, of pollutant across any section is the sum of these two fluxes; that is,

$$F(x) = Qc - SA\frac{dc}{dx} \qquad (1)$$

If the pollutant is conservative (does not decay with time), the net flux, $F(x)$, must be constant downstream of the source of pollutant, and must be zero upstream of it. Some important pollutants, such as bacterial and atomic pile wastes, are not conservative, and their concentrations decay even when not subject to the dispersing influence of the estuary.

The concentration of such a non-conservative pollutant in an isolated container, may decrease with time according to the exponential decay law—

$$c = c_0 e^{-t/\tau} \qquad (2)$$

—in which τ is the time required for the concentration to decay from the concentration c_0 to c_0/e. The time, τ, is slightly larger than the half-life of the pollutant, or

$$0.693\tau = \text{(half-life)}$$

The net flux, $F(x)$, cannot be the same for all values of x if the pollutant is non-conservative, but must diminish in the following manner:

$$\frac{d}{dx}F(x) = -\frac{S}{\tau}c \qquad (3)$$

The steady-state equation (Eq. 1) may be written in the form

$$\frac{d}{dx}\left[Qc - SA\frac{dc}{dx}\right] + \frac{S}{\tau}c = 0 \qquad (4)$$

or

$$\frac{d}{dx}\left[Qc - SA\frac{dc}{dx}\right] + \frac{S}{\tau} = \psi \quad \text{at outfall} \qquad (4a)$$

where ψ is the total rate of pollutant supply at the outfall.

For a given pollutant and given estuary it is evident that the quantities Q, S, and τ are known. If A can be determined, then the distribution of $c(x)$ should be easily calculated.

Determination of the Eddy Diffusivity

The eddy diffusivity, A, may be computed from a knowledge of the concentration of any other property in the estuary. The concentration of fresh water, $f(x)$, is a convenient conservative property. In some estuaries where ground water, or precipitation, or evaporation, is important, it might be almost impossible to use the concentration of fresh water as a means of computing A. Let it be supposed for the immediate purpose that all the fresh water comes from one river, and that little is added or subtracted by other means. How to treat more complicated cases will be evident when the principles for this simple case are understood.

If the concentration of fresh water, f, is written for c in Eq. 1, the equation

takes the following form because in this case $F(x) = Q$:

$$A = \frac{Q(f-1)}{S\,df/dx} \qquad (5)$$

The concentration of fresh water, f, is dimensionless (for example, pure fresh water is represented by 1.0; a mixture of one part fresh water and three parts sea water, is given by $f = 0.25$, etc.) The river discharge, Q, is in cubic feet per second; the cross-sectional area, in square feet; and distance in the x direction, in feet. The dimensions of the eddy diffusivity A are, therefore, in square feet per second.

The easiest way to compute A is to segment the estuary along its axis, the intervals being equally spaced a feet apart (Figure 2).

The average value of f is indicated at each segment. Eq. 5 may now be written in finite difference form for numerical computation:

$$A_n = \frac{Q2a(1-f_n)}{S_n(f_{n-1}-f_{n+1})} \qquad (6)$$

In general, f_n is less than unity, and f_{n+1} is less than f_{n-1}, so that A_n is expected to be positive. The values of A_n at points far upstream (where $f_n \to 1$ and $f_{n-1} \to f_{n+1}$), are indeterminate from the fresh-water distribution; this is also true beyond the mouth of the estuary in the ocean.

Calculation of the Concentration of Pollutant

Eq. 4 is written in finite difference form and the various coefficients gathered together, as follows:

$$P_n c_{n-1} + Q_n c_n + R_n c_{n+1} = 0 \qquad (7)$$

in which

$$P_n = -\frac{1}{2a}\left[Q - \left(\frac{A_{n+1}S_{n+1} - A_{n-1}S_{n-1}}{2a}\right)\right] - \frac{A_n S_n}{a^2}$$

$$Q_n = \frac{2A_n S_n}{a^2} + \frac{S_n}{\tau}$$

$$R_n = \frac{1}{2a}\left[Q - \left(\frac{A_{n+1}S_{n+1} - A_{n-1}S_{n-1}}{2a}\right)\right] - \frac{A_n S_n}{a^2}$$

Eq. 7 must hold at each of the segments, with one exception. In addition, there are certain additional constraints. At the ocean, where $f = 0$, the value of $c = 0$; also, far upstream $c = 0$. At the segment where the outfall of the pollutant is located one further condition is imposed: the difference in flux upstream and downstream must be equal to the total rate of input of pollutant ψ. The segment at which the source (outfall) of pollutant is nearest may be designated as $n = s$.

In place of Eq. 7, which holds at all points except at $n = s$, the equation at $n = s$ becomes

$$P_s c_{s-1} + Q_s c_s + R_s c_{s+1} = \frac{\psi}{2a} \qquad (7a)$$

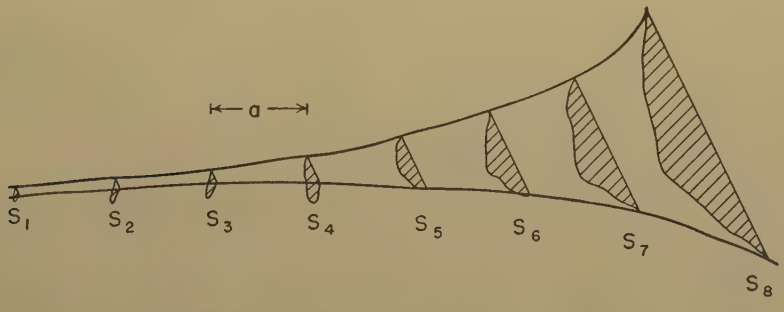

FIGURE 2.—Segmentation of estuary for computation of the eddy diffusivity.

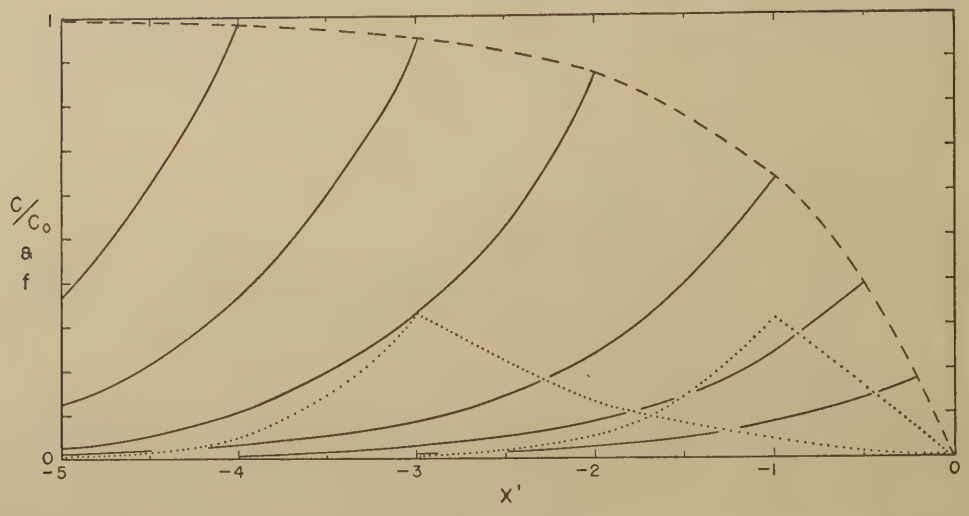

FIGURE 3.—Plot of computation results for estuary of uniform section.

The equations having been obtained, the solution is easily carried through by relaxation methods.

Simple Example, Estuary of Uniform Section

Before proceeding with a numerical example, it may be of interest to consider a simple example to illustrate certain fundamental properties of the problem. An example is chosen which admits an analytical solution.

Consider an estuary of uniform cross section, S, which opens abruptly into the sea at $x = 0$. If the eddy diffusivity, A, is a constant, then the concentration of fresh water has a very simple analytical form:

$$f = 1 - e^{x'} \tag{8}$$

in which

$$x' = \frac{Q}{AS}x$$

The water is entirely fresh far upstream ($f = 1$), but diminishes to $f = 0$ at the mouth, as shown by the dashed line in Figure 3. In this graph the distance along the estuary is plotted in dimensionless units, x', the value being negative within the estuary.

Now consider the concentration of pollutant due to an outfall at $x = L$. The analytical solution of Eq. 4 is composed of two separate parts:

$c_1(x)$ applies upstream of the outfall;
$c_2(x)$ applies downstream of the outfall;

and

$$\frac{c_1(x)}{c(L)} = e^{k_1(x'-L')} \tag{9}$$

$$\frac{c_2(x)}{c(L)} = \frac{e^{k_2x'} - e^{k_1x'}}{e^{k_2L'} - e^{k_1L'}} \tag{9a}$$

in which

$$c(L) = c_0(e^{k_2L'} - e^{k_1L'}),$$
$$k_1 = \tfrac{1}{2}(1 + \sqrt{1 + Z}),$$
$$k_2 = \tfrac{1}{2}(1 - \sqrt{1 + Z}),$$
$$Z = 4AS^2/(\tau Q^2),$$

and

$$c_0 = \psi/Q, \quad L' = \frac{Q}{AS}L$$

The quantity c_0 is the concentration of pollution which would result at the outfall if there were no diffusion or decay; in other words, the simple dilution by river flow alone.

Figure 3 displays certain of these solutions. The abscissa is expressed in a dimensionless fashion. The ocean is located at the extreme right-hand side. Toward the left is the upstream direction. The dashed line is the solu-

tion of Eq. 8 for the concentration of fresh river water, f. The solutions of the problem of the distribution of a conservative pollutant introduced at $x' = -4, -3, -2, -1, -0.5$, and -0.2 are shown as solid black curves, terminating at the dashed curve at each of the outfall locations respectively. The remainder of the solution (downstream of the outfall) falls along the dashed line. The peak concentration is at the outfall. It is immediately clear, then, in this simple case of an estuary of uniform cross-section and eddy-diffusivity, that the pollution extends far upstream of the outfall, no matter what the location of the outfall, but that the concentration is everywhere reduced upstream of the outfall if the location of the outfall is moved toward the sea.

A seaward displacement of the outfall also reduces the peak concentration at the outfall, but downstream the concentration of a conservative pollutant is not affected by such a displacement.

The dotted curves in Figure 3 represent solutions for a non-conservative pollutant whose decay time is

$$\tau = AS^2/(2Q^2)$$

for outfall locations at $x' = -3$ and -1. The remarkable feature of these curves is that the peak concentration, even at the outfalls, is much reduced from what it is in the case of the conservative pollutant. The general equation for the peak concentration is

$$\frac{c(L)}{c_0} = \frac{1}{\sqrt{1+Z}}\left(1 - e^{L'\sqrt{1+Z}}\right) \quad (10)$$

The non-conservative pollutant extends both upstream and downstream of the outfall, but, unlike the conservative

TABLE I.—Numerical Example of Pollution Computation

n	S_n (1,000 sq.ft.)	f_n	A_n sq. ft./sec.	P_n	Q_n	R_n	c_n*	X_n	c (lb./cu.ft. $\times 10^4$)
0	7.7	1.000	—	—	—	—	—	—	—
1	7.7	1.000	—	—	—	—	—	—	—
2	8.9	0.929	180	—	—	—	—	—	—
3	8.2	0.840	280	−0.147	0.062	0.100	—	—	—
4	12.8	0.679	290	−0.134	0.099	0.080	—	—	—
5	15.4	0.536	500	−0.182	0.184	0.029	—	—	—
6	14.0	0.465	960	−0.237	0.296	−0.032	0	—	0
7	18.0	0.393	1,040	−0.282	0.410	−0.191	1	0.0	0.05
8	27.3	0.350	1,000	−0.377	0.601	−0.169	2	+0.1	0.1
9	75.0	0.308	390	−0.419	0.735	−0.166	4	−0.1	0.2
10	102.0	0.265	280	−0.384	0.781	−0.192	13	0.0	0.6
11	84.0	0.215	510	−0.464	1.024	−0.393	44	+0.7	2.2
12	117.0	0.200	570	−0.793	1.567	−0.533	100	+95.9	5.0
13	151.0	0.172	270	−0.496	1.123	−0.236	48	−0.4	2.4
14	254.0	0.125	192	−0.572	1.487	−0.406	21	−0.4	1.1
15	285.0	0.108	210	−0.656	1.767	−0.541	8	0.0	0.4
16	410.0	0.072	190	−0.274	2.378	−1.283	1.5	—	0.07
17	424.0	0.065	740	−2.714	7.123	−3.560	0.7	—	0.03
18	525.0	0.061	570	−2.937	7.035	−2.676	0.5	—	0.02
19	855.0	0.059	280	−2.468	6.498	−2.321	—	—	—
20	1,091.0	0.046	295	−3.147	8.618	−3.290	—	—	—
21	1,372.0	0.043	234	−3.139	9.168	−2.879	—	—	—
22	1,268.0	0.036	190	−2.218	7.357	−1.958	—	—	—
23	1,748.0	0.029	110	−1.942	7.341	−1.682	—	—	—
24	2,070.0	0.018	95	−2.078	8.073	−1.855	—	—	—
25	2,496.0	0.011	80	—	—	—	—	—	—
26	2,915.0	0.000	—	—	—	—	—	—	—

* Arbitrary units.

pollutant, can be reduced at a point below the outfall by an upstream displacement of the outfall.*

Consideration of this simple case also shows clearly the effect of a change in the river discharge, Q. Increase of river discharge increases the fresh-water concentration at every position, foreshortens the extent of pollution upstream, reduces the peak concentration of pollution at the outfall, and even reduces the concentration of a conservative pollutant downstream.

Numerical Example

As an example of computation of concentration of pollution by numerical methods, a particular distribution is computed for the Severn estuary, for which good salinity data are available (4). Stations are chosen beginning at Gloucester ($n = 0$); the sections are spaced about 2 mi. apart ($a = 10{,}000$ ft). Cross-section areas are given in Table I, in the column headed S_n. The fresh-water concentration, f_n, from actual summertime survey data, is also tabulated.

The eddy diffusivity, A_n, is computed at each station by Eq. 6, using a value of $Q = 360$ cu. ft. per sec. as the fresh-water discharge during the summer dry period. It is interesting to note that the highest values of A_n occur at Stations 6, 7, and 8, which happen to be the location of the Severn bore.

Suppose now that a pollutant outfall is located at Sharpness ($n = 12$), and that this pollutant has a half-life of 4 days ($\tau = 5 \times 10^5$ sec.) The coefficients P_n, Q_n, and R_n of Eq. 7 are tabulated in Table I. An estimated distribution of pollutant is initially entered into Table I, and the sum $\bar{X}_n$ (called the residual) is formed:

$$P_n c_{n-1} + Q_n c_n + R_n c_{n+1} = \bar{X}_n \quad (11)$$

Eq. 7 requires that all residuals except that at the outfall should vanish. In fact, it is seen that this is far from true for the estimated pollution distribution. The values of c_n can be adjusted by successive steps (relaxation method) because it is obvious that if Δc_n units are added to any c_n, not only will the residual $\bar{X}_n$ be changed by the addition of $Q_n \Delta c_n$, but also the residual $\bar{X}_{n+1}$ will be increased by $P_{n+1} \Delta c_n$ and the residual $\bar{X}_{n-1}$ by $R_{n-1} \Delta c_n$. These adjustments are made step by step, removing the worst residuals first, and from time to time recomputing the residuals from the newly adjusted c_n by Eq. 11. When the residuals have all been reduced to a point where further readjustments of c_n are below the precision of the required result (say 1 to 5 per cent), the relaxation procedure may be regarded as completed: namely, a set of values of c_n has been obtained which satisfy Eq. 7. In the example shown, 54 adjustments of c_n were necessary in all. The computation took about 3 hr. Arbitrary units have been used for c_n, which must now be converted to units of actual pollution concentration. If it be supposed that the discharge of pollutant at Station 12 is 10 lb. per sec., the concentration due to dilution by a river flow of 360 cu. ft. per sec. alone (if there were no diffusion or decay) would be 28×10^{-3} lb. per cubic foot.

The value of $\bar{\psi}$ (= 10 lb. per sec.) is put into Eq. 7*a*. Then $\bar{\psi}/2a$ should be equal to the residual, $\bar{X}_s$. If all the concentrations in arbitrary units are multiplied by 5×10^{-6}, the value of $\bar{X}_s$ comes out properly. The values of the concentration of pollution thus computed are shown in the last column of Table I.

Acknowledgment

The work reported herein was supported by funds made available by the

* In commenting on the manuscript of this paper, A. C. Redfield pointed out to the author that some of these conclusions have already been deduced numerically for the special case of the Raritan River. These results were obtained using Ketchum's analysis in the course of consultation over the placement of the outfall sewer, but were not published.

Office of Naval Research under contract No. N6onr-27701(NR-083-004).

References

1. Ketchum, B. H., "The Flushing of Tidal Estuaries." THIS JOURNAL, 23, 2, 198 (Feb., 1951).
2. Arons, A. B., and Stommel, H., "A Mixing-Length Theory of Tidal Flushing." *Trans. Amer. Geophysical Union*, 32, 419 (1951).
3. Pritchard, D., "Estuarine Hydrography." Recent Advances in Geophysics, 1 (1952).
4. Bassindale, R., "Studies on the Biology of the Bristol Channel. II. The Physical Environment and Intertidal Fauna of the Southern Shores of the Bristol Channel and Severn Estuary." *Jour. Ecology*, 31, 1 (1943).

Contribution No. 641

PLEISTOCENE CLIMATIC RECORD IN A PACIFIC OCEAN CORE SAMPLE

JACK L. HOUGH

Reprinted for private circulation from
THE JOURNAL OF GEOLOGY
Vol. 61, No. 3, May 1953
PRINTED IN U.S.A.

PLEISTOCENE CLIMATIC RECORD IN A PACIFIC OCEAN CORE SAMPLE[1]

JACK L. HOUGH
University of Illinois

ABSTRACT

A core sample of the bottom in the southeastern Pacific Ocean contains several layers of red clay and globigerina ooze. The highly calcareous ooze is correlated with warm-water conditions, whereas the red clay, which is low in carbonate, is correlated with cold-water conditions because the carbonate is more soluble in cold water. The core is interpreted as a record of climate. Age determinations made by W. D. Urry, using the "percentage of equilibrium method" for uranium, ionium, and radium give dates for the various layers covering a period of several hundred thousand years.

The detailed interpretation of this core gives dates for the end of the Kansan glacial stage (about 700,000 years ago), for three substages of the Illinoian glacial stage (330,000; 310,000; and 274,000 years ago), for six substages of the Wisconsin glacial stage (64,000; 51,000; 37,000; 26,000; 15,000; and 11,000 years ago), and for a postglacial thermal maximum centering at 6,000 years ago. There is good correlation between the Pacific red-clay (cold-water) zones of Wisconsin age and the North Atlantic and Antarctic glacial marine zones of the same age.

INTRODUCTION

Two core samples were taken by the writer in the southeastern Pacific Ocean during "Operation Highjump," the United States Navy Antarctic Expedition of 1946–1947. The sediment of these cores has been dated by W. D. Urry, so that a time scale in years is available for use with the lithologic logs of the samples. Several hundred thousand years are represented by this sediment. One of the samples, numbered N-1, contains several layers of red clay and of globigerina ooze and is, therefore, of interest as a possible record of climatic fluctuations in a considerable part of the Pleistocene epoch. This core is the principal subject of this paper. The other core, N-2, consists of red clay throughout and thus presents no evidence of changing conditions of deposition.

The locations from which the cores were taken are shown in figure 1. Core N-1 was taken at lat. 08°56′.2 S., long. 92°05′.2 W., from a depth of 3,930 meters (12,900 feet). The length of the core is 194 cm. and, according to Urry's estimate, it is 990,000 years old at its bottom end. Core N-2 was taken at lat. 32°21′.0 S., long. 105°55′.0 W., from a depth of 3,620 meters (11,880 feet). The length of the core is 138 cm., and it is 1,231,000 years old at its bottom end according to Urry's estimate.

The core samples were collected with an apparatus which was designed by the writer and constructed in the shops of the Woods Hole Oceanographic Institution. The core barrel of the apparatus carried a transparent plastic liner which receives the core. When the apparatus is brought on deck after a sample is obtained, the water above the core is poured off carefully to minimize the loss of poorly compacted sediment at the top of the core, the liner containing the core is removed from the apparatus, sawed off just above the core, and both ends of the liner are stoppered and sealed.

[1] Contribution No. 641, Woods Hole Oceanographic Institution. Manuscript received August 14, 1952.

FIG. 1.—Map showing locations of core samples N-1 and N-2, and the Peru current of the southeastern Pacific Ocean.

METHODS OF STUDY

The cores were opened in the laboratory, at the Carnegie Institution of Washington, by splitting liner and core into halves parallel to their long axis. Dr. W. D. Urry then removed samples from various points in half of each core, for use in making age determinations. The points sampled in core N-1 are indicated in figure 2. The age determinations were made by the per cent of equilibrium method for uranium, ionium, and radium, described by Urry in 1942. Urry's results on these cores have been published (1949), and, in addition, detailed time-depth curves were sent to the writer (personal communication, 1948).

A photograph was taken, and a lithologic log of core N-1 was made, immediately after it was opened, before any appreciable shrinkage or color change had taken place. These, supplemented by later examination with a binocular microscope, examination of the material after drying, and a few determinations of acid-soluble content at random points in the core were used in constructing the final log of the core shown in figure 2. The red clay, when still wet, was chocolate-brown in color where its carbonate content was lowest, whereas the purest globigerina ooze was chalky white. Various shades between chocolate-brown and white represented mixtures of red clay and globigerina ooze.

Foraminifera are abundant in the lighter-colored portions of the core and are very rare in the darker portions. A study of the Foraminifera was planned but not carried out, and the writer has decided to present the lithologic log and its time scale without waiting longer for the biological data.

PRESENTATION OF DATA

Figure 2 shows a log of core sample N-1, drawn to correct depth scale and reduced. Black color on this log represents the purest red clay with no appreciable carbonate content, white represents the purest globigerina ooze with no appreciable clay content, and the patterns of black lines represent various proportions of red clay in relation to the amount of black in the pattern. Figure 2 shows, in addition, the points sampled by Urry for age determination, the age in years at each lithologic boundary as interpolated from Urry's time-depth curve for the core, and, finally, an interpretation of the possible climatic significance of the core. The interpretation will be discussed below.

Figure 3 presents portions of the log of core N-1 and logs of other dated cores, from the North Atlantic Ocean (Bramlette and Bradley, 1940; Piggot and Urry, 1942) and from the Ross Sea, Antarctica (Hough, 1950), all drawn on the same time scale, for comparison.

EVALUATION OF DATA

The first assumption made in interpreting the log of core N-1 is that the red clay was deposited during periods of colder climate and that the globigerina ooze may be attributed to periods of warmer climate. This assumption is discussed more fully by Kuenen (1950, p. 369) and apparently is generally quite acceptable for application to any deep-sea bottom having stratified red clay and globigerina ooze.

Core N-1 was collected from a point on the sea bottom which for two reasons may be expected to be sensitive to changes in climate. One reason is that the depth is intermediate between the normal depths for accumulation of red clay and globigerina ooze, respectively. A review of the bottom information at 66 stations in the southeastern Pacific Ocean shows that only red clay occurs below 4,100 meters, whereas only glo-

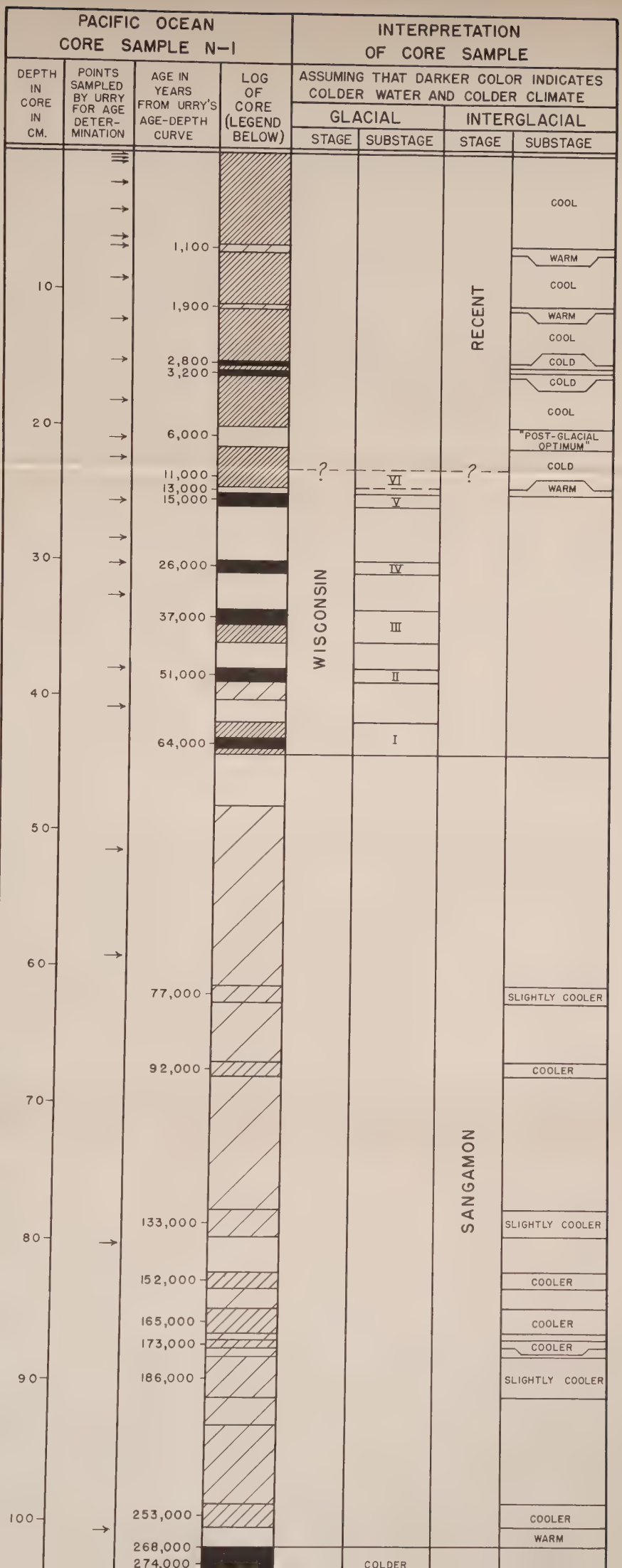
PACIFIC OCEAN
CORE SAMPLE N-I
INTERPRETATION
OF CORE SAMPLE
ASSUMING THAT DARKER COLOR INDICATES
COLDER WATER AND COLDER CLIMATE
DEPTH IN CORE IN CM.
POINTS SAMPLED BY URRY FOR AGE DETER-MINATION
AGE IN YEARS FROM URRY'S AGE-DEPTH CURVE
LOG OF CORE (LEGEND BELOW)
GLACIAL
INTERGLACIAL
STAGE
SUBSTAGE
STAGE
SUBSTAGE
1,100
1,900
2,800
3,200
6,000
11,000
13,000
15,000
26,000
37,000
51,000
64,000
77,000
92,000
133,000
152,000
165,000
173,000
186,000
253,000
268,000
274,000
10
20
30
40
50
60
70
80
90
100
WISCONSIN
VI
V
IV
III
II
I
RECENT
SANGAMON
COOL
WARM
COOL
WARM
COOL
COLD
COLD
COOL
"POST-GLACIAL OPTIMUM"
COLD
WARM
SLIGHTLY COOLER
COOLER
SLIGHTLY COOLER
COOLER
COOLER
COOLER
SLIGHTLY COOLER
COOLER
WARM
COLDER

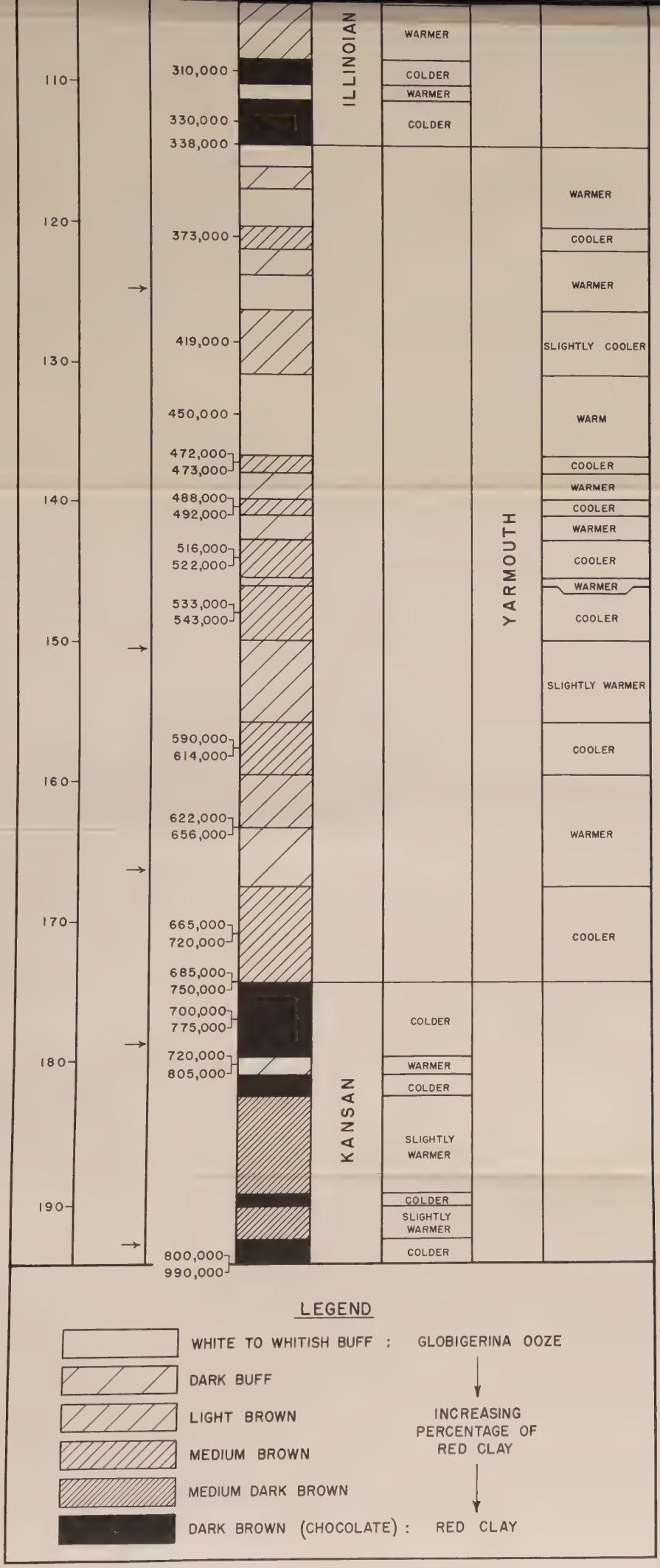

FIG. 2.—Log of core N-1, and interpretation of the log

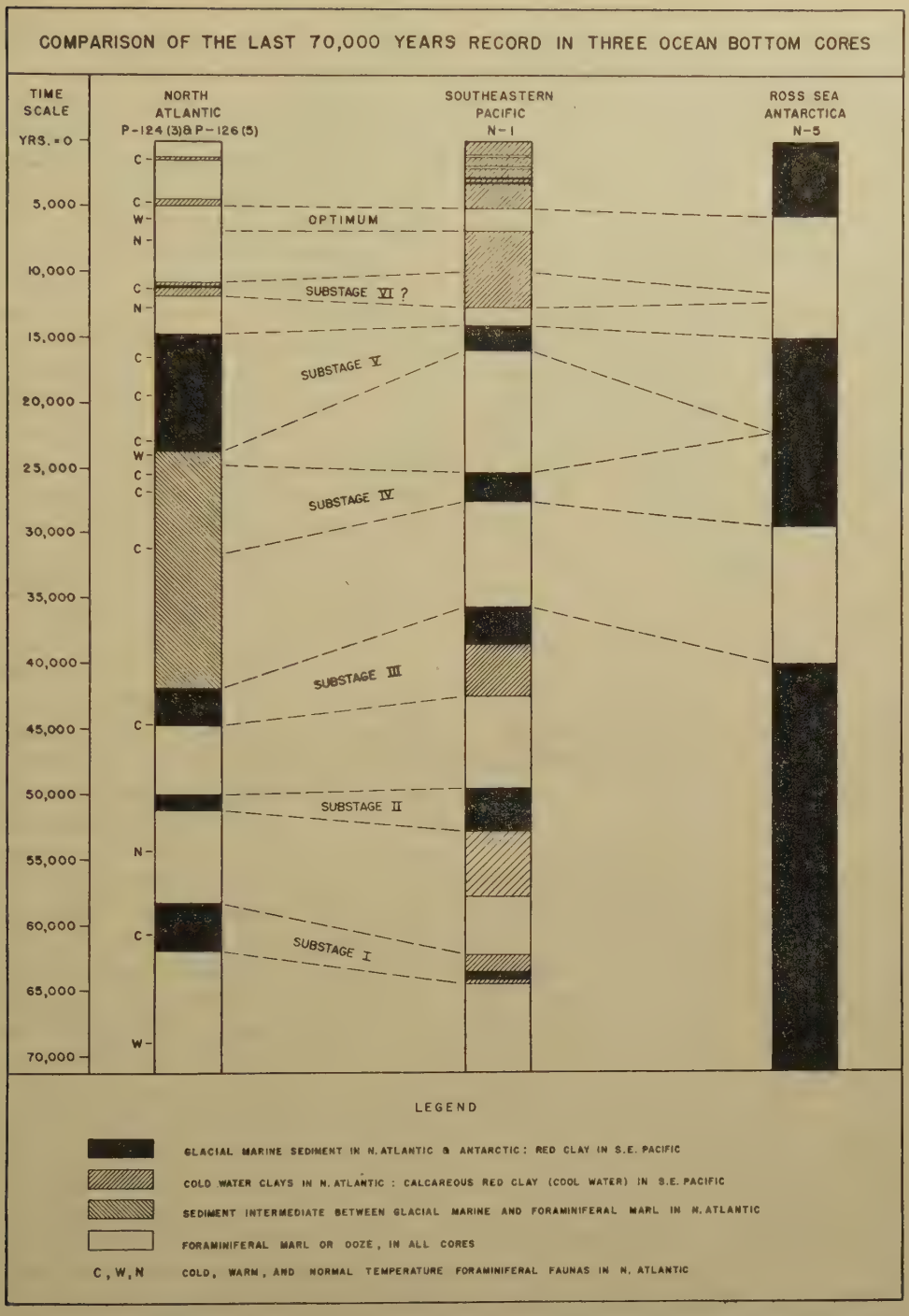

FIG. 3.—Comparison of records of the last 70,000 years in cores from the north Atlantic Ocean, the southeastern Pacific Ocean, and the Ross Sea, Antarctica. All three were dated by W. D. Urry.

bigerina ooze occurs above 3,600 meters; between these two depths either red clay or globigerina ooze occurs, depending on the locality. Inasmuch as core N-1 came from a depth of 3,930 meters, it may be considered as being in a sensitive zone. The second reason for supposing that the point where core N-1 was taken would be sensitive to changes in climate is that it is in the path of a surface current (see fig. 1) which moves from extreme southern latitudes, bringing subantarctic water northward up the west coast of South America, and swings westward (Sverdrup, Johnson, and Fleming, 1942, p. 702). Variations in the temperature or volume of this current might be expected to result from climatic changes, and these in turn should affect the type of sediment deposited.

Core N-2 was collected from a shallower point within the postulated sensitive depth range, but from a location 23° farther from the equator than was core N-1; apparently cold-water conditions existed at this point throughout the period of deposition of the material in core N-2.

Slumping as a mechanism for producing alternations of red clay and globigerina ooze in some localities has been discussed by Kuenen (1950, pp. 247, 270). The writer does not believe that slumping was involved in producing the sequence of deposits shown in core N-1. The time-depth curve of Urry indicates more rapid deposition of the more highly calcareous zones of the core; but this is to be expected in the normal process of sedimentation. In so far as the topography of the bottom is known in the vicinity of where the core was taken, there are no great differences in elevation, but the location of core N-1 is somewhat shallower than the general bottom depths for several miles around. Apparently there is no shallower bottom near by from which material could have slumped.

The accuracy of the time scale is the next question of importance. Piggot and Urry (1942) and Urry (1942) describe the dating method as applying to the last 300,000 years but give no indication of the percentage of error involved throughout this range. Perhaps the best method of evaluating the error is to compare ocean-bottom cores which have been dated by this method and which contain records of the same events. This has been done in figure 3, where events of the last 70,000 years in the North Atlantic, the southeastern Pacific, and the Ross Sea, Antarctica, are found to correlate sufficiently well to give considerable confidence in the dating method for at least the latter part of its applicable range.

For dates beyond 300,000 years Urry's "percent of equilibrium" method does not apply, but Urry has extrapolated his time scale for core N-1 to 990,000 years by making certain assumptions regarding rates of deposition of the various sediments involved, the degree of their compaction, and the probable amount of thinning of layers by lateral squeezing during the coring operation. The writer does not agree with Urry's estimate of the importance of thinning by lateral squeezing, and questions the larger age values assigned to the lower part of the core. Urry's time-depth curve is essentially a straight line from 150,000 to 460,000 years, and if this line is extrapolated without adjustment, the age at the bottom of the core is 800,000 years instead of 990,000 years. The total age may be even less, because a zone of the purest globigerina ooze in the core occurs below the 300,000-year level, and, because the ooze generally accumulates faster than red clay, this would decrease the assigned time interval. The writer

proposes, however, a straight-line extrapolation of the time curve. In figure 2 the two dates given for each boundary below the 338,000-year level are those obtained by extrapolation by the writer and by Urry, respectively, from Urry's data.

INTERPRETATIONS

Using the intensity of reddish-brown color in the core (black in fig. 2) as an approximate index to coolness of climate and correlating the darkest color with glacial stages, a detailed sequence of events can be established which are believed to have occurred from the time of the Kansan glacial stage to the present. The ages in years assigned to the events are derived from Urry's data. The time scale is believed to be of the correct order of magnitude only, but the sequence of events appears to be valid.

RECENT EPOCH

The climate of the Recent epoch has been relatively cool compared with that of the Yarmouth and Sangamon interglacial stages. The trend has been from warmer to cooler conditions in the last 6,000 years; this trend is corroborated in part by data from the bottom of the Ross Sea, Antarctica (Hough, 1950, pp. 258–259), which indicate that the northern limit of the pack ice moved northward more than 100 miles between 6,000 and 4,000 years ago.

There was a brief warmer period of several years' duration approximately 1,100 years ago, or about A.D. 850. Another brief warmer period occurred approximately 1,900 years ago, centered about A.D. 50. Two brief abnormally cool periods occurred approximately 2,800 years ago (850 B.C.) and 3,200 years ago (1250 B.C.).

There was a distinctly warm period of nearly two thousand years' duration centered at a time about 6,000 years ago. Presumably this is the "climatic optimum" which is generally recognized by students of the Recent epoch (Flint, 1947, p. 487).

WISCONSIN GLACIAL STAGE

An abnormally cool period, represented by red clay in core N-1, occurs from 7,000 to 12,700 years ago. In the North Atlantic core [P-124(3)], which is represented in the uppermost 12,000-year portion of figure 3, there is a zone of less calcareous mud with a cold-water fauna between the ages of 10,800 and 11,800 years, and within this zone, at 11,000 years, is an "anomalous" coarser-grained zone which was attributed to submarine slumping by Piggot and Urry (1942, p. 1196) but which may represent glacial marine deposition. In the Ross Sea, Antarctica, core N-5 (fig. 3) there is a single (probably ice-rafted) pebble at the 11,000-year level. These features of the three ocean-bottom cores are interpreted as representing a glacial substage. This substage, numbered VI in figure 3, may be correlated with the Mankato substage of the North American continent.

The Mankato substage, in the vicinity of its type locality in the state of Iowa, has been dated by the radiocarbon method as follows: samples of wood incorporated in the lower portion of the Mankato till are 11,952 $\pm$ 500 years and 12,200 $\pm$ 500 years old (Libby, 1952). At Kimberly, Wisconsin, wood from a varved clay deposit which apparently accumulated adjacent to the retreating Mankato (locally Valders) ice front has been dated as 10,676 $\pm$ 750 years old (Libby, 1952).

At Two Creeks, Wisconsin, the Valders (Mankato) till overlies and contains within its lower portion logs and branches of trees, and tree stumps in growth

position occur below the till. The average date of five samples of wood from the till is 11,404 ± 350 years (Arnold and Libby, 1951). Because it appears that the Valders ice overrode standing trees (Flint, 1947, p. 251), the radiocarbon date for the trees may be considered as a date within Valders (or Mankato) time, before maximum development of the ice sheet in the Michigan Basin.

From the foregoing evidence it appears that the Mankato glacial substage may be correlated with glacial substage VI of the ocean-bottom core samples.

Preceding substage VI (correlated with the Mankato substage) in the southeastern Pacific core N-1 is a globigerina ooze zone representing a distinctly warm period of approximately 1,000 years' duration.

Five additional substages of the Wisconsin appear to be clearly represented in core N-1 by distinct layers of dark-red clay which are separated or bounded by globigerina ooze. These substages are here numbered I to V, and their median dates to the nearest 1,000 years are given in table 1.

TABLE 1

Wisconsin Substage	Approximate Medium Age (Years)
VI	11,000
V	15,000
IV	26,000
III	37,000
II	51,000
I	64,000

In their study of North Atlantic core samples, Bramlette and Bradley (1940) recognized only four glacial marine zones in their supposed Wisconsin stage, but they described the material between their two uppermost glacial marine zones as "sediment intermediate in texture and composition between glacial marine deposits and foraminiferal marl." On the basis of the comparison made in figure 3 it is suggested by the present writer that this material is the representative of a glacial substage. The North Atlantic core material has been dated by Piggot and Urry (1942) since the report by Bramlette and Bradley (1940) was published. The lithologic information on North Atlantic core P-126(5) is plotted on the appropriate time scale in figure 3. Comparison of this sequence with that of Pacific core N-1, plotted on the same time scale, shows a remarkable correlation between the four original glacial marine zones of the North Atlantic with four of the red-clay zones of the southeastern Pacific. It should be noted that the Pacific cold-water substages designated I, II, III, and V correlate well with definite glacial marine zones in the North Atlantic. This leaves substage IV without a representative in the North Atlantic cores, unless the "sediment intermediate in texture and composition between glacial marine deposits and foraminiferal marl" is that representative. This possibility is supported by the indications of water temperature found by Cushman and Henbest in a study of Foraminifera (Bramlette and Bradley, 1940, pl. 4). These water temperature indications are reproduced in figure 3 of the present paper by means of the letters *C*, *W*, and *N*, standing for cold, warm, and normal. It can be seen that cold-water species of Foraminifera occur in the zone correlated with substage IV and that this zone is separated from substage V above by a warm-water fauna.

The number of distinct glacial substages on the North American continent during the Wisconsin is not known. Four substages are generally accepted at the present time: the Iowan, Tazewell, Cary, and Mankato (Ruhe, 1952). An additional substage, the Farmdale, has been

proposed by Leighton and Willman (1950). The Farmdale is represented in the Mississippi Valley by a loess lying on the mature Sangamon profile of weathering on the Illinoian drift, itself having a youthful profile of weathering and being overlain by Iowan loess. These relationships, along with the relationship of the loess to the major river valleys of the region, were interpreted by Leighton and Willman as implying "an extension of an ice sheet during the Farmdale substage into the drainage basin of the ancestral Mississippi prior to the Iowan substage but not yet recognized in the series of drift sheets because it fell short of subsequent ice lobes." The Farmdale, proposed as probably the first Wisconsin substage in North America, is here presented as a possible correlative of substage I of the ocean-bottom cores.

Because no dates are available for the continental glacial substages older than Mankato, further correlations of specific North American substages with the numbered oceanic substages are conjectural. If the Farmdale is the equivalent of substage I, there remain only three of the presently accepted North American substages (Iowan, Tazewell, and Cary) to be correlated with four oceanic substages (II, III, IV, and V). The writer suggests a tentative correlation of the Port Huron, which is late Cary according to Bretz (1951), with substage V, centered at 15,000 years. He suggests that the Valparaiso correlates with substage IV, centered at 26,000 years. The Cary substage then includes substages IV and V and the intervening time. This correlation is consistent with the records in the North Atlantic and Ross Sea columns of figure 3, where cold water conditions generally are indicated in the period between substages IV and V.

The warm-water indication at 24,000 years in the North Atlantic may correlate with the post-Fort Wayne, pre-Defiance (post-Valparaiso, pre-Tinley) glacial retreat. A major retreat in the Erie basin at this time is suggested by a study of the mechanical composition of tills in eastern Ohio by Shepps (1953). Because the Defiance till contains a much higher percentage of silt and clay than the older Cary till, it is suggested that silt and clay were deposited in the Erie basin during a retreat of the ice and were incorporated in the Defiance till during the next ice advance.

The Defiance and Tinley moraines, in the Erie and Michigan basins respectively, are suggested as correlatives of the cold-water deposit at 23,000 years in the north Atlantic, and the Lake Border moraines, in both the Erie and Michigan basins, then were deposited during the period centered at approximately 19,000 years (fig. 3).

Substages II and III remain as possible correlatives of the generally accepted Iowan and Tazewell substages of North America.

If the foregoing tentative correlations are correct, correlatives have been found for all six of the oceanic Wisconsin substages. In Illinois, the Shelbyville and Bloomington morainic systems appear to be sufficiently distinct to be considered as separate substages which could be correlated with oceanic substages II and III. If these correlations are correct, and if the Farmdale represents substage I, the Iowan must be the equivalent of substage II and therefore the equivalent of the Shelbyville.

One additional point should be mentioned in the comparison of the oceanic record with that in North America. Figure 3 indicates a twofold division of the Wisconsin stage in the Ross Sea, Antarctica, column. Substages I, II, and III of

the southeastern Pacific and of the North Atlantic correlate with the lower division, while substages IV and V correlate with the upper division (substage VI is weakly developed in all the cores and is younger than the upper division). The North American substages are grouped into two divisions of the Wisconsin, with the major break occurring between the Tazewell and Cary substages (Ruhe, 1952).

SANGAMON INTERGLACIAL STAGE

Below the five dark-red clay zones of core N-1, which were interpreted as substages of the Wisconsin glacial stage, there is a generally light-colored section of the core, 58 cm. long, which is interpreted as representing the Sangamon interglacial stage. According to Urry's time scale, the Sangamon lasted approximately 200,000 years. Several minor fluctuations within this stage are indicated, including some more or less definite cool periods. The more distinct cool periods are centered at about 92,000, 152,000, 165,000, 173,000, and 253,000 years. The less distinct cool periods are centered at about 77,000, 133,000, and 186,000 years.

ILLINOIAN GLACIAL STAGE

The Illinoian glacial stage appears to be represented in core N-1 by three red-clay layers, which are interpreted as representing three glacial substages. According to Urry's time scale, these are centered at the ages of 274,000, 310,000, and 330,000 years. The Illinoian stage as a whole lasted 70,000 years. For comparison with this record for the southeastern Pacific Ocean reference is made to the occurrence of three Illinoian subdivisions, represented by the Buffalo Hart, Jacksonville, and Payson moraines, in central North America (Leighton and Willman, 1950).

YARMOUTH INTERGLACIAL STAGE

Below the three red-clay zones of core N-1, which were interpreted as substages of the Illinoian glacial stage, there is a generally very light-colored section of core, 60 cm. long, which is interpreted as representing the Yarmouth interglacial stage. This section lies below the level dated at 340,000 years and therefore is beyond the time range within which Urry's dating method is applicable. However, by extrapolation of Urry's time-depth scale, estimated dates can be obtained for the lower, older portions of the core. The beginning of the Yarmouth, at the top of the underlying red clay, is given an estimated date of 685,000 years ago by the writer, extrapolating Urry's data, and is given a date of 750,000 years ago if Urry's extrapolation of his data is used. The duration of the Yarmouth is, therefore, estimated as between 340,000 and 410,000 years.

The Yarmouth section of the core generally is more highly calcareous than the Sangamon section, presumably indicating generally warmer climatic conditions. One zone 6 cm. thick near the middle of the Yarmouth section (age approximately 450,000 years) is a chalky white, essentially pure globigerina ooze, and this appears to represent the warmest period of the entire core section.

Several minor fluctuations within the Yarmouth are indicated by various shades of color between white and light brownish-red. There are seven fairly definite darker, or cool-climate, zones. The estimated dates of these may be read from the time scale in figure 2.

KANSAN GLACIAL STAGE

The upper part of the Kansan glacial stage appears to be represented in core

N-1 by dark brownish-red clay which extends from a depth of 174 cm. to the bottom of the core at 194 cm. The date of the end of the Kansan, as stated above, is estimated as between 680,000 and 750,000 years ago.

The occurrence of one considerably lighter zone and other slightly lighter zones within this section suggests that the Kansan is divisible into substages. Since the entire Kansan is not represented, the number of substages cannot be stated.

DISCUSSION

The sediment of a core sample has been interpreted as a record of climatic fluctuation during a large part of the Pleistocene epoch. This interpretation, if correct, applies strictly only to the southeastern Pacific Ocean, where the core sample was taken. If it is assumed that the major climatic fluctuations were approximately contemporaneous throughout the world during the Pleistocene, we may expect major events which are influenced by climate to be susceptible to correlation from one region to another. It is possible, however, that regional variations in some climatic factors may have been sufficiently pronounced to cause an exaggeration or a suppression of the general climatic condition, and thus to introduce an anomalous event in a particular region.

Ocean-bottom core samples, if taken from appropriate locations, may be expected to contain more complete records of climate-influenced sediment than can be found in continental deposits. Because core samples from the southeastern Pacific and from the North Atlantic oceans have been found to contain records of similar climate at approximately similar dates during the last 70,000 years, it appears reasonable to give some credence to the details of the longer record in the southeastern Pacific, which extends back into the Kansan glacial stage according to the present interpretation.

ACKNOWLEDGMENTS.—The writer, as research associate of the Woods Hole Oceanographic Institution, was given the opportunity to take part in the United States Navy Antarctic Expedition of 1946–1947 under a contract between the Institution and the Hydrographic Office of the Navy. Bottom-core samples were collected from the U.S. Coast Guard Cutter "Northwind," and the interest and co-operation of Captain C. W. Thomas of that vessel is appreciated. Mr. W. G. Metcalf, the writer's colleague of the scientific staff, rendered able assistance in the bottom-sampling work. The co-operation of the Carnegie Institution of Washington, and especially of Dr. W. D. Urry of that Institution, is gratefully acknowledged.

REFERENCES CITED

ARNOLD, J. R., and LIBBY, W. F. (1951) Radiocarbon dates: Science, vol. 113, p. 117.

BRAMLETTE, M. N., and BRADLEY, W. H. (1940) Geology and biology of North Atlantic deep-sea cores between Newfoundland and Ireland. Pt. 1, Lithology and geologic interpretations: U.S. Geol. Survey Prof. Paper 196, pp. 1–34.

BRETZ, J H. (1951) The stages of Lake Chicago: their causes and correlations: Am. Jour. Sci., vol. 249, pp. 422–424.

FLINT, R. F. (1947) Glacial geology and the Pleistocene epoch, New York, John Wiley & Sons, Inc.

HOUGH, J. L. (1950) Pleistocene lithology of Antarctic ocean-bottom sediments: Jour. Geology, vol. 58, pp. 254–260.

KUENEN, PH. H. (1950) Marine geology, New York, John Wiley & Sons, Inc.

LEIGHTON, M. M., and WILLMAN, H. B. (1950) Loess formations of the Mississippi Valley: Jour. Geology, vol. 58, pp. 599–623.

LIBBY, W. F. (1952) Chicago radiocarbon dates. III: Science, vol. 116, p. 675.

PIGGOT, C. S., and URRY, W. D. (1942) Time relations in ocean sediments: Bull. Geol. Soc. America, vol. 53, pp. 1187–1210.

RUHE, R. V. (1952) Classification of the Wisconsin glacial stage: Jour. Geology, vol. 60, pp. 398–401.

SHEPPS, V. C. (1953) Correlation of the tills of northeastern Ohio by size analysis: Jour. Sedimentary Petrology, vol. 23, pp. 34–48.

SVERDRUP, H. U.; JOHNSON, M. W.; and FLEMING, R. H. (1942) The oceans, New York, Prentice-Hall, Inc.

URRY, W. D. (1942) The radio-elements in non-equilibrium systems: Am. Jour. Sci., vol. 240, pp. 426–436.

——— (1949) Radioactivity of ocean sediments. VI. Concentrations of the radio-elements in marine sediments of the Southern Hemisphere: *ibid.*, vol. 247, pp. 257–275.

Contribution No. 642

PROCEEDINGS OF THIRD CONFERENCE

ON

COASTAL ENGINEERING

CAMBRIDGE, MASSACHUSETTS

OCTOBER 1952

Edited by

J. W. JOHNSON

PROFESSOR OF HYDRAULIC ENGINEERING

UNIVERSITY OF CALIFORNIA
BERKELEY

PUBLISHED BY

COUNCIL ON WAVE RESEARCH
THE ENGINEERING FOUNDATION

1953

CHAPTER 6
CIRCULATION IN ESTUARIES [1]

Bostwick H. Ketchum
Woods Hole Oceanographic Institution
Woods Hole, Massachusetts

In discussing the circulation in estuaries, an apparent paradox must always be kept in mind. In the first place the problems of estuarine circulation are unique, being different from the problems of the open sea, and from the problems of river hydrology. Estuarine circulation and related problems consequently constitute a valid field for investigation. In contrast to this viewpoint is the tremendous range of conditions found in various estuaries - no two are alike. This inherent variability of estuaries discourages generalizations about the circulation.

The paradox thus lies in the recognized fact that estuaries are similar enough to constitute an integrated field of investigation, but at the same time estuaries are so different in details that generalizations are dangerous. The state of our knowledge is still so imperfect that one is never certain whether a general principle or a unique detail is being studied. Therefore it is difficult and sometimes impossible to apply methods which have been found useful in one estuary as the basis for predictions in others.

When asked to present a paper "summarizing the present state of the art and science" it seemed particularly important to attempt to classify our knowledge so as to indicate, on the one hand, principles which are generally applicable and tend to make estuaries similar, and, on the other hand, to contrast the circulation in various estuaries so as to indicate the wide variety of differences which may be encountered. Since our knowledge is meagre, this can be done only in a qualitative way.

Let us first consider what is meant by an estuary. Many definitions have been given, but one suggested by Pritchard (1952a) seems particularly applicable to studies of the circulation. "An estuary is a semi-enclosed coastal body of water having a free connection with the open sea and containing a measurable quantity of sea salt." The most common type of estuary is one in which the enclosed water is fresher than that of the open sea, since the increments of fresh water from precipitation and runoff exceed the loss of water by evaporation. Such locations have an estuarine type of circulation. In some enclosed bodies of water evaporation exceeds precipitation and runoff, and the water becomes more saline than that of the open sea. These may logically be included among estuaries, since the same processes must determine their circulation, even though everything is working in reverse. Redfield (1951) has called the

---

[1] Contribution No. 642 from the Woods Hole Oceanographic Institution.

circulation in this type of embayment anti-estuarine. Little is known about anti-estuarine circulation (Collier and Hedgpeth, 1950) and the remainder of this paper will deal only with the positive type.

Among the positive type of estuaries in which the water within the estuary is fresher than pure sea water, three major types can be enumerated. The drowned river valley is the common type of estuary of the Atlantic and Gulf coasts. For example, the Delaware, Hudson and Chesapeake Bay systems are drowned river valleys. These estuaries are generally shallow relative to their width and have a tidal range which is substantial in proportion to the total depth. The sides of the estuary slope gradually in a shallow V shape and the surrounding coast is relatively low.

The Scandinavian coasts and the coasts of northern United States and of Canada are frequently indented by fjord type estuaries which present many contrasts. The depth is great relative to the width of the estuary, being not uncommonly equal to the width. There is frequently a sill at the entrance which isolates the deeper water within the estuary from coastal water at equal depths. The estuary is steep sided giving essentially a U shaped trench in contrast to the shallow V shape of the drowned river valley. The total depth of water is generally great relative to the range of tides.

Estuaries may also be formed by the development of an offshore barrier beach, having a narrow entrance to an enclosed bay. Such estuaries are found along the south shore of Long Island, and along our Southern Atlantic coast. The largest estuary of this sort on the Atlantic coast is the Pamlico Sound system in North Carolina. In general these estuaries are even more shallow relative to the width than are the drowned river valleys. However, the entrance to the sea is generally so narrow that the tidal wave is damped and consequently the range of tides in such estuaries is not as great in proportion to the total depth as it is in the drowned river valley. The wave may indeed be sufficiently damped so that within the embayment no predictions of tidal variations are possible.

In each of the above categories, estuaries of various sizes and shapes will be found. It is this variation which discourages generalizations about the circulation in estuaries. All of the positive type estuaries, however, have the following properties in common:

1. Fresh water additions exceed evaporation. The principle of the continuity of volume requires that the circulation remove the excess fresh water at a rate which, over a period of time, equals the rate of addition.

2. There is a gradual increase of salinity from the source of fresh water to the sea. As the salt content increases a greater volume of mixed water must move out in order to transport a unit

volume of fresh water seaward. The principle of continuity of salt requires that the circulation provide enough sea salt to maintain the salinity distribution and to balance the salt removed.

3. The volume of water within the estuary varies periodically with the stage of the tide.

4. The currents within the estuary vary periodically with the stage of the tide. These currents are directly related to the tidal change in volume, though in some locations the relationship may be obscure and unpredictable.

5. Net movements of water, or non-tidal drifts, result from inequalities in the direction, velocity or duration of flood and ebb tidal currents.

The circulation of water is the net result of two processes operating simultaneously and in three dimensions. These are advection and turbulent mixing. Advection is the mass transport of water, whereas turbulence involves random motions of water and the resultant intermixture of adjacent waters. Theoretically, at least, either one of these processes alone could produce a circulation in an estuary which would satisfy the requirements of the continuity of volume and the continuity of salt. Actually the two processes are combined in various ways to produce the diversity of circulation patterns which is so apparent and troublesome to students of estuaries.

To show the range of conditions which may be found in different estuaries the salinity variation with distance for four examples is plotted in Figure 1. In all cases the salinity increases along the length of the estuary, but the shape of the distribution curve is quite different. The ratio between the volumes of water entering the two ends of the estuary during each tidal cycle is informative in connection with this figure. In the Bay of Fundy, where the salinity increases so rapidly, the tidal flow exceeds mean river flow by a factor of about 900. This factor is about 300 for the Raritan system, 150 for the Delaware and the two volumes are nearly equal in the Connecticut. As this ratio decreases the change of salinity with distance becomes more gradual in the upper end of the estuary. It seems probable that the ratio of these two volumes will have a direct effect on the pattern of salinity distribution in all estuaries, though the circulation can be determined by so many combinations of the turbulent and advective processes that no simple relationship can be expected.

Let us consider first the advective processes, neglecting for the moment the horizontal transport resulting from turbulent mixing. In order to remove the fresh water increment there must be a net transport seaward. As the water moves seaward there is continuous admixture of more saline water, and the gross seaward transport of water must increase

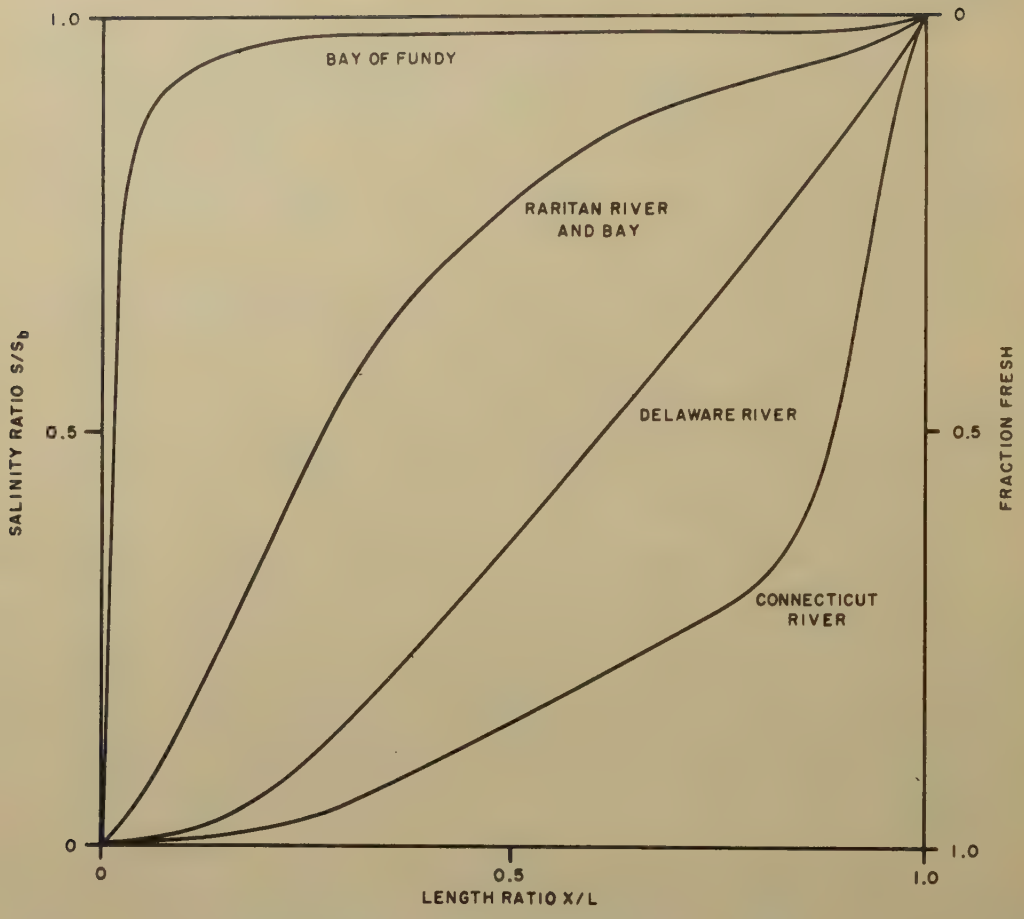

Fig. 1. The distribution of salinity along the length of four estuaries. Data for Delaware Bay from Mason and Pietsch (1940); for Connecticut River from Howard (1940).

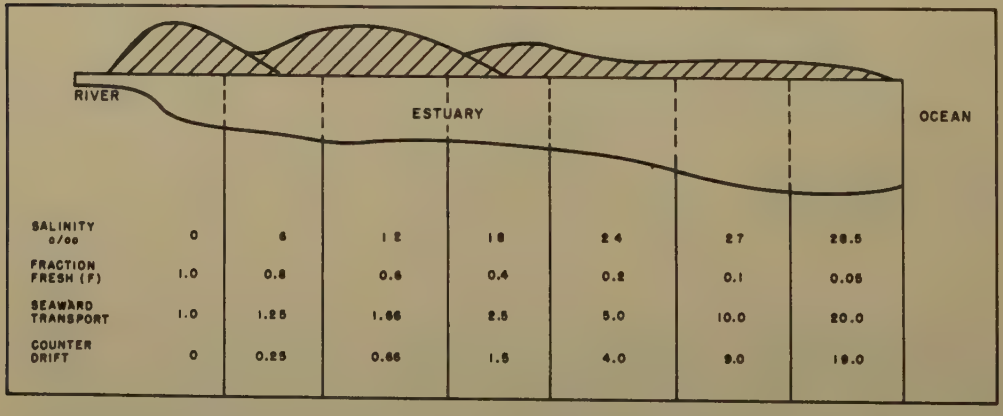

Fig. 2. The changes in mean salinity and in the volume of water which must be transported in order to maintain the steady state distribution in a hypothetical estuary.

directly in proportion to its salt content. At the same time a landward transport of salt must take place to satisfy the salt balance. For example, where the mixture contains half sea water and half fresh water two volumes must move seaward in order to carry one volume of fresh water seaward. A direct consequence of this simple relationship is that the total circulation in the estuary increases enormously in volume as the water moves from the river towards the sea. This is illustrated in a diagrammatic way in Figure 2 which shows the increase in seaward transport of mixed water and the compensating landward transport of salt, expressed in terms of the equivalent volume of pure sea water.

These seaward and landward advective transports may be separated vertically to produce two or three layered flow systems, or they may be horizontally separated. In still other cases there may not be a division into two distinct advective drifts, so that the horizontal transport in one direction must be due to rather large, horizontal mixing processes.

The relative importance of the advective and turbulent mixing processes has been assessed by Pritchard (1952) in the estuary of the James River. In this location the two most important processes were horizontal advection and vertical random mixing. Of secondary, but significant, importance was the vertical advection and lateral random mixing related to the change in width of the estuary with depth. Horizontal random mixing was negligible. The horizontal advection in this case was clearly separated into two layers, with a net seaward transport in the surface and a net landward transport in the deeper layer. Pritchard's measured tidal currents as a function of depth, and the resultant non-tidal drifts are shown in Figure 3.

As mentioned above there may be no separation of the system into two clear advective drifts such as those observed in the James River. As an example of such a case Table I presents the transport of water by the ebb and flood tidal currents in the mouth of the Raritan River. At this location both the surface and deeper water showed seaward non-tidal drifts, and no landward countercurrent was found. The seaward drift calculated from the river flow and the mean fraction of fresh water in the section indicates a volume of gross seaward transport intermediate in magnitude between the surface and deeper transports. In such a case turbulent mixing must be the mechanism which provides the salt required to maintain the salt balance.

The admixture of salt water into the system as the water moves seaward is clearly an important process. Two sets of evidence are available to indicate that the rate of admixture is correlated with the velocity of the tidal currents. These are given in Figure 4. The left-hand figure is from Tully (1949) who was describing the circulation in Alberni Inlet, a fjord type estuary where the deepest layer was essentially completely isolated from a two layered surface system. This shows that the total admixture of salt, whether it resulted from turbulence or from vertical advection, into the surface layers is directly

Table I

Tidal Excursions and Non-Tidal Drifts in Mouth of Raritan River
Negative values indicate seaward motion
(feet per tidal cycle)

Surface:-	Excursion on Flood	$+12.1 \times 10^3$
	Excursion on Ebb	-26.8×10^3
	Non-tidal drift	-14.7×10^3
Bottom:-	Excursion on Flood	$+16.5 \times 10^3$
	Excursion on Ebb	-22.1×10^3
	Non-tidal drift	-5.6×10^3

Average Non-Tidal Drift Calculated from Salinity:

$$NTD = \frac{-R}{FA} = \frac{-23 \times 10^6}{0.12 \times 27 \times 10^3} = -7.1 \times 10^3$$

Where R = River flow (cubic feet per tidal cycle),
F = Average fraction of fresh water,
A = Cross sectional area.

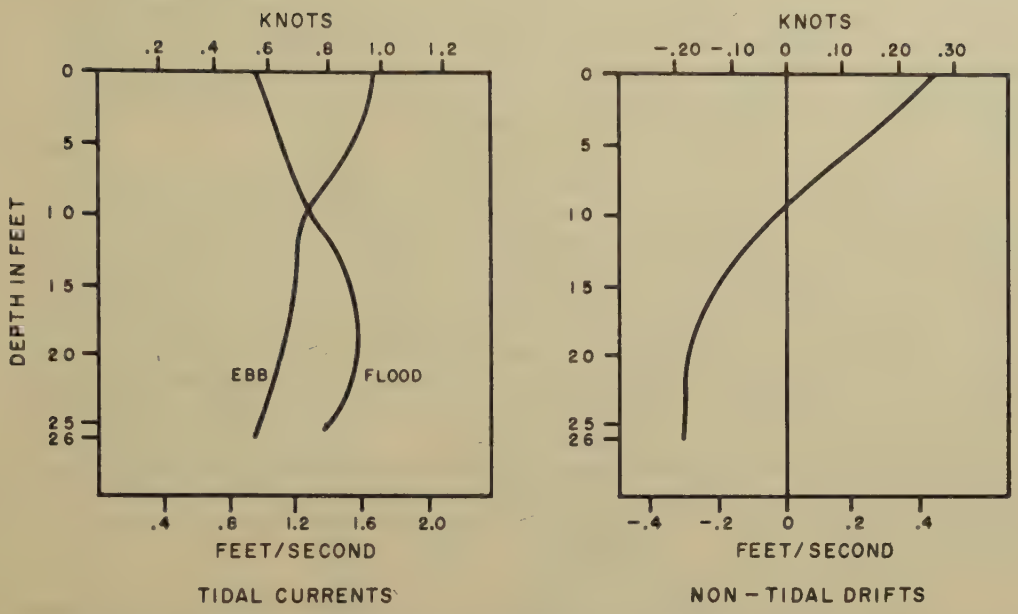

Fig. 3. Tidal currents and non-tidal drifts observed by Pritchard (1952) at various depths in the James River.

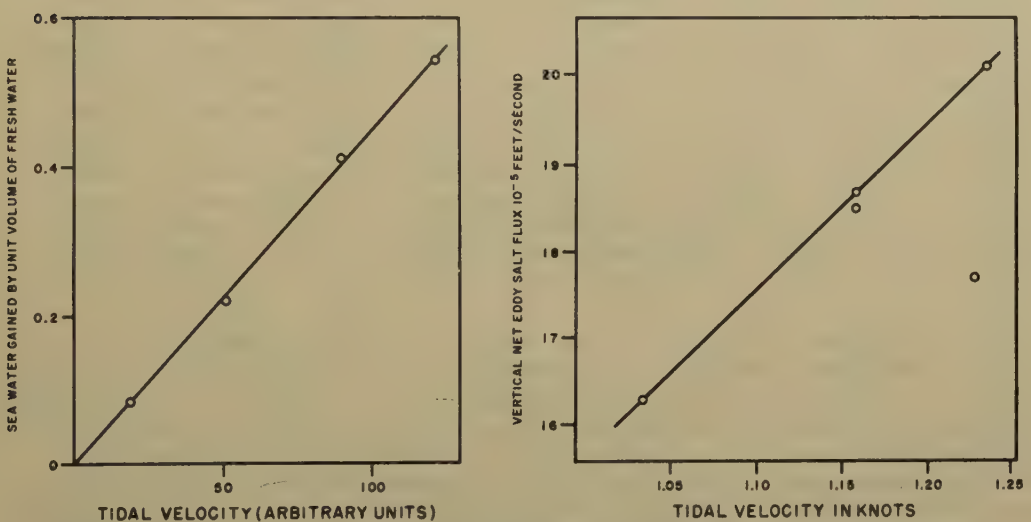

Fig. 4. The rate of admixture of salt into the freshened surface water in Alberni Inlet (at left, Tully, 1949) and in the James River (at right, Pritchard, 1952).

related to tidal velocity. The right-hand figure is from Pritchard's (1952) analysis of the James River, and shows that the random eddy flux, excluding the admixture of salt due to vertical advection, is a direct function of tidal velocity. These relationships between salt entrainment and tidal flow emphasize the importance of tidal currents in effecting the mixing between salt and fresh water.

As the estuary widens the seaward drift of freshened water may be horizontally separated from the landward counter drift. The distribution of salinity in Raritan Bay just off the mouth of the Raritan River illustrates this condition (see Figure 5). A similar effect is shown in Figure 6 for Mount Hope Bay. This effect is the result of the rotation of the earth, and is generally found in the wider parts of estuaries. Even in the narrow parts the effect may be present, but the change from one side to the other is so small that it frequently cannot be detected. In localities where additional river flow enters a bay along one side the distortion of the salinity distribution may be augmented, as it seems to be in the Chesapeake Bay (Pritchard, 1952) and in the Bay of Fundy (Ketchum and Keen, in press), or it may be decreased or completely obliterated, as seems to be the case in the lower Delaware Bay (Mason and Pietsch, 1940).

So far, we have been talking of estuaries in which mixing between salt and fresh water occurs throughout the length of the estuary. We have mentioned cases in which the landward counter drift and the seaward drift are separated vertically or horizontally, and in which only one advective drift can be identified. There are, of course, other possibilities. Tully (1949) clearly describes in Alberni Inlet, a case in which three layers are identifiable, the deepest being essentially isolated from the upper two. Farmer and Morgan (1953) will discuss in the next paper the salt wedge, which is a special case of two layer flow in which vertical mixing is very slight. There is evidence that in some estuaries intense mixing takes place in a certain region and that little additional mixing occurs as the freshened water flows seaward. Hachey (1934) has studied localized mixing phenomena in a small model and applied the results to the conditions in the upper end of Passamaquoddy Bay. There he finds a surface fresher layer mixing with a deep saline layer to produce an intermediate layer of intermediate properties.

In the Strait of Juan de Fuca - Strait of Georgia system in the Pacific Northwest, the San Juan islands, combined with rapid tidal flows, appear to provide a similar localized mixing. The resultant water masses and their distribution are shown in Figure 7. In this case water from mid depths of the Pacific Ocean enters through the Strait of Juan de Fuca unchanged until it is mixed with surface water from the Strait of Georgia in the San Juan channels. This mixed water then becomes the deep water of the Strait of Georgia and the surface water of the Strait of Juan de Fuca (Redfield, 1950). The volume of water flowing into the system from the Pacific Ocean in the countercurrent is about 15 times greater than the volume of fresh water introduced by the rivers. This

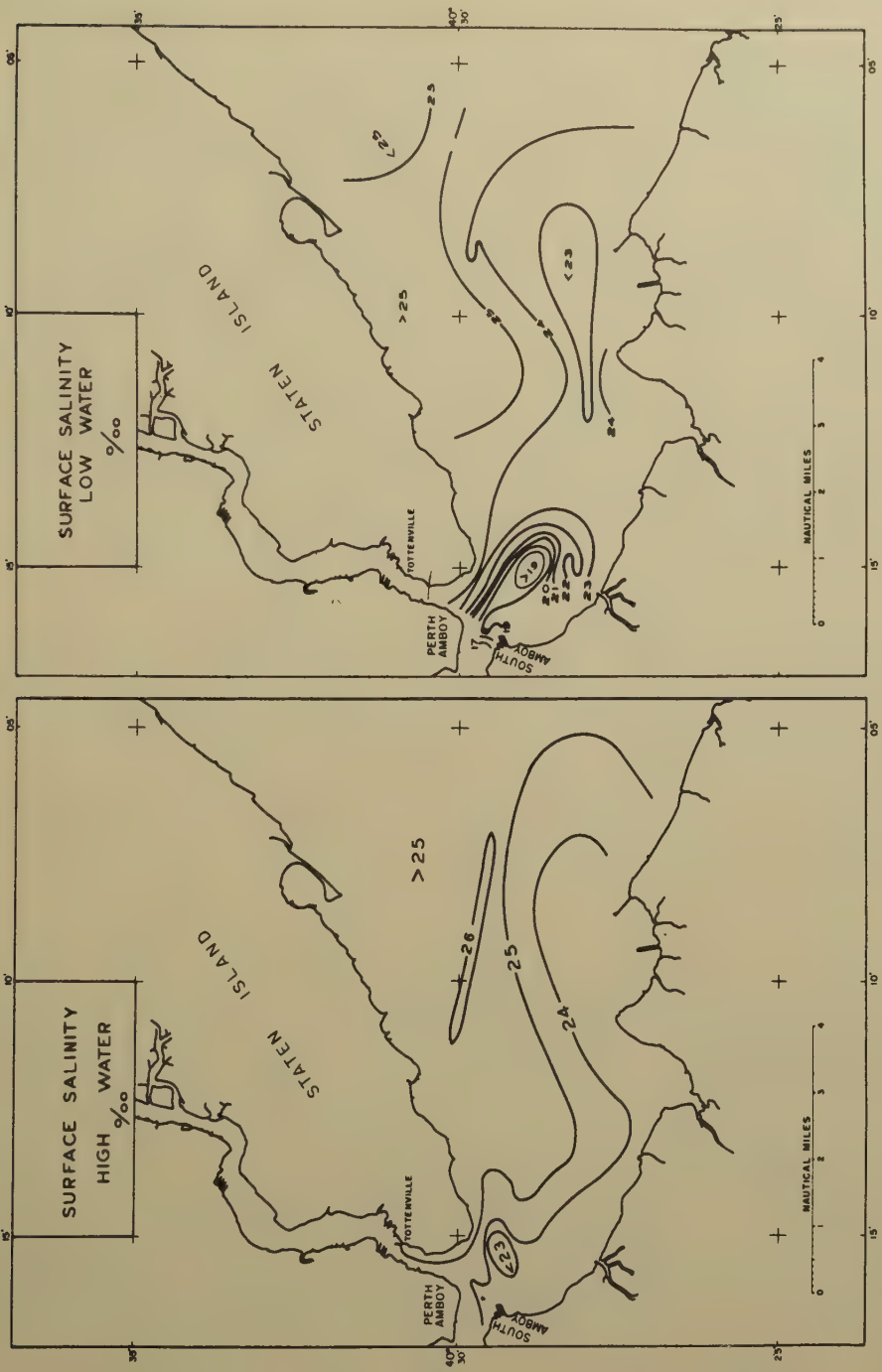

Fig. 5. Surface distribution of salinity at high and at low tide in Raritan Bay.

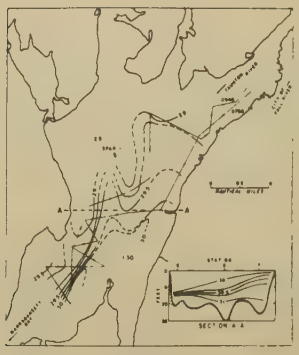

Fig. 6.

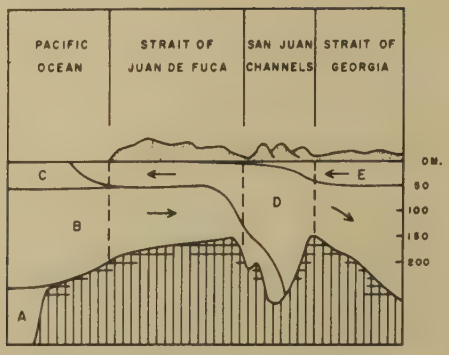

Fig. 7.

Fig. 6. Surface distribution of salinity in Mt. Hope Bay, and a cross section showing the slope of the isohaline surfaces.

Fig. 7. Diagrammatic chart of the distribution of various water masses in a section running from the Pacific Ocean through the Strait of Juan de Fuca to Georgia Strait (after Redfield, 1950).

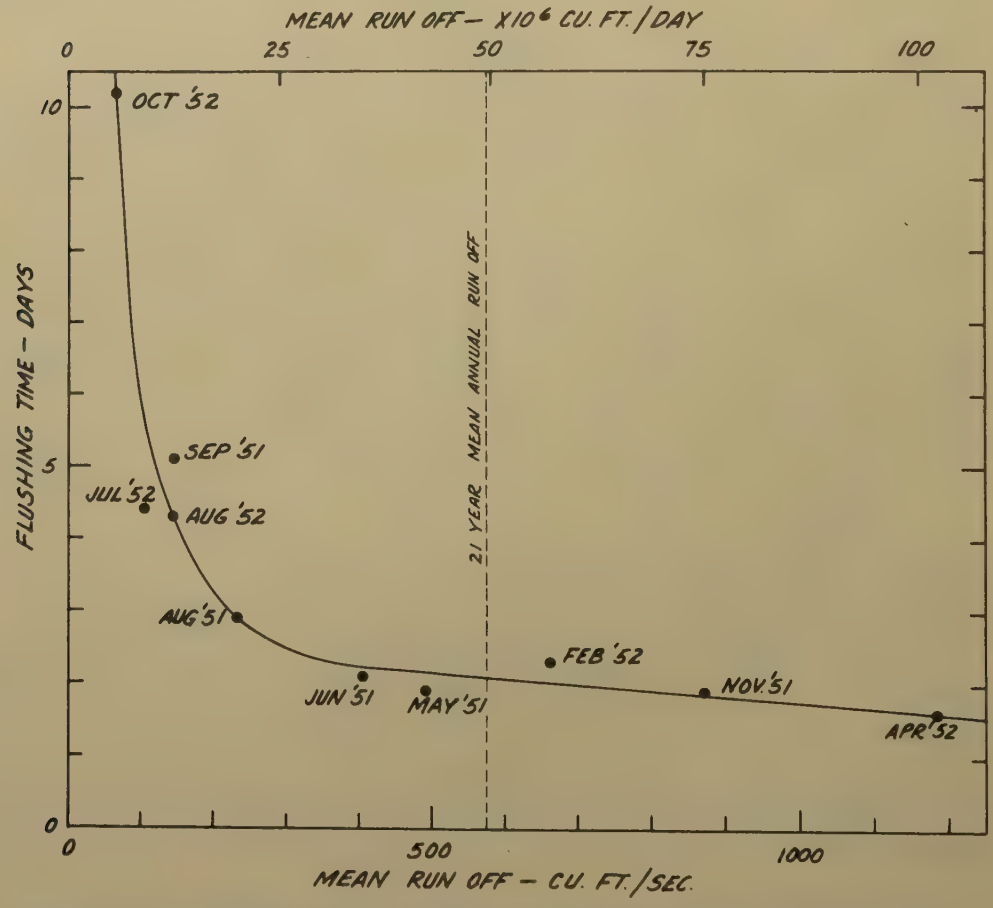

Fig. 8. The relationship between flushing time and river flow in Boston Inner Harbor (after Bumpus, 1952).

is a case of three layered flow in which all three layers have an active part in the circulation.

The importance of the tides as the effective force producing mixing has been emphasized. Empirical predictions of the distribution of fresh and salt water which are based upon the concept of tidal mixing have been shown to be applicable to a variety of estuaries (Arons and Stommel, 1951; Ketchum, 1951, 1951a; Ketchum and Keen, in press). What effect does variation in river flow have upon the circulation? Obviously increased river flow requires an increased transport of fresh water through each part of the estuary. This could be accomplished by increasing the fraction of fresh water in the mixed water which moves seaward, which would result in the movement downstream of the whole pattern of salinity distribution. It could also be accomplished by a more rapid circulation of the water with essentially no change in the salinity distribution. Once again both phenomena exert their influence. In the upper reaches of the estuary the rate of the circulation appears to increase as the river flow increases. Bumpus (1952) has determined the accumulation of fresh water in Boston Harbor and shows that the flushing time decreases from about ten days during low flow to about two days at the mean annual rate of flow. Further increases in runoff had only a slight additional effect on the rate of the circulation. His results are given in Figure 8.

As the water moves seaward, however, the fresh water is a smaller and smaller proportion of the mixture, and the effect of changes in fresh water volume is similarly decreased. In the offing of the Hudson River, for example, where the volume of sea water was about 100 times greater than the volume of fresh water in the mixture, variations in river flow had no measurable effect on the flushing time (Ketchum, Redfield and Ayers, 1951). It seems likely that river flow will, in all estuaries, have a direct effect on the rate of the circulation in the upper reaches, and a progressively smaller effect in the seaward region where the mixture moving seaward contains so much more sea water than fresh.

This paper has attempted to indicate the fundamental similarities in estuaries, and to point out the wide variety of detail in circulation which may be expected. It seems probable that the examples cited are isolated pieces of a continuous range of conditions extending from one extreme to the other. This is almost certainly true of the vertically stratified estuaries. In temperate latitudes, at least, the same geographical estuary can change from the vertically homogeneous type to the vertically stratified type at different seasons of the year as a result of changing runoff and temperature. As yet no unified theory is available which is comprehensive enough to permit application to a wide variety of conditions, though some success in interpreting quasi semi-state conditions in particular estuaries has been achieved. The recently expanded interest in estuarine circulation promises great advances in the art and science of such studies in the future.

REFERENCES

Arons, A. B. and Stommel, H. (1951). A mixing-length theory of tidal flushing: Trans. Amer. Geophys. Union, vol. 32, pp. 419-421.

Bumpus, D. F. (1952). Unpublished records from Woods Hole Oceanographic Institution files.

Collier, A. and Hedgpeth, J. W. (1950). An introduction to the hydrography of tidal waters of Texas: Pub. Inst. Mar. Sci., I, pp. 125-194.

Farmer, H. G. and Morgan, G. W. (1953). The salt wedge: Proc., Third Conference on Coastal Engin. Council on Wave Research.

Hachey, H. B. (1934). Movements resulting from mixing of stratified waters: J. Biol. Bd. Can. I, pp. 133-143.

Howard, C. S. (1940). Salt-water intrusion in the Connecticut River: Trans. Amer. Geophys. Union, vol. 21, pp. 455-457.

Ketchum, B. H. (1951). The exchanges of fresh and salt waters in tidal estuaries: Sears Found. J. Mar. Res., vol. 10, pp. 18-38.

Ketchum, B. H. (1951a). The flushing of tidal estuaries: Sewage and Industrial Wastes, vol. 23, pp. 198-209.

Ketchum, B. H. and Keen, D. J. Exchanges of fresh and salt water in the Bay of Fundy and in Passamaquoddy Bay: J. Fish. Res. Bd. Can. (in press).

Ketchum, B. H., Redfield, A. C. and Ayers, J. C. (1951). Oceanography of the New York Bight: Pap. Phys. Oceanog. and Meteorol., vol. 12, no. 1, pp. 1-46.

Mason, W. D. and Pietsch, W. H. (1940). Salinity movement and its causes in the Delaware River estuary: Trans. Amer. Geophys. Union, vol. 21, pp. 457-463.

Pritchard, D. W. (1952). The physical structure, circulation and mixing in a coastal plain estuary: Chesapeake Bay Inst. of The Johns Hopkins Univ. Tech. Report III, Reference 52-2.

Pritchard, D. W. (1952a). Estuarine hydrography: Advances in Geophysics I, pp. 243-280.

Redfield, A. C. (1950). Notes on the circulation of a deep estuary: Proceedings of the Colloquium on The Flushing of Estuaries. Woods Hole Oceanographic Institution, Reference 50-37.

Redfield, A. C. (1951). The flushing of harbors and other hydrodynamic problems in coastal waters: Hydrodynamics in Modern Technology. Mass. Inst. Tech., pp. 127-135.

Tully, J. (1949). Oceanography and prediction of pulp mill pollution in Alberni Inlet: Bull. Fish. Res. Bd. Can., vol. 83, 169 pp.

Contribution No. 643

SALT NUCLEI IN MARINE AIR AS A FUNCTION OF ALTITUDE AND WIND FORCE

By A. H. Woodcock

Woods Hole Oceanographic Institution [1]

(Manuscript received 24 February 1953)

ABSTRACT

Large differences are shown to occur in the numbers and sizes of sea-salt particles in marine air over the sea as the altitude, position, and the time of sampling are varied. Increases in the amount of air-borne salt near cloud base are related to increases in wind force at the sea surface. The greatest proportionate increase in particle number occurs at the large end of the weight range. Most of the samples reported here were taken near the Hawaiian Islands. The differences in nuclei number and size with increasing altitude in the lower atmosphere are similar in pattern in Hawaii, Florida and South Australia.

It is suggested that bursting air bubbles in "white caps" on the open sea are a major source of the salt nuclei, and that a greater portion of the sea surface may act as a source of these particles during average winds than might be judged from the relatively small area usually covered by white caps.

1. Introduction

Recent developments in the study of rain-forming mechanisms have indicated the importance of very large condensation nuclei in the formation of rain by accretion [2;10]. Large sea-salt nuclei have been found at cloud levels in marine air over land, and their number and weight have been shown to agree in part with the assumption that each salt particle becomes a raindrop [19]. The purpose of the present paper is to indicate some of the great variations which occur in the number and size of large air-borne salt particles at cloud levels in marine air, as a contribution to the detailed study of the role of sea-salt in atmospheric processes. For example, knowledge of the details of these variations is essential to study the relationship of the salt particles in the clear air in the environment of clouds to the precipitation elements within these clouds [14;19].

2. Methods

The salt particles impinge upon and adhere to small glass slides which are exposed from aircraft. The slides are then taken to the laboratory where measurements and counts are made with a microscope of the sizes of individual particles at a relative humidity of 90 per cent, the weight being computed from these size measurements using an isopiestic method [6]. The values for salt-nuclei weight derived in this manner have been tested by direct titration of chlorides. Details concerning sampling methods have been published by Woodcock and Gifford [17] and Woodcock [19], and no further discussion of them will be given here.

3. Increasing wind force and increasing salt content of air

Moore [12] and Fournier [5] have measured an increase in the number and size of large salt particles in the air near the sea surface as the wind speed increases. For cloud physics studies, however, it seems necessary to know the distribution of these particles at cloud heights.

Over the sea in Hawaii, salt-particle samples were taken at cloud levels on thirty-seven days. On twenty-four of these days, most of the range of particle size present on the sampling slides was counted and measured. The average size distributions of the particles in the air on these twenty-four days are given on fig. 1. (On the remaining days only the large nuclei were measured.)

The distribution curves on fig. 1 show that greater wind force in the Hawaiian area is associated with a rather consistent pattern of increase in numbers and sizes of particles near cloud base. It is expected that a comparable pattern of increase will probably be found in most marine atmospheres having a similar fetch, and which also have a similar water-vapor, temperature and velocity distribution throughout the previous several days of movement of the air.

The differences between the values obtained at a given wind force in Hawaii, Australia and Florida, are attributed primarily to differences in the history of the air preceding its arrival at the time and place of sampling, and to errors inherent in estimations of wind force. Note on fig. 6 that the observed force

[1] Contribution No. 643 of the Woods Hole Oceanographic Institution, Woods Hole, Mass. This study was supported by the Office of Naval Research, under Contract Nonr-798(00) (NR-085-001).

3–4 winds are associated with a salt distribution near cloud base (790 m) equal to the average found during a force 5 wind in Hawaii, as shown on fig. 1. Conversely, on fig. 7 note that the observed force 6 wind is associated with a salt distribution curve near cloud base (640 m) which falls between the force 3 and 5 curves on fig. 1. A further discussion of sources of error in relating wind force to salt particle distribution

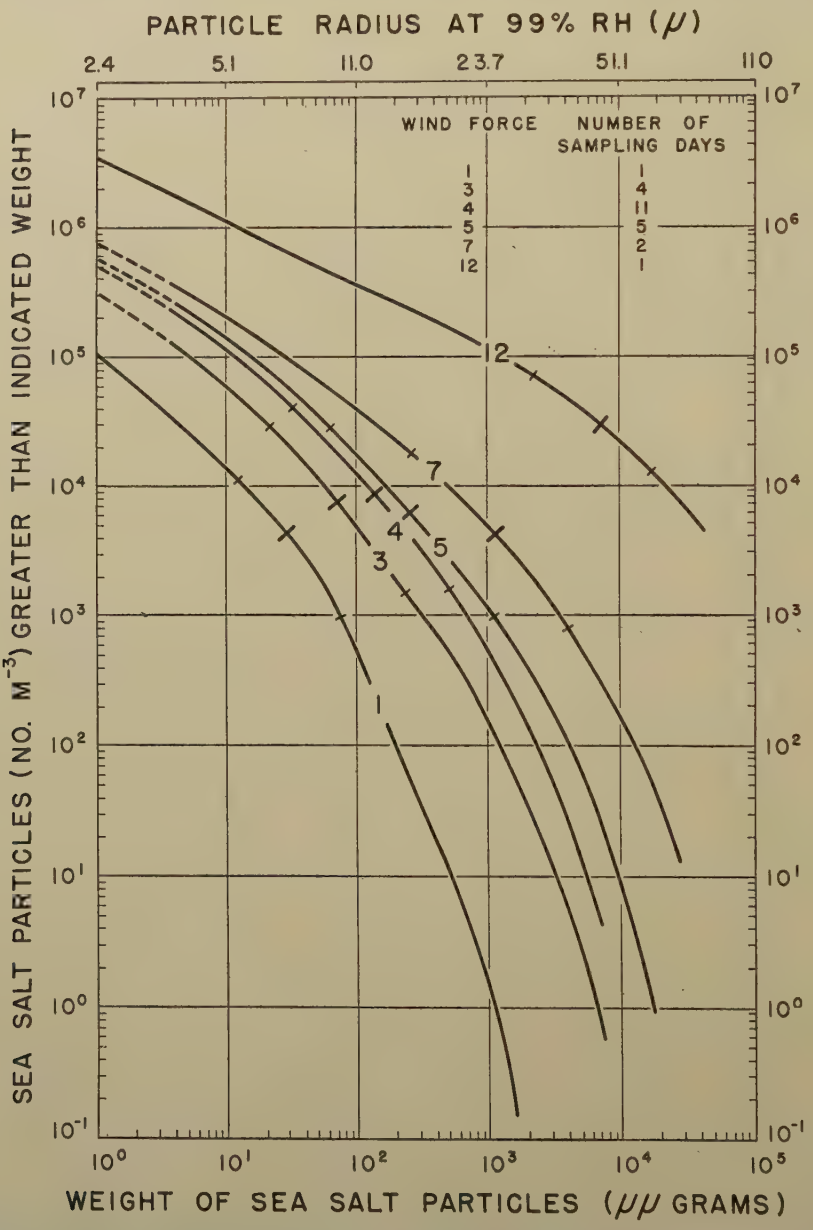

Fig. 1. Effects of varying wind force upon number and weight of large sea-salt particles near cloud base over sea in Hawaii area. Smoothed distribution curves for forces 3, 4, 5 and 7 based upon averaging of results obtained on days when these forces were observed (see legend). Curves for forces 1 and 12 based upon observations for one day only. Three short transverse lines on each curve mark first quartile, median and third quartile weight-distribution points, reading left to right. Distribution curves are read as follows: in force 5 wind, there are about 10,000 particles m^{-3} larger than 170 $\mu\mu$g. Force 12 curve based upon measurements made in Florida within a tropical storm, and included here as indication of probable maximum amount of airborne salt.

seems unnecessary at the present stage of the study.

As indirectly indicated in fig. 1, a great increase is observed in the total amount of sea salt in the air as wind force increases. This is shown by fig. 2, which gives values for all of the thirty-seven sampling days,[2] and also a few measurements obtained in hurricane force winds. Measurements made by Jacobs [7] at La Jolla, California, are also shown on fig. 2. The marked difference in the amounts of salt given by Jacobs and the author is probably due to the fact that Jacobs' samples were taken on the shore at La Jolla behind the surf line, whereas most of the samples reported here were taken near cloud base.

Emphasis should be given to the fact that the individual values for total sea salt on fig. 2 represent, in each case, averages obtained along flight paths thousands of meters in length, and that they cannot be regarded as representing the salt present in any small portion of the paths traversed. As an indication of the variability along flight paths of similar length, seven salt samples were taken on a 65-km horizontal run with constant course in the cloud layer, at an altitude of 1220 m. Each sample represented an averaging in 2700 m of air, with a 7200-m interval between them. Surface winds were force 3. These seven samples showed a variation in total weight of sea salt of from 2×10^{-6} to 4×10^{-6} g m^{-3}. If the sampling had been limited to shorter air paths, a greater variability would probably have been found.

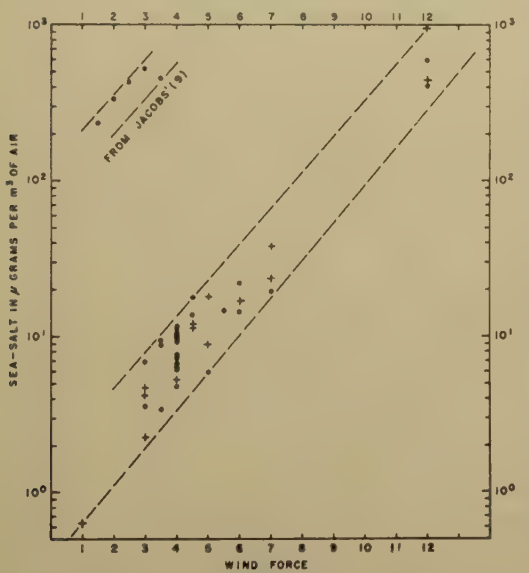

FIG. 2. Variation in total amount of air-borne sea salt as wind force varies. Most of samples taken at cloud levels in Hawaii, June 1951 to July 1952. Upper symbols represent data taken from Jacobs [7]. His measurements were obtained near seashore at Scripps Institute, La Jolla, Calif. Dashed lines are added as aid to note broad trend of observed values.

[2] As previously noted, only the larger nuclei (>10 to 100 $\mu\mu$g) were measured on some of the sampling days. To save time and effort, these data were not included in deriving the average curves on fig. 1. There is no indication that their inclusion would significantly modify these curves. The addition of the total salt values from these data to fig. 2 is useful, however, and is justified by the fact that the larger nuclei which were measured contain most of the salt (see mass distribution points on fig. 1).

It is expected that further measurements, made during winds in excess of force 7, will reveal the presence at cloud levels of particles as large or larger than 10^5 $\mu\mu$g. At the small end of the weight spectra the curves shown on fig. 1 are ended at about 4 $\mu\mu$g because, on many of the sampling days, the smaller particles on the slides were not counted.

The great increase in the number and size of sea-salt particles at cloud level, which is associated with higher winds, is thought to be due primarily to an increase in the number of bubbles produced in "white caps" at the sea surface. In the laboratory, the bursting of air bubbles (estimated diameters 50 to 500μ) at the surface of sea water is found to project small droplets of various sizes into the air. These droplets contain sea salt which has a weight range comparable to that observed among particles found in the air over the sea. Other laboratory observations concerning this bubble-droplet mechanism have been made in distilled water by Stuhlman [16], and in sea water by Aliverti [1] and Facy [4]. As suggested by the above laboratory tests, the bubble patches which result from breaking waves at the sea surface are found by the author to be sources of miniature clouds of droplets which are rapidly dispersed by the wind. Similar observations of bubbles as a source of nuclei have been made by Boyce [3] in the surf on a Carolina beach. As the foam patches on the open sea become more numerous and greater in extent with higher winds, a larger proportion of the sea surface becomes a source area for particles. Individual foam patches, during a force 5 wind, remain clearly visible from aircraft as turbid or cloudy areas for more than two minutes, indicating the presence of bubbles slowly rising to the surface long after the occurrence of the obvious white cap. Thus a larger proportion of the sea surface is probably a source of particles arising from bursting bubbles than might be judged from the number of readily visible white caps.

As a result of the above preliminary observations, a further study is now being made of the role of bursting bubbles in the formation of salt nuclei in the air overlying the sea.

4. Increasing altitude and decreasing salt

Some indication of the variability of salt content with altitude and with wind force in Hawaii is shown on figs. 3, 4 and 5. In both the subcloud and cloud layers of air there is a general increase in the amount

of salt as the wind increases. At the highest sampling levels, in cloud-free dry air, the quantity of salt is very low and the variations in the amount present seem to be unrelated to surface wind.

The most obvious feature of the distribution curves on figs. 3, 4 and 5 is the rapid decrease of salt with height. On the basis of these and other samples [19], the lower atmosphere in the trades can be divided roughly into three layers: the layer extending from about 50 m above the sea to cloud base, the layer from cloud base up to the trade-wind inversion where the clouds are usually stopped [13], and the air above the inversion. Ascent from one of these layers to the next always reveals a marked decrease in salt. This decrease also appears in samples taken in marine air in Florida and Australia (see figs. 6 and 7). The altitudes of the clouds and the temperature distributions are shown by the insert graphs on each figure.

The environment of cumulus clouds (which develop in the air represented by figs. 3 through 8) is, there-

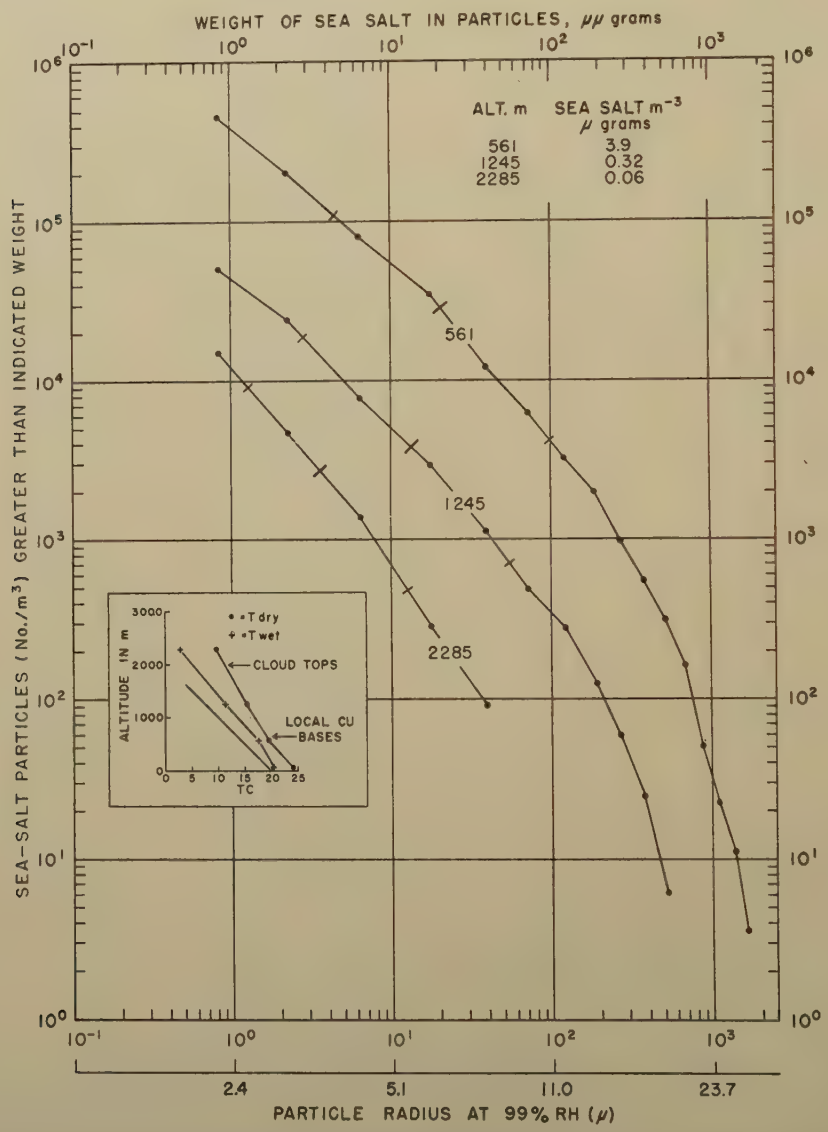

Fig. 3. Vertical distribution of salt particles over sea in Hawaii (21°30′N, 157°40′W), 4 June 1951, 1230 local time. Surface wind 60 deg, force 3. Widely scattered cumulus clouds. See legend to fig. 1.

fore, one of rapid change in the numbers and sizes of salt particles. The clouds may draw much of their air from the subcloud layer, while their tops commonly extend up into relative salt-free air. The number of large salt particles found within these clouds at any given height will depend, in part, upon the relative

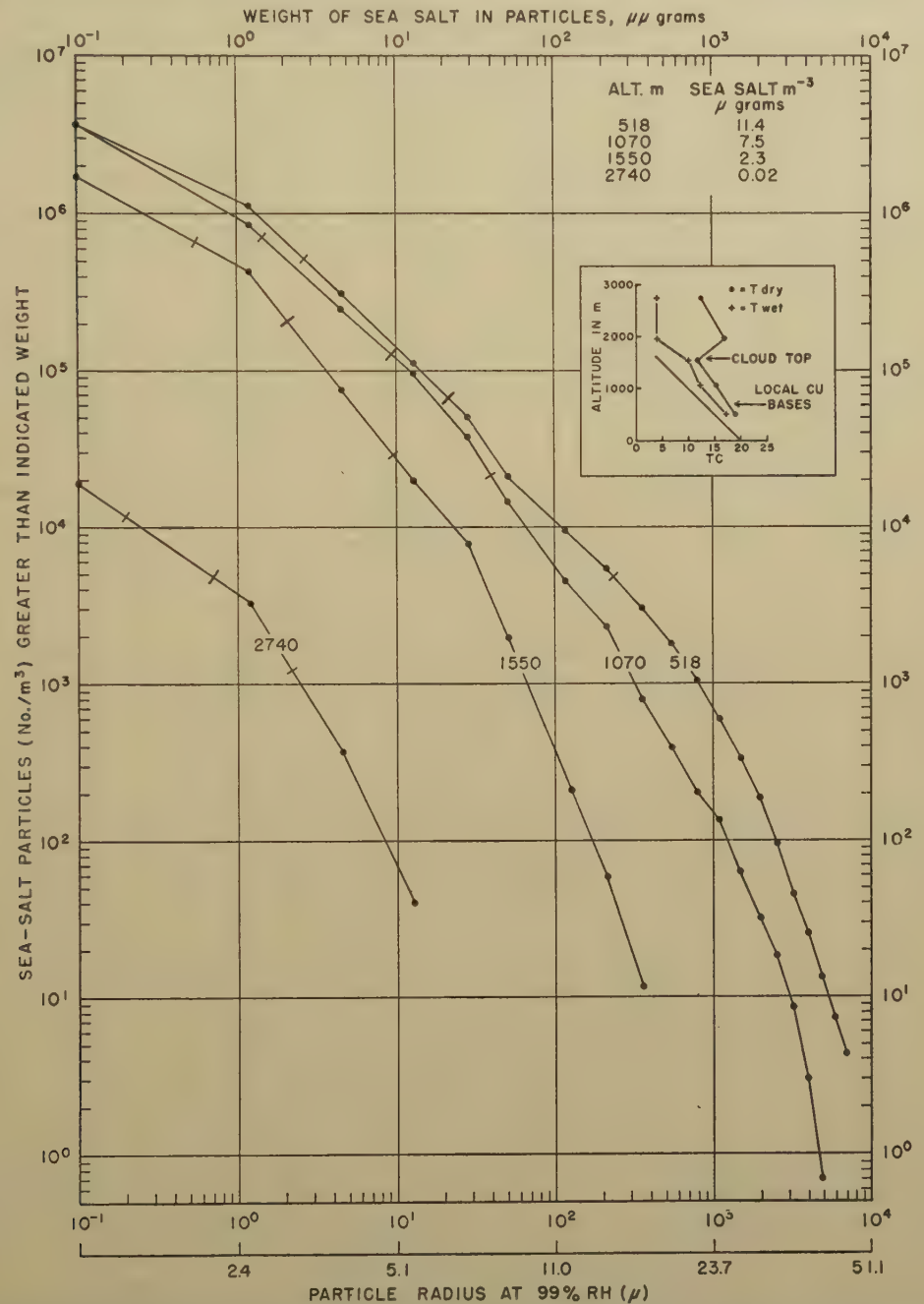

FIG. 4. Vertical distribution of sea-salt particles over sea in Hawaii (21°30'N, 157°40'W), 30 May 1952, 1300 local time. Surface wind 80 deg, force 4 to 5. Height of scattered cumulus cloud bases varied from 640 to 760 m. Temperature at 2740 m, 12.8C. See legend to fig. 1.

proportions of cloud air which are "entrained" as the cloud ascends [11;15]. Thus it may prove to be difficult to assign very definite numbers to the nuclei which should be found within a cumulus cloud at various levels, on the basis of measurements of the nuclei sizes in the clear air near the cloud base.

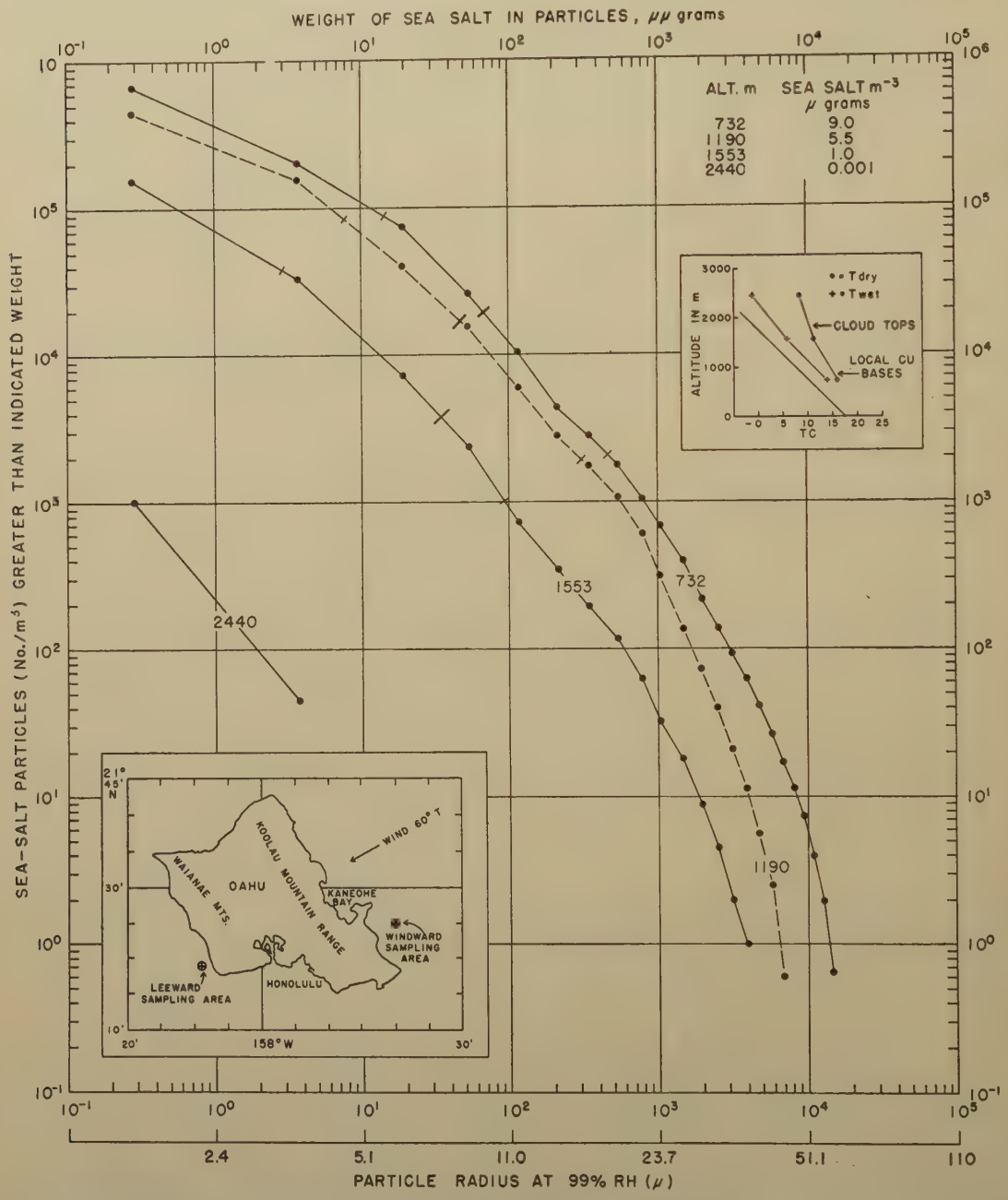

Fig. 5. Vertical distribution of salt particles over sea (21°25'N, 157°40'W) on windward side of Oahu on 22 April 1952, 1140 local time. Surface wind 70 deg, force 5. See legend to fig. 1. Observed points connected by dashed line (1190 m) represent particle distribution on lee side of Oahu (see map), 1500 local time, 22 April 1952.

At present, little is known about the relationship between the numbers of large salt particles in the clear air and the numbers of the sparsely distributed large droplets within the clouds, though a beginning has been made in a recent study by Squires and Woodcock of cumulus and strato-cumulus clouds in maritime air in southern Australia [14]. Many similar observations are needed to enable us to relate the size distribution of the largest cloud droplets in the numerous cloud types to the size distribution of the salt nuclei in the clear air surrounding the cloud.

Most of the studies of salt distribution (figs. 3–8) have been made in regions of large scale divergence and sinking within the atmosphere. Samples taken in the same areas during periods of large scale convergence and ascent should reveal a very different graphical picture of the distribution, the salt aerosols in this case being carried to much higher levels.

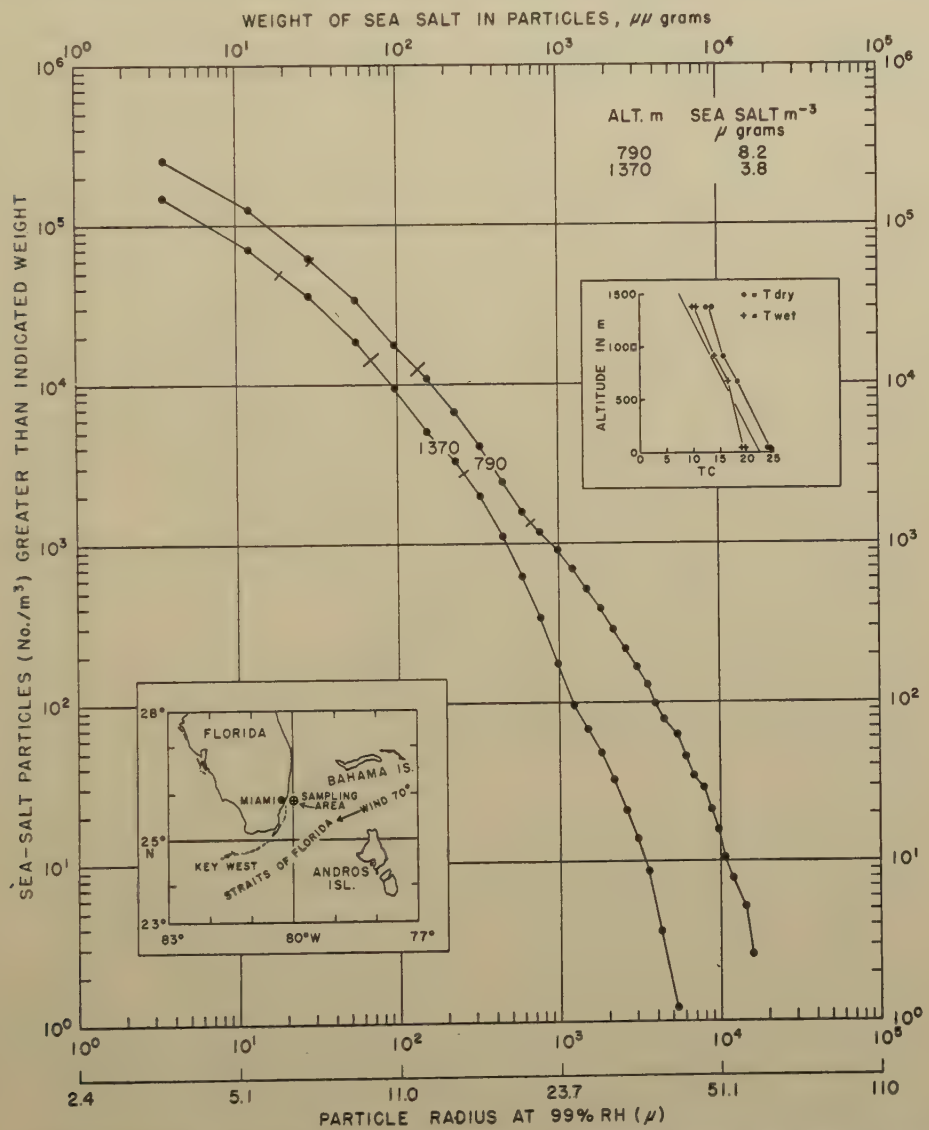

FIG. 6. Average distribution of sea-salt particles in oceanic air over sea east of Florida (see insert map), 8 and 14 November 1951. Surface winds force 3 to 4, 65 deg. Data from 790 m represent samples taken about 100 m below local cumulus clouds, and data from 1370 m represent samples taken in clear air among clouds. See legend to fig. 1.

5. Modification of salt-particle distribution by passage over islands

On 22 April, 1952, samples were taken on the windward and leeward sides of the island of Oahu (see positions on insert map, fig. 5). The continuous lines on fig. 5 show the distribution of particles on the windward side before the air arrived over the island, and the broken line shows the distribution just below cloud base after the air had passed over the island. No profound change has occurred in the numbers of particles as a result of passage over about 32 km of land and over a mountain range having an average altitude of about 600 m. It was observed that no rain was falling in the mountain areas at the time of the lee-side sampling.

On the large island of Hawaii however, a very great decrease was found in the amount of salt near the bases of large cumulus clouds over land, when a com-

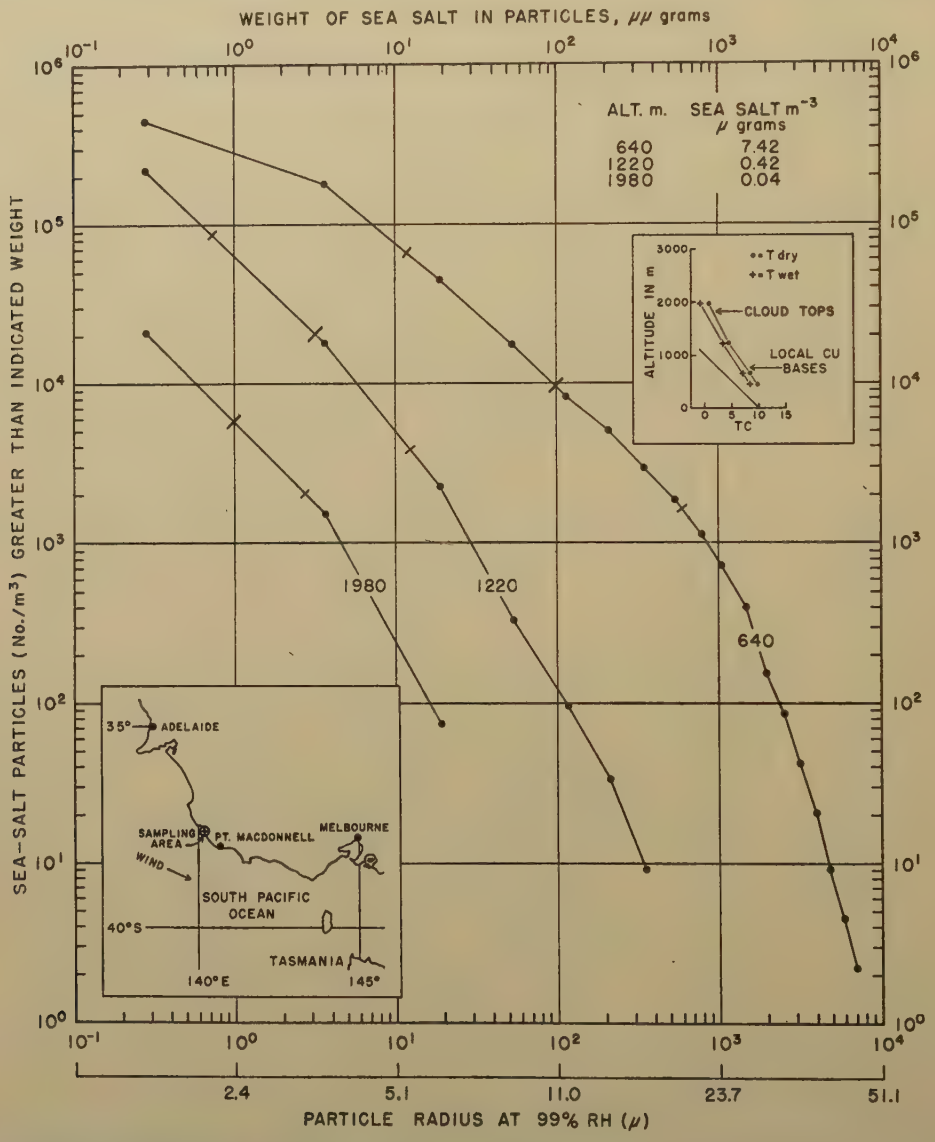

Fig. 7. Vertical distribution of sea-salt particles over Southern Ocean, off coast of S. Australia (37°40′S, 140°12′E), 9 August 1952, 1630 local time. Surface wind 300 deg, force 6. Height of scattered cumulus cloud bases varied from 305 m to 790 m during observation period; tops from 1830 to 1980 m. Rain showers visible during flight. Temperature at 1980 m, 0.5 to 1.4C. See legend to fig. 1.

parison was made with the amount present near cloud base over the windward sea (see comparative distribution curves and sampling positions on fig. 8). The curve representing salt particles over land is, in this case, similar to those derived from samples taken at the highest levels over the sea (see figs. 3

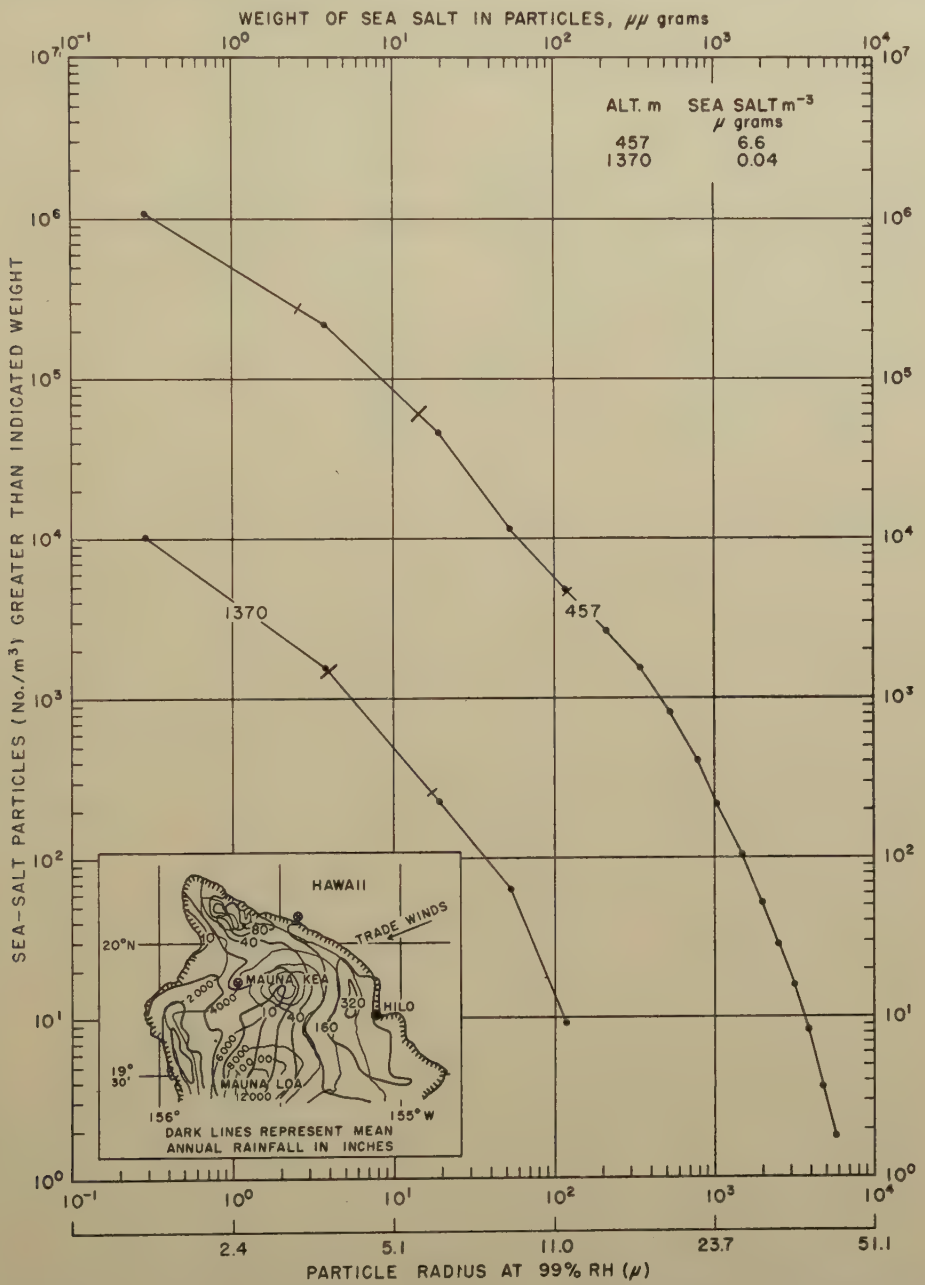

FIG. 8. Comparison of amounts of salt at height of 457 m over sea on windward side of Hawaii, and that over land on lee side of great mountain Mauna Kea at altitude of 1370 m. Sampling positions shown by circled X marks on map. Samples taken on 20 and 21 March 1952, about 100 m below bases of local cumulus clouds. Isohyets on map taken from Leopold [10].

and 4). The great decrease observed over the land area is tentatively attributed to rain-out of the large salt nuclei in the windward high-rainfall areas (see isohyetal lines on map), and perhaps in smaller part to descent of salt-free high level air in a "land-breeze" which, according to Leopold [9], occurs at night on the windward face of the great mountain Mauna Kea.

The presence of well developed cumulus clouds over land in air relatively free from large salt particles is of interest to those concerned with inducing rain by accretion processes. Initially, these clouds will most probably contain very few large droplets, as compared to clouds developed in the air flowing in from the sea on the windward shore (see relative particle sizes on scale at base of diagram, fig. 8). If it is assumed that the larger particles grow to raindrop size more rapidly [8], it is reasonable to suppose that clouds containing smaller salt particles will require more time to produce rain naturally [10]. Exploration of the frequency of occurrence of relatively salt-free and moist air in Hawaii and other regions may prove useful, for the seeding of clouds formed in this air with larger water or salt particles, is more likely to reduce markedly the time required for them to produce rain.

Acknowledgments.—The writer is indebted to Mr. W. A. Mordy of the Pineapple Research Institute, Experiment Station of the Hawaiian Sugar Planters' Association and the Territorial Cattleman's Council, for the opportunity to work in Hawaii, and to Dr. E. G. Bowen of the Commonwealth Scientific and Industrial Research Organization, Sydney, for the opportunity to work in South Australia. The writer is also grateful to Dr. G. Walton Smith for the use of the facilities of the Marine Laboratory, University of Miami, Coral Gables, Florida.

REFERENCES

1. Aliverti, G., and G. Lovera, 1950: Sui nuclei de condensazions de origine marittime. *Geofis. pura applic.*, **16**, 133–135.
2. Bowen, E. G., 1950: The formation of rain by coalescence. *Austr. J. sci. Res.*, A, **3**, 193–213.
3. Boyce, S. G., 1951: Source of atmospheric salts. *Science*, **113**, 620–621.
4. Facy, L., 1951: Éclatement des lames minces et noyaux de condensation. *J. sci. Meteor.*, Paris, **3**, 86–98.
5. Fournier, D. E. M., 1951: Sur les embruns marins *Bull. Inst. Oceanogr. Monaco*, **48**, No. 995, 7 pp.
6. Glasstone, S., 1946: *Textbook of physical chemistry.* Van Nostrand Co., New York, 2nd ed., 1320 pp.
7. Jacobs, W. C., 1937: Preliminary report of a study of atmospheric chlorides. *Mon. Wea. Rev.*, **65**, 147–151.
8. Langmuir, I., 1948: The production of rain by chain reaction in cumulus clouds at temperatures above freezing. *J. Meteor.*, **5**, 175–192.
9. Leopold, L. B., 1949: The interaction of trade wind and sea breeze, Hawaii. *J. Meteor.*, **6**, 312–320.
10. Ludlam, F. H., 1951: The production of showers by the coalescence of cloud droplets. *Quart. J. r. meteor. Soc.*, **77**, 402–417.
11. Malkus, J. S., 1952: The slopes of cumulus clouds in relation to wind shear. *Quart. J. r. meteor. Soc.*, **78**, 531–542.
12. Moore, D. J., 1952: Measurements of condensation nuclei over the North Atlantic. *Quart. J. r. meteor. Soc.*, **78**, 596–602.
13. Riehl, H., *et al.*, 1951: The north-east trade of the Pacific Ocean. *Quart. J. r. meteor. Soc.*, **77**, 598–626.
14. Squires, P., and A. H. Woodcock, 1953: Simultaneous observations on sea-salt nuclei and cloud droplets. Manuscript.
15. Stommel, H., 1947: Entrainment of air into a cumulus cloud. *J. Meteor.*, **4**, 91–94.
16. Stuhlman, O., Jr., 1952: The mechanics of effervescence. *Physics*, **2**, 457–466.
17. Woodcock, A. H., and M. M. Gifford, 1949: Sampling atmospheric sea salt. *J. marine Res.*, **8**, 177–197.
18. Woodcock, A. H., 1950: Sea salt in a tropical storm. *J. Meteor.*, **7**, 397–401.
19. ——, 1952: Atmospheric salt particles and raindrops. *J. Meteor.*, **9**, 200–212.

Contribution No. 644

Reprinted from SCIENCE, June 5, 1953, Vol. 117, No. 3049, pages 639–640.

Rapid Aerial Survey of Gulf Stream with Camera and Radiation Thermometer[1]

During the cold half of the year a sharp discontinuity of surface temperature (often amounting to 20° F in less than 100 yd) occurs along the northern border of the Gulf Stream. The recent discovery (*1*) of meanders in the Gulf Stream has stimulated efforts to devise rapid means for surveying its course, and we (Parson and Stommel) decided to investigate the possibility of tracing the thermal discontinuity on the ocean surface by flying an infrared detector along it.

A Goylay detector (*2*) is exposed alternately to the sea surface and to a reference black body in the instrument by means of a rotating shutter. The temperature of the black body is adjusted by admitting hot or cold water into it until the chopped signal from the Golay cell is nulled. Were there no absorption and emission of thermal radiation by the atmosphere between the cell and the sea, the temperature of the black body would be that of the sea surface. In practice, however, a minimum altitude of 1000 ft is safe over long ocean flights. Enough radiation from the sea penetrates the lowest 1000 ft of the atmosphere to make the sharp thermal discontinuity easily detectible, although the actual temperature of the sea surface is not indicated by that of the black body.

To date three surveys have been made. Positions of the thermal discontinuity on Nov. 26, 1952 are shown in Fig. 1 by dots; the visual evidence of the northern edge of the Stream cited by Kielhorn (*3*) (contrast in color and sea-state) was confirmed. A wide angle (80°) time lapse (72 frames/min) motion picture camera directed straight ahead (von Arx) recorded visual evidence of the edge of the Stream at positions marked by segments of curves on the figure. The general appearance of the course of the Stream is similar to that obtained by ship (*4*).

[1] Contribution No. 644 of the Woods Hole Oceanographic Institution, work supported by the Bureau of Aeronautics and the Office of Naval Research. A Navy PBY airplane carried the apparatus.

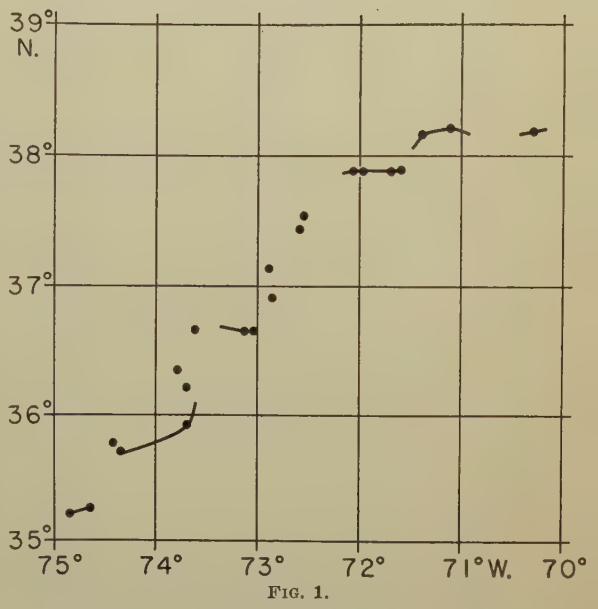

FIG. 1.

The primary obstacle to extending this type of survey to areas further to the east is the range and endurance of aircraft; but it does seem quite clear that an airborne infrared detector is capable of providing an almost synoptic oceanographic chart of surface thermal gradients over a much greater area and in a shorter time than can be obtained using surface vessels.

HENRY STOMMEL
W. S. VON ARX
D. PARSON
W. S. RICHARDSON
Woods Hole Oceanographic Institution
Woods Hole, Massachusetts

References

1. FUGLISTER, F. C., and WORTHINGTON, V. *Tellus*, **3**, 1 (1951).
2. GOLAY, M. J. E. *Rev. Sci. Instruments*, **18**, 357 (1947).
3. KIELHORN, M. V. Unpublished manuscript (1950).
4. ISELIN, C. O'D., and FUGLISTER, F. C. *J. Market Research*, **7**, 317 (1948).

Contribution No. 645

EXAMPLES OF THE POSSIBLE ROLE OF INERTIA AND STRATIFICATION IN THE DYNAMICS OF THE GULF STREAM SYSTEM[1]

By

HENRY STOMMEL

Woods Hole Oceanographic Institution

ABSTRACT

An hypothesis is offered to explain certain major features of the Florida Current: (1) the large axial gradient of vorticity, (2) the fact that seasonal fluctuations in the Miami-Cat Key tide gauge difference are twice the amplitude of those in the Key West-Havana tide gauge difference, and (3) the fact that the Havana-Cat Key difference is at a maximum during the period of minimum flow—the opposite of what might ordinarily be expected. An elementary perturbation theory of meanders in a wide stratified current is presented and its possible application to Gulf Stream meanders is discussed.

1. *Introduction.* Recent successful oceanographic studies of the steady-state wind-driven ocean circulation (Munk, 1950; Hidaka, 1949) do not require inclusion of the effects of density stratification or of inertia terms. Transient or periodic phenomena in general involve both inertia and stratification explicitly, and it seems to this author that results obtained from theoretical consideration of homogeneous models may omit important features. For example, Ichiye (1951) has obtained an interesting solution for the wind-driven ocean circulation due to a periodic wind-stress acting on a homogeneous ocean. In a stratified ocean, however, the mass movements which must accompany changes in the circulation are many hundredfold those occurring in a homogeneous ocean, and changes in potential energy are correspondingly greater. This raises the question as to whether or not the time-constants which characterize the response of a stratified ocean to a periodic wind-stress will be the same as those obtained by Ichiye's solution. This paper does not attempt to answer this difficult question. Instead, it treats two problems, the mass distribution of the Florida Current and the stability and size of Gulf Stream meanders, in which stratification and inertia play essential roles.

2. *Florida Current Tide and Current Data.* Numerous studies of tide gauge data have been made (Montgomery, 1938, 1941; Iselin, 1940; Hela, 1952) to obtain information about seasonal fluctuations

[1] Contribution No. 645 from the Woods Hole Oceanographic Institution.

Reprint from SEARS FOUND. JOURN. MAR. RES.

in the cross-stream slope of the sea surface, and, by the geostrophic equation, to compute seasonal fluctuations of the mean surface velocity of the Florida Current. In addition to the tide gauge data already published for Key West, Miami, and Cat Key, tide gauge data for Havana are now available for the first time. These data are obtained from a gauge installed by the U. S. Coast and Geodetic Survey in 1946. Table I shows the monthly means of sea level (in feet)

TABLE I. Monthly Means of Sea Level (Feet), Each Referred to Separate Local Datum

Month	*Cat Key 1938–early 1941*	*Key West 1930–1948*	*Havana 1947–1951*	*Miami Beach 1935–1944*
Jan.	3.75	4.88	4.82	3.34
Feb.	3.77	4.83	4.80	3.34
Mar.	3.82	4.82	4.92	3.22
Apr.	3.90	4.93	4.95	3.34
May	3.94	5.01	5.10	3.48
Jun.	3.98	5.03	5.09	3.41
Jul.	4.07	5.03	5.06	3.33
Aug.	4.18	5.17	5.26	3.46
Sep.	4.29	5.37	5.37	3.79
Oct.	4.18	5.53	5.47	4.07
Nov.	3.94	5.33	5.06	3.84
Dec.	3.84	5.06	4.94	3.74

measured at these stations, averaged over different sets of years, uncorrected for atmospheric pressure, and each referred to a different datum. A leveling survey has been made between Key West and Miami (Montgomery, 1941), but obviously it is impossible to connect Havana or Cat Key to the same datum by ordinary means. Therefore we cannot obtain true differences in sea level across the Straits, but we can obtain fluctuations in the differences of sea level at two stations, as shown in Fig. 1. At all four stations there is a maximum sea level in September-October which is apparently caused by the summer heating of the water. This average rise does not appear in the differences.

It is interesting to note that the fluctuation in the Miami-Cat Key differences is about twice that of the Key West-Havana differences. The maximum cross-stream slopes occur during July when the flow is strongest (Fuglister, 1951), at which time the maximum downstream slope from Key West to Miami also occurs. These relations of slopes to surface velocity are quite what might be expected from the most elementary considerations of Bernoulli's equation and the geostrophic

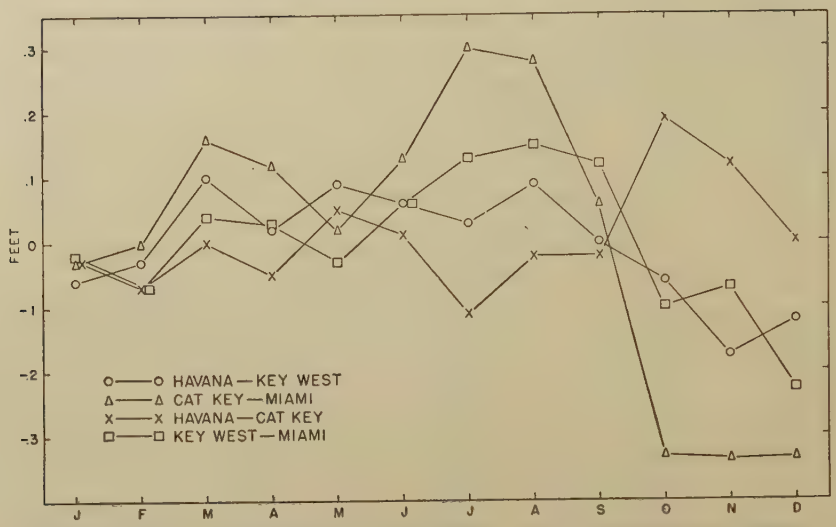

Figure 1. Monthly mean tide gauge differences for various pairs of stations, adjusted so that the annual mean of the differences vanishes.

equation. But at first sight it is rather startling that the fluctuations of the differences at Miami-Cat Key are larger than those at Key West-Havana and that the downstream slope between Havana and Cat Key is smaller in July rather than larger, hence an explanation is required.

Another noteworthy feature of the Florida Current is the extensive region of anticyclonic vorticity in the section off Miami. So far as direct velocity measurements from an anchored vessel are concerned, the data are scanty. The only observations at different depths are those of Pillsbury (1890), and these show a rapid decrease of velocity with depth. The axis of maximum surface velocity is not in the center but is displaced toward Miami; and this feature has been verified from many crossings of the Current off Miami by Murray (1952). Fig. 3 shows measurements with towed electrodes during one of these crossings, but it should be emphasized that towed electrodes are apt to give particularly misleading readings of velocity in the Florida Straits. Nevertheless, the general fact is that a wide zone of anticyclonic vorticity (of approximately $-[0.5 \pm 0.1]f$, where f is the local Coriolis parameter) seems to be established and also requires explanation. It is impossible, of course, for the variation of the Coriolis parameter with latitude to cause such shear over so short a distance as the length of the Florida Straits.

The channel at Miami is only about half as deep and half as wide as that at Key West, as shown in Fig. 2. The change in depth can

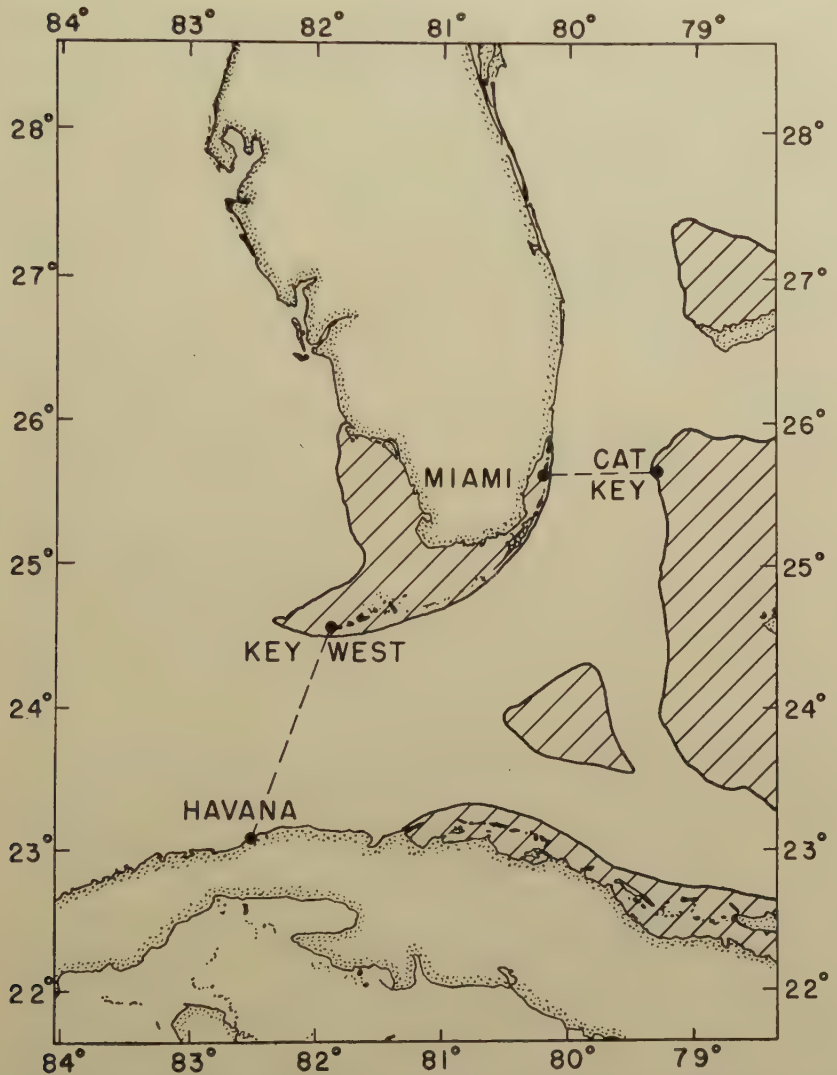

Figure 2. Chart of the Florida Straits showing the positions of the tide gauges.

have no important influence on the flow because the bottom water does not have an appreciable velocity at either section. On the other hand, the narrowing of the channel at Miami is important hydrographically because the water, in order to pass through it, is accelerated, and this requires a small drop in the level of the free surface from Key

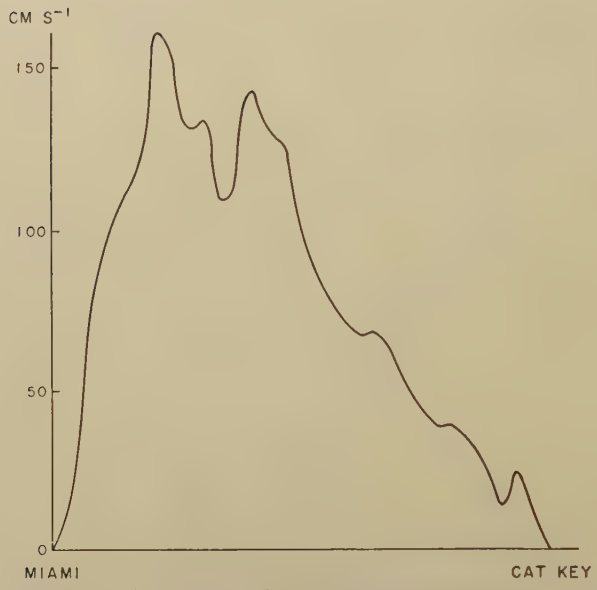

Figure 3. One of Murray's cross-stream surface velocity profiles made across the Florida Current off Miami.

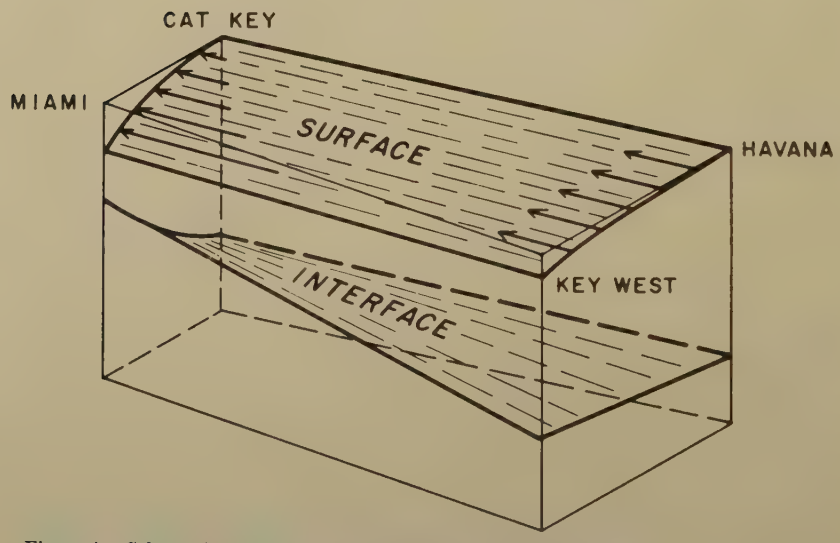

Figure 4. Schematic diagram showing configuration of the free surface (exaggerated scale) and of the interface in the hypothetical model of the Florida Current.

West to Miami. Since the lower layers are at rest (except for tides), the isopycnic surfaces must slope upward from Key West toward Miami to counteract the axial pressure gradient in the upper accelerating layers. Because this slope must be some 500 times the drop of the free surface, it produces a marked decrease in the thickness of the surface layers as Miami is approached. By virtue of the principle of conservation of absolute vorticity, this vertical shrinking produces an anticyclonic shear and magnifies the transverse geostrophic slope of the free surface. A crude quantitative analysis based on a two-layer model is presented in the following section. Fig. 4 illustrates the average hydrographic structure of the Florida Current envisaged in this hypothesis.

3. *Application of the Vorticity Theorem to the Florida Current.* Consider a layer of water of density ρ_1, depth D, overlying a deep resting layer of density ρ_2. The upper layer has a velocity U at the Key West-Havana section ($x = 0$) and its vorticity is taken as zero. Further downstream ($x = \Delta x$), at the narrower Miami-Cat Key section, the stream has accelerated by a drop in the free surface Δh. Because the lower layer is at rest, the interface must slope upwards to offset the effect of the free surface. If the axial pressure gradient vanishes in the lower layer then the following relation must hold:

$$\frac{\rho_2 - \rho_1}{\rho_2} \frac{\partial D}{\partial x} = \frac{\partial h}{\partial x} .$$

The vorticity equation in this simple case may be written as follows, where ζ is the vorticity of the upper layer:

$$U \frac{\partial}{\partial x} \left(\frac{\zeta + f}{D} \right) = 0 ,$$

where a steady state of motion is presumed. Since the vorticity vanishes at Key West, that at Miami is given approximately by

$$\Delta\zeta = f \frac{\Delta h}{D} \frac{\rho_2}{\rho_2 - \rho_1} .$$

The actual acceleration observed at Miami corresponds to a value of Δh of about $-$ 20 cm (this is somewhat in excess of the $-$ 4.9 cm obtained by leveling between Key West and Miami, according to Montgomery, 1941). The density difference of the two layers is approximately $(\rho_2 - \rho_1)/\rho_2 \cong 2 \times 10^{-3}$. The initial depth D of the current is roughly 250 m, which yields a value of the vorticity increase between Key West and Miami of $\Delta\zeta \cong -0.4f$, which corresponds

within the limit of observational error to the observed value given above.

If the high anticyclonic vorticity at Miami is actually due to the vertical shrinking of the upper layers, then it should be possible to test this hypothesis by careful hydrographic observations on the two sections to try to detect the average rise of about 100 m in the isopycnic surface at 100–300 m depth. It will be difficult and tedious to measure this hypothetical rise because it may be partly masked by the large cross-stream slope of the isopycnic surfaces and by variations in depth due to tides. Present data are insufficient to attempt a satisfactory test.

4. *Gulf Stream Meanders.* The Gulf Stream meanders observed on the Multiple Ship Survey of June 1950 (Fuglister and Worthington, 1951) have inspired several theoretical studies. It has been suggested that they are analogous to the waves in the atmospheric jet stream, but both their small scale (100–400 km) and small velocities of propagation suggest that the variation of the Coriolis parameter with latitude is not a dominant factor in their dynamics. Haurwitz and Panofsky (1950) have constructed several models of currents in a homogeneous ocean with cross-stream velocity profiles similar to those observed in the true Gulf Stream and have carried out an intricate perturbation analysis to show the existence of unstable waves with reasonable velocities of propagation. These waves are a result of the shearing instability of the Stream.

It seemed to the writer that, if stratification were taken into account, certain types of meanders might exist in which horizontal divergence was dynamically important. In order to illustrate such a system, meanders in a wide current were studied. To simplify the analysis, the realistic cross-stream velocity profiles of Haurwitz and Panofsky were abandoned. The density stratification of the real ocean is approximated by a two-layer system such as that used in Section 3.

5. *A Simple Meander Theory for a Wide Current in a Stratified Ocean.* Let us suppose that the lower layer is sufficiently deep so that the horizontal pressure gradients vanish in it at all times. In the undisturbed state a steady current U flows in the x-direction in the upper layer. Associated with this current is a cross-stream pressure gradient of the following form:

$$fU = -g\frac{\partial h}{\partial y} = -g\frac{\partial D}{\partial y}\frac{\Delta\rho}{\rho}.$$

We now suppose that small perturbations, u, v, the velocity components, and h, the elevation of the free surface, occur, and that these

quantities are independent of y, the cross-stream co-ordinate. The perturbation equations may be written in the form:

$$\left(\frac{\partial}{\partial t} + U\frac{\partial}{\partial x}\right)u - fv = -g\frac{\partial h}{\partial x}, \tag{1}$$

$$\left(\frac{\partial}{\partial t} + U\frac{\partial}{\partial x}\right)v + fu = 0, \tag{2}$$

$$\left(\frac{\partial}{\partial t} + U\frac{\partial}{\partial x}\right)\left(\frac{\rho}{\Delta\rho} + 1\right)h + D\frac{\partial u}{\partial x} + v\frac{\partial D}{\partial y} = 0. \tag{3}$$

If the perturbations are all in the form $e^{i(kx-\sigma t)}$, we obtain the following frequency equation, taking f = constant:

$$k^2U^2(1-p)^3 - \left[f^2 + gk^2\frac{\Delta\rho}{\rho}D\right](1-p) + f^2 = 0,$$

where $p = \dfrac{c}{U} = \dfrac{\sigma}{kU} = p' + ip''$, the real part ($p'$) of which is the ratio of the velocity of propagation of the wave to the velocity of the current, and the imaginary part (p'') of which gives the instability of the wave motion. For the particular range of parameters involved, no one of these terms is small compared to the others. It is convenient to rewrite this equation in the form:

$$y^3 + 2 = \P y,$$

where $\P = 2\left(\dfrac{f^2}{2k^2U^2}\right)^{\frac{1}{3}}\left(\dfrac{f^2 + gk^2\frac{\Delta\rho}{\rho}D}{f^2}\right)$ and $y = \left(\dfrac{f^2}{2k^2U^2}\right)^{-\frac{1}{3}}(1-p)$.

The roots of this equation are all real provided $\P \geqslant 3$, in which case there are three types of stable waves present. If $\P < 3$, there is a region of unstable waves. These are of most interest to us because they are the only ones that are likely to grow large enough to be noticed on a ship survey. Examination of the coefficients of the frequency equation reveals that for $U^2 < g\dfrac{\Delta\rho}{\rho}D$, all waves are stable. At $U^2 = g\dfrac{\Delta\rho}{\rho}D$, a single wave number given by $k = f/(\sqrt{2}\,U)$ becomes "just unstable," whereas all other wave numbers are stable. For slightly larger values of U^2 there is a narrow range of wave numbers about $k = f/(\sqrt{2}\,U)$ in which waves are unstable. In the critical case of marginal stability the "just unstable" wave is stationary.

One objection to the application of this model to the meanders observed in the Gulf Stream is that the real Stream is not very wide. A more sophisticated theory would include lateral boundaries to the Stream and would provide for resting layers of water on each flank beyond the boundaries. Also a perturbation theory such as this applies only to waves of infinitesimal amplitude, whereas meanders often grow to large amplitude. Therefore it is important to regard this treatment of meanders as merely indicative of the possible role of divergence terms in the meandering of a stratified current. Their physical reality must be tested by actual observation of the depth of the current in the crests and troughs of meanders.

6. *Application to the Actual Gulf Stream.* Rossby (1951) has shown that velocity of the Gulf Stream does in fact approach the critical value $\sqrt{g\frac{\Delta\rho}{\rho}D}$. In a steady state one might expect the Stream to become progressively shallower downstream, gradually approaching the critical condition. Because of the paucity of hydrographic sections of the Stream in any one year or season it is necessary to construct a composite series of sections in order to determine whether or not there is a noticeable change in the depth of the Stream along its axis. A number of sections, all made in early June of several years, have been assembled and recomputed: (1) one at Hatteras at about 74° W; (2) two more on the Montauk Point to Bermuda line surveyed in Iselin's (1940) studies; (3) one at 58° W; and (4) two Ice Patrol sections along the 50° W meridian. The geostrophic transports at different depths were computed. In order to exhibit any changes in the depth of the Stream, the percentage of the total transport below certain selected depths was computed. The results are given in Table II; it is clear that there is no striking change in the depth of the Stream as indicated by these sections. The inference to be drawn from this is that the Stream is near to the critical velocity almost everywhere from Cape Hatteras to the tail of the Grand Banks and that unstable meanders of a single wavelength might be expected anywhere.

We may ask ourselves what the size of the meanders predicted by our two-layer meander theory might be expected to be. A surface layer 200 m thick moving at 200 cm sec^{-1} and having a density difference ratio of $\Delta\rho/\rho = 2 \times 10^{-3}$ is critical. The wavelength of the "just unstable" perturbation corresponding to this choice of parameters is 180 km. All other wavelengths are stable and do not grow. It is remarkable that this wavelength corresponds closely to that of

the large stationary meander which was observed during growth and detachment into an eddy (Fuglister and Worthington, 1951).

During the process of growth this observed meander diverted momentum at right angles to the mean direction of the Stream; from mixing-length ideas we may calculate the order of magnitude of the local gross coefficient of lateral eddy viscosity due to this eddy: $A = U\,2\pi/k$, where k is wavelength of the detaching meander. Sub-

TABLE II. Percentage of Total Transport Below Selected Depths at Different Hydrographic Sections Along the Gulf Stream
(AT. = Atlantis; IP. = Ice Patrol)

Depth (*m*)	*74° W AT. 4570–4565*	*68° W AT. 2871–2867*	*68° W AT. 3058–3054*	*58° W AT. 2620–2616*	*50° W IP. 2715–2719*	*50° W IP. 4175–4184*
0	100	100	100	100	100	100
50	94	92	92	92	91	92
100	88	85	84	84	82	84
200	74	71	69	69	65	69
300	61	58	55	56	50	56
400	49	46	43	44	37	45
600	30	38	23	26	19	28
900	12	13	7	9	6	12
1200	4	7	2	3	2	4
1600	1	1	0	1	0	1
2000	0	0	0	0	0	0

stituting numerical values above, we obtain $A = 3.6 \times 10^9 \mathrm{cm^2 sec^{-1}}$, a value much in excess of that used by Munk (1950) in his wind-driven ocean circulation theory. If it is recalled that Munk assumed a uniform viscosity over the entire length of the Gulf Stream System and if it is assumed that there is usually but one detaching eddy at a time, then the discrepancy is not so glaring. The above value of A acts on only 90 km of the Stream, but if it is averaged over the entire length of 4,500 km, a value of 7×10^7 cm^2 sec^{-1} is obtained which agrees rather well with Munk's value 5×10^7. It is inferred, therefore, that the meanders alone produce sufficiently large scale lateral mixing processes for Munk's theory of the climatological mean Gulf Stream.

Since a thin filament of anomalously fresh water preserves its integrity all along the Gulf Stream proper (Ford, Longard, and Banks, 1952), it seems that the influence of mixing processes of a scale smaller than meanders must be negligible. The physical explanation of the process which determines the width and vertical structure of the instantaneous Gulf Stream is quite obscure.

In concluding, it is important to emphasize that the meander theory presented here is not complete or proven. It is merely suggestive of a type of wave-motion which may possibly dominate the dynamics of meanders. It is interesting to note that if the energy of meanders is absorbed from the potential energy of the cross-stream mass distribution instead of from the kinetic energy of the flow, the meanders are then a part of the thermohaline circulation of the ocean.

ACKNOWLEDGMENT

The writer wishes to express his indebtedness to Dr. Arnold Arons for many stimulating discussions of the subject matter of Section 2, to Mr. Sainsbury Strack for discussions of Section 5, to Commander Floyd Soule for advice concerning Section 6, and to the Office of Naval Research for financial assistance.

REFERENCES

Ford, W. L., J. R. Longard, and R. E. Banks
1952. On the nature, occurrence and origin of cold low salinity water along the edge of the Gulf Stream. J. Mar. Res., *11* (3): 281–293.

Fuglister, F. C.
1951. Annual variations in current speeds in the Gulf Stream System. J. Mar. Res., *10* (1): 119–127.

Fuglister, F. C. and L. V. Worthington
1951. Some results of a multiple ship survey of the Gulf Stream. Tellus, *3* (1): 1–14.

Haurwitz, B. and H. A. Panofsky
1950. Stability and meandering of the Gulf Stream. Trans. Amer. geophys. Un., *31* (5): 723–731.

Hela, I.
1952. The fluctuations of the Florida Current. Bull. mar. Sci. Gulf and Caribbean, *1* (4): 241–248.

Hidaka, Koji
1949. Mass transport in ocean currents and lateral mixing. Geophys. Notes, Tokyo, *2* (3): 1–4.

Ichiye, T.
1951. On the variation of oceanic circulation. (1st paper). Oceanogr. Mag., Tokyo, *3* (2): 79–82.

Iselin, C. O'D.
1940. Preliminary report on long-period variations in the transport of the Gulf Stream System. Pap. phys. Oceanogr. Meteorol., *8* (1): 1–40.

Montgomery, R. B.
1938. Fluctuations in monthly sea level on eastern U. S. coast as related to dynamics of western North Atlantic Ocean. J. Mar. Res., *1* (2): 165–185.
1941. Sea level difference between Key West and Miami, Florida. J. Mar. Res., *4* (1): 32–37.
1941. Transport of the Florida Current off Habana. J. Mar. Res., *4* (3): 198–220.

Munk, W. H.
1950. On the wind-driven ocean circulation. J. Meteor., *7* (2): 79–93.
Murray, K. M.
1952. Short period fluctuations of the Florida Current from geomagnetic electrokinetograph observations. Bull. Mar. Sci. Gulf and Caribbean, *2* (1): 360–375.
Pillsbury, J. E.
1890. The Gulf Stream . . . Report of the Superintendent, U. S. Coast and Geodetic Survey, for 1890, Appendix No. 10: 459–620.
Rossby, C.-G.
1951. On the vertical and horizontal concentration of momentum in air and ocean currents. Tellus, *3* (1): 15–27.
Wüst, G.
1924. Florida- und Antillenstrom . . . Veröff. Inst. f. Meereskunde, Berlin, N. F. A, *12:* 1–48.

Contribution No. 648

Reprinted from THE JOURNAL OF EXPERIMENTAL ZOOLOGY
Vol. 124, No. 1, October 1953

AUDITORY RESPONSE OF A BOTTLENOSED PORPOISE, TURSIOPS TRUNCATUS, TO FREQUENCIES ABOVE 100 KC [1]

WILLIAM E. SCHEVILL AND BARBARA LAWRENCE
Woods Hole Oceanographic Institution, Woods Hole, Massachusetts, and Museum of Comparative Zoology, Cambridge, Massachusetts

TWO FIGURES

INTRODUCTION

In the course of our studies of cetacean communication, we recently performed a simple conditioned response experiment on a small toothed whale, *Tursiops truncatus* (Montagu), commonly called bottlenosed porpoise or dolphin. This investigation, exploring the upper part of the range of frequencies responded to by this species, is part of a program of study of the sounds made by whales.[2] Our interest in the general subject includes the ways in which the sounds are made and heard, as well as the respective acoustic spectra involved, and especially the significance of these sounds to the whale. This paper deals with only one aspect of the problem of hearing. The earlier work leading up to it is briefly reviewed below (see Discussion, p. 158).

Since a cetacean is environmentally and anatomically cut off from the normal mammalian way of hearing, it necessarily depends on bone (body) conduction as the means of transmitting sound to the inner ear. From reports like that of Pumphrey ('50) on ultrasonic "hearing" by bone conduction in man, it is apparent that a cetacean may be expected to respond to a much wider band of frequencies than it can hear

[1] Contribution no. 648 from the Woods Hole Oceanographic Institution.

[2] This work, begun in 1948, has been largely supported by the Woods Hole Oceanographic Institution, and by the U. S. Navy Office of Naval Research under its Contract Nonr-167(00).

in the restricted sense of being able to discriminate pitch. It would be more precise, though more cumbersome, to say, instead of pitch, such characteristics of the auditory stimulus as frequency and intensity. It is not clear whether this ultrasonic hearing by bone conduction, at least in man, is anything more than a presence or absence sensation. As a first step in learning a porpoise's audible range, we set up the simple conditioned response experiment here described, showing the upper range of frequencies to which the animal responds. We intend in future to try some more complex tests, in the hope of learning such things as the range of frequency and intensity discrimination, as well as localization.

MATERIALS AND METHODS

Site and subject

For the site of this experiment we chose Marine Studios, near St. Augustine, Florida, which, as on many other occasions, were most hospitable in allowing the fullest use of their excellent facilities. Although they suggested that we work with the collection of *Tursiops truncatus* and *Stenella plagiodon* on exhibition in their Circular Oceanarium, we avoided the use of these specimens, since we distrusted the acoustics of that steel cylinder, 22.8 m in diameter and 3.6 m deep, with its complex background noises, and because we were suspicious of the uncertain psycho-physical effects of prolonged captivity. Moreover, the difficulties of assessing responses among a crowd of a dozen active porpoises of two species seemed unnecessarily large. Therefore we requested one fresh-caught, wild, adult *Tursiops,* which was installed in a separate enclosure. In spite of the fact that such a test as this would be more meaningful if made on a large series of individuals, we felt that at this stage of the problem a reconnaissance investigation of even a single animal would be informative.

The work was done in an enclosure at the end of a turbid mud-bottomed tidal inlet off the Matanzas River. Here the porpoise could swim about in an area approximately 20 by

55 m with a greatest depth of about 2.5 m at low water, and a tidal range of about 1 m. The fence was of coarse wire mesh, through which fish as large as 1 kg could pass easily. The water was so murky that a white object could not be seen through it at a greater distance than 30 cm. This pool was essentially anechoic, no echoes or reverberations being detected. However, it had a deplorably high background, chiefly caused by a relatively sparse population of snapping shrimp. This background noise level normally varied some 3 to 6 decibels, apparently to some extent with the tide, and ranged in general from about + 3 to — 4 db, in the band below 50 kc, to — 18 to — 24 db at 135 kc. (These levels are referred to a pressure of 1 dyne/cm^2 at the monitor hydrophone.) At times the high frequency background was considerably more variable than this general statement indicates. For example, at 130 kc the background was sometimes as high as — 13 to — 14 db and even — 10 db. The lowest background measured was — 25 db at 140 kc. Individual shrimp snaps, presumably quite near the monitor hydrophone, were usually 4 to 12 db above the general background to which our figures refer.

Equipment

There were two sections in the acoustic equipment, transmitting and monitoring (fig. 1). The transmitting system included a signal generator, a driver, and one of three underwater sound projectors. The signal generator was a commercial oscillator capable of producing tones from .02 to 153 kc; the driver was a 20-watt amplifier with flat response from .015 to 120 kc and with less than 10 db drop to 153 kc; the projectors were a 1K (inertia-controlled moving coil, .1 to 10 kc, used from a .15 to 7.5 kc), a 6B (Y-cut Rochelle salt crystal, 6 to 70 kc, used from 8 to 60 kc), and a 5A (ADP crystal, 20 to 150 kc, used from 70 to 153 kc); in addition there were meters for controlling the output. The monitoring system included either an AX-40 barium titanate hydrophone, designed to give a flat response from .05 to 200 kc, or a more

sensitive AX-58C Rochelle salt crystal hydrophone with a flat response from .05 to 10 or 20 kc. The hydrophone was connected either to a WHOI sound level meter (Suitcase) for frequencies below 60 kc, or to a National Company's HRO-M tuned receiver with an electronic voltmeter for frequencies between 50 and 196 kc. Calibration of the tuning of the HRO-M receiver provided a much more precise control of the fre-

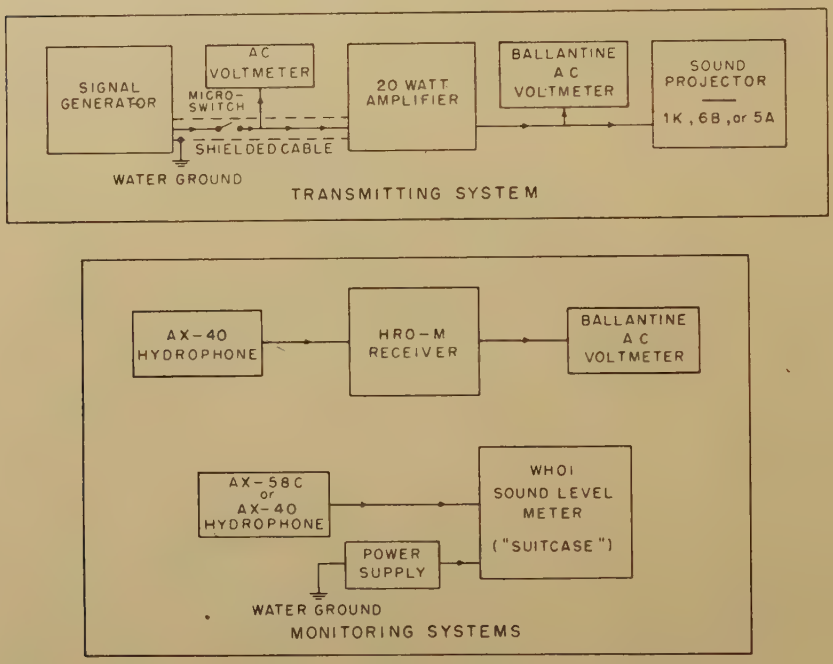

Fig. 1 Diagram of apparatus.

quencies used than the relatively crude and inaccurate scale of the oscillator, and also enabled us to be sure that our transmissions never contained more than one frequency detectable above the background. The projectors were hung just outside the fence, to protect them from possible molestation by the porpoise, at about 1 m depth at low tide, and carefully trained so that the main lobe centered on the monitor hydrophone, which was at the same depth at a measured range of 33.5 m,

near the middle of the pool; the highly directional AX-40 was of course trained directly on the projectors.

All sound levels given here are those of the *sound field at the monitor hydrophone,* and are stated in decibels referred to a pressure of one dyne per square centimeter. These levels may be taken as equivalent to or greater than those experienced by the porpoise, since we normally called her only when she was at ranges from about 28 to 55 m, most of the time very close to 33 m.

With this equipment we were able to expose our porpoise to tones between .15 and 153 kc, which was the upper limit of our signal generator. The signals were given by pressing a microswitch for a few seconds, generally between 3 and 5 (occasionally signals as short as 2 or even 1.6 seconds were used, and some as long as 10 seconds when checking negative responses). This gave the porpoise ample time to receive the signal even through the interference of nearby snapping shrimp. It was of course essential that the transmitting switch be entirely inaudible, and for the following reasons we feel that it was indeed effectively silent: No response was elicited from the porpoise when the switch was keyed with the oscillator gain cut down, even though it was tuned to frequencies to which the animal responded briskly when the gain was higher; likewise there was no response to signals at normal gain, but well outside the frequency range of the projector, as once when the oscillator was connected to the 6B and tuned to 3 kc; and then there were the repeated instances of no response to signals at the higher frequencies, alternating with brisk responses to lower frequencies.

The transmitted level at the hydrophone was uncontrollably erratic, and led to variations for successive signals of as much as 6 to 13 db in the sound field at the hydrophone, with constant transmitter input. Nearly half the time this variation averaged 3 to 4 db, but values over 6 were by no means rare. This sort of fluctuation is commonly observed in underwater

sound transmission experiments. The signal level was sometimes down in the background and sometimes well above it.

Behavior of the Tursiops and assessment of responses

An experiment like this is psycho-acoustic, and it must be remembered that the acoustic part cannot stand alone. Without a proper understanding of the behavior of the animal, the acoustic measurements have no significance. Our animal was a cow *Tursiops truncatus* whose well-worn teeth indicated that she was old; she was 252 cm long, and at the end of our tests, when she was a little thin, weighed 148 kg. Simply stated, the first part of our problem was to teach her to acknowledge an acoustic signal by coming to accept a fish from the hand. Hand feeding was important because in this way we could be sure that she was not being attracted by the slap of a thrown fish on the water, and because this was the only way in which we could be sure that she actually got the fish when she responded properly to our signal. The second part of our problem was to discourage prospecting on her part. By prospecting we mean independent trips to the feeding platform in the absence of an acoustic signal.

Previous work of this sort has not been reported in the literature, and the conditions under which we worked differ so from those which obtain in the more usual conditioned response experiments with land mammals that the methods used for training and interpreting her behavior had to be arrived at empirically as we went along. Our greatest difficulty lay in our inability to keep track of what our animal was doing. As stated above, the water was so opaque that she could not be seen through it for as much as .3 m; she was rarely seen at the surface except when she came up for her typically hasty blow, and, as is true of porpoises in general, she kept on the move. All of this meant that we could tell some of the time in what part of the pool she was, and less of the time which way she was heading. To this should be added that we could communicate with her only by sound, and that we

in no sense controlled her environment. Mullet, a normal food, were always present, and extraneous sounds, some quite disturbing to her, could not be shut out. We further had to arrange to get results with a limited number of feedings each day. Butterfish, *Poronotus triacanthus,* were the smallest fish readily available, and we had to use these whole since it became apparent early in the work that it would take far too long to teach her to eat cut fish.

Eight days after conditioning was begun she was thoroughly trained to come to the end of the feeding platform for a fish when we struck a length of two-inch iron pipe hung partly in the water, and we were satisfied that this was the only signal that brought her. We now substituted a single 15 kc note for the pipe signal. A few of these reinforced by simultaneous pipe banging were enough to teach her what the new signal meant. After that, no matter how drastically we varied the frequency, we never had to teach her anew the meaning of the signal, so that there was no problem of deciding whether failure to respond meant failure to understand.

Once we started exploring for the upper limits of her response, we constantly checked and rechecked her behavior, spreading the feeding of her 70-odd fish over most of the daylight hours to allow ample time for observation between responses. Because she never learned not to prospect, this was essential in order to be sure that what appeared to be positive or negative responses were true responses, not behavior initiated by her. Any response, no matter how convincing, was assessed doubtful if her behavior before or after suggested in any way that she might be acting independently. Moreover, at times when we did not signal her, we repeatedly set up and went through the motions of being about to feed without doing so, in order to make sure that she was not coming for some visual indication.

Careful watching showed that her behavior varied from day to day with no well marked diurnal pattern, although often in the early morning, when we first started to feed her, she was much too eager, coming in fast from any part of the

pool with or without a signal. At such times she was impossible to work with. Later in the morning she was calmer, circling the pool on a variety of paths. At any given time these paths and the places where she chose to blow were fairly constant and soon predictable, but from day to day they varied in haphazard fashion. At times she would loaf near the surface with her body arched and her head bent down, preoccupied with something. Sometimes, for no apparent reason, she would swim erratically and very fast from one end of the enclosure to the other, occasionally jumping clear of the water. Sometimes we saw her apparently feeding, with mullet jumping near her. At other times she would dive repeatedly and steeply in the same place. Her behavior when she hoped for fish was various. In the early mornings she might approach the platform just as fast when she was prospecting as when she had been signaled. Sometimes, when called two or three times in a row from a particular spot, she would go back and touch base, as it were, and then return immediately to the end of the platform. Given the above variations in her behavior, before assessing her responses we checked them in different ways, depending on what she was doing. At those times when she was circling the inlet along a particular track, passing near the end of the platform each time around, we would try to deflect her when she was headed away. At such times a positive response was clearly indicated by a fast, abrupt turn to come to the platform. After such a response we would let her make her loop a few times without calling her, to make sure she did not use that same spot in the inlet as a starting point for prospecting trips. Whenever she repeatedly prospected along a particular line we never called her from it, and, of course, we never scored a response if we did not know where she was when called, which way she was going, and how fast. At other times when her swimming was less regular, but slow, we could tell a positive response by the increased speed of her approach after a signal. This was especially easy to see on still days or when the tide was low, for she made a very conspicuous V-shaped surface wave as

she hurried in. Another obvious response was when she could be distracted while loafing at the surface, while rushing from one end of the pool to the other, or while engaged in deep diving. When she interrupted these activities to come for a signal, the response was clearly positive, since she never abruptly broke off otherwise. On the other hand a negative response at such times was not significant, as, when she was thus occupied, she often did not choose to heed a signal that we knew she could hear. Of the approximately 1,200 fish which we fed her during the time when we were testing her with signals of known frequencies, only about five-sixths produced responses which were definite and thus useful as data. When we were working in the higher frequencies where her responses fell off, it was especially hard not to retard the work by reinforcing bad behavior. If her response was slow and we withheld the fish, it confused her instead of making her come in faster next time, and on the other hand, if we mistook a prospecting trip for a slow response and gave her a fish, it encouraged her to prospect. The most satisfactory way of dealing with the marginal frequencies was, after an uncertain response, to drop down to a frequency to which she had always responded, send her 4 signals which would bring her in fast, getting fed each time, and then to go back up again, staying at the high frequency until we had another uncertain response.

After conditioning, the actual working time with the porpoise was about 100 hours, spread over 10½ consecutive days; during this time we assessed 1006 responses. As indicated above, it often took all day to dispense the 70-odd fish that were at once the animal's ration and reinforcement; we were unable to average more than about 95 signals a day, though on some days it was possible to get in as many as 140 assessments.

Responses to tones ranging from .15 to 153 kc were noted. As the critical region became defined, the effort was concentrated there, so that most work was done between 100 and 150 kc. However, we rarely stayed long in any one frequency

region, and thus repeatedly checked the porpoise's responses all up and down the scale.

The data were analyzed by grouping the responses into narrow frequency bands, one or occasionally 2 or 3 kc wide. The percentage of positive responses was then found, and plotted against frequency. Our points show considerable scatter, which is not surprising in view of the small and uneven number of responses, which in this region average only about 16 per frequency band, the largest number being 46. Hardly a basis for statistical study!

RESULTS

The disturbingly high background in the test enclosure effectively prevented us from learning anything of the porpoise's minimum audible field, as we had hoped we might; it is evident that her threshold was well below this noise level. In general, both she and the observer could detect signals which were so far down into this background that the sound level meter could not respond to them, either on the broad band system below 50 kc or on the sharply tuned receiver used for higher frequencies. The few indications of anything like threshold occurred only at the highest frequencies used, and they are not compellingly convincing; there are two few low intensity points to make this appearance much more than probable. Therefore we consider our data as essentially one-dimensional, bearing only on the frequency range.

The porpoise was exposed to signals of no great intensity, the sound levels falling mostly between 0 and 10 db above 1 dyne/cm^2, although some ranged down to -25 and up to $+28$ db; at frequencies above 120 kc less than 10% of the signals were at levels below 0 db. In comparing these figures for sea water with familiar levels in air, it is helpful to remember that the difference in characteristic impedance between these media implies that for the same acoustic pressure in each, the intensity of the sound in sea water is only about 1/3200 of its intensity in air, or 35 db down.

From .15 to 120 kc, there was essentially uniform positive response, the occasional negatives being clearly attributable to psychology rather than to acoustics. Above 120 kc there appeared a marked falling off in positive responses, which by 126 kc had dropped to a 50% incidence; above 130 kc (30%) the curve flattened somewhat, and the lowest percentage reached was in the highest band, 13% for 151–153 kc (see fig. 2). We were unable to carry this any higher, for 153 kc

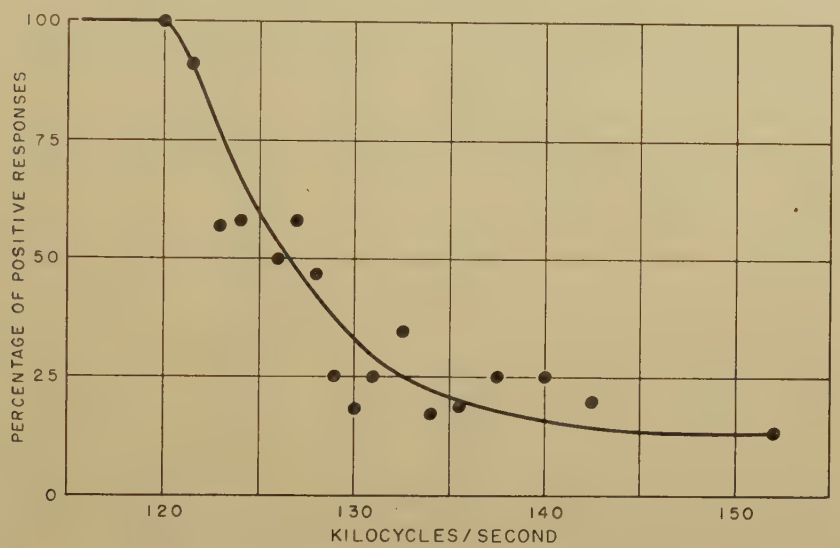

Fig. 2 High frequency cut-off of auditory response of a *Tursiops truncatus*. Doubtful responses (see text) occurred throughout the frequency range, and their inclusion would merely displace the entire curve downward a few per cent. More data at the high frequency end would doubtless make the curve less asymptotic.

was the absolute upper limit of our signal generator; although our 5A projector was not calibrated above 150 kc, it is probable that it would have functioned satisfactorily at somewhat higher frequencies since its output had continued dependable and strong.

These figures should be compared, not with data based on air-coupled hearing, but on bone conduction, which has been most extensively studied in man, for which animal it is known that while an average upper frequency limit by air-coupled

hearing is 15 kc, bone conduction brings an extension past 100 kc, but with an important and striking difference. A critical feature of hearing is frequency discrimination, which functions through most of the human air-coupled range. By bone conduction, however, one distinguishes pitch up to the limits of ordinary hearing, and beyond that one experiences an auditory sensation without further rise in pitch. In other words, one continues to hear the highest pitch that is normally audible, even while exposed to much higher frequencies. A readily accessible note on this has been published by Pumphrey ('50). Kunze and Kietz ('49) have published curves reaching 128 kc for man, without any sign of a break in the upper end of the curve; they also report some individuals, presumably normal by air-coupled hearing, who can evidently discriminate tones on the basis of frequency up to 60 kc by bone conduction. Deatherage, Jeffress, and Blodgett ('53) have also noted this phenomenon. It may be significant that the sound levels reported in these human experiments are of the order of 60 db or more above 1 dyne/cm^2, or from 300 to 1000 times the sound pressure of most of our signals.

In the light of all this, it is not surprising that the porpoise responded to tones as high as it did. What is remarkable is the indication of an upper limit for this presumably colorless kind of response, which, as far as we know, has not been reported for any other mammal. Our simple conditioned response test does not give any indication of the upper limit of pitch perception of this animal; for all we know, our *Tursiops* may have had a highly monotonous time during much of this test.

DISCUSSION

Earlier work

For a good many years it has been well-known to seagoing people in general and naval men in particular that many whales, especially the smaller ones, responded to sounds and made them over a wide range of frequencies. (At this point we would like to emphasize that the usual distinction

between sonic and ultrasonic frequencies is a purely subjective human one, and has no significance for animals with different ranges of hearing.) Our own experience has included both standard and experimental underwater sound equipment, and has confirmed what others have also noticed, that porpoises will often depart from a ship when an echo-sounder or any other intense sound source is turned on. This had been observed for both sonic and ultrasonic frequencies, up to 60 kc.

Similarly, sounds presumably made by cetaceans, as well as by other marine animals, have often been a cause of trouble to acousticians, but without definite identification of the source. In 1948 we were able to establish the connection between a particular cetacean, *Delphinapterus leucas* (the beluga), and some of these underwater sounds, and later we recorded them (Schevill and Lawrence, '49, '50). Since then we have listened to and recorded similar but not identical sounds produced by *Tursiops, Stenella, Globicephala,* and *Grampus (G. griseus),* as well as a few unidentified cetaceans. It may be noted that all those identified as soniferous are odontocetes, or toothed whales, and that so far all our listening to mysticetes, or whalebone whales *(Balaenoptera, Megaptera,* and *Eschrichtius),* has resulted in our hearing no underwater sound whatsoever from them.

Our earlier observations at Marine Studios had shown that the porpoise sounds were made without expulsion of air, although one sound (the squeal) was usually accompanied by the release of the string of small bubbles reported by previous observers (e.g., McBride, '40; Fraser, '47). We believe these sounds to be made in the larynx, although, as our dissections confirm, true vocal cords are lacking; this will surprise no laryngologist. In support of this belief we have phonographic recordings of sounds made by pumping air through the larynx of dead *Stenella* and *Delphinus* both before and after removal from the carcass.

One of the ways of studying the significance of these sounds is to record them and then play them back, noting the resulting reactions. We feel that this requires the highest at-

tainable fidelity in the record-playback system, which should accordingly be a broad-band system approximating the animal's audible range.

Even though we had no data on the audible range of any porpoise, beyond the knowledge that an unidentified pelagic species had reacted to 60 kc, we did nevertheless attempt such a playback experiment in 1951, although we feared our equipment was inadequate by at least one octave. With the aid of Magnecord, Inc., of Chicago, who kindly supplied a special recorder, we arranged a record-playback system with good response to 30 kc, broad band. With this we worked in the waters near St. Augustine, Florida, and actually succeeded in attracting wild *Tursiops truncatus;* these experiments were too limited, however, to give definitive results. The need to know the hearing range of these animals was emphasized; the next step was the experiment here reported, which was carried out in May and June 1952.

A paper by Kellogg and Kohler ('52) would appear to have dealt with this matter. These investigators report projecting high frequency sound into the Marine Studios Circular Oceanarium, using a 1K projector which they state "was capable of faithfully transmitting vibrations in water up to 200,000 cps." They assessed responses on the basis of bursts of fast swimming by the group of 12 porpoises in the tank, and conclude that "the range of hearing as measured by this method extended from 100 to 50,000 cps." In a footnote on page 251 they refer to a later test in which the "upper threshold . . . was found to be closer to 80,000 cps than to 50,000 cps." We find it difficult to compare this experiment of Kellogg and Kohler with our much simpler one. It seems likely that the shallow cylindrical shape of the tank, 22.8 m in diameter, had a critical effect on their signals; this could account for the peculiar reactions of the porpoises to "frequencies between 100 and 400 cps" (wave lengths of about 15 to 3.75 m, respectively). Here the repeated reflection of sound from the curved walls of the tank will have produced well-spaced regions of high intensity, which may well have caused discom-

fort to the porpoises (cf. Morse, '48, pp. 384, 401). It seems unnecessary to postulate non-auditory sensation to explain this reaction, as do Kellogg and Kohler (p. 251). Their statement that their equipment worked well up to 200 kc makes it hard to explain their cut-off at the relatively low frequency of 50 kc (or even somewhere below 80 kc). The explanation may lie partly in the nature of their sound projector, a 1K (described above, in our equipment), which is designed for reliable operation between .1 and 10 kc. We have found that above 10 kc this instrument has such variable output that the study of any frequency dependent phenomenon is made very difficult, even with the exercise of extreme care.

Acoustic conduction in whales

From the first, it has been apparent that whales must hear by bone (body) conduction, since they are totally immersed in water and thus cut off from the normal sound transmission path of land mammals, which include their ancestors. In order for sound to be perceived (heard), it is of course necessary for it to reach the receptor, in mammals the organ of Corti, which is not at the surface of the body. For a terrestrial beast, surrounded by air, sounds are not efficiently transmitted from the air into the body tissues. The difficulty is met by the mechanism of the middle ear, which by means of a mechanical system (the tympanic membrane and the auditory ossicles) couples the air-borne sound directly to the cochlea. An animal immersed in water has not this problem, for sound is transmitted from water into its body with small loss. Another way of expressing this is to say that animal tissue presents a serious acoustic mismatch with air, while it is a good match with water. The minor internal mismatches between different kinds of tissue, such as bone and blubber, are negligible compared with the large acoustic discrepancy between air and water. Thus, in general, sound passing through water will have very little difficulty penetrating animal tissue in its path, whereas air-borne sound will not readily penetrate the body of an animal. It is consequently not surprising

to find that the normal mammalian ear has been greatly modified in the Cetacea, who have lost the use of the air-adapted mechanical coupling system which they no longer need. Not only is the external auditory meatus extremely small, but it is to a large extent occluded. The tympanic membrane is said to be coarsened and slack, its normal concavity has been exaggerated (in the mysticetes it is reversed to an extreme convexity which has been likened to a glove-finger), and the connection between this membrane and the malleus has become remote and much reduced. The malleus is fused with the tympanic bone, and the incus and stapes are described as essentially immobilized. (These anatomical details are from Boenninghaus, '04; Lillie, '10; Turner, '13; and Hanke, '14). Although the acoustic role of the air-filled cephalic sinuses is not entirely clear to us, it may be said that sound can reach the inner ear only through the body tissues, that is, by what is called bone conduction (although the soft tissues are also involved). This path entails no disadvantage to an aquatic animal.

Similarly, the Cetacea have no need for the mouth as a speaker or sound projector, for sounds originating in the larynx travel outward through the body and readily pass into the surrounding medium (the water). In fact, the mouth and gullet are devoted to biting and swallowing, and play no part in breathing or phonation.

The question of directionality and localization, both in phonation and in hearing, will not be dealt with here, but is reserved for a later study. For the present, it will suffice to say that we have noted no indication that a cetacean has any difficulty in determining the direction of a sound, and that our test *Tursiops* showed no preference for any aspect (orientation) in responding to our signals.

Phonation frequencies

During this experiment, our *Tursiops* was often heard "talking" over the entire range of frequencies used. However, since she was by herself, she did not "talk" very much. (This is

a trait in which porpoises appear to differ from man.) When the work was finished, the monitoring system, together with a tape recorder, was transferred to the Circular Oceanarium containing the exhibit of 10 *Tursiops* and 2 *Stenella,* where there was a great deal of vocal activity; the approximate upper limit of their sound production (phonation) is still unknown, for some of their calls were still noticeable (8 to 10 db above background) at 196 kc, the extreme upper limit of our receiver. While the precise significance of these figures is uncertain, since we made no study of the acoustic effects in this tank, there seems little reason to doubt that these high frequencies are part of the calls of these porpoises.

That cetaceans may make use of these sounds for echo-location has suggested itself to a great many people, most of whom have evidently felt, as we do, that there is no observational proof of this possibility. Since Kellogg and Kohler ('52, p. 251) speculate on it at some length, it may be pointed out that we have long searched in vain for evidence of echo-location by cetaceans, and are still waiting for someone to demonstrate it. In the course of the experiment we have just reported, our porpoise swam through very opaque water (Secchi disk reading .3 m), a presumably propitious situation for the use of echo-location. Nevertheless, although we listened continuously and attentively over the entire band of frequencies used, we never heard any sound from the porpoise that could in any way be related to her swimming or food-getting. It might be noted that most of the time she swam no faster than about 4 knots (about 2 m per second).

SUMMARY

The auditory response of a bottlenosed porpoise, *Tursiops truncatus,* is seen to extend as high as 120 kc, with a sharp cut-off above this frequency, the response being only 13% at 152 kc; below 120 kc to .15 kc, the lowest frequency used, the response was uniformly practically 100%. This cut-off is in marked contrast with what is known of comparable (bone conduction) response in man, in which animal no upper cut-off

has been reported. Nothing was learned of the porpoise's frequency range of pitch discrimination, or of its minimum audible field.

ACKNOWLEDGMENTS

Among those who have aided us during this study, we especially wish to mention the following: Dr. J. B. Hersey of the Woods Hole Oceanographic Institution for patient encouragement and advice, and for allowing Mr. M. E. Edwards to serve as electronics technician; Prof. W. A. Rosenblith of the Massachusetts Institute of Technology for helpful suggestions; at Marine Studios, Messrs. W. F. Rolleston, F. G. Wood, Jr., F. Essapian, and H. M. Lightsey for great and varied assistance during the data taking; and also Drs. C. P. Lyman, M. H. Lurie, C. B. Officer, and Mr. H. E. Sawyer. We have likewise profited greatly by discussion with Drs. R. Galambos and J. V. Brady of the Walter Reed Hospital in Washington.

For the generous loan of field equipment we are indebted to Mr. Oakes A. Spalding of Woods Hole, Mass., and to the U. S. Navy Underwater Sound Reference Laboratory, which also calibrated the sound projectors and hydrophones.

LITERATURE CITED

Boenninghaus, G. 1904 Das Ohr des Zahnwales. Zoologische Jahrbücher, Abt. Anat. und Ont., *19:* 189–360.

Deatherage, B. H., L. A. Jeffress and H. C. Blodgett 1953 Audibility of intense ultrasonic sound. Acoustical Soc. Am., J., *25:* 190.

Fraser, F. C. 1947 Sound emitted by dolphins. Nature (London), *160:* 759.

Hanke, H. 1914 Ein Beitrag zur Kenntnis der Anatomie des äusseren und mittleren Ohres der Bartenwale. Jenaische Ztschr. f. Naturwissenschaften, *51:* 487–524.

Kellogg, W. N., and R. Kohler 1952 Reactions of the porpoise to ultrasonic frequencies. Science, *116:* 250–252.

Kunze, W., and H. Kietz 1949 Ueber Hörempfindungen im Ultraschallgebiet bei Knochenleitung. Archiv f. Ohren-, Nasen-, Kehlkopfheilkunde, *155:* 683–692.

Lillie, D. G. 1910 Observations on the anatomy and general biology of the larger Cetacea. Proc. Zool. Soc. London, 1910, pt. 3, October, pp. 769–792.

McBride, A. F. 1940 Observations on captive porpoises. Florida Acad. Sciences, Proc., *4:* 282, August, 1940.

MORSE, P. M. 1948 Vibration and sound, 2nd edition. McGraw-Hill, New York. Pp. xix + 468.

PUMPHREY, R. J. 1950 Upper limit of frequency for human hearing. Nature (London), *166:* 571.

SCHEVILL, W. E., AND B. LAWRENCE 1949 Underwater listening to the white porpoise *(Delphinapterus leucas).* Science, *109:* 143–144.

———— 1950 A phonograph record of the underwater calls of *Delphinapterus leucas.* Woods Hole Oceanographic Institution, Reference No. 50-1, January, 3 pp. and phonograph disk.

TURNER, W. 1913 Observations on the auditory organ in the Cetacea. Roy. Soc. Edinburgh, Proc., *34:* 10–22.

Contribution No. 649

Cartographic Principles Applied to Wide-Field Photography

William S. von Arx

Woods Hole Oceanographic Institution

ABSTRACT—Most photographic lenses are designed to produce an image having the properties of the gnomic or central perspective projection of a sphere. This convention imposes limitations on the maximum field of view and indirectly on the speed of wide angle photographic objectives. Alternative perspective projections of a sphere relieve these limitations to some extent. Two-stage optical systems can be used to approximate the alternative projections which make it possible to accept fields of view on flat film which range to and somewhat beyond a hemisphere in some instances, and to nearly a full sphere in one other.

The optical systems have been adapted to both motion picture and still photography. Color and other narrow latitude emulsions can be exposed successfully by locating the system stop in such a way that the effect of the $\cos^4$ law is small.

The original angular dimensions of the object space can be reproduced for purposes of measurement or study by projecting the film image on a spherical screen. Ordinary narrow field projection equipment and standard light sources are suitable provided the screen is of ordinary size. The center of perspective usually coincides with the center of curvature of the screen, but with practice, the image is also intelligible from other points of view or on a flat screen.

Three experimental cameras utilizing the orthographic projection have been built for aerial and other studies of oceanographic and meteorological phenomena. One of these is described in some detail and other applications are mentioned.

1. Introduction

The lens design criteria to be described are an outgrowth of some experiments in which time-lapse methods were used in photographing the earth, the sea surface, and cloud forms from an aircraft in flight. In this problem an unusually wide field of view is required since conditions often are such that large objects are screened from sight at more than moderate ranges, and it is not always known in advance what objects may prove to be of interest or where they may lie with respect to the path of flight. It was found helpful to be able to study an unfamiliar object or pattern from a variety of points of view. Fields as large as 150° total angle were found desirable for oceanographic and meteorological surveys from the air, and larger fields are desirable in some work from the ground.

Contribution No. 649 from the Woods Hole Oceanographic Institution.

Presented at the Third Annual Conference, Society of Photographic Engineers, May 20-22, 1953, West Point, N. Y.

2. Review of Methods for Obtaining Ultra-wide-field Photographs on Flat Film

The range of horizontal vision from aircraft is usually limited only by atmospheric haze or the true horizon. Hence the object space is radially symmetrical and can be assumed to be either spherical or

even cylindrical or toroidal rather than plane. Each assumption has a number of possible consequences in photographic procedures utilizing flat film.

A procedure for photographic reproduction of cylindrical object-spaces on a flat surface is already implemented by the panoramic camera. In a familiar case, such as the members of a convention standing in a semicircle around the camera, one obtains a cylindrical projection (similar to Mercator's) of the group on a flat film which is curved during exposure. This method is practicable in terms of motion picture mechanisms having a cylindrical gate but in aircraft the time required for the lens and narrow slit to cover the focal surface would allow the image to be distorted in proportion to the change of point of view during each exposure. A similar solution of the toroidal problem would yield a different cylindrical projection but would suffer from the same displacement effect.

It is also possible to adapt the tri-metrogon principle to motion picture photography to produce broad but not high fields of view. This has already been done in the Cinerama technique. Three cameras and films are required and later on, three projectors, all fairly well synchronized and aligned to form a single image and provide a common center of perspective.

It is also conceivable that a broad field might be generated with one camera trained on successive azimuths either directly or by means of a rotating or oscillating mirror so that every second or third frame, for instance, might represent a sequence of views in one direction. Were a similar rotating mirror system to be placed before the projector, the reversion of the camera mirror would be canceled and very wide fields of view be generated presumably on folded flat screens. The view on each screen would have its own center of perspective unless these are brought together at the rotating mirror by using a projection lens having the same focal length as the camera lens. Except for the mirror or training mechanisms, these principles could be applied with standard cameras and projection equipment. These are essentially photo-mosaic techniques.

Finally, there is a group of possibilities offered if a suitably distorted image of a wide field of view is formed and then photographed with an ordinary camera on flat film. If the distortion of the primary image accords with one or another of the perspective projections of a sphere, the distortion can be removed by projecting the image on a spherical screen. Thus the distorted image on the original film can be considered to be an intermediate step in the photographic process and not a final result. Since the group of perspective projections are mutually transformable by simple operations that can be approximated optically, the transformation of the particular perspective projection on the film to a final image having the angular properties of the original (spherical) object can be achieved without passing light backward through the camera system, although this is always possible. Rather, it is better in some ways to project the image with conventional projection equipment on a spherical screen so arranged that the normals to the sphere at various points in the field of view intersect at the center of curvature of the sphere, at the same angles as did the lines of sight to the original objects from the position of the camera lens when the exposure was made.

This latter possibility has been given some empirical study. Cartographic principles have been taken directly from the literature on that subject and optical procedures were developed experimentally with the components at hand. The systems have not been given thorough study from the standpoint of optical design nor has the relationship of the optical and cartographic aspects of the problem received critical mathematical analysis. Therefore, the results of such examinations may require that some of the statements in this paper be modified.

3. Perspective Projections of Spherical Object Space

As a matter of background it may be helpful to summarize the cartographer's methods and nomenclature concerning the various ways in which the surface of a sphere can be represented on a flat chart. The crux of the problem is that a sphere is non-developable; that is, the spherical shell cannot be made flat without tearing, folding, or bending the surface in some manner. Eliminating the operations in-

volving tearing or folding the surface as optically unsuitable, one has left the group of perspective projections of the sphere which differ only in the adoption of different points of view.

The group of perspective projections (which includes the gnomonic, stereographic, and orthographic cases shown in Fig. 1 and to be discussed in turn) have a number of properties in common. They are all *azimuthal*; that is, all great circles cutting the center of projection are represented as straight lines at proper angles to each other. All points equally distant from the centers of these projections are displaced by equal angles from a given point on the axis of projection and lie on concentric circles of equal distortion. Transformation of one projection to another can be accomplished by adjusting only the radii of these circles.

Perspective projections differ from one another only in the distance of the point of view from the center of the sphere. When the point of view is taken at the center of the sphere the projection on a (usually tangent) plane is *gnomonic*. When the point of view is taken at the surface of the sphere opposite the point of tangency, the projection is *stereographic*. When the eyepoint is removed to infinity the projection is *orthographic*. From any intermediate point of view the projection is generally *exterior* and has nearly the properties of an *equidistant* projection when the eyepoint is somewhat less than a diameter away from the center of the sphere. In all the exterior projections except the orthographic somewhat more than one hemisphere can be shown.

Each perspective projection has its own set of properties which may be favorable or unfavorable to the problem in view. The gnomonic projection is well chosen as the basis for most optical designs in that all straight lines in space are represented as straight lines in projection. However, lines of equal altitude in spherical space coordinates are reproduced as hyperbolas (Fig. 2) except for the lines cutting the center of projection which remain straight in all perspective projections. Since the planes of all great circles contain the center of projection in the gnomonic case, great circles are also represented as straight lines.

In the stereographic projection all circles great and small are represented by arcs of circles. The scale of projection increases outward but becomes infinitely large only in the projection of a full sphere. The increase in scale from the center to the limits of the stereographic hemisphere is in the ratio of the length of the radius of the projection to the arc length of one quadrant at the perimeter. Vertical circles and almucantars (lines of equal altitude) cross at right angles.

In the orthographic projection (Fig. 3) almucantars are represented as parallel straight lines but vertical circles are ellipses of different eccentricity. Thus an object subtending a given vertical angle in orthographic projection is represented by a figure of constant height regardless of the azimuth of the object. However, it is compressed laterally as it is moved toward the periphery of the projection. Marked as this compression is, it is not disturbing since it provides the impression of a turning globe. Given the feeling of hemispherical relationships emphasized by the shapes of objects, it is always clear that the normal appearance of these objects is presented when they occupy the center of the projection.

Finally, there is a combined optical and cartographic projection which will accommodate nearly a full sphere on a small flat surface. The sphere is first imaged by reflection from a small concentric hemispherical mirror. The reflection serves to reduce the sphere to a hemispherical image by halving all but the azimuthal angles. Following this operation the image can be projected orthographically. The resulting projection is azimuthal. The diminution of radial scale on this projection is half that of the orthographic projection; hence the projection of the first hemisphere involves less than 30 percent shrinkage of radial scale at the perimeter. If a full sphere is to be projected the central mirror must be convex but the projection of a hemisphere may be accomplished with a concave mirror if desired. The concave system has certain optical advantages over direct cartographic projection which have been turned to astronomical uses by Henyey and Greenstein (1945). The increase of field in the convex case has attracted the attention of many photographers who have entered gardens equipped with gazing globes.

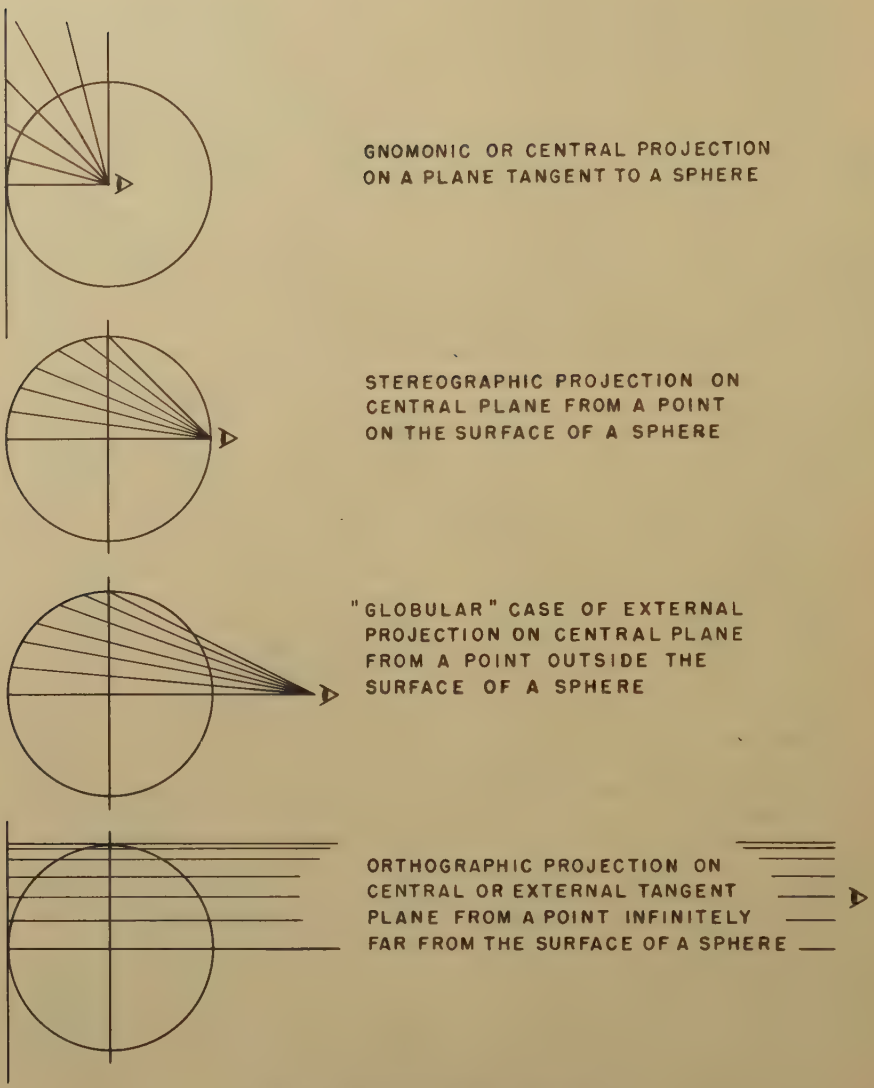
GNOMONIC OR CENTRAL PROJECTION
ON A PLANE TANGENT TO A SPHERE
STEREOGRAPHIC PROJECTION ON
CENTRAL PLANE FROM A POINT
ON THE SURFACE OF A SPHERE
"GLOBULAR" CASE OF EXTERNAL
PROJECTION ON CENTRAL PLANE
FROM A POINT OUTSIDE THE
SURFACE OF A SPHERE
ORTHOGRAPHIC PROJECTION ON
CENTRAL OR EXTERNAL TANGENT
PLANE FROM A POINT INFINITELY
FAR FROM THE SURFACE OF A SPHERE

Fig. 1—Common perspective projections.

4. Optical Systems

A number of two-tage optical systems will produce an external projection of a spherical object space on a flat film, Fig. 4. In all cases the field angle is first compressed to a spherical miniature of the world outside and then this image is focused on the film plane by conventional objectives. The distance of the camera from the field compressor influences the type of external projection obtained much less than the design of the field compressor. These designs may be classed as positive systems in which at least two real images are formed in succession; or negative systems in which the first image is virtual and only the second is real. The positive systems employ either positive

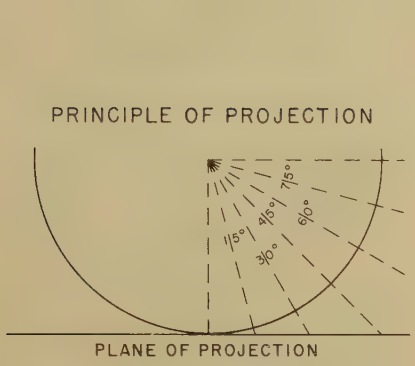

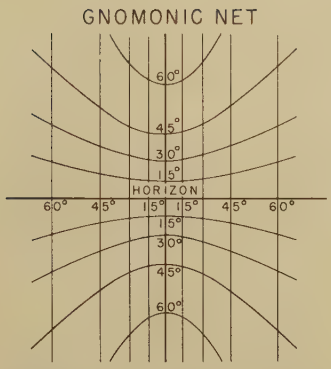

GNOMONIC PROJECTION OF THE HORIZON SYSTEM OF COORDINATES. VERTICAL CIRCLES ARE STRAIGHT AND PARALLEL. CIRCLES OF EQUAL ALTITUDE ARE HYPERBOLIC.

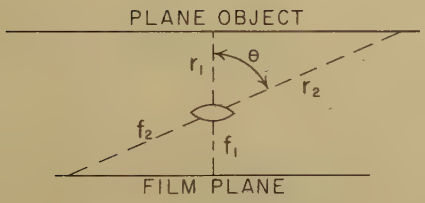

$$\frac{r}{f} = \text{CONST.}$$

$$r, f \sim \text{SEC } \theta$$

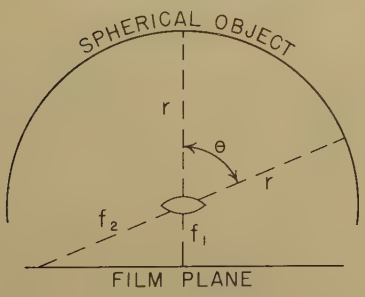

$$r = \text{CONST.}$$

$$f \sim \text{SEC } \theta$$

Fig. 2—Gnomonic projection.

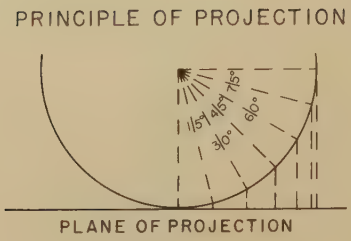

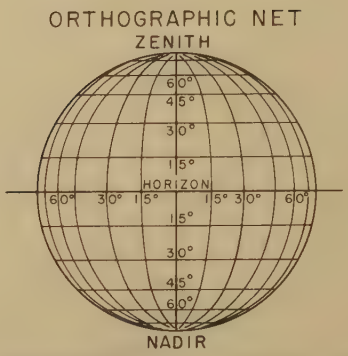

ORTHOGRAPHIC PROJECTION OF THE HORIZON SYSTEM OF COORDINATES. VERTICAL CIRCLES ARE ELLIPTICAL. CIRCLES OF EQUAL ALTITUDE ARE STRAIGHT AND PARALLEL.

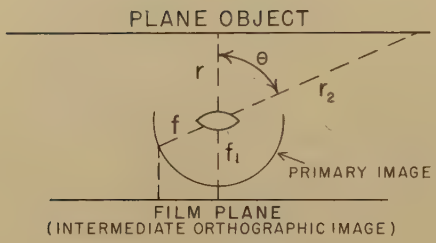

$f = \text{CONST.}$
$r \sim \text{SEC } \theta$
} IN PRIMARY IMAGE AND FINAL IMAGE WHEN FORMED ON A SPHERICAL SCREEN

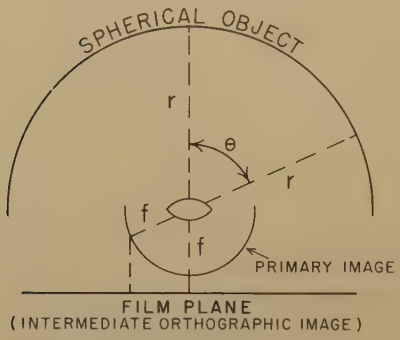

$\frac{r}{f} = \text{CONST.}$
$r, f \sim \text{SEC } \theta$
} IN PRIMARY IMAGE AND FINAL IMAGE WHEN FORMED ON A SPHERICAL SCREEN

Fig. 3—Orthographic projection.

lenses or concave reflectors as field compressors while negative systems utilize either negative lenses or convex reflectors for that purpose.

Reflecting systems should be composed of first surface mirrors so that the doubling of bright images is avoided. The optical quality of the mirrors need not be high but ground and polished surfaces of at least ophthalmic accuracy are required. In refracting systems attention must be given to achromatization but the Abbe condenser system can be utilized in positive systems covering less than 180° and modifications of this type of system can be used behind negative field compressors covering more than one hemisphere.

It is almost futile to attempt to compare all the merits and demerits of refracting and reflecting systems as they may be used in different programs of study. It is significant to note, however, that while field compressors of the reflecting type offer some optical advantages, being achromatic and single surfaced, the curves must be aspheric to provide an orthographic image. (Spheric and aspheric reflectors offer a group of possibilities all their own which are of great interest.) These systems also require either secondary reflecting elements or that the camera mechanism be placed in the field of view if the whole field is to be utilized.

Refracting systems with spherical surfaces are readily adapted to external projection geometry and are characteristically free of folded light paths which are inconvenient in applications to aircraft. In this application it is advantageous to arrange the first real image provided by the positive refracting field compressor located inboard. This makes it possible to insert reticles or notes written on translucent plastic slips into the plane of the first image to be recorded directly on the film. The slips are illuminated by the first image so that the exposure is adequate and the note is properly placed in the time sequence of the photographic record.

Each of these field compressor systems can, of course, be used as a field expander ahead of a standard projector. In such uses the center of perspective of the projected image then lies very close to the field expander and is therefore relatively inaccessible or inconvenient to occupy. If the screen is large enough to surround the observer a high intensity light source is needed to produce acceptable levels of illumination on the screen. Alternatively, it is more convenient to relate the cartographic projection of the image on the film to a small spherical screen in such a way that the center of perspective lies at the radius of curvature as in Fig. 5.

5. An Experimental Orthographic System

One of the optical systems that has been used experimentally at the Woods Hole Oceanographic Institute in a PBY-6A consists of a high quality 5x gunsight telescope (M71) placed wrong-end-to before a 16 mm magazine-load Bell and Howell camera fitted usually with a 44 mm $f/3.2$ objective (Fig. 6). The eyepiece of the telescope either alone or with auxiliary lenses is in effect a positive field compressor which reduces the true field of view of 65°, 80°, or 145°, to about 12°. The erecting system is not essential but in performing its designed function it permits the camera to be run in an upright position. The objective of the telescope acts as a collimator so that the image projected by the field compressor appears to be at infinity. The camera lens, therefore, produces a sharp final image when it is focused for infinity. As there is no limiting aperture in the optical train ahead of the iris diaphragm in the camera lens, this acts as the system stop. Thus the lens manufacturer's stop markings remain correctly calibrated. There are light losses due to the added absorption and reflections in the optical train, but these are constant and can be compensated by either determining the "filter factor" of the system or by making equivalent corrections of the effective film speed.

The 65° field provided by the unmodified field telescope eyepiece is fairly free of negative distortion, but is a little small for aerial survey work over the ocean. This field was increased to 146° by means of a negative auxiliary lens.

It is characteristic of the class of positive field compressors that all the oblique rays within the limits of the field cross the axis a short distance ahead of the first glass surface to form a caustic, which was the eye point of the original telescope system. The angle at which the extreme rays may enter this caustic can be in-

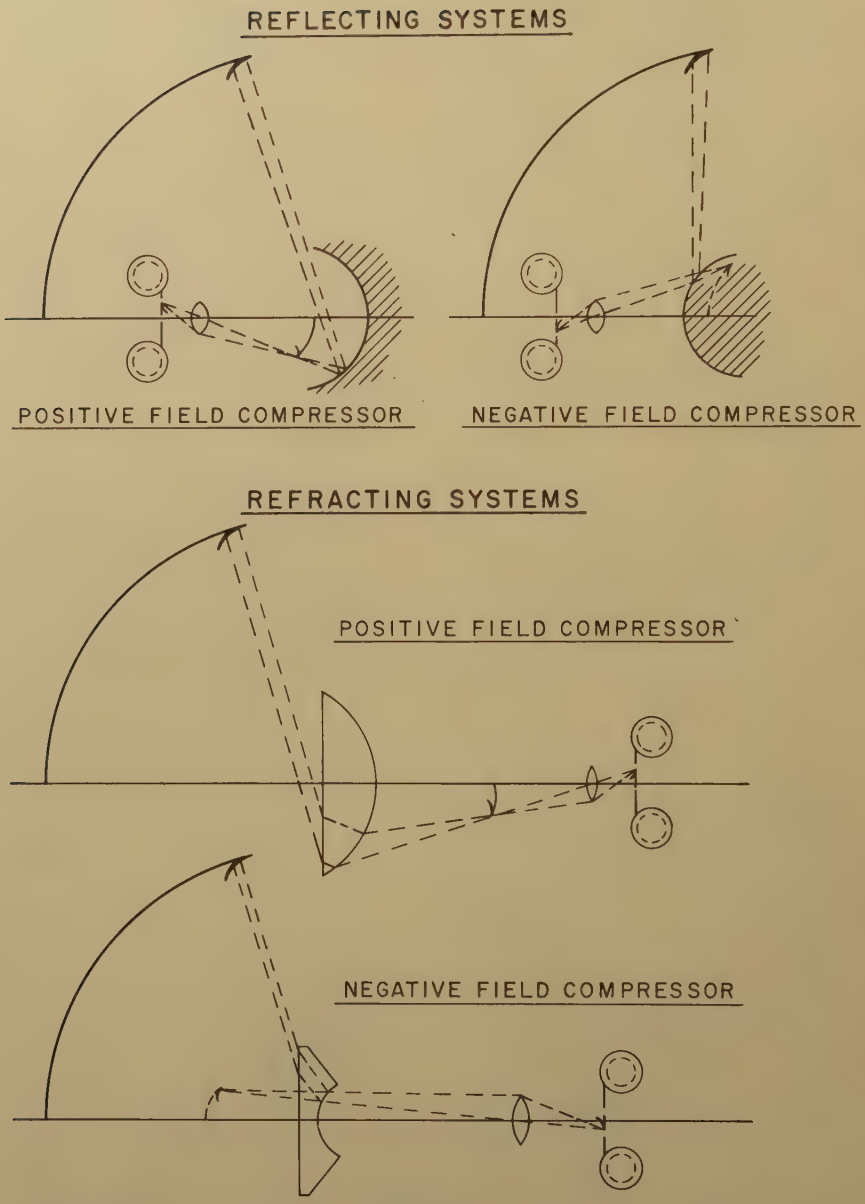
REFLECTING SYSTEMS
POSITIVE FIELD COMPRESSOR
NEGATIVE FIELD COMPRESSOR
REFRACTING SYSTEMS
POSITIVE FIELD COMPRESSOR
NEGATIVE FIELD COMPRESSOR

Figure 4.

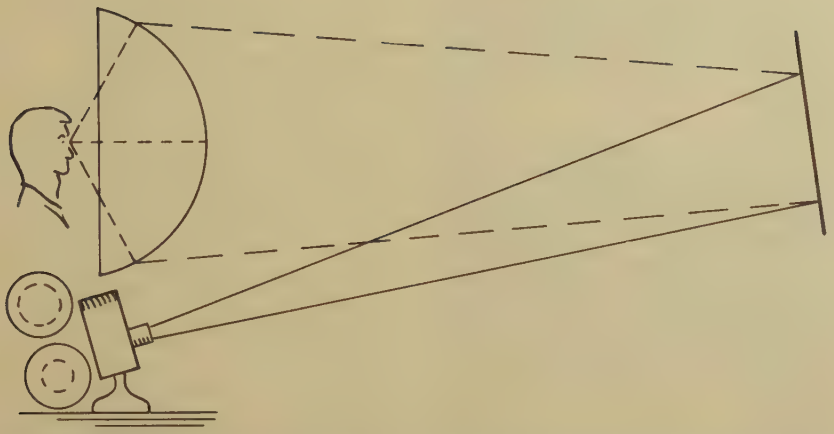

Fig. 5—Method of projection which permits eye to occupy the center of perspective and to have projector near at hand. Reflection from the plane mirror compensates reversal of left and right otherwise occasioned by a transmission screen.

creased by increasing the total power of the field compressor system. This may be accomplished by increasing the power of the original field lens or more conveniently, by placing a positive lens inside the caustic or a negative lens beyond it. In the latter cases adjustment of negative distortion can be made not only through a choice of radii but also through changes in the position of the auxiliary lens with respect to the caustic. It is found that plano-convex positive elements and plano-concave negative elements mounted with their plane surfaces facing the object space are most suitable. A field of nearly 180° total angle for orthographic projection can be obtained with either negative or positive elements. This angle can be exceeded with negative meniscus auxiliaries for other external projections. Because of the rapid radial reduction of the image scale it seemed unprofitable to press the angle of view very much beyond 140° on the 16 mm film format used in these experiments. The effect of the auxiliary lens and other components was adjusted by inspection at the final image in such a way that if R is the radius of the field extended to include objects of 90° off axis, the radial scale of the final orthographic image should decrease as $R \cos \theta$. When this convention is satisfied almucantars remain straight and parallel to each other across the full width of the field. The spacing of almucantars also decreases as $R \cos \theta$ toward the upper and lower limits of the field. The field compressor and auxiliaries were first adjusted to render the almucantars parallel in the final image. Further adjustments were then required to focus the collimator and camera.

Curvature of field is almost certain to be present in the primary image of the field compressor, whether the system be positive or negative, reflecting or refracting. This can be removed at either the initial or the final image plane, but it can be neglected if the field curvature is small enough to be accommodated within the limits of the depth of field of the camera objective. A camera objective of short focal length has a deep field and at the same time may work at high relative aperature in proportion to the diameter of the entrance pupil. The latter is of consequence since the diameter of the largest bundle of rays entering the system stop must be kept small (under one centimeter) so that the astigmatism associated with the caustic may not become too pronounced.

These optical difficulties prevent existing systems from covering the whole width of field with uniformly high image quality at all useful relative apertures. At $f/1.9$ acceptably stigmatic images can be recorded over the central steradian of field. Ordinarily, in the air the required stops may

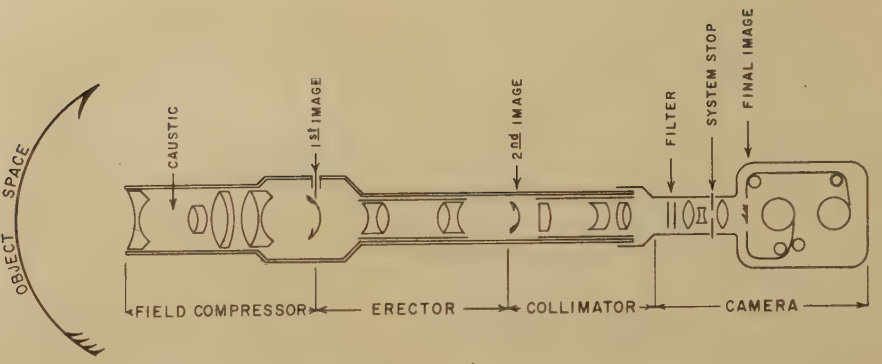

Fig. 6a—Optical train of the PBY bow camera. (schematic.)

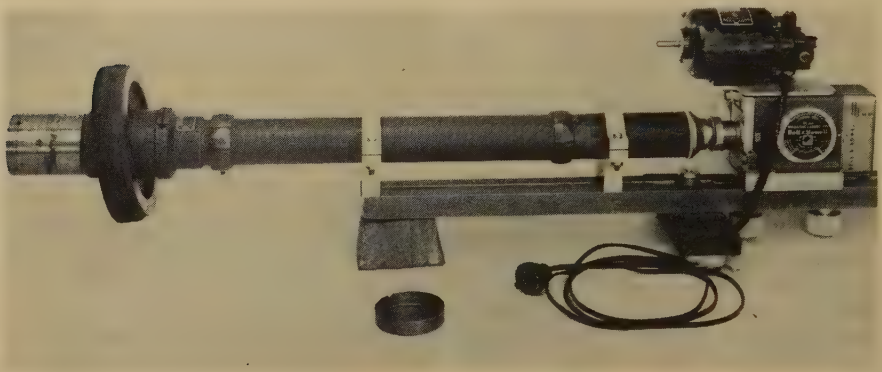

Fig. 6b—Experimental optical train covering a field of 146° and utilizing the orthographic projection.

be in the range $f/8$ to $f/11$, hence the image quality is improved and becomes fairly uniform to the edge of much wider fields (Figs. 7a and 7b). Although the image quality is not up to the best standards, neither should it be classed with the worst. Illumination over the full field width is remarkably uniform.

Owing to the position of the system stop the $\cos^4\theta$ law of decreasing illumination does not hold for the total field but only for the limited angle of view accepted by the camera lens. Thus it is possible to utilize color films having a latitude of only about 2 stops. An effect related to the $\cos^4\theta$ law does apply to the true field later on however because of the obliquity of the projected light on the rim zones of the spherical screen. Since the eye can tolerate a very much wider range of brightnesses than any emulsion, this deferment of an inevitable effect is desirable.

While illumination is uniform enough within the optical system, there is often a wide range of brightness from one part of the field to another. The direct rays of the sun may be included at times so that the system must be designed to minimize internal reflection or flare.

Exposures must be measured over the whole field of view. This may be done by scanning the field with a narrow angle meter, such as the G.E. Type DW-68, a special wide-angle meter, or by incident light readings with adjustment for the albedo of the subject. It seems best to underexpose color films made from the air. When the range of brightness (other than directly into the sun) is as great as 3 stops, it is best to place the 2 stop range

of the film at the high end of the brightness range. This means that the exposure is correct only for the upper two stops of the brightness range, and that the color is oversaturated in the darker portions of the photograph. This turns out to be preferable to either centering the exposure or favoring the less bright portions of the field. Half-field neutral filters might be useful.

The contrast of these wide angle films often seems to be unusually high especially when studied on a flat screen or from a point well behind the center of perspective. This is mainly illusory and arises from the compression of the familiar gradients of color or brightness. Still a useful purpose is served in calling attention to gradients that are weaker than those readily perceived by the unaided eye. Stratiform clouds, for example, often seem featureless to the eye, but exhibit surprising amounts of detailed structure on wide angle films. It is found that slicks on the sea surface seem more numerous in these photographs than to the eye because many of them are quite broad and involve subtile differences in the reflected color or intensity of light originating in closely adjacent portions of the sky.

It is found that some contrast is lost when the image is formed on an opaque concave spherical screen because of light scattered across the bowl. The concave screen does possess an accessible center of perspective but the observer's head will obscure part of the image if he occupies it. The center of perspective of the opaque convex spherical screen is inaccessible. Figure 5 shows an arrangement utilizing a translucent spherical screen and one plane reflector to revert the image. The screen also reflects some light so that the image is visible to more than the observer at the center of perspective.

It is clear from the cartographic principles discussed earlier than an orthographic image can be restored to spherical shape only when projected on a spherical screen from an infinite distance away. At a finite distance it is necessary to utilize another exterior projection taken from a point geometrically similar to that occupied by the projector with respect to the spherical screen. This refinement was neglected because of the necessity in such cases of turning the concave side of the

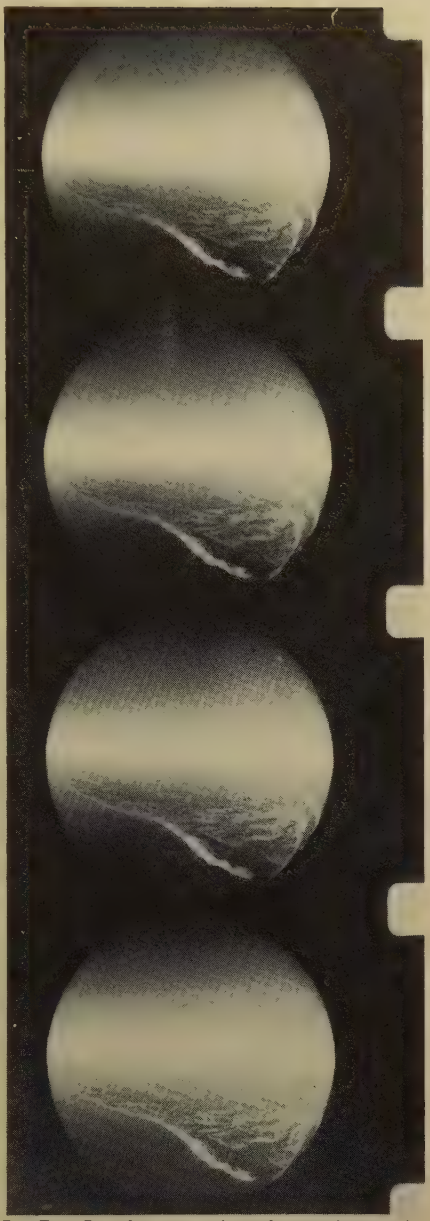

Fig. 7a—Four frames made at 1-second intervals from an altitude of 6000 feet above a point approximately 3 miles SSE of Chatham, Mass., with the 146° lens system. The visibility is about 40 miles. Most of Cape Cod and Cape Cod Bay is shown in each of these pictures. Original exposures on Kodachrome.

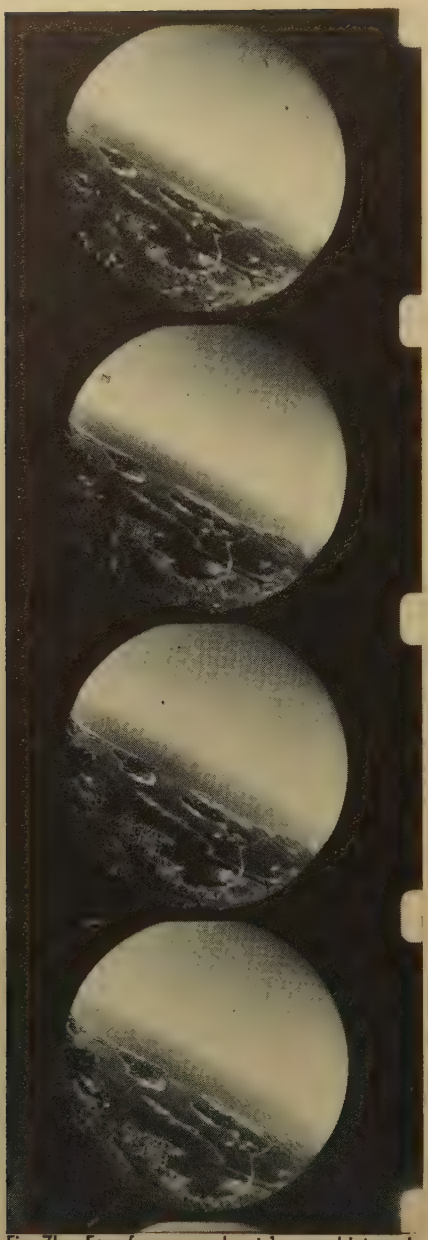

Fig. 7b—Four frames made at 1-second intervals from an altitude of 1000 feet above West Falmouth, Mass., with the 146° lens system. About 3 miles of shore line are included although the distance to the nearest part of the beach is under ¾ of a mile. Original on Kodachrome.

screen toward the projector, which produces some loss of contrast due to light scattering. Were the screen to be placed with its convex side toward the projector, one would be forced to consider the exterior projection of the proximal hemisphere on the equatorial plane of the sphere. This is a cartographic possibility that is not ordinarily utilized.

6. Installation

The mechanical arrangements for installation and operation of the bow camera in the PBY were simplified by the existence of a hawse hole in the bow. The hawse cover has been replaced by a sponge rubber cover which contains a hole large enough to hold the field compressor of the camera. This cushion acts as the forward shock mount and wind screen. The camera is run out through the hole until the slit for written notes is just inside the skin of the airplane. The optical train is about three feet long so that the winding key, stop control, and magazine compartment are beside the bowman in the forward turret. The inboard end of the camera is bolted through shock mounts to temporary framing. The shock mounts are designed to damp vibrations mainly in the range 1200 to 2000 cycles, and seem to be satisfactory. Actually, the image scale is so small that engine vibration or even landing shock has little effect on the image quality. Shock mounting is necessary mainly to keep bolts and the set screws of the optical components from being shaken loose over a period of hours. Film magazines are also less likely to jam if they are not subjected to intense vibration.

Two kinds of time-lapse triggering mechanisms have been used. The first was simply a 6 volt Permag motor fitted with an eccentric which tripped the single frame button on the camera through a bell crank. The camera was wound by hand every five minutes. When others found use for the bow camera there were greater demands on the time of the bowman so that it seemed desirable to provide a motor drive (Fig. 8). This drive consists of a 110 volt, 60 cycle Bodine motor turning at 60 rpm which will trigger the single frame button once each revolution and at the same time turn the

going barrel of the camera spring 1/60th of a revolution, which in this case restores the spring tension lost during each exposure. The camera spring requires three inch-pounds of torque to be wound, hence the motor drive is a fairly powerful affair. If the film magazine jams, the stop-work on the going barrel of the camera spring will stall the drive sufficiently to shear a pin before there is risk of damage to the camera.

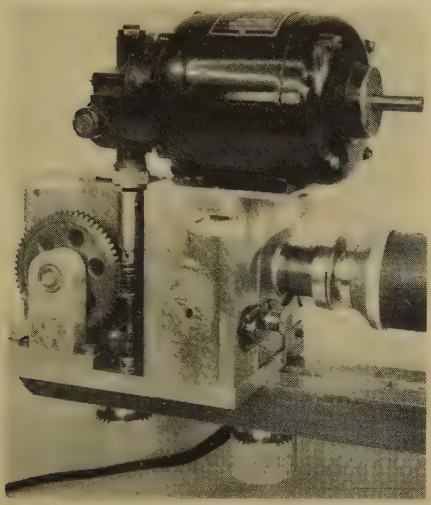

Fig. 8—The motor drive for the time lapse camera shown in Fig. 6b.

7. Time Lapse Film as a Flight Log

At a time lapse of one second between frames the events of an hour of flight are recorded on approximately 100 feet of 16 mm film which serves as a flight log. The changes in successive images are small enough to give the illusion of hurried but acceptably smooth progress at ordinary projection rates if the flight was made at altitudes above 500 feet and at speeds in the order of 100 knots.

The film record may be reviewed qualitatively in 1/16th the original flight time, when projected at 16 frames per second; and stopped or reversed as necessary. When stretched out along the direction of flight, the film represents a dead reckoning plot of the flight and indicates the relative positions of successive objects or events. The scale of the dead recokoning plot is compressed by the ratio of the length of film advanced between exposures to the distance traveled by the airplane in the same interval of time. For the one-second time lapse the ratio falls in the range from 1/5000 for slow aircraft and would be as much as 1/30,000 for the fastest. The angular dimensions of distant objects can be reduced to approximate linear dimensions from a knowledge of the airspeed and time required to close with them after sighting. More exact linear measurements are possible if the perspective geometry of the changing point of view and distortions of the optical system are taken into account.

8. Other Possibilities and Applications

While these experiments with ultra-wide-field time-lapse systems were undertaken merely to find means to develop an instrument for a specific purpose, they may have application to other problems, particularly those in which haze makes it difficult to place the camera very far from the subject and inequalities of illumination are troublesome, such as underwater photography. Presumably in photographing the sea bottom the camera would be pointed straight up into a reflecting field compressor so that it would be possible to mount the light source directly below the camera. This would reduce the length and increase the obliquity of the illuminating paths to effect some decrease in backward scattering. Such a system might be made to operate at higher relative apertures than those in present use and the light requirements reduced correspondingly. The depth of field in any system utilizing field compressors is very large so that focusing might be less of a problem than at present. The reflecting system has the advantage that the law of reflection applies without reference to the refractive index of the matrix medium. Presumably suitable reflectors would be constructed of corrosion-resistant alloys to survive immersion in sea water and rough usage. A compass might be centrally mounted in the focal surface of the field compressor where otherwise the camera image would appear, and a vent cut through the reflector behind the compass to release trapped air.

The extreme depth of field possessed by these systems is useful and is a conse-

quence of the fact that the field compressor has a short focal length and does not form its image on a sensitized surface. The small conjugate motions of the primary image are reduced still more at the plane of the final image. When a collimator is mounted immediately ahead of the final image-forming component the focus of the entire system can be altered by focusing the collimator alone. This permits the system to be used conveniently at ranges in the order of the focal length of the field compressor without requiring allowance for changes in the calibration of the iris diaphragm in the camera lens. Some experiments utilizing this principle have been made on photography of minute objects such as the smaller flowers, the structure of compound flowers, insects, and so on (Fig. 9). Exposure offered no problem and the combination of intimate perspective with orthographic projection seemed to have unusual pictorial possibilities which are not available with conventional double or triple extension techniques.

Fig. 9—Example of macrophotography in orthographic projection showing a common garden spider. Hand-held pentaprism reflex camera, 65° auxiliary lens-system designed for aerial photography. Original photograph on 35mm Kodachrome.

9. Conclusion

Little of the material in this paper is new and yet it is difficult to find very much discussion of these particular properties of optical trains either in texts or in journals devoted to optical subjects. A list of some of the sources referred to during these experiments may be helpful to others who find their possibilities of interest.

10. References

Jacobs, D. H., 1943: *Fundamentals of Optical Engineering*. McGraw-Hill, New York 487 pp.

Deetz, Charles H., and Oscar S. Adams, 1945: Elements of Map Projection With Applications to Map and Chart Construction. *Special Publication No. 68, U. S. Coastal and Geodetic Survey*. 226 pp. with 15 plates.

Henyey, Louis G. and Jesse L. Greenstein, 1945: Wide Field Fast Cameras. *Final Report of Section 16.1 NDRC; OSRD Report No. 4504*. Yerkes Optical Bureau, University of Chicago 30 pp.

Henyey, Louis G. and Jesse L. Greenstein, 1945: Miscellaneous Optical Designs. *Final Report of Section 16.1 NDRC; OSRD Report No. 4505*. Yerkes Optical Bureau, University of Chicago 53 pp.

Kingslake, Rudolph, 1951: *Lenses in Photography*. Garden City Books, New York 246 pp.

Eastman Kodak Company, 1951: *Motion Picture Films for Professional Use*. Published by the Eastman Kodak Company, Rochester, N. Y. 80 pp.

Editorial Staff, American Society of Photogrammetry, 1952: *Manual of Photogrammetry*. Published by the Society, Washington, D. C. 876 pp.

11. Acknowledgements

Thanks are due Dr. Jesse L. Greenstein now of Mount Wilson and Palomar Observatories staff and formerly of the Yerkes Observatory staff for helpful correspondence concerning his designs for wide field reflecting systems. Dr. Dow Smith of the Optical Research Laboratory of Boston University and Mr. F. Claude Ronne of this Institution have given much helpful advice. The cooperation of Mr. Ronne, Mr. David H. Frantz, Captain Norman Gingrass, and members of the crew of the Navy PBY 46683 who have participated in the test flights and several long over-ocean flights at low altitude is gratefully acknowledged as is the support of the Office of Naval Research which under Contract N6onr-27701, has provided both the PBY aircraft and funds for the oceanographic and meteorological researches of which these optical experiments are a by-product.

Contribution No. 655

PROCEEDINGS

Minnesota International Hydraulics Convention

A Joint Meeting of

International Association for Hydraulic Research

and

Hydraulics Division, American Society of Civil Engineers

University of Minnesota — Minneapolis, Minnesota

September 1-4, 1953

Local Arrangements by

NORTHWESTERN SECTION, AMERICAN SOCIETY OF CIVIL ENGINEERS

Assembly and Arrangement of Papers
For Publication by

ST. ANTHONY FALLS HYDRAULIC LABORATORY

August, 1953

Minneapolis, Minnesota

Copyright 1953
by
International Association
for
Hydraulic Research

Manufactured by WM. C. BROWN CO. INC., Dubuque, Iowa
Printed in U. S. A.

THE ROLE OF DENSITY CURRENTS IN ESTUARIES

Henry Stommel
Woods Hole Oceanographic Institution
United States

This paper is contribution No. 655 from the Woods Hole Oceanographic Institution.

ABSTRACT

Estuaries provide large-scale examples of density currents produced by mixing. Because these currents influence pollution dispersal and sedimentation processes they are of practical importance. Examples of types of density distribution and flow that occur in estuaries are given, together with some examples of mixing mechanisms. The control action of the mouth of the estuary on both the velocity distribution and maximum possible salinity of the estuary is discussed.

Perhaps the simplest example of density current in an estuary is that present in South West Pass of the Mississippi River. A salt wedge of the type portrayed in Fig. 1 penetrates for many miles from the jetties at the mouth of South West Pass upstream. The fresh water of the river flows out over this salt wedge and accelerates toward the jetties where it is discharged into the Gulf of Mexico. Because of the changes of discharge in the river and the small tides in the Gulf of Mexico, it is seldom possible for this salt wedge to be in a steady state and, in fact, it is usually moving slowly toward equilibrium in response to changes of the river discharge and sea level. The discontinuity between the density of the salt water

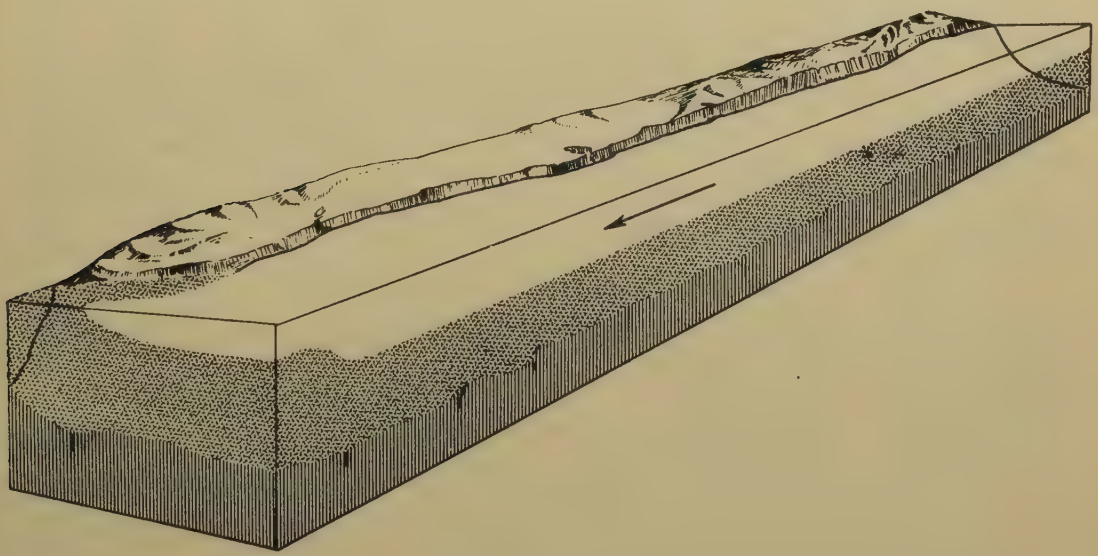

Fig. 1 - Estuary with negligible mixing. The fresh water from the river overrides a motionless salt-water wedge. The mouth of the estuary, opening into the ocean at the left of the figure, acts as a control on the depth of the interface between the fresh and salt water. Density is proportional to shading.

below and the fresh water above is remarkably sharp as compared to that in most estuaries. The depth of the fresh-water layer at the jetties is controlled by a critical interfacial Froude number [1]. Fair agreement between computed and observed depths of the fresh layer at the jetties as functions of river discharge has been obtained. Upstream of the jetty the slope of the salt wedge seems to be determined by the magnitude of the frictional stresses of the moving upper layer on the more sluggish salt wedge below. Attempts at an analysis of the shape of the wedge have been made [2]. Due to the lack of a priori knowledge of the magnitude of the frictional stresses to be expected and the uncertainty as to whether the wedge as observed is in a steady state, it is impossible to apply these theories directly to the Mississippi River, although good agreement is obtained for laboratory flume studies of the salt wedge. One sees, therefore, that the same rather artificial division of phenomena into those occurring at transitions and controls and those of gradually varied flow which is so useful in the study of the ordinary open channel flow of a homogeneous medium is also useful for the study of two-layer flow.

Another type of estuary is the deep fjord-like estuary such as Alberni Inlet [3]. In this case a deep layer of sea water extends right to the head of the estuary and the fresh water is confined to a very shallow surface stratum. In moving through the fjord from the river to the open sea, this surface stratum apparently picks up a great deal of salt from the lower water. The depth of the surface stratum at the mouth of the estuary again appears to be controlled by the interfacial Froude number. The shape of the boundary between the fresh water and the salt water upstream of the mouth exhibits some very interesting features, the most important of which is that the addition of salt water to the upper layer as it moves toward the mouth does not deepen the upper layer, but if anything causes it to become shallower.

There does not appear to be any quantitative relationship available for computing how much of the deep water should be entrained by the upper layer. In the case of an actual estuary like Alberni Inlet, the amount of entrainment can be computed from the downstream increase in salinity of the upper layer. Keulegan [4] has published results for entrainment in a small flume, but these cannot be extrapolated to the large scale of an estuary.

From theoretical considerations it can be shown that the ratio of relative increase of thickness $\Delta D/D$ of the upper layer to relative increase in discharge $\Delta q/q$ should be given by

$$\frac{q}{D}\frac{\Delta D}{\Delta q} = (4 F_i - 1)/2 (F_i - 1)$$

where F_i, the interfacial Froude number, is $F_i = U^2/g \nu D$, U is the velocity of the upper layer, g is the acceleration of gravity, and ν is the density difference of the two strata divided by the density of the lower layer. It will be seen that entrainment of salt water into the fresh layer causes the thickness of the upper layer to increase only for internal Froude numbers less than 0.25, but for the range of internal Froude numbers between 0.25 and unity the thickness of the fresh layer diminishes. This latter behavior is similar to that which tends to concentrate the momentum flux in the upper layers of a stratified fluid (not subject to mixing) subject to momentum losses as pointed out by Rossby [5] and Craya [6]. This behavior of the thickness of the upper layer (Fig. 2b) is, of course, quite the opposite of that occurring due to entrainment in an unstratified medium (Fig. 2a).

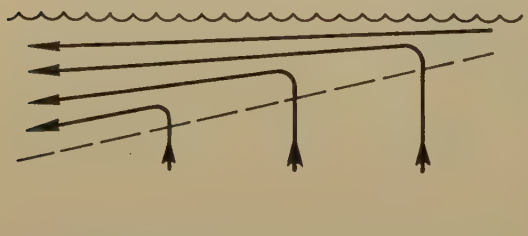

a. Effect of entrainment on the depth (dashed line) of a moving surface layer in a homogeneous medium.

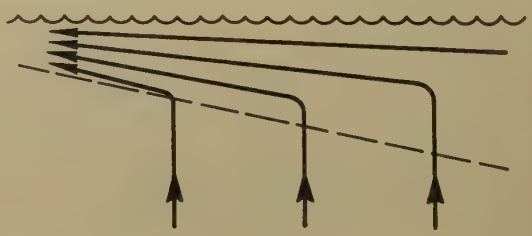

b. Effect (on the depth of a moving surface layer) of entrainment from a lower layer of denser water.

Fig. 2 - Streamline patterns.

In a very large number of estuaries, entrainment plays a minor role in transporting salt as compared to random turbulent vertical transport of salt. The Kennebec Estuary is an example of such a turbulent estuary. There is so much vertical mixing in this estuary that the difference of salinity between the surface and the bottom is only a small fraction of that between the ocean and fresh river water (Fig. 3). The Kennebec Estuary is subject to strong tidal currents. The vertical mixing in this estuary is partly due to eddies stirred up from

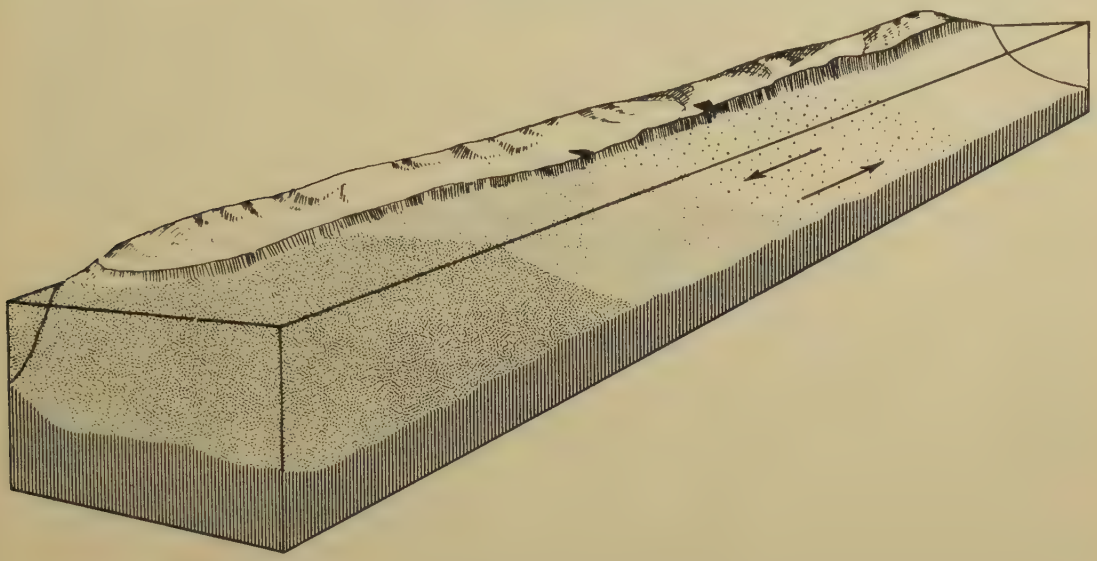

Fig. 3 - Estuary with moderate mixing. There is some vertical stratification of density, and the density currents (shown by arrows) are strongly developed. Density is proportional to shading.

roughness elements on the bottom by the tidal currents, and partly due to eddies generated by the mean velocity gradients associated with the density flow in the estuary. Fig. 4 shows the type of density flow produced by the mixing at a station in the Kennebec. The tidal currents are averaged out by computing averages over a complete tidal cycle. Near the mouth of the estuary the discharges both in the bottom and surface layers are many times the river discharge, and the kinetic energy represented by these massive discharges is very much greater than that of the entering river. This very large excess of kinetic energy is extracted from the energy of the intense mixing. This is not a violation of the second law of thermodynamics: the mixing increases the potential energy of the mass distribution in the estuary, and it is from this potential energy that the large excess of kinetic energy is drawn.

In the case of some estuaries, the mixing of the water is so very intense that all measurable vertical stratification is destroyed, although the horizontal gradient of density from the river to the ocean is, of course, still present. The Severn Estuary, with its very large tides, seems to be such a case. Fig. 5 illustrates the nature of the density distribution in a completely vertically mixed estuary. In such a case, density currents, such as those observed in the Kennebec, simply do not exist; and the transfer of salt upstream against river flow appears to be entirely produced by horizontal diffusion. Such vertically mixed estuaries are particularly well adapted for simple computation of distribution of pollutants. Several methods of computation have been proposed [7, 8]. These computational schemes depend upon using the fresh water as a tracer from which the mixing characteristics of the estuary can be computed, and hence the distribution of the pollutant predicted. In an estuary of this kind, the forces due to the small differences of density between the fresh water and ocean water are not dynamically significant.

The three types of estuary shown in Figs. 1, 3, and 5 are different chiefly because of the relative amount of mixing occurring in them.

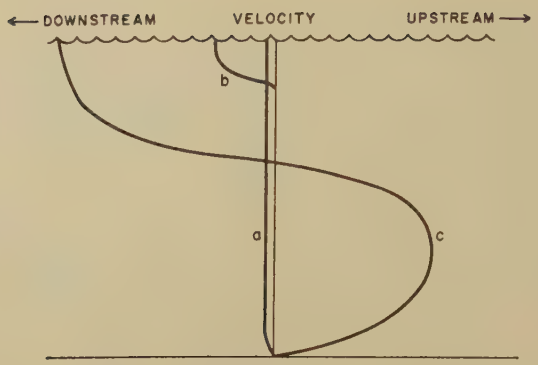

Fig. 4 - Plot of velocity against depth, to show effect of mixing on density flow. If there were no density difference between the ocean and a river, the discharge of the river would be distributed over the entire depth as shown schematically by profile (a). Allowing for the fact that the ocean is more dense than the river, but not allowing mixing, the same river discharge would be confined to a shallow upper layer (b). If mixing is permitted, a very large two-layer density current may develop such as shown by profile (c).

In an estuary with no mixing at all (Fig. 1), the salt water wedge may extend upstream for great distances. Were there no friction or entrainment at the interface, the upstream extent of the salt water would be limited only by the slope of the estuary bottom and the critical control condition at the mouth. The salt water, of course, would be at rest.

Moderate mixing tends to "short circuit," so to speak, the salt wedge with the fresh water flow above, and thus actually tends to freshen the estuary as a whole, and induces the familiar two-layer flow shown in Fig. 3.

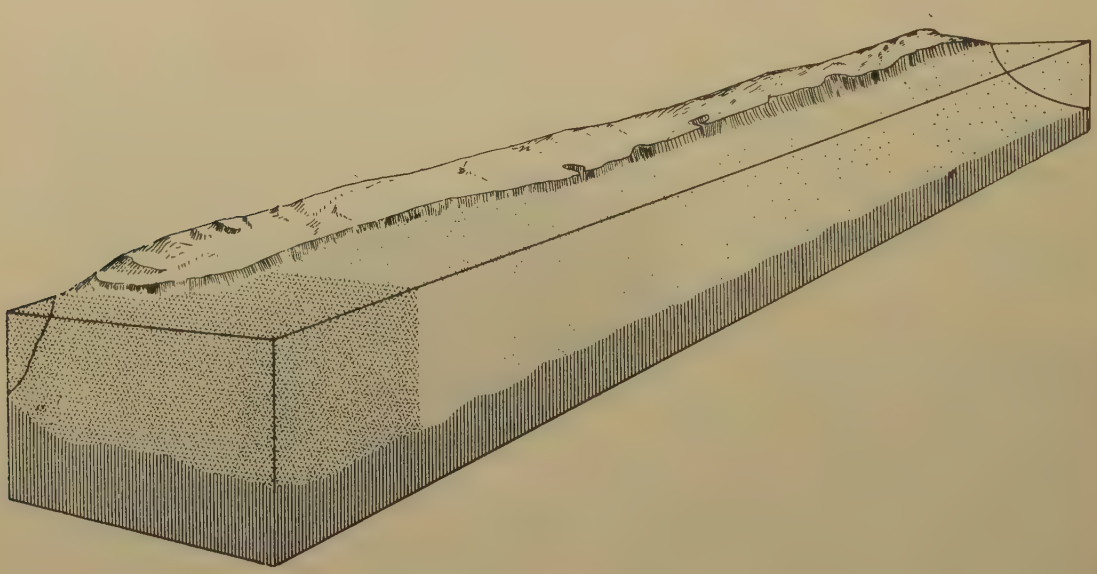

Fig. 5 - Intensely mixed estuary. The density currents are destroyed. The net motion at all depths is downstream, and the salt is carried upstream by horizontal diffusion. Density is proportional to shading.

Very intense mixing destroys the two-layer density flow, but transports salt upstream by horizontal diffusion and, if too intense, actually increases the over-all salinity of the estuary again as shown in Fig. 5. Theoretically, in the limit, the salt could extend even further upstream than in the case of no mixing because the bottom slope would then have little direct influence.

In addition to the types of mixing process which have already been mentioned, there are many others which are frequently encountered. A promontory (Fig. 6) extending out into a tidal current provides a back eddy alternately on one side and then on the other. These back eddies produce large-scale lateral mixing not so much by violent motion but because they retard portions of water which upon the reversal of the tide are assimilated in an entirely different environment. For example, at low tide the water at the promontory is likely to be freshest. As flood begins, more saline water passes the promontory; but a pocket of fresh water may be caught in the back eddy behind the promontory. At the beginning of ebb the dynamical reason for the back eddy ceases to exist and the fresh eddy is incorporated in the highly saline environment.

A very interesting type of vertical mixing is frequently induced by a transition in width of the channel. There are a number of these transitions, for example, in the Kennebec Estuary which we can use as an example. At the moment of the beginning of ebb we may suppose that in the narrow section upstream there is water almost vertically mixed and slightly less dense than the water in the wider part of the channel downstream. As the ebb progresses the fresh water does not push the heavy water back downstream but, because of the control action of the sudden widening in the channel, passes through critical velocity and flows out over the lower, heavier water with supercritical velocity, probably forming somewhere further downstream an internal hydraulic jump. This supercritical flow induces a great deal of mixing between the

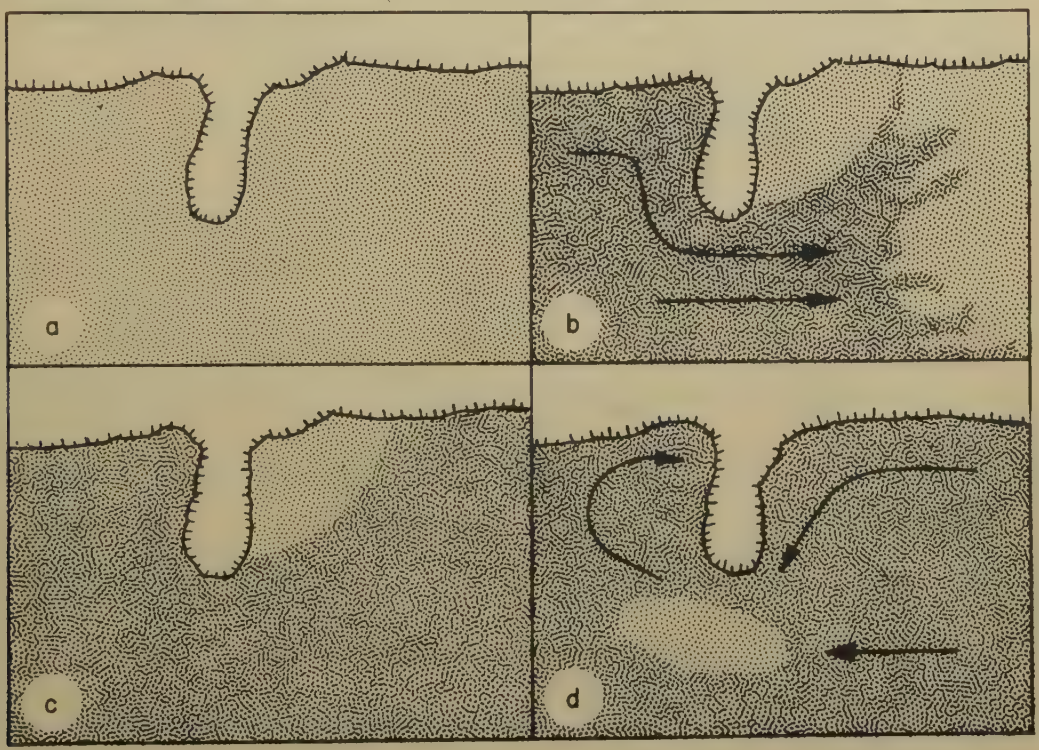

Fig. 6 - A promontory acting as agent for large-scale horizontal mixing. Fresh water upstream of the promontory (a) is caught in a back eddy during flood (b), as density of environment increases (c). At beginning of ebb, the fresh eddy is flushed out into tidal stream (d) and mixed with surrounding water.

rapidly flowing surface layers and the stagnant lower layers in the wider section of the channel. Upstream, of course, in the narrow section, the water is homogeneous and has a large velocity right down to the bottom of the channel. As time goes on, fresher and fresher water comes from further upstream and because the lower layer in the wider section is retarded the stratification increases. On the reversal of the tide, the transition ceases to act as a control, and both the surface and bottom water move upstream together where they are mixed apparently more by other processes such as back eddies and turbulence produced by roughness elements on the bottom.

As a final example of curious density current phenomena that occur in estuaries, I mention the process of "overmixing" [9]. Suppose that there is a large harbor basin connected to the sea by a narrow channel such as shown in Fig. 7 and that a river also flows into the basin. If

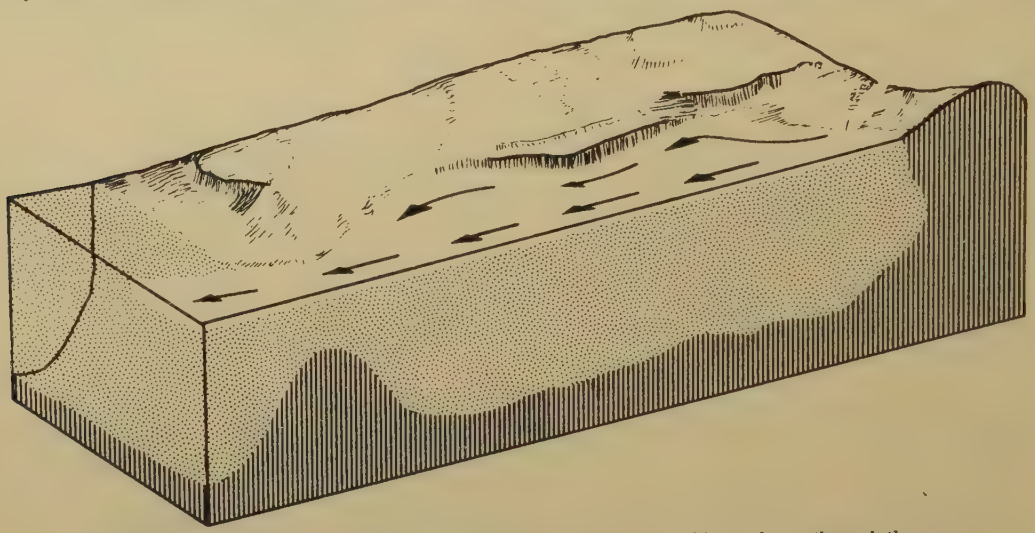

a. In the absence of mixing in an estuary the river water flows out as a thin top layer through the narrows to the sea.

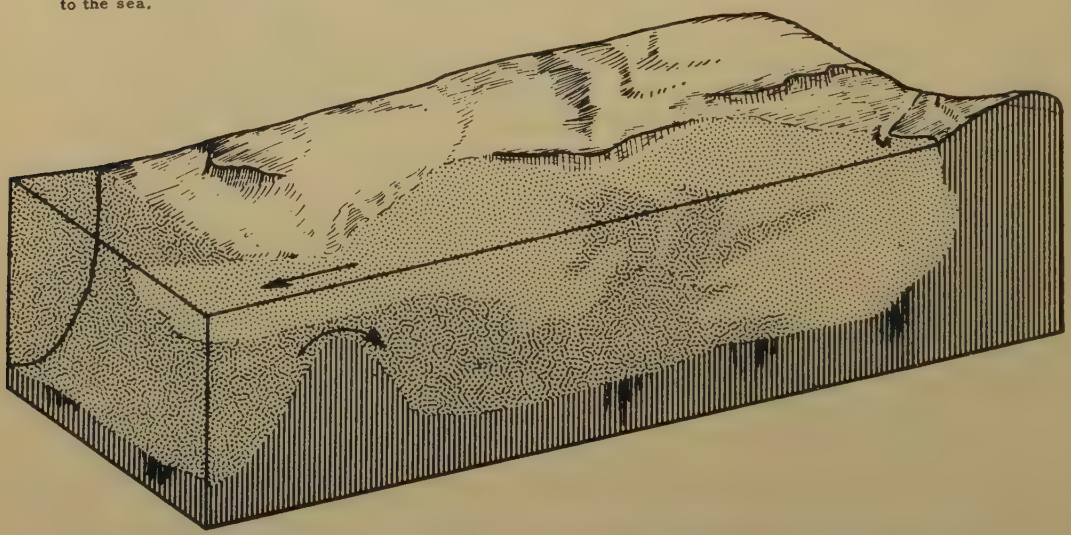

b. A limit on the salinity of the estuary under extreme mixing is imposed by control action of the narrows.

Fig. 7 - Overmixing.

there is no mixing at all in the large basin, the fresh water of the river flows out in a thin surface layer over the heavy ocean water which fills the basin and out through the channel where it is dispersed in the sea. If, however, there is some mixing in the basin, a two-layer flow is induced in the channel consisting of an outflowing mixture of sea water and river water at the surface and an inflowing layer of ocean water along the bottom. As the amount of mixing in the basin is increased, there is a corresponding increase in the discharges of these two superposed density currents in the channel. When the mixing in the large basin has reached a certain amount, however, the control action of the connecting channel restricts any further inflow of ocean water and outflow of mixture. Further intensification of mixing in the basin then has no effect on the salinity of the mixture. It is interesting in this simple situation to reflect upon the fact that the density currents in the channel which are produced by the mixing in the basin are able to restrict the amount of mixture when the mixing processes have exceeded a certain limit. This relationship can be derived theoretically and has been tested in an experimental flume [9]; it appears to be an important criterion in determining the salinity of harbors such as New York and St. John, New Brunswick.

Density currents in estuaries should be of interest to hydraulic engineers for a number of reasons:

(1) They occur on a fairly large scale (but in many cases, at least, are not complicated by the Coriolis forces which are so important in larger scale motions of the atmosphere and ocean),

(2) There is such a wide variety of estuaries in the world that practically every possible complicating effect can be found somewhere,

(3) Density currents in estuaries can be of considerable practical importance for those interested in the movement of sediments and of pollution in harbors.

The invasion of salt into an estuary is a matter of considerable economic concern in some places in the world and considerable thought has been given to controlling the salinity of the estuary. A very drastic solution is employed on the Nile. Every dry season a temporary dam is built across the river mouth. One of the remedial measures often suggested is a sill along the bottom of the estuary near the mouth. If the estuary is a well mixed one with a well developed upstream flow in the lower layer, such a sill is bound to be effective. In the case of a very poorly mixed estuary with very little flow in the salt wedge, a bottom sill is not likely to be very effective unless it extends very nearly to the height of the interface. In such a case a sill is actually likely to be worse than nothing at all because it will impound salt water when the river discharge increases and the wedge would normally recede. A horizontal narrowing of the mouth of the estuary, however, would have the result of decreasing the salinity in both cases: in the mixed case the narrowing tends to throttle the density flow through the mouth and hence reduce the over-all salinity of the estuary; in the case of the unmixed estuary the narrowing tends to depress the level of the interface at the mouth and hence reduce the volume of the salt wedge. In estuaries of the type shown in Figs. 1 and 3 an artificial increase in the vertical mixing might possibly be used to reduce the over-all salinity of the estuary; however, the practical realization of this measure of control may be fraught with engineering difficulties. In estuaries of the type shown in Fig. 5, an increase in mixing might have the opposite effect, hence in such a case an effort could be made to reduce mixing.

BIBLIOGRAPHY

[1] Stommel, Henry and Farmer, H. G. "Abrupt Change in Width in Two-layer Open Channel Flow." Journal of Marine Research, Vol. 11, No. 2, pp. 205-214. 1952.

[2] Farmer, H. G. and Morgan, G. W. "The Salt Wedge." Proceedings, Third Conference on Coastal Engineering, 1952 (in press).

[3] Tully, J. P. "Oceanography and Prediction of Pulp Mill Pollution in Alberni Inlet." Bull. 83, Fisheries Research Board of Canada, 1949.

[4] Keulegan, G. H. "Interfacial Instability and Mixing in Stratified Flows." Journal of Research National Bureau of Standards, Vol. 43, pp. 487-500. 1949.

[5] Rossby, C. G. "On the Vertical and Horizontal Concentration of Momentum in Air and Ocean Currents." Tellus, Vol. 3, No. 1, pp. 15-27. 1951.

[6] Craya, A. "Critical Regimes of Flows with Density Stratification." Tellus, Vol. 3, No. 1, pp. 28-42. 1951.

[7] Ketchum, B. H. "The Exchanges of Fresh and Salt Waters in Tidal Estuaries." Journal of Marine Research, Vol. 10, No. 1, pp. 18-38. 1951.

[8] Arons, A. B. and Stommel, H. "A Mixing-length Theory of Tidal Flushing." Transactions, American Geophysical Union, Vol. 32, No. 3, pp. 419-421. 1951.

[9] Stommel, Henry and Farmer, H. G. "Control of Salinity in an Estuary by a Transition." Journal of Marine Research, 1953 (in press).

Contribution No. 656

The Commonwealth of Massachusetts

DEPARTMENT OF CONSERVATION
Arthur T. Lyman, Commissioner

DIVISION OF MARINE FISHERIES
Francis W. Sargent, Director

FIFTH REPORT ON

INVESTIGATIONS OF THE SHELLFISHERIES OF MASSACHUSETTS

Prepared by the
WOODS HOLE OCEANOGRAPHIC INSTITUTION
In Accordance with Contract
Effective July 1, 1952

PREFACE

The following report, prepared by Harry J. Turner, Jr., Biologist of the Woods Hole Oceanographic Institution, is a summary of the investigations of methods of improving the shellfish resources of Massachusetts which were carried out in 1952 by the Woods Hole Oceanographic Institution under contract with the Division of Marine Fisheries, Massachusetts Department of Conservation.

The investigations were conducted under the leadership of Mr. Turner. Those participating were Edward Chin, J. Arthur Posgay, and James E. Hanks, graduate assistants, and Robert Bagg, summer assistant. The work was greatly aided by counsel from Dr. David L. Belding, former Biologist for the Massachusetts Department of Fisheries and Game who is now a member of the staff of the Woods Hole Oceanographic Institution.

The Institution has worked in close cooperation with the U. S. Fish and Wildlife Service which is conducting investigations in Essex County and in other parts of New England under a federal appropriation for the improvement of the soft and hard clam fisheries. Members of the Institution served on the Committee of Clam Technicians sponsored by the Atlantic States Marine Fisheries Commission of which Massachusetts is a member.

The Woods Hole Oceanographic Institution wishes to express its appreciation to Mr. Francis W. Sargent, Director of the Division of Marine Fisheries, and to Mr. Charles L. Wheeler, Biologist of the Division for their valuable suggestions and close cooperation.

Alfred C. Redfield
Associate Director
Woods Hole Oceanographic Institution

December 31
1952

FIFTH REPORT ON INVESTIGATIONS OF THE SHELLFISHERIES OF MASSACHUSETTS *

BY
HARRY J. TURNER, JR.

INTRODUCTION

During the past year biological investigations of the Woods Hole Oceanographic Institution on commercial shellfish resources of Massachusetts have been mainly concerned with the soft clam fishery in the moderately contaminated areas. Records supplied by the Massachusetts Division of Marine Fisheries have been analyzed to determine the effect of digging on trends in production and abundance, to provide a basis for any regulatory measures that may become necessary. A comprehensive field survey of the moderately contaminated areas of Boston Harbor has been completed and all important accumulations of soft clams have been mapped.

A series of observations was made on an exceptional set of soft clams near Raccoon Island, Quincy, and important information was obtained on the behavior of soft clams after setting. This information has made it possible to determine the probable sequence of events which lead to the formation of certain populations of adult clams.

Experimental work has been continued on the boring snail, *Polynices*. Feeding rates of both the oceanic species, *P. heros,* and the estuarine species, *P. duplicata* have been related to temperature and salinity, so that the destructive capabilities of each species in various environmental conditions may be estimated.

The following investigations were also made and the results are summarized below:

Experiments performed to determine whether boring snails drill by chemical or mechanical means have demonstrated that the mechanism is basically mechanical.

One cruise was made to the sea scallop beds in the vicinity of Nantucket Shoals and a number of photographs of the beds were taken with an improved camera. The new series of pictures confirmed the previous determinations of the probable density of sea scallops in areas under commercial exploitation.

Preliminary attempts at salt water pond culture of commercial shellfish failed because of excessive seepage of fresh water in artificial ponds excavated at the chosen site. The experiments demonstrated the presence of fresh water in marshy areas and the danger of its seepage in localities that may be otherwise suitable for the excavation of salt ponds.

* Contribution No. 656 from the Woods Hole Oceanographic Institution.

THE SOFT CLAM FISHERY IN THE MODERATELY CONTAMINATED AREAS OF MASSACHUSETTS

The future of the soft clam fishery in the moderately contaminated areas of Massachusetts has been a matter of concern for the past few years, because these areas have been the only dependable source of soft clams and the demands upon them have been greatly increased by the decline in the yield of the uncontaminated areas. Recently, diggers in increasing numbers have been complaining of a decrease in the level of abundance of soft clams in the moderately contaminated areas and the difficulty of finding localities where digging is worth while. They believe this is to be indicative of a downward trend which may ultimately result in a collapse of the fishery unless checked by some system of management.

The fundamental problem in the management of a shellfishery is the evaluation of the effect of exploitation so that it can be regulated to produce the highest long term yield. The problem is complicated by natural fluctuations in abundance resulting from variations in setting and survival. It is generally believed, however, that over-exploitation tends to exaggerate these fluctuations by depressing the average level of abundance, lengthening periods of low abundance, and retarding recovery. The conventional remedy is prohibitive or restrictive regulation, which may include limitations of the catch, seasonal closure, regulations of sizes, and others designed to prevent the total catch from exceeding the basic natural supply.

The degree of exploitation of the moderately contaminated areas of Massachusetts is automatically restricted by measures designed to protect the public health. These regulations require that all diggers obtain a special license and dig only under the immediate supervision of a bonded master digger. The master digger is required to process all the clams in an approved purification plant before placing them on the market. The number of diggers is thus limited to those willing to take the trouble of obtaining a special license, and the total catch is restricted by the capacity of the available purification plants.

In the past these sanitary regulations have also had a profound effect on digging patterns and have in effect resulted in a system of management. Master diggers have generally directed their crews to areas which would provide large daily yields in order to offset the expenses of trucking and purification. They have also tended to dig over one area after another systematically instead of here and there at random. This has developed a system of crop rotation with periods of recovery between successive diggings.

Recent increases in the number of master diggers and the sizes of their crews have lead to a breakdown of this self-management system. Productive areas are now being dug over with increasing frequency and the scope of activities of various crews have been so expanded that none of the productive areas are permitted as much time to recover as formerly. It will be shown that this has actually increased the total annual yield of clams. However, the catch of each individual digger has declined. The implications insofar as they affect the future of the fishery will be discussed in a later section.

The soft clam fishery in the moderately contaminated areas has been well documented from its beginning in 1931 when purification plants were first put into operation. All master diggers have been required to make frequent reports of their operations indicating the general locality, the total catch, the

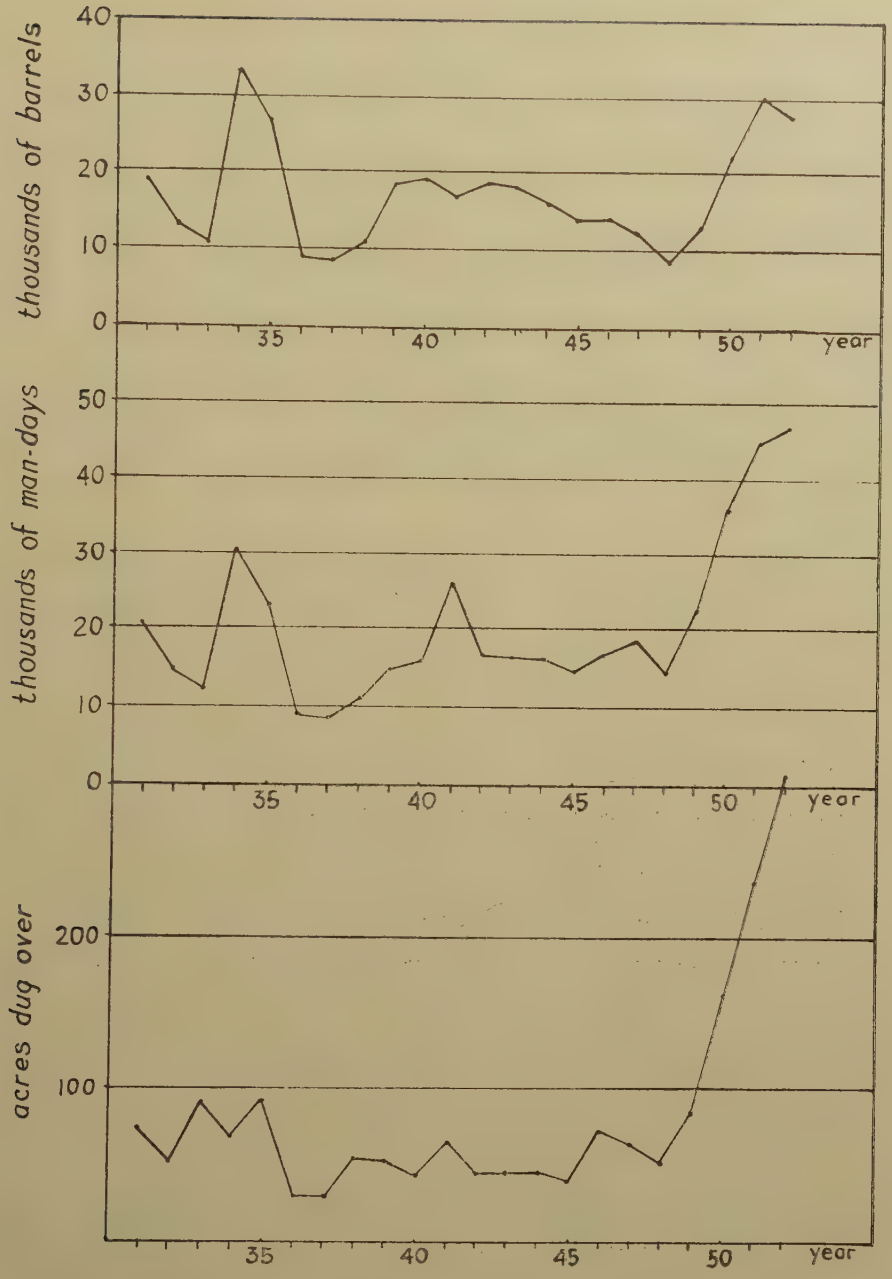

Figure 1. Graphs of the data pertaining to the soft clam fishery of the moderately contaminated areas of Massachusetts.

Upper graph—Gross annual production
Middle graph—Annual effort
Lower graph—Area reported dug over annually

number of diggers employed, and the total area dug over. The reports have been compiled on an annual basis.

Records of annual production reported by all the master diggers have been found to agree closely with records of the purification plant, indicating a high degree of accuracy. Similarly, the total annual effort (man days) can be considered to be accurate because each master digger pays off his employees each day and keeps records of his financial transactions. On the other hand, reports of the total area dug over depend on the subjective judgments of individual clammers and may contain both random and systematic errors. Random errors result from variations in the ability to judge area and may be compensating with the underestimates of some diggers balanced by the overestimates of others. Systematic errors result from the tendency of most diggers to exaggerate both favorable and unfavorable circumstances. When clams are abundant, diggers tend to report less area than they actually dig over, and when clams are scarce the area may be magnified. Thus considerable confidence may be placed on conclusions derived from analyses of records of production and effort, which are accurate, but all conclusions derived from reports of the areas dug over must be viewed with caution.

The compiled data are illustrated graphically in Figure 1. Essentially parallel trends are evident in the curves of production and effort showing that annual yields of this fishery during its entire history have depended primarily on the number of man-days of digging. The total area dug over each year shows some departure from this but the general trends appear to follow those of production and effort when due consideration is given to the inherent inaccuracies in the data.

The average catch per man per day illustrated in graph Figure 2 is a more instructive indication of changes in the condition of the soft clam populations. This curve shows that the average digger could find clams in sufficient densities to permit the catch of approximately one barrel per day from the beginning of the fishery in 1931 through 1945. After 1945 clams became progressively less dense so that by 1947 the average digger could manage to obtain only about 0.65 barrels per day, a level which has remained fairly constant to the present.

There is no clear indication from the trends in production and effort that the average density of clams has at any time been directly affected by exploitation. It remained essentially constant throughout the first 9 years of the fishery in spite of wide fluctuations in the annual removal. During the next 5 years effort and yield remained essentially constant as well so that the decline in average density after 1945 was not preceded by any exceptional event. Likewise, the unprecedented increase in effort that occurred after 1948 has not appeared to have affected the average density during the following period.

The trend of changes in average density calculated from the reported areas reveals a somewhat different situation. Graph Figure 2 illustrates the average number of clams removed from 1 sq. ft. each year as calculated from the annual production and the reported square footage. This is based on the assumption that the commercial catch consists primarily of clams averaging just over 2″ in length. Annual fluctuations are much wider than those indicated by the catch per man per day and probably reflect the inaccuracies in the data. The average was approximately 30 clams per square foot with no indication of any definite trend. Beginning in 1946, however, there was a progressive decline terminating in a low figure of 8 per sq. ft. in 1952.

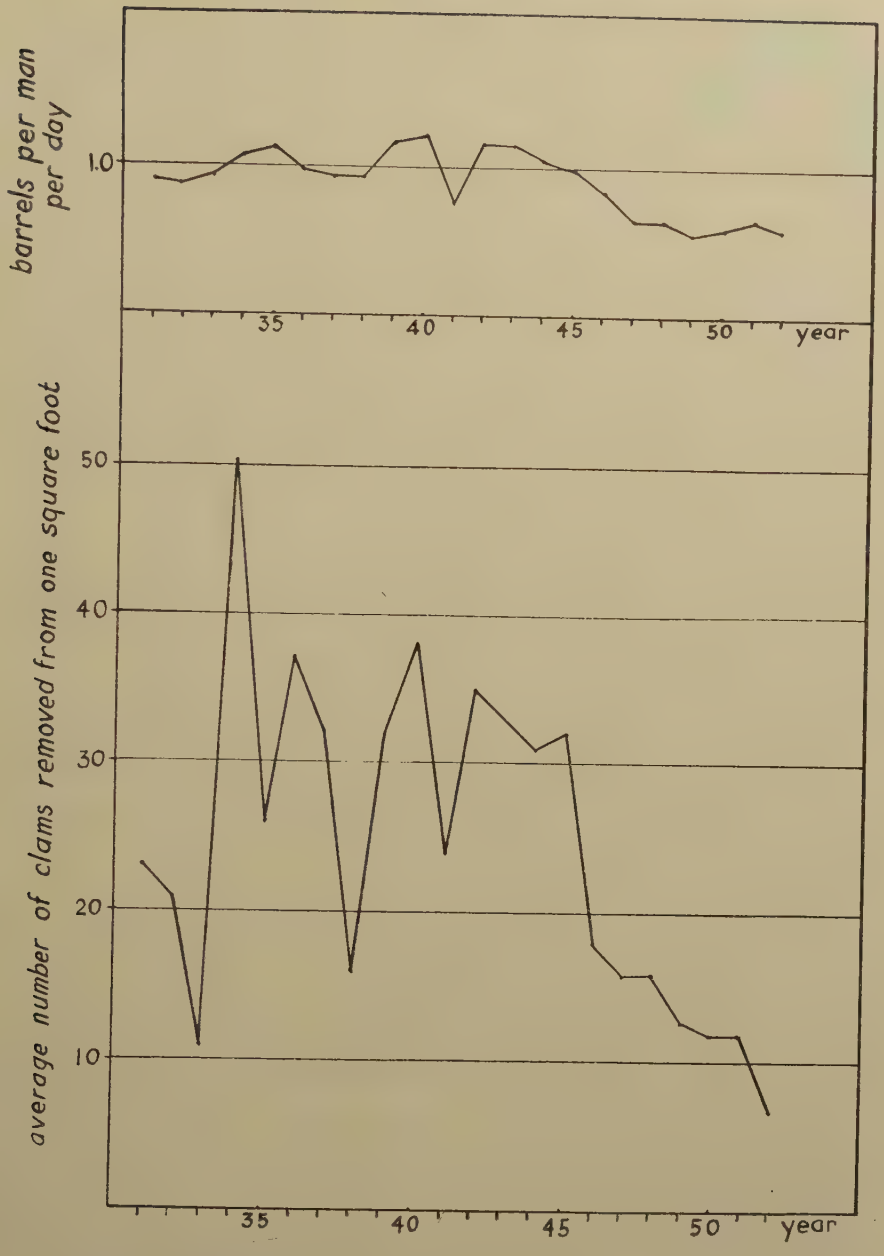

Figure 2. Upper graph—Catch per unit of effort
Lower graph—Average removal of soft clams calculated from annual yield and area reported dug over

The beginning of the decline corresponds in time with the decline in the catch per man per day but the magnitude is considerably greater. The catch per man per day indicates a relative reduction of approximately 40%, while that determined from the calculated average density is 74%. Field evidence which will be discussed in another section, has shown that densities of legal size clams in excess of 10 per sq. ft. were rare in 1952 so that the removal of 8 clams per sq. ft. is a reasonable figure. Likewise, experience has shown that it is unlikely that clams ever attain such high densities under normal conditions that diggers can remove as many clams per sq. ft. as were calculated for some of the pre-1945 years. Beds of stunted clams numbering 50 or more per sq. ft. have been observed, but it is unlikely that they could have accounted for the high average densities reported for the early period.

It is highly probable that the prevailing average densities of soft clams in the areas under exploitation during the pre-1945 period ranged between 15 and 20 per sq. ft. The subsequent decline would thus appear less drastic and would more nearly match that indicated by the catch per unit of effort. The exaggerated average densities calculated for the pre-1945 period are undoubtedly due to gross underestimates of the areas dug over.

The expansion of the total area dug over annually in the post-1945 period suggests that the rate of rotation of digging may have been increased and interviews have revealed greater utilization of less productive areas. The field investigations have shown that productive localities have generally been dug over at least twice per year while the less desirable ones have been worked on in increasing amounts. Originally, a crew would dig over an area, removing about 60% of the legal clams and abandon it until growth of a new crop plus the 40% missed brought the population back to an acceptable level. However, the increased demands in recent years have reduced the level of abundance considered worth digging so that repeated exploitation after short intervals has become common. The system which once permitted longer periods of recovery has thus broken down and the productive areas are now being dug over so frequently that they remain in a marginal condition.

The practice of repetitive digging appears to have brought about a more complete utilization of all soft clam resources by forcing the exploitation of marginal areas. As long as digging was limited to areas of high density there were vast expanses of marginal flats where clams were going to waste because they were too scattered to interest the commercial digger. With densities in productive areas maintained at low levels by repetitive digging these marginal areas have become relatively more attractive and their yield has been added to the total catch.

The question of future production depends on how the younger stocks are affected by this present high level of exploitation and how well the marginal areas will stand up. There is no evidence that the parent stocks are being reduced to a level where propagation is endangered because the reproductive biology of the soft clam has been shown to be influenced more by environmental conditions than by the size of the parent stock. One real danger lies in the predator-prey relationships that may be altered by reduction of the standing crops and another is the physical destruction of undersized clams by too frequent digging.

It has been shown that propagation and growth must exceed the rate of removal by predator activity and other forms of natural mortality to provide a surplus for digging. There must also be some margin of safety to provide for

fluctuations in the abundance of predators and to compensate for excessive mortalities from other sources. Excessive removal may reduce the supply to a level at which growth is insufficient to satisfy the predators. This level varies from one locality to another depending on the abundance of predators, intensity and regularity of setting, and rate of growth. There is no evidence that the situation is at all serious at present in the moderately contaminated areas of Boston Harbor, but a sudden influx of predators might alter conditions radically.

The physical destruction of small clams by excessive digging has received a considerable amount of attention in recent years. Numerous investigators have made observations which show that a certain amount of actual breakage or other fatal injury does occur and that it varies with the digging practices and the character of the soil. Soft, muddy soils minimize breakage and favor the re-establishment of small clams and breakage tends to be high in gravel and stony soils. Thus the frequent reworking of certail areas may reduce the long term yield because of the cumulative effects of digging on clams of sublegal size.

If the better localities in the moderately contaminated areas of Massachusetts are becoming less productive because of overexploitation, the effect has been hidden by the expanded utilization of marginal areas. However, some attempts have been made to improve desirable localities by closing areas where good setting has occurred. This can form a realistic basis for a general management policy if these areas can be shown to benefit by closure. Good prospective areas may then be protected until the maturation of their crops with the bulk of the digging effort being absorbed by the marginal areas in the interim.

The universal preference for clams just over the 2 inch legal minimum limits the extent to which the yield can be augmented by management because no significant increases in volume can be obtained by allowing time for added growth. Thus no advantage can be achieved by prolonged closure of good growing areas. An ideal management program would provide for the protection of the young and would permit their immediate removal upon reaching legal size.

THE SOFT SHELL CLAM RESOURCES OF BOSTON HARBOR

Boston Harbor contains the most extensive and heavily exploited moderately contaminated soft clam areas of the entire coast of Massachusetts. For the past three years field investigations have been conducted to determine the condition of the soft clam fishery as reflected by the actual standing abundance. The changing nature of the clam populations as influenced by setting, growth, and removal has made it impossible to formulate a description that would apply to the entire locality at any one time, but sufficient coverage has been made to permit a generalized description of this fishery and its resources. Practically all the moderately contaminated localities in Boston Harbor have been visited at least once. Wherever clams occurred in appreciable abundance representative samples of the flats were screened and the clams measured to determine the assortment of sizes. This information was supplemented by estimates of the number of syphon holes and the catch of the diggers. Rough estimation was often necessary because the total area was too great to permit adequate determinations by screen sampling within a reasonable time. Diggers, shellfish officers, and local residents were interviewed for digging history and personal im-

pressions. Notes were made of the character of the soil, presence or absence of predators and competitors, and the prevailing species of incidental organisms. A few representative clean and grossly contaminated areas were examined for comparison.

The important information derived from the investigation which bears on the future of the fishery is the ratio of the density of legal (2 inch) clams to that of the smaller sizes which are to form the future crops. The maps included in this section are shaded to show the approximate extent of the clam bearing areas with the numbers of legal clams per square foot obtained by screening encircled and the numbers of sublegal clams in squares. Estimates made without screening are so indicated. Management policies for individual localities are suggested. The Hingham Bay section which was reported previously is included again in greater detail.

Hull: There are two moderately contaminated areas in Hull, one to the north and around Hog Island, and one south of Sunset Point. Both were examined in 1951. The northern area shown in Map I was sparsely populated with the greatest concentration in the cove shown in the figure. The low abundance of legal clams and the scarcity of sublegal ones indicates poor prospects for this area. Two portions of the area south of Sunset Point showed greater promise. See Map II. The sandspit halfway out the southern shore of the point was of particular interest because it showed no evidence of recent digging. The ratio of 14 legal to 31 small clams was indicative of future prospects. The head of the cove, in contrast, showed evidence of heavy digging and the clams were only half as dense with a ratio of only 4 legal to 19 small.

These areas illustrate three different conditions that would be met in any attempt to regulate digging for future interests. The northern area is barely marginal and would not be improved by any restrictive measures. The cove is a more productive area which would profit by closure for about two years, the density of legal clams being low. The sandspit, on the other hand, presents a peculiar problem. The legal clams were sufficiently numerous to justify immediate removal, but the younger stocks were present in sufficient abundance to justify some protection. In this case it would be necessary to weigh the advantages of obtaining an immediate crop against the possibility of a larger future one.

Hingham: The moderately contaminated areas of Hingham occur in Weir River and along the Weymouth Back River shores. These areas were all examined in 1951 with the exception of those near Stodder's Neck on Weymouth Back River, which were examined in 1952. The Weir River areas were variable. See Map II. The most productive locality was on World's End Island with a ratio of 10 legal to 31 sublegal clams per sq. ft. The remaining flats in Weir River were generally infested with mussel beds with small accumulations of clams scattered among them. Most of the Weymouth Back River shore consisted of stony gravel with sparse accumulations of clams in densities of 5 to 10 of all sizes per sq. ft. See Map III. The cove east of Stodder's Neck examined in 1952 exhibited a considerable variability in the abundance of clams with good prospects for the future. The muddy areas in the middle of the cove contained small clams exclusively and it was reported that they appeared every year but died before maturing. Gravel patches on the east side of the cove were reported to have been cleaned out. However, the ratio of 144 sublegal to 14 legal clams per sq. ft. forecasted good future crops if closed for two years or more since the majority of the smaller ones were less than an inch long. The firm mud flat at the mouth of the cove was being dug at the time of the investigation and

was practically cleaned out as indicated by the ratio of 4 legal to 18 sublegal clams per sq. ft. This area also contained a sprinkling of a new set too small to be retained by the screens.

The Stodder's Neck section appears to be the only part of Hingham that might benefit from management except for the uncontaminated areas which are under the jurisdiction of the town authorities. The Weir River section contained spotty accumulations which would be unsuitable for management and much of the Weymouth Back River shore is naturally unproductive because of physical features. However, the abundance of small clams in the Stodder's Neck section would justify serious consideration.

Weymouth: The soft clam resources of Weymouth are situated along the north shore of the Back River, south shore of the Fore River and around Grape Island. All areas were examined in 1952 except Grape Island. See Map III. The density of legal clams was low in all the Weymouth areas, but future prospects appear bright for the inner section of the Back River which contained a heavy set averaging about 200 three-quarter inch clams per sq. ft. with legal clams averaging less than 10 per sq. ft. The growth lines of the legal clams indicated that it would take at least three years for the set to mature. All other areas had been reported to have been dug clean and the densities of remaining clams indicated in Map III did not include appreciable numbers of small ones so that there is little prospect of improvement in the immediate future. Grape Island soft clams were generally limited to the southern shore. In 1951 the legal clams averaged 5 per sq. ft. in scattered patches as is shown in Map III.

The soft clam areas of Weymouth are limited in spite of the relatively long coastline. The greater part of the shore along Weymouth Fore River is exposed and rocky so that productive areas are limited to those just described. The absence of clean areas which might absorb some of the digging pressure makes it difficult to rotate areas in a cycle that is long enough to provide for adequate growth. Considerable benefit might result from closure of certain portions of the Back River shore for two or three years.

Quincy: The Quincy coast extends from Weymouth Fore River to the Neponset River and contains some of the most heavily worked clam areas in Boston Harbor. They fall into three groups geographically: (1) the Hough's Neck section; (2) the Wollaston Beach section; and (3) the Squantum-Neponset River section.

The important areas of the Hough's Neck section lie in Town River Bay and Rock Island Cove. See Map IV. Town River Bay was visited in 1950 and Rock Island Cove in 1951. In 1950 the clams in Town River Bay consisted of a single year class averaging 30 to a sq. ft. The size range was narrow with the clams distributed fairly evenly each side of the 2 inch legal length. In 1951 the clams in Rock Island Cove were distributed along the upper reaches in scattered patches too irregular for accurate sampling. A heavy set covering a large part of the Cove and numbering hundreds per sq. ft. was reported in 1952. Clamming has been marginal along Manet Beach and the north shore of Hough's Neck, but a heavy set in 1951 between Rock Island Head and Raccoon Island indicated good future possibilities for a limited area. This set is discussed in detail in a separate section.

The Wollaston Beach section extending from the base of Hough's Neck to Squantum is uncontaminated as far as the Wollaston Beach Yacht Club and is a public fishing area. It has been worked over continuously by all classes of

diggers because of its proximity to the main highway which makes it easily accessible to all the residents of greater Boston. It is described here to show the effect of unrestricted digging. A portion of the western end of Wollaston Beach called the Willows had been closed for some time for conservation. See Map IV. This measure appears to be completely justified because of the abundance of small clams which fall in two separate size groups, one just under two inches and the other much smaller. In the adjacent open area called the Half Moon, legal clams were limited to the lower levels of the Beach. Accumulations of small clams just under legal size were found in the adjacent Cove but in insufficient numbers to indicate substantial future crops. The remaining portions of the uncontaminated area extending from Black's Creek to the Wollaston Yacht Club are directly accessible to tourists driving along Wollaston Boulevard. The entire locality had been so thoroughly dug over by August 1952 that it was impossible to find a single representative area for sampling. Scattered large clams occurred in the lower levels of the beach but only in sufficient numbers to provide a bucket full (¼ bu.) per tide for casual diggers. One sample taken north of Black's Creek gave 5 legal and 3 sublegal clams per sq. ft. See Map V.

The only portion of the uncontaminated section of Wollaston Beach with good future prospects was the small portion in the Willows that was closed at the time of examination. The density of the clams and distribution of sizes would make elaborate management of the area somewhat of a problem. The number of clams expected to reach legal size in the near future appeared to be sufficient to justify their utilization at the expense of the smaller size group that would mature at a much later date. The overcrowded condition of the smaller size group might easily lead to stunting or reduced growth so that the smallest clams might never become available unless the larger ones were removed upon reaching legal size.

The moderately contaminated northwest portion of Wollaston Beach had just been dug over when it was examined in August 1952. See Map V. Representative samples were unobtainable as a result. Legal size clams had been reduced to 3 or 4 per sq. ft. and those of smaller sizes were too scattered to permit an accurate determination. Diggers reported that they had been able to get from ½ to 1½ barrels per tide when they first entered the area. A similar undug area south of Moonhead Causeway was examined for comparison. See Map VI. Digging was prohibited because the area was grossly contaminated and it was situated where illegal digging could be readily detected and prevented. The clams numbered 54 to the sq. ft. with lengths distributed between 1 and 2½ inches.

The Squantum-Neponset River section is situated around the Squantum Naval Base. See Map VI. The cove east of the Base contained 9 legal clams to 43 sublegal clams per sq. ft. in August 1952. Diggers working in the area said they were getting 2/3 to 1 1/3 barrels depending upon the duration of the tide. The substratum of very soft mud appeared to favor the re-establishment of the smaller clams turned up in digging so there were good prospects for the future.

Considerable variation in density was found around the northwest corner of the Naval Base with large clams predominating. Inaccessibility discouraged frequent use of the area but 15 diggers managed to obtain approximately 1 barrel of 2½ to 3 inch clams apiece per day during part of August. Accumulations of small clams were limited to the areas around the tip of Squantum Point as is shown in Map VI.

The extent and diversity of the soft clam resources of Quincy make them reasonably well suited to management programs. Good digging may be expected in the Rock Island Cove and Raccoon Island areas if they are kept closed long enough to permit maturation of the present crop of small clams. In the meantime there is enough marginal area to permit the fishery to continue at its present level.

South Boston: The entire shoreline of South Boston is grossly contaminated with the exception of a stretch from Columbus Park to Castle Island. See Map VII. Much of this section is primarily a bathing beach with loose sand at the upper levels and a sharp transition to soft mud near the low tide mark. Clams are limited to the soft mud level because the beach sand is unsuitable for their existence. Local regulations prohibit clamming during the summer season. In 1952 clams were all found to be very large and averaged 5 to 10 per sq. ft. and diggers showed little interest in them.

East Boston: The East Boston soft clam resources are sitauted on the south and east sides of the Logan International Airport. Artificial extensions of the Airport have connected Apple Island and Governor's Island so that their flats are now continuous. See Map VIII. In 1950 the Governor's Island flats were densely populated with stunted clams of fairly uniform size. Large portions of these flats contain as many as 300 clams per sq. ft. with approximately 100 just over 2 inches in length. Clams became progressively less abundant toward the eastern end of the area with the flats adjacent to Apple Island containing about 50 per sq. ft. The size ratios remained about the same with 20 just over 2 inches long and 30 just under. The Apple Island flats had been dug over constantly for some time up to two months previous to the day of examination but had been abandoned in favor of the Governor's Island flats where the legal size clams were more numerous.

The Governor's Island and Apple Island flats between them contained the most extensive dense population of legal or near legal size clams of any one locality in Boston Harbor. The population undoubtedly originated as a single set where conditions permitted such a high percentage of survival that the clams became overcrowded and growth was retarded. The extremely crowded conditions with a narrow range of size approximating the 2 inch legal minimum has made it difficult for the diggers to dig efficiently and select only the legal size clams. Thus the relative yield of the area has probably been lower than that of other areas in spite of the enormous standing crop. Such an area would be an ideal source of small clams for transplantation if mechanical devices could be used for efficient harvesting. However, the poor success that has resulted from transplantation and the adverse attitude of the diggers have discouraged this practice.

The average level of abundance of legal size clams observed in practically all the moderately contaminated areas of Boston Harbor has confirmed the statistical evidence on the condition of the fishery. All areas investigated contained legal clams in low abundance with the exception of isolated localities such as Town River Bay and the Logan Airport flats, both of which were examined in 1950. It is quite apparent that clams are being removed about as fast as they grow to legal size, although it is not clear how this will affect subsequent production. There is some indication of destruction of the young, particularly where the soils are stoney, but the erratic periodicity of setting prevents any determination of this with complete certainty. It is likely that considerable

benefit might be derived from closure of areas containing dense sets, but it would be necessary to follow the progress of these sets with care to prevent stunting from overcrowding.

It is fairly certain that the present high level of total production is a direct result of increased effort and the willingness of new diggers to expand into marginal areas. Future production will depend on whether or not the intensified digging affects the younger stocks adversely so that they fail to mature. It will also depend on the ability of the marginal areas to support continued exploitation.

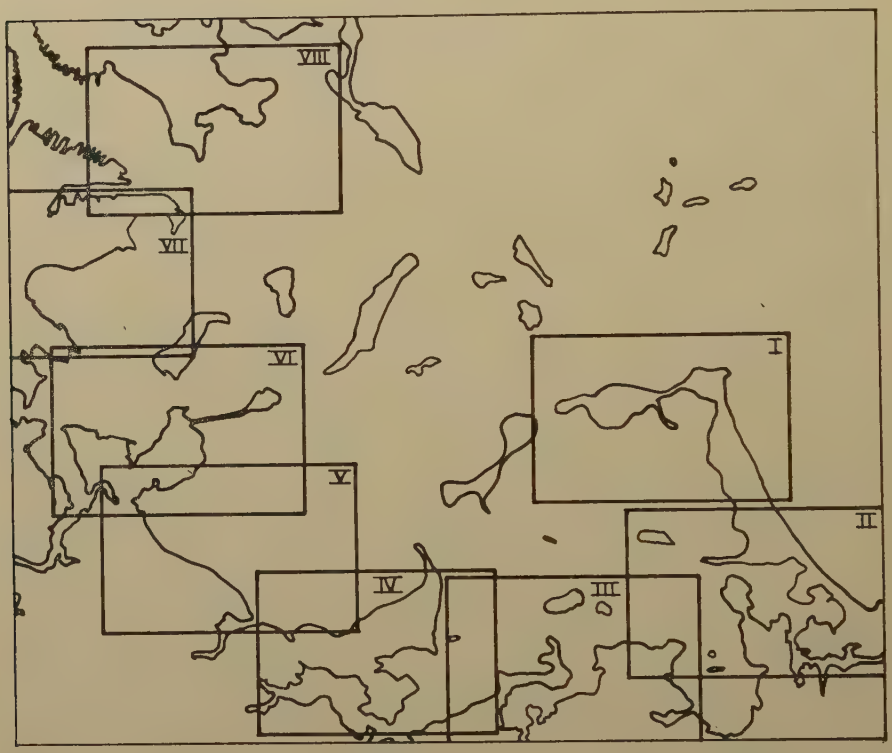

Map of the coastline of Boston Harbor showing locations of maps in the following series.

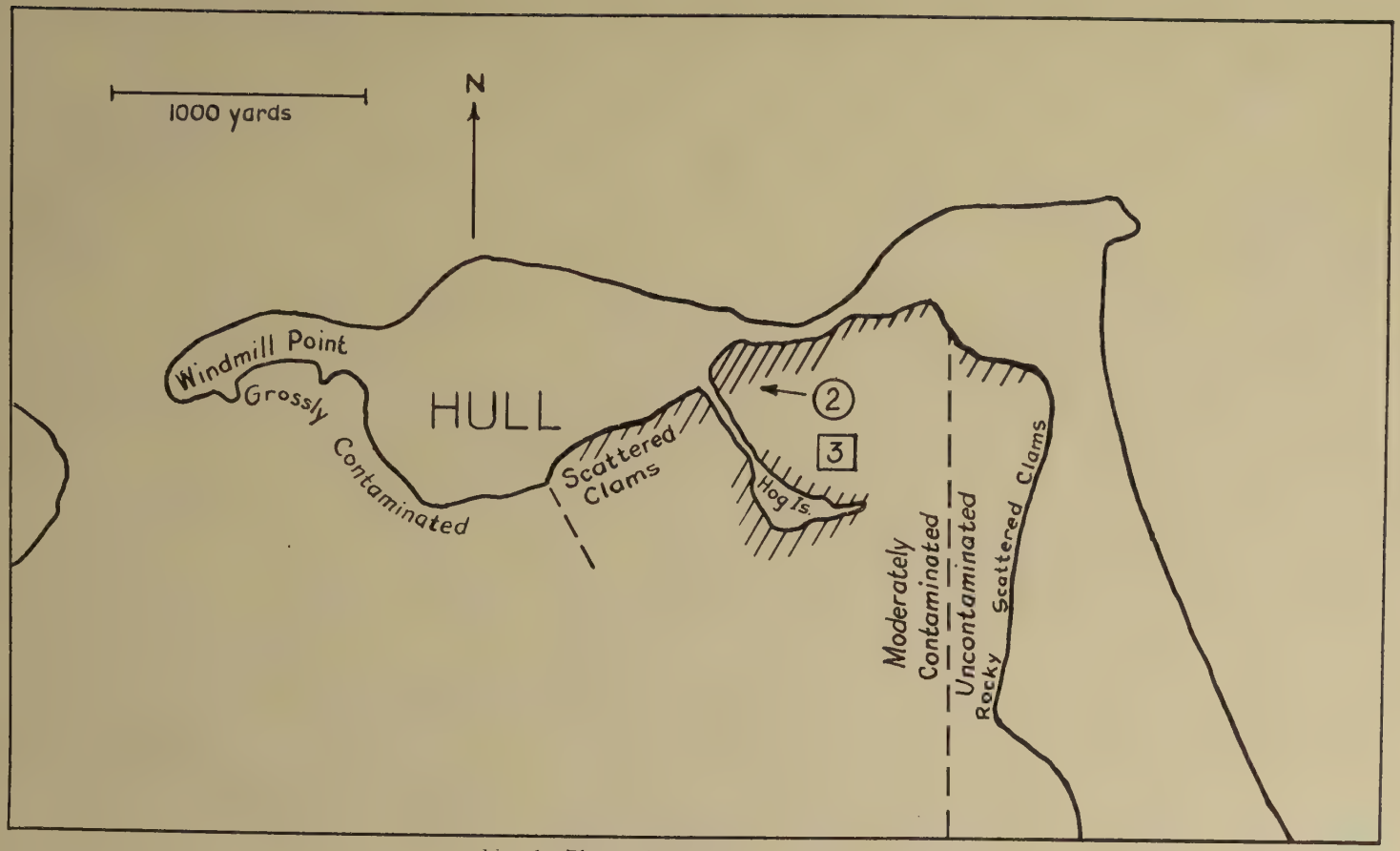

Map 1 The northern section of Hull

Map 2 The southern section of Hull and the eastern section of Hingham

Map 3 Hingham and Weymouth

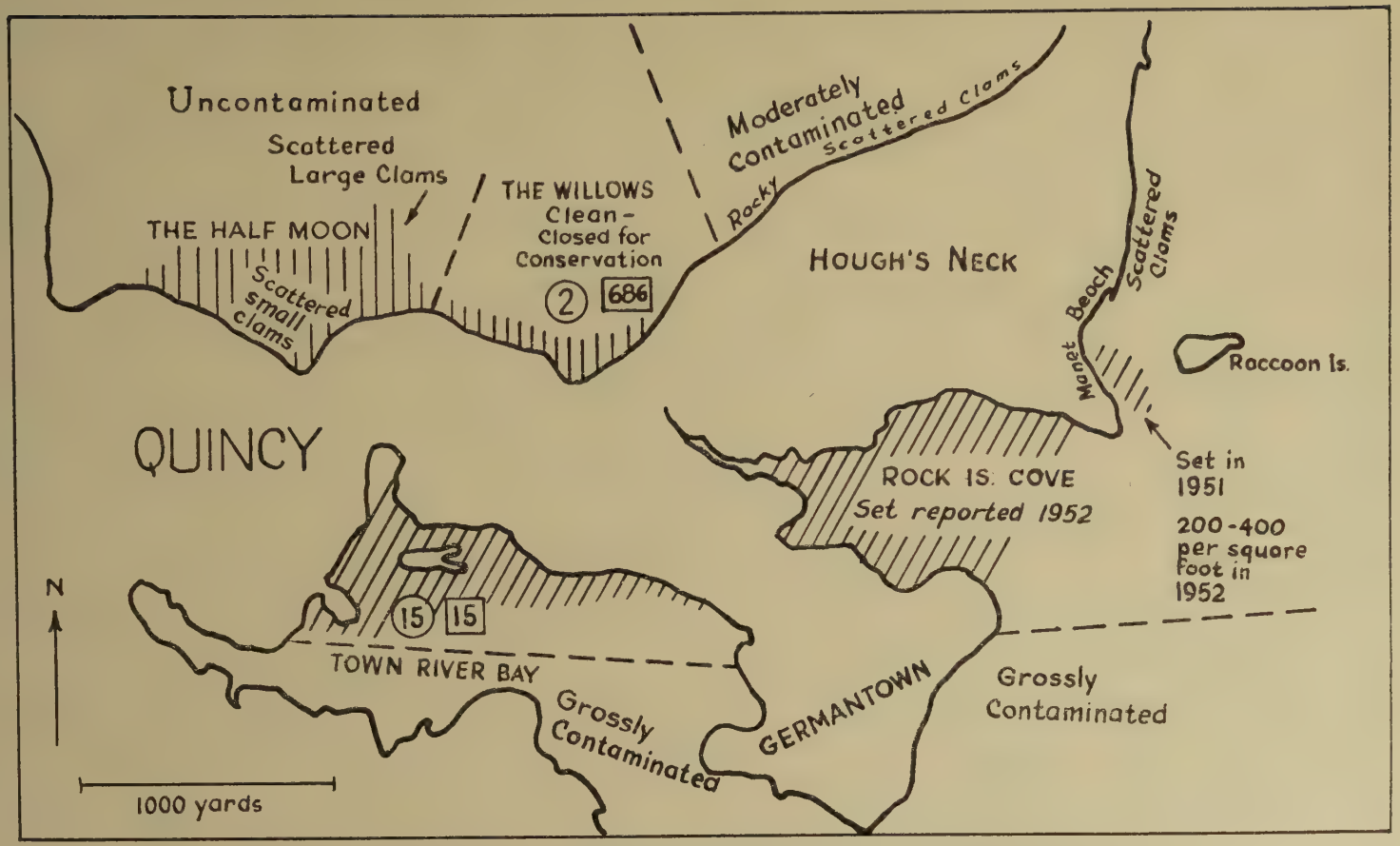

Map 4 The Hough's Neck section of Quincy including "The Willows" and "The Half-Moon"

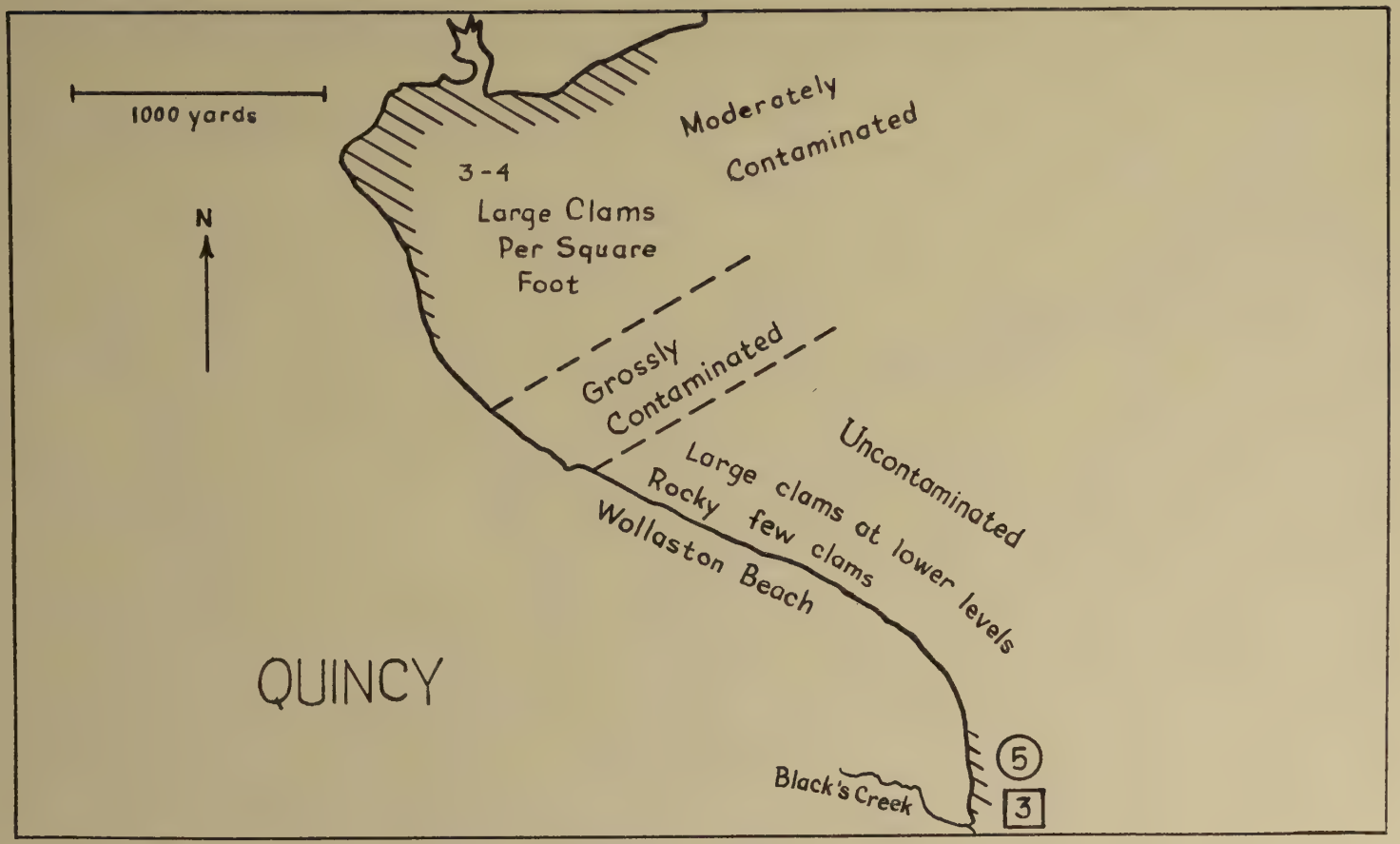

Map 5 The Wollaston Beach section of Quincy

Map 6 The Squantum-Neponset section of Quincy

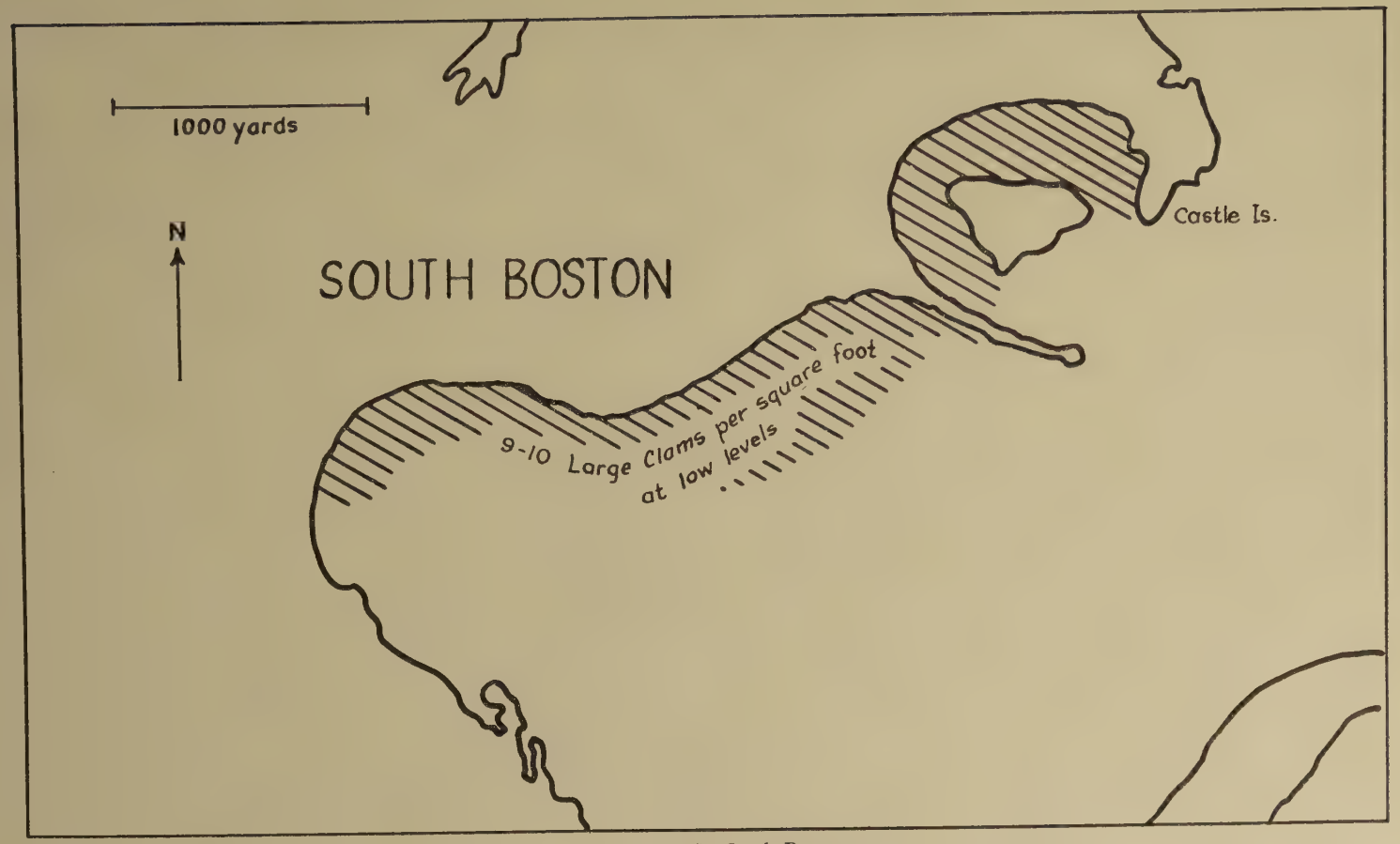

Map 7 South Boston

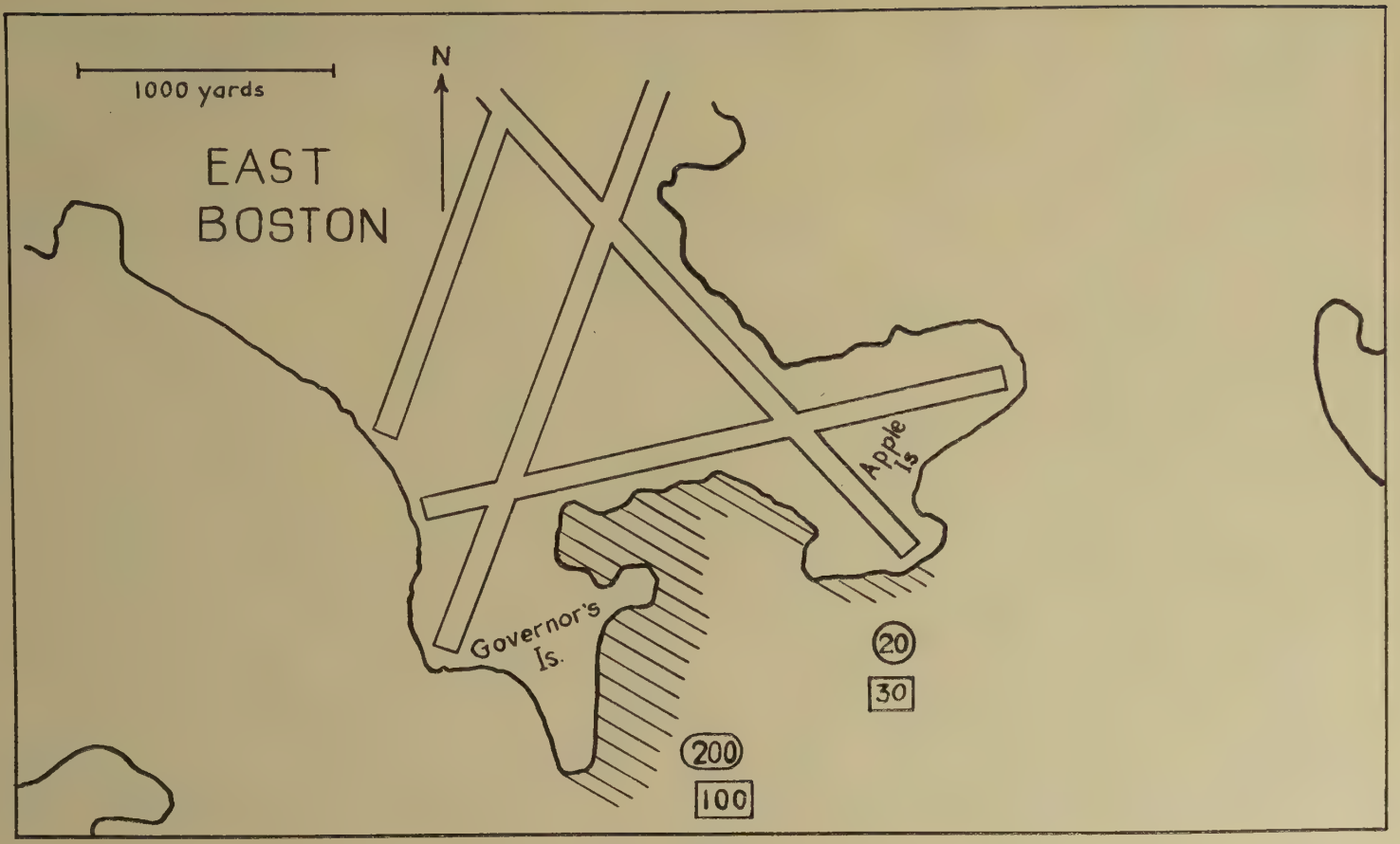

Map 8 East Boston

RACCOON ISLAND SET

An exceptional set of soft clams discovered near Raccoon Island, off Manet Beach, Houghs Neck, Quincy, (see Map IV) in August 1951 was examined at intervals until September 1952. The original condition of the set was described in a previous report.

The physical characteristics of the area in which the set occurred are typical of a considerable portion of the shoreline of Boston Harbor. The upper beach consists of stoney gravel and slopes steeply down to a point just above the low tide mark. Here it changes abruptly to a firm sand flat which extends seaward with a gentle slope for a considerable distance. Some distance beyond mean low water the soil changes abruptly from sand to soft yielding mud. See Figure 3.

In August 1951 the sand zone contained 10,000 or more clams per square foot averaging ⅜ of an inch long. There was no set beyond the sand-mud boundary on the seaward side, and none in the gravel beach on the landward side. There were no large clams either in the sand or mud but the gravel beach contained scattered clams averaging two inches long.

During September and October the largest of the clams of the set began to disappear from the seaward side of the sand flat and the average density throughout the area declined to less than 2000 per sq. ft. by November. See Figure 3. During this time windrows of paired shells formed near the high water mark. It was apparent that clams were being removed as fast as they grew to ½ inch in length and were being washed up the beach where the violent interaction of the waves and pebbles crushed their shells or otherwise injured them fatally. A few managed to survive and establish themselves in the gravel beach between the half tide mark and its lower border. These survivors numbered 400 per sq. ft. and varied from 0.7 to 1.0 inches long in August 1952.

The geological structure of the Raccoon Island region gives some indication of the mechanisms responsible for the appearance of the set and its subsequent history. The steep gravel beach with the broad sand and mud flats extending seaward occurs where there is difference between force of waves as they approach the shore and the force of the returning backwash. The action of the waves is strong enough to transport particles as large as the largest pebbles up the beach, while the returning backwash is only strong enough to return the sand and mud particles.

The force of the backwash diminishes as it flows seaward and the heavier sand particles settle out in a narrow zone along the low tide mark. The lighter particles are retained to be deposited farther out where the force becomes still more reduced. In this manner, a random assortment of particles within the influence of the action of the waves may be transported shoreward and sorted for size in definite zones by selective deposition from the backwash. The location of the various zones depends on the intensity of the water movements, the size of the particles and their specific gravity. The same water movements may act on clams before they establish themselves deep enough to prevent dislodgment. However, the sorting characteristics of the clams would differ from that of pebbles and sand grains because of their lower specific gravity.

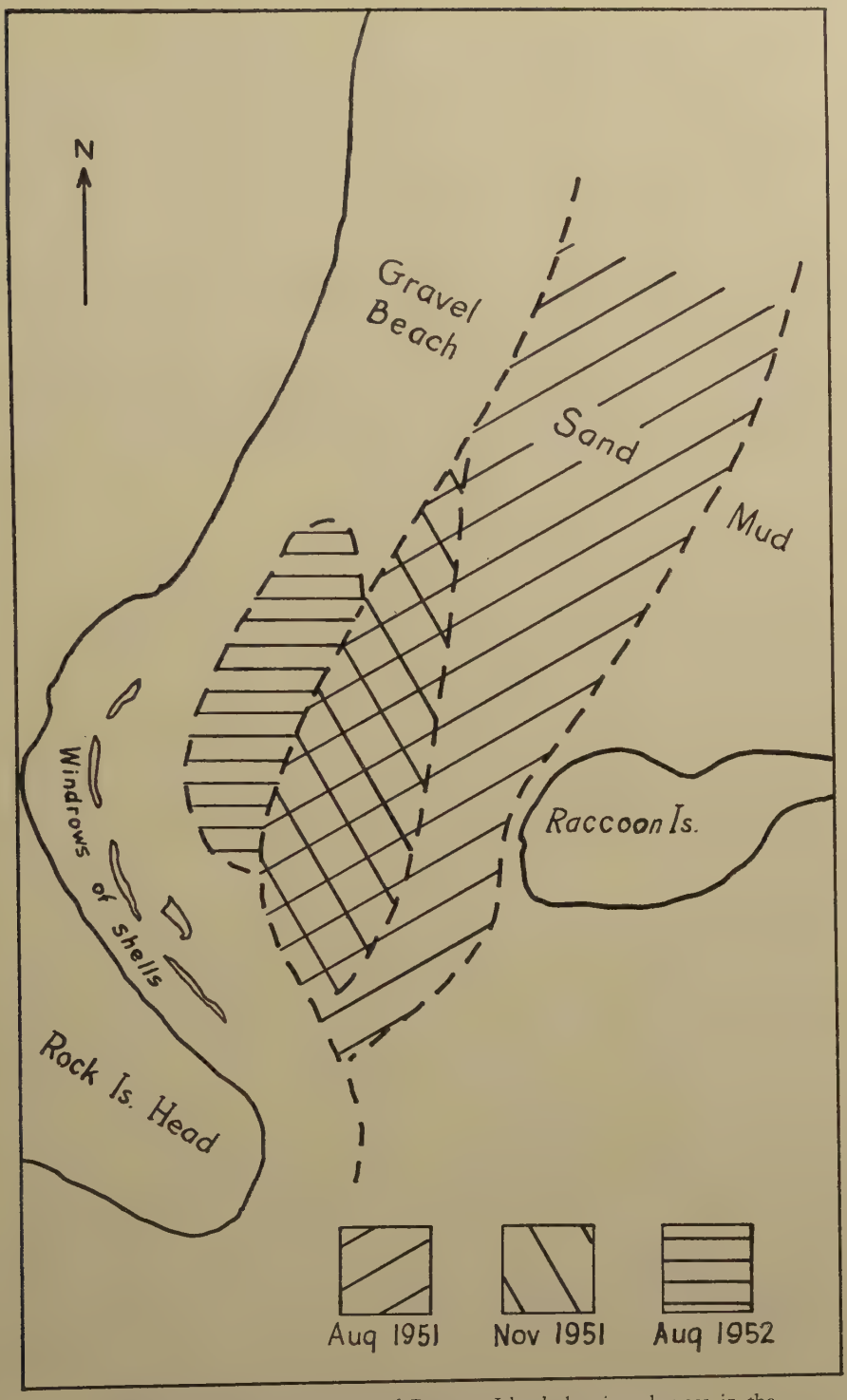

Figure 3—Map of the vicinity of Raccoon Island showing changes in the distribution of soft clams of the set of 1951

This mechanism provides a plausible explanation of the initial concentration of clams in the sand zone near Raccoon Island, and their subsequent transferral to the gravel beach. The gentle seaward slope of the beach near the low tide line forms a broad expanse of bottom under the influence of wave action. Young clams setting throughout this area were probably dislodged, transported, and sorted by water currents which finally deposited them in the sand zone. This zone thus became an area of concentration. As long as the clams remained within a certain size range they were returned to the same zone if dislodged by the waves. As soon as the clams grew to ½ inch in length, their sorting characteristics probably changed and they became comparable to the pebbles. Water movements then transferred them to the gravel beach. During the final transfer, their greater weight probably prevented the clams from being carried in suspension, but caused them to be washed along the bottom instead. The violence of the waves and the grinding action of the pebbles accounted for the high percentage of mortality so that comparatively few survived to establish themselves between the tide lines.

THE EFFECT OF CHANGES IN WATER TEMPERATURE AND SALINITY ON THE FEEDING HABITS OF THE BORING SNAILS,

POLINICES HEROS and *POLINICES DUPLICATA**

BY

JAMES E. HANKS

There are two species of boring snail, *Polinices heros* and *Polinices duplicata,* which are considered serious predators of the soft shell clam (*Mya arenaria*) and the bay quahog (*Venus mercenaria*) on the coastal flats of the Commonwealth. They are distributed along the Atlantic Coast as follows (Miner 1950):

Species	Range
P. heros	Gulf of St. Lawrence to North Carolina
P. duplicata	Massachusetts Bay to the Gulf of Mexico

It has been observed by Turner (1949) and Sawyer (1950) that *P. heros* primarily frequents the rather constant and high salinity waters prevailing along the open coast, while *P. duplicata* is an inhabitant of the variable and generally lower salinity waters of bays and harbors. Thus, it would appear that *P. heros* is an oceanic species and *P. duplicata* is an estuarine species.

Taking into consideration the known north-south distribution of the snails and the annual water temperature gradient over this same area, it appears probable that water temperature exerts some influence on this distribution. Similarly, it seems probable that the low to high salinity gradient occuring from inland tidal waters to the open ocean is responsible, at least in part, for the observed estuarine preference of *P. duplicata* in contrast to the oceanic habitat of *P. heros.*

Previous feeding studies by Sawyer (1950) on *P. duplicata* had shown a reduction in feeding rate of approximately 4/5ths when the water temperature was lowered from 70°F. to 50°F. This was a considerable amount in that the consumption of clams by 10 snails went from 202 at 70°F. down to 46 at 50°F. during one month feeding periods. This work showed that the water temperature had a direct effect on the feeding rate and suggested that at some low temperature level *P. duplicata* would cease feeding.

It was considered that additional studies on the effect of changes in temperature and salinity on the rate of feeding of both species of snails would be of value in estimating the destructive potential of these shellfish predators. In order to study these factors, a series of experiments was conducted at the Woods Hole Oceanographic Institution during the fall and winter of 1952-53. Temperature experiments were carried out in compartmented, wooden tanks with a two inch layer of sand on the bottom covered by about five inches of running sea water. Various water temperatures were provided by the use of heating and refrigerating units controlled by suitable thermostats. The salinity experiments were conducted in wooden buckets in which different salinities were

* A summary of material submitted as a master's thesis at the Univ. of New Hampshire.

maintained by mixing appropriate amounts of salt and fresh water. Since this water had to remain stagnant, it was necessary to aerate it with compressed air. Feeding periods ranged from 7 - 10 days. Three to five snails, of various size groups, and twenty to thirty clams (*Mya arenaria*), ranging in size from 15 - 30 mm, were used in each feeding compartment.

A. Temperature experiments. (see Table I for a summary of results).

These experiments were conducted in water of a constant salinity of 32 o/oo. Both *P. heros* and *P. duplicata* fed at similar rates at a water temperature of 21°C., five snails consuming up to 25 clams in a 7 day feeding period. It was not possible to determine the feeding rate at higher temperatures, since the heating unit was not capable of raising the water temperature higher than 21°C. from existing fall water temperatures. As the water temperature was lowered 3° to 5°C. every few weeks, the feeding rate of both species of snail showed a decrease. With the first 5°C. drop in water temperature, from 21°C. to 16°C., both *P. heros* and *P. duplicata* showed a 50% reduction in feeding rate. The feeding rate of both species compared quite closely at all temperatures down to and including 7°C.

P. duplicata first stopped feeding at 5°C. and did not feed for three successive feeding periods (22 days) at this temperature. *P. heros,* on the other hand, fed at progressively lower rates at temperatures down to and including 2°C. However, the rate of feeding by *P. heros* at this temperature (0.05 clams per snail per day) was so low that one snail would consume only one clam every twenty days. Experiments attempted at 0°C. were unsuccessful due to equipment difficulties.

The limiting temperature, with respect to feeding, for *P. heros* and *P. duplicata* was not lethal to either species. Although *P. duplicata* did not feed at a temperature of 5°C., all snails survived this temperature for periods of up to three weeks and when returned to warmer water resumed feeding. How long they could have gone without food is not known, but it is probable that they could withstand this low temperature restriction on feeding for any period at which these temperatures prevail in New England waters.

B. Salinity experiments. (see Table II for a summary of results.)

These experiments were conducted at a water temperature ranging between 14° - 18°C. *P. heros* fed at a slightly higher rate than *P. duplicata* at a salinity of 32 o/oo. However, with the first lowering of the salinity to 25 o/oo, both species of snail had a similar feeding rate. Thus, while *P. heros* showed a decrease in feeding rate with the lowering of salinity by 7 o/oo, *P. duplicata* maintained a similar rate for both a salinity of 32 o/oo and 25 o/oo. This suggests that at salinities above 32 o/oo the feeding rate of *P. duplicata* might decrease, which would agree with their known concentration in estuarine waters.

The feeding rate of *P. heros* declined with each lowering of the salinity down to 18 o/oo, but remained relatively the same as the feeding rate of *P. duplicata* at these salinities. However, the feeding rate of *P. heros* dropped off sharply at salinities of 14 and 12 o/oo and this species stopped feeding entirely at a salinity of 10 o/oo.

P. duplicata, although similarly showing a decline in feeding rate with each lowering of the salinity below 25 o/oo, fed fairly well at salinities down to

TABLE I.

Feeding rate of *P. heros* and *P. duplicata* at various temperatures (expressed as "clams per snail per day".)

Feeding rate of *P. heros*					Feeding rate of *P. duplicata*			
Temp. °C.	Days of feeding	Clams consumed	No. snails	Feeding rate	Days of feeding	Clams consumed	No. snails	Feeding rate
21.0	7	25	5	0.63	7	25	5	0.63
16.0	7	62	30	0.29	7	63	30	0.30
14.0		No data			7	63	40	0.18
12.0	7.5	59	30	0.26	7	46	30	0.21
10.0	7	78	45	0.24	7.5	46	30	0.20
7.0	7	11	15	0.10	7	24	30	0.11
5.0	7	12	30	0.06	22	0	15	0.00
2.0	7	16	45	0.05				

TABLE II.

Feeding rate of *P. heros* and *P. duplicata* at various salinities (expressed as "clams per snail per day".)

Feeding rate of *P. heros.*					Feeding rate of *P. duplicata*			
Sal. o/oo	Days of feeding	Clams consumed	No. snails	Feeding rate	Days of feeding	Clams consumed	No. snails	Feeding rate
32	8.5	27	6	0.53	8.5	23	6	0.45
25	7	10	3	0.47	7.5	21	6	0.47
18	7	10	9	0.16	7	14	9	0.23
14	7	1	6	0.02	7	7	6	0.17
12	14	3	6	0.04		No data		
10	14	0	6	0.00	7	10	12	0.12
8					14	2	3	0.05
6					14	0	6	0.00

10 o/oo. The feeding rate at this salinity (0.12 clams per snail per day) would have resulted in one snail consuming one clam every 9 days. It is interesting to note that *P. heros* fed at about this same rate by the time the salinity had been lowered to 18 o/oo. *P. duplicata* ceased to feed at a salinity of 6 o/oo.

P. duplicata proved much less sensitive to low salinities than *P. heros* not only in its feeding rate index but also for survival. *P. heros* kept in water of 10 o/oo for periods of over one week did not live, even though returned to higher salinity water. Only one *P. duplicata* out of nine died at a salinity of 6 o/oo after a period of three weeks, and the remaining eight snails resumed feeding when placed in higher salinity water.

C. Conclusions and Discussion.

On the basis of this experimental data, it is possible to make the following conclusions:

1. The rate of clam consumption by both species of snail decreases as the temperature of the water is lowered (within the limits set by the experiments).

2. The rate of clam consumption by both species of snail decreases as the salinity of the water is lowered (within the limits set by the experiments).

3. *Polinices duplicata* does not feed at water temperatures of 5°C. or lower, nor at salinities of 6 o/oo or lower.

4. *Polinices heros* feeds at water temperatures down to and including 2°C., but does not feed at salinities of 10 o/oo or below.

The results of this study indicate that the effect of water temperature and salinity on the feeding habits of these snails may be one facor influencing the distribution of both species. In addition, *P. heros* appears to have an advantage over *P. duplicata,* in that it can feed throughout the annual temperature range for New England waters. Also it is not restricted to inter-tidal waters, but can feed in the cold bottom waters offshore, where populations of the surf clam (*Mactra solidissima*) and the ocean quahog (*Artica islandica*) are abundant. *P. duplicata,* while restricted by low temperatures, has the advantage of being able to feed at lower salinities than *P. heros* and therefore is able to concentrate its feeding on the stocks of soft shell clams that are present in estuarine waters. As high temperature limits were not obtained, it cannot be stated what their effect would be on the distribution or feeding rate.

The feeding rates established in this study agree favorably with those resulting from summer field experiments by Mead and Barnes (1903) in Rhode Island and Belding (1930) in Massachusetts, as well as the laboratory experiments of Sawyer (1950). Thus, when the water temperature is near 21°C. (70°F.) both species of snail can consume approximately one clam every two days.

BIBLIOGRAPHY

BELDING, DAVID L., 1930: The Soft-Shelled Clam Fishery of Mass., Commonwealth of Mass., Dept. of Conservation, Div. Fish and Game, Marine Fisheries Section, Marine Fisheries Series, No. 1, Boston.

MEAD, A. D. and E. W. BARNES, 1903: Observations on the Soft-shelled Clam. Ann. Reports, Comm. Inland Fisheries, Rhode Island.

MINER, R. W., 1950: Field Book of Seashore Life, G. P. Putnam's Sons, New York.

SAWYER, DAVID B., 1950: Feeding Activities of the Boring Snail, *Polynices duplicata.* Third Report on Investigations of Methods of Improving the Shellfish Resources of Mass., Commonwealth of Mass., Dept. of Conservation, Div. of Marine Fisheries, Boston.

TURNER, HARRY J. JR., 1949: Report on Investigations of Methods of Improving the Shellfish Resources of Mass., Commonwealth of Mass., Dept. of Conservation, Div. of Marine Fisheries, Boston.

Contribution No. 658

RAINDROP SIZE-DISTRIBUTION IN HAWAIIAN RAINS

By Duncan C. Blanchard

Woods Hole Oceanographic Institution[1]

(Manuscript received 8 June 1953)

ABSTRACT

A brief survey of the major techniques of raindrop size-sampling is given. The filter-paper technique, finally adopted for use in this study, adapts itself admirably to the sampling of Hawaiian orographic rains.

The change in the drop-size distribution of rain as it falls from cloud to ground may be considerable. It is affected by wind shear, gravity separation, evaporation and drop collision. The evaporation error alone can be appreciable. The many small drops of the Hawaiian orographic rains may completely evaporate in a sub-cloud fall of only 1000 m. The evaporation problem was eliminated, and the others minimized, by sampling all the orographic rain at cloud base or within the cloud itself.

Drop-size distributions were obtained in such non-orographic rains as thunderstorms and cyclonic storms. The pertinent meteorological parameters, such as liquid-water content, median drop diameter, and radar reflectivity, agree reasonably well with the values given by other investigators.

The measurements made in orographic rains from non-freezing clouds, however, lead to considerably different values of these factors. The raindrop distributions are narrow, with the largest drops rarely exceeding 2 mm in diameter. In general, the higher the intensity, the more numerous are the drops at the large end of the spectrum. At the small end of the drop spectrum (<0.4 mm), however, increased intensity is accompanied by a decrease in the drop count. Distributions of this type indicate the absence of any chain-reaction process.

Concentrations of drops less than 0.5 mm in diameter often are in excess of 40,000 m^{-3}. These large numbers of small drops give low values for median drop diameter and radar reflectivity, but high values of liquid-water content.

All of the drop distributions have been put into three categories: (1) non-orographic rain, (2) orographic rain at cloud base, and (3) orographic rain within the cloud and near cloud top. In each case, regression equations have been developed to express the meteorological parameters as a function of rain intensity.

1. Introduction

In October 1951, the writer and Mr. A. H. Woodcock went to the Hawaiian Islands to begin a joint ten-months study with the Meteorology Department, Pineapple Research Institute and Hawaiian Sugar Planters' Association. The study was aimed toward a better understanding of the basic mechanism of warm-cloud rain. It is believed that large salt particles of marine origin form the nuclei from which raindrops develop, first by condensation and later by accretion (Woodcock, 1952). To test this hypothesis further, three separate programs of study were carried out: (1) measurements were made of the air-borne salt particle distribution beneath, at and above the cloud layer, (2) the variation of rainwater chloride-content *vs.* intensity was studied, and (3) the raindrop size-distributions at various points within the cloud were obtained.

Inasmuch as the meteorological literature, with the exception of Anderson's (1948) work, contains little information on raindrop size-distributions from non-freezing clouds, it was felt that the data obtained in connection with this third program would be of of sufficient interest to warrant publication. It is becoming increasingly more evident that a study of the drop distribution may enable us better to understand the growth mechanism of the drops.

One of the earliest papers on raindrop size described observations of splash pattern on slates (Lowe, 1892). At about this time, the idea of exposing chemically treated filter papers to the rain was suggested, but it remained for Wiesner (1895) to publish the first detailed results. A novel approach to raindrop size-measurements was achieved with the flour technique (Bentley, 1904). The raindrops, on falling into a flour-filled container, produced hard dough pellets whose size was a function of the diameter of the original raindrops. This method has subsequently been used by several investigators (Laws and Parsons, 1943; Chapman, 1948; Blanchard, 1949a). An account of European investigations of raindrop size and accompanying instrumentation prior to 1942 can be found in an excellent survey paper by Neuberger (1942).

In an effort to develop a drop-size measuring technique which would eliminate the splashing and spreading of the large drops on contact with the sampling surface, the writer (Blanchard, 1949b) experimented with soot-coated 100- and 50-mesh brass screens. Raindrops, in passing through the screen, removed a circular area of soot whose diameter

[1] This study was supported by the Office of Naval Research, Contract Nonr-798(00) (NR-085-001). Contribution No. 658 of the Woods Hole Oceanographic Institution, Woods Hole, Massachusetts.

was a function of the drop size. This method was considerably improved when nylon screens were substituted for wire screens (Mt. Washington Observatory, 1951a). The nylon screens were treated with a petroleum ether-lanolin solution and then covered with powdered sugar. In this manner, some excellent raindrop samples have been obtained. Mr. Woodcock recently attempted to use these screens from aircraft flying at speeds of 60–80 mi/hr. With low speeds and low relative humidities, a drop-size distribution can be obtained; but in the high humidity region near cloud base, and within the rain area, the hygroscopic sugar particles absorb water and render the screen useless. It would appear, from some brief experiments in sooting nylon screens, that the hydrophillic soot particles from acetylene smoke would serve in lieu of powdered sugar for measurements of drop size from aircraft.

Electronic techniques have been developed in an attempt to obtain continuous measurements of drop size in flight. Cooper (1951) has used a balloon-borne instrument for telemetering raindrop size. An instrument, similar in principle, has been used in France (Maulard, 1951). In the United States, a number of reports, dealing with both optical and momentum devices, have been issued on air-borne instrumentation (Katz, 1952). At the time of this writing, few of these instruments have been put into use.

In Australia, a raindrop spectrograph has been used to obtain continuous drop-size measurements at the ground (Bowen and Davidson, 1951). This ingenious and relatively simple technique permits a direct determination of raindrop size.

2. Hawaiian climate

As any study of this type should be made with cognizance of the influence of the local topographical and meteorological conditions, a brief discussion of these factors and their influence on Hawaiian rainfall will be given.

The eight Hawaiian Islands, some 2400 mi southwest of San Francisco, are oriented northwest-southeast and extend from a latitude of 19 to 22°N. The entire island chain is located within the Pacific northeast trades. These trades are characterized by a temperature inversion with a modal elevation of 6000 ft. Below the inversion, the air is moist and turbulent with an average lapse rate of 8.3C/1000m. As one passes up through the inversion, the air becomes quite dry and free from turbulence. The usual convective and orographic clouds are normally limited by the inversion. It is only on the relatively infrequent occasions when the trade winds are weak or subside completely that the clouds remain over the islands for a sufficient time to build up convectively to high altitudes. As these conditions are so infrequent, it has proved difficult to evaluate properly the results of dry-ice seeding in Hawaii (Leopold and Mordy, 1951).

A marked departure from the normal trade-wind weather is introduced by the passage of easterly waves in the trade-wind current and by the Kona storm (Simpson, 1952). The Kona storms, occurring perhaps 2–3 times during the winter and spring, are cyclonic storms which develop to the northwest of Hawaii. During the day or two of Kona-type weather, heavy rainfall is experienced throughout the islands.

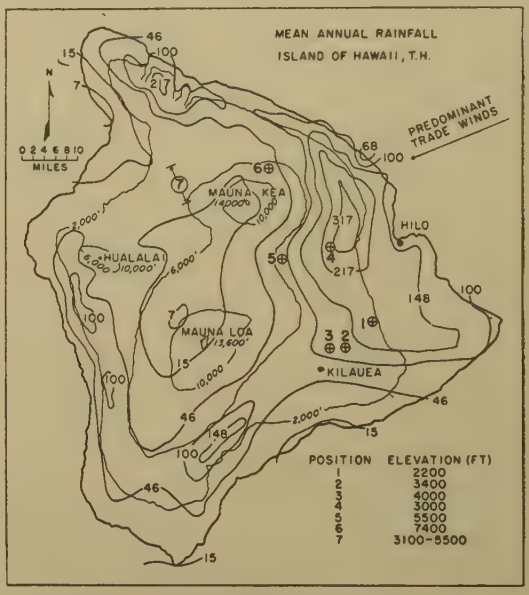

FIG. 1. Isohytal map of island of Hawaii, with location of the seven sampling positions.

The topography of the islands is the major factor in the formation of the orographic clouds. This is effectively shown in the isohyets of the annual rainfall, especially those of the island of Hawaii (see fig. 1). Strong isohyetal gradients are set up in critical areas of trade-wind flow. For example, note the marked increase in annual rainfall from sea level to a point some 10 mi up the east flank of Mauna Kea. In this distance, the annual rainfall increases by 250 in. A rapid decrease of annual rainfall with altitude is found at higher elevations. An explanation for this rainfall maximum has been given by Leopold (1949), who attributes it to the splitting of the trade winds by the huge volcanic cones. He states: "Streamlines drawn in accordance with the observed splitting of the trades by each of the two cones, Mauna Loa and Mauna Kea, would converge directly over the observed zone of greatest rainfall."

TABLE 1. Summary of 113 rain samples made during study.

Sample no.	Date	Time (Hawaiian Standard)	Position	R (mm/hr)	W (mg/m³)	Z (mm⁶/m³)	d_0 (mm)	Number of drops per cubic meter within 0.2-mm size interval centered about indicated size (mm)																		
								0.1	0.3	0.5	0.7	0.9	1.1	1.3	1.5	1.7	1.9	2.1	2.3	2.5	2.7	2.9	3.1	3.3	3.5	3.7	3.9
1	3-27-52	0814	6	1.6	230	76	0.39	11,200	5,800	590	172	80															
2	3-27-52	0842	6	3.5	181	2,112	1.3	*	250	100	44	24.5	43	15	13	9.2	5.7	—	2.6	—	2.35						
3	3-27-52	0845	6	3.1	148	2,285	1.75	*	182	25	31	25	14	6.1	7.3	6.7	1.6	7.4	2.85	1.37	1.3						
4	3-27-52	0858	6	2.95	154	1,668	1.69	*	248	92	49	25	16	8	7.4	11.8	7.8	3	1.4	1.4							
5	3-27-52	0908	6	4.4	220	2,980	1.75	*	315	125	42	32	22	9.7	22	2	11.3	3.55	5	1.62	1.52						
6	3-27-52	0914	6	5.5	324	1,954	1.28	*	630	260	158	109	60	35	41	4.8	8.8	—	4								
7	3-27-52	1118	6	2.9	165	1,130	1.41	*	191	110	35	32.5	37.5	20.8	15.5	8.6	7.9	—	1.2								
8	3-27-52	1120	6	2.8	166	1,039	1.36	*	430	23.5	36	53	41	17	20	4.7	5.8	2.7									
9	3-27-52	?	6	2.7	174	758	1.17	*	420	162	45	82	43	30.5	13	3	5.5										
10	3-27-52	1412	6	1.7	183	132	0.55	5,700	1,500	900	162	61	36.5														
11	3-27-52	1420	6	1.4	147	279	0.47	8,100	2,600	430	59	26	16.8	9.6	—	—	3.6										
12	3-27-52	1640	6	2.5	154	960	1.3	*	520	252	72	47	18.3	3.2	14.5	7.9	2.5	4.7									
13	3-27-52	2025	6	0.28	31	21	0.55	521	471	100	28.5	10.2	5.75														
14	1-19-52	1031	8	2.9	185	1,241	1.19	9,300	700	120	50	56	50	22	15	8	—	—	1.7	1.6							
15	1-19-52	1056	8	1.8	95	811	1.42	2,200	160	39	9.2	17	15.5	16	8.6	5.7	2.1	—	0.94	0.9							
16	1-19-52	1108	8	7.0	325	8,210	1.88	14,000	560	130	49	7.6	46	5.8	15.5	14.5	8.8	4.2	—	3.8	3.7	—	—	3.4			
17	1-19-52	1135	8	10.7	468	13,040	2.26	11,000	1,050	82	34	55	19	—	29	13.5	—	8.8	11.5	2.7	10	—	2.45	2.4			
18	1-19-52	1150	8	127	5,330	153,000	2.32	*	*	1,650	320	165	185	124	135	34	73	170	230	63	61	33	8.2	24			
19	1-19-52	1514	8	6.7	334	4,090	1.68	1,240	230	94	31	37	52	46	12	3.7	21	10	6.2	3							
20	1-19-52	1516	8	12.1	524	12,790	2.04	1,600	225	41	48	11	23	12	44	20	22	12	11	2.7	7.7	—	—	—	2.3		
21	1-19-52	1525	8	20.8	851	18,480	2.0	460	190	94	77	54	70	15	36	38	59	15	28	6.7	3.2	—	—	—	3.1		
22	1-19-52	1533	8	17.5	764	12,990	1.88	1,500	700	150	39	68	31	50	70	42	24	17	22	9	—	—	2.9				
23	2-11-52	1354	8	0.8	33	434		—	—	—	—	1.5	0.7	0.5	3.1	1.4	4	1.3	0.4								
24	2-11-52	1355	8	3.6	146	6,000		—	—	2.8	—	1.8	1.5	1.4	—	1.15	1.02	1	2.8	2.7	4.4	1.5	1.44	0.7			
25	2-11-52	1356	8	1.25	57	885		—	—	2.1	10.5	4.1	2.3	1.0	2.8	2.5	3.2	3	1.4	0.7							
26	2-11-52	1401	8	8.8	470	16,300	2.0	2,900	360	120	54	24	10	14	32	22	17	3.3	3.1	6	8.6	—	—	—	—	—	2.5
27	2-11-52	1402	8	27.5	1,170	23,440	2.05	11,200	680	230	55	120	66	65	44	34	50	36	17	27	10	5					
28	2-11-52	1404	8	12.0	640	7,680	1.65	2,400	480	86	13	25	21	52	70	50	32	5.4	2.6	4.8	4.6						
29	2-11-52	1409	8	5.25	293	3,630	1.42	3,600	690	210	95	105	26	26	20	15.5	8.5	—	2.6	—	—	—	2.2				
30	2-11-52	1419	8	2.9	154	2,330	1.71	3,500	140	13.5	5.6	29	—	1.6	19	4.1	5	3.6	1.15	1.1	1.04	1					
31	7- 8-52	1423	1	1.5	156	73	0.59	—	440	970	300	43															
32	7- 8-52	1433	1	3.4	351	189	0.59	830	2,240	1,880	530	139	13														
33	7- 8-52	1437	1	9.2	610	2,220	1.05	—	1,640	356	510	310	160	93	10.3	28.8	8.8										
34	7- 8-52	1442	1	3.9	379	235	0.64	—	850	2,000	660	208	9.3														
35	7- 8-52	1445	1	6.2	550	673	0.74	730	2,000	2,050	720	153	180	31													
36	7- 8-52	1451	1	7.3	522	1,114	0.98	—	1,010	472	236	464	240	35	20.4												
37	7- 8-52	1509	1	2.6	235	273	0.62	—	592	1,320	282	79	17	15	6.6												
38	7- 8-52	1517	1	6.5	494	870	0.89	—	340	920	660	208	235	32	7.3												
39	7- 8-52	1526	1	2.8	338	314	0.69	—	1,150	1,280	535	175	56	8.1													
40	7- 8-52	1539	1	3.8	398	173	0.52	—	1,740	3,100	450	92	13.2														
41	7- 8-52	1545	1	1.8	196	58	0.46	122	2,100	1,670	180	17.7															
42	7- 8-52	1605	1	5.1	448	473	0.76	—	870	1,460	620	375	71	10													
43	7- 8-52	1617	1	8.7	682	1,080	0.92	—	740	1,240	680	490	320	31													
44	7- 8-52	1629	1	5.3	652	230	0.47	245	7,400	6,000	300	18.2															
45	7- 8-52	1655	1	0.31	79	5	0.22	20,000	2,700	28	23																
46	7- 8-52	1714	1	5.05	660	200	0.47	75,000	6,600	4,200	460	146															
47	7- 8-52	2142	4	13.3	1,243	1,400	0.73	45,000	10,900	2,200	1,700	540	332	55													
48	7- 8-52	2146	4	3	330	140	0.57	1,600	3,400	1,650	520	98															
49	7- 8-52	2150	4	3.6	369	257	0.62	4,700	4,600	810	635	177	23	6.7													
50	7- 8-52	2155	4	4.7	672	154	0.41	29,200	13,700	4,000	248	98															
51	7- 8-52	2203	4	1.8	298	47	0.39	9,000	9,400	1,030	152	10.8															
52	7- 8-52	2208	4	8.2	816	531	0.61	4,600	2,480	4,400	1,400	280	83														

* Splashing of large drops by wind prevented accurate determination of the concentration of these drops. It is believed that the count would have been <500 m^{-3}.

TABLE 1. (Continued)

Sample no.	Date	Time (Hawaiian Standard)	Position	R (mm/hr)	W (mg/m³)	Z (mm⁶/m³)	d_0 (mm)	Number of drops per cubic meter within 0.2-mm size interval centered about indicated size (mm) 0.1	0.3	0.5	0.7	0.9	1.1	1.3	1.5	1.7	1.9	2.1
53	5- 6-52	1648	4	1.02	160	19.6	0.4	2,270	4,200	1,058								
54	5- 6-52	1654	4	1.5	196	60	0.5	3,870	3,210	890	287	19.8						
55	5- 6-52	1710	4	0.95	149	20	0.39	4,800	4,050	790	41							
56	5- 6-52	1718	4	0.51	76	10.2	0.41	2,000	1,600	580								
57	5- 6-52	1721	4	2.6	262	168	0.71	2,000	2,170	524	590	168						
58	5- 6-52	1732	4	8.5	490	2,326	1.4	*	790	280	82	87	121	65	125	13.5		
59	5- 6-52	1735	4	4.2	334	390	0.87	1,580	1,080	137	355	550	31					
60	4-28-52	1656	5	0.056	52	0.11	0.1	48,700	85									
61	4-28-52	1724	5	1.82	423	26.5	0.27	116,000	11,500	1,150								
62	4-28-52	1735	5	0.21	82	1.5	0.2	41,500	2,040									
63	4-28-52	1807	5	0.046	31	0.21	0.16	25,400	243									
64	4-28-52	1820	5	0.15	100	0.76	0.17	78,500	930									
65	4-28-52	1835	5	0.11	115	0.11	0.1	110,000										
66	5- 5-52	2038	5	0.77	250	7.4	0.20	101,000	7,030	144								
67	5- 5-52	2051	5	1.8	371	29	0.31	65,000	11,200	1,120	27							
68	5- 5-52	2117	5	0.62	208	5.2	0.2	80,800	6,400	33								
69	5- 5-52	2132	5	0.18	95	1.1	0.17	66,200	1,360									
70	5- 5-52	2150	5	0.15	156	0.15	0.1	149,000										
71	5- 5-52	2216	5	0.33	99	2.6	0.21	29,500	3,600									
72	5- 5-52	2230	5	0.55	168	4.5	0.21	51,000	6,100									
73	5- 5-52	2255	5	1.08	249	12.4	0.26	19,400	11,000	280								
74	4-29-52	1742	5	1.15	190	19.9	0.39	4,300	6,100	900	11.2							
75	4-29-52	1800	5	2.5	319	81	0.45	2,450	5,400	2,060	270	24.2						
76	4-29-52	1813	5	2.1	381	36	0.38	16,000	13,000	1,540	19.6							
77	4-29-52	1847	5	0.17	97	0.9	0.19	71,300	1,170									
78	4-29-52	1909	5	0.66	162	11.9	0.34	10,500	6,100	480								
79	3-21-52	1645	7	1.12	141	42.7	0.47	2,380	2,050	900	110	27						
80	3-21-52	1655	7	0.11	29	1.05	0.25	2,550	1,350	4.4								
81	3-21-52	1702	7	1.9	203	87	0.59	820	1,150	1,160	400	41						
82	3-21-52	1705	7	4.44	393	475	0.69	1,470	1,780	1,290	601	159	63.6	25	5.6			
83	3-21-52	1718	7	0.24	63	2.2	0.23	8,800	2,800	12								
84	3-21-52	1727	7	1.44	190	32	0.45	7,800	2,800	1,640	34							
85	3-21-52	1745	7	1.14	160	47.5	0.4	4,600	3,950	580	94	47						
86	3-21-52	1803	7	0.51	122	4.5	0.27	4,600	6,200									
87	3-21-52	1814	7	0.061	21	0.5	0.2	8,310	666									
88	3-21-52	1837	7	0.083	54	0.4	0.17	43,000	495									
89	3-21-52	1850	7	0.12	119	0.12	0.1	114,000										
90	3-25-52	1812	7	0.9	90	68	0.59	730	470	490	134	8.2	14.3	3.1				
91	3-25-52	1813	7	2.54	212	243	0.82	640	129	600	240	195	58					
92	3-25-52	1815	7	3.1	239	443	0.91	490	400	215	390	92	94	27	4			
93	3-25-52	1825	7	1.74	154	142	0.79	640	420	400	215	170	11.3					
94	5- 1-52	1326	1	1.3	137	56	0.58	600	360	920	270	18						
95	5- 1-52	1341	1	3.6	303	430	0.83	2,000	1,500	385	390	265	52	26				
96	5- 1-52	1344	1	20.5	1,095	7,430	1.45	1,308	1,282	369	76	206	164	198	202	22.5	55.2	6.6
97	5- 1-52	1555	2	13	933	1,915	0.96	1,300	305	248	800	950	405	65	21.8			
98	5- 1-52	1608	2	3.4	374	127	0.54	534	804	3,470	436	39.6						
99	5- 1-52	1625	2	9.6	647	1,570	1.08	1,100	385	169	245	305	540	83				
100	5- 1-52	1638	2	2.8	321	97	0.53	1,010	2,950	2,350	440	10.8						
101	5- 1-52	1500	3	3	450	70	0.41	—	8,300	3,860	30.5							
102	5- 1-52	1505	3	1.1	157	25	0.43	270	2,820	1,350	12.5							
103	5- 1-52	1513	3	0.77	147	12	0.35	800	5,800	485								
104	5- 4-52	1707	3	0.75	187	7.1	0.26	20,000	8,600	56								
105	5- 4-52	1735	3	0.46	132	3.9	0.23	28,500	5,400									
106	5- 4-52	1810	1	0.95	152	19	0.39	1,358	4,320	855	21.1							
107	5- 4-52	1815	1	1.2	168	28	0.43	2,000	3,200	1,300	43							
108	5- 4-52	1820	1	1.3	214	27	0.37	4,750	6,900	971	21.1	8.4						
109	5- 4-52	1827	1	0.23	63	2.2	0.23	11,400	2,610	18.8								
110	5- 4-52	1833	1	3.6	331	277	0.73	620	1,700	850	620	225	39.5					
111	5- 4-52	1844	1	2.4	262	106	0.57	370	1,800	1,770	390	40.5	5.8					
112	5- 4-52	1846	1	24.8	1,555	5,180	1.15	—	290	196	251	710	850	410	85	11.2		
113	5- 4-52	1850	1	8.5	622	1,065	0.91	—	111	520	690	670	194	54				

* Splashing of large drops by wind prevented accurate determination of the concentration of these drops. It is believed that the count would have been $<500\ m^{-3}$.

3. Measurements of drop-size distribution

Prior to the field experiments, provision was made to obtain drop-size measurements both with nylon screens and with chemically treated filter papers. In view of the difficulties encountered with the screens at high humidities, plus the fact that a low power microscope is essential for accurate determination of the drop size, the filter-paper method was adopted. An objection to using filter papers is that the papers are sensitive to changes in relative humidity (Niederdorfer, 1932). The writer found that this was especially true at relative humidities above 70 per cent. Inasmuch as the measurements of drop sizes carried out in this study were usually made at some point within the cloud, it became necessary to store the filter papers in such a manner as to keep the relative humidity below 70 per cent. This was accomplished by storing the papers in a vertical position, 6 mm apart, in a box containing several desiccating bags. Some 40 papers could be stored in this manner.

Whatman No. 1 filter papers, dusted with methylene blue dye, were held between two brass rings. These were exposed to the rain, with the aid of a small aluminum cover and a stopwatch, for any desired period of time. The exposure times, filter-paper number, time of day, and other pertinent meteorological information were recorded with pencil on painted metal strips. Data were recorded in this manner in heavy rain and cloud without any smearing whatever.

With the aid of a calibrated scale, raindrop sizes were read, in 0.2-mm intervals, directly from the filter papers. This scale was designed from a calibration curve constructed from data obtained with water drops of known size at terminal velocity. The calculation of the space distribution of the drop sizes, $N_D(\text{m}^{-3}\ 0.2\ \text{mm}^{-1})$, from the filter-paper distribution involves a knowledge of the effective filter-paper area (252 cm^2), time of exposure, drop count in each 0.2-mm size interval, and a representative terminal velocity for the drops within each size interval. The terminal velocities used in this work were those experimentally determined by Gunn and Kinzer (1949). As these velocities were determined for water drops falling in still air, it is apparent that the presence of vertical air velocities within a rain area may give rise to errors in the distribution of drops per cubic meter as computed from the filter-paper measurements. In the case of the measurements made in the orographic rain, these errors are negligible. The orographic rain samples were obtained on slopes of only 3 deg. The upslope wind was usually very low. The vertical velocity of the air, i.e., the vertical component of the upslope wind, would have little effect on the terminal velocity of the drops and, therefore, the computed spatial distributions should be correct. This, of course, applies only for the spatial distributions near the sampling area.

A rapid rate of change of terminal velocity with drop diameter is encountered with drops less than 0.2 mm in diameter.[3] For this reason, all computations of N_D for drops less than 0.2 mm are subject to error. The mass of water represented by these drops is negligibly small, when compared to the total. Therefore, computations of liquid-water content W and radar reflectivity Z are, in most cases, little affected.

The intensity of rainfall R(mm/hr) was computed from the filter-paper drop distribution. Within each 0.2-mm interval, an average mass (milligrams) was determined. This average mass, multiplied by the drop count in that particular interval, defined its contribution to the intensity. The writer realizes that such a method of determining intensities may be

[3] Unless otherwise noted, all drop sizes in this paper will be understood to be in mm diameter.

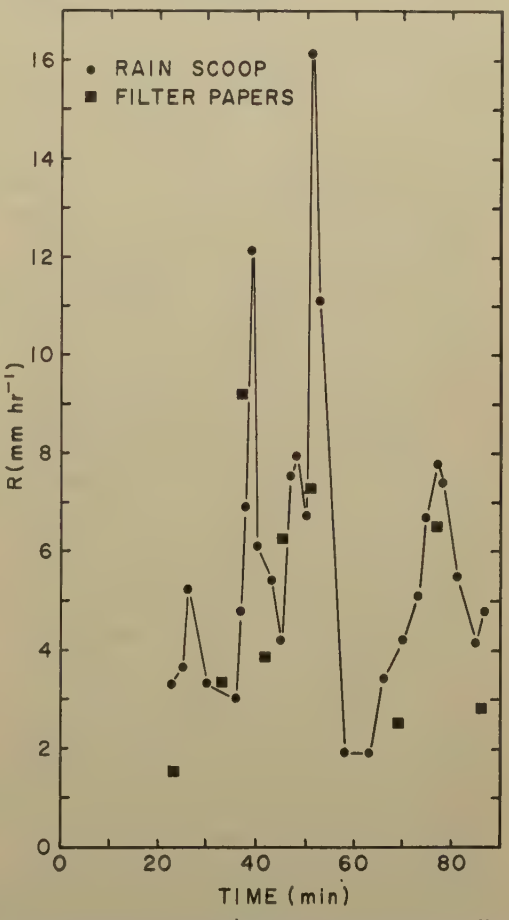

FIG. 2. Comparison of determination of rain intensity from filter papers and 80-cm diameter "rain scoop."

subject to error when the drop distributions containing large drops (>3 mm) are considered. Here the distribution of drops arriving at a horizontal surface is usually skewed, with a long tapering tail reaching into the region of large drops. In this region the distribution is often statistically inadequate and, as these large drops represent the majority of the water, incorrect intensities are computed. This is not the case, however, with the orographic rain of Hawaii. The drop-size distributions have low standard deviations, with the largest drops seldom exceeding 2 mm.

The intensities computed from filter papers have been found to agree reasonably well with those obtained with a 0.5-m² stainless steel funnel (see fig. 2). With the aid of a plywood cover and two flexible automobile windshield-wipers, both mounted to rotate around the inner surface of the funnel, sufficient water for intensity calculations could be collected in 10 to 200 sec. On several occasions, two such funnels were used at the same location. The results were, as expected, nearly identical. As shown in fig. 2, the average intensities as computed from funnel measurements vary considerably. The nearly instantaneous intensities computed from filter papers follow this trend probably as well as can be expected.

4. Changes in drop-size distribution in passage through sub-cloud layer

It appears that most, if not all, of the raindrop size-measurements reported in the literature were made at a considerable distance below cloud level. The changes in the spatial distribution of drops as they fall in the sub-cloud air can be considerable, depending upon the fall distance, temperature and relative humidity, relative drop sizes, and wind shear. These effects were recognized many years ago (Bentley, 1904), but received little attention as few measurements were then being made of raindrop sizes. The measurements reported in this paper, with the exception of those made in the thunderstorm and Kona storm (samples 14–30 of table 1) were obtained either at cloud base or at some point within the cloud system. This was made possible by roads which led up to elevations of many thousands of feet on both Mauna Kea and Mauna Loa.

The above-mentioned factors and their effects on the drop size distribution will be briefly discussed.

Wind shear and relative fall velocities.—If we at first consider the case of zero shear, it becomes apparent that, due to the relative fall velocities alone, large changes may occur in a spatial drop distribution between cloud and ground level. For example, consider a distribution at cloud level to contain drops ranging in size from 0.2 to 4 mm. With a cloud to ground distance of 2000 m, the 0.2-mm drops would arrive at the ground some 40 min after the 4-mm drops, with the intermediate drops arriving at successively earlier times. At ground level the distribution would be transient, not reaching the steady state until 40 min after the arrival of the largest drops. At the onset of natural rains, it is often observed that large drops precede the smaller ones by several minutes but seldom by times exceeding 10 min. This would suggest that either the drops originated at different times or positions within the cloud, or that small drops evolved as a result of continual growth and breakup of the larger drops.

If we now consider the usual case, in which horizontal winds increase with altitude, the problem becomes quite complex. It is apparent that, to have drops of several sizes arriving simultaneously at a given point on the ground, it is necessary that the large and small drops originate at different levels within the cloud or else originate at the same level with the smallest drops forming first. Both of these explanations have been considered, with the former tentatively accepted, as one explanation of observed drop distribution at the beginning stages of a shower (Atlas and Plank, 1952). However, regardless of which explanation is used, it requires that the large and small drops constituting the ground sample have their origin at different locations within the cloud.

Evaporation of raindrops.—Recent experimental work (Kinzer and Gunn, 1951) on the evaporation of falling water drops has resulted in a table of evaporation rates, at several relative humidities, for drops of various diameters. The writer has expressed this table in functional form and combined it with an expression relating terminal velocity to drop diameter. The resulting differential equation was integrated, to obtain an equation relating drop size and distance fallen. At a relative humidity of 90 per cent and an isothermal atmosphere of 20C, it was found that small drops can completely evaporate in a fall of about 1000 m. For example, a 1.5-mm drop will evaporate to only 1.42 mm in a fall of 2000 m, while a 0.5-mm drop will evaporate completely in a little over 1000 m. It is interesting to note that these calculations agree relatively well with the more detailed theoretical calculations of Best (1952).

The calculations indicate that large changes in the drop-size distribution are to be expected among the smallest drops. The evaporation of the small drops is serious, in that it deprives us of any knowledge of their distribution. This knowledge is extremely vital to the question of the mechanism of rain formation, as these drops represent the great majority of the total drops present. The great difference in numbers of small drops in rains from freezing and non-freezing clouds is pointed out later in the paper.

Drop collision in the sub-cloud layer.—As a direct consequence of the differences in fall velocities of the

various sized drops, it is to be expected that raindrop collisions in the sub-cloud layer will tend to modify the distribution which existed at cloud base. Calculations of these effects, plus those of evaporation, have been made by Rigby and Marshall (1952). They find that the collision effect tends to increase the number for large drops while decreasing it for the small ones. Evaporation effects, on the other hand, will tend to decrease the number at all sizes. On combining both evaporation and collision effects, they found that the change in distribution for the larger drops was not as pronounced as that caused by collision effects alone. The distribution of the small drops, which was decreased by both collision and evaporation, naturally departed even more from its initial state when both effects were considered. The general conclusion arrived at by Rigby and Marshall was that the basic form of the drop-size distribution would not be seriously affected by any of the aforementioned factors. It might be added that their work was based on distributions which extended into drops of 3 mm. As a majority of the drop distributions of orographic rain from warm clouds have 50 per cent of the water contained in drops smaller than 1 mm, it is to be expected that evaporation effects would be quite pronounced. In fact, the occurrence of virga, the result of evaporation, is a most common event associated with the warm clouds of Hawaii.

5. Raindrop size-distributions from clouds extending above the freezing level

On three different occasions, drop-size samples were obtained in rains whose origins most likely were associated with ice-crystal formation.

Windward Mauna Kea.—On 27 March 1952, raindrop measurements were taken on the northeast flank of Mauna Kea at an elevation of 7500 ft. These are represented by distributions 1–13 of table 1. At 0630 the weather was as follows: winds light and downslope, temperature 6.3C, and a light drizzle falling from an overcast which was solid only near the mountain. At about 0840 both the drizzle and the wind increased in intensity. Sample 2 of table 1, as compared with sample 1, shows the change in the nature of the drop distribution.[3] The absence of any drops over 1 mm and the large numbers of drops smaller than 0.5 mm in sample 1 are typical of the distributions from non-freezing clouds (see samples 31–113). The sudden increase in maximum drop size and corresponding decrease in small drops, as indicated by sample 2, was shown by all subsequent measurements until 1412 and sample 10. The change in distribution of sample 10 was no doubt associated with a wind shift to east at 1400, plus a lowering of cloud base 100 ft or more to the sampling position. At 1700 the winds became very irregular and strong. The rain continued until about 2100. At sunrise on 28 March it was observed that all of Mauna Kea above the 10,000-ft level was covered with snow. It was then realized that the rain of the previous day had probably originated as snow.

The pronounced change in drop distribution from sample 1 to sample 2 was accompanied by a marked change in the chloride content of the rain. Chloride determinations on five rainwater samples taken between 0730 and 0842 showed the expected trend towards an inverse relationship between rain intensity and chloride content (Woodcock, 1952). During this time, the chloride concentration dropped from 20 to 0.4 ppm. From 0842 through 1802, twenty rainwater samples were obtained. Although the samples were obtained in intensities ranging from 1.6 to 13 mm/hr, the chloride concentration was never above 0.3 ppm. Rain from the typical Hawaiian orographic cloud usually has chlorides present in amounts from 0.5–20 ppm. The small amounts found above would suggest that the larger saline droplets had been eliminated from the cloud by raining out at lower elevations.

The Kona storm.[4]—Heavy and continuous rain fell throughout the day of 19 January 1952. For a period of some 20 hr, the weather was entirely dominated by a Kona or cyclonic storm. From 1031 through 1533, samples 14–22 were obtained at the Pineapple Research Institute, Honolulu. The cloud base was estimated at 200 ft. The temperature at 1200 was 20.7C, with a wet-bulb depression of 0.4C. The winds were light, with occasional strong gusts.

The drop-size measurements covered a wide range of intensities, ranging from 1.8 to 127 mm/hr. A few minutes after sample 18 was taken, the intensity rose from 127 to 242 mm/hr. This latter measurement was made with the 0.5-m² sampling funnel.

The thunderstorm.—On 11 February 1952, weak trade winds were indirectly responsible for the formation of cumuli over the island of Oahu. By 1300, large cumuli were forming over the city of Honolulu. Extreme vertical depth was suggested by the intense darkening of the cloud base. The first rain fell at 1352 and continued on for about 35 min. During that time, sporadic thunder was heard and small hail pellets were reported.[5]

Eight drop-size measurements (samples 23–30) were obtained. With the exception of the first three measurements, the drop distribution was, in general, similar to that found in the Kona storm. Sample 23,

[3] Hereafter in the paper all reference to table 1 will be in terms of the sample number only.

[4] Kona is the Hawaiian word for leeward. A Kona storm approaches from the leeward side of the islands, with respect to the trade winds; hence, its name.

[5] According to newspaper reports, hail was reported several miles from the sampling position.

obtained 2 min after the start of the rain, contained no drops smaller than 0.8 mm. A few minutes later, at 1355, a few drops in the 0.5-mm range had arrived. At 1356 drops as small as 0.4 mm were present, although in small numbers. From 1401 on, all samples indicated the existence of drops smaller than 0.2 mm.

The drop distributions of fig. 3 show the gradual increase of small drops with time. The two dashed lines are the distributions of Laws and Parsons (1943), as presented by Marshall and Palmer (1948), for intensities of 25 and 1 mm/hr. Note how the transient is characterized by a positive slope which decreases with time. Sample 26 (R = 8.8 mm/hr), the first to contain drops smaller than 0.4 mm, is the first distribution that has a pronounced negative slope.

An explanation for this behavior is beset with many difficulties, arising mainly from a lack of knowledge of the drop distribution and vertical air-velocities at cloud base. With an estimated cloud to ground distance of 1000 m, and a distribution of drops of all sizes simultaneously starting their fall from cloud base, it is evident that the slower falling smaller drops will reach the ground some time after the large ones. Approximately 3 min will elapse between the arrival of drops larger than 2.4 mm and those of 0.8 mm. It is to be noted that sample 23, taken 2 min after the beginning of the rain, contains no drops smaller than 0.8 mm. Subsequent samples, obtained three or more mintues after the initial rain, contain increasing numbers of drops smaller than 0.8 mm. Thus, the time of appearance of the 0.8-mm drops agrees with the estimated time of 3 min. On the other hand, the drops smaller than 0.2 mm should not appear until some 21 min after the initial rain. Clearly this is not the case. It is, therfore, probable that the large and small drops had their origin at different altitudes, or at the same altitude but at different times (see section 4, above). The other alternatives are: (1) smaller drops are being produced by drop disintegrations resulting from collisions and turbulence (Blanchard, 1950), or (2) downdrafts created by the large drops tend to decrease the total fall time of the small drops and, consequently, decrease the elapsed time between their respective arrivals at the earths surface. In the absence of any data on the turbulence and downdrafts associated with the thunderstorm in question, it is impossible to obtain any quantitative information.

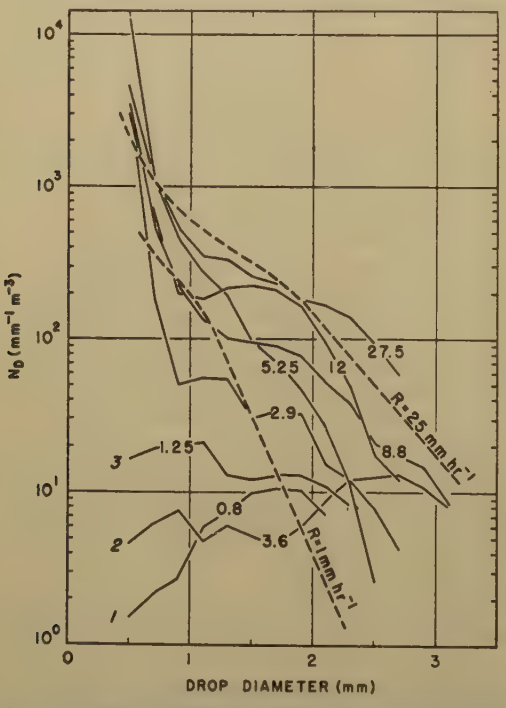

FIG. 3. Raindrop distribution (solid lines) of thunderstorm data (samples 23–30). Dashed lines represent smoothed distributions of Laws and Parsons data. Numbers in lower left-hand corner indicate the three transient distributions in a chronological order.

6. Liquid-water content as a measure of the drop distribution

It is not always convenient to compare two sets of rain measurements by comparing their drop-size distributions. It would be far more desirable to represent a drop-size distribution graphically by a single point. Of course, such a representation would tell nothing of the total drop count per cubic meter, but it could indicate whether the distribution had a large or narrow spread.

This is essentially what is measured by the liquid-water content W (mg/m^3). For example, let us consider

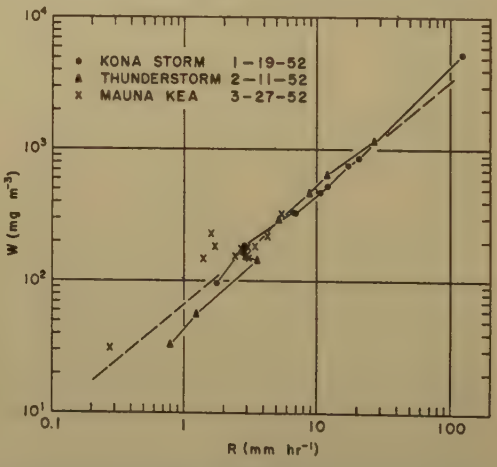

FIG. 4. Liquid-water content W as function of rain intensity R for samples 1–30. Dashed line is locus obtained by Best (1950). Lines connecting points are visual aids only.

the hypothetical distribution of 1 drop per m^3. This defines an intensity R, and a liquid-water content W. Let this drop be split into two equal-sized smaller drops. Although the liquid-water content is unchanged, the slower falling, smaller drops lower the intensity. One or more of these smaller drops will, therefore, have to be added to attain the original intensity. It is apparent that this process can be repeated indefinitely. At each sequence the intensity is held constant by adding drops, the liquid-water content rises, and the drop distribution tends toward smaller and more numerous drops.

The liquid-water contents of the drop-size distributions of the three storms represented by samples 1–30 are shown in fig. 4 as a function of the intensity R. The dashed line is the locus $W = 67\,R^{0.84}$ (Best, 1950), representing the mean value of data obtained by other investigators. With the exception of six points, the present data agree reasonably well with this locus. Note that three drop-distributions from the windward Mauna Kea rain, representing intensities less than 2 mm/hr, have liquid-water contents considerably higher than the locus would suggest. This, of course, implies a drop distribution of relatively small spread and numerous drops. Reference to samples 1, 10 and 11 shows that this is the case. In each of those samples, from 7000 to 17,000 drops per m^3 are smaller than 0.4 mm. The spread in drop distribution is about half that of the other samples.

The three anomalous thunderstorm samples indicate the opposite trend, that of a wide distribution coupled with a scarcity of small drops. These are samples 23–25, representing the transient period at the start of the storm. In each case the drop spread is greater than or equal to the other thunderstorm samples, and the sum total of drops smaller than 0.8 mm, as compared to the remaining samples, is negligibly small.

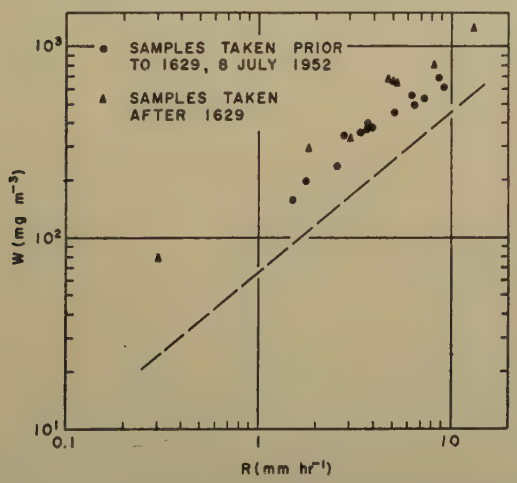

FIG. 5. *W vs. R* relationship for samples 31–52. Dashed line is locus obtained by Best (1950).

7. Drop-size distributions in orographic clouds

All samples in table 1 from 31 on were obtained on the island of Hawaii, at cloud base or within the clouds. This type of sampling will eliminate or at least minimize the factors which tend to change the distribution (see section 4, above). Measurements made over a period of several months show variations in drop size for a given intensity. The liquid-water content W, as reflected by these variations, will be used to demonstrate the changes in drop distributions.

Raindrop size-distribution from clouds of windward Hawaii.—A complete overcast existed over Hilo on 8 July 1952. A light drizzle was falling at Hilo and on up through position 1 (see fig. 1). The cloud base fluctuated from ground level at position 1 to perhaps 50 ft elevation. At 1525 the temperature was 21.5C, with a wet bulb of 21.3C.

Samples 31–46 were obtained throughout a period of nearly 3 hr extending from 1423 to 1714. The trend of the drop distributions, as indicated by the liquid-water content W, is shown in fig. 5. Prior to sample 44 at 1629, the distributions fall on a common locus. All samples after 1629, with the exception of 48 and 49, have higher liquid-water contents for similar intensities. Table 1 shows this change, as might be expected, accompanied by a large increase in the drop count for drops smaller than 0.4 mm. In fact, sample 50, with its concentration of 13,700 and 4000 drops per m^3 in the 0.2-mm intervals centered on 0.3 and 0.5 mm, is one of the highest obtained by the writer. For a given R, W is 2 to 2.5 times as large as that indicated by Best's (1950) data.

Samples 53–59 were taken on 6 May 1952 at position 4. The rain-producing clouds were forming in the vicinity of the islands, as there existed an area free of

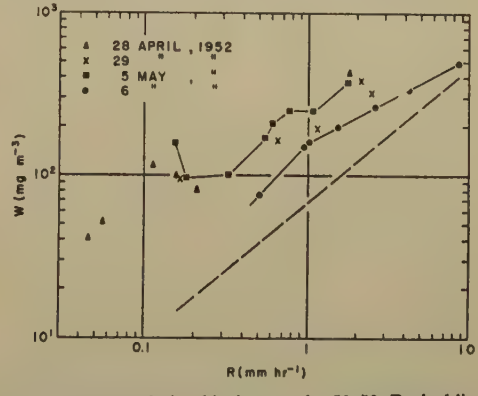

FIG. 6. *W vs. R* relationship for samples 53–78. Dashed line is locus obtained by Best (1950). Lines connecting points are visual aids only.

clouds along the east coast of Hawaii in the Hilo region. Cloud bases were approximately 100 ft above the sampling position. The dry-bulb temperature was 14.5C, and the wet bulb 14.2C. Fig. 6 shows the relative position of the W vs. R locus as compared with that of samples 60–78. Note how the points tend to approach Best's locus at the upper end.

Samples 60–65 were obtained on 28 April 1952 at position 5, at an elevation of 5500 ft. The cloud base was at 2000 ft. All but one of these samples are of intensities less than 0.2 mm/hr. With the exception of one sample, the drops are all smaller than 0.4 mm with a majority smaller than 0.2 mm. This large number of small drops can give rise to an error in the calculated intensity. This probably explains the anomalous distribution of the data.

On 5 May 1952 samples 66–73 were obtained at position 5, well within the cloud. The wind was upslope at 0.6 m/sec. The temperature was 10.8C, with a wet bulb of 10.7C. The liquid-water content for sample 70 was abnormally high. A glance at table 1 shows that all drops in sample 70 were smaller than 0.2 mm and in concentrations of 149,000 m^{-3}. This is the highest concentration of drops smaller than 0.2 mm found in the present study.

On 29 April 1952, position 5 was at or near the upper dissipating edge of the cloud. At 1640 a fine mist-like rain began to fall. The temperature was 14.4C, with a wet bulb of 13C. At 1725 the wind was steady at 1.3 m/sec. By 1740 the clouds moved in over the area, with a light drizzle which lasted throughout the time of sampling. From 1742 to 1909, samples 74–78 were collected. It is interesting to note that these distributions are similar, both in number and maximum drop size, to those obtained by Bowen (1950) from an aircraft flying through the top of a non-freezing cululus cloud.

Simultaneous with the drop-size distribution measurements at position 5, rain-intensity measurements were being made at position 4. Twenty-six measurements, from 1605 to 1905, indicated intensities ranging from 0.5 to 13.3 mm/hr. During the entire time, the cloud base was approximately at the elevation of position 4. At 1708 the dry- and wet-bulb temperatures were 16.8 and 16.7C, respectively, and at 1818 both were 15.8C.

Raindrop distributions in a dissipating orographic cloud.—In some respects, the drop-size distributions obtained on 21 March 1952 are the most interesting. For they are measurements not only made in a dissipating cloud system, but they were made at many points within the cloud system ranging from cloud base to near the cloud top.

It will be well to discuss briefly the topographical and meteorological features of the area in which this cloud forms. The region of position 7, in the lee of Mauna Kea, has little possibility of being influenced by the trade-wind flow, as is the region around positions 1–5. Leopold (1949) has shown that the 14,000-ft low-angle cones formed by Mauna Kea and Mauna Loa are sufficient to split the trade-wind flow into two components. Apparently the inversion is sufficient to prevent the flow from rising over mountains extending up through the inversion. Leopold has studied, in some detail, the formation of clouds in the lea of the 10,000-ft cone of Haleakala on the island of Maui. He found that a sea breeze was the dominant factor in the formation of the afternoon orographic clouds. In the late afternoon, this sea breeze gives way to a downslope land breeze. In many respects, we may expect a somewhat similar mechanism of cloud formation in the lee of Mauna Kea.

At 1645 on 21 March 1952, the writer was at cloud base at position 7 at an elevation of 3100 ft. The wind was nearly dead calm, and a light rain was falling. Sample 79 was taken at this point. Samples 80–83 were taken at approximately 2-mi intervals up through the cloud. Fig. 7 indicates these positions, and shows the gradual uniform rise of the slope and a schematic representation of the cloud-top positions at various times. Note the vertical structure of the cloud edge. Its 1000-ft height is based on a visual estimate.

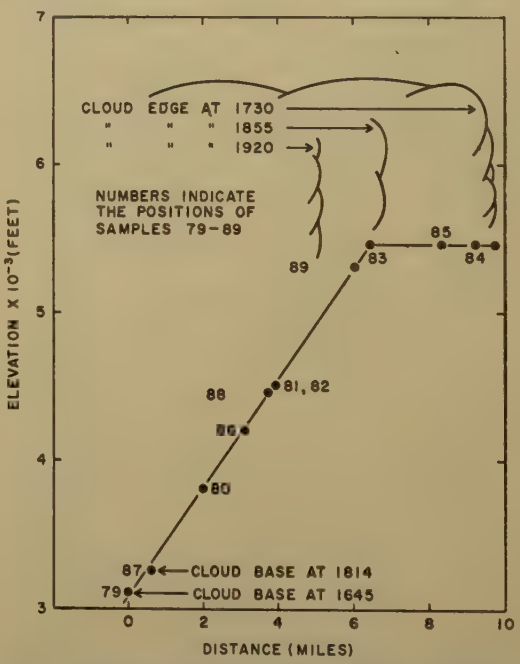
CLOUD EDGE AT 1730
" " " 1855
" " " 1920
NUMBERS INDICATE THE POSITIONS OF SAMPLES 79-89
ELEVATION X 10⁻³(FEET)
DISTANCE (MILES)
CLOUD BASE AT 1814
CLOUD BASE AT 1645

FIG. 7. Uniform slow rise of terrain (370 ft/mi) at area where samples 79–89 were obtained. Numbers alongside points indicate position of samples. Although abscissa indicates horizontal distance between points, it is to be taken as distance measured along the slope. (Actually the difference is negligible.)

Samples 85–87 were taken on the first downward traverse. During this time the cloud top was receding slowly, and the drop distribution was shifting toward the small end. This trend in the drop distribution continued during the second upward traverse, as the remaining samples, 88 and 89, were taken. From sample 86 on, a decrease was found in the number of drops in the 0.3-mm size interval and, concurrently, a steady increase in the drop count in the 0.1-mm size interval. In fact, the increase of the number of drops smaller than 0.2 mm is exponential. The equation $N = 4000\, e^{7.1\times10^{-3}t}$ can be used to express the number at t min after the time of sample 86, 1803. Within 15 min after sample 89, the cloud was void of drops of sufficient size to register on the filter paper. The apparent "drying out" of this cloud was by no means confined to these data. On other occasions the writer has been in this cloud in the early evening and has experienced the decrease in size and eventual disappearance of raindrops.

The liquid-water–intensity relationship (fig. 8) shows a fairly uniform trend with the exception of the last two samples. The large increase in W associated with these is what would be expected. Note that for the same liquid-water content of sample 89, a 17-fold increase in intensity would be required to fit Best's (1950) results.

The existence of trade-wind eddies in the lee of Mauna Kea, and high-level air flowing from east to west through the Mauna Kea-Mauna Loa saddle (Leopold, 1949), makes it very difficult to ascertain the past history of the air in this area. Woodcock's measurements have shown that significant differences in the distributions of air-borne salt particles are a function of not only wind velocities but, in some cases, of the topographical features over which the air flows.

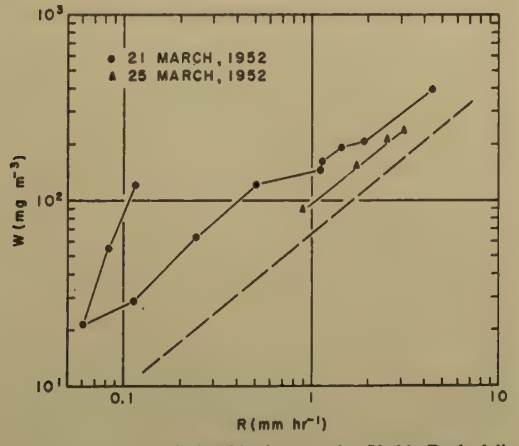

FIG. 8. *W vs. R* relationship for samples 79–93. Dashed line is locus obtained by Best (1950). Lines connecting points are visual aids only.

On 21 March 1952, the estimated winds to windward of the island were Beaufort force 4–5. At such speeds, the concentrations of air-borne salt particles at cloud base would be of the order of 6000–10,000 particles per m³ between 10^2 and 10^4 $\mu\mu$g. (The equilibrium diameters of salt particles of 10^2 and 10^4 $\mu\mu$g at a relative humidity of 99 percent are 22 and 102 μ, respectively.) And yet, on this particular day, measurements obtained from aircraft just below cloud base to leeward from Mauna Kea failed to show the existence of any salt particles heavier than 10^2 $\mu\mu$g. Ordinarily this would be typical of air only above the inversion. Whether the explanation is that this air is high-level air which has flowed down the mountain during the night, or whether it represents salt-depleted air which has passed through the saddle area from clouds on the windward side of the island, the writer cannot say. It seems apparent, however, that the presence or absence of these large salt particles should profoundly effect the rain-producing characteristics of the clouds.

Three days later, on 25 March 1952, samples 90–93 were taken at the 5500-ft level. In fig. 8 and table 1, the difference in the characteristics of the two "lee-side" distributions is obvious. A scarcity of droplets exists in the first two size-intervals. As no aircraft salt-measurements were made on this day, it is impossible to tell if the salt-particle distribution resembled that of 21 March.

Drop distributions at cloud top and base.—On 1 May 1952 a series of ten drop-distribution measurements, samples 94–103, was obtained at cloud base, an intermediate point, and near the cloud top. These are positions 1, 2 and 3 on fig. 1, with elevations of 2200, 3400, and 4000 ft, respectively. Samples 94–96, obtained at position 1, contain some of the largest drops found in orographic rain. Samples 97–100 were obtained at position 2, 6.6 mi upslope from position 1.

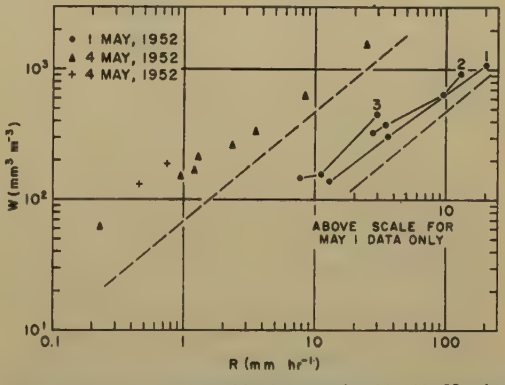

FIG. 9. *W vs. R* relationship for samples 94–113. Numbers alongside 1 May data indicate sampling position. 4 May data, indicated by crosses, were obtained at position 3. Dashed line is locus obtained by Best (1950).

The remaining samples were obtained at position 3, 8.8 mi upslope from position 1. At position 3, near the upper dissipating edge of the cloud, a great increase in numbers of drops between 0.2 and 0.6 mm was found. Fig. 9 shows the difference in drop distribution at the three positions, expressed in terms of the liquid-water content.

On 4 May 1952, samples 104–113 were obtained at positions 1 and 3. At 1730, at position 3, both wet- and dry-bulb readings were 13.4C. The difference in drop distribution between the two positions is illustrated in fig. 9. This difference becomes numerically clear by inspection of table 1. The large number of drops smaller than 0.4 mm is sufficient to cause a high liquid-water content.

8. Median volume diameter as a function of rain intensity

Many of the data of table 1 have been expressed in fig. 10 in terms of median volume diameter d_0. The d_0 is that diameter which divides the drop distribution into two parts, such that each represents half of the liquid-water content W. It is obtained by plotting a cumulative per-cent curve of the liquid-water content. The percentage corresponding to any drop diameter is the percentage of the total liquid-water content contained in the drops smaller than the drop in question. The drop diameter at the 50 percent ordinate is, therefore, the median drop diameter d_0.

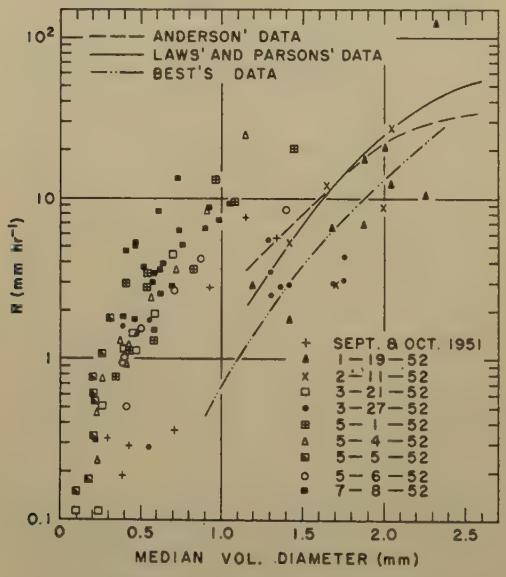

FIG. 10. Median volume diameter as related to rain intensity. Data labeled Sept.–Oct. 1951 were obtained at Woods Hole, Mass. Median volume diameters, as found in orographic rains, are considerably less than those found in non-orographic rains.

In addition to the data from the Hawaiian orographic rains, data from non-orographic rains (samples 1–30 and drop distributions obtained at Woods Hole, Massachusetts) have been included in fig. 10. With the exception of four of the samples from the Mauna Kea and Woods Hole data, all the median diameters greatly exceed those found in orographic rains of the same intensity. Note that the three Mauna Kea samples (1, 10 and 11 in table 1) which fall into the orographic grouping have drop distributions representative of orographic rains. The median diameters of the non-orographic samples alone show considerable spread at all intensities. In view of the differences already pointed out in the $W-R$ relationship, this spread is to be expected.

The solid line was drawn from the data of Laws and Parsons (1943), the dashed line from the data of Anderson (1948), and the dash-dot line from the data of Best (1950). Laws and Parsons used the flour technique for drop-size sampling (Bentley, 1904) and calculated the intensity of rainfall from the exposures, area, and drop distribution of the sample. All of their rain samples were obtained at ground level at Washington, D. C.

Anderson's results are extremely interesting, in that they were taken on the island of Hawaii in the vicinity of position 4 (fig. 1). Some 60 samples were obtained with the blotting-paper method over a period of 5 hr. The disagreement of Anderson's data with the present data, and the relatively good fit with that of Laws and Parsons, and Best, suggests that Anderson's sampling was in a particular rain not representative of the general Hawaiian rains. Of the 60 samples, only three were taken at intensities less than 8 mm/hr and none at intensities less than 2.5 mm/hr. Anderson states,[6] however, that the rain appeared to be orographic in nature and was accompanied by light winds. Nevertheless, it is possible that this rain was similar in origin to that of samples 1–13, evolving from snow from high-level supercooled clouds. From a meteorological point of view, this was quite possible. Anderson's work was carried out on 16 March 1945, the same time of the year as samples 1–13. During the winter months, and extending through March, it is not an infrequent occurrence to have rain of this nature.

The quartile deviation for orographic rain, a measure of the spread of the liquid-water content, is considerably lower than that reported by Anderson.

The present data indicate values ranging from 0.01 to 0.15 mm, as compared to Anderson's measurements of 0.1 to 0.8 mm. The writer finds, as did Anderson, that the quartile deviation is roughly proportional to the median diameter. This, of course, implies a decreasing slope of the cumulative per-cent curve

[6] Private communication.

between the first and third quartiles with increasing median diameter. According to Anderson, this is contrary to the cumulative per-cent curves of Laws and Parsons, which show a nearly constant slope between the first and third quartiles at all median diameters.

9. Radar reflectivity

The success of radar in determining the intensity of precipitation is dependent on a knowledge of the size distribution of the precipitation elements. The power received at a radar from a rain target is proportional to the radar reflectivity $Z = ND^6\,\delta D$, where N is the number of drops per cubic meter of diameter D in the size interval δD. It is apparent that the sixth-power-of-the-diameter factor allows the relatively few large drops greatly to influence the radar reflectivity.

Wexler (1948) and Marshall and Palmer (1948) have computed, from their own data and that of other investigators, the relationship between Z and rain intensity R. Recently, similar relationships have been found to hold for various spectrums of cloud droplets (Atlas and Boucher, 1952). Marshall and Gunn (1952) report that the Z *versus* R relation has been found to be interchangeable for rain and snow. That is, for equal rates of precipitation, whether rain or snow, they obtain the same values of Z. Twomey (1953) has presented the results of Z calculations made in Australia. He points out that, for a given intensity, the drop-size distribution may vary considerably. This, of course, implies a corresponding variation in Z. Twomey has presented a list of $Z-R$ equations obtained by many investigators at widely separated localities. Considerable disagreement exists in these equations. They range from $Z = 23.5\ R^{2.028}$ to $Z = 1600\ R^{1.4}$. The Australian results alone indicate that the rain intensity, as deduced by radar, may be in error by a factor as great as four.

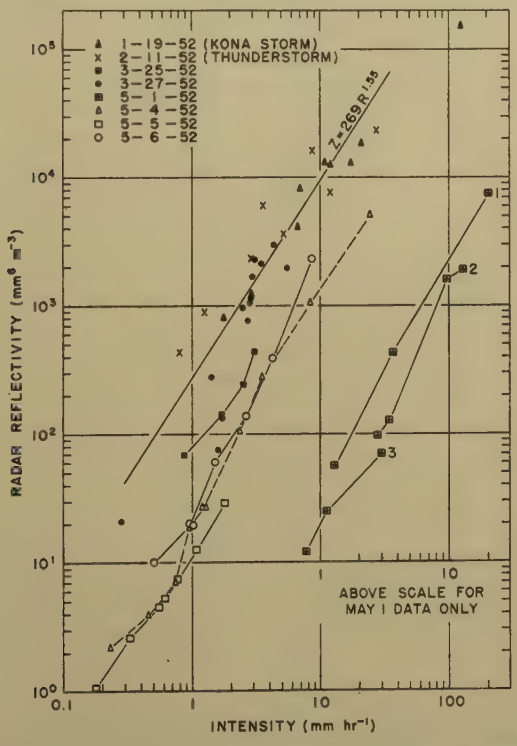

FIG. 11. Radar reflectivity as function of rain intensity. Locus $Z = 269\ R^{1.55}$ is not that of present data, but one obtained by staff of Mt. Washington Observatory in least-squares analysis of Z *vs.* R relation of continuous and shower-type rain at Cambridge, Mass. Numbers connected with 1 May data represent sampling positions. Lines connecting points are visual aids only.

These variations in the $Z-R$ equations are not surprising. They undoubtedly represent rains whose origins lie in snow-producing clouds, non-freezing cumuliform clouds, and orographic-type clouds. Further variations are probably introduced by the evaporation and collision of drops in the sub-cloud region (see section 4, above). Fig. 11 shows how the Hawaii data alone vary in Z for a given R. The $Z-R$ relationship for samples 1–30, the non-orographic rains, most nearly corresponds with that of other workers. The regression line shown was not drawn on the basis of these data. It represents the least-squares regression of 63 rain samples, both from continuous and shower-type rain, taken at Cambridge, Massachusetts (Mt. Washington Observatory, 1951b). The regression for the three types of rain represented by samples 1–30, excluding samples 1 and 10, is $Z = 290\ R^{1.41}$. Samples 1 and 10, as seen from table 1 and discussed in section 5, above, are representative of orographic rain and would, therefore, show relatively low values of Z.

The Hawaiian orographic rains of low intensity (less than 2 mm/hr), as compared with the non-orographic rains, may give lower values of Z by as much as a factor of 30.[7] At intensities greater than 10 mm/hr a factor of from four to ten is found. Inasmuch as day-by-day variations exist, it is not felt necessary to present any least-square fits. However, it can be easily seen from inspection of fig. 11 that the coefficient in the $Z-R$ equation will be from 10 to 100, considerably lower than those found elsewhere. The data of 1 May 1952, obtained at three different positions within the cloud, illustrate the small but noticeable difference in Z in various parts of the cloud.

If the type of rain, *i.e.*, thunderstorm, frontal, orographic, is not known, a large error may be made

[7] A factor of 15 is probably the usual case. The factor of 30 was based on the 5 May 1952 data, obtained at position 5. Only in the case of a subsiding cloud (samples 79–89) would one expect to find such a drop distribution at cloud base.

in determining R by radar. In agreement with the Australian findings, the error indicated here may be as large as a factor of four.

10. Generalized nature of the drop distribution

The variations in the drop distributions.—The discussions above, and figs. 5–9, have dealt with the changing drop-distributions that exist from day to day and from one position to the next. The writer feels that an adequate explanation for these apparent anomalies is to be found only by considering the past history of the cloud. For example, one would want to know just how long a cloud system has been raining prior to the time that the raindrop samples are obtained. Some of the present samples were obtained when it was observed that the rain area extended many miles to windward. On the other hand, other samples were obtained at or near the beginning of the rain area. If large airborne salt-particles are the nuclei upon which the raindrops form (Woodcock, 1952), it is to be expected that these particles will rain out as the cloud system advances and, therefore, provide a variation in the drop distribution.

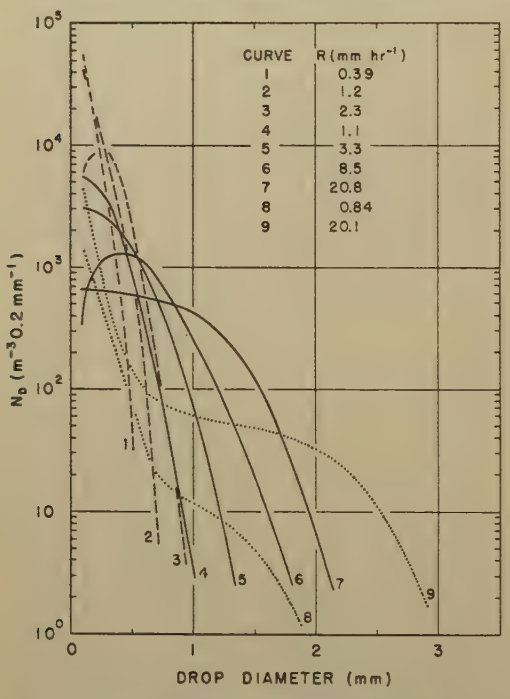

FIG. 12. Raindrop distributions, as averaged from data of table 1. Curves 1–3 are for measurements made at or near dissipating edge of non-freezing orographic clouds (positions 3 and 5), while curves 4–7 represent data taken at cloud base (positions 1 and 4). Curves 8–9 are for non-orographic rain distributions (samples 1–30). It should be noted that these curves were drawn for best fit to the averaged data. In all cases, with exception of curve 7, little or no "smoothing" of curves was required. In case of curve 7, however, data showed considerable scatter about "smoothed" line.

Fig. 12 represents, then, an average drop-size distribution around which systematic fluctuations can and do occur. The three dashed curves represent the averaged distributions of positions 3 and 5, while the solid curves are for distributions obtained at positions 1 and 4. It is immediately apparent that the distributions well up in the cloud (positions 3 and 5) are markedly different, for the same rain intensity R, than those at cloud base (positions 1 and 4). For example, curves 2 and 4, representing nearly identical intensities of 1.2 and 1.1 mm/hr, respectively, show large differences at each end of the drop spectrum. The number of drops smaller than 0.2 mm is nearly a factor of ten greater within the cloud than at cloud base. On the other hand, the number of drops per cubic meter between 0.6 and 0.8 mm is a factor of ten less within the cloud than at cloud base. A somewhat similar picture is presented by curves 3 and 5.

A second feature of these curves is that, in general, the number of drops per cubic meter at the small end of the spectrum is an inverse function of the intensity. It is believed that the scarcity of small drops at high intensities is due to accretion with the large drops. It will be noted that the numbers of large drops, as well as the maximum size, increase with intensity.

The two dotted curves are for some of the data from the non-orographic rains (samples 1–30). In all respects, they are markedly different from the other curves. The inverse relationship of intensity *vs.* raindrop concentration at the small end of the spectrum is not obtained, and the curves exhibit a more uniform distribution of drops beyond 0.7 mm. Without further data on this type of rain, one can only speculate as to why these curves differ from those of the orographic rain. As it is most probable that these curves represent rain evolving from snow falling through the freezing level, it is likely that the size distribution of the snowflakes and the manner in which they melt determine the basic shape of the raindrop distribution curve.

If one closely considers the nature of the drop distribution curves for the orographic rain, it becomes apparent that Langmuir's (1948) "chain reaction" process does not take place. This hypothesis postulates the existence of updrafts and cloud thicknesses which must exceed a critical value. Raindrops are presumed to grow to a point where turbulence or drop collision causes breakup into two or more smaller drops which, in turn, repeat the same process. This cannot occur here, for, in the first place, vertical velocities and cloud thicknesses of the order necessary for chain reaction are not observed in Hawaiian non-freezing orographic clouds. Secondly, and perhaps more important, a necessary condition for chain reaction is

the presence of drops of some 5 mm.[8] The absence of drops larger than 2 mm is quite apparent in the present data. Any chain-reaction process would certainly provide a spectrum of drops between 2 and 5 mm. It is much more likely that the raindrops are the product of a simple accretional growth process. The evidence in support of this process is being prepared for publication at the present time.

Regressions equations and determination of the median volume diameter.—The important meteorological parameters, liquid-water content W, radar reflectivity Z, and the median volume diameter d_0, have been determined for the distributions of fig. 12, and have been plotted against the intensity R. The regression equations relating these data are given in table 2. Note that the Z regression equation for the non-orographic rain is in good agreement with that of fig. 11, while the equation for W is similar to that given by Best (1950), $W = 67\ R^{0.87}$. The regression equations for the orographic rain are, as must be expected, considerably different than those for the non-orographic rain. For example, the coefficients for the three Z equations vary by a factor of 17.

[8] It is at about this size that raindrops are thought to become unstable. The writer (Blanchard, 1950) has observed that waterdrops up to 8 mm are stable in non-turbulent air. It is only when an 8-mm drop encounters a high degree of turbulence that breakup will occur. This turbulence may be part of the air structure itself, or it may be set up by the aerodynamic interaction of two drops about to collide. The droplets resulting from the breakup, in either case, will have a variety of sizes. Drops of only 3 or 4 mm, on the other hand, are stable even when falling in turbulent air or when colliding amongst themselves.

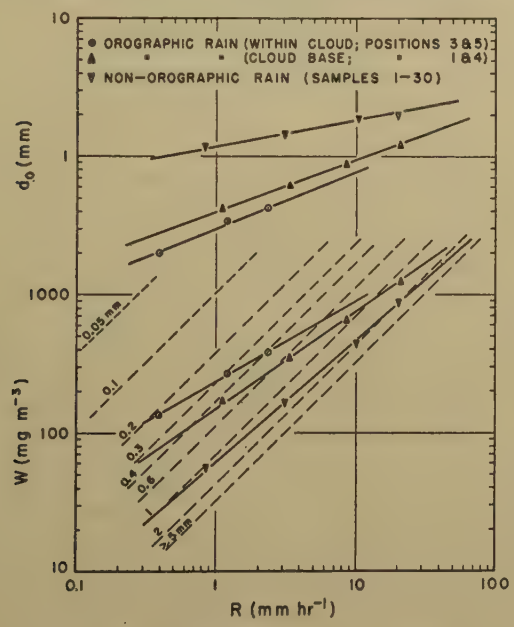

FIG. 13. Average distributions of fig. 12 represented as regression lines for parameters d_0 (upper set of lines) and W (lower set of lines) as function of R. Dashed lines on W-R graph constitute a family of lines of uniform drop size. Subject to standard deviations given in text, these lines may be considered as lines representing d_0.

TABLE 2. Regression equations for raindrop-distribution parameters W, d_0 and Z, for both orographic and non-orographic rains. (R in mm/hr.)

Type of rain	W (mg/m^3)	d_0 (mm)	Z (mm^6/m^3)
Orographic rain within the cloud (positions 3 and 5)	$235\ R^{0.67}$	$0.302\ R^{0.4}$	$16.6\ R^{1.88}$
Orographic rain at cloud base (positions 1 and 4)	$150\ R^{0.70}$	$0.397\ R^{0.37}$	$31\ R^{1.71}$
Non-orographic rain (Samples 1–30)	$61\ R^{0.89}$	$1.175\ R^{0.19}$	$290\ R^{1.41}$

The d_0 and W data from the averaged distributions are shown in fig. 13 as functions of R. The dashed lines, with a slope of one, are for a collection of drops of uniform size. These lines illustrate that, for any given intensity, the liquid-water content will increase as the drop size decreases (this was discussed in section 6, above). The plotting of these lines on the same graph as the regression lines enables one to make a reasonably accurate estimate as to the median volume diameter d_0 of the drop distribution. As an example, consider the regression line for the orographic rain within the cloud. At an intensity of 1 mm/hr, the liquid-water content is 235 mg/m^3. The dashed line for drops of 0.3 mm crosses the regression line at this point. This value of 0.3 mm is identical with the value of d_0 found with the aid of the upper group of lines of fig. 13. At an intensity of 2.1 mm/hr, the regression line crosses the line for drops of 0.4 mm. Again this is seen to coincide with the actual d_0. It is interesting to note that the dashed lines reach a limiting position at a drop size of about 5 mm. At this size, the terminal velocity has effectively reached a maximum.[9] A further increase of drop size, say to 10 mm, will give rise to an eight-fold increase in W and, as the terminal velocity remains unchanged, a similar increase in R. Thus, the new position on the W–R graph will still be on the line for 5-mm drops. If any drop distribution has values of W and R which locate it to the right of the line for 5-mm drops, a mistake in the calculations of W or R is implied, or else terminal velocities exceeding those with respect to a stationary reference must be inferred. The latter case presumably could be found in downdrafts or at high altitudes.

The median volume diameters were individually determined for each of the drop samples of table 1. These were compared with the value estimated by the method explained above. The standard deviation of d_0 for the non-orographic rain (samples (1–30) was 15.6 per cent and, for the orographic rain, only 11 per cent. It is interesting that, for the non-orographic

[9] In reality, the terminal velocity continues to increase with drop size beyond 5 mm. This increase, less than 1 per cent, can be neglected in the present study.

samples, the estimated d_0 was less than the actual d_0 in about 75 per cent of the cases, while for the orographic rain the estimated d_0 exceeded the actual d_0 in 70 per cent of the cases. Regardless of this, the relatively small standard deviation allows one to use the dashed lines of fig. 13 as lines of constant d_0.[10]

The validity of using the lines of constant drop size as lines of constant d_0 was confirmed even for cloud-droplet distributions. The parameters R, W, Z and d_0 were obtained for the nine cloud-droplet distributions published by Squires and Gillespie (1952). With the exception of the first three distributions, which extended well into the drizzle range, the standard deviation of the estimated d_0 was only 4.2 per cent. These distributions gave intensities from 0.1 to 0.4 mm/hr and liquid-water contents in the region of 1000 mg/m³.

The function $Z = f(d_0, W)$, identical for cloud and raindrop distributions.—In a paper on the reflection and transmission characteristics of microwaves in clouds, Bartnoff and Atlas (1951) presented the equation $Z = 6\pi^{-1} G(n) d_0^3 W$, where $G(n)$ was a factor depending on the spread of the cloud-drop distribution. In a later paper (Atlas and Boucher, 1952) over 100 cloud samples were analyzed, with the result that $G(n)$ could be taken as a constant of 1.35 with a standard deviation from regression of 35 per cent.

The value $d_0^3 W$ was computed for each distribution of the present study and plotted against Z.[11] The regression line was calculated to be $Z = 6\pi^{-1}$ (1.37) $d_0^3 W$, with a standard deviation from regression of 30 per cent for the coefficient. The exponent of $d_0^3 W$ was 1.007, near enough to unity to insure the reliability of the exponents 3 and 1 on d_0 and W, respectively. The cloud-drop distributions (Squires and Gillespie, 1952) gave a regression line of $Z = 6\pi^{-1}$ (1.32) $d_0^3 W$, with a standard deviation from regression of 13 per cent for the coefficient. The good agreement of these three regression equations indicates uniqueness for cloud- and raindrop-distributions alike.

11. Summary and conclusion

1. A given drop-size distribution can be modified by wind shear, relative fall among the drops, evaporation, and drop coalescence in the fall from cloud to ground. Although some of these factors are at work within the cloud itself, it is certain that drop-size sampling at the cloud base will minimize the errors contributed by these factors. The evaporation will be most important, especially in the case of the semi-tropical orographic rains discussed in the present study. In these rains, the many thousands of drops per cubic meter smaller than 0.5 mm that are normally present may evaporate completely in a sub-cloud fall of 1000 m. This evaporation was eliminated in the present work by obtaining the orographic drop distributions on the sides of the volcanoes of the island of Hawaii at cloud base or within the cloud itself.

2. Drop distributions have been obtained in rain which presumably began as snow in freezing clouds. The differences in drop distribution, liquid-water content, median volume diameter, and radar reflectivity from that of orographic rains are apparent from table 1 and figs. 4–11. The liquid-water content W has been used as a measure of the drop distribution. A wide distribution with relatively few drops, both large and small, will give a lower value of W, for the same intensity, as will a narrow distribution composed of many small drops. W-R relationships for non-orographic rains have been found to agree reasonably well with that of Best (1950).

3. The distribution of raindrops in semi-tropical, non-freezing orographic clouds is decidedly different from the drop distributions presented in the literature. In general, the number of drops per cubic meter at the small end of the raindrop spectrum is an inverse function of the rain intensity. The number of large drops is a direct function of the intensity. The maximum drop size seldom exceeds 2 mm and concentrations of drops smaller than 0.5 mm often exceeds 25,000 per m³. These distributions of drops are not the result of chain reaction. It seems probable that these drops evolve first by condensation on large air-borne salt particles, and then by accretional processes with the numerous cloud droplets. The evidence for this hypothesis will be presented in the near future. The raindrop distribution near the top of orographic clouds is concentrated at the small end of the spectrum. The appearance of drops larger than 0.6 mm is exceptional.

4. The median volume diameter, the drop diameter at which the total volume of water per cubic meter is divided equally, has been presented as a function of the intensity of rainfall. For a given intensity in an orographic rain, the median volume diameter is about half that found in thunderstorm and frontal type rains.

5. The radar reflectivity Z in an orographic rain is a factor of 10–20 less than that found in thunderstorm-type rains. Variations of Z have been found in orographic rain from day to day.

6. Regression equations for the parameters d_0, W and Z as a function of R illustrate the basic differences between orographic rain from non-freezing clouds and the type of rain which develops by the Bergeron-Findeisen process. The regression $Z = f(d_0, W)$ is identical for all the drop distributions of the present study and for the cloud distributions of Squires and Gillespie (1952). The median volume diameter d_0 can be found with reasonable accuracy from a W-R plot of a family of lines of constant drop size. This indicates that, in general, a drop distribution can be represented by a uniform collection of drops with a drop size equal to d_0. The parameters W, Z and R will be unchanged in either case.

Acknowledgments.—The writer would like to thank Mr. Alfred H. Woodcock for his assistance in obtaining many of the data used in this study. He is grateful to Mr. W. A. Mordy of the Pineapple Research Institute, Experiment Station of the Hawaiian Sugar Planters' Association, and the Territorial Cattlemen's Council, for the opportunity to work in Hawaii.

[10] A somewhat similar method for determining d_0 for cloud-droplet distributions was used by Atlas and Boucher (1952), by using a W-Z graph.

[11] The Z values for the data ranged from 10^{-1} to 10^5. Some ten or more points with $Z < 3$ were not used in computing the regression line. As most of these points represented drop samples with a spread of only 0.2 to 0.4 mm, it was felt that the small errors in determining the drop diameters would be magnified in the calculation of Z.

REFERENCES

Anderson, L. J., 1948: Drop-size distribution measurements in orographic rain. *Bull. Amer. meteor. Soc.*, 29, 362–366.

Atlas, D., and R. J. Boucher, 1952: The relation of cloud reflectivity to drop-size distribution. *Proc. 3rd Radar Wea. Conf.* Montreal, McGill Univ., 240 pp.

Atlas, D., and V. G. Plank, 1952: The starting transient of a shower. *Proc. 3rd Radar Wea. Conf.* Montreal, McGill Univ., 240 pp.

Bartnoff, S., and D. Atlas, 1951: Microwave determination of particle-size distribution. *J. Meteor.*, **8**, 130–131.

Bentley, W. A., 1904: Studies of raindrops and raindrop phenomena. *Mon. Wea. Rev.*, **32**, 450–456.

Best, A. C., 1950: The size distribution of raindrops. *Quart. J. r. meteor. Soc.*, **76**, 16–36.

——, 1952: The evaporation of raindrops. *Quart. J. r. meteor. Soc.*, **78**, 200–225.

Blanchard, D. C., 1949a: *The distribution of raindrops in natural rain.* Schenectady, Genl. Elect. Res. Lab. (Occas. Rep. 15, Project Cirrus), 16 pp.

——, 1949b: *The use of sooted screens for determining raindrop size and distribution.* Schenectady, Genl. Elect. Res. Lab. (Occas. Rep. 16, Project Cirrus), 11 pp.

——, 1950: The behavior of water drops at terminal velocity in air. *Trans. Amer. geophys. Union*, **31**, 836–842.

Bowen, E. G., 1950: The formation of rain by coalescence. *Austral. J. appl. Sci.*, **3**, 193–213.

——, and K. A. Davidson, 1951: A raindrop spectrograph. *Quart. J. r. meteor. Soc.*, **77**, 445–449.

Chapman, G., 1948: Size of raindrops and their striking force at the soil surface in a red pine plantation. *Trans. Amer. geophys. Union*, **29**, 664–670.

Cooper, B. F., 1951: A balloon-borne instrument for telemetering raindrop-size distribution and rainwater content of cloud. *Austral. J. appl. Sci.*, **2**, 43–55.

Gunn, R., and G. D. Kinzer, 1949: The terminal velocity of fall for water droplets in stagnant air. *J. Meteor.*, **6**, 243–248.

Katz, I., 1952: A momentum disdrometer for measuring raindrop size from aircraft. *Bull. Amer. meteor. Soc.*, **33**, 365–368.

Kinzer, G. D., and R. Gunn, 1951: The evaporation, temperature and thermal relaxation-time of freely falling waterdrops. *J. Meteor.*, **8**, 71–83.

Langmuir, I., 1948: The production of rain by a chain reaction in cumulus clouds at temperatures above freezing. *J. Meteor.*, **5**, 175–192.

Laws, J. O., and D. A. Parsons, 1943: The relation of raindrop-size to intensity. *Trans. Amer. geophys. Union*, **24**, 452–460.

Leopold, L., 1949: The interaction of trade wind and sea breeze, Hawaii. *J. Meteor.*, **6**, 312–320.

——, and W. A. Mordy, 1951: 1948–1949 trials of the Schaefer-Langmuir cloud-seeding technique in Hawaii. *Tellus*, **3**, 44–52.

Lowe, E. J., 1892: Rain drops. *Quart. J. r. meteor. Soc.*, **18**, 242–245.

Marshall, J. S., and K. L. S. Gunn, 1952: Measurement of snow parameters by radar. *J. Meteor.*, **9**, 322–327.

Marshall, J. S., and W. McK. Palmer, 1948: The distribution of raindrops with size. *J. Meteor.*, **5**, 165–166.

Maulard, J., 1951: Measure du nombre de gouttes de pluie. *J. Sci. Météor.*, **10**, 69–73.

Mt. Washington Observatory, 1951a: Research Report, Quarterly Progress report, January 23.

——, 1951b: Research Report, Quarterly Progress report, October 23.

Neuberger, H., 1942: Notes on measurement of raindrop sizes. *Bull. Amer. meteor. Soc.*, **23**, 274–276.

Niederdorfer, E., 1932: Messungen der Grösse der Regentropfen. *Meteor. Z.*, **49**, 1–14.

Rigby, E. C., and J. S. Marshall, 1952: *The modification of rain with distance fallen.* Montreal, McGill Univ. (Sci. Rep. MW-3, Stormy Wea. Res. group), 52 pp.

Simpson, R. H., 1952: Evolution of the kona storm, a subtropical cyclone. *J. Meteor.*, **9**, 24–35.

Squires, P., and C. A. Gillespie, 1952: A cloud-droplet sampler for use on aircraft. *Quart. J. r. meteor. Soc.*, **78**, 387–393.

Twomey, S., 1953: On the measurement of precipitation intensity by radar. *J. Meteor.*, **10**, 66–67.

Wexler, R., 1948: Rain intensities by radar. *J. Meteor.*, **5**, 171–173.

Wiesner, J., 1895: Beiträge zur Kenntnis des tropischen Regens. *Sitzber. k. Akad. Wiss. Wien*, Math.-naturw. Kl., **104**, 1397–1434.

Woodcock, A. H., 1952: Atmospheric salt particles and raindrops. *J. Meteor.*, **9**, 200–212.

Contribution No. 659

A SIMPLE RECORDING TECHNIQUE FOR DETERMINING RAINDROP SIZE AND TIME OF OCCURRENCE OF RAIN SHOWERS

Duncan C. Blanchard

(Contribution No. 659 of the Woods Hole Oceanographic Institution)

Abstract--This paper describes an easily constructed instrument for the purpose of obtaining a continuous record of the time of occurrence and duration of shower-type rains and their range of raindrop sizes. A battery-driven motor pulls paper tape, previously treated with the water-soluble dye, methylene blue, past an opening exposed to the rain. The spot diameters left by the rain on the tape may be related to raindrop size by laboratory calibration. During a week's run on the island of Oahu, Hawaii, a total of 119 rains were recorded. Although many of these passed in a minute or so and were only a few minutes apart, less than 40 were recorded by nearby recording rain gages.

Introduction--The drop recorder described in this paper is a simple instrument which records the imprint of raindrops on a moving paper tape. Although it was designed for one specific job, the simplicity of its construction coupled with the interesting data it has obtained may render it useful for other investigations as well. It was initially designed to satisfy the need of obtaining the frequency of occurrence and the predominant drop sizes of rain on the windward and leeward sides of the island of Oahu, Hawaii.

The prime advantages of the recorder are: (1) Compactness and lightweight (3.2 kg). (2) Relatively simple and inexpensive to build. With the exception of the small six-volt motor, all parts should be obtainable in any machine shop. (3) Portability. As the motor is driven by a six-volt dry cell, the drop recorder can be used in locations relatively inaccessible to many instruments. The present model uses two 15-watt, 115-volt lamps for drying the exposed tape. To make it completely independent of a 115-volt power supply, a self-enclosed unit could be made by winding a heating element powered by, for example, a Burgess 4F4H six-volt battery. It should be possible to utilize the heaters to a higher efficiency than at the present time. In such case, it may be possible to get by with ten or 15 watts.

Design of drop recorder--The entire unit was built up around the six-volt, one-rpm motor (see Fig. 1). At this speed some 300 meters of tape would be wound on the take-up reel A in a day's time. Consequently, two reduction gears were used to reduce the speed to a point where about 20 m of tape per day was exposed. The tape, which was coated with methylene blue dye, was 16 mm wide and reasonably water resistant. The reels for the tape were Kodak 16-mm × 100 ft movie reels. After exposure (through opening B, Fig. 1) the tape passed over two 15-watt cylindrical lamps. This insured sufficient drying, even in the heaviest rain, to prevent any smearing of the drop record on the take-up reel.

The entire unit, including battery, was placed within the small metal box C. The rain fell through a 30 × 40-mm opening, thus giving an effective tape exposure area of 6.4 cm^2. As the recorder was designed and used in Hawaiian orographic rains, which are composed mainly of drops less than two mm in diameter, the 6.4-cm^2 area was adequate for the job. However, calibration of the tape showed that a 2.75-mm diameter drop at terminal velocity produced a spot 16 mm in diameter, the width of the tape. Thus, for use in areas where convective type and frontal storms are common, one would have to use a tape of sufficient width to handle raindrops in excess of four mm. A tape width of perhaps 60 mm would be desirable. It would probably be necessary to change the gear ratio to increase the tape speed to some 40 m per day. As the tape is easily treated with the water-soluble methylene blue dye, the added area will pose no problem to the treating process. The optimum values of tape width and speed will depend on the general drop-size distributions in the particular region where the recorder is used.

No attempt was made to drive the tape at constant speed. Time marks were placed on the tape about every ten hours. From these checks and previous laboratory calibrations, a curve of the relationship of time to exposed tape length was made. The time of occurrence of the rain spots on the tape was picked off this curve.

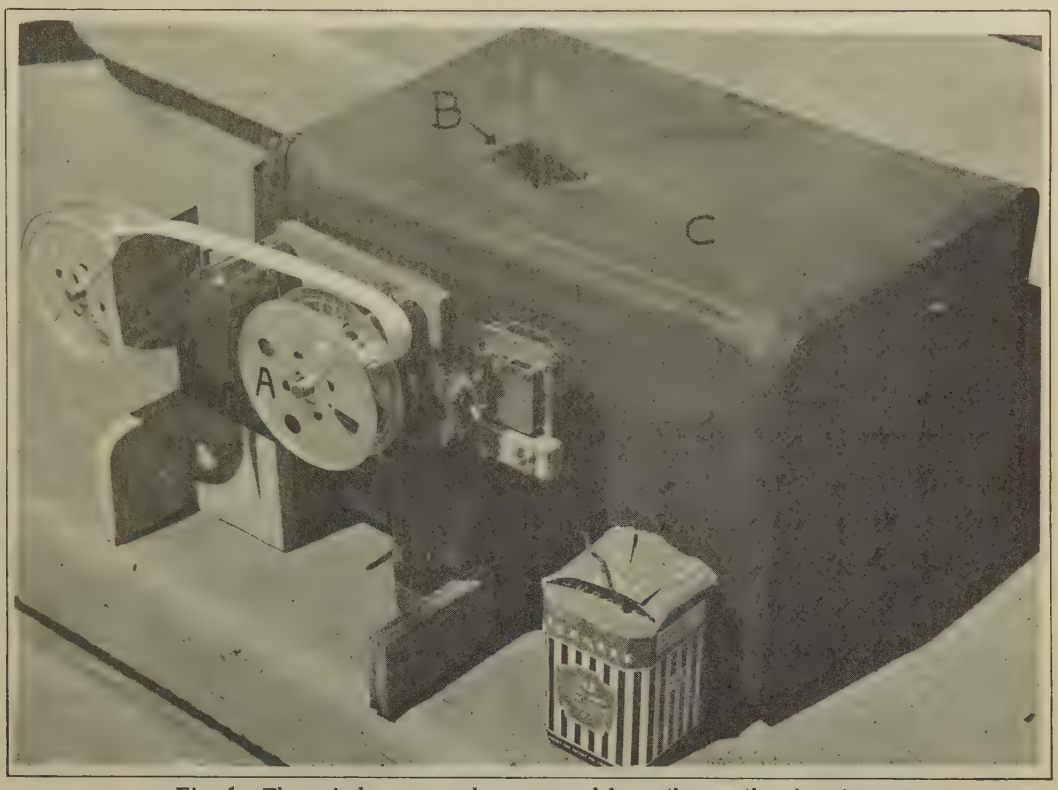

Fig. 1--The raindrop recorder removed from the weather housing

Some results of the drop recorder--During the period June 16-18 and June 25-July 1, 1952, a detailed cloud-physics study was carried out on the island of Oahu, Hawaii, by the Meteorology Department of the Pineapple Research Institute of Hawaii and A. H. Woodcock and the writer, both of the Woods Hole Oceanographic Institution. The primary purpose of this study was to obtain as much detailed information as possible on the formation of cloud and rain on the southern end of the Koolau mountain range. To this end, special attention was given to the sea-salt hypothesis [WOODCOCK, 1952]. It is believed that the orographic rain of Hawaii develops from sea-salt particles which grow initially by condensation and then by accretion. The growth of the salt particles to raindrop size would require considerably more time than is available during the orographic lifting of the cloud. This requires that either rain be falling from the clouds as they pass over the windward shore of the island or that large droplets be present within the cloud. In either case the orographic lifting causes additional condensation of water and should bring about an accelerated growth of the small droplets already present.

Two raindrop recorders were used to determine the percentage of showers on the central part of the island that were preceded by rain to windward. One recorder was located on the windward side of the island (Recorder 1) at the edge of the sea and the other at a point 6.5 miles downwind and in the lee of the 3000-ft Koolau mountain range (Recorder 2). The mean annual rainfall at the position of the first recorder is about 35 inches, increasing to 150 inches at the position of the downwind raindrop recorder.

Both recorders were kept running for seven consecutive days (with the exception of Recorder 1, which was not running on the last day). Although Recorder 1 was not equipped with the drying lamps, the relatively infrequent rain showers were seldom heavy enough to cause extreme flooding of the tape. Some of the interesting characteristics of the orographic rains, as obtained from the tapes, are listed in Table 1. It is seen that Recorder 2 received rain on each of the seven days. Expressed percentagewise (the ratio of the number of hours of rain to the 24 odd hours of tape exposure), the days were increasingly wetter with rain falling 72 pct of the time on June 29-30, 1952.

Table 1--Comparison of data from the two raindrop recorders

Date and time				Rain occurrence[a]		Number of showers		Max. shower duration		Drop-size change[b]		Flooding[c]	
From		To		Rec 1	Rec 2	Rec 1	Rec 2	Rec 1	Rec 2	Rec 1	Rec 2	Rec 1	Rec 2
1952	h m	1952	h m	pct	pct			min	min			pct	pct
June 25	11 38	June 26	09 47	0	0.15	0	2	0	1	0	0	0	0
June 26	10 01	June 27	09 36	4	26	7	14	48	169	1	8	0	23
June 27	09 48	June 28	07 55	14	28	9	22	103	60	3	2	20	63
June 28	08 04	June 29	08 12	4.4	35	10	30	11	60	1	2	52	40
June 29	08 20	June 30	08 34	2.2	72	6	23	17	188	0	12	19	32
June 30	08 48	July 1	08 37	0.3	11	5	13	1	19	0	0	20	20
July 1	08 48	July 2	10 11	. .[d]	15	. .[d]	15	. .[d]	69	. .[d]	1	. .[d]	67

[a]Percentage of exposure time that rain was falling.

[b]Minimum number of marked drop-size variations during maximum shower (during flooding it is impossible to ascertain drop-size change).

[c]Per cent of rainy period that rain intensity was sufficient to cause flooding.

[d]Recorder 1 was not running during the last day.

During the week's run 119 separate showers were recorded. Although many of these showers were separated by intervals as small as five minutes and consisted of only a brief fall of drizzle-type drops, it is interesting to note that two weighing-type rain gages gave no indication of the frequent occurrence of showers. The records of these two recording gages, located about 0.7 mile on either side and nearly on a line normal to the prevailing tradewinds, indicated the passage of 34 and 40 showers respectively. The similarity between the two rain traces makes it reasonable to suspect that this rainfall pattern was similar in the area between the gages and, in particular, at the site of Recorder 2. If this is true, it is apparent that some 70 pct of the showers were not being detected. These discrepancies are no doubt due to the evaporation of the light rain which adheres to the sloped sides of the collectors of the recording gages or to accumulation on the collector of several such rains. In the latter case, the water from these rains will eventually reach the receiver but will be recorded as a single shower. (This is especially true in the light Hawaiian rains. In the course of obtaining rainwater for chemical analysis, the writer used stainless-steel funnels of 0.5 m^2 effective area. On many occasions, ten to 20 minutes would elapse while rain continued to adhere to the hydrophobic surface of the funnel. Only after 100 or more milliliters had accumulated would any pass into the collector bottle.)

In the course of examining the tapes, an arbitrary method of classifying the drop distributions was adopted. Each drop distribution in the showers was listed as having many or few, small drops, large drops, large and small drops, or flooding. Flooding referred to an overabundance of drops which rendered the tape a uniform blue. Fifty-five per cent of the showers were classified as having few drops. These occasions probably represent those in which evaporation on the collector prevented any indication of the rain on the gage. A worthwhile project would be to use a standard recording gage and drop-size recorder side by side. The lack of sensitivity of the gage to brief light rains would then become apparent.

The showers at Recorder 2 lasted from one minute to over three hours. The flooding of the tape, indicative of medium to heavy rain, occurred a maximum of 67 pct of the total time of rainfall. Recorder 1, on the windward side of the island, indicated considerably lower values in nearly every category. The maximum amount of rain, at least as measured by elapsed time, was 14 pct on the third day. During the same time it rained 28 pct of the time at Recorder 2. On June 29-30, Recorder 1 indicated rain only 2.2 pct of the time as compared to 72 pct at Recorder 2. It should not be inferred from this that the majority of the showers completely develop during the time it takes the clouds to travel between the two recorder stations. It seems probable, as already discussed, that many of the clouds have already developed to the drizzle stage by the time they pass over Recorder 1.

Ten sections of the tape records are shown in Figure 2. Tape 1 illustrates the relatively splash-free pattern associated with the larger drops. The spots, some six mm in diameter, indicated raindrops of 1.7-mm diameter. Tapes 2-6 show the large and small drops that represent the low-intensity rains. The low number per sq m is realized when one considers that approximately 2.6 minutes are required for the tape to move the four cm across the exposure opening (see time scale on Tape 1). Tape 7 shows both large and small drops alike. Tape 8 illustrates the wind effect on the small drops. The turbulent nature of the wind is apparent from the varied direction of the

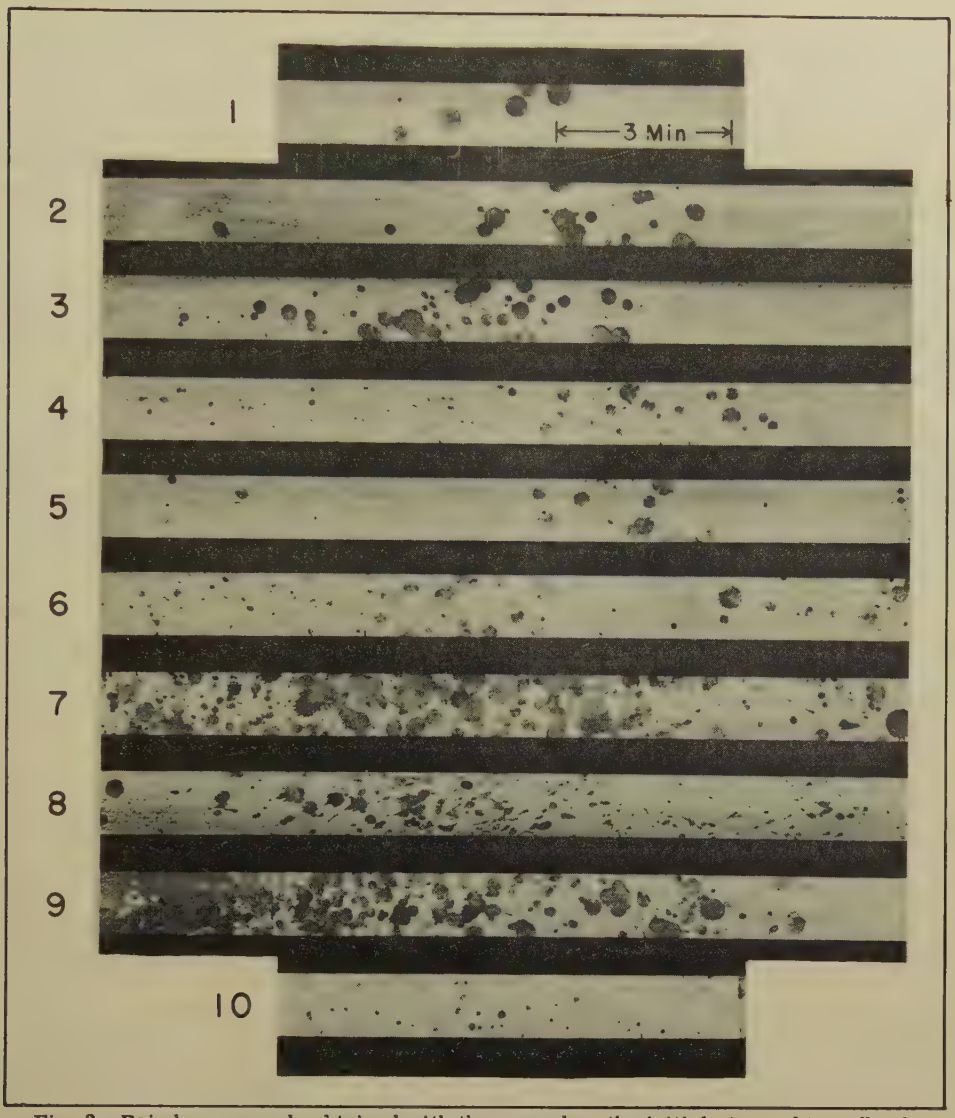

Fig. 2--Raindrop records obtained with the recorder; the initial stage of tape flooding is shown on the left hand end of Tape 9

"tails" of the spots. Tape 9 shows the beginning of a shower. Although relatively few drops fell during the first six or seven minutes, the intensity increased and eventually caused a flooding of the tape. Tape 10 is typical of the fine rain which is so common in the Hawaiian Islands. The drops pictured are <0.7 mm diameter and, as explained earlier, often fail to register on standard rain gages.

Conclusions--The drop recorder has proved quite useful for the purpose for which it was designed. It succeeded in giving a continuous record of the occurrence and duration of showers in Hawaiian rains. It was also possible to obtain the maximum drop size and some idea of the relative frequency of appearance of the smaller drops in light to medium rains.

It is realized that the present drop recorder has many limitations, some briefly touched upon in this paper. For example, there would be considerable doubt as to the accuracy of calculations of the spatial distribution of drops. At the best, they would represent, not point distributions, but distributions averaged over a thousand or more meters of vertical height. A wider tape running

at a higher speed would be needed to minimize this problem. The problem of tape flooding in rains of moderate to high intensity could, in all probability, be eliminated by using a horizontally mounted sheet-metal disc as a protective shield for the tape. This disc could be rotated by the tape-drive motor, on an axis normal to its plane, by either pulley or gear drive. A slot cut in the disc would pass over the moving tape for each revolution of the disc. Thus, by varying the disc speed and slot width and distance from the disc axis, a wide choice of exposure times and frequency could be obtained. The intermittent exposures would probably be short enough to prevent flooding in rain of high intensities, and yet be frequent enough to obtain the times of starting and ending of the rain.

In addition to using two recorders as described in this paper, it would be interesting to utilize several such recorders located at intervals along the path of a shower. A similar study would involve locating recorders at points along the fall line of a mountain against which orographically formed rain is falling. In this way the variations in raindrop size from cloud top to bottom could be found.

Acknowledgments--The writer would like to thank his co-worker, Alfred H. Woodcock, who first suggested the possible advantages of a drop recorder in studying Hawaiian rains. He is indebted to W. A. Mordy of the Pineapple Research Institute, Experiment Station of the Hawaiian Sugar Planters' Association, and the Territorial Cattlemen's Council, for the opportunity to work in Hawaii. He is grateful to David Johnson and Laurence Eber, also of the Pineapple Research Institute, for their assistance in obtaining data. This study was supported by the Office of Naval Research under Contract Nonr 79800 (NR-085-001).

Reference

WOODCOCK, A. H., Atmospheric salt particles and raindrops, J. Met., v. 9, pp. 200-212, 1952.

Woods Hole Oceanographic Institution,
Woods Hole, Massachusetts

(Communicated manuscript received February 13, 1953;
open for formal discussion until January 1, 1954.)

Contribution No. 660

NOTES

Hawaii as a Cloud Physics Laboratory

Reprinted from PACIFIC SCIENCE
October, 1953

NOTES

Hawaii as a Cloud Physics Laboratory

The major islands of the Hawaiian chain lie across the Pacific northeast trade winds near north latitude 21°, about 2,400 miles southwest of San Francisco. It is the purpose of this note to discuss very briefly the great advantages of one of these islands (Hawaii) as a place to study the relationships between the precipitation elements in clear marine air and these elements present in clouds formed in this air.

Recent developments in the study of rain formation have led to the hypothesis that large sea-salt particles are the basic nuclei upon which many raindrops initially form (Ludlam, 1951, Quart. Jour. Roy. Met. Soc. 77: 402–417; Woodcock, 1952, Jour. Met. 9: 200–212; Squires and Woodcock, MS.). These developments have re-emphasized the need in cloud physics for further detailed physical-chemical studies of rain which will enable us to ". . . know how nature operates to produce precipitation" (Byers, 1953, Indian Acad. Sci., Proc. 37(A): 237–247).

In order to make preliminary tests of the salt particle-raindrop hypothesis by making measurements of natural rains, it was necessary to find a geographic location where the contents of the lower atmosphere could be determined before, during, and after the formation of cloud and rain. Recent work has indicated that the windward side of the island of Hawaii, in the region of Hilo, is almost ideal for this study (see Fig. 1). Here, on most of the days throughout the year, rain falls near area A from orographic clouds which have formed over the island and within the trade-wind stream. If one follows the streamlines of this trade-wind air upwind of area A and over the sea, only scattered cumulus clouds are found upon arrival near area B. If the air is followed downstream from A, the clouds are found to dissipate, leaving clear air at C. Hence it is possible to determine, by appropriate measurement, the contents of a parcel of clear air at B, the nature of the precipitation within clouds formed in this air when it arrives at A, and the final modified parcel after the clouds have dissipated at C, a distance of about 30 miles.

Much of the mountain slope near Hilo is readily accessible on paved roadways. Rain and cloud drop sizes may be sampled within the orographic clouds from the 2,000 foot level to the 6,500 foot level on these roadways, thus avoiding the problems of evaporation, accretion, etc., which can greatly modify rains falling through clear air from cloud base to ground.

The presence of the trade-wind inversion at an average height of about 6,000 feet over the sea concentrates the clouds and water vapor in the lower air (Riehl *et al.*, 1951, Quart. Jour. Roy. Met. Soc. 77: 598–626; U.S. Weather Bureau, Staff Members, Honolulu, MS.; Leopold, 1949, Jour. Met. 6: 312–320). The inversion also limits the vertical extent of the salt nuclei, as shown in Figure 2. The distribution curves representing salt particles at the 1,550 and 2,740 meter altitudes show a great reduction in the number and weight of particles at the base of the inversion and above it (see temperature on insert diagram,

FIG. 1. Streamlines and mean annual rainfall on NE part of Hawaii. Isohyetal lines are in inches. The arrows represent the hypothetical mean streamlines of the flow of the trade winds in this part of the island, as given by Leopold (1949). (Scale in statute miles.)

Fig. 2). This concentration of the precipitation elements (i.e., clouds, water vapor, and nuclei) in the lower air is found during most of the year in this area and is one of the major advantages of Hawaii for precipitation studies such as those discussed here. Measurements of water vapor, temperature, salt nuclei, etc., can therefore be limited to the lower atmosphere, and there is usually no need to be concerned with the higher levels.

A further result of the presence of the trade-wind inversion is that the great majority of the clouds never ascend to heights at which the temperature is below freezing. Thus, most of the time there is no confusion as to whether or not the Bergeron rain-forming process may have occurred. It seems clear that accretional processes must account for practically all the rains in this region, and hence it is an excellent area in which to attempt to relate the

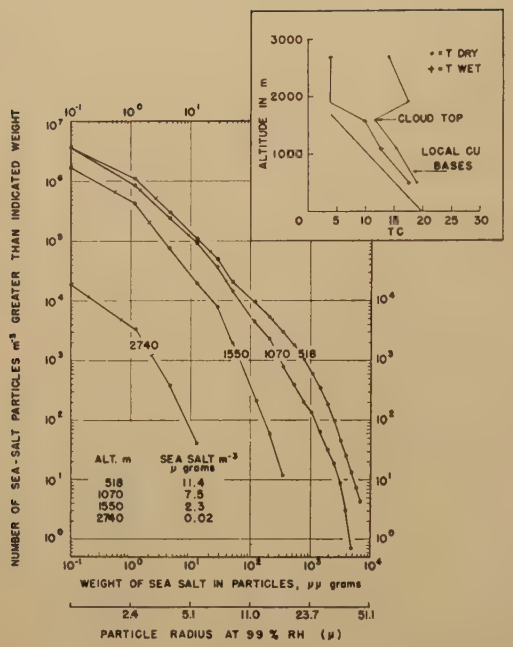

FIG. 2. Vertical distribution of sea-salt particles over the sea in Hawaii (21°30'N, 157°40'W), May 30, 1952, 1300 local time. Surface wind 80°, force 4 to 5. Height of scattered cumulus cloud bases varied from 690 to 820 meters. Temperature at 2,740 meters 12.8°C. The short transverse lines on the distribution curves mark the first quartile, median, and third quartile weight distribution points, reading left to right. The distribution curves are read as follows: at a height of 518 meters there are about 10,000 particles larger than 100 $\mu\mu$ grams.

detailed physical changes in the air associated with these frequently recurring processes.

The presence of the great mountain Mauna Kea (see Fig. 1), extending up to almost 14,000 feet, makes it possible to obtain direct visual estimates of maximum cloud heights among the orographic clouds over the high-rainfall region during extended time periods which make air craft observation impracticable. These estimates can be made at the same time that rain and cloud drops are being sampled within the cloud along the roadway below. One can drive a car up to a point at the 9,500 foot level, which is near a site overlooking the high-rainfall region A.

In this area of Hawaii, nature is producing rain very regularly and under simple conditions usually uncomplicated vertically by multiple layering of air masses of different origin and physical history. Geophysical events of the past and present seem to have fortuitously conspired to produce a setting in which simple natural experiments in rain-making are an almost daily occurrence. Through the use of local roadways and aircraft, the whole experimental area is readily accessible for study, and the observations of one day can commonly be tested or extended on the following day under the nearly constant natural conditions. The author knows of no other geographical setting so uniquely advantageous for cloud physics studies.

The importance of rainfall to the economy of the Hawaiian Islands has led to extensive activity by local organizations in the study of various weather factors and in the accumulation of data from numerous observing stations. These organizations—the U. S. Weather Bureau, the Pineapple Research Institute, the Experiment Station of the Hawaiian Sugar Planters' Association, and the Territorial Cattlemen's Council—located at Honolulu, Hawaii, are interested in fostering cloud physics research and are able to supply valuable climatological data from long-period records as well as current radiosonde and other data from numerous local stations. — *A. H. Woodcock, Woods Hole Oceanographic Institution.* (Contribution No. 660 of the Woods Hole Oceanographic Institution.)

Contribution No. 663

Reprinted from THE JOURNAL OF THE ACOUSTICAL SOCIETY OF AMERICA, Vol. 25, No. 5, 1016–1017, September, 1953
Copyright, 1953, by the Acoustical Society of America.
Printed in U. S. A.

High-Frequency Auditory Response of a Bottlenosed Porpoise, *Tursiops truncatus* (Montagu)*

WILLIAM E. SCHEVILL, *Woods Hole Oceanographic Institution, Woods Hole, Massachusetts*

AND

BARBARA LAWRENCE, *Museum of Comparative Zoology, Harvard College, Cambridge, Massachusetts*

(Received June 25, 1953)

Conditioned responses of a bottlenosed porpoise (*Tursiops truncatus*) showed its upper frequency limit of auditory response to be about 120 kc. The analogy of human bone-conduction ultrasonic "hearing" is considered. Some aspects of phonation and echo-location are commented on.

THIS experiment with a fresh-caught, wild, adult bottlenosed porpoise, *Tursiops truncatus* (a small whale), deals with only one aspect of the problem of hearing, the high-frequency auditory response. Whales are completely aquatic mammals, with the mammalian external ear modified nearly to the vanishing point; this is no obstacle to their hearing, for the body is well-coupled and well-matched to the surrounding water. Thus a cetacean necessarily depends on bone (or body) conduction for transmitting sound to the inner ear.

The work was done in a turbid mud-bottomed tidal inlet at Marineland, Florida. This pool was essentially anechoic, no echoes or reverberations being detected. However, it had a deplorably high background, chiefly caused by snapping shrimp; this prevented our determining the porpoise's minimum threshold. The acoustic equipment included three underwater sound projectors covering the range from 100 cycles to 153 kc and a monitor hydrophone designed for flat response from 50 cycles to 200 kc, connected to a sound level meter. The hydrophone was 33.5 meters from the projectors. The signals were generally between 3 and 5 seconds long, which gave the porpoise ample time to receive them even through the interference of nearby snapping shrimp. All sound levels are those of the sound field at the monitor hydrophone, and are referred to a pressure of 1 dyne/cm². They approximate the sound field to which the porpoise was exposed, since we called her only when she was within about 5 meters of the hydrophone. The signal level was sometimes down in the background and sometimes well above it, the pressures falling mostly between 0 and 10 db, with extremes at −25 and +28 db; less than 10 percent of the signals were below 1 dyne/cm². After the porpoise was taught to acknowledge an acoustic signal by coming to accept a fish from the hand, we assessed 1006 responses during about 100 working hours spread over 10½ consecutive days.

We tested her with tones ranging from 0.15 kc to 153 kc, rarely staying long in any one frequency region, and thus repeatedly checked the porpoise's responses all up and down the scale. From 0.15 kc to 120 kc these were essentially uniformly positive, the occasional negatives being clearly attributable to psychology rather than to acoustics. The positive responses fell off abruptly above 120 kc, and dropped to 50 percent by 126 kc; above 130 kc (30 percent), the curve seems to flatten somewhat, dropping to 13 percent for 151–153 kc, the absolute upper limit of our signal generator.

These figures are presumably comparable with data based not on air-coupled hearing, but on bone-conduction, which has been most extensively studied in man, for which animal an average upper frequency limit by air-coupled hearing is 15 kc, while bone-conduction may bring an extension past 100 kc, but with an important and striking difference. A critical feature of hearing is frequency discrimination, which functions through most of the human air-coupled range. By bone-conduction, however, one distinguishes pitch up to the limits of ordinary hearing, and beyond that one continues to hear the highest pitch that is normally audible, even while exposed to much higher frequencies. Kunze and Kietz[1] have published curves reaching 128 kc for man, without any sign of a break in the upper end of the curve; they also report some individuals, presumably normal by air-coupled hearing, who can evidently discriminate tones on the basis of frequency up to 60 kc by bone conduction. See also Pumphrey[2] and Deatherage, Jeffress, and Blodgett.[3]

In the light of all this, it is perhaps not surprising that the porpoise responded to tones as high as it did. What is remarkable is the indication of an upper limit for this presumably colorless kind of response, which as far as we know has not been reported for any other mammal. Our simple conditioned response test does not give any indication of the upper limit of pitch perception by this animal. There is probably significance in the contrast in signal levels between our experiment with the porpoise, where above 100 kc the levels were almost all between 0 and 20 db above 1 dyne/cm², and the human bone-conduction work with thresholds of the order of 60 db or higher. In conversation, Dr. D. R. Griffin has suggested that the various human bone-conduction experiments, with their high levels, may represent paradoxical stimulation rather than true auditory response. If this is so, it would make it likely that the porpoise might have been discriminating pitch over all or nearly all of the very wide range of frequencies to which it responded, since we subjected it to no intensities likely even to approach paradoxical levels. We plan to test this experimentally on both porpoises and human beings.

A few points concerning sound production (or phonation) may be of interest.

Although all our evidence shows that cetaceans are highly directional in hearing, it seems probable that in phonation they are essentially a point source of sound. This is a corollary of the good match between animal tissue and water, and is borne out by a number of experiments of ours. Sound originating in the larynx, as we have demonstrated they produce, would thus travel almost spherically outward through the body tissues. The cetaceans have no need for the mouth as a speaker, and use this organ only for biting and eating; it plays no part in phonation or breathing.

While we have not made a detailed study of the spectrum of porpoise calls (Kellogg, Kohler, and Morris[4] have reported on those of *Tursiops truncatus*), we have learned that most of the energy appears to be concentrated in the lower end of their spectrum; nevertheless, their upper frequency limit is still undetermined, for we have noted some components still 8 to 12 db above background at 196 kc, the extreme upper limit of any of the gear we have ever used.

Ever since it has been widely realized that cetaceans produce underwater sounds, the attractive idea that they use these sounds for echo-location and navigation has occurred to a great many people, most of whom have evidently felt, like us, that in spite of much field work, observational evidence was lacking. In the test we have just described, which was not focused on this problem, our porpoise swam through more than usually opaque water, and though we listened continuously and attentively over the entire band of frequencies used, we never heard any sound from her that could be in any way related to her navigation or food-getting.

* This note (a condensation of a paper presented at the Forty-fifth Meeting of the Acoustical Society, May 1953) is a partial summary of a paper in press in the Journal of Experimental Zoology. The work was supported by the U. S. Office of Naval Research, and the experiment was carried out with the cordial help of Marine Studios, Marineland, Florida. Contribution No. 663 from the Woods Hole Oceanographic Institution.

[1] W. Kunze und H. Kietz, Arch. Ohren-, Nasen-, u. Kehlkopfheilk. ver. Z. Hals-, Nasen -u. Ohrenheilk. 155, 683–692 (1949).

[2] R. J. Pumphrey, Nature 166, 571 (1950).

[3] Deatherage, Jeffress, and Blodgett, J. Acoust. Soc. Am. 25, 190 (1953).

[4] Kellogg, Kohler, and Morris, Science 117, 239–243 (1953).

Contribution No. 669

Reprinted from
BULLETIN OF MARINE SCIENCE
OF THE GULF AND CARIBBEAN
Vol. 3, No. 2, pp. 83-95
SEPTEMBER, 1953

PLANKTON OF THE FLORIDA CURRENT. III. THE CONTROL OF THE VERTICAL DISTRIBUTION OF ZOOPLANKTON IN THE DAYTIME BY LIGHT AND TEMPERATURE

HILARY B. MOORE, HARDING OWRE, EVERETT C. JONES and T. DOW.[1]

The Marine Laboratory, University of Miami

ABSTRACT

The four groups, pteropods, siphonophores, chaetognaths and copepods, have been studied separately and together in the plankton of the Florida Current. Vertical diffuseness of plankton was found to be under the control mainly of light at its upper levels and of temperatures at lower levels. This is true both within a population of a single species and, to some extent, between species living at different depths. Finally, in the copepods only, changes in level in response to temperature and light changes are superimposed on a seasonal change in level of the population which may be correlated with the presence of successive broods.

INTRODUCTION

In a study of the zooplankton of the Bermuda area (Moore, 1949), certain generalizations were made with regard to the behaviour and distribution of the organisms. The one to which the present work relates was the fact that the spread, or degree of vertical diffuseness, was slight in shallow-living species, but became progressively greater in deeper-living ones. In studies of the deep scattering layer and euphausids (Moore, 1950, 1952) it was shown that a workable explanation of the day-time vertical distribution could be obtained if it was assumed that two opposing factors were operative, temperature and illumination. During the descent and ascent periods of diurnal migration, illumination appeared to be the predominant control ex-

[1]Contribution No. 669 from Woods Hole Oceanographic Institution. Contribution No. 111 from the Marine Laboratory, University of Miami.

cept at the greatest depths reached. During the latter, that is to say around noon, temperature usually superceded illumination as the controlling factor.

Finally, in a study of the siphonophores of the Florida current (Moore, 1953), it was found that the mid-day level occupied by the various species varied in close correlation with the changes in level of the isotherms. In fact the regression of change in level of the species on change in level of the 15°C. isotherm was 95%.

The behaviour of very few marine plankton species has been studied, either experimentally or by deduction from field observations. Experiments have suffered from the great difficulties of reproducing natural conditions and obtaining consistent results. For this reason, or because of wide differences in specific behavior patterns, little generalization has been possible with regard to the characteristics of plankton as a whole. In the Bermuda studies, the characteristics of each species were determined, and the resulting data treated as a whole for correlation studies. It was felt that the generalized view so obtained clarified points not readily seen in studies of single species. In addition, of course, it greatly increased the amount of material available for statistical analysis. The same method has been followed in the present work.

Material and Methods

The field work, and part of the study of the material was carried out as a joint program of the Marine Laboratory of the University of Miami and the National Geographic Society. An account of methods used as well as of the hydrographic conditions observed, has been published by Miller *et al.* (1953). An account of the siphonophores has also been published (Moore, 1953). The study on chaetognaths is part of a doctorate thesis to be submitted by H. Owre at the University of Michigan. That on copepods, by E. C. Jones, was incorporated in part in a masterate thesis at the University of Miami, and that on pteropods, by T. Dow, is part of a masterate thesis to be submitted at the same university. The work on the individual groups is that of the authors indicated, while the coordination is that of the senior author. This coordinated study is part of an investigation of the scattering layer carried out by the Marine Laboratory for the Office of Naval Research under contract number NObsr-57146. It was also carried out in part at Woods Hole Oceanographic Institution under Bureau of Ships contract number NObsr-43270. The authors wish to express

their gratitude to all those members of both laboratories who have assisted in the work, and also to Mr. W. Shoemaker of Rochester Institute of Technology who helped greatly in obtaining the information on illumination.

A depth-distance recorder (Miller *et al.*, 1953) was used with all plankton hauls, and the counts of all species were corrected to a standard of one mile of towing. Generally, six or seven depths were sampled on each occasion. Owing to the strong currents in the area, it was not possible to hold the nets very close to a desired depth, but in general the water column was well sampled by a series of oblique hauls. The mid-depth of each haul was calculated, and from these, the depths half-way between each pair of hauls. It was assumed that each count was representative of the water column between two such half-way depths. The uppermost haul was assumed to extend to the surface, and the lowest, to the deepest recorded depth reached. For each species, and on each day, the total content of the water column was then integrated by cumulative multiplication of the counts and the lengths of the sections of water column to which they applied. A second integration was then performed from the top down, using the same figures, and the depths were noted at which 25, 50 and 75 percent of the above total were reached. In earlier work (Moore, 1949, 1953), the 50 percent depth so obtained was defined as the mean day level of the species, and the distance between the 25 and 75 percent levels as the spread. The mean day level, of course, varies widely in different species. In much of the present work it was convenient to eliminate the effects of such variation by expressing the values for each day as deviations from the annual mean for the species, the latter being the mean of all days for which data were available. In such cases, a positive value implies a depth greater than the mean, and a negative value, less than the mean. All depths are given in metres.

Only those species which occurred fairly consistently in adequate numbers, have been included. Not all these species were adequately represented on every day, so the numbers of pairs of figures available for comparison varies slightly throughout. The following species were included:

PTEROPODA

Limacina trochiformis (D'Orb.)
L. inflata (D'Orb.)
Creseis virgula Rang
C. acicula Rang
Diacria quadridentata (Lesueur)
Cavolinia longirostris (Lesueur)

SIPHONOPHORA

Chelophyes appendiculata (Esch.)
Diphyes bojani (Esch.)
D. dispar Chamisso & Eysenhardt
Eudoxoides mitra (Huxley)
E. spiralis (Bigelow)
Abylopsis eschscholtzii Huxley
A. tetragona Otto
Bassia bassensis (Quoy & Gaimard)

CHAETOGNATHA

Sagitta enflata Grassi
S. hexaptera D'Orb.
S. lyra Krohn
S. bipunctata Quoy & Gaimard
S. serratodentata Krohn
S. minima Grassi
S. decipiens Fowler
Pterosagitta draco (Krohn)
Krohnitta subtilis (Grassi)

COPEPODA

Neocalanus gracilis (Dana)
Undinula vulgaris (Dana)
Eucalanus attenuatus (Dana)
E. monachus Giesbr.
Rhincalanus cornutus (Dana)
Calocalanus pavo (Dana)
Euaetidius giesbrechti Cleve
Euchaeta marina (Prestand)
Scolethrix danae (Lubbock)
Temora stylifera (Dana)
T. turbinata (Dana)
Lucicutia flavicornis (Claus)
Haloptilus longicornis (Claus)
Candacia pachydactyla (Dana)
C. bispinosa (Claus)
Lubbockia squillimana (Claus)
Copilia mirabilis (Dana)
Acartia negligens (Dana)

At the station, approximately ten miles east of Miami, where this material was collected, the surface waters vary in origin. Water which has come through the Yucatan Channel is about 5°C. warmer than that from the Gulf of Mexico. None of the zooplankton species are restricted to one water mass only, although most show some relative variation in abundance in the two. The depth of the 15°C. isotherm was taken as a temperature standard. Its mean depth for the period was 151 meters, and its range, from 87 to 184 meters. The mean depth of the 50 percent level of the plankton, combining all species, was 93 meters. The selected isotherm is, therefore, deeper. However, the mean depth-temperature curve for the whole period was almost linear over the range of depths covered here, so the value of the standard temperature selected does not seriously affect the discussion.

Illumination was calculated by the method used in previous work (Moore, 1950), but making a small allowance for the effect of cloud.

The isolume selected was that with a value of 10^{-2}, which is approximately equivalent to one foot-candle. The mean depth of this for the period was 143 meters, and the range from 124 to 157 meters, which is considerably less than the temperature range. As with the 25, 50 and 75 percent levels of the plankton, the daily values for isotherm and isolume have, in most cases, been used as deviations from the mean for the period. Depths greater than the mean have a positive value, and lesser ones a negative value.

The Relation of Mean Day Level to Temperature and Illumination

Study of scattering layer records had indicated that, except in regions of slight temperature stratification, the mid-day level of the organisms concerned was likely to be under the almost complete control of temperature, with illumination exerting but little influence. An initial study of the Florida Current siphonophores showed a significant correlation between mean day level and the depth of the 15°C. isotherm. The regression of organism depth on isotherm depth was 95%. It should be noted that the latter figure differs from ones given later in the present paper since additional data have been incorporated in the present analysis. The coefficients of correlation between deviations from annual mean day levels and deviations of the depth of the 15°C. isotherm from its annual mean were worked out with the results shown in Table 1. The values are given for the four groups separately and for all species combined.

TABLE I

Coefficients of Correlation between Deviations of Mean Day Levels of the Species from their Annual Means and Deviations of the Depth of the 15°C. Isotherm from its Mean. Values with a Significance of P=>5% Are in Parentheses. P Is the Frequency with which the Observed Results Might Be Expected To Occur by Chance.

Pteropods	+.26
Siphonophores	+.33
Chaetognaths	+.24
Copepods	(+.04)
All species	+.18

Similar correlations between mean day level deviations and deviations in the depth of the 10^{-2} isolume showed no significant values, although the coefficient for the chaetognaths was sufficiently large to suggest the possibility of a relationship there. No significant change

was observed when the relationships to temperature and illumination were treated as partial correlations.

In the Bermuda work, no relationships were found between behaviour and temperature since there was so little day-to-day variation in the vertical temperature distribution. Night reaction to moonlight was rather closely correlated with the day level occupied by the species, but daytime reaction to cloudiness appeared to be a specific characteristic, not correlated with the depth of the species. It showed some correlation, however, with the extent of diurnal migration of the species, and the latter, in turn, was correlated with the depth of the day level of the species. In the Florida Current material, the closeness of correlation between day level deviations and isotherm deviations showed no relation to depth. On the other hand, it did appear to be a group characteristic. The pteropods did not give a significant value, probably because too few species were available for study. The coefficients were about the same, though, for pteropods, siphonophores, and chaetognaths. On the other hand, the copepods, with more data available than any other group, showed no correlation at all.

It is known that, in temperate waters, some chaetognaths and copepods change level seasonally (Russell, 1936). These level changes do not correspond with seasonal movements of either isotherms or isolumes, and appear to be specific characteristics of the successive broods, on which the adjustments of diurnal migration, and day-to-day level changes, are superimposed. It seemed possible that a correlation between day level and isotherm level might be masked in the Florida copepods by a similar seasonal rhythm. To test this possibility, partial correlations were calculated between deviations of day level and isotherm deviations, as well as between day level deviations and isolume deviations, but including a third variable, deviation from a given date. A series of six alternative dates was tested, namely the first of October, November, December, January, February and March. Of these, October 1 gave the highest partial correlation with change in day level, and was therefore used to recalculate the partial correlations of day level deviations with isotherm and isolume deviations. Allowing for the seasonal level change, these now became +.57 and +.40 respectively, both significant with a value of $P = < 1$ percent. To demonstrate the nature of the seasonal vertical rhythm of the copepods, the partial regression coefficients of level deviation on isotherm and isolume deviations were calculated. These were +105 percent and +81 percent respectively. Using these factors, the effects of the daily

differences in isotherm and isolume depths were allowed for, and Figure 1 shows what the seasonal changes in day level of an average copepod would have been had there been no changes in temperature or light. The pteropod data were inadequate for such treatment, but

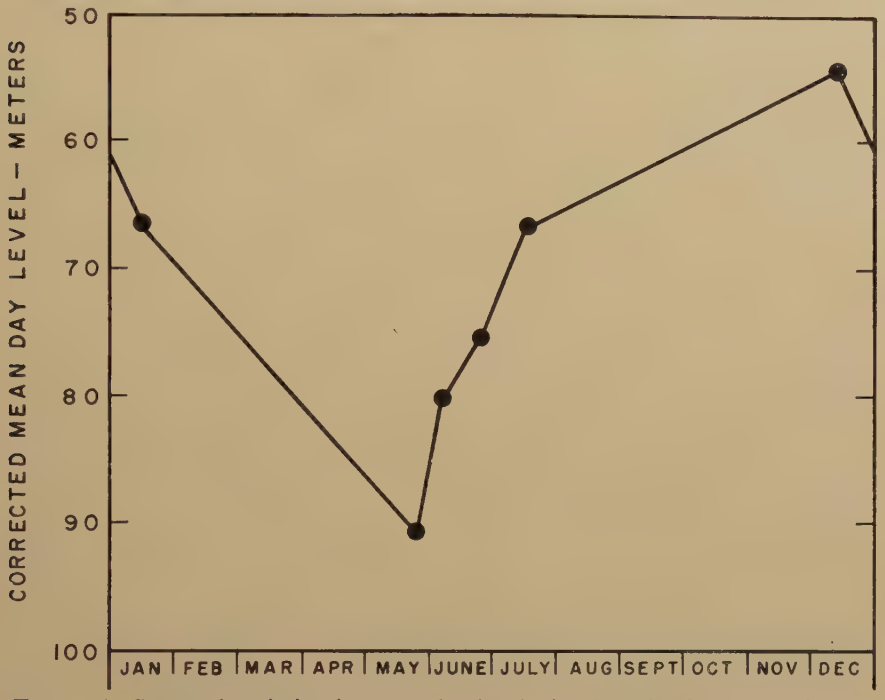

FIGURE 1. Seasonal variation in mean day level of copepods after correction for effects of variations in temperature and illumination.

neither siphonophores nor chaetognaths showed any significant seasonal level shift of this type. It remains possible, of course, that within these groups, individual species do show such a seasonal rhythm, but that these rhythms are not sufficiently similar in phase to appear as a group characteristic.

THE RELATION OF SPREAD TO TEMPERATURE AND ILLUMINATION

The vertical distribution pattern of a typical plankton species may be roughly represented by a kite, where the diameter of the figure at any depth corresponds to the concentration of the organisms there. In such a kite, the lower tail is characteristically longer than the upper part. A more accurate picture would probably be given if the sides

of the kite were skewed normal distribution curves. However, lacking adequate information as to the form of the curve, we have chosen the 25 and 75 percent levels as useful parameters for considering the outlying parts of the population. The distance between the two, or spread, has been used as an index of the diffuseness of the population.

The Bermuda data showed that, for all species combined, there was a significant increase in spread in the deeper-living species. This held true in the Florida material also, the correlation coefficient between spread and mean day level being +.44 ($P=<1\%$). The separate groups all showed positive correlations, but only that for the copepods was significant ($r=+.55$; $P=<1\%$).

In one group or another it has been shown that the degree to which the mean day level is correlated with temperature and illumination is itself dependent on the depth characteristically occupied by the species in question. It is probable, then, that a similar difference in reaction to these two factors exists at different levels in a population of a given species. Reactions at the 25 percent level may differ from those at the 75 percent level. If this is so, then variations in spread may be more simply explained in terms of reactions at the two limits which define it. Partial correlation coefficients were therefore calculated for each level with isotherm and isolume deviations. Significant values were obtained in most groups at one level or the other. Since we are concerned with the reaction of the plankton to movements of the isotherms and isolumes, it is clearer if the results are shown as regression coefficients. This is done in Table II, where the figures indicate the percentage response of the plankton to a given shift of an isotherm or isolume. For completeness, the responses of the 50 percent level also have been included. Since responses of the 50 percent level of copepods had been

TABLE II

COEFFICIENTS OF REGRESSION OF THE DEVIATIONS OF THE 25, 50 AND 75% LEVELS ON DEVIATIONS OF THE 15°C. ISOTHERM (ABOVE) AND OF THE 10^{-2} ISOLUME (BELOW). VALUES IN PARENTHESES ARE SIGNIFICANT WITH A VALUE OF $P>5\%$.

	Pteropods	Siphonophores	Chaetognaths	Copepods	All Species
25%	(+20%)	+32%	+ 36%	+ 62%	+ 22%
50%	+66%	+61%	+ 39%	+105%	+ 31%
75%	+71%	+76%	+ 41%	+151%	+ 42%
25%	— 7%	(+67%)	+116%	+ 75%	+137%
50%	(+10%)	(+21%)	(+ 84%)	+ 81%	+ 31%
75%	(+29%)	(+26%)	(— 52%)	(+ 22%)	+ 43%

found to be largely masked by the seasonal rhythm present, allowance has been made for this in calculating the partial regression coefficients in that group. Since, however, this seasonal effect has not been found in the other groups, the seasonal effect on copepods has not been allowed for in calculating the values for all species combined, and the values in this column are, therefore, probably somewhat lower than they should be. If the regression coefficients are considered as an index of the response of the plankton to changes in level of isotherms and isolumes, it is clear that there is a general tendency for the upper levels of the plankton to be more under the control of light and the the lower levels more under the control of temperature. This is not to be interpreted as a difference in response between shallow and deep species, since the effects of the differing characteristic levels occupied by the various species have been eliminated. The response differences exist between the upper and lower parts of the populations of a single species.

It appears that, if light penetrates deeper, the upper levels of the plankton move deeper also, but the lower levels show little response. On the other hand if the isotherms move upwards, the lower plankton levels move upwards, and there is little response in the upper plankton levels. The spread of the plankton is therefore related to the relative positions of isotherms and isolumes. To test this, the distance between the selected 15°C. isotherm and 10^{-2} isolume was calculated for each occasion. The deviations of this from its mean value for the period were then compared with the spread deviations with the results shown in Table III.

TABLE III

Coefficients of Correlation (above) and of Regression (below) between Deviations of the Distance between the 15°C. Isotherm and the 10^{-2} Isolume and Deviations of Spread. The Pteropod Data were Inadequate for Inclusion. All Figures Are Significant with a Value of $P=<1\%$.

	Siphonophores	Chaetognaths	Copepods	All Species
r	+.66	+.63	+.40	+.48
b	+95%	+89%	+51%	+62%

As would be expected, the copepods agree well with the other groups in this case, since their seasonal rhythm affects all levels together and not spread. With more data available, some seasonal rhythm might well be looked for in spread in all groups, since, in most areas, there is some seasonal change in the depths of both isotherms and isolumes. The present locality is unusual in that such

effects are likely to be masked by much greater changes due to water mass variation.

It was found, in Bermuda, that the spread of the plankton as a whole increased with depth. After elimination of the effects of isotherm and isolume movements, such relation was found also in the Florida material as shown in Table IV. Only the values for chaetognaths were not significant.

TABLE IV

PARTIAL CORRELATION COEFFICIENTS BETWEEN SPREAD AND THE 50% LEVEL OF THE SPECIES, OMITTING THE EFFECTS OF CHANGES IN ISOTHERM AND ISOLUME DEPTHS. THE VALUES FOR CHAETOGNATHS ARE NOT SIGNIFICANT, BUT THE REST ARE SIGNIFICANT WITH A VALUE OF P=<1%. PTEROPOD DATA WERE INADEQUATE FOR INCLUSION.

	Siphonophores	Chaetognaths	Copepods	All Species
r	+.53	+.19	+.29	+.32

The regression coefficients were only small: —23 percent for all species combined.

A residual increase in spread with depth has been found. Spread is itself a resultant of differential movements of the upper and lower parts of the population. These upper and lower parts differ in the relative strength of their reactions to light and temperature. Some correlation may therefore be looked for between the strengths of these reactions of the upper and lower levels and the depths characteristically occupied by the species in question. For each species, the coefficient of regression of deviation of the 25 percent level on deviations of the 10^{-2} isolume were determined. The coefficient of correlation between these regression coefficients and the mean 25 percent level of the species was then calculated. It was significant only in the case of the siphonophores, with a value of —.72 (P=<5%). Where the correlation was made with the 50 percent level of the species, the chaetognaths showed a significant value of —.73 (P=2%). The direction of the correlation is as might be expected. The upper levels of a deep-living species tend to be less responsive to light changes than those of a shallow species.

A similar comparison was made between response to temperature at the 75 percent level and the 75 percent level of the species. Using regression coefficients, as above, no significant values were obtained. Using, instead, the coefficients of correlation between 75 percent level deviations and isotherm deviations, a value of +.74 (P=2%) was obtained in the case of the chaetognaths. There is, therefore, some

indication that the lower levels of the population are more closely controlled by temperature in deep-living species than in shallower ones.

Discussion

The present study has been limited to conditions in the middle of the day when it is assumed that an equilibrium has been established after the morning descent. Scattering layer records indicate that such an equilibrium is rapidly established, and that, in fact, the organisms responsible for the phenomenon can migrate vertically faster than is needed to keep pace with the changing illumination. This is probably true also of even such small organisms as copepods, for which very rapid ascents and descents have been recorded. The basic data used were the levels occupied on different occasions by selected fractions of the plankton and by a selected isotherm and isolume. The three values being compared are, therefore, all depths. Within the range of depths under consideration, the rate of change with depth of both illumination and temperature is approximately linear. Changes in depth of isotherms and isolumes may therefore be considered as indices of the strength of temperature and illumination stimuli, and as having an approximately linear relation to them. It seems reasonable, then, to consider movement of the plankton in relation to movement of an isotherm or isolume as equivalent to a measure of response to a given temperature or light stimulus. Then a value of +100 percent, obtained as the regression coefficient of plankton movement on isotherm movement, indicates a response of the plankton exactly sufficient to maintain it under conditions of constant temperature.

In general, when some ecological condition of an organism is shown to be under the simultaneous control of two factors, and can be expressed as functions of each, then the condition resulting from the simultaneous variation of both factors is best expressed as the product of the two factors. In the present case it has been assumed that the deviation of the plankton level from its mean position may be considered as the sum of the movements which would have resulted had temperature or light operated alone. Whether or not this is strictly true is open to question, and will probably not be settled until more data are available. The assumption has, however, been made since it greatly simplifies the partial regression analysis. It can, however, be shown that the assumption that the reaction of the plankton is a function of the product of the temperature and illumination changes

results in values, the sum of the squares of whose errors is about four times that obtained assuming that the effects of the two factors are additive.

It is found that the mean day level of the various species studied followed the isotherm changes, but was influenced little, if at all, by light changes. This is in agreement with what is most usually found in the scattering layer in the North Atlantic. In the Mediterranean, where there is only very slight temperature stratification, this does not hold for the scattering layer. In Bermuda, where the temperature at the level concerned varied very little throughout the year, a correlation was found between the mean day level of the zooplankton as a whole and the cloudiness of the sky, but no more exact information on the vertical distribution of illumination is available.

Comparison of the responses of the plankton at its 25, 50 and 75 percent levels showed a transition from dominant light control at the top to dominate temperature control below. Three possible conditions are suggested which might produce such results. The responses of all the individuals in the population might be similar, and the observed vertical distribution might reflect either random "diffusion" around a center of distribution, or random movement more or less modified by the light and temperature conditions encountered away from this center. This is inherently unlikely since individual variation in reactions would be expected to occur in a population. The second alternative is that the observed vertical variation in relative reaction to light and temperature directly reflects the distribution within the population of individual reactions to these two factors. The distribution curves tentatively arrived at so far cast doubt of the likelihood of this. The third alternative combines the second with a modification of individual reaction by some third factor such as pressure. Further discussion of these alternatives must await considerable further analysis and probably calls for the examination of night levels also, and of the levels occupied during the morning descent and evening ascent.

When allowance was made for the effects of temperature and illumination on the 25 and 75 percent levels of the plankton, and through them on the spread, there still remained some residual tendency for the spread to be greater in deep-living than in shallower-living species. This agreed with observations in Bermuda. Furthermore, there was some slight indication that the upper (25 percent) levels are more responsive to light in shallow-living than in deep-living species, and conversely that the deeper-living species are the more responsive to

temperature at their lower levels. These two effects were, however, not universal.

Finally, in the case of the copepods, there was a residual seasonal change in level after variations due to temperature and illumination had been allowed for, and it was suggested that this resulted from different levels being characteristically occupied by successive broods, over and above any responses to temperature and light conditions. Such a seasonal vertical range has previously been demonstrated in a few plankton species.

REFERENCES

Jones, E. C.
1952. A preliminary survey of the copepods of the Florida Current. Master's Thesis, The Marine Laboratory, University of Miami.

Miller, S. M., H. B. Moore and K. R. Kvammen
1953. Plankton of the Florida Current. I. General conditions. Bull. Mar. Sci. Gulf and Caribbean, *2*(3):465-485.

Moore, H. B.
1949. The zooplankton of the upper waters of the Bermuda area of the North Atlantic. Bull. Bingham oceanogr. Coll., *12*(2):1-97.
1952. Physical factors affecting the distribution of euphausids in the North Atlantic. Bull. Mar. Sci. Gulf and Caribbean, *1*(4):278-305.
1953. Plankton of the Florida Current. II. Siphonophora. Bull. Mar. Sci. Gulf and Caribbean, *2*(4):559-573.

Russell, F. S.
1936. A review of some aspects of zooplankton research. Rapp. Cons. Explor. Mer., *95*(1):3-30.

Contribution No. 673

(*Reprinted from Nature, Vol.* 172, *p.* 1144, *December* 19, 1953)

Giant Condensation Nuclei from Bursting Bubbles*

Among cloud physics workers there is increasing recognition that the larger of the salt nuclei that are found in the air may initiate rain by coalescence in clouds. Hence mechanisms which produce these nuclei at ocean surfaces are of special interest. Köhler[1] has suggested that they result from spray formed by the action of strong winds on wave crests. More recently, Aliverti and Lovera[2] have related the production of minute salt particles to the presence of bursting bubbles at the sea surface, and Facy[3] has suggested that the particles result from the shattering of the thin water-films present in clusters of bubbles.

At the Woods Hole Oceanographic Institution, high-speed motion pictures (more than 3,000 frames $sec.^{-1}$) of small bubbles bursting at the water surface have revealed one of the processes which bring about the formation of the larger salt nuclei. Fig. 1 illustrates some of the stages in the collapse of small bubbles and the production of jets, and Fig. 2 shows a jet producing droplets. Smaller bubbles are observed to form jets more rapidly and to eject much smaller droplets into the air. The bubble cavities and jets observed are similar in form to some of Worthington's 'splashes'[4], and confirm Stuhlman's[5] assumption that jets are formed by small bubbles bursting at the surface of distilled water.

Each bubble ejects about five droplets, the heights of projection ranging from about 0·5 to 15 cm. Photographic studies have been made of bubbles ranging in size from 0·2 to 0·02 cm. diameter, though smaller bubbles are also observed to form jets and droplets. When bubbles burst in sea water, evaporation of the water from the droplets formed by the jets is observed to leave a salt residue which in many cases is similar in weight to salt nuclei found in the atmosphere. It is inferred that many of the larger sea-salt nuclei found in the atmosphere[6] originate in this manner from bubbles naturally formed in surface waters of the seas.

More complete information about this photographic study of bursting bubbles is to be published in the near future.

* Contribution No. 673 from the Woods Hole Oceanographic Institution.

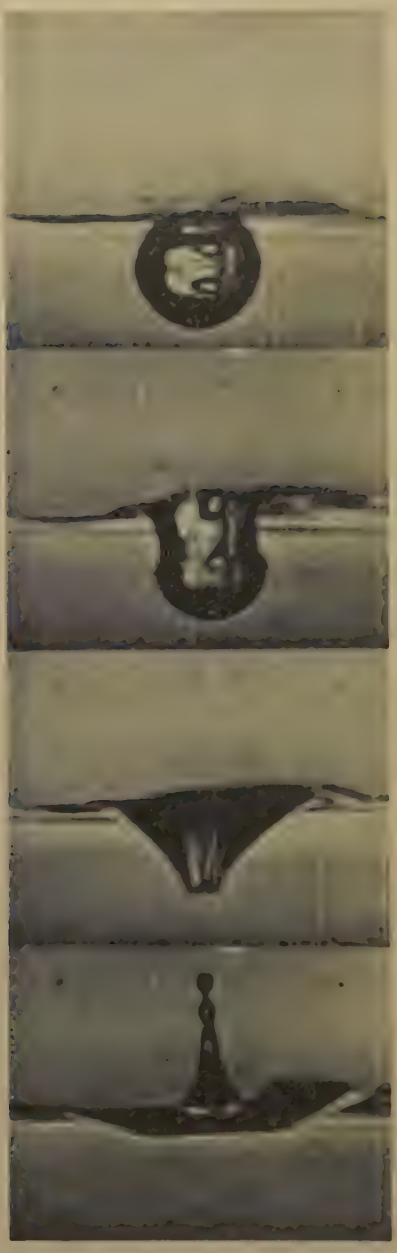

Fig. 1. Composite photograph of high-speed motion pictures illustrating some of the stages in the collapse of small bubbles and the formation of jets. Time interval between top and bottom frames about 2·3 milliseconds. Bubble diameter, 1·7 mm.; angle of view horizontal through glass wall. (Surface irregularities due to meniscus.)

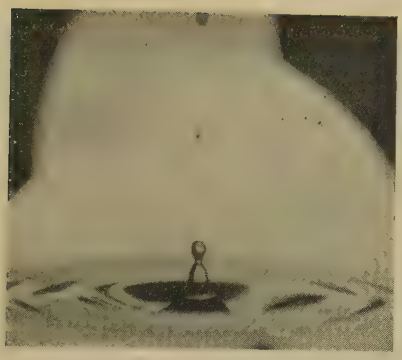

Fig. 2. Oblique view of jet from 1·0 mm. diameter bubble. Diameter of smallest droplet shown, 0·09 mm. Exposure time, 30 μsec.

This study was supported by the Office of Naval Research, under contract number Nonr–798(00) (NR–082–124).

A. H. Woodcock
C. F. Kientzler
A. B. Arons
D. C. Blanchard
Woods Hole Oceanographic Institution,
Woods Hole, Mass.

Oct. 14.

[1] Köhler, H., *Nova Acta Reg. Soc. Sci. Upsaliensis*, (4), **12**, No. 6 (1941).
[2] Aliverti, G., and Lovera, G., *Atti. R. Accd. Sci., Torino*, **74**, 573 (1939).
[3] Facy, L., *J. Sci. de la Met.*, **3**, (11), 86 (1951).
[4] Worthington, A. M., and Cole, R. S., *Phil. Trans. Roy. Soc.*, A, **189**, 137 (1897).
[5] Stuhlman, jun., Otto, *Physics* (*J. App. Phys.*), **2**, (6), 457 (1932).
[6] Woodcock, A. H., *J. Met.*, **10**, No. 5 (1953).

Printed in Great Britain by Fisher, Knight & Co., Ltd., St. Albans.

Contribution No. 677

Reprinted from
BULLETIN OF MARINE SCIENCE
OF THE GULF AND CARIBBEAN
Vol. 3, No. 3, pp. 157-167
DECEMBER, 1953

SEASONAL CHANGES IN THE SURFACE WATER MASSES AND IN THEIR PLANKTON IN THE BERMUDA AREA

ILMO HELA, HILARY B. MOORE AND HARDING OWRE
Marine Laboratory, University of Miami, and
Woods Hole Oceanographic Institution[1]

ABSTRACT

Bermuda plankton studies showed seasonal differences in the fauna which suggested different origins of the water in summer and winter. Studies of the geographical distribution of typical summer and winter species confirmed this, showing widely different centers of distribution for the two seasonal groups. Previous studies of currents and of the distributions of temperature and transparency suggested an eddy of the Gulf Stream, reaching Bermuda from the east or southeast. The present current studies confirm the indications of the plankton distribution in showing that Bermuda summer water comes from the North Equatorial Current, while the winter water comes from an eddy of the Gulf Stream approximately along the 30° parallel.

In an earlier study of the zooplankton of the Bermuda area (Moore, 1949), it was shown that the plankton was distinctly different in summer and winter. There was a sharp transition in October, and a second, less well defined, in late winter or spring. The change was apparent in the species comprising the zooplankton, in the number of species present, and in the total volume of plankton per standard haul at a single station. These changes are shown in Figure 1. The volume changes at a single station were shown to be due to a shift in the position of a plankton-rich area which lay to the east of the islands in summer and to the west in winter. This shift strongly suggested a change in the circulation system around the island, which was borne out by the nature of the summer and winter faunas.

[1]Contribution No. 677 from the Woods Hole Oceanographic Institution.
Contribution No. 206 from the Bermuda Biological Station.
Contribution No. 113 from the Marine Laboratory, University of Miami.

It was hoped that some of the typically summer and winter zooplankton species might be used as indicators of the origin of their respective water masses, and with this in view, a study of the Atlantic

FIGURE 1. Seasonal variation in number of species present and in size of catch at a standard station off Bermuda.

distribution of a series of selected forms was commenced in 1947. The study was begun at the Woods Hole Oceanographic Institution and later continued at the Marine Laboratory of the University of Miami. At the latter, Hela undertook a study of the seasonal surface drift of the Bermuda area, which was part of a more general survey of the North Atlantic (Hela, 1954).

ZOOPLANKTON STUDIES

The following species, all of which showed marked seasonal fluctuation in numbers at Bermuda, were selected as possible indicator forms:

SUMMER SPECIES	WINTER SPECIES
SIPHONOPHORA	
Diphyes dispar Chamisso & Eysenhardt	*Diphyes bojani* (Eschscholtz)
	Eudoxoides spiralis (Bigelow)
	Abylopsis eschscholtzii Huxley
	A. tetragona Otto
	Bassia bassensis (Quoy & Gaimard)

CHAETOGNATHA

Sagitta bipunctata Quoy & Gaimard
S. hexaptera D'Orbigny
S. lyra Krohn
Sagitta planktonis Steinhaus
Pterosagitta draco (Krohn)
Krohnitta subtilis (Grassi)

The groups chosen were limited to those with widespread records from the North Atlantic. Unfortunately these did not include the Pteropoda, which otherwise would have been ideal. Also a considerable series of hauls, referred to below and examined by us, had not been properly preserved. Their examination was delayed by World

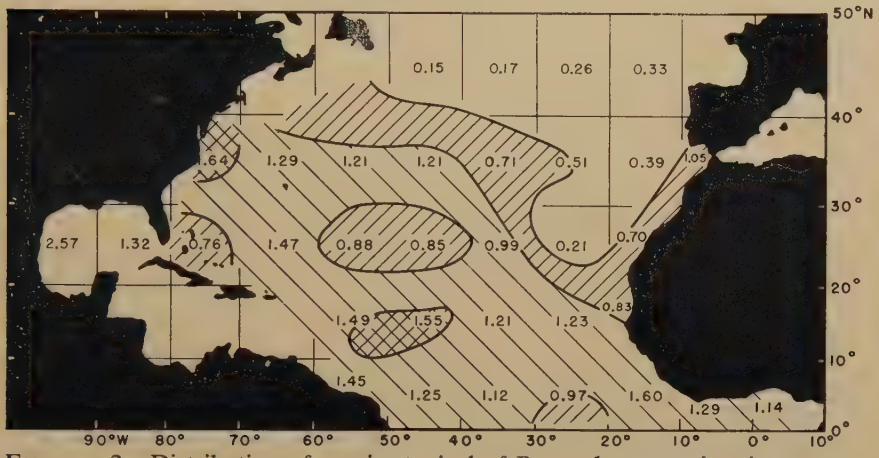

FIGURE 2. Distribution of species typical of Bermuda waters in winter.

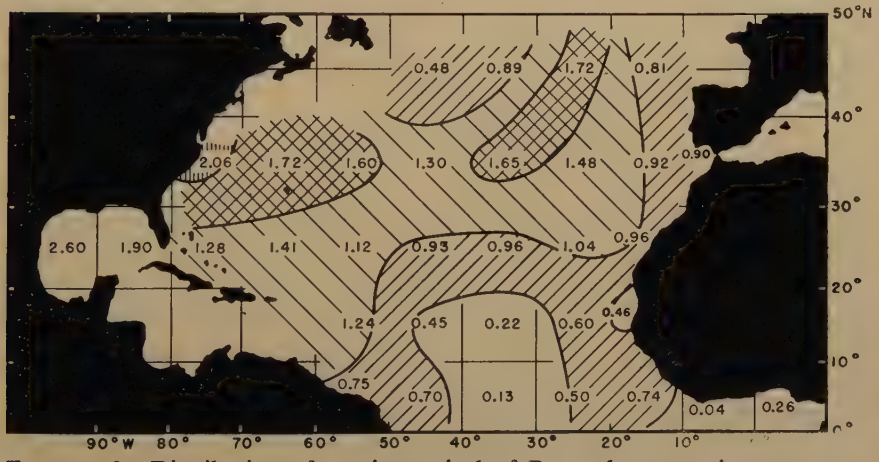

FIGURE 3. Distribution of species typical of Bermuda waters in summer.

War II, and after a lapse of several years they had become decalcified and many of the pteropods were no longer identifiable. However, the larger pteropods did provide verification for the belief that the seasonal changes mentioned above recurred in successive years. In material collected by Dr. M. V. Lebour in the summer of 1947, they were very scarce, as they had been in the summers previously studied. These appear to be typically winter forms in Bermuda.

Abstracts were made from the published records of all expeditions which have worked in the North Atlantic[2]. They were grouped by 10° squares, and presence or absence of each of the selected species was noted. The percentage occurrence of each species was then calculated for each square. Allowance was made for the varying relative total abundance of the different species by weighing each value in proportion to the total number of records of the species for the whole area. Finally, for each 10° square, a mean value was obtained for the combined winter forms, and for the combined summer forms. Figures 2 and 3 show these values, expressed in arbitrary units, and it is clear that those species which are common in Bermuda waters in winter have characteristically different distributions from those common in summer.

These two charts indicate the centers of abundance of the Bermuda summer and winter forms. However, at these centers, the species in question may occur more abundantly than they do in the Bermuda area at the appropriate season. An attempt was therefore made to locate the areas where the frequency of occurrence most closely approximated that found around Bermuda. It would have been desirable to separate the published data into two groups according to whether the hauls were made in summer or winter, omitting those made in the transition periods, but this would have reduced the available data unduly. The best that could be done was to determine those areas in which mean annual conditions most closely approximated those found in the Bermuda area in summer and winter respectively. For the Bermuda area, sufficient seasonal data were already available. The results (Figure 4) show that Bermuda winter conditions are most closely matched by a band of water lying well to the south of the islands, and extending from the West Indies across to the African coast at approximately 20° north latitude. Summer conditions are most closely matched by a band of water lying roughly along the course of

[2]Bedot, 1904; Bigelow, 1918; Burfield, 1930; Chun, 1897; Fowler, 1906; Germain and Joubin, 1916; Haeckel, 1888; Leloup, 1933; Leloup and Hentschel, 1935; Moser, 1925; Ritter-Zahony, 1911, 1911a; Thiel, 1938; Totton, 1936.

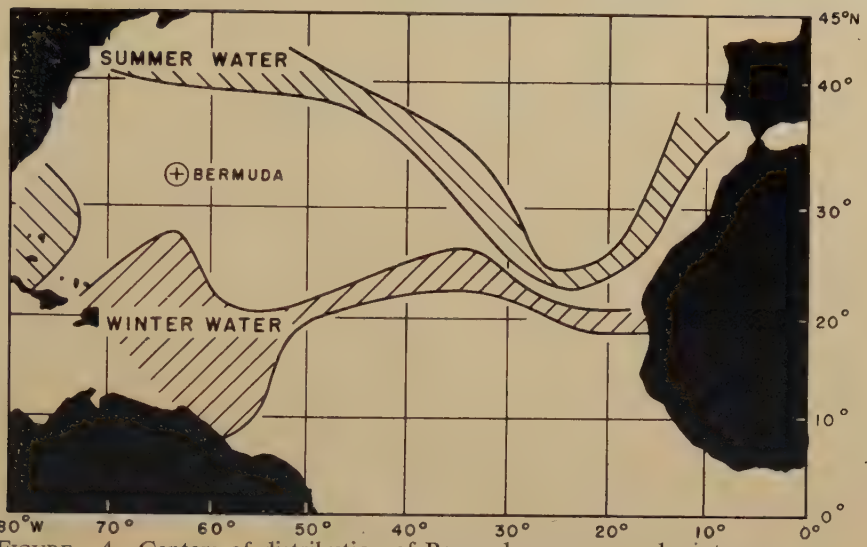

FIGURE 4. Centers of distribution of Bermuda summer and winter species.

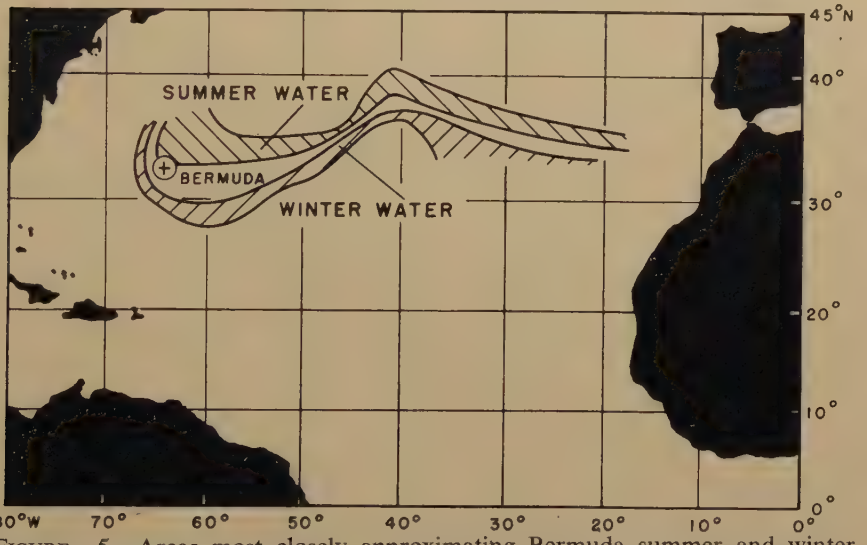

FIGURE 5. Areas most closely approximating Bermuda summer and winter conditions.

the Gulf Stream from Florida to the northeast of Bermuda, and swinging southward to the east.

Most of the expedition reports give records of presence or absence,

but do not include counts of the relative abundance of the different species. The latter give a far more reliable picture of distribution, but are available for only a limited series of stations. In order to extend these data, the *Atlantis* has collected plankton samples, usually night surface hauls, on a number of cruises extending widely over the North Atlantic. The siphonophores and chaetognaths have been counted in all of these hauls. For each selected siphonophore species, a value was calculated expressing its numerical abundance as a percentage of the total summer siphonophore population in the Bermuda area. A winter value was obtained in the same way. Similarly, the chaetognaths were expressed as percentages of the total chaetognath population. Finally, weighted values which expressed the typical ratio of total summer to total winter forms in the area in each season were obtained. The ratio of Bermuda summer species to winter species was calculated in the same way for those parts of the North Atlantic where these species occurred and a chart of the distribution of this ratio was prepared. From this, the areas in which the annual mean values most closely approximate Bermuda summer and winter conditions, respectively, were determined and are shown in Figure 5. There is some resemblance between these and the areas indicated from other data in Figure 4, but in this case the two areas lie considerably closer together.

Both methods indicated that the water masses whose plankton most closely corresponded with Bermuda summer and winter conditions lie respectively further north and further south. The fact that mean annual plankton, rather than appropriate seasonal plankton, was compared, has masked any possible seasonal change within these areas, but their separation is still marked. However, both areas extend for a considerable distance, more or less along the line of flow of the Gulf Stream. It has not, therefore, been possible to associate any very circumscribed area with the Bermuda plankton. Such information must be sought in a study of the current system.

Current Systems

Bermuda lies well to the east of the Gulf Stream system and within the Sargasso Sea, but there are some indications that it may, at least on occasions, be influenced by an eddy of the main stream. Iselin (1936) has indicated the existence of such an eddy in a generalized way (Figure 6). Fuglister (personal communication) has prepared charts showing the distribution of temperature (Figure 7) and salinity

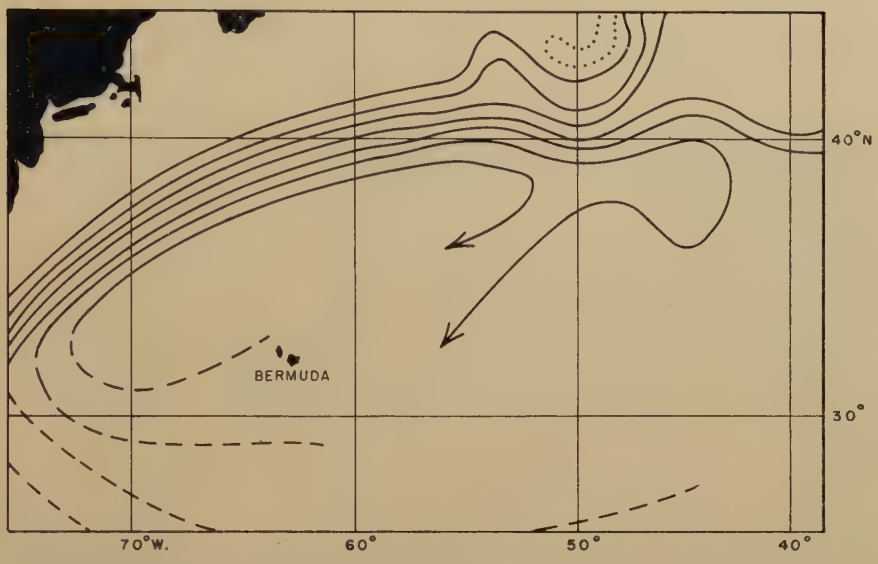

FIGURE 6. Portion of the Gulf Stream System, according to Iselin (1936).

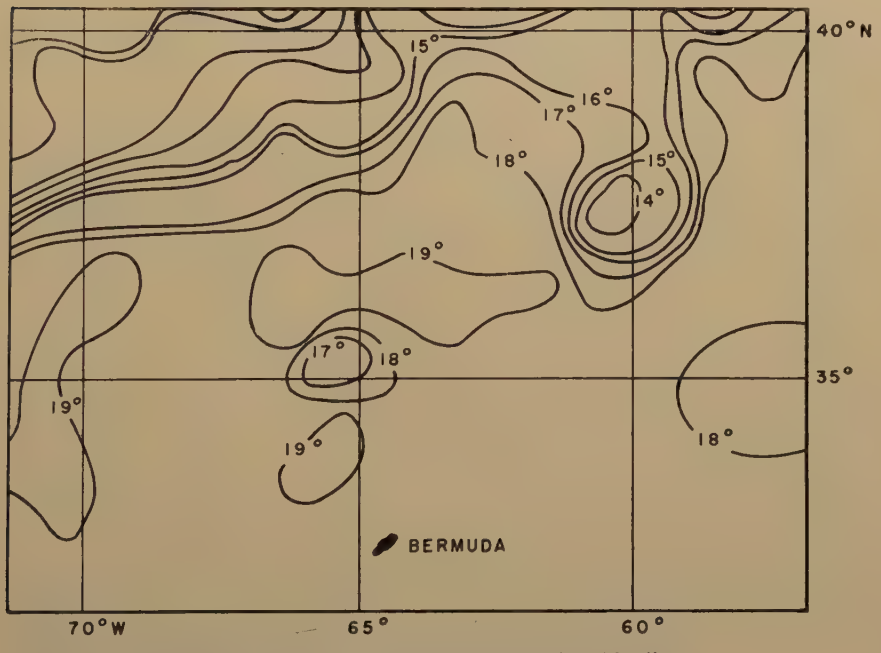

FIGURE 7. Temperature (°C.) at 200 meters, after Fuglister.

at a depth of 200 meters in the North Atlantic, and finally Moore (1952) has published a chart of water transparency in the area (Figure 8). Both of these suggest the presence of such an eddy in the

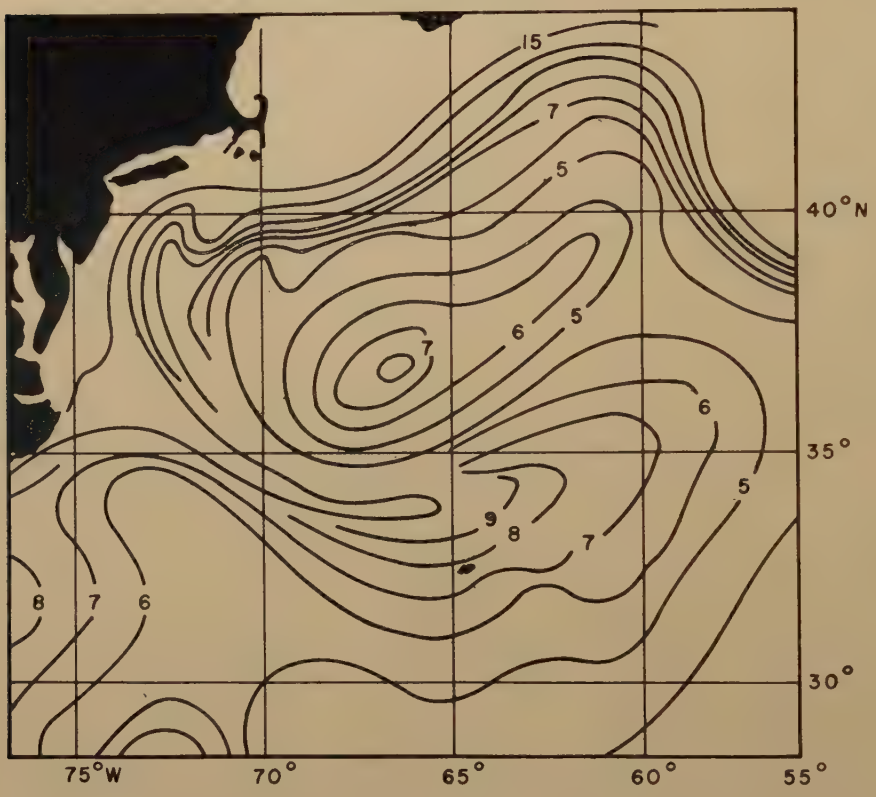

FIGURE 8. Extinction coefficients (× 100), according to Moore (1952).

neighborhood of Bermuda. One may assume that a comparatively slight seasonal shift might well bring summer and winter plankton populations from widely separated areas into the vicinity of Bermuda.

Hela (1954) has computed the resulting surface currents of every degree square and for the different seasons separately by means of the monthly current charts published by the U. S. Navy Hydrographic Office (H. O. Publ. 571, sheets 1 through 12). The winter and summer current conditions are given schematically in Figures 9 and 10. In the winter chart (Figure 9), the eddy pointed out by Iselin (Figure 6) can be seen distinctly. The shaded area has been copied from

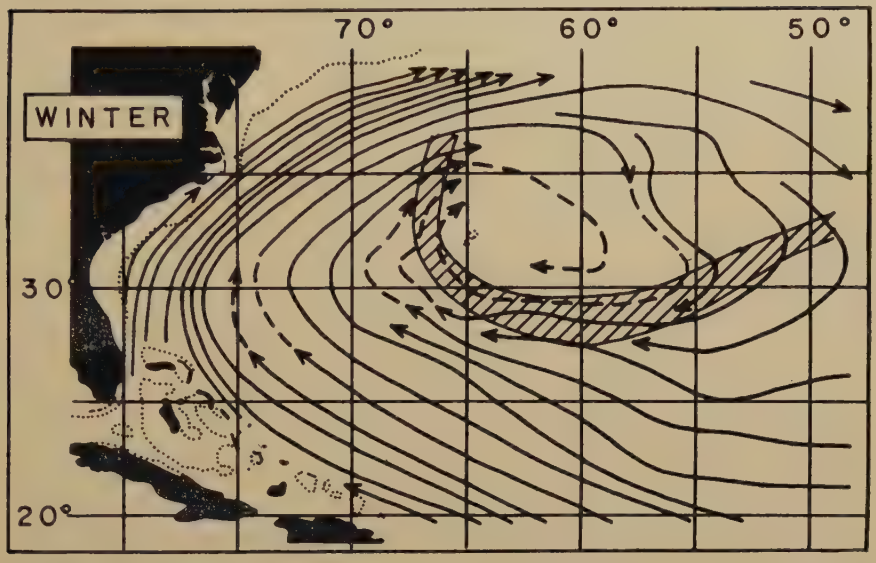

FIGURE 9. Winter current conditions with the "winter water" area (shaded) from Figure 5 included.

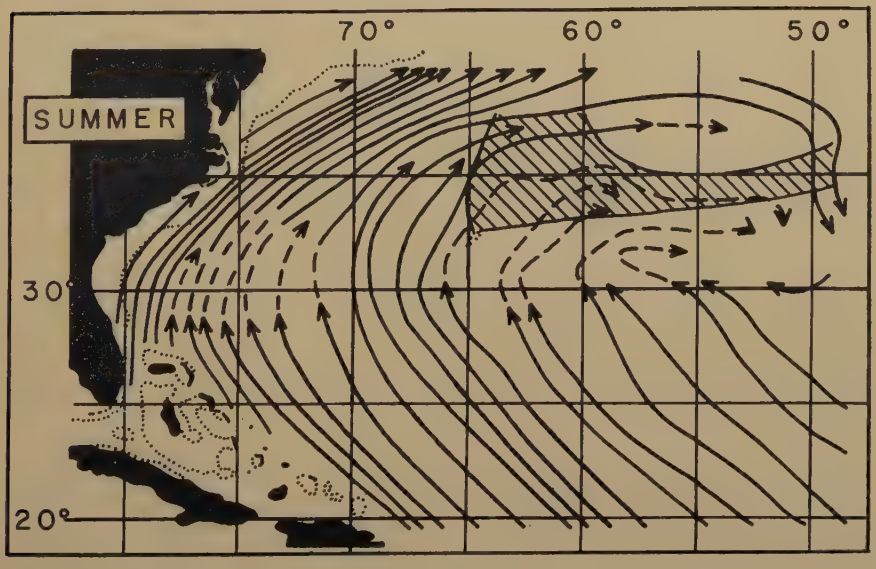

FIGURE 10. Summer current conditions with the "summer water" area (shaded) from Figure 5 included.

Figure 5 and corresponds to the "winter water" area south and west of Bermuda. In the summer chart (Figure 10), no indication whatsoever can be seen of the above eddy. In this case the shaded area has similarly been copied from Figure 5 and corresponds to the "summer water" area north and northeast of Bermuda.

The difference in the current system between winter and summer can be simply interpreted as follows. In winter the waters reaching Bermuda seem to come from the southeast and east roughly along the 30° north latitude parallel. These waters build the eastern and southern sections of an eddy of the Gulf Stream south of it, as indicated in Figure 9. Thus the "winter water" which is to be found south and southeast of Bermuda during the winter is nothing else but the south and westbound eddy of the Gulf Stream.

In summer the waters reaching Bermuda seem to come, directly from the south and southeast, from the North Equatorial Current. The mean direction of the surface currents (usually called Antilles Current) in the area seems to be roughly 300° in winter and 330° in summer. There are some indications, too, that in summer, in addition to the regular Antilles Current, another current branch exists with an approximate path from 20°N. and 60°W. to 30°N. and 67°W. Thus the "summer water" which is to be found west and southwest of Bermuda during the summer is just water coming directly from the North Equatorial Current.

The evidence from the geographical distribution of the plankton indicates the passage of waters of different origins around Bermuda in winter and summer. The above interpretation of the surface current systems is consistent with the indications from the plankton. The water, and its fauna, which passes Bermuda in winter has a more southerly origin than that which passes there in summer.

REFERENCES

Bedot, M.
1904. Siphonophores provenant des campagnes du yacht *Princesse-Alice* (1892-1902). Résult. Camp. sci. Monaco, *27*: 1-27.

Bigelow, H. B.
1918. Some Medusae and Siphonophorae from the Western Atlantic. Bull. Mus. comp. Zool. Harv., *62*(8):365-442.

Burfield, S. T.
1930. Chaetognatha. Brit. Antarct. Terra Nova Exped., Nat. Hist. Rept., Zool., *7*(4):203-228.

Chun, Carl
1897. Die Siphonophoren der Plankton-Expedition. Ergebn. Atlant. Planktonexped., *2*(K.b.):1-126.

FOWLER, G. H.
1906. The Chaetognatha of the Siboga expedition. Siboga Exped., *21*:1-86.

GERMAIN, LOUIS AND LOUIS JOUBIN
1916. Chétognathes provenant des campagnes des yachts *Hirondelle* et *Princesse-Alice* (1885-1910). Résult. Camp. sci. Monaco, *49*:1-118.

HAECKEL, ERNEST
1888. Report on the Siphonophorae collected by H.M.S. *Challenger* during the years 1873-1876. Rep. sci. Res. *Challenger*, Zool. *28*:1-380.

HELA, ILMO
1954. The surface current field in the western part of the North Atlantic. Bull. Mar. Sci. Gulf and Caribbean, in press.

ISELIN, C. O'D.
1936. A study of the circulation of the western North Atlantic. Pap. phys. Oceanogr., *4*(4):1-101.

LELOUP, EUGÈNE
1933. Siphonophores calycophorides provenant des campagnes du Prince Albert Ier de Monaco. Résult. Camp. sci. Monaco, *87*:1-64.

LELOUP, EUGÈNE AND ERNST HENTSCHEL
1935. Die Verbreitung der calycophoren Siphonophoren im Südatlantischen Ozean. Wiss. Ergebn. dtsch. atlant. Exped. 'Meteor', *12*(2):1-31.

MOORE, HILARY B.
1949. The zooplankton of the upper waters of the Bermuda area of the North Atlantic. Bull. Bingham oceanogr. Coll., *12*(2):1-97.
1952. Physical factors affecting the distribution of Euphausids in the North Atlantic. Bull. Mar. Sci. Gulf and Caribbean, *1*(4):278-305.

MOSER, F.
1925. Die Siphonophoren der Deutschen Südpolar-Expedition, 1901-1903. Dtsch. SüdpolExped., *17*(Zool. 9):1-541.

RITTER-ZAHONY, RUDOLF VON
1911. Die Chätognathen der Plankton-Expedition. Ergebn. Atlant. Planktonexped., *2*:1-33.
1911a. Revision der Chätognathen. Dtsch. SüdpolExped., *13* (Zool. 5):1-71.

THIEL, M. E.
1938. Die Chätognathen-Bevölkerung des Südatlantischen Ozeans. Wiss. Ergebn. dtsch. atlant. Exped. 'Meteor', *13*(1): 1-110.

TOTTON, A. K.
1936. Plankton of the Bermuda oceanographic expeditions. VII. Siphonophora taken during the year 1931. Zoologica, N. Y., *21*(4):231-240.

Contribution No. 686

AN EXPERIMENT TO DETERMINE THE HYDRODYNAMIC FORCES ON A CABLE INCLINED TO THE DIRECTION OF FLOW

By

E. E. WATSON

Queen's University, Kingston, Ontario;
Woods Hole Oceanographic Institution[1]

ABSTRACT

The hydrodynamic force on a cable inclined to the direction of flow, though derived previously, is not widely known. A simple experiment is described which verifies the magnitude and direction of this force, showing that it is normal to the cable, not parallel to the flow.

In oceanographic research, when instruments are lowered from a ship by cable or wire, it is easy to observe the length of wire paid out and the wire angle at the surface. But unless the true depth of the instrument is measured directly by means of some pressure-sensitive device in the instrument itself, then it becomes necessary to estimate the depth of the instrument on the basis of observations which can be easily obtained. Some knowledge of the vertical distribution of current relative to ship will be required, and the forces acting on each element of the cable must be known in order to determine by integration the shape of the whole cable.

Experiments performed at the David Taylor Model Basin of the U. S. Navy, and probably elsewhere, have determined both the nature and the approximate magnitude of these forces, but unfortunately these results are not widely known, as is indicated in Mossby's (1952)[2]

[1] Contribution No. 686 from the Woods Hole Oceanographic Institution.

[2] Mossby, H. 1952. Wire-angle in oceanography. Årb. Bergens Mus., Naturv. Rekke, Nr. 2.

Reprint from SEARS FOUND. JOURN. MAR. RES.

recent paper which is based on incorrect equations for the forces acting on an inclined wire. He states that the frictional forces between the water and a wire towed lengthwise are neglected, which is equivalent to saying that the resistance is perpendicular to the wire at every point. Therefore the resistance will have both vertical and horizontal components except when the wire is vertical. Yet the equations given contain no vertical component of the resistance. Since the wire-angle corrections to depth are derived from these equations, their accuracy must be questioned. The errors may be negligible at small wire angles, but they will become increasingly important as the wire angle increases.

The purpose of this paper is to (1) derive the hydrodynamic force acting on an inclined element of wire in a stream from the force on a wire perpendicular to the stream and (2) present an experiment which demonstrates the validity of the assumptions and of the results obtained. The experiment requires no elaborate apparatus.

Theory. A long cylindrical rod held in a stream at right angles to the direction of flow experiences a force in the direction of flow. The force, arising from the pressure differences and frictional stresses developed by the flow of fluid around the rod, is proportional to the cross section of the rod, the density of the fluid, and the square of the velocity. For the case of a rod which is held at an angle ϕ to the direction of flow (see *OB* in Fig. 1), the velocity of the fluid may be resolved into components $v \sin \phi$ normal to the rod and $v \cos \phi$ parallel to the rod, thus giving rise to two corresponding components of resistance. If R is the resistance per unit length for a rod held at right angles to the flow, and if R' is the normal component of resistance per unit inclined length for the same rod when it is inclined at an angle ϕ to the flow, then

$$R = \text{const} \times v^2, \text{ and } R' = \text{const} \times (v \sin \phi)^2 = R \sin^2 \phi .$$

The component of resistance parallel to the rod will be due to frictional stresses only and will be small in comparison with the normal resistance. When a wire was towed longitudinally and then transversely, the longitudinal drag was found to be less than 2% of the transverse drag.

It is concluded that the total force per unit length on an inclined cylindrical rod, cable, or wire which is at an angle ϕ to the direction of flow is given by $R \sin^2 \phi$ normal to the cable, where R is the resistance per unit length of the same cable when it is perpendicular to the same flow.

Some writers have assumed that, for a cable inclined to a horizontal stream, the force is horizontal and equal to that on the vertical pro-

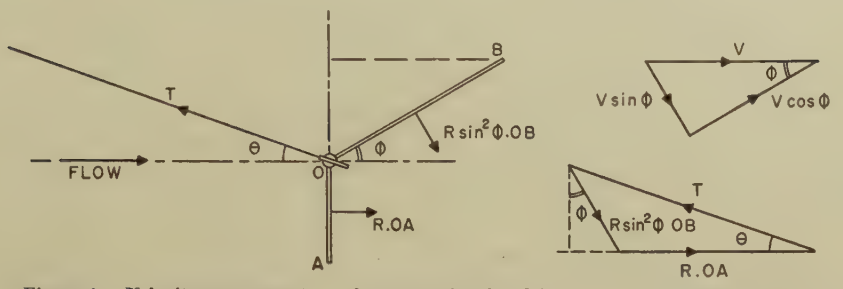

Figure 1. Velocity components and vector triangle of forces for an experimental model of a wire inclined to the flow.

jection of the cable. This gives the same component that we have derived above, $R \sin^2 \phi$ normal to the cable, but in addition it gives a component $R \sin \phi \cos \phi$ tangentially along the cable. Furthermore, the assumption of a purely horizontal force leaves out the "lift" component which has a considerable effect on the shape of the cable.

Experiment. The following experiment will demonstrate the validity of the theoretical conclusion as to the force on an inclined cable. Two lengths of ¾″ diameter wooden dowel are mounted in a small cylindrical wooden hub (see Fig, 1) so that the angle ϕ is about 30°. When the lengths are mounted they are adjusted so that $OA = OB \sin \phi$. A metal pin is driven through the center of the hub perpendicular to the plane AOB, and a strip of brass is bent into a U-shaped bracket to serve as a bearing for this axle pin; the towing line is then attached to the bracket. Holes drilled in the ends A and B provide space for lead weights and are closed by corks trimmed flush with the ends of the rods. Weights at O, A and B are adjusted so that the whole assembly has no net buoyancy when immersed in sea water.

The apparatus is towed by a small line leading from O to a sinker weight (any piece of iron weighing from one to two pounds) which is suspended in the water and moved at uniform velocity at about 9″ below the surface. At the start, AOB is submerged and held in a horizontal plane, with OA perpendicular to the direction of towing. It will be found that, during the towing, OA remains perpendicular to the direction of motion, but for equilibrium the towline must set at an angle θ to the direction of motion.

If the resistance of OB is parallel to the flow and equal to $R.OB \sin \phi$, then the tension will also be parallel to the flow. However, if the resistance of OB is $R \sin^2 \phi.OB$ normal to OB, it is easily shown, from the vector triangle of forces, that T must be in a direction given by

$$\tan \theta = \frac{(R \sin^2 \phi.OB) \cos \phi}{R.OA + (R \sin^2 \phi.OB) \sin \phi} = \frac{\sin 2\phi}{2\,(1 + \sin^2 \phi)} = \frac{\tan \phi}{1 + 2 \tan^2 \phi}.$$

In either case, provided $OB \sin \phi = OA$, the total moment about O is zero, so that there should be no tendency for OA to swing away from the position perpendicular to the flow.

In the experiment performed, OB was nearly 3 feet, the angle θ was 58°, and the assembly was towed by walking along the edge of a dock at a speed of about 1½ knots. The theoretical expression for $\tan \theta$ gives $\theta = 19.3°$ while the experimental value was $20° \pm 1°$. It should be noted that any tangential friction along OB would tend to reduce the value of θ. If R_t is the tangential resistance per unit length, R_n the normal resistance per unit length, and $r = R_t/R_n$, then an analysis of the vector polygon of forces gives for the direction θ' of the tension T

$$\tan \theta' = \frac{\sin \phi \cos \phi - r}{1 + \sin^2 \phi + r \cot \phi} .$$

In the actual experiment described, if r had been as large as 0.02 we should have obtained $\theta' = 18.1°$ instead of 19.3°. Thus the experimental result of $20° \pm 1°$ indicates that we are quite justified in neglecting the tangential resistance of a cable and using for the normal resistance the expression $R \sin^2 \phi$, where R is the resistance per unit length for the same velocity when $\phi = 90°$.

Contribution No. 718

Reprinted from NAVIGATION, Vol. 3, Nos. 1 & 2,
Sept. – Dec., 1951, pages 23 - 29

Contribution No. 718 from the Woods Hole Oceanographic Institution

SOME SUGGESTIONS FOR MORE PRECISE LORAN NAVIGATION

ARTHUR R. MILLER
Woods Hole Oceanographic Institution

The Loran system of navigation enables one to find his exact position at any time regardless of weather or visibility. While Loran and other related systems represent a tremendous advance in navigational science, a deep insight is needed into the difficulties and confusions that sometimes arise in their use. Since the science of navigation is obviously a critical science, it is a credit to most navigators not to accept Loran information too readily without the proper understanding of the whys and wherefores of Loran discrepancies. The purpose of this article is to discuss the apparent errors of Loran observations and to promote procedures which will enable the critical navigator to use Loran lines of position with confidence and reliability.

In recent years, Loran has become an indispensable tool in investigations of ocean currents, for during these investigations, positional data is almost entirely dependent upon frequent or continuous Loran measurements. The nature of the Loran system, providing immediate access to positional information, recommends it for this work. It also allows for a statistical evaluation of the reliability of the system, because of the frequency with which these fixes can be taken.

The successful use of Loran for precision navigation in the study of ocean currents requires much more frequent observations than routine navigation. In a statistical sense, the accuracy of the system is probably best appreciated by those ships participating in investigation of the Gulf Stream between the Straits of Florida and Cape Hatteras. The program calls for hourly observations along five northbound and three southbound tracks to determine the most useful routes to follow with respect to the Stream itself. The frequent periodic Loran observations clearly prove the value of the system; each fix bears out the worth of the preceding one.

If Loran reception were perfect, the value of frequent observations would not be so obvious. Unfortunately, there are times when Loran bearings may lead to an impossible fix or to confusion of position. For instance, in some areas Loran reception may be poor, due to weak signals that are difficult to measure.

To gauge the value of the system it is necessary to understand why Loran can be misleading and what steps can be taken to prevent misinterpretation. Apparent errors in the Loran system can be found through its characteristics. These errors are understood if one takes into account the requisites for a perfect Loran fix and where they may be lacking. The ideal fix, that is, one composed of true lines of position, is assured by fulfillment of the following conditions:

One—The microsecond lines from each pair of stations are closely spaced.

Two—Three pairs of stations are received, their microsecond lines crossing each other at suitable angles.

Three—Reception occurs during the daytime or with minimum interference from sky wave trains.

Four—Reception is free from atmospheric or internal interference.

These conditions are rarely satisfied in toto.

The first and second of these conditions are fixed, geographically, depending on the locations of the Loran stations. Broadly speaking, the ideal combination of these two conditions occurs several hundred miles out to sea. Along the coast the ideal conditions break down until the navigator can make use of but one pair of stations, the others usually represented by base-line extensions or wide-spaced microsecond lines paralleling the coast. The ideal fix location is partially fulfilled near the coast of the Carolinas where closely spaced microsecond lines from two pairs of stations cross each other.

An example, in which the reception of a single set of signals was confusing during a coastal run, follows. A vessel was on a passage from New York to Norfolk in which most of the run involved night time operation. In the early morning the ship's dead reckoning position placed her in the vicinity of Winter Quarter Lightship. Occasional Loran readings, however, indicated that the ship was far south of the estimated D. R. Due to the hash that sometimes interferes with night time Loran operation, inconsistent readings, and lack of Loran experience, these Loran lines were not accepted. At daybreak, in a thick fog, the ship made a Light Vessel that was thought to be Winter Quarter but which turned out to be the Chesapeake Lightship, a position 60 miles south of the dead reckoning position.

In this instance modern navigational aids were not particularly useful to the ship. Her track was over a more or less unchanging depth, so soundings were not practical for determining latitude. Land was beyond radar range and a cloud cover made celestial observations impossible. Only Loran could give positive proof of position. Since one pair of stations was received with fair to poor reception the set was assumed to be malfunctioning. The radio compass might have given a bearing but the ship's dead reckoning position was considered to be reliable. This was apparently confirmed by soundings and by the comparative short distance from a known position.

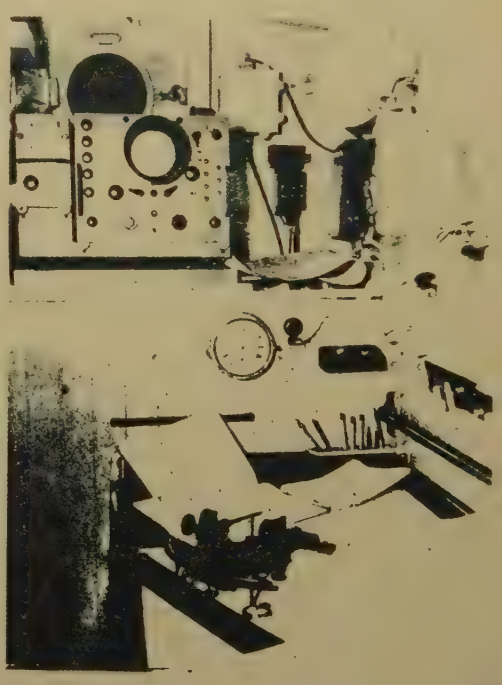

Figure 1. The old and the new. Chartroom of the Atlantis shows the radio-navigation Loran receiver and standard celestial navigation equipment, tables and plotting chart.
Photo: *Woods Hole Oceanographic Institution.*

Although the conditions prevailing at the time gave them no reason to doubt the D. R., this serious error would not have occurred had the ship's officers known how to evaluate the reliability of the Loran signal. The error in D. R. was presumably due to underestimation of ship's speed and to a southerly set during the passage.

If such a mistake can occur during a short coastal passage, one wonders how many errors in position might occur in the open ocean. From the standpoint of safety, it is not absolutely necessary to know one's precise position in the open sea. For that matter, it would be very difficult to confirm the accuracy of deep sea fixes. In Loran, however, we have this opportunity simply by weight of the number and frequency of observations, if nothing else.

The third and fourth requirements for ideal fixes are most likely to be absent at some distance from shore. At night time, especially, it is occasionally very difficult to distinguish and match the proper pips. The situation can be misleading, for, if one pair of stations is mismatched, it could lead to a consistent error over a period of time. In a case like this, the human factor may be seriously involved; a change of watch might put a different interpretation on the picture.

An example of this kind occurred during a passage from Bermuda to Norfolk in which a great many periodic readings were taken. About a day's sailing from Bermuda atmospheric interference hampered the Loran reception and consequently, readings became confused and erratic. After a change of the watch, the signals slightly improved and positions were plotted. These positions were reasonable among themselves but the ship would have had to travel at an impossible speed to reach them. However, with the next watch change and further signal improvement, the ship was back on its normal track. The positions during the previous watch were in error.

The art of navigation consists of weighing the variables of information obtained by various means and deducing position from the order of their importance. Although Loran information is accessible at any time while in range, it is sometimes very difficult to reconcile this information with one's dead reckoning position. Therefore, another factor should be taken into account. The navigator does not know, with certainty, what direction or how fast a current may be moving his ship. He has charts and directions to guide him, but these are based, for the most part, on average conditions which are not necessarily true for the time of passage.

For instance, the smooth line describing the axis of the Gulf Stream beyond Cape Hatteras in North Atlantic charts shows only its average position. However, the full velocity of the stream has been met as much as a hundred miles on either side of this line due to the stream's meandering nature. Average values also cut down its virtual speed which can easily reach five knots and often does, as shown by recent investigations. Its direction may be any point of the compass in spite of its general east and northeast movement.

It is small wonder that the navigator may sometimes doubt his Loran position or, for that matter, his position determined by celestial observation, when there is a sharp disagreement from the dead reckoning position. In the open ocean there exists a strong tendency to upset his calculations where the combination of variable currents, variable Loran readings and celestial observations could tend to mislead rather than confirm positions. In coastal navigation greater accuracy is needed and all the factors of information assume greater importance. Further analysis of the Loran system will show how Loran readings can be evaluated, so that a constant check may be maintained on the dead reckoning position.

Imagine a ship traveling in an area covered by Loran. She maintains constant speed and a straight course; her track is unaffected by currents or weather; she receives perfect Loran signals—a totally uneventful passage. We can illustrate an important principle with this model cruise. We step off equal time intervals along the ship's track and note the readings for each pair of Loran stations. Then, by graphing these readings with coordinates of

microseconds and time, a *smooth line* for each pair of stations will be demonstrated.

This principle gives us a powerful means for evaluating the Loran reading. Suppose we eliminate the reception of perfect signals in the above qualification and introduce some static or interference making it difficult to interpret the Loran signal. In this example,

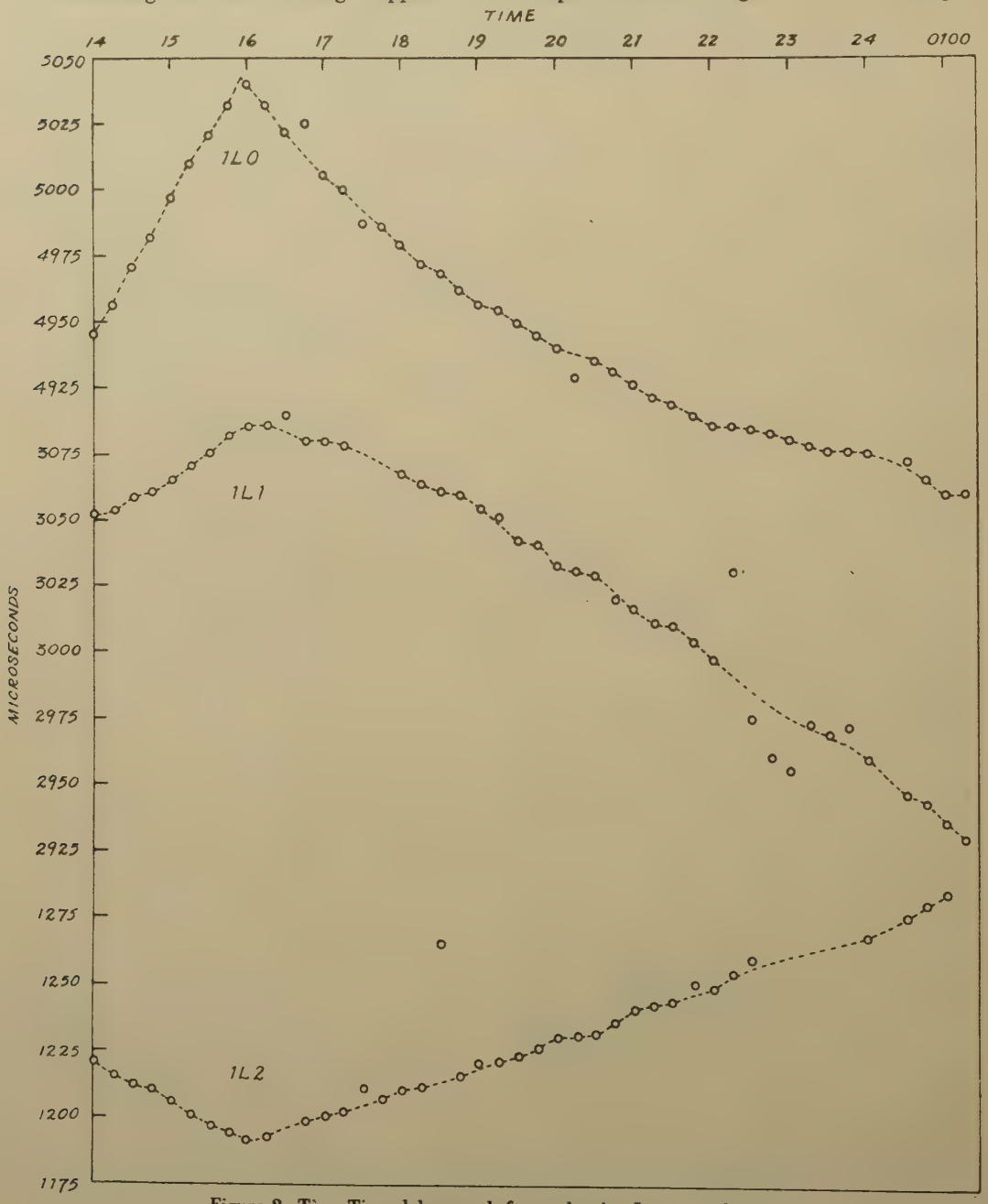

Figure 2. Time-Time delay graph for evaluating Loran readings.

we know the plotted line will be a smooth line because of the constant speed and course of the vessel; consequently, the greater the deviation from this line, the less weight that reading should have for evaluating position.

In actual practice, what ship, except when maneuvering, does not maintain a fixed course and speed over a period of time? Figure 2 illustrates the principle in action. Three stations were received; therefore, three lines were plotted. It will be noted that each set of readings allows a smooth line to be plotted. Occasionally a reading appears off the line. Normally, a fix based on such a reading shows a large triangle with no way of knowing which line of position was off; the graph clearly points out the sour reading. Between 2200 and 2400 reception was very poor. This is demonstrated by the variable readings of stations 1L1 and 1L2. The extension of the lines until good reception was resumed allows us to interpolate the missing readings.

Change the speed or course and a corresponding shift will occur in the direction of the smooth line. Changes due to current and weather amount to the same thing as altering ship's speed or course. The graphed lines for all stations received should shift together, along with any shift of the track (all, provided of course, the shift is not parallel to a microsecond line). Needless to say, the method, in this example, resulted in satisfactory pinpoint fixes, consequently certainty of position was assured.

The method requires that frequent readings be taken: ordinarily, one an hour should be sufficient. Since time is involved, it should be recorded for each pair of stations rather than a set of stations. After all, one phase of the problem is to surmount difficulties of poor reception, and, in such cases, a set of readings may take 10 or 15 minutes instead of the usual two minutes when reception is excellent.

In areas where only one pair of stations can be received, the principle is useful for evaluating the Loran line of position. This is particularly applicable to areas where base line extensions predominate or in the fringe zones of Loran coverage. A line of position in a fringe zone can then be compared with bearings or soundings obtained by other means.

The region of Florida and the West Indies is a fringe area where only one station (1H7) is useful. Here is a region where precise knowledge of position is exceptionally desirable, especially for ships traveling against the swift current of the Gulf Stream. If another set of microsecond lines were to cross the lines of 1H7 another navigational aid would be added to the region. It could be accomplished with a Loran station installed in Bermuda.

Bermuda is about 600 miles from land in two directions—on a line to Cape Hatteras and another to Nantucket. There are Loran installations in both these regions. However, this distance is about the maximum which can be used between master and slave of a pair of stations. Probably, for this reason, such an installation has not been contemplated. Much is to be gained by considering the possibility. Two Loran stations are obtained for one installation by tying in with Nantucket to the North and Hatteras to the West (Figure 3). The area covered by these would extend along the entire eastern coast of the United States. In addition to this large coverage, the Bermuda installation could conceivably overcome the base line extension problem, for its related microsecond lines would intersect present lines normal to the coast.

Because of the extreme distance involved in the operation of a Bermuda installation complications of ground wave and sky wave reception may arise. The distance however, tends to minimize the seriousness of this possibility. A glance at Loran coverages for each pair of stations shows that, the shorter the distance between master and slave stations, the smaller the number of microsecond lines between them. Since the spacing of microsecond lines fanning out between the stations determines the accuracy, it is reasonable to assume that the increased number of lines resulting from a Bermuda installation could be used with accuracy and would minimize the seriousness of ground wave-sky wave complication.

For the present I would like to recommend the taking of Loran bearings at frequent,

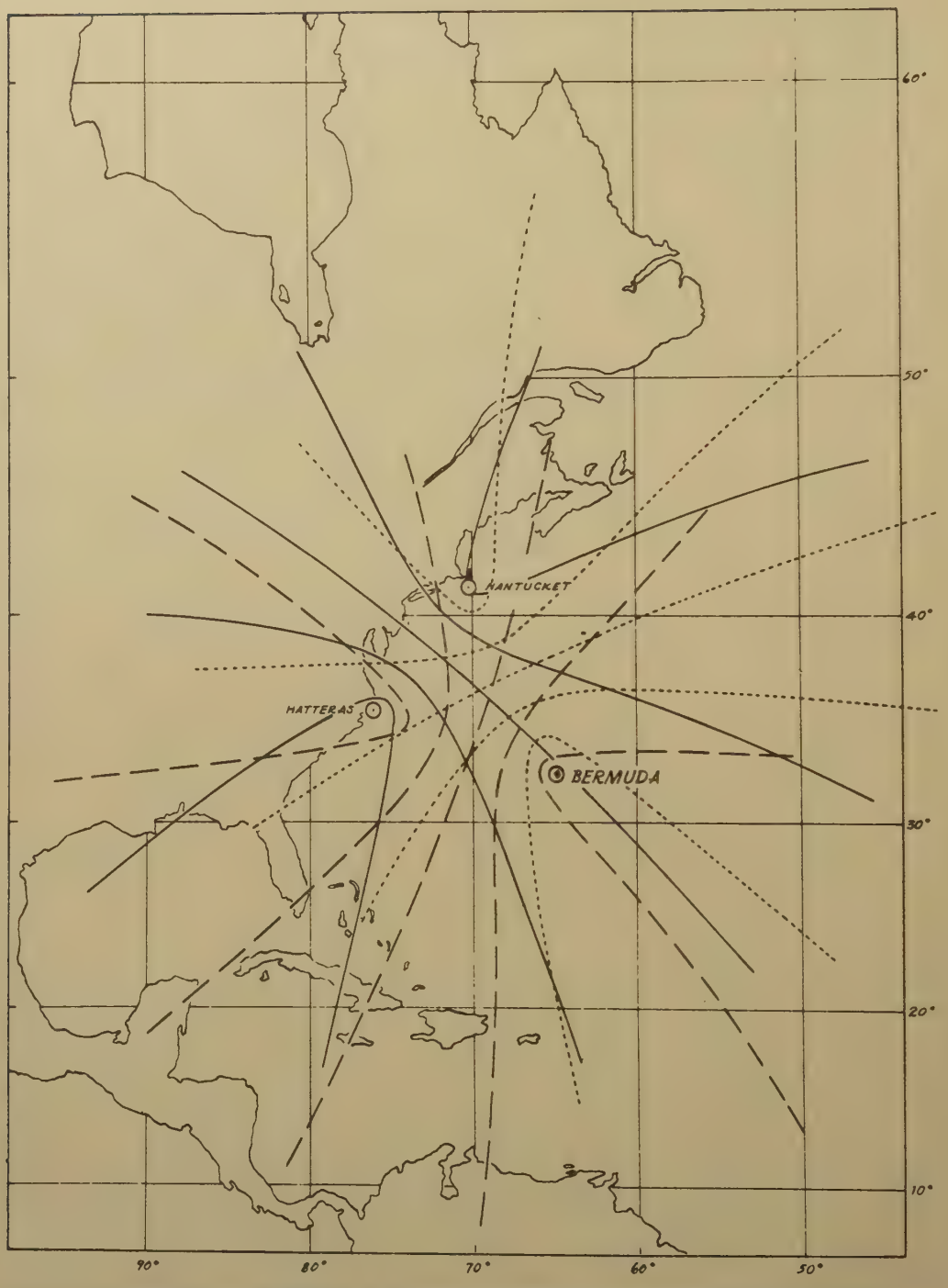

Figure 3. Suggested Loran installation in Bermuda with approximate coverage over area involved.

periodic intervals bearing in mind that, should navigational discrepancies and difficulties be encountered during a cruise, a graph of these bearings will clearly show the fault. Many positions will be saved by this method and the increased accuracy and number of positional data will prove valuable to general navigational science. The installation of a Bermuda Loran station, with the successful usage of its central location, could make the western North Atlantic as well charted as the roads and highways of the United States by elimination of the coastal base line extension difficulty and by the increased coverage over the open ocean.

Report of the year 1953

THE WOODS HOLE OCEANOGRAPHIC INSTITUTION

REPORT FOR THE YEAR 1953

1954

HENRY BRYANT BIGELOW

Director of the Woods Hole Oceanographic Institution, 1930–1940, President, 1940–1950, and Chairman of the Board of Trustees since 1950

"The purposes of the Woods Hole Oceanographic Institution are: to prosecute the study of oceanography in all its branches; to maintain a laboratory or laboratories, boats and equipment; and hold money and property of any kind, whatsoever and wherever situated, and whether received through bequest, devise, gift or otherwise —."

TABLE OF CONTENTS

		PAGE
I.	Trustees, as of December 31, 1953	4
II.	Members of the Corporation, as of December 31, 1953	5
III.	Research Staff	6
IV.	Director's Report	9
V.	Treasurer's Report	30
	Appendix	39

I. TRUSTEES

(As of December 31, 1953)

Honorary Trustees

HENRY B. BIGELOW, Museum of Comparative Zoology, Cambridge, Mass.
MARION EPPLEY, 510 Park Avenue, New York, N.Y.
ALEXANDER FORBES, 610 Harland Street, Milton, Mass.

To serve until 1957

ERIC G. BALL, Harvard Medical School, Shattuck Street, Boston, Mass.
L. O. COLBERT, 4408 29th Street, N.W., Washington, D.C.
FRANK A. HOWARD, 30 Rockefeller Plaza, New York, N.Y.
COLUMBUS O'D. ISELIN, Woods Hole Oceanographic Institution, Woods Hole, Mass.
RAYMOND STEVENS, c/o Arthur D. Little Inc., 30 Memorial Drive, Cambridge, Mass.
E. BRIGHT WILSON, JR., Department of Chemistry, Harvard University, Cambridge, Mass.

To serve until 1956

DETLEV W. BRONK, Rockefeller Institute for Medical Research, York Avenue and 66th Street, New York, N.Y.
DANIEL MERRIMAN, Bingham Oceanographic Laboratory, Yale University, New Haven, Conn.
ALFRED C. REDFIELD, Woods Hole Oceanographic Institution, Woods Hole, Mass.
LAWRASON RIGGS, Riggs, Ferris and Geer, 74 Trinity Place, New York, N.Y.
HENRY L. SHATTUCK, 10 Milk Street, Boston, Mass.
GERARD SWOPE, JR., c/o International General Electric Co., 570 Lexington Avenue, New York, N.Y.

To serve until 1955

J. S. COLES, Bowdoin College, Brunswick, Maine.
CARL H. ECKART, Scripps Institution of Oceanography, La Jolla, Cal.
ROSS G. HARRISON, Osborn Zoological Laboratory, Yale University, New Haven, Conn.
MILFORD R. LAWRENCE, Siders Pond Road, Falmouth, Mass.
HARLOW SHAPLEY, Harvard College Observatory, Cambridge, Mass.
FRANCIS C. WELCH, 73 Tremont Street, Boston, Mass.

To serve until 1954

CHARLES FRANCIS ADAMS, 15 State Street, Boston, Mass.
HORACE S. FORD, 77 Massachusetts Avenue, Cambridge, Mass.
ARNAUD C. MARTS, 521 Fifth Avenue, New York, N.Y.
ALBERT E. PARR, American Museum of Natural History, Central Park West at 79th Street, New York, N.Y.
ATHELSTAN F. SPILHAUS, Institute of Technology, University of Minnesota, Minneapolis 14, Minn.
SELMAN A. WAKSMAN, Institute of Microbiology, Rutgers University, New Brunswick, N.J.

Ex. Officio

EDWIN D. BROOKS, JR., P.O. Box 1135, Boston 3, Mass.
MARY SEARS, Woods Hole Oceanographic Institution, Woods Hole, Mass.
EDWARD H. SMITH, Woods Hole Oceanographic Institution, Woods Hole, Mass.

OFFICERS

ARNAUD C. MARTS, President of the Corporation, 521 Fifth Avenue, New York, N.Y.
HENRY B. BIGELOW, Chairman of the Board of Trustees, Museum of Comparative Zoology, Cambridge, Mass.
EDWIN D. BROOKS, JR., Treasurer, P.O. Box 1135, Boston 3, Mass.
MARY SEARS, Clerk of the Corporation, Woods Hole Oceanographic Institution, Woods Hole, Mass.

II. MEMBERS OF THE CORPORATION

Charles Francis Adams, 15 State Street, Boston, Mass.

Oliver Ames, III, North Easton, Mass.

Philip Armstrong, Medical Center of Syracuse, State University of New York, Syracuse, N. Y.

Eric G. Ball, Department of Biological Chemistry, Harvard Medical School, Boston, Mass.

Henry B. Bigelow, Museum of Comparative Zoology, Cambridge, Mass.

Lindsay Bradford, 215 East 72nd Street, New York, N.Y.

Detlev W. Bronk, Rockefeller Institute for Medical Research, York Avenue and 66th Street, New York, N.Y.

Edwin D. Brooks, Jr., P.O. Box 1135, Boston 3, Mass.

L. O. Colbert, 4408 29th Street, N.W., Washington, D.C.

J. S. Coles, Bowdoin College, Brunswick, Maine.

Carl H. Eckart, Scripps Institution of Oceanography, La Jolla, Cal.

Harrison P. Eddy, c/o Metcalf & Eddy, 1300 Statler Building, Boston, Mass.

Marion Eppley, 510 Park Avenue, New York, N.Y.

Alexander Forbes, 610 Harland Street, Milton, Mass.

Horace S. Ford, 77 Massachusetts Avenue, Cambridge, Mass.

Ross G. Harrison, Osborn Zoological Laboratory, Yale University, New Haven, Conn.

Frank A. Howard, 30 Rockefeller Plaza, New York, N.Y.

Columbus O'D. Iselin, Woods Hole Oceanographic Institution, Woods Hole, Mass.

Milford R. Lawrence, Siders Pond Road, Falmouth, Mass.

Lamar R. Leahy, 910 Park Avenue, New York, N.Y.

Alfred L. Loomis, Room 2420, 14 Wall Street, New York, N.Y.

Arnaud C. Marts, 521 Fifth Avenue, New York, N.Y.

Daniel Merriman, Bingham Oceanographic Laboratory, Yale University, New Haven, Conn.

Henry S. Morgan, 2 Wall Street, New York, N.Y.

Albert E. Parr, American Museum of Natural History, Central Park West at 79th Street, New York, N.Y.

Alfred C. Redfield, Woods Hole Oceanographic Institution, Woods Hole, Mass.

Lawrason Riggs, Riggs, Ferris and Geer, 74 Trinity Place, New York, N.Y.

George H. Richards, 68 William Street, New York, N.Y.

Francis C. Ryder, Massachusetts Institute of Technology, Cambridge, Mass.

Mary Sears, Woods Hole Oceanographic Institution, Woods Hole, Mass.

Athelstan F. Spilhaus, Institute of Technology, University of Minnesota, Minneapolis, Minn.

Lyman Spitzer, Jr., Princeton University Observatory, 14 Prospect Avenue, Princeton, N.J.

Harlow Shapley, Harvard College Observatory, Cambridge, Mass.

Henry L. Shattuck, 10 Milk Street, Boston, Mass.

Edward H. Smith, Woods Hole Oceanographic Institution, Woods Hole, Mass.

Raymond Stevens, c/o Arthur D. Little Inc., 30 Memorial Drive, Cambridge, Mass.

Gerard Swope, Jr., c/o International General Electric Co., 570 Lexington Avenue, New York, N.Y.

Selman A. Waksman, Institute of Microbiology, Rutgers University, New Brunswick, N.J.

Francis C. Welch, 73 Tremont Street, Boston, Mass.

E. Bright Wilson, Jr., Department of Chemistry, Harvard University, Cambridge, Mass.

William D. Winter, c/o Atlantic Mutual Insurance Co., 49 Wall Street, New York, N.Y.

III. RESEARCH STAFF

(As of December 31, 1953)

Director

EDWARD H. SMITH

Senior Scientists

COLUMBUS O'D. ISELIN, Associate Professor of Physical Oceanography, Harvard University and Research Oceanographer, Museum of Comparative Zoology; Senior Oceanographer.

BOSTWICK H. KETCHUM, Senior Biologist.

ALFRED C. REDFIELD, Professor of Physiology, Harvard University; Senior Biologist.

Scientists

ARNOLD B. ARONS, Professor of Physics, Amherst College; Associate in Physical Oceanography.

JOHN C. AYERS, Assistant Professor of Oceanography, Department of Conservation, Cornell University; Associate in Marine Biology.

DAVID L. BELDING, Professor of Bacteriology and Experimental Pathology (Emeritus), Boston University; Consultant, U. S. Fish and Wildlife Service; Associate in Marine Biology.

HENRY B. BIGELOW, Professor of Zoology (Emeritus), Harvard University; Associate in Oceanography.

DEAN F. BUMPUS, Oceanographer.

ANDREW F. BUNKER, Meteorologist.

WILLIAM S. BUTCHER, Geologist.

CORNELIA L. CAREY, Associate Professor in Botany (retired), Barnard College; Associate in Marine Bacteriology.

GEORGE L. CLARKE, Associate Professor of Zoology, Harvard University; Marine Biologist.

WILLARD DOW, Electronics Engineer.

WILLIAM MAURICE EWING, Professor of Geology, Columbia University; Director, Lamont Geological Observatory; Associate in Geophysics.

CHARLES J. FISH, Professor of Marine Biology, University of Rhode Island and Director, Narragansett Marine Laboratory; Associate in Marine Biology.

FREDERICK C. FUGLISTER, Physical Oceanographer.

BERNARD HAURWITZ, Professor of Meteorology and Chairman of the Department of Meteorology and Oceanography, New York University; Associate in Meteorology.

JOHN B. HERSEY, Physical Oceanographer.

LOUIS W. HUTCHINS, Associate in Marine Biology.

BENJAMIN B. LEAVITT, Assistant Professor of Biological Sciences, University of Florida; Associate in Marine Biology.

JOANNE S. MALKUS, Meteorologist.

WILLEM V. R. MALKUS, Physical Oceanographer.

RAYMOND B. MONTGOMERY, Visiting Professor of Oceanography, Brown University; Associate in Physical Oceanography.

HILARY B. MOORE, Associate Professor in Marine Biology and Assistant Director, Marine Laboratory, University of Miami; Associate in Marine Biology.

DANIEL R. NORTON, Research Chemist, U. S. Geological Survey, Washington, D.C.; Associate in Chemical Oceanography.

CHARLES B. OFFICER, JR., Fulbright Fellow in Geophysics, U. S. Educational Foundation, New Zealand; Geophysicist.

ROY L. RATHER, JR., Associate in Underwater Acoustics.

FRANCIS A. RICHARDS, Chemical Oceanographer.

WILLIAM S. RICHARDSON, Physical Chemist.

GORDON A. RILEY, Associate Professor of Marine Biology, Yale University; Associate in Marine Physiology.

HELEN M. ROBERTS, Assistant Professor of Mathematics, University of Connecticut; Associate in Mathematics.

CARL-G. ROSSBY, Director, Institute of Meteorology, University of Stockholm; Meteorologist.

MARSHALL SCHALK, Assistant Professor of Geology and Geography, Smith College; Associate in Geology.

PER L. SCHOLANDER, Physiologist.

WILLIAM C. SCHROEDER, Associate Curator of Fishes, Museum of Comparative Zoology, Harvard University; Ichthyologist.

MARY SEARS, Planktonologist.

EDWARD H. SMITH, Director, Woods Hole Oceanographic Institution; Physical Oceanographer.

PAUL F. SMITH, Assistant Professor of Oceanography, University of Miami; Associate in Oceanography.

FLOYD M. SOULE, Principal Senior Oceanographer, U. S. Coast Guard; Associate in Physical Oceanography.

ATHELSTAN F. SPILHAUS, Dean, Institute of Technology, University of Minnesota; Associate in Physical Oceanography.

HENRY C. STETSON, Research Oceanographer and Alexander Agassiz Fellow in Oceanography, Museum of Comparative Zoology, Harvard University; Submarine Geologist.

HENRY M. STOMMEL, Physical Oceanographer.

PARKER D. TRASK, Research Engineer, University of California; Associate in Submarine Geology.

HARRY J. TURNER, JR., Marine Biologist.

ALLYN C. VINE, Physical Oceanographer.

WILLIAM S. VON ARX, Physical Oceanographer.

EDMOND E. WATSON, Professor of Physics, Queen's University, Kingston, Ontario; Associate in Physical Oceanography.

RAYMOND WEXLER, Research Meteorologist, Harvard University and Massachusetts Institute of Technology; Associate in Meteorology.

ALFRED H. WOODCOCK, Oceanographer.

GEORGE P. WOOLLARD, Professor of Engineering Geology and Geophysics, University of Wisconsin; Associate in Geophysics.

(*Research Staff continued on page 8*)

Research Associates

Richard H. Backus, Research Associate in Marine Biology.
Duncan C. Blanchard, Research Associate in Meteorology.
Robert H. Brockhurst, Research Associate in Physics.
Elizabeth T. Bunce, Research Associate in Physics.
Joseph Chase, Research Associate in Meteorology.
Frank T. Dietz, Research Associate in Physics.
Harlow G. Farmer, Jr., Research Associate in Hydraulics.
David H. Frantz, Jr., Research Associate in Engineering.
John F. Holmes, Research Associate in Engineering.
Henry R. Johnson, Research Associate in Underwater Acoustics.
John W. Kanwisher, Research Associate in Biophysics.
Charles H. Keith, Research Associate in Chemistry.
Sydney T. Knott, Jr., Research Associate in Engineering.
Wilbur Marks, Research Associate in Mathematics.
Donald P. Martineau, Research Associate in Physical Oceanography.
Frank J. Mather III, Research Associate in Ichthyology.
Kenneth G. McCasland, Research Associate in Meteorology.
William G. Metcalf, Research Associate in Physical Oceanography.
Arthur R. Miller, Research Associate in Physical Oceanography.
D. Jane Roberg, Research Associate in Physics.
John H. Ryther, Research Associate in Marine Biology.
Harold E. Sawyer, Research Associate in Engineering.
Irving I. Schell, Research Associate in Meteorology.
William E. Schevill, Research Associate in Physical Oceanography.
Karl E. Schleicher, Research Associate in Physics.
Levie van Dam, Research Associate in Physiology.
Robert G. Walden, Research Associate in Engineering.
George W. Wheeler, Research Associate in Physics.
L. Valentine Worthington, Research Associate in Physical Oceanography.
Ralph F. Wyrick, Research Associate in Underwater Acoustics.
John W. Zeigler, Research Associate in Geology.

ADMINISTRATIVE STAFF

Edward H. Smith, Director.
Alfred C. Redfield, Associate Director.
Ronald A. Veeder, Assistant to the Director.
Helen F. Phillips, Secretary to the Director.
John McGilvray, Business Manager.
Norman T. Allen, Administrator.
Harvey MacKillop, Controller.
John F. Pike, Port Captain.
Delmar R. Jenkins, Purchasing Agent.
Otis E. Hunt, Laboratory Services.
Jan Hahn, Public Information.

IV. DIRECTOR'S REPORT

Introduction

ALTHOUGH research is characteristically slow and one may become impatient at times with progress, there are always compensations when dealing with such a fascinating scientific study as that of the ocean. Our investigations ranged this year from studies of microscopical water droplets formed by bursting sea crests, to the physics of cumulus clouds of the Trade Wind belt. One zealous staff member, journeyed some forty miles by dog team over the ice of Frobisher Bay during the spring of 1953 searching for certain cold water fishes. Some of the year's features include:

(*a*) A second summer expedition along the continental slope, Virginia to Nova Scotia, trawling beyond commercial fishing depths.

(*b*) The filament pattern of the inshore edge of the Gulf Stream as observed from the air,— thermally and optically.

(*c*) The use of freed radio telemetering buoys in the vicinity of Bermuda to record wind-drift currents.

(*d*) The discovery of a chain of sea mounts which trend offshore from the New England shelf.

(*e*) Blood studies of Arctic fishes with reference to their physiological adaptation to sub-zero environment.

Due acknowledgments are again made to generous sponsors of oceanographic research at Woods Hole among whom are the U. S. Department of Defense, the National Science Foundation, the Commonwealth of Massachusetts and others.

Support on a broader basis than in the past is one of the established aims of the Institution. The year witnessed in this respect an encouraging growth in our newly established Woods Hole Oceanographic Associates whose numbers now exceed fifty. It is desired to express appreciation in behalf of the Institution to the Associates. Extension of the program to include membership of corporations and institutions is planned. Further comment on these activities is contained under an appropriate subsequent section.

The report of the year's work of the Research Staff as submitted by Drs. Redfield and Iselin follows.

Scientific Program

During the last twelve years an extensive file of North Atlantic temperature and salinity data has gradually been assembled and organized under

the direction of Mr. F. C. Fuglister. Many of the longer cruises, especially during recent years, have been planned with the purpose of filling in gaps in the geographic and seasonal coverage of these basic data. During the past six months Mr. Fuglister has carried out a general review of the situation in descriptive physical oceanography. Has the time come to get out a new atlas of the North Atlantic and would this be markedly superior to the one published in 1936 as part of the reports on the "Meteor" Expedition? How much longer will it be profitable to process all bathythermograph records and average them by one degree squares? With sub-surface temperature data are we approaching the point that was reached some time ago for surface observations where the Law of Diminishing Returns has begun to operate?

Mr. Fuglister's study has brought out a number of new and interesting points. As was suspected, too many data produce the same sort of over-simplification as do too few. The averaging process in the case of the Gulf Stream reduces the maximum temperature marking the warm core of the current and shifts it south of its usual position. In other words, the highest temperatures on the average chart will be along the limit of extreme southward meanders. On the other hand, by plotting the maximum range of temperature by one degree squares where there are sufficient data the regions of strong current are clearly shown, for at any one time the current coincides with a band of closely spaced isotherms, and as it migrates back and forth across a given one degree field a large temperature range will be recorded in the course of time. In this way, Mr. Fuglister's new charts clearly locate the mean positions of the three main branches of the Gulf Stream east of the longitude of the Grand Banks. Surprisingly, very little of this warm current system reaches the Norwegian Sea directly, as most previous charts have shown. No strong currents exist in the northeastern area of the main Atlantic Basin. The Norwegian Sea has its own anti-clockwise system of currents which carry relatively warm water northward along the edge of the Norwegian continental shelf, but rather little of this has entered from the open North Atlantic via the Faero-Shetland Channel. Thus the circulation of the Norwegian Sea is largely maintained by regional thermohaline differences.

Another striking feature of the new 200-meter temperature chart is that in mid-latitudes in the east, the currents are generally weak, the terminal branches of the Gulf Stream being well separated from the beginnings of the Northern Equatorial Current. In this respect the North Atlantic is quite different from the South Atlantic or the South Pacific where relatively strong equator-ward flowing currents appear to exist in the east. Unfortunately the comparative approach in descriptive oceanography will not become really profitable until the southern hemisphere oceans have been more adequately surveyed.

Having established a more or less reliable picture of the average current system over the North Atlantic, it is to be hoped that during the next few years studies will be made that will show up the variations in the system, both seasonally and over longer periods.

Mr. Henry Stommel and Mr. Gunther Wertheim have continued to study the fluctuations in transport through the Florida Straits. Their measurements of the difference in electrical potential between Key West and Havana now cover more than a year. There is evidence that the diurnal tide which is characteristic of the Gulf of Mexico strongly influences the short period variations of flow through the Florida Straits, which have a pronounced 25 hour rhythm.

Mr. von Arx and Dr. Richardson have been studying these pulses as they travel down stream. At least it is their present belief that these pulses are the cause of the interrupted nature of the inshore edge of the current as they observe surface temperature from the PBY-6A by means of the radiation thermometer. A number of successful flights have followed the current northward from the Florida Straits to Cape Hatteras and in a few cases beyond. As seen from the air the inshore edge of the Florida Current consists of overlapping filaments from 50 to 100 miles in length, along each of which the surface waters are strongly converging. When one of these is followed down stream it trends somewhat to the right of the mean direction of the axis of the current. Just before a given filament becomes diffusive and difficult to follow, a new one will be originating 10 or 15 miles further inshore.

Using the CARYN off the Carolinas, Mr. von Arx attempted last spring to examine the variations in surface velocity and the subsurface temperature structure across different parts of these overlapping streaks of surface convergence. Although the CARYN proved to be rather slow for this work and the data are still being analyzed, the original hypothesis has by no means had to be abandoned, namely that the periodic outpouring through the Florida Straits of tidal origin continue to exert an influence on the current for many miles down stream.

During August the CARYN again worked back and forth across the Gulf Stream measuring the variations in the velocity profile that are associated with seaward and landward meanders as located by the ATLANTIS.

It had been expected that during the summer we would have the help of Dr. C-G. Rossby in developing a theory that could begin to account for some of the newly observed characteristics of the Gulf Stream. Unfortunately sickness delayed his visit to Woods Hole until the winter. His assistant, Dr. Chester Newton has been collaborating with Mr. Fuglister and others in a comparative study of the dynamics of the Gulf Stream and of the atmospheric jet streams. Meanwhile, Dr. Willem Malkus has been elaborating one of Dr. Rossby's early theories and feels that he is on the threshold of some new advances.

It has long been a considerable embarrassment that so little progress has been made in observing the characteristics of wind currents. This is the one problem in physical oceanography where the classical theory has remained unchallenged by the observational approach. Ekman's famous spiral is still the best picture available of a wind current.

Mr. Stommel has undertaken to remedy the situation. He chose the Bermuda area in March as most nearly satisfying two of Ekman's simplifying assumptions: namely a deep layer of homogeneous water and an ocean surface that is large compared to the local wind system. The results were inconclusive for a number of significant reasons, but some new insight has been gained into the nature of the problem.

In the first place, he found that in winter the surface waters down to a considerable depth are subject to quite rapid inertial oscillations. These large, more or less eddy-like motions are presumably due to distant storms and can be readily observed with the G. E. K. The currents due to the local winds, at least in weather that permits effective operation of the *Caryn*, are shallower and weaker, and of course superimposed. To say the least this very much complicates the observational problem, for at no easily reached level can the water be considered approximately still.

A further difficulty was due to the fact that the local winds never blew for long steadily or in one direction. New wind currents kept forming on top of old ones. Nothing remotely approaching the simple Ekman spiral was observed. Furthermore, the high eddy viscosity near the surface due to waves was clearly exerting a major influence. The surface water, more often than not, simply moved down wind and not at 45° to the right as the theory calls for. It is clear that only by taking a very large number of observations can one hope to show up the effect of the earth's rotation in the statistical sense.

Although the current poles with large metal drags at various depths were easily set out, and a good technique was developed for handling the piano wire which connected the drags to the floats, when the winds approached force 5 the *Caryn* could no longer be maneuvered so as to measure the distances and bearings of the various markers.

As a result of this experience, during the spring and early summer, Mr. Stommel and his assistants have been developing a free floating, radio buoy from which current meters can be suspended at several depths, and which also records the direction and velocity of the wind.

In September Mr. Stommel and his assistants shifted their base of operation to Bermuda. The *Atlantis* carried down many tons of batteries and buoys. From the outset the operation was an unqualified, if somewhat puzzling, success. Buoys have been launched at intervals of approximately

three weeks and have been monitored continuously out to distances of approximately 60 miles. They report at fixed intervals, usually every three hours, wind velocity and direction, and the difference in direction and velocity between the surface water and the water at some deeper selected level. They have continued to function satisfactorily in winds of over 35 miles per hour. Since early October at least one buoy has been functioning continuously off Bermuda. In general the buoys confirm the importance of inertial currents first detected by the *Caryn* last winter. Usually the buoy circles to the right relative to the water at 300 feet, but occasionally it can circle to the left. Almost never does the buoy progress for long in a persistent down wind direction.

Mr. Arthur R. Miller returned to Woods Hole in April after a year's leave of absence during which time he took part in a survey of Delaware Bay. As part of this survey several temporary tide gauges were set out and these records provide excellent material for a study of meteorological effects on the tides in a large shallow bay. Since his return Mr. Miller has made excellent progress in analyzing these data, and he and Dr. Alfred Redfield have organized a similar study in Nantucket and Vineyard Sounds.

Mr. Donald P. Martineau has been working on two problems of a very different sort. Last winter he undertook a study of the accumulated bathythermograms from the standpoint of diurnal warming. Although few of the observations had been secured with this particular purpose in mind, he found that in a qualitative way it was in general possible to judge the relative importance of the several factors which influence the depth and intensity of the diurnal thermocline. In this way he was able to work out a fairly successful method of predicting the characteristics of the diurnal thermocline on the basis of the wind strength, the cloud cover, the altitude of the sun and the difference in temperature between the air and the water. Mr. Martineau more recently has undertaken a study of the origins and trajectories of the so-called Antarctic intermediate water in the South Atlantic. He finds that isentropic mixing is as well able to account for the observed distribution of temperature and salinity in the layer as the mass movements postulated by the German and British oceanographers who carried out the original surveys.

Mr. Irving Schell has been studying the so-called southern oscillation and has been looking for evidence that the ocean currents are the link whereby persistence effects are carried over long distances. He hopes to be able to show that a change in the index of the southern oscillation is followed by a change in transport of the northward flowing currents in the southern hemisphere oceans. In the case of the Atlantic, an increase of transport of the Southern Equatorial Current, which was brought about in

this way, could be expected to cross the Equator via the Guiana Current and still later to influence the Gulf Stream. While the validity of the southern oscillation is generally recognized in meteorology, Mr. Schell's study seems to be the first attempt to link the oceanic circulation with the gradual weather changes.

Mr. Joseph Chase has completed a study which correlates the varying success of each year class of haddock on Georges Bank with the strength and duration of northwest winds during the winter and early spring months. He could easily show that during its pelagic stage the haddock is very vulnerable to prolonged northwest gales over the bank, but it was much more difficult to deduce from the available data how the time of spawning varies from year to year.

Our meteorological program has begun to attract increasing attention, and each summer more meteorologists are acquiring the habit of coming to Woods Hole. It is evident that without much additional effort our laboratory can become an important focus point in meteorological research.

It happens that during most of the year the members of our permanent staff interested in weather phenomena over the ocean have been mainly occupied with report writing. Mr. Alfred Woodcock and Mr. Duncan C. Blanchard have been working up the data on warm rain clouds secured at Hawaii last year. Dr. Arnold Arons and Dr. Charles H. Keith have completed an experimental and theoretical study of the growth of droplets forming on salt nuclei.

Dr. Joanne Starr Malkus completed a study of observations secured in two trade cumulus clouds in 1952 and then during the early spring took part in a new observational program in the Virgin Island area. The 1953 field work in the tropics included a cooperative program with a group of British meteorologists who were based on Anagada Island. Dr. Malkus is planning soon to spend a year at the Imperial College, London, in order to knit the two groups even more closely together. Dr. R. S. Scorer, one of the leaders of the British group concerned with the dynamics of low level meteorology, visited Woods Hole during the autumn and gave a series of lectures on convective phenomena.

Mr. Andrew F. Bunker has continued to study the modifications of air masses as they pass over long stretches of water. During recent months he has been particularly concerned with the measurement of shearing stresses present in the air at altitudes between 50 feet and 5000 feet. He has also carried on studies of the dynamics of the plane as a means of exploring turbulence. Thus the plane itself has become a calibrated meteorological instrument. It is perhaps worth nothing that the interests of the oceanographers and the meteorologists in the characteristics of a plane do not coincide. The former would like a fairly fast plane of great endurance. The latter are well satisfied with the present PBY-6A because it is so slow.

Research in underwater acoustics, under the direction of Dr. J. B. Hersey, has continued to emphasize increasingly refined measurements at sea of transmission phenomena, reverberation, bottom reflectivity and ambient noise. Of recent months particular emphasis is being placed on scattering of biological origin as a function of frequency. The BLUE DOLPHIN has been chartered for the summer for the specific purpose of catching the biological scatterers that the BEAR with her acoustical gear has located. Thus at long last we hope we have means of making certain in reverberation measurements of the effects of the number of organisms present, their size and their body characteristics. Until now we have usually only been able to secure half of the data necessary to gaining a better understanding of such phenomena.

Advances have also been made in our knowledge concerning the distribution and importance in acoustical transmission of the air bubbles present just below the sea surface. These are of course introduced into the sea by breaking waves. Observations made last winter during periods of strong, cold winds showed that at times down to depths of 50 feet or more the whole water column can become so filled with air bubbles that its ability to transmit high frequency sound almost disappears.

Dr. Hersey and his group have continued to collaborate closely with other laboratories working in underwater acoustics and more and more the importance of the environmental factors is becoming generally recognized.

Mr. Henry Stetson's and Dr. Parker D. Trask's reports on the sediments of the Western Gulf of Mexico have been published and Mr. Stetson's work on the newer samples from the Eastern Gulf is nearing completion.

A new program of studying the changes in underwater topography along the outer Cape Cod beaches has recently gotten under way. Mr. John M. Zeigler who has completed his graduate studies at Harvard in sedimentary geology and who has recently joined our staff has been practicing at aqualung diving. This will enable him to study the underwater transportation of sand at first hand. Mr. L. D. Hoadley has completed a time lapse underwater camera capable of taking up to five thousand pictures. This will be used to study sand ripples and scour.

Mr. Zeigler has on three occasions carried out a survey of the bottom topography in deep water off the southern edge of Georges Bank. A most interesting chain of sea mounts has been discovered trending in a southeasterly direction. These are not only of considerable geological interest, but also since they cross the mean track of the Gulf Stream they should provide almost ideal mooring points for a line of instruments to record variations in the path of the current. So far nine sea mounts have been found with an average separation of about 35 miles.

During the past year considerable effort has been devoted to devising means of obtaining records of the energy spectrum of ocean waves. Under Mr. Robert Walden's direction a capacitance type wave recorder has been developed. This is a moored instrument and therefore only useful in relatively shallow water. Mr. John Holmes has been working on a free floating instrument. Both instruments seem capable of obtaining accurate records in waves up to about 8 feet in height. They are being tested under the high bridge across Narragansett Bay near Jamestown where stereophotographs of the sea surface can conveniently be obtained.

Reliable measurements of the characteristics of relatively small waves are being carried out for the David Taylor Model Basin with the launch *Risk*. The purpose of this work, which is being carried on by Mr. Wilbur Marks, is to test the new St. Denis-Pierson theory of the motion of ships in confused seas. It is hoped that out of this rather precise study of the statistical characteristics of small waves a reliable means will evolve of gaining similar information on storm waves.

In reviewing the work of the marine biologists, in progress since the first of the year, I would like first to mention the investigations done with the support of various civil agencies.

The contract with the Commonwealth of Massachusetts for investigations of the shell fisheries is continuing. At the request of the Department of Conservation Mr. Turner is surveying the crab fishery conducted in Boston Harbor, in order to obtain a basis for their administrative decisions on the desirable length of the open season. This is a matter on which controversy exists between two factions of the fishermen. Like the sea scallop, the rock crab supports a locally important fishery which is being conducted without benefit of any adequate knowledge of its natural history.

Mr. Posgay has been working for several years on the biology of the sea scallop and has attempted to determine the rate at which the scallops grow. To this end he has tagged a large number of sea scallops after measuring them and has liberated them on the fishing grounds. Recently he has been rewarded by the recapture of a considerable number of tagged specimens which are giving the answer to this important question.

The Institution has been represented by Dr. Ketchum as a consultant to the New York City Board of Water Supply in connection with litigation arising from the proposed diversion of water from the Delaware Watershed by New York. Here the question at issue is the effect of the proposed diversions on the salinity of Delaware Bay, particularly in the regions occupied by the New Jersey oyster industry.

This spring the Creole Petroleum Corporation proposed that we send representatives to Lake Maracaibo, Venezuela to outline a program of

observations to enable them to follow the changes in the salt content of the Lake expected to follow the purposed deepening of the channel to the sea. Their immediate concern was with the effects on the corrosive quality of the water, its potability and its use for industrial purposes. Drs. Redfield and Ketchum spent two weeks in Venezuela about the first of June and were able to secure a very complete picture of the hydrography of the Lake. This proved to be a most welcome opportunity since little is known of the character of embayments in tropical regions. Our observations revealed that the Lake has several novel characteristics which we hope to have an opportunity to study further.

Some years ago Dr. Mary Sears was invited by the Peruvian guano interests to examine the plankton in Peruvian waters, which supply the food for the birds on which the industry depends for its raw material. In the course of her studies Dr. Sears has examined the characteristics of the water present at the times of El Nino, when unusual warmth of the surface water is associated with catastrophic destruction of marine life, causing the guano birds to forsake the area. This condition is known to arise when a slackening of the coastal current permits an intrusion of warm water from the north, or from offshore, to invade the coast. Dr. Sears' studies now indicate that conditions may from time to time cause the local coastal water to become destructively warm without recourse to major changes in the circulation. The causes of the destructive condition are thus multiple and more complex than had been supposed.

Dr. Sears, who is well recognized as a marine biologist, and is an authority on the Siphonophores, now qualified as a significant contributor to general oceanography. It may be noted with regret that present conditions do not permit her to carry out her work at sea in person except through engagements with foreign agencies.

Turning to the work supported solely by the Institution, I will mention first the studies of Mr. Schroeder. In continuing the exploration of the fish fauna of the local coast he has made three trips this summer on the chartered dragger *Cap'n Bill II*. These have extended the range southward to Cape Charles and outward to 730 fathoms. Valuable information has been obtained on the southward extension of the range of northern species, but curiously enough little new has been discovered on the extension of the northern range of southern species into this area. As the work has extended deeper the numbers of fish caught has declined without much change in the composition of the catch. On the practical side red fish have been found again and, in more substantial numbers, off Nova Scotia in depths not exploited by commercial fishermen and deep sea red crabs, previously taken in goodly numbers off New England were found in undiminished supply to the southward.

Drs. Scholander and Van Dam accompanied Mr. Schroeder on two of their fishing expeditions in order to continue their studies of the gas contained in the swim bladder of deep living fishes, and the properties of the blood of such fishes which might be concerned with the secretion of the gas under very great pressure. These trips have been so successful that this phase of the investigation is now complete. The study is almost unique as an examination of physiological phenomena which occur under the high pressures of the deep sea.

In March Dr. Scholander made an expedition to Frobisher Bay in Baffin Land with the support of a grant from the Arctic Institute. The problem was to discover how Arctic fish survive at temperatures lower than those at which fish blood is known to freeze (about −0.6°C). With the aid of airplane and dog-sled Dr. Scholander succeeded in finding a hole in the ice where requisite low temperatures existed and in catching six small fishes. Examination of the blood showed that it did not freeze at temperatures higher than the local sea water (about −2°C) and indicated that this condition was due to the unusually high salt content of the blood. These observations promise to add a new chapter to the very interesting history of the development of renal function in fishes and to provide a concrete example of a mechanism by which physiological adaptation to environmental conditions is accomplished.

One of the central points of interest in marine biology today is the productivity of ocean water. By productivity is meant the rate at which energy is absorbed from sunlight to be used in the synthesis of organic matter. It is perhaps analogous to the fertility of the soil. The simplest method of measuring productivity at present is to confine a sample of sea water, with its normal biological content, to a bottle and to expose it to the local conditions of temperature and illumination for 24 hours. By subsequent determination of the oxygen content of the bottle conclusions may be drawn on the rate of production of organic matter by photosynthesis. The current rather extravagant claims for the great productivity of the ocean, relative to the land, are based primarily on measurements made by Dr. Riley using this method.

Recently an alternate method has been devised in Denmark using Carbon 14 as an indicator of carbon assimilation. This method results in very much smaller estimates of the productivity of tropical seas. Dr. Ryther and Mr. Vaccaro, of our staff, have compared the two methods simultaneously on controlled laboratory cultures and have shown that the results agree well, although the Carbon 14 method is the more precise when productivity values are low. This work will clarify the interpretation of much existing information and should lead to rapid advances in our knowledge of this fundamental problem.

The rise in sea level which has occurred during post glacial times, and is still continuing at rates measured by tide gauge records is a matter of interest in geology and oceanography alike. During the summer Mr. Patrick Butler, a student of botany at Harvard, who held a summer fellowship at the institution has studied the pollen buried in the peat of the salt marsh at Barnstable. Since the marsh has built upward as sea level rose, the pollen entrapped at different depths provides an indication of the changes in vegetation during the time sea level has risen. The latter may be related to changes in climate, which can be dated from other evidence. Mr. Butler has distinguished in this way a research of climatic change thought to have occurred some 5000 years ago, and now lying at a depth of 29 feet. This indicates an average rise in sea level of six or seven inches per hundred years — a rate about that given by recent tide gauge records.

Forty-two scientific papers have been published in 1953. These include the "Fishes of the Gulf of Maine," a book of 577 pages by Dr. Bigelow and Mr. Schroeder. A second book of similar proportions by the same authors will bear the 1953 date line, although it will not appear before mid–1954. One number of *Papers in Physical Oceanography and Meteorology* with two rather long papers was also published in 1953. The following contributions of the Institution for 1953 are listed by author and title:

	Contr. No.
Bigelow, H. B., and W. C. Schroeder. Fishes of the Gulf of Maine. Revised edition. *Fish Bull.* 74, *Fish Bull., Fish and Wildlife Service*, 53:1–577, 288 text figs.	592
Bigelow, H. B., W. C. Schroeder and S. Springer. New and little known sharks from the Atlantic and from the Gulf of Mexico. *Bull. Mus. Comp. Zool., Harvard Coll* , 109(3):213–276, 10 text figs.	596
Blanchard, D. C. Raindrop size-distribution in Hawaiian rains. *J. Meteorol.*, 10(6):457–473, 13 text figs.	658
Blanchard, D. C. A simple recording technique for determining raindrop size and time of occurrence of rain showers. *Trans. Amer. Geophys. Union*, 34(4):534–538, 2 text figs.	659
Bunker, A. F. On the determination of moisture gradients from radiosonde records. *Bull. Amer. Meteorol. Soc.*, 34(9):406–409, 2 text figs.	605
Bunker, A. F. Diffusion entrainment and frictional drag associated with non-saturated, buoyant air parcels rising through a turbulent air mass. *J. Meteorol.*, 10(3):212–218, 4 text figs.	631
Farmer, H. G., and G. W. Morgan. Ch. 5. The salt wedge. *Proc. Third Conf. Coastal Eng.*, Cambridge, Mass., Oct. 1952:54–64, 4 text figs.	638
Francis, J. R. D. A note on the velocity distribution and bottom stress in a wind-driven water current system. *J. Mar. Res.*, 12(1):93–98, 4 text figs.	639
Hela, Ilmo, H. B. Moore and H. Owre. Seasonal changes in the surface water masses and in their plankton in the Bermuda area. *Bull. Mar. Sci., Gulf and Caribbean*, 3(3):157–167, 10 text figs.	677

	Contr. No.
Hough, J. L. Pleistocene climatic record in a Pacific Ocean core sample. *J. Geol.*, 61(3):252–262, 3 text figs.	641
Ketchum, B. H. Ch. 6. Circulation in estuaries. *Proc. Third Conf. Coastal Eng.*, Cambridge, Mass., Oct. 1952:65–76, 8 text figs.	642
Ketchum, B. H., and D. J. Keen. The exchange of fresh and salt waters in the Bay of Fundy and in Passamaquoddy Bay. *J. Fish. Res. Bd., Canada*, 10(3):97–124, 11 text figs.	593
Malkus, J. S., and M. E. Stern. The flow of a stable atmosphere over a heated island. Pt. 1. *J. Meteorol.*, 10(1):30–41, 6 text figs.	624
Malkus, W. V. R. A recording bathypitotmeter. *J. Mar. Res.*, 12(1):51–59, 5 text figs.	634
Moore, H. B., H. Owre, E. C. Jones and T. Dow. Plankton of the Florida Current. III. The control of the vertical distribution of zooplankton in the daytime by light and temperature. *Bull. Mar. Sci., Gulf and Caribbean*, 3(2):83–95, 1 text fig.	669
Officer, C. B., Jr. The refraction arrival in water covered areas. *Geophysics*, 18(4):805–819, 9 text figs.	629
Redfield, A. C. Interference phenomena in the tides of the Woods Hole region. *J. Mar. Res.*, 12(1):121–140, 9 text figs	636
Roelofs, E. W., and D. F. Bumpus. The hydrography of Pamlico Sound. *Bull. Mar. Sci., Gulf and Caribbean*, 3(3):181–205, 11 text figs.	547
Said, Rushdi. Foraminifera of Great Pond, Falmouth, Massachusetts. *Contr. Cushman Found. Foram. Res.*, 4(1):7–14, 3 text figs.	588
Schevill, W. E., and Barbara Lawrence. Auditory response of the bottle-nosed porpoise, *Tursiops truncatus*, to frequencies above 100 kc. *J. Exper. Zool.*, 124(1):147–165, 2 text figs.	648
Schevill, W. E., and Barbara Lawrence. High-frequency auditory response of a bottle-nosed porpoise, *Tursiops truncatus* (Montagu). *J. Acoust. Soc., Amer.*, 25(5):1016–1017	663
Scholander, P. F., and L. Van Dam. Composition of the swimbladder gas in deep sea fishes. *Biol. Bull.*, 104(1):75–86, 5 text figs.	632
Sears, Mary. Notes on siphonophores. 2. A revision of the Abylinae. *Bull. Mus. Comp. Zool., Harvard Coll.*, 109(1):1–119, 29 text figs.	602
Soule, F. M., P. S. Branson, and R. P. Dinsmore. Physical oceanography of the Grand Banks region and the Labrador Sea in 1951. *U.S.C.G. Bull.*, No. 37:17–85, 21 text figs. (dated 1952)	601
Stern, M. E., and J. S. Malkus. The flow of a stable atmosphere over a heated island. Pt. II. *J. Meteorol.*, 10(2):105–120	625
Stetson, H. C. The sediments of the western Gulf of Mexico. Pt. 1. The continental terrace of the western Gulf of Mexico: its surface sediments, origin and development. *Pap. Phys. Oceanogr. Meteorol.*, 12(4): 1–45, 18 text figs.	646
Stommel, Henry. Computation of pollution in a vertically mixed estuary. *Sewage and Ind. Wastes*, 25(9):1065–1071, 3 text figs.	640
Stommel, Henry. The role of density currents in estuaries. *Proc. Minnesota Int. Hydraulics Conv.*, Sept. 1–4, 1953:305–312, 7 text figs.	655

Contr. No.

STOMMEL, HENRY. Examples of the possible role of inertia and stratification in the dynamics of the Gulf Stream System. *J. Mar. Res.*, 12(2):184–195, 4 text figs. 645

STOMMEL, HENRY, and H. G. FARMER. Control of salinity in an estuary by a transition. *J. Mar. Res.*, 12(1):13–20, 4 text figs. 587

STOMMEL, HENRY, W. S. VON ARX, DONALD PARSON and W. S. RICHARDSON. Rapid aerial survey of Gulf Stream with camera and radiation thermometer. *Science*, 117(3049):639–640, 1 text fig. 644

TRASK, P. D. The sediments of the western Gulf of Mexico. Pt. II. Chemical studies of sediments of the western Gulf of Mexico. *Pap. Phys. Oceanogr. Meteorol.*, 12(4):47–120, 21 text figs. 647

TURNER, H. J., JR. The drilling mechanism of the Naticidae. *Ecology*, 34(1):222–223 630

TURNER, H. J., JR. Fifth report on investigations of the shellfisheries of Massachusetts. Comm. Mass., Dept. Conserv., Div. Mar. Fish.:1–37, 3 figs., 8 maps. (Dated 1952) 656

VAN DAM, L., and P. F. SCHOLANDER. Concentration of hemoglobin in the blood of deep sea fishes. *J. Cell. Comp. Physiol.*, 41(3):522–524 633

VISHNIAC, H. S., and S. W. WATSON. The steroid requirements of *Labyrinthula vitellina* var. *pacifica*. *J. Gen. Microbiol.*, 8:248–255 623

VON ARX, W. S. Cartographic principles applied to wide-field photography. *Photogr. Eng.*, 4(2):60–73, 9 text figs. 649

WATSON, E. E. An experiment to determine the hydrodynamic forces on a cable inclined to the direction of flow. *J. Mar. Res.*, 12(3):245–248, 1 text fig. 686

WOODCOCK, A. H. Salt nuclei in marine air as a function of altitude and wind force. *J. Meteorol.*, 10(5):362–371, 8 text figs. 643

WOODCOCK, A. H. Hawaii as a cloud physics laboratory. *Pacific Science*, 7(4):522–524, 2 text figs. 660

WOODCOCK, A. H., C. F. KIENTZLER, A. B. ARONS and D. C. BLANCHARD. Giant condensation nuclei from bursting bubbles. *Nature*, 172(4390):1144–1145, 2 text figs. 673

WORTHINGTON, L. V. Oceanographic results of Project Skijump I and Skijump II in the Polar Sea, 1951–1952. *Trans. Amer. Geophys. Union*, 34(4):543–551, 4 text figs. 628

Vessels

The winter season in New England waters is not a favorable time for oceanographic field work, yet ATLANTIS was able to get in a few short cruises. Early in March saw her departing on a southern cruise from which she did not return until early June. During the first part of the period ATLANTIS conducted field work out of Guantanamo, Cuba, then in April she joined company with the schooner VEMA, chartered by Lamont Geological Observatory, under Dr. Maurice Ewing to carry out a seismic survey of the Caribbean and Gulf of Mexico waters.

Following ATLANTIS' return to Woods Hole and the semi-annual refit

at Boston, she sailed on a Gulf Stream cruise. Later, in September, found her in Bermuda waters, where she had a close call from stranding in a hurricane which passed over that island. The latter part of 1953 witnessed additional short trips across the continental shelf in the New England area. Total mileage approximated 20,000 in 193 days at sea.

CARYN made two trips to Bermuda, one in the Spring to establish a base party to study wind drift currents, and later in July in company with ATLANTIS. About six weeks CARYN was used in Gulf Stream observations out of Morehead City, North Carolina, part of the time in conjunction with our Navy loaned PBY-6A airplane. In October in the interests of economy CARYN was decommissioned for the remainder of the year.

The BEAR, which was purchased in 1952 under a contract with the Bureau of Ships, proved to be a useful and active unit in acoustical field operations. Due to her somewhat off-shore limitations, her cruises were a matter of days in and out of Woods Hole. In company with the schooner BLUE DOLPHIN which was chartered for the summer, these two vessels carried out bio-physical observations in the area south of Martha's Vineyard. The BLUE DOLPHIN's charter ran from 13 June to 27 August.

Another charter refers to the previous year's deep trawling fishery expedition along the continental slope, Virginia to Nova Scotia, when again the dragger CAP'N BILL II was used on three cruises of seven to eight days duration each. Again as last year some rare specimens were caught, and fish and crab populations met which indicate possibilities of development of economic proportions.

The boat pool of the Institution consisting of ASTERIAS and CLAIR was employed in similar miscellaneous local operations as in former years. The MYTILUS which had been kept as a spare hull in reserve, appeared to have no future use, and was therefore sold.

The sport fishing cruiser ALLURE, a gift to the Institution last year by an Associate, was found unsuitable for the usual field work, and was disposed of in the early summer.

The PBY-6A Navy airplane operated by our own personnel kept active throughout the year with time out only for prescribed engine and structural inspections. The craft's meteorological-oceanographic activities included visits to the West Indies, Newfoundland, Nebraska, and three flights along the inshore boundaries of the Gulf Stream, Miami to Cape Hatteras. The airplane completed operations over the waters around Bermuda during December.

By the year's end two factors were only too evident. Hurricanes had once again greatly decreased the effectiveness of the operations during the latter part of the summer. Perhaps more fundamental is that Loran navi-

gation is becoming marginal for our needs. Although this was a great stimulus to research on the circulation problem when it first became available, it is not sufficiently accurate to help solve several of the critical problems. We need a still more precise system of navigation, and until this has been developed progress in our understanding of the details of ocean currents is not likely to be spectacular. To be able to measure the depth to the bottom in deep water within a fathom or so and at the same time not to know one's geographical position within half a mile or more is not a very satisfactory situation.

The situation regarding the main field instrument of the Institution,—its sea-going fleet, has not improved during the last year for maintenance continues relatively higher than what it would be on newer ships, and age is becoming increasingly apparent. Not only is this true in the rate of material deterioration but also it is met at every turn such as in the efficient operation of the scientific equipment and in the sea-comfort of those on board.

In an effort to ultimately replace existing American craft with more modern designed oceanographic ships, a study and recommendations were completed during the year which received favorable comment from naval circles. Marked improvement in reduction of the noise factor on shipboard was a feature of the study. A committee continues under a research contract between our Institution and the Office of Naval Research on which representatives of several oceanographic activities, in and out of the government, plan to prepare design drawings and estimates. It is hoped that out of this work will come appropriations and the actual construction of a modern ocean-class research ship.

For detailed information on the itineraries of the research vessels and airplane, please refer to Appendix.

Plant

The crowded conditions of the laboratory which have prevailed for several years received no immediate alleviation. Yet the ever growing construction next door of the Office of Naval Research's new Laboratory of Oceanography, augured well for a not too distant relief of cramped working spaces. The new construction in those floor areas used by existing activities such as the garage and stock room, necessitated some interruptions of the normal work to accommodate to the new building.

In order to adjust temporarily the parking of employees' automobiles, an area in the rear of the Institution's village property was leveled and surfaced to accommodate 84 vehicles. Through the kindness, furthermore, of Mr. Wilbur A. Dyer, the Dyer's Dock parking area was made available at no charge for winter use.

The so-called Hall property belonging to the Institution across Main Street from our main laboratory was connected with the town sewer line, and the main building, formerly leased as a grocery store, was utilized during the summer as a temporary office for visiting scientists. Maintenance of the dock and several buildings was provided on a current level sufficient to a neat appearance and the overall utilitarian value of the property.

Personnel

The Research Staff in 1953 numbered 190. Below is shown a tabulation of all Institution personnel (Research Staff and Administrative Staff), as of July 1, 1953. The table for 1952 is included for comparison.

	1952		*1953*	
RESEARCH STAFF				
Full time:				
At Woods Hole	96		79	
Off Campus	6		29	
Secretaries and Clerks	4		8	
Part time:				
At Woods Hole	45		43	
Off Campus	21		17	
Fellowship Holders	14		10	
Visiting Investigators	7	193	4	190*
ADMINISTRATIVE STAFF				
Department Heads and Assistants	11		12	
Secretaries and Clerks	18		19	
General Maintenance and Service Personnel	55		59	
Crews of Vessels	41	125	51	141
Grand Total		318		331

* Includes 71 Staff Appointees and 119 others

It is with pleasure that we record the following additions to and promotions within the Research Staff:

Dr. Carl-G. Rossby, Director, Institute of Meteorology, University of Stockholm, already an associate on our staff, was appointed meteorologist as of September 1.

Dr. Bostwick H. Ketchum, marine microbiologist, was promoted to senior biologist as of December 1.

Appointments to the Research Staff for a period of one year from September 1 were made to the following:

JOHN W. KANWISHER	Research Associate in Biophysics
BENJAMIN B. LEAVITT	Associate in Marine Biology
WILBUR MARKS	Research Associate in Mathematics

William S. Richardson	Physical Chemist
John H. Ryther	Research Associate in Marine Biology
Marshall Schalk	Associate in Geology
Robert G. Walden	Research Associate in Engineering
Raymond Wexler	Associate in Meteorology
George W. Wheeler	Research Associate in Physics
John M. Zeigler	Research Associate in Geology

In accordance with the policy of the Institution to constantly improve and strengthen the Research Staff, the Board of Trustees voted in August to provide a fund for a sabbatical leave of a top scientist, or to afford the opportunity for a younger scientist to continue his formal education. In the Fall, Mr. William S. von Arx was granted sabbatical leave for a period of approximately one year to pursue earth science courses at the Massachusetts Institute of Technology.

It is with regret that we accepted the resignation of Dr. Charles H. Keith, Dr. William S. Butcher, and Captain Adrian K. Lane. The latter who had been on the Administrative Staff of the Institution for approximately seven years, spent all but the latter one in command of Atlantis, logging many thousands of miles at sea.

The Institution lost through death, the services of Mr. Marcus Conlan, Property Custodian, who passed away May 4th, after more than ten years of faithful and untiring service.

Other changes of note is the transfer of Captain John F. Pike from command of Atlantis to become Port Captain on July 1, and the assignment of Captain W. Scott Bray as the new master of Atlantis.

Dr. Bostwick H. Ketchum attended the Sixth International Congress of Microbiology at Rome, Italy in September. He also represented the Institution at the fifty-first annual meeting of the International Council for the Exploration of the Sea at Copenhagen, and visited several marine stations in Scandanavia, England and Scotland.

Dr. George L. Clarke attended the meeting of the Pacific Scientific Congress held in November at Manila, Philippine Islands.

The following persons were awarded honoraria, grants or fellowships during the year:

Ayers, John C.	Fofonoff, Nick	Moore, J. R., III
Bergeron, Tor	Francis, J. R. D.	Riley, Gordon
Butler, Patrick	Gilbert, Theo. W., Jr.	Scorer, R. S.
Conover, John T.	Harris, Eugene	Stefanssen, Unnstein
Cousteau, Jacques-Yves	Lawton, C. S.	Voss, G. L.
Doe, L. A. Earlston	Montgomery, Raymond B.	Watson, Edmond E.
Ewing, William M.		

It is desired to acknowledge with appreciation grants from the National Science Foundation to Dr. Per L. Scholander in the sum of $8500 for studies on the mechanism of gas secretion in fishes; also another grant to Dr. John H. Ryther from the National Science Foundation in the sum of $3000 for studies of the etiology of plankton blooms.

Previous reference has been made to the new supporting organization of the Institution — the Woods Hole Oceanographic Associates. It had its growth quite naturally from small groups of persons in the Woods Hole Community who were welcomed by a tour of the laboratory.

The Associates on May 21 held what they called a Spring Dinner at the appropriate quarters of the New York Yacht Club, and this was followed by a day's excursion in Vineyard Sound, August 1st, of over one hundred Associates and their friends on board the vessels ATLANTIS and BLUE DOLPHIN. On board each vessel several of the oceanographers' instruments were demonstrated, such as water sampling, coring, BT casts and the netting of plankton. Thus the day, which was one of beautiful weather, proved very enjoyable as well as instructive.

The annual meeting which was held on board ATLANTIS resulted in the re-election of the following:

GERARD SWOPE, JR., President
JOHN GIFFORD, Secretary
EDWIN D. BROOKS, JR., Treasurer

and the following Executive Committee:

WINSLOW CARLTON	N. B. MCLEAN	THOMAS J. WATSON, JR.
RACHEL L. CARSON	EDWARD A. NORMAN	JAMES H. WICKERSHAM
GEORGE F. JEWETT	MALCOLM S. PARK	WILLIAM D. WINTER
HENRY S. MORGAN		

By the end of the year plans were well along to offer certain industrial corporations and institutions, interested in the scientific study of the oceans, an opportunity to become members of the Woods Hole Oceanographic Associates.

The following visitors were among those who spent from one day to a few weeks at the Institution at one time or another during the year:

MR. M. AHMED, Central Fisheries Department, Ministry of Foreign Agriculture, Karachi, Pakistan
HIS IMPERIAL HIGHNESS AKIHITO, Crown Prince of Japan
DR. H. BENOIT, University of Strasbourg, France
DR. TOR BERGERON, University of Upsala, Sweden
DR. BERT BOLIN, University of Stockholm, Sweden
MR. E. L. BOUSFIELD, National Museum of Canada, Ottawa, Canada
DR. S. CHANDRASEKAR, Yerkes Observatory, Williams Bay, Wisconsin
MR. H. CHARNOCK, National Institute of Oceanography, England
COMMANDANT JACQUES-YVES COUSTEAU, French Navy

Dr. T. B. Davie, Vice-Chancellor, University of Capetown, South Africa
Mr. Edgar Deacon, C.S.I.R.O., Sydney, Australia
Dr. G. E. R. Deacon, National Institute of Oceanography, England
Dr. Maxwell Doty, University of Hawaii
Mr. E. T. Eady, Imperial College of London
Commander K. P. Farrell, Royal Canadian Navy
Dr. S. Jones, Central Fisheries, Barrackpore, India
Mr. D. J. Kim, University of Korea
Mr. B. J. Mason, Imperial College, London
Mr. H. J. McLellan, Fisheries Research Board of Canada
Dr. Fritz Moller, University of Mainz, Germany
Mr. Wendell A. Mordy, Pineapple Research Institute, Hawaii
Dr. C. H. Mortimer, Freshwater Biological Association, Ambleside, Westmoreland, England
Dr. A. W. H. Needler, Fisheries Research of Canada
Dr. Fergus J. O'Rourke, National University, Dublin, Ireland
Commander E. N. Poland, British Joint Services Mission
Lieut. Pinich Pukasab, Thailand Navy
Lt. Commander J. E. Ruse, Royal Canadian Navy
Dr. R. S. Scorer, Imperial College of Science and Technology, London, England
Mr. Unnsteinn Stefansson, University Research Institute, Department of Fisheries, Reykjavik, Iceland
Dr. Amar Nath Tandom, Poona, India
Mr. H. L. A. Torr, Fisheries Research Board, Vancouver, British Columbia

The persons whose names are listed below were members of the Institution (additional to those otherwise listed) for a period of six months or more during the calendar year 1953.

RESEARCH ASSISTANTS, ENGINEERS, AND TECHNICIANS

Anderson, Nellie T.
Athearn, William D.
Bergstrom, Stanley W.
Bradshaw, Alvin L.
Brainerd, Suzanne
Cain, Henry A.
Cangiamila, Angelo
Carter, Alwyn L.
Chute, Nancy W.
Conover, John T.
Corwin, Nathaniel
Creitz, Grace I.
Davis, Lee C.
Davis, Priscilla A.
Day, C. Godfrey
Duys, Gerrit, Jr.
Edwards, Melville E.
Fee, Frances M.
Gessner, Robert E.
Hanks, James E.
Hayes, Carlyle R.
Hoadley, Lloyd D.
Hodgson, Sloat F.
Kiernan, Clayton F.
Lufburrow, Robert A.
Newton, Chester W.
Owen, David M.
Parson, Donald, Jr.
Pasley, Gale G., Jr.
Pierce, Phebe
Pingree, Frederick deW.
Poole, Stanley E.
Posgay, Julius A.
Purinton, Charles S.
Raiche, Shirley A.
Rose, John C.
Ryan, Dorothy S.
Schroeder, Elizabeth H.
Shultz, William S.
Spencer, Allard T.
Thayer, Mary C.
Tollios, Evangeline P.
Vaccaro, Ralph F.
Volkmann, Gordon H.
Walsh, Martha A.
Whitney, Geoffrey G., Jr.
Wilkins, Charles H.
Witzell, Warren E.

TECHNICAL CLERKS AND SECRETARIES

Allen, Ethel B.
Atwood, Barbara
Bergstrom, Eileen J.
Bloedel, Pamela
Bowman, Phyllis R.
Bradley, Mabel D.
Brailey, Leola R.
Chase, Allison E.
English, Jean
Glaeser, Florence E.
Kerner, Patty Jo
Mellor, Florence
Ostiguy, Betty P.
Parker, Evelyn M.
Perry, Barbara L.
Posgay, Marjorie F.
Scharff, Margaret
Soderland, Eloise M.
Souza, Cecelia
Stewart, Doris H.
Wilson, Esther N.

ADMINISTRATIVE AND SECRETARIAL PERSONNEL

Backus, Jeanne M.
Behrens, Henry G.
Broadbent, Madeline P.
Bryant, Edwin T.
Casiles, Phyllis B.
Cook, Carol B.
Crocker, Marion W.
Dingwell, Eva Z.
Donald, Mary
Douthart, Dorothy E. S.
Ferris, Alice H.
Ferris, George A.
Griffin, T. S. Perry
Hatzikon, Kaleroy L.
Ortolani, Mary
Sandblom, John D.
Souza, Jane C.
Young, Anita M.

TECHNICAL SERVICES PERSONNEL

Allen, John L.
Bailey, Frank A.
Barstow, Elmer H.
Bennett, Paul E.
Blake, Forrest W.
Bodman, Ralph H.
Bowman, Warren O.
Chute, Edward H.
Condon, J. William
Dimmock, Richard H.
Dingwell, Paul E.
Dunkle, William M., Jr.
Eldridge, Stanley N.
Emery, Beverly S.
Feldman, Joel
Fisher, Stanley O.
Gallagher, Gloria S.
Gallagher, William F.
Gaskell, Fred
Gifford, James E.
Grant, Carleton
Hammond, Willis T.
Hodgkins, Harry L.
Howland, Myron P., Jr.
Morrison, Kenneth
Manning, Mary
Nelson, Dona E.
Rennie, Thomas D.
Ronne, F. Claude
Spooner, Charles E.
Spooner, Joanne C.
Stimpson, John W.
Thayer, Lawrence A.
Vail, Phyllis L.
Weeks, Robert G.
Wing, Carleton R.

MAINTENANCE, HOUSING, AND CUSTODIAL PERSONNEL

Backus, Harold
Christian, John A.
Cross, Donald E.
Fielden, Frederick E.
Polley, Robert E.
Salthouse, James
Solberg, Otto
Sparks, Elizabeth C.
Stansfield, Richard
Turner, Catherine
Wilde, Phillips B.
Wing, Nathaniel R.
Woodward, Fred C., Jr.
Yando, Anthony J.
York, Javan D.

OFFICERS AND CREW MEMBERS OF VESSELS, BOATS, AND AIRCRAFT

Adams, Malcolm H.
Backus, Cyril
Bailey, James S.
Barros, George M.
Bisaillon, Ralph
Bray, Winfield S.
Buck, Leo M.
Cabral, John V.
Casiles, David F.
Cavanaugh, James J.
Childs, Ashley B., Jr.
Clarkin, James J.
Colburn, Arthur D., Jr.
Conley, William J.
Cook, Hans
Copestick, Louis B.
Culliton, John F.
Day, Joseph V.
Ellis, Kenneth B.
Fay, Donald H.
Fournier, Richard A.
Gingrass, Norman
Hennessey, Richard F.
Howe, Paul M.
Howland, Paul C.
Karlson, Arvid
Lambert, Joseph L.
Lyon, Thomas
Mackey, Malcolm R.
Mathews, Francis S.
Merchant, Floyd L.
Mysona, Eugene J.
O'Brien, Warren E., Jr.
Palmieri, Michael
Peterson, Edward J.
Roderick, Milton
Rose, Lawrence
Seibert, Harry H.
Shields, William J.
Silva, Manuel F., Jr.
Smith, John J.
Speight, Carl W.
Waters, Francis V.
Williams, David H.

V. TREASURER'S REPORT

The accounts for the year 1953 have been audited by Messrs. Seamans, Stetson & Tuttle, Certified Public Accountants of Boston.

Endowment Fund Assets and Endowment Fund

The Endowment Fund cash plus the quoted market value of the investments in bonds and stocks at December 31, 1953 totaled $3,557,401.88, a decrease of $43,589.02 from the December 31, 1952 total. Of the total amount, $10,023.88 was in cash, $1,251,563.00 in bonds, a decrease of $11,741.43 from the book value, and $2,295,815.00 in stocks, an increase of $864,459.47 over the book value.

During the year bonds costing $105,344.62 were sold or redeemed for $102,911.25 which, after adding applicable amortization of bond premiums in the amount of $19.62, resulted in a realized loss of $2,413.75. Stocks and rights with book or assigned values of $125,214.57 were sold for $188,684.69, resulting in a net gain of $63,470.12. The total net gain from all sales or exchanges amounted to $61,056.37, thus bringing the accumulated net realized gain to the Endowment Fund to $285,263.88.

During the year, from the proceeds of the above sales and cash, $152,814.12 was invested in bonds and $130,987.00 in stocks, leaving $10,023.88 uninvested at the year-end.

Plant Assets and Plant Funds

Plant Assets decreased $30,818.84 during the year. This decrease resulted from the sale of the motor boats Allure and Mytilus for a total of $23,650.00. Proceeds of the sales were credited in the case of the Allure to Unexpended Balance of Gifts and in the case of the Mytilus to Surplus. Plant Assets were decreased by the book value of these two boats amounting to $50,458.30. The additions to the Plant Account were principally Laboratory Equipment and Library Books, and totaled $19,639.46. The decreases and additions combined to produce a net decrease in the Plant Assets of $30,818.84.

Current Assets and Current Liabilities

Cash and Accounts Receivable exceeded Accounts and Notes Payable and Unexpended Grants by $96,776.19, an improvement of $113,976.05 over last year. The Notes Payable were reduced $45,000 during the year.

Deferred Expenses decreased $41,613.78 during the year. The benefit of these expenses extends over several years, and each year a proportionate part is added to Current Costs.

Included in Deferred Expenses are the items "Boat Expenses" and "Motor Vessel BEAR". $6,317.36 was added to "Boat Expenses" during the year, and $1,053.14 to the "Motor Vessel BEAR." During the year $30,419.07 of Deferred Boat Expenses were charged to Current Boat Costs, and $17,500.00 of the Deferred Motor Vessel BEAR expense was charged to Current Boat Costs.

The item "Maintenance of Homestead" under Deferred Expenses covers costs of improvement of the parking lot at the Homestead property. This should be fully amortized by the end of 1955.

The Surplus Account decreased from $104,636.47 at the end of 1952 to $17,979.94 at the end of 1953. However, this decrease is principally the result of the transfers to the new General Plant and Equipment Reserve shown on the balance sheet. This reserve was set up by combining the depreciation recovered in past years by charges to overhead expenses which were credited to surplus, the depreciation so recovered in the current year, the periodic replacement fund, and the reserve for equipment purchases. The Reserve is available for replacements or acquisitions of new buildings, boats and equipment or other items for use by the Institution.

The Unexpended Balance of Gifts, amounting to $20,103.26, consists of a $3,258.74 unexpended balance of Woods Hole Oceanographic Associates' dues and contributions, and a $16,844.52 balance remaining from the proceeds of the sale of the ALLURE which was received as a gift from an Associate in 1952.

The Income and Salary Stabilization Reserve was established pursuant to a vote of the Executive Committee for the purpose of having reserve income available in case the income from investments is reduced, and to provide a reserve to meet salary commitments in the event of sudden termination of our Government contracts. At the beginning of each year the Finance Committee votes a percentage on original book value of the endowment to be allocated to the Year's budget. The balance is added to the Income and Salary Stabilization Reserve. The 1953 percentage so voted was 5.3%.

INCOME AND EXPENSES

The total income of the Institution from investments after deducting custodian fees and amortization of bond premiums amounts to $151,862.36, compared to $153,685.24 for the previous year. Of this $23,633.36 was added to the Income and Salary Stabilization Reserve and the balance of $128,229.00 went into the current income. Other income included grants and fees, which brought the total to $183,856.04.

The Institution does contract work for various governmental agencies

on a cost reimbursement basis, and during 1953 received a fee for work under these contracts amounting to $44,032.97, which amount is included in the Institution income.

The Housing and Mess were operated at losses of $4,580.27 and $1,685.12 respectively, which losses were included in overhead costs. The Hall property produced a net income of $105.06. The three comparable figures for the previous year were: Housing, loss of $5,845.21; Mess, loss of $3,001.32; and Hall property, net income of $1,048.49.

In the Income and Expense Statement the item "Cooperative Projects, $10,723.83" represents the expenditures by the Institution on Cooperative Projects, amounting to $57,381.76, less the total of grants and contributions, amounting to $46,657.93 received from the following: Arctic Institute of North America; Research Corporation; Commonwealth of Massachusetts; The Rockefeller Foundation; National Science Foundation and E. I. duPont de Nemours & Company.

Total cost of the operation of vessels during the year was $391,041.27. Of this amount $1,042.41 was charged to Cooperative and Institution Projects. The balance was charged to Government contracts and others.

The return on the investments held at the year-end was at the rate of 4.3% on the market value, 5.6% on the book value, and 6.3% on the original book value of the Endowment.

The Balance Sheets and Statement of Income and Expenses are appended.

BALANCE SHEET

As of December 31, 1953

ENDOWMENT FUND ASSETS

Bonds (Less Reserve for Amortization of Bond Premiums $2,880.33)		$1,263,304.43	
Quoted Market Value	$1,251,563.00		
Stocks		1,431,355.53	$2,694,659.96
Quoted Market Value	2,295,815.00		
	$3,547,378.00		
Cash			10,023.88
			$2,704,683.84

Note: Bonds having a book value of $399,809.43 are specifically allocated as collateral on the Institution's indebtedness to The New England Trust Company.

PLANT ASSETS

Laboratory Plant:			
Land		$27,072.32	
Buildings		336,564.86	
Laboratory Equipment		98,337.63	
Library		24,400.00	$486,374.81
Ketch "Atlantis":			
Construction	$218,674.47		
Equipment	41,462.50	260,136.97	
Ketch "Caryn"		98,275.43	
Small Boats and Equipment		6,570.55	364,982.95
Hall Property			26,500.00
Homestead			134,803.36
			$1,012,661.12

BALANCE SHEET

As of December 31, 1953

ENDOWMENT FUNDS

Endowment Fund — General	$2,000,000.00	
Endowment Fund — for Upkeep of Plant	419,419.96	$2,419,419.96
Add accumulated Net Gain on Securities Called or Sold		285,263.88
		$2,704,683.84

PLANT FUNDS

Plant Fund — General	$ 640,328.79
Plant Fund Reserve	372,332.33
	$1,012,661.12

BALANCE SHEET

As of December 31, 1953

(Concluded)

CURRENT ASSETS

CASH:		
Main Account	$153,846.14	
Operating Accounts	16,212.50	
Office and Boat Funds	1,419.02	$171,477.66
ACCOUNTS RECEIVABLE:		
Governmental Agencies:		
Invoiced	$72,561.13	
Not Invoiced	192,059.59	
	$264,620.72	
Co-operating Institutions	1,874.00	
Other Accounts Receivable	7,501.02	273,995.74
Total Cash and Accounts Receivable		$445,473.40
SUPPLIES AND WORK-IN-PROCESS		33,866.11
DEFERRED EXPENSES:		
Boat Expenses	$30,005.36	
Motor Vessel "Bear"	18,553.14	
Insurance Premiums	8,401.71	
Maintenance of Homestead	3,543.36	60,503.57
		$539,843.08

BALANCE SHEET

As of December 31, 1953

(Concluded)

CURRENT LIABILITIES

ACCOUNTS PAYABLE:			
Sundry Creditors		$11,328.15	
Withheld from Employees for Taxes, Insurance, etc.		11,666.89	
Sundry Accrued Expenses		4,692.28	$27,687.32
NOTES PAYABLE (SECURED BY BONDS HAVING A BOOK VALUE OF $399,809.43)			295,000.00
UNEXPENDED GRANTS			26,009.89
Total Accounts and Notes Payable and Unexpended Grants			$348,697.21
INCOME AND SALARY STABILIZATION RESERVE			23,633.36
UNEXPENDED BALANCE OF GIFTS			20,103.26
GENERAL PLANT AND EQUIPMENT RESERVE			129,429.31
SURPLUS:			
Balance, December 31, 1952		$104,636.47	
Deduct:			
Transfer to General Plant and Equipment Reserve:			
Depreciation Charged to Overhead	$77,081.57		
Periodic Replacement Fund	18,322.82		
Transfer to Unexpended Balance of Gifts	1,025.19	96,429.58	
		$8,206.89	
Add:			
Excess of Income	$2,919.63		
Prior Year Adjustments	6,203.42		
Sale of Motor Boat "Mytilus"	650.00	9,773.05	
Balance, December 31, 1953			17,979.94
			$539,843.08

INCOME AND EXPENSE STATEMENT

Year Ended December 31, 1953

INCOME:			
Investments:			
Interest	$ 36,985,79		
Dividends	115,813.73	$152,799.52	
Less:			
Reserved for Income and Salary Stabilization	$ 23,633.36		
Amortization of Bond Premiums	937.16	24,570.52	$128,229.00
Fees on Government Contracts			44,032.97
Other Income:			
Sundry Projects Credits (Non-Government)		$ 8,379.05	
Donations		1,110.00	
Sale of Equipment		1,150.00	
Hall Property (Net)		105.06	
Miscellaneous		849.96	11,594.07
			$183,856.04
EXPENSES:			
Operating		$98,072.27	
Institution Projects		46,544.86	
Co-operative Projects		10,723.83	
Interest Paid		9,856.05	
Operation of Vessels		627.92	
Adjustment of Contract		600.00	166,424.93
			$ 17,431.11
PAYMENT FOR PLANT ITEMS FROM CURRENT FUNDS:			
Laboratory Equipment		$11,460.53	
Library Books		1,200.00	
Equipment at Homestead		250.95	
		$12,911.48	
Reserved for Equipment Purchases		1,600.00	14,511.48
Excess of Income to Surplus			$ 2,919.63

APPENDIX

ATLANTIS

Cruise No.	Departure and Return	Days Duration	Ports of Call	Scientist-in-Charge
	1–10 February		Local trips	Vine
182	11 February		To Continental Shelf	Hersey
	12 February	2	To Woods Hole	
183	17 February		To Continental Shelf	Hersey
	20 February	4	Woods Hole	
184	6 March		Woods Hole to	Vine
	9 March	4	Bermuda	
	12 March		Bermuda to	
	15 March	4	Guantanamo Bay	
	16 March		To sea	
	26 March	11	Guantanamo Bay	
	28 March		Guantanamo Bay to	
	4 April	8	Kingston, Jamaica	
	6 April		Kingston to	
	9 April	4	Guantanamo Bay	
	11 April		Guantanamo Bay to	
	15 April	5	San Juan	
185	17 April		San Juan	Ewing
	21 April	½	San Juan to Roosevelt Roads	
	21 April		Roosevelt Roads to	
	23 April	3	San Juan	
	23 April		San Juan to	
	5 May	13	Guantanamo Bay	
	8 May		Guantanamo Bay to	
	27 May	20	Galveston, Texas	
	29 May		Galveston to	
	10 June	13	Woods Hole	Ewing
186	7 July		Woods Hole to	Officer
	13 July	7	St. Georges	
	15 July		St. Georges to	
	20 July	6	Woods Hole	
187	23 July		Woods Hole to	Wheeler
	31 July	9	Woods Hole	
	1 August	1	Associates Cruise	
188	7 August		Woods Hole to	Richards
	13 August	7	Norfolk	
	15 August		Norfolk to	
	1 September	18	Woods Hole	

ATLANTIS (Continued)

Cruise No.	Departure and Return	Days Duration	Ports of Call	Scientist-in-Charge
189	10 September		Woods Hole to	Stommel
	13 September	4	St. Georges	
	20 September		St. Georges to	
	22 September	3	St. Georges	
	26 September		St. Georges to	
	30 September	5	Woods Hole	
190	14 October		Woods Hole to	Volkman
	18 October	5	Woods Hole	
191	21 October		Woods Hole to	Vine
	26 October	6	Woods Hole	
192	29 October		Woods Hole to	Zeigler
	7 November	10	Woods Hole	
193	10 November		Woods Hole to	Fuglister
	14 November	5	Woods Hole	
194	22 November		Woods Hole to	Schultz
	25 November	4	Woods Hole	
195	7 December		Woods Hole to	Zeigler
	17 December	11	Woods Hole	

CAPTAIN BILL II (CHARTERED)

4	25 June		Woods Hole to Continental Shelf	Schroeder
	1 July	7	Woods Hole	
5	10 July		Woods Hole to Continental Shelf	Schroeder
	17 July	8	Woods Hole	
6	23 July		Woods Hole to Continental Shelf	Schroeder
	30 July	8	Woods Hole	

BLUE DOLPHIN (CHARTERED)

BD 6	13 June		Woods Hole to	Worthington
	24 June	12	St. Georges	
	26 June		St. Georges to	
	30 June	5	Woods Hole	
BD 7	11–19 July	9	Woods Hole	Backus
BD 8	22–30 July	9	Woods Hole	Leavitt
	1 August		Associates' Cruise	
BD 9	4– 8 August	5	Woods Hole	Backus
BD 10	11–14 August	4	Woods Hole	Backus
BD 11	17–27 August	11	Woods Hole	Backus

CARYN

Cruise No.	Departure and Return	Days Duration	Ports of Call		Scientist-in-Charge
56	15–17 January	3	Woods Hole	(Local)	Duys
57	22 January	1	Woods Hole	(Local)	Backus
58	27 January	1	Woods Hole	(Local)	Hersey
59	29 January	1	Woods Hole	(Local)	Hersey
60	30 January	1	Woods Hole	(Local)	Hersey
61	1 February		Woods Hole to		Dietz
	2 February	2	Boston		
	4 February	1	Boston	(Local)	
	5 February		Boston to		
	6 February	2	Woods Hole		
62	17–20 February	4	Woods Hole		Officer
63	1 March		Woods Hole to		Malkus
	5 March	5	Bermuda		
	10–11 March	2	Bermuda	(Local)	Stommel
	15–16 March	2	Bermuda	(Local)	
	16–20 March	5	Bermuda	(Local)	
	23 March	1	Bermuda	(Bermuda)	
	24–30 March	7	Bermuda	(Local)	
	2 April	1	Bermuda	(Local)	
	3– 6 April	4	Bermuda	(Local)	
	10 April		Bermuda to		
	16 April	7	Woods Hole		
64	8 May		Woods Hole to		von Arx
	14 May	7	Morehead City		
	16–20 May	5	Morehead City	(Local)	
	22–31 May	10	Morehead City	(Local)	
	4–11 June	8	Morehead City	(Local)	
	13 June		Morehead City to		
	20 June	8	Woods Hole		
65	28 June–2 July	5	Woods Hole	(Local)	Shultz
66	7 July		Woods Hole to		Johnson
	13 July	7	Bermuda		
	15 July		Bermuda to		
	20 July	6	Woods Hole		
67	23–31 July	7	Woods Hole	(Local)	Bergstrom
68	17–26 August	10	Woods Hole	(Local)	W. Malkus
69	31 August–6 September	7	Woods Hole	(Local)	Johnson
70	14–24 September	11	Woods Hole	(Local)	Fuglister

BEAR

Cruise No.	Departure and Return	Days Duration	Ports of Call	Scientist-in-Charge
	January through December		Short but frequent trips to sea	Hersey, Vine

PBY-6A, BUNO 46683

Flight No.	Departure and Return	Days Duration	Bases	Scientist-in-Charge
	January	13	Local flights	
P-41	10 Feb.		New Bedford to Kindley AFB	Malkus & Bunker
	11 and 12 Feb.		Local from Kindley	
	14 Feb.	5	Kindley AFB to New Bedford	
P-44	24 Feb.		Otis to Cherry Point	vox Arx
	25 Feb.		Cherry Point to Miami	
	26 Feb.		Miami to Jacksonville	
	27 Feb.	4	Jacksonville to New Bedford	
P-46	9 Mar.		New Bedford to Cherry Point	Malkus
	10 Mar.		Cherry Point to Miami	
	11 Mar.		Miami to San Juan	
	12 Mar.		San Juan to St. Thomas	
	14 Mar.		St. Thomas to San Juan	
	15 Mar. to 7 April		San Juan-St. Thomas and Anegada Area	
	8 April		San Juan to Jacksonville	
	9 April	32	Jacksonville to New Bedford	
P-47	30 April		New Bedford to Quebec	Richardson
	1 May		Quebec to Goose Bay, Newfoundland	
	2 May		Goose Bay to Bluie West 1	
	3 May		Bluie West Local	
	6 May		Bluie West to Rekjavik AFB	
	7 May		Rekjavik to Keflavik	
	9 and 11 May		Keflavik-Keflavik	
	12 May		Keflavik to Bluie West 1	
	13 May		Bluie West to Argentia	
	18–19 May		Argentia local	
	20 May	21	Argentia to Otis AFB	
P-48	2 June		Otis AFB to Cherry Point	Richardson
	3 to 6 June		Daily—Cherry Point local	
	7 June	6	Cherry Point to Otis AFB	
	7 July–19 July	6	Local flights	
P-55	20 July		Otis-Gulf Stream-Cherry Point	Richardson
	21 July		Cherry Pt.-Gulf Stream-Cherry Pt.	
	22 July	3	CherryPt.-Gulf Stream-New Bedford	
	27 July–18 Aug.	8	Local flights	

PBY-6A, BUNO 46683 (Continued)

Cruise No.	Departure and Return	Days Duration	Bases	Scientist-in-Charge
P-62	19 Aug.		Otis AFB to Columbus, Ohio	
	20 Aug.		Columbus to Omaha, Neb.	Bunker
	21 to 28 Aug.		Daily flights to O'Neil area	
	29 Aug.		Omaha to Cleveland	
	30 Aug.	12	Cleveland to Otis AFB	
P-66	25 Sept.		Otis to Cherry Point	Woollard
	27 Sept.		Cherry Point–Montgomery	
	28 Sept.		Montgomery–Houston	
	3 Oct.		Houston–Columbus, Ohio	
	4 Oct.	10	Columbus to Otis AFB	
	7 Oct. to 5 Nov.	11	Local flights	
P-78	8 Nov.		Otis to Kindley AFB	Richardson
	9 Nov.		Kindley to Otis AFB	
	10 Nov.		Otis to Kindley AFB	
	11 Nov.–20 Nov.		Daily local flights over Bermuda	
	23 Nov.	16	Kindley–Quonset	
	7–8 Dec.		Local flights	
P-82	9 Dec.		Otis-Quonset to Kindley	Richardson
	10 to 13 Dec.		Local flights over Bermuda	
	15 Dec.	7	Kindley to Quonset	
	17 to 31 Dec.	4	Local flights	

List of Contributions

No. 315. Gordon A. Riley. The Relationship of Vertical Turbulence and Spring Diatom Flowerings. *Sears Found., Jour. Mar. Res.*, Vol. 5, No. 1, pp. 67–87. 1942.

No. 316. Earl H. Myers. Biological Evidence as to the Rate at which Tests of Foraminifera are Contributed to Marine Sediments. *Jour. of Paleontology*, Vol. 16, No. 3, pp. 397–398. 1942.

No. 317. Richard E. Lee. The Hypophysis of the Broad-billed Swordfish, *Xiphias gladius* L. *Biol. Bull.*, Vol. 82, No. 3, pp. 401–412. 1942.

No. 318. Athelstan F. Spilhaus. Maps of the Whole World Ocean. *Geog. Rev.*, Vol. 32, No. 3, pp. 431–435. 1942.

No. 319. Gordon A. Riley. Physiological Aspects of Spring Diatom Flowerings. *Bull. Bingham Oceanographic Coll.*, Vol. 8, Art 4, pp. 1–53. 1943.

No. 320. Olga Hartman. Report on the Scientific Results of the *Atlantis* Expeditions to the West Indies under the joint auspices of the University of Havana and Harvard University. The Polychaetous Annelida. *Mem. Soc. Cub. Hist. Nat.*, Vol. 16, No. 2, pp. 89–104. 1942.

No. 321. Theodor von Brand, Norris W. Rakestraw and J. William Zabor. Decomposition and Regeneration of Nitrogenous Organic Matter in Sea Water. V. Factors Influencing the Length of the Cycle; Observations upon the Gaseous and Dissolved Organic Nitrogen. *Biol. Bull.*, Vol. 83, No. 2, pp. 273–282. 1942.

No. 322. Fenner A. Chace, Jr. Reports on the Scientific Results of the *Atlantis* Expeditions to the West Indies, under the joint auspices of the University of Havana and Harvard University. The Anomuran Crustacea. I. Galatheida (Families Chirostylidae, Galatheidae and Porcellanidae). *Torreia*, No. 11, pp. 1–106. 1942.

No. 323. William Schallek. The Reaction of Certain Crustacea to Direct and to Diffuse Light. *Biol. Bull.*, Vol. 84, No. 1, pp. 98–105. 1943.

No. 324. Richard E. Lee. Notes on the Color Changes of the Sea Robin (*Prionotus strigatus* Cuvier) with special reference to the Erythrophores. *Jour. Exper. Zool.*, Vol. 91, No. 2, pp. 131–153. 1942.

No. 325. Selman A. Waksman, Donald B. Johnstone and Cornelia L. Carey. The Effect of Copper upon the Development of Bacteria in Sea Water and the Isolation of Specific Bacteria. *Sears Found., Jour. Mar. Res.*, Vol. 5, No. 2, pp. 136–152. 1943.

No. 326. Robert W. Pyle. The Histogenesis and Cyclic Phenomena of the Sinus Gland and X-Organ in Crustacea. *Biol. Bull.*, Vol. 85, No. 2, pp. 87–102. 1943.

No. 327. Earl H. Myers. Life Activities of Foraminifera in Relation to Marine Ecology. *Proc. Amer. Philos. Soc.*, Vol. 86, No. 3, pp. 439–458. 1943.

No. 328. George L. Clarke, E. Lowe Pierce and Dean F. Bumpus. The Distribution and Reproduction of *Sagitta elegans* on Georges Bank in Relation to the Hydrographical Conditions. *Biol. Bull.*, Vol. 85, No. 3, pp. 201–226. 1943.

No. 329. A. A. Abramowitz, F. L. Hisaw and D. N. Papandrea. The Occurrence of a Diabetogenic Factor in the Eyestalks of Crustaceans. *Biol. Bull.*, Vol. 86, No. 1, pp. 1–5, 1944.

No. 330. Richard E. Lee. A Quantitative Survey of the Invertebrate Bottom Fauna in Menemsha Bight. *Biol. Bull.*, Vol. 86, No. 2, pp. 83–97. 1944.

No. 331. Alfred H. Woodcock. A Theory of Surface Water Motion deduced from the Wind-Induced Motion of the Physalia. *Sears Found., Jour. Mar. Res.*, Vol. 5, No. 3, pp. 196–205. 1944.

No. 332. Louis W. Hutchins. An Annotated Check-List of the Salt-Water Bryozoa of Long Island Sound. *Trans. Conn. Acad. Arts Sci.*, Vol. 36, pp. 533–551. 1945.

No. 333. Henry B. Bigelow and William C. Schroeder. New Sharks from the Western North Atlantic. *Proc. New Engl. Zool. Club*, Vol. 23, pp. 21–36. 1944.

No. 334. W. J. Clench and C. G. Aguayo. A New Tropical Buccinum From Cuba. *Rev. Soc. Malacol.*, Vol. 2, No. 2, pp. 67–68. 1944.

No. 335. Bostwick H. Ketchum, John D. Ferry, Alfred C. Redfield and Arthur E. Burns, Jr. Evaluation of Anti-fouling Paints by Leaching Rate Determinations. *Ind. Eng. Chem.*, Vol. 37, pp. 456–460. 1945.

No. 336. George T. Scott. The Influence of H-ion Concentration on the Mineral Composition of *Chlorella pyrenoidosa*. *Jour. Cell. and Comp. Physiol.*, Vol. 25, No. 1, pp. 37–44. 1945.

No. 337. George T. Scott. The Mineral Composition of Phosphate Deficient Cells of *Chlorella pyrenoidosa* during the Restoration of Phosphate. *Jour. Cell. and Comp. Physiol.*, Vol. 26, No. 1, pp. 35–42. 1945.

No. 338. Fred B Phleger, Jr. Vertical Distribution of Pelagic Foraminifera. *Amer. Jour. Sci.*, Vol. 243, pp. 377–383. 1945.

No. 339. Warren H. Yudkin. Occurrence of Thiaminase in Marine Teleosts. *Proc. Soc. Exper. Biol. and Med.*, Vol. 60, pp. 268–269. 1945.

No. 340. Irwin M. Newell. Studies on the Morphology and Systematics of the Family Halarachnidae Oudemans 1906 (Acari, Parasitoidae). *Bull. Bingham Oceanographic Coll.*, Vol. 10, Art. 4, pp. 235–266. 1947.

No. 341. Nelson Marshall. Observations on the Comparative Ecology and Life History of two Sea Robins, *Prionotus carolinus* and *Prionotus evolans strigatus*. *Copeia*, No. 3, pp. 118–144. 1946.

No. 342. John D. Ferry and Dayton E. Carritt. Action of Antifouling Paints. I. Solubility and Rate of Solution of Cuprous Oxide in Sea Water. *Ind. Eng. Chem.*, Vol. 38, pp. 612–617. 1946.

No. 343. M. Juul Hvorslev and Henry C. Stetson. Free-Fall Coring Tube: A New Type of Gravity Bottom Sampler. *Bull. Geol. Soc. Amer.*, Vol. 57, pp. 935–950. 1946.

No. 344. Fred B Phleger, Jr. and Walter A. Hamilton. Foraminifera of two Submarine Cores from the North Atlantic Basin. *Bull. Geol. Soc. Amer.*, Vol. 57, pp. 951–966. 1946.

No. 345. John D. Ferry and Gordon A. Riley. Action of Antifouling Paints. II. Solubilities of Antifouling Toxics in Sea Water. *Ind. Eng. Chem.*, Vol. 38, pp. 699–701. 1946.

No. 346. John D. Ferry and Bostwick H. Ketchum. Action of Antifouling Paints. III. Maintenance of the Leaching Rate of Antifouling Paints Formulated with Insoluble, Impermeable Matrices. *Ind. Eng. Chem.*, Vol. 38, pp. 806–810. 1946.

No. 347. Bostwick H. Ketchum, John D. Ferry and Arthur E. Burns, Jr. Action of Antifouling Paints. IV. Maintenance of Leaching Rate of Antifouling Paints Formulated with Soluble Matrices. *Ind. Eng. Chem.*, Vol. 38, pp. 931–936. 1946.

No. 348. Maurice Ewing, Allyn Vine, and J. L. Worzel. Photography of the Ocean Bottom. *Jour. Optical Soc. Amer.*, Vol. 36, No. 6, pp. 307–321. 1946.

No. 349. C. M. Pomerat and C. M. Weiss. The Influence of Texture and Composition of Surface on the Attachment of Sedentary Marine Organisms. *Biol. Bull.*, Vol. 91, No. 1, pp. 57–65. 1946.

No. 350. Marshall Schalk. A Study of Textural Changes in a Beach by repeated Samplings. *Jour. Sed. Petrology*, Vol. 16, No. 2, pp. 43–51. 1946.

No. 351. Maurice Ewing, G. P. Woollard, A. C. Vine, and J. L. Worzel. Recent Results in Submarine Geophysics. *Bull. Geol. Soc. Amer.*, Vol. 57, pp. 909–934. 1946.

No. 352. Gordon A. Riley and Dean F. Bumpus. Phytoplankton-Zooplankton Relationships on Georges Bank. *Sears Found., Jour. Mar. Res.*, Vol. 6, No. 1, pp. 33–47. 1946.

No. 353. Gordon A. Riley. Factors Controlling Phytoplankton Populations on Georges Bank. *Sears Found., Jour. Mar. Res.*, Vol. 6, No. 1, pp. 54–73. 1946.

No. 354. H. R. Seiwell. Military Oceanography in Tactical Operations of World War II. *Trans. Amer. Geophys. Union*, Vol. 27, No. 5, pp. 677–681. 1946.

No. 355. Henry Stommel. A Summary of the Theory of Convection Cells. *Annals N. Y. Acad. Sci.*, Vol. 48, Art. 8, pp. 715–726. 1947.

No. 356. A. H. Woodcock and Jeffries Wyman. Convective Motion in Air over the Sea. *Annals N. Y. Acad. Sci.*, Vol. 48, Art. 8, pp. 749–776. 1947.

No. 357. R. B. Montgomery. Introduction: Problems Concerning Convective Layers. *Annals N. Y. Acad. Sci.*, Vol. 48, Art. 8, pp. 707–713. 1947.

No. 358. Richard A. Craig. Observations of Vertical Temperature and Humidity Distributions in the Convective Layer above the Sea Surface. *Annals N. Y. Acad. Sci.*, Vol. 48, Art. 8, pp. 783–788. 1947.

No. 359. H. A. Panofsky. Radiative Cooling in the Lowest Layers of an Atmosphere Warmer than the Ground. *Jour. Meteorology*, Vol. 4, No. 1, pp. 35–37. 1947.

No. 360. George L. Clarke. Poisoning and Recovery in Barnacles and Mussels. *Biol. Bull.*, Vol. 92, No. 1, pp. 73–91. 1947.

No. 361. R. B. Montgomery. Over-water Refraction of 10-cm. Electromagnetic Radiation. *Bull. Amer. Meteorol. Soc.*, Vol. 28, No. 1, pp. 1–8. 1947.

No. 362. Richard A. Craig. Measurements of Temperature and Humidity in the lowest 1000 feet of the Atmosphere over Massachusetts Bay. *Papers in Physical Oceanography and Meteorology*, Vol. 10, No. 1, pp. 1–47. 1946.

No. 363. George L. Clarke. Dynamics of Production in a Marine Area. *Ecological Monographs*, Vol. 16, No. 4, pp. 322–335. 1946.

No. 364. Fred B. Phleger, Jr. Foraminifera of three Submarine Cores from the Tyrrhenian Sea. *Kungl. Vet.-o. Vitterh. Samh. Handl.*, F. 6, Ser. B, Bd 5, No. 5, pp. 1–19. 1947.

No. 365. Henry Stommel. Entrainment of Air into a Cumulus Cloud. *Jour. Meteorology*, Vol. 4, No. 3, pp. 91–94. 1947.

No. 366. Bostwick H. Ketchum. Plankton Algae and their Biological Significance. In: Manual of Phycology — an Introduction to the Algae and their Biology, Ch. 17, pp. 335–346. Gilbert M. Smith, Editor. Published by The Chronica Botanica Co., Waltham, Mass. 1951.

No. 367. Henry Stommel. Note on the Use of the T-S Correlation for Dynamic Height Anomaly Computations. *Sears Found., Jour. Mar. Res.*, Vol. 6, No. 2, pp. 85–92. 1947.

No. 368. Gordon A. Riley. A Theoretical Analysis of the Zooplankton Population of Georges Bank. *Sears Found., Jour. Mar. Res.*, Vol. 6, No. 2, pp. 104–113. 1947.

No. 369. Gordon A. Riley. Seasonal Fluctuations of the Phytoplankton Population in New England Coastal Waters. *Sears Found., Jour. Mar. Res.*, Vol. 6, No. 2, pp. 114–125. 1947.

No. 370. William S. von Arx. A Salinometer for use in Brackish Water. *Sears Found., Jour. Mar. Res.*, Vol. 6, No. 2, pp. 139–145. 1947.

No. 371. Norris W. Rakestraw and Theodor von Brand. Decomposition and Regeneration of Nitrogenous Organic Matter in Sea Water. VI. The Effect of Enzyme Poisons. *Biol. Bull.*, Vol. 92, No. 2, pp. 110–114. 1947.

No. 372. Alfred H. Woodcock and Gordon A. Riley. Patterns in Pond Ice. *Jour. Meteorology*, Vol. 4, No. 3, pp. 100–101. 1947.

No. 373. Alfred H. Woodcock and Henry Stommel. Temperatures Observed near the Surface of a Fresh-Water Pond at Night. *Jour. Meteorology*, Vol. 4, No. 3, pp. 102–103. 1947.

No. 374. Louis W. Hutchins. The Bases for Temperature Zonation in Geographical Distribution. *Ecological Monographs*, Vol. 17, No. 3, pp. 325–335. 1947.

No. 375. Norris W. Rakestraw. Oxygen Consumption in Sea Water over long Periods. *Sears Found., Jour. Mar. Res.*, Vol. 6, No. 3, pp. 259–263. 1947.

No. 376. Frances L. Parker. Foraminifera of the Continental Shelf from the Gulf of Maine to Maryland. *Bull. Mus. Comp. Zool.*, Vol. 100, No. 2, pp. 213–241. 1948.

No. 377. Bostwick H. Ketchum. The Biochemical Relations between Marine Organisms and their Environment. *Ecological Monographs*, Vol. 17, No. 3, pp. 309–315. 1947.

No. 378. F. G. Walton Smith. Mechanical Control of Ship-Bottom Fouling by means of Air Bubbles. *Jour. Fla. Acad. Sci.*, Vol. 9, Nos. 3–4, pp. 153-161. 1947.

No. 379. H. R. Seiwell. Oceangraphic Factors in Underwater Depth Determination by Aerial Photography. *Photogrammetric Eng.*, Vol. 15, No. 1, pp. 171–176. 1949.

No. 380. H. J. Turner, Jr., D. M. Reynolds and A. C. Redfield. Chlorine and Sodium Pentachlorophenate as Fouling Preventives in Sea Water Conduits. *Ind. Eng. Chem.*, Vol. 40, pp. 450–453. 1948.

No. 381. H. R. Seiwell. Resume of Military Oceanography in World War II. *The Military Engineer*, Vol. 39, No. 259, pp. 202–210. 1947. (Not included in *Collected Reprints.*)

No. 382. H. R. Seiwell. Tidal Illumination Diagrams. *Science*, Vol. 106, No. 2743, pp. 76–77. 1947.

No. 383. R. B. Montgomery and P. A. Sheppard. Comments on P. A. Sheppard's Direct Measurement of Ground Stress. *Quart. Jour. Roy. Meteor. Soc.*, Vol. 73, Nos. 317–318, pp. 459–463. 1947.

No. 384. Edward S. Deevey, Jr. Life Tables for Natural Populations of Animals. *Quart. Rev. Biol.*, Vol. 22, No. 4, pp. 283–314. 1947.

No. 385. Charles M. Weiss. The Comparative Tolerances of some Fouling Organisms to Copper and Mercury. *Biol. Bull.*, Vol. 93, No. 1, pp. 56–63. 1947.

No. 386. H. R. Seiwell. Investigation of Underwater Pressure Records and Simultaneous Sea Surface Patterns. *Trans. Amer. Geophys. Union*, Vol. 28, No. 5, pp. 722–724. 1947.

No. 387. Frederick C. Fuglister. Average Monthly Sea Surface Temperatures of the Western North Atlantic Ocean. *Papers in Physical Oceanography and Meteorology*, Vol. 10, No. 2, pp. 1–25. 1947.

No. 388. R. B. Montgomery. Viscosity and Thermal Conductivity of Air and Diffusivity of Water Vapor in Air. *Jour. Meteorology*, Vol. 4, No. 6, pp. 193–196. 1947.

No. 389. Alfred H. Woodcock. Note Concerning Human Respiratory Irritation Associated with High Concentrations of Plankton and Mass Mortality of Marine Organisms. *Sears Found., Jour. Mar. Res.*, Vol. 7, No. 1, pp. 56–62. 1948.

No. 390. Charles M. Weiss. An Observation on the Inhibition of Marine Wood Destroyers by Heavy Fouling Accumulation. *Ecology*, Vol. 29, No. 1, p. 120. 1948.

No. 391. Georgiana B. Deevey. The Zooplankton of Tisbury Great Pond. *Bull. Bingham Oceanographic Coll.*, Vol. 12, Art. 1, pp. 1–44. 1948.

No. 392. Charles M. Weiss. Observations on the Abnormal Development and Growth of Barnacles as Related to Surface Toxicity. *Ecology*, Vol. 29, No. 1, pp. 116–119. 1948.

No. 393. J. C. Decius. Dimensional Analysis: An Approach from Transformation Theory and a Criterion for Scaling Model Experiments. *Jour. Franklin Inst.*, Vol. 245, No. 5, pp. 379–387. 1948.

No. 394. Alfred C. Redfield. Characteristics of Sea Water. In: The Corrosion Handbook, pp. 1111–1122. H. H. Uhlig, Editor. Published by John Wiley & Sons, New York. 1948.

No. 395. George C. Whiteley, Jr. The Distribution of Larger Plankton Crustacea on Georges Bank. *Ecological Monographs*, Vol. 18, No. 2, pp. 233–264. 1948.

No. 396. William C. Schroeder. Notes on the Diet of the Goosefish, *Lophius americanus*. *Copeia*, No. 3, p. 201. 1947.

No. 397 Louis W. Hutchins and Margaret Scharff. Maximum and Minimum Monthly Mean Sea Surface Temperatures chartered from the "World Atlas of Sea Surface Temperatures". *Sears Found., Jour. Mar. Res.*, Vol. 6, No. 3, pp. 264–268. 1947.

No. 398. Bostwick H. Ketchum. Action of Antifouling Paints. V. Use of Glycine Solutions as Accelerated Test of Availability of Toxic. *Ind. Eng. Chem.*, Vol. 40, pp. 249–253. 1948.

No. 399. Bostwick H. Ketchum and John C. Ayers. Action of Antifouling Paints. VI. Effect of Nontoxic Pigments on the Performance of Antifouling Paints. *Ind. Eng. Chem.*, Vol. 40, pp. 2124–2127. 1948.

No. 400. Charles M. Weiss. The Effect of Illumination and Stage of Tide on the Attachment of Barnacle Cyprids. *Biol. Bull.*, Vol. 93, No. 3, pp. 240–249. 1947.

No. 401. W. S. Butcher. A New Species of *Nonion* (Foraminifera) from the Woods Hole Region. *Contr. Cushman Lab. Foram. Res.*, Vol. 24, (1), No. 308, pp. 21–23. 1948.

No. 402. Edward S. Deevey, Jr. On the Date of the Last Rise of Sea Level in Southern New England, with Remarks on the Grassy Island Site. *Amer. Jour. Sci.*, Vol. 246, pp. 329–352. 1948.

No. 403. Charles M. Weiss. The Abnormal Development of Tunicates Attached to Glass Surfaces Adjacent to Antifouling Paints. *Ecology*, Vol. 29, No. 2, pp. 215–218. 1948.

No. 404. Charles M. Weiss. The Seasonal Occurrence of Sedentary Marine Organisms in Biscayne Bay, Florida. *Ecology*, Vol. 29, No. 2, pp. 153–172. 1948.

No. 405. R. B. Montgomery. Vertical Eddy Flux of Heat in the Atmosphere. *Jour. Meteorology*, Vol. 5, No. 6, pp. 265–274. 1948.

No. 406. Hilary B. Moore. The Zooplankton of the Upper Waters of the Bermuda Area of the North Atlantic. *Sears Found., Jour. Mar. Res.*, Vol. 12, Art. 2, pp. 1–97. 1949. (Not included in *Collected Reprints*.)

No. 407. H. R. Seiwell. Evaluation of Sea-Surface Roughness from Underwater-Pressure Recordings. *Trans. Amer. Geophys. Union*, Vol. 29, No. 2, pp. 197–201. 1948.

No. 408. Henry Stommel. The Westward Intensification of Wind-Driven Ocean Currents. *Trans. Amer. Geophys. Union*, Vol. 29, No. 2, pp. 202–206. 1948.

No. 409. Sidney C. Hsiao. The Simple Micromethod for Rapid Extraction of Lipids. *Science*, Vol. 107, No. 2766, pp. 24–25. 1948.

No. 410. Austin H. Clark. Some Interesting Starfishes and Brittle-Stars Dredged by the *Atlantis* in the Mid-Atlantic. *Jour. Wash. Acad. Sci.*, Vol. 38, No. 2, pp. 75–78. 1948.

No. 411. Alfred C. Redfield and Charles M. Weiss. The Resistance of Metallic Silver to Marine Fouling. *Biol. Bull.*, Vol. 94, No. 1, pp. 25–28. 1948.

No. 412. J. B. Hersey and H. B. Moore. Progress Report on Scattering Layer Observations in the Atlantic Ocean. *Trans. Amer. Geophys. Union*, Vol. 29, No. 3, pp. 341–354. 1948.

No. 413. Gardner Emmons. Vertical Distributions of Temperature and Humidity over the Ocean between Nantucket and New Jersey. *Papers in Physical Oceanography and Meteorology*, Vol. 10, No. 3, pp. 1–89. 1947.

No. 414. W. T. Edmondson and Yvette H. Edmondson. Measurements of Production in Fertilized Salt-Water. *Sears Found., Jour. Mar. Res.*, Vol. 6, No. 3, pp. 228–245. 1947.

No. 415. J. Lamar Worzel and Maurice Ewing. Propagation of Sound in the Ocean: Explosion Sounds in Shallow Water. *Mem. Geol. Soc. Amer.*, 27, pp. i–vi, 1–53. 1948.

C. L. Pekeris. Propagation of Sound in the Ocean: Theory of Propagation of Explosive Sound in Shallow Water. *Mem. Geol. Soc. Amer.*, 27, pp. i–viii, 1–117. 1948.

Maurice Ewing and J. Lamar Worzel. Propagation of Sound in the Ocean: Long-Range Sound Transmission. *Mem. Geol. Soc. Amer.*, 27, pp. i–v, 1–35. 1948. (Not included in *Collected Reprints*.)

No. 416. Sidney Cornell. The Collapse of Long Cylindrical Shells under External Pressure. *Soc. Exper. Stress Analysis*, Vol. 6, No. 1, pp. 111–114. 1948.

No. 417. Alfred H. Woodcock. The Swimming of Dolphins. *Nature*, Vol. 161, p. 602. 1948.

No. 418. J. M. Richardson, A. B. Arons and R. R. Halverson. Hydrodynamic Properties of Sea Water at the Front of a Shock Wave. *Jour. Chem. Physics*, Vol. 15, No. 11, pp. 785–794. 1947.

No. 419. Bostwick H. Ketchum and Jean Keen. Unusual Phosphorus Concentrations in the Florida "Red Tide" Sea Water. *Sears Found., Jour. Mar. Res.*, Vol. 7, No. 1, pp. 17–21. 1948.

No. 420. C. A. Barnes, D. F. Bumpus and John Lyman. Ocean Circulation in Marshall Islands Area. *Trans. Amer. Geophys. Union*, Vol. 29, No. 6, pp. 871–876. 1948.

No. 421. William S. von Arx. The Circulation Systems of Bikini and Rongelap Lagoons. *Trans. Amer. Geophys. Union*, Vol. 29, No. 6, pp. 861–870. 1948.

No. 422. William L. Ford. Radiological and Salinity Relationships in the Water at Bikini Atoll. *Trans. Amer. Geophys. Union*, Vol. 30, No. 1, pp. 46–54. 1949.

No. 423. R. B. Montgomery. Ivory's Psychrometric Formula and the Concepts of Equivalent Temperature and Wet-Bulb Temperature. *Jour. Meteorology*, Vol. 5, No. 3, pp. 113–115. 1948.

No. 424. Parker D. Trask, Fred B Phleger, Jr., and Henry C. Stetson. Recent Changes in Sedimentation in the Gulf of Mexico. *Science*, Vol. 106, No. 2759, pp. 460–461. 1947.

No. 425. George L. Clarke and David W. Bishop. The Nutritional Value of Marine Zooplankton with a Consideration of its Use as an Emergency Food. *Ecology*, Vol. 29, No. 1, pp. 54–71. 1948.

No. 426. J. Lamar Worzel. Ocean Bottom Sampler for Ships Under Way. *Geophysics*, Vol. 13, No. 3, pp. 452–456. 1948.

No. 427. Clinton M. Osborn. Factors Influencing the Growth of Integumentary Pigment in Fishes. I. The Role of Light. *Proc. Soc. Exper. Biol. and Med.*, Vol. 67, pp. 440–445. 1948.

No. 428. A. W. Jacobson. An Instrument for Recording Continuously the Salinity, Temperature, and Depth of Sea Water. *Trans. Amer. Inst. Elec. Eng.*, Vol. 67, pp. 1–9. 1948.

No. 429. Fred B Phleger, Jr. Foraminifera of a Submarine Core from the Caribbean Sea. *Kungl. Vet.-o. Vittern. Samh. Handl.*, F. 6, Ser. B, Bd. 5, No. 14, pp. 1–9. 1948.

No. 430. A. B. Arons, J. P. Slifko and A. Carter. Secondary Pressure Pulses due to gas Globe Oscillation in Underwater Explosions. I. Experimental Data. *Jour. Acoust. Soc. Amer.*, Vol. 20, No. 3, pp. 271–276. 1948.

No. 431. A. B. Arons. Secondary Pressure Pulses due to Gas Globe Oscillation in Underwater Explosions. II. Selection of Adiabatic Parameters in the Theory of Oscillation. *Jour. Acoust. Soc. Amer.*, Vol. 20, No. 3, pp. 277–282. 1948.

No. 432. Talbot H. Waterman. Studies on Deep-Sea Angler-Fishes (Ceratioidea). III. The Comparative Anatomy of *Gigantactis longicirra* Waterman. *Jour. Morphology*, Vol. 82, No. 2, pp. 81–149. 1948.

No. 433. L. N. Liebermann. Reflection of Sound from Coastal Sea Bottoms. *Jour. Acoust. Soc. Amer.*, Vol. 20, No. 3, pp. 305–309. 1948.

No. 434. Charles M. Weiss. Seasonal and Annual Variations in the Attachment and Survival of Barnacle Cyprids. *Biol. Bull.*, Vol. 94, No. 3, pp. 236–243. 1948.

No. 435. H. R. Seiwell. Sea Surface Roughness Measurements in Theory and Practice. *Annals N. Y. Acad. Sci.*, Vol. 51, Art. 3, pp. 483–501. 1949.

No. 436. H. R. Seiwell. Results of Research on Surface Waves of the Western North Atlantic. I. Investigation of Bottom Pressure Fluctuations and Surface Waves. II. Results of Sea Roughness Determinations in the Vicinity of Woods Hole, Massachusetts and Bermuda. *Papers in Physical Oceanography and Meteorology*, Vol. 10, No. 4, pp. 1–56. 1948.

No. 437. A. B. Arons and R. H. Cole. Design and Use of Piezoelectric Gauges for Measurement of Large Transient Pressures. *Review of Sci. Instruments*, Vol. 21, No. 1, pp. 31–38. 1950.

No. 438. Arthur A. Klebba. Details of Shore-Based Wave Recorder and Ocean Wave Analyzer. *Annals N. Y. Acad. Sci.*, Vol. 51, Art. 3, pp. 533–544. 1949.

No. 439. Athelstan F. Spilhaus. Drop Size, Intensity and Radar Echo of Rain. *Jour. Meteorology*, Vol. 5, No. 4, pp. 161–164. 1948.

No. 440. Athelstan F. Spilhaus and Arthur R. Miller. The Sea Sampler. *Sears Found., Jour. Mar. Res.*, Vol. 7, No. 3, pp. 370–385. 1948.

No. 441. Gordon A. Riley and Samy Gorgy. Quantitative Studies of Summer Plankton Populations of the Western North Atlantic. *Sears Found., Jour. Mar. Res.*, Vol. 7, No. 2, pp. 100–121. 1948.

No. 442. Alfred C. Redfield. The Exchange of Oxygen across the Sea Surface. *Sears Found., Jour. Mar. Res.*, Vol. 7, No. 3, pp. 347–361. 1948.

No. 443. Patricia A. Langwell. Inhomogeneities of Turbulence, Temperature, and Moisture in the West Indies Trade-wind Region. *Jour. Meteorology*, Vol. 5, No. 5, pp. 243–246. 1948.

No. 444. Fred B. Phleger, Jr. Origin and Deposition of Deep Sea Sediments. *Trans. Amer. Geophys. Union*, Vol. 30, No. 2, pp. 180–182. 1949.

No. 445. B. Haurwitz. The Effect of Ocean Currents on Internal Waves. *Sears Found., Jour. Mar. Res.*, Vol. 7, No. 3, pp. 217–228. 1948.

No. 446. Bostwick H. Ketchum, Cornelia L. Carey and Margaret Briggs. Preliminary Studies on the Viability and Dispersal of Coliform Bacteria in the Sea. *In* Limnological Aspects of Water Supply and Waste Disposal. Ed. F. R. Moulton and and Florence Hitzel. *Publ. Amer. Assoc. Adv. Sci.*, pp. 64–73. 1949.

No. 447. Henry B. Bigelow and William C. Schroeder. New Genera and Species of Batoid Fishes. *Sears Found., Jour. Mar. Res.*, Vol. 7, No. 3, pp. 543–566. 1948.

No. 448. Hilary B. Moore. A Camera for Producing One-Dimensional Reduction in Narrow Records. *Sears Found., Jour. Mar. Res.*, Vol. 8, No. 1, pp. 21–23. 1949.

No. 449. A. B. Arons and D. R. Yennie. Energy Partition in Underwater Explosion Phenomena. *Rev. Modern Physics*, Vol. 20, No. 3, pp. 519–536. 1948. (Not included in *Collected Reprints.*)

No. 450. J. B. Hersey and Maurice Ewing. Seismic Reflections from beneath the Ocean Floor. *Trans. Amer. Geophys. Union*, Vol. 30, No. 1, pp. 5–14. 1949.

No. 451. C. O'D. Iselin and Frederick C. Fuglister. Some Recent Developments in the Study of the Gulf Stream. *Sears Found., Jour. Mar. Res.*, Vol. 7, No. 3, pp. 317–329. 1948.

No. 452. Norris W. Rakestraw and Dayton E. Carritt. Some Seasonal Chemical Changes in the Open Ocean. *Sears Found., Jour. Mar. Res.*, Vol. 7, No. 3, pp. 362–369. 1948.

No. 453. Henry Stommel. The Theory of the Electric Field Induced in Deep Ocean Currents. *Sears Found., Jour. Mar. Res.*, Vol. 7, No. 3, pp. 386–392. 1948.

No. 454. Parker D. Trask. Oceanography and Geosynclines. *Sears Found., Jour. Mar. Res.*, Vol. 7, No. 3, pp. 679–685. 1948.

No. 455. L. N. Liebermann. Reflection of Underwater Sound from the Sea Surface. *Jour. Acoust. Soc. Amer.*, Vol. 20, No. 4, pp. 498–503. 1948.

No. 456. Lewis F. Richardson and Henry Stommel. Note on Eddy Diffusion in the Sea. *Jour. Meteorology*, Vol. 5, No. 5, pp. 238–240. 1948.

No. 457. Joanne Starr Malkus. Effects of Wind Shear on Some Aspects of Convection. *Trans. Amer. Geophys. Union*, Vol. 30, No. 1, pp. 19–25. 1949.

No. 458. Alfred H. Woodcock and Mary M. Gifford. Sampling Atmospheric Sea-Salt Nuclei over the Ocean. *Sears Found., Jour. Mar. Res.*, Vol. 8, No. 2, pp. 177–197. 1949.

No. 459. William L. Ford. The Field Use of a Salinity-Temperature-Depth Recorder. *Sears Found., Jour. Mar. Res.*, Vol. 8, No. 1, pp. 84–96. 1949.

No. 460. William E. Schevill and Barbara Lawrence. Underwater Listening to the White Porpoise (*Delphinapterus Leucas*). *Science*, Vol. 109, No. 2824, pp. 143–144. 1949.

No. 461. H. R. Seiwell and George P. Wadsworth. A New Development in Ocean Wave Research. *Science*, Vol. 109, No. 2829, pp. 271–274. 1949.

No. 462. Harry J. Turner, Jr., John C. Ayers and Charles L. Wheeler. Report on Investigations of the Propagation of the Soft-Shell Clam, *Mya arenaria*. *Com. Mass., Dept. Cons., Div. Mar. Fish.*, pp. 1–61. 1948.

No. 463. Floyd M. Soule and E. R. Challender. Discussion of some of the Effects of Winds on Ice Distribution in the Vicinity of the Grand Banks and the Labrador Shelf. *U. S. Coast Guard Bull.*, No. 33, pp. 59–61. 1949.

No. 464. Gordon A. Riley, Henry Stommel and D. F. Bumpus. Quantitative Ecology of the Plankton of the Western North Atlantic. *Bull. Bingham Oceanographic Coll.*, Vol. 12, Art. 3, pp. 1–169. 1949. (Not included in *Collected Reprints*.)

No. 465. A. F. Bunker, B. Haurwitz, J. S. Malkus and H. Stommel. Vertical Distribution of Temperature and Humidity over the Caribbean Sea. *Papers in Physical Oceanography and Meteorology*, Vol. 11, No. 1, pp. 1–82. 1949.

No. 466. David M. Pratt. Experiments in the Fertilization of a Salt Water Pond. *Sears Found., Jour. Mar. Res.*, Vol. 8, No. 1, pp. 36–59. 1949.

No. 467. Floyd M. Soule, H. H. Carter and L. A. Cheney. Oceanography of the Grand Banks Region and Labrador Sea, 1948. *U. S. Coast Guard Bull.*, No. 33, pp. 67–118. 1950.

No. 468. Richard A. Craig. Vertical Eddy Transfer of Heat and Water Vapor in Stable Air. *Jour. Meteorology*, Vol. 6, No. 2, pp. 123–133. 1949.

No. 469. Henry Stommel. Trajectories of Small Bodies Sinking Slowly through Convection Cells. *Sears Found., Jour. Mar. Res.*, Vol. 8, No. 1, pp. 24–29. 1949.

No. 470. Henry W. Menard, Jr. Synthesis of Sand Mixtures. *Jour. Sed. Petrology*, Vol. 19, No. 2, pp. 71–77. 1949.

No. 471. Austin H. Clark. Echinoderms from the Mid-Atlantic Dredged by the *Atlantis* in the Summer of 1948. *Jour. Wash. Acad. Sci.*, Vol. 39, No. 11, pp. 371–377. 1949.

No. 472. Gordon A. Riley and Ruth Von Arx. Theoretical Analysis of Seasonal Changes in the Phytoplankton of Husan Harbor, Korea. *Sears Found., Jour. Mar. Res.*, Vol. 8, No. 1, pp. 60–72. 1949.

No. 473. Bostwick H. Ketchum, Lois Lillick and Alfred C. Redfield. The Growth and Optimum Yields of Unicellular Algae in Mass. Culture. *Jour. Cell. and Comp. Physiol.*, Vol. 33, No. 3, pp. 267–279. 1949.

No. 474. Bostwick H. Ketchum and Alfred C. Redfield. Some Physical and Chemical Characteristics of Algae Grown in Mass. Culture. *Jour. Cell. and Comp. Physiol.*, Vol. 33, No. 3, pp. 281–299. 1949.

No. 475. Joanne Starr Malkus. Cumulus, Thermals and Wind. *Soaring*, Vol. 13, Nos. 9–10, pp. 6–9, 12. 1949.

No. 476. Henry W. Menard. Transportation of Sediment by Bubbles. *Jour. Sed. Petrology*, Vol. 20, No. 2, pp. 98–106. 1950.

No. 477. B. Haurwitz. Internal Waves of Tidal Character. *Trans. Amer. Geophys. Union*, Vol. 31, No. 1, pp. 47–52. 1950.

No. 478. Richard A. Craig and R. B. Montgomery. Evaporation (Measured) from Ocean into Hydrostatically Stable Air. *Jour. Meteorology*, Vol. 6, No. 6, pp. 426-427. 1949.

No. 479. Athelstan F. Spilhaus, A. Ehrlich and Arthur R .Miller. Hydrostatic Instability in the Ocean. *Trans. Amer. Geophys. Union*, Vol. 31, No. 2, pp. 213–215. 1950.

No. 480. Maurice Ewing, J. L. Worzel, N. C. Steenland and Frank Press. Geophysical Investigations in the Emerged and Submerged Atlantic Coastal Plain. Part V: Woods Hole, New York, and Cape May Sections. *Bull. Geol. Soc. Amer.*, Vol. 61, pp. 877–892. 1950.

No. 481. Mary Sears. Notes on Siphonophores. I. Siphonophores from the Marshall Islands. *Sears Found., Jour. Mar. Res.*, Vol. 9, No. 1, pp. 1–16. 1950.

No. 482. R. B. Montgomery. The Taylor Diagram (Temperature against Vapor Pressure) for Air Mixtures. *Arch. Meteor. Geoph. und Bioklim.*, Serie A: Meteor. und Geoph., Bd. II, Heft 2–3, pp. 163–183. 1950.

No. 483. Maurice Ewing, J. L. Worzel, J. B. Hersey, Frank Press and G. R. Hamilton. Seismic Refraction Measurements in the Atlantic Ocean Basin. (Part I). *Bull. Seismol. Soc. Amer.*, Vol. 40, No. 3, pp. 233–242. 1950.

No. 484. Fred B. Phleger. The Foraminifera. *In* The Boylston Street Fishweir II. *Papers Robert S. Peabody Found. Archaeol.*, Vol. 4, No. 1, pp. 99–108. 1949.

No. 485. Fred B. Phleger. Submarine Geology and Pleistocene Research. A Review by the Members of the Committee on Interrelations of Pleistocene Research, National Research Council. 8. Submarine Geology and Pleistocene Research. *Bull. Geol. Soc. Amer.*, Vol. 60, pp. 1457–1461. 1949.

No. 486. H. R. Seiwell. The Principles of Time Series Analyses Applied to Ocean Wave Data. *Proc. Nat. Acad. Sci.*, Vol. 35, No. 9, pp. 518–528. 1949.

No. 487. Henry C. Stetson. The Sediments and Stratigraphy of the East Coast Continental Margin: Georges Bank to Norfolk Canyon. *Papers in Physical Oceanography and Meteorology*, Vol. 11, No. 2, pp. 1–60. 1949.

No. 488. Martin J. Pollak. Notes on Determining the Depths of Sampling in Serial Oceanographic Observations. *Sears Found., Jour. Mar. Res.*, Vol. 9, No. 1, pp. 17–20. 1950.

No. 489. Alfred H. Woodcock. Subsurface Pelagic Sargassum. *Sears Found., Jour. Mar. Res.*, Vol. 9, No. 2, pp. 77–92. 1950.

No. 490. A. B. Arons and D. R. Yennie. Phase Distortion of Acoustic Pulses Obliquely Reflected from a Medium of Higher Sound Velocity. *Jour. Acoust. Soc. Amer.*, Vol. 22, No. 2, pp. 231–237. 1950.

No. 491. Rushdi Said. Foraminifera of Narragansett Bay. *Contr. Cushman Found. Foram. Res.*, Vol. 2, (3), pp. 75–86. 1951.

No. 492. William L. Ford. Seagoing Photoelectric Colorimeter. *Analytical Chemistry*, Vol. 22, No. 11, pp. 1431–1435. 1950.

No. 493. Henry W. Menard. Current-Ripple Profiles and their Development. *Jour. Geology*, Vol. 58, No. 2, pp. 152–153. 1950.

No. 494. Jack L. Hough. Pleistocene Lithology of Antarctic Ocean-Bottom Sediments. *Jour. Geology*, Vol. 58, No. 3, pp. 254–260. 1950.

No. 495. Martin J. Pollak. The Water Structure in the Brownson Deep. *Trans. Amer. Geophys. Union*, Vol. 31, No. 3, pp. 393–397. 1950.

No. 496. Henry Stommel. Horizontal Diffusion Due to Oceanic Turbulence. *Sears Found., Jour. Mar. Res.*, Vol. 8, No. 3, pp. 199–225. 1949.

No. 497. David M. Pratt. Experimental Study of the Phosphorus Cycle in Fertilized Salt Water. *Sears Found., Jour. Mar. Res.*, Vol. 9, No. 1, pp. 29–54. 1950.

No. 498. Ivan Tolstoy and Maurice Ewing. North Atlantic Hydrography and the Mid-Atlantic Ridge. *Bull. Geol. Soc. Amer.*, Vol. 60, pp. 1527–1540. 1949.

No. 499. William S. von Arx. An Electromagnetic Method for Measuring the Velocities of Ocean Currents from a Ship Under Way. *Papers in Physical Oceanography and Meteorology*, Vol. 11, No. 3, pp. 1–62. 1950.

No. 500. Floyd M. Soule and C. A. Barnes. Physical Oceanography of the Ice Patrol Area in 1941. *U. S. Coast Guard Bull.*, No. 31, pp. 1–62. 1950.

No. 501. Alfred H. Woodcock. Condensation Nuclei and Precipitation. *Jour. Meteorology*, Vol. 7, No. 2, pp. 161–162. 1950.

No. 502. Andrew F. Bunker. Fluctuations of the Vertical Component of the Wind Associated with the Outflow of Cold Air from a Thunderstorm. *Bull. Amer. Meteorol. Soc.*, Vol. 31, No. 5, pp. 178–180. 1950.

No. 503. Henry Stommel. The Gulf Stream. A Brief History of the Ideas Concerning Its Cause. *The Scientific Monthly*, Vol. 70, No. 4, pp. 242–253. 1950.

No. 504. H. R. Seiwell. A New Mechanical Autocorrelator. *Review of Sci. Instruments*, Vol. 21, No. 5, pp. 481–484. 1950.

No. 505. H. R. Seiwell. Problems in Statistical Analyses of Geophysical Time Series. *Science*, Vol. 112, No. 2905, pp. 243–246. 1950.

No. 506. Ralph F. Vaccaro, Margaret P. Briggs, Cornelia L. Carey and Bostwick H. Ketchum. Viability of *Escherichia coli* in Sea Water. *Amer. Jour. Public Health*, Vol. 40, No. 10, pp. 1257–1266. 1950.

No. 507. Fred B. Phleger and William R. Walton. Ecology of Marsh and Bay Foraminifera, Barnstable, Mass. *Amer. Jour. Sci.*, Vol. 248, pp. 274–294. 1950.

No. 508. Jan Hahn. Some Aspects of Deep Sea Underwater Photography. *Jour. Photo. Soc. Amer.*, Sect. B. Phot. Sci. Tech., Vol. 16, No. 6, pp. 27–29. 1950.

No. 509. William S. von Arx. Some Current Meters Designed for Suspension from an Anchored Ship. *Sears Found., Jour. Mar. Res.*, Vol. 9, No. 2, pp. 93–99. 1950.

No. 510. Harry J. Turner, Jr. Report on Investigations of Methods of Improving the Shellfish Resources of Massachusetts. *Com. Mass., Dept. Cons., Div. Mar. Fish.*, pp. 1–22. 1949. (Included in Collected Reprints for 1950.)

No. 511. Henry B. Bigelow and William C. Schroeder. New and Little Known Cartilaginous Fishes from the Atlantic. *Bull. Mus. Comp. Zool.*, Vol. 103, No. 7, pp. 385–408. 1950.

No. 512. Henry W. Menard. Sediment Movement in Relation to Current Velocity. *Jour. Sed. Petrology*, Vol. 20, No. 3, pp. 148–160. 1950.

No. 513. B. Haurwitz and H. A. Panofsky. Stability and Meandering of the Gulf Stream. *Trans. Amer. Geoph. Union*, Vol. 31, No. 5, pp. 723–731. 1950.

No. 514. Alfred C. Redfield. Some Applications of Oceanography to Engineering Problems. *Jour. Boston Soc. Civil Eng.*, Vol. 37, No. 3, pp. 275–295. 1950.

No. 515. Bostwick H. Ketchum. Hydrographic Factors Involved in the Dispersion of Pollutants Introduced into Tidal Waters. *Jour. Boston Soc. Civil Eng.*, Vol. 37, No. 3, pp. 296–314. 1950.

No. 516. Bostwick H. Ketchum. The Exchanges of Fresh and Salt Waters in Tidal Estuaries. *Sears Found., Jour. Mar. Res.*, Vol. 10, No. 1, pp. 18–38. 1951.

No. 517. Alfred H. Woodcock. Impact Deposition of Atmospheric Sea Salts on a Test Plate. *Amer. Soc. for Testing Materials*, Vol. 50, pp. 1151–1166. 1950.

No. 518. Arthur R. Miller. A Study of Mixing Processes over the Edge of the Continental Shelf. *Sears Found., Jour. Mar. Res.*, Vol. 9, No. 2, pp. 145–160. 1950.

No. 519. Vern O. Knudsen, Alfred C. Redfield, Roger Revelle, and Robert R. Shrock. Education and Training for Oceanographers. *Science*, Vol. 111, No. 2895, pp. 700–703. 1950.

No. 520. George L. Clarke. Conservation and the Productivity of the Sea. *The Gamma Alpha Record*, Vol. 40, No. 4, pp. 95–101. 1950.

No. 521. H. R. Seiwell. Ocean Wave Analyses. In: Symposium on Applications of Autocorrelation Analysis to Physical Problems, Woods Hole, Massachusetts, 13–14 June 1949, *Office of Naval Research*, NAVEXOS-P-735, pp. 74–79. 1950.

No. 522. Alfred H. Woodcock and A. F. McBride. Wave-riding Dolphins. *Jour. Exper. Biol.*, Vol. 28, No. 2, pp. 215–217. 1951.

No. 523. John Northrop and Bruce C. Heezen. An Outcrop of Eocene Sediment on the Continental Slope. *Jour. Geology*, Vol. 59, No. 4, pp. 396–399. 1951.

No. 524. Henry Stommel. An Example of Thermal Convection. *Trans. Amer. Geophys. Union*, Vol. 31, No. 4, pp. 553–554. 1950.

No. 525. Alfred C. Redfield. Hemocyanin. In: Copper Metabolism, A Symposium on Animal, Plant and Soil Relationships, W. D. McElroy and B. Glass, Editors, Johns Hopkins University Press, pp. 174–190. 1950.

No. 526. William S. von Arx. Dead Reckoning by Surface Current Observation. *Jour. Inst. Navigation* (London), Vol. 4, No. 2, pp. 117–125. 1951.

No. 527. Patricia A. Langwell. Forced Convection Cell Circulation in Clear Air. *Trans. Amer. Geophys. Union*, Vol. 32, No. 1, pp. 7–14. 1951.

No. 528. Alfred H. Woodcock. Sea Salt in a Tropical Storm. *Jour. Meteorology*, Vol. 7, No. 6, pp. 397–401. 1950.

No. 529. Alfred C. Redfield. The Analysis of Tidal Phenomena in Narrow Embayments. *Papers in Physical Oceanography and Meteorology*, Vol. 11, No. 4, pp. 1–36. 1950.

No. 530. G. L. Clarke and D. F. Bumpus. The Plankton Sampler — An Instrument for Quantitative Plankton Investigations. *Amer. Soc. Limnol. and Oceanogr.*, Spec. Publ. No. 5 (revised), pp. 1–8. 1950.

No. 531. H. R. Seiwell. Experimental Correlogram Analyses of Artificial Time Series (with Special Reference to Analyses of Oceanographic Data). In: Proc. Second Berkeley Symposium on Mathematical Statistics and Probability, Univ. Calif. Press, pp. 639–666. 1951. (Published posthumously.)

No. 532. Henry Stommel. An Elementary Explanation of Why Ocean Currents are Strongest in the West. *Bull. Amer. Meteorol. Soc.*, Vol. 32, No. 1, pp. 21–23. 1951.

No. 533. Henry Stommel. Entrainment of Air into a Cumulus Cloud II. *Jour. Meteorol.*, Vol. 8, No. 2, pp. 127–129. 1951.

No. 534. Joanne Starr Malkus, Andrew F. Bunker and Kenneth McCasland. A Formation of Pileus-like Veil Clouds over Cape Cod, Massachusetts. *Bull. Amer. Meteorol. Soc.*, Vol. 32, No. 2, pp. 61–66. 1951.

No. 535. Hilary B. Moore. The Relation between the Scattering Layer and the Euphausiacea. *Biol. Bull.*, Vol. 99, No. 2, pp. 181–212. 1950.

No. 536. Bostwick H. Ketchum. The Flushing of Tidal Estuaries. *Sewage and Industrial Wastes*, Vol. 23, No. 2, pp. 198–209. 1951.

No. 537. Henry Stommel. Streaks of Natural Water Surfaces. In: International Symposium on Atmospheric Turbulence in the Boundary Layer. Mass. Inst. Tech., 4–8 June, 1951. *Geophys. Res. Pap., Air Force Cambridge Research Center*, No. 19, pp. 145–154. 1952.

No. 538. Henry Stommel. Streaks on Natural Water Surfaces. *Weather*, Vol. 6, No. 3, pp. 72–74. 1951.

No. 539. Edward S. Castle. Electrical Control of Marine Fouling. *Ind. Eng. Chem.*, Vol. 43, No. 4, pp. 901–904. 1951.

No. 540. Rushdi Said. Organic Origin of some Calcareous Sediments from the Red Sea. *Science*, Vol. 113, No. 2940, pp. 517–518. 1951.

No. 541. Rushdi Said. Preliminary Note on the Spectroscopic Distribution of Elements in the Shells of some Recent Calcareous Foraminifera. *Contr. Cushman Found. Foram. Res.*, Vol. 2, Pt. 1, pp. 11–13. 1951.

No. 542. Gordon A. Riley. Oxygen, Phosphate and Nitrate in the Atlantic Ocean. *Bull. Bingham Oceanographic Coll.*, Vol. 13, Art. 1, pp. 1–126. 1951. (Not included in *Collected Reprints*.)

No. 543. J. Lamar Worzel and Maurice Ewing. Gravity Measurements at Sea, 1947. *Trans. Amer. Geophys. Union*, Vol. 31, No. 6, pp. 917–923. 1950.

No. 544. Arnold B. Arons and Henry Stommel. A Mixing-length Theory of Tidal Flushing. *Trans. Amer. Geophys. Union*, Vol. 32, No. 3, pp. 419–421. 1951.

No. 545. Arthur A. Klebba and Henry Stommel. A Simple Demonstration of Coriolis Force. *Amer. Jour. Physics*, Vol. 19, No. 4, p. 247. 1951.

No. 546. Henry W. Menard and A. J. Boucot. Experiments on the Movement of Shells by Water. *Amer. Jour. Sci.*, Vol. 249, No. 2, pp. 131–151. 1951.

No. 547. E. W. Roelofs and D. F. Bumpus. The Hydrography of Pamlico Sound. *Bull. Mar. Sci. Gulf and Caribbean*, Vol 3, No. 3, pp. 181–205. 1953.

No. 548. Frederick C. Fuglister and L. V. Worthington. Some Results of a Multiple Ship Survey of the Gulf Stream. *Tellus*, Vol. 3, No. 1, pp. 1–14. 1951.

No. 549. Bostwick H. Ketchum, Alfred C. Redfield and John C. Ayers. The Oceanography of the New York Bight. *Papers in Physical Oceanography and Meteorology*, Vol. 12, No. 1, pp. 1–46. 1951.

No. 550. Floyd M. Soule. Physical Oceanography of the Grand Banks Region, the Labrador Sea and Davis Strait in 1949. *U. S. Coast Guard Bull.*, No. 35, pp. 49–116. 1951.

No. 551. Floyd M. Soule. Physical Oceanography of the Grand Banks Region and the Labrador Sea in 1950. *U. S. Coast Guard Bull.*, No. 36, pp. 61–127. 1951.

No. 552. Henry Stommel. Determination of the Lateral Eddy Diffusivity in the Climatological Mean Gulf Stream. *Tellus*, Vol. 3, No. 1, p. 43. 1951.

No. 553. Henry Stommel and Alfred H. Woodcock. Diurnal Heating of the Surface of the Gulf of Mexico in the Spring of 1942. *Trans. Amer. Geophys. Union*, Vol. 32, No. 4, pp. 565–571. 1951.

No. 554. Henry B. Bigelow and William C. Schroeder. A New Genus and Species of Anacanthobatid Skate from the Gulf of Mexico. *Journ. Wash. Acad. Sci.*, Vol. 41, No. 3, pp. 110–113. 1951.

No. 555. Henry B. Bigelow and William C. Schroeder. Three New Skates and a New Chimaerid Fish from the Gulf of Mexico. *Journ. Wash. Acad. Sci.*, Vol. 41, No. 12, pp. 383–392. 1951.

No. 556. Martin J. Pollak. The Sources of the Deep Water of the Eastern Mediterranean Sea. *Sears Found., Jour. Mar. Res.*, Vol. 10, No. 1, pp. 128–152. 1951.

No. 557. Frederick C. Fuglister. Annual Variations in Current Speeds in the Gulf Stream System. *Sears Found., Jour. Mar. Res.*, Vol. 10, No. 1, pp. 119–127. 1951.

No. 558. Donald Parson and Andrew F. Bunker. A Recording Computer for the Direct Measurement of the Turbulent Heat Exchange in the Atmosphere. In: International Symposium on Atmospheric Turbulence in the Boundary Layer. Mass. Inst. Tech., 4–8 June, 1951. *Geophys. Res. Pap., Air Force Cambridge Research Center*, No. 19, pp. 369–379. 1952.

No. 559. Ivan Tolstoy. Submarine Topography in the North Atlantic. *Bull. Geol. Soc. Amer.*, Vol. 62, No. 5, pp. 441–450. 1951.

No. 560. Hilary B. Moore. The Seasonal Distribution of Oceanic Birds in the Western North Atlantic. *Bull. Mar. Sci. Gulf and Caribbean*, Vol. 1, No. 1, pp. 1–14. 1951.

No. 561. Bostwick H. Ketchum, John C. Ayers and Ralph F. Vaccaro. Processes Contributing to the Decrease of Coliform Bacteria in a Tidal Estuary. *Ecology*, Vol. 33, No. 2, pp. 247–258. 1952.

No. 562. J. B. Hersey, H. R. Johnson and L. C. Davis. Recent Findings about the Deep Scattering Layer. *Sears Found., Jour. Mar. Res.*, Vol. 11, No. 1, pp. 1–9. 1952.

No. 563. Alfred H. Woodcock. Atmospheric Salt Particles and Raindrops. *Jour. Meteorol.*, Vol. 9, No. 3, pp. 200–212. 1952.

No. 564. Harry J. Turner, Jr., David B. Sawyer, Carl N. Shuster, Jr., and Julius A. Posgay. Third Report on Investigations of Methods of Improving the Shellfish Resources of Massachusetts. *Com. Mass., Dept. Cons., Div. Mar. Fish.*, pp. 1–31. 1951.

No. 565. Fred B. Phleger. Ecology of Foraminifera, Northwest Gulf of Mexico. Part I. Foraminifera Distribution. *Mem. Geol. Soc. Amer.*, No. 46, pp. 1–88. 1951. (Not included in *Collected Reprints.*)

No. 566. Fred B. Phleger and Frances L. Parker. Ecology of Foraminifera, Northwest Gulf of Mexico. Part II. Foraminifera Species. *Mem. Geol. Soc. Amer.*, No. 46, pp. 1–64. 1951. (Not included in *Collected Reprints.*)

No. 567. Bostwick H. Ketchum and William L. Ford. Rate of Dispersion in the Wake of a Barge at Sea. *Trans. Amer. Geophys. Union*, Vol. 33, No. 5, pp. 680–684. 1952.

No. 568. Patricia A. Langwell. The Onset of Rain from Cumuli. *Jour. Meteorol.*, Vol. 8, No. 5, pp. 354–356. 1951.

No. 569. Stefan Machlup. A Theoretical Model for Sound Scattering by Marine Crustaceans. *Jour. Acoust. Soc. Amer.*, Vol. 24, No. 3, pp. 290–293. 1952.

No. 572. Andrew F. Bunker. Recognition of the Presence of Convective Currents within a Nonsaturated Turbulent Layer of the Atmosphere. In: International Symposium on Atmospheric Turbulence in the Boundary Layer. Mass. Inst. Tech., 4–8 June, 1951. *Geophys. Res. Pap., Air Force Cambridge Research Center*, No. 19, pp. 309–322. 1952.

No. 573. John Northrop. Ocean-bottom Photographs of the Neritic and Bathyal Environment South of Cape Cod, Massachusetts. *Bull. Geol. Soc. Amer.*, Vol. 62, No. 12, pp. 1381–1384. 1951.

No. 574. I. I. Schell. Stability and Mutual Compensation of Relationships with the Iceberg Severity off Newfoundland. *Trans. Amer. Geophys. Union*, Vol. 33, No. 1, pp. 27–31. 1952.

No. 575. D. B. Ericson, Maurice Ewing and Bruce C. Heezen. Deep-sea Sands and Submarine Canyons. *Bull. Geol. Soc. Amer.*, Vol. 62, No. 8, pp. 961–965. 1951.

No. 576. R. B. Montgomery. The Present Position of the Study of Exchange across the Ocean-Atmosphere Interface. In: International Symposium on Atmospheric Turbulence in the Boundary Layer. Mass. Inst. Tech., 4–8 June, 1951. *Geophys. Res. Pap., Air Force Cambridge Research Center*, No. 19, pp. 131–140. 1952.

No. 577. Gordon A. Riley. Parameters of Turbulence in the Sea. *Sears Found., Jour. Mar. Res.*, Vol. 10, No. 3, pp. 247–256. 1951.

No. 578. Gordon A. Riley. Hydrography of the Long Island and Block Island Sounds. *Bull. Bingham Oceanographic Coll.*, Vol. 13, Art. 3, pp. 5–39. 1952.

No. 579. Gordon A. Riley. Phytoplankton of Block Island Sound, 1949. *Bull. Bingham Oceanographic Coll.*, Vol. 13, Art. 3, pp. 40–64. 1952.

No. 580. Woods Hole Oceanographic Institution. Marine Fouling and its Prevention. U. S. Naval Inst., Annapolis, Md. 388 pp. 1952. (Not included in *Collected Reprints.*)

No. 581. Hilary B. Moore. Physical Factors Affecting the Distribution of Euphausids in the North Atlantic. *Bull. Mar. Sci. Gulf and Caribbean*, Vol. 1, No. 4, pp. 278–305. 1952.

No. 582. Henry A. Kierstead. Bottom Pressure Fluctuations due to Standing Waves in a Deep, Two-Layer Ocean. *Trans. Amer. Geophys. Union*, Vol. 33, No. 3, pp. 390–396. 1952.

No. 583. J. B. Hersey, Charles B. Officer, H. R. Johnson, and S. Bergstrom. Seismic Refraction Observations North of the Brownson Deep. *Bull. Seismol. Soc. Amer.*, Vol. 42, No. 4, pp. 291–306. 1952.

No. 584. Frederick C. Fuglister. Multiple Currents in the Gulf Stream System. *Tellus*, Vol. 3, No. 4, pp. 230–233. 1951.

No. 585. Gerald B. Collins. Factors Influencing the Orientation of Migrating Anadromous Fishes. Fish and Wildlife Service, Vol. 52, *Fish. Bull.* 73, pp. 375–396. 1952.

No. 586. Alfred C. Redfield and Lionel A. Walford. A Study of the Disposal of Chemical Waste at Sea. Report of the Committee for Investigation of Waste Disposal. *Nat. Res. Council*, Publ. 201, 49 pp. 1951.

No. 587. Henry Stommel and Harlow G. Farmer. Control of Salinity in an Estuary by a Transition. *Sears Found., Jour. Mar. Res.*, Vol. 12, No. 1, pp. 13–20. 1953.

No. 588. Rushdi Said. Foraminifera of Great Pond, East Falmouth, Massachusetts. *Contr. Cushman Found. Foram. Res.*, Vol. 4, Pt. 1, pp. 7–14. 1953.

No. 589. Frances L. Parker. Foraminifera Species off Portsmouth, New Hampshire. *Bull. Mus. Comp. Zool.*, Vol. 106, No. 9, pp. 391–423. 1952.

No. 590. Frances L. Parker. Foraminiferal Distribution in the Long Island Sound-Buzzards Bay Area. *Bull. Mus. Comp. Zool.*, Vol. 106, No. 10, pp. 427–473. 1952.

No. 591. Fred B. Phleger. Foraminifera Ecology off Portsmouth, New Hampshire. *Bull. Mus. Comp. Zool.*, Vol. 106, No. 8, pp. 315–390. 1952.

No. 592. Henry B. Bigelow and William C. Schroeder. Fishes of the Gulf of Maine. Fish and Wildlife Service, Vol. 53, *Fish. Bull.* 74, pp. i–viii, 1–577. 1953. (Not included in *Collected Reprints*.)

No. 593. Bostwick H. Ketchum and D. Jean Keen. The Exchanges of Fresh and Salt Waters in the Bay of Fundy and in Passamaquoddy Bay. *Jour. Fish. Res. Bd. Canada*, Vol. 10, No. 3, pp. 97–124. 1953.

No. 594. I. I. Schell. The Problem of the Iceberg Population in Baffin Bay and Davis Strait and Advance Estimate of the Berg Count off Newfoundland. *Jour. Glaciology*, Vol. 2, No. 11, pp. 58–59. 1952.

No. 595. Joanne Starr Malkus. Recent Advances in the Study of Convective Clouds and their Interaction with the Environment. *Tellus*, Vol. 4, No. 2, pp. 71–87. 1952.

No. 596. Henry B. Bigelow, William C. Schroeder and Stewart Springer. New and Little Known Sharks from the Atlantic and from the Gulf of Mexico. *Bull. Mus. Comp. Zool.*, Vol. 109, No. 3, pp. 213–276. 1953.

No. 599. Frank J. Mather, III. Three Species of Fishes, Genus *Seriola*, in the Waters of Cape Cod and Vicinity. *Copeia*, No. 3, pp. 209–210. 1952.

No. 600. Jeffries Wyman, Jr., P. F. Scholander, G. A. Edwards and L. Irving. On the Stability of Gas Bubbles in Sea Water. *Sears Found., Jour. Mar. Res.*, Vol. 11, No. 1, pp. 47–62. 1952.

No. 601. Floyd M. Soule, P. S. Branson and R. P. Dinsmore. Physical Oceanography of the Grand Banks Region and the Labrador Sea in 1951. *U. S. Coast Guard Bull.*, No. 37, pp. 17–85. 1952.

No. 602. Mary Sears. Notes on Siphonophores. 2. A Revision of the Abylinae. *Bull. Mus. Comp. Zool.*, Vol. 109, No. 1, pp. 1–119. 1953. (Not included in *Collected Reprints*.)

No. 603. I. I. Schell. On the Role of the Ice off Iceland in the Decadal Air Temperatures of Iceland, and some other Areas. *Jour. du Conseil*, Vol. 18, No. 1, pp. 11–36. 1952.

No. 604. D. B. Ericson, Maurice Ewing and Bruce C. Heezen. Turbidity Currents and Sediments in the North Atlantic. *Bull. Amer. Assoc. Petrol. Geol.*, Vol. 36, No. 3, pp. 489–511. 1952.

No. 605. Andrew F. Bunker. On the Determination of Moisture Gradients from Radiosonde Records. *Bull. Amer. Meteorol. Soc.*, Vol. 34, No. 9, pp. 406–409. 1953.

No. 606. Frank J. Mather, III and Howard A. Schuck. Additional Notes on the Distribution of the Blackfin Tuna (*Parathunnus atlanticus*). *Copeia*, No. 4, p. 267. 1952.

No. 607. Mary Sears. Notes on Siphonophores. 3. *Nectopyramis spinosa* n. sp. *Breviora*, No. 3, pp. 1–4. 1952.

No. 608. W. V. R. Malkus and M. E. Stern. Determination of Ocean Transports and Velocities by Electromagnetic Effects. *Sears Found., Jour. Mar. Res.*, Vol. 11, No. 2, pp. 97–105. 1952.

No. 609. Joanne Starr Malkus. The Slopes of Cumulus Clouds in Relation to External Wind Shear. *Quart. Jour. Roy. Meteor. Soc.*, Vol. 78, No. 338, pp. 530–542. 1952.

No. 610. Henry B. Bigelow and William C. Schroeder. A New Species of the Cyclostome Genus *Paramyxine* from the Gulf of Mexico. *Breviora*, No. 8, pp. 1–10. 1952.

No. 611. Frank J. Mather, III. Sport Fishes of the Vicinity of the Gulf of Honduras, certain Caribbean Islands, and Carmen, Mexico. *Proc. Gulf and Caribbean Fish. Inst.*, pp. 118–129. 1952.

No. 612. C. O'D. Iselin. The Gulf Stream System. *Proc. Amer. Philos. Soc.*, Vol. 96, No. 6, pp. 660–662. 1952.

No. 613. Frederick B. Laidlaw. The History of the Prevention of Fouling. *U. S. Naval Inst. Proc.*, Vol. 78, No. 7, Whole No. 593, pp. 768–779. 1952.

No. 615. Harry J. Turner, Jr. Fourth Report on Investigations of the Shellfisheries of Massachusetts. *Com. Mass., Dept. Cons., Div. Mar. Fish.*, pp. 1–21. 1951.

No. 616. Henry Stommel and Harlow G. Farmer. Abrupt Change in Width in Two-Layer Open Channel Flow. *Sears Found., Jour. Mar. Res.*, Vol. 11, No. 2, pp. 205–214. 1952.

No. 617. Joanne Starr Malkus and Andrew F. Bunker. Observational Studies of the Air Flow over Nantucket Island during the Summer of 1950. *Papers in Physical Oceanography and Meteorology*, Vol. 12, No. 2, pp. 1–50. 1952.

No. 618. Andrew F. Bunker. Measurements of the Vertical Water Vapor Transport and Distribution within Unstable Atmospheric Ground Layers and the Turbulent Mass Exchange Coefficient. *Papers in Physical Oceanography and Meteorology*, Vol. 12, No. 3, pp. 1–42. 1952.

No. 619. William L. Ford and A. R. Miller. The Surface Layer of the Gulf Stream and Adjacent Waters. *Sears Found., Jour. Mar. Res.*, Vol. 11, No. 3, pp. 267–280. 1952.

No. 621. William S. von Arx. Notes on the Surface Velocity Profile and Horizontal Shear across the Width of the Gulf Stream. *Tellus*, Vol. 4, No. 3, pp. 211–214. 1952.

No. 622. William S. von Arx. A Laboratory Study of the Wind-driven Ocean Circulation. *Tellus*, Vol. 4, No. 4, pp. 311–318. 1952.

No. 623. Helen S. Vishniac and S. W. Watson. The Steroid Requirements of *Labyrinthula vitellina* var. *pacifica*. *Jour. Gen. Microbiol.*, Vol. 8, No. 2, pp. 248–255. 1953.

No. 624. Joanne Starr Malkus and Melvin E. Stern. The Flow of a Stable Atmosphere over a Heated Island, Part I. *Jour. Meteorology*, Vol. 10, No. 1, pp. 30–41. 1953.

No. 625. Melvin E. Stern and Joanne Starr Malkus. The Flow of a Stable Atmosphere over a Heated Island, Part II. *Jour. Meteorology*, Vol. 10, No. 2, pp. 105–120. 1953.

No. 626. William E. Schevill. On the Nomenclature of the Pacific Gray Whale. *Breviora*, No. 7, pp. 1–3. 1952.

No. 627. Alfred C. Redfield. The Flushing of Harbors and other Hydrodynamic Problems in Coastal Waters. In: *Hydrodynamics in Modern Technology*, Mass. Inst. Tech., pp. 127–135, December 1951.

No. 628. L. V. Worthington. Oceanographic Results of Project Skijump I and Skijump II in the Polar Sea, 1951–1952. *Trans. Amer. Geophys. Union*, Vol. 34, No. 4, pp. 543–551. 1953.

No. 629. Charles B. Officer, Jr. The Refraction Arrival in Water Covered Areas. *Geophysics*, Vol. 18, No. 4, pp. 805–819. 1953.

No. 630. Harry J. Turner, Jr. The Drilling Mechanism of the Naticidae. *Ecology*, Vol. 34, No. 1, pp. 222–223. 1953.

No. 631. Andrew F. Bunker. Diffusion, Entrainment and Frictional Drag Associated with Non-Saturated, Buoyant Air Parcels rising through a Turbulent Air Mass. *Jour. Meteorology*, Vol. 10, No. 3, pp. 212–218. 1953.

No. 632. P. F. Scholander and L. van Dam. Composition of the Swimbladder Gas in Deep Sea Fishes. *Biol. Bull.*, Vol 104, No. 1, pp. 75–86. 1953.

No. 633. L. van Dam and P. F. Scholander. Concentration of Hemoglobin in the Blood of Deep Sea Fishes. *Jour. Cell. and Comp. Physiol.*, Vol. 41, No. 3, pp. 522–524. 1953.

No. 634. Willem V. R. Malkus. A Recording Bathypitotmeter. *Sears Found., Jour. Mar. Res.*, Vol. 12, No. 1, pp. 51–59. 1953.

No. 636. Alfred C. Redfield. Interference Phenomena in the Tides of the Woods Hole Region. *Sears Found., Jour. Mar. Res.*, Vol. 12, No. 1, pp. 121–140. 1953.

No. 638. Harlow G. Farmer and George W. Morgan. The Salt Wedge. *Proc. Third Conf. on Coastal Engineering*, Cambridge, Mass., October 1952, pp. 54–64. 1953.

No. 639. J. R. D. Francis. A Note on the Velocity Distribution and Bottom Stress in a Wind-Driven Water Current System. *Sears Found., Jour. Mar. Res.*, Vol. 12, No. 1, pp. 93–98. 1953.

No. 640. Henry Stommel. Computation of Pollution in a Vertically Mixed Estuary. *Sewage and Industrial Wastes*, Vol. 25, No. 9, pp. 1065–1071. 1953.

No. 641. Jack L. Hough. Pleistocene Climatic Record in a Pacific Ocean Core Sample. *Jour. Geology*, Vol. 61, No. 3, pp. 252–262. 1953.

No. 642. Bostwick H. Ketchum. Circulation in Estuaries. *Proc. Third Conf. on Coastal Engineering*, Cambridge, Mass., October 1952, pp. 65–76. 1953.

No. 643. A. H. Woodcock. Salt Nuclei in Marine Air as a Function of Altitude and Wind Force. *Jour. Meteorology*, Vol. 10, No. 5, pp. 362–371. 1953.

No. 644. Henry Stommel, W. S. von Arx, D. Parson and W. S. Richardson. Rapid Aerial Survey of Gulf Stream with Camera and Radiation Thermometer. *Science*, Vol. 117, No. 3049, pp. 639–640. 1953.

No. 645. Henry Stommel. Examples of the Possible Role of Inertia and Stratification in the Dynamics of the Gulf Stream System. *Sears Found., Jour. Mar. Res.*, Vol. 12, No. 2, pp. 184–195. 1953.

No. 646. Henry C. Stetson. The Sediments of the Western Gulf of Mexico. Part I. The Continental Terrace of the Western Gulf of Mexico: its Surface Sediments, Origin and Development. *Papers in Physical Oceanography and Meteorology*, Vol. 12, No. 4, pp. 1–45. 1953.

No. 647. Parker D. Trask. The Sediments of the Western Gulf of Mexico. Part II. Chemical Studies of Sediments of the Western Gulf of Mexico. *Papers in Physical Oceanography and Meteorology*, Vol. 12, No. 4, pp. 47–120. 1953.

No. 648. William E. Schevill and Barbara Lawrence. Auditory Response of a Bottlenosed Porpoise, *Tursiops truncatus*, to Frequencies above 100 kc. *Jour. Exper. Zool.*, Vol. 124, No. 1, pp. 147–165. 1953.

No. 649. William S. von Arx. Cartographic Principles Applied to Wide-Field Photography. *Photogr. Engineering*, Vol. 4, No. 2, pp. 60–73. 1953.

No. 655. Henry Stommel. The Role of Density Currents in Estuaries. *Proc. Minnesota Int. Hydraulics Conv.*, Sept. 1–4, 1953, pp. 305–312. 1953.

No. 656. Harry J. Turner, Jr. Fifth Report on Investigations of the Shellfisheries of Massachusetts. *Com. Mass., Dept. Cons., Div. Mar. Fish.*, pp. 1–37. 1952.

No. 658. Duncan C. Blanchard. Raindrop Size-Distribution in Hawaiian Rains. *Jour. Meteorology*, Vol. 10, No. 6, pp. 457–473. 1953.

No. 659. Duncan C. Blanchard. A Simple Recording Technique for Determining Raindrop Size and Time of Occurrence of Rain Showers. *Trans. Amer. Geophys. Union*, Vol. 34, No. 4, pp. 534–538. 1953.

No. 660. A. H. Woodcock. Hawaii as a Cloud Physics Laboratory. *Pacific Science*, Vol. 7, No. 4, pp. 522–524. 1953.

No. 663. William E. Schevill and Barbara Lawrence. High-Frequency Auditory Response of a Bottlenosed Porpoise, *Tursiops truncatus* (Montagu). *Jour. Acoust. Soc. Amer.*, Vol. 25, No. 5, pp. 1016–1017. 1953.

No. 669. Hilary B. Moore, Harding Owre, Everett C. Jones and T. Dow. Plankton of the Florida Current. III. The Control of the Vertical Distribution of Zooplankton in the Daytime by Light and Temperature. *Bull. Mar. Sci. Gulf and Caribbean*, Vol. 3, No. 2, pp. 83–95. 1953.

No. 673. A. H. Woodcock, C. F. Kientzler, A. B. Arons and D. C. Blanchard. Giant Condensation Nuclei from Bursting Bubbles. *Nature*, Vol. 172, No. 4390, pp. 1144–1145. 1953.

No. 677. Ilmo Hela, Hilary B. Moore and Harding Owre. Seasonal Changes in the Surface Water Masses and in their Plankton in the Bermuda Area. *Bull. Mar. Sci. Gulf and Caribbean*, Vol. 3, No. 3, pp. 157–167. 1953.

No. 686. E. E. Watson. An Experiment to Determine the Hydrodynamic Forces on a Cable Inclined to the Direction of Flow. *Sears Found., Jour. Mar. Res.*, Vol. 12, No. 3, pp. 245–248. 1953.

No. 718. Arthur R. Miller. Some Suggestions for more precise Loran Navigation. *Navigation*, Vol. 3, Nos. 1 and 2, pp. 23–29. 1951.

No. 719. Henry B. Bigelow and Isabel Pérez Farfante. Fishes of the Western North Atlantic. Lancelets. *Mem. Sears Found. Mar. Res.*, No. 1, Pt. 1, Ch. 1, pp. 1–28. 1948. (Not included in *Collected Reprints*.)

No. 720. Henry B. Bigelow and William C. Schroeder. Fishes of the Western North Atlantic. Cyclostomes. *Mem. Sears Found. Mar. Res.*, No. 1, Pt. 1, Ch. 2, pp. 29–58. 1948. (Not included in *Collected Reprints*.)

No. 721. Henry B. Bigelow and William C. Schroeder. Fishes of the Western North Atlantic. Sharks. *Mem. Sears Found. Mar. Res.*, No. 1, Pt. 1, Ch. 3, pp. 59–576. 1948. (Not included in *Collected Reprints*.)

SEP 1954
LIBRARY
POFI
FISH & WILDLIFE
SERVICE